

---

# FOUNDATIONS OF SPACE BIOLOGY AND MEDICINE

---

(NASA-SF-374-Vol-1) FOUNDATIONS OF SPACE  
BIOLOGY AND MEDICINE. VOLUME 1: SPACE AS A  
HABITAT (NASA) 458 p MF \$2.25; SOD HC  
\$11.75

N76-26799  
THRU  
N76-26808  
Unclass  
41839

H1/52

# ОСНОВЫ КОСМИЧЕСКОЙ БИОЛОГИИ И МЕДИЦИНЫ

Совместное советско-американское издание

в трех томах

под общей редакцией

ОЛЕГА Г. ГАЗЕНКО (СССР) и МЕЛЬВИНА КАЛЬВИНА (США)

Том I

КОСМИЧЕСКОЕ ПРОСТРАНСТВО

КАК СРЕДА ОБИТАНИЯ



ИЗДАТЕЛЬСТВО «НАУКА» МОСКВА 1975

National Aeronautics and Space Administration, USA

Academy of Sciences of the USSR

Национальное управление по аэронавтике  
и исследованию космического пространства США

Академия наук СССР

**ORIGINAL CONTAINS  
COLOR ILLUSTRATIONS**

# FOUNDATIONS OF SPACE BIOLOGY AND MEDICINE

Joint USA/USSR Publication  
in Three Volumes

General Editors

MELVIN CALVIN (USA) and OLEG G. GAZENKO (USSR)

## Volume I SPACE AS A HABITAT



*Scientific and Technical Information Office*  
NATIONAL AERONAUTICS AND SPACE ADMINISTRATION  
*Washington, D.C. 1975*

*Dedicated to the memory of*

**HUGH LATIMER DRYDEN**

*and*

**ANATOLIY ARKADIEVICH BLAGONRAOV**

for their pioneering efforts to establish cooperation in  
the peaceful exploration and use of space between the  
National Aeronautics and Space Administration of the  
United States of America and the Academy of Sciences  
of the Union of Soviet Socialist Republics.

ON BEHALF OF the US National Aeronautics and Space Administration (NASA) and the USSR Academy of Sciences, we welcome the publication of this joint US/USSR review of space biology and medicine.

*Foundations of Space Biology and Medicine* is a comprehensive scientific and technical treatise summarizing the results achieved in this new field of knowledge during the last 15 years. It includes not only the results of biomedical investigations carried out during laboratory and flight experiments, but also a discussion of numerous factors which bear on the safety of manned space missions.

We believe that these three volumes are noteworthy for their content and for their demonstration of successful cooperation between US and Soviet scientists.

We believe, also, that this publication represents an important achievement in scientific cooperation in space research between our two nations which began with negotiations between Dr. Hugh L. Dryden, who was Deputy Administrator of NASA, and Academician Anatoliy A. Blagonravov, who was Chairman of the Commission on the Exploration and Use of Outer Space, USSR Academy of Sciences.

The US National Aeronautics and Space Administration and the USSR Academy of Sciences are, at present, well-advanced in preparations for the experimental Apollo-Soyuz flight of 1975 to test compatible rendezvous and docking systems for spacecraft and stations.

We are pleased that, in so short a time, we have progressed from joint efforts in scientific publication to joint efforts in actual flight operations. This points to a future in which we can work more closely together and with other nations in exploring the space environment which all men share.

  
JAMES C. FLETCHER  
*Administrator*  
US National Aeronautics  
and Space Administration

  
M. V. KELDYSH  
*President*  
Academy of Sciences of  
the USSR

### **Editorial Board**

M. Calvin, R. W. Krauss, J. P. Marbarger,  
O. E. Reynolds, J. M. Talbot (USA)  
A. I. Burnazyan, P. V. Vasil'yev, O. G. Gazenko,  
A. M. Genin, A. A. Imshenetskiy, G. I. Petrov,  
V. N. Chernigovskiy (USSR)

### **Executive Secretaries**

W. L. Jones (USA), E. F. Panchenkova (USSR)

### **Volume I Editors**

R. W. Krauss (USA)  
A. A. Imshenetskiy, G. I. Petrov (USSR)

### **Редколлегия:**

А. И. Бурназян, П. В. Васильев, О. Г. Газенко  
А. М. Генин, А. А. Имшенецкий, Г. И. Петров,  
В. Н. Черниговский (СССР)  
М. Кальвин, Р. В. Краусс, Дж. П. Марбаргер,  
О. Е. Рейнольдс, Дж. М. Тальбот (США)

### **Ответственные секретари**

Э. Ф. Панченкова (СССР). У. Л. Джонс (США)

### **Редакторы I тома**

А. А. Имшенецкий, Г. И. Петров (СССР)  
Р. В. Краусс (США)

## FOREWORD

**FOUNDATIONS OF SPACE BIOLOGY AND MEDICINE** is a collective scientific work which reviews the most important problems, achievements, and prospects for the development of space biology and medicine. Its purpose is to make available to specialists, and those who will become specialists, summarized and systematized data on the most important problems of space biology and medicine, accumulated in man's study and mastery of space during the first years of the space effort. The text is published in three volumes, in authentic English and Russian versions.

This joint work began with an exchange of correspondence between the US National Aeronautics and Space Administration and the Academy of Sciences, USSR, with the objective of developing cooperation in matters relating to space. The correspondence, under the general leadership of Dr. Hugh L. Dryden and Academician Anatoliy A. Blagonravov, resulted in a series of agreements, one of which, reached in October 1965, called for preparation and publication of a joint scientific work, *Foundations of Space Biology and Medicine*.

In order to carry out this agreement, a Joint Editorial Board was established early in 1966, under the cochairmanship of Professor Melvin Calvin and the late Academician Norair M. Sisakyan (replaced in March of that year by Professor Oleg G. Gazeiko). Members of the US portion of the Joint Editorial Board were: Professors Robert W. Krauss, John P. Marbarger, the late Loren D. Carlson and Wolf V. Vishniac; Dr. Orr E. Reynolds, and Brigadier General John M. Talbot, USAF, MC (Retired). Members of the Soviet portion were: Academicians Alexander A. Imshenetskiy, Vladimir N. Chernigovskiy, Georgiy I. Petrov, the late Vasiliy V. Parin (replaced upon his death in 1971 by Professor Dr. Pavel V. Vasil'yev), Professor Drs. Avetik I. Burnazyan and Abram M. Genin.

Initial discussions among Dr. Orr E. Reynolds, Professors Robert W. Krauss, and Anatoliy A. Nichiporovich involved questions on the structure and content of the joint work. In a series of meetings that followed, members of the Joint Editorial Board carefully developed and coordinated plans for chapters, procedures for completing the work, and instructional materials for authors. All materials were to be divided into 45 chapters, to comprise three volumes.

Volume I. SPACE AS A HABITAT. Editors: the late Professor Wolf V. Vishniac (replaced in December 1973 by Professor Robert W. Krauss) (USA) and Academicians Alexander A. Imshenetskiy and Georgiy I. Petrov (USSR).

Volume II. ECOLOGICAL AND PHYSIOLOGICAL FOUNDATIONS OF SPACE BIOLOGY AND MEDICINE. Editors: Professor John P. Marbarger (USA) and the late Academician Vasiliy V. Parin (replaced in 1971 by Professor Dr. Pavel V. Vasil'yev) (USSR).

Volume III. SPACE MEDICINE AND BIOTECHNOLOGY. Editors: Brigadier General John M. Talbot, USAF, MC (Retired) (USA), and Professor Dr. Abram M. Genin (USSR).

The work undertaken by the Joint Editorial Board was unprecedented in nature and scope, at least for those concerned with it. It was deemed necessary to develop special procedures for preparation of the joint work and to determine the sequence and schedule of the individual stages. For example, in order to assure the most careful and complete selection of materials for each chapter, each segment of the Joint Editorial Board named review composers (referred to in each chapter) to prepare summaries of works and bibliographies on their respective national materials and to utilize the most important data from the world literature. The material collected was exchanged and evaluated. Then, each segment suggested a list of authors for the corresponding chapters, the Joint Editorial Board making the final selection of authors. As a result, 19 chapters were prepared by US authors, 20 by USSR authors, and six were prepared jointly.

With few exceptions, chapters were written by different authors. Their views on individual problems, as well as on broader aspects of the discipline, understandably did not always agree. This posed a difficult task—to establish relationship between chapters, coordinate and illuminate contradictory points of view wherever possible, and fill gaps. Detailed plans for each chapter were developed and sent to all authors with general rules for preparing the manuscripts. All chapters were reviewed by Soviet and US experts.

In spite of our best efforts, probably we may not have completely achieved a homogeneous presentation with harmonious views and the clearest sequencing of material. However, utmost effort has been made to give authors the greatest freedom possible, in the belief that their competence and expertise fully compensate for structural shortcomings.

These three volumes represent successful completion of one of the cooperative projects between the US National Aeronautics and Space Administration and the Academy of Sciences, USSR, in space biology and medicine. The work is commended to specialists worldwide for study and use. It is believed that it is of value not only for scientific and technical content, but also as evidence that scientists of the two nations can work together effectively to achieve a common goal.

We believe that the Joint Editorial Board's efforts in preparing this work have been effective, useful, and pleasant, providing an opportunity for fuller understanding between two peoples, to become more familiar with the science, culture, and traditions of the two nations, and to work with mutual aid for constructive solutions of problems encountered in space biology and medicine.

The effective effort by members of the Joint Editorial Board, during some eight years, is officially noted here. The result is successful completion of this complex work. Significant contributions made by others include the Executive Secretaries of both sections of the Editorial Board, Drs. Walton L. Jones and Eleanora F. Panchenkova; past Executive Secretaries: Virginia M. Bolton and Drs. George J. Jacobs, Stanley C. White, and Edward J. McLaughlin; assistants to

the Executive Secretaries: Walter B. Sullivan, Jr., Rebecca R. Wise, and Irvin C. Mohler (USA); and Galina Ya. Tverskaya, Tatyana B. Kasatkina, and Lyudmila Zille (USSR); Scientific Secretary to the USSR Academy of Sciences Commission on Exploration and Use of Outer Space Genrikh S. Balayan; consultants on international aspects, Dr. Oscar E. Anderson, Philip A. Thibideau, and Yuri P. Khomenko; and the staffs of the US Embassy in Moscow and the Soviet Embassy in Washington, who facilitated contacts and the exchange of material.

The Joint Editorial Board expresses warm gratitude to personnel in the two respective publishing houses who made every effort toward this work being attractive and convenient for the reader.



MELVIN CALVIN  
*University of California  
at Berkeley, California, USA*



OLEG G. GAZENKO  
*Institute of Medical and Biological  
Problems  
USSR Ministry of Public Health,  
Moscow*

Volume I

SPACE AS A HABITAT

## CONTENTS

### VOLUME I

Introduction.....	xv
PART 1. PHYSICAL PROPERTIES OF SPACE AND THEIR BIOLOGICAL SIGNIFICANCE	
Chapter 1. Theories of the Origin and Nature of the Universe..... A. G. W. CAMERON	3
Chapter 2. Physical Characteristics of Interplanetary Space..... S. N. VERNOV, YU. I. LOGACHEV, AND N. F. PISARENKO	32
PART 2. PLANETS AND SATELLITES OF THE SOLAR SYSTEM FROM PHYSICAL AND ECOLOGICAL POINTS OF VIEW	
Chapter 3. The Moon and Its Nature..... HAROLD C. UREY	115
Chapter 4. Earth-Type Planets (Mercury, Venus, and Mars)..... M. YA. MAROV AND V. D. DAVYDOV	133
Chapter 5. Planets and Satellites of the Outer Solar System, Asteroids, and Comets..... RAY L. NEWBURN, JR. AND SAMUEL GULKIS	197
PART 3. PROBLEMS OF EXOBIOLOGY	
Chapter 6. Biological Effects of Extreme Environmental Conditions..... A. A. IMSHENETSKIY	271
Chapter 7. Theoretical and Experimental Prerequisites of Exobiology..... A. I. OPARIN	321
Chapter 8. Search for and Investigation of Extraterrestrial Forms of Life... A. B. RUBIN	368
Chapter 9. Planetary Quarantine: Principles, Methods, and Problems..... LAWRENCE B. HALL	403
Authors' Addresses.....	431
Index.....	433

## INTRODUCTION

The last decade has witnessed the beginning of man's exploration of the Universe with an entirely new potentiality—manned and instrumented space vehicles capable of bringing observations closer to celestial bodies than had been deemed possible a few years ago. How far into the Universe this exploration will ultimately lead is in the hands of future generations. However, the solar system is already highly instrumented, with data being recorded hourly both directly and indirectly. A vast amount of information is accumulating, the resolution of which will take painstaking effort for many years. In short, mankind has achieved familiarity with the Sun and its planets in a comparatively short time.

Understanding of the physical and chemical characteristics of the solar system has impelled man's curiosity to seek solutions to problems long considered beyond reach. Experiments on forces, matter, and radiation, discovered in interplanetary space, can now be conducted expeditiously and with high precision. Cosmological concerns with the origin of the Universe have uncovered new data suggesting refinements in our understanding of how matter and energy were scattered over the wide framework of the cosmos. Through the direct exploration of space, tools have evolved that are far more powerful than anticipated, but which are still primitive and inadequate for solving the problems that lie ahead. Opportunities exist for testing theories concerning the origin of life, not only in this planetary system, but also conceivably in other stellar clusters and other galaxies. The launching of space probe after space probe has not only brought to man an awareness of his physical insignificance in the Universe, but also has given him a quiet confidence in his ability to understand it all—given sufficient time and freedom for re-

search. Scientists worldwide have joined in the desire to compare views and lay groundwork for a cosmology that will ultimately merge with the development of unified field theory for physics in general.

In Volume I of this series, an effort is made to lay the physical groundwork for biologists and physicians to appreciate current data about the structure of the Universe, especially the nature of our solar system and its galaxy. The intent of the authors in their contributions to Volume I is to provide for the serious student, as well as for the lay reader, an intellectual base toward appreciation and understanding of the problems faced by biologists—not only in the exploration of space and testing of theories, but also in simple survival in that vast area now being explored by cosmonauts and astronauts.

Volume I is essentially in two major parts. The first five chapters are designed to present the nature of the Universe built from a cosmological point of view. It is important that the reader will understand the characteristics not only of the planets of the solar system, but also of the space occupying most of the void between them. The Moon, the most thoroughly explored extraterrestrial body, has been described in detail and is a type study to characterize the geology, geochemistry, and geophysics of other celestial bodies. Data included in Volume I from classical astronomy and from recent instrumented space flights tell much about the structure of the other planets close to us in the total scheme of space, but which are very distant in terms of the current limitations to man's space travel at the present stage of space vehicle engineering.

The remaining chapters of the first volume, chapters 6 through 9, are directed toward an understanding of some of the biological strategies

for life on other celestial bodies. Exobiology is described in the context of modern biochemistry and biophysics. At the same time, efforts are directed toward explaining the dilemma facing scientists in designing apparatus to provide unequivocal answers on the existence of extraterrestrial life. All of this writing indicates that the severe environmental stresses of planetary surfaces, including those of the Earth, govern the limits within which life must originate and evolve.

The coeditors of Volume I have taken few liberties with the chapters. By and large, they represent the individual responses of American and Soviet colleagues to the requests made of them. In all cases, each author was provided with information available in the literature outside his own nation. An author is generally more familiar with research in his own country than elsewhere, which is to be expected. The editors have made an effort to stimulate inclusion of material which otherwise might be omitted, but the responsibility for that which has been included remained entirely with the authors. Every effort has been made to collect pertinent data from any necessary source. Material which is important to those attempting a basic comprehension of physical astronomy and cosmology has been included. Succeeding authors have laid a groundwork for the review of parameters which must be taken into account, whether space serves as an exploratory laboratory for biological theories developed on Earth, or if it is to be approached as a hostile

environment that must be occupied for varying periods by man.

The space beyond the Earth's atmosphere is perhaps not as hostile as it is demanding. The pioneering thus far has proved that men are capable of surviving in the space environment and pursuing scientific curiosity while there. This can be considered no less than a gigantic step for mankind in its search for intellectual absolutes.

This introduction would not be complete without recognition of the contributions by the late Dr. Wolf Vishniac of the University of Rochester [N.Y.], who shared in early plans for the development of these volumes, and who contributed both spirit and substance to the content of all chapters in Volume I. Dr. Vishniac's superb command of both the English and Russian languages did much to remove linguistic barriers and to expedite the completion of this work. His untimely death in the pursuit of exobiological data saddened all of us. It is with profound respect and affection for our late colleague that the current coeditors dedicate this volume to his memory.

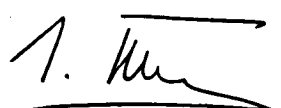
The coeditors also express profound appreciation to the compilers and reviewers who shared materials to assist the authors; a complete list of these contributors is at the end of the volume. Without their supporting expertise, the quality of this publication would have been diminished. The editors join the authors in expressing sincere gratitude to the collaborators.



ROBERT W. KRAUSS  
*College of Science*  
*Oregon State University*  
*Corvallis, Oregon, USA*



A. A. IMSHENETSKIY  
*Institute of Microbiology*  
*USSR Academy of Sciences*  
*Moscow, USSR*



G. I. PETROV  
*Institute of Space Exploration*  
*USSR Academy of Sciences*  
*Moscow, USSR*

## **Part 1**

# **PHYSICAL PROPERTIES OF SPACE AND THEIR BIOLOGICAL SIGNIFICANCE**



Trifid Nebula in Sagittarius (NGC6514; Messier 20). The Trifid is a typical emission nebula and is excited to luminosity by the presence of hot early-type stars. The nebula is about 2300 light-years from Earth and its diameter is estimated to be 30 light-years. (Copyright by the California Institute of Technology and Carnegie Institution of Washington. A Hale Observatories photo.)

REPRODUCIBILITY OF THE  
PAGE IS POOR

## Chapter 1

## THEORIES OF THE ORIGIN AND NATURE OF THE UNIVERSE

A. G. W. CAMERON<sup>1</sup>

Harvard College Observatory, Cambridge, Massachusetts USA

**COSMOLOGY**

Radio and optical telescopes enable us to see only a very small fraction of the universe. All of our knowledge of physics and astronomy is limited to a relatively local part of the universe; it is necessary to extrapolate this knowledge to a much larger scale of time and distance. The cosmologist starts by assuming a broad, physical, "cosmologic principle" to govern his theory of behavior of the universe, which is subject to experimental and observational verification like any other law of physics. The cosmologist can, at present, only assume his broad principle and some framework of the physics of general relativity, work out the mathematical consequences of a model of the universe, and determine if the predicted phenomena are experimentally or observationally verifiable [36, 46, 56 or 58].

Most systems of cosmology are based upon a cosmologic principle, according to which, on a large-scale average, every point in space is indistinguishable from every other point in space, at a given cosmologic time.

Individual points in space are not observable as such, only objects in space. Consequently, the cosmologic principle can only be applied to the contents of space which can be observed. Each piece of matter in space has its own hierarchy

of structure, and possesses its own intrinsic motion. Therefore, it is necessary to consider the average motion of many pieces of matter existing in a particular region of space as representing the general behavior of that region of space. The cosmologist must also ignore that in observable space, matter is collected into compact bodies while most of the intervening space is relatively empty. He assumes, in constructing his theory, that the mass of compact bodies in space is smeared out into a medium of average density, and he ignores special effects which may be caused by condensation of matter into compact bodies.

*"Big Bang" theory.* A consequence of general relativity, as formulated by Einstein, and applied to cosmology by Friedmann, is that only a universe containing no matter at all can be truly static. If matter is present, then the universe must be in either a state of expansion or contraction. Observations indicate that our observable universe is in a state of expansion. Distant matter in the universe, not gravitationally bound to our local system of galaxies, is receding from us. According to cosmologic principle, on any one of those distant pieces of matter, the same behavior would be observed from the point of view in space that we see in our own: all distant masses will be receding from the observer.

If distant masses in the universe are receding at present with a velocity proportional to their

---

<sup>1</sup> The work of A. A. Mikhailov (USSR) in the compilation of material for this chapter is gratefully acknowledged.

distance from us, then, going into the past, it would be found that local density of matter becomes progressively higher. If one goes far enough into the past, it would be discovered that matter in the universe progressively draws closer together, until at some finite time in the past, matter would appear to be gathered together at a single point. Such a picture is described as a "Big Bang" cosmology, matter exploding away from infinite density at a finite time in the past, which can be regarded as a sort of creation event. The relatively simple mathematical models of cosmology based upon this point of view are generally called Friedmann universes, on which most discussions of cosmologic processes are based.

*Steady state cosmology.* A number of British cosmologists were not satisfied with the "Big Bang" cosmologic principle. One of the corollaries of Einstein's general theory of relativity is that time has many dimensional attributes similar to those of space. Since space and time are joined in a four-dimensional geometry of space-time, it was therefore asked why the cosmologic principle should apply only to space, and not also to time. A broader, cosmologic principle, the "perfect cosmologic principle," was proposed which postulates that every observer in the universe, on a large-scale average, should see the same picture at every point in space and at every time.

The universe will always exhibit the same average behavior, according to this principle. Since the universe is observed to be expanding, and since the perfect cosmologic principle requires that the average density of matter in space should remain constant, then it is also necessary to postulate that additional matter must be created in space to replace loss through expansion. Since matter being lost is observed in the form of galaxies and clusters of galaxies, it is necessary to postulate that newly created matter must condense to form new systems of galaxies. This general picture is called steady state cosmology.

The continuous creation of matter, it must be emphasized, is a postulate of a physical process which has never been observed experimentally. Thus, the perfect cosmologic principle requires assuming new and untested laws of physics which

need not be invoked in the cosmologies based only upon the ordinary cosmologic principle.

When Einstein first applied his theory of general relativity to cosmology, it was widely assumed that the universe was static. He realized that his ordinary theory of general relativity predicted either an expanding or contracting universe, experimented with the form of his equations, and found that by adding a term to his general equation, called the "cosmologic constant," it had the property of rendering the universe nearly static for very long periods. After it was discovered that the universe appears to be expanding, Einstein dropped his experiments with the cosmologic constant, although other cosmologists have continued such experiments, producing various types of cosmologic models based upon this constant.

The expansion of the universe was discovered by Hubble, resulting from his work on measuring the spectra of galaxies. The fainter the galaxy, he found, the greater the shift toward the red of the characteristic spectral lines in the light of that galaxy. The red shift of the spectral lines is interpreted as a Doppler shift, indicating that distant galaxies are receding from us. A distant galaxy is receding from us at a rate which appears to be proportional to its distance, a relationship known as the "Hubble law." If motions of distant galaxies are extrapolated backwards in time, it appears that the "Big Bang" must have occurred between 1 and  $2 \times 10^{10}$  years ago.

The red shifts of galaxies were essentially the only concrete observational data available to cosmology until the mid-1960s.

*Background radiation.* In 1965, Penzias and Wilson discovered microwave background radiation, and found that radio waves, at a wavelength of 7.5 cm, are constantly impinging on the Earth with an equal intensity from all directions in space. Other investigators have corroborated this throughout the observable radio wavelength region, and observations based upon interstellar molecules have confirmed that the radiation has approximately a blackbody shape down to a wavelength of about 1 mm at 2.7° K. The simplest interpretation of this background radiation is that it is a relic of a hot early stage in the universe, when matter in the universe was closely

compacted and much higher in temperature than at present. When density of matter and temperature are high enough, then matter becomes ionized and fully in equilibrium with blackbody radiation. When temperature falls low enough so that matter, primarily composed of hydrogen, can recombine to neutral form, interaction between radiation and matter becomes very small, and radiation is free to expand into space with the universe. This expansion dilutes radiation, and photons suffer a red shift, so that the shape of the spectrum remains that of a blackbody while temperature is progressively decreased.

The idea of a very hot initial medium was proposed by Gamow [17] who predicted a temperature of  $6^{\circ}\text{K}$  instead of the actual  $2.7^{\circ}\text{K}$  for the present epoch. Doroshkevich and Novikov [11] pointed out that relic radiation would exceed the combined radiation of radio sources and stars in the 1–10 cm wavelength region. Dicke et al [10], beginning an experimental search for relic radiation, learned of the findings of Penzias and Wilson, and were immediately able to explain the results.

That isotropic background radiation is necessarily thermal in origin or that it has a Planck shape is not agreed upon by all astronomers. Suggestions have been made that radiation could arise from great numbers of unknown emitters isotropically distributed in space. Most suggestions involve very complex models of these unknown emitters and numerous arbitrary assumptions. An alternative model, complex though it may be, is necessary if the true cosmologic model should be steady state, for example, which never undergoes a high-density, high-temperature phase.

Within the context of a Friedmann model of the expanding universe, if density of matter presently in the universe is less than a critical value of a little less than  $10^{-29} \text{ g/cm}^3$ , the universe will always expand, and is described as an open universe. On the other hand, if density is greater than the critical value, expansion of the universe will coast to a halt, and the universe will start to contract again toward infinite density. This cosmologic model is called a closed universe. Critical density depends upon the precise value of the constant of proportionality in the Hubble law.

Many variations of Einstein's general theory of relativity have been suggested, all of which produce slight variations in their associated cosmologies. Only one of these is mentioned here because it has received a fair amount of attention in recent years: the scalar-tensor theory of general relativity. Einstein's theory of relativity is characterized by a tensor gravitational field, and added to this is a scalar gravitational field. This theory can predict some differences in the behavior of a cosmologic model compared to those in a Friedmann universe, including a very rapid expansion in the early history of the cosmologic model, and a variation with time of the gravitational "constant" in the Newtonian force law of mass attraction between bodies. The directly measurable consequences of addition of a scalar to a tensor field are very small, and it has not yet been possible to make an experimental choice between the two theories [36].

## PHYSICS OF THE EARLY UNIVERSE

Considerable interaction between high energy particle physics and cosmology during the last few years has been stimulated by the discovery of microwave background radiation, which implies that the universe was once highly dense, very hot, and originated from a big bang. This interaction raises the very important issue of whether the universe is symmetric in matter and antimatter, or unsymmetric with an excess of one over the other. This difference can have an important influence on the behavior of the very early universe; some aspects of the difference may persist until the present; allowing a possible test of the degree of symmetry of the universe. In discussing initially the behavior of the unsymmetric universe, it is assumed that all galaxies visible in space are composed of ordinary matter.

### Unsymmetric Universe—Open Model

The story begins when the universe was approximately  $10^{-43} \text{ s}$  old. The characteristic length associated with the universe, known as the "Hubble radius," is  $r=ct$ , the age of the universe multiplied by the velocity of light, a distance of only  $3\times 10^{-33} \text{ cm}$ . This is much smaller than the

characteristic radius of any of the elementary particles with which we deal in the universe today, called the "Compton radius," which is inversely proportional to the mass of the particle. Ordinary neutrons and protons have radii around  $10^{-13}$  cm so it might be said that the universe is not yet old enough to contain ordinary neutrons and protons at  $10^{-43}$  s [19].

If any matter exists in the universe at this time, it must consist either of a highly excited baryonic state of the neutron or proton, or of some completely unknown form of matter. In any case, particles in the universe at  $10^{-43}$  s can be expected to have masses of the order of  $10^{-5}$  g in order to fit into the Hubble radius. Such particles are entirely hypothetical, lying far beyond the scope of the existing particle theory and its extrapolations.

The universe at this time is best described as chaotic. The Hubble radius has a value comparable to expected quantum fluctuations in the structure of the universe, if general relativity is to be unified with quantum mechanics in some way. If the age of the universe is multiplied by the energy content, including rest mass, of the volume contained within a Hubble radius, the result is a number of the order of Planck's constant,  $\hbar$ . This is the cosmologic expression of the Heisenberg uncertainty principle. It does not make any physical sense to inquire what happened in the universe earlier than  $10^{-43}$  s, because such times are not meaningful due to the energy uncertainty.

As the universe grows older, the Hubble radius grows and encompasses many types of particle. These particles can interact and achieve a thermodynamic equilibrium, and the mass of particles which can exist in the universe becomes progressively lower as the Hubble radius increases.

The character of physics at this expansion epoch is rendered uncertain by the unknown form of the mass excitation spectrum of the baryon. Hagedorn has suggested that the number of baryon states per unit mass interval rises exponentially, which leads to an expectation that the universe will have a finite maximum temperature that could have been attained in early times, of the order of  $10^{12}$  °K. This limiting temperature is asymptotically attained as the rest mass of the baryons present goes to infinity. In the Hagedorn

version of early cosmology, the early universe would have this limiting temperature, and as it expands, the characteristic masses of particles present would progressively decrease [18]. Significant variations in the ratio of baryons to antibaryons may exist in this picture. Only when the universe has expanded enough so that most of the particles expected to be present are neutrons and protons, would the temperature decrease appreciably below  $10^{12}$  °K.

However, if the number of mass states of the baryon should increase with mass at a rate slower than exponential, then there is no upper limit on the temperature of matter, and this can become arbitrarily high. In such a case, the earliest universe would contain both matter and antimatter in profusion, but with a slight excess of matter over antimatter, at least in that region of the universe which will form our own galaxy. In this version of cosmology, matter and antimatter progressively annihilate, until, when temperature falls below  $10^{12}$  °K, only baryons which are in excess of antibaryons remain unannihilated, and the local part of the universe then contains only matter in the form of baryons (see under next section, **Symmetric Universe—Open Model**).

At temperatures in the universe between  $10^{11}$  and  $10^{12}$  °K, it is not possible for baryonic pairs to exist together, but pi and mu mesons can exist in profusion. As expansion occurs and the universe cools, the pi mesons disappear, followed by the mu mesons which also disappear. This leaves matter consisting of some neutrons and protons, electron-positron pairs with a small excess of electrons, muon neutrinos and antineutrinos, and electron neutrinos and antineutrinos, as well as photons. After mu mesons have disappeared, mu meson neutrinos and antineutrinos no longer interact with the rest of the particles. When temperature falls below  $10^{10}$  °K, electron neutrinos and antineutrinos no longer interact with ordinary matter, and shortly afterwards, electron-positron pairs disappear through annihilation [33, 56, 58]. Both electron and muon neutrinos and antineutrinos contribute energy density and pressure which help to drive the expansion of the universe, but it is only in this indirect way that these particles can have further influence upon physical events in the universe [36].

During the time that electron-positron pairs were present in the expanding universe, they were interacting with neutrons and protons present, causing interconversion of one into the other. This sets up an equilibrium between neutrons and protons, in which protons are somewhat more abundant than neutrons, since their mass is slightly less than that of neutrons. About seven times as many protons as neutrons are expected at the time that electron-positron pairs disappear through annihilation [36].

When temperature falls to  $10^9$  °K, it becomes possible for complex nuclei to exist. The first nucleus formed, deuterium, results from combination of a neutron with a proton with the emission of a photon. At the same time, absorption of photons from the radiation field by the resulting deuterium nuclei will result in their photodisintegration back into neutrons and protons. At first, photodisintegration greatly predominates, and very little deuterium can be present. However, as the temperature falls, equilibrium shifts toward deuterium in the medium.

Deuterium can in turn capture neutrons to form tritium. This nucleus is radioactive with a half-life of 12 years, which is very long compared to the expansion time in this discussion, when the expansion age of the universe is just a few minutes. Thermonuclear reactions then take place between deuterium and tritium, forming helium. At the expected matter densities for this stage in the expansion of the universe, these reactions go nearly to full completion, converting almost all of the neutrons in the mixture into helium. Since there were more protons present than neutrons, excess protons are left over following completion of nuclear reactions. About one-fourth of the matter becomes helium under these conditions. Very little deuterium and tritium is left when universal expansion has reached an age of half an hour [36].

The amount of helium formed in this way is comparable to that which appears to exist in all stars, both very old and quite new. The amount of helium produced by cosmologic nucleosynthesis varies from about 28% in a closed universe, to about 24% in an open universe. A variety of observational and theoretical evidence indicates

that this is an approximately universal abundance of helium observed in stars everywhere in space, but it is not yet known whether the abundance of helium in these stars is sufficiently close to a single value to indicate that the uniform process of cosmologic nucleosynthesis has been responsible.

The amount of deuterium and  $^3\text{He}$  produced in a closed universe model is negligible, but in an open universe it is quite possible to produce amounts of deuterium and  $^3\text{He}$  comparable to those inferred in the primitive solar nebula from which the solar system evolved. If no alternative method should be found for producing deuterium and  $^3\text{He}$ , this would constitute strong evidence in favor of this unsymmetrical model of the universe, and would identify our universe as an open model [39, 53]. However, this claim cannot yet be made because not all alternative methods of producing deuterium and  $^3\text{He}$  have yet been ruled out.

As the universe continues to expand, it is composed of hydrogen, helium, electrons, and photons, with various types of neutrinos and antineutrinos arising from interaction with other particles. Photons continue to interact strongly with matter, and because most of the pressure is in photons, matter is unable to fragment into self-gravitating bodies, such as galaxies or clusters of galaxies at this stage in the expansion of the universe.

When the expansion of the universe is nearly 1 million years old, the temperature of matter and radiation will have fallen close to  $3000^\circ$  K. Already, helium will have recombined to the neutral form, and, at this temperature, hydrogen also recombines to form neutral hydrogen atoms. This makes a tremendous difference in the interaction between matter and radiation. As long as hydrogen was ionized, radiation photons could move only relatively short distances before undergoing Compton scattering on the free electrons. However, after recombination, only Rayleigh scattering is possible with neutral hydrogen atoms, and the mean free path of photons becomes larger than the Hubble radius of the universe. Hence, photons can expand indefinitely into space after recombination, and these constitute the isotropic background microwave radiation with a present temperature of  $2.7^\circ$  K in this type of

cosmologic model. It is possible for gravitational instabilities in matter to grow only after decoupling from radiation.

### Symmetric Universe—Open Model

What is necessary in a symmetric universe? There is, at present, as much matter as antimatter among visible galaxies in the universe. It can be assumed that imbalance between matter and antimatter arose from fluctuations in the relative numbers of baryons and antibaryons at different places in the early expanding universe. This type of assumption has an ad hoc character which does not lead to a natural explanation for anything. An attempt to find processes which can lead to separation of matter and antimatter on at least the galactic scale, starting from an intimate microscopic mixture of baryons and antibaryons, has been carried out in recent years by Omnes. The following theoretical developments are generally ascribed to him.

First, new developments have been reported by Parker at the Aspen Workshop, June 1972, on The Physics of the Early Universe. Returning to a universal age of  $10^{-43}$  s and universal chaos, chaos is defined as different parts of the universe, merging with Hubble radii of  $3 \times 10^{-33}$  cm which introduce fluctuating gravitational potentials containing tremendous energy. Parker investigated the consequences of rapid nonisotropic expansion of the universe under these circumstances, and found that baryon-antibaryon creation can occur in which strong chaotic gradients in the gravitational potential are largely converted into rest mass and kinetic energy of baryon-antibaryon pairs. Furthermore, pair creation occurs over distances slightly greater than the Hubble radius, thus introducing a possible mechanism which can lead to large-scale homogeneity in expansion of the universe. This mechanism predicts production of equal numbers of baryons and antibaryons with any microscopic volume.

Zel'dovich and Starobinsky pointed out the importance of pair creation in an anisotropically expanding universe. The influence of created pairs on expansion tends to make expansion isotropic, which is a step toward an explanation of the Friedmann expansion law.

At temperatures greater than about  $3 \times 10^{12}$  °K (Omnes' basic hypothesis), there exists a phase separation between baryons and antibaryons [29]. The existence of these phases is very controversial and according to Omnes, in a statistical sense, baryons and antibaryons cannot approach each other too closely and retain their identity, whereas baryons can approach indefinitely closely to baryons, and antibaryons to antibaryons. This leads to an expected separation of baryons and antibaryons into two condensed phases, with separate blobs of baryons and antibaryons growing to dimensions of around  $3 \times 10^{-4}$  cm by the time the temperature has fallen to about  $3 \times 10^{12}$  °K, each patch of material containing about 10 kg of material.

After the temperature has fallen below  $3 \times 10^{12}$  °K, the thermodynamic condition which favored separation of the baryon from the antibaryon phase would no longer be the lowest thermodynamic energy state. Therefore, Omnes expects baryons and antibaryons in the separated patches to start diffusing together, leading to mutual annihilation. This mutual annihilation will continue until temperature has fallen to around  $3 \times 10^8$  °K. At this time, most of the original matter and antimatter will have disappeared in mutual annihilation, feeding energy into the photon field, and reducing the number of baryons or antibaryons to about  $10^{-8}$ /photon.

At this stage, separate patches of matter and antimatter still exist. These patches continue to annihilate baryons and antibaryons along the borders between patches, but as temperature in the universe continues to fall, a new process sets in which Omnes calls the coalescence stage. Annihilation causes relative motions among patches of matter and antimatter, with a matter patch being repelled from an antimatter patch due to annihilation along the common boundary, but with mergers occurring when a matter patch meets other matter patches, or antimatter patches meet other antimatter patches.

These conditions have prevented the formation of helium or other light elements when the temperature was approximately  $10^9$  °K. Under these conditions, there is no longer an electron-positron pair plasma present everywhere in space, hence there is no longer interconversion of neu-

trons to protons at that temperature. Because neutrons, which have remained after disappearance of electron-positron pairs, can diffuse faster than protons, there has been preferential annihilation of neutrons and antineutrons during the annihilation stage. Thus, in this type of symmetric universe there is no formation of large quantities of primordial helium (or antihelium), and some other type of event would be required to form large quantities of helium in the pregalactic stage of evolution of the universe.

As the universe expands, material in separate patches of matter and antimatter during the coalescence phase continues to grow rapidly. This is partially due to rather rapid motions of matter and radiation taking place within the universe at this time, because the speed of sound is not much less than the speed of light. However, when the characteristic radiation temperature falls to  $3000^{\circ}$  K, so that hydrogen recombines to the neutral form, the speed of sound in the decoupled matter decreases drastically, and the motion of such matter in the universe is greatly decreased. In effect, this brings the coalescence stage to an end and practically ends the mutual annihilation of matter and antimatter on the boundaries between their separate patches. Omnes has estimated that the patches contain an amount of matter at least as great as that of a typical galaxy at this stage. It is not out of question that the patches should contain enough matter to form clusters of galaxies. The discussion in the section that follows, THE PREGALACTIC ERA, would be more consistent with the Omnes cosmology if the separate patches had grown to the size of clusters of galaxies.

In summary, symmetric and unsymmetric types of cosmology lead to very similar results throughout the universe, with symmetric cosmology predicting that clusters of galaxies may tend to be either all of matter, or all of antimatter, and the unsymmetric cosmology predicting that visible galaxies are all composed of matter. There is no practical way to distinguish between these pictures by direct observation. However, the symmetric cosmology predicts that helium will not be formed in large amounts by cosmologic nucleosynthesis, and the unsymmetric cosmology not only predicts such a large cosmologic nucleo-

synthesis of helium, but also possibly that of deuterium and  $^3\text{He}$  as well, if we live in an open cosmologic model.

### THE PREGALACTIC ERA

The problem of gravitational instability within a large self-gravitating medium was first considered many years ago by Sir James Jeans. There is a critical length, called the Jeans length, such that disturbances of wavelengths longer than the Jeans length are unstable against gravitational contraction within the medium, whereas disturbances of wavelengths smaller than the Jeans length will be damped out and will propagate as giant sound waves.

Peebles and Dicke [37] postulated that following hydrogen recombination in the universe, matter may contain density perturbations over a wide range of scales, and that the most frequent of the perturbations which can become gravitationally unstable will have wavelengths close to the Jeans length. However, there is no theoretical basis at present to estimate the expected magnitude of such density fluctuations within the universe at a particular time. If the density fluctuation is very small, then it takes a long time for it to be felt within the expanding universe, and for the matter associated with the fluctuation to fragment and condense away from its neighboring matter. Thus, fragmentation time within the expanding universe may be very long.

A comprehensive study of perturbations superimposed on the isotropic homogeneous Friedmann solution (carried out by Lifshitz [24]) included simultaneous perturbations of radiation and matter density, rotational motion, and gravitational waves. Doroshkevich, Novikov, and Zel'dovich [12] added the perturbation of matter density on the unperturbed radiation (photon) background. This type of perturbation remains hidden until recombination occurs.

At the time of the hydrogen atom recombination, both matter and radiation are expanding with the universe. Following recombination, radiation continues to expand uniformly with the universe. Matter has a large outward expansive velocity, and density perturbations can only grow comparatively slowly. Thus, any given blob of matter

must continue to expand for a long time before its self-gravitational forces are able to prevail and bring expansion to a halt, to be followed by subsequent contraction toward a denser state.

The smaller the density fluctuations within matter following recombination, the greater the subsequent expansion of a blob of matter before it reaches its minimum density. For example, if density fluctuation following recombination should amount to about 1%, then the subsequent expansion and recollapse of matter will take about 3 or  $4 \times 10^9$  years. Rapid formation of galaxies within the universe is only possible if density fluctuations should be much larger than 1%. Perhaps such density fluctuations are more likely to occur in a violently stirred universe such as that of Omnes than in a rather uniform unsymmetric universe.

### Primitive Globular Clusters

Following recombination, the Jeans length in matter encompasses nearly  $10^6$  solar masses of material. On this basis, a theory was formulated [37] of the formation of primitive globular clusters, noting that globular clusters have about  $10^5$  to  $10^6$  solar masses of stars. However, this value of  $10^6$  solar masses may not have much significance, since it is merely the minimum mass which is unstable against gravitational collapse. All density fluctuations representing larger masses of material are also unstable against collapse. Such density fluctuations may include large galactic masses or galactic material clusters. Such large-scale density fluctuations presumably are of smaller scale than smaller density fluctuations near the Jeans length, hence it is more likely that smaller density fluctuations will grow faster within the expanding universe. Thus, the emerging picture is one in which gravitational instability can occur on a very wide range of scales, with individual masses of the order of  $10^6$  solar masses condensing, and these in turn falling toward mutual gravitating centers, which in turn fall toward other centers on a larger scale, and so on.

However, as matter continues to expand toward its minimum density configuration, the Jeans length includes less matter. Matter is now decou-

pled from radiation, so that it can become extremely cold near the position of its maximum expansion. Temperature in matter may fall below  $1^\circ\text{K}$ . Under these circumstances, the Jeans length may enclose only 1000 solar masses. Thus, it is possible that the most frequent fluctuations which develop within the expanding universe have masses more characteristic of a few thousand solar masses.

As matter falls back from its position of maximum expansion, the rise in temperature due to adiabatic compression eventually becomes limited due to cooling processes within the gas. The most important of the cooling processes results from hydrogen molecule formation due to a few electrons left over from the recombination stage in the expansion of the universe. These electrons can be captured by hydrogen atoms, forming negative hydrogen ions which readily capture other hydrogen atoms, forming hydrogen molecules, and again releasing the electron. Thus, the electron acts as a catalyst in the process as long as it does not encounter a positive hydrogen ion and becomes captured, forming a neutral hydrogen atom. When temperature is high enough, of the order of  $250^\circ\text{K}$ , to produce significant excitation of the lower excited states of the hydrogen molecule, infrared radiation from de-excitation of the molecules can lead to cooling within the contracting gas. As gas contraction accelerates, formation of hydrogen molecules is limited through gradual elimination of all remaining electrons, and the increasingly rapid gas compression gradually raises the temperature until thermal decomposition of hydrogen molecules takes place. At this time, when the density has risen to about  $10^{10}$  hydrogen atoms/cm<sup>3</sup>, the Jeans length in the compressing material encloses only about 60 solar masses. Presumably, the gas can thus fragment into stars having masses in the range  $10^2$ – $10^3$  solar masses [54].

### Pregalactic Stars

There is a natural expectation that the immediate result of expansion and contraction of matter in the early universe is to form a set of pregalactic stars, all quite massive. These stars may be composed of pure hydrogen, if the symmetric universe

is a correct model, or they may have about one-fourth their mass as helium. In either case, they do not behave like ordinary stars in the universe today. Massive stars composed of only hydrogen and helium have been studied by Ezer and Cameron [14]. These stars become much more compact than ordinary stars of the same mass, owing to very high internal temperatures needed to convert hydrogen into helium without initially such catalyst nuclei as those of carbon, nitrogen, and oxygen. This means that the radii of stars are abnormally small, and their surface temperatures are approximately  $10^5$  °K. These stars will emit a tremendous flood of ultraviolet radiation, which will certainly ionize any residual hydrogen and helium in the universe which have not been formed into stars at this stage.

Stars composed of pure hydrogen, corresponding to the symmetric universe, have been studied little so far. It is possible that the dynamic collapse which forms these stars may lead to such high central temperatures that there is sudden conversion of hydrogen to neutrons by electron capture, followed by massive helium formation and explosion of stars back into space. If stars can form stable objects, they should behave much the same as the hydrogen-helium stars described above. The major question is whether such stars can form so much helium and eject it into space, so as to contaminate the remaining gas in space to the extent of one-fourth by mass of helium, in order to account for the essentially universal hydrogen-to-helium ratio in stars throughout space, which seems to require a pregalactic helium formation.

Stars in this massive range may eventually explode in supernova explosions or collapse to form black holes. It is tempting to argue that both events will occur. This primordial generation of stars is presumably concentrated in space into masses at least of the order of clusters of galaxies. The visible amount of matter in galaxies in clusters of galaxies is inadequate, by approximately 1 order of magnitude, to provide for the gravitational binding of such clusters of galaxies, keeping them together against dispersion in space during the history of the universe. This mass discrepancy could be accounted for if a majority of the primordial generation of stars were to

collapse to form black hole remnants, distributed more or less uniformly throughout the volume occupied by a cluster of galaxies [50].

Evidence, on the other hand, indicates that supernova explosions could also occur among the primordial generation of stars. It seems difficult to account for the observed heavy element content of stars in the galactic halo, unless the heavy metal content of these stars was also formed in the pregalactic era. If supernova explosions occur among some of the hydrogen-helium or pure hydrogen stars formed in the primordial stellar generation, some conversions into heavier elements are likely to take place (to be described in a subsequent section). These heavy elements will spread in the gas which will subsequently condense into galaxies [50].

In any event, it appears that unconsolidated gas, which did not succeed in becoming incorporated in the primordial generation of stars, together with gas ejected from stars in supernova explosions or as a result of stellar variability and stellar winds, is subject to a great deal of heating. Intense ultraviolet output from the primordial generation of stars is likely to heat gas at relatively low densities to a temperature of the order of  $10^5$  °K. In addition, supernova explosions occurring in this gas may provide heating to somewhat higher temperatures, which has been stressed [12]. This will probably lead unconsolidated gas to expand throughout the volume occupied by a cluster of galaxies, forming a common gas envelope throughout all of this volume. Into this common gas envelope will be injected in a random manner the products of stellar nucleosynthesis, including heavy metals, and possibly large amounts of helium. The heavy metals, in particular, should greatly enhance the cooling efficiency of the gas, leading to local cool spots within the gas. Since local cooling within the gas leads to a reduction in local pressure, such cool spots will undergo density increases, thus forming density fluctuations about which gravitational instabilities can grow within the gas. This is a probable mode of nuclei formation of galaxies within the common gas envelope filling a cluster of galaxies. After a galactic nucleus is formed, matter is likely to continue falling toward such galactic nuclei, allowing the

galaxies to grow in size. There is considerable indication that such mass infall is still continuing within our galaxy today [30].

How newly formed galaxies acquire their angular momentum has been the subject of debate. It was suggested [34] that the galactic angular momentum is acquired as a result of tidal distortion during the fragmentation process in the expansion stage of the universe. This theory has been quantitatively questioned by Oort [30], but further defended by Peebles [35]. Oort, in turn, preferred a picture in which the expanding universe contains highly turbulent matter, and presumed that the galaxies have acquired their angular momentum as a result of vortices within the turbulent matter. The turbulent theory is developed also by Ozernoy et al [31]. The point of view that initial perturbations are characterized by acoustical waves in a photon-ionized gas mixture is advocated by Doroshkevich, Sunyaev, and Zel'dovich [13, 58].

### THE EVOLUTION OF GALAXIES

Whatever the mechanism which initiates the collapse of galactic masses of gas to form galaxies, quite a bit about the nature of this collapse can be inferred from morphologic forms exhibited by the resulting galaxies. Galaxies show a tremendous variety of forms, and likely these arise largely from subtle differences in the angular momentum distribution of the initially collapsing gas clouds.

*Elliptical galaxies.* The nearly spherically symmetric distribution in space of stars in elliptical galaxies can be maintained only if the stars have nearly radial orbits; such stars fall close to the center of their galaxy and then recede outward to large distances from the center. Such galaxies have very little total angular momentum. As the total angular momentum of a galaxy increases, the degree of flattening of the distribution of stars increases. When the system of stars becomes rather flattened, gas and dust start to appear in the central plane of the galaxy, and as the degree of flattening becomes even greater, large amounts of gas and dust appear. Evidently stars in such galaxies have orbits which are more nearly circular, and

certainly stars formed from gas and dust lying in the central plane of the galaxy will have almost circular orbits.

Systems with a great deal of gas and dust usually exhibit spiral arms; these are rendered more prominent because spiral arms are the locations of current star formation in such galaxies, and the hot, massive blue stars form effective markers for these arms. Spiral arms exhibit a wide range of curvature and numbers of turns about the center of the galaxy. In some of these galaxies, central stars exhibit an approximately spherical distribution, but in others they form an elongated bar. Central bars of barred spiral galaxies are thought to arise from details of angular momentum distribution of infalling gas; if this gas, upon forming a disk, rotates with approximately constant angular velocity, it is unstable against deformation into a bar. Some galaxies have no strong concentration whatever of stars toward the center; these systems, which contain a large ratio of gas to stars, are called irregular galaxies.

*Spiral galaxies.* Knowledge of the features of spiral galaxies is the most complete of any type of galaxy, since our own galaxy is apparently a typical spiral.

The time required for primordial galactic gas to collapse from the volume of space presently occupied by the galactic halo to form the disk is about  $2 \times 10^8$  years. This estimate is necessarily rough, since the initial volume occupied by gas at the start of collapse may have been considerably greater than that now occupied by stars in the approximately spherical galactic halo. It is natural to suppose that stars in the halo were formed by condensation from gas during the collapse stage. The motions of these halo stars have large radial components.

The abundances of heavier elements in halo stars are less than in the Sun, typically by a factor of about 3, although in a few extreme cases, by factors of several hundred. It is rather unlikely that the collapsing gas had time to form an initial population of stars which could evolve and form heavy elements by nucleosynthesis, eject these elements back into the collapsing gas in supernova explosions, to be followed by formation of a second generation of stars incorporating

these heavy elements. Thus, the existence of heavy elements in these stars provides an argument for a stage of pregalactic stellar nucleosynthesis.

After gas has collapsed into the form of a disk, subsequent star formation will be of stars in approximately circular orbits in the plane of the disk. When such a star has been formed, its orbit may suffer gravitational perturbations as it approaches other stars, star clusters, or interstellar gas clouds. As a result of such perturbations, the star may swing to increasingly greater distances away from the central plane of the galaxy as it grows older. Older stars within the disk population in our galaxy have a distribution in distance away from the central plane of the galaxy corresponding to a thickness of about 400 parsecs. Stars formed in more recent galactic history, on the other hand, are confined to a narrower thickness of about 200 parsecs.

### Density Wave Theory

The most quantitative and promising modern theory of spiral arms appears to be the density wave theory [25, 26, 41, 42]. According to this theory, stars in the galactic disk can undergo collective gravitational clustering for significant periods, and the gravitational cluster, or density wave, progresses through the stellar distribution in the disk of the galaxy at about half the rate of rotation of the stars. For example, at the solar distance from the center of the galaxy, a star such as the Sun can be expected to spend about  $10^8$  years traveling in the interarm region from one spiral arm to the next, and then an additional  $10^8$  years within the next spiral arm which it encounters. At the end of this total interval, it has made approximately 1 revolution around the center of the galaxy, according to a simple two-armed model of a spiral galaxy. The actual model for our own galaxy may be slightly more complicated.

In order to understand how star formation currently takes place within our galaxy, it is necessary to consider first properties of the interstellar medium [47] which consists of gas and dust between the stars. The dust is composed of small solid particles with dimensions slightly less than 1  $\mu\text{m}$ , intimately mixed with gas in the inter-

stellar medium. The dust is responsible for extensive absorption of starlight in certain directions within our galaxy, showing up as dark patches on photographs of portions of the Milky Way.

Interstellar gas resembles the Sun in composition; about  $\frac{3}{4}$  of the mass is hydrogen, about  $\frac{1}{4}$  is helium, and only about 1.5% is in the form of heavier elements, mostly condensed into interstellar grains.

### Hydrogen Ionization

When electromagnetic radiation, having photon energies greater than 13.6 electron volts (eV), is incident on interstellar hydrogen atoms, that radiation is capable of ionizing hydrogen. Consider some hydrogen located close to a very hot, massive, highly luminous star. Such a star, because of its high surface temperature, will emit most of its radiation far into the ultraviolet portion of the spectrum. Most of its emitted photons may have energies  $\leq 13.6$  eV. Hence, hydrogen close to the star will be ionized very quickly by the enormous ultraviolet flux, incident upon it.

Now consider a continuous hydrogen gas cloud surrounding this star which extends a considerable distance into the interstellar medium. Ultraviolet radiation from the star will start ionizing nearby hydrogen. As hydrogen becomes ionized, it no longer absorbs the outpouring radiation from the star, so that ultraviolet rays from the star can reach farther and farther into space, ionizing hydrogen on the way. If hydrogen were to stay ionized, this process could go on indefinitely, and it would be expected that the star could ionize hydrogen gas to indefinite distances.

Hydrogen, however, will not stay ionized indefinitely. Internal recombination will take place continuously, leading again to neutral hydrogen. Such a neutral atom will not remain in this state for very long before becoming ionized again by ultraviolet light. However, the greater the distance at which the star succeeds in ionizing hydrogen surrounding it, the greater the region in which hydrogen recombination will occur simultaneously, with consequent weakening of the ultraviolet radiation which proceeds to further distances as neutral hydrogen is again ionized.

A natural limit is created in this way for the distance to which starlight can ionize hydrogen. This limit is reached when the total number of neutral hydrogen atoms which are being ionized in every second becomes equal to the total number of hydrogen atoms which are recombining to the neutral state in every second. In this way, a hot star can create a sphere of ionized hydrogen surrounding it, with the result that there is a remarkably sharp transition from ionized hydrogen to neutral hydrogen at the surface of the sphere.

### *Neutral Hydrogen Regions*

Absorption of ultraviolet photons by neutral hydrogen results in heating of the resulting ionized hydrogen. Most of the absorbed photons have an energy somewhat greater than 13.6 eV. Hence, in the absorption process, 13.6 eV are used to split up the hydrogen atom, and the remaining energy appears as kinetic energy of the proton and electron which are emitted. This excess energy is rapidly shared with other particles, leading to high temperature of the ionized gas.

Ionized gas can cool in various ways. The typical process involves collisions between a proton and an electron in which a photon can be emitted but the proton and electron remain ionized, with the electron departing from the proton having less kinetic energy than when it approached. The photon which is emitted is generally free to escape from the region in which it is created, thus removing some of the heat energy from that region.

Energy input into an ionized hydrogen region is limited by the number of photons from the hot star which neutral hydrogen atoms in the region can absorb. On the other hand, the rate of radiation from collisions between protons and electrons increases rapidly with temperature, hence a balance will be achieved at a temperature where the rate of energy input from absorption of ultraviolet photons is balanced by the rate of energy radiation from collisions between protons and electrons. The temperature which gives this equality between absorption and radiation of energy from ionized hydrogen gas is ca 10 000° K.

Thus, in a region in the interstellar medium in which hydrogen gas is neutral, the ultraviolet spectrum of interstellar starlight has been cut off above 13.6 eV, the ionization potential of the hydrogen atom. Photons more energetic than this limit have been absorbed in ionizing hydrogen in the ionized region.

Some of the elements with ionization potentials below 13.6 eV, including all the heavier elements, will be ionized in a neutral hydrogen region. The main elements which will not be ionized, in addition to hydrogen, are helium, nitrogen, oxygen, and neon. About three-fourths of the ions in the neutral hydrogen region are of carbon.

Ionization processes within neutral hydrogen regions also provide heat input to these regions, although of a considerably smaller magnitude than in the ionized regions. A variety of cooling processes are also present in neutral hydrogen regions, involving collisions among electrons, ions, neutral atoms, molecules, and interstellar grains. These collisions result in cooling when they raise one of the particles into a more highly excited energy state, from which deexcitation by radiation can occur, with radiation escaping from the neutral hydrogen region. The balance between heating and cooling of gas typically occurs at a temperature of about 100° K, somewhat lower in denser neutral hydrogen regions [21].

### *Pressure Equilibrium*

Pressure in gas is proportional to density, also to temperature. In considering adjacent regions of neutral and ionized hydrogen, if each of these regions were to have about the same number density of particles, pressure in the ionized region would be about 100 times that in the neutral region, and gases would then be set into violent dynamic motion due to pressure imbalance. Pressure equality could be achieved if density in the ionized hydrogen region were 100 times less than density in the neutral hydrogen region, in inverse proportion to the temperatures in these two regions. It appears that the interstellar medium always seeks to achieve such a pressure equilibrium throughout, so that in general, ionized hydrogen regions are of much

lower density than neutral hydrogen regions. However, newly formed stars and supernova explosions provide continual variation in local rates of heat input into the interstellar medium, so that the readjustment process of the configuration, in order to approach pressure equality, is ongoing, leading to significant dynamic motions of gas within the interstellar medium.

Comparable amounts of ionized and neutral hydrogen appear to be in the interstellar medium. Since the density of ionized gas is much less than that of neutral gas, the neutral gas will obviously occupy only a small fraction of the volume in the interstellar medium. The neutral hydrogen clumping which thus occurs leads to the description of the interstellar medium as consisting of neutral hydrogen clouds embedded within an ionized region.

The foregoing description is oversimplified. Other sources of ionization exist in the interstellar medium, such as cosmic rays and soft x-rays, which modify the details of the description given, but not its most essential features.

In a typical interstellar cloud, self-gravitational forces which would tend to make the cloud collapse are generally very much weaker than thermal pressure forces which attempt to expand the cloud. Expansion is prevented by a lower density medium surrounding the cloud, which has the same pressure as that in the cloud; the pressure throughout the interstellar medium is a consequence of the gas being held within the general gravitational potential field of the galaxy. Thus, under normal conditions, there is no tendency for collapse of any part of the interstellar medium, and hence no reason for star formation to take place.

#### *Spiral Arm Shock*

Consider the sequence of events which occurs when gas in the interstellar medium flows into a spiral arm [41, 42]. Since the spiral arm consists of a concentration of stars forming a gravitational potential well, gas undergoes shock deceleration when it flows into the arm, becoming hotter and denser. The interstellar magnetic field, whose lines of force are tied to interstellar gas via the ions within the gas, and which must

move with the gas, is also compressed and strengthened in passing through the spiral arm shock. Instabilities will probably then arise in the magnetic field configuration, with large parts of the field becoming buoyant and rising out of the galactic plane, allowing gas attached to the lines of force to collect into pockets, or clouds, near the galactic plane by sliding along the lines of force, which it is free to do. This appears to be the general mechanism in which interstellar clouds can be formed as gas flows into a spiral arm.

After a cloud has formed, there is gradual diminution of heavier elements and ions within the cloud, many of which are mainly responsible for cooling processes within the cloud. These atoms and ions are likely to stay attached to interstellar grain surfaces when they strike those surfaces in the normal course of their thermally agitated motion within the gas. Thus, the newly formed cloud may start out with relatively low temperature, but as time goes on, temperature in the cloud will rise as its cooling agents decrease in number.

As temperature in the cloud rises, density correspondingly decreases, and probably when gas emerges from the spiral arm after residing there about  $10^8$  years, the clouds expand and disappear into a medium which again has become rather homogeneous in density. There is no evidence that interstellar gas clouds exist in the region between spiral arms.

#### **New Star Formation**

The optimum time for causing collapse of an interstellar cloud to form stars appears to occur at its formation, since some clouds may be formed with somewhat greater density than others, so that self-gravitational forces become stronger. However, some clouds may suffer dynamic compression at a later stage, being subjected to surface heating if there is nearby formation of a number of hot, massive stars, or nearby explosion of a supernova.

A typical interstellar cloud may have a mass a few hundred or few thousand times that of the Sun; the more massive clouds appear more likely to undergo collapse to form stars. A repeated

process of fragmentation of the cloud into separate condensation centers evidently takes place during collapse of the cloud, so that the ultimate product of the collapse is formation of a great number of new stars. If only a portion of gas is formed into new stars, and the remaining gas is quickly expelled from the region of star formation through ultraviolet ionization when new hot stars are formed, then the newly formed stars are not gravitationally bound together, but are free to expand into space. Numerous examples of such expanding associations, containing stars which are massive and very luminous, have been observed in the galaxy.

It is likely that a certain minimum density of gas in the interstellar medium is needed in order that star formation can follow the flow of gas into the spiral arm shock [38]. It might be expected that this minimum density is closely approached through depletion of gas by star formation soon after collapse of the gas to form the galactic disk. In an isolated galaxy, the star formation process could occur subsequently only from gas returned to the interstellar medium as a result of stellar evolution. While this process is observed to occur, it is doubtful that the amount of gas thus returned to the interstellar medium is nearly enough to account for the number of new stars currently observed to be formed in the galaxy.

A number of high-velocity clouds observed in the galactic halo have been interpreted as gas infalling to the galaxy for the first time from intergalactic space [30]. If there is a continuous infall of this sort of gas, which would not be entirely unexpected according to the description in the preceding section, then this gas would collect in the interstellar medium and provide the excess density needed to maintain a steady state of star formation when gas passes into the spiral arms [38].

In an elliptical galaxy, only the first stages of this type of galactic evolution can occur. Infal of gas to form the galaxy presumably results in direct formation of stars from the collapsing gas. Because of the small amount of angular momentum in the system, residual gas, which does not form stars during the collapse process, is likely to collect near the center of the galaxy, forming stars in the vicinity of the center. Henceforth,

introduction of new gas into such a system will result in collection of that gas near the center, with additional star formation there, and so on. However, the formation rate of new stars in such a galaxy is likely to be rather small unless there is a fairly substantial continuing input of gas from the intergalactic medium, which there appears to be in our own galaxy.

No existing theory describes the interaction between gas and stars in irregular galaxies. The geometry of such systems is too irregular and complicated for application of the density wave theory, but it is evident from the presence of many hot young stars in irregular galaxies that star formation is a vigorous and continuing process.

## STELLAR EVOLUTION AND NUCLEOSYNTHESIS

A star is a large sphere of hot gas held together under its own gravitational forces (for details of stellar structure, see [9]). The structure of the star does not vary appreciably with time. It can therefore be concluded that the interiors of stars are in hydrostatic equilibrium; there is an exact balance between the force of gravity, directed downwards, and expansive thermal pressure of gas, opposing the pull of gravity. At any given point in the star interior, the gas pressure must be high enough to support the weight of overlying layers. Moving inward from that point, there is more matter in the overlying layer, hence, higher pressure is needed to sustain this increased weight.

Pressure increases from the surface of the star toward the center, and in general, density and temperature of the gas also increase from the surface toward the center. Typically, in the central regions of ordinary stars, such as the Sun, temperature will be a few million degrees Kelvin. Under such conditions, electrons are stripped from their atomic orbits, and constituents of the gas become fully ionized. Hence, the gas continues to act like a perfect gas even at densities more than 100 times that of water, which is characteristic of the center of the Sun, because atomic nuclei are very much smaller than atoms in size, hence, the particles have

plenty of room to move about between collisions.

A star generates energy in the interior and radiates this energy electromagnetically from the surface, under ordinary circumstances. In order for energy to reach the surface from the deep interior where it is generated, it is necessary that temperature continually decrease from a high value at the center to a low value at the surface. In principle, this energy flow can occur in the deep interior of a star in three ways: conduction, radiation, and convection. Conduction is very inefficient in the interior of the star and usually contributes negligibly to the flow of energy. If the temperature gradient in the interior of the star is not very strong, energy transport is mainly by radiative transfer. In this process, radiation is emitted at any given point in the interior, but since it is emitted proportionally to the 4th power of temperature, more radiation is emitted in a region of higher temperature rather than lower temperature. Thus, photons diffuse in the interior of a star from higher to lower temperature regions.

If temperature gradients become sufficiently high, convection is possible. This is mass transport of heat. A blob of gas in the interior starts rising because of buoyancy forces, and after traveling some distance, it will break up and individual parts will mix into the surroundings. Gas moving vertically upwards in the interior will, under these circumstances, be hotter than the surrounding gas into which it mixes, thus, energy can be efficiently transported by the mass motion of the gas.

Theoretical determination of the structure of a star requires not only a precise balance of pressure at every point, a condition of hydrostatic equilibrium, but also determination of how energy flows in the interior. In successful models of stars, the various differential equations describing these processes are solved simultaneously.

The energy emitted from a star over billions of years is derived from nuclear reactions in its deep interior. These are fusion reactions, in which two relatively light nuclei collide and fuse to make a heavier one, releasing energy as a result. Since thermonuclear reaction rates are extremely sensitive to temperature, energy re-

leased from these reactions is strongly concentrated toward the center of the star, where temperature is highest.

In a typical star like the Sun, three-fourths of the mass is composed of the lightest element, hydrogen; since there is only one unit of charge on each nucleus, two protons will have the least coulomb repulsive forces between them of any possible combination of nuclei. Consequently, hydrogen nuclei will fuse in thermonuclear reactions at the lowest temperatures, since the least amount of relative kinetic energy is needed to bring two protons sufficiently close together. It also happens that the most efficient energy generation processes are those which involve hydrogen nuclei.

Four protons can fuse to make one helium nucleus in a variety of ways. Some of these processes commence with the proton-proton reaction, which makes deuterium. Deuterium in turn can capture another proton, making  $^3\text{He}$ . The  $^3\text{He}$  nuclei may combine with one another, making  $^4\text{He}$  with the release of two protons. Alternatively, a  $^3\text{He}$  nucleus can combine with a  $^4\text{He}$  nucleus to make an isotope of beryllium,  $^7\text{Be}$ , and after several more nuclear reactions, an additional proton is captured making a  $^4\text{He}$  nucleus and releasing the original  $^4\text{He}$  nucleus which acted as a catalyst for these reactions.

Still other nuclear reactions involve the combination of hydrogen with isotopes of carbon, nitrogen, and oxygen. These reactions form a linked triplet of nuclear reaction cycles in which carbon, nitrogen, and oxygen nuclei are successively transformed into one another. Thus, they act as catalysts in the process, resulting in four hydrogen nuclei combined to form one  $^4\text{He}$  nucleus.

### Main Sequence Stars

Stars converting hydrogen into helium at the centers are called main sequence stars. Since the bulk of available nuclear energy release from nuclear transformations occurs in the hydrogen-to-helium burning stage, the stars spend most of their active lifetimes in this stage. The Sun is expected to take about  $10^{10}$  years to convert its central hydrogen into helium; it is about halfway through this process. When

approximately the central 10% of a star like the Sun has fully burned its hydrogen into helium, then it is no longer stable for long periods, but starts to change its structure relatively quickly.

After all hydrogen has been converted into helium in the core of such a star, energy generation ceases there. The energy flow from the center of the star to the surface must continue, therefore energy which had been generated by nuclear reactions at the center must instead be generated by contraction of the central regions, releasing gravitational potential energy. However, this contraction does not last very long, since shrinkage of the star's core leads to a temperature rise of the material not only at the center, but also in the rest of the star's inner parts. Soon this temperature rise is enough to ignite the hydrogen burning thermonuclear reactions in the region surrounding the core which still contains hydrogen. These reactions then form a shell source of energy generation, which provides the energy flow toward the surface needed to maintain the star once again in a state of relatively long-term equilibrium, although the structure is changing at a rate considerably higher than previously during the main sequence hydrogen burning. Since the structure again becomes relatively stabilized, the higher temperature at the center of the core is no longer needed to maintain energy generation, hence, energy flow away from the center to regions of lower temperature tends to make the inner core, now completely helium, have much the same temperature throughout.

*Red giant stars.* As time passes, the hydrogen burning shell source converts a considerable amount of hydrogen into helium in the star's interior, then this added helium becomes part of the helium core of the star. Meanwhile, the hydrogen burning shell source moves outward in the mass of the star. The core continues to grow in mass and continues to contract slowly, remaining approximately isothermal. However, the outer parts of the star behave differently. Stellar evolution calculations show that, with a hydrogen-burning shell source, and corresponding discontinuity in composition between the helium core and largely hydrogen envelope, as this core contracts, the outer envelope of the

star must expand. At the same time, because energy generation lies closer to the surface relative to mass distribution in the star, the star's luminosity increases. Meanwhile, the outer envelope of the star expands. Hence, the surface area of the star increases, and for a given luminosity, the temperature needed to radiate energy output of the star decreases. The surface of the star thus decreases in temperature, and the now relatively giant stars tend to appear red. Hence, they are called red giants.

Reliable calculations of stellar evolution extending beyond the red giant stage are relatively few. However, these calculations do indicate several features of stellar evolution. When a star becomes a red giant, enough mass has been added to the core by the hydrogen-burning shell so that the core starts to contract relatively rapidly. There is no longer time for energy to flow out of the core at a rate sufficient to maintain an approximate isothermal condition; hence, the central core temperature rises considerably above the temperature in the hydrogen-burning shell source. When this temperature reaches a value in the range  $1-2 \times 10^8$  °K, helium-burning thermonuclear reactions commence. In these reactions, three helium nuclei can fuse together to make a nucleus of  $^{12}\text{C}$ , and then a further helium nucleus captured by the  $^{12}\text{C}$  nucleus to make  $^{16}\text{O}$ .

*Horizontal branch stars.* In a star of relatively low mass, the onset of helium-burning causes quite a large expansion of the core. While the preceding contraction of the core caused expansion of the envelope, expansion of the core now causes contraction of the envelope, and the surface of the star increases in temperature. The star, then, is no longer a red giant, but the tendency is to call it a "horizontal branch star," from its position in a diagram in which luminosity of the star is plotted as a function of surface temperature (Hertzsprung-Russell diagram). In more massive stars, basically the same happens, but contraction of the outer envelope is much less pronounced.

Stellar evolution calculations that are available suggest that helium-burning will finish in the core, and the core will again start to contract. This will ignite helium-burning thermonuclear

reactions in the material surrounding the carbon and oxygen core, so that the star in this stage may possess both hydrogen and helium-burning shells. These shells will again progress outward in the mass of the star, adding helium to the region below the hydrogen-burning shell, and adding carbon and oxygen to the central core below the helium-burning shell. At this stage, if the star is not more massive than the upper limit of stability of a white dwarf star, about 1.4 solar masses, it appears likely that the helium-burning shell source will die out after a certain time and the hydrogen-burning shell source will approach the surface quite closely.

*White dwarf stars.* Under these circumstances, it appears probable that the great bulk of the star at this stage in its evolution will form a white dwarf star. In this star, the electrons form a degenerate gas, thus contributing sufficient pressure to maintain the star against further gravitational contraction. The outer layer of hydrogen, which may still exist when the star is in this late stage of evolution, is probably expelled by one means or another. Possible mechanisms include stellar wind, bulk ejection of a shell of material leaving behind the nucleus of a planetary nebula, or nova explosions in which the hydrogen shell is ejected explosively. Details of the evolution which may lead to one of these possibilities are not yet understood. Since a considerable amount of mass may have been lost from the star during the red giant phase of its evolution, probably by a stellar wind process, the masses of stars which may end as white dwarfs can initially have been considerably larger than one solar mass, perhaps as much as five solar masses.

### **Further Evolutionary History of a Star**

Among theoretical astrophysicists, there is considerable dispute about details of the ultimate evolutionary history of a star too massive to form a stable white dwarf. The general course of its evolution must lead the core of the star toward higher temperatures and higher densities. The two main pathways which may be followed are either complete collapse of the star (implosion) or nuclear explosion of the star [49].

*Supernova explosions.* Stars with initial masses of 4–8 solar masses were thought, until recently, to be destroyed in supernova explosions. In this sequence, as the carbon and oxygen core grows in size, and the hydrogen and helium-burning shells progress outward in the mass of the star, the core gradually contracts faster and faster, and temperature starts to rise rapidly. When temperature exceeds  $10^9$  °K, there is ignition of carbon thermonuclear reactions with two carbon nuclei reacting with each other to form various heavier nuclei. Because the core contains a degenerate electron gas, the equation of state is very dissimilar to that in a perfect gas, rather, there is an almost unique relation between pressure and density, with very little dependence of pressure on temperature. Thus, rising temperature in the core has very little effect on its structure. However, since thermonuclear reactions burn at rates that depend upon a high power of temperature, the ignition of carbon thermonuclear reactions will lead to a rapidly increasing rate of energy generation, hence a thermal runaway at the center of the star. This runaway can progress until carbon thermonuclear reactions have exhausted the carbon, and oxygen thermonuclear reactions have begun. In these reactions, two oxygen nuclei react to form heavier nuclei. All these reactions can be expected to be completed before significant changes in the structure have occurred, but meanwhile, the temperature will have risen so high that the center of the core is no longer degenerate.

The sequence of reactions would be sufficient to commence a detonation wave which would progress outward in the core, exploding the carbon and oxygen nuclei there, and probably allowing thermonuclear reactions to burn all the way to the vicinity of iron. Here, the nuclei have the greatest possible nuclear binding energy per nucleon, where their abundances are determined by principles of nuclear statistical equilibrium. If this process could continue, then all of the energy generated by thermonuclear explosion in the core would form a gigantic shock wave which would race through the outer layers of the star, ejecting them into space. This would result in a supernova explosion.

One apparent difficulty with this scheme,

however, has been that it should lead to the complete explosion of the star, leaving no stellar remnant behind. While statistics of supernovae in our galaxy and others indicate that stars with masses as low as four solar masses are undoubtedly required to participate in the supernova process, the statistics of pulsars, which are believed to be neutron star remnants of supernova explosions, indicate that such neutron stars should be formed in the majority of supernova explosions in this mass range.

Resolution of this puzzle may have been provided by Paczynski [32]. He noted that when ignition of carbon thermonuclear reactions starts in the core of the star, convection commences at the center, in order to carry away some of the heat generated by carbon reactions. At this point the URCA convection process starts which is a powerful cooling mechanism. At high densities in the core, degenerate electrons may have a Fermi energy of a few MeV. These electron energies will be high enough to initiate electron capture on some of the heavier nuclei present in the core. When such a nucleus is transported by convection to higher densities, electron capture will take place, with emission of a neutrino, and when the same nucleus is subsequently transported toward lower densities, it can emit an electron, transforming back to the original nucleus, with emission of an antineutrino. Neutrinos and antineutrinos emerging from the core of the star can thus carry away tremendous amounts of energy, preventing the thermonuclear ignition from running away to explosive conditions, but nevertheless permitting continued burning of carbon. Under these circumstances, carbon- and oxygen-burning may take place in the core, followed by silicon-burning and formation of the iron equilibrium peak, if, in the meantime, the core has not initiated extensive electron capture, leading to collapse toward nuclear densities in the core, and the formation of a neutron star remnant. It is possible that the pulsar emission mechanism, which is still not understood, but which apparently derives its energy from the rotational energy of a neutron star, may provide enough prompt energy generation in the center to blow off the outer envelope of the star and provide the supernova explosion.

*Black hole formation.* Among more massive stars, carbon and oxygen-burning is expected to take place at lower densities, before the core of the star undergoes electron degeneracy. When the core of such a star eventually undergoes collapse to form a neutron star remnant, the mass of overlying layers may be too great to be ejected by radiation emitted by the newly formed pulsar. As the mass continues to accrete onto this neutron star remnant, the neutron star may be overwhelmed by general relativistic effects, and collapse to form a general relativistically collapsed object, called a black hole. In such cases, a supernova explosion would not be seen.

Among still more massive stars, perhaps about 50 solar masses or more, a different effect is expected. Such stars can achieve very high temperatures, about  $10^9$  °K, through large parts of their mass, even though density in most of these parts of the mass is relatively low. Under these circumstances, electron-positron pairs come into equilibrium with the radiation field of photons, having been created from energy in the photons, and this renders the star unstable against collapse [16]. However, the region in which pairs form contains tremendous amounts of carbon and oxygen, and collapse will progress only until thermonuclear detonation occurs in this carbon and oxygen. The result should be a thermonuclear explosion in which all massive outer layers of the star are ejected into space. If a stellar remnant would be formed under these circumstances is not clear, but in any case, a supernova explosion can be expected.

### Nucleosynthesis

During the last decade, a great deal of progress has been made in understanding how nuclear reactions taking place during stellar evolution are related to the abundances of elements in nature [49]. This understanding has, to a great extent, resulted from construction of a good abundance distribution curve for elements in solar system material, which has relied in part upon spectroscopic determinations of the abundances of elements in the Sun, but these are rarely better than a factor of 2 for any given element.

Some of the more striking regularities of

nuclear abundances are not brought out by using the fairly crude data available for solar abundances. Abundances determined in terrestrial materials are of little value, because the Earth has been extensively differentiated chemically, and it is very difficult to determine the total abundance of any given Earth element. On the other hand, certain types of meteorites have been an extremely valuable source of abundance information, and it appears that among non-volatile elements, meteorites of the fragile stony variety, known as Type I carbonaceous chondrites, appear to exist with essentially non-volatile constituents in the original proportions in which they existed in the interstellar medium.

#### *Elements in Solar System Material*

Hydrogen constitutes about three-fourths of the mass of solar system material, and helium is the second most abundant element with about one-fourth of the mass. The bulk of helium may have been created by cosmologic nucleosynthesis (described above), or possibly in the first generation of stars formed prior to formation of the galaxies, following the original collapse of matter in the universe after it decoupled from radiation. The remaining elements add up to only about 1.6% of the mass: among these, the third most abundant element, oxygen, has only  $10^{-3}$  as many atoms as hydrogen in the solar system.

The next elements, lithium, beryllium, and boron, have extremely small abundances, whereas carbon, nitrogen, and oxygen are in much greater abundance. Helium-burning in stars jumps directly from helium to carbon and oxygen, and the intervening elements are destroyed in stellar interiors. It can thus be understood how this striking feature of element abundances is directly related to features of nuclear reactions in stellar interiors. Nitrogen is a product of coupled cycles involving carbon, nitrogen, and oxygen isotopes, in which hydrogen is converted into helium in main sequence stars.

Current calculations in the theory of nucleosynthesis indicate that elements in the neon through nickel range are made by explosive carbon, oxygen, and silicon-burning processes in supernova explosions. This range of elements

has an intermediate abundance in nature, but, of course, it contains the most important elements present in a planet such as Earth. Of the non-volatile elements in this range, the most abundant are magnesium, silicon, and iron, which have comparable abundances. Such elements as sodium, aluminum, and calcium are considerably less abundant. Sulphur is half as abundant as silicon, but because it is more volatile than the other elements named, its abundance varies widely in the solid materials of the solar system. Of the various supernova environments previously described, the one most consistent with production of these elements involves massive stars, of 50 solar masses and more, which undergo supernova explosions as a result of the electron-positron pair instability process.

*Formation of elements.* Current studies of nucleosynthesis have also shown how elements beyond nickel can be formed by a variety of secondary reactions during the process of stellar evolution. Some elements are made by a process of neutron capture taking place on a slow time scale, in which neutrons produced by thermonuclear reactions on relatively minor constituents of the medium during helium-burning are captured on the nuclei of the iron peak which happen to be present in the medium. This leads these nuclei, by a succession of neutron captures and beta decays, toward the heavy element region. This process can form elements only as heavy as lead and bismuth, and it forms only a few isotopes at most of each element.

Another process which has produced heavy elements is neutron capture taking place on a rapid time scale. Current calculations indicate that the most likely astrophysical environment in which this will occur is composed of material in the outer part of a stellar core which has imploded to nuclear densities. This material is compressed and largely converted to neutrons by capture of electrons on protons, before being ejected, by a process not yet understood. It has been shown that in the expansion of material of this sort, charged particle reactions build a variety of nuclei of medium mass number, which then can capture the remaining neutrons in which they are imbedded to form much heavier nuclei. This process is responsible for producing all the

elements beyond bismuth which exist in nature, including all of the heavy radioactive nuclei present in nature.

The remaining isotopes of heavy elements which are not formed by neutron capture on some time scale, are likely to be formed by a process of proton capture taking place on a rapid time scale in supernova explosions. Such processes can occur in the outer regions of an exploding star when the supernova shock wave sweeps through a region still containing the original hydrogen. Heavy elements incorporated in this material at the time the star was formed may then capture protons and form neutron-deficient nuclei.

At present, the nuclear physical aspects of nucleosynthesis in stars are generally understood quantitatively better than the astrophysical aspects. Observations of the element abundances in stars show that very few stars are depleted in elements heavier than helium, relative to the Sun, by factors of 100 or more. Most stars in space appear to have abundances of these elements within a factor of 3 of that which is found in the Sun. From these results, together with some attempts to trace the history of nucleosynthesis in our galaxy, it has been concluded that the rate of star formation was probably very rapid in the early history of our galaxy or even in the pregalactic period, so that the formation of heavier elements occurred quite promptly on the galactic time scale [50]. As a consequence, most of the stars likely formed in space after that very early period of rapid star formation, contained sufficient heavy elements to be able to possess planetary systems containing planets having earthlike conditions accompanying them.

### **FORMATION OF THE SOLAR SYSTEM**

The problem of the origin of the solar system has occupied scientists for more than three centuries, since the time of Descartes. For most of this time, the number of facts about the solar system which scientific theories attempted to explain were pitifully few: the regularity of planetary orbits, the alignment of angular momentum vectors within the solar system, and the slow rotation of the Sun. It now appears that the last

of these features may have nothing to do with the origin of the solar system; an initially rapidly rotating Sun can easily have been slowed down to its present rate of rotation as a result of magnetic interaction of the Sun with the outflowing solar wind. It is not surprising that such a small number of boundary conditions could give rise to a very large number of widely different theories to explain them. During the last two decades, the whole problem of the origin of the solar system has been greatly transformed through acquisition of new boundary conditions of a physical and chemical character, resulting from meteorite research, from space probe analyses of distant bodies within the solar system, and from manned exploration of the Moon. This has required theories of the origin of the solar system to become more sophisticated, although several varieties are still current.

Nearly all the cosmogonical theories of the solar system developed within the last three centuries can be classified as either monistic or dualistic. In a monistic theory, the development of the Sun and planets occurs within a closed system, in which there is no interaction with any external system. A dualistic theory is one in which an external system, usually another star, is involved in the cosmogonical process. It is possible for a theory to start with dualistic features, and to end with essentially monistic features. Despite such possible ambiguities, the classification is useful.

The first monistic theory was proposed by Descartes, who published a vortex gaseous theory on formation of the solar system in 1634. The first dualistic theory appeared in 1745 when Buffon suggested that a comet made a grazing collision with the Sun, tearing from it sufficient material to form the planets. In those days, comets were thought to have masses comparable to the Sun, so this was the first of the invading star dualistic theories. Since these two theories were advanced, and until three decades ago, opinion has swung back and forth between proponents of monistic and dualistic theories. The review by Ter Haar and Cameron [48] relates this historical development.

Any form of dualistic theory has, at present, been almost universally discounted by astrono-

mers. There are many difficulties associated with attempts to explain formation of the planets by material withdrawn from the Sun. These include various hydrodynamic difficulties: the amount of material drawn from the Sun would be very hot, hence would tend to expand and disperse in space, rather than undergo chemical condensation to form the planets. If matter is drawn from the Sun at the time of close passage of another star, by far the overwhelming bulk of this material would gain so little angular momentum that it would fall back into the Sun after the other star had departed.

The modern theory of solar evolution indicates that the Sun would have destroyed any initial deuterium in its constitution by thermonuclear reactions at an early stage in its evolution, at the time it was fully convective and hence fully mixed. Thus, the deuterium present in the oceans of Earth could not have come from the Sun at any time following its very early deuterium-burning stage, leading to supposition that the remaining material in the Earth was not derived from the Sun either.

Most current theories of the formation of the solar system are monistic, involving some assumptions about the properties of a primitive solar nebula from which the planets and possibly the Sun were believed to have been formed.

The major exception to this general picture among currently advocated theories is perhaps that of Arrhenius and Alfvén [3], who believe that nonequilibrium plasma processes were dominant in formation of the planets and their satellites. They postulate that interstellar gases become enhanced in density and partially ionized as they approach the Sun, so that the resulting plasma flows through the solar system, where some of it may be trapped by magnetic fields, and where various solid grains can condense from the plasma and accumulate into larger bodies via gravitational self-focusing processes forming "jet streams." According to this theory, the Sun was formed as an isolated body by an unspecified mechanism, and at the time the planets were formed, the Sun had a magnetic field which was very much stronger than at present, and no solar wind was in operation which would prevent convergence of the interstellar plasma upon the

immediate neighborhood of the Sun. This may be regarded as a dualistic theory, although the external system involved is gas in the interstellar medium, rather than an invading stellar body, and no material is required to be torn from the Sun to form the planets.

### Solar Nebula Theories

Modern theories of the primitive solar nebula may be divided into two subclasses: the minimum solar nebula and the massive solar nebula. The minimum solar nebula contains about 0.01 solar masses of material, containing just enough condensable matter to form the present planets, with a large amount of excess volatiles which must be removed following planetary formation. The massive solar nebula may contain about 2 solar masses of material, and is distinguished from the minimum solar nebula through not having the Sun initially present at its center; it is a pure rotating disk of gas from which the Sun is required to form.

*Minimum solar mass theories.* Most solar nebula theories discussed within the last three decades have been minimum solar mass theories. The earliest involved discussions by von Weizsäcker, Kuiper, and Ter Haar [48], stressing the role of turbulence in physical processes within the primitive solar nebula. In fact, although turbulence is likely to be important within the solar nebula, it probably does not have the overwhelmingly important role ascribed to it in these theories. The authors assumed that turbulence must be present if the Reynolds number of the system should be very large, which is practically an inescapable situation in any large cosmic system of gas. However, they did not provide specific mechanisms, calculated in any detail, by which energy could be fed into large eddies in the turbulence, thus maintaining turbulence against natural dissipation processes. Nevertheless, these theories were very important historically, since they marked the first introduction of turbulence as a process which must be taken into account in the theory of the origin of the solar system. They also showed that gas dynamic processes can lead to a remarkably rapid dissipation of the solar nebula, the time scale for the dissipation being only some  $10^2$  or  $10^3$  years.

Meanwhile, monistic theories were being proposed in Russia. Schmidt [45] proposed a theory of the origin of the solar system in which the Sun was assumed to capture a swarm of smaller particles into a surrounding disk, suggesting that these small particles accreted to form planets. He later modified this to include gas together with the dust in the surrounding nebula. These ideas were further developed and modified by Levin [23] and Safronov [44], who attempted to calculate details of the formation of planets from the disk of dust and gas and to consider dissipation processes taking place within it.

The term *minimum solar nebula* describes a quantitative process carried out by Hoyle [20] in a theory developed a decade ago, and later elaborated by Fowler, Greenstein, and Hoyle [15]. It was noted by Hoyle that the icy and rocky components of solar matter constitute about 0.015 of the mass, and that the rocky constituents alone make up about 0.003 of the mass. Thus, the minimum amount of mass required to have been present in the solar nebula constitutes about 300 times the masses of the inner planets, which are rocky in composition, together with the masses of Jupiter and Saturn, which he assumed to be essentially solar in composition, with 60 or 70 times the masses of Uranus and Neptune, which he assumed to be composed mainly of ice and rock. Such minimum solar nebula theory requires that suitably condensed material be collected into planets with nearly 100% efficiency.

In Hoyle's theory, a fragment of a collapsing interstellar cloud was assumed to lose a great deal of angular momentum as a result of torque applied by an interstellar magnetic field interacting with the interstellar surroundings of the cloud. Material was then assumed to collapse to a radius somewhat less than that occupied by the orbit of Mercury. Part of the interstellar magnetic field was assumed to be compressed with collapsing material into the proto-Sun; when the collapse had been completed, this magnetic field was assumed to exert a torque on the equatorial regions of the proto-Sun, spinning them off in the form of a nebula, and increasing the radius of this nebula to some tens of astronomical units (AU).

In the elaboration of this theory, Fowler, Greenstein, and Hoyle suggest that chemical condensations will occur within this nebula, and chemically condensed material will form bodies typically tens of meters in diameter, which would be left behind as the magnetic field accelerated the gas toward larger radial distances. Following this, it was assumed that a great deal of magnetic energy would be dissipated in the proto-Sun, and that part of the dissipation would result in acceleration of charged particles to energies of several hundred million electron volts. These energetic particles were then supposed to bombard condensed bodies left behind in the inner part of the solar system, and to produce by nuclear spallation reactions the lighter elements which are not produced in the normal course of nuclear reactions in stellar interiors: lithium, beryllium, and boron. Deuterium in meteorites and in the Earth was assumed to be formed as a result of direct spallation, also by capture of spallation-produced neutrons by hydrogen in ice in the bodies.

The particle bombardment aspects of the theory of Fowler, Greenstein, and Hoyle have fallen into general disfavor because of predicting variations in certain isotopic ratios of some elements in meteorites which have been diligently searched for but not found. The theory had made very specific predictions concerning the presence of such variations, which stimulated a great deal of research on meteorites to search for these variations. However, other aspects of the discussion of formation of the solar nebula in this and other minimum solar nebula theories tend not to be predicted in any detail, thus, these aspects of the theories tend not be easy to test, to accept, or to reject.

*Massive solar nebula theories.* The principal advocate of a massive solar nebula has been Cameron [5, 7, 8]. This theory attempts to link formation of the solar system to the processes by which stars appear to be formed in space within the galaxy, which has been discussed previously. Random turbulence in the collapsing interstellar gas cloud is considered to have contributed so much total angular momentum to that fragment of the cloud which will form the solar system that gas is forced to form a flattened disk,

without any stellar body at the center. The amount of material needed in this massive primitive solar nebula is considerably greater than the mass of the Sun for two reasons:

newly formed stars are observed to be rapidly losing mass into space in what is called their T Tauri stages, and not all mass within the primitive solar nebula can be dissipated into the Sun;

some must remain at large distances to take up the angular momentum lost by material dissipating to form the Sun, and this gas will later be ejected when the T Tauri phase mass loss of the Sun begins.

Cameron and Pine [8] have calculated detailed numerical models of the massive primitive solar nebula, with thermodynamic conditions linked to the history of the interstellar cloud collapse stage. They found that certain parts of their models were unstable against thermally driven convection, whereas other parts tended to be in radiative equilibrium. They postulated that these models would be dissipated to form the Sun in a few thousand years, due to internal angular momentum transport associated with circulation currents within the disk.

These recurring short dissipation times constitute a challenge to all theories of the primitive solar nebula. It is very much easier to accumulate solids into larger bodies in the presence of a gas than in a vacuum. Solid bodies collide under vacuum conditions today in the asteroid belt, resulting in shattering of the bodies into smaller pieces, rather than their assemblage into a larger body. The presence of a gas assures that different size bodies will move with different relative velocities, thus promoting collisions between them, and under most circumstances preventing the collisions from being rapid enough to cause shattering.

Cameron [7] has investigated general accumulation processes in the context of his massive primitive solar nebula theory. He finds the key to the rapid assembly of planetary bodies in the presence of gas is the start of accumulation processes during the collapse stage of the interstellar cloud which will form the primitive solar

nebula. In the presence of turbulence in such gas, interstellar grains acquire significant relative velocities, and if it is assumed that they stick together upon collision, they will accumulate into bodies several centimeters in radius by the time the primitive solar nebula is formed. Such bodies can accumulate fairly rapidly near the central plane of the gaseous primitive solar nebula, where pressure gradients in the gas will induce relative velocities among the condensed solids, leading to their rapid accumulation into much larger bodies.

It has been estimated by Cameron that bodies of planetary size can be built up in times of the order of a few thousand years throughout much of the primitive solar nebula, from regions of relatively small radial distance where terrestrial-type planets would form, to much greater distances where the planets formed would be largely icy in composition. Perhaps the greatest uncertainty in these calculations is associated with the assumption that bodies stick upon contact; far too little is known about the character of the surfaces of chemically condensed material in the primitive solar nebula to evaluate the sticking probability upon collision at different velocities.

Theories of formation of the solar system, as they undergo further development, will undoubtedly benefit from important new developments in the study of meteorites from which physical conditions in the primitive solar nebula can be inferred. This is the development of cosmothermometers and cosmobarometers by Anders and colleagues [1]. When meteorites accumulate at some temperature in the primitive solar nebula, many elements will be completely condensed from gas and be quantitatively incorporated into meteorites, other elements will remain mostly in the gas and only traces of them will appear in the meteorites, but some elements will be partially condensed, and their abundances may be highly variable in the meteorites. These last elements constitute a form of cosmothermometer; a meteorite containing a larger amount of such an element will have been formed at a lower temperature than one which contains little of the element, and a precise thermodynamic analysis of the

spread in abundances allows estimates to be made of these temperatures.

These techniques tend to indicate that ordinary chondritic meteorites accumulated in the primitive solar nebula at 400°–500°K, whereas carbonaceous chondrites have tended to accumulate closer to 300° K. Relative oxygen isotope ratios also act as a cosmothermometer. The precise mineral phases in which certain elements are condensed can act as crude cosmobarometers, as can the partial pressure of absorbed gases, such as argon in meteorites. These clues tend to indicate that ordinary chondritic meteorites accumulated at total pressures in the primitive solar nebula of the order of  $10^{-5}$  atm. These thermodynamic conditions exist simultaneously at a suitable radial distance in the massive primitive solar nebula models of Cameron; however, minimum solar nebula models tend to have much lower pressures than are indicated by these cosmobarometers, although such models can be somewhat arbitrary since it is usually assumed that temperature distribution in such models arises from solar heating, with usually some partial dust-shielding.

### THE EARTH-MOON SYSTEM

Problems associated with the formation of the Moon have, for the most part, been discussed independently of the general cosmogonies of the solar system outlined above. The Moon is a rather anomalous body within the solar system with a much greater mass relative to the mass of its primary planet than any of the other satellites in the solar system. It has a remarkably low density of only 3.34 g/cm<sup>3</sup>, on the average, which is less than the density of meteorites, and very much less than the mean density of the inner terrestrial planets. These unusual characteristics have suggested to many that the formation of the Moon involved some rather unusual event within the history of the solar system.

### Origin of the Moon

Four general theories have been advanced to explain the origin of the Moon [22, 28]: fission theories, atmospheric condensation

theories, twin planet theories in which the Moon is assumed to be assembled in orbit about Earth, and capture theories in which the Moon is assumed to be formed elsewhere in the solar system and captured by Earth. All these theories have their modern advocates. Recent investigations of the Moon and of lunar materials have provided a large number of boundary conditions which must be satisfied by such theories, but apparently they have not yet allowed the unique selection of one class of theory.

*Fission.* In a fission theory, the Moon is postulated to be placed in orbit about the Earth as the result of some kind of disruption of the Earth. George Darwin was the first to suggest such a theory in the last years of the 19th century. He assumed that the initial Earth would be rotating with a period of about 4 hours, which he believed to be about twice the resonant period of Earth, so that huge tides would be raised on Earth, leading to separation of one of the tidal bulges to become the Moon. This theory was rejected by H. Jeffreys in 1930 on the grounds that the tidal dissipation would be too large for the separation to occur. More recently, in modified forms of the tidal theories suggested, the Earth is assumed to be rotating even faster in its initial state, close to rotational instability, which is assumed to occur when the formation of the iron core of the Earth takes place, reducing the moment of inertia and increasing the rotation rate above that required for disruption. If the Earth were rotating fast enough for this, its initial angular momentum would be much greater than that presently possessed by the Earth-Moon system, and a major process for removal of angular momentum is required.

*Atmospheric condensation* theories, or precipitation theories, as Ringwood [40] calls them, are motivated by the desire to form the Moon with little content of internal iron. These theories rely upon the assumption that the Earth formed very quickly in space, so that a great deal of the gravitational energy of accumulation was retained by the growing Earth, and its outer layers would be so hot that silicates would be contained in gaseous form, together with their decomposition products. If this system collides with a major planetesimal, which sets it spinning

rapidly, the outer part of the atmosphere can be shed into orbital motion, from which the silicate materials required to form the Moon are then precipitated [5]. The Moon is then assumed to form from this silicate debris in orbit about Earth.

*Twin planet.* Many have suggested that the Moon was formed near Earth as an independent body at the time the solar system was formed. The major problem faced by this kind of hypothesis is to account for the low density of the Moon, and no simple mechanism has been suggested by which the Moon could form with a very much smaller density than Earth if the materials from which the two bodies were assembled were similar. The Moon would have to be formed rather close to the Earth; some calculations backwards in time of the orbital motions of the Moon tend to indicate that the Moon was close to Earth much later than the time at which Earth formed, but these calculations generally assume a constant tidal phase lag, and the uncertainty in the actual phase lag introduces corresponding uncertainties into the time scale.

Various modifications of a simple twin planet formation have been suggested. For example, MacDonald [27] suggested two possible theories: (1) a small terrestrial satellite was formed in orbit about the Earth, which acted as a target which collided with a larger incoming body, thus allowing capture of the larger body; and (2) many smaller bodies are assumed to accumulate in orbit about the Earth, very similar to satellites of the giant planets, with the innermost one being more massive and receding from Earth due to tidal drag, gobbling up the others in the course of its recession.

*Capture.* Many different lunar capture hypotheses have both a geochemical and a dynamical aspect. In a geochemical version of a capture theory, possible conditions are discussed whereby the low mean density of the Moon can be produced, but the tendency is not to consider the details of capture dynamics. A dynamic theory tends not to be concerned with geochemical details, but to deal with the mechanism by which the independent motion of the Moon can be dissipated, leading to capture, and of the subsequent dynamic history of the lunar orbit.

Dynamic theories have recently been discussed in some detail by Kaula [22]. In their original form, as suggested by Gerstenkorn, capture theories required that the Moon initially approach the Earth in a retrograde orbit, with the subsequent elliptical orbit flipping over the poles of the Earth to become a prograde orbit. Various difficulties have been encountered with these versions of the theory, resulting from neglecting important dynamic details, and the most recent formulation of a dynamic theory of prograde capture is due to Singer. Kaula concludes that dynamic capture theories are improbable but not impossible.

All of these classes of theory must attempt to cope with the fundamental importance of the low mean density of the Moon. One of the major aspects of both fission and atmospheric condensation theories is to provide a single interactive system within which chemical differentiation can occur prior to the separation of Earth and the Moon into two distinct bodies. This essential interactive feature is missing from theories in which the Moon is assumed to be independently assembled in orbit about Earth from similar material, and this constitutes a prime objection against such theories. There is a little more freedom in capture theories, provided conditions can be found elsewhere in the solar nebula in which a body of lunar composition might be assembled.

*Other theories.* Several years ago it was believed that the Sun contained a much smaller abundance of iron relative to silicon than meteorites and terrestrial planets. This led Urey [52] to a theory of formation of the Moon, assuming that the Moon was formed from the condensable fraction of solar material, thereby being relatively low in iron and having a small mean density. It was supposed to be but one of a large number of primary condensation objects within the solar system. A great majority of these were assumed to collide with one another, producing fractionation of silicates and iron, leading to a concentration of iron in the surviving planets. The Moon was then supposed to be left over from this process, a surviving primary object, which was captured by the Earth. However, errors have been discovered recently in

the oscillator strengths of the iron lines used to determine the solar abundance of iron; it now appears that the iron-to-silicon ratio in the Sun is essentially the same as in meteorites and terrestrial planets.

Analyses of lunar samples recently have indicated that the upper portion of the Moon is abnormally rich in aluminum, calcium, and titanium. Since oxides and silicates of these metals are the first major refractory substances to condense out of gas at high temperature, this has led P. W. Gast to propose that when the Moon was assembled, the outer layers were made from such very high temperature condensates. This point of view has recently been extended by Anderson [2], who has suggested that the entire Moon resulted from a complete chemical fractionation of such high temperature condensates. If this is correct, it must place the formation of the Moon in a part of the primitive solar nebula where the temperature is much higher than that in which the main part of Earth was formed. Cameron [6] has suggested that this locates the formation site of the Moon inside the orbit of Mercury, so that perturbations of the initial lunar orbit by Mercury can cause the Moon to acquire a highly elliptical orbit from which it can be captured by Earth, and at the same time, the surprisingly high orbital eccentricity of Mercury can be produced.

Earth scientists have turned up a great deal of evidence bearing on the physical and chemical history of the Earth. Nevertheless, major controversies remain as a result of their investigations, which render knowledge of the earliest history of Earth very unreliable. The oldest rocks, determined from a decay of radioactivities in the Earth, are only some  $4 \times 10^9$  years old. On the other hand, a great deal of information indicates that the solar system is  $4.6 \times 10^9$  years old. The first several hundred million years of Earth's history remain an enigma as far as direct geological investigation is concerned.

### **Formation of the Earth**

A major controversy is whether Earth was formed in a very cold or very hot state. In the early years of this century, geologists favored a

picture of an entirely molten Earth in its earliest stages. No doubt this point of view was influenced by dualistic theories for the origin of the solar system, in which the Earth was pictured as hot condensation from a filament of hot gases torn from the Sun. However, some two decades ago, this prevailing point of view was challenged by Urey [51], who pointed out that certain of the more volatile elements present in large quantities in the Earth could not be present if Earth were to form from condensates of such a gas filament at high temperature. Urey concluded that the condensed material which assembled to form the Earth was cold, not more than a few hundred degrees Celsius. However, it is sufficient that small condensed bodies which accumulate upon Earth be rather cool, since the accumulation process may produce a very hot body, but the more volatile elements can be retained by this body as soon as it has an appreciable mass.

The initial temperature in the Earth's interior is a strong function of the time interval required for accumulation of the Earth. If a body is pictured where growth is steady by accumulation of relatively small particles onto a much larger nucleus, then the particles will release gravitational potential energy when their infall is stopped by contact with the surface of the growing body. The bulk of released gravitational potential energy would then be radiated away from the surface into surrounding space. However, the faster the rate of accumulation, the higher the required surface temperature would be which would radiate the bulk of energy into space. This radiating surface temperature becomes a measure of the Earth's interior temperature.

If the Earth forms on a time scale characteristic of gaseous dissipation of the primitive solar nebula, of the order of  $10^3$  years, then interior terrestrial temperatures of the order of 5000 to  $10\,000^\circ\text{K}$  would be produced [7]. At these high temperatures, the bulk of solid materials could only exist in gaseous form, and would form a hot extended atmosphere of the Earth. This is the basis for atmospheric condensation theories of the Moon's origin. However, this hot atmosphere would soon lose the bulk of its heat by radiation into space, and likely it would have condensed into liquid rock form in a few thousand years.

Related to these uncertainties in the thermal history of Earth are problems of the origin of the atmosphere and oceans of Earth. A great deal of geologic evidence was assembled by Rubey in 1951 [43] to show that the oceans had been outgassed from the interior of Earth. He concluded that the outgassing was a continuing process, the outgassing of water still occurring at present. Subsequently, however, no evidence has accumulated that any completely primitive water is still being outgassed from the interior of the Earth, with present evidence suggesting that the bulk of water now being outgassed has been recirculated from the surface through the interior of the Earth.

At about the same time, Brown [4] pointed out that the abundances of oxygen and nitrogen in Earth's atmosphere were several orders of magnitude greater than the abundances of rare gases. Thus, this implied that the atmosphere had originated largely in a secondary fashion by outgassing from the interior of Earth, since only chemically combined elements could be brought into the Earth in large amounts by small cold bodies which participated in the accumulation process. Present evidence indicates that both oceans and atmospheres of the Earth have been formed largely as a result of outgassing from the interior. The abundances of rare gases do not exhibit the solar abundance pattern, but rather a highly fractionated pattern which is characteristic of the abundances of rare gases absorbed in meteorites. Even the small amounts of rare gases present in Earth's atmosphere probably were also brought into the Earth by small-sized bodies.

### *Origin of Life*

These considerations have important bearing upon problems of the origin of life on Earth. The

present indication is that any primordial atmosphere that the Earth had, resulting from accumulation from the primitive solar nebula, was probably swept away by the very intensive T Tauri stage of the solar wind. Subsequently, the present atmosphere and oceans of the Earth were outgassed from the interior. Many biochemical investigations relating to the origin of life have assumed that the primitive atmosphere of Earth should be basically derived from solar composition, so that gases would be composed essentially of hydrogen, methane, ammonia, and water vapor. However, a secondary atmosphere will have much less hydrogen. Nitrogen may be outgassed partly in the form of ammonia, and carbon in the form of methane or other gaseous organic compounds, but the bulk of carbon is likely to be outgassed as carbon dioxide. Hence, such biochemical investigations of the early history of life on Earth might better proceed from the assumption that the composition of gases was mainly water vapor and carbon dioxide, with somewhat more minor constituents of excess hydrogen in the form of ammonia and methane.

The origin of life on Earth is thus seen arising as a natural consequence of a long series of physical and chemical processes taking place in association with the evolution of the universe, many details of which are still being unraveled. The seeming inevitability of this long sequence of events has led to the prevalent view that planetary systems are extremely widespread throughout our galaxy and the universe, that planets suitable for life exist in a large fraction of these planetary systems, and that the general geochemical conditions associated with such planets will be rather similar to those on Earth, so that the development of life and possibly of intelligent beings should be an exceedingly widespread phenomenon.

### REFERENCES

1. ANDERS, E. Physico-chemical processes in the solar nebula as inferred from meteorites. In, Reeves, H., Ed. *On the Origin of the Solar System*, pp. 179–201. Paris, Cent. Nat. de Rech. Sci., 1972.
2. ANDERSON, D. L. Structure and composition of terrestrial planets. In, Cameron, A. G. W., Ed. *Cosmochemistry*. Boston, Reidel, 1973.
3. ARRHENIUS, G., and H. ALFVÉN. Fractionation and condensation in space. *Earth Planet. Sci. Lett.* 10:253–267, 1971.
4. BROWN, H. Rare gases and the formation of the Earth's atmosphere. In, Kuiper, G. P., Ed. *The Atmospheres of*

- the Earth and Planets*, pp. 258–266. Chicago, Univ. Chicago Press, 1952.
5. CAMERON, A. G. W. Formation of the Earth-Moon system. *EOS, Trans. Am. Geophys. Union* 51:628–633, 1970.
  6. CAMERON, A. G. W. The orbital eccentricity of Mercury and the origin of the Moon. *Nature* 240(5379):299–300, 1972.
  7. CAMERON, A. G. W. Accumulation processes in the primitive solar nebula. *Icarus* 18(3):407–450, 1973.
  8. CAMERON, A. G. W., and M. R. PINE. Numerical models of the primitive solar nebula. *Icarus* 18(3):377–406, 1973.
  9. COX, J. P., and R. T. GIULI. *Principles of Stellar Structure*, Vol. I, II. New York, Gordon and Breach, 1968.
  10. DICKE, R. H., P. J. E. PEEBLES, P. G. ROLL, and D. T. WILKINSON. Cosmic black-body radiation. *Astrophys. J.* 142(7):414–419, 1965.
  11. DOROSHKEVICH, A. G., and I. D. NOVIKOV. Average density of radiation in the metagalaxy and some problems of relativistic cosmology. *Dokl. Akad. Nauk SSSR* 154(4):809–811, 1964.
  12. DOROSHKEVICH, A. G., Ya. B. ZEL'DOVICH, and I. D. NOVIKOV. The origin of galaxies in an expanding universe. *Astron. Zh.* 44(2):295–303, 1967.
  13. DOROSHKEVICH, A. G., R. A. SUNYAEV, and Ya. B. ZEL'DOVICH. The formation of galaxies in Friedmannian universes. In, Longair, M., Ed. *International Astronomical Union Symposium* 63:200, 1973.
  14. EZER, D., and A. G. W. CAMERON. The evolution of hydrogen-helium stars. *Astrophys. Space Sci.* 14:399–421, 1971.
  15. FOWLER, W. A., J. L. GREENSTEIN, and F. HOYLE. Nucleosynthesis during the early history of the solar system. *Geophys. J.* 6:148–220, 1962.
  16. FRALEY, G. S. Supernovae explosions induced by pair-production instability. *Astrophys. Space Sci.* 2:96–114, 1968.
  17. GAMOW, G. On the temperature of the hot universe. *Kgl. Dan. Videns. Selsk. Mat. Fys. Medd.* 27(10), 1953.
  18. HAGEDORN, R. Thermodynamics of strong interactions at high energy and its consequences for astrophysics. *Astron. Astrophys.* 5:184–205, 1970.
  19. HARRISON, E. R. Particle barriers in cosmology. *Comments Astrophys. Space Phys.* 4:187–191, 1972.
  20. HOYLE, F. On the origin of the solar nebula. *Quart. J. Roy. Astron. Soc.* 1:28–55, 1960.
  21. KAPLAN, S. A., and S. B. PIKEL'NER. *Mezhzyozdnaya Sreda*. Moscow, Izv. Akad. Nauk SSSR, Ser. Fiz., 1963. (Transl: *Interstellar Environment*). Cambridge, Mass., Harvard Univ. Press, 1970.
  22. KAULA, W. M. Dynamical aspects of lunar origin. *Rev. Geophys. Space Phys.* 9:217–238, 1971.
  23. LEVIN, B. Yu. Structure of the earth and planets and meteoritic hypothesis of their origin. *Priroda* 10:3–14, 1949.
  24. LIFSHITZ, E. M. On gravitation stability of the expanding world. *J. Exp. Theor. Phys.* 16:587, 1946.
  25. LIN, C. C., and F. H. SHU. On the spiral structure of disk galaxies. *Astrophys. J.* 140:646–655, 1964.
  26. LIN, C. C., and F. H. SHU. On the spiral structure of disk galaxies. III. Comparison with observations. *Astrophys. J.* 155:721–746, 1969.
  27. MACDONALD, G. J. F. Tidal friction. *Rev. Geophys.* 2(8):467–541, 1964.
  28. MARSDEN, B. G., and A. G. W. CAMERON, Eds. *The Earth-Moon System*. New York, Plenum, 1966.
  29. OMNES, R. On the origin of matter and galaxies. *Astron. Astrophys.* 10:228–245, 1971.
  30. OORT, J. H. The formation of galaxies and the origin of the high-velocity hydrogen. *Astron. Astrophys.* 7:381–404, 1970.
  31. OZERNOY, L. M., and A. D. CHERNIN. The fragmentation of matter in a turbulent metagalactic environment. *Astronom. Zh.* 44(6):1131–1138, 1967. (Transl: *Sov. Astron.*) 11(3):907–913, 1968.
  32. PACZYNSKI, B. Carbon ignition in degenerate stellar cores. *Astrophys. Lett.* 11:53–55, 1972.
  33. PEEBLES, P. J. E. Primeval helium abundance and the primeval fireball. *Phys. Rev. Lett.* 16:410, 1966.
  34. PEEBLES, P. J. E. Origin of the angular momentum of galaxies. *Astrophys. J.* 155:393–401, 1969.
  35. PEEBLES, P. J. E. Rotation of galaxies and the gravitational instability picture. *Astron. Astrophys.* 11(3):377–386, 1971.
  36. PEEBLES, P. J. E. *Physical Cosmology*. Princeton, N.J., Princeton Univ. Press, 1972.
  37. PEEBLES, P. J. E., and R. H. DICKE. Origin of the globular star clusters. *Astrophys. J.* 154(12):891–908, 1968.
  38. QUIRK, W. J. On the gas content of galaxies. *Astrophys. J.* 176:L9–L14, 1972.
  39. REEVES, H., J. AUDOUZE, W. A. FOWLER, and D. N. SCHRAMM. On the origin of light elements. *Astrophys. J.* 179:909, 1973.
  40. RINGWOOD, A. E. Origin of the Moon. (Clarke Memorial Lecture) *Earth Planet. Sci. Lett.* 8:131–140, 1970.
  41. ROBERTS, W. W. Large-scale shock formation in spiral galaxies and its implications on star formation. *Astrophys. J.* 158:123–143, 1969.
  42. ROBERTS, W. W., Jr., and C. YUAN. Applications of the density wave theory to the spiral structure of the Milky Way system. III. Magnetic field: large-scale hydromagnetic shock formation. *Astrophys. J.* 161:877–902, 1970.
  43. RUBEY, W. W. Geologic history of sea water. An attempt to state the problem. *Bull. Geol. Soc. Am.* 62:1111–1148, 1951.
  44. SAFRONOV, V. S. Dimensions of the largest bodies falling on planets in the process of their formation. *Astron. Zh.* 42(6):1270–1276, 1965.
  45. SCHMIDT, O. Y. The astronomical age of the earth. *Dokl. Akad. Nauk SSSR* 46:293–295, 1945.
  46. SCIAMA, D. W. *Modern Cosmology*. New York, Cambridge Univ. Press, 1971.
  47. SPITZER, L., Jr. *Diffuse Matter in Space*. New York, Wiley, 1968.
  48. TER HAAR, D., and A. G. W. CAMERON. Historical re-

- view of theories of the origin of the solar system. In, Jastrow, R., and A. G. W. Cameron, Eds. *Origin of the Solar System*, pp. 4–37. New York, Academic, 1963.
49. TRURAN, J. W. Theories of nucleosynthesis. In, Cameron, A. G. W., Ed. *Cosmochemistry*. Boston, Reidel, 1973.
50. TRURAN, J. W., and A. G. W. CAMERON. Evolutionary models of nucleosynthesis in the galaxy. *Astrophys. Space Sci.* 14:179–222, 1971.
51. UREY, H. C. *The planets, Their Origin and Development*. New Haven, Yale Univ. Press, 1952.
52. UREY, H. C. Primary and secondary objects. *J. Geophys. Res.* 64:1721–1737, 1959.
53. WAGONER, R. V., W. A. FOWLER, and F. HOYLE. On the synthesis of elements at very high temperatures. *Astrophys. J.*, Pt. 1, 148(4):3–49, 1967.
54. YONEYAMA, T. On the fragmentation of a contracting hydrogen cloud in an expanding universe. *Pub. Astron. Soc. Japan* 24(1):87–98, 1972.
55. WHEELER, J. A. *Magic Without Magic*. New York. W. H. Freeman, 1972.
56. ZEL'DOVICH, Ya. B., and I. D. NOVIKOV. *Relativistic Astrophysics*. Moscow, Nauka, 1967.
57. ZEL'DOVICH, Ya. B., and A. A. STAROBINSKIY. The birth of particles and vacuum polarization in an anisotropic gravitation field. *Zh. Eksp. Teor. Fiz.* 61(6):2161–2175, 1971. (Transl: *J. Exp. Theor. Phys.*) 39(6):1159–1166, 1972.
58. ZEL'DOVICH, Ya. B., and I. D. NOVIKOV. *Relativistic Astrophysics*, Vol. 2. Chicago, Univ. Chicago Press, 1975. (In press)

N 76-26801

## Chapter 2

# PHYSICAL CHARACTERISTICS OF INTERPLANETARY SPACE<sup>1</sup>

S. N. VERNOV, Yu. I. LOGACHEV

Scientific Research Institute of Nuclear Physics, Moscow State University, USSR

AND

N. F. PISARENKO

Institute of Space Research, Academy of Sciences USSR, Moscow

### THE SUN

The properties of interplanetary space are determined, to a considerable extent, by the central body of the solar system—the Sun—which is the source of powerful streams of corpuscular and electromagnetic radiation, and is responsible for the structure of the interplanetary magnetic fields.

Many phenomena on the Earth are closely related to processes occurring on the Sun. The mechanism of this relationship is not yet fully understood, but it is clear that the solar wind, the corpuscular streams, and short-wave electromagnetic radiation of the Sun play a prominent

role in these processes. Before describing the manifestations of Sun-Earth relationships, the elements of solar activity should be discussed.

### Solar Activity

Solar activity, a combination of various phenomena occurring in the atmosphere of the Sun, is distinguished by significant changes in the physical characteristics of the various strata of the solar atmosphere. The close relationship between the active processes in the photosphere (spots, faculae), chromosphere (flares, flocculi), and corona (protuberances, condensation, radiating areas), and the decisive role of the magnetic field in these processes are obvious.

The magnetic fields, the presence of which has been detected everywhere in the solar atmosphere, play a significant, and in many cases the primary role in the physical processes on the Sun. A general magnetic field of the Sun has also been detected; the field of the Sun is different at different latitudes. In the polar areas ( $|\phi| > 55^\circ$ ), its intensity is about 1 G, and differs slightly from a dipole field. The magnetic field force lines over the poles, judging from the configuration of the coronal rays, diverge more slowly

<sup>1</sup> Translation of, *Fizicheskaya Kharakteristika Mezoplanetnogo Prostranstva*, Volume 1, Part 1, Chapter 2, of *Osnovy Kosmicheskoy Biologii i Meditsiny (Foundations of Space Biology and Medicine)*, Moscow, Academy of Sciences USSR, 1973, 149 pages.

The authors acknowledge with appreciation the significant work by J. Van Allen in the preliminary preparation of data for this chapter, as well as A. G. Aiken. They also sincerely thank S. L. Mandel'shtam, Yu. I. Gal'perin, K. I. Gringauz, O. L. Vaysberg, T. N. Nazarov, Ye. V. Gorchakov, and S. N. Kuznetsov for help in compiling the review. Contributors from the USSR were R. I. Ivanov and M. Sugiura; from the USA, W. M. Alexander, S. J. Bauer, J. P. Heppner, W. N. Hess, C. W. McCracken, G. D. Mead, N. Ness, R. Palmeira, G. Pieper, and I. A. Zhulin.

than for an ordinary dipole, and show no tendency to bend in the direction of the Equator. This field with about 1 G intensity observed near the poles of the Sun in the photosphere decreases to 0.5 G at an altitude of about  $3 \cdot 10^5$  km. High-resolution measurements have shown that the overall field consists of a multitude of fine elements of different polarities and sizes. The field intensity in some of these elements reaches 10–20 G, with one polarity usually predominating. Coarse observations show a weak field of one sign due to averaging.

In the moderate and low latitudes ( $|\phi| < 50^\circ$ ), local magnetic fields which generally coincide with active formations on the Sun are observed. Large-scale local formations include bipolar (BM), which are most frequently observed and unipolar (UM) magnetic areas. The field intensity in these areas varies over broad limits from 0.2 G to hundreds of G, the sign of the field differing in different parts of the area. The field intensity in a BM area and the area dimensions are inversely related. The area follows a certain cycle of development from the beginning to the end of its existence (several months); the greatest intensity is observed after about 27 d, then it decreases as the area begins to increase in size, possibly reaching about  $0.3 R_\odot$ .

Within a BM, there may sometimes be a group of spots ranging in field intensity from about 500 to 4000 G. The BM areas are apparently the primary cause of groups of spots developing. BM fields and spots are usually stretched out along a parallel, corresponding with the direction of general Sun rotation. The first parts of regions and of spot groups are called the leading ones and are designated by the letter "r," and the latter ones are called the closing ones and designated by the letter "f." Fields of leading spots and BM fields have opposite polarity in the northern and southern hemispheres of the Sun and change their sign at the beginning of each new cycle of solar activity (Hoyle polarity laws). These polarity laws are more closely followed for BM areas than for spots.

The unipolar magnetic (UM) areas have weaker field intensity, greater area, and longer life than the BM areas; field intensity is  $\leq 2$  G, dimensions are about  $0.1 R_\odot$ , and lifetime is about

6–8 months. UM fields apparently terminate in high-latitude fields and are the remainders of disappearing BM areas. The development of BM and UM areas, preceded by the appearance of active areas on the Sun, is terminated after their disappearance.

Observations using modern, high-resolution instruments have revealed short-lived small-scale magnetic fields, intermediate in intensity between the BM group fields and the fields of the spots. They are related to the flocculi, pores, small spots, and other active formations in the atmosphere of the Sun.

*Sunspots*, the dark areas on the surface of the Sun, consist of umbras and penumbras. Granulation is observed in the area of an umbra, while the area of a penumbra consists of radial fibers. The umbra of a sunspot is below the photosphere, while the penumbra forms a sort of funnel. The effective temperature of the umbra is about  $4270^\circ$  K; that of the penumbra about  $5380^\circ$  K. Gas flows from the center of the spot into the penumbra (Evershed effect) at about 2 km/s, the motion disappearing at the edge of the penumbra. The outflow velocity decreases with altitude and changes its direction at the limits of the chromosphere, so that the gas at this point is flowing back toward the center of the spot. There are some indications of rotary motion of the spot as a whole. A light ring forms around the penumbra which is 3%–4% brighter than the photosphere. The diameters of spots range from thousands to tens of thousands of km. The smallest spots, pores, which have no penumbras, make up the majority of all spots. Spots are rarely individual, but usually observed in groups stretching to 100 000 km.

Groups are classified according to polarity: unipolar (type  $\alpha$ , 10% of all groups)—spots of identical polarity; bipolar (type  $\beta$ , 90%)—two main spots of opposite polarity; and complex (type  $\gamma$ , about 1%)—spots of different polarities scattered without order. Groups of spots are observed in the so-called "regal zones" ( $5^\circ \leq |\phi| \leq 45^\circ$ ).

The number of spots visible on the surface of the Sun changes cyclically with a mean period of about 11.2 years. The measure of the number of spots is the relative number of spots (Wolf

number):  $W = k(10g + f)$ , where  $g$  is the number of groups of spots,  $f$  is the number of individual spots, and  $k$  is a reduction factor on the order of 1. Information on the number of sunspots is published [72, 131].

The placement of spots on the visible disk of the Sun changes with the phases of the solar activity cycle, although the position of a spot changes little during its existence. At the beginning of the cycle, spots arise at latitudes of  $\pm 35^\circ$ , near the maximum at latitudes  $\pm 16^\circ$ , while at the end of the cycle—at about  $\pm 8^\circ$  (Speer law). Some refinements have been made to this regularity in recent years.

The magnetic field at the center of a spot's umbra is almost vertical and never less than 200 G, reaching 2000–4000 G during the maximum phase of development. In the penumbra, the field is horizontal in direction and at the edge is about 300 G. The role of convective transfer of energy, slight in the photosphere, apparently increases in the area of the spots. Groups of spots are usually extended along parallels, but the leading spot is located near the Equator. A typical group begins to develop with the appearance of pores, from which the spots develop; their area and magnetic field increase for several days. The group reaches its maximum development and begins to break out in 2–3 weeks. The tail spot and most of the smaller spots disappear first, and the group becomes unipolar; the leading spot is retained until its diameter becomes less than 30 000–45 000 km, after which it breaks up rapidly. A group may exist for a few hours to a few months.

### *Faculae*

Sunspots are always accompanied by faculae, light fibrous formations in the photosphere, which also may exist independently of spots. Faculae appear before spots and remain for several revolutions of the Sun after the spots disappear. The range of their latitudes is somewhat greater than that of spots. In white light, faculae are not visible at the center of the disk. For 3–4 d, faculae may be observed near the eastern and western edges of the disk; the upper parts of the faculae are hotter than the surrounding photosphere by about  $200^\circ$ – $300^\circ$ , the lower

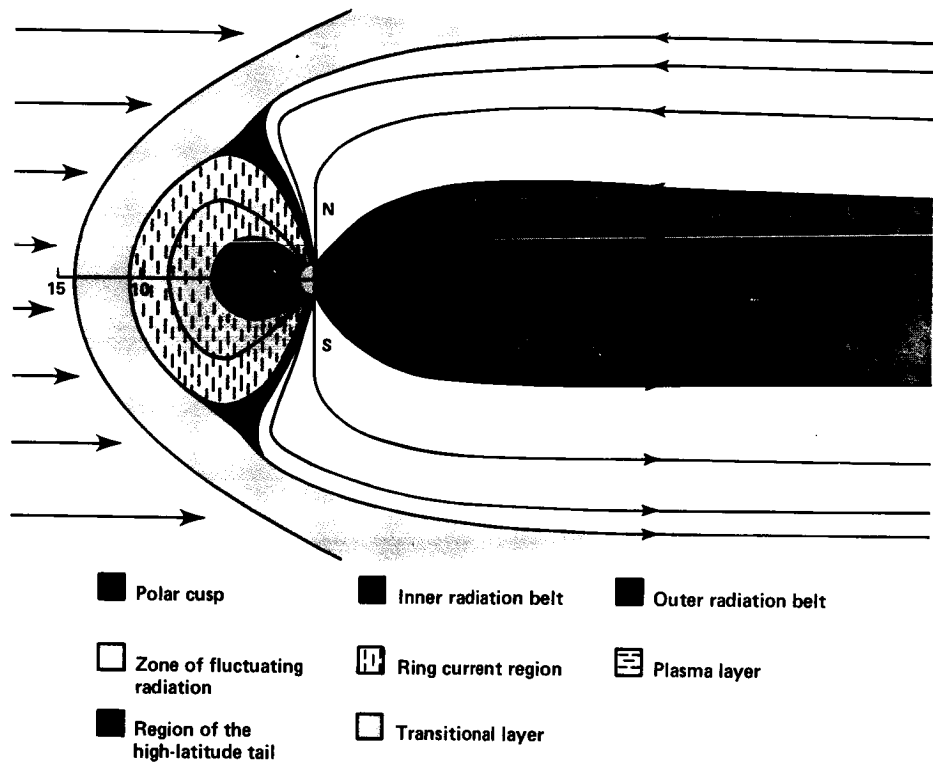
parts are cooler. Faculae are localized in areas where the magnetic field intensity  $H > 2$ –5 G. At latitudes around  $\pm 70^\circ$ , polar faculae are observed, which are smaller (about 2000 km), shorter lived (about 0.5 h), and circular in form.

### *Flocculi*

The upper layers of photospheric faculae become chromospheric faculae or flocculi, which can be observed in the violet lines of ionized calcium H and K (calcium flocculi) and in the red line of hydrogen H (hydrogen flocculi). The latter are smaller and less stable. Flocculi are heterogeneous formations with great fluctuations in brightness, temperature, rate of movement, and magnetic field intensity at various points. The lifetime is greater than that of spots, from a few days to a few months. Flocculi are also observed without spots, but they are less stable. In contrast to spots, they are located throughout the visible disk, but near the poles are less bright, unstable, and rounder. The fine structures of flocculi are closely related to the magnetic fields; most of their fibers are oriented along the lines of forces of the magnetic field. The intensity of flocculi increases on days of appearance and disappearance of spots.

*Solar flares*, the most active formations on the Sun, appear suddenly over a small area (tens of thousands km). Weak flares last 5–10 min; powerful flares last several hours. They appear in the upper chromosphere or corona, always above a field of faculae near complex groups of type  $\gamma$  spots and near neutral lines of the longitudinal magnetic field, where high field gradients are observed. Large flares correspond to gradients of 0.1 G/km. The number of grade 1 flares is an order of magnitude higher than the number of grade 3 flares. The classification of flares is shown in Table 1 [73].

A flare is accompanied by sporadic UV, x-ray, and radio radiation and by the ejection of particles of various energies up to high-energy solar cosmic rays (see section, THE INTERPLANETARY MEDIUM). Apparently, the generation of high-energy particles is a basic characteristic of flares. Hard x-rays arise in the area of flares or above them as a result of bremsstrahlung of electrons



Profile of the magnetosphere of the Earth.

accelerated in the flare, while a cm-band radio burst occurs simultaneously as a result of synchrotron radiation of the same electrons.

The ejection of matter apparently is a characteristic of all flares. The most frequent type of ejection of matter is a protuberance which returns; ejection velocity is 50–5000 km/s, and the stream of matter falls back to the Sun. Ejection of matter into interplanetary space must occur at velocities greater than the escape velocity, which is determined by the Sun's gravity.

The emission of solar cosmic rays at high energies has almost always been observed with very strong flares. It has been discovered that, in addition to rare cases of high-energy particle emission, the Sun radiates low-energy particles much more frequently, also related to flares.

Type IV radio radiation (continuous) and sudden disturbances in the terrestrial ionosphere usually accompany the generation of energetic protons during proton flares. This results from increased ionization of the lower portion of the D area of the ionosphere by solar x-rays with  $\lambda \leq 5 \text{ \AA}$ . The total energy of solar cosmic rays ejected by a powerful flare reaches  $10^{31}–10^{32} \text{ erg}$ .

The relationship between complex phenomena in flares and the generation of solar cosmic rays has not yet been explained. The appearance of flares is assumed to be related to instabilities near the neutral lines with high field gradients of complex configuration in the chromosphere, which results in conversion of the magnetic energy to other forms [127, 128]. After a flare, the magnetic field is usually simplified, the gradients are decreased, and the field is weaker. Energy estimates have shown that neutralization of a field of 50–100 G is sufficient to compensate for the energy liberated.

*Protuberances* are masses of comparatively cold, dense gas ( $n \approx 10^{10}–10^{11} \text{ cm}^{-3}$ ), rising over the chromosphere. At the edge of the disk, protuberances are visible as light clouds; at the center of the disk they appear as dark fibers called hydrogen fibers. Near the Equator, they are located along the meridians; at high latitudes they fall along the parallels. Three types of protuberances are distinguished: quiet, active, and eruptive. Quiet protuberances are encountered at the boundaries of active areas primarily on the high latitude side, but sometimes within the area. These are about 100 000–200 000 km in length with a height of several thousands of km and a thickness of about 10 000 km. Their lifetime is several months and the rate of movement of individual streams is about 10 km/s. Active protuberances are small, encountered within active areas, frequently near spots, and related to flares. Their shape is varied and changes rapidly; their lifetime is several hours or days. The rate of movement of individual elements is up to 100 km/s. Eruptive protuberances, a rare type, are distinguished by extremely rapid development, instability of shape, sudden increase in velocity of motion of hundreds of km/s and sudden disappearance. Their lifetime is but a few minutes.

The temperature of protuberances is about  $10^4 \text{ }^\circ\text{K}$ ; their density is about 100 times greater than the surrounding coronal gas. This indicates that protuberances may condense from the coronal matter as a result of cooling related to a decrease in the magnetic field at the base of the corona, or may be formed by compression of a certain volume by some external force, for example a magnetic field. Figure 1 shows various elements of solar activity across the disk of the Sun [21].

#### *Centers of Activity*

The development of various active formations throughout the solar atmosphere is a single process, which can be looked upon as development of a center of activity (centers of activity were formerly called active areas, and referred only to a facular area with spots and flares). The development of a typical center of activity can be divided into four stages:

TABLE 1.—*Classification of Flares*

Estimate of relative brightness	2.0 Subflare	Adjusted area in square degrees			
		2.1–5.1	5.2–12.4	12.5–24.7	24.7
f—faint	sf	1f	2f	3f	4f
n—normal	sn	1n	2n	3n	4n
b—bright	sb	1b	2b	3b	4b

Stage 1, which lasts several days, is characterized by the appearance of a weak (or complex configuration) UM field, plus a bright facula and development of flocculi in the chromosphere. At the brightest point of the flocculi, dark spots (pores) appear, from which spots develop. The field area increases and becomes BM.

Stage 2, which lasts several weeks, is the active state characterized by rapid and unstable development. During this time, the size and intensities of the M areas and flocculi reach their maximum, flares appear,

and active protuberances are seen. After a month, the group of spots begins to break up while the flocculi grow but become darker.

Stage 3, the stable state, lasts several months. The group of spots becomes unipolar and disappears; faculae and flocculi gradually weaken although quiet protuberances and a significantly weakened M area are temporarily retained.

Stage 4 lasts several months. The protuberances disappear and the BM area is converted to a UM area before it dissipates.

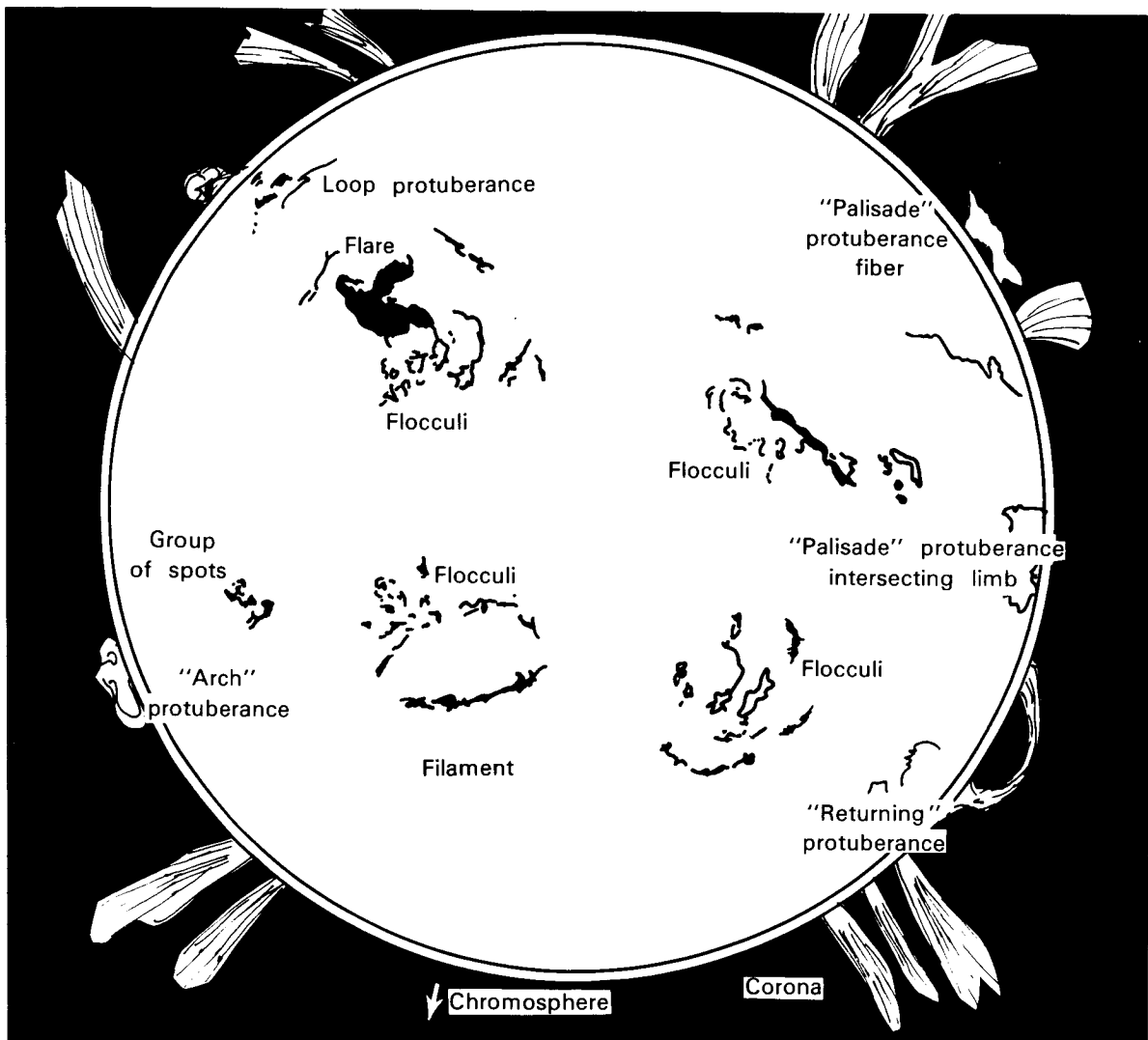


FIGURE 1.—Diagram of the active Sun, showing flares, flocculi, spots, protuberances, the chromosphere, and corona.

Centers of activity are unevenly distributed in the solar atmosphere. The primary latitudes are the "regal zones," but during the years of maximum activity, centers also appear at latitudes of more than  $\pm 40^\circ$ , although they are less stable here. The intervals of longitude in which centers of activity most frequently develop are called "active longitudes."

The active longitudes are retained for two or more 11-year cycles, although they fluctuate in different directions, obviously unaffected by the presence of differential motion in the layers of the atmosphere. Consequently, the active longitudes characterize the physical state of the deep internal photosphere layers, where the differential rotation is replaced by rigid rotation.

Solar activity can be characterized by various indices [72, 122, 131]:

1. index of the relative number of spots—the Wolf number
2. index of the summary area of groups of spots
3. index of the maximum magnetic field intensity of the spots
4. flare index
5. index of the summary area of protuberances
6. corona index (mean intensity of lines)
7. index of the flux of radio radiation at a given wavelength (from over 1 m to cm); most commonly used is,  $\lambda = 10$  cm.

### *Cycles of Solar Activity*

Solar activity is also characterized by cycles of various lengths; those of greatest interest are the 11- and 22-year cycles which have perturbations, and the 80-year cycle.

The 11-year cycle of solar activity is most clearly seen by measuring the number of groups of spots. The cycles are numbered beginning with the zero cycle in 1745. The 11-year cycles, which vary in length (7–17 years) with a mean length of about 11.2 years, are asymmetrical; the transition from the maximum number of spots to the minimum (descending branch) occurs at an average 6.7 years, while transition from the minimum number of spots to maximum (ascending branch) occurs in about 4.6 years. The cycles also differ

in mean annual maximum values of Wolf number ( $W=46$ –190); in late 1957, the mean quarterly Wolf number was  $W=235$ . The intensity of the cycle is related to its length: the more powerful the cycle, the shorter its length; the shorter the growth branch, the greater the asymmetry of the cycle and the higher the latitudes at which its first groups of spots appear. In weak cycles, the ascending branch is almost equal to the descending branch; in very weak cycles, the normal proportion may even reverse. The polarity of the leading spots in the northern and southern hemispheres changes from cycle to cycle. Eras of the maximum in the hemispheres sometimes differ by 1 or 2 years. The most powerful phenomena of solar activity are usually not observed in the year of the maximum of sunspots, but at the end of the ascending branch or at the beginning of the descending branch.

*The 22-year magnetic cycle* is characterized by a change in sign of the overall magnetic field and the fields of magnetic areas and spots. In odd cycles, the leading spots and the overall field have positive signs in the northern hemisphere and negative signs in the southern hemisphere. The 22-year cycle begins with an even 11-year cycle. Apparently, the 22-year cycle also governs the index of mean area of groups of spots, the index of frequency of flares, and the sum of mean annual Wolf numbers.

*The 80-year cycle* is a quasi-periodic change in maxima of the 11-year cycles. The maxima of 80-year cycles have fallen approximately in 1775, 1855, and 1930; the minima, in 1815, 1900, and next to be in 1980. The next few minima in the 11-year cycle of solar activity are expected to be deeper than the past few. Studies and descriptions of solar activity are the subject of an extensive literature [41, 46, 57, 58, 93, 121].

### **Electromagnetic Radiation of the Sun**

The spectrum of solar electromagnetic radiation extends from the radio range to the x-ray area. The shortwave boundary of the spectrum usually lies at a few ångströms ( $1 \text{ \AA} = 10^{-8} \text{ cm}$ ; the energy of a quantum with wavelength  $\lambda = 1 \text{ \AA}$  is 12.4 keV) under "quiet" Sun conditions and may shift to several hundred keV during flares.

The solar constant outside the Earth's atmosphere is  $1.36 \cdot 10^6$  erg/cm $^2$  s, or 1.95 cal/cm $^2$  min. Direct measurement of the solar constant considering the short wave portion of the spectrum was first achieved in late 1967. The accuracy of this determination is about 1.0%. Distribution of energy in the various areas of the solar spectrum is presented in Table 2. The general form of the solar spectrum outside the Earth's atmosphere is presented in Figure 2 [85].

The Earth's atmosphere fully absorbs solar radiation at wavelengths of less than 2900 Å. From 3000 Å to 40 000 Å, the atmosphere is transparent (the so-called "optical window"). The next window of transparency begins at millimeter wavelengths and extends to approximately 15 m (the so-called "radio window"). Radio radiation is significantly attenuated by the ionosphere at wavelengths longer than 15 m and fully cut off at a wavelength of about 40 m.

### *Visible Light*

Most of the visible light is emitted from the surface of the photosphere in the form of a continuous spectrum, onto which the Fraunhofer absorption lines are superimposed. The light that arises deep within the Sun in the form of high-energy x-ray photons after traveling the path from the deep layers to the solar atmosphere, generates the continuous spectrum of radiation in the process of multiple energy exchange by radiation and absorption over a broad range of frequencies. The energy of the visible light ( $\lambda = 3800\text{--}7600$  Å) represents about 20% of the total energy of solar radiation.

The matter of the photosphere has a high coefficient of radiation absorption and becomes practically nontransparent at a depth of about 300–400 km. Tens of thousands of Fraunhofer absorption lines are superimposed on the con-

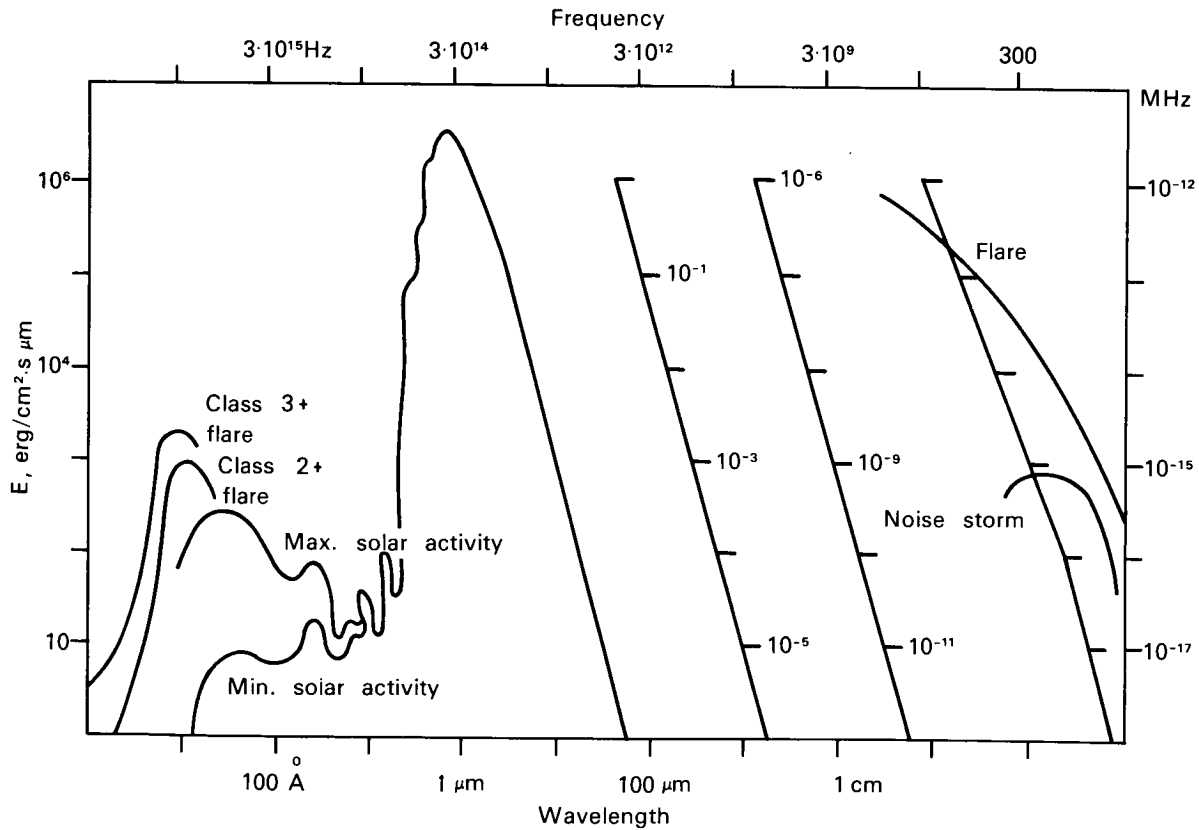


FIGURE 2.—Distribution of energy in the spectrum of the Sun.

tinuous spectrum, most of which are formed in the upper layers of the photosphere, some in the chromosphere. The absorption lines significantly change the distribution of energy in the spectrum of solar radiation. Thirteen elements have over 100 absorption lines each, two of these (Ti and Cr) have over 1000, and one, Fe, over 3000 absorption lines. The observed erosion of the Fraunhofer lines generally results from the combined influence of the Doppler effect and various types of attenuation (Table 3).

Radiation in the visible area is almost constant; in the UV and radio areas it changes about every 11 years. The Earth's atmosphere, opaque to a significant portion of the radiation, also distorts sunlight in the form of extinction (the general weakening of the spectrum, stronger at the violet end), telluric lines, and molecular absorption bands, the density of which also increase

toward the violet end; in the red area they even predominate over the solar absorption lines.

### *Shortwave Radiation of the Sun*

Radiation with wavelengths shorter than 3000 Å, corresponding to energy of quanta over 4 eV, is generally called shortwave radiation. Compared to the corpuscular ionizing radiation of solar flares, the energy of shortwave radiation quanta is low. However, the energy flux of shortwave radiation is thousands of times greater than the maximum energy flux of other types of ionizing radiation recorded in space. The shallow penetration depth of shortwave radiation can significantly change the surface properties of various structural materials. Thus, when space conditions are simulated under laboratory conditions, detailed knowledge of energy fluxes in various areas of the Sun's spectrum of shortwave radiation is required.

The photosphere makes the primary contribution to the shortwave radiation of the Sun down to 1600–1500 Å; the intensity of this radiation remains practically unchanged with time. In the area of the spectrum with wavelengths shorter than 1500 Å, the primary contribution is made by the chromosphere and the corona, while at wavelengths less than 300 Å, by the corona of the Sun. Radiation with wavelengths shorter than 1300 Å and in particular, shorter than 100 Å, changes sharply depending on the level of solar activity.

Variations in solar radiation flux during the 11-year cycle of activity are known, as well as 27-day variations caused by the visible movement of active areas across the disk as the Sun rotates. The greatest increase in radiation flux, particularly near the shortwave boundary of the spectrum, is observed during brief x-ray bursts, which frequently accompany chromospheric flares. The length of these bursts, depending on class and on the wavelength of the x-ray radiation, is from a few minutes to some hours. For example, in the spectrum area shorter than 10 Å, bursts lasting some tens of minutes are observed, comparable in duration to chromospheric flares. However, in the area shorter than 1 Å, the duration is generally not more than a

TABLE 2.—*Spectral Distribution of Solar Radiation at the Upper Boundary of the Earth's Atmosphere for Mean Sun-Earth Distance*

$\lambda(\text{\AA})$	$f_\lambda, \frac{\text{erg}}{\text{cm}^2 \text{s} \text{\AA}}$	Relative energy, %, for area shorter than $\lambda$
10	$10^{-6}$	$10^{-9}$
100	$10^{-3}$	$10^{-5}$
1000	$10^{-3}$	$10^{-4}$
2000	1.4	$10^{-2}$
3000	61	1.3
5260	196	26
6070	178	36
6880	148	46
10 000	73	73
20 000	11	95
30 000	2.7	98
50 000	0.4	99.8

TABLE 3.—*Strongest Fraunhofer Lines in the Visible Area*

Å	Atom	Å	Atom	Å	Atom
3820.44	Fe	4226.74	Ca	5172.70	Mg
3933.68	Ca <sup>+</sup>	4340.48	H <sub>γ</sub>	5185.62	Mg
3968.49	Ca <sup>+</sup>	4383.56	Fe	5889.97	Na
4045.82	Fe	4861.34	H <sub>β</sub>	5895.94	Na
4101.75	H <sub>δ</sub>	5167.33	Mg	6562.81	H <sub>α</sub>

few minutes. The development of a characteristic x-ray flare with time is shown in Figure 3 [151].

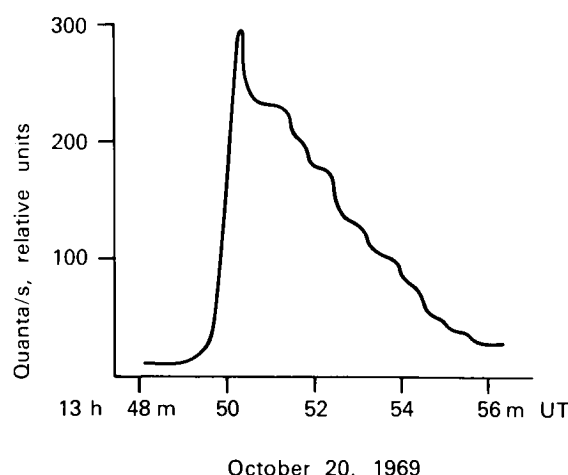


FIGURE 3.—Development of x-ray flare in the spectral area shorter than 1 Å (observed October 20, 1969 at 13:50).

Table 4 shows the absolute values of the radiation flux in the area of the spectrum shorter than 3000 Å when there are no flares ("quiet Sun"), near the minimum phase of the 11-year activity cycle. Between the minimum and the maximum of the 11-year cycle of solar activity, the summary flux shorter than 1300 Å increases by a factor of 2–3 times. During each 27-day period of variation, the summary flux shorter than 1300 Å may change by 1.5–2 times. The flux in the most intensive hydrogen line  $L_\alpha$  at 1215.7 Å varies by from 3–6 erg/cm<sup>2</sup> · s. Brief changes in radiation flux in the area shorter than 1300 Å are apparently slight.

The flux in the spectrum area shorter than 100 Å apparently varies from 0.1 to 1 erg/cm<sup>2</sup> · s during each 11-year solar cycle and may vary from 3 to 5 times within a few hours or days. The flux of the "quiet" Sun in the area of the spectrum shorter than 10 Å increases by two orders of magnitude from the minimum to the maximum of the solar cycle and may change dozens of times during a 27-day cycle; during solar flares, the flux may reach  $5 \cdot 10^{-2}$  erg/cm<sup>2</sup> · s. The flux in the area shorter than 5 Å for the "quiet" Sun apparently reaches  $10^{-6}$  erg/cm<sup>2</sup> · s and may increase by almost three orders of magnitude

during flares. In the spectral area shorter than 1 Å, the flux during flares may reach  $10^{-4}$  erg/cm<sup>2</sup> · s.

The distribution of energy in the shortwave spectrum of the Sun is shown in Figures 4 and 5, [22]. Figure 5 relates to the "quiet" Sun near the

TABLE 4.—*Flux of Solar Energy and Shortwave Area of Spectrum ( $\lambda < 3000 \text{ \AA}$ ) Above the Earth's Atmosphere at a Distance of 1 AU*

Boundaries of intervals, Å	Energy flux, erg/cm <sup>2</sup> s	Boundaries of intervals, Å	Energy flux, erg/cm <sup>2</sup> s
3025	3050	1100	0.09
2975	3150	1050	0.17
2925	2600	1000	0.13
2875	1700	950	0.14
2825	1200	900	0.18
2775	1100	850	0.12
2725	1250	800	0.10
2675	1000	750	0.05
2625	700	700	0.05
2575	560	650	0.13
2525	380	600	0.10
2475	390	550	0.07
2425	340	500	0.08
2375	320	450	0.06
2325	360	400	0.13
2275	350	350	0.41
2225	310	300	0.19
2175	240	250	0.23
2125	145	200	0.36
2075	90	180	0.39
2025	70	160	0.07
1975	55	140	
1925	41	120	0.04
1875	28	100	0.02
1825	19	80	0.06
1775	12	60	0.05
1725	8.2	40	0.04
1675	5.0	30	0.02
1625	3.2	20	0.005
1575	1.7	10	0.002
1525	0.95	< 10	0.00001
1475	0.50		
1425	0.26		
1375	0.26		
1325	0.18		
1275	0.37		
1225	5.10		
1200	0.19		
1150	0.10		
1100			

minimum of the 11-year cycle of activity and shows the most intensive lines, their ordinates being numerically equal to the energy flux in a line ( $\text{erg}/\text{cm}^2 \cdot \text{s}$ ). Near lines are combined; the ordinate here corresponds to the summary flux.

Experimental material on shortwave solar radiation is still limited. The data in Table 4 were produced at various times by various

methods. Some of the measurements were made by rockets and the results extrapolated beyond the Earth's atmosphere. Thus, the data must be looked upon as approximate, and will be refined in the future. Shortwave radiation of the Sun is the subject of several works [8, 9, 23, 69, 109, 129].

#### *Radio Radiation of the Sun*

The radio radiation of the Sun can be observed on the surface of the Earth only in the radio window at wavelengths from  $\lambda=8 \text{ mm}$  to  $\lambda=15 \text{ m}$ . The shortwave boundary is determined by absorption by molecules of  $\text{H}_2\text{O}$  and  $\text{O}_2$ ; the longwave boundary, by the critical frequency of the ionosphere.

The Sun is a variable radio star. Radio waves are radiated by the solar atmosphere, basically by the chromosphere and the corona, i.e., by a plasma varying in temperature from  $10^4$  to  $10^7 \text{ }^\circ\text{K}$  with electron concentration  $10^7$  to  $10^4 \text{ cm}^{-3}$ . The Sun emits three types of radio emission:

1. constant continuum of the quiet Sun (background), observed throughout the entire spectrum

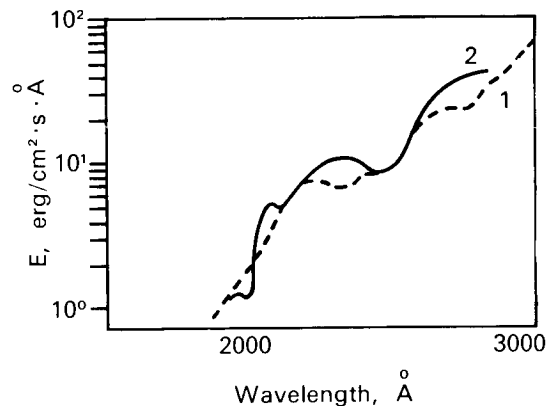


FIGURE 4.—Distribution of solar energy in the spectral region 2000–3000 Å.

1—April 19, 1960[129];  
2—January 13, 1967[22].

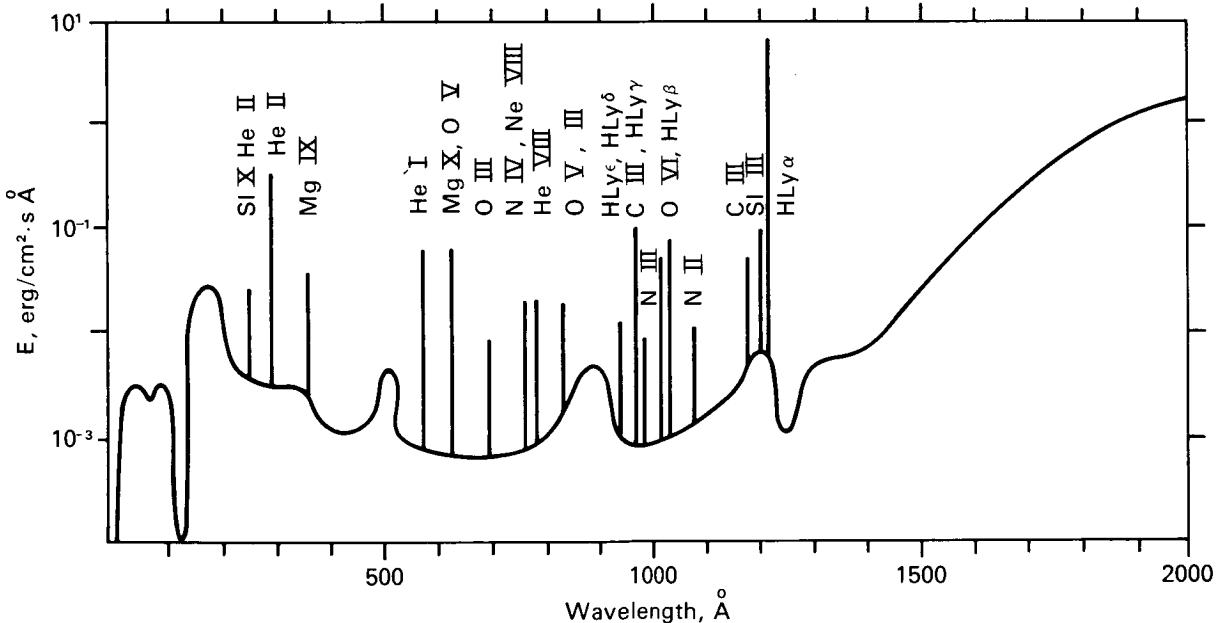


FIGURE 5.—Distribution of solar energy in the spectral region shorter than 2000 Å.

2. slowly changing component, best observed at wavelengths of 3–60 cm, related to spots and flocculi
3. sporadic radio emission—noise storms, five types of microwave bursts and the decimeter continuum; the sources are related to centers of activity, and certain types of bursts correlate directly with flares.

In the equilibrium high temperature plasma of the quiet Sun, radiation of electrons is thermal and incoherent. Nonthermal radiation appears with a deviation from the Maxwellian distribution of velocities and is related to active formations on the Sun and plasma oscillations. For thermal radiation, the influence of the general magnetic field of the Sun can be ignored. Sporadic nonthermal radio emission is related to the areas of the solar atmosphere where strong local magnetic fields are present; therefore, it is polarized and observed in the form of ordinary and extraordinary components.

Electrons generate three types of solar radio emission: bremsstrahlung, magnetic bremsstrahlung (for relativistic electrons called synchrotron radiation, for nonrelativistic electrons—cyclotron radiation), and Cherenkov radiation, which make different contributions to different types of solar radio emission.

The concept of “effective” or “brightness” temperature  $T_{\text{eff}}(\lambda)$  is frequently used for thermal and nonthermal radio emission, but it is not always identical to the temperature of the source of the radiation. Rather, it is a measure of the intensity of the radiation, since the observed radiation may contain contributions from various layers of the solar atmosphere.

The placement of thermal radiation sources is different for the different wavelengths. The chromosphere and corona, transparent for visible light and short radiowaves, become nontransparent for the wavelengths which they themselves radiate. The observed radiation at millimeter wavelengths comes from the lower chromosphere, at centimeter wavelengths—from the chromosphere, and at meter wavelengths—from the corona. The radius of the “radio Sun,” near the radius  $R_{\odot}$  of the optical disk at millimeter wave-

lengths, increases with increasing  $\lambda$  and in the meter waveband reaches about  $(1.5\text{--}3.0) R_{\odot}$ .

*Radio emission of the “quiet” Sun* (background or B component), observed throughout the entire wave range from millimeter to meter waves, is the lower boundary of radio emission of the Sun and is determined during the time of least solar activity. The frequency spectrum, characterized by  $T_{\text{eff}}(\lambda)$ , varies from  $6 \cdot 10^3$  °K for millimeter waves to about  $10^6$  °K in the meter waveband.  $T_{\text{eff}}(\lambda)$  is a nonmonotonic function, with a maximum at  $\lambda = 4$  mm, and a minimum at  $\lambda = 6$  mm. It then increases strongly to the meter waveband. The question of 11-year variations of the B component is still undetermined. The B component is thermal, is not polarized in the stationary atmosphere of the Sun, and is basically electron bremsstrahlung with some Cherenkov radiation. As the millimeter waves are generated in the lower chromosphere, the height of the area of generation increases with increasing  $\lambda$ , and the meter waves come from the corona. The B component is a continuum of radiation types, i.e., it is stable and has a broad frequency spectrum, indicating a noncoherent mechanism of generation.

*The slowly changing component* (S component) of continuum type is observed in the wavelength  $3 \leq \lambda \leq 50$  cm and at a few percent in the millimeter waveband for up to 30 d as a smooth increase in the signal received above the “quiet” Sun level. Periodicity of 27 d is observed, correlating well with the Wolf number and with the overall area of spots; i.e., it is related to the cycle of solar activity. Its sources are local areas on the disk of the Sun at a height of about  $0.03 R_{\odot}$  from the surface of the Sun, i.e., at the boundary between the chromosphere and corona; it is closely related to the spots, particularly the flocculi and, apparently, is located at spots in the areas of high electron concentration in the lower corona over the centers of activity containing spots and flocculi. The slowly changing component exists longer than the flocculi with which it is associated. Observations of the S component over active areas can be used to predict proton flares. Most proton flares occur when the ratio of flux densities of S component at  $\lambda = 3.2$  cm and  $\lambda = 7.5$  cm is higher than 1.

*The sporadic radio emission of the Sun* is related to solar activity, is heterogeneous in composition and most intensive and varied in the meter waveband. For classification, it is best to assume a dynamic spectrum of radio emission (dependence of frequency on time), which facilitates the search for mechanisms of generation.

Solar activity is related to: the slowly changing component (S component), noise storms and type I, II, III, and IV bursts, microwave bursts, and the decimeter continuum.

If the slowly changing component, related to centers of activity, is generated during the stable mode of the Sun and is thermal radiation, all other types of sporadic radio emission would arise during the "active" phase of development of centers of activity and would be nonthermal radiation.

*Noise storms and type I bursts* are continuum-type radio emissions with superimposed narrow bursts. They are observed primarily in the meter waveband, are less frequent and less intense in the decimeter band. The greatest intensity observed is at  $\lambda=2-4$  m, with a frequency interval range not over 250 MHz. The increase in flux during bursts may be  $10^2-10^3$  times greater than at the mean quiet level. The continuum usually arises gradually, is observed for several hours or days, and has many brief type I bursts with lengths of a fraction of a second to a minute.

The emissions of noise storms and type I bursts are strongly polarized, do not drift in frequency and are nonthermal in type. The mechanism of their generation is not exactly known; it may be incoherent magnetic bremsstrahlung. It is assumed that the area of noise storms generation forms a sort of reservoir, which retains energetic particles in a "trap" formed by the BM fields of the spots. Type I bursts appearing against the background of a noise storm can apparently be explained by additional acceleration of fast electrons over a limited area of the corona. Another possible source might be plasma waves, which have an attenuation time comparable to the lifetime of type I bursts.

*Type II bursts* (slowly drifting in frequency) are powerful bursts of radio emission in the meter and decimeter bands lasting a few to tens of minutes. Type II bursts arise at high frequencies,  $f \approx 200$  MHz, then shift to lower frequencies; the

majority attenuate at a frequency  $f=25$  MHz ( $\lambda=12$  m). The frequency drift rate is about a fraction of a MHz/s. The intensity is 100–1000 times greater than the background. Type II bursts are among the rarest phenomena in the radio emissions of the Sun; even during the period of maximum activity, an average of one burst is observed each 50–100 h. Type II bursts usually arise during large grade 2 and 3 flares. The delay of a type II burst relative to the maximum of an optical flare averages about 7 min. The width of the frequency band of a burst at each moment is about  $0.3f$ , where  $f$  is the frequency of maximum intensity. Polarization is slight.

Type II bursts are clearly distinguished by the appearance of a second harmonic (in 75%–80% of cases); the structure of the bursts at the main frequency and second harmonic is identical. They appear simultaneously and at great altitude in the corona, although the second harmonic is apparently generated deeper in the corona than the main tone.

The frequency drift in the direction of low frequencies, visible in the dynamic spectrum of type II bursts, can be explained by the "plasma" hypothesis of movement of an agent from the area of a flare through the corona. The "plasma" hypothesis relates the frequency of radio radiation to the natural frequency of oscillations of the plasma. With increasing distance from the photosphere, the concentration of electrons decreases; consequently, the frequency drift of a type II burst will be in the direction of lower frequencies. Type II bursts might be caused by shock waves in plasma with a magnetic field frozen in. These arise in the explosive phase of a flare and move at a speed of  $10^3$  km/s. Bursts are generated in the process of passage, of the leading edge of the shock wave which runs before the bundle of plasma, through the corona.

The relationship of type II bursts to the ejection of material from the area of a flare and to solar geoactive streams is confirmed by the appearance of geomagnetic perturbations 1 to 2 d after strong type II bursts and the agreement of the velocity of a bundle and of these streams. The  $A_p$  and  $K_p$  indices increase 1.5–2.2 d after type II bursts; magnetic storms and polar auroras begin only after 45% of type II bursts.

*Type III bursts* (rapidly drifting bursts) are observed in the meter waveband. Similar to type II bursts, they consist of nonthermal radiation, created upon transformation of plasma waves into electromagnetic waves in a system consisting of a corpuscular stream and the coronal plasma. The corresponding stream of particles, which leave the area of the flare, moves through the corona at about  $10^5$  km/s.

The main difference between type III and II bursts is that type III bursts drift rapidly in frequency, i.e., develop about 100 times more rapidly than type II bursts, and have a duration of about 3–15 s. The velocity of the agent causing type III bursts in the corona is two orders of magnitude higher than in type II. Type III bursts are observed much more frequently than type II bursts; for each 100 hours observation, an average of 300 type III bursts are observed, compared with less than one type II burst. The beginning of a type III burst is usually related to the beginning, not the maximum of an optical flare. Type III bursts frequently appear in groups. About half of all bursts are strongly polarized (30–70%). Type II and III bursts are closely related; 60–80% of type II bursts are accompanied by type III bursts, with a mean delay of 5.5 min.

The U burst is one variety of type III burst, which occurs when the direction of motion of the exciting agent reverses, so that the frequency drift first is downward toward lower frequencies, then toward higher frequencies. This type of burst rarely appears and results either from a special configuration of the magnetic field of bipolar groups of spots, or from local heterogeneities in the corona.

*Type IV bursts* frequently (about 70%) follow type II bursts, are related to strong flares, and reach a maximum 10 to 30 min after the flash phase of the optical flare. Type IV bursts are radiation of the continuum type, covering a wide frequency band (sometimes more than 8 octaves). The length, from minutes to several hours, and the intensity gradually decrease. The greatest intensity is in the meter waveband ( $\lambda > 1.2$  m). A gradual frequency drifting in the direction of low frequencies is observed.

These bursts differ from the continuum of

noise storms (with which they are generally not observed) by their more stable nature, briefer duration, broader range of frequencies (in the high-frequency direction), close relationship to type II bursts, mechanism of generation, and movement of the generation area in the corona over distances greater than approximately  $6 R_{\odot}$ .

The structure of type IV bursts is very complex; they are divided into several subtypes, but as yet there is no standard classification. The dynamic spectrum frequently has three maxima: in the meter waveband (type IV m), decimeter waveband (type IV dm), and centimeter waveband (type IV cm). In the meter waveband, two subtypes are differentiated, stationary and moving, which differ in the distance of motion of the source. There are two classes of type IV bursts related to the chromospheric or coronal flares.

The great correlation of type II and IV bursts and movement of their areas of generation at approximately the same velocity indicate that apparently both phenomena are caused by the same agent, for example, shock waves in plasma, moving in the corona from a flare area at a velocity of  $10^3$  km/s. Although the defining factor for type II bursts is the velocity of the shock wave, type IV bursts are generated by the synchrotron radiation of relativistic electrons behind the shock wave front and are related to ambient magnetic fields. The acceleration of electrons to the necessary energies may occur directly within the bundle during the existence stage of the type II burst. Polarization of radiowaves confirms the hypothesis of the synchrotron mechanism of generation.

Type IV bursts have narrow directionality and are less frequently observed away from the center of the solar disk. Type IV bursts correlate well with various phenomena: geomagnetic storms with sudden onset, appearance of solar cosmic rays, and polar blackouts. The probability of appearance of a magnetic storm increases if a type IV burst follows a type II burst. The time of onset of polar blackouts is determined by the geometry of the magnetic fields in the solar atmosphere and in interplanetary space, and, under favorable conditions, begins about

40 min after a type IV burst. At times they may begin simultaneously with the magnetic storm, i.e., within 1 or 2 days.

*Type V bursts* consist of broad, continuous radiation in the meter waveband. The frequency band ranges from tens to hundreds of MHz. They are observed only at frequencies less than 150 MHz ( $\lambda \geq 2m$ ), with the maximum intensity usually  $\lambda \geq 3 m$ . The lifetime of a burst is about 0.5–3.0 min with no observed frequency drift. The velocity of motion of the source is about  $3 \cdot 10^3$  km/s. Type V bursts differ from type IV in their close relationship with type III bursts, are about two orders lower in intensity, and consist of directed radiation. They follow type III bursts, excited by streams of fast particles (apparently electrons) moving at about  $10^5$  km/s. Possibly these particles serve as the source of type V bursts, when they reach the higher layers of the corona, by synchrotron radiation of the electrons captured between points of reflection of an arc-shaped magnetic field. A close correlation has been found between type III and V events, centimeter bursts and flares.

*Microwave radiation*, continuous-type radiation primarily in the centimeter waveband, is more varied and has been less studied than the radiation in the meter waveband. It is divided into three types as a function of the form, duration, and dimensions of the area of generation:

Type A—rise and fall rapid, lifetime, 1–5 min, generation area, small (diam 1–1.6 min), polarized;

Type B—fast rise and slow fall, lifetime—several min to several h, generation area, large (greater than 2.5–3.0 min);

Type C—rise and fall gradual, lifetime about 30 min to several h, generation area, small (0.8 min).

These three types may exist individually or be superimposed on one another. The most powerful bursts are of type A or B and are accompanied by a decimeter continuum.

The sources of emission are localized in three regions of the disk of the Sun, from which the slowly changing component originates. The radiation may be nonthermal for strong bursts

and thermal for weaker bursts. The assumed mechanisms of generation are: type A—magnetic bremsstrahlung of energetic electrons appearing in a flare in the local magnetic fields of a center of activity; types B and C—the combined action of magnetic bremsstrahlung and bremsstrahlung mechanisms in the corona over a portion of centers of activity.

Powerful microwave bursts are closely related to flares, and the x-radiation of the Sun, which in turn are related to geophysical phenomena observed practically simultaneously with events on the Sun (sudden ionospheric disturbances, and polar blackouts). The polar blackouts are more closely correlated with microwave bursts than with type IV bursts; they practically always follow a microwave burst.

A direct dependence has been established between the flux of protons recorded after a flare and the intensity of microwave bursts in the range of  $\lambda = 3-10$  cm; however, this dependence is at times masked by the propagation conditions of protons in interplanetary space.

An overall picture of sporadic radio emission can be represented approximately as: the centers of activity (flocculi, groups of spots) stimulate the formation of areas of increased plasma density in the lower corona, serving as sources of the slowly changing (S) components, detected primarily in the centimeter waveband. In the higher layers of the corona, to which the strong magnetic fields of the spots penetrate, noise storms with gradual onset and type I bursts are generated in the meter waveband. During flares, noise storms arise near active groups of spots that have rapid onset, reinforcing existing sources of noise storms. Streams of charged particles apparently are accelerated, generating type III bursts, which drift rapidly in frequency as they move through the less dense layers of the corona at about  $10^5$  km/s. Type III bursts are accompanied by x-ray and microwave bursts in the centimeter band.

A large flare is accompanied by an intensive microwave burst, the spectrum of which extends into the decimeter waveband; a type III burst appears simultaneously in the meter waveband. Radio emission then continues as type II bursts, drifting slowly in frequency over the meter waveband, apparently created by shock waves

in plasma with magnetic fields "frozen in," spread from the area of the flare into the corona at about  $10^3$  km/s. An intensive type IV continuum is immediately emitted by the area of the bundle of charged particles moving in the corona. The appearance of the two types of radiation, either one of them or neither, depends on the intensity of the field in the bundle and its velocity. Figure 6 shows an idealized dynamic spectrum of the sporadic radio emission. The radio emission of the Sun has been described [41, 46, 110, 120, 148].

### Corpuscular Radiation of the Sun

The corpuscular radiation of the Sun can be divided into constant, continuous emission of particles—the solar wind—and sporadic expulsion of intensive streams of plasma and charged particles—the corpuscular streams and solar cosmic rays. This division is arbitrary, reflecting the time-dependence of these types of radiation, emphasizing the constant existence

of the solar wind, variations in its velocity and density never falling below minimum values, of 250 km/s and 0.5 particles/cm<sup>3</sup>, respectively, at the level of the Earth's orbit. The stronger streams of solar plasma observed sporadically, i.e., the reinforced streams of the solar wind, are generally considered separately as solar corpuscular streams. This concept was introduced to science before the discovery of the solar wind, to explain various geophysical phenomena which correlated with certain phenomena on the Sun. The solar corpuscular streams reach velocities of about 1600 km/s at particle densities up to 100 cm<sup>-3</sup>. After their formation, these intense streams move through the quiet, slow portions of the solar wind, disrupt the stable structure of interplanetary space, and cause various disturbances (described below). The solar wind and corpuscular streams are the most important components of solar corpuscular radiation, and determine conditions in interplanetary space. The solar wind, solar corpuscular streams, and solar cosmic rays

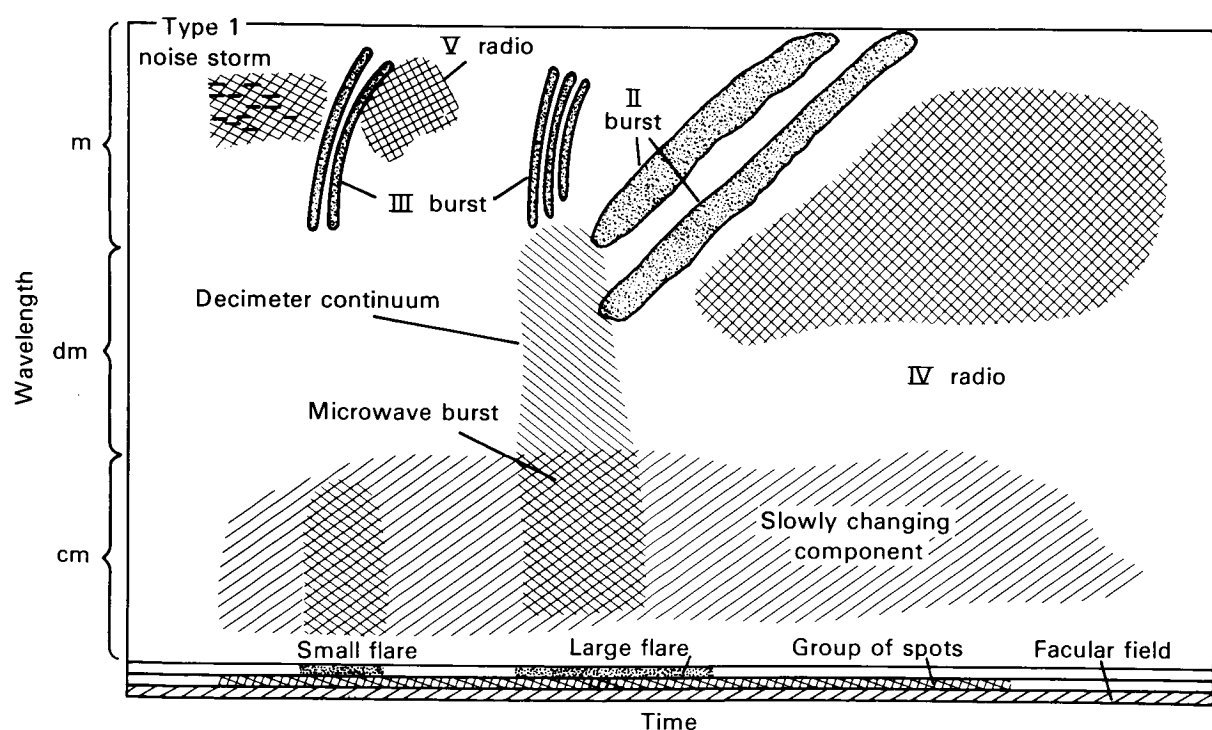


FIGURE 6.—Idealized dynamic spectrum of sporadic radio radiation from a center of activity.

will be described in detail in a subsequent section, THE INTERPLANETARY MEDIUM.

Solar corpuscular radiation causes the Sun to lose an average of a million tons of matter per second, which corresponds to  $10^{-22}$  solar masses per second, assuming spherical symmetry of the solar wind. The basis for this assumption is experimental data produced by Biermann [17], who observed type I comet tails. However, other published data indicate that the solar wind is not spherically symmetrical [123].

Another type of corpuscular radiation, solar cosmic rays, consists of high-energy charged particles (from 30–50 keV/nucleus to several GeV/nucleus). Recent studies indicate that every bright chromospheric flare on the Sun probably generates solar cosmic rays.

Solar cosmic rays are apt tools for the study of interplanetary space; they illuminate the solar system and allow determination of various of its characteristics. After large solar flares, great fluxes of solar cosmic rays sometimes represent a serious radiation danger for space flight.

## THE INTERPLANETARY MEDIUM

Properties of the interplanetary medium must be considered during flights in space. The most important are the characteristics of interplanetary plasma (solar wind), magnetic field, galactic and solar cosmic rays, and micrometeorite material. Another component of the interplanetary medium is the electromagnetic radiation of the Sun, stars, and galaxy, which will be briefly analyzed.

### The Solar Wind and the Interplanetary Magnetic Field

The general concept of the existence of solar corpuscular streams (the solar wind) was based on many geomagnetic observations, studies of gaseous tails of comets deflected from the radial direction away from the Sun, and variations in galactic cosmic rays [17, 18]. Comets have been observed in various parts of the sky, indicating that corpuscular streams fill all of interplanetary space. The theoretical basis for streams of solar plasma was adduced by Parker [105, 107], who showed that the solar corona can provide the

constant presence, in interplanetary space, of streams of solar plasma moving away from the Sun at supersonic speeds. The main reason for the expansion of the corona is its high temperature (about  $10^6$  °K).

The first direct observations of the solar wind were made by the Soviet lunar spacecraft Luna 2 and 3 and Venera 1 interplanetary space station [60, 64]. According to these data, the flux of the solar wind was about  $10^8 \text{ cm}^{-2} \text{ s}^{-1}$ , a result which was confirmed [21]. The solar wind arrives from the Sun at a velocity of about 300 km/s [21]. Numerous studies of the parameters of the solar wind have produced an extensive literature [123].

The coronal plasma distorts the lines of force of the solar magnetic field during its supersonic expansion. The conductivity of the plasma is very high; the magnetic field frozen in the plasma is carried away by the solar wind, forming the interplanetary magnetic field. The dynamic state of the solar wind can be arbitrarily divided into quiet and perturbed, according to modern concepts.

### *The Quiet Solar Wind*

This term, the quiet solar wind, relates to the average dynamic and kinetic characteristics of the stable flux of solar plasma, without the influence of individual active processes on the Sun. The time picture of density, velocity, and temperature of the solar wind, as well as the magnetic field for various periods of solar activity, have been studied [123]. Table 5 presents the mean macroscopic parameters of the solar plasma under quiet conditions and with strong perturbations at a distance of 1 AU from the Sun.

The chemical composition is an important characteristic of the solar wind. The solar corona chemical composition determined by spectroscopic measurements, includes protons (90%), helium nuclei (~ 9%) and heavier ions ( $^{16}\text{O}$ ,  $^{14}\text{N}$ ,  $^{56}\text{Fe}$ ) in quantities of less than 1%. Observations of the chemical composition of the interplanetary plasma are quite preliminary. Measurement of charge composition, using electrostatic analysis and selection of velocities, shows that protons and helium nuclei are recorded with good resolution (Fig. 7 [11]). The mean ratio of helium to hydrogen for 1962–1967 was about 4.5%,

fluctuating between 1.5% and 5%. The ions of oxygen, nitrogen, and carbon, i.e., elements with identical mass-to-charge ratio, cannot be differentiated by this method. In a very quiet, unperturbed solar wind with low temperature (less than  $10^4$  °K), individual peaks of  ${}^3\text{He}$  can be resolved, as well as singly or doubly ionized atoms of nitrogen, oxygen, and carbon. Stronger perturbations, such as shock waves from chromospheric flares, frequently increase the content

of helium in the interplanetary medium, at times raising it to 20%.

### Interplanetary Magnetic Fields

Measurements of the interplanetary magnetic fields have led to determination of the mean unperturbed picture of the magnetic field in space and its distortions during various types of solar activity [28, 29, 97, 99, 101].

TABLE 5.—Mean Macroscopic Parameters of the Solar Plasma

Parameters of solar wind and magnetic field	Quiet conditions at 1 AU	With strong perturbations at 1 AU	Dependence on distance from Sun
Velocity, solar wind, km/s	320–400	to 1600	weak
Density, solar wind, cm <sup>-3</sup>	8–10	to 100	$\sim r^{-2}$
Mean temperature, ions, °K	$10^4$	to $5 \cdot 10^4$	weak
Mean temperature electrons, °K	$10^5$	to $5 \cdot 10^5$	weak
Magnetic field intensity, gammas	5	to 50	$H_r \sim r^{-2}$ $H_\phi \sim r^{-1}$

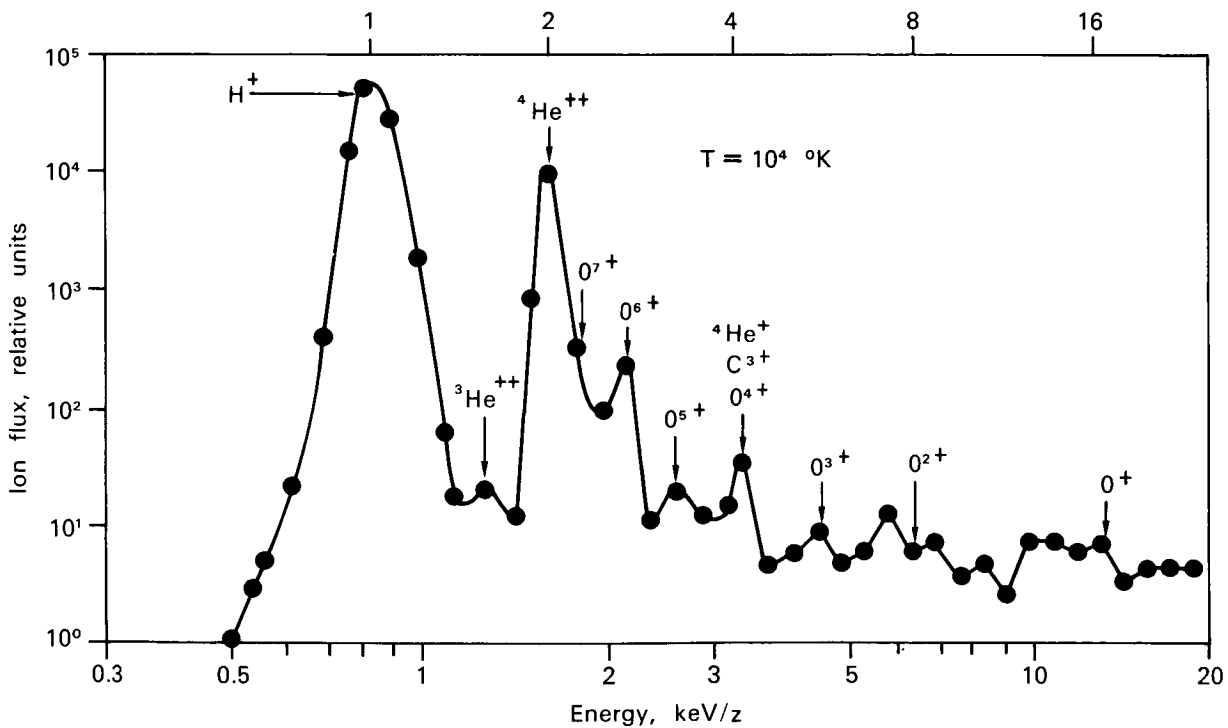


FIGURE 7.—Charge composition of the solar wind, determined October 8, 1965, by the Vela-2A satellite. Arrows indicate peaks of ions of each type. Oxygen, helium, and carbon ions with identical mass to charge ratio are not separated.

The coronal plasma, during supersonic expansion extends the lines of force of the solar magnetic field due to its high conductivity. At the orbit of the Earth, the energy density of the interplanetary field is much less (about 1%) than the kinetic energy density of the solar wind. The geometry of the unperturbed interplanetary magnetic field is reminiscent of an Archimedes spiral. Radio fading and radio transmission studies have shown that at 15–20 Sun radii, the magnetic field has an energy density much less than the kinetic energy density of the plasma, and its direction is almost radial, i.e., even at these distances the interplanetary field is determined by the dynamics of the solar plasma flow.

The radial and tangential magnetic field components  $H_r$  and  $H_\phi$  are defined from the condition of conservation of magnetic flux considering the rotation of the Sun:

$$H_r = H_{r_0} \left( \frac{r_0}{r} \right)^2 \quad (1)$$

$$H_\phi = H_{r_0} \frac{r_0 \Omega}{u_r} \left( \frac{r_0}{r} \right) \sin \theta \quad (2)$$

$r_0$  is the minimum distance, at which the velocity of the plasma is supersonic;  $u_r$  is the supersonic radial velocity of the wind;  $\Omega$  is the angular speed of rotation of the Sun;  $\theta$  is the angle between the line of force and the radial direction.

The angle between a line of force and the radial direction at the orbit of the Earth,  $\theta = \arctan r\Omega/u_r$ . For  $r=1$  AU and  $u_r=400$  km/s, angle  $\theta=47^\circ$  ( $\Omega=2.9 \cdot 10^{-6}$  rad/s). At distances of less than 1 AU, the field is primarily radial; at the orbit of Jupiter, the field is basically tangential.

*Sectorial structure.* During low solar activity, a sectorial structure to the interplanetary field (Fig. 8) is formed by elongated areas in which the interplanetary field is regular either from the Sun or to the Sun. These sectors, with an appearance related to the large active local magnetic areas in the photosphere, where there are large areas of directed field, rotate at a rate determined by the rotation rate of the Sun around its axis. The sectors differ in size, averaging  $100^\circ$  in the plane of the ecliptic, and correspond to a 6- to

7-d time of passage of one sector near the Earth. Recent measurements have shown the sectorial structure to be defined by the number of areas on the Sun's surface in which the magnetic field is of the same sign; the number of sectors may change. The sectorial structure is only a large-scale picture of the interplanetary field. Variations in velocity of the solar wind tend to wash out the precise boundaries of a sector.

The data of IMP-1 (December 1963–February 1964), indicate a certain structure within the limits of each sector (Fig. 9 [97]). The plasma density is maximal near the leading (western) boundary, and inversely correlates with velocity, so that generally, the flux of the solar plasma is conserved. The magnetic field reaches its maximum during the second day, but does not totally vanish even at the boundaries. Since these observations are true for the orbit of the Earth, the measured parameters may differ significantly from corresponding parameters near the Sun. Figure 10 shows a model of the development of a sectorial boundary based on the pictures of the lines of force in the corona [115]. At the boundary of a bipolar area, the magnetic field prevents acceleration of the plasma. As distance from the

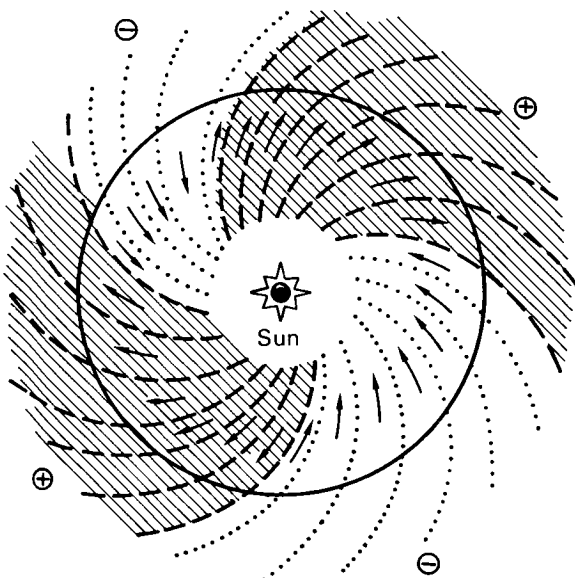


FIGURE 8.—Schematic of sectorial structure of the interplanetary magnetic field during periods of low solar activity.

boundary increases, the field can no longer hold the plasma. Since the dimensions of bipolar areas represent a small fraction of the total area of the solar disk, the magnetic fields probably can only form streams with different acceleration in the overall quasi-radial flow of the solar wind. In regard to the distribution of the flux parameters within a sector, the density maximum near the sector boundary might be created when a rapid stream (about 500 km/s) catches up with a slower stream (about 300 km/s).

At distances  $> 5$  AU, the sectorial formations and interaction of streams with different velocities apparently form large-scale magnetic heterogeneities with dimensions of 1 AU and greater.

Information on the dynamics of these fluctuations in the field can be produced by analyzing long-period variations (such as the 11-year variations) in galactic cosmic rays in the energy area  $E_p \approx 10^9$  eV. Measurements of spectral density of the fluctuations in the magnetic field at distances of  $\leq 2$  AU show a very low-frequency branch of the spectrum ( $f \approx 10^{-6}$  s $^{-1}$ ), which may indicate the presence of large-scale field variations ( $L > 1$  AU).

### *Perturbations in the Solar Wind*

In this case, unstable behavior of the interplanetary plasma is observed; various types of

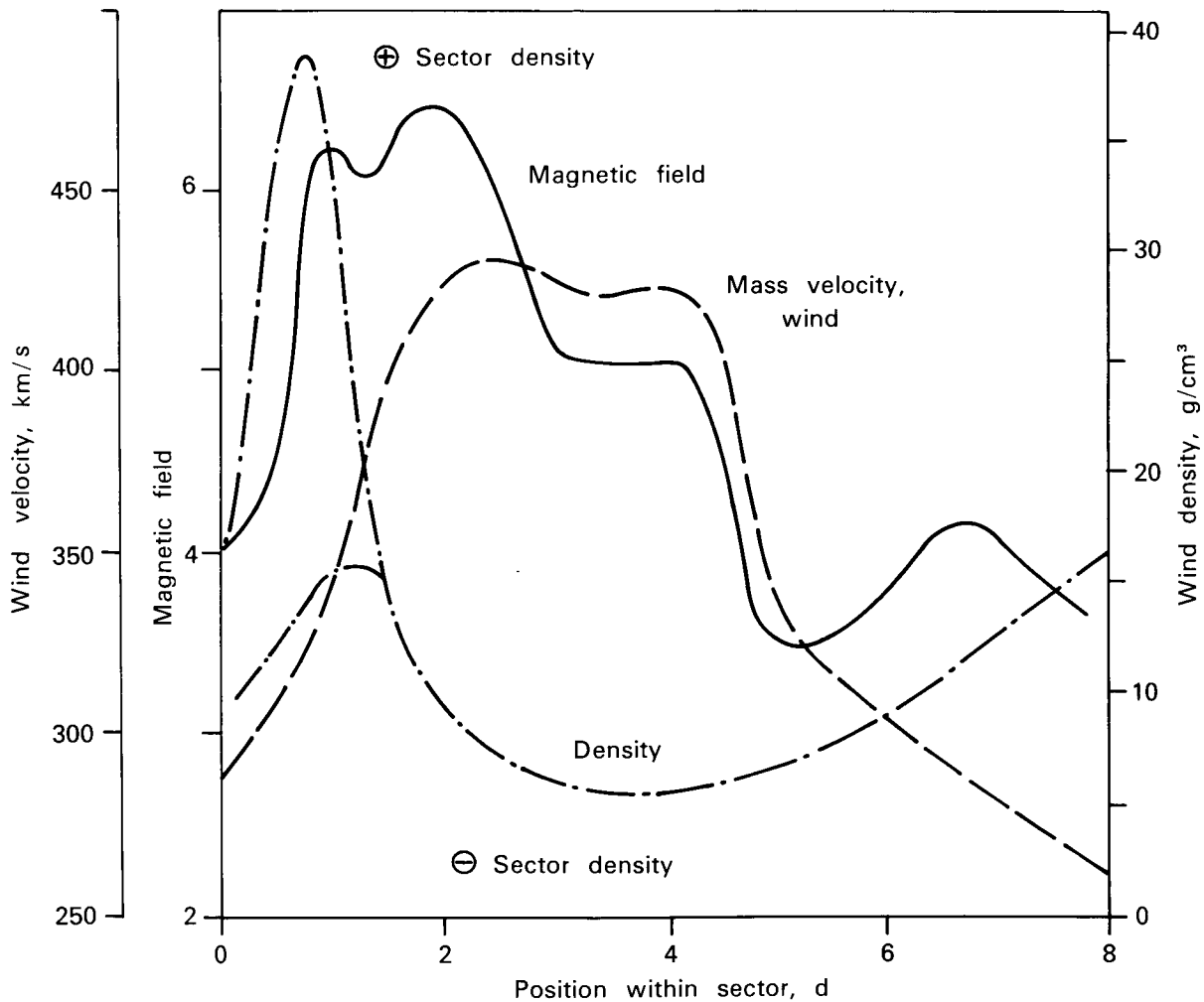


FIGURE 9.—Mean values of interplanetary magnetic field intensity, density and velocity of solar wind produced by the method of superimposition of eras.

magnetohydrodynamic perturbations such as hydromagnetic waves, nonspherical rapid jet flows, fast streams of plasma from chromospheric flares, and so forth, propagate with the supersonic stream from the wind. In these cases, the rapid development of solar activity such as chromospheric flares, the actions of individual active areas, and jet flows in the corona is predominant.

Such concepts as the corpuscular flow no doubt relate to the perturbed solar wind. The term "corpuscular flow" arose before discovery of the solar wind and has come to mean a strong flow of plasma, moving in the solar wind after bursts or as a recurrent phenomenon.

The section of reinforced solar wind or corpuscular flow is distinguished by the slightly greater velocity or density of the plasma and the increased magnetic field. An increase in the velocity and density of the plasma leads to reinforcement of the effects of the solar wind on the magnetosphere of the Earth, whereas the strengthened magnetic field slightly decreases and modulates the flux of galactic cosmic rays in those areas in space experiencing corpuscular flows. The clearest manifestation of unstable perturbations in the solar wind are shock waves, which will be described in more detail.

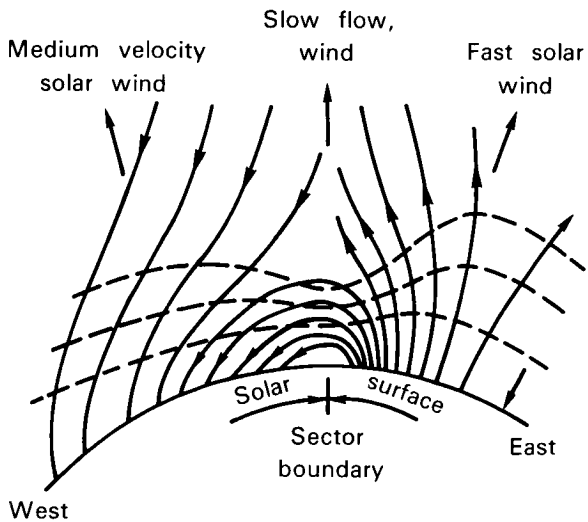


FIGURE 10.—Possible conditions for development of sectorial structure of interplanetary field in the corona. Dashed lines show isothermal surfaces. Solid curves with arrows show lines of force of the coronal magnetic field.

### *Shock Waves in Interplanetary Space*

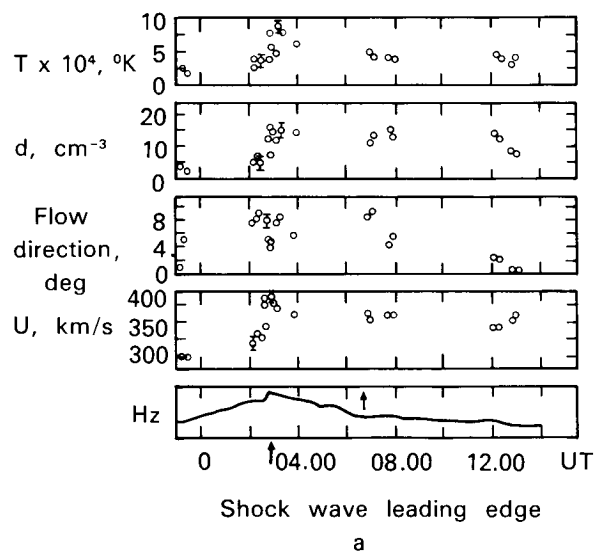
The stable state of the supersonic flow of the solar wind is disrupted during strong eruptions of the coronal plasma, which result from chromospheric flares on the Sun. Sharp expansion of the plasma in a flare region leads to formation of shock waves, usually having velocities of 1000 km/s, indicated by the type II radio radiation observed. The shock waves in interplanetary space propagate through the stable solar wind. Shock waves at distances of 0.7–1.5 AU from the Sun are now firmly established; they have sudden changes in macroscopic and kinetic parameters of the plasma, energetic particles, and deep modulation of the galactic cosmic rays, called Forbush effects.

The shock wave is characterized by the movement of matter through the discontinuity (wave front); the pressure is discontinuous, while all the laws of conservation of mass, momentum, and energy are observed. The density, velocity, and temperature behind the leading edge of the wave are greater than before the leading edge in the unperturbed area of the plasma. Analyses of the plasma parameters and measurement of low-energy solar protons penetrating the interplanetary magnetic field over the past 11-year cycle have shown that near 1 AU, the interplanetary shock waves can be characterized by values of relative velocity  $U_{\text{wave}} - U_{\text{wind}}$  of 50 to 200–300 km/s, and by doubling of the density, temperature, and the magnetic field intensity of the plasma across the wave front (see Fig. 11-a, b) [70]. There are discussions in the literature of two physical concepts of shock waves.

One concept, based on the possibility of unambiguous identification of cosmic phenomena (plasmas, fields, and increasing intensity of cosmic rays of solar origin) with events on the Sun (flares), assumes that a flare generates a strong shock wave (velocity 1000–3000 km/s in the corona) which, as it propagates, undergoes significant deceleration, so that at the Earth's orbit, waves of weak or moderate intensity are measured (with Mach No. 2–3). The area of space containing the shock wave is a trap for solar protons with energies of  $\leq 30$  MeV, which are recorded simultaneously with arrival of the shock

wave. Processing of experimental observations based on these assumptions shows that the velocity of the shock wave decreases very rapidly ( $\approx r^{-3}$ ), which means that some strong dissipative mechanism must be present. In this case, it is assumed that the shock waves are spherically symmetrical and propagate radially from the Sun.

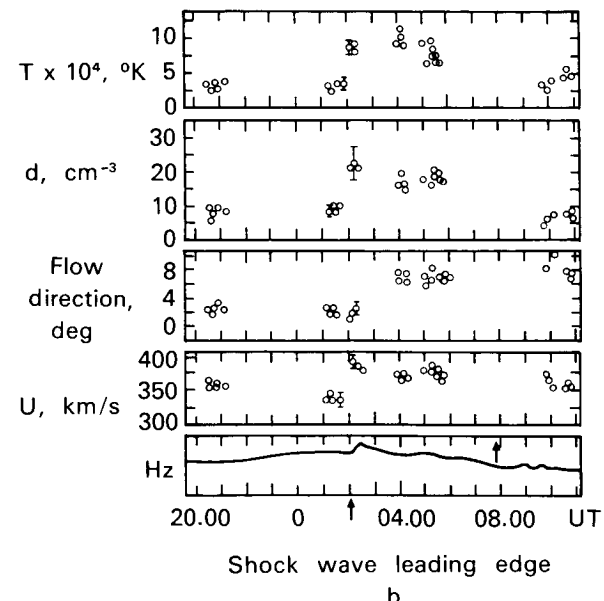
The other concept [71] assumes that shock waves in interplanetary space usually have moderate intensity, do not decelerate significantly during propagation from the Sun to the Earth's orbit and cannot be identified precisely with events on the Sun. In other words, the shock waves observed near 1 AU may be generated either on the Sun (perhaps by several weak flares) or in interplanetary space at distances of  $20\text{--}100 R_\odot$ , as a result of the action of plasma fluxes ejected from the corona. This concept is based partially on experimental estimates of the energy of flares from optical observations, measurements of radio and x-ray radiation, which determine the total energy of grade 2B-4B flares as around  $2 \cdot 10^{31}\text{--}5 \cdot 10^{32}$  erg, and partially on results of gas dynamic studies of various flow modes of unstable gas streams in a medium, the density of which decreases as  $r^{-2}$ .



a

Many researchers have found that solar flares only indicate active regions on the Sun, some of which are responsible for geomagnetic activity. Geomagnetic perturbations should not always be related to shock waves propagating through the solar wind; frequently, they result from passage of a sectorial boundary contact surface in the interplanetary magnetic field.

Contemporary experimental and theoretical ideas on plasma phenomena in the interplanetary medium do not allow preference for either concept. Physical interpretations have not yet gone beyond the level of working hypotheses, but a number of important qualitative conclusions may be drawn and quantitative estimates made. The conditions of propagation of collision-free shock waves in interplanetary space are largely determined by the dynamics of the coronal plasma during a flare and status of the solar wind plasma before a flare. Optical observations and measurements of x-ray and radio radiation from the Sun indicate that the nature of a flare plasma flow may vary quite widely, and result in a highly complex process of shock wave generation in



b

FIGURE 11.—Changes in temperature, density, direction, and velocity of solar wind protons: (a) for October 4–5, 1965, according to measurements of Vela-3B satellite; (b) for January 19–20, 1966, according to observations of Vela-3A satellite. Bottom graphs show sudden change in horizontal component of terrestrial magnetic field  $H_z$ , indicating sudden onset of magnetic storm. Direction  $0^\circ$  corresponds to radial flow from the Sun. Typical measurement errors are indicated.

the solar wind. Combined study of perturbations in the interplanetary medium following powerful flares (about 3B) permits sketching the dynamics of plasma flow at the Earth's orbit in many cases.

The event of February 15, 1967, was related to a grade 4B flare with coordinates  $20^{\circ}$  N,  $10^{\circ}$  W, which occurred on February 13. On February 15, the Earth satellites Vela 3A and Explorer 33 simultaneously recorded the first jump in plasma parameters and field intensity, which was interpreted as arrival of the leading edge of the shock wave (see Fig. 12). The geometric position of the satellites and the simultaneity of recording the shock wave showed that the direction of propagation of the leading edge of the wave (normal to the leading edge) made an angle of about  $60^{\circ}$  with the plane of the ecliptic. Measurements of the interplanetary field and recording the sudden beginning of the geomagnetic perturbation (SC) by surface geomagnetic stations permitted measurement of the mean direction of the normal to the leading edge of the shock wave. This also indicated an angle of about

$50^{\circ}$ – $70^{\circ}$ , forcing the assumption that the plasma flow following the flare was not spherical.

Measurements of the velocity, density, and magnetic field on February 15 and 16 (see Fig. 12) showed that the shock wave was pushed by the expanding coronal plasma. The "pusher" or, as it is more commonly called in gas dynamics, the "piston," was recorded about 9 h after passage of the leading edge of the wave and was saturated with helium. The plasma analyzers of Vela 3A showed a fivefold increase in content of  $\alpha$ -particles [70]. Measurements of the structure of the interplanetary field by Explorer 33 showed that between the leading edge of the shock wave and the leading edge of the helium layer there was a tangential discontinuity. These important experimental facts have been noted by other researchers, who found that the shock wave is frequently accompanied by several tangential discontinuities and a three- to fivefold change in the relative content of helium to hydrogen. This increase in the content of helium in the interplanetary plasma has been observed repeatedly, but no single theoretical interpretation of it has been developed.

Based on analysis of parameters of solar proton plasma and fluxes during 1965–1970, data on shock waves in the interplanetary medium can be summarized:

flares on the Sun can be precisely identified with shock waves in interplanetary space in some cases;

shock waves generally propagate with Mach numbers 2–5, while the density, temperature, and magnetic field in the shock wave usually double in comparison with the unperturbed status of the interplanetary medium;

the shock wave is often pushed by a "piston" of dense plasma, rich in helium;

plasma flows in which the propagation of shock waves is not spherically symmetrical have been observed;

the plasma area between the leading edge of the shock wave and the leading edge of the helium piston generally contains one or more tangential discontinuities, and rotary discontinuities may develop;

aspherical shock waves are frequently

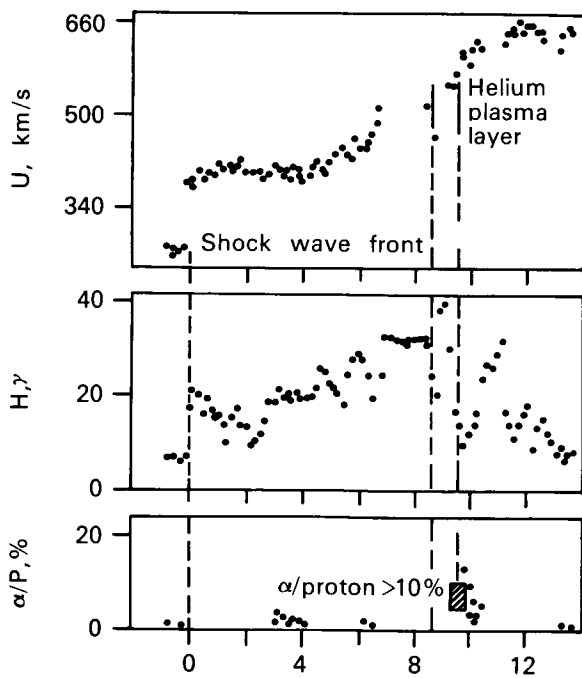


FIGURE 12.—Perturbations in the interplanetary medium following a chromospheric flare.  $U$ , velocity of solar wind;  $H$ , intensity of interplanetary magnetic field;  $\alpha/P$ , percent content of helium in the solar wind in relation to hydrogen.

interpreted as propagation of a spherical wave with a displaced center.

### Galactic Cosmic Rays

Galactic cosmic rays, the most energetic component of corpuscular flow in interplanetary space, consist of nuclei of chemical elements, primarily hydrogen, of very high energies. Galactic cosmic rays (except the neutrino) exceed all other types of radiation in penetrating capacity. The mean energy of the primary particles observed near the Earth is about  $10^{10}$  eV; the energy of some individual particles may reach  $10^{20}$  eV and higher. The energy spectrum of galactic protons at energies over  $10^4$  MeV can be represented as:

$$\frac{dN}{dE} = 2.14 \cdot 10^9 E^{-2.7} (\text{m}^{-2} \cdot \text{s}^{-1} \cdot \text{sr}^{-1} \cdot \text{MeV}^{-1}) \quad (3)$$

where  $E$  is expressed in MeV.

For lower energies, the flux of the particles depends on solar activity: at the maximum and minimum of solar activity, the total flux of galactic cosmic rays with energies  $E > 30$  MeV (nucleon is about  $2000 \text{ m}^{-2} \text{ s}^{-1} \text{ sr}^{-1}$  and  $6000 \text{ m}^{-2} \text{ s}^{-1} \text{ sr}^{-1}$  respectively).

The chemical composition of galactic cosmic rays in the high-energy area is sufficiently known (see Table 6). The flux of nuclei represented in Table 6 relates to particles with energies  $E > 2.5 \cdot 10^3$  MeV/nucleon.

The chemical composition of primary cosmic rays differs slightly from the composition of elements in the Earth's crust, meteorites, solar atmosphere, and atmosphere of certain stars,

TABLE 6.—Flux of Nuclei

Nuclei, groups	Symbol	Charge	Mean number, nucleons/nucleus	Flux of particles $\text{m}^{-2} \cdot \text{s}^{-1} \cdot \text{sr}^{-1}$	Percent total flux
Proton	P	9	1	1500	≈ 94
Helium nuclei	$\alpha$	2	4	90	5.5
Light	L	3-5	10	2	
Medium	M	6-9	14	5.6	
Heavy	H	10-19	30	1.9	0.6
Very heavy	VH	20-28	48	0.7	

which is known from spectroscopic analysis. Cosmic rays are characterized by relatively lower content of hydrogen and helium, and predominance of the heavier elements, particularly noticeable in the area of light nuclei (Li, Be, B group), where the difference reaches several orders of magnitude. This doubtless reflects the nature of the sources of cosmic rays, mechanism of their acceleration, and status of interstellar space, which the cosmic rays penetrate on their path to the Earth. It serves as a serious argument in favor of the theory of the origin of cosmic rays and their subsequent fragmentation upon collision with nuclei of interstellar material. In addition to the nuclei of the chemical elements, the galactic cosmic rays contain a slight flux of electrons and gamma quanta.

The energy spectra of various particles observed in interplanetary space at a distance of 1 AU from the Sun are shown in Figure 13. As distance from the Sun increases, the flux of

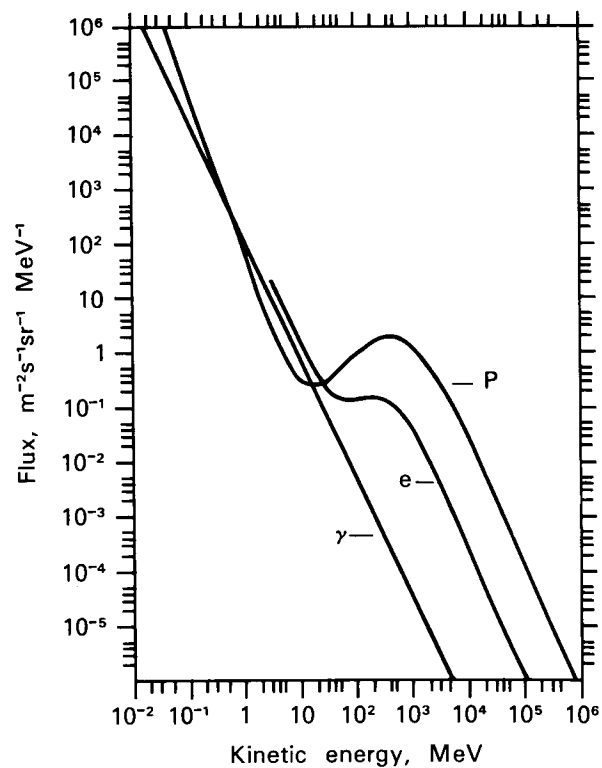


FIGURE 13.—Idealized spectrum of galactic protons, electrons, and  $\gamma$ -rays.

galactic cosmic rays can only increase, because the magnetic fields in the solar system, carried away from the Sun by the solar wind, prevent penetration of cosmic rays into the inner areas of the solar system. This same mechanism, the modulation mechanism, causes the difference in fluxes of particles in different phases of the solar activity cycle. Increased flux of cosmic rays cannot continue without limit. At some distance from the Sun, the solar wind density or interplanetary magnetic field intensity will no longer exceed the corresponding parameters of interstellar space and at these distances, modulation of galactic cosmic rays will cease. The area of modulation of galactic cosmic rays is estimated to be about 10–30 AU.

The differential energy spectra of charged particles have a minimum in the area of 30–60 MeV (Fig. 14). It is assumed at present that particles with energies less than 30–60 MeV are of solar origin, i.e., can be considered solar cosmic rays. Experimental and theoretical aspects of galactic cosmic rays have been widely studied [45, 55, 94, 117, 118, 141].

### Solar Cosmic Rays, Definition and Classification

The Sun is a source of corpuscular radiation over a broad range of energies. Solar cosmic rays form the high-energy portion of the Sun's corpuscular radiation. Fluxes of protons and

electrons observed in interplanetary space, with energies of tens of keV to several hundred MeV, and originating in various forms of solar activity will be discussed here.

The study of high-energy particles generated by the Sun began in 1942. Until early 1957, only five events were studied when high-energy particles reached the Earth. Since then, experiments performed at high altitudes using balloons, satellites, and rockets, and observations with rheometers, have shown that fluxes of solar protons with energies of 100–300 MeV appear in the area of the Earth approximately once a month during the time near the solar maximum. Since 1964, practically continuous (monitor) observations using Earth satellites and spacecraft have been made outside the terrestrial magnetosphere. During this time, the energy threshold of recording protons has been significantly reduced to a few hundred keV and the installation of low- and medium-energy electron detectors on spacecraft began. Experiments beginning in 1967 have shown that electrons with energies from 10 keV to several MeV and protons with energies of tens of keV to several hundred MeV are generated by the Sun during flares [134].

Fluxes of charged particles observed in interplanetary space at about 1 AU from the Sun can be divided arbitrarily, according to their relationship to various forms of solar activity, into these groups.

1. Increases in protons with energies up to several hundred MeV and high-energy electrons with energies up to 10 MeV, immediately follow large (class 1B and higher) solar flares. These show a rapid increase in the intensity of particles, and arrival of the particles from the Sun at the point of measurement according to their velocity, i.e., the more energetic particles appear before less energetic particles. At the maximum of large flares, the intensity of the proton flux with energy  $E_p > 1$  MeV reaches values of about  $10^5$  particles/cm<sup>2</sup> · s. The drop of these streams usually shows a characteristic exponential shape with a time constant  $\tau$  of about 10–30 h.

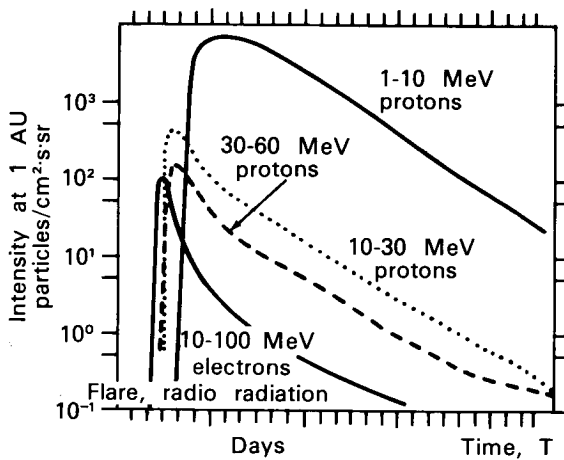


FIGURE 14.—Typical increase in flux of solar cosmic rays observed immediately after a major chromospheric flare.

2. An increase in low-energy electrons with energies of 10 to several hundred keV is generally observed following small flares. These increases differ from increases in group I and therefore are considered separately.
3. Long-lived streams of protons and electrons of low and moderate energies, apparently form after large flares and rotate with the Sun. These streams, when observed by spacecraft, have a relatively smooth rise and fall; the duration of recording these streams (characterizing their angular width in the plane of the ecliptic) is 6–30 h. Some streams, particularly during minimum solar activity, may exist for several solar revolutions, and are called recurrent streams.
4. Streams of protons and electrons are observed near the Earth simultaneously with shock waves from large solar flares. The passage of these particles has not yet been definitely established. It is possible that these particles move with the shock wave from the Sun in a trap, or are accelerated in the shock wave itself as it moves through interplanetary space or, if they exist for some time, are transferred by the shock wave with tubes of force lines to the point of observation. Since it has been assumed in some studies that these particles are accelerated behind the leading edge of the shock wave (causing a magnetic storm on the Earth), the electrons and protons in these streams, in earlier works, were frequently called “energetic storm particles.”
5. A minimal background flow of protons with energy  $E_p < 20$  MeV and, possibly, electrons with energy  $E_e < 3$  MeV, not directly related to flares, change slowly with changes in the overall level of solar activity.

*Properties of Solar Cosmic Ray Events  
During Large Flares*

Large flares characteristically occupy a vast area of the Sun's surface and are observed in the

H $\alpha$  line for long periods (about 2 h). These flares are accompanied by intensive x-ray and complex microwave bursts, frequently followed by type II and IV radio radiation.

During a solar flare, particles are ejected from the Sun, which, at a distance of 1 AU, is observed as a time change in the flux, with a rapid increase to its maximum value and a slow, exponential drop. The development of events in time for these situations is shown in Figure 14.

The maximum fluxes of particles, for example protons with energies  $> 1$  MeV, recorded in interplanetary space following large solar flares, reach  $10^5$  particles  $\cdot \text{cm}^{-2} \cdot \text{s}^{-1} \cdot \text{sr}^{-1}$ . These fluxes are observed rarely and only after the largest flares. The fluxes of protons usually observed are  $10^2$ – $10^3$  particles  $\cdot \text{cm}^{-2} \cdot \text{s}^{-1} \cdot \text{sr}^{-1}$ . The number of events recorded increases with decreasing intensity.

Electrons from flares with energies of 10 to several hundred keV were first observed, 1965–1966, in interplanetary space. Streams of electrons with energies of  $40 \text{ keV} \leq E_e \leq 300 \text{ keV}$ , recorded in mixed electron-proton events, act differently from protons and relativistic electrons. The properties of streams of low-energy electrons will be considered in detail separately; this section deals with the properties of streams of protons and electrons with energies at  $E > 1$  MeV.

In spite of the serious interest in solar cosmic rays, detailed study of the chemical composition has been performed with photographic plates launched on rockets for only four flares. The flare of November 12, 1960, was most thoroughly studied, during which several research rockets were launched and hardness spectra were produced for protons, helium nuclei, and nuclei with charge  $6 \leq Z \leq 9$ . The spectra are in Figures 15 and 16 [19]. Within limits of accuracy, all three groups of nuclei have identical dependence on hardness. The ratio of fluxes of helium nuclei and nuclei of group “M” ( $6 \leq Z \leq 9$ ) remained constant during measurement, whereas the relative flux of protons changes, which is evident from comparison of the scales of Figures 15 and 16.

During the flare of July 18, 1961, an upper limit of the ratio of fluxes of “L” nuclei ( $3 \leq Z \leq 5$ ) to “M” nuclei of 0.07 was produced. The relation-

ship between the flux of helium nuclei and that of group "M" nuclei remained the same as in the flare of November 12, 1960. The mean ratio of these fluxes for all measurements was  $62 \pm 7$ . Figure 17 shows the charge spectrum of solar cosmic rays [20]. The relationship of fluxes of nuclei of oxygen and carbon differs from this ratio in primary cosmic rays and agrees well with the composition of the photosphere of the Sun.

#### *Increases in Fluxes of Particles*

Near the Earth, an increase in intensity of solar cosmic rays is most frequently recorded following flares near longitudes of  $60^\circ$  W. These longitudes serve as the sole origin for the lines of force of the interplanetary magnetic field

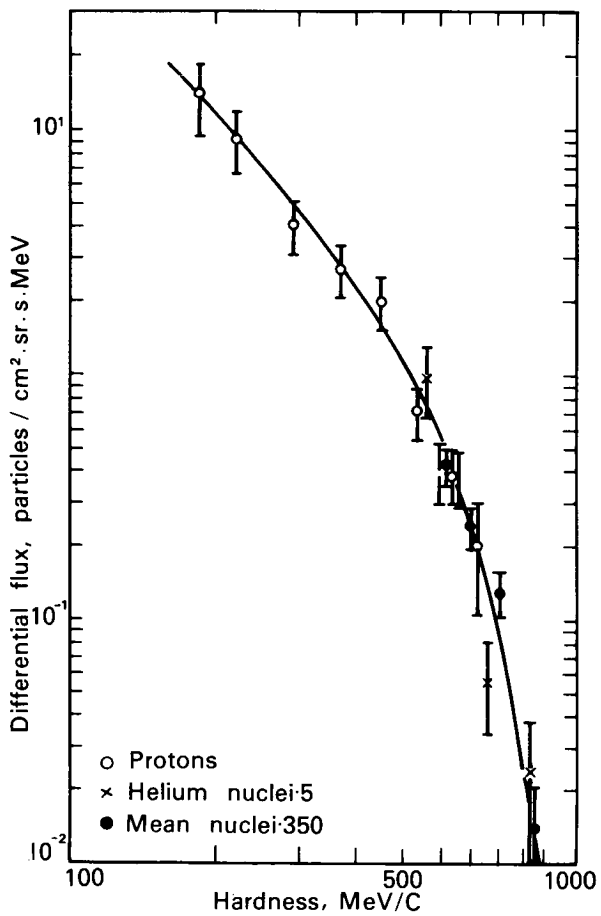


FIGURE 15.—Hardness spectrum of solar protons, helium nuclei, and nuclei with charge  $6 \leq Z \leq 9$ , measured during flare of November 12, 1960, at 18:40 UT [19].

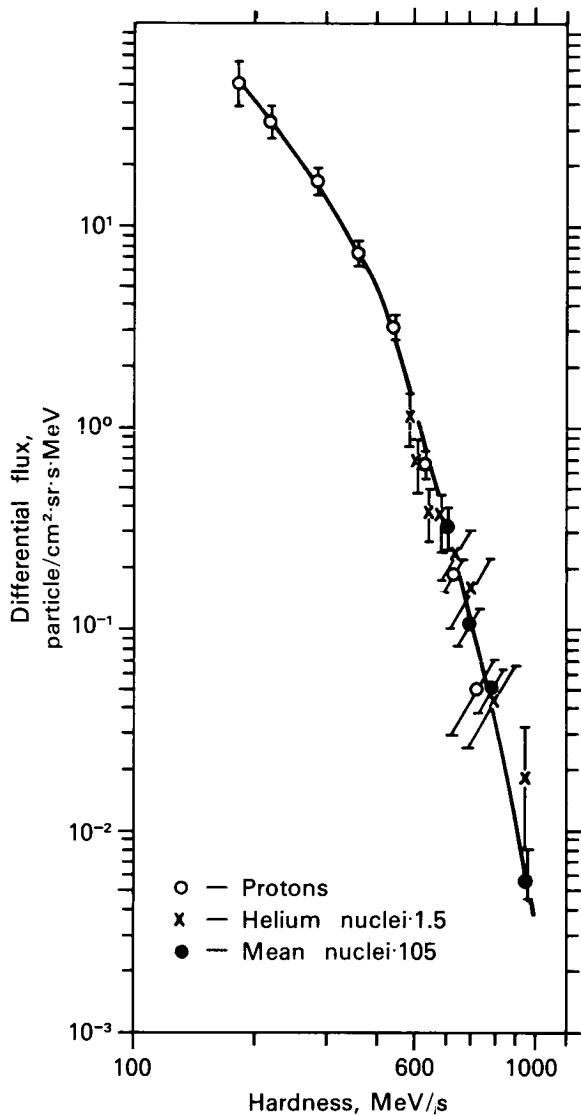


FIGURE 16.—Hardness spectrum of solar protons, helium nuclei, and nuclei with charge  $6 \leq Z \leq 9$ , measured after flare of October 12, 1960. Data relate to 16:03 UT, November 13 [19].

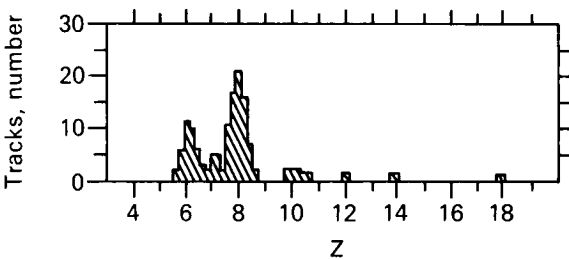


FIGURE 17.—Charge spectrum of solar cosmic rays for flare of November 12, 1960 [20].

passing by the Earth at the mean velocity of the solar wind  $u \approx 400 \text{ km} \cdot \text{s}$ . However, this does not mean that particles generated in flares outside of these longitudes are not recorded near the Earth. The increases caused by eastern and western flares, as well as flares at higher latitudes greater than  $15^{\circ}$ – $20^{\circ}$  are also observed near the Earth. The rise front in these events is usually less steep ( $t \approx 5$ – $10$  h) than for increases produced by flares at low latitudes of the Sun and at longitudes of  $50^{\circ}$ – $60^{\circ}$  W.

### *Solar Flares with Various Levels of Activity*

Solar particles in interplanetary space depend directly on the activity of the Sun. During years near the minimum solar activity, large flares are rare; likewise, generation of cosmic rays. Spacecraft flying during 1964–1965 often did not record a single event for months.

The statistics of proton ( $E_p > 15$  MeV) increases measured at the beginning of the 20th cycle of solar activity by the IMP series satellites are shown in Figure 18 [83]; the number increased sharply in 1966–1967. High-energy electrons appear more frequently in interplanetary space during years near the maximum of solar activity. For observations in near-Earth orbits, the time required to reach the maximum is usually a half to several hours following the beginning of a flare, indicating the mean distance traveled by

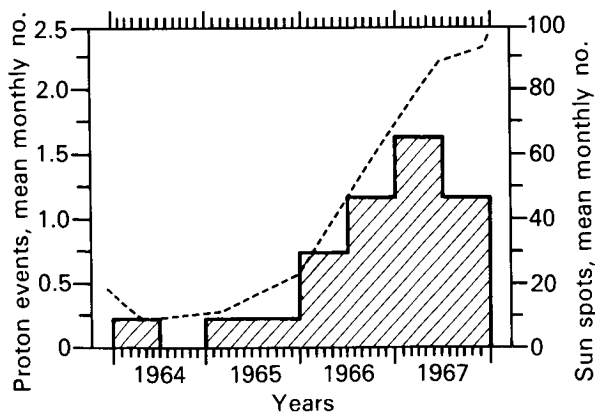


FIGURE 18.—Number of proton increases  $E_p > 15$  MeV recorded by IMP satellites as a function of mean number of sunspots. —— number of sunspots; —— proton events.

most particles is greater than 1 AU. This is particularly noticeable in a flare at the base of force lines of the interplanetary magnetic field not connected with the Earth, for example in the far western and eastern longitudes, or the far southern or northern latitudes.

Figure 19 shows the dependence of observed particle fluxes in various energy intervals on the path traveled by these particles for the flares of July 7, 1966 (a) [83], February 25, 1969 (b) [13], and September 28, 1961 (c) [141]. These figures show that the points for protons of various energies and relativistic electrons, within the limits of measurement error, fall on the same curve. This agreement indicates that protons and relativistic electrons travel the same path from the moment of acceleration to the moment of recording. The mean length of this path, determined on the basis of the maximum of the increase, is near 8–10 AU.

A curve for low-energy electrons is shown in Figure 20. These electrons arrive at the point of observation before the protons and relativistic electrons, which is characteristic for such mixed electron-proton events. The intensity of the fluxes of protons and electrons in impulse events decreases with time according to an exponential rule with  $\tau_0 \approx 0.5$ – $1.5$  d. This rule is well fulfilled for times of 5–6  $\tau$ .

### *Energy Spectra of Solar Particles*

Measurements of the energy spectra of solar cosmic rays performed in the stratosphere and by remote satellites have shown that the energy spectra of solar protons can be described by an exponential function of the form  $N(\geq E) = AE^{-\gamma}$  for a broad range of energies (from several MeV to several hundred MeV), where  $N(\geq E)$  is the number of particles with energies higher than  $E$ , while  $A$  and  $\gamma$  are constants for a specific flare. For various flares, the values of  $A$  change over several orders of magnitude; the exponent  $\gamma$  has a range of about 1–5, and is most frequently 3 or 4.

Detailed measurements of the energy spectra are rare, and have been performed by different methods and in different energy intervals. Several examples of energy spectra for various increases in solar cosmic rays are presented below. Figure

20a shows the differential spectrum of protons for the flare of February 25, 1969 [13]. This event has been carefully studied over a broad energy inter-

val. The spectrum presented was produced 14 h after the beginning of the event; its index over a broad energy interval is  $\gamma = 2.7$ .

Figure 20b [35] shows a spectrum of electrons for the same flare, which also follows the rule  $E^{-\gamma}$ , where  $\gamma \sim 3-4$  as shown in Figure 20b. The index of the integral spectrum of relativistic electrons for most events is  $\gamma \approx 4$ . Figure 21 [25] shows energy spectra of solar protons for the flares of September 28, 1961, and October 29, 1962, extrapolated in time to the moment of the flare, i.e., the energy spectra formed in the process of acceleration.

The spectra both of protons and of energetic

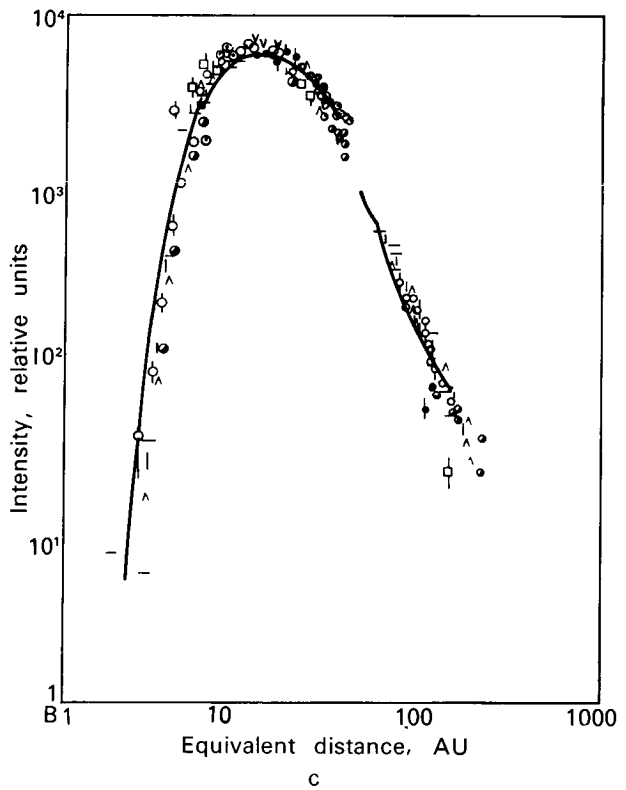
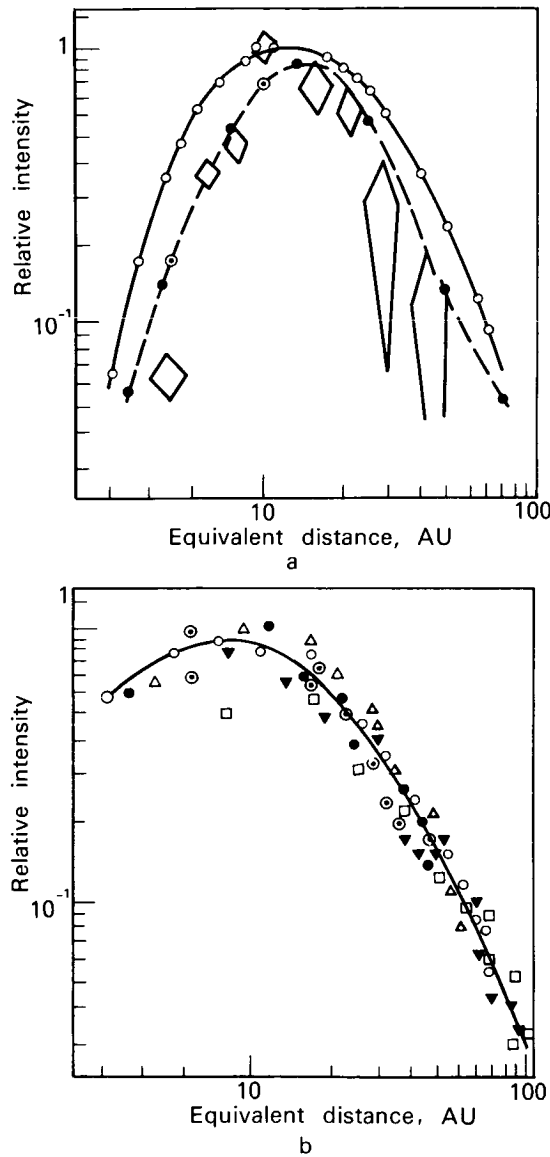


FIGURE 19.—Intensity of particle flux (normalized at maximum) as a function of path traveled by particles of various energies. Path defined as product of particle velocity by time elapsed between moment of injection and moment of recording.

- (a) for protons and electrons of various energies from flare of July 7, 1966 [83]: ○,  $\geq 45$  keV electrons, with  $\beta \approx 0.4$ ; ◇, 3+12 MeV electrons,  $\beta \approx 0.99$ ; ●, 19+45 MeV protons,  $\beta = 0.20 + 0.30$ ; ○, 16+38 MeV protons,  $\beta = 0.18 + 0.28$ ;
- (b) for protons of various energies in flare of February 25, 1969 [71]: ○, 30 MeV; ●, 45 MeV; △, 67 MeV; ○, 98 MeV; ▼, 160 MeV; □, 282 MeV;
- (c) for protons of various energies in flare of September 28, 1961 [140]: √, 2.2 MeV; ●, 3.8 MeV; ○, 5.7 MeV; ○, 7.9 MeV; ○, 14.5 MeV; ●, 87 MeV; |, 135 MeV; ▲, 175 MeV; △, 230 MeV; ○, 295 MeV.

electrons, measured some time (about 20–30 h) after the flare, apparently have the same form with  $\gamma \approx 3$ , regardless of the magnitude of the flare. When solar cosmic rays are observed simultaneously with the arrival of a shock wave, the energy spectra are greatly softened (Fig. 22 [34]).

*Anisotropy of streams.* Considerable experimental material has been accumulated on the angular distribution of streams of protons and of low-energy electrons. Measurements have not been made of the angular distributions of high energy electrons. If the angular distribution of particles is expressed as

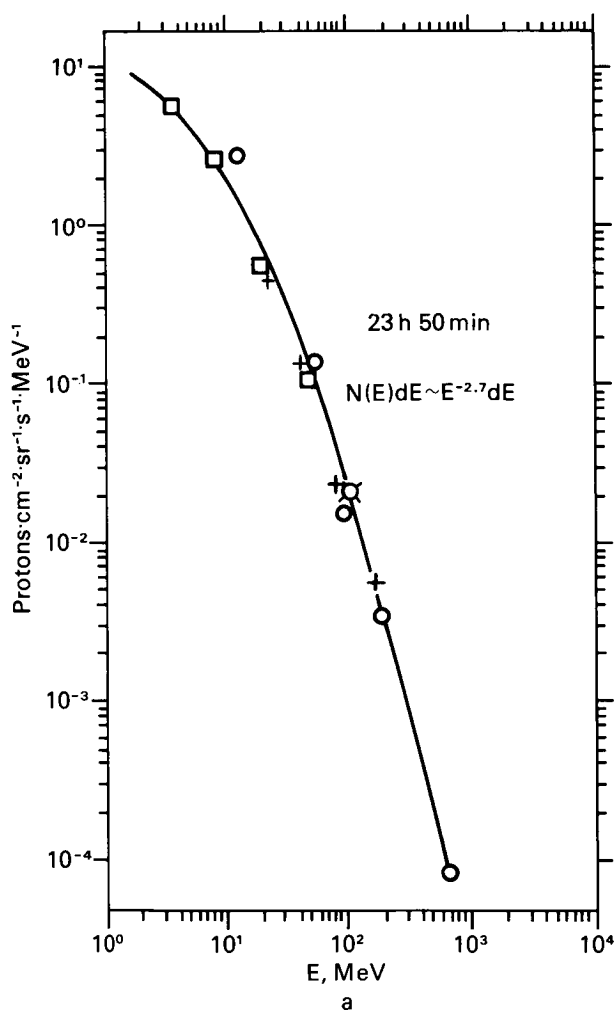


FIGURE 20.—Energy spectra of solar cosmic rays for flare of February 25, 1969.

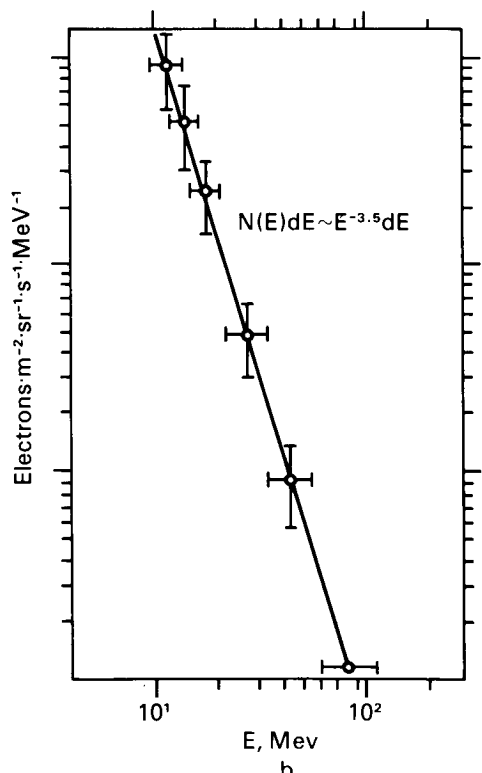
(a) according to [13]; (b) according to [35]

$$F(\theta) = a + b \sin (\theta + \phi), \quad (4)$$

then the quantity  $A = a/b$  defines the anisotropy of the stream, while angle  $\phi$  is the anisotropy direction. With more complex angular distribution, the stream may have more than one maximum, and there may be so-called bidirectional anisotropy. If the measurements are performed in two directions, for example, "toward the Sun" and "from the Sun," the anisotropy is

$$A = \frac{n_+ - n_-}{n_+ + n_-} \quad (5)$$

where  $n_+$  is the flux from the Sun;  $n_-$  is the flux toward the Sun. Simultaneous measurements of the flux of particles and the direction of the interplanetary magnetic field have shown that there is a strong correlation between the direction of the angular distribution maximum and the direction of the magnetic field at the point of observation (Fig. 23 [87]). Simultaneous measurements of the anisotropy of streams of protons and



low-energy electrons in mixed proton-electron events have shown that the directions of maximum arrival of protons and electrons coincide. Figure 24 shows an example of such correlation between streams of electrons and protons [104].

The amplitude of anisotropy for low-energy protons and for low-energy electrons in mixed proton-electron events reaches 70%–80%. For events related to eastern flares and far western flares, with a slower rise front ( $\tau \approx 10$  hours), the anisotropy is slightly less,  $A \approx 30\%-50\%$ . The amplitude of anisotropy decreases, after reaching the maximum of intensity, although the maximum of the flux remains directed toward the field.

The time course of intensity of tones with

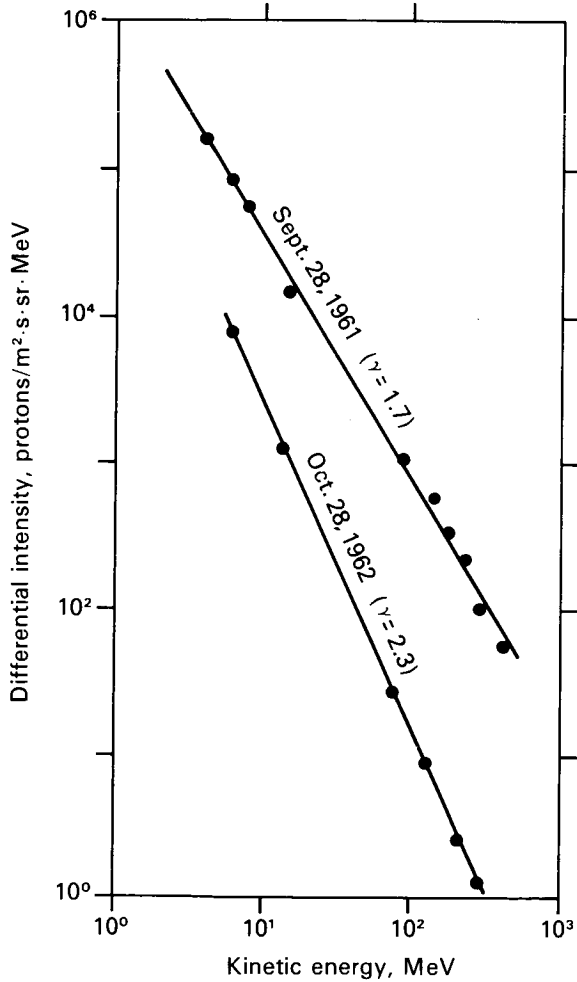


FIGURE 21.—Differential energy spectra of protons extrapolated to moment of flare [25].

$E = 7.5\text{--}45.0$  MeV is presented in Figure 25 [90] for the flare of November 18, 1968, which was near the western limb of the Sun  $18^\circ$  N,  $84^\circ$  W, at 10 h 30 min UT, and was accompanied by types II and IV radio bursts. Figure 26 [104] shows a vector diagram for changes in anisotropy of protons of  $0.7\text{--}7.6$  MeV in the time following a flare. During the initial period  $T < 2$  d, during the phases of increase and decrease, the anisotropy reaches 50% (western flare). The direction of the anisotropy is near the mean direction of the interplanetary magnetic field. The value of anisotropy is related to the energy of particles so that  $A$  is greater for particles with lower velocity.

During later stages of an event, for times  $1\text{--}2 < T < 4$  d, when the flux of particles is not great, there is also some anisotropy of protons, with a value directly proportional to the velocity of the solar wind,  $u$ , and inversely proportional to the velocity of the particles,  $v$ . This anisotropy, as shown below, is caused by transport of particles from the space near the Sun by the solar wind and is called "equilibrium" anisotropy, the area of which is directed radially from the Sun.

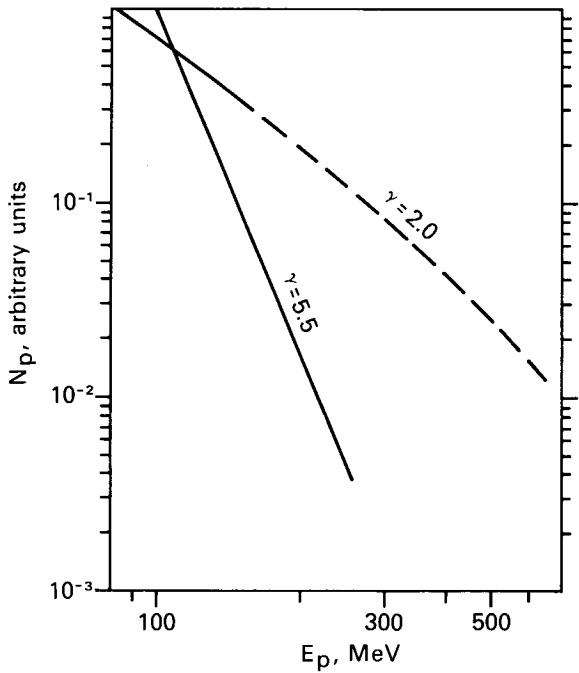


FIGURE 22.—Mean integral spectra of solar protons for energies over 100 MeV during magnetically quiet periods (dashed line) and during magnetic storms (solid line) [34].

In the last phase, decreasing flux of solar protons for  $T > 4$  d, the anisotropy becomes eastern making an angle of  $45^\circ$  from the Sun-spacecraft line with a value of anisotropy  $A \approx 5\text{--}10\%$ . Equilibrium anisotropy in this late period is also inversely proportional to the velocity of the particles.

### *Increases in Fluxes of Low-Energy Electrons*

Electrons with energies of 10–100 keV are the most common and most frequently encountered types of particle emitted by the Sun during mild and moderate flares. During the 20th solar cycle, from 1964 to mid-1970, about 230

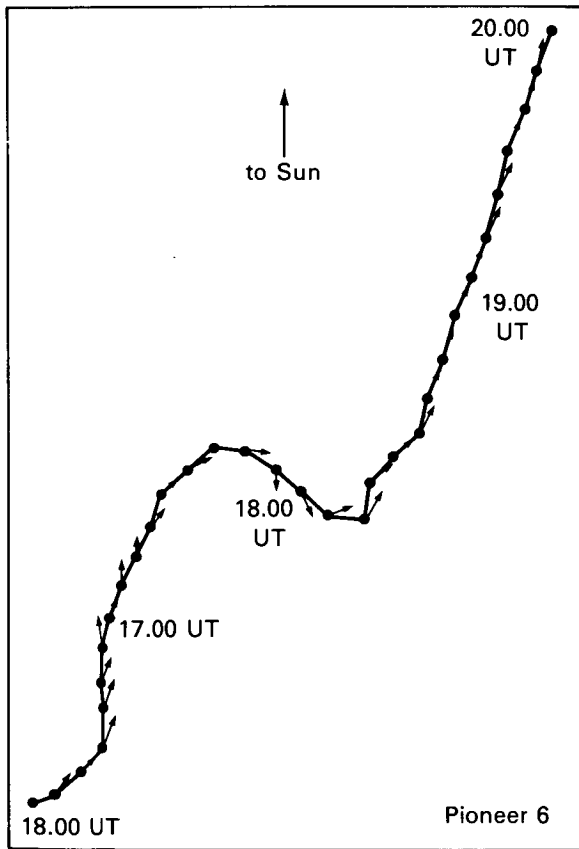


FIGURE 23.—Direction of interplanetary magnetic field in the plane of the ecliptic (azimuth) and anisotropy of cosmic rays during period 16:00–20:00 UT, December 30, 1965 [87].

- azimuth of field lines;
- direction of anisotropy of cosmic rays.

such events were recorded by spacecraft near the Earth. The properties of electrons emitted by small solar flares are:

1. Streams of electrons can almost always be correlated to an optical flare, which may have small areas, but are bright in the  $H_\alpha$  line.
2. The intensity of streams of electrons observed near the Earth after individual flares may reach about  $10^4$  particles  $\cdot cm^{-2} \cdot s^{-1} \cdot sr^{-1}$  for energies  $E_e > 40$  keV. In most cases, fluxes of  $10\text{--}1000$  particles  $cm^{-2} \cdot s^{-1} \cdot sr^{-1}$  were recorded at the maximum of each event [83]. The electrons are not usually accompanied by significant streams of protons. The energy spectra of solar electrons in interplanetary space in most cases can be represented in exponential form:

$$N(E) dE = K \cdot E^{-\gamma} dE \quad (6)$$

where  $\gamma \approx 3$  in the interval of energies of 20–45 keV; over 100–200 keV the spectrum falls very rapidly ( $\gamma \geq 5$ ). This means that particles with energies of over 200–300 keV are not present in these streams.

3. The delay of arrival of electrons to the

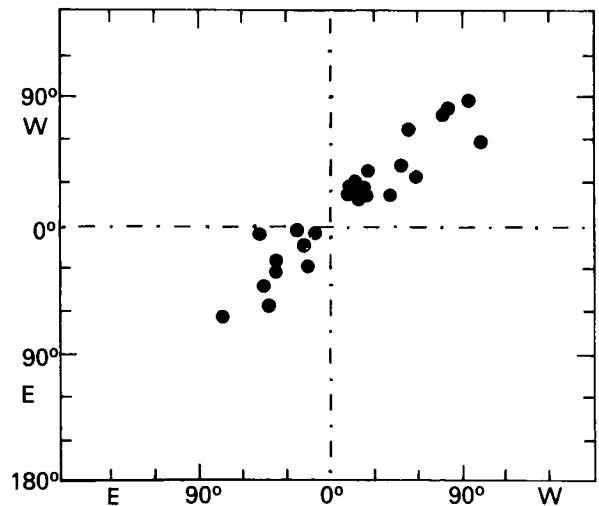


FIGURE 24.—Correlation between direction of arrival of streams of protons and electrons in mixed electron-proton events [104].

Earth in relationship to the burst of x-rays usually is 15–60 min. The rise time to the maximum is much briefer than the rise time of the flux of protons following large flares (usually 5–50 min). The drop in intensity has a dual nature. In some cases, an exponential decrease in intensity is noted from the maximum at  $\tau \approx 12$  h [83]. In other cases, there is a rapid drop with  $\tau$  on the order of the rise time, followed by a much slower drop in intensity as soon as it has reached 10% of its maximum value.

4. When the active area moves across the solar disk, electrons from this area reach the Earth only when the area falls within a certain interval of helio-longitudes. Statistical analysis of the electron increases leads to the conclusion that most of the electrons recorded at the Earth are produced by flares located  $60^\circ \pm 30^\circ$  W solar longitude (see Fig. 27 [83]). These conclusions lead to the concept of "cones of propagation," with a width of  $30^\circ$ – $90^\circ$ , within which low-energy

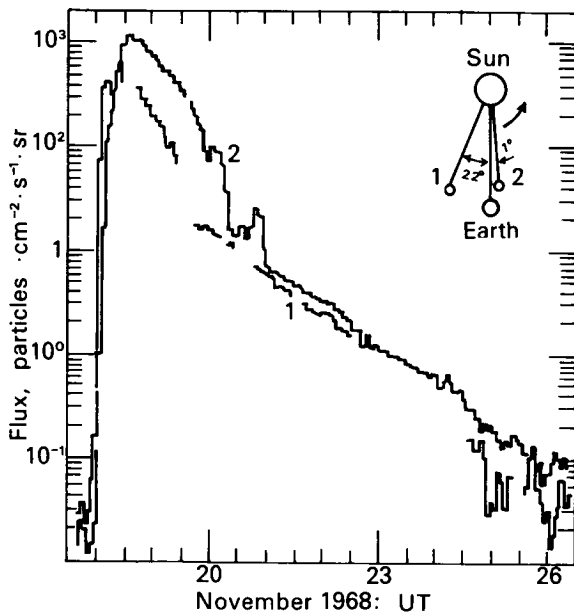


FIGURE 25.—Time behavior of flux of protons with energies  $E_p = 7.5$ – $45$  MeV [90].

1—Pioneer 8  
2—Pioneer 9

electrons propagate in interplanetary space (Fig. 28 [83]). If this is true and the electrons are emitted only in the "cone of propagation," only a portion of all the electron events generated on the Sun can be recorded on the Earth.

5. The anisotropy of streams of electrons has recently been measured. The initial anisotropy is great and directed along the interplanetary magnetic field, after which it falls much lower than the anisotropy of proton events, reaching an equilibrium value of about 2.5%. This indicates

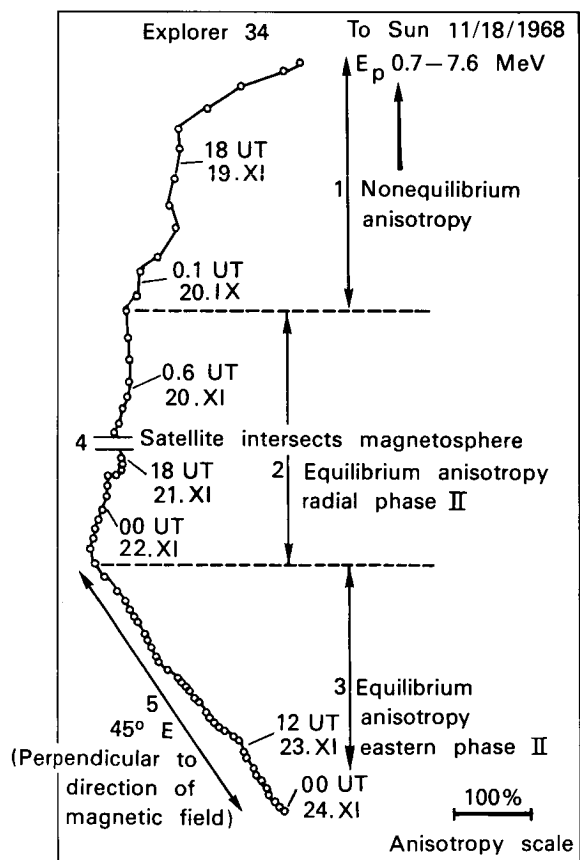


FIGURE 26.—Vector diagram of change in direction of anisotropy with time for flare of November 18, 1968. Anisotropy in initial nonequilibrium phase of event (1–2 d) directed along lines of force of field and value near 50%. Vector diagram construction: each vector represents the mean for a certain interval of anisotropy. The length of each vector corresponds to the amplitude of anisotropy, the direction—to the direction of the maximum flux of particles in the plane of the ecliptic [104].

that the nonequilibrium anisotropy exists for a long time during the phase of decreasing electron flux. The question of anisotropy is still far from answered and requires many more experiments.

#### *Solar Particles Localized in Space*

Streams of high-energy particles are almost always related to flares on the Sun. Low-energy particles (protons with energies of 0.3–20 MeV and electrons with energies of 20–100 keV) may appear in interplanetary space at times other than immediately after a flare. An increase in streams of particles is frequently observed which cannot be related to a visible flare, or for which the interval of time between the optical flare and the rise in the flux of low-energy particles is much greater than the direct flight time of the particles. Measurements by spacecraft of such delayed fluxes have shown that the time course of intensity is almost identical for protons with energy  $E_p \sim 0.5$  MeV and  $E_p \sim 10$ –20 MeV. When this type of increase is recorded, the spacecraft is intersecting a stream of particles localized in space, moving with the solar wind. The magnetic field of this area modulates the intensity of the galactic cosmic rays, and causes a Forbush reduction; the flux of plasma, colliding with the magnetosphere of the Earth, may cause geomagnetic disturbances.

These localized areas are usually tubes of force lines extended in space and rotating with the Sun. These “rotating” fluxes are frequently so long-lived that they are observed over several rotations of the Sun as recurrent events, repeating with

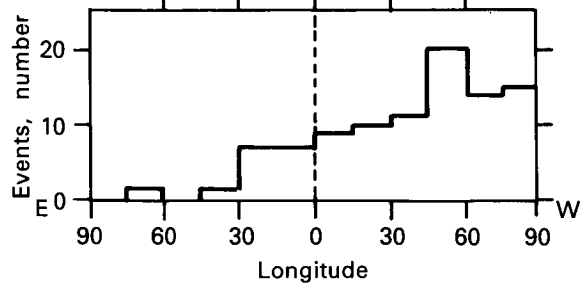


FIGURE 27.—Dependence of recording of electron increases on heliographic longitude of flare [83].

periods of 27 d. Long-lived streams of protons with energies of several MeV are usually related to active areas on the Sun. The initial sources of long-lived protons are assumed to be solar flares, supporting extended expulsion of plasma after the flare from the same active area. Subsequently, the stream remains attached to the same active area.

The magnetic field frozen in the plasma of the solar wind fully determines the motion of particles in these streams; i.e., the particles move within a certain cone of lines of force of the magnetic field, carried outward from the Sun by the solar wind. Therefore, when the same stream is measured at two points in interplanetary space, a shift in the time of recording the increase  $\Delta T$  is observed. This is related to the velocity of the solar wind,  $u$ , and the distance between the points of observation:

$$\Delta T = \frac{\Delta R + \Delta\phi \cdot R}{u} \cdot \cot \theta = \frac{\Delta R}{u} + \frac{\Delta\phi}{\Omega} \quad (7)$$

where  $\Delta\phi$  is the angular distance between the spacecraft;

$\Delta R$  is the radial distance between the spacecraft;

$u$  is the speed of the solar wind;

$\Omega \approx 13.3^\circ/d$  is the angular rate of rotation of the Sun;

$\cot \theta$  is the angle of inclination of the lines of force of the magnetic field in the plane

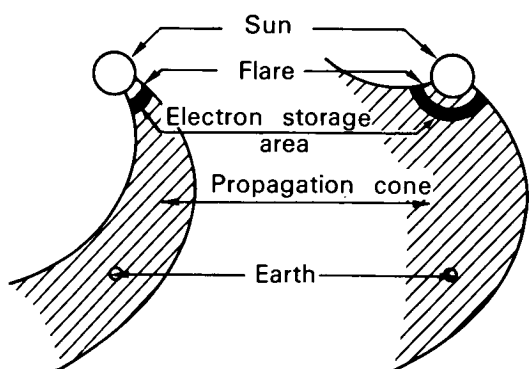


FIGURE 28.—Concept of the “cone of propagation” of electrons in interplanetary space.

of the ecliptic to the radius at the given point;

$R$  is the distance from the Sun.

This shift in recording time of two spacecraft separated in longitude allows an unambiguous increase in particles in rotating streams to be separated from all other types of increase in the case of simultaneous presence of spacecraft at different points in space.

Figure 29 is an example of the recording of such an increase by the Zond-3 and Venera-2 spacecraft [138]. The mutual placement of the spacecraft during recording of the localized stream is to the right.

The properties of such streams, characteristic for most recorded increases, are summarized briefly.

1. The intensity of particles in long-lived streams is usually low:  $N \approx 10-100 \text{ cm}^{-2} \cdot \text{s}^{-1} \cdot \text{sr}^{-1}$ . For protons with energies of  $E_p \approx 0.5 \text{ MeV}$  and electrons with energies of  $E_e \gtrsim 40 \text{ keV}$ , the intensity may sometimes reach  $10^4 \text{ cm}^{-2} \cdot \text{s}^{-1} \cdot \text{sr}^{-1}$ .
2. The energy of particles populating these streams is usually not great:  $E_e \approx 40-300 \text{ keV}$ ,  $E_p \approx 0.5-20 \text{ MeV}$ . In several cases,

electrons of high energies have been recorded in rotating streams (Fig. 30 [88]).

3. The energy spectra of electrons and protons recorded in long-lived streams are usually softer than those of particles observed during flare bursts.
4. The long-lived streams may consist only of protons or electrons, but sometimes both.
5. When streams of protons and electrons are recorded, an electron maximum is frequently followed by a proton maximum [6].
6. Rotating streams sometimes have a broad halo of  $70^\circ-90^\circ$  longitude; the halo is of harder particles of relatively low intensity. At the center of the stream, where the particles have lower energy, the concentration of particles is higher. The duration of recording the central portion of a stream is usually 6–12 h, indicating that the angular width of the central stream is  $3^\circ-6^\circ$ .
7. The anisotropy of long-lived streams is usually low, 10%–20%, sometimes reaching 30%–40%; however, very few reliable measurements have yet been made.
8. A shock wave called a standing shock wave is sometimes recorded simultane-

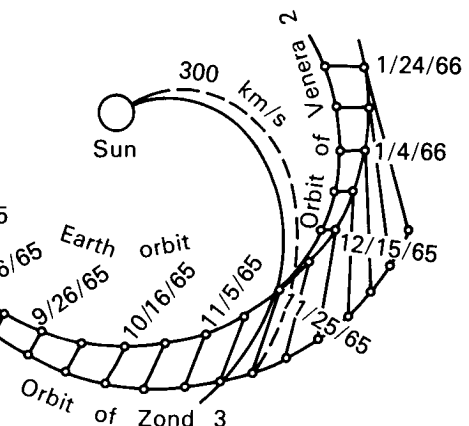
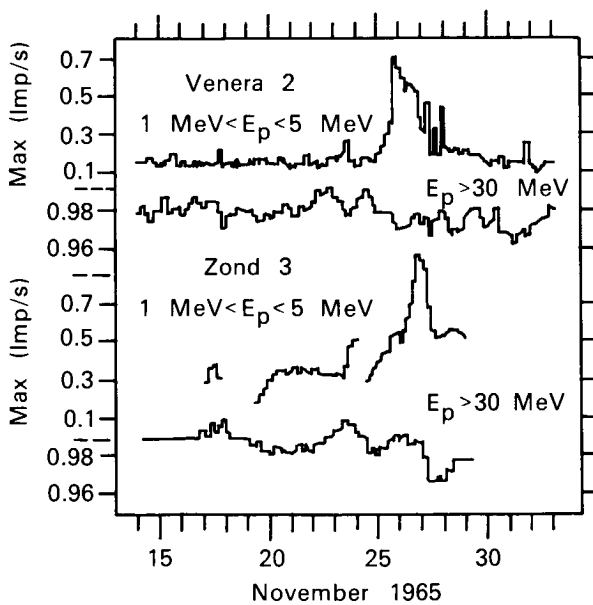


FIGURE 29.—Recording of long-lived flux by Zond 3 and Venera 2 spacecraft [138].

ously with the rotating stream, bounding the stream on the side of the interplanetary medium, and a magnetic storm is observed.

#### *Solar Cosmic Rays and Shock Waves*

An increase in the intensity of cosmic rays is frequently observed in interplanetary space, coinciding in time with the passage of a shock wave, generated in a large flare. In relationship to the initial flare, these particles are delayed, like the particles in the long-lived streams. It is possible that both types of increases represent the same phenomenon. The recording of such particles is always accompanied by a Forbush decrease in the intensity of galactic cosmic rays and geomagnetic storms on the Earth, caused by interaction of the shock wave with the Earth's magnetosphere. Figure 31 shows an example of such an increase [136].

The mean propagation velocity of shock waves from flares at 1 AU is about 600 km/s; therefore, the usual delay of such particles appearing at the Earth in relationship to a flare generating the shock wave is 50–60 h. In the case of flares in the central portion of the limb, two phenomena

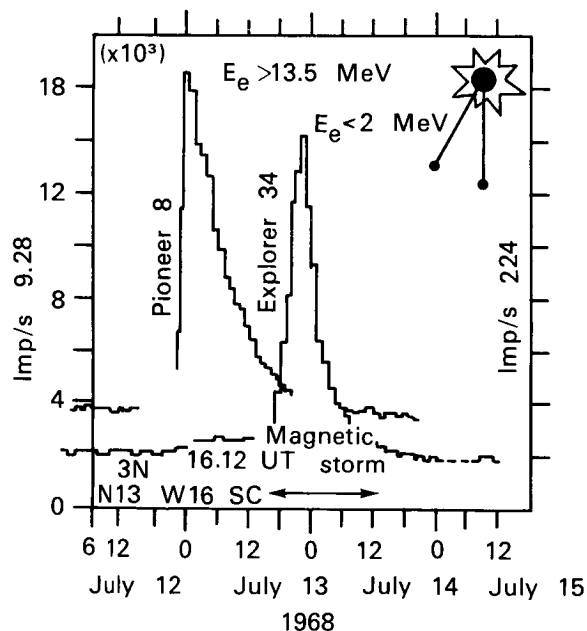


FIGURE 30.—Recording of long-lived stream of relativistic electrons [88].

may be superimposed: a rotating stream of particles and those related to the movement of the shock wave. When strong waves with a mean propagation velocity of about  $2500 \text{ km} \cdot \text{s}^{-1}$  are observed, the energetic particles are observed approximately 1 d following the flare. The criterion for selecting such events is the accompaniment by a shock wave, propagating from the solar flare into interplanetary space. The differentiation of a shock wave from all other types of perturbations in the interplanetary medium is difficult and can be achieved unambiguously only by simultaneous measurement of the parameters of the plasma and magnetic field by satellite. A summary of the basic known properties of such streams of particles accompanied by shock waves is presented.

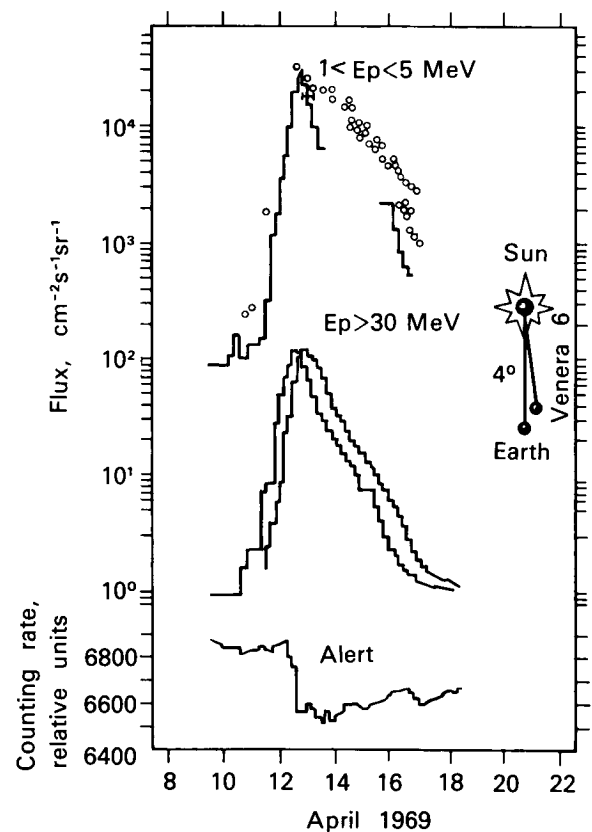


FIGURE 31.—Increase in flux of particles related to shock wave for protons with energy  $1 \leq E_p \leq \text{MeV}$  and  $E_p > 30 \text{ MeV}$  according to data by Venera 6, Molniya 1, and Explorer 34 spacecraft, April 10–15, 1968. Bottom curve shows indications of neutron monitor in alert [138].

1. The rise time is 6–24 hours. Usually, the rise begins before the arrival of the shock wave is recorded. At the moment of passage of the leading edge of the shock wave, an additional narrow burst lasting 10–20 min is recorded.
2. The streams may be either pure proton streams with energies  $0.5 \leq E_p \leq 100$  MeV, or may contain electrons with  $E_e \approx 40$ –300 keV.
3. Simultaneous arrival at the observation point of particles of various energies is observed, with identical rise rates of the fluxes of particles at different energies.
4. The energy spectra of such particles are usually much softer than the spectra of the diffusion components against the background of which they are recorded.
5. The anisotropy of such streams has been insufficiently studied. The anisotropy may be great, but the direction of the maximum arrival of particles changes rapidly with time, apparently synchronously with rapid fluctuations in the magnetic field behind the leading edge of the shock wave.
6. The appearance of particles is always accompanied by Forbush reduction of the intensity of galactic cosmic rays and geomagnetic storms with sudden onset.

#### *Solar Cosmic Rays During "Quiet" Periods*

A minimum background flux of protons occurs during quiet periods when there are no solar flares. Low fluxes and the spectra of such particles with energies of 30 MeV against the background of the significantly greater flux of galactic cosmic rays are difficult to measure; therefore, data produced so far are not distinguished by great accuracy. The mean flux of protons with energies  $E_p > 1$  MeV, according to various measurements, is about  $10^{-2}$  particles/ $\text{cm}^2 \cdot \text{s} \cdot \text{sr}$ . The differential spectral index for the energy area 0.03–5 MeV is  $\gamma \approx 3$ .

*Generation of solar cosmic rays during flares.* There is reason to assume that the generation of solar electrons and protons occurs in two stages, both directly during the period of the explosive phase of a flare, when the brightness in the

$H_{\alpha}$  line is maximum (stage 1), and after the explosive phase, when the hydromagnetic shock wave formed during the large flare explosion interacts with the intensive magnetic fields in the sunspots (phase 2). Thus, there are probably two accelerating mechanisms, acting in sequence, i.e., acceleration in the explosive phase is the injector of particles accelerated in the second phase.

Direct generation of particles during the explosive phase is a possibility which is indicated by observation of type III radio bursts. The velocity of movement of the source of type III bursts is from  $0.2 c$  to  $0.8 c$ ; the agent exciting these plasma oscillations can be identified as electrons with energies of 10 to several hundred keV. The movement of such a source of type III radio bursts from the Sun to a distance of  $200 R_{\odot}$  was observed [119], and it was found that the velocity of motion remained constant, equal to  $(0.4\text{--}0.5) \cdot c$ , while the source itself was a compact formation with linear dimensions of  $10^6$  km. An estimate of the number of electrons causing a type III radio burst in the corona is  $N_e \approx 10^{35}\text{--}10^{36}$ , which is similar to the number of solar electrons ( $N_i$ ) observed directly in interplanetary space after a flare ( $N_i \approx 3 \cdot 10^{33}\text{--}10^{34}$  for  $E_e \geq 22$  keV). This yields a value of 0.1–1% for the effectiveness of departure of electrons from the corona into interplanetary space [83]. With a type III radio burst generated in the corona, there are simultaneous microwave bursts in the cm radio range and x-ray bursts in energies ranging to 100 keV (Figs. 32 and 33). Since type III radio

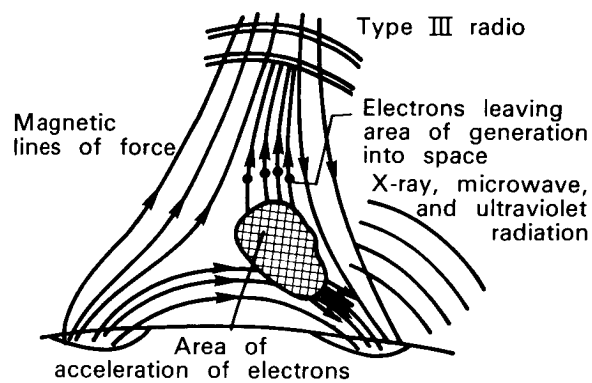


FIGURE 32.—Model of generation of electrons in a flare.

bursts are observed from particles moving outward, microwave bursts may arise as magnetic bremsstrahlung in the chromosphere when a portion of the stream of accelerated particles moves in the direction parallel to the boundary of the chromosphere. The x-radiation of this phase results from bremsstrahlung of electrons moving into the denser layers of the solar atmosphere. That all of these particles belong to the same area of generation shows similarity of the time form of a burst for various types of electromagnetic radiation. The ratio between intensities of these groups of electromagnetic radiation may vary, even to the point that individual forms may be totally absent, depending on the situation and specific conditions of acceleration.

If the acceleration of particles in this phase is achieved by electric fields arising upon dissipation near the zero points of oppositely directed magnetic fields, acceleration to identical hardnesses probably occurs. If the electrons are accelerated to energies of about 300 keV, the protons are accelerated only to 200 eV, i.e., their energy is lower than the kinetic energy of the solar wind. Observations in interplanetary space have shown that after flares of low intensity, only the first phase of acceleration occurs, accelerating mostly electrons. If there is any mechanism of acceleration, for example, accelerating a particle to identical energy, a low energy (up to a few hundred keV) proton component should be observed after a low-intensity

flare. The scarcity of experimental data does not yet allow drawing any reliable conclusions in this respect.

The primary portion of the protons is accelerated to energies of hundreds of MeV, while the electron component is accelerated to energies of tens of MeV, apparently in the subsequent phase of the flare phenomenon, in which the shock wave formed in the explosion interacts with the strong magnetic fields of the spots. This shock wave is noted on the basis of type II radio bursts several minutes after the beginning of large solar flares. There apparently is an energy threshold of formation of a shock wave, since it generally does not follow low-intensity flares.

Finally, the interaction (mentioned above) causing acceleration of particles is indicated by type IV radio storms, resulting from synchronous radiation of electrons captured in the corona. These storms are varied in form, often last for many hours, and cover areas that drift slowly in the corona. The proton component of solar cosmic rays correlates rather well with the appearance of these type IV radio storms. It has been assumed that the corona, similar to such type IV areas, also contains areas occupied by type I radio storms, a broad continuum of radio noise, sometimes lasting for several days. In type IV radio storms, these regions are occupied by energetic electrons and protons, but in type I radio storms, they consist of captured electrons with energies of tens of keV.

Thus, at a stage in the flare phenomenon in the corona, near the base of the lines of force carried by the solar wind out into interplanetary space, broad regions are formed, populated with charged particles, and frequently quite distant from the location of the flare. At some moment, the particles are liberated and enter the interplanetary magnetic field.

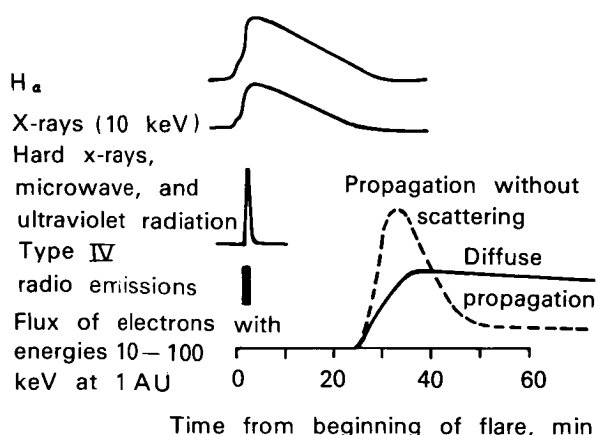


FIGURE 33.—Model of generation of electrons in a flare (time picture).

#### *Propagation of Solar Cosmic Rays in Interplanetary Space*

The interplanetary magnetic field is the basic factor defining the nature of motion of charged particles in interplanetary space. Protons injected by the Sun propagate in the interplanetary spiral

magnetic field formed by the solar wind. The spectrum of the heterogeneities related to the inconstancy of solar wind parameters is superimposed on this basically ordered interplanetary magnetic field structure. Corresponding to this structure of the interplanetary magnetic field, the motion of a charged particle can be divided into motion along the spiral mean regular field and scattering on magnetic heterogeneities.

With movement in a regular field, changing as a function of  $R$ , the magnetic moment of a particle  $M = E \cdot 1/B$  is conserved (first adiabatic version), leading to conservation of the value of  $\sin^2\alpha/B$ , where  $\alpha$  is the angle between the direction of the velocity of the particle and the line of force. The intensity of the magnetic field decreases as  $B_r(R) \approx 1/R^2$ ,  $B_\phi(R) \approx 1/R$ . Since the value of the field at the orbit of the Earth is decreased by  $10^4$  times in comparison to the intensity at the surface of the Sun, the pitch angle of the particle  $\alpha$  would be very slight  $\alpha \leq 1^\circ$  (even for a particle which departed the Sun at an angle of about  $90^\circ$ ), if the particle were not scattered on magnetic field heterogeneities.

When a particle interacts with field heterogeneities, it is scattered, i.e., changes its pitch angle and the direction of motion. The particle is most effectively scattered on field heterogeneities with dimensions  $\ell$  on the order of the Larmor radius of the particle  $\rho\lambda = pc/ZeB$  where  $p$  is the momentum of the particle,  $B$  is the mean intensity of the field in the heterogeneity. Where  $\ell \gg \rho\gamma$ , particles are scattered on heterogeneities to very slight angles; when a particle moves along the line of force, it either runs around a heterogeneity so that the scattering angle is also slight, or is reflected from it.

Most increases in solar particles recorded in the past 15–20 years (as stated above) have been gradual during several hours from the moment of the first particles at the recording point, to the maximum of intensity with subsequent slower decrease. The solar flares responsible for these increases last from  $\frac{1}{2}$  to 3 h; the phase of the flare in which hard x-ray and radio radiation is observed lasts for much less time (Fig. 33). Therefore, the longer leading edges of the time profiles of particles are interpreted as the effect of diffusion of particles.

The model of isotropic diffusion is the simplest model describing the process of propagation of particles when strong scattering is present, which is suggested at the very beginning of the study of solar cosmic rays. This simple model, in the case of an unlimited medium and constant diffusion factor, yields the time-dependence of the flux of particles:

$$n(R, v, t) = \frac{N(v)}{(4\pi \cdot D \cdot t)^{-3/2}} \cdot e^{-\frac{3t_m}{2t}} \quad (8)$$

where  $n$  is the density of the particles;

$R$  is the heliocentric distance to the point of observation;

$D(R, v)$  is the diffusion factor;

$v$  is the velocity of the particles;

$t_m = R^2/6D$  is the moment in time when

$n(R, v, t)$  has its maximum value.

*Isotropic diffusion.* The model of isotropic diffusion assumes that the particle is injected in a pulse over a very short time near the maximum of a flare or the maximum of a burst of x-rays and moves in a spherically symmetrical volume encountering heterogeneities, leading to isotropic scattering of the particles. The density of heterogeneities in space must be such that the length of the free path of a particle  $\lambda$  is much less than the distance  $L$  from the source to the point of observation.

The time-dependences of intensity of solar cosmic rays are sometimes fairly well-described by isotropic diffusion, particularly if the source of particles is located in the eastern or central portion of the Sun. Agreement of the time-dependence can be improved by considering the dependence of diffusion factor  $D$  on heliocentric distance  $R$ .

However, isotropic diffusion does not explain the spatial anisotropy of the flux of solar protons observed in the initial stages of a flare; the maximum of the flux in the process of isotropic diffusion should be observed in the direction from the Sun. Actually, the maximum flux is directed at an angle of  $\phi \approx 50^\circ$  to the Earth-Sun line and is displaced to the east. Isotropic diffusion also cannot explain the greater effectiveness of the western half of the Sun from the standpoint of arrival of solar cosmic rays. Measurements in

interplanetary space have indicated that the fluxes of particles in space depend strongly on the heliolongitude of the location of the solar flare, which also does not fit the isotropic diffusion theory.

Furthermore, experiments frequently indicate a free path length for protons with  $E_p < 50$  MeV which is comparable to 1 AU, contradicting one of the conditions of applying the diffusion theory [89].

All of this indicates that isotropic diffusion produces an acceptable description of the late stage of an increase, with the exception of the properties of anisotropy. However, it must be recalled that most particles are recorded at the maximum of an increase. Consequently, isotropic diffusion can describe the behavior of not more than 10% of particles emitted by the Sun.

*Anisotropic diffusion.* Models of anisotropic diffusion have been developed in recent years. Some are based on the assumption that the diffusion of particles occurs not only in interplanetary space, but also in the solar corona, with the relative roles of coronal and interplanetary diffusion depending on the time of observation; when a particle moves along lines of force, scattering predominates over transfer across the lines of force. In other words, the effective diffusion factor along the field  $D_{||}$  is significantly greater than  $D_{\perp}$ —the factor across the lines of force ( $D_{||} \approx 100 D_{\perp}$ ).

Based on these assumptions, a theory of scattering of particles as to pitch angles has been developed for description of the physical relationship between the scattering of particles and the observed fluctuations in the magnetic field [78, 84]. A theory of anisotropic diffusion has been developed under the same assumptions [54, 56], considering transfer of particles by the solar wind, time behavior of fluxes and anisotropy of solar cosmic rays in the nonequilibrium phase of the phenomenon, when diffusion is significant. It is indicated that the anisotropy  $A \approx R/2 vt$ , where  $R$  is the distance from the source to the observer along a line of force,  $v$ , the velocity of the particle, and  $t$ , the time since the moment of injection of the particle into the solar system. Consequently, the anisotropy of electrons, even of low energies ( $E_e \geq 100$  keV) should decrease

much more rapidly than for protons with  $E_p \geq 10$  MeV, which agrees with the experimental data [104].

In one model [27], it is assumed that at a certain heliocentric distance  $R_1$  ( $R_1$  is comparable to 1 AU), the nature of scattering of solar particles by the interplanetary magnetic field changes so that particles reaching this distance do not return to the area of diffusion. This boundary condition for the decreasing intensity phase leads to the exponential dependence of particle fluxes on time up to the moment in time  $t \geq t_D$ , where  $t_D$  is the mean time of diffusion of particles from source to boundary. Within the framework of the models studied, the value and direction of “equilibrium” anisotropy observed in the late stage of increases in solar cosmic rays for  $T > 2$  d can be produced.

After the increase in solar cosmic rays begins, when the solar particles have propagated by several AU, long-term anisotropy may be caused by: (1) convective transfer of solar protons along lines of force in the magnetic field  $B$ , (2) drift of particles due to movement of the magnetic field relative to the particles, where the velocity of drift is directed perpendicular to the magnetic field force line, and (3) constant injection of particles by the Sun. The drift of particles has a very significant effect, particularly for low-energy particles. The radial equilibrium anisotropy existing 1–4 days after a flare, arises because of drift of particles due to convection along field lines  $B$ .

The movement of the particles at this time is fully determined by the solar wind. Consequently, a current of particles is perpendicular to the line of force due to drift motion, as well as along the line of force, caused by collision of a particle with magnetic heterogeneities moving along the lines of force of the field at velocity  $u \cos \theta$ .

The total equilibrium anisotropy is independent of the direction of the interplanetary field vector. For an observer at rest, the anisotropy of the cosmic rays will be directed along the radius and its value  $A_{eq} = (2 + \gamma)u/v$ , where  $u$  is the velocity of the solar wind,  $v$  is the velocity of the particles,  $\gamma$  is the differential spectral index of the particles.

In the late stage of the increase in solar cosmic rays, for moments more than 4 d after the flare, the equilibrium anisotropy is observed about  $45^\circ$

to the east of the Sun-spacecraft line. This anisotropy is fully determined by drift movement of solar cosmic rays; the component of the anisotropy parallel to the lines of force of the magnetic field disappears due either to lack of deflection of solar cosmic rays by magnetic field heterogeneities, or to compensation of this anisotropy by the reverse flow of particles accumulated during the first phases of the increase at the periphery of the solar system. In the latter case, a significant positive (i.e., increase of flux of particles with increasing distance from the Sun) radial gradient of solar cosmic rays should be observed. With full compensation of the convective anisotropy, only the drift anisotropy remains, the value of  $A = (2 + \gamma)u/v \sin \theta$ , where  $\theta$  is the angle between the direction of the lines of force of the magnetic field and the direction to the Sun.

The increase in solar cosmic rays related to the arrival at the point of observation of shock waves caused by flares on the Sun has not been fully determined. The existing hypotheses of the origin of these energetic particles do not describe all aspects of the phenomenon observed. The most natural "trap" hypothesis assumes that the solar particles were accelerated in a flare on the Sun, then moved in interplanetary space with the shock wave from the same flare in a certain adiabatic or diffusion trap. Another hypothesis assumes that within the shock wave, there are conditions capable of accelerating particles to the observed energies. It would follow that the solar cosmic rays observed with the shock wave are not inherently solar, but interplanetary. A third hypothesis states that the particles were created on the Sun, remained near the Sun for a long time and fed a group of force tubes, which the shock wave has pushed outward to the point of observation. The nature of this phenomenon will not be discussed in detail, because there are not sufficient data to support any of the hypotheses listed.

Based on current knowledge of particles of solar origin, the magnetic field of the Sun and the interplanetary magnetic field, a phenomenological picture can be constructed of the propagation of solar cosmic rays.

Particles generated during a flare diffuse in the solar corona far from the point of the flare. The

shock wave, propagating in the chromosphere and corona of the Sun, facilitates this diffusion of particles. The particles are then injected along neutral lines into interplanetary space over a broad range of angles, frequently reaching 90°, propagate along the lines of force of the field, forming a "cone of propagation," and dissipate little over the range of 1 AU. The particle population of lines of force departing from the area of a flare, or the area into which the maximum concentration of accelerated particles has diffused, is much greater than in neighboring areas. When the particles have traveled far from the Sun (2–3 AU), they begin to scatter intensively, causing isotropization of flow in the propagation cone and filling the entire space near the Sun with particles, i.e., erosion of the cone. If the injection process lasts many hours, the increased intensity of particles and great anisotropy in the bundle of lines of force departing from the area of the flare will also be retained for a long time. However, the spectrum of such particles will become softer than the first time following the flare, since the more energetic particles disappear sooner at the boundaries of the diffusion volume.

If the shock wave generated in the flare propagates into interplanetary space, it is greatly perturbed and changes the distribution of particles (or serves as a source of reflection of particles, possibly changing their energy). Therefore, when a shock wave passes spacecraft, a change in the characteristics of the particle stream is recorded. After the shock wave passes, the interplanetary medium gradually returns to its quiet state. Since shock waves propagate from the Sun at speeds of 500–800 km/s, 4 to 5 d after a flare, the primary process of propagation of particles will be transfer of particles by the solar wind from the solar system.

#### *Streams of High-Energy Solar Protons*

The greatest radiation danger for man and for various materials within spacecraft is the high-energy solar protons which penetrate freely through the skins of contemporary spacecraft. The energies of such protons can be, arbitrarily, 100 MeV. This section provides a summary of the increases in solar cosmic rays during which pro-

tons with energies greater than 100 MeV have been observed.

During the past two cycles of solar activity, over 100 flares of solar cosmic rays containing protons with energies  $E_p > 100$  MeV have been observed. The most powerful of these, as well as the integral flux of particles in each flare [67, 92], are presented in Table 7. The values of fluxes in Table 6 were from varied data; the accuracy of their determination can be assumed to be within the limits of a factor of 2. Figure 34 shows the time-dependence of the summary flux of solar cosmic rays over a year, and the time-dependence of the smoothed number of sunspots.

### Meteorite Material

Meteor material in interplanetary space consists of a multitude of small bodies moving freely in the Sun's field of gravity and generally unrelated physically to the planets. These bodies range broadly in dimension, from asteroids (tens of km in diameter) to tiny dust particles, comparable in size to the wavelength of sunlight. The number of particles in interplanetary space

increases rapidly with decreasing dimensions.

The study of small bodies in the solar system is undoubtedly of theoretical and practical interest. The distribution of small bodies into classes of comets, asteroids, meteorites, and cosmic dust is more deeply based physically than mere differences in dimensions of bodies, phenomena, or related methods of observations, and reflects their characteristic features. Explanation of the physi-

TABLE 7.—*Flares of Solar Cosmic Rays*

Date of flare	Flux of protons with energy $E_p > 100$ MeV/cm <sup>2</sup> for entire flare
2/23/56	$3.5 \cdot 10^8$
5/10/59	$8.5 \cdot 10^7$
7/10/59	
7/14/59	$3.7 \cdot 10^8$
7/16/59	
11/12/60	
11/15/60	$4 \cdot 10^8$
11/20/60	
8/02/72	
8/04/72	$2.4 \cdot 10^9$ (Estimate for pro-
8/07/72	tons with $E > 60$ MeV)

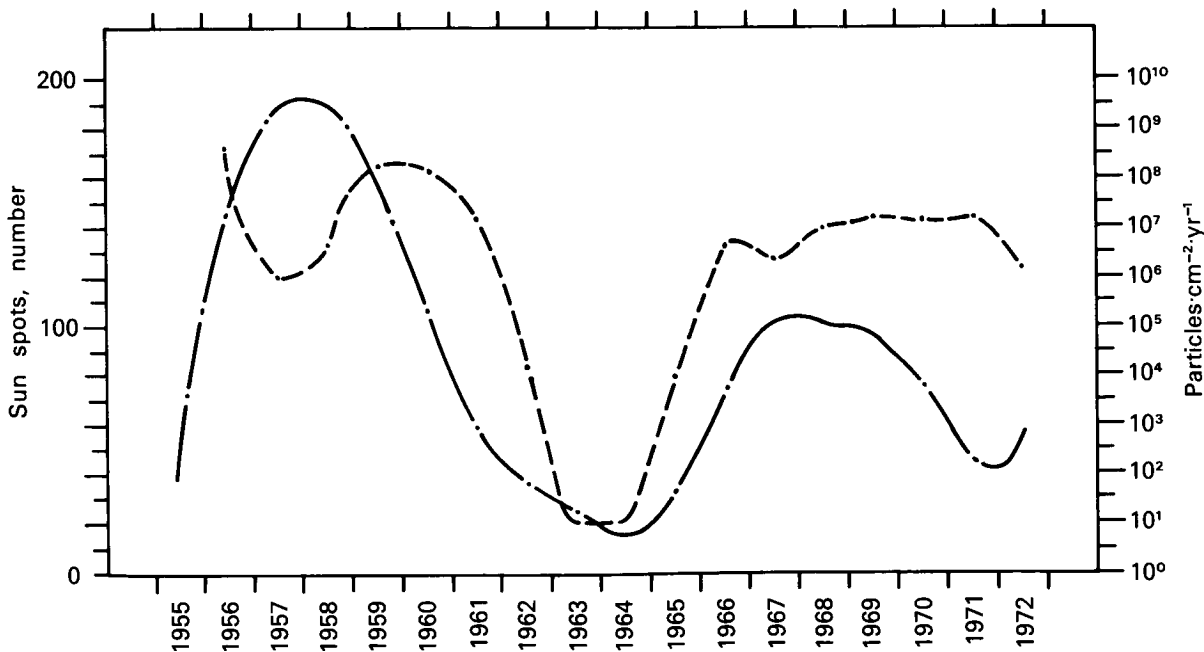


FIGURE 34.—Summary flux of protons from Sun/yr as a function of time (dashed line) and number of sunspots (solid curve).

cal structure and chemical composition of small bodies in the solar system, their origin and age, and establishment of the evolutionary relationships between comets, asteroids, and meteorites may be highly significant for the development of solar system cosmogony.

These problems are frequently interwoven closely with other problems of space physics and the immediate surroundings of the Earth. Investigation of meteorite material interactions and, in particular, comets with fluxes of radiation and corpuscular radiation is an effective means of obtaining information on properties of the interplanetary medium, the solar wind plasma, and magnetic fields in space. A comprehensive study of meteorites can yield important information on the structure of the upper atmosphere and the physical processes within it, as well as on the propagation of radiowaves.

The effects of meteorite bombardment on the surface of the Moon provide a basis for study of the history of the Moon, and to determine the flux of meteorite material and its evolution in the solar system. Analysis of the properties of meteorites reaching the Earth allows judgment of their nature, origin, and age, and the effects and properties of cosmic rays.

Special problems in the study of meteorite bodies and cosmic dust are connected with the problem of meteorite danger for space flights. There are two potential types of danger represented by solid particles for satellites, rockets, and spacecraft. Collision with a sufficiently large particle can cause serious damage to a spacecraft, even in an individual event. On the other hand, continuous bombardment with tiny particles causes erosion of surfaces and may lead, for example, to failure of optical devices or changes in the optical properties of heat exchange surfaces and temperature regulation systems. Determination of the degree of meteorite danger is necessary in the design of spacecraft and the development of protective measures when necessary.

Studies and experience show that the meteorite danger during flights in the region of the Earth's orbit is slight, but extrapolation of these data over a great range of heliocentric distances is unjustified; experimental data must be developed on the meteorite situation for long interplanetary flights

beyond the limits of the orbits of Mars and Venus.

Main channels of information on the presence and properties of meteorites in the solar system are from studies of meteors, meteorites, zodiacal light, optical phenomena in the upper atmosphere, stratospheric dust, and meteorite dust reaching the Earth's surface. Most of the information on the meteorite component of the interplanetary medium is from surface investigation.

The development of rocket and space technology over the past two decades has made possible direct studies of micrometeorite particles in the upper atmosphere of the Earth and in space, using special equipment which utilizes various recording principles. In contrast with surface observations, these studies have produced information on individual particles with masses down to  $10^{-14}$  g, their spatial density, physical properties, and chemical composition. The phenomena studied, related solid interplanetary particles, frequently have practical applications. Observations of meteorite tracks are used to determine the direction and velocity of winds in the upper atmosphere, and the ionization created by meteorites is used in some communications systems.

The meteorite material rotating around the Sun at a distance of about 1 AU consists of rock and iron particles primarily of iron, nickel, and iron sulfide. The chemical composition of rock meteorites is reminiscent of that of terrestrial rock. The density of rock meteorites is about  $3 \text{ g/cm}^3$ , that of iron meteorites about  $7.8 \text{ g/cm}^3$ . Meteorite bodies may form conglomerates, with very low density, approximately  $0.5 \text{ g/cm}^3$ . The velocity of meteorite particles relative to the Earth varies from 12 to 72 km/s. The significant fraction of these bodies is combined into clusters extended along their orbit or concentrated in small sections.

Meteorite bodies which cannot be classified in any meteorite stream are called the meteorite background or sporadic meteorites, which belong to weak meteorite streams not yet defined.

Meteorite matter has been studied using spacecraft in the areas of the Earth, the Moon, and interplanetary space along the spaceflight trajectories to Venus, Mars, and beyond the orbit of Mars in the asteroid belt [86].

Measurements of micrometeorite material by

acoustical methods near the Earth have indicated that the number of micrometeorite particles with masses less than  $10^{-6}$  g is higher, by several orders of magnitude, near the Earth than the interplanetary background level. These results have led to formulation of the hypothesis of a dust belt or dust cloud around the Earth. Two possible sources have been considered for these particles: interplanetary dust particles captured by the gravitational field of the Earth, and dust particles separated from the Moon.

However, careful study of these mechanisms [37, 38, 47, 116] has shown that these phenomena could not support the observed concentration of dust particles. At the same time, doubts have

been expressed concerning the experimental reliability of the results produced; many scientists currently believe that the fluxes of powder particles in near-Earth and interplanetary space are the same. However, recent studies using sensors of various types have shown that there is spatial density of particles with masses of  $\leq 10^{-7}$  g elevated by approximately an order of magnitude in the area around the Earth in comparison to their similar density in the area of the Moon and in interplanetary space (Fig. 35). The presence of a dust belt of this concentration near the Earth is not difficult to explain. Nevertheless, the accumulation of experimental data to answer this question finally must be continued.

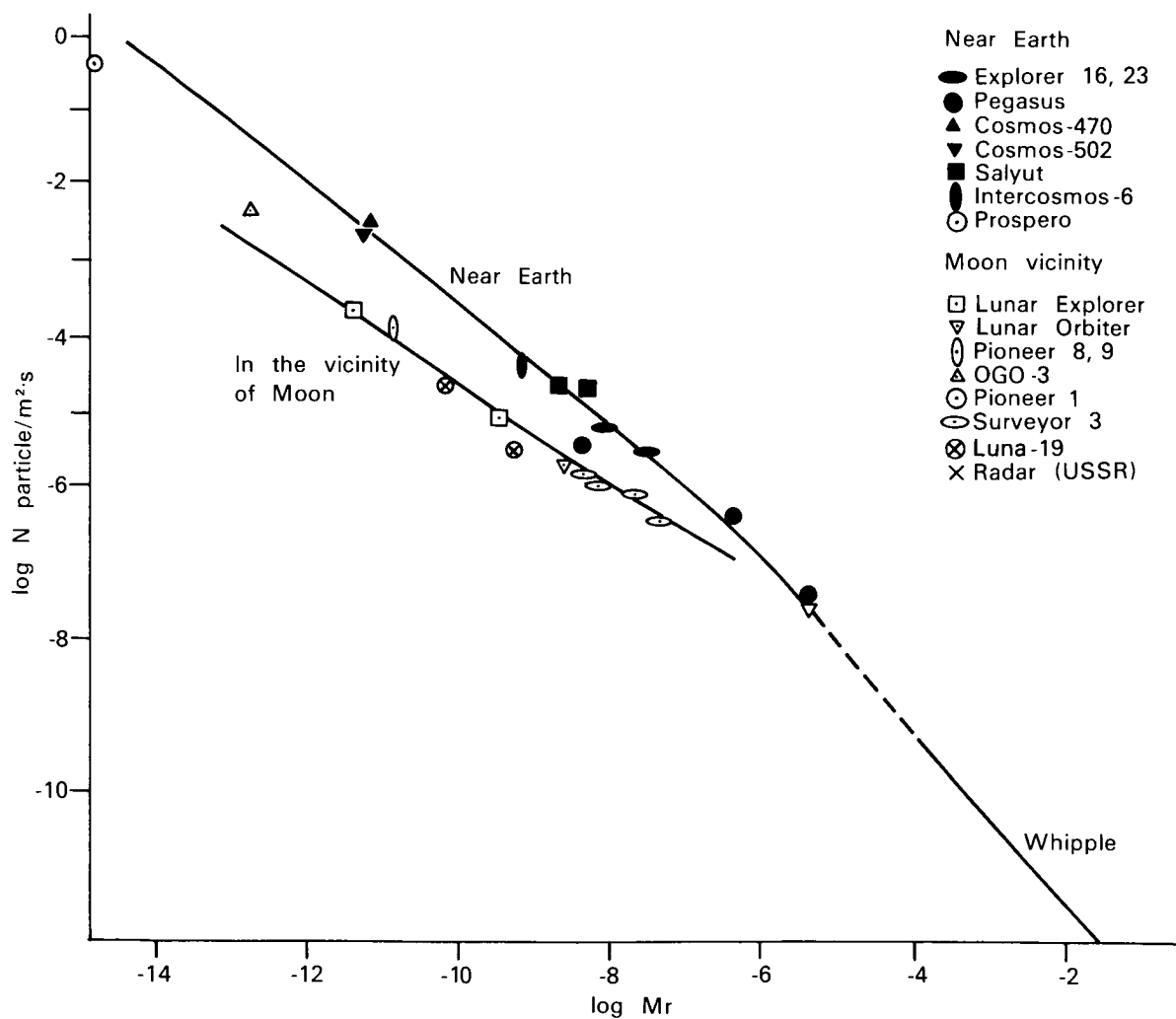


FIGURE 35.—Results of measuring meteor bodies.

QUALITY OF THE  
PAGE IS POOR

In Figure 35, parameter  $S$ , characterizing the exponential law of propagation of meteorite bodies by mass, for the mass range  $m = 10^{-12} - 10^{-7}$  g, near the Moon and interplanetary space is  $S \approx 0.6$  in comparison to  $S \approx 0.8$  near the Earth, i.e., the shortage of particles with decreasing mass in the area of the Moon and in interplanetary space is greater than near the Earth.

Preliminary results of measurement by Pioneer 10 spacecraft have shown that in the asteroid belt, the flux of particles increases sharply with the main mass of asteroid belt particles having dimensions of 0.01–1 mm. The number of particle impacts with the Pioneer 10 spacecraft has been greater than expected before launch, but there is not great danger of serious damage to the spacecraft [1].

#### *Micrometeorite Matter at the Surface of the Moon*

There is no atmosphere around the Moon; therefore, meteorite bodies collide with its surface at high velocities. When a particle impacts with the surface, an explosion occurs, and the mass of soil particles ejected is many times greater than the mass of the impacting particle. Experiments with models in the US have shown that many of the particles ejected in such an explosion have a mass of about  $10^{-11}$  g. Ninety-nine percent of these particles fly over ballistic trajectories at velocities of about 1 km/s, and only 1% achieves a velocity greater than 2.4 km/s, sufficient to depart the Moon. Secondary particles and impacts should not greatly increase the danger of materials penetrating the surface of the Moon due to their primarily low velocities; however, the erosive effect of repeated impacts, even at low impacting particle speeds, might present a problem for operation of individual structural elements.

When large meteorites strike the Moon (a rare occurrence), a great quantity of rock is ejected from the surface. Experiments by the Pegasus, Explorer 16, and Explorer 23 spacecraft have been very valuable for the study of meteorite danger, which used penetration-type sensors recording the penetration frequency of an envelope as a function of its thickness, and considered

the specifics of rupture of the envelopes when particles strike at an angle (due to the isotropic model of the incident stream used). These figures are presented in Figure 36, together with the calculated data of Whipple. In the area with thickness of less than 1 mm, the experimental and calculated data agree well.

For medium-range flights in the area of the Earth and Moon, this figure shows that meteorite danger can be ignored, while for long flights (about 1 year or more) in little-studied areas of the solar system, the meteorite danger must be taken into consideration.

The recording of micrometeorites in meteorite streams is of a particular interest; this represents a unique phenomenon in the solar system. The point of view generally accepted is that there is a genetic relationship between meteorite streams and comets, and the processes of rupture of these are the sources for formation of streams and their constant new supply of meteorite bodies. A hypothesis has been set forth and actively developed [81, 82, 138] which assumes that all meteorites, including sporadic ones, are of comet origin, and the breakup of comets and scattering of meteorite streams maintain the quasi-stable state of the zodiacal cloud of cosmic dust. The meteorite streams, like sporadic meteorites, have been intensively studied by surface visual, photographic, and radio observation. There is, understandably, great interest in the study, related to the technical capabilities of direct observation in space, of micrometeorites belonging to meteorite streams by means of satellites and rockets.

Extrapolation of the data from surface optical and radio observations of sporadic meteorites and meteorite streams indicates that the probability is slight of recording small particles with masses of  $10^{-8}-10^{-11}$  g in meteorite streams [37, 38, 82]. This is due primarily to the different distributions of particles by masses of sporadic meteorites and meteorite streams; the contribution must be slight of meteorite streams to the total counting rate of micrometeorites with masses of less than  $10^{-6}$  g. It is important that with decreasing dimensions of particles, the significance of nongravitational forces acting on such particles increases, essentially limiting their lifetime in the solar system. The decrease in the

steepness of the integral distribution of sporadic micrometeorites with masses of  $10^{-7}$ - $10^{-11}$  g to a value of 0.6, compared with mean value  $S=1.2$  for meteorites in the optical and radio ranges, is characteristic. The effects of such forces on the particles in streams can lead to selective removal from orbit of particles of small dimensions. This makes the recording of small particles in the streams more difficult.

Based on experiments with micrometeorite material, the mean density of meteorite material in the solar system is about  $2 \cdot 10^{-22}$  g/cm<sup>-3</sup> and the mean rate of accretion of interplanetary matter by the Earth is 40 t/d.

## MAGNETOSPHERE OF THE EARTH

### Terrestrial Magnetosphere Structure

The physical conditions near the Earth differ greatly from conditions in interplanetary space because of the terrestrial magnetic field. The structure of the magnetosphere of the Earth, washed in the solar wind, is shown in Figure 37 for the spring and fall (magnetic axis of the Earth perpendicular to the direction to the Sun) [98]. Figure 38 is for June (significant inclination of magnetic axis to Earth-Sun line) [112]. Differentiation can be made on the figures between the stable magnetic field of the Earth (described in this section), and the area perturbed by disturbances (under the subsequent section, SUN-EARTH CONNECTION).

#### *Stable Magnetic Field of the Earth*

The terrestrial magnetic field is described in the first approximation by a dipole field with magnetic moments  $\vec{M}=8.07 \cdot 10^{25}$  G·cm<sup>3</sup>, placed at the center of the Earth. The axis of the dipole intersects the surface of the Earth at two opposite points with coordinates  $78.3^\circ$  N,  $69.0^\circ$  W, and  $78.3^\circ$  S,  $111.0^\circ$  E. In the second approximation, the magnetic dipole is shifted from the center of the Earth by 436 km in the direction toward the point with coordinates  $15.6^\circ$ N,  $150.0^\circ$ E. A stricter approximation of the geomagnetic field can be produced using an expansion with respect to spherical harmonics.

Some properties of the dipole field should be

considered at this point which will be needed in later exposition.

A magnetic line of force is produced by the equation:

$$r = R_e \cos^2 \phi \quad (9)$$

where  $R_e$  is the distance from the center of the dipole to the line of force in the equatorial plane ( $\phi=0$ );  $\phi$  is the geomagnetic latitude; and  $r$  is the distance from the center of the dipole.

The unit of distance used is the radius of the Earth  $R_0$ , equal to  $6.37 \cdot 10^8$  cm.

Then  $L = \frac{R_e}{R_0}$ ;  $R = r/R_0$ ; the equation for a line

of force can be rewritten as

$$R = L \cos^2 \phi \quad (10)$$

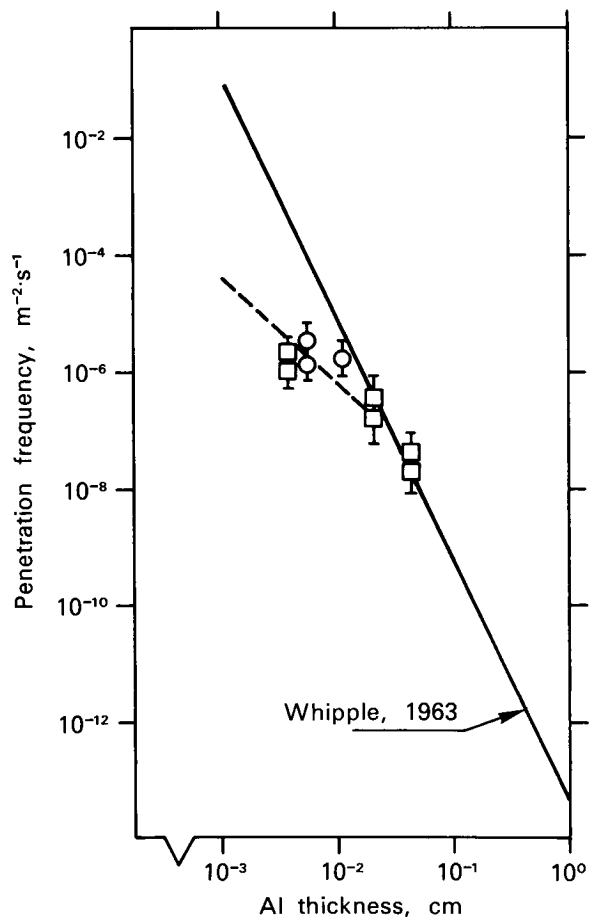


FIGURE 36.—Frequency of penetrations of solid barrier in area of the Earth's orbit.

The intensity of the field in the plane of the equator  $B_e$  can be calculated by the formula

$$B_e = \frac{0.312}{L^3} [\text{G}] \quad (11)$$

The intensity of the field at any point on a line of force can be determined by the expression:

$$\frac{B}{B_e} = \frac{\sqrt{4 - 3 \cos^2 \phi}}{\cos^6 \phi} = \frac{\sqrt{4 - 3R/L}}{(R/L)^3} \quad (12)$$

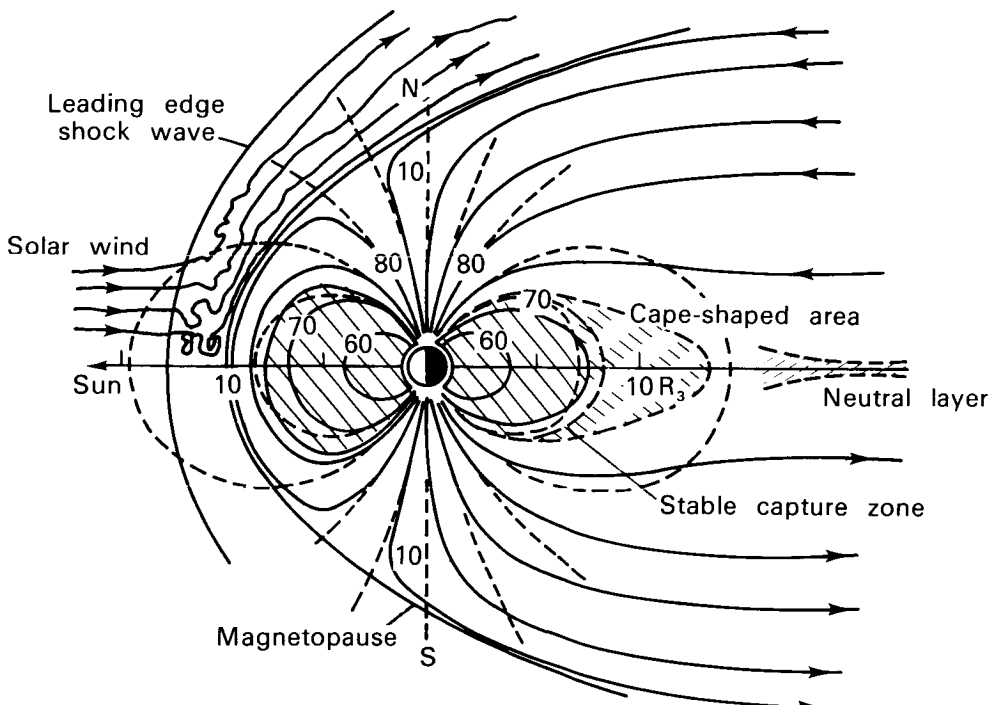


FIGURE 37.—Magnetosphere structure.

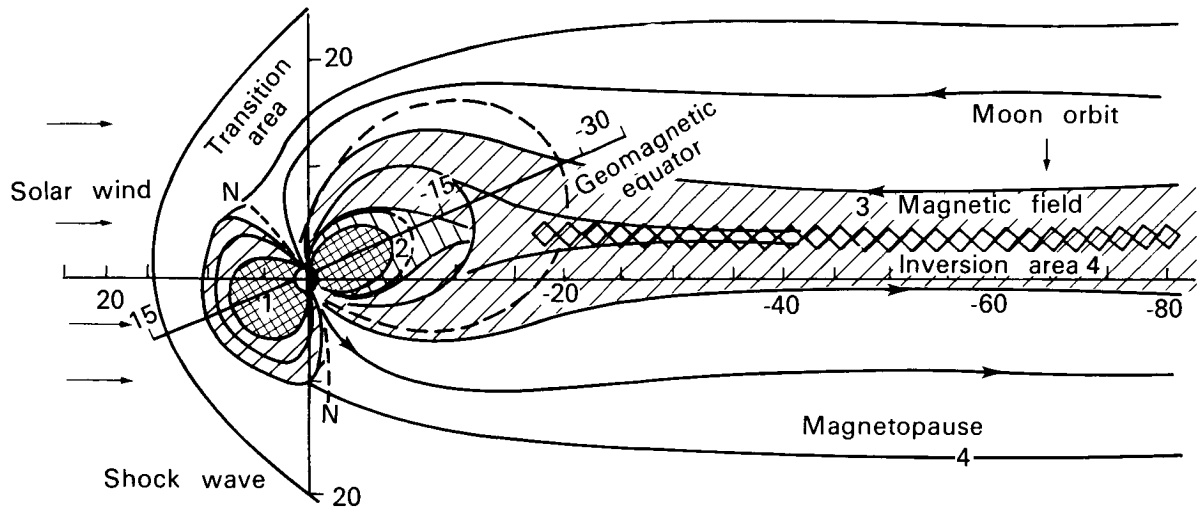


FIGURE 38.—Structure of the Earth's magnetosphere. 1, radiation belts; 2, quasi-capture area; 3, plasma layer; 4, neutral layer.

Angle  $\gamma$  between a line of force and the radius-vector is determined by the relationships:

$$\tan \gamma = 1/2 \cot \phi \quad (13)$$

The "inclination" of the field  $I = \frac{\pi}{2} - \gamma$ .

At great distances, the structure of the geomagnetic field differs significantly from that of a dipole, due to the interaction of the Earth's magnetic field with the solar wind (see Fig. 37).

*Movement of particles in the geomagnetic field.* The movement of particles with  $E < \text{GeV}$  can be represented as the superposition of three independent motions [5]: the Larmor rotation of the particle in the plane perpendicular to the magnetic field; oscillations of the instantaneous center of rotation (leading center) along the lines of force; and drift of the leading center around the Earth.

The Larmor rotation has a period of:

$$\tau_1 = \frac{7 \cdot 10^{-7}}{B} (E_k + E_0) \text{ [s]} \quad (14)$$

where:  $E_k$  is the kinetic energy of the particles in MeV;  $E_0$  is the rest energy of the particle in MeV; for an electron  $E_0 = 0.51$  MeV, for a proton  $E_0 = 938$  MeV.

The Larmor frequency  $1/\tau$  of electrons near the Earth is about 1 MHz, of protons about 1 kHz, the frequency decreasing as  $I/R^3$  with increasing distance from the Earth. The Larmor radius of rotation of a particle can be determined from the relationship

$$\rho = \frac{33 \sin \alpha}{B} E_0 \sqrt{\epsilon^2 + 2\epsilon} \text{ [M]} \quad (15)$$

or  $pc = 300 B \rho$

where  $\alpha$  is the angle between the velocity vector of the particle and the direction of the magnetic field force line (pitch angle),  $\epsilon = E_k/E_0$ ,  $p_1$  is the momentum of the particle in eV/s.

The Larmor radius of electrons in the geomagnetic field does not exceed a few kilometers, whereas for protons it may reach several hundreds of kilometers.

As a particle moves along a line of force, this relationship is fulfilled:

$$\sin^2 \alpha/B = \text{const.} \quad (16)$$

From this, the intensity at the point of reflection can be determined:

$$B_{\text{ref}} = B_e / \sin^2 \alpha_e. \quad (17)$$

The period of oscillation of a particle between points of reflection is given by the formula

$$\tau_2 = 8.5 \cdot 10^{-2} \cdot L \frac{1 + \epsilon}{\sqrt{\epsilon^2 + 2\epsilon}} \cdot T(\alpha) \text{ [s]}, \quad (18)$$

where  $T(\alpha) = 1.3 - 0.563 \sin \alpha_e$ .

The longitude drift around the Earth is opposite for particles with opposing charges (electrons move toward the east, protons toward the west).

The period of drift around the Earth  $\tau_3$  is defined by the expression

$$\tau_3 = 88 \frac{1 + \epsilon}{2 + \epsilon} \cdot \frac{K}{L \cdot E_k} \text{ [min]} \quad (19)$$

where  $K = 1.25 - 0.25 \cos^2 \alpha_e$ .

$$\text{For nonrelativistic particles, } \tau_3 = \frac{44}{LE_k} \text{ [min].} \quad (20)$$

All three types of motion studied correspond to certain quantities which are conserved approximately constant for the entire time of motion of a particle, if the change in the magnetic field with time characteristic for a given type of motion ( $\tau_1$ ,  $\tau_2$ ,  $\tau_3$ ) is slight in comparison to the value of the magnetic field

$$B / \frac{\partial B}{\partial t} \gg \{\tau_1, \tau_2, \tau_3\}; \rho \frac{(\text{grad } B)}{B} \ll 1 \quad (21)$$

These quantities are the adiabatic invariants of motion in the magnetic field.

The first adiabatic invariant is the magnetic moment of particle  $\mu = P_1^2/2\gamma mB$ ; (where  $v \ll c$ ,  $\mu = E_{k1}/B$ ), where  $\gamma = 1/\sqrt{1 - (v/c)^2}$ ,  $P_1$  and  $E_{k1}$  are the components of momentum of the particle perpendicular to the magnetic field.

The second or longitudinal invariant (longitudinal action invariant) is defined as  $j = \phi mv_{||} ds = p\phi \sqrt{1 - B/B_{\text{ref}}} ds$ . Using these two invariants, as well as that  $E_k = \text{const}$  in a constant magnetic field, it can be shown that particles on one line of force but with different pitch angles describe practically the same envelope as they drift around the Earth as they would in a dipole field. Therefore, the captured radiation can be characterized by a function of two coordinates  $L$  and  $B$  [91].

Calculation of  $L$ ,  $B$  coordinates is a rather cumbersome task, performed by computer.

If the points of reflection of the captured particles are at low altitudes over the surface of the Earth, the influence of the atmosphere on the captured particles is considered by introducing the parameter  $h_{min}$ , representing the minimum altitude over the surface of the Earth at which a particle descends onto a given drift envelope  $L$ .

The third invariant  $\phi$  is defined as the magnetic flux through the surface intersecting the drift envelope of a particle around the Earth and the limited trajectory of the point of reflection of the particle. Each  $L$  envelope corresponds to a unique value of invariant  $\phi$ . In the case where  $B / \frac{\partial B}{\partial t} \approx \tau_3$ , the third invariant is not con-

served, but since in this case  $B / \frac{\partial B}{\partial t} \gg \{\tau_1; \tau_2\}$ , the first two invariants  $\mu$  and  $j$  are conserved. The magnetic field for a given  $L$  envelope will change. In this case  $E_k/B = \text{const}$ , due to the conservation of  $\mu$ , also the particle can shift to another  $L$  envelope with the corresponding change in  $E_k$ . If  $B / \frac{\partial B}{\partial t} \approx \{\tau_1; \tau_2\}$ , the equivalent pitch angle of the particle changes,  $E_k$  may change and in this case either  $\mu$  or  $j$  is disrupted. Finally, the particle enters the ionosphere. Movement of particles in the magnetic field has been reported [68, 112, 130, 133].

#### *Movement of a Particle in the Presence of an Electrical Field*

Many phenomena in the magnetosphere of the Earth can only be explained by assuming the existence of an electrical field perpendicular to the magnetic field in the plane of the Equator. In this case, drift in the direction perpendicular to the electric and magnetic fields is superimposed on the rotation of the leading center around the Earth, with the velocity

$$v_\epsilon = 10^8 \frac{\epsilon}{B}$$

where  $\epsilon$  is the electric field intensity in v/cm. The trajectory of motion of the leading center in the plane of the equator ( $\alpha_e = 90^\circ$ ) can be calculated

on the basis of the rules of conservation of energy and magnetic moment:

$$E_k + V = \text{const}, \mu = \text{const}$$

where  $V$  is the electrical potential of the given point in space. The form of the trajectories for a homogeneous electrical field [7] is shown in Figure 39. The trajectories moving at great distances from the Earth are open. The particles in closed orbits belong to the radiation bands. The critical trajectory dividing the two types (open and closed) is shown by the dotted line in Figure 39.

The branching point  $L_{cr}$  on the critical orbit can be found by assuming the electrical drift velocity  $v_\epsilon$  and magnetic drift velocity around the Earth  $v_m = \frac{2\pi R_0 L}{\tau_3}$  to be equal. For nonrelativistic particles

$$L_{cr} = 4.75 \cdot 10^{-3} \frac{E_k}{\epsilon}$$

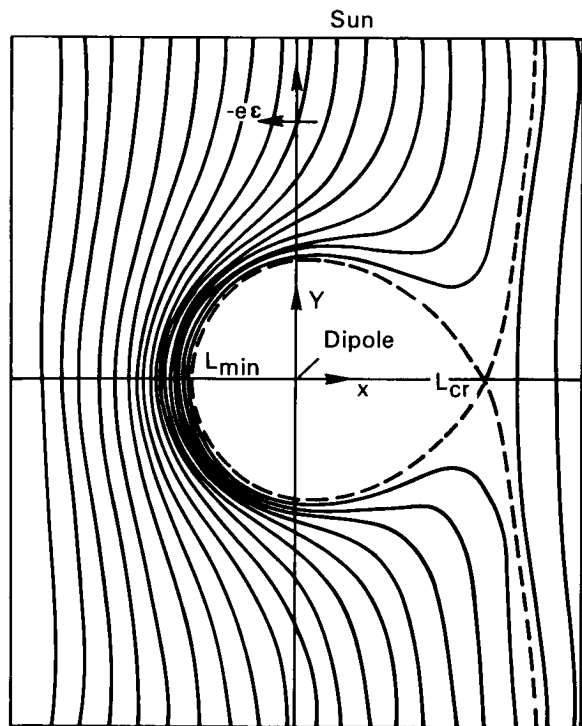


FIGURE 39.—Drift of electrons in equatorial plane of magnetic dipole field with superimposed homogeneous magnetic field in a homogeneous electric field parallel to the equatorial plane. Solid lines show typical trajectories of center of rotation.

From this formula, particles with energies at a given distance can be defined as belonging to the radiation bands. On the other side, particles pass at a minimum distance from the Earth  $L_{min} = L_{cr}/1.78$ .

### *Theoretical Models, Earth's Magnetic Field*

The coordinates  $L$  and  $B$  are unsuitable for analysis of captured radiation at  $L > 6$ , where the influence of the solar wind on the Earth's magnetosphere is significant. The effect of the wind causes the trajectory of movement of captured particles to depend on local time. More complex models of the geomagnetic field must be used to study the motion of particles.

The theoretical models of the magnetosphere have the purpose of analytic or numerical description of the area where the source of the magnetic field is the terrestrial magnetic dipole. These models are necessary for qualitative description of various processes occurring in this field. The bases of such processes are the radiation bands of the Earth, polar auroras, dynamics of magnetospheric perturbations, phenomena in the high-latitude conjugate points, and propagation of low-energy cosmic rays.

Two models of the magnetosphere are theoretically best developed; one empirical model has been constructed.

*The Williams-Mead model* [145] is based on consideration of currents at the boundary of the magnetosphere by spherical harmonics, as well as internal field sources. A plate with a homogeneous point in the plane of the geomagnetic equator on the night side of the Earth imitates the neutral layer of the tail of the magnetosphere.

For this model there are four parameters:  $R_s$ —the distance from the center of the Earth to the subsolar point of the boundary of the magnetosphere,  $R_h$  and  $R_f$ —distances from the Earth to the near and far edges of the plate with the current, and  $B_t$ —the field of the plate with the current.

Usually,  $R_s = 10R_0$ ,  $R_h = 10R_0$ ,  $R_f = 200R_0$  and  $B_t = 15\gamma$ .

The two-dipole model [7] is based on the possibility of imitating the perturbing effect of the solar

wind, under certain assumptions, by an additional dipole. The field of the neutral layer is imitated by the field of a plate with current. Characteristic for this model are:  $\alpha$ —the distance from the Earth to the perturbing dipole,  $\beta$ —the value showing the number of times by which the perturbing dipole is greater than the terrestrial dipole  $M_{pd} = \beta M_e$ .  $R_h$  and  $R_f$  are the distances to the near and far boundaries of the plate with current from the Earth.  $B_t$  is the field of the plate with current. For ordinary conditions, when  $R_s = 10R_0$ ,  $\alpha = 33-40R_0$ ,  $\beta = 12.7-27$ ,  $R_h = 11R_0$ ,  $R_f = 51R_0$ ,  $B_t = 16\gamma$ .

*Empirical model of the magnetosphere* [48]. So much data has recently been produced on the magnetic field at distances  $> 5R_0$ , that it is possible to construct an empirical model of the magnetosphere, which has been done by Fairfield [48].

Calculation of various theoretical models has been made to explain the position of certain characteristic points of the magnetosphere and the topology of motion of charged particles in the magnetosphere. In the field and in models in the equatorial plane, the magnetic field is greater on the day side than on the night side (see Figs. 40 and 41). However, in the figure, the value of the field near the boundary is different for all models, in spite of the approximately identical position of the magnetosphere's boundary. The form of the magnetic lines of force near the boundary of the magnetosphere differs notably for different models.

Figure 40a, b, c, shows the meridional cross section of the magnetosphere for all three models in the day-night direction. The qualitative similarity of all the models is evident but the approximation of the infinitely thin plate with current is too rough for description of the field near the neutral layer; also evident is the different position of the neutral points at the boundary of the magnetosphere with the day side of the Earth and their projection over the lines of force on the Earth.

The figure shows good agreement of the line of force configuration for various models, although there is some quantitative divergence.

*Envelopes of magnetic drift.* The study of the motion of captured charged particles around the Earth indicates that  $R \lesssim 5 R_0$ , the influence of

external field sources (currents at the boundary and in the tail of the magnetosphere), can be ignored, and the  $L$ ,  $B$ , coordinates described above can be used. In this case, particles located on a single line of force and having different pitch angles drift around the Earth practically around a single drift envelope. At great distances from the Earth, the drift envelopes split.

Figure 42 shows the distribution of particles of various energies in the magnetosphere of the Earth [113]. Four areas are easily distinguishable.

*The area of the polar cap (area I).* The lines of force departing from the day side of the Earth at latitudes  $\lambda \geq 78^\circ$  and on the night side at lati-

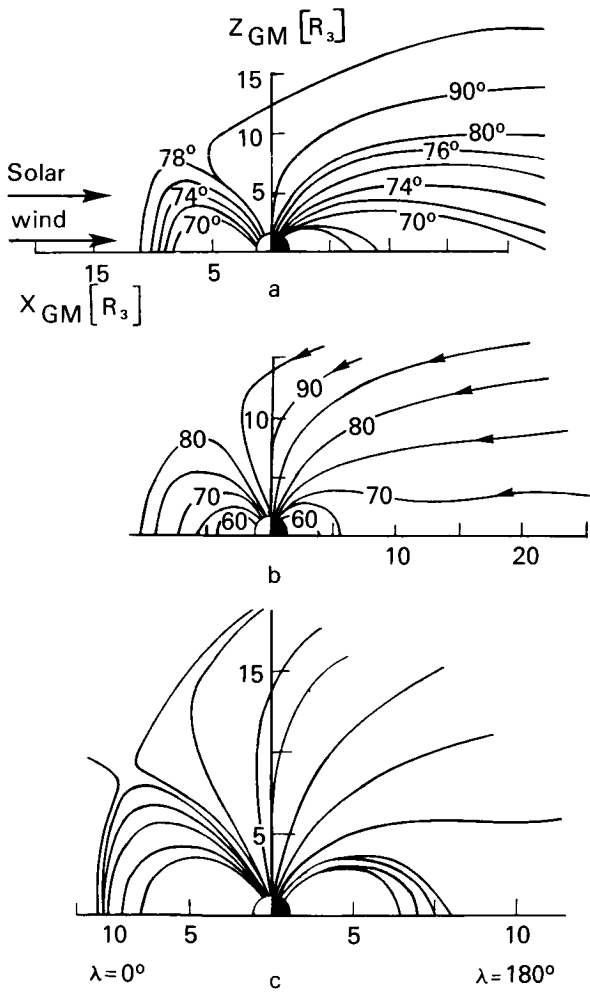


FIGURE 40.—Contours of even geomagnetic field intensity in equatorial plane [2]. (a) For empirical models; (b) for Williams-Mead models; (c) for two-dipole model.

tudes  $\lambda \geq 73^\circ$  move out into interplanetary space or close far from the Earth. Here it is primarily a plasma of ionospheric origin with temperature  $T \approx 3-5 \cdot 10^4$  °K, which moves out to great altitudes along the magnetic lines of force and, apparently, can extend into interplanetary space.

*The area of the plasma layer on the night side*

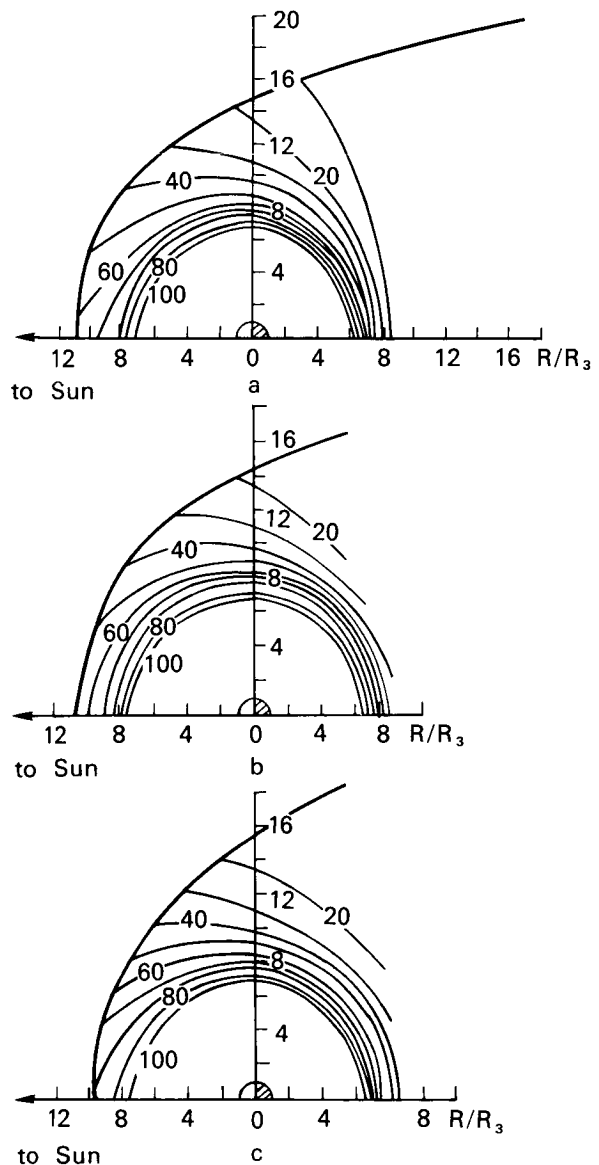


FIGURE 41.—Magnetic field of the Earth, perturbed by solar wind, in meridional day-night cross section. Latitudes of intersection of the surface of the Earth by lines of force—(a) empirical model [48]; (b) Williams-Mead model [145]; (c) two-dipole model [7].

*and neutral points on the day side of the Earth (area II).* On the day side, this area is located at  $\lambda \approx 76^\circ\text{--}80^\circ$ , where the neutral point is projected along the magnetic lines of force (latitude of polar drop on the day side of the Earth). On the night side this area is projected along the magnetic lines of force at latitude  $\lambda \approx 68^\circ\text{--}73^\circ$  (latitude of polar drop on the night side of the Earth). The source of the plasma of this area is the solar wind, penetrating into the magnetosphere of the Earth. The mean energy of particles in this area fluctuates from a few hundred eV to several keV.

*The area of the plasmosphere (area III)* is located at the center of the magnetosphere of the Earth, extending from the ionosphere to  $4\text{--}5 R_\oplus$ , limited on the high latitude end by  $\lambda \approx 60^\circ\text{--}65^\circ$ . This area is characterized by increased concentration of electrons and ions of ionospheric origin. Near the ionosphere, the concentration of ions  $N_i \approx 10^5 \text{ cm}^{-3}$ , while at a distance of  $4 R_\oplus$  the concentration decreases to about  $10^3 \text{ cm}^{-3}$ . The energy of particles is about a few eV.

*Area of the radiation belts of the Earth (area IV).* The area of the magnetosphere is populated by particles with energies of several tens of keV to hundreds of MeV. A characteristic feature of the particles at these energies is rapid magnetic drift around the Earth in a time much less than the rotation period of the Earth around its axis.

If area I is related to the open lines of force of the geomagnetic field, areas II and III form

under the influence of the weak electric field, about  $2\text{--}4 \cdot 10^{-6} \text{ V/cm}$  in the plane of the equator, directed from morning toward evening.

The source of ions in area III is within the magnetosphere (ionosphere of the Earth), while the source of ions in area II is outside the magnetosphere (solar wind).

For particles of area IV, the influence of the electric field on their drift trajectories can be ignored. The boundary of this area is at a distance where the electric field carries the particles beyond the limits of the magnetosphere. From the standpoint of dynamics of the magnetosphere and effects on space objects, characteristics of particles in areas II and IV are most important.

The most detailed measurements of plasmas in the tail of the magnetosphere have been performed by the Vela and OGO satellites. Information on direct measurements of the plasma near the neutral point have not yet been published, but data are available on low-energy particles, produced near the Earth on lines of force connecting with the area of the neutral points. Based on these measurements, the position of area II in the magnetosphere of the Earth is shown in Figure 42. On the night side of the Earth, the neutral layer of the magnetosphere tail is surrounded by a plasma layer with a thickness  $h \approx 4 R_\oplus$  near the midnight meridian; closer to the morning and evening sides, the thickness of the layer increases to  $h \approx 6 R_\oplus$ . The streams of electrons can reach values of  $10^9 \text{ electrons/cm}^{-2} \text{ s}^{-1}$ . The mean energy of electrons fluctuates from about 10 eV to about 5 keV.

During magnetic disturbances, the thickness of the plasma layer first decreases to  $h \approx 1 R_\oplus$ , then increases to  $h \geq 6 R_\oplus$  by the end of the geomagnetic disturbance (during which time magnetic disturbances develop at latitudes  $\phi \approx 75^\circ\text{--}83^\circ$ ). During this time, electrons appear in the plasma layer with energies of at least 40 keV.

Plasma-layer particles drifting in the crossed electric and magnetic fields may reach the morning, evening, and day sides. From the day side, particles of the solar wind may penetrate into the magnetosphere of the Earth through the neutral points. Although the fluxes of particles have not yet been measured near the neutral points, at altitudes of several hundred to several

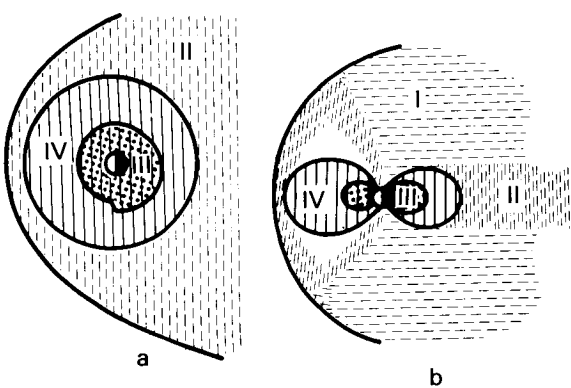


FIGURE 42.—Distribution of charged particles in magnetosphere of the Earth; (a) equatorial cross section; (b) meridional cross section.

thousand kilometers at latitudes  $\phi \approx 75^\circ - 83^\circ$ . Electron fluxes have been recorded with  $E_e > 100$  eV, reaching values of  $N (E > 100 \text{ eV}) \approx 10^8 \text{ cm}^{-2} \text{ s}^{-1} \text{ sr}^{-1}$  with a spectrum of  $N (> E) \approx E^{-1}$ . Since the fluxes are isotropic, it can be assumed that they have the same value in the area of the neutral points. The energy density of these electrons corresponds to that of the magnetic field with an intensity of  $5 \gamma$ .

In area II, electron fluxes with  $E_e \gtrsim 100 \text{ keV}$  are also sometimes observed. If electrons at this energy level, observed on the morning and day sides, can be accelerated in the tail of the magnetosphere, the origin of the electrons in the plasma layer is uncertain. Observation of electrons of such energies near the morning side is more probable than near the evening side.

The spectrum of the electrons from the zone of the polar aurora on the night side is frequently similar to the spectrum of electrons in the plasma layer, indicating that this is the same area. The polar auroras are closely related to ionospheric and geomagnetic disturbances caused by various manifestations of solar activity, which will be discussed in the section, SUN-EARTH CONNECTIONS.

### Radiation Belts of the Earth

The area of radiation belts of the Earth is shown in Figure 43 (area IV). Since high-energy particles can be recorded outside this area as a

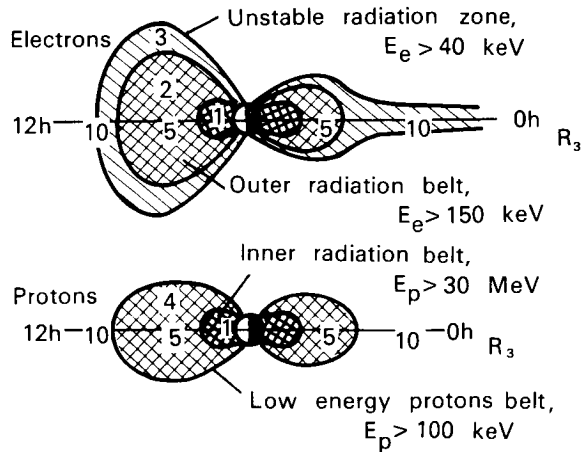


FIGURE 43.—Structure of radiation belts.

result of various physical factors, the placement of electrons with energies of several tens of keV differs from the placement of the areas of the belts. Figure 43 shows schematically the areas of recording high-energy particles in the magnetosphere of the Earth. The area of distribution of electrons with energies  $> 40 \text{ keV}$ , noted by the slanted shading, does not belong to the radiation belt, since the drift orbits in this area for particles are open. Therefore, the high-energy particles at great distances from the Earth are not particles of the radiation belts, but are expelled from the magnetosphere in a time less than 1 period of drift around the Earth.

Two areas of radiation belts are mentioned in the literature: the inner and outer radiation belts [68, 130]. Although this separation was initially caused by imperfections in the detectors used to study the radiation belts, it was later found that for certain groups of particles this separation does have a physical sense. This will be discussed in greater detail.

### Protons of Earth Radiation Belts

The distribution of protons of various energies, from  $100 \text{ keV}$  extending to  $500 \text{ MeV}$  at  $L \leq 6$  [144], is shown in Figure 44. For  $L \geq 6$ , the distribution of particles becomes a function of local time. Figure 44 shows that as the energy increases, the maximum intensity shifts to lower  $L$ , at which the spectrum of protons becomes harder. The meridional cross section of the belt of pro-

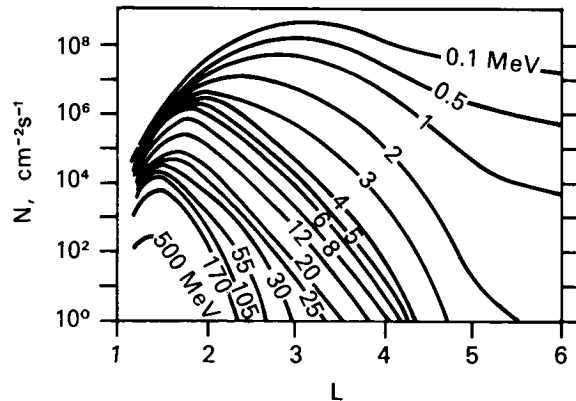


FIGURE 44.—Radial profiles of time-averaged global intensity of protons with energies over a fixed value in the plane of the geomagnetic Equator [144].

tons with energies  $E > 1.0$  MeV and  $E > 30$  MeV is shown in Figure 45.

Important characteristics of the radiation belts include the distribution in the plane of the Equator, and distribution of particles along lines of force, usually approximated by the function  $N(B)_{L=\text{const}} \approx B^n$ . Analysis of the data shows that for low-energy protons ( $E_p < 30$  MeV), this approximation satisfies the experimental data well,  $n$  increasing with decreasing  $L$ . For high-energy protons, the dependence of intensity on  $L$  is more complex. Protons of these energies are more concentrated in the plane of the Equator; with increasing  $L$ , the altitude course increases. Examples of altitude courses for protons with  $E > 1$ ,  $E > 30$  and  $E > 110$  MeV are presented in Figure 46 [139]. Analysis of the spectra shows that for low-energy protons, the energy spectrum is well-approximated by an exponential function:

$$N(>E) \approx \exp(-E/E_0) \quad (22)$$

where  $E_0 \approx L^{-3}$  (for  $L=6$ ,  $E_0 \approx 60-100$  keV). High-energy protons have an exponential energy spectrum  $N(>E) \approx E^{-x}$ .

At the maximum of the belt ( $L \approx 1.5$ ),  $x=1$ ; at  $L=2$ ,  $x \approx 2$ .

These peculiarities of high- and low-energy protons are explained by their difference in origin. It is assumed that their origin differs; the source of high-energy protons is neutrons in the cosmic ray albedo, interacting with the atmosphere of the Earth; the source of low-energy protons is the solar wind. The protons of the solar wind are captured by the magnetosphere of the Earth and, diffusing into the magnetosphere, fill

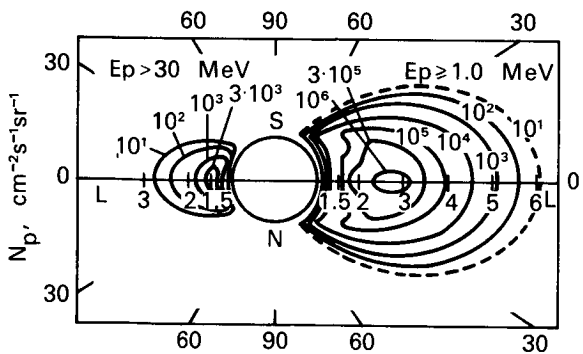


FIGURE 45.—Meridional cross section of belt of protons with energies  $E_p > 1.0$  MeV and  $E_p > 30$  MeV.

the core of the magnetosphere. The area of protons with  $E_p < 50$  keV, detected on the evening side of the Earth, can be interpreted as an intermediate stage between the proton belt and solar wind. Figure 47 shows the distribution of protons in the radiation belt and protons with  $E_p < 50$  keV as functions of  $L$  [144]. The intensity maximum of protons with  $E_p < 50$  keV is observed at  $L=7-8$ . During magnetic storms, the intensity of protons with  $E_p < 50$  keV at the maximum increases by an order of magnitude or more, and the maximum is shifted to  $L \approx 4$ . Protons with  $E_p \leq 50$  keV at this time cause a  $D_{st}$  variation in the magnetic field.

The death of protons is due to ionization losses in the upper layer of the atmosphere.

#### $\alpha$ -Particles in Radiation Belts Around the Earth

Since the solar wind contains both protons and  $\alpha$ -particles, it is natural to assume that the radiation belts of the Earth would also contain  $\alpha$ -particles. However, their flux should be quite low, since ionization losses of  $\alpha$ -particles are greater than those of protons and the concentration of  $\alpha$ -particles in the solar wind is 10 times less than the concentration of protons.

A profile of the belt of  $\alpha$ -particles, according to Soviet data [53], is shown in Figure 48, while Figures 49 and 50 show the spectrum and relative intensity of  $\alpha$ -particles. These figures show the data of other authors as well [144].

*Electrons in the radiation belts of the Earth.* The distribution of electrons of various energies in the plane of the Equator in 1966 is shown in Figure 51. The area where captured electrons are recorded is divided into the external and internal radiation belts. The boundary between these belts follows approximately  $L=3$ , where electrons with energies of several hundred keV have minimal lifetimes in comparison to the surrounding  $L$  envelopes.

The electron source in the inner radiation belt is neutrons of the cosmic ray albedo, interacting with the atmosphere of the Earth. During the strongest magnetic storms, particles are injected not only into the external radiation belt, but also into the internal radiation belt at  $L \geq 2$ . Subse-

...ILITY OF THE  
RE IS POOR

quently, during the process of diffusion, these electrons may penetrate to even lower  $L$ . The data relating to the inner belt (Fig. 51) can char-

acterize the natural electrons of the inner radiation belt [147]. By 1966, electrons with  $E_e \leq 690$  keV injected by the Starfish explosion had

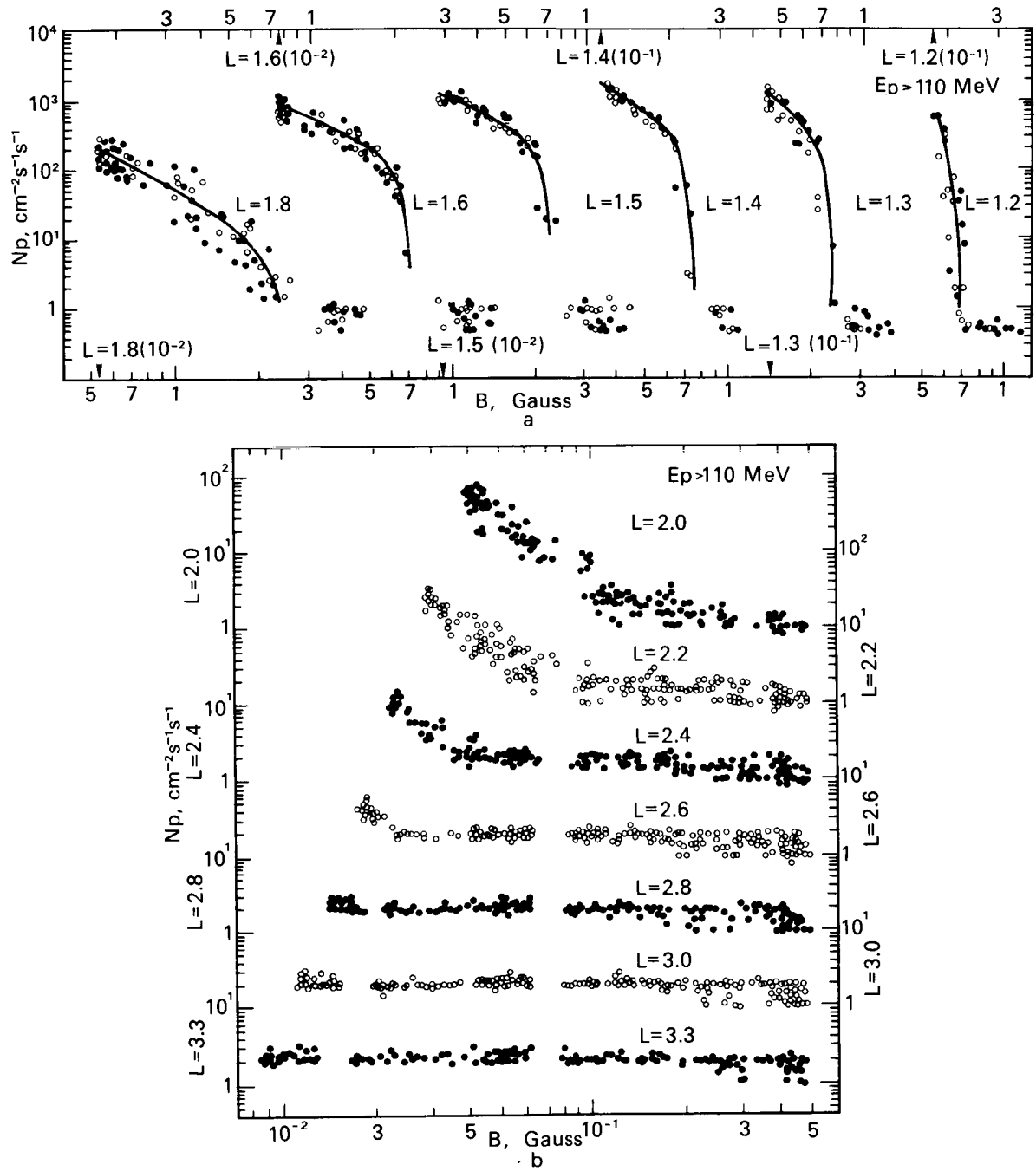


FIGURE 46.—Distribution of protons with energies  $\geq 110$  MeV with respect to  $B$  in various  $L$  envelopes (from  $L = 1.2$  to  $L = 3.3$ ) according to data from electron satellites. Light points—February; dark points—July 1964. (a) Area  $1.2 \leq L \leq 1.8$ ; (b) area  $2.0 \leq L \leq 3.3$ .

almost completely disappeared. The altitude course of electrons in the inner belt can be approximated by the expression  $N \approx B^{-1}$ .

The distribution of electron fluxes with energy  $E_e \geq 150$  keV in the outer radiation belt in the

plane of a meridian is presented in Figure 52 [137]. The electrons of the solar wind are the sources of electrons for the outer radiation belt whose maximum intensity is at  $L = 4-5$ .

The altitude course of the electrons in the outer belt becomes weaker with transition from the outer boundary to the gap. As  $L$  changes from 6 to 4, the mean altitude course changes from  $N \approx B^{-1}$  to  $N \approx B^{-0.3}$ . If a magnetically quiet situation is retained for 4-5 days, at  $L \sim 4$  the altitude course disappears and  $N = \text{const}$  with variations in altitude of  $\sim 6000$  km to the Equator.

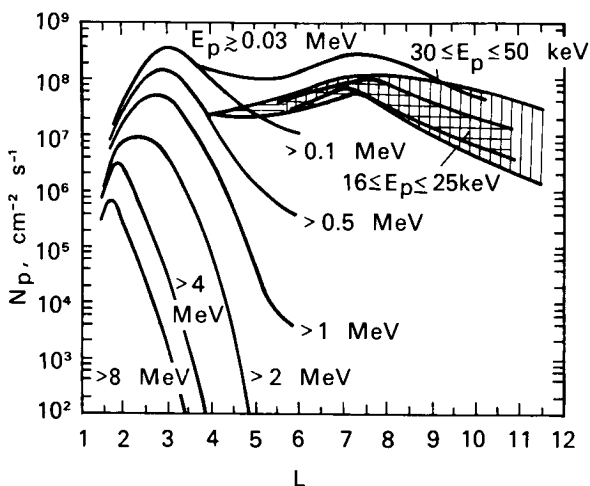


FIGURE 47.—Radial profiles of equatorial omnidirected flux of low-energy protons.

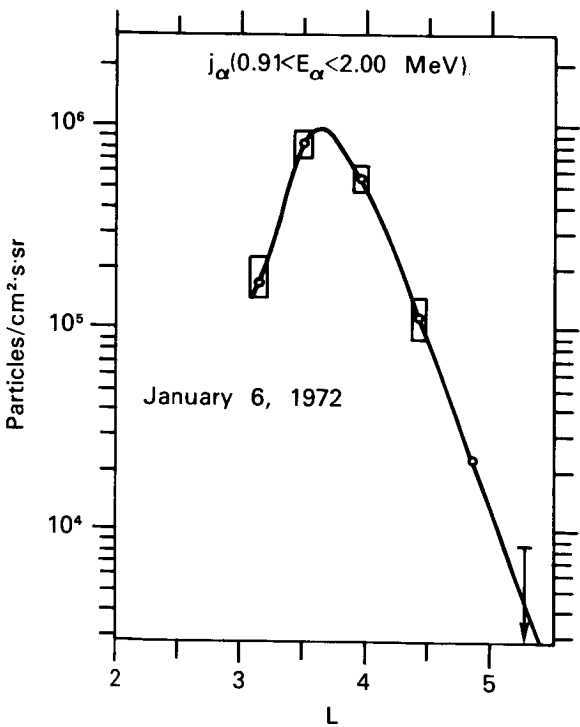


FIGURE 48.—Equatorial cross section of belt of low-energy  $\alpha$ -particles.

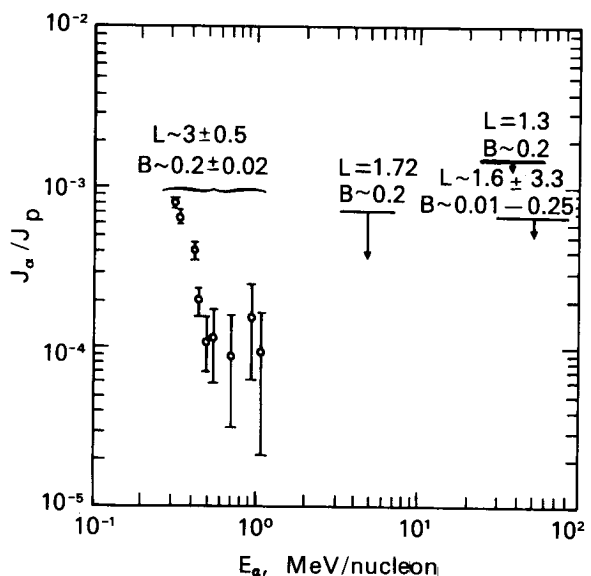


FIGURE 49.—Data on energy spectrum of  $\alpha$ -particles in radiation belts.

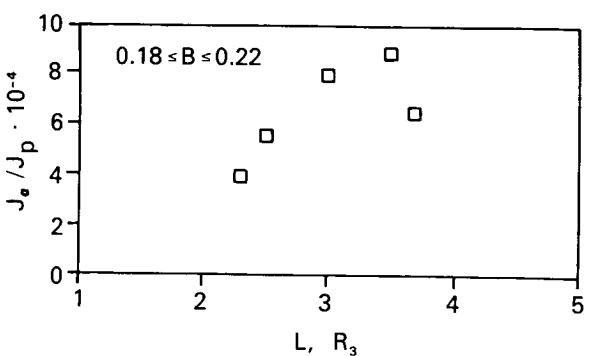


FIGURE 50.—Relative intensity of  $\alpha$ -particles with energies over 0.31 MeV/nucleon as a function of  $L$ .

### Sources of Particles in Radiation Belts

The particles causing the Earth's radiation belts have already been noted; consideration will be given to the mechanisms by which the radiation belts of the Earth are filled, and these can be divided into two groups:

- slow continuous filling of the radiation belts with particles;
- rapid "impulse" injection of particles.

The slow, continuous filling of the radiation belts with high-energy particles occurs as neutrons of the cosmic ray albedo interact with the atmosphere of the Earth. This process is the source of particles for the proton belt with energies  $E > 30$  MeV and the electron belt at  $L \leq 2-3$ . Many calculations have been made of the intensity of protons in the inner radiation belt, the source of which is the albedo neutrons [68, 130]. The actual altitude course of intensity differs significantly from the calculated course. Apparently, neither the change or flux of neutrons with altitude, nor the mechanism of proton death (usually only ionization losses are considered) is well-known.

This filling also occurs in the process of diffusion of particles from the outer areas of the magnetosphere to its core. The theory of the process

has been well-developed [40, 106, 130]. It is assumed that the diffusion of particles occurs during sudden impulses of the geomagnetic field, frequently recorded by magnetic observatories. The diffusion of particles may also occur during magnetic substorms. This process leads to acceleration of the diffusion of electrons at low  $L$  ( $L < 2$ ).

The change in the profile of the electron belt with  $E_e > 1.6$  MeV in the process of diffusion is shown in Figure 53 [50]. The leading edge of the belt during the process of diffusion moves at  $v = 33 \cdot 10^{-7} L^9 R_e$  per day. The rate of movement of the maximum of the belt is approximately one-fourth as great. This figure shows the dependence of the rate of diffusion of electrons with energies of 0.15–5 MeV on  $L$  [139].

During the process of diffusion, the proton belts of the Earth with  $E_p < 30$  MeV and the outer electron belt are formed. The maximum intensity of particles of various energies is formed at the  $L$  for which diffusion time for the boundary of the belt is approximately equal to the lifetime of the particles.

Rapid increases in the intensity of particles in the belt occur during magnetospheric substorms, and involve strengthening of the large-scale electric field in the terrestrial magnetosphere. Three modifications of the acceleration mechanism can be noted.

First, particles are injected from the tail of the magnetosphere under the influence of a strengthened electric field. Higher energy particles in this case appear in more distant drift envelopes; electrons with  $E_e \gtrsim 40$  keV appear at  $L \geq 4.0$ . Drift orbits of accelerated particles under the influence of the reinforced electric field are open, become closed only when it weakens.

Second, particles of the belt are redistributed under the influence of relatively weak electric fields, changing with time. The drift orbits of the particles remain closed in this case, but rapid diffusion of the particles occurs to the  $L$  envelope, for which the period of rotation of the particles around the Earth  $\tau_3$  is equal to the period of influence of the electric field, since

$\tau_3 \sim \frac{1}{E_k L}$  so that high-energy particles increase their intensity less than lower energy particles.

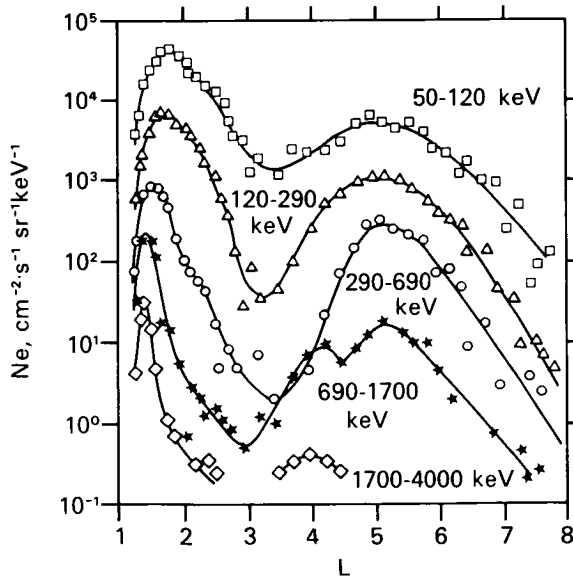


FIGURE 51.—Radial profiles of electron intensity at  $L \geq 1.75$ .

Third, at the beginning of any magnetospheric substorm, the field in the tail of the magnetosphere is increased by transition of lines of force from the core of the magnetosphere into the tail. Upon completion of a storm, the lines of force return. The field at the tip of a line of force increases and the energy of particles located on a given line of force increases correspondingly ( $E/B = \text{const}$ ). At the end of a magnetospheric substorm, an accelerating induction electric field appears in the tail of the magnetosphere [146].

The mechanism of development of the quasi-stable electric field is not yet clear. Possibly, charges separate at the boundary of the magnetosphere. They may arise in the region of the proton belt, where the current responsible for the  $D_{st}$  variation of a magnetic storm is formed (to be discussed later).

### *Death of Particles in the Earth's Radiation Belts*

The general picture of the intensity of particles in the radiation belts drawn above reflects the state of dynamic equilibrium between the death of particles and their arrival. The mechanisms of death for particles of various types are different.

For protons and  $\alpha$ -particles, the basic mechanism of death is a decrease in the energy of the particles due to ionization losses upon interaction with the traces of atmosphere at high altitudes. The disruption of the first adiabatic invariant is significant only for protons with  $E_p \geq 100$  MeV.

For electrons, Coulomb scattering is more effective than ionization losses. It defines the lifetime of electrons at less than 1.5. For higher  $L$ , the lifetime decreases, indicating that there is a new, more effective mechanism leading to departure of electrons from the belts. This mechanism is scattering of electrons on low-frequency waves such as whistling atmospherics and natural cyclotron radiation.

The decrease in intensity of electrons in various  $L$  envelopes during magnetically quiet periods can be approximated by a function such as:

$$N \approx \exp(-t/\tau) \quad (23)$$

where  $\tau$  is called the lifetime of the electrons. A summary of the lifetime of electrons in various

$L$  envelopes is presented in Figure 54, which shows the dependence of lifetime of electrons with  $E_e \geq 1.2$  MeV and  $E_e \geq 300$  keV on  $L$  [144].

The intensity at which the flux of particles is reduced by a factor of 2 in 1 day is called the limiting intensity. At intensities near  $N_{np}$ , the lifetime of electrons with  $E_e > 40$  keV and  $E_e > 300$  keV drops sharply. The decrease in intensity is not exponential, but a power function:  $N \approx t^{-1}$  [81]. When the intensity reaches the value  $N \approx \frac{N_{np}}{0.69} \tau$ , the power drop in intensity becomes exponential with lifetime  $\tau$ . The decrease in the lifetime of electrons with an increase in intensity is related to the development of cyclotron instability and scattering of electrons on their own cyclotron radiation. The ionosphere in this case has a stabilizing influence on the belt, since it absorbs the cyclotron radiation of electrons with a frequency near the low-frequency radio radiation band. The death of particles occurs primarily on the night side of the Earth, where the ionization density is less and the absorption of cyclotron radiation is weaker.

The scattering of electrons can be conveniently observed on the basis of the accumulation of particles in forbidden drift trajectories, which descend into the denser layers of the atmosphere or to the Earth.

Figure 55 shows the change in intensity of electrons with  $E_e \geq 400$  keV at  $L=2$  at the drift trajectory with  $h_{\min}=100$  km. It can easily be seen that at the departure from the anomaly, the flux of such particles is slight and increases with drift around the Earth.

The peculiarities of the pouring of electrons with  $E_e \sim 100$  keV around the entire Earth can be seen in Figure 56, likewise the increased pouring of electrons during the night hours at  $L \geq 2$  to the east of the Brazilian anomaly ( $0^\circ$ – $60^\circ$  W), a phenomenon which is related to conical instability. This pouring and death of particles occurs constantly even under quiet geomagnetic conditions. In addition to this stable death of particles, sporadic pourings of electrons and protons are observed in the belts. These phenomena are related to geomagnetic, ionospheric, and solar disturbances and will be described in the section on Sun-Earth connections.

## SUN-EARTH CONNECTIONS

### Geomagnetic Activity—Storms and Ionospheric Disturbances

Most geophysical phenomena in the upper atmosphere of the Earth are directly or indirectly related to active phenomena on the Sun. The most characteristic manifestations of this connection are geomagnetic storms, arising as a result of interaction of streams of solar plasma from flares with the magnetic field of the Earth. Geomagnetic storms, together with the geo-

magnetic and ionospheric disturbances accompanying these storms, form a complex group of phenomena called geomagnetic activity. Typical manifestations of geomagnetic activity are phenomena such as the polar auroras, absorption of cosmic noise in the polar caps, and atmospheric reduction and disturbances in the F layer of the ionosphere.

Ionospheric disturbances and polar auroras are among the outstanding phenomena related to geomagnetic storms. Study of the behavior of the ionosphere relates directly to determination of

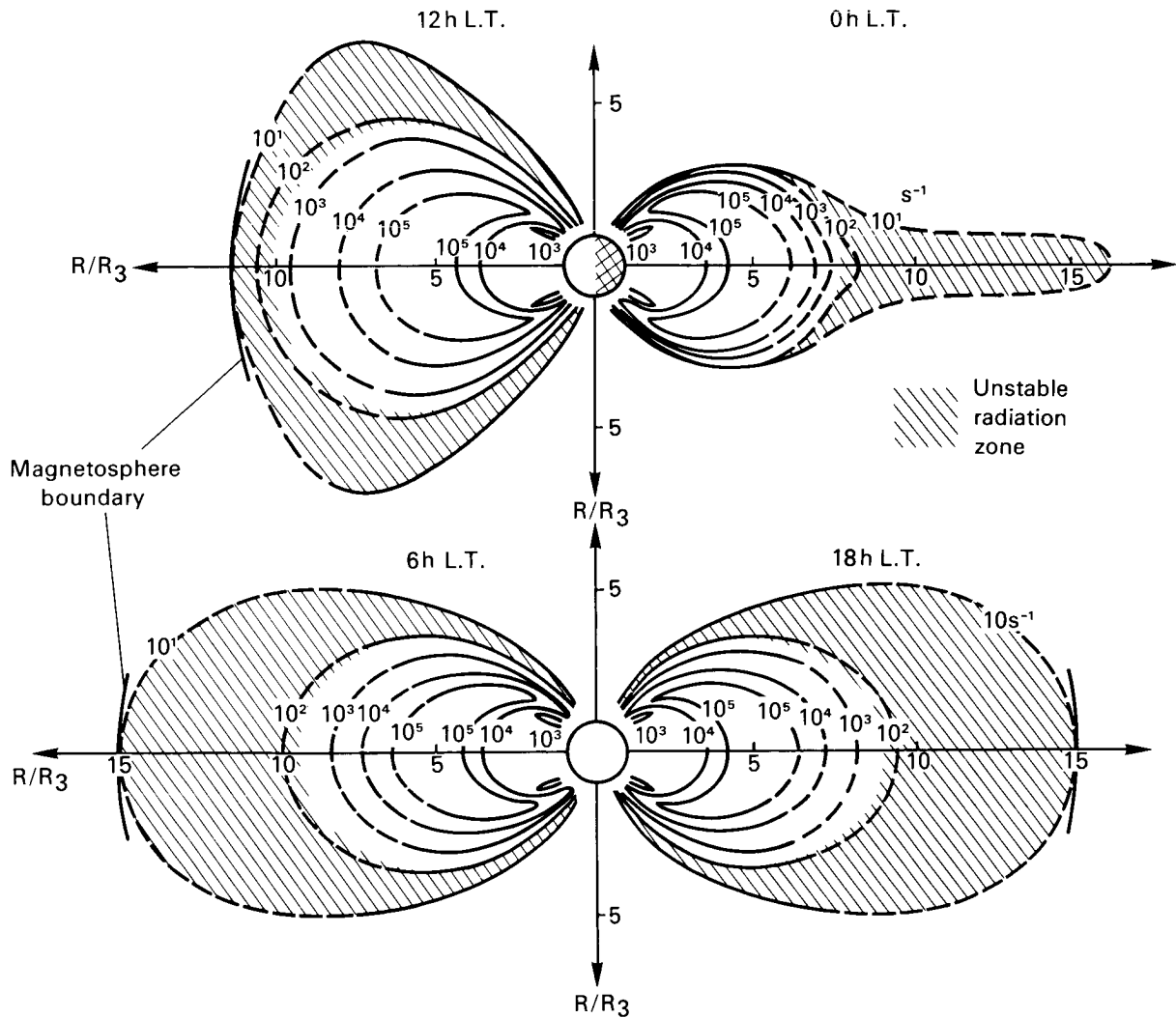


FIGURE 52.—Distribution of electrons with energies  $E_e \geq 150$  keV in the terrestrial magnetosphere. To produce flux of electrons per  $\text{cm}^2 \cdot \text{s}$ , figures by curves must be multiplied by a factor of about 100. Zone of unstable radiation shaded. Top—cross section through day-night line; bottom—morning-evening.

the mechanism of geomagnetic storms, since the primary current systems responsible for magnetic disturbances apparently lie in the ionosphere, while study of the auroras provides unique information on pouring of particles from the magnetosphere.

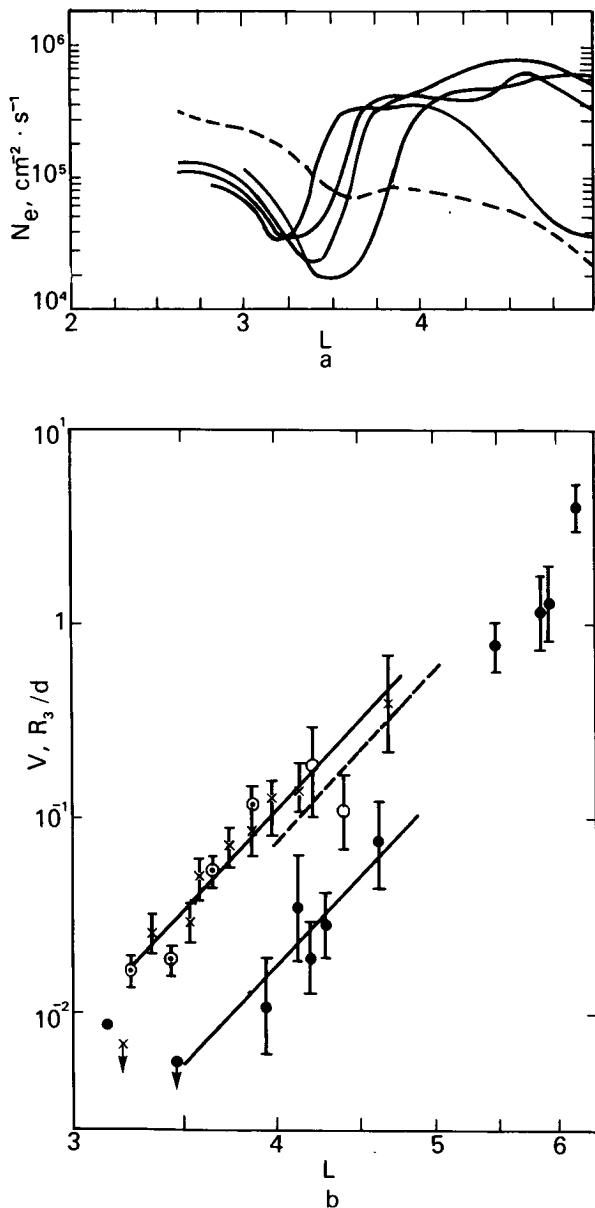


FIGURE 53.—(a) Change in profile of intensity of electrons with  $E_e > 1.6 \text{ MeV}$  as a result of radial diffusion [39]. (b) Velocity of radial diffusion of electrons with energy  $E \sim 0.15 + 50 \text{ MeV}$  as a function of  $L$  [81].

Geomagnetic activity is complexly dependent on a number of parameters of the interplanetary medium, the magnetosphere, and the ionosphere, and on the physical processes which occur in them. Its most common measure is the magnetic index, represented as  $K$  or  $A$  (depending on the

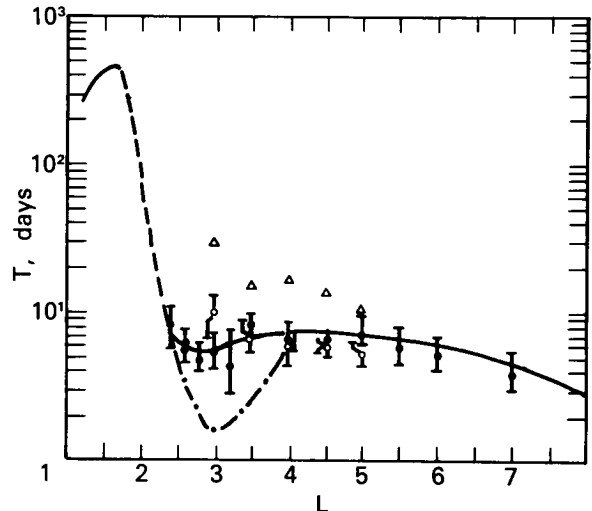


FIGURE 54.—Lifetime of electrons with  $E_e > 300 \text{ keV}$  and  $E_e > 1.2 \text{ MeV}$  as a function of  $L$ .  $\triangle$   $> 1.2 \text{ MeV}$ ;  $\circ$   $> 300 \text{ keV}$  (Explorer 26);  $\bullet$   $> 300 \text{ keV}$  (1963–38°C). Dot-dash line, possible reduction in lifetime; solid line, lifetime of electrons with  $E_e > 300 \text{ keV}$ ; dashed line, no data available.

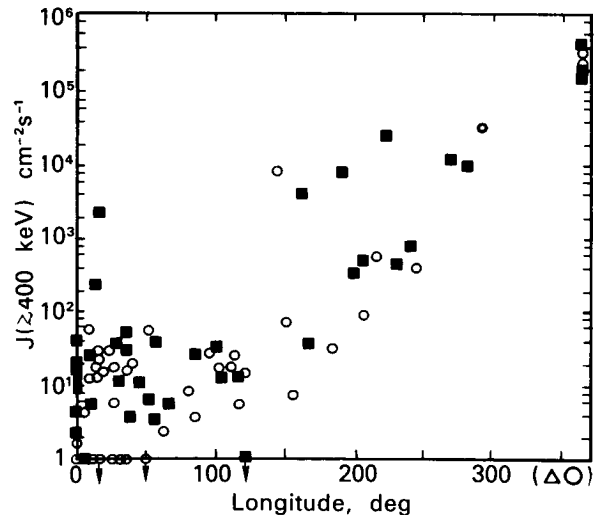


FIGURE 55.—Flux of electrons with  $E_e > 400 \text{ keV}$  at  $L = 2.0$  as a function of longitude, to east of Brazilian anomaly.  $\triangle$   $\circ$ , longitude interval between point of measurement and point  $h_{\min} = 100 \text{ km}$ ,  $\circ$   $- T_m \sim 12$ ,  $\blacksquare$   $- T_m \sim O_h$ .

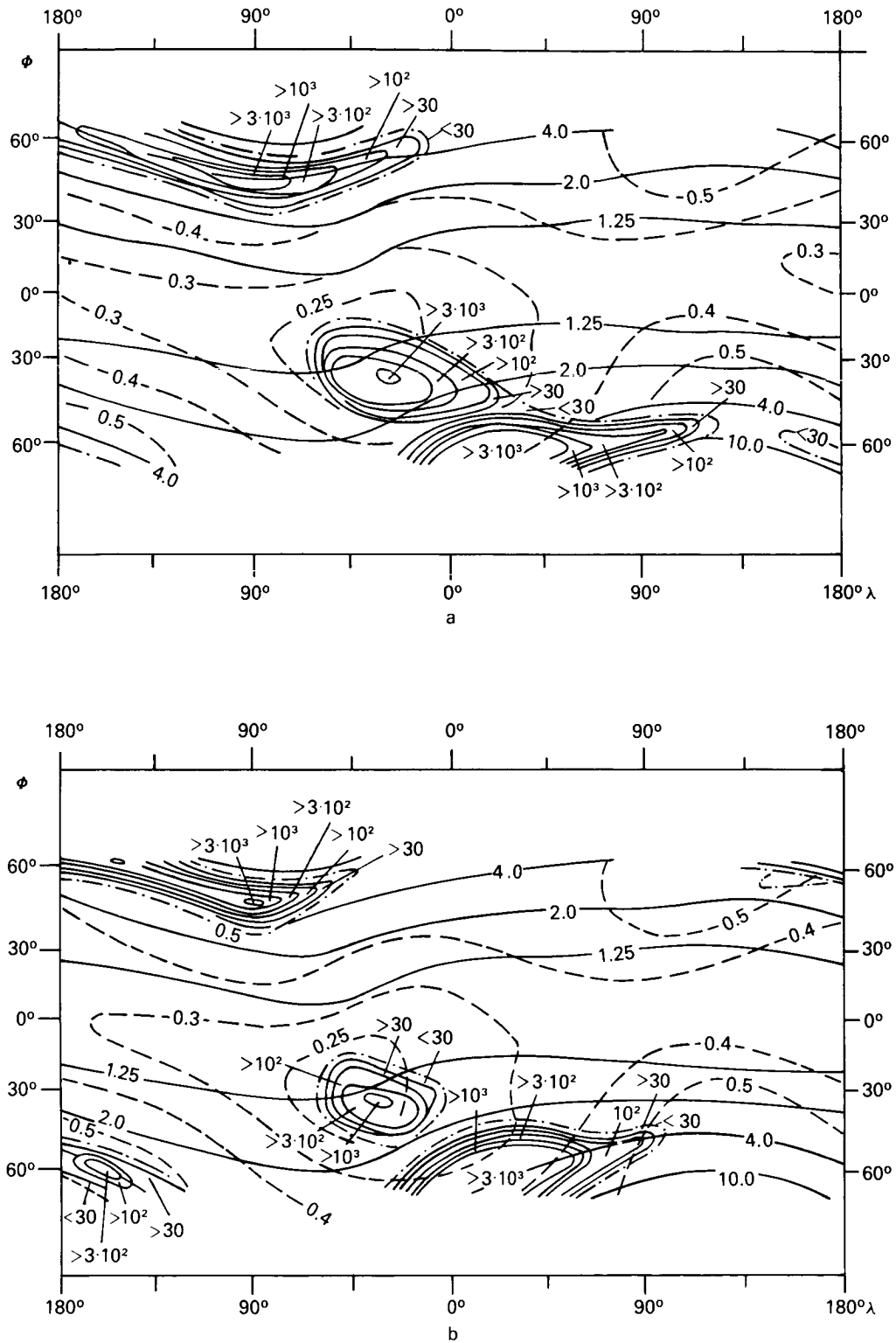


FIGURE 56.—Distribution of precipitation of electrons with  $E_e > 100$  keV for local time. (a) LT 18:00–5:00 (night); (b) LT 6:00–17:00 (day). Intensity is expressed in particles/cm · s.

use of the quasi-logarithmic or linear scale), characterizing the maximum change in the geomagnetic field over 3 hours.

Variations in geomagnetic activity observed are both periodic (27-day and 11-year variation) and sporadic in nature. The 11-year variation is closely related to the cycle of solar activity and correlates well with it; the 27-day variation indicates a relationship between the phenomena observed and certain active areas on the Sun. The perturbing agent may be either recurrent corpuscular streams from the active areas, or hard electromagnetic radiation. Increases in geomagnetic activity are observed as the Earth intersects streams of high-velocity solar plasma. Some increase in activity is observed as the Earth crosses the boundary of the sector of the interplanetary magnetic field where the velocity of the solar plasma frequently reaches values of 700–850 km/s. As the sector boundary is passed, a change is recorded in the intensity of cosmic rays, the index of magnetic activity A increases, and the intensity of captured electrons in the outer radiation belt changes. This represents the influence of the quasi-stable sectorial structure of the interplanetary magnetic field on geomagnetic activity. Study of the interaction of the solar wind with the magnetic field of the Earth has been reviewed [26, 208].

#### *Interaction of the Solar Wind with the Earth's Magnetic Field*

The solar wind and clouds of solar plasma, striking the magnetic field of the Earth as they propagate from the Sun, deform it in a way so that on the Sun side it is somewhat compressed, while on the opposite (shadow) side it extends outward, forming a long, geomagnetic tail. The particles of the solar plasma are partially deflected by the geomagnetic field. Flowing around the magnetosphere, they continue farther into interplanetary space, and are partially captured by the field, forming belts of charged particles or zones of captured radiation around the Earth.

Near-Earth space can be divided into three areas with regard to its physical characteristics:

- (1) interplanetary space, where the properties of the interplanetary medium are not

disturbed by the Earth and its magnetic field;

- (2) the transition region or magnetosheath resulting from interaction of the solar wind with the geomagnetic field;
- (3) the magnetosphere—the area of space occupied by the geomagnetic field.

The magnetosphere can in turn be divided into two parts: the portion of the magnetosphere which encompasses primarily the zones of captured radiation, and the remaining portion, including the magnetic tail (magnetotail) of the Earth with a magnetic neutral plasma layer.

These three areas of space are separated by two characteristic boundaries: the collisionless head shock wave and the magnetopause. The collisionless shock wave separates the unperturbed interplanetary medium from the magnetosheath; the magnetopause (boundary of the magnetosphere) separates the magnetosheath from the magnetosphere (see Fig. 37).

A boundary of the geomagnetic field and its motion were first discovered by the Explorer 10 satellite. The first measurements of captured particles, the magnetic field, and the plasma at the boundary of the geomagnetic field were made in 1961 by Explorer 12 [30, 52]. The geomagnetic field is compressed by the stream of the solar wind on the Sun side at a distance of about  $8.2 R_0$  along the Sun-Earth line. In addition to the limitation of the regular geomagnetic field, a limitation of the quasi-thermalized plasma was discovered, which was interpreted as the leading edge of a collisionless shock wave.

Further investigations finally established that there is an area which serves as a division boundary between the strong, regular geomagnetic field within the magnetosphere and the rapidly fluctuating weak magnetic fields of interplanetary origin in the transition area (Fig. 37). In the transition area, the low-energy solar plasma is retained and thermalized upon transition through the area of the collisionless shock wave. In both the shock wave and the magnetosphere, significant fluctuations of the magnetic field are observed. Later measurements of the magnetosphere boundary indicated a slightly higher value than the first measurements for its distance

from Earth, and showed that the position of both boundaries may change, displacements reaching 20% of the nominal values of the boundary distances. These variations in position of the boundary surfaces result from time variations in the density and velocity of the solar wind and related interplanetary fields.

The boundary of the magnetosphere on the Sun side is assumed to be approximately spherical in shape with a radius of curvature of about  $14 R_0$ , and its center displaced by  $3.5 R_0$  toward the night side along the Earth-Sun line. The shock wave is approximately parabolic in shape and intersects the Sun-Earth line at a distance of  $14 R_0$ . The axis of symmetry of the magnetosphere boundary in the plane of the ecliptic is rotated relative to the Sun-Earth direction by a slight angle ( $5^\circ$ ), a result of the effect of aberration due to the orbital motion of the Earth around the Sun.

The head shock wave is recorded by sharp change in physical properties of the plasma medium (appearance of low-energy plasma in the transition area). Observations on satellites such as Vela [39] have shown that the flux of electrons recorded by satellites in the area of the assumed head shock wave undergoes sudden and sharp changes. The general nature of the change in proton and electron fluxes agrees with the idea that turbulence results from interaction of the solar wind plasma with the shock wave. Protons of the solar wind lose some of their energy, while the electrons of the solar wind increase their energy and the direction of motion of the particles becomes more chaotic. The global flux of electrons with  $E_e > 350$  eV, upon transition from interplanetary space to the transition area, increases from not more than  $10^7$  to about  $5 \cdot 10^8 \text{ cm}^{-2} \text{ s}^{-1}$ . The temperature of the protons increases from about  $10^5$  (typical value for interplanetary space) to about  $10^6$  °K. The electron temperature behind the leading edge of the shock wave is about  $10^6$  °K, although higher values are frequently observed (up to about  $5 \cdot 10^6$  °K).

In the transition area approximately between  $10$  and  $15 R_0$ , near-isotropic but varying streams of protons and electrons have been observed with intensities of  $10^9 \text{ cm}^{-2} \text{ s}^{-1}$ . A significant increase in the ion temperature and a sharp decrease in the

intensity of streams of protons and electrons have also been observed near the magnetopause ( $R_m \approx 10.5 R_0$ ). Measurements have shown that the concentration of protons in the transition area is 8 to 10 times higher than in the solar wind. The magnetopause is easily detected not only by the change in the magnetic field, but also by the sharp decrease in the flux of protons with  $E_p < 10$  keV and the appearance of electrons with  $E_e > 40$  keV within the magnetosphere. Both boundaries (the head shock wave and the magnetopause) sometimes diffuse, making identification more difficult.

On the night side of the Earth, the lines of force of the geomagnetic field are extended far away from the Sun, forming a long loop, extending to a distance over  $80 R_0$ , i.e., beyond the orbit of the Moon [43, 44, 61].

A tail is indicated as far out as  $R = 1000 R_0$  [101]. The diameter of the tail of  $30 R_0$  is about  $40 R_0$ , at the geocentric distance of  $80 R_0$  about  $50 R_0$ . The geomagnetic tail is assumed to form as a result of extension of the lines of force of the geomagnetic field from the polar areas by the solar wind. It is shaped like a slightly flattened cylinder with a  $\theta$ -shaped cross section, consisting of two individual magnetic force tubes. In the southern tube, the magnetic lines of force from the south polar area are directed away from the Earth; in the northern tube the magnetic lines of force, connected to the north polar area, are directed toward the Earth. These tubes are separated by a magnetically neutral layer with very low field intensity, almost coinciding with the layer of hot plasma, balancing the pressure upward and downward from the neutral layer.

The neutral layer, according to observations [16, 17], is very thin; its thickness is not over the radius of the Earth (changes within limits of 500–5000 km have been recorded). When a satellite crosses the neutral layer, the sign of the field reverses; thus the existence is presumed of a layer of plasma and an equivalent electrical current, connected to the field gradient. Measurements made by the IMP-1 satellite show the neutral layer to be frequently in motion; the lines of force have a small component connecting the lines of force on opposite sides of the neutral layer. During magnetic storms, the magnetic tail is strongly deformed and changes [144].

The intensity of the magnetic field in the tail ( $H_x$ ) decreases with increasing geocentric distance  $r_{se}$  according to the rule  $H_x \approx (r_{se})^{-\gamma}$ ,  $\gamma 0.5 \pm 0.2$ . At the distance  $r_{se} = 10-15 R_0$ ,  $H_x = 20-30 \gamma$ . At  $r_{se} = 40 R_0$ ,  $H_x \sim 10-18 \gamma$ , while at  $r_{se} = 80 R_0$ ,  $H_x \approx 6-12 \gamma$ . The value of the component perpendicular to the neutral layer is  $H_z \approx 1-4 \gamma$  [129]. According to measurements by Explorer 33 [100], the field intensity of the geomagnetic loop at the orbit of the Moon is 10-18  $\gamma$ ; the direction of the field is almost parallel to the Earth-Sun line. The form of the geomagnetic tail depends largely on the flux of plasma at its surface and, like the mechanism of the tail formation, is still debated [15].

### *Geomagnetic Disturbances*

The instability of solar plasma fluxes leads to fluctuations in the position of the outer boundary of the magnetosphere, which can be recorded on Earth as pulsations of the geomagnetic field. Comparison of variations in parameters of the solar wind flux, made from observations by Venera 2, 4, and 6, with pulsations of the geomagnetic field [66], show that the primary parameter of the solar wind, determining the nature of geomagnetic field pulsations, recorded

on the Earth, is the concentration of the proton component.

The stronger geomagnetic disturbances are caused by high-energy fluxes of solar plasma from solar flares and recurrent fluxes of solar plasma. These disturbances may be periodic (smooth and regular) or sporadic; the most intensive are called geomagnetic storms. The intensity of the geomagnetic field, equal to about 0.3 Oe (30 000  $\gamma$ ) at the surface of the Earth near the Equator, may vary as much as 1%-2% during the strongest geomagnetic storms.

A geomagnetic storm usually passes through three phases of development: the initial phase, a smooth or sudden change of field; the main phase, a significant decrease in the horizontal component of the field in the middle and low latitudes; and a phase of gradual recovery, developing approximately 1 day after the beginning of a storm and continuing for several days (Fig. 57).

Correlation of the time variation of the field of a storm  $D_{st}$  with the position of the magnetopause on the day side, shows that in the initial phase of a magnetic storm, the magnetosphere is compressed, apparently due to an increase in the solar plasma flux, while during the recovery phase there is general expansion. In geomagnetic

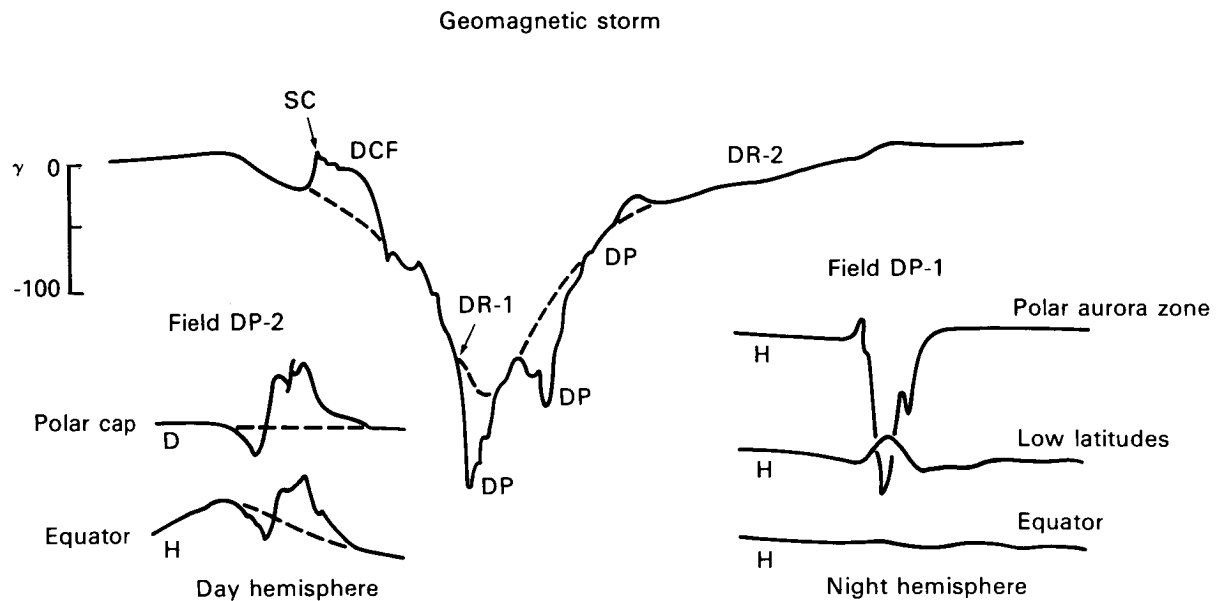


FIGURE 57.—Change of magnetic field during a geomagnetic storm.

storms with a clearly expressed main phase, there are great increases in the distance to the head shock wave and in the thickness of the transition, and a tendency toward increased storm intensity with increasing transition area thickness. Formation of the broader transition area may facilitate generation and transmission of magnetohydrodynamic waves into the magnetosphere, causing an increase in the viscous interaction and subsequent transfer of magnetic lines of force into the Earth tail, which increases the intensity of the storm.

There is a relationship between the position of the flare responsible for a storm on the solar disk and the nature of the storm. Storms caused by central flares are usually more sudden in onset SC and show a well-developed main phase; flares near the edges of the solar disk cause storms with milder, more extended initial phases; the development of the main phase is not always the same during such storms. The flux of energy responsible for geomagnetic storms can be assumed to be concentrated in a narrow cone, with an axis directed radially outward from the area of the flare. The appearance of flares responsible for storms with sudden onset at any point on the solar disk also shows that the leading edge of the plasma flow expands almost hemispherically as it propagates, and forms an extended envelope. These concepts can be combined into a single picture, presumably, of the distortion of the shock wave generated, as plasma is thrown outward from the area of a solar flare [59].

#### *Morphology of Geomagnetic Disturbances*

The analysis of the morphology of geomagnetic disturbances presented here is based largely on the detailed review by Obayashi [102]. Chapman suggested that the field of a disturbance  $D$  be formally divided into two areas to describe the rather complex nature of a geomagnetic storm: the axisymmetrical area  $D_{st}$  and the asymmetrical area  $DS$ :

$$D = D_{st} + DS \quad (24)$$

The field  $D_{st}$  corresponds to variations during the storm. For a typical geomagnetic storm, this

portion begins with a sharp change in the field at the moment of the sudden onset SC and continues with the longer initial phase (Fig. 57). The main phase of the storm shows a significant decrease in the horizontal component of the field  $D_{st}$  in the middle and lower latitudes. Field  $DS$  is disturbed, depending on local time; the average of  $DS$  is called the disturbed solar-diurnal variation  $DS$ . Field  $DS$  predominates, generally, in the high latitudes and is most active during the main phase of the storm [33].

In the polar auroral areas, particularly along the auroral belt, the magnetic disturbances are very intense. These disturbances, polar substorms or geomagnetic bays, usually last no more than a few hours and may reach several hundred gammas. They may appear during planetwide geomagnetic storms, or under quiet magnetic conditions. The most significant feature of these disturbances is the development of strong stream currents in the ionosphere along the night side of the auroral belt, the auroral electric streams. These disturbances are represented as field  $DP-1$  (Fig. 57).

With the auroral electric stream  $DP-1$ , another ionospheric current system, responsible for the  $DP-2$  field, consists of two current vortices with opposite directions, located in the polar area, with centers approximately along the morning-evening meridian. The field of  $DP-2$  disturbances arises and exists over the entire Earth (from the pole to the Equator), i.e., has a wider distribution in space than field  $DP-1$ . The frequency of current systems  $DP-2$ , excluding cases of SC and SI, is comparable to the frequency of  $DP-1$  polar magnetic substorms.

#### **Upper Atmosphere of the Earth – the Ionosphere**

Short-wave radiation from the Sun carries sufficient energy to cause significant photoionization of the terrestrial atmosphere at high altitudes, creating a partially ionized area in the upper atmosphere, the ionosphere. The ionosphere extends from about 50 km to the boundary of the magnetosphere. It is usually divided into several parts: the  $D$  area (50 to 90 km),  $E$  area (90 to 120–140 km),  $F$  area (120–140 to 600–1500 km), and protonosphere (1200–5000 km to the

boundary of the magnetosphere). The *F* area is divided into the *F*<sub>1</sub> and *F*<sub>2</sub> layers, the *E* area is sometimes divided into the *E*<sub>1</sub> and *E*<sub>2</sub> layers. The separation into areas is defined by the processes of their formation and composition of ions they contain. The *D*, *E*, and *F* areas are primarily molecular ions O<sub>2</sub><sup>+</sup> and O<sup>+</sup>, the *F*<sub>2</sub> area consists of O<sup>+</sup>, and the protonosphere consists of H<sup>+</sup>.

Atmospheric conditions in areas of the ionosphere differ greatly. The temperature varies from about 200 to 1000–2000° K, the concentration of neutral particles *n* varies by a factor of a million: from 10<sup>15</sup> cm<sup>-3</sup> in the *D* area to 10<sup>9</sup> cm<sup>-3</sup> in the *F* area. The electron concentration *n*<sub>e</sub> depends on the phase of the solar cycle and the time of day. The maximum concentration of ions and electrons is reached in the uppermost layer, in the *F*<sub>2</sub> layer above 300 km altitude. At altitudes over 110 km, the degree of ionization *n*<sub>e</sub>/*n* in the daytime is about 10<sup>-7</sup>, while at altitudes of about 300 km it reaches 10<sup>-3</sup>. Upon transition from day to night, the electron concentration in the *F*<sub>2</sub> area decreases by about 3–10 times, whereas in the *E* and *D* area it drops by 1.5 and 2.5 orders of magnitude. The time and geographic variations of the day *E* layer are quite regular. The maximum ion concentration in the *E* layer depends almost entirely on the activity and zenith distance of the Sun. The *E* layer has almost no sharp disturbances, such as those observed in the *D* and *F* layers.

Ionization by solar radiation dominates throughout the ionosphere over *h* ≈ 80 km, with the primary portion of shortwave solar radiation absorbed at altitudes of 100–200 km. Over 85 km at the minimum of solar activity and over 70 km at the maximum of solar activity, the primary source of ionization is x-radiation with  $\lambda \leq 10 \text{ \AA}$ . Radiation in *L*<sub>a</sub> is also significant at 70  $\leq h \leq 90$  km. Below 65–70 km, at the middle latitudes, the effect of cosmic rays predominates even in the daytime. The flux of cosmic rays increases by a factor of 3 from the minimum to the maximum of solar activity. In the 65–80 km area in the daytime and  $\geq 80$  km at night, ionization by corpuscular streams of particles, pouring into the lower portion of the atmosphere, predominates. During magnetic disturbances, the flux of poured

particles increases and ionization correspondingly increases (even at 100–110 km on the day side).

The total flux of ionizing radiation from the Sun varies between 2.5 and 8 erg · cm<sup>-2</sup> · s. Cosmic rays expend 3 · 10<sup>-3</sup> erg · cm<sup>-2</sup> · s on ionization of the terrestrial atmosphere in the middle latitudes. Of this energy, over 90% goes to ionization of the atmosphere below 40 km. Particles poured in during periods of high solar activity expend up to 1 erg · cm<sup>-2</sup> · s on ionization during the daytime and 10<sup>-2</sup> erg · cm<sup>-2</sup> · s at night.

The most significant changes in parameters of the Earth's upper atmosphere are related to changes in the flux of shortwave solar radiation. Dependence of ionospheric parameters on solar shortwave radiation is manifested as periodic (27-day and 11-year) changes and sporadic disturbances, a result of sharp increases in the flux of x-ray and ultraviolet radiation during active phenomena on the Sun.

A change is observed in the parameters of the ionosphere during the course of the day from day to night. The temperature changes most strongly in the 100–200 km altitude range. Over *h* ≈ 250–300 km is an area of isothermy. The daily maximum temperature *T*<sub>ex</sub> in this area is at 14:00–16:00, the minimum at 4:00–5:00 local time, indicating the inertial properties of the temperature of the atmosphere. Upon transition from day to night, *T*<sub>ex</sub> decreases by 20%–40% with low activity and 1.5–2 times with high activity of the Sun, from 1000° to 800° K and 1800° to 1100° K respectively. At altitudes less than 200–250 km, the change in temperature is much more complex. As solar activity increases, the density of the atmosphere increases significantly. The overall atmospheric density at 200 and 300 km increases by 2 and 3–4 times respectively upon transition from minimum to maximum activity. Atmosphere temperature also correlates well with the planetary geomagnetic index *A*<sub>p</sub>. The increase in the geomagnetic index during geomagnetic storms corresponds to an increase in pressure, i.e., density and temperature changes (in the upper atmosphere) are generally recorded 5–7 h after a magnetic storm begins. The upper atmosphere of the Earth and the ionosphere have been widely studied [75, 96, 111].

### *Ionospheric Disturbances*

Disturbances in the ionosphere include processes of two main types: reinforcement of ionization in the lower ionosphere (*D* and *E* areas) and complex aerochemical and dynamic processes relating to the *F* area (Fig. 58 [102]). That the anomalous ionization in the lower ionosphere results from bursts of solar radiation or outpouring of energetic particles is generally accepted.

The plan of disturbances in the *E* area, including the auroras, is shown in Figure 59 from [102]. During solar flares, ionization of the atmosphere, particularly below 100 km, increases sharply. In the *D* layer, following intensive solar flares, it increases by  $10^2$ – $10^4$  times as a function of the altitude in the atmosphere and the intensity of the flare. This increase in ionization, a sudden ionospheric disturbance (SID), is determined primarily by increase in intensity of solar x-radiation in the 0–20 Å range. The increase in electron density at various altitudes is determined by the increase in the flux of radiation in the 0–20 Å range, and change in spectral distribution of this radiation. The duration of SID is a few minutes to a few hours.

Sudden ionospheric disturbances encompass the lower portion of the ionosphere in the *D* area,

although an increase in  $n_e$  sometimes occurs in the *E* and *F* layers. Recording of sudden increase in ionization in an area is based on sudden phase anomalies in reflected radio signals (SPD), sudden increases in atmospherics and atmospheric whistles (SEA and SES) at altitudes below 70 km, fading of shortwave signals (SWF), and sudden absorption of cosmic radio radiation (SCNA) between 60 and 100 km.

The strong increase in the Sun's ultraviolet and x-radiation during a flare leads, in a few minutes, to an increase in the system of electrical currents in the ionosphere, responsible for the daily variations in the magnetic field, and is noted on magnetograms as sudden slight excursions—“crumbs.” Crumbs are observed on the sunlit side of the Earth and are most clearly expressed near the subsolar point. Almost all crumbs have been observed during periods of increasing x-radiation. The beginning of radio bursts in the centimeter range and the beginning of crumbs usually coincide.

Perturbations in the *F* area, related to geomagnetic storms, have been studied for many years. Analysis of data from the world network of ionospheric sounding stations has revealed many important peculiarities of variations in the elec-

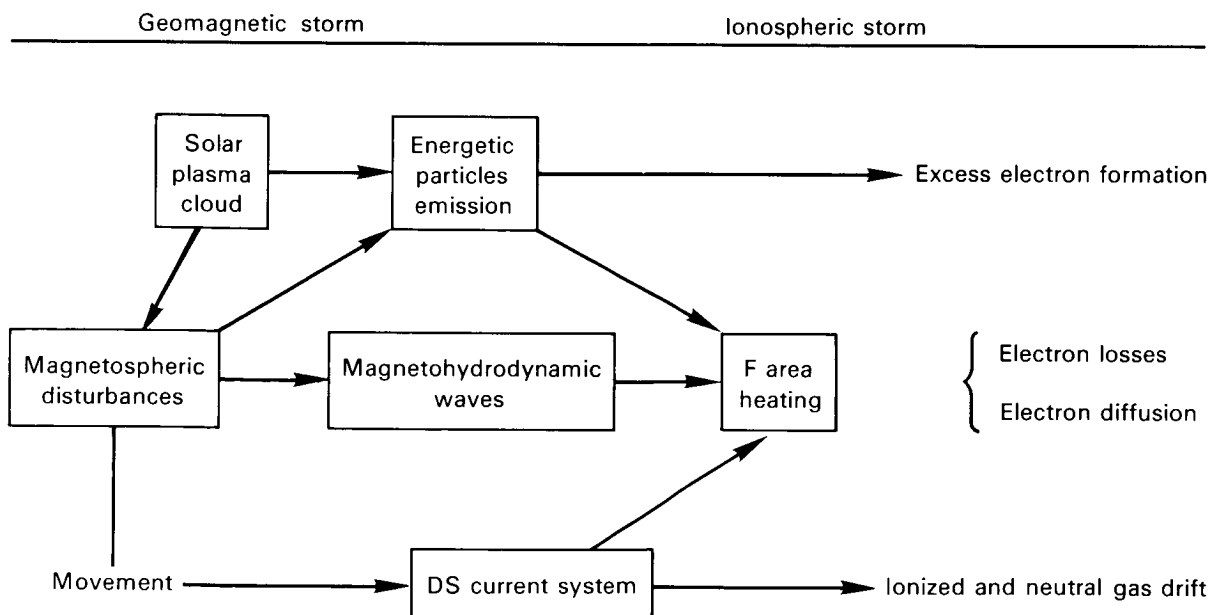


FIGURE 58.—Possible mechanism of ionospheric storm in *F* area.

tron concentration in the ionosphere. However, the theories set forth to explain the mechanism of these disturbances in the *F* area are debatable; there is still no satisfactory explanation for the main peculiarities of the storms. This situation is caused by the complex processes of formation of the *F* layer and poor understanding of the electro-

dynamics of the upper atmosphere. Nevertheless, two factors should be important in solving the problem: the change in the temperature of the ionosphere during magnetic disturbances and the drift electrodynamic motions of electrons under the influence of electric fields arising in the ionosphere.

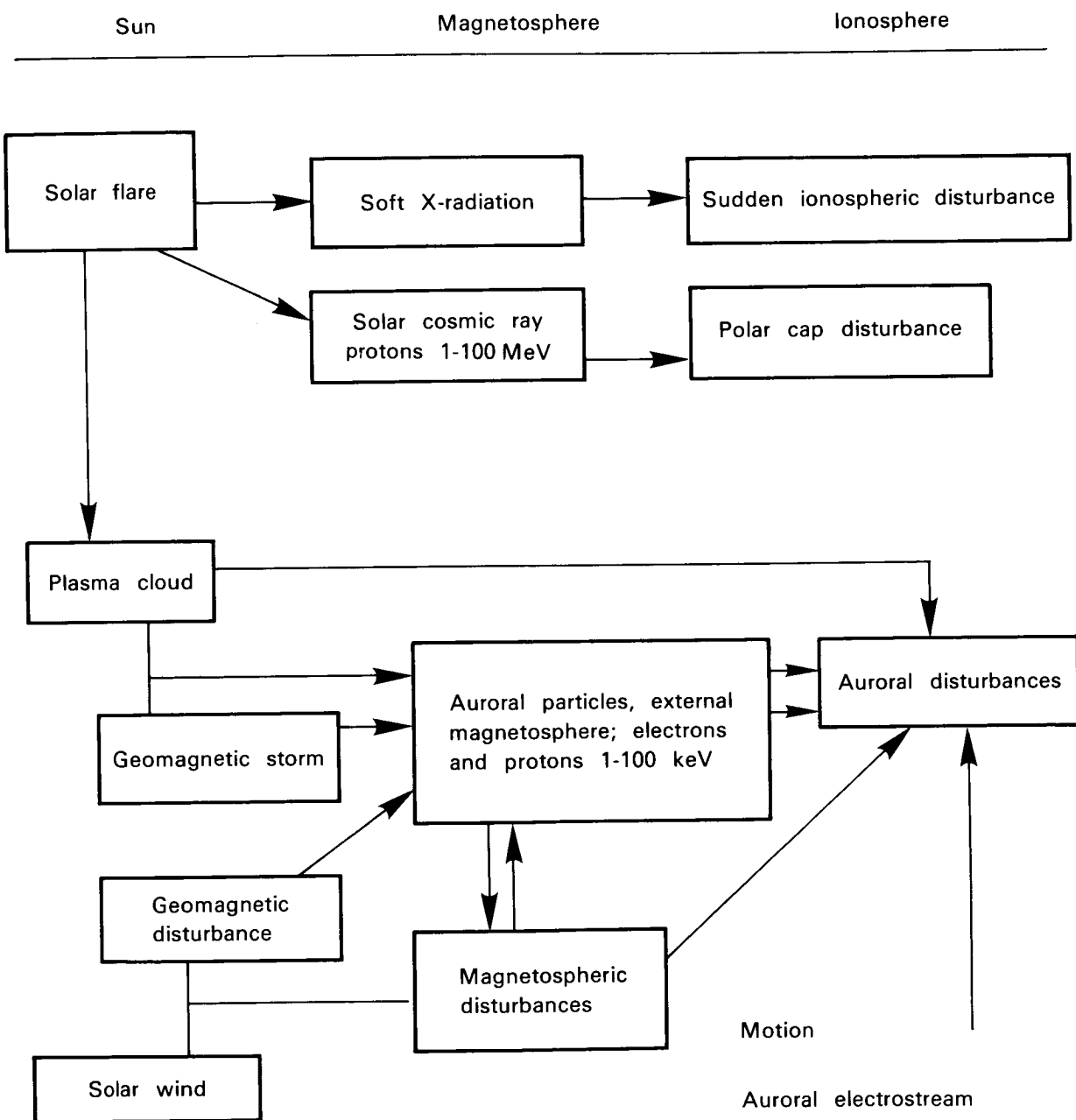


FIGURE 59.—Sources and mechanism of development of primary disturbances in the *F* area.

The temperature in the *F* area obviously increases during geomagnetic storms. Observations of the atmospheric braking of satellites have shown that general heating of the ionosphere occurs in altitudes 200 to 700 km; the temperature rise correlates well with the rise in geomagnetic activity. Increased temperature in the *F* layer leads to significant changes in equilibrium as a result of the electrodynamic drift motion of electrons, caused by interaction of the geomagnetic and electrical fields, related to the currents flowing in the ionosphere.

### Polar Auroras and Auroral Phenomena

One manifestation of the Sun-Earth connection is the polar auroras, the only visible manifestation of the interaction of charged particles with the upper atmosphere and ionosphere. This phenomenon varies in the form of the glowing areas and their brightness, color, mobility, and duration (Fig. 60 [31]). The polar aurora has been the subject of many works [2, 12, 31, 32, 74, 76, 77, 80, 96, 111].

All auroras are divided into two structural classes: ray type and homogeneous. The first includes forms of individual rays coinciding in

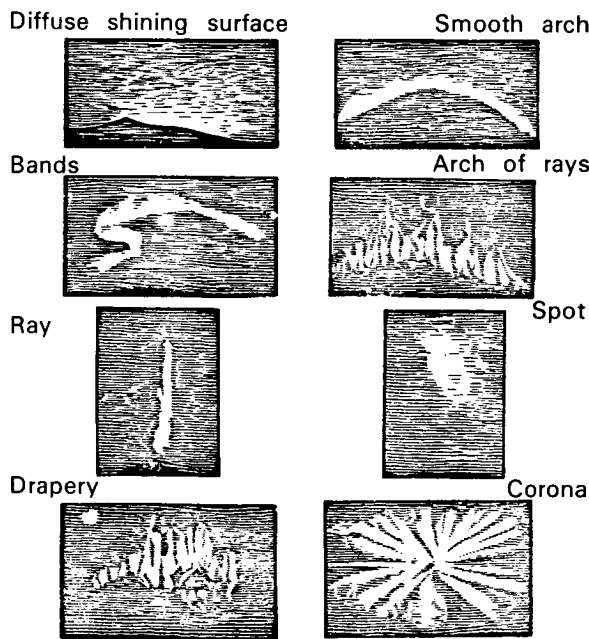


FIGURE 60.—Primary forms of polar auroras.

direction with the geomagnetic lines of force; the second, of a homogeneous diffuse glow. Auroras with ray structure are usually very mobile, while homogeneous forms stay at rest.

Study of the polar auroras, closely related to ionospheric and geomagnetic disturbances, can produce indirect information about parameters of the magnetosphere and its charged particles. The timespan of individual forms of auroras varies from a few seconds (ray forms) to several hours (homogeneous forms). The thickness (width) of the arcs falls within 1.5 to 23 km, with a mean value of 10 km; as the geomagnetic disturbance increases, the thickness of the arcs increases. The thickness of the rays amounts to a few hundred meters. The vertical extent of homogeneous arcs is about 30 km, arcs of rays  $\geq 40$  km, and individual rays about 100 km, sometimes up to several hundred km. The altitude of an aurora is usually the altitude of the lower boundary of the glow (Fig. 61 [147]). Several arcs may be present simultaneously in the sky. The minimum distance observed between them is about 10 km, the maximum distance about 200 km, and the most probable distance, 30–40 km.

Arcs have been observed repeatedly stretching over  $180^\circ$  of longitude, i.e., extending about 7000 km, which is apparently not the limit, since the length of individual forms in the longitude interval  $> 180^\circ$  has never been studied. As the level of geomagnetic disturbance increases, the length of the arcs decreases and their regular form is disrupted.

Auroras become visible to the naked eye when their brightness exceeds the night sky glow. The brightest auroras are 1000 times as bright as the glow of the night sky. The international 4-grade scale of brightness (see Table 8) is based on the

TABLE 8.—Physical Properties of Auroras

Brightness, arbitrary grades	I	II	III	IV
Intensity of 5577 Å (kR)	1	10	100	1000
Light flux ( $\text{erg}/\text{cm}^2 \cdot \text{s}$ )	0.01	0.1	1	10
Flux energy of particles ( $\text{erg}/\text{cm}^2 \cdot \text{s}$ )	3–5	30–50	300–500	3000–5000

absolute intensity [2] of the 5577 Å emission. The Rayleigh is used as a unit of measurement. An auroral intensity of 1 Rayleigh corresponds to the emission of  $10^6$  quanta/s in a column of atmosphere with a cross section of  $1 \text{ cm}^2$ .

The overall spectra of electrons (shown in Fig. 62 [77]) is according to the data from rockets and satellites for the high and middle latitudes. In both cases, electrons with  $E = 1\text{--}10 \text{ keV}$  carry

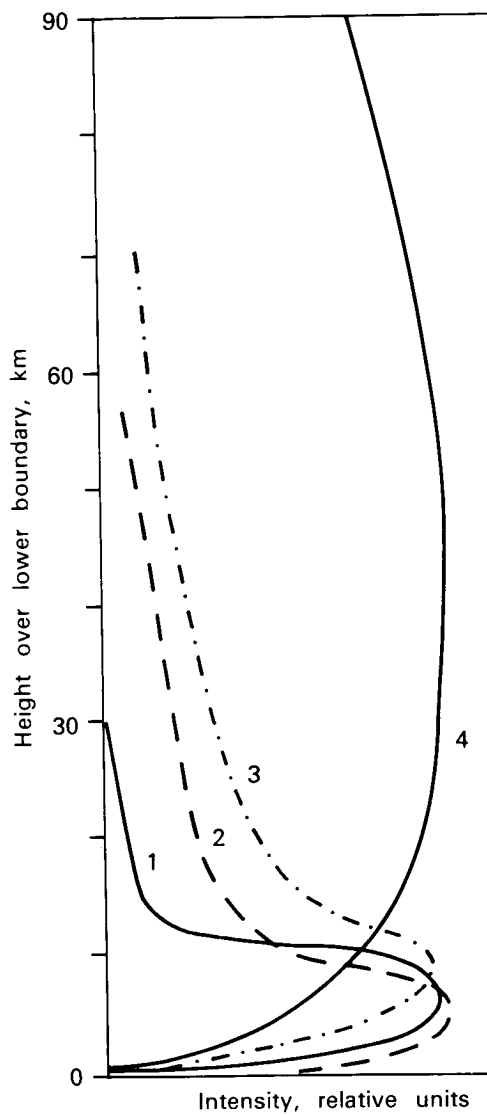


FIGURE 61.—Vertical cross section of intensity of glow of various types of polar auroras: 1, smooth arches; 2, arches of rays; 3, bands of rays; 4, rays.

the primary energy of the stream, although at the auroral latitudes their intensity is significantly higher. These electrons are most effective in formation of the polar auroras and ionization at the altitude of the *E* layer.

The area in space in which polar auroras can be observed at a given fixed moment in time is an irregular circle, asymmetrical relative to the magnetic pole; on the night side of the Earth, the circle passes over latitudes  $\phi \sim 67^\circ\text{--}68^\circ$ ; on the day side—over  $\phi \sim 75^\circ\text{--}77^\circ$  (Fig. 63a). The radius of the circle is  $18^\circ\text{--}19^\circ$  latitude. The probability of appearance of auroras at local times along the entire circle is almost constant and at its maximum, equal to about 0.8 (slightly decreasing toward the day meridian [79]).

The area of latitudes lying within the circle of auroras is called the *polar cap*. The probability of appearance of auroras in the polar cap is not over 0.2. Usually, a weak diffuse glow or weak, short, and short-lived homogeneous arc which arises and develops separately from the glow of the polar oval may be seen. Figure 63b shows typical distribution of the form of auroras in the polar oval and the polar cap during a moderate substorm. During quiet times, the auroras do not disappear completely, but only one fine arc may remain on the night portion of the oval, with groups of separate rays on the day portion.

The altitude of the auroras changes along the oval: the most probable altitudes are 100 km, 125, and 150 km in the night, evening, and day portions respectively. No data are yet available concerning the altitudes in the morning sector; there is reason to assume that it is even lower than at night.

The spatial position of the polar oval is shown in Figure 63a, which is for the winter hemisphere, the geographic axis combined with the geomagnetic axis. The probability is about 0.8 of this glowing ring appearing. The brightness of the auroras in the day portion of the oval is always less, apparently a result of their greater altitude; the auroras here arise in the less dense layers of the atmosphere.

All that has been stated is true of electron auroras. Much less information is available about proton auroras. It can only be said that they are also located in an asymmetrical ring, but it is

somewhat displaced relative to the ring of the electron auroras; during the evening hours, proton auroras are found in lower latitudes, during the morning, in higher latitudes. Around midnight, these two rings cross.

The most active and brightest manifestations of the polar auroras arise in the midnight sector of the auroral belt [3]. This system of manifestations is subject to repeated large-scale expansions and contractions, which may go beyond the limits of the field of vision of an individual station. These large-scale auroral activities, which arise during development of a single phenomenon, have been called auroral substorms.

Auroral substorms are closely related to magnetic disturbances. Akasofu and Chapman [4] have shown that intensive auroral substorms frequently appear during the stage of development of the main phase of a storm, not during the quiet initial phase. Significant displacement of auroral arcs toward the Equator is observed during the large main phases of geomagnetic storms.

In addition to the ordinary polar auroras, two other types, which are not visible, have been discovered: subauroral red arcs, and a glow in the area of the polar caps. The stable red arcs (6300 Å), which cannot be seen by eye, appear in the zone of middle latitudes during geomagnetic storms. These arcs are located in the *F* area of the ionosphere, extend over about 500 km of

latitude and form magnetic continuous bands, at least for the night half of the Earth. The intensity of the arcs increases with increasing geomagnetic activity.

Observations of emissions in the oxygen line at 6300 Å in the upper atmosphere of the Earth ( $h > 200$  km) during geomagnetic disturbances have shown that emissions on the 6300 Å line are closely related to solar activity. In particular, a close relationship has been observed between the intensity of the 6300 Å line and the flux of solar radio radiation at  $I_{10.7\text{-cm}}$  wavelength. For sufficiently large geomagnetic disturbances ( $D_{st} > 100 \gamma$ ), the logarithm of intensity of the emission line is linearly related to the indices  $D_{st}$  and  $I_{10.7\text{-cm}}$ .

The glow in the area of the polar caps is observed in close connection with absorption in the polar caps (PCA). This form of polar aurora is usually an intense glow, covering the entire polar cap; the intensity of the glow changes according to changes in the flux of solar cosmic rays. The polar auroras of this type arise at altitudes of 60–100 km, and their spectrum characteristically shows radiation in the bands of molecular nitrogen, blending with weak hydrogen radiation with broad Doppler profile of the line. These peculiarities show that the glow in the area of the polar caps results primarily from the protons of solar cosmic rays with energies of 1–10 MeV.

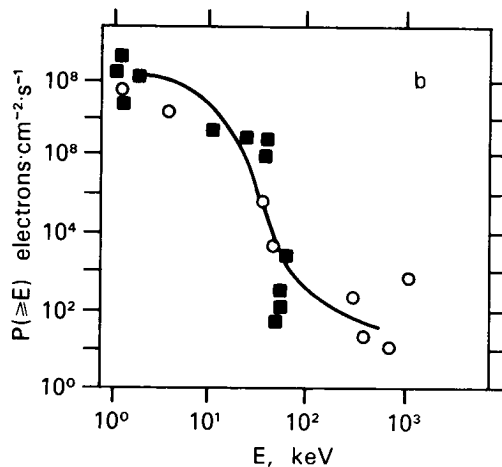
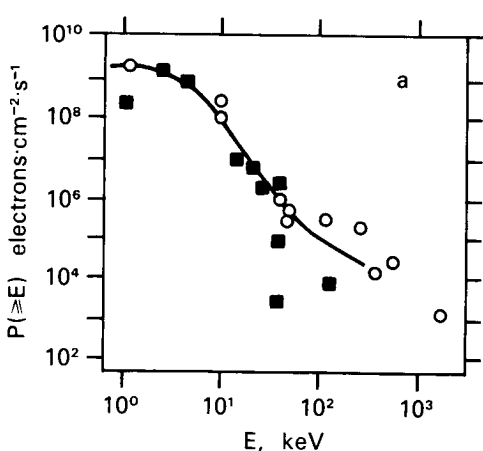


FIGURE 62.—Generalized spectrum of electron precipitation: (a) at latitudes of auroral zone; (b) at middle latitudes. Circles show satellite data; squares show rocket data.

### *Absorption in the Polar Caps*

When the stream of high-energy particles enters the terrestrial atmosphere from solar flares, one of the first results is the absorption of cosmic radio noise in the polar caps (PCA) or, as it is sometimes called, polar cap blackout [49]. This absorption results from anomalously great ionization of the ionosphere in the area of the polar caps by the flux of high-energy particles with energies of 1–30 MeV. Absorption in the polar cap begins approximately 1 hour after a flare and may continue for several days. The main ionizing agent responsible for PCA during a grade 2B flare on May 13, 1967, was protons with energies of 10–20 MeV during the day and protons with energies of 5–10 MeV at night. The stream of protons had an energy spectrum  $N(E) = k \cdot E^{-\gamma}$ ,  $\gamma = 2.2-3.5$ ,  $k = 2.7 \cdot 10^4 - 2 \cdot 10^6$ , and reached a maximum value at the Earth at

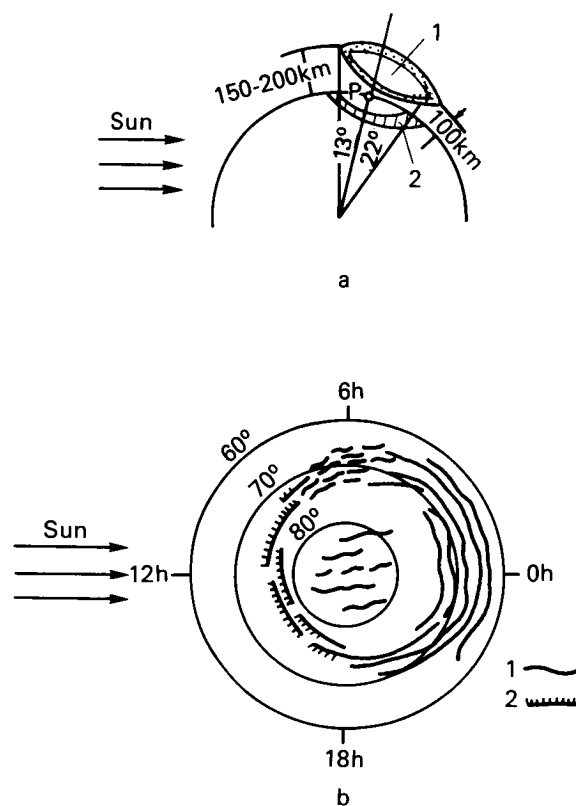


FIGURE 63.—Form on Earth from evening side. (a) 1—auroral ring; 2—projection of the ring on Earth's surface, and distribution of aurora forms along the instantaneous zone. (b) 1—homogeneous arcs; 2—rayed arcs.

all energies 40 hours after the flare. In addition to absorption in the polar caps, auroral absorption (auroral blackout) is also observed, caused by auroral particles (particles poured into the auroral area during strong geomagnetic disturbances).

Distribution of the PCA is in the form of a circle with its center at the geomagnetic pole. Distribution of the auroral absorption differs slightly, depending on the specific conditions of geomagnetic activity. During a strong geomagnetic storm, distribution of anomalous ionization is in the form of a spiral, falling along the belt of polar auroras; the greatest intensity of ionization relates to the morning and midnight sectors. However, during the time of an isolated bay-shaped disturbance (polar substorm), the greatest increase in ionization relates to the midnight section of the polar auroral belt. The auroral blackouts, as a rule, are associated with visible manifestations of polar auroras and localized influx of electrons and protons with energies on the order of keV. An intensive sporadic  $E$  layer, known as the auroral  $E$  layer, frequently appears in the ionosphere along with the auroral blackouts. During the sudden onset of a storm, there is a brief, sudden increase in ionization resulting from the x-ray bremsstrahlung of the energetic electrons, which penetrate into the denser layers of the atmosphere along the polar auroral belts [24].

### *Influx of Particles in the Upper Atmosphere*

The main part of the auroral phenomena results from the influx of energetic particles, usually called auroral, i.e., responsible for the polar auroras and associated phenomena. Since the discovery of radiation belts, there have been extensive studies of the relationships between the auroral and captured energetic particles. In this respect, there is significant interest in the zone of pouring of particles.

In a review of satellite results relating to the pouring of particles [103], it was concluded that two pouring zones existed. Zone 1 occupies the area of geomagnetic latitudes between 60° and 70°. In this zone, electrons with energies primarily over 10 keV are poured out, with a broad maximum of pouring in the morning-noon sector. Zone

2, in the night sector, overlaps zone 1, but is displaced near noon to the latitude  $75^\circ$ – $80^\circ$ . Electrons entering this zone have lower energies than in zone 1.

The pouring of particles in zone 1 is diffuse and stable and encompasses a broad area; pouring in zone 2 is discrete and impulselike, usually localized in space, and subject to rapid, strong fluctuations. All this information, produced by direct measurement of particle fluxes and indirect methods (altitudes of development of various phenomena in the atmosphere), indicates that the phenomena in zone 1 result from streams of relatively hard electrons, in zone 2, from streams of soft electrons.

The line of intersection of the captured radiation belt outer boundary with the ionosphere roughly coincides with the oval of polar auroras and the division boundary between zones 1 and 2. Comparison of the position of the outer boundary of the radiation belt to the boundary according to the model of the geomagnetic field in the magnetosphere [145] shows that zone 2 corresponds to the entry of the lines of force or the set of closed and open lines of force directly related to the division boundary, or passes very close to it. In other words, this zone is directly related to the magnetically neutral layer in the geomagnetic tail of the Earth.

During geomagnetic storms, the position of the pouring zones generally shifts toward the Equator. Changes in zone 2 are particularly noticeable during auroral substorms accompanied by repeated expansion, with subsequent contraction, of the width of the belt.

Auroral particles, intensive bursts of streams of electrons with energies primarily less than 10 keV, are assumed to be responsible for the visible auroral substorms. These streams may correspond to the “islands” of electrons discovered in the geomagnetic tail.

High energy particles, 10–100 keV, are poured out in addition to low-energy auroral particles, energies less than 10 keV; this pouring is usually related to the active polar auroras along the  $60^\circ$ – $70^\circ$  latitude band. Some of these particles may be high-energy particles from the solar plasma, but most are a result of acceleration in the magnetosphere rather close to the Earth.

The acceleration might possibly be due to fluctuating electrostatic fields along the lines of force of the geomagnetic field.

In smaller scales, the pouring of particles occurs (constantly and sporadically) in the moderate latitudes as well. Streams of electrons with energies of 1–10 keV at altitudes of 200–500 km in the daytime reach about  $0.3 \text{ erg/cm}^2\cdot\text{s}$ , a significant (up to 10%) share of the energy flux from shortwave solar radiation. At altitudes below 150–200 km, the flux of poured electrons begins to weaken. The full energy of the flux of electrons with  $E \gtrsim 1$ –3 keV, measured during the Soviet “Sun-atmosphere” experiment of April 18–23, 1969, at altitudes of  $\gtrsim 125$  km, varied from 0.07 to  $0.01 \text{ erg/cm}^2\cdot\text{s}\cdot\text{sr}$  [78]. Many scientists consider these data elevated by 1 to 2 orders of magnitude. At altitudes of about 100 km, the recorded radiation flux was 3–4 times less than at  $\sim 125$  km. The energy spectrum can be approximated by the exponent  $N \approx \exp(-E/E_0)$ ,  $E_0 = 10$ –12 keV. The flux of electrons with  $E > 40$  keV in the area of altitudes around 85 km varied significantly, within limits of 1–1.5 orders of magnitude, as well as varying in the energy spectrum, particularly in the 40–60 keV energy range.

Fast reductions (less than 3 h) in the intensity of electrons and protons in the outer radiation belt also result from dumping of particles during magnetospheric substorms. The death of particles in this case occurs during magnetic disturbances type DP-1 in the area where the current responsible for the  $D_{st}$  variation is formed, during the beginning of formation of the current. This is indicated by one condition being necessary for rapid death of particles: good development of the evening ionospheric electrojet and a strong reduction in the field at low latitudes in the evening sector of the Earth (18:00–24:00 local time). During magnetic storms, when  $D_{st}$  variations are increased, the rapid reduction in intensity encompasses  $L$  envelopes closer to the Earth.

The polar magnetic and auroral substorms are related to sudden decreases in the field of the geomagnetic tail, according to observations. This led to hypothesizing that the auroral phenomena are caused by particles accelerated in the neutral layer of the geomagnetic tail. The decrease in the geomagnetic tail field can be represented as

attachment (contact) of the tail's lines of force through the neutral layer. The conversion of magnetic energy to kinetic energy which occurs in this case can cause heating of the particles to about 1 keV, and acceleration to about 1–10 keV.

There is still no quantitative theory of annihilation of the magnetic field of the tail applicable to details of the effects of auroral storms. The quietness of conditions during periods between successive phenomena apparently indicates that the process of annihilation of the field in the tail is relatively brief. This process may be caused by macroinstability developing in the plasma of the tail, with conversion defined by changes in the parameters of the solar wind. Another possibility might be realized with a change in direction of the outer magnetic field, leading to disruption of the equilibrium of the system [124]. Observations of the intensity of streams of low-energy electrons with  $E_e \geq 100$  eV on the Luna-1, Luna-2 [65], Mars-1 [63] spacecraft and the Explorer 12 satellite at distances of over  $8 R_0$  show that the position of the streams of high-intensity electrons corresponds to the beginning of strong deformation of the field of the tail in the direction away from the Sun, measured by the IMP-1 and Explorer 14 satellites. The observed electron energy flux of some tens of  $\text{erg/cm}^2 \cdot \text{s}$  (energy density on the order of  $10^{-8} \text{ erg/cm}^3$ , if  $E_e$  is on the order of several keV), is sufficient for maintenance of the neutral layer if the intensity of the field in neighboring areas is about 30  $\gamma$ . The high intensities of streams of electrons of such energies might indicate that the area of the tail is, at least partially, a reservoir or area for acceleration of particles producing the polar auroras.

### Sources and Transmission of Energy in the Magnetosphere

The flux of solar plasma is the primary source of energy responsible for large-scale disturbances in the magnetosphere. The effects of the flux of solar plasma on the magnetosphere can be represented by normal and transverse components. The normal components lead to general compression or a return to the initial state of the magnetospheric cavity in the stream of solar plasma and,

consequently, is a field source [32]. The transverse components influence the general form of the magnetosphere, primarily by leading to formation of a tail.

Dissipative effects in the magnetopause lead to transverse stresses in the magnetosphere plasma, causing formation of a geomagnetic tail with a neutral layer and a plasma convection system in the magnetosphere [10]. The *DP* fields and related disturbances are believed to result primarily from processes in the geomagnetic tail. Theories explaining the field depression during the period of the main phase of storms (*DR* field) are still in question. Essentially, the mechanism for transmitting the energy of the solar plasma to circular current located deep within the magnetosphere remains unknown.

The total energy of an average geomagnetic storm has been estimated as  $10^{22}$ – $10^{23}$  erg [51]. Dissipation of energy occurs in three forms: (a) formation of polar auroras about  $10^{18}$  erg/s; (b) heating of the ionosphere about  $10^{18}$  erg/s; and (c) swelling of the magnetosphere (circular currents) about  $10^{18}$ – $10^{19}$  erg/s.

The energy of circular currents in the final analysis is dissipated during the phase of restoration, which may last several days, but the energy must be injected in a few hours. Thus, any theory of magnetic storms and polar auroras must be capable of explaining a transfer through the magnetopause of at least  $10^{18}$ – $10^{19}$  erg/s. On the other hand, since the solar plasma energy flux is assumed to be  $1$ – $10 \text{ erg} \cdot \text{cm}^2 \cdot \text{s}$ , the total influx of energy throughout the surface of magnetosphere ( $R \approx 20 R_0$ ) is estimated as  $10^{22}$  erg/s. Therefore, approximately  $10^{-3}$ – $10^{-4}$  of the entire influx of energy must be transmitted from the solar plasma to the magnetospheric plasma.

The inward transmission of energy to the magnetosphere can be achieved by:

- (1) deformation of the magnetosphere, a result of the pressure of the medium (causing generation of magnetohydrodynamic waves and heating of the thermal magnetic plasma);
- (2) direct injection of energy;
- (3) a mechanism of reconnecting magnetic force lines of the interplanetary and geomagnetic fields with subsequent

formation of the magnetic tail of the Earth, believed responsible for many magnetic disturbances;

- (4) the mechanism of viscous interaction of the solar wind with the magnetosphere.

A great contribution to geomagnetic activity may be made by fluctuations in the magnetospheric circular current and currents of the ionosphere as well as by the instability of the magnetopause and instability and accelerating processes within the magnetosphere itself [10, 14, 123]. It must be noted that present experimental data and theoretical analysis do not yet warrant giving definite preference to any given theory or mechanism of transmission of energy of the interplanetary medium into the magnetosphere.

### RADIATION CONDITIONS NEAR OTHER PLANETS OF THE SOLAR SYSTEM

Radiation conditions near the planets of the solar system are determined, to a significant extent, by the presence or absence of an internal magnetic field of the planet. This field, if it exists, determines the nature of interaction of the solar wind with the planet.

The characteristics of the planets of the solar system and the Moon, along with certain characteristics of the solar wind near these planets,

are listed in Table 9. In this table, the radius of the heliosphere is assumed to be about 40 AU, the convective velocity of the solar wind about  $400 \text{ km} \cdot \text{s}^{-1}$ .

When the magnetic field or properties of the ionosphere of the planet were unknown, the dimensions of the magnetopause were taken to be equal to the diameter of the planet. For Venus and Mars, the effective diameter of the magnetopause was determined by measurements of the shock wave and is the upper limit of the measured quantity. For Jupiter, this quantity was based on radio astronomy observations.

*Moon.* There are no radiation belts near the Moon, according to observations. Attempts to measure the constant magnetic field have indicated that the magnetic moment of the Moon is  $10^{-6}$  of the magnetic moment of the Earth. This means that radiation conditions of the Moon's surface are completely determined by the radiation in interplanetary space considering the geometric shielding provided by the body of the Moon. There is no shock wave near the Moon, and the flow of the solar wind around it is well-described by hydrodynamic equations. The Moon has no significant influence on the characteristics of the solar wind [142]. Similar interactions might be expected between solar wind and the planets Uranus, Pluto, and Neptune.

*Venus.* There is also no radiation field around Venus, indicating a weak internal magnetic

TABLE 9.—*Characteristics of Planets of the Solar System, Moon, and Solar Wind*

Physical properties	Celestial body									
	Mercury	Venus	Earth	Moon	Mars	Jupiter	Saturn	Uranus	Neptune	Pluto
Radius in $\text{km}^3$	2.42	6.08	6.38	1.74	3.38	71.35	60.40	23.80	22.20	3.00
Distance from Sun, AU	0.39	0.72	1.0	1.0	1.52	5.2	9.5	19.2	30.0	39.4
Dipole moment, $M_{\text{planet}}/M_z$	?	$2 \cdot 10^{-3}$	1	$1 \cdot 10^{-6}$	$2 \cdot 10^{-4}$	$4 \cdot 10^5$	—	?	?	?
Solar wind velocity, $\text{km/s}$	300	350	400	400	400	400	400	400	400	400
Density of protons, $\text{m}^{-3}$	34.0	9.5	5.0	5.0	2.1	0.19	0.055	0.018	0.006	0.003
Mean temperature of protons, $T, 10^4 \cdot \text{K}^\circ$	6.9	4.7	4.0	4.0	3.2	1.8	1.3	0.92	0.73	0.64
Magnetic field, gammas	24.7	8.26	5.0	5.0	3.12	1.72	0.39	0.19	0.12	0.09
Angle of Archimedes spiral, deg.	$30^\circ$	$42^\circ$	$47^\circ$	$47^\circ$	$59^\circ$	$80^\circ$	$84^\circ$	$87^\circ$	$88^\circ$	$89^\circ$
Magnetopause diameter, $\text{km}^3$	4.84	30.4	268.0	1.74	18.0	34 000	120.8	47.6	44.4	6.00

field [62, 135]. Detailed study of data about the magnetic field shows that the field, down to an altitude of about 200 km over the surface of the planet, is the interplanetary magnetic field; that the magnetic moment of Venus is  $\bar{M}_v \lesssim 10^{-4}$  of the magnetic moment of the Earth. However, a shock wave is observed near Venus which apparently is related to a dense ionosphere around this planet. The high conductivity of the ionospheric plasma does not allow the interplanetary magnetic field to penetrate to the surface of the planet. Therefore, an obstacle is produced, causing a shock wave in the stream of the solar wind.

*Mars.* Radiation belts are not around this planet. An estimate of the magnetic moment of Mars indicates a value of  $2 \cdot 10^{-4}$  of the moment of the Earth. A shock wave is observed near the planet in the solar wind, apparently, as is true for Venus, a result of a small ionosphere [132].

*Jupiter.* Strong sources of decimeter and decameter radio radiation have been detected near this planet. Analysis has shown that the decimeter radiation is polarized and reminiscent of synchrotron radiation from relativistic electrons. Numerical estimates have led to these values: if the magnetic field has a value of about 1 gauss, and the energies of electrons of 2.5–25 MeV the flux should be about  $5 \cdot 10^7$  electrons  $\cdot \text{cm}^2 \cdot \text{s}$ ; with a field of 0.1 G and energies of 10–100 MeV, the flux of electrons should be about  $5 \cdot 10^8$  electrons  $\cdot \text{cm}^2 \cdot \text{s}$  [95]. Analysis of the decameter radiation has led to an estimate of the magnetic moment of Jupiter as  $10^4$  times the magnetic moment of Earth. Thus, the radiation belts and magnetosphere around this planet should be the strongest in the solar system. The dynamics of the radiation belts apparently are the same as around the Earth, although they may be complicated by interaction of the planets with its satellites. The magnetosphere of Jupiter

is apparently reminiscent of that of the Earth with a distance to the magnetopause of about  $4 \cdot 10^6 \text{ km}$  [114].

The space probe Pioneer 10 approached the planet in December 1973 and found a magnetosphere which extends to distances of  $96R_s$  (the angle of approach to the planet was formed along the Jupiter-Sun line at about  $35^\circ$ ) [36]. A standing shock wave and the transition field were observed from distances of  $109R_s$ . Within the magnetosphere a disklike distribution of charged particles was observed in a magnetic field resembling the field in the tail end of the Earth magnetosphere. At distances from  $96\text{--}25R_s$ , the field has the value of  $\sim 5 \gamma$  and does not change significantly. It increases in the part from 50 to  $25R_s$ , where its intensity reaches values of about  $20 \gamma$ . In this case, electron fluxes with an energy of 0.4–1.0 MeV reach values from  $10^3$  to  $10^5 \text{ e}^- \cdot \text{cm}^2 \cdot \text{s}$ . Proton fluxes with  $E$  from 5.6 to 21 MeV amount to a value of  $1\text{--}10^2 \text{ p} \cdot \text{cm}^2 \cdot \text{s}$ . Particles are within a thin layer close to the equator.

Beginning with distances  $R$  about  $20R_s$ , the magnetic field starts to increase essentially as it approaches the planet and has a bipolar character. Its intensity increases up to values of about 0.2 gauss for  $R$  at  $2.8R_s$ . Within this field, which essentially represents the radiation belts of Jupiter, the intensity of the particle fluxes increases rapidly: at distances of about  $5R_s$  the intensity of electron fluxes with  $E > 3$  MeV reaches  $5 \cdot 10^8 \text{ cm}^2 \cdot \text{s}^{-1}$ , and with an energy  $E > 50 \text{ MeV} = 10^7 \cdot \text{cm}^2 \cdot \text{s}^{-1}$ , proton fluxes  $E > 50 \text{ MeV}$  at these distances amount to  $4 \cdot 10^6 \cdot \text{cm}^2 \cdot \text{s}^{-1}$ . The distribution in space of various spectral components of particles is fairly complicated and seems to be connected with the interaction of these particles with the satellites of Jupiter, Io, Europa, and Ganymede.

## REFERENCES

1. Anon. Surprises for Pioneer 10 in the asteroid belt. *Aerospace. Dly* 58(8):62, 1972.
2. AKASOFU, S. I. *Polar and Magnetospheric Substorms*. Dordrecht, Holl., D. Reidel; New York, Springer, 1968.
3. AKASOFU, S. I. The development of the auroral substorm. *Planet. Space Sci.* 12:273–282, 1964.
4. AKASOFU, S. I., and S. CHAPMAN. Magnetic storms: the simultaneous development of the main phase (DR) and of polar magnetic substorms (DP). *J. Geophys. Res.* 68(10):3155–3158, 1963.
5. ALFVÉN, H., and G. G. FÄLTHAMMAR. *Cosmical Electrodynamics*, 2nd ed. Oxford, Clarendon, 1963.
6. ANDERSON, K. A. Electrons and protons in long-lived

- streams of energetic solar particles. *Solar Phys.* 6:111–132, 1969.
7. ANTONOVA, A. E., and V. P. SHABANSKIY. The structure of the geomagnetic field at great distances from the Earth. *Geomagn. Aeron.* 8:801–811, 1968.
  8. ARNOLDY, R. L., S. R. KANE, and J. R. WINCKLER. Energetic solar flare x-rays observed by satellite and their correlation with solar radio and energetic particle emission. *Astrophys. J.* 151(2, Pt. 1):711–736, 1968.
  9. ATHAY, R. G. Sources of solar ultraviolet radiation. *J. Geophys. Res.* 66(2):385–390, 1961.
  10. ALEXANDER, W. I. Viscous interaction between the solar wind and the Earth's magnetosphere. *Planet. Space Sci.* 12:45–53, 1964.
  11. BAME, S. J., A. I. HUNDEHAUSEN, J. K. ASBRIDGE, and I. B. STRONG. Solar wind ion composition. *Phys. Rev. Lett.* 20:393–395, 1968.
  12. BARBIER, D. Introduction to the study of the aurora and airglow. In, DeWitt, C., J. Hieblot, and A. Lebeau, Eds. *Geophysics, The Earth's Environment*, pp. 301–368. New York, Gordon & Breach, 1963.
  13. BAROUCH, E., J. ENGELMANN, M. GROS, L. KOCH, and P. MASSE. Observations of the spectra and time history of protons in interplanetary space, February 25–28, 1969. In, Manno, V., and D. E. Page, Eds. *Intercorrelated Satellite Observations Related to Solar Events*; Proc., 3rd ESLAB/ESSRIN Symp., Noordwijk, Neth., Sept., 1969 (Astrophysics and Space Science Library), Vol. 19, pp. 448–459. Dordrecht, Holl., Reidel, 1970.
  14. BEARD, D. B. The interaction of the terrestrial magnetic field with the solar corpuscular radiation. *J. Geophys. Res.* 65:3559–3568, 1960.
  15. BEHANNON, K. W. Mapping of the Earth's bow shock and magnetic tail by Explorer 33. *J. Geophys. Res.* 73:907–930, 1968.
  16. BERNSTEIN, W., R. W. FREDERICKS, and F. L. SCARF. A model for a broad disordered transition between the solar wind and the magnetosphere. *J. Geophys. Res.* 69(7):1201–1210, 1964.
  17. BIERMANN, L. Kometenschweife und Solare Korpuskularstrahlung. (Transl: Comets' tails and solar corpuscular radiation). *Zs. Astrophys.* 29:274–286, 1951.
  18. BIERMANN, L. Über den Schweif des Kometen Halley in Jahre, 1910. (Transl: The tail of Halley's Comet in 1910). *Zs. Naturforsch.* 7(Pt. A):127–136, 1952.
  19. BISWAS, S., C. E. FICHTEL, and D. E. GUSS. Study of the hydrogen helium and heavy nuclei in the Nov. 12, 1960 solar cosmic event. *Phys. Rev.* 128:2756–2771, 1962.
  20. BISWAS, S., C. E. FICHTEL, D. E. GUSS, and C. J. WADDINGTON. Hydrogen, helium and heavy nuclei from the solar event in Nov. 15, 1960. *J. Geophys. Res.* 68:3109–3122, 1963.
  21. BONETTI, A., H. S. BRIDGE, A. S. LAZARUS, B. ROSSI, and F. SCHERB. Explorer 10 plasma measurements. *J. Geophys. Res.* 68(13):4017–4063, 1963.
  22. BONNET, R. M. Stigmatic spectra of the Sun between 1800 Å and 2800 Å. In, Mitra, A. P., L. G. Jacchia, and W. S. Newman, Eds. *Life Sciences and Space Research* (Proc. 10th Plenary COSPAR Meet., London, July 1967), Vol. 8, pp. 458–472. Amsterdam, North-Holland, 1968.
  23. BRANDT, J. C., and P. W. HODGE. *Solar System Astrophysics*. New York, McGraw-Hill, 1964.
  24. BROWN, R. R. Electron precipitation in the auroral zone. *Space Sci. Rev.* 5:311–387, 1966.
  25. BRYANT, D. A., T. L. CLINE, U. D. DESAIR, and F. B. McDONALD. Studies of solar protons with Explorers XII and XIV. *Astrophys. J.* 141:478–499, 1965.
  26. BRYUNELLI, B. Ye. Processes in near-Earth space and geomagnetic disturbances. In, Trudy 5-y Vsesoyuznoy Yezhegodnoy Zimney Shkoly po Kosmofizike (Transl: Works of Fifth All-Union Annual Winter School on Astrophysics), p. 212. Apatity, 1968.
  27. BURLAGA, L. F. Anisotropic diffusion of solar cosmic rays. *J. Geophys. Res.* 72(17):4449–4466, 1967.
  28. BURLAGA, L. F. Nature and origin of directional discontinuities in the solar wind. *J. Geophys. Res.* 76:4360–4365, 1971.
  29. BURLAGA, L. F., and N. F. NESS. Macro and micro structure of the interplanetary magnetic fields. *Can. J. Phys.* 46:S962–S965, 1971.
  30. CAHILL, L. F., and P. G. AMAZEEN. The boundary of the geomagnetic field. *J. Geophys. Res.* 68(7):1835–1843, 1963.
  31. CHAMBERLAIN, J. W. *Physics of the Aurora and Airglow*. New York, Academic, 1961.
  32. CHAPMAN, S. Solar plasma, geomagnetism and aurora. In, DeWitt, C., J. Hieblot, and A. Lebeau, Eds. *Geophysics, The Earth's Environment*, pp. 371–502. New York, Gordon & Breach, 1963.
  33. CHAPMAN, S., and V. C. A. FERRARO. A new theory of magnetic storm. *Terr. Magn. Atmos. Electr.* 36:77–97, June 1931.
  34. CHARAKHCH'YAN, A. N., V. F. TULINOV, and T. N. CHARAKHCH'YAN. The energy spectrum and time dependence of the intensity of solar cosmic ray protons. *Zh. Eksp. Teor. Fiz.* 41(3):735–746, 1961. (Transl: *Sov. Phys. JETP*) 14:530–537, 1962.
  35. CLINE, T. L., and F. B. McDONALD. *Relativistic Electrons from Solar Flares*. Greenbelt, Md., Goddard Space Flight Cent., 1968. (NASA TM-X-63210)
  36. [Collected reports on Pioneer 10 mission to Jupiter.] *Science* 183(4122, Jan. 25):301–324, 1974.
  37. COLOMBO, G., D. A. LAUTMAN, and I. I. SHAPIRO. The Earth's dust belt: fact or fiction? 2. Gravitational focusing and Jacobi capture. *J. Geophys. Res.* 71:5705–5717, 1966.
  38. COLOMBO, G., I. I. SHAPIRO, and D. A. LAUTMAN. The Earth's dust belt: fact or fiction? 3. Lunar ejecta. *J. Geophys. Res.* 71:5719–5731, 1966.
  39. COON, J. H. Vela satellite measurements of particles in the solar wind and the distant geomagnetosphere. In, McCormac, B. M., Ed. *Radiation Trapped in the Earth's Magnetic Field*, pp. 231–255. Presented

- at Adv. Stud. Inst., Bergen, 1965. Dordrecht, Holl., D. Reidel, 1966.
40. DAVIS, L., Jr., and D. B. CHANG. On the effect of geomagnetic fluctuations on trapped particles. *J. Geophys. Res.* 67:2169–2179, 1962.
  41. DE JAGER, C. Structure and dynamics of the solar atmosphere. In, Flügge, S., Ed. *Handbuch der Physik, (Astrophysik III: Das Sonnensystem)*, Vol. 52, pp. 80–362. Berlin, Springer, 1959.
  42. DOHNAHYI, J. S. On the origin and distribution of meteoroids. *J. Geophys. Res.* 75:3468–3493, 1970.
  43. DOLGINOV, Sh. Sh., Ye. G. YEROSHENKO, L. N. ZHUGOV, and N. V. PUSHKOV. Measurements of the magnetic field in the area of the Moon by the Luna 10 satellite. *Dokl. Akad. Nauk SSSR* 170(3):574–577, 1966.
  44. DOLGINOV, Sh. Sh., Ye. G. YEROSHENKO, L. N. ZHUGOV, and I. A. ZHULIN. Possible interpretation of results of measurements performed by the lunar satellite Luna 10. *Geomagn. Aeron.* 7(3):436–441, 1967. (Transl: *Geomagn. Aeron.*) 7(3):352–356, 1967.
  45. DORMAN, L. I. *Variatsii Kosmicheskikh Luchey i Issledovaniye Kosmosa* (Transl: *Variations in Cosmic Rays and Space Studies*). Moscow, Akad. Nauk SSSR, 1963.
  46. ELLISON, M. A. *The Sun and Its Influence*. London, Routledge, 1955.
  47. ERICKSON, J. E. Mass influx and penetration rate of meteor streams. *J. Geophys. Res.* 74:576–585, 1969.
  48. FAIRFIELD, D. H. Average magnetic field configuration of the outer magnetosphere. *J. Geophys. Res.* 73:7329–7338, 1968.
  49. FISK, L. A. and W. I. AXFORD. Anisotropies of solar cosmic rays. *Solar Phys.* 7:486–498, 1969.
  50. FRANK, L. A. Inward radial diffusion of electrons of greater than 1.6 million electron volts in the outer radiation zone. *J. Geophys. Res.* 70:3533–3540, 1965.
  51. FRANK, L. A. On the extraterrestrial ring current during geomagnetic storms. *J. Geophys. Res.* 72:3753–3767, 1967.
  52. FREEMAN, J. W., J. A. VAN ALLEN, and L. J. CAHILL. Explorer 12 observations of the magnetospheric boundary and the associated solar plasma on September 13, 1961. *J. Geophys. Res.* 68(8):2121–2130, 1963.
  53. FRITZ, T. A., and D. J. WILLIAMS. *Initial Observations of Geomagnetically Trapped Alpha Particles at the Equator*. Boulder, Colo., Nat. Oceanic Atmos. Adm., Space Environ. Lab., 1972. (NOAA-TM-ERL-SEL-20)
  54. FROMAN, M. A. The equilibrium anisotropy in the flux of 10 MeV solar flare particles and their convection in the solar wind. *J. Geophys. Res.* 75(16):3147–3153, 1970.
  55. GINZBURG, V. L., and S. I. SYROVATSKIY. *Proishkhozhdenie Kosmicheskikh Luchey* (Transl: *The Origin of Cosmic Rays*). Moscow, Akad. Nauk SSSR, 1963.
  56. GLEESON, L. J., and W. I. AXFORD. The Compton-getting effect. *Astrophys. Space Sci.* 2(4):431–437, 1968.
  57. GNEVYSHEV, M. N. On the 11-year cycle of solar activity. *Solar Phys.* 1(1):107–120, 1967.
  58. GNEVYSHEV, M. N. The 11-year cycle of solar activity. *Usp. Fiz. Nauk (Transl: Successes Phys. Sci.)* 90(2):291–301, 1966.
  59. GOLD, T. Plasma and magnetic fields in the solar system. *J. Geophys. Res.* 64:1665–1674, 1959.
  60. GRINGAUZ, K. I. Some results of experiments in interplanetary space by means of charged particle traps on Soviet space probes. In, Van de Hulst, H. C., C. de Jager, and A. F. Moore, Eds. *Life Sciences and Space Research* (Proc., 2nd COSPAR Int. Space Sci. Symp., Florence, 1961), Vol. 2, pp. 539–553. Amsterdam, North-Holland; New York, Interscience, 1961.
  61. GRINGAUZ, K. I., V. V. BEZRUKIKH, M. Z. KHOKHLOV, L. S. MUSATOV, and A. P. REMIZOV. Indications of intersection of the Earth's magnetospheric tail by the Moon according to charged particle traps on the first artificial satellite of the Moon. *Dokl. Akad. Nauk SSSR* 170(3):570–573, 1966.
  62. GRINGAUZ, K. I., V. V. BEZRUKIKH, L. S. MUSATOV, and T. K. BREUS. Plasma measurements performed near Venus by Venera 4. *Kosm. Issled.* 6:411–419, 1968.
  63. GRINGAUZ, K. I., V. V. BEZRUKIKH, J. S. MUSATOV, R. Ye. RYBCHINSKY, and S. M. SHERONOVA. Measurements made in the Earth's magnetosphere by means of charged particle traps aboard the Mars 1 probe. In, Muller, P., Ed. *Life Sciences and Space Research* (Proc., 4th COSPAR Int. Space Sci. Symp., Warsaw, June 1963), Vol. 4, pp. 621–626. Amsterdam, North-Holland; New York, Wiley, 1964.
  64. GRINGAUZ, K. I., V. V. BEZRUKIKH, V. D. OZEROV, and R. Ye. RYBCHINSKIY. Study of interplanetary ionized gas, energetic elements and corpuscular radiation of the Sun using three electrode charge particle traps on the second Soviet space rocket. *Dokl. Akad. Nauk SSSR* 131(6):1301–1304, 1960.
  65. GRINGAUZ, K. I., V. G. KURT, V. I. MOROZ, and I. S. SHKLOVSKIY. Results of observations performed with charge particle traps on Soviet space rockets up to about 100 000 km. *Astron. Zh.* 37:716–735, 1960. Transl. in *Sov. Astron. AJ* 4:680–695, Jan./Feb. 1961.
  66. GRINGAUZ, K. I., V. A. TROITSKAYA, E. K. SOLOMATINA, and R. V. SHCHEPETNOV. Variations of the solar wind flux observed with Venera 2, 4, 5, and 6, and pulsations of the geomagnetic field connected with them. Presented at Int. Symp. on Solar Terrestrial Physics, Leningrad, May 1970. Also, Variations of solar wind flux observed by several spacecraft and related pulsations of the Earth's electromagnetic field. *J. Geophys. Res.* 76:Feb. 1, 1065–1069, 1971.
  67. HAFFNER, H. W. *Radiation and Shielding in Space*. New York Academic, 1967.
  68. HESS, W. N. *Radiation Belt and Magnetosphere*. Waltham, Mass., Bleisdell, 1968.
  69. HINTEREGGER, H. E., and L. A. HALL. Solar extreme ultraviolet emission in the range 260–1300 Å observed

- from OSO-111. *Solar Phys.* 6(12):175–182, 1969.
70. HIRSHBERG, J., A. ALKSNE, D. S. COLBURN, S. J. BAME, and A. J. HUNDHAUSEN. Observations of a solar flare, induced interplanetary shock and helium-enriched driver gas. *J. Geophys. Res.* 75:1–15, 1970.
  71. HUNDHAUSEN, A. J. Composition and dynamics of the solar wind plasma. *Rev. Geophys. Space Phys.* 8:729–811, 1970.
  72. International Astronomical Union. *Quarterly Bulletin on Solar Activity*. Zurich, Eidgenossische Sternwarte, 1932–
  73. International Astronomical Union. *Report*. Zurich, Eidgenossische Sternwarte, Aug. 1966.
  74. ISAYEV, S. I. *Morfologiya Polyarnykh Siyanyy* (Transl: *The Morphology of Polar Auroras*). Leningrad, Nauka, 1968.
  75. IVANOV-KHOLODNIY, G. S., Ed. *Fizika Verkhney Atmosfery* (Transl: *Upper Atmosphere Physics*). Leningrad, Gidrometizdat, 1971.
  76. IVANOV-KHOLODNIY, G. S., T. V. KAZACHEVSKAYA, G. A. KOKIN, and V. V. MIKHNEVICH. In, Mikhnevich, V. V., and A. D. Danilov, Eds. *Issledovaniya Atmosfery i Ionosfery v Period Povyshennoy Solnechnoy Aktivnosti* (Transl: *Studies of the Atmosphere and Ionosphere During a Period of Increased Solar Activity*), pp. 143–153. Leningrad, Gidrometeo, 1970.
  77. IVANOV-KHOLODNIY, G. S., and G. M. NIKOL'SKIY. *Solntse i Ionosfera* (Transl: *The Sun and the Ionosphere*). Moscow, Nauka, 1969.
  78. JOKIPII, J. R., and E. N. PARKER. Stochastic aspects of magnetic lines of force with application to cosmic-ray propagation. *Astrophys. J.* 155:777–798, 1969.
  79. KHOROSHEVA, O. V. Space-time distribution of polar auroras. In, *Mezhdunarodnyi Komitet po Provedeniyu Mezhdunarodnogo Geofizicheskogo Goda*. IV. *Razdel Programmy MGG: Polyarnyye Siyaniya*. Moscow, Nauka, 1967.
  80. KRASOVSKIY, V. I. *Shtili i Shtormy v Verkhney Atmosfere* (Transl: *Calms and Storms in the Upper Atmosphere*). Moscow, Nauka, 1971.
  81. KUZNETSOV, S. N., and B. A. TVERSKOY. Monotonic decrease of the intensity of electrons in the radiation belts of the Earth. *Geomagn. Aeron.* 11(1):3–10, 1971. (Transl: *Geomagn. Aeron.*) 11(1):1–6, 1974.
  82. LAUTMAN, D. A., I. I. SHAPIRO, and G. COLOMBO. The Earth's dust belt: fact or fiction? 4. Sunlight-pressure air-drag capture. *J. Geophys. Res.* 71:5733–5741, 1966.
  83. LIN, R. P. The emission and propagation of ~40 keV solar flare electrons. I. The relationship of ~40 keV electron to energetic proton and relativistic electron emission by the Sun. *Solar Phys.* 12:266–303, 1970.
  84. LIN, R. P., S. W. KAHLER, and E. C. ROELOF. Solar flare injection and propagation of low energy protons and electrons in the event of July 7–9, 1966. *Solar Phys.* 4(3):338–360, 1968.
  85. MALITSON, H. H. The solar energy spectrum, *Sky Telesc.* 29(3):162–165, 1965.
  86. MAZETS, E. P. Cosmic dust and meteor showers. In, Kondratyev, K. Ya., M. J. Rycroft, and C. Sagan, Eds. *Life Sciences and Space Research* (Proc., 13th COSPAR Plenary Meet., Leningrad, May 1970), Vol. 11, pp. 363–369. Berlin, Ger. (E.), Akademie, 1971.
  87. McCracken, K. G., and N. F. NESS. The collimation of cosmic rays by the interplanetary magnetic field. *J. Geophys. Res.* 71:3315–3318, 1966.
  88. McCracken, K. G., R. A. R. PALMEIRA, R. P. BUKATA, U. R. RAO, F. R. ALLUM, and E. P. KEATH. A co-rotating solar cosmic ray enhancement observed by Pioneer 8 and Explorer 34 on July 13, 1968. Presented at 11th Int. Conf. on Cosmic Rays, Budapest, 1969.
  89. McCracken, K. G., U. R. RAO, and R. P. BUKATA. Cosmic ray propagation processes. I. A study of the cosmic-ray flare effect. *J. Geophys. Res.* 72:4293–4324, 1967.
  90. McCracken, K. G., U. R. RAO, R. P. BUKATA, and E. P. KEATH. The decay phase of solar flare events. *Solar Phys.* 18:100–132, 1971.
  91. McILWAIN, C. E. Coordinates for mapping the distribution of magnetically trapped particles. *J. Geophys. Res.* 66:3681–3691, 1961.
  92. MCKINNON, J. A. *August 1972 Solar Activity and Related Geophysical Effects*. Boulder, Colo., Nat. Oceanic Atmos. Adm., Space Environ. Lab., 1972. (NOAA-TM-ERL-SEL-22)
  93. MENZEL, D. H. *Our Sun*. Cambridge, Mass., Harvard Univ. Press, 1959.
  94. MEYER, P. Cosmic rays in galaxy. In, Goldberg, L., Ed. *Annual Review of Astronomy and Astrophysics*, pp. 1–38. Palo Alto, Calif., Annual Reviews, 1969.
  95. MICHAUX, C. M. *Handbook of the Physical Properties of the Planet Jupiter*. Washington, NASA, 1967. (NASA SP-3031)
  96. MITRA, S. K. *The Upper Atmosphere*, 2nd ed. Calcutta, Asiatic Soc., 1952.
  97. NESS, N. F. Measurements of the magnetic fields in interplanetary space and the magnetosphere. In, *Proceedings, 9th International Conference on Cosmic Rays*, London, Sept. 1965, Vol. 1, pp. 14–25. London, Inst. Phys. Phys. Soc., 1966.
  98. NESS, N. F. Observations of the interaction of the solar wind with the geomagnetic field during quiet conditions. In, King, J. W., and W. S. Newman, Eds. *Solar Terrestrial Physics*, pp. 57–89. (Presented at Inter-Union Symp. on Solar-Terrestrial Physics, Belgrade, Aug. 1966.) London, Academic, 1967.
  99. NESS, N. F. Simultaneous measurements of the interplanetary magnetic field. *J. Geophys. Res.* 71(13):3319–3324, 1966.
  100. NESS, N. F., K. W. BEHANNON, S. C. CANTARANO, and C. S. SCEARCE. Observations of the Earth's magnetic tail and neutral sheet at 510 000 kilometers by Explorer 33. *J. Geophys. Res.* 72(3):927–933, 1967.
  101. NESS, N. F., and J. M. WILCOX. Extension of the photospheric magnetic field into interplanetary space. *Astrophys. J.* 143:23–31, 1966.
  102. OBAYASHI, T. The interaction between solar wind and geomagnetic field during active periods. In, King,

- J. W., and W. S. Newman, Eds. *Solar Terrestrial Physics*, pp. 107–167. (Presented at Inter-Union Symp. on Solar-Terrestrial Physics, Belgrade, Aug. 1966.) London, Academic, 1967.
103. O'BRIEN, B. J. Rocket and satellite observations of energetic particles during P. C. A. events. In, Smith-Rose, R. L., Ed. *Life Sciences and Space Research* (Proc., 7th COSPAR Int. Space Sci. Symp., Vienna, May 1966), Vol. 7, Pt. 2, pp. 806–818. Amsterdam, North-Holland, 1967.
104. PALMEIRA, R. A. R., F. R. ALLUM, K. G. McCACKEN, and U. R. RAO. Low energy solar proton and electron propagation in interplanetary space. In, *Trudy Mezhdunarodnogo Seminara po Probleme Generatsiya Kosmicheskikh Luchey na Solntse* (Transl: *Proceedings, International Seminar on Solar Cosmic Ray Generation*), pp. 75–151. Moscow, 1971.
105. PARKER, E. N. Dynamics of the interplanetary and magnetic fields. *Astrophys. J.* 128:664–676, 1958.
106. PARKER, E. N. Geomagnetic fluctuations and the form of the outer zone of the Van Allen radiation belt. *J. Geophys. Res.* 65:3117–3130, 1960.
107. PARKER, E. N. *Interplanetary Dynamic Processes*. New York, Interscience, 1963.
108. PARKER, E. N. Solar wind interaction with the geomagnetic field. *Rev. Geophys.* 7(7):3–10, 1969.
109. POUNDS, K. A. Recent solar x-ray studies in the United Kingdom. *Ann. Astrophys. (Paris)* 28(1):132–145, 1965.
110. *Radioizlucheniye Solntsa* (Transl: *Radio Radiation of the Sun*), Collect. No. 1. Leningrad, Leningrad State Univ., 1969.
111. RATCLIFFE, J. A., Ed. *Physics of the Upper Atmosphere*. New York, Academic, 1960; Moscow, Fizmatizdat, 1963.
112. ROEDERER, J. G. *Dynamics of Geomagnetically Trapped Radiation (Physics and Chemistry in Space)*, Vol. 2. Berlin, New York, Springer, 1970.
113. ROEDERER, J. G. Quantitative models of the magnetosphere. *Rev. Geophys.* 7:77–96, 1969.
114. SCARF, F. L. Characteristics of the solar wind near the orbit of Jupiter. *Planet. Space Sci.* 17:595–608, 1969.
115. SCHATTEN, K. H., J. M. WILCOX, and N. F. NESS. A model of interplanetary and coronal magnetic fields. *Solar Phys.* 6:442–455, 1969.
116. SHAPIRO, I. I., D. A. LAUTMAN, and G. COLOMBO. The Earth's dust belt: fact or fiction? 1. Forces perturbing dust particle motion. *J. Geophys. Res.* 71:5695–5704, 1966.
117. SHAPIRO, M. M., and R. SILBERBERG. Heavy cosmic ray nuclei. In, Segre, E., Ed. *Annual Review of Nuclear Science*, Vol. 20, pp. 323–392. Palo Alto, Calif., Annual Reviews, 1970.
118. SIMPSON, J. A. Galactic sources and the propagation of cosmic rays. In, *Invited and Rapporteur Papers, 12th International Conference on Cosmic Rays*, Hobart, Aust., Aug. 1971, pp. 324–355. Hobart, Univ. Tasmania, 1972.
119. SLYSH, V. I. Observations of radio radiation of the Sun at long wave lengths by the Luna 11 and Luna 12 artificial lunar orbiters. *Kosm. Issled.* 5(6):897–910, 1967.
120. SMITH, F. G. *Radio Astronomy*. London, Penguin, 1960.
121. SMITH, H. J., and E. VAN P. SMITH. *Solar Flares*. New York, Macmillan, 1963.
122. *Solnechnyye Dannye* (Transl: *Solar Data*). Leningrad, Nauka, 1954–(Monthly)
123. SONETT, C. P., P. J. COLEMAN, Jr., and J. M. WILCOX, Eds. *Solar Wind*. Washington, D.C., NASA, 1972. (NASA SP-308)
124. SONNERUP, B. U. Ö. On the stability of the closed magnetosphere. *J. Geophys. Res.* 70(5):1051–1060, 1965.
125. SPEISER, T. W., and N. F. NESS. The neutral sheet in geomagnetic tail; its motion, equivalent currents and field line connection through it. *J. Geophys. Res.* 72:121–141, 1967.
126. SVESTKA, Z. PCA events and forbush effects. Presented at Inter-Union Symp. on Solar-Terrestrial Physics, Belgrade, Aug. 1966.
127. SYROVATSKIY, S. I. The development of current layers in the plasma with frozen magnetic lines of force. *Zh. Eksp. Teor. Fiz.* 60:1727–1741, 1971. (Transl: *Sov. Phys.-JETP*) 33:933–940, 1971.
128. SYROVATSKIY, S. I. The formation of polar and equatorial condensations of plasma in the proximity of a changing magnetic dipole. *Astrophys. Space Sci.* 4:240–251, 1969.
129. TOUSEY, R. Ultraviolet spectroscopy of the Sun. In, Liller, W., Ed. *Space Astrophysics*, pp. 1–16. New York, McGraw-Hill, 1961.
130. TVERSKOV, B. A. *Dinamika Radiatsionnykh Poyasov Zemli* (Transl: *Dynamics of the Radiation Belts of the Earth*). Moscow, Nauka, 1968.
131. U.S. Environmental Science Service Administration. *Solar Geophysical Data*. Boulder, Colo., ESSA Res. Labs., 1966–1970.
132. VAISBERG, O., and A. BOGDANOV. About structure and variation solar wind–Mars interaction region. *J. Geophys. Res.* (In press)
133. VAN ALLEN, J. A. Dynamics, composition and origin of corpuscular radiation trapped in the Earth's magnetic field. In, LeGalley, D. P., Ed. *Space Science*, pp. 226–274. New York, Wiley, 1963.
134. VAN ALLEN, J. A., and S. M. KRIMIGIS. Impulsive emission of ~ 40 keV electrons from the Sun. *J. Geophys. Res.* 70(23):5737–5751, 1965.
135. VERNOV, S. N., S. N. CHUDAKOV, P. V. VAKULOV, E. V. GORCHAKOV, P. P. IGNATIEV, N. N. KONTOR, S. N. KUZNETSOV, et al. A study of solar and cosmic radiation from the Venus 4 space probe. In, Champion, K. S. H., P. A. Smith, and R. L. Smith-Rose, Eds. *Life Sciences and Space Research* (Proc., 11th COSPAR Plenary Meet., Tokyo, May 1968), Vol. 9, pp. 203–214. Amsterdam, North-Holland, 1969.
136. VERNOV, S. N., A. E. CHUDAKOV, P. V. VAKULOV, E. V. GORCHAKOV, N. N. KONTOR, Yu. I. LOGACHEV, G. P. LYUBIMOV, N. V. PERESLEGINA, and G. A. TIMOFEEV. Propagation of solar and galactic cosmic rays of low energies in the interplanetary medium.

- In*, Somogyi, A., Ed. *Acta Physica, Acad. Scient. Hung.*, Proceedings, 11th Conference on Cosmic Rays, Budapest, 1969, Vol. 29, Suppl. 2, pp. 459–469. Budapest, Akademiai Kiado, 1970.
137. VERNOV, S. N., E. V. GORCHAKOV, S. N. KUZNETSOV, Yu. I. LOGACHEV, E. N. SOSNOVETS, and V. G. STOLPOVSKIY. Particle fluxes in the outer geomagnetic field. *Rev. Geophys.* 7:257–280, 1969.
138. VERNOV, S. N., P. V. VAKULOV, E. V. GORCHAKOV, V. G. KURT, Yu. I. LOGACHEV, G. P. LYUBIMOV, and G. A. TIMOFEEV. The nature of propagation of fast particles in interplanetary space at various stages of increases in solar cosmic ray fluxes. *In, Trudy Mezhdunarodnogo Seminara po Probleme Generatsiya Kosmicheskikh Luchey na Solntse*, 1970. (Transl: *Proceedings, International Seminar on Solar Cosmic Ray Generation*), pp. 64–74. Moscow, 1971.
139. VERNOV, S. N., P. V. VAKULOV, and Yu. I. LOGACHEV. The radiation belts of the Earth. *In, Blagonravov, A. A., Ed. Uspekhi Sovetskogo Soyuza v Issledovanii Kosmicheskogo Prostranstva* (Transl: *Successes of the Soviet Union in Space Studies*), pp. 106–148. Moscow, Nauka, 1968.
140. WEBBER, W. R. Review of solar cosmic ray events. *In, Hess, W. N., Ed. NASA Symposium on the Physics of Solar Flares*, pp. 215–255. Washington, D.C., NASA, 1963. (NASA SP-50)
141. WEBBER, W. R. The spectrum and charge composition of the primary cosmic radiation. *In, Flügge, S., Ed. Handbuch der Physik (Kosmische Strahlung II)*, Vol. 46, pp. 181–264. Berlin, Springer, 1967.
142. WHANG, Y. C., and N. F. NESS. Observations and interpretation of the lunar Mach cone. *J. Geophys. Res.* 75:6002–6010, 1970.
143. WHIPPLE, F. J. A comet model. II. Physical relations for comets and meteors. *Astrophys. J.* 113:464–474, 1951.
144. WILLIAMS, D. J. Sources, losses, and transport of magnetospherically trapped particles. *In, Solar Terrestrial Physics, 1970. The Magnetosphere* (Proc., Int. Symp., Leningrad, May 1970), Pt. 3, pp. 66–130. Dordrecht, Holl., D. Reidel, 1972.
145. WILLIAMS, D. J., and G. D. MEAD. Nightside magnetosphere configuration as obtained from trapped electrons at 1100 kilometers. *J. Geophys. Res.* 70(13):3017–3029, 1965.
146. WILLIAMS, D. J., and N. F. NESS. Simultaneous trapped electrons and magnetic tail field observations. *J. Geophys. Res.* 71(21):5117–5128, 1966.
147. WINCKLER, J. R. The origin of energetic electrons in the Earth's environment. *In, Proceedings, International Seminar on Space Research*, p. 130. Leningrad, 1969.
148. ZHELEZNYAKOV, V. V. *Radioizlucheniye Solntsa i Planet* (Transl: *Radio Radiation of the Sun and Planets*). Moscow, Nauka, 1964.

## **Part 2**

# **PLANETS AND SATELLITES OF THE SOLAR SYSTEM FROM PHYSICAL AND ECOLOGICAL VIEWPOINTS**



The Moon. This photograph of the full Moon was taken from the Apollo 11 spacecraft at a distance of 18 500 kilometers during its journey homeward. Aboard Apollo 11 were astronauts Neil A. Armstrong, Michael Collins, and Edwin E. Aldrin, Jr. (NASA 69-H-1374)

THE POSSIBILITY OF THE  
IMAGE IS POOR

! N 76 - 26802

## Chapter 3

### THE MOON AND ITS NATURE

HAROLD C. UREY<sup>1</sup>

University of California, San Diego, La Jolla, California USA

The Moon and its relation to the Earth and Sun have been observed by men from ancient times to the present with ever-increasing intensity and effectiveness. Results of these studies up to the most recent years have been recorded in numerous treatises and textbooks. For present purposes, it is not necessary to review the older work, which will be referred to without detailed discussion whenever it bears on very recent work.

The lunar surface consists predominantly of many craters produced by great collisions. This applies particularly to the far side and the terrae areas of the near side. The great circular maria, Imbrium, Serenitatis, Crisium, Nectaris, Humorum, and Orientale, were produced by great collisions; the shallow, irregular maria consist of flooded areas with igneous materials over previous terrain similar to the terrae areas. These shallow maria have mountainous masses protruding through the dark, smooth material, and may cover areas that are collision maria, the outlines of which have been obscured by subsequent events. If such collisions have occurred on the

Earth, which appears to be a necessary conclusion, all Earth rocks laid down prior to this collisional history would have been converted to rubble. Since well preserved igneous and sedimentary rocks are preserved in the Earth's surface from some 3.5 aeons ago, these numerous collisions must have occurred before that time. The ray craters, many smaller ones, and some larger craters without rays, have surely been formed during all geologic time. The great maria have the appearance of lava flows, ash or ignimbrite flows, or lakes of water. They certainly are not the last, shown by absence of water in the lunar rocks, but the choice between the others remains open. There are also explosive craters of internal origin and it is sometimes maintained that some caldera exist on the Moon. This writer has doubts in regard to the presence of any large caldera. Recent work is reviewed somewhat in the time sequence of discovery and study.

The physical constants of the Moon and its orbit are well-known, some of which are listed in Table 1.

#### GRAVITATIONAL FIELD

<sup>1</sup>This work was supported by NASA grant NGR 05-009-150-2. I wish to thank J. R. Arnold, W. Compston, K. Marti, W. H. Munk, J. F. Gilbert, H. Suess, L. T. Silver, M. Tatsu-mota, S. P. Vinogradov, G. J. Wasserburg, and G. Latham for their critical advice in the preparation of this manuscript.

Special thanks are due the Russian compilers G. A. Leikin, B. Yu. Levin, L. N. Bondarenko, V. S. Troitskiy, T. V. Tikhonov, and A. N. Gavrilov, who provided Soviet material for this chapter.

The gravitational field of the Moon has been investigated in great detail using orbiter satellites [37, 42, 43]. This field can be represented by the usual series in spherical harmonics only with the use of many terms; Michael et al [42] have given

the most comprehensive tables for constants in the equation

$$V(r, \phi, \lambda) = \frac{GM}{r} \left\{ 1 + \sum_{n=2}^{\infty} \sum_{m=0}^n \left( \frac{a}{r} \right)^n P_n^m (\sin \phi) (C_{n,m} \cos m\lambda + S_{n,m} \sin m\lambda) \right\} \quad (1)$$

where  $r, \phi, \lambda$  are the polar coordinates. They show that terms to the 13th order are necessary to describe the field, and even then, the constants are not decreasing, indicating that the field of the Moon is far from that expected for a weak body under gravitational forces of the Earth, Moon, and Sun and the centrifugal forces of rotation. In this latter case, the terms beyond  $C_{2,0}$  should be zero, but this is not true. It must be concluded that some very irregular distribution of mass exists within the Moon.

The values of the constants

$$\alpha = \frac{C-B}{A}, \quad \beta = \frac{C-A}{B}, \quad \gamma = \frac{B-A}{C}$$

where  $A, B$ , and  $C$  are the moments of inertia,  $A$  about the axis pointing to the Earth,  $B$  that about the east-west axis, and  $C$  that about the polar axis, have been carefully studied by Koziel [29] who gives 3.984, 6.294, and 2.310, all  $\times 10^{-4}$  for these constants from lunar librations. Kopal obtains similar values for these constants [27]. The calculated values for a plastic Moon under tidal and centrifugal forces are 0.94, 3.75, and 2.81, all  $\times 10^{-5}$ . Again, these constants indicate that the Moon is a very rigid body and has been since early in its history. Estimates of moments of inertia have been made, indicating that these moments are close to  $0.4 Ma^2$ , where  $M$  and  $a$  are the mass and radius of the Moon. This value is characteristic of a sphere with uniform density

TABLE 1.—Physical Constants of the Moon

Mass	$7.35 \times 10^{25} \text{ g}$
Radius	1737 km
Surface force of gravity	162 cm/s <sup>2</sup>
Orbital mean radius	384 403 km
Orbital eccentricity	0.05490
Velocity of escape	2.38 km/s
Sidereal month	27. <sup>d</sup> 32 166

throughout. The surface regions, for some depth, must consist of low-density material and should lower the moments of inertia to some extent. This low density is located predominantly on the far side—possibly 30 km thick—and is responsible mostly for the Moon's irregular shape, moments of inertia, and displacement of the center of mass relative to the center of figure—2 to 3 km [26].

The triaxial, ellipsoidal, nonequilibrium shape of the Moon is a puzzle of long standing, for which various explanations have been offered.

1. The Moon may be sufficiently rigid to support the irregularity, although this does not explain its origin.
2. The lower temperature at the poles should result in greater density material and smaller radii in these regions [35], but this does not explain the difference between the A and B moments of inertia.
3. Convection in the Moon in two cells rising at the poles and sinking at the Equator should give less mass at the poles and higher mass at the Equator [57], but again, the A and B moments should be equal. Possibly a special combination between the second and third suggestions is possible.
4. The Moon accumulated from objects of variable density which should give variations in moments of inertia [87]. If convection occurs, the Moon must have been melted greatly at some point in its history, since two-cell convection requires a small core, according to Chandrasekhar [12]. The convection must be deep enough in the Moon so that no folded mountains are produced, as on the Earth. Booker [8] proposed a single-cell convection which may have produced the higher level of the far side if the rising current was in the region of the near side.

### Anomalies

Muller and Sjogren [44, 45, 46] showed that substantial mass concentrations, called mascons, exist in various locations on the near side of the Moon which are associated mostly with the

circular collision maria and probably always where definite localized masses occur. The mascons were discovered and mapped by observing flights of the orbiters and measuring their velocities directly. Muller and Sjogren believe that the observations are reliable for longitudes between 100 and  $-100^{\circ}$  and latitudes between  $-50$  and  $50^{\circ}$ . The marked positive gravity anomalies in Maria Imbrium, Serenitatis, Crisium, Nectaris, and Humorum are evident, as is a positive anomaly slightly to the northwest of the center of the lunar disk. Mare Orientale appears to have an anomaly which is partly positive and partly negative. Other positive and negative anomalies are probably within observational error. A negative anomaly in Sinus Iridum is regarded as real by the authors. They also noted negative anomalies in Ptolemaeus and Albategnius of some 87 milligals (mGal) from observations of the Apollo 12 flight in its approach to the landing site. Booker et al [8] estimated the excess masses required to produce the observed anomalies of the order of  $10^{21}$  G and produce excess pressures below these masses of about 100 bars. Since all these features are very old, the gravity anomalies have been supported by the Moon for several aeons, indicating that it has, and has had, very high rigidity.

Two distinct classes of explanations for these effects have been offered. (1) It is presumed that material from the lunar interior has risen by various processes into excavations produced by the objects which produced the maria [7, 25, 48, 95]. (2) It is suggested that the mascons consist of remnants of the colliding objects themselves, together with substantial material filling the excavation produced by the collision [27, 67, 85, 88].

If lava flows from the interior are responsible for the mascons, it must be possible to account for the excess pressure required to produce these deposits, i.e., about 50–100 bars. No satisfactory source of such pressure exists. Possibly material has flowed into the great excavations, produced by large colliding objects from surrounding areas. Probably Van Dorn's [90] great waves in a highly fragmented surface layer of the Moon would bring this about, but special assumptions are necessary to account

for the excess mass per unit area. If lava flows from beneath neighboring areas into the mare regions occurred, the excess mass might be explained. Sjogren concluded recently that the extra mass of Mare Serenitatis consists of a near surface slab which may have been produced by such lava flows.

Another assumption is that the interior rocks of the Moon moved as solid material into the great cavities produced when the maria were produced, and that these rocks were of higher density than the rocks more on the surface. If they moved until reaching isostatic equilibrium, no gravitational anomalies would be observed, but if they did not quite reach this position, negative anomalies would be observed. If the rocks exceeded this, due to high momentum of the rising material or fill-in over the mass by lava flow or fragmented materials, there would be a positive anomaly, as observed. In this case, great strength in the highly broken material below must be postulated, which may be possible but does not seem probable.

It has been suggested that the outer parts of the Moon have considerable tensile strength, and that the heating within the Moon produces liquid that is forced up into the basins of the maria [25]. Such partial melting on Earth produces rocky materials which are less dense in the solid state and even more so in the liquid state than the rocks from which they are produced. On Earth, lava flows produce mountainous masses with positive gravity anomalies; on the Moon, these occur in the low-lying maria. Possibly the high-density titaniferous basalt could supply such material. However, the many cracks or regular rills in the Moon's surface do not favor the view that an outer shell of great tensile strength exists.

These suggested origins require that a net throwout equal to a volume of the area of the maria to a depth of some 50 km existed, and this requires a throwout layer of one-tenth this thickness over an area of ten times the area of Maria Imbrium and Serenitatis, for example. This writer is quite unconvinced that this is true on the basis of available photographs.

The suggestion that the mascons are the residues of colliding objects is based on several assumptions: that the objects arrived at velocities

not much greater than the lunar escape velocity; that collision energies extrapolated from those of atomic explosions can be applied to the lunar maria; and that the volume of the net throwout of lunar rock is equal to the volume of the colliding object. This explanation requires considerable "fill-in" of some kind. Because of the difficulty of supporting the mascons if the lunar interior is at melting temperatures, it is assumed that this material was filled in during the collision by processes of the type discussed by Van Dorn [90]. Significantly, there seems to be approximate agreement between the masses required to produce the mascons and the masses required to produce the maria. The great excess mass of the mascon of Mare Imbrium and of those of other maria and their persistence for aeons (probably  $4.0 \times 10^9$  years), indicates that the Moon is now, and has been, much more rigid and at lower temperature than the Earth, which establishes isostasy in some  $10^7$  years. It seems that immense lava flows and very large movements of material from the interior beneath the maria are inconsistent with the support of these massive structures during several aeons.

The Apollo 15 laser altimeter showed that great differences in altitude of lunar surface areas exist. The near side areas are generally depressed by about 2 km, and the far side elevated relative to the sphere centered on the center of mass. Also, the deeper points observed so far are in circular maria, which means of course, that some especially high-density masses must lie below the surface in these regions. The irregular Van de Graff crater on the far side is also very deep, and one wonders if a mascon exists in this area (see [55]).

## SURFACE

The lunar surface is covered by craters and extensive smooth areas. The craters are mostly of collisional origin, but some volcanic craters are surely present. The collisional craters vary in size from the microscopic to the great collisional areas of the lunar maria, i.e., hundreds of kilometers in diameter. They are of varying ages—a very dense covering of older ones possibly 4.0 to 4.6 billion years old and a sparse covering of those which have been formed during

all of geologic time. These craters, which have been studied by many with regard to numerous details, are, however, mostly random events with little more to reveal about the history of the Moon. Ptolemaeus and Albategnius have negative gravitational anomalies of approximately 87 mGal [45], and thus show that these old craters were formed on a rigid Moon early in lunar history, and that this rigidity has persisted to the present. Unfortunately, it appears difficult to state exactly what temperature regime would be consistent with this fact. The larger craters have central peaks indicating that some rebound of the material below has occurred, or that some residue of the colliding object remains; probably the former is the correct explanation.

Volcanolike craters are present on the Moon. Certainly the halo craters which are surrounded by black areas and rows of craters along winding cracks are such. The Davy rill is nearly a straight line of craters which may be of internal origin, or collisional craters from an object such as a comet head which broke into many fragments due to effects of the lunar gravitational field. In many cases, it is difficult to state whether other smaller craters also belong to this class, much effort having been directed to this problem. Many of these craters have wide mouths as though they were produced by emission of gases. (Steam is the most prominent volcanic gas on earth! What were these gases on the very dry Moon? Did water react with iron somewhere below to produce hydrogen, or was it carbon monoxide or something else?) Definite localized lava flow structures are observed in several places, particularly in Maria Imbrium and Serenitatis. Also, the Marius Hills in the western equatorial regions appear to have definite volcanic features.

The great maria represent extensive eruptive flows, generally thought to be lava, but which may be volcanic ash or ignimbrite. Lava flows to the Earth's surface are regularly frothy, and such flows to the lunar surface, where at present at least a hard vacuum exists, should have this character even if there are fewer volatiles in these melts. Soils are observed at present which consist of finely divided crystalline and glassy particles in which sizeable crystalline rocks are imbedded. These rocks have some cavities with

smooth walls which must have crystallized from a melt containing macroscopic bubbles of gas, with the appearance of having solidified at some depth beneath an insulating surface layer. The soil has been partly produced by collisions of micrometeoroids on the soil and rocks, although probably it is partially of ignimbrite origin as well [50].

The great shallow maria—Oceanus Procellarum, Tranquillitatis, Fecunditatis, and Nubium—do not show marked and consistent gravity anomalies. Hence, the flows are in isostatic equilibrium indicating that the material of the flows probably originated below the surfaces where they lie, or isostasy was established for masses over large areas on the surface but not for the mascons lying some distance beneath the surface. These dark materials must be very thick (up to several kilometers), since the collisional mountains present originally in these areas are largely covered by these flows. These mountains may have been partly shaken down by the violent collisional process which produced the circular maria, but deep pockets and shallow areas must be present in these maria. A popular hypothesis for many years has been that these dark maria are deep lava flows from the lunar interior, and this opinion remains popular today. However, the seismic data are so different from those observed on the Earth that it is necessary to postulate some marked differences in surface structures in order to explain these differences.

Substantial differences exist in estimates of the thickness of the regolith. Shoemaker et al [64] find evidence for very small depths, some 3 to 6 m, in the crater near the Apollo 11 landing site. Kopal [28] argues from the depths of the rills for some hundreds of meters depth and Seeger [63] from the structure of the Dawes crater suggests 1 km as the depth at this point. Gold and Soter [20] argue for a depth of fragmented material of 6–9 km. These estimates are for mare material. The intense collisional processes in the terrae regions must have produced a highly fragmented material, and of course, the terrae surfaces have been subjected to the same micro- and macrometeoroid bombardment as the mare areas since their formation.

The great circular maria were produced by

massive collisions. Van Dorn [90] has applied wave theory to these collisions and, particularly in regard to Mare Orientale, found satisfactory agreement between calculated and observed radii of wavelike structures surrounding this mare and others, if a liquid layer 50 km deep is assumed. However, it cannot be presumed that a liquid was present 50 km deep, and at the same time, suppose that a rigid crust supporting mountainous masses existed. A highly fragmented layer of solid materials possibly would behave as an imperfect liquid supplying waves under high energy which “froze” as energy densities fell to lower values.

The far side of the Moon is more elevated than the near side by approximately 3 to 4 km, and the center of figure is displaced about 2 to 3 km away from 25°E longitude [26]. This probably indicates that the crust is some 30 km thick on the far side of the Moon, consists of minerals rich in CaO, Al<sub>2</sub>O<sub>3</sub> and SiO<sub>2</sub>, and contains little FeO.

The physical evidence for the lunar surface strongly favors the view that there is a substantial fragmented layer of silicate materials in the surface of the maria and highlands, that the body of the Moon is remarkably rigid to a considerable depth, and has been during most of its age.

## SEISMIC OBSERVATIONS

Seismic instruments were landed on the Moon by the Apollo missions, and the information received proved of great importance for understanding the lunar interior [34, 71]. The first most striking observation was that the rate of decay of seismic signals was far less than for terrestrial signals. The lunar module of Apollo 12 was dropped at a velocity 1.68 km/s, an energy of  $3.36 \times 10^{16}$  erg, and at a distance of 73 km from the seismometer. A signal recorded rose to maximum value in about 7 min and slowly decreased until it was hardly detected 54 min later. When the third stage of the Apollo 13 was dropped at 2.58 km/s and an energy of  $4.63 \times 10^{17}$  erg, 135 km from the seismometer, a similar record was obtained, lasting for more than 200 min. If the velocity of sound were 6 km/s, the sound would have traveled 21 600 km or 6 times the diameter of the Moon within 1 hour. Both P-

and S-waves, i.e., compressional and shear waves, were recorded. Similar effects have been observed more recently. Such results differ greatly from observations on the Earth, where the signals would have died out in a few minutes. Other weaker signals, quite similar, have been observed, which are believed due to meteorite collisions. Other groups of signals have also been received, where the detailed pattern of vibrations is repeated exactly, indicating that successive members of a group come from the same location on the Moon and travel in identical paths from their sources to the seismometers.

The waves and vibrational energy for long period vibrations appear to be confined to a very limited volume, probably a layer on the surface of the Moon, mostly in the immediate neighborhood of the source. Such slow attenuation is not observed on the Earth, and hence, important differences in the surfaces of the two planets must exist. The most obvious is the more highly fragmented character of the lunar surface and high vacuum, resulting in absence of gas in the fragmented rocks of the Moon. Both Oceanus Procellarum and Mare Tranquillitatis must have a highly fragmented layer similar to that of the highland underlying the dark soil and rocky layer of the maria. Latham et al [34] discussed this structure, and Gold and Soter [20] presented calculations using a model of dust layer some km in thickness with sound velocities increasing linearly with depth, and with reflections from the top surface of the maria. The two models are quite similar, if it is remembered that blocks of rocks smaller than the wavelengths would make little difference in the flow and reflection of sound waves. It is probable that sheets of solid silicates would not behave in a similar way.

Some signals are precisely repeated and cannot be ascribed to meteorites, hence, are indigenous; these are more frequent at perigee, therefore appear to be triggered by a tidal effect. Reflections from various masses and surfaces must occur, hence, extensive heterogeneities must be present. These moonquakes mean that mechanical or potential energy from some source is being dissipated as vibrational energy and heat. Several sources of such energy can be considered.

1. The mascons are settling into deeper layers.
2. The irregular shape of the Moon is settling into a more spherical shape.
3. The ellipsoidal shape of the Moon's orbit is becoming more nearly circular with a lesser major axis; this effect would be superimposed on other changes in orbit due to other causes.
4. Convection in the lunar interior or lava flows cause terrestrial-type quakes.
5. As the Moon moves away from the Earth due to tidal effects, it keeps the same face toward the Earth, its velocity of rotation decreases, and this probably requires moonquakes, the decreased rotational energy supplying the energy.
6. Slight contraction or expansion occurs due to changing temperature of the Moon.
7. Rocks are falling from cliffs; however, it would seem probable that this would have been completed after billions of years.

These moonquakes appear to come from depths of some 800 km, and slight reflections come from similar depths indicating that some layering exists at these depths. However, definite evidence for a metal core has not been observed as yet. There appears to be a layer below the 20-km regolith or basaltic layer to 60-km depth having a compressional sound velocity equal to that of anorthosite, and below this material, to an undetermined depth, having a sound velocity of dunite. Thus, the layering seems to be approximately 20 km of fragmented basalt, 40 km of anorthosite, and then dunite to an unknown depth with a source of moonquakes and slight reflection at some 800-km depth with no evidence as yet for any metallic core. However, later data indicate that there is a central region which will not transmit S-waves, probably consisting of partially melted silicates. This central "core" has a radius of about 700 km [31].

The Moon is much quieter than the Earth which has immense sources of energy, the most important being convection in the mantle driven by radioactive heating. This builds the immense mountain chains, great gravity anomalies both positive and negative, produces the great vol-

canoes and lava flows, and moves the continental masses over the Earth's surface. If convection occurs (or has occurred) in the Moon, it must produce very minor effects compared to its effects on Earth.

The explanation of the seismic effects, due to a fragmented layer on the surface, argues strongly against a conventional bed of solidified lava below the surface. But there are rocks scattered in the soil which were produced by a melting process, and the complicated and detailed patterns from the moonquakes indicate that complicated structures exist below the surface.

### CHEMICAL COMPOSITION

The most recent values for the radius of the Moon give a mean density of  $3.36 \text{ g/cm}^3$ , and the highly fragmented character of the surface suggests that the fraction of voids may not be negligible when estimating the density for the whole Moon. Also, the interior density may be lowered more by high temperatures than it is raised by high pressures. Again, this suggests higher true mineral densities at laboratory temperature and pressure; possibly  $3.4 \text{ g/cm}^3$  is a reasonable estimate for the average of this quantity (see [88, 93]). Mean densities of chondritic meteorites of the L and H types under low pressures run about  $3.57$  and  $3.76 \text{ g/cm}^3$  [86] or  $3.68$  and  $3.85 \text{ g/cm}^3$ , if high density minerals are present. The Earth's density at low temperatures and pressures may be about  $4 \text{ g/cm}^3$ .

The Moon contains either less iron or larger quantities of water and carbonaceous compounds than the Earth. The low concentrations of water and carbon compounds in the surface materials dispute the second hypothesis. Silicate minerals observed in meteorites with iron content limited to some 10% by weight would give the required estimated density. Carbonaceous chondrites Type III also have this density. The concentration of potassium is lower in these meteorites than in other chondrites, i.e., about 360 instead of 850 ppm. This lower abundance of potassium and comparable abundances of uranium and thorium would permit an initially cool Moon to remain below the melting point of silicates during geologic time.<sup>2</sup>

In a very thorough paper that reviewed the chemistry of the Moon [91], the conclusion was that the Moon's surface materials can be regarded as a mixture of two components: one condensed at high temperature, and another of average meteoritic composition. The ratio of K to U is about 2000, whereas this ratio in chondritic meteorites is about 60 000 or 90 000 due to greatly increased concentration of U and other high-temperature condensing elements. This ratio for Earth rocks is about 10 000 indicating that the Earth also has an increased high-temperature condensate fraction.

The first observational data on lunar composition were obtained in Surveyor flights 5, 6, and 7 [73, 74, 75, 76], showing that the maria contained basalt with high titanium content, and the highlands contained high concentrations of aluminum, calcium, and low concentrations of iron. These results were completely confirmed by the precise measurements on returned Apollo samples. Several distinct types of siliceous materials are on the lunar surface. The maria areas appear to consist mostly of basaltic-type rocks and finely divided material. The highland areas consist of rocks having high concentrations of calcium feldspars, so-called anorthositic-type materials. Then the area near Fra Mauro where Apollo 14 landed consists of so-called KREEP, high in potassium, rare earths, and phosphorus. No meteorites of the anorthositic or KREEP type have been observed, nor has any other rock type been exactly duplicated by meteorites. Other rock types found are apparently rare. Certain marked chemical differences exist between lunar terrestrial and meteoritic materials.

One very curious chemical difference concerns europium, an element which is divalent under highly reducing conditions and trivalent under less reducing conditions. In the lunar surface rocks, it has a strong tendency to follow the divalent strontium and decreased tendency to follow the other trivalent rare earths. This indicates that the lunar surface materials were formed under rather highly reducing conditions. Only small bits

<sup>2</sup> In a recent paper, Tozer [72] discusses convection in planetary objects and points out that much greater cooling might occur in the Moon than would be expected if thermal conduction only was effective.

of metallic iron-nickel are observed, and it is uncertain whether these are native to the Moon or are fragments of meteorites. Iron sulfide is present only in small amounts; titanium contents, strikingly, are much higher in some lunar basalts than in terrestrial basalts.

The physical condition of these siliceous materials is of interest: the basaltic soil consists of finely divided crystalline and glassy chips, and the breccia appears to have the physical structure of sintered soil. Rocks are present which crystallized from a liquid melt, which sometimes contain smooth bubbles, indicating that gas was present when they solidified. The "genesis" rock 15415 consists entirely of glass spherules of calcium feldspar. The lunar materials often contain rounded silicate objects which are physically similar to chondrules of meteorites, but of different chemical composition. Only a few recognizable bits of meteorites have been observed, indicating that meteorites which must have fallen on the Moon have been broken into very small fragments. One or 2 percent of the lunar surface is of meteoritic composition.

Since the Moon has no atmosphere, it is possible to observe the high-energy radiation emitted by radioactive elements, i.e., rays at great heights above the lunar surface. Such observations were planned by Arnold very early in the lunar space program, and have recently been successful on Apollos 15, 16, and 17 [5]. These studies show that the maria areas have higher concentrations of K, U, and Th than have the terrae areas, also that there is some variation in concentrations of these elements over considerable mare areas. Also, the K/U ratio is considerably less in all areas than in terrestrial rocks. These results confirm analyses on returned samples, showing that the chemical differences apply to great areas of the Moon.

The study of fluorescent x-rays emitted by the lunar rocks under bombardment of solar x-rays showed the highland areas to be generally high in elements of anorthositic-type rocks [2]. Unfortunately, there are not more such detailed and extensive studies of the Moon.

Continuous melting of some kind on a limited scale appears likely from the earliest years of lunar history until about 3 aeons ago. The small

lava flows reported at various locations may be more recent. If they come from the deep lunar interior, they may provide information regarding the chemical composition of the Moon's deep interior, which will be very informative. It was thought that Apollo 16 which landed near Descartes would find more recent volcanic materials, but this area proved to be covered with ancient anorthositic-type rocks and soil. The landing area of Apollo 17 near Littrow was carefully planned to be a recent lava flow area, but proved not to be so. At present, there is no evidence for more recent lava flows. It was hoped that Apollo 17 would provide examples coming from the deep lunar interior, but this proved not to be true.

## CARBONACEOUS MATERIALS

Evidence for living or fossil forms on the Moon has not been found. The total concentrations of carbon in all lunar samples range from about 30 to 230 ppm, the concentrations in the soils ranging higher than in the crystalline rocks. Nitrogen concentrations are somewhat less.

Evidence was obtained for carbon-hydrogen, carbon-hydrogen-oxygen, and nitrogen compounds, but generally in such low concentrations that it is difficult to be certain that these are indigenous and not due to terrestrial contaminations. The gas chromatograph and mass spectrometer are so sensitive that contaminations in the range of parts per  $10^9$  of some compounds can be detected.

In general, all investigators found many carbon-hydrogen compounds containing up to some six or more carbon atoms and the more common and simple compounds of carbon with oxygen, hydrogen, and nitrogen. The more interesting compounds suggestive of those commonly present in living organisms were observed by a few. Nagy et al [47] reported glycine, alanine, and ethanalamine in addition to urea and ammonia. Glycine and alanine in nonhydrolyzed water extractions were reported, as well as glutamic acid, aspartic acid, serine, and threonine in extracts after hydrolysis. Amounts were in the range of 50 parts per  $10^9$  [17]. Porphyrin, while reported [24], was believed due to rocket exhaust.

The evidence for these compounds should be checked in other samples and, in view of the small concentrations reported, particularly great care should be taken in regard to contaminations. Likely, many compounds apparently are produced when chemical solutions are applied to the soils which contain highly activated carbon and other atoms from the solar wind. It has been shown particularly that  $\text{CD}_4$  is produced when  $\text{D}_2\text{O}$  is used instead of  $\text{H}_2\text{O}$  [1]. Water is present in such low concentrations that it is very difficult to distinguish between indigenous water and terrestrial contaminations.

### AGES

Two types of calculation have been considered in studying the age of lunar materials. Assuming that lunar materials were derived from meteoritic-type materials, we ask for the time since the materials of the lunar surface were separated from such meteoritic material, which is known as the "model age." It is assumed in calculating the  $\text{Rb}^{87}-\text{Sr}^{87}$  age or the uranium-lead and thorium-lead ages that the ratios of concentrations of rubidium to strontium or of uranium and thorium to lead have not changed since the separation process.

The second type age measures the time since the sample was last melted or since the isotopes of the elements were last uniformly distributed between the minerals of the sample in question, the latter age known as the "isochron age."<sup>3</sup> The  $\text{Rb}^{87}-\text{Sr}^{87}$  model age in the case of many lunar samples is about 4.6 aeons ( $10^9$  years), this being the time required for the  $\text{Sr}^{87}$  in bulk

<sup>3</sup> If an isotope with concentration  $x$  disintegrates to another isotope with present concentration  $y$ , and the concentrations  $t$  years ago were  $x_0$  and  $y_0$ , all relative to a stable isotope of concentration  $r$ , then

$$\frac{y}{r} - \frac{y_0}{r} = \frac{x}{r} (e^{\lambda t} - 1) \quad (2)$$

where  $t$  is the age and  $\lambda$  is the disintegration constant. This is the fundamental dating equation. If  $y/r$  and  $x/r$  are measured and  $y_0/r$  is assumed to be known from measurements on meteorites, the time  $t$  can be calculated. This is the model age. If  $y_0/r$  is unknown, but different crystals in the sample have varying values of  $y/r$  and  $x/r$ , these can be plotted on a graph, and the slope of the straight line is  $(e^{\lambda t} - 1)$  and the intercept on the  $y/r$  axis is  $y_0/r$ . The age can be calculated from the slope, and this is the isochron age [53].

samples to have evolved from the primitive strontium of 4.6 aeons ago as determined from the basaltic achondritic meteorites commonly referred to as BABI [51]. Isochron ages vary from 3.3 to 4.1 aeons. This means that the overall composition with regard to rubidium and strontium was acquired 4.6 aeons ago and was not changed in the reheating processes at later isochron dates. Ash flows at these later dates did not separate the liquid melt from a solid residue. This was probably due to the low gravitational field of the Moon where pockets of partially melted masses did not separate into liquid and solid layers, or it was due to complete melting of basaltic pockets so that no fractionation occurred.

The  $\text{K}^{40}-\text{Ar}^{40}$  ages agree generally with the  $\text{Rb}^{87}-\text{Sr}^{87}$  isochron ages, since argon would escape in the latest heating process. The U, Th-Pb ages of rocks are more complicated and do not agree with the  $\text{Rb}^{87}-\text{Sr}^{87}$  ages, apparently due to loss of lead to the surroundings, probably by volatilization. An isochron plot for bulk soils and many rocks gives ages of 4.3–4.6 AE [52]. Since the soils and rocks have varying compositions, the volcanic flows occurred from isolated pockets which did not mix from the time of 4.6 AE until the flows occurred, i.e., 3.3 to 4.0 AE ago. Whether igneous activity occurred prior to 4.0 AE or after 3.3 AE is unknown.

An alternative suggestion is that the basaltic components were made by the usual terrestrial type of flow in which the basaltic liquid is separated from a solid fraction which remains at depth, and that uranium, thorium-lead, rubidium, and strontium were added later in varying amounts to the soil from some source materials which were produced 4.6 AE ago. In this case, it must be assumed that these initial basaltic rocks with low concentrations of these elements were produced by melting processes which regularly, in terrestrial cases, do produce basalts containing these elements. This seems most improbable, and it seems likely that the closed system melting explains these data and results from the low gravitational field.<sup>4</sup>

<sup>4</sup> This is a brief summary of results obtained by several laboratories headed by G. J. Wasserburg, M. Tatsumoto, L. T. Silver, and W. Compston. (See refs. [3, 13, 14, 52, 56, 65, 68, 69, 70, 92].)

Two ages which are particularly interesting depend on the K<sup>40</sup>-Ar<sup>40</sup> ages as developed by Turner [77, 78, 79, 80], also on these and Rb<sup>87</sup>-Sr<sup>87</sup> ages reported by Schaeffer et al [61]. The "genesis rock" 15415 and anorthositic rocks of Apollo 16 have ages of about 4.1 AE. It was thought that some anorthositic rock ages might be 4.6 AE on the basis of the most primitive melting period occurring at that time, and that the anorthositic rocks were produced then. What reset the K<sup>40</sup>-Ar<sup>40</sup> clocks? Was it a hot Sun, an intense collisional process due to a collision catastrophe in the asteroidal belt, both of these, or something else?

### LUNAR HISTORY

The highland areas of the Moon are known at present to consist of an anorthositic-type rock, and that this material and the titaniferous basalt acquired their composition through a melting process  $4.6 \pm 0.1$  aeons ago. Later melting produced the rocks of Mare Tranquillitatis and Oceanus Procellarum. Mascons were produced during this interval and were supported by very rigid rocks from the time of formation until the present. The maximum subsurface temperatures consistent with support of the mascons are not known, but the subsurface temperatures of the Earth appear to be too high. Exact comparison is difficult because of the higher gravitational field of the Earth and its higher pressures in the outer layers. If the evidence for melting could be ignored, a low temperature history can be favored. If the mascons could be ignored, a high temperature history is immediately favored, i.e., if the evidence for the moments of inertia is ignored or explained. If all evidence is considered, a complicated history seems inevitable. In any case, the magnetic rocks are puzzling.

If the Moon was originally completely melted, it must have solidified and fractionated 4.5-4.7 aeons ago. The anorthositic layer solidified and floated at the surface, the pyroxene-olivine layer settled to the interior, and the titaniferous basaltic layer was between, or remained mixed with, other layers to be separated by subsequent closed system melting. The outer parts must have become cold enough to support the negative grav-

itational anomalies in Ptolemaeus and Albategnius and presumably in such craters over the entire surface. This occurred when the concentrations of radioactive elements were at maximum values [15, 16].

Many studies of lunar thermal histories have been made, which show how difficult it is to cool down a melted Moon in an aeon, even in the absence of radioactive elements. Possibly convection, as Tozer [72] points out, would be more effective. This has not happened to the Earth in 4.6 aeons, and positive gravitational anomalies are still not supported except through great convection cells. As long as lava flows occurred, the interior of the Moon would remain at high temperatures, and only an outer layer of rigid rocks would be possible, as with the Earth. It seems improbable, if not impossible, to explain the observations in this way. Without the evidence of the mascons, this postulated history would probably be more consistent with more lava flows than have been present, and particularly such a very high temperature history should have produced more general melting over the entire surface. The absence of great mare-type areas in the large craters of the far side suggests that the melting processes were just marginally possible.

If the moments of inertia indicated by orbiter and astronomical data are correct, an extensive layer of low-density anorthositic material, a small iron core, and high-density silicates on the interior are impossible without the addition of some high-density layer near the surface. It appears to be impossible that such a high-density layer was formed and supported, if the Moon was completely melted early in its history. But possibly the moment of inertia data are in error!

The suggestion has been made that the initial melting 4.5-4.7 aeons ago was limited to an outer layer of an initially cool Moon, and that the mascons were supported by the cool interior, and the negative anomalies of Ptolemaeus and Albategnius and other craters by an outer layer which had cooled rather rapidly. The sources of heating in this model are presumed to be:

- (1) surface heating in a large gas sphere or during accumulation in such a sphere [6],
- (2) surface heating by tidal effects during capture of the Moon,

- (3) magnetic fields sweeping over the lunar surface and thus generating electric currents in silicate material preheated by some previously acting mechanism,
- (4) heating in an accumulation process where rapid accumulation of solid objects occurred in the terminal stages; in cooling, the separation into several layers occurred with the titaniferous basalt solidifying last somewhere beneath the surface. Method (4) would appear to provide a very stirred condition not favorable for separation of the different layers indicated by the chemical studies.

The basalt was later melted and expelled from deeper layers. Radioactive heating was possible because of the very low thermal conductivity of a highly thermal-insulating dust layer at the surface. The shallow maria, consisting of ash flows over a very irregular surface, must have deep layers as well as shallow layers, and the deep layers should warm up markedly during hundreds of millions to a billion years, even if initially they were at low temperatures, i.e., 0° C, which need not have been the case. This is the model favored by the present writer [89, 97].

Previous suggestions assumed that the collisional history of early craters, maria, and mascons were produced early in lunar history, but if it is supposed that a catastrophic collision occurred in the asteroidal belt some 4 aeons ago, producing many large and small objects, and that these fell on the Earth, Moon, and other planets during some hundreds of millions of years, another history for the lunar surface can be devised. No record of such collisions would be retained on Earth if this occurred prior to the time the oldest terrestrial rocks were formed.

It must be assumed that the mascons result from rebound of the lunar rocks, and that the gravitational anomalies are supported in spite of a most massive and vigorous movement of rocky materials, since collisions of this kind should be at high velocities. Hence, the masses of such high-velocity colliding objects must be too small to account for the gravity anomalies. With this assumption, there may be little difficulty in having a sufficiently cold lunar surface in order

to support the gravitational anomalies of Ptolemaeus and Albategnius. But the problem of supporting the mascons remains, if it is assumed that the titaniferous basaltic rocks flowed out on the surface from melts beneath the surface, which would seem the appropriate hypothesis for this suggestion of early lunar history.

Partial remelting in the lunar interior some 3.1 to 4.0 aeons ago, which is favored by some, would almost certainly fractionate rubidium and strontium relative to each other, hence, the model ages of the titaniferous basalts would almost certainly not be near 4.5 aeons. This is a strong argument against the origin of these materials by partial melting in the lunar interior.

From this discussion, it is concluded that the Moon was formed at comparatively low temperatures, heated on its surface by external heat sources, cooled sufficiently and at adequate depth to permit large craters, 150 km in diameter, to retain negative gravitational anomalies, and was able to support mass concentrations on the rigid interior. The differentiation of anorthosite, titaniferous basalt, and other fractions occurred during the cooling process. The soil resulted mostly from an ash flow and was remelted in limited amounts by radioactive heat due to the low thermal conductivity of the soil. This suggested history is complicated and will most probably be revised as more evidence is obtained.

The seismologists, Toksöz et al [71], secured evidence for an anorthositic layer extending to some 60 km below the surface and an interior below this of dunitic-type rocks rich in pyroxene and olivine. (This was discussed previously.) Very mild moonquakes (compared to earthquakes) occur, some of which originate repeatedly at points beneath the surface at depths of about 700–800 km. There are also reflections from structures at about the same depth which cannot be due to a metal core, but may be due to the boundary of some other type of central structure. This evidence favors the proposition that there was very deep or complete melting early in lunar history, but the evidence is not conclusive. The observations have been made over a very limited area and in regions relatively near the areas of the great mascons and collisional maria.

## THE MAGNETIZED ROCKS OF THE MOON

A dipole magnetic field has not been detected on the Moon, but magnetized rocks of ages 4 to 3.1 aeons have been located at the Apollo landing sites, hence, magnetic fields must have been present up to that time or to later times, and the rocks cooled below the Curie point in this magnetic field. Also, rather large areas of the Moon are magnetized. The origin of the magnetic field responsible for producing these magnetized rocks is a puzzle to all students of this subject, and this question has an important bearing on lunar origin.

After the magnetic field of the Earth and a possible field from the Sun are discarded, we turn to a possible lunar dipole field which must have disappeared later than 3.1 aeons ago. One proposal advanced particularly [57] has been an iron core smaller than that of the Earth which, therefore, must have rotated very rapidly in order to produce the required field. This seems unlikely, and no iron core has been detected in the seismic observations which, however, may not be conclusive. If such a circulating iron core was present in the early period before 3.1 aeons ago, it has been suggested that it froze and, hence, no field would exist today. Another suggestion was that the interior of the Moon accumulated at low temperatures and magnetizable particles, i.e., iron, accumulated in a primitive magnetic field of the Sun to form a permanent magnetic dipole field which would persist until radioactive heating raised the temperature above the Curie point. However, in this case, the surface regions must have melted in order to produce the highly differentiated surface regions and ash flows on the surface.

A popular view is that the Moon accumulated from solid objects, at first at low temperatures, because of the low gravitational energy and rate of accumulation, and later at high gravitational energy and velocity of accumulation, thus producing a cold interior and a melted surface. It is estimated that the accumulation must have occurred in about 2000 years or less, in order to produce surface melting in spite of radiation loss. Also, this bombardment must have been

terminated rather suddenly. It is difficult to specify a place in the solar nebula where this could occur. An alternative method is provided by the gas spheres [88]. In this case, the solids settle to the interior of the sphere when it is cold, but as the sphere contracts, the temperature of the sphere's interior rises, thus, the interior could form cold and the surface could accumulate at higher temperatures [6]. The Moon cooled after the high-temperature Sun blew the gas sphere away and, whichever way the Moon accumulated, the magnetic field carried by the cold interior magnetized the cooling surface rocks and disappeared when radioactive heating raised the temperature of the cold interior above the Curie point. It has been mentioned that this is a most interesting problem and one that has surprised many who study the Moon. (See reviews [58, 66].)

## ORIGINS OF THE MOON

A discussion of the origin of the Moon requires considering the origin of the planets and their satellites—in fact, the origin of the solar system. Jupiter and its inner moons have the general orbital structure of the Sun and its planets, and the axis of Jupiter's rotation is nearly perpendicular to the plane of the ecliptic. If the other planets and their satellites resembled this planet in general structure, there would be no great disagreement in regard to questions of origin. It would be supposed that the planets and their satellites accumulated from smaller objects both solid and gaseous. However, the Earth, Venus, Mars, and major planets other than Jupiter have axes of rotation not perpendicular to the ecliptic, and this probably requires collisions of very massive objects to form the planets. This alone indicates the presence of such objects early in the solar system history.

If all the terrestrial planets had large moons similar to that of the Earth, it would be supposed that these planets and satellites formed as double planets, i.e., accumulation from solid or liquid silicate compounds in the immediate neighborhood of each other. Again, the problem of the Moon's origin would not have been discussed for many decades in this case. It is the uniqueness

of the Moon as a single, very large satellite that poses the interesting and controversial question of its origin. But if the double planet origin is the rule, the absence of a large moon of Venus and some fairly large moons of Mercury and Mars becomes the disturbing question.

Cameron [9] and Ringwood [54] favored the view that the Earth and Moon accumulated quickly in some  $10^3$  or  $10^4$  years at very high temperatures and as a double body. The Moon accumulated from a volatilized mass of high-temperature material moving in a ring about planet Earth. The mass of the Earth, plus its proportion of solar gases, would be approximately equal to that of Jupiter originally dispersed over a disk surrounding the Sun. At some time, it is necessary that the 0.3% of the terrestrial-type material destined to form solid bodies separate from the 99.7% of gases and accumulate into a limited volume. This, seemingly, could only occur if these materials were at a sufficiently low temperature to condense to liquids or solids. Possibly, if solids settled to the median plane of the nebula, this would be possible. The model resembles, and in a way is identical with, protoplanets of Kuiper [30], which have the obvious difficulty of losing a mass of gas equal to that of Jupiter. Urey [81] argued that this is impossible and, up to the present, no satisfactory method of removing gases has been proposed. It may be, but is not certain, that the magnetic fields of the rotating magnetic dipole Sun may have provided such a mechanism. Soviet authors, especially Schmidt, Safronov, and Levin [36, 60, 62] are inclined to favor a theory suggesting the accumulation of a multitude of small satellites which surrounded the Earth during its synthesis and growth over 100 million years.

Ringwood [54] argues that the loss of volatiles so evident in lunar surface material shows that the Moon must have separated from high-temperature gases.<sup>5</sup> This is a very good argument especially if these elements have been depleted in the entire Moon—an untested assumption at present. The abundance of the more abundant elements in lunar materials are so similar to

those expected from the fractionation of silicate materials by melting that it would appear that extreme volatilization methods are not required. Moreover, mechanisms for tilting the axis of the Earth and moving the Moon's orbit in some way are required, since Goldreich [21] showed that the present orbit of the Moon could not have originated in the plane of the Earth's orbit. Both these effects require the presence of other sizeable bodies which collided with the Earth and Moon to produce these effects. If they existed, similar objects colliding with other planets would produce similar effects.

That Venus does not have a moon and rotates in the reverse sense is probably the most damaging evidence in regard to this theory for Earth and lunar origin. Marcus [40] and Safronov [59] pointed out that such collisions were necessary, and Urey [82, 83] suggested methods of producing such objects. It has recently been proposed that large preplanetary objects existed and collided to form the Earth at high temperatures, and a Moon volatilized from the Earth, according to Ringwood's model. Elements volatile at 1500° K and lower are missing from the lunar surface, but there appears to be no reason to assume any important fractionation between silicon on the one hand and aluminum, magnesium, and calcium on the other, even though great differences in volatilities exist. This writer doubts the correctness of Ringwood's gaseous silica, alumina [etc] atmosphere as an origin for the Moon.

Possibly, if samples of rocks from the deeper layers of the Moon could be secured and showed low abundances of the very volatile elements, this would indicate that the materials of the Moon had been heated to some 1000–1500° C in fairly finely divided form, and that the volatiles were swept away with the residual gases. Those who believe that the titaniferous basalts are indeed lava flows from the interior will now accept this point as proven. This writer would like to see samples from what appear to be limited lava flows in various locations on the Moon and which might come from great depths, before accepting this conclusion.

Sir George Darwin suggested that the Moon escaped from the Earth, which has been discussed pro and con during this century. This

<sup>5</sup> Ringwood has recently withdrawn his sponsorship of these suggestions.

discussion has been reviewed [49, 94]. The density of the Moon approximates that of the Earth's mantle, and this troublesome problem is solved immediately by this hypothesis. Much effort has been expended in showing that such a separation would be possible. Recently, this hypothesis has not been favored partly, and possibly decisively, by studies on the chemical composition of the lunar surface. The lunar basalts have definitely higher concentrations of iron and titanium and definitely lower concentrations of the more volatile elements than the Earth. It is certainly not impossible that these differences in a complicated high-temperature separation process could be produced, but it does appear improbable. The ages of lunar rocks would restrict the time of separation to before 4.5 aeons. One thing evident from the older data is important! If Venus and Earth evolved by similar processes at comparable distances from the Sun, why does the Earth-Moon system have a very large positive angular momentum relative to the orbital angular momentum, and Venus a small and negative value for this quantity? Why did not Venus also accumulate with a large axial rotation and separate into a double planet? These questions could have been asked many years ago. Today, separation of the Moon from the Earth is not favored and seems very unlikely.

The capture hypothesis has been especially popular since Gerstenkorn [18, 19] investigated this problem, and it has been discussed by others [4, 38]. This mechanism has the obvious advantage that it is an incidental origin, and it is not necessary to explain the absence of satellites of the other terrestrial planets. However, it must be assumed that many moons were present at some time in the early period of the solar system unless multiple, highly improbable assumptions are made. There is small probability of capture of the Moon in any orbit about the Earth rather than capture by impact on the Earth. These problems have been discussed in detail by Urey and MacDonald [88]. Gerstenkorn [19] concludes that capture occurred in a reverse orbit which turned over the Earth's poles and became direct. It was proposed that the minimum orbit was near the Roche limit of 2.9 Earth radii for an object of lunar density.

In this capture process, a great deal of energy must be dissipated as heat, i.e., some  $10^{11}$  ergs per gram of the Moon. Part of this would be dissipated in the Moon, probably in the outer layers, and may have contributed to the production of its melted surface layer (discussed above). Such a melting process would be more concentrated in the hemisphere near the Earth and may aid in accounting for the more extensive maria areas in the nearer hemisphere. If such heating became general, the support of the mascons would be jeopardized. Urey and MacDonald [88] suggest that collisions with other objects moving about the Earth may have aided in the capture process, and that the initial orbit may have been much larger, thus avoiding the heating difficulty. Also, their proposal permits the angular momentum density of the initially accumulated Earth to lie on the empirical curve of MacDonald [38], who shows that the logarithm of the angular momentum densities of the planets plotted against the logarithms of the masses is a straight line of slope of about 0.82.

This model for lunar origin requires the premise that the Moon accumulated elsewhere. The method of accumulation and general chemical composition present problems for which solutions must be offered if the capture process is to be accepted. Until the present, only the gas sphere model of Urey [41, 82, 84] has been proposed, but others are possible, although difficult to calculate realistically. It is supposed that two dimensional gravitational instabilities occurred in a flat disk nebula following formulas first developed by Jeans and revised by Chandrasekhar [11]. The formulas are approximate when applied in this way, since the presence of solids probably increases the instability. Calculated temperatures in the nebula required to make lunar-sized objects are very low, and the calculated mass of the nebula is a substantial fraction of a solar mass. Some substantial loss of mass of this kind must have occurred in order to decrease the angular momentum of the primitive Sun as usually assumed by the Alfvén magnetic field mechanism, and Herbig [23] requires dust clouds of approximate solar mass in T Tauri stars.

Accumulation of lunar masses at the center of

such gaseous objects due to gravitation with the energy of accumulation being absorbed by the great mass of gas could occur at low temperatures while the radii are large. If the gas mass contracted to smaller radii subsequently, the surface regions of the central lunar object could be heated to high temperatures, and reduced liquid iron would remove the siderophiles, and liquid iron sulfide would remove the chalcophiles (see [6]). With slow removal of the gas spheres, there would be slow cooling of the central mass, and, with complete removal of the gases, more rapid cooling to low temperatures. The composition remains a serious problem. With a low abundance of iron in the Sun relative to other elements (which has been fashionable for many years), the Moon consisted of primitive, nonvolatile solar matter, but with revised solar abundances, the density of primitive, solar nonvolatile matter becomes close to 4 g/cm<sup>3</sup> and does not agree with the lunar density.

If capture theory is to be seriously considered, explanation of this problem must be made. Carbonaceous chondrites are fairly abundant as observed falls, and the Type III Vigarano-type group have proper densities and a low abundance of potassium, so that a rigid interior of the Moon could be maintained if the central body had composition of this kind or similar. However, these meteorites contain water and considerable carbon. The low abundances of both these substances in the lunar surface are very unfavorable, but not fatal to this suggestion for the lunar interior.

Other methods [22, 39, 40, 59] have been discussed for accumulated sizeable objects from smaller solid objects without the presence of gases, which will certainly be necessary if the more volatile elements are missing from the interior of the Moon. In this case, successive events must provide for loss of volatiles at some 1500°K, and these must be driven out of the neighborhood

where the Moon and Earth will accumulate before that accumulation takes place. If the volatiles are present in the deep interior of the Moon, then the accumulation of the Moon in a gas sphere is indicated, and the Earth accumulated from fragments of such objects.

Cameron [10] suggests that the Moon condensed from the gaseous solar nebula inside the orbit of Mercury where the least volatile elements, CaO and Al<sub>2</sub>O<sub>3</sub>, condensed. These accumulated into the Moon which was thrown by Mercury into an orbit crossing the orbits of Venus and the Earth, and was then captured by the Earth. Thus, the Moon was condensed in a region of the solar nebula where iron remained in the gaseous form to a considerable extent, and in this way, the low lunar density and possibly the chemical composition are accounted for. Both these mechanical events appear to be highly improbable, although not impossible.

If the Moon was captured, it was formed independently from the Earth and as a separate primitive planet. The present ages indicate that the Moon was present as a body at about the time the meteorites were formed, and all possibility of dating the Earth in the same way has been lost.

Jupiter and its satellites appear to be a small solar system (as stated previously) and a strong prejudice favors the formation of these satellites in the neighborhood of their primary. The seven moons of approximately lunar size in the solar system, and all other satellites and the asteroids having a combined mass of about 0.25 of one lunar mass, suggest that lunar-sized objects were favored in the solar system. The tilts of axes of the planets hint that some large objects were about and collided with the accumulating planets during the terminal stages of accumulation. Possibly our Moon is not such a unique object as it is often thought to be!

## REFERENCES

- ABELL, P. I., P. H. CADOGAN, G. EGLINTON, J. R. MAXWELL, and C. T. PILLINGER. Survey of lunar carbon compound. I. The presence of indigenous gases and hydrolyzable carbon compounds in Apollo 11 and Apollo 12 samples. In, *Proceedings, Second Lunar Science Conference*, Houston, Jan. 1971, Vol. 2, pp. 1843–1863. Cambridge, Mass., MIT Press, 1971.
- ADLER, I., J. TROMBKA, J. GERARD, P. LOWMAN, R. SCHMADEBECK, H. BLODGET, E. ELLER, L. YIN, R. LAMOTHE, P. CORENSTEIN, and P. BJORKHOLM. Apollo 15 geochemical x-ray fluorescence experiment: preliminary report. *Science* 175:436–440, 1972.

3. ALBEE, A. L., D. S. BURNETT, A. A. CHODOS, O. M. EUGSTER, J. C. HUNEKE, D. A. PAPANASTASSIOU, F. A. PODOSEK, G. P. RUSS II, H. G. SANZ, F. TERA, and G. J. WASSERBURG. Ages, irradiation history, and chemical composition of lunar rocks from the Sea of Tranquility. *Science* 167:463–466, 1970.
4. ALFVEN, H. The early history of the Moon and the Earth. *Icarus* 1(4):357–363, 1963.
5. ARNOLD, J. R., J. I. TROMBKA, L. E. PETERSON, R. C. REEDY, and A. E. METZGER. Lunar orbital gamma-ray measurements from Apollo 15 and Apollo 16. In, *Space Research XIII, Proceedings, 15th Plenary Meeting*, Madrid, May 1972, Vol. 2, pp. 927–933. Berlin, Akademie, 1973.
6. BAINBRIDGE, J. Gas imperfections and physical conditions in gaseous spheres of lunar mass. *Astrophys. J.* 136(1):202–210, 1962.
7. BALDWIN, R. B. Lunar mascons: another interpretation. *Science* 162:1407–1408, 1968.
8. BOOKER, J. R. Thermal state of the Moon. *Trans. Am. Geophys. Union* 51(11):774, 1970.
9. CAMERON, A. G. W. The pre-Hayashi phase of stellar evolution. In, Kumar, S. S., Ed. *Low Luminosity Stars*, pp. 423–431. New York, Gordon and Breach, 1969.
10. CAMERON, A. G. W. Properties of the solar nebula and the origin of the Moon. *The Moon* 7:377–383, 1973.
11. CHANDRASEKHAR, S. The gravitational instability of an infinite homogeneous medium when a coriolis acceleration is acting. In, Beer, A., Ed. *Vistas in Astronomy*, Vol. 1, pp. 344–347, 1955.
12. CHANDRASEKHAR, S. *Hydrodynamic and Hydromagnetic Stability*. New York, Oxford Univ. Press, 1961.
13. COMPSTON, W., H. BERRY, M. J. VERNON, B. W. CHAPPELL, and M. J. KAYE. Rubidium-strontium chronology and chemistry of lunar material from the Ocean of Storms. In, *Proceedings, Second Lunar Science Conference*, Houston, Jan. 1971, Vol. 2, pp. 1471–1485. Cambridge, Mass., MIT Press, 1971.
14. COMPSTON, W., B. W. CHAPPELL, P. A. ARRIENS, and M. J. VERNON. The chemistry and age of Apollo 11 lunar material. In, Levinson, A. A., Ed. *Proceedings, Apollo 11 Lunar Science Conference*, Vol. 2, pp. 1007–1027. New York, Pergamon, 1970.
15. CROZAZ, G. Evidence for extinct Pu<sup>244</sup>: implications of extinct Pu<sup>244</sup> in lunar material. In, Watkins, C., Ed. *Abstracts of Third Lunar Science Conference*, Houston, Jan. 1972, p. 165. Houston, Lunar Sci. Inst., 1972. (No. 88)
16. CROZAZ, G., R. DROZD, H. GRAF, C. M. HOHENBERG, M. MONNIN, D. RAGAN, C. RALSTON, M. SEITZ, J. SHIRCK, R. M. WALKER, and J. ZIMMERMAN. Evidence for extinct Pu<sup>244</sup>: implications for the age of the Pre-imbrium crust. In, Watkins, C., Ed. *Abstracts of Third Lunar Science Conference*, Houston, Jan. 1972, p. 164. Houston, Lunar Sci. Inst., 1972. (No. 88)
17. FOX, S. W., K. HARADA, P. E. HARE, G. HINSCH, and G. MUELLER. Bio-organic compounds and glassy micro-particles in lunar fines and other materials. *Science* 167:767–770, 1970.
18. GERSTENKORN, H. Über Gezeitenreibung beim zweikörper Problem. *Z. Astrophys.* 36:245, 1955.
19. GERSTENKORN, H. The model of the so-called “weak” tidal friction and limits of its applicability. In, Runcorn, S. K., Ed. *Mantles of the Earth and Terrestrial Planets*, pp. 228–234. New York, Wiley (Interscience), 1967.
20. GOLD, T., and S. SOTER. Apollo 12 seismic signal: indication of a deep layer of powder. *Science* 169:1071–1075, 1970.
21. GOLDRICH, P. History of the lunar orbit. *Rev. Geophys.* 4(4):411–439, 1966.
22. HARTMANN, W. K. Growth of planetesimals in nebulae surrounding young stars. *Mem. [8°] Soc. Roy. Sci. Liege, 5th Ser.* 19:13–26, 1970.
23. HERBIG, G. H. Pre-main sequence stellar evolution: introductory remarks. *Mem. [8°] Soc. Roy. Sci. Liege, 5th Ser.* 19:13–26, 1970.
24. HODGSON, G. W., E. PETERSON, K. A. KVENVOLDEN, E. BUNNENBERG, B. HALPERN, and C. PONNAMPERUMA. Search for porphyrines in lunar dust. *Science* 167:763–765, 1970.
25. KAULA, W. M. Moon: gravitational field. In, *McGraw-Hill Yearbook of Science and Technology*, pp. 222–224. New York, McGraw-Hill, 1969.
26. KAULA, W. M., G. SCHUBERT, R. E. LINGENFELTER, W. L. SJOGREN, and W. R. WOLLENHAUPT. Lunar topography from Apollo 15 and 16 laser altimetry. In, *Proceedings, 4th Lunar Science Conference*, Houston, Tex., March 1973, pp. 2811–2819. New York, Pergamon, 1973.
27. KOPAL, Z. *The Moon*, p. 88. Dordrecht, Holl., Reidel, 1969.
28. KOPAL, Z. On the depth of the lunar regolith. *The Moon* 1:451, 1970.
29. KOZIEL, K. Differences in the Moon’s moments of inertia. *Proc. Roy. Soc. London, Ser. A* 296:248–253, 1967.
30. KUIPER, G. P. On the origin of the lunar surface features. In, *Proceedings, National Academy of Science*, Vol. 40, pp. 1096–1112. Washington, D.C., Nat. Acad. Sci. 1954.
31. LATHAM, G., J. DORMAN, F. DUENNEBIER, M. EWING, D. LAMMLEIN, and Y. NAKAMURA. Moonquakes, meteoroids, and the state of the lunar interior. In, *Proceedings, 4th Lunar Science Conference*, Houston, Tex., March 1973, pp. 2515–2527. New York, Pergamon, 1973.
32. LATHAM, G. V., M. EWING, F. PRESS, G. SUTTON, J. DORMAN, Y. NAKAMURA, N. TOKSÖZ, R. WIGGINS, J. DERR, and F. DUENNEBIER. Passive seismic experiment. *Science* 167:455–457, 1970.
33. LATHAM, G. V., M. EWING, F. PRESS, G. SUTTON, J. DORMAN, Y. NAKAMURA, N. TOKSÖZ, R. WIGGINS, J. DERR, and F. DUENNEBIER. Apollo 11 passive seismic experiment. In, Levinson, A. A., Ed. *Proceedings, Apollo 11 Lunar Science Conference*, Houston, Jan. 1970, Vol. 3, p. 2309. New York, Pergamon, 1970.
34. LATHAM, G. V., M. EWING, F. PRESS, G. SUTTON, J. DORMAN, Y. NAKAMURA, N. TOKSÖZ, R. WIGGINS, and R. KOVACH. Passive seismic experiment. In,

- Apollo 12 Preliminary Scientific Report*, pp. 39–53. Washington, D.C., NASA, 1970. (NASA SP-235)
35. LEVIN, B. J. Thermal effects on the figure of the Moon. *Proc. Roy. Soc. London, Ser. A* 296:266–269, 1967.
  36. LEVIN, B. Yu. Origin of the Earth. *Izv. Akad. Nauk SSSR, Fiz. Zemli* (7):5–21, 1972.
  37. LORELL, J., and W. SJOGREN. Selenodesy experiment. In, *Space Program Summary*, Vol. 3, pp. 47–50. Pasadena, Calif., Jet Propul. Lab., 1968.
  38. MACDONALD, G. J. F. Origin of the Moon; dynamical considerations. In, Marsden, B. S., and A. G. W. Cameron, Eds. *The Earth-Moon System*, p. 170. New York, Plenum, 1966.
  39. MARCUS, A. H. Positive stable laws and the mass distribution of planetesimals. *Icarus* 4(3):267–272, 1965.
  40. MARCUS, A. H. Formation of the planets by accretion of planetesimals: some statistical problems. *Icarus* 7(3):283–296, 1967.
  41. MARTI, K., G. W. LUGMAIR, and H. C. UREY. Solar wind gases, cosmic ray spallation products and the irradiation history of Apollo 11 samples. In, Levinson, A. A., Ed. *Proceedings, Apollo 11 Lunar Science Conference*, Vol. 2, pp. 1357–1367. New York, Pergamon, 1970.
  42. MICHAEL, W. H., Jr., and W. T. BLACKSHEAR. Recent results on the mass, gravitational field, and moments of inertia of the Moon. *The Moon* 3:388–402, 1972.
  43. MICHAEL, W. H., Jr., W. T. BLACKSHEAR, and J. P. GACPYNISKI. Results on the mass and the gravitational field of the Moon as determined from dynamics of lunar satellites. In, Morando, B., Ed. *Dynamics of Satellites, Proceedings, 12th COSPAR Plenary Meeting*, Prague, May 1969, pp. 42–56. Berlin, Springer, 1970.
  44. MULLER, P. M., and W. L. SJOGREN. Mascons: lunar mass concentrations. *Science* 161:680–684, 1968.
  45. MULLER, P. M., and W. L. SJOGREN. Lunar gravimetrics. In, Donahue, T. M., Ed. *Space Research X*, pp. 975–983. Amsterdam, North-Holland, 1970.
  46. MULLER, P. M., and W. L. SJOGREN. Private communication. 1970.
  47. NAGY, B., C. M. DREW, P. B. HAMILTON, V. E. MODZEL-ESKI, M. E. MURPHY, W. M. SCOTT, H. C. UREY, and M. YOUNG. Organic compounds in lunar samples: pyrolysis products, hydrocarbons, amino acids. *Science* 167:770–773, 1970.
  48. O'KEEFE, J. A. Isostasy on the Moon. *Science* 162:1405–1406, 1968.
  49. O'KEEFE, J. A. Origin of the Moon. *J. Geophys. Res.* 74(10):2758–2767, 1969.
  50. O'KEEFE, J. A., and W. S. CAMERON. Evidence from the Moon's surface features for the production of lunar granites. *Icarus* 1(3):271–285, 1962.
  51. PAPANASTASSIOU, D. A., and G. J. WASSERBURG. Initial strontium isotopic abundances and the resolution of small time differences in the formation of planetary objects. *Earth Planet. Sci. Lett.* 5:361–376, 1969.
  52. PAPANASTASSIOU, D. A., and G. J. WASSERBURG. Rb-Sr age of a Luna 16 basalt and the model age of lunar soils. *Earth Planet. Sci. Lett.* 13:368–374, 1972.
  53. REYNOLDS, J. H. Determination of the age of the elements. *Phys. Rev. Lett.* 4:8, 1960.
  54. RINGWOOD, A. E., and E. ESSENE. Petrogenesis of Apollo 11 basalts, internal constitution and origin of the Moon. In, Levinson, A. A., Ed. *Proceedings, Apollo 11 Lunar Science Conference*, Houston, Jan. 1970, Vol. 1, p. 769. New York, Pergamon, 1970.
  55. ROBERSON, F. I., and W. M. KAULA. Apollo 15 laser altimeter. In, *Apollo 15 Preliminary Science Report*, pp. 25:48–50. Washington, D.C., NASA, 1972. (NASA SP-289)
  56. ROSHOLT, J. N., and M. TATSUMOTO. Isotopic composition of thorium and uranium in Apollo 12 samples. In, *Proceedings, Second Lunar Science Conference*, Houston, Jan. 1971, Vol. 2, pp. 1577–1584. Cambridge, Mass. MIT Press, 1971.
  57. RUNCORN, S. K. Convection in the Moon and the existence of a lunar core. *Proc. Roy. Soc. London, Ser. A* 296:270–284, 1967.
  58. RUNCORN, S. K., and H. C. UREY. A new theory of lunar magnetism. *Science* 180:636–638, 1973.
  59. SAFRONOV, V. S. Sizes of the largest bodies falling onto the planets during their formation. *Astron. Zh.* 42(6):1270–1276, 1965. (Transl: *Sov. Astron. J.*) 9(3):987–991, 1966.
  60. SAFRONOV, V. S. *Evolvutsiya doplanetnogo Oblaka i Obrazovanie Zemli i Planet*. Moscow, Nauka, 1969. (Transl: *Evolution of the Protoplanetary Cloud and Formation of the Earth and the Planets*.) Washington, D.C., NASA, 1972. (NASA TT-F-677)
  61. SCHAEFFER, O. A., L. HUSAIN, J. SUTTER, J. FUNKHOUSER, T. KIRSTEN, and I. KANEOKA. The ages of lunar material from Fra Mauro and the Hadley Rille-Apennine front area. In, Watkins, C., Ed. *Abstracts of Third Lunar Science Conference*, Houston, Jan. 1972, p. 677. Houston, Lunar Sci. Inst., 1972.
  62. SCHMIDT, O. Yu. *A Theory of Earth's Origin; Four Lectures*, 3d ed. Moscow, Akad. Nauk SSSR, 1957; Moscow, Foreign Lang. Pub. (transl.), 1958.
  63. SEEGER, C. R. A geological criterion applied to Lunar Orbiter V photographs. *Mod. Geol.* 1(3):203–210, 1970.
  64. SHOEMAKER, E. M., M. H. HAIT, G. A. SWANN, D. L. SCHLEICHER, D. H. DAHLEM, G. G. SCHABER, and R. L. SUTTON. Lunar regolith at Tranquillity Base. *Science* 167:452–455, 1970.
  65. SILVER, L. T. Uranium-thorium-lead isotopes in some Tranquillity Base samples and their implications for lunar history. In, Levinson, A. A., Ed. *Apollo 11 Lunar Science Conference*, Houston, Jan. 1970, Vol. 2, pp. 1533–1574. New York, Pergamon, 1970.
  66. SONETT, C. P., and S. K. RUNCORN. Electromagnetic evidence concerning the lunar interior and its evolution. *The Moon* 8(9):308–334, 1973.
  67. STIPE, J. G. Iron meteorites as mascons. *Science* 162:1402–1403, 1968.
  68. TATSUMOTO, M., and J. N. ROSHOLT. Age of the Moon:

- an isotopic study of uranium-thorium-lead systematics of lunar samples. *Science* 167:461–465, 1970.
69. TATSUMOTO, M., R. J. KNIGHT, and B. R. DOE. U-Th-Pb systematics of Apollo 12 lunar samples. In, *Proceedings, Second Lunar Conference*, Houston, Jan. 1971, Vol. 2, pp. 1521–1546. Cambridge, Mass., MIT Press, 1971.
70. TERA, F., and G. J. WASSERBURG. Oxygen isotope composition of the Luna 16 soil. *Earth Planet. Sci. Lett.* 13:455, 1972.
71. TOKSÖZ, M. N., F. PRESS, K. ANDERSON, A. DAINTY, G. LATHAM, M. EWING, J. DORMAN, D. LAMMLEIN, G. SUTTON, F. DUENNEBIER, and Y. NAKAMURA. Lunar crust: structure and composition. *Science* 176:1012–1016, 1972.
72. TOZER, D. C. The Moon's thermal state and an interpretation of the lunar electrical conductivity distribution. *The Moon* 5:90–105, 1972.
73. TURKEVICH, A. L., E. J. FRANZGROTE, and J. H. PATTERSON. Chemical analysis of the Moon at the Surveyor V landing site. *Science* 158:635–637, 1967.
74. TURKEVICH, A. L., J. H. PATTERSON, and E. J. FRANZGROTE. Chemical analysis of the Moon at the Surveyor VI landing site: preliminary results. *Science* 160:1108–1110, 1968.
75. TURKEVICH, A. L., E. J. FRANZGROTE, and J. H. PATTERSON. Chemical analysis of the Moon at the Surveyor VII landing site: preliminary results. *Science* 162:117–118, 1968.
76. TURKEVICH, A. L., E. J. FRANZGROTE, and J. H. PATTERSON. Chemical composition of the lunar surface in Mare Tranquillitatis. *Science* 165:277–279, 1969.
77. TURNER, G.  $^{40}\text{Ar}/\text{Ar}^{39}$  dating of lunar rock samples. In, Levinson, A. A., Ed. *Proceedings, Apollo 11 Lunar Science Conference*, Vol. 2, pp. 1665–1684. New York, Pergamon, 1970.
78. TURNER, G.  $\text{Ar}^{40}/\text{Ar}^{39}$  ages from the lunar maria. *Earth Planet. Sci. Lett.* 11:169–191, 1971.
79. TURNER, G.  $\text{Ar}^{40}/\text{Ar}^{39}$  age and cosmic ray irradiation history of the Apollo 15 anorthosite 15415. *Earth Planet. Sci. Lett.* 14:169–175, 1972.
80. TURNER, G., J. C. HUNEKE, F. A. PODOSEK, and G. J. WASSERBURG.  $\text{Ar}^{40}/\text{Ar}^{39}$  ages and cosmic ray exposure ages of Apollo 14 samples. *Earth Planet. Sci. Lett.* 12:19–35, 1971.
81. UREY, H. C. Some criticisms of "On the origin of the lunar surface features" by G. P. Kuiper. *Proc. Nat. Acad. Sci.* 41(7):423, 1955.
82. UREY, H. C. The early history of the solar system as indicated by the meteorites (Hugo Mueller Lecture). *Proc. Chem. Soc. (London)*, pp. 67–78, 1958.
83. UREY, H. C. Chemical evidence relative to the origin of the solar system. *Mon. Nat. Roy. Astron. Soc.* 131(3): 199–223, 1966.
84. UREY, H. C. III. Origin of the Moon. In, Runcorn, S. K., Ed. *Mantles of the Earth and the Terrestrial Planets*, pp. 251–260. New York, Wiley (Interscience), 1967.
85. UREY, H. C. Mascons and the history of the Moon. *Science* 162:1408–1410, 1968.
86. UREY, H. C., and H. CRAIG. The composition of the stone meteorites and the origin of the meteorites. *Geochim. Cosmochim. Acta* 4(1/2):36, 1953.
87. UREY, H. C., W. M. ELSASSER, and M. G. ROCHESTER. Note on the internal structure of the Moon. *Astrophys. J.* 129(3):842–848, 1959.
88. UREY, H. C., and G. J. F. MACDONALD. Origin and history of the Moon. In, Kopal, Z., Ed. *Physics and Astronomy of the Moon*, 2nd ed., Vol. 1, Chap. 6, pp. 213–289. New York, Academic, 1971.
89. UREY, H. C., K. MARTI, J. W. HAWKINS, and M. K. LIU. Model history of the lunar surface. In, *Proceedings, Second Lunar Science Conference*, Houston, Jan. 1971, Vol. 2, pp. 987–998. Cambridge, Mass., MIT Press, 1971.
90. VAN DORN, W. G. Lunar maria: structure and evolution. *Science* 165:693–695, 1969.
91. WÄNKE, H. Chemistry of the Moon. *Top. Curr. Chem.* 44:115–154, 1974.
92. WASSERBURG, G. J., G. TURNER, F. TERA, F. A. PODOSEK, D. A. PAPANASTASSIOU, and J. C. HUENKE. Comparison of Rb-Sr, K-Ar and U-Th-Pb ages: lunar chronology and evolution. In, Watkins, C., Ed. *Abstracts of Third Lunar Science Conference*, Houston, Jan. 1972, p. 788. Houston, Lunar Sci. Inst., 1972. (No. 88)
93. WETHERILL, G. W. Lunar interior: constraint on basaltic composition. *Science* 160:1256–1257, 1968.
94. WISE, D. U. An origin of the Moon by rotational fission during formation of the Earth's core. *J. Geophys. Res.* 68(5):1547–1554, 1963.
95. WISE, D. U., and M. T. YATES. Mascons as structured relief on a lunar "Moho". *J. Geophys. Res.* 75(2):261–268, 1970.
96. WOOD, J. A. Petrology of the lunar soil and geophysical implications. *J. Geophys. Res.* 75(33):6497–6513, 1970.
97. WOOD, J. A. Thermal history and early magnetism in the Moon. *Icarus* 16(2):229–240, 1972.

## Chapter 4

EARTH-TYPE PLANETS (MERCURY, VENUS, AND MARS)<sup>1</sup>M. Ya. MAROV<sup>2</sup>

Institute of Applied Mathematics, Academy of Sciences USSR, Moscow

AND

V. D. DAVYDOV<sup>2</sup>

Institute of Space Research, Academy of Sciences USSR, Moscow

Tremendous progress has been made in the study of planets of the solar system, particularly of those closest to the Earth—Venus and Mars. Spacecraft flights combined with improvements in techniques of Earth-based observations and the reliability of interpretation of data have provided new knowledge that, in many cases, has revolutionized previous concepts of the nature of these planets.

The Earth, Venus, Mars, and the planet closest to the Sun, Mercury, are usually called the planets of the Earth group. This generalization is based on their similar mean densities (see Table 1), which indicates that these planets are composed, as is the Earth, primarily of the rather heavy elements, Si, Fe, Ca, Al, Mg, and their oxides which are widespread in the solar system. The atmospheres of these planets

contain gases consisting of the most common elements, H, C, O, N, and their compounds, which are oxidizing in nature, in contrast to the atmosphere of planets in the Jupiter group. It is generally believed that atmosphere is a portion of the volatile fraction liberated by degassing of the core during the process of differentiation of planet materials into shells.

For the planets of the Earth group, localized within 1.5 astronomical units (AU)<sup>3</sup> from the Sun, moderate differences in geometric dimensions and in distribution of mass are characteristic. The Earth and Venus are similar in mass, while Mars and Mercury are less massive than the Earth, by approximately 10 and 20 times respectively. Of all the planets, only the Earth has a satellite comparable in size to Mercury, so that from the standpoint of planetary dynamics, it is actually more correct to speak of the Earth-Moon system; the satellites of Mars, Phobos

<sup>1</sup> Translation of, Planety Zemnogo Tipa: Merkuriy, Venera, Mars, in *Osnovy Kosmicheskoy Biologii i Meditsiny (Foundations of Space Biology and Medicine)* Volume I, Part 2, Chapter 2, 138 pp. Moscow, Academy of Sciences USSR, 1973.

<sup>2</sup> The section on Venus was written by M. Ya. Marov; the sections on Mercury and Mars by V. D. Davydov.

The authors acknowledge the great efforts of D. G. Rea (US) and V. M. Vakhnin (USSR) in the preliminary preparation of data for this chapter, and express gratitude to all their colleagues who cooperated closely in work on this chapter.

<sup>3</sup> The astronomical unit, AU, equal to the large half-axis of the ellipse of the Earth's orbit, is  $149 \cdot 10^6$  km; according to the most recent and precise measurements [53], it is equal to the distance traveled by light in the time interval  $449.004780 \pm 0.000001$  s, whereas the speed of light in a vacuum (also a fundamental constant)  $c = 299772.4562 \pm 0.0011$   $\text{km} \cdot \text{s}^{-1}$  [215].

TABLE 1.—*Geometric, Spin, and Mass Characteristics of Planets of the Earth Group*

Planet	Equatorial half diameter Linear (km)	Geometric polar flattening Maximum angular	Oblliquity— inclination of plane of Equator to plane of orbit	Direction of axial rotation	Sidereal day	Mean solar day	Solar days per orbital revolution	Mass of planet in units of Earth mass	Mean density (g/cm <sup>3</sup> )	g at Equator (cm/s <sup>2</sup> )	Critical escape velocity (km/s)
Mercury	$\approx 2450$	$\approx 6.3''$	?	< 3°	Direct	58.65 <sup>1</sup>	175.9 <sup>1</sup>	0.500	$0.05526 \pm 0.0048$	$5.38 \pm 0.08$	$\approx 370$
Venus	$6050 \pm 5$	$31.9''$	Not detected 1/296	$< 3^\circ$ $23^\circ 27'$	Reverse Direct	243.0 <sup>1</sup> 23 h 56 min 1 s	116.8 <sup>1</sup> 365 1/4	1.924 24 h 0 min 0 s	0.8150 1.0000	5.24 5.52 (without Moon)	876 981
Earth	6378	—									10.2 11.2
Mars	$3397 \pm 3$	$12.5''$	$\approx 0.0051$	$25.0^\circ \pm 0.3^\circ$	Direct	24 h 37 min 22.7 s	24 h 39 min 35 s	$6682/3$	$0.10744 \pm 0.00003$	3.94	371
											5.0

<sup>1</sup>In units of mean solar days of universal time.



Surface of Mars. This photograph, taken by the Mars-5 spacecraft, was synthesized from three photographs in the blue, green, and red wavelengths. (Precise color reconstruction is difficult, not only because of differences in lighting and viewing geometry between frames at the time the photos were taken, but also because of the contrast between colors during development and reproduction.)

REPRODUCIBILITY OF THE  
ORIGINAL PAGE IS POOR

and Deimos, are incomparably smaller than the planet itself. However, the study of the planet-satellite system is significant for understanding the long-term evolution of an astronomical body, particularly as it concerns interactions related to energy exchange.

In this chapter, attention will be concentrated on three planets: Mercury, Venus, and Mars. A complete presentation would require at least brief mention of the nature of the Earth, the best studied member of the Earth group of planets, although until recently the methods used to study the Earth and its neighboring planets differed quite basically. Essentially, launching the first artificial Earth satellite was the beginning of the modern era of investigation, allowing the Earth to be looked upon as a planet and to determine such important characteristics as its radiation, gravitational and magnetic fields, and the peculiarities of its interaction with surrounding space. Comparison of these results with analogous characteristics of other planets has permitted combined analysis and a number of generalizations. In turn, geological and geophysical methods used to study the Earth and successful studies of its internal structure have served as necessary bases for understanding the complex nature of other astronomical bodies. This combination of the traditional Earth sciences with planetary studies, until recently confined entirely to observational astronomy, has led to the birth of a new and rapidly growing area of science—planetary physics. The development of this discipline will facilitate the solution of basic problems related to the formation and evolution of the entire planetary system.

The limited space allocated for this section does not permit including the Earth. The authors considered it more expedient to utilize the space for a more detailed presentation of contemporary concepts of other planets of the Earth group, particularly since the abundant new information on their nature made even this task quite difficult. Naturally, the review which we present here has no pretensions of absolute completeness and, to a certain extent, reflects the subjective points of view and interests of the authors. The sparsity of the presentation is often compensated somewhat by references to prime sources.

## MERCURY

Mercury is the closest to the Sun of the nine large planets; in our sky, it is never farther than  $28^\circ$  from the Sun, making it quite difficult to observe from the Earth. From time to time, the planet can be seen by the naked eye as a barely noticeable bright spot among the colors of a sunrise or sunset. Through the telescope, Mercury appears as a crescent or part circle; the changes in its shape as it orbits the Sun clearly show that we are actually observing a sphere illuminated on one side by the Sun. In its closest position to the Earth (mean minimum 92 million km, minimum minimorum 80 million km), Mercury is unfortunately located next to the Sun in the sky, and turns its dark (night) hemisphere toward the Earthbound observer. This hindrance in observing Mercury from terrestrial observatories adds to the already great difficulties resulting from the small angular dimensions of the object, weakness of the energy flux arriving from it, and interference of Earth's atmosphere. Nevertheless, researchers have learned much through improvement of complex apparatus and methods of observation. All the information (rather extensive) now available on Mercury has been produced by terrestrial observation.

Excellent reviews have been written about Mercury [5, 110, 158, 167]; however, in recent years some of the information in these reviews has been refined. The present review attempts to present the factual material on the physics of this planet using, where possible, the latest data.

### Diameter, Mass, and Derived Quantities

Precise knowledge of the dimensions and mass of a planet is necessary to determine a number of parameters characterizing the physical conditions on the surface, which are important for astronautics.

The linear diameters of all planets, determined from the angular diameters measured from the Earth, are quantities derived from the numerical value of an astronomical unit of length. Due to possible refinement of these values, the diameters of the planets are traditionally not expressed in linear measure, but rather in angular seconds at a distance of 1 AU. Measure-

ments of the equatorial diameter of Mercury are in more than reasonable agreement and fall between 6.2 and 6.9 s. Reviews of the primary results are available [47, 158, 240]. New measurements yield  $6.73 \pm 0.03$  s, corresponding to a linear measure of  $4882 \pm 30$  km [132]; by the Hertzsprung method,  $D \geq 6.79$  s, [197], i.e., 4920 km.

The best method for determining the mass of a planet is to study the rotation periods of its satellites. Since Mercury has no satellites, its mass is calculated by the difficult method of observing the effects of its gravitational interactions with other astronomical bodies. The data of various authors [72, 107, 190], produced to three or four significant digits, agree with an accuracy only extending to the second decimal point. The limitation of this accuracy will be observed in this review. The mass of Mercury in units of the ratio of the mass of the Sun to the mass of the planet is near  $6.0 \cdot 10^6$ . Estimates of the mass and diameter of the planet can be used to determine, quite easily, the acceleration of the force of gravity and the parabolic (escape) velocity at the surface; the former amounts to about 38% of its value on the Earth, the latter to about 4.3 km/s.

The first tests on Mercury were carried out from space by automatic instruments on the US Mariner 10 on March 29, and September 21, 1974. Photographs of the planet surface were communicated to Earth. The radius of Mercury, inferred from radio-eclipsed measurements, is  $2440 \pm 2$  km at a latitude of  $2^\circ$  and  $2438 \pm 2$  km at a latitude of  $68^\circ$ . Analysis of track data precisely defined the mass of Mercury; in units of the ratio of the mass of the Sun to that of the planet it amounts to  $6\,023\,600 \pm 600$ . The new value of the average density of the planet is  $5.44 \text{ g} \cdot \text{cm}^{-3}$  [83].

From the values of the mass and diameter, a mean density of 5.30 to 5.46 is calculated [196]. The high mean density of Mercury (compared with the density of substances in the Earth at the level of the corresponding pressure) is explained by an abundance of the heavy elements. The chemical composition of Mercury apparently is mostly iron [18, 108, 195]. The high content of iron and, consequently, the limited

content of silicates, indicate a significantly lower content of radioactive substances in Mercury than in the substance of chondrite meteorites. However, it is known that the decomposition of the radioactive elements contained in the silicates is one factor in the internal heating of the planets. Consequently, the thermal history and present state in the depths of Mercury depend, to a considerable degree, on the average chemical composition. The still unknown factors must also be considered, such as the velocity of the planet's conglomeration from the substance of the protoplanetary cloud, abundance and composition of radioactive elements in this substance, and radiant energy obtained from outside at early evolutionary stages.

Calculations [145] of the thermal history of Mercury have shown that in all stages of its evolution, the temperature deep in the planet has never reached the value necessary to melt silicate substances or iron. This indicates that substances in Mercury would not be segregated according to specific gravity, with iron in the central core. Lamination of the substance according to the specific rate (gravitational differentiation) in the solid depths of the planet is considerably slower than in the case of melting. Nonetheless, some specialists consider it possible that Mercury has a nucleus. Various models of the internal structure of Mercury have been described [121]; models with homogeneous distribution of metallic iron and with iron segregated in the core were both studied.

### **The Surface: Photometric Properties and Modern Data on Relief**

The surface of Mercury appears bright in sunlight, but measurements have shown that it is rather dark, more precisely, dark brown. The visual Bond albedo<sup>4</sup> for Mercury is 0.056 [79];

<sup>4</sup>Bond albedo (or spherical albedo) is expressed by a fraction, the numerator of which shows the flux of solar radiation reflected by the daylighted hemisphere of a planet in all directions. The denominator shows the flux of solar radiation striking the planet. To the name of the albedo we add a word indicating either absence of limitations of spectral range—integral albedo, or the type of spectral sensitivity of the radiation receiver used, for example—visual albedo.

the integral albedo is 0.09 [157]. The mean brightness of the Mercury surface increases sharply as the phase angle approaches zero. Curves of the variation of brightness as a function of phase angle for Mercury and the Moon practically correspond [74, 79]. The spectral reflectivity increases with increasing wavelength, at least up to  $1.6 \mu\text{m}$  [157]. The results of measurement of spectral reflectivity of Mercury, ad-

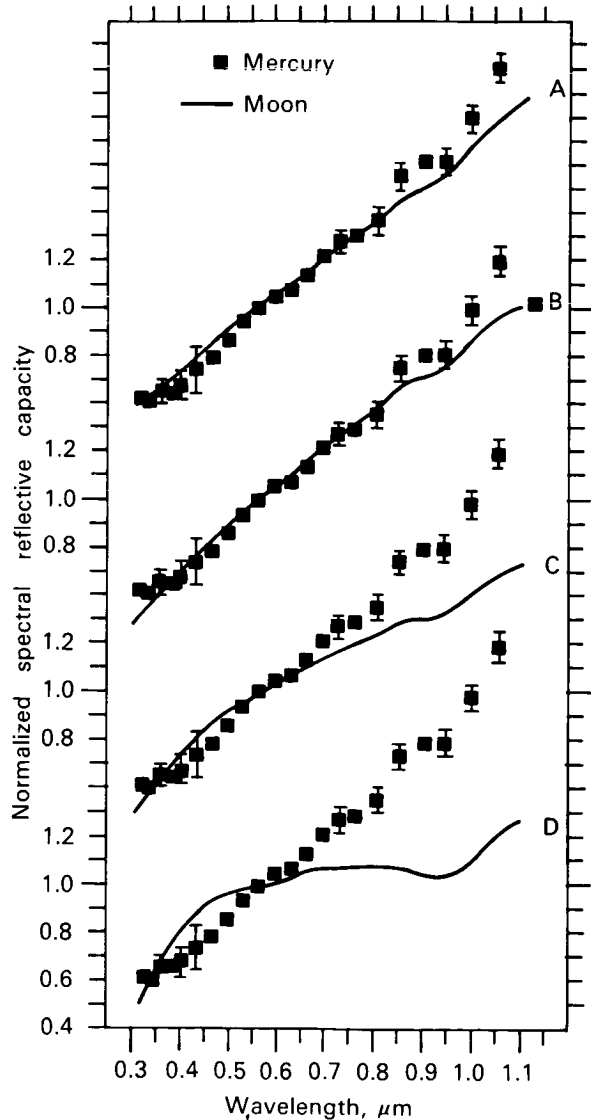


FIGURE 1.—Spectral reflective capacity of Mercury and its comparison with reflection spectra of various territories of the Moon: (A) mountains; (B) sea; (C) bright craters in mountain areas; (D) bright crater (from [147]).

justed to zero phase, within the limits of  $0.32$  to  $1.05 \mu\text{m}$  are shown in Figure 1 (from [147]). The curve of the reflectivity of Mercury is similar to that of mountainous and maria areas of the Moon's surface and differs from the curve from the floors of lunar craters. With these results, it was concluded that the surface of Mercury is probably covered with Moonlike solid matter, rich in dark volcanic glass, such as pyroxene. The reason for the low albedo may be the high content of iron and titanium in the minerals [147].

Under exceptionally favorable conditions, which are rather rare, light and dark spots can be seen on the surface of Mercury through a telescope. Repeated attempts to map Mercury have been made. Historical maps will not be studied here, since their composers used erroneous data on the period of axial rotation of the planet. New attempts to map Mercury according to modern concepts have been reported [20, 21, 32]. The best modern map of details of the Mercury surface, showing the coordinates of details drawn, was composed in 1972 from photographic and visual observations in 1942–1970 in the astronomical observatories of Pic-du-Midi in France and New Mexico in the US [172].

The new map is shown in Figure 2. Longitudes are given according to the new system, recommended at the Fourteenth Session of the International Astronomical Union (Brighton, 1970 [172]). The composers of the map concluded that the visible contrast of details on the surface of Mercury is somewhat less than the contrast between the maria and continental areas on the Moon. Possibly, the decrease in contrast results from eroded images of dark details during observations of Mercury, since the angular resolution produced is 300 times poorer than that of observations of the Moon. The area between  $350^\circ$  and  $90^\circ$  hermographic<sup>5</sup> longitude, occupying over one-fourth of the surface of the planet, shows practically no large contrast details. The authors [172] noted that the details on the surface of Mercury remained

<sup>5</sup>The term for the system of coordinates on the surface of Mercury comes from the Greek name for this planet—Hermes.

unchanged during more than 30 years of observation, and that no atmospheric haze was observed in any area of the planet.

Studies of the surface relief of Mercury are beyond the capabilities of optical methods of Earth-based astronomy. During the past decade, radar has been used successfully to study the surfaces of the closest planets. The capabilities of radar have been increased both through improvements in apparatus and through new methods of data analysis. However, Mercury is difficult to investigate since a radio echo signal returning from Mercury is approximately 1% as strong as a signal returning from Venus.

Before 1970, researchers at MIT attempted to use two-dimensional radar spectra (delay time and frequency) to estimate the profile of the surface of Mercury [227] but were unsuccessful. The reflected signal was too weak to permit differentiation of significant relief details or determination of the inclination of the Mercury surface from the surface of a sphere. Two radar studies of Mercury conducted in 1970–1971 by Goldstein at the Jet Propulsion Laboratory, California Institute of Technology, at a wavelength of 12.5 cm, and at Haystack Observatory (MIT) at a wavelength of 3.8 cm, achieved sufficient sensitivity to study the scattering characteristics. Both the scattering function and the

polarization of radiation at 12.5 cm showed that the surface of Mercury is significantly rough with respect to small irregularities [66]. Measurements at 3.8 cm [86] in several areas of the equatorial portion of the planet showed that the mean slope was approximately 10°. This value changes significantly with longitude. Topographical details were observed with variations in the radius of the planet on the order of 1–3 km.

Radar studies have measured the “reflection factor” of the planet in the microwave band. It was approximately the same as that of the Moon. The scattering cross section<sup>6</sup> of Mercury varied during observations within limits of 4%–8% from the optical cross section.

### Parameters of Axial (Diurnal) Rotation

Repeated attempts were made to determine the period of axial rotation of the planet by observation of spots on the surface. These visual observations led to the mistaken conclusion that Mercury always turns the same hemisphere toward the Sun, i.e., to the conclusion that the

<sup>6</sup>The radar cross section of a planet is found from the total power of reflected radio radiation, and is defined as the geometric cross section of an ideally conducting sphere at the same distance as the planet being studied and yielding the same radio echo power; it is usually expressed as a percent of the geometric cross section of the planet.

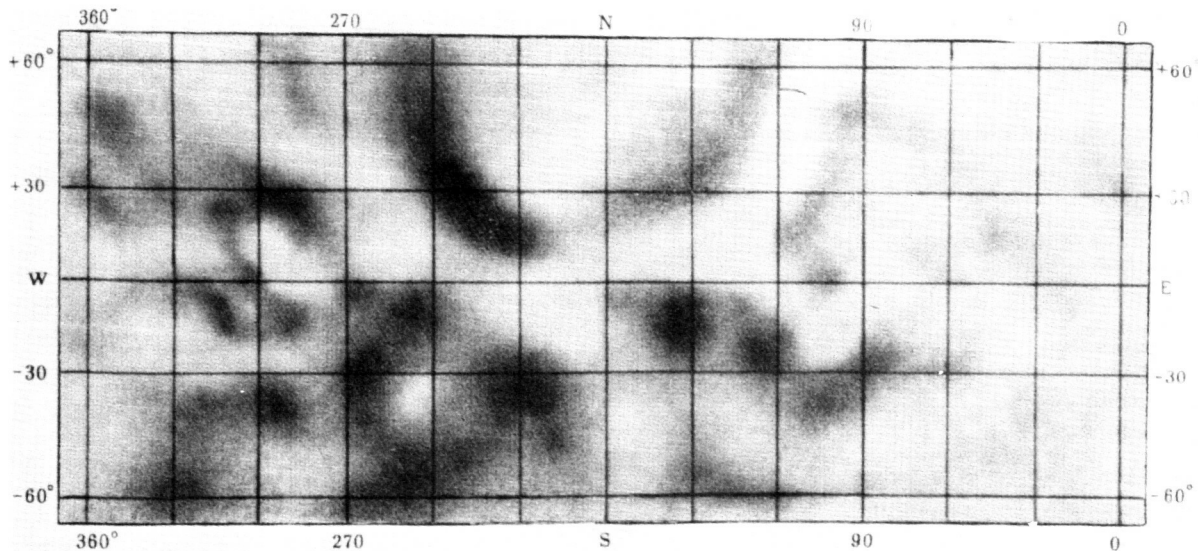


FIGURE 2.—Map of the surface of Mercury (after [172]).

sidereal period of axial rotation was equal to the sidereal<sup>7</sup> period of orbital rotation (87.97 d). This erroneous opinion was held until the discoveries of Pettengill and Dyce [180], who found, by radar studies, that the sidereal period of axial rotation of Mercury is  $59 \pm 3$  d. This value was subsequently refined. Thus, Mercury does rotate, but so slowly that its axial rotation is difficult to observe during the short interval favorable for visual observations.

Many authors explain the long life of the erroneous hypothesis of synchronous rotation of the planet as the result of the "fatal" quasi-comparability of the period of this rotation with the period of recurrence of conditions most favorable for observations of Mercury (in one astronomical observatory outside the tropical belt—with this refinement, the statement is correct). The necessary combination of factors repeats itself every 3 synodic periods, i.e., every 348 d, during which time Mercury turns by approximately a whole number of rotations in relationship to both the Sun and the Earth. In this case, the apparent displacement of details on the planetary disk and the position of the subsolar point among them recur with hardly noticeable changes.

Optical observations, incidentally, have helped to refine the period of rotation of Mercury after its rough but reliable estimation by the radar method. A period of  $58.67 \pm 0.03$  d was determined on the basis of data from the archives of the Pic-du-Midi Observatory for 1942–1966 [20]. On the evidence of photographic archives built up over many years, a period of rotation of  $58.663 \pm 0.021$  d was reported [228]. The accuracy of the radar observations has been consistently improved and now approximates the accuracy of optical methods. New radar observations [66] indicate a period of 58.65 d, with an error of not over 0.4%. The earlier photographs and drawings of Mercury were supplemented with new optical observations made at the Pic-du-Midi and New Mexico Observatories and a rotation period of  $58.644 \pm 0.009$  d was determined [172]. The axis of the planet's rotation has been found to be perpendicular to the plane

of its orbit with a probable deviation of not over 3°.

The period of axial rotation of Mercury is not a random figure; an interval of 58.6462 d is precisely two-thirds of the orbital period of Mercury. This is an interesting example of resonance in spin oscillations, caused by the gravitational effects of the Sun on the planet, within which the placement of mass cannot be considered strictly concentric. A rotation period two-thirds that of orbital rotation should be stable [26]; the small axis of the ellipsoid of inertia of the planet is oriented toward the Sun each time Mercury returns to its perihelion. It is demonstrated [64] that development of a 3/2 spin-orbital resonance requires a compression of the ellipsoid of inertia in the equatorial plane  $(B - A)/C \geq 10^{-5}$ , i.e., very slight.

### The Atmosphere of Mercury

An atmospheric pressure at the surface of Mercury of approximately 1 millibar (mbar) was reported on the basis of measurements of the polarization of the light scattered by the planet in various areas of the spectrum [45, 46]. An estimate of the same order of magnitude ( $\text{CO}_2$  content of 0.3–7.0 g/cm<sup>2</sup>) was produced from observations of the excess absorption in the  $\text{CO}_2$  band (1.6  $\mu\text{m}$ ) in the spectrum of Mercury over that of the Earth [157]. The peculiarities of polarization of Mercury were attributed to surface properties alone, without the participation of atmospheric effects [175]. Belton, using measurements in the 1.05  $\mu\text{m}$  band determined an upper limit for the content of  $\text{CO}_2$  on Mercury of 5 m · atm (partial pressure at the surface less than 0.35 mbar); while Bergstrahl, observing the band around 1.20  $\mu\text{m}$ , evaluated this upper limit as not over 0.58 m · atm (partial pressure approximately 0.04 mbar). These data place in doubt the results indicating detection of  $\text{CO}_2$  on Mercury.

For gas molecules to be retained on Mercury, they would have to be (1) rather heavy, and (2) resistant to dissociation under the influence of sunlight. These criteria are satisfied by  $^{40}\text{Ar}$ , widely distributed in the solar system. Observations do not exclude an argon atmosphere with a pressure at the surface of Mercury of 1 mbar or

<sup>7</sup>The term sidereal refers to the movement of the object in the system of coordinates coupled to the fixed stars.

less, but its existence is only hypothetical. The similar surface photometric properties of Mercury and the Moon suggest that the surface of Mercury has been influenced by the solar wind. On this assumption, the upper limit of atmospheric pressure at the surface of the planet was estimated at approximately  $10^{-5}$  mbar [175, 202]. Another group, using calculations on the rate of dissipation, produced an upper limit of around  $10^{-6}$  mbar. In a discussion of various models of the atmosphere of Mercury, Banks [11] allows for the possibility of an exospheric model consisting of  $^4\text{He}$ ,  $^{20}\text{Ne}$ , and  $^{40}\text{Ar}$ , with a summary upper limit of  $2 \cdot 10^{14}$  particles in a unit column. The structure of the model is determined by the solar wind.

An ultraviolet (UV) experiment by Mariner 10 showed that Mercury is surrounded by a thin atmosphere with full pressure at the surface of not more than  $2 \cdot 10^{-9}$  mbar [17]. The upper limits of various gases were determined; the most abundant components may be Ne, Ar, and Xe. Among other gases, in particular, He was found, the partial pressure of which at the surface amounts to  $2 \cdot 10^{-12}$  mbar.

### Insolation and Surface Temperature

Because of the combined effects of axial and orbital rotation, 1 solar day on Mercury exactly equals 3 stellar days or 2 Mercurian years, i.e., 176 mean solar Earth days. The Sun has variable size in the Mercurian sky, and moves from east to west unevenly, due to the eccentricity of the orbit and the periodic changes in heliocentric angular velocity of the planet. Twice each solar day (namely at each perihelion), the Sun increases in size and stops, after which its motion reverses for some 100 hours, after which the Sun stops once more, then takes up its course toward the west.

The quantity of solar energy received per unit time and unit area perpendicular to the rays of the Sun (the so-called solar constant, equal to  $2.00 \pm 0.04 \text{ cal} \cdot \text{cm}^{-2} \cdot \text{min}^{-1}$  at the upper boundary of the Earth's atmosphere) on Mercury at the perihelion is approximately double the value at the aphelion, and is 10 times greater than on the Earth, i.e., reaches  $14 \text{ kW} \cdot \text{m}^{-2}$ . The

daily cycle of illumination is not the same at different geographic longitudes on the Equator. Around longitudes  $0^\circ$  and  $180^\circ$ , the Sun has its maximum angular size at the upper culmination and moves very slowly in the sky, whereas around longitudes  $90^\circ$  and  $270^\circ$ , its minimum angular dimensions are at noon and it crosses the sky relatively rapidly, delaying only at the horizon.

The daily heating of the surface decreases with increasing latitude right up to the poles of rotation. At the poles, continuous or near-continuous illumination is observed. The Sun moves along the mathematical horizon with a period of 176 d; the center of the Sun dips below the horizon every 38 d by a quantity equal to the inclination of the Equator of the planet to its orbit (an inclination  $< 3^\circ$ ); the upper edge of the Sun, if it disappears, does so only briefly, since the immersion depth of the center beneath the line of the mathematical horizon is approximately equal to the radius of the Sun as seen from Mercury.

The long days and nights on Mercury produce great temperature differences between the noon and midnight sections of the surface. The planet's closeness to the Sun and its low albedo result in great surface heating during the day. The temperature on Mercury has been determined on the basis of changes in the planet's natural thermal radiation in the portion of the infrared (IR) range where the contribution of reflected solar radiation is negligible. At the mean distance from the Sun, the brightness temperature<sup>8</sup> of the surface at the subsolar point of Mercury corresponds to the Planck radiation of an absolutely black body at a temperature  $T_b = 613^\circ\text{K}$  [182]. The color temperature (according to the ratio of intensities at  $\lambda = 2.2$  and  $3.4 \mu\text{m}$ ) at the perihelion has been found to be  $T_c = 670^\circ \pm 20^\circ\text{K}$  [158].

Infrared thermometry of the dark side of

---

<sup>8</sup> The brightness temperature is the temperature of an absolutely black body of the same dimension and the same luminance as the body observed in a limited spectral range. The color (or spectrophotometric) temperature is parameter  $T$  in the well-known formula of Planck, with the value of the parameter selected so as best to approximate the observed distribution of energy of radiation of the body in a given wavelength interval.

Mercury involves greater technical difficulties, since in addition to high angular resolution of the apparatus and ideal atmospheric conditions, it requires reliable protection of the apparatus from the radiation of the crescent of the bright hemisphere of the planet and extremely high sensitivity of the detector. Nevertheless, measurements of such difficulty have been successfully performed. Murdock and Ney [170], studying the  $3.75\text{--}12.0 \mu\text{m}$  range, found a nighttime surface temperature of  $111^\circ \pm 3^\circ \text{ K}$ . Thus, the amplitude of diurnal fluctuations in temperature on Mercury is over  $500^\circ \text{ K}$ .

Modern observations of Mercury's thermal radiation have not been limited to the IR band. Radioastronomy measurements in the microwave band have determined the thermal mode of the subsurface layers of the planet at various depths and the physical properties of the outer cover of the planet. The greater the radiation wavelength used, the greater the depth responsible for its origin. The penetration depth of electromagnetic oscillations (i.e., depth of the radio radiating layer)  $l_e = 1/\kappa$ , where  $\kappa(\lambda)$  is the electromagnetic wave-absorption factor, and  $\lambda$  is the wavelength. Equally important is another expression of the same quantity:  $l_e = \delta l_t$ , where  $\delta$  is a coefficient which depends on the properties of the material, and  $l_t$  is the depth of penetration of the temperature wave, defined by a decrease in amplitude of fluctuations of temperature by  $e$  times in comparison to the value on the surface. At a depth three to four times  $l_t$ , the fluctuations in temperature are practically nil. This determines the thickness of the surface layer of material heated by the Sun during the course of the day. The theory of this problem has been presented in detail [109].

The temperature measured in the microwave band depends on the relationship between the thickness of the layer heated by the Sun and the thickness of the radio-radiating layer. Reviews of results of radiometric observations of Mercury at wavelengths of  $0.19\text{--}11.3 \text{ cm}$  are available [65, 67, 167]. The numerical values of the heat-physical parameters of Mercury are presented at the end of this section.

The heat-physical behavior of the outer cover

of the planet indicates its exceptionally low heat conductivity. The amplitude of diurnal fluctuations in temperature at a certain depth, as would be expected, is considerably less than that indicated by measurements in the IR band. The data from microwave radioastronomical observations indicate that the brightness temperature, averaged over the entire visible disk of Mercury, varies both with phase angle ( $i$ ) and with longitude ( $L$ ) from the center of the disk, also depends on the ratio ( $\delta$ ) of the penetration depth of the electrical and thermal waves. The most complex results of observations, processed by the method of least squares, are:

$$\begin{aligned} \lambda = 0.33 \text{ cm}; T_1 (\text{°K}) = & 296 + 127 \cos(i + 16^\circ) \\ & \pm 7 \quad \pm 9 \quad \pm 4^\circ \\ & + 16 \cos(2L + 16^\circ); \delta/\lambda = 1.0 \text{ cm}^{-1} [92]; \\ & \pm 9 \quad \pm 28^\circ \end{aligned} \quad (1)$$

$$\begin{aligned} \lambda = 3.75 \text{ cm}; T_2 (\text{°K}) = & 380 + 55 \cos(i + 32^\circ) \\ & \pm 4 \quad \pm 3 \quad \pm 4^\circ \\ & + 11 \cos(2L - 8^\circ); \delta/\lambda = 1.3 \text{ cm}^{-1} [126]; \\ & \pm 3 \quad \pm 11^\circ \end{aligned} \quad (2)$$

where  $\lambda$  is the electromagnetic radiation wavelength;  $i$  is the Sun-planet-Earth angle; and  $L$  is the hermographic longitude in the system of longitudes described [32]. The position of the zero meridian in this system differs from its position in the International Astronomical Union (IAU) system of 1970.

The great differences between the expressions of temperature in the millimeter and centimeter wavebands cannot be explained solely by the differences in effective depth of the radiating layer. In applying the theory of radio radiation developed for the Moon to Mercury, it is necessary to consider the temperature-dependence of heat-physical parameters in the case of Mercury [60]. The average brightness temperature of Mercury has been calculated in various bands of thermal radiation as a function of phase angle and position in its orbit, with the dependence of heat conductivity on temperature taken into account [166, 167].

An IR radiometer on Mariner 10 measured thermal radiation of the planet in a spectrum region of about  $45 \mu\text{m}$ , given minimal sizes of the observed surface element as  $40 \text{ km}$ . In the

periequatorial scan the lowest brightness temperature, 100° K, was registered next to the local midnight. The law of temperature decrease after sunset is the same as in the case of homogeneous porous material with thermal inertia  $0.0017 \text{ cal} \cdot \text{cm}^{-2} \cdot \text{s}^{1/2} \cdot ^\circ\text{K}^{-1}$  with fluctuations of this value up to 0.003 in some regions [24].

### **Similarities Between External Layers of Mercury and of the Moon**

A comparison of the above-mentioned calculations [166, 167] with the most reliable observations permitted selection of the most probable values of parameters characterizing thermal and electrical properties of the outer layer of Mercury. Some of these parameters are:

$$\text{Density } (\rho) = 1.5 \pm 0.4 \text{ g} \cdot \text{cm}^{-3};$$

$$\text{Thermal inertia } (\gamma) = (kpc)^{1/2} = (15 \pm 6) \cdot 10^{-6} \text{ cal} \cdot \text{cm}^{-2} \cdot \text{s}^{-1/2} \cdot ^\circ\text{K}^{-1};$$

Parameter  $\delta/\lambda = 0.9 \text{ cm}^{-1} \pm 0.3 \text{ cm}^{-1}$ , where the ratio of the depth of penetration of the thermal and electrical waves ( $\lambda$ ) is the wavelength of electromagnetic radiation in cm;

$$\text{Heat conductivity factor } (k) = (4 \pm 2) \cdot 10^2 \text{ cal} \cdot \text{cm}^{-1} \cdot \text{s}^{-1} \cdot ^\circ\text{K}^{-1};$$

$$\text{Depth of penetration of thermal wave } l_t = 11 \pm 6 \text{ cm};$$

$$\text{Dielectric constant } (\epsilon) = 2.9 \pm 0.5;$$

$$\text{Loss angle tangent } (\tan \Delta) = (0.9 \pm 0.4) \cdot 10^{-2}.$$

Similar characteristics of Mercury and the Moon indicate that there are no sharp differences in the structure of the outer layers of these two bodies. However, caution must be exercised in considering the similarity of the mineral composition of their surfaces. Until experimental data about the surface composition of Mercury are available, ideas in this regard depend on the solution of another problem: Was the planet subjected to internal melting and gravitational differentiation? It is known that the Moon contains melted products from the depths in its external layers. The extremely high average density of Mercury suggests models of its internal structure which, it seems, could not have been subjected to melting. Possibly the external similarity of the surface of Mercury to that of

the Moon resulted from similar processing of minerals into regolith by external factors.

These are the basic contemporary concepts of the nature of Mercury. Further growth in the level of knowledge of this planet apparently can be significantly accelerated only by means of spacecraft.

### **VENUS**

Venus, the inner planet closest to the Earth and the brightest light in the sky after the Sun and the Moon, has been a subject for astronomers' constant attention for many centuries. Until the mid-1950s, it was considered possible that well-developed forms of life might exist on Venus. Although this attractive idea has been abandoned at present, interest in the planet has not decreased, but more probably has increased, since Venus has been found a very special and surprising world in terms of its natural conditions, full of riddles and surprising facts.

The capabilities of automatic spacecraft have probably been demonstrated best in the study of Venus. For several years, a program of studies of Venus has been conducted in the Soviet Union. The Venera 4, 5, 6, 7, and 8 automatic spacecrafts conducted a broad range of studies of the lower atmosphere and planet surface, essentially discovering the world of Venus. A considerable contribution to the study of the atmosphere above the visible cloud border and the surrounding space was made by measurements from flyby trajectories of US spacecraft Mariner 5 and 10. Improved methods of astronomical Earth observations, especially in radioastronomy and radiolocation, clarified a number of newly discovered physical characteristics of this planet. The results of complex studies conducted during the recent decade are of fundamental scientific significance and serve as the basis for current conceptions of Venus [137].

### **Basic Astronomical Characteristics**

Venus moves in a near circular orbit within that of the Earth about 108.1 million km from the Sun, or 0.723 AU. The velocity of the orbital motion of the planet is approximately 5 km/s greater than the orbital velocity of the Earth, at 34.99 km/s. The time required for one rotation

of the planet around the Sun (the sidereal period) is 224.7 Earth days. The synodic period (time between two successive identical conjunctions or two phases of Venus) averages 584 days. The phases of Venus are similar to those of the Moon. The planet is located at its minimum distance from the Earth (about 40 million km) in the lower conjunction, in the position between the Earth and the Sun (at phase angle  $\alpha=180^\circ$ ), at which time it turns its dark side toward the Earth. Near the upper conjunction, when the planet is located beyond the Sun ( $\alpha=0$ ) its almost fully lighted disk is observed. The intermediate positions ( $0 < \alpha < 180^\circ$ ) correspond to intermediate phases of partial illumination of Venus for the terrestrial observer, from a narrow crescent to a nearly full disk. The visible angular diameter of the planet varies between the upper and lower conjunctions by almost 6.5 times, from 9.9 to 64.0 s.

Venus is brightest (stellar magnitude about  $-4.3$ ) at its maximum angular distance from the Sun, reaching up to  $48^\circ$  under the most favorable conditions, in the position of the so-called "pauses." The angular diameter of the disk at these moments is about 40 s. The period of the

beginning of visibility of the planet at twilight corresponds to passage of the upper conjunction, after which its angular distance from the Sun increases, then decreases; at the same time, the visible diameter of the disk increases, while its illuminated portion decreases. The morning ascent of Venus in the east is accompanied by passage of the lower conjunction, after which the visible diameter of the disk begins to decrease, while its illuminated portion increases. The difference between Venus and the Sun in rising and setting reaches almost 4 h. Due to this peculiarity of the visibility of Venus, it has long been called the morning or evening "star."

Observations of Venus in its lower conjunction indicate that the plane of its orbit is inclined to the ecliptic at angle  $i=3^\circ 23' 39''$ . Therefore, the disk of the planet during periods of conjunctions is usually not projected on the disk of the Sun. The transit of Venus across the Sun occurs only when at the moment of a lower conjunction, both planets are located on the line of intersection of their orbits. These events, schematically illustrated in Figure 3, are comparatively rare, periodically repeating at intervals of 8 and slightly over 100 years (see [12]). Obser-

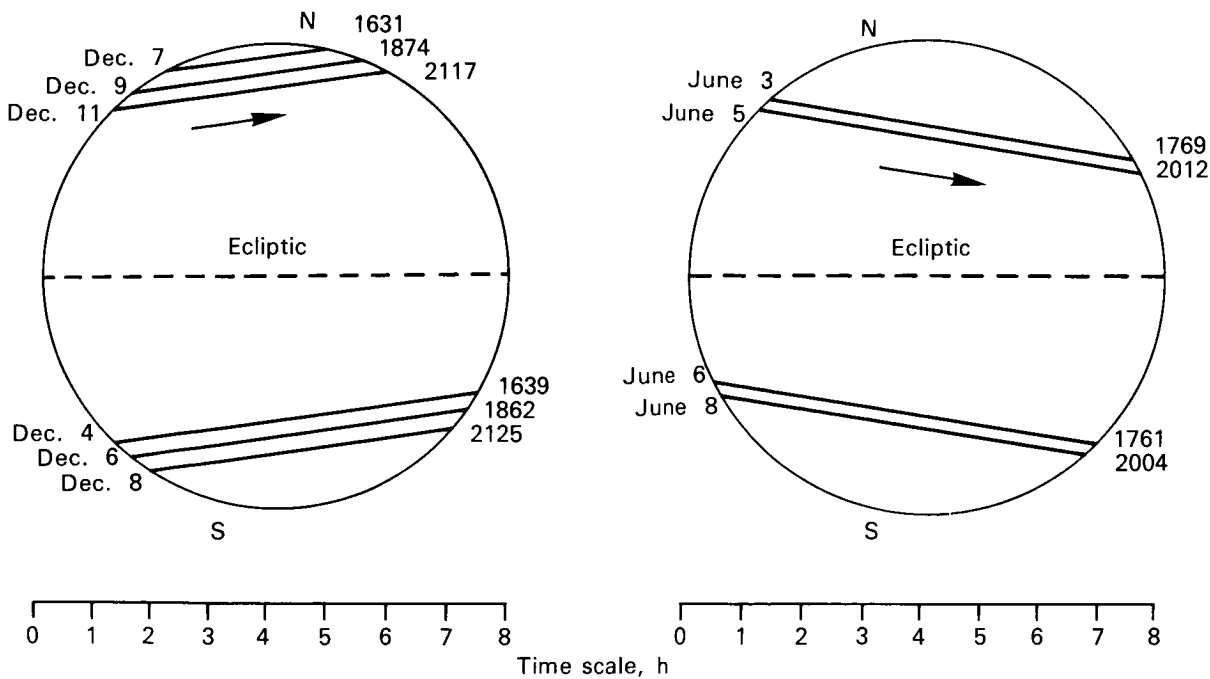


FIGURE 3.—Moments of Venus passage over the Sun's disk.

vation of the transit of Venus across the disk of the Sun, July 6, 1761, allowed the Russian scientist, Lomonosov [125], to make the fundamental discovery of an atmosphere on the planet.

Of all the planets of the solar system, Venus most nearly resembles Earth in its dimensions, mass, and mean density. Its radius is 0.948 Earth radii ( $R_\oplus=6050 \pm 0.5$  km [72]). The ratio of the mass of the planet to the mass of Earth is about 0.81, while its mean density is  $5.24 \text{ g} \cdot \text{cm}^{-3}$  as compared to  $5.52 \text{ g} \cdot \text{cm}^{-3}$  for Earth. Based on measurements of the orbit of the Mariner 5 spacecraft, the mass of Venus is  $408\,522 \pm 3$  times less than the mass of the Sun. The primary parameters characterizing elements of the Venus orbit, its geometry, mass, and related quantities are presented in Tables 1 and 2; corresponding parameters of the Earth are also shown for comparison [215].

For considerable time, the characteristics of the rotation of Venus about its axis and the ecliptical coordinates of its poles were subjects of animated debate; i.e., the tilt of the axis of rotation in relation to the plane of its orbit around the Sun. Many visual, photographic, and later, spectral observations were made in the visible, IR, and UV areas of the spectrum in attempts to follow the visible movement of characteristic details (individual spots and bands) across the disk of the planet. However, the peculiarities observed, parts of the cloud layer which constantly cover the planet, were generally unstable, and the subjectivity of the observer had a strong influence on any conclusions concerning periodicity of repetition. Values of a few days to a few months were reported, with most observers assuming synchronous rotation of the planet.

Significant progress in defining the nature of the rotation of Venus was made only after radar studies began in 1958 [189]. The first successful radiolocation measurements of Venus, close to the inferior conjunction, were carried out in 1961 in the USSR by a group of specialists of the Institute of Radiotechnology and Electronics [105, 106]. Studies were pursued in the US at the MIT Lincoln Laboratory [179], Jet Propulsion Laboratory of the California Institute of Technology [135, 242], and in England at the Jodrell Bank Radioastronomy Observatory [236]. More

complete and exact data resulted from measurements made close to the inferior conjunction of Venus in 1964. The measurements of Kotel'nikov and others [104] gave a rotation period of  $230 \pm 25$  d, reverse rotation direction. According to measurements at the Arecibo Ionosphere Laboratory of Cornell University [53], the rotation period of Venus is  $T = 244.3 \pm 2$  d, reverse rotation direction. The most accurate data on the rotation characteristics of the planet are based on the periodicity of appearance of details of increased reflection in the course of several inferior conjunctions. According to data of the Arecibo Observatory [93], the rotation period equals  $243.0 \pm 0.1$  Earth d, reverse rotation direction, coordinates of the North Pole of the rotation axis  $\alpha = 272.7^\circ \pm 0.7^\circ$ ;  $\beta = 65.3^\circ \pm 1^\circ$ . According to observations [23] at the Jet Propulsion Laboratory, the rotation period of Venus in reverse direction amounts to  $242.98 \pm 0.04$  d, the pole coordinates  $\alpha = 274.1^\circ \pm 3^\circ$ ;  $\beta = 71.4^\circ \pm 1^\circ$  (for an epoch 1950.0).

Venus has a clockwise rotation when observed from the North Pole of the World, in contrast to the other planets of the solar system. The combination of the annual motion and the reverse diurnal rotation of the planet means that 1 Venusian year includes 2 days, each lasting 116.8 Earth days. This means that during a Venusian year, the Sun rises and sets twice. An observer on the surface of Venus would be surprised to see the Sun rise in the west and set in the east, and would find himself under conditions similar to the "polar night" and "polar day," lasting some 2 Earth months, both in the equatorial and the moderate latitudes. The measured coordinates of the rotation vector (direct ascension  $\alpha$  and inclination  $\delta$ ) lead to the conclusion that the axis of rotation of Venus is almost perpendicular to the plane of its orbit: the angle between the plane of the equator and the plane of the orbit is less than  $3^\circ$ . This means that there are practically no seasonal changes in the annual rotation of the planet.

Repeated results show that the rotation period of Venus, which equals 243.16 Earth days, is very close to the planet's resonance rotation in respect to Earth. In this case, at each inferior conjunction, Venus is turned to Earth with one

TABLE 2.—*Mean Orbital Elements of Planets of the Earth Group in System of Coordinates with Ecliptic and Point of Vernal Equinox of Earth in Epoch 1950.0*

Planet	Mean distance from Sun		Rotation period <sup>1</sup>		Eccentricity	Inclination	Longitude of ascending node	Annual change	Longitude of perihelion	Annual change	Mean longitude of planet in initial epoch	Mean velocity of motion in orbit, (km/s)	Mean angular velocity of motion in orbit/d
	Millions of km	AU	Sidereal	Mean synodic									
Mercury	57.91	0.38710	87.97	115.88	0.2056	7° 1' 14"	47° 44' 19"	+0.71"	76° 40' 39"	+0.93"	33° 10' 6"	47.83	4° 5' 32"
Venus	108.21	0.72333	224.70	583.92	0.0068	3° 23' 39"	76° 13' 39"	+0.54	130° 52' 3"	+0.84	81° 34' 19"	34.99	1° 56' 8"
Earth	149.60	1.00000	365.26	779.94	0.0167	1° 51' 0"	49° 10' 19"	+0.46	102° 4' 50"	+1.03	99° 35' 18"	29.76	0° 39' 8"
Mars	227.94	1.5237	686.98	779.94	0.0934				335° 8' 19"	+1.10	144° 20' 7"	24.11	0° 31' 27"

<sup>1</sup> In units of mean solar days of universal time.

side. Such resonance rotation in relation to Earth is, obviously, caused by the gravitational impact of Earth on the asymmetric figure of the planet. A detailed explanation of the methods and a more complete summary of the results of radiolocation measurements are available [114, 200].

### Figure, Topography, Surface

Information on the nature of the solid body of Venus is quite limited. The results of measurements, performed in 1968–1969 at a wavelength  $\lambda = 3.8$  cm [85, 237], have shown that, in the equatorial plane, the cross section of the planet is an ellipse, the difference of the half axes of which amounts to  $1.1 \pm 0.25$  km. The long axis of the ellipse forms an angle of  $55^\circ$  (clockwise) with the direction toward the Earth in the lower conjunction. The center of mass is displaced relative to the center of the planet's figure by  $1.5 \pm 0.25$  km.

In topography and physical properties, the results of mapping the reflective properties of the Venus surface in the radioband are of interest. These experiments [85] indicated local areas of increased reflectivity extending for hundreds and thousands of kilometers. The map of the surface reflective properties, limited by longitudes  $0^\circ$  and  $-80^\circ$  and latitudes of  $-50^\circ$  to  $+40^\circ$ , is shown in Figure 4. The most characteristic areas are  $\alpha$  and  $\beta$ . Large circular formations like the lunar maria (*shaded*) have also been found, as well as individual specific details within them (*Roman numerals*). The nature of the areas of increased reflection can be explained, not only by possible rough surface and elevations leading to a decrease in the effective absorptive layer of the atmosphere, but also by differences in surface material and, consequently, dielectric permeability ( $\epsilon$ ). The mean value of  $\epsilon$ , concluded from radar measurements, falls within limits of 4–4.5.

Altitude differences of 3–5 km on the surface of Venus have been detected from radar studies. The region of greatest elevation is at a longitude of about  $31^\circ$  (according to the Ingalls-Evans system [85], in which the meridian passing through the  $\alpha$  area is taken as the zero meridian). Relief differences of the planet's surface may

possibly be expressed still more sharply. However, data on polarization of radio waves reflected by the planet show that the polarization of most of the waves' energy corresponds to mirror reflection, and that the ratio of depolarized reflection to polarized reflection for Venus is significantly less than for the Moon. This indicates that the microstructure of the Venus surface is, on the average, smoother than that of the Moon.

The available experimental data from radar probing indicate, in general, significant variation in the physical properties of the Venus surface, and, apparently, a rather smooth topography.

Theories of a smooth topography were recently supported by a radiolocation experiment conducted in the equatorial region [67]. A reflected signal was received by two antennas 22 km apart. This made possible a stereoscopic depiction of a surface area about 1500 km in diameter (coordinates  $\lambda = 320^\circ$ ,  $\theta = +2^\circ$ ) at a height range of 200 m and a surface range of up to 10 km. More than 10 ring craters with diameters from 35 to 150 km were found which, in their form, resemble Moon craters. Their depth, however, is insignificant. A crater 150 km in diameter has a depth of not more than 0.5 km. The entire region studied turned out to be flat, with a relative difference in heights of less than 1 km. Such distinct flatness is not strange under conditions of a very dense atmosphere subjected (to be explained later) to considerable motion and, possibly, containing aggressive admixtures which advance the erosion processes on the surface.

The flight of Venera 7 yielded the first estimates of the physical and mechanical properties of the Venus surface. A qualitative analysis of the spacecraft's landing conditions was made on the basis of changes in signal power received on the Earth at the moment of contact with the surface. The vertical velocity of the spacecraft was damped in less than 0.2 s, probably corresponding to hard soil. Had the vehicle struck a low-viscosity fluid or a thick dust layer, the process of spacecraft deceleration and drop in signal level would have been significantly slower. Considering data on spacecraft strength,

an upper estimate can be made of the soil strength  $P_s \leq 80 \text{ kg/cm}^2$ . On Earth, this level of soil strength corresponds to rocks such as volcanic tuffs. However, comparison of the nature of change in signal power at the moment of Venera 7 touchdown with test results involving impacting of a descending vehicle against various soils indicates that the soil strength is sig-

nificantly lower than this upper limit, not over  $2 \text{ kg/cm}^2$  [140].

During flight of Venera 8, changes in the energy of radio waves reflected by the surface of the planet as the spacecraft descended were used to estimate the dielectric permeability, which differs significantly (by a factor of about 1.5) from that indicated by radar data. This

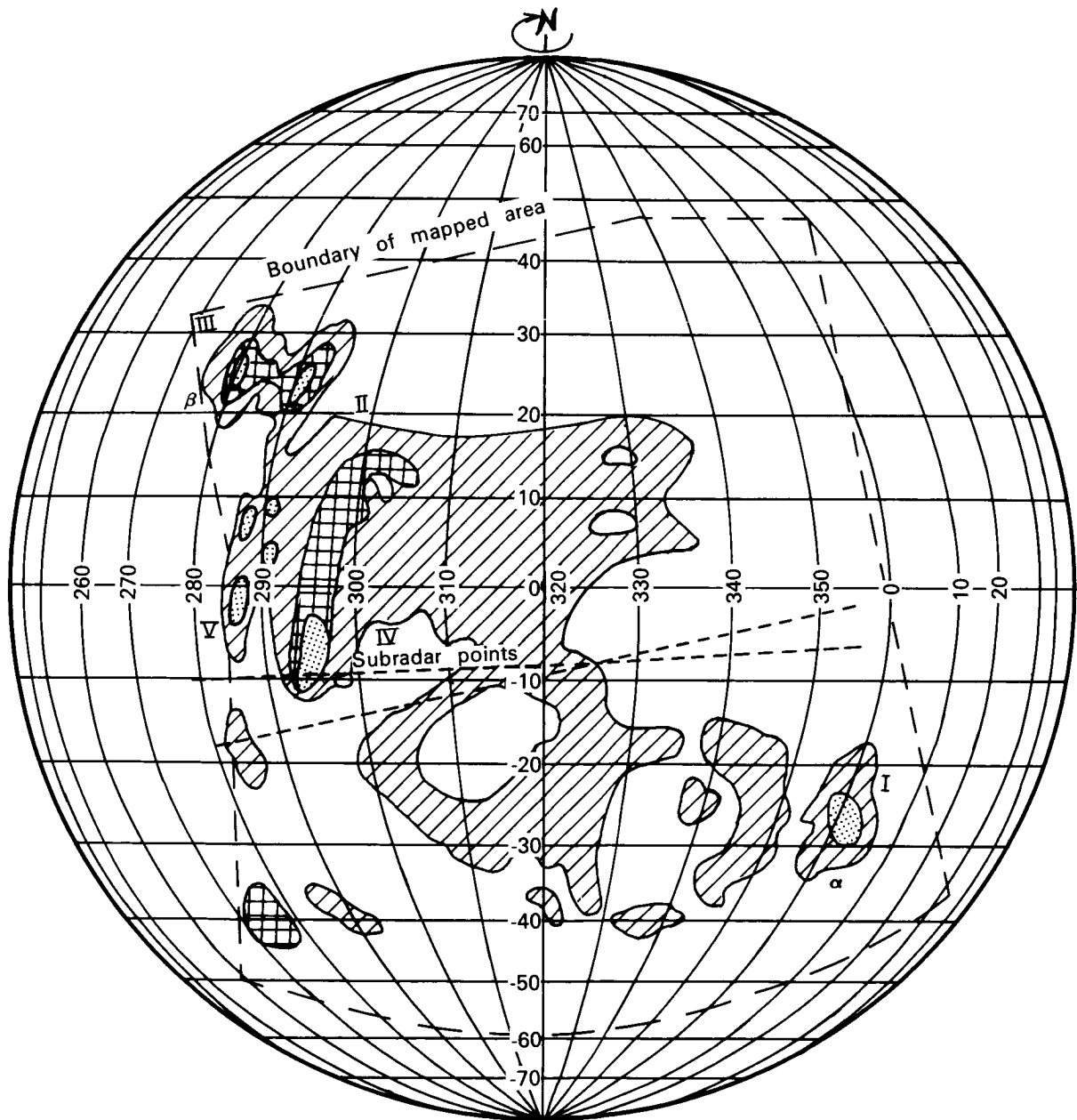


FIGURE 4.—Map of reflective properties of the Venus surface.

means that the surface layer of the planet in the descent region of Venera 8 is rather loose and, most probably, consists of crushed rock. Its density is about  $1.5 \text{ g/cm}^3$  [3]. The analyses of the Venusian surface rock by Vinogradov et al [246] with the gamma spectrometer installed on Venera 8 are of tremendous significance for our understanding of the geology of Venus. Preliminary study of the spectrum and the summary intensity of gamma radiation created by the natural radioactive elements contained in the surface layer (U, Th, K) indicates that the material of the Venusian surface in the area of the spacecraft landing contained 4% K, 0.0002% U, and 0.00065% Th. The content of these elements and their ratio indicate that the material of the surface is similar in composition to the granites common on Earth.

### Atmosphere of Venus

The dense, almost uninterrupted cloud layer of Venus generally prevents observation of its surface in the visible area of the spectrum. However, observations in the visible and particularly in the IR range, which have become possible due to advances in IR spectrophotometry, have yielded information on the atmosphere of this planet. The presence of  $\text{CO}_2$ ,  $\text{H}_2\text{O}$ , CO, HF, and HCl in the Venusian atmosphere has been recorded. Estimates have been made of possible impurities content in the upper limits and of the temperature and pressure near the cloud boundary visible from the Earth [158]. However, even with the resolution of  $0.1 \text{ \AA}$  achieved in the near IR area of the spectrum, these measurements indicated only the relative contents of individual gases, and have not answered the question of the Venusian atmosphere's primary composition.

Determination of the absolute concentrations of components and the possibility of extrapolation of temperature and pressure values at the tops of the clouds into the atmosphere beneath the clouds is hindered by the uncertainty regarding the optical properties of the cloud layer. The clouds significantly influence estimates of the effective formation depth of the absorption lines and the processes of radiation transfer, while the various

characteristics of scattering, and the spectrum of particle dimensions and their nature, allow the parameters of reflection from the cloud layer to vary over a broad range; at the same time, the cloud boundary itself is not sharp. As a result, estimates of parameters of the atmosphere at the level of the clouds depend on selection of an idealized model. Optical measurements, naturally, cannot answer questions on the properties of the atmosphere beneath the clouds or the temperature and pressure at the planet's surface.

Radio astronomy measurements, developed intensively since the late 1950s, unexpectedly detected a surprisingly high radio brightness temperature for Venus—about  $600^\circ$ – $659^\circ \text{ K}$ . The first attempt of this nature was carried out by Mayer and others [143] who measured the 3.15-cm wave  $T_{\text{eq}} = 560^\circ \pm 73^\circ \text{ K}$ . This result was later repeated many times by measurements within the centimeter and decimeter range. A detailed summary is available [114, 184].

Radio brightness temperature was several times higher than those of the Earth and Mars, which correspond approximately to the mean surface temperatures of these planets. At first it was assumed that the surface of Venus, which radiates intensively at centimeter wavelengths, for which the atmosphere is almost transparent, was actually heated to this temperature. In this case, however, such attractive and popular hypotheses as the existence of oceans and luxurious vegetation on the planet would have to be abandoned, which was difficult even from the purely psychological standpoint. Attempts were made to make the observed microwave spectrum agree with the idea of a moderate climate on Venus. Hypotheses were set forth of a superdense ionosphere, of glowing electrical discharges in the atmosphere, of generation of radiation by movement of electrons in a magnetic field and other mechanisms, each of which could be a source of nonthermal radio radiation or a hot atmosphere. Further analysis indicated these mechanisms were inadequate to explain the available experimental data. Nevertheless, the question of the source of the high radio brightness temperature and, consequently, of the temperature of the atmosphere and surface of Venus remained unanswered.

Still greater uncertainty existed in estimates of the pressure at the surface of the planet. With the known chemical composition of the atmosphere, even assuming that the surface of Venus was hot, values from a few atm to several hundred atm were proposed. There was no information on the nature of temperature change below the clouds, or on the depth of the atmosphere. Spacecraft were called upon to answer these fundamental questions. One of the most important results of the Venera spaceflights was direct determination of the chemical composition of the atmosphere [245]. The Venera 4, 5, and 6 spacecraft were equipped with simple gas analyzers and amplitude and threshold methods were used to estimate the content of CO<sub>2</sub>, N<sub>2</sub>, O<sub>2</sub>, and H<sub>2</sub>O vapor. A coloristic method was used by Venera 8 to determine the NH<sub>3</sub> content [3]. Measurements were performed at several levels at pressures of 0.6, 2, and 10 atm. In contrast to earlier beliefs that the atmosphere was predominantly N<sub>2</sub>, it was found to consist almost entirely (93%–100%) of CO<sub>2</sub>, while the volumetric content of N<sub>2</sub> (if it is present at all) is not over 2%. The Venusian atmosphere contains less than 0.1% O<sub>2</sub>; H<sub>2</sub>O vapor near the cloud layer amounts to not over 0.1%–1.0% and the NH<sub>3</sub> content is 0.01%–0.1%.

Terrestrial spectroscopy indicates lower upper limits for the content of O<sub>2</sub>, H<sub>2</sub>O vapor and NH<sub>3</sub> (10<sup>-3</sup>%, 10<sup>-3</sup>%, and 10<sup>-5</sup>% respectively). For O<sub>2</sub>, this result agrees with the threshold estimate of the gas analyzers, but for H<sub>2</sub>O and NH<sub>3</sub>, the different levels of the atmosphere to which the direct and spectroscopic measurements relate, and the possibility of "precipitation" of H<sub>2</sub>O vapor and ammonium salts must be considered due to condensation. Probably, the upper spectroscopic estimates are correct for the atmosphere above the cloud layer. The maximum estimate is yielded by analysis of the microwave spectrum of Venus. The absence of any notable attenuation in the intensity of emissions near the line of resonance absorption of H<sub>2</sub>O vapor ( $\lambda = 1.35$  cm) can be interpreted as an indication that the maximum content of H<sub>2</sub>O is not over 0.1%. The most probable chemical composition of the Venusian atmosphere corresponds to a value of mean molecular weight  $\mu_m = 43.3$ . The chem-

ical composition of the Venusian atmosphere, compiled from results of all measurements, is presented in Table 3.

To measure temperature and pressure, Venera 4–8 carried simple, reliable instruments for measurement of the heat-physical parameters of a dense gas with resistance thermometers and membrane (aneroid) manometers [8, 9, 138, 139, 140] (Fig. 5). The altitude profile of temperature on the sunlit side measured by Venera 8 was quite similar to the results of earlier measurements in the night atmosphere by Venera 7 and 8 (747° ± 20° and 734° ± 8° K respectively).

Radioastronomy measurements taken within a 10-cm range of wavelengths in which the atmosphere of Venus is most transparent (radio irradiation is basically surface irradiation), and in which fairly accurate radioastronomy measurements were made, shows that, given the value of dielectric permittivity of  $\epsilon = 5$ , the average surface temperature on the night side of the planet was  $T_n = 720^\circ \pm 30^\circ$  K. Corrected for measurement errors, this value coincides with the results of direct measurements.

The pressure at the surface, measured by Venera 7, was 90 ± 15 kg/cm<sup>2</sup>. At the point of landing of Venera 8, the pressure was 93 ± 1.5 kg/cm<sup>2</sup>. The altitude variations in pressure in the Venusian atmosphere are also shown in Figure 5. In the areas which they both surveyed (from 300° to 440° K in temperature and 0.6 to 7 kg/cm<sup>2</sup> in pressure), the measurements of the Venera spacecraft and the data of Mariner 5 and 10 generated by the radio refraction method as the spacecraft went behind the planet [58] are in good agreement. The probing field on Mariner 10 was somewhat smaller, up to 40 km at a frequency of 2295 MHz and up to 51 km at a frequency of 8115 MHz. Comparison with the data of Mariner 5, when related to the distance to the gravitational center of the planet, indicates that the regions of landing of Venera 7 and 8 correspond to a planetocentric distance  $r = 6051$ –6052 km. These local values agree well with available data on the mean radius of Venus, calculated from radar measurements.

Figure 5 shows that the experimental profiles of atmospheric parameters determined from the measurements of Mariner 5 cover the altitude

interval between 35 and 90 km. Also shown are the calculated curves  $T(h)$ , produced in the approximation of radiant equilibrium for a "gray" stratosphere [136], and according to the stricter recent measurements of Dickenson [41]. These latter measurements take into account the effect of heating of the atmosphere between the 65 and 115 km level by absorption of solar radiation in the near IR area of the spectrum and the refined characteristics of

cooling due to radiation in the fundamental 15- $\mu\text{m}$  band of CO<sub>2</sub>. The resulting equilibrium temperature profile (*dot-dash line*) indicates a drop in temperature from 250°K at an altitude of 66 km to approximately  $T_m \approx 160^\circ\text{K}$  near 90 km, which agrees closely with the experimental curve, the ambiguity and inversion nature of which in the area of the beginning of measurements by Mariner 5 (Fig. 5) are determined by selection of boundary conditions for integra-

TABLE 3.—*Chemical Composition of the Atmosphere of Venus and Upper Limits of Possible Impurities*

Component	Relative content	Method of determination	References	Note
CO <sub>2</sub>	0.97 <sup>+0.03</sup> —0.04	Venera 4, 5, 6	[245]	
N <sub>2</sub> (including inert gases)	2.10 <sup>-2</sup>	"	"	
H <sub>2</sub> O	(0.6–1.1) · 10 <sup>-2</sup>	"	"	
H <sub>2</sub> O	(0.4–2) · 10 <sup>-3</sup>	Radio-astronomy	[91]	
H <sub>2</sub> O	≈ 7.10 <sup>-5</sup>	Spectroscopy	[112]	
O <sub>2</sub>	< 10 <sup>-3</sup>	Venera 5, 6	[245]	
O <sub>2</sub>	< 10 <sup>-5</sup>	Spectroscopy	( <sup>1</sup> )	
CO	(1–3) · 10 <sup>-5</sup>	"	[28]	
HCl	2.10 <sup>-7</sup>	"	[27]	
HCl	< 10 <sup>-6</sup>	OAO	[176]	With 1 atm-km CO <sub>2</sub>
HF	(1–3) · 10 <sup>-9</sup>	Spectroscopy	[27]	
CH <sub>4</sub>	< 10 <sup>-6</sup>	"	"	
CH <sub>3</sub> Cl	< 10 <sup>-6</sup>	"	"	
CH <sub>3</sub> F	< 10 <sup>-6</sup>	"	"	
C <sub>2</sub> H <sub>2</sub>	< 10 <sup>-6</sup>	"	"	
HCN	< 10 <sup>-6</sup>	"	"	
O <sub>3</sub>	< 10 <sup>-8</sup>	Spectroscopy	[92]	
O <sub>3</sub>	< 3.10 <sup>-9</sup>	OAO	[176]	With 1 atm-km CO <sub>2</sub>
SO <sub>2</sub>	< 3.10 <sup>-8</sup>	Spectroscopy	[33]	
SO <sub>2</sub>	< 10 <sup>-8</sup>	OAO	[176]	"
COS	< 10 <sup>-6</sup>	Spectroscopy	[31]	
COS	< 10 <sup>-8</sup>	"	[112]	
COS	< 10 <sup>-7</sup>	OAO	[176]	"
C <sub>3</sub> O <sub>2</sub>	< 5.10 <sup>-7</sup>	Spectroscopy	[111]	
C <sub>3</sub> O <sub>2</sub>	< 10 <sup>-7</sup>	OAO	[176]	"
H <sub>2</sub> S	< 2.10 <sup>-4</sup>	Spectroscopy	[31]	
H <sub>2</sub> S	< 10 <sup>-7</sup>	OAO	[176]	"
NH <sub>3</sub>	< 3.10 <sup>-8</sup>	Spectroscopy	[112]	
NH <sub>3</sub>	10 <sup>-4</sup> –10 <sup>-3</sup>	Venera 8	[3]	Where P = 2–10 kg/cm <sup>2</sup>
NH <sub>3</sub>	< 10 <sup>-7</sup>	OAO	[176]	With 1 atm-km CO <sub>2</sub>
NH <sub>3</sub>	< 10 <sup>-5</sup>	Radio-astronomy	[115]	
NO	< 10 <sup>-6</sup>	OAO	[176]	"
NO <sub>2</sub>	< 10 <sup>-8</sup>	"	[176]	"
N <sub>2</sub> O <sub>4</sub>	< 4.10 <sup>-8</sup>	"	"	"
HCHO	< 10 <sup>-6</sup>	"	[176]	"
CH <sub>3</sub> CHO and higher order aldehydes	< 10 <sup>-6</sup>	"	"	"
CH <sub>3</sub> COCH <sub>3</sub> and higher order ketones	< 10 <sup>-6</sup>	"	"	"

<sup>1</sup> Belton, M. J. S., D. M. Hunten, and M. B. McElroy. A search for an atmosphere on Mercury. *Astrophys. J.* 150:1111, 1967.

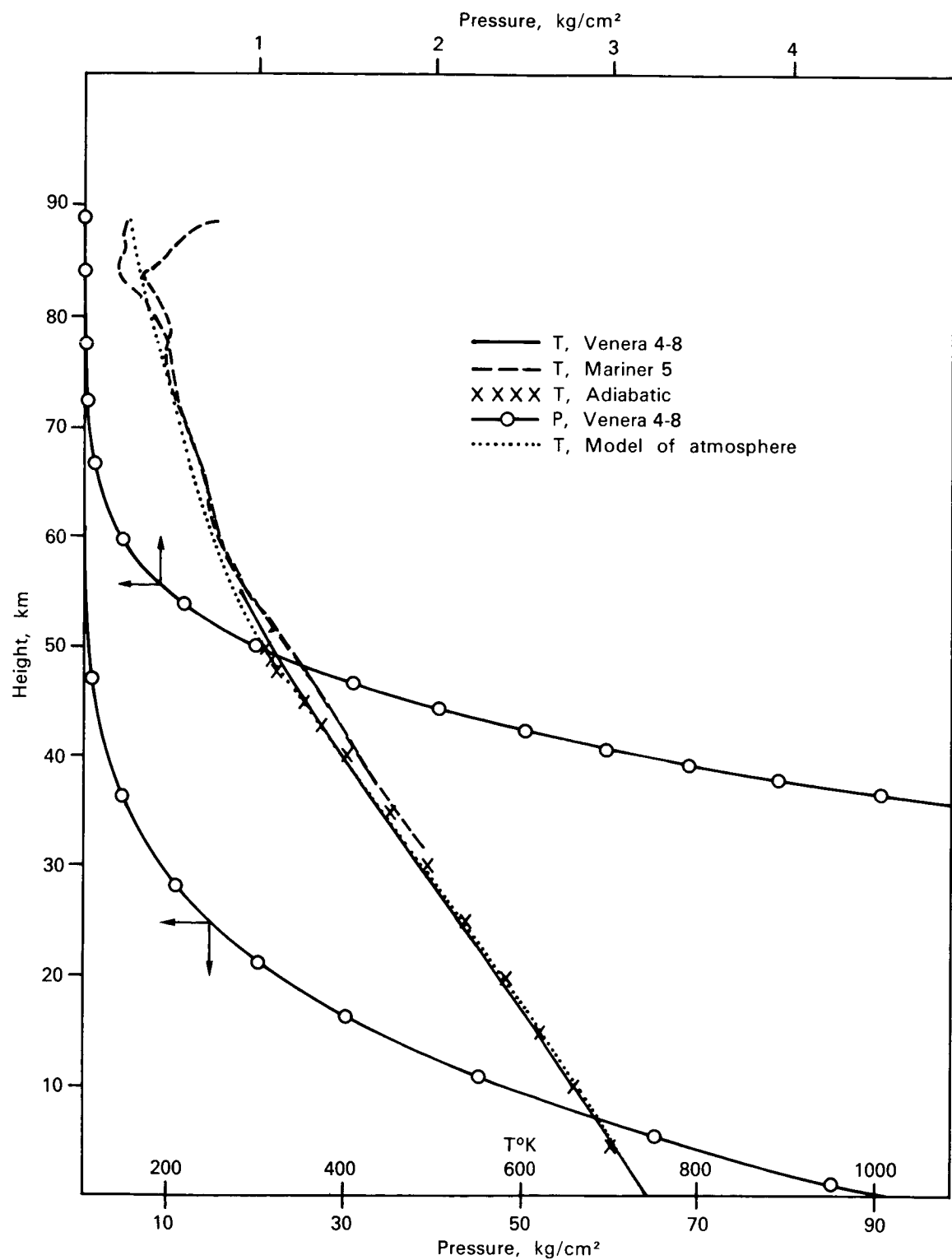


FIGURE 5.—Altitude profiles of temperature and pressure in the atmosphere of Venus according to Venera 4-8 and Mariner 5.

tion of the dependence of index of refraction of height selected.

In contrast to the simple approximation of radiant equilibrium, leading to a minimum temperature value of about  $195^{\circ}$  K at an altitude of 105 km, according to the calculations of [41], a second temperature minimum  $T \approx 180^{\circ}$  K is reached at about the 120-km level, with a slight peak in the area between at  $T \approx 190^{\circ}$  K. An additional criterion for determination of the altitude distribution of atmospheric parameters in the area from approximately 60 to 120 km, which by analogy with the Earth can be called the stratosphere, is the estimate of the atmospheric density and gradient of its change, based on results of photometric measurements of attenuation of the radiation from Regulus ( $\alpha$  Leo) as it was occluded by Venus in 1959 [241]. The characteristics produced at the level of eclipse ( $h_R = 120$  km) place a definite boundary condition on the rate of decrease in temperature (scale of altitudes) in the area beneath that level, determining the intensity of "settling" of the atmosphere.

The  $T(h)$  profile below 60 km corresponds in general to the distribution of temperature in the atmosphere with convective equilibrium. The temperature gradient, within the limits of possible measurement errors of  $T$  and  $h$ , is near the mean adiabatic gradient ( $dT/dh$ )  $\approx 8.6^{\circ}$   $\text{km}^{-1}$ . A thermodynamic analysis of the measurement curves of the gas state in the atmosphere of Venus at the corresponding temperature and pressure confirms this conclusion. However, certain peculiarities in the gas state, particularly in the 15–37-km area, are indicated by the analysis of the radio refraction profiles and microwave losses produced from measurements of Mariner 5 [58]. Below 40 km, according to measurements of densimeters carried on Venera 4 and 5, significant deviations were also observed from monotonic density change [137].

The observed value of microwave weakening cannot be explained by absorption of the  $\text{CO}_2$  and  $\text{H}_2\text{O}$  mixture. These losses measure  $\sim 10^{-3}$  dB/km at a level of 37 km for each of these components, i.e., two to three times less than is required for coordinating them with the data of Mariner 5 (Fig. 6) [58]. However, the microwave

spectrum, according to ground radio measurements, generally agrees with the model of the atmosphere with surface pressure of 80–100 atm, consisting of  $\text{CO}_2$  with a concentration of  $\text{H}_2\text{O} \sim 10^{-3}$  [184]. To explain these special features in the spectrum, it can be assumed that additional admixtures exist whose height distribution is accompanied by phase transitions which cause them to be located at certain levels. Relatively small concentrations of admixtures, especially in the liquid or solid states (which do not affect the molecular weight and, therefore, do not show up in pressure measurements) could, by their structural characteristics, also influence the readings of densimeters.

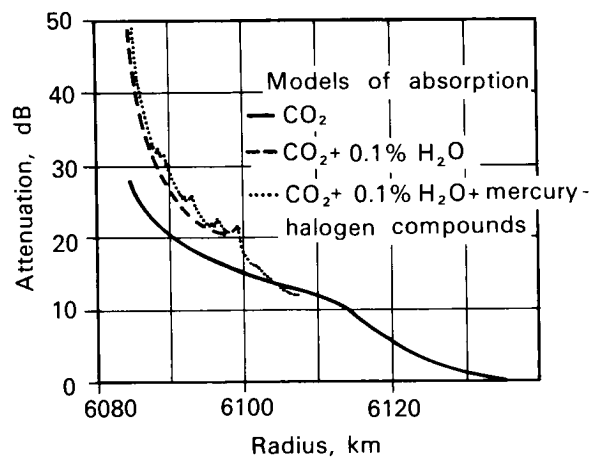


FIGURE 6.—Attenuation nature of radio signals in the atmosphere of Venus compared with approximating models.

### Clouds

The problem of Venus clouds must be approached by assuming the existence of different admixtures in the atmosphere. There is no agreement about the structure and nature of the clouds at present. The basic sources of information are the optical characteristics of the planet, observed from Earth (Fig. 7a) which relate to the upper part of the visible cloud layer (Fig. 7b). On the basis of these observations, assessments of the average size of cloud particles ( $\sim 1.1 \mu\text{m}$ ), the reflection characteristics (albedo) in various spectrum fields, the refraction indicator, the coefficient of volumetric scattering, and other data were derived [89, 137, 159].

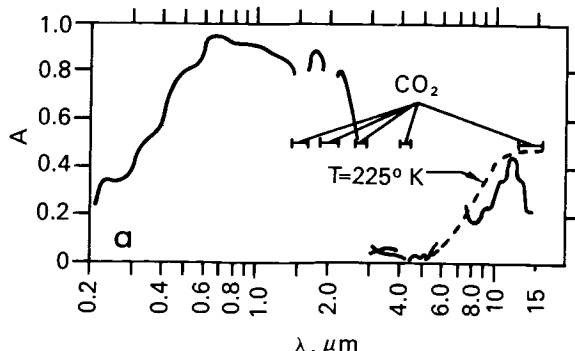


FIGURE 7a.—Basic reflective and emission characteristics of Venus.

The optical characteristics, combined with data on the altitude profiles of temperature and pressure, however, can give no information about the chemical nature of the Venusian clouds. In principle, a stratified cloud structure that includes various components cannot be excluded. Given the surface temperature of Venus (about 750° K), many components could pass from the lithosphere to the atmosphere and exist as vapors and condensates at various levels. Possible geochemical equilibrium reactions for the lithosphere-atmosphere system were discussed in detail by Lewis [122, 123], who studied conditions related to the formation of mercury-halogen clouds in the atmosphere which condense at temperatures of 250° K ( $HgCl_2$ ) to 450° K ( $Hg_2I_2$ ). Rasool [192] indicated the possible depth of such clouds on the basis of analysis of weakening radio signals from Mariner 5. It was also assumed that ammonium compounds exist which sublime at  $T > 330^{\circ}K$ , but form bonds with carbonic acid, water, hydrogen chloride and other gases at higher levels in the atmosphere of Venus [234].

The most attractive assumption is that Venus has water-ice clouds. This is based on the measurements by the Venera spacecraft, which indicate a rather high moisture content of the upper portion of the planet's troposphere. Water clouds (probably including solutions of certain salts, also true for terrestrial clouds) could exist regardless of the presence of condensates of other substances. With an  $H_2O$  concentration of about 1%, the lower boundary of such clouds should be at 59 km; the effective thickness of the

cloud layer then would be about 10–15 km. However, when the concentration of  $H_2O$  is less than 0.1%, the level at which condensation begins should be at 68 km. With  $T_m \approx 160^{\circ} K$ , sublimation would continue up to about 110 km (Fig. 8).

The strongest arguments against  $H_2O$  clouds include: (1) absence of depressions at 1.5 and 2  $\mu m$  that are characteristic for ice, (2) the excessive divergence in the index of refraction (polarimetric observations of Venus indicate  $\eta = 1.45$ , while for ice  $\eta = 1.31$ ), the slight transparency of the clouds for waves of  $\lambda > 0.6 \mu m$ , and (3) the low concentration of water vapor as indicated by spectroscopic data at the level of formation of  $H_2O$  bands by which the brightness temperature of the planet  $T_b = 240 \pm 10^{\circ} KV$  is measured [78, 186, 207].

In the light of the available spectroscopic and polarimetric data, the presence of many previously assumed compounds such as  $C_3O_2$ ,  $SiO_2$ , carbohydrates and various chlorides such as  $FeCl_2$ ,  $NaCl$ ,  $NH_4Cl$  can no longer be considered [112, 156]. Lewis assumed cloud formation by an HCl-in-water solution compared with its relatively low content in a gas environment [124]. The basis of his theory is that a 6 M (25%) HCl solution in clouds corresponds to the stage of equilibrium of  $H_2O$  and HCl according to spectroscopic data. It is favorable that the refractive index of an HCl-in-water solution increases with decreasing temperature, coming close to the measured value at the upper border of the clouds of Venus. This condition, however, is achieved at  $T < 200^{\circ} K$  which is considerably different from  $T_0 \approx 240^{\circ} K$ . An interesting recent hypothesis, independently put forth by Young [249] and Sill [219], concerns cloud formation by a concentrated water solution (on the order of 75%–80%) of sulfuric acid. This hypothesis avoids the serious difficulty of coordinating assessments of the water vapor content at the formation level of spectral lines ( $pH_2O \leq 10^{-5}$  mbar) with the results of direct measurements of the absolute humidity in the lower atmosphere. This is caused by the remarkable drying properties of  $H_2SO_4$ . The special reflection features (albedo) of Venus in the spectrum field close to the IFR, especially the characteristic depression between 3 and 4  $\mu m$  and the emission spectrum in the field 8–13

$\mu\text{m}$  (Fig. 7), are in satisfactory agreement with this assumption. As far as the depressions at  $\lambda\lambda 1.4; 1.6; 2.0$ ; and  $2.8 \mu\text{m}$  are concerned, they must obviously be attributed to the absorption of  $\text{CO}_2$  [183]. The refractive index of a 75%  $\text{H}_2\text{SO}_4$  solution corresponds precisely to the indicator measured for Venus. The assumed liquid-drop state of clouds at a temperature of about  $-30^\circ \text{C}$  and the extremely low content of sulfur compounds can be explained by the data of ground spectrometry (Table 3), also testified to by polarimetry measurements [124]. This fact does not agree with the cosmic distribution of sulfur and its evolution from the planet's depths due to volcanic exhalations.

According to the assessments of Young [249], the observed optical characteristics of clouds—visible from Earth within limits of one optical thickness  $\tau \approx 1$ —are supported by the comparatively thin layer of a 75%  $\text{H}_2\text{SO}_4$  solution at a pressure of  $P \sim 50 \text{ mbar}$  (a homogeneous layer of drops with a diameter of  $2.2 \mu\text{m}$ ). In this case, the necessary acid concentration would amount to  $0.29 \text{ mg/cm}^2$ , or to  $2.3 \cdot 10^{-6}$  based on the  $\text{CO}_2$  content. However, if it is assumed that the weight ratios of  $\text{H}_2\text{O}$  and  $\text{H}_2\text{SO}_4$  remain constant below the level of visible clouds, and that 99% of the water at this level is bonded by sulfuric acid, then, given  $p\text{H}_2\text{O} \sim 10^{-3} \text{ mbar}$ , the  $p\text{H}_2\text{SO}_4$  content would be approximately three orders higher. The

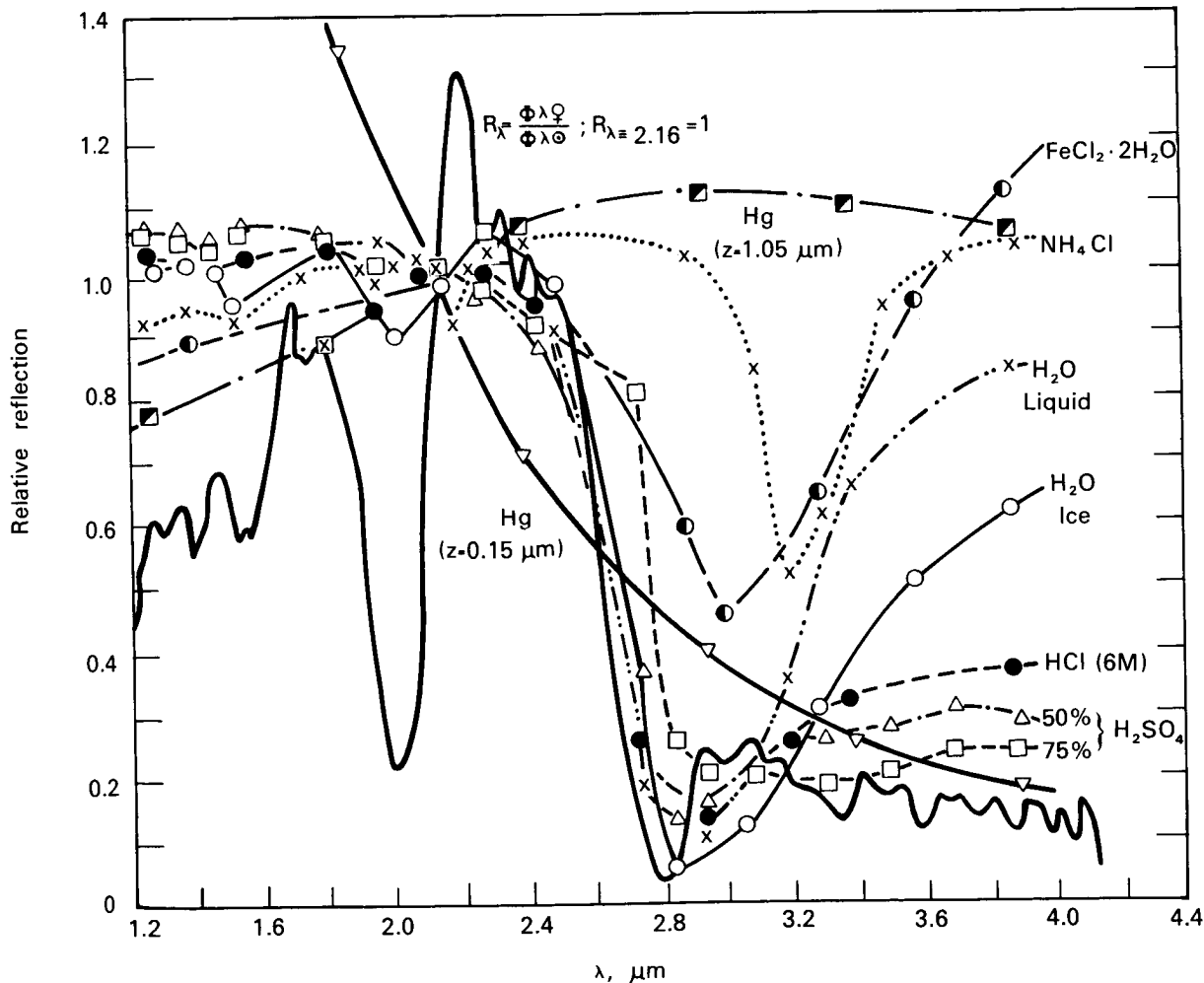


FIGURE 7b.—Spectrum of Venus on a close infrared field in comparison with laboratory spectra of a number of compounds assumed to exist in Venus clouds.

indefiniteness in this case is connected with scattering while measuring the degree of precipitation which depends on the mixing intensity.

The water content in an extended cloud must increase with depth through release of bonded water from drops of solution at increased temperatures. This will bring about a change in the concentration of the  $\text{H}_2\text{SO}_4$  solution. The extension of clouds, in its turn, depends on the total water content in the atmosphere.

Young [249], proceeding from assessments of the equilibrium ratio between the gas stage and cloud drops at various levels in the atmosphere (given the constancy of weight fractions of  $\text{H}_2\text{SO}_4$  and  $\text{H}_2\text{O}$  at each level), found that, given  $p_{\text{H}_2\text{O}} \approx 10^{-3}$  mbar (to which a 75%  $\text{H}_2\text{SO}_4$  solution corresponds at a level with a temperature  $T = 273^\circ \text{ K}$ ), clouds could extend up to the boiling point, where  $T = 533^\circ \text{ K}$  and  $P = 14$  atm ( $h \approx 26$  km) and the solution con-

centration of  $\text{H}_2\text{SO}_4$  reaches  $\sim 98.3\%$ . If, however,  $p_{\text{H}_2\text{O}} \approx 10^{-5}$  mbar, then the initial concentration of the  $\text{H}_2\text{SO}_4$  solution must be higher (not less than 85% at a level of  $T = 250^\circ \text{ K}$ , which is not in good agreement with polarimetry measurements) and the lower border turns out to be at the level of  $T = 373^\circ \text{ K}$  and  $P = 2.4$  atm ( $h \approx 44$  km). Finally, given  $p_{\text{H}_2\text{O}} \approx 10^{-4}$  mbar, the clouds must end at a height of  $h \approx 35$  km where a strong change is found in the character of weakening solar radiation energy with depth according to data from *Venera 8* [138].

Thus, numerous data support the  $\text{H}_2\text{SO}_4$  hypothesis, which at first glance seems rather exotic, and permit elimination of the contradictions found in other assumptions. Nevertheless, more detailed analysis of this fresh and interesting idea is required, followed by direct measurements, which will permit obtaining the

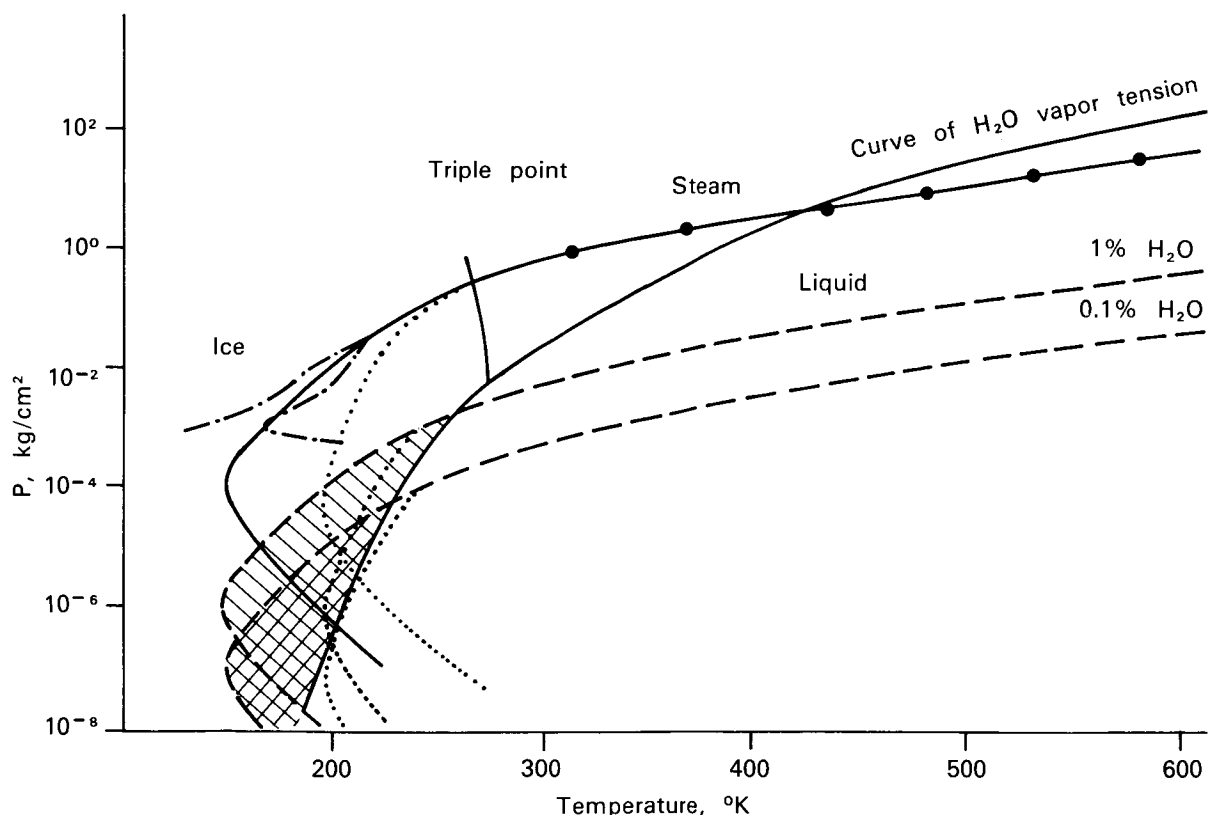


FIGURE 8.—Phase diagram of  $\text{H}_2\text{O}$  with estimates of condensation levels and extent of clouds with concentrations of  $\text{H}_2\text{O}$  at 1% and 0.1% for various atmospheric models.

best answer to the question of the nature of the Venusian clouds.

### Illumination

Whether sunlight penetrates to the surface of Venus or is fully absorbed by the dense atmosphere and clouds has been the subject of discussion for many years. The degree of trans-

parency of the atmosphere in the visible area of the spectrum will determine both conditions of illumination at the surface and the nature of high temperatures on the planet. This important question, however, has been answered only recently as a result of direct measurements below the clouds visible from the Earth. These measurements were performed by the Venera 8 automatic spacecraft using special photometric

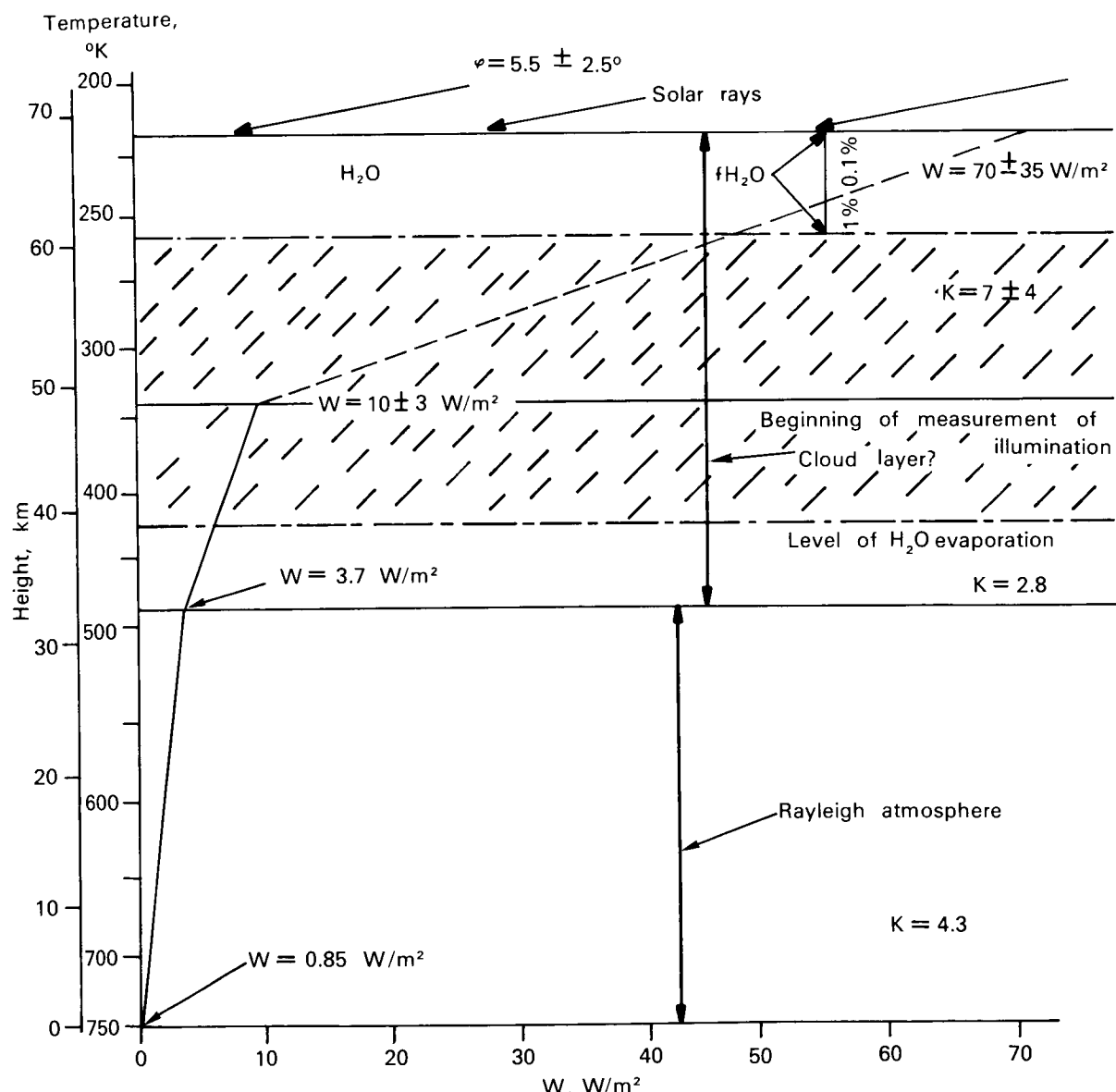


FIGURE 9.—Changes in luminance in Venus atmosphere with altitude according to Venera 8 measurements.

devices with sulfur-cadmium photoresistors as receptors. These devices retain their efficiency after extended exposure to temperatures up to 500°C and pressures up to 100 atm. The range of spectral sensitivity of the receptor is from 0.4 to 0.8 μm, with its maximum of 0.62 μm. The index of the sensor allowed it to record both direct rays at all zenith angles and diffuse radiation [7].

The results of the measurements, performed with a zenith angle of the Sun at the point of landing of  $84.5^\circ \pm 2.5^\circ$ , are in Figure 9, showing the nature of attenuation of solar energy (in  $\text{W}/\text{m}^2$ ) in the atmosphere of Venus from an altitude of about 50 km to the surface. The nature of attenuation of the radiant flux is uneven with altitude. From the upper boundary of the visible clouds (about 70 km) to the level of beginning of measurements, light is attenuated by a factor of approximately 7, while between 50 and 35 km it is attenuated by an additional factor of approximately 3, followed by an additional attenuation factor of approximately 4 in the layer below 35 km. This means that, as the physical density of the atmosphere increases, its optical density decreases. The break in the curve near  $35 \pm 3$  km is quite characteristic. The attenuation of light from this altitude to the surface is explained by molecular (Rayleigh) scattering in a carbon dioxide atmosphere at the ambient pressure. Above 35 km, the presence of aerosol scattering or significant true absorption must be assumed in order to explain the nature of the attenuation. The models calculated under these two assumptions are satisfied with high values of optical thickness  $\tau_0 \approx 50$  and unit scattering albedo  $\omega \approx 1$ , respectively, or for  $\tau_0 \approx \tau_{\text{ray}} = 3.5$  and  $\omega_0 \approx 0.9$ . Consideration of the degree of elongation of the scattering indices has a certain influence on these estimates [129].

Optical measurements in the atmosphere have given additional information on the structure of the clouds on Venus. The significant attenuation of light down to 35 km can be interpreted to mean that the cloud cover extends down to this level. However, the level of the beginning of condensation of  $\text{H}_2\text{O}$ , it has been noted, is almost 25 km higher. This inconsistency can be explained if the possibility is recalled of existence of phase

transitions, in particular of mercury-halide clouds. The boundary of  $\text{HgS}$  clouds in this case would fall at an altitude of about 35 km. Another possibility is the existence of liquid-drop water (precipitation of "rain") approximately down to this level (*dot-dash line*, Fig. 7b), near which the water-steam phase conversion would occur at the corresponding  $P$  and  $T$  [7]. Finally, as mentioned earlier, 35 km is the "boiling" level of a concentrated solution of sulfuric acid for a model with a relatively small content of water vapor in the atmosphere ( $p\text{H}_2\text{O} \approx 10^{-4}$  mbar). It can then be assumed, that within the framework of the  $\text{H}_2\text{SO}_4$  hypothesis, there is a homogeneous cloud layer with a thickness of the order 30–35 km.

If slight deformation of the spectrum composition of solar radiation upon penetration through the atmospheric mass is assumed, the conversion from the measured radiant energy to values of illumination can be performed using the conversion factor  $\zeta \approx 350 \text{ lx}/\text{W} \cdot \text{m}^{-2}$ , determined from the results of calibration. In this case, the expected surface illumination at the point of landing should be about 300 lx, or at zero solar zenith angle—over 3000 lx. Thus, although only about 1% of the light flux striking Venus reaches the surface, this would create significant illumination (approximately the same as an extremely cloudy day on Earth). The light reaching the surface is repeatedly scattered and is diffuse. It is difficult as yet to estimate reliably the range of visibility under such conditions or the color characteristics. These characteristics are of both physical and practical interest, particularly because of possible curious effects resulting from the strong refraction of light rays in such a dense gas. If the atmosphere is sufficiently transparent, the horizon would seem elevated in all directions, and an observer on the surface would have the illusion of standing in the bottom of a giant bowl.

### Thermal Mode

The data from measurements of the solar radiant energy in the Venus atmosphere, and calculations of radiation loss and transfer, confirm the hypothesis (Sagan [201]) that the high temperature at the surface of the planet is

most probably due to the greenhouse effect. The physical basis of this mechanism is simple. Visible solar light, only partially absorbed by the atmosphere and clouds, reaches and heats the surface of the planet; the heated surface radiates longer IR waves that are retained by the dense Venusian atmosphere.

A similar mechanism, more strongly expressed, operates in the terrestrial atmosphere and is widely used in greenhouses, which also prevents convective heat transfer. Calculations of Marov and Shari [142] and Shari [214] have shown that even if a slight portion of the solar radiation reaches the surface of Venus, carbon dioxide gas along with a small quantity of water vapor ( $p_{H_2O} \approx 5 \cdot 10^{-5} - 10^{-4}$ ) would create a strong screening effect for departing thermal radiation (Fig. 10). With increasing temperature and pressure, the degree of screening increases. The conditions on the planet apparently developed as a result of gradual self-heating and now correspond to an equilibrium state. Obviously, this is not only a temperature equilibrium, but also a geochemical equilibrium, which corresponds to the measured content of  $CO_2$  gas and atmospheric pressure. Possibly the Venusian clouds, reflecting a certain portion of the departing radiation back from their lower boundary, also influence the distribution of the field of thermal radiation in the atmosphere.

The heat fluxes for measured atmospheric parameters of Venus change significantly with altitude (Fig. 10) [142]. Near the surface, the gas retains radiation so strongly that the surface makes practically no contribution to the departing heat flux. Radiant equilibrium is apparently achieved only near 40–50 km. The thermal balance at lower altitudes can be provided only by additional heat transfer. Since the measured temperature profile is near adiabatic, most probably this additional heat transfer mechanism is convection.

Studies of the convective activity in the atmosphere of Venus have indicated that the rate of convection in the lower layers of the atmosphere of Venus is probably less than 0.05–0.2 m/s [10]. This agrees with estimates produced independently by calculation of the vertical currents using equations relating the

aerodynamics of the parachute descent of the Venera spacecraft to measured values of  $P$  and  $T$ . It should be noted that in this case convection can reach higher areas of the atmosphere, so that the convective zone becomes greater than the area of atmospheric instability. Although models have been constructed only for an area limited to approximately 40 km alt, it can be assumed that convective transfer is effective throughout the entire troposphere and, in particular, that it is important in forming the structure of Venusian clouds.

The Venusian atmosphere, because of its tremendous heat content, should have great thermal inertia, so that the difference between the day and night sides is very slight; the maximum diurnal variation at the surface is less than 1°. Temperature measurements by the Venera 8 spacecraft on the sunlit side confirm these theoretical assumptions. Equalization of temperature throughout the day, also between the equatorial and polar areas, is confirmed by recent measurements of the brightness temperature of the planet by terrestrial radiointerferometry at wavelengths of 11 and 13 cm, relating to the surface and the lower atmosphere respectively [59, 220]. According to these results, there is no significant phase ( $\Delta t_f < 12^\circ \pm 6^\circ$ ) or latitude ( $\Delta T_1 < 18^\circ \pm 9^\circ K$ ) change in temperature across the disk of Venus. The IR brightness temperature also is essentially independent of phase. Averaging over the disk yields  $T_b = 220^\circ \pm 10^\circ K$ , in 8–14  $\mu m$  wavelength corresponding to an altitude of about 70 km; diurnal changes in temperature near this level are also practically nil [174].

### Dynamics of the Atmosphere

The dynamics of the Venusian atmosphere, particularly large-scale planetary circulation, are directly related to the problem of thermal mode of the atmosphere. One mechanism of this type is the model of deep circulation suggested by Goody and Robinson [71], until recently considered a probable mechanism for explaining heat exchange on Venus in the case of nontransparency for solar rays of the atmosphere below the clouds. Other attempts to calculate the

structure of planetary circulation and estimate theoretically the intensity of atmospheric movement have been made by methods of numerical modeling or the use of similarity relationships [69, 252]. Apparently, latitude-longitude circulation influences the thermal mode of the planet; in particular, transfer of hot, dense gas in the meridional direction should facilitate transfer of heat into the polar regions.

Measurements of the radial velocity of different portions of the parachute descent of the Venera spacecraft are of great significance for investigation of the dynamics of the Venusian atmosphere. Interesting data were yielded on the nature of horizontal motions, as well as ideas on the structure of small scale (turbulent) fields [96, 97, 98]. The results of all measurements of horizontal velocity, shown in Figure 11,<sup>9</sup> relate to local areas of descent of each spacecraft. However, due to the tremendous heat capacity of the

Venusian atmosphere and the resulting time of thermal relaxation at the surface which is on the order of  $10^{10}$  s, it can be assumed that equalization of irregularities of the thermal fields is due to large-scale motions rather than local winds. From this point of view, the data of Figure 11 can be looked upon as reflecting, to some degree, the structure of global circulation on the planet.

The rather convincing agreement of individual measurements is noteworthy, indicating stable zonal circulation in the direction corresponding to

<sup>9</sup> The geostrophic wind is the characteristic, horizontal, even straight-line movement of air characteristic for altitudes of over 1 km (in the terrestrial atmosphere), for which the pressure gradient is balanced by the Coriolis force, while the force of friction is negligible. The wind is directed along an isobar, and its velocity  $U = (1/2\omega\rho \cdot \sin \phi \Delta)(\Delta P/\Delta n)$ , where  $\omega$  is the angular velocity of rotation of the planet,  $\rho$  is the density of the gasses,  $\phi$  is the latitude of the point,  $\Delta P$  is the pressure difference, and  $\Delta n$  is the distance between corresponding isobars.

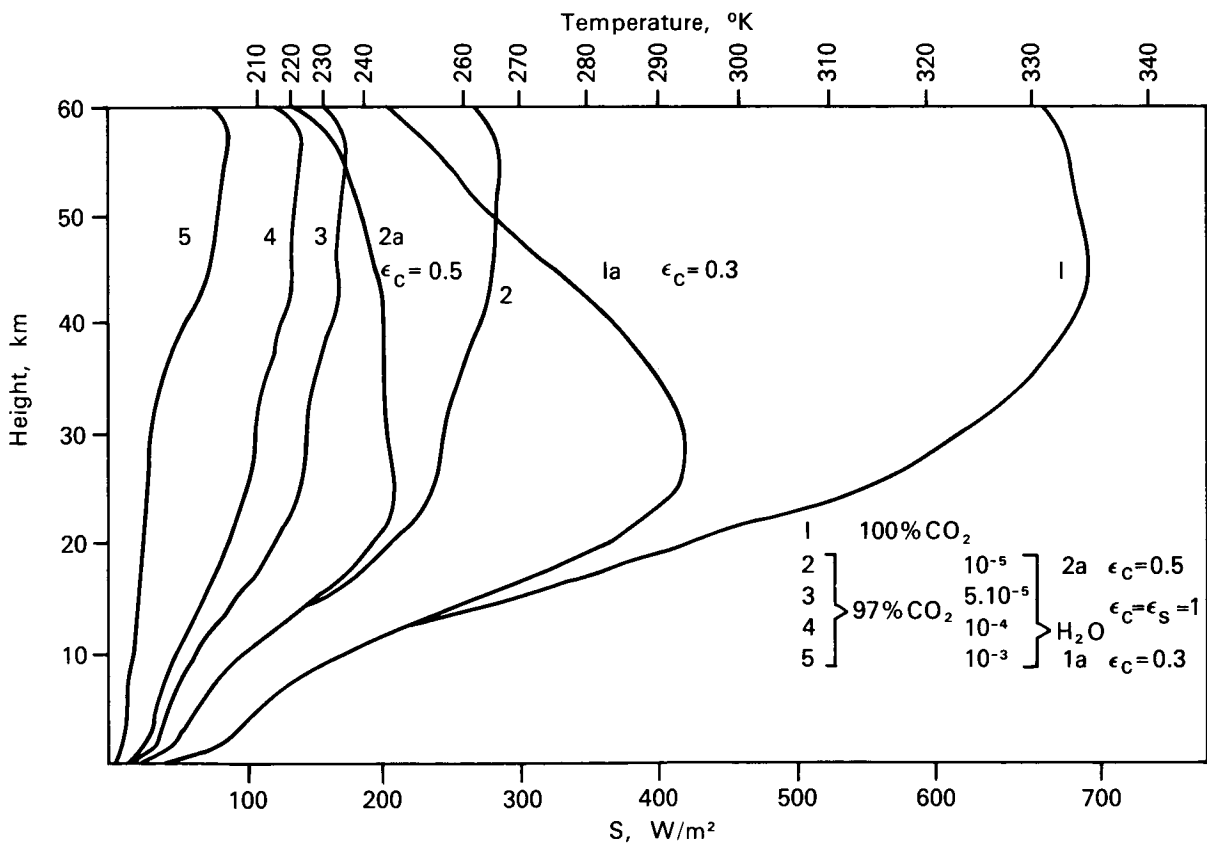


FIGURE 10.—Profiles of radiation fluxes of departing (summary) radiation under various conditions.

the natural rotation of the planet, at least above 30 km. The most complete measurements, made by Venera 8, indicated the highest wind speeds on the illuminated side to be near the morning terminator. It is evident that the horizontal component of wind velocity varies strongly with altitude: at altitudes of about 45–50 km, it reaches almost 100 m/s, decreasing to less than 1 m/s below 10–12 km. The altitude range between 18 and 30 km is interesting, since the windspeed remains almost unchanged in this range, whereas above and below this area the gradient reaches 5 m/s · km.

The low windspeeds in the surface layer of the atmosphere indicate immediately that there cannot be much dust in the atmosphere. It has been noted that this agrees with illumination measurements. At the higher altitudes, there is an inference of a direct relationship between measured windspeed and the mechanism of stratospheric circulation, manifested as drift of the so-called "ultraviolet clouds." When terrestrial observations are made in the UV area of the spectrum, individual contrasting details

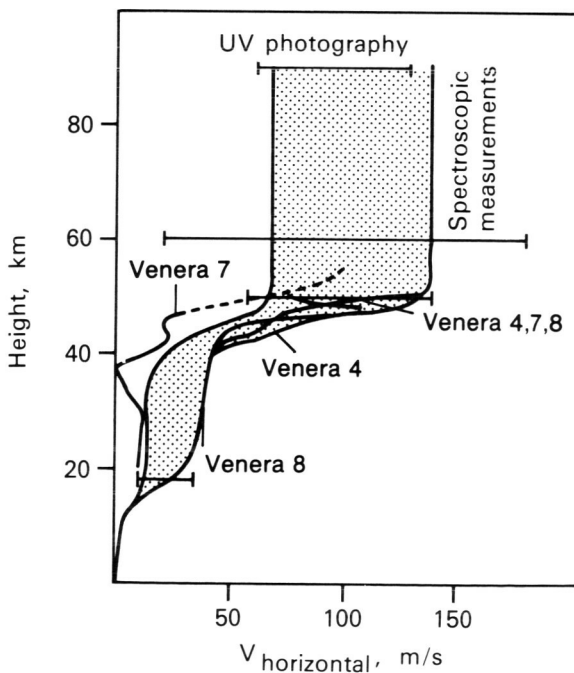


FIGURE 11.—Velocities of horizontal movements in the atmosphere of Venus according to measurements of Venera 4, 7, and 8.

are apparent which cannot be seen in the visible area of the spectrum (Fig. 12a and b). It has been established that the movement of these details across the disk of the planet is approximately 60 times more rapid than the natural rotation of the planet, which would correspond to a mean drift rate of about 100 m/s [225]. Leading rotation of the atmosphere on the Earth is noted, with a velocity ratio of not over 1.2–1.4, found only at significantly higher altitudes of 150–400 km.

The observed irregularities in the Venusian clouds in the UV range are some 25 km higher than the boundaries of the cloud cover in visible light. The periodic repetition of details apparently

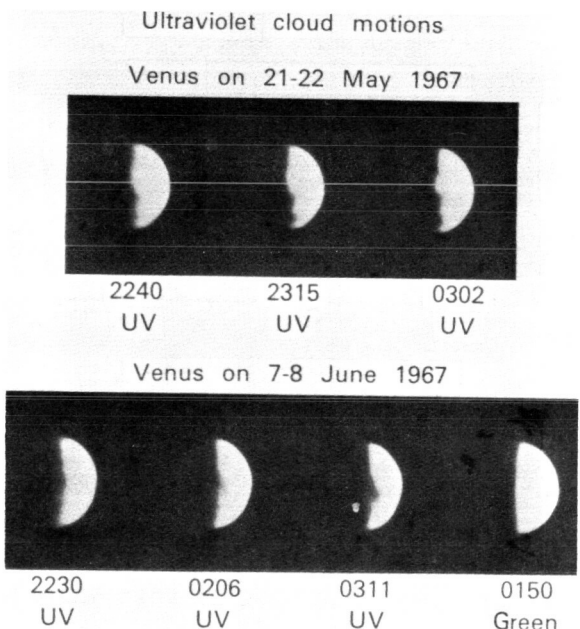


FIGURE 12a.—Photograph of Venus in UV rays (according to [225]).

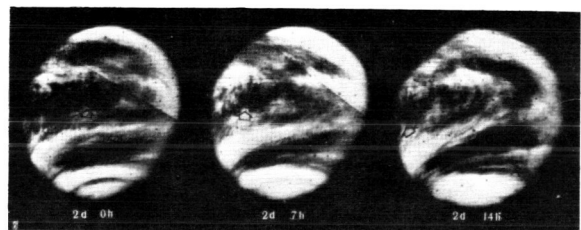


FIGURE 12b.—Contrasting details in UV area of Venus spectrum.

reflects the general nature of global circulation in the troposphere and stratosphere of Venus.

These ideas are confirmed by the photographs of the planet from Mariner 10 [171]. Successive pictures of Venus under a UV filter ( $\lambda_{\max} = 3550 \text{ \AA}$ ), with a range from 130 km to 100 m, indicate characteristic motions that are directly connected with the fields of the upper troposphere and lower stratosphere. There were also clear drift motions in the equatorial zone, reflecting a system of more stable 4-d zonal circulation, distinguished by separate belts up to 100 km wide in which increases in angular velocity were related to increases in width; also a clearly distinguishable spiral structure and lower structure at the poles (Fig. 12a). At a latitude of  $50^\circ$  the circulation appears to have a period of only about 2 d, i.e., the velocity of motion reaches 200 m/s. At lower latitudes, the meridional motions are small; there are no local large-scale vortexes resembling Earth cyclones. Adjoining in the field of the subsolar point, within the limits of several dozens of grades by longitude and latitude, these are found as symptoms of a large-scale cell convection which is preserved against the background of stable zonal motions. The interactions of these two forms of motion may cause disturbances which can be observed in the form of wave motions close to the midday meridian.

Preference for one or the other of these theoretical models is difficult at present; they are developed to explain special features of the global circulation on Venus. It is obvious, however, that the circulation mechanism is not asymmetric. Ideas about the appearance of a zonal stream, as a consequence of the asymmetry of convex motions at the expense of insulation periodicity at the peak of the atmosphere, found an expression in the bimolecular models of Schubert and Young [213] and Giersch [61]. They considered the results of modeling circulation in cylinders with a liquid, where insulation periodicity is imitated by a rotating burner; the appearance of zonal currents in the liquid in the direction opposite the burner motion could be shown.

Experiments on circulation modeling in a two-level model of the Venus atmosphere were carried out by Zilitinkevich and others [252], which pro-

duced a comparatively simple two-cell diagram with the center of low pressure on the day side which shifted to the evening terminator. The center of high pressure was located on the night side close to the morning terminator. Malkus [131] studied a trimolecular model and concluded that there was possible appearance, close to the peak of the troposphere, of a weak cell of the Galleev type with transition at the expense of temperature contrasts between the Equator and energy pole and at the expense of the angular moment toward high latitudes.

With this model, it is possible to correlate the experimental data about space motions received by Mariner 10, if it is also assumed that there is a great influence by the subsolar field of high pressure on the circulation structure. Meridional pressure gradients emerging in this case must bring about acceleration with increase of latitude of streams orthogonal to isobaric surfaces, with the formation of spiral motions and jet currents. Energy will be lost in polar vortexes as a consequence of vectors of motion velocities converging at the poles under low pressures [171]. In this way, the idea developed that transition of the moment of motion quantity in the meridional direction must be important in the atmosphere dynamics of Venus. The structure of the atmosphere in equatorial and polar fields shows noticeable differences primarily manifested in differences of temperature profiles, in vertical and horizontal velocities, and in motion direction. Further study of these special features will advance the understanding of regularities in formation of the present climatic conditions on the planet.

### Upper Atmosphere and Space Around the Planet

The structure of the atmosphere of Venus at high altitudes, in the areas of the thermosphere and exosphere, and the physical structure of fields in space around the planet present a separate problem. Available data on the upper atmosphere of Venus are based on measurements made by Venera 4 and Mariner 5, during a time corresponding to conditions of moderate solar activity. The value of exospheric temperature

$T = 650^\circ \text{ K}$  for these conditions is consistent with the most probable estimate produced by measurement of resonant emission in the Lyman alpha-spectral line of hydrogen ( $L_\alpha 1216 \text{ \AA}$ ) [14, 58]. Results of theoretical modeling agree closely with this estimate and indicate a probable temperature difference on the day and night sides of the planet of  $400^\circ\text{--}900^\circ \text{ K}$  [85, 88, 218], as well as possible significant variation in  $T$  as a function of the phase of the 11-year solar cycle.

Spectrophotometric measurements of resonant scattering in the characteristic lines of atomic oxygen (O), made by high-altitude rockets and spacecraft [113, 155], have been used to estimate the O content in the upper atmosphere of Venus. These are of great interest since they determine the degree of photodissociation of CO<sub>2</sub>, the primary component of the atmosphere, by the UV radiation of the Sun, forming O and CO. If the upper atmosphere of Venus were in photochemical equilibrium, then, as simple calculations show, at altitudes of 200–300 km, atomic oxygen would be the predominant component, as it is on Earth, where it is formed as a result of dissociation of molecular oxygen. However, the content of O is estimated as 1%–10% of the total density [49], which leads to the assumption of highly effective reverse recombination mechanisms in the thermosphere of Venus, which prevent accumulation of O by dissociation of CO<sub>2</sub>.

The assumption of a predominance of CO<sub>2</sub> up to altitudes of around 200–300 km is also confirmed by theoretical calculations of the profile of electron concentration in the ionosphere of Venus and their comparison with the results of measurements by Mariner 5 [134, 149, 153]. These results are shown in Figure 13. The bundles of lines characterize the slopes of profiles for calculated values of the altitude scale corresponding to various ions for several values of plasma temperature,  $t_p$ . Up to 300 km, the best agreement is provided for the CO<sub>2</sub>+ion. The maximum electron concentration in the ionosphere on the day side, reaching  $(5.0\text{--}5.5) \cdot 10^5 \text{ cm}^{-3}$ , corresponds to an altitude of 142–145 km, i.e., slightly over half as high as the maximum of the F<sub>2</sub> layer in the terrestrial ionosphere (in which the O<sup>+</sup> ion predominates), with approximately half the electron concentration. In the night

ionosphere the electron density, on the average  $\eta_e \leq 10^3 \text{ cm}^{-3}$ , with maximums at levels of 120 and 140 km, reaches  $\eta_e \sim 10^4 \text{ cm}^{-3}$ .

Numerous attempts have been made to find an adequate mechanism to explain the primarily CO<sub>2</sub> composition of the thermosphere of Venus, as well as the thermosphere of Mars, where the situation is similar. Study of the martian thermosphere has progressed greatly due to remarkable results of UV spectrometry from spacecraft [15, 16]. In particular, the discovery of strong emissions in the radiation spectra of the martian atmosphere similar to the resonant emission of O belonging to the system of Cameron bands of CO and the bands of CO<sub>2</sub><sup>+</sup> was quite unexpected. This indicates significant losses of energy from the atmosphere by radiation in the UV area of the spectrum, in addition to significant cooling in the long waveband, primarily due to oscillating conversions of CO<sub>2</sub>. It can be assumed that similar mechanisms are operating in the thermosphere of Venus which, incidentally, explains the comparatively low temperature of the upper atmosphere of the two planets. In regard to the retention of a steady concentration of CO<sub>2</sub>, the idea of the intensity of dynamic processes of macrocirculation transfer from the day side to the night side and turbulent diffusion is widely accepted. In other words, O is rapidly carried away from the areas of dissociation [42, 218].

In the denser, lower lying atmosphere, recombination processes are significantly more effective. Intensive turbulent diffusion assures constant delivery of molecules of CO<sub>2</sub> to the upper atmosphere. Although the required values of turbulent diffusion factors are rather high ( $10^7\text{--}10^8 \text{ cm}^2/\text{s}$ , i.e., approximately an order of magnitude greater than the figures for the Earth), these are quite possible for the conditions of the upper atmospheres of Venus and Mars. The actual sequence of chemical conversions accompanying the processes of circulation or diffusion mass transfer should be explained, considering the maximum concentrations of the components participating and the rate constants of the corresponding reactions.

According to present estimates, the effectiveness of the most probable mechanism of recombi-

nation of O drops significantly at levels below 300 km. This, obviously, should lead to appearance of a comparatively thin layer of O, with He having a certain influence above this layer. The measured electron concentration profiles in the night atmosphere of Venus, shown in Figure 13, can be explained by photoionization of He on the day side at a rate of  $3 \cdot 10^7 \text{ cm}^{-2} \cdot \text{s}^{-1}$  above 250 km with subsequent horizontal transfer of  $\text{He}^+$  ions to the nonilluminated hemisphere. If the delivery of He to the Venusian atmosphere by radioactive decomposition of uranium and thorium within the planet corresponds approximately to its delivery to the atmosphere of the Earth (about  $3 \cdot 10^6 \text{ atm} \cdot \text{cm}^{-2} \cdot \text{s}^{-1}$ ), the neces-

sary balance between delivery and thermal dissociation of He is provided, if additional transfer is assumed of about 10% of the quantity of  $\text{He}^+$  ions formed on the day side of the planet by the solar wind [150].

Above approximately 1000 km the atmosphere of Venus apparently becomes primarily hydrogen, which is apparent in Figure 13. The hydrogen corona of Venus, directly measured by spacecraft [12, 113], is similar to the hydrogen corona of the Earth, but at the lower exospheric temperature it is smaller. Measurements of Mariner 5 showed a curious peculiarity of hydrogen emission from the day side of the planet—a rapid increase in intensity of the glow in the direction

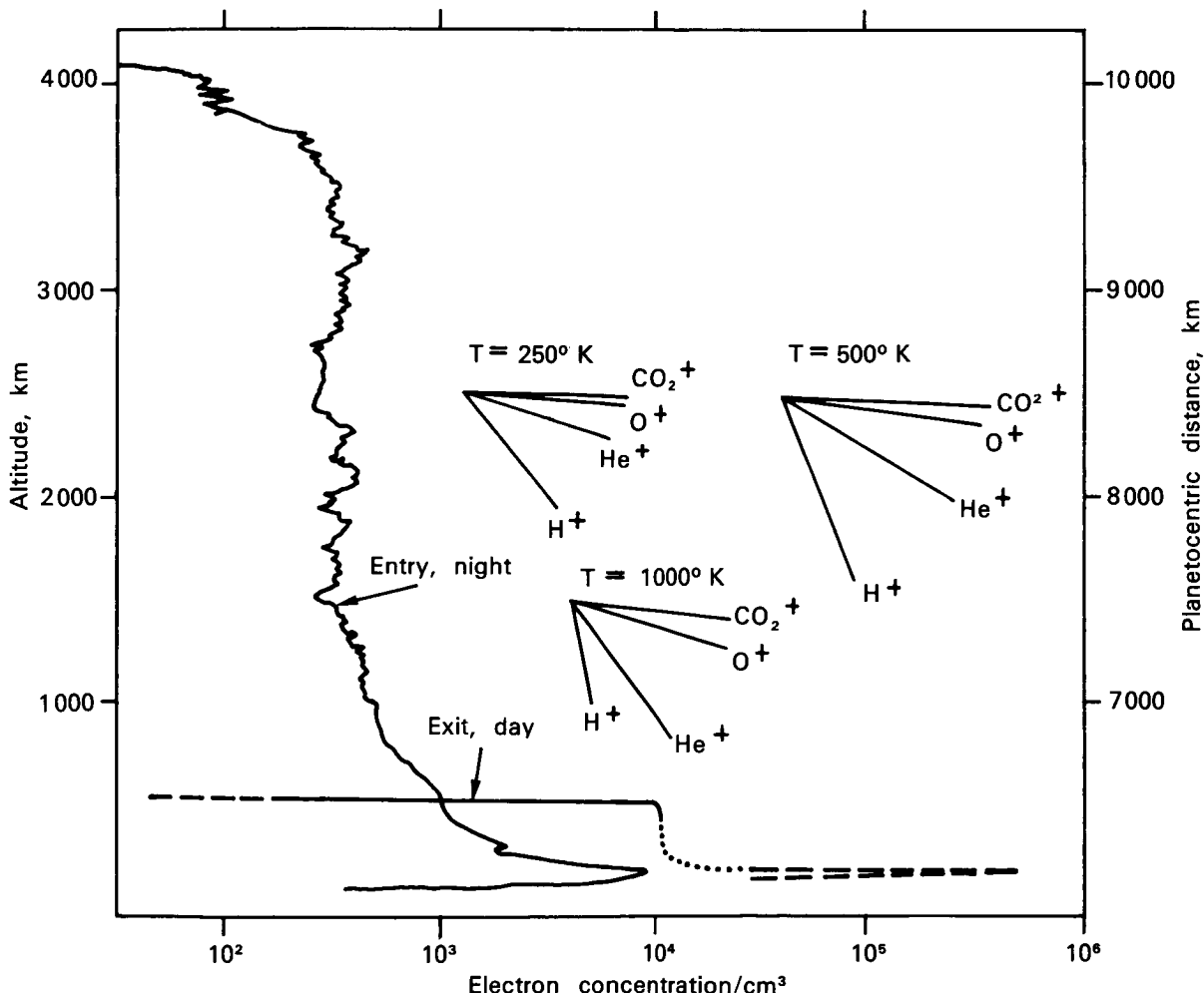


FIGURE 13.—Change in electron concentration with altitude on night and day sides according to measurements of Mariner 5, with estimates of corresponding values of scale of altitudes. (According to [134])

toward the limb (in the altitude range from 3000 to 450 km), corresponding to a decrease in the scale of altitudes by approximately a factor of 2. Although this high intensity of glow from the day side of the planet was not confirmed by the rocket experiments of Moos et al [155], various hypotheses have been advanced to explain this interesting phenomenon.

The most feasible hypothesis is based on the significant content of deuterium in the base of the Venus hydrogen corona. However, it requires assuming that the relative content of deuterium on Venus ( $n_D/n_H \approx 0.1$ ) is significantly greater than in the Earth's atmosphere. This ratio is difficult to explain within the framework of the mechanism of thermal fractionation of hydrogen and effects at the base of the exosphere. However, for a planet practically free of a regular magnetic field (its intensity is some 1/3000 that of the Earth [43]), one additional and quite effective mechanism might be transfer of particles ionized by solar UV radiation by the electric field arising in the "induced ionopause" of Venus on the day side as solar plasma flows toward the planet.

The concept of the *induced ionopause* is illustrated by Figure 13, which shows a sharp (by almost 3-order magnitude) drop of electron concentration in the hemisphere illuminated by the Sun, in contrast to the even drop on the night side. This results from formation of a shock wave in the area where the pressure of the solar wind is comparable to the pressure of the induced magnetic field. The ionopause on Venus is similar, to some extent, to the magnetopause on Earth, which prevents direct penetration of the solar plasma into the magnetosphere—the area of the regular geomagnetic field. Therefore, the magnetopause is located significantly farther from the surface, at a distance on the order of 10 R<sub>⊕</sub>. Since Venus has no strong perturbing influence on the structure of the interplanetary field, it is natural to assume that the solar wind flowing around it practically does not change its characteristics on the night side [229].

The nature of the physical structure of the Venus atmosphere up to an altitude of about 1000 km is summarized in Figure 14, according to a model [141], containing the primary physical parameters of the atmospheric gas.

## Origin and Evolution

The hypothesis of the single origin of all the planets of the solar system from a gigantic protoplanetary gas-dust cloud prompts the seeking of common features among the planets of the Earth group. However, investigations during the past decade have provided convincing evidence that Earth, Mars, Venus, and Mercury differ strongly. These differences can be explained, to a certain extent, by differences in the current stages of evolution of the planets. How the Earth developed can be imagined with some reliability; the natural conditions on the Earth millions of years ago were doubtless different from the present. The nature of this evolution depends on many conditions: primarily the geometric and mechanical characteristics of the planet, distance from the Sun, changes occurring within the planet, and fragmentation of rock. These processes are accompanied by formation and evolution of the planetary atmosphere, which therefore reflects the most important characteristics of each stage.

The gas composition of the atmospheres of planets of the Earth group resulted primarily from volcanic emissions, accompanied by processes of differentiation of the substance of the planet into envelopes, due to heating of the interior by radioactive decay. Within the planet, water vapor and carbon dioxide make up the major fraction of volcanic gases. It is, therefore, not surprising that these gases, along with the carbon monoxide, hydrogen chloride, and hydrogen fluoride, determined by spectroscopic measurements, are present in the atmosphere of Venus (nor is it surprising that the possibility of sulfurous gases, confirming the hypothesis of clouds of H<sub>2</sub>SO<sub>4</sub>, may be present).

The atmosphere of the Earth probably had similar composition over a billion years ago. However, processes of photosynthesis and the appearance of free oxygen due to development of the biosphere apparently had a decisive influence on the formation of the terrestrial atmosphere. This, in turn, resulted in oxidation of ammonia, also contained in volcanic gases, which liberated large quantities of nitrogen into the atmosphere. The carbon dioxide, hydrogen

chloride, hydrogen fluoride, and sulfur compounds entered into reactions with the biosphere, hydrosphere, and the solid substances of the planet. With the moderate surface and atmospheric temperatures, the Earth retained its water, most of which was concentrated in the oceans [243, 244].

The greater proximity of Venus to the Sun probably caused the evolution of its atmosphere to be different. The primary factor leading to the present conditions apparently was the loss of

water by the planet. Water loss is probably the key question in the evolution of Venus.

If the improbable assumption is eliminated that water was not liberated from the core of the planet in volcanic activity during its evolution, which apparently occurred on the Earth, it must be explained why the water content in the atmosphere of Venus is at least 1000 times less than on Earth. One possible explanation is that the temperature of the coldest area in the upper atmosphere of Venus (the mesopause) is some-

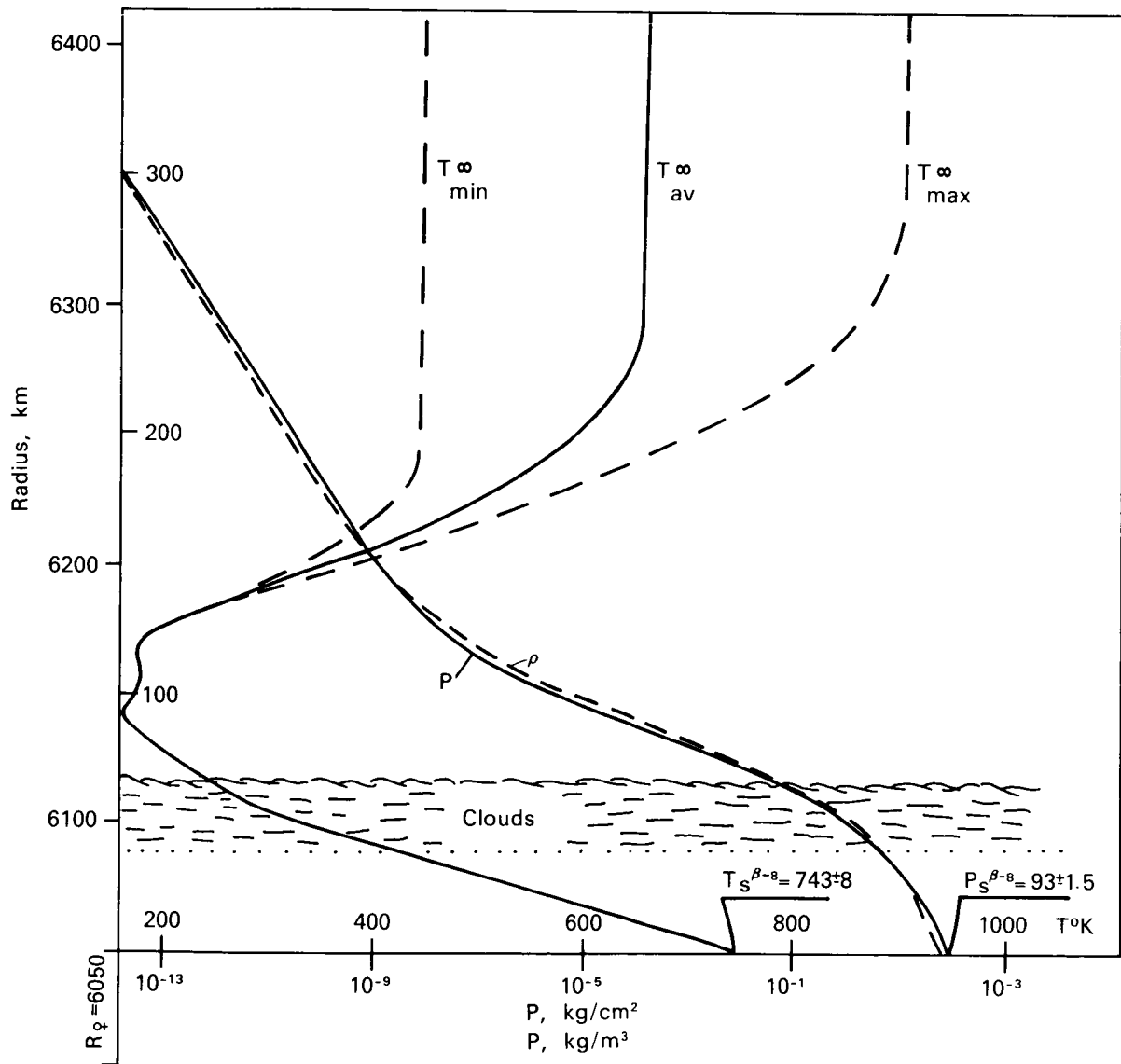


FIGURE 14.—Physical structure of the Venus atmosphere according to model of Marov and Ryabov [141].

what higher, and that hard UV radiation can penetrate more deeply, than on Earth. The result would be more intensive decomposition of water into oxygen and hydrogen and more energetic dissipation of light hydrogen from the atmosphere into space. The oxygen would then be bound by the solid substances on the surface of the planet.

High temperature, high pressure, very low content of water, and almost total absence of oxygen—all present peculiarities of the Venus atmosphere which are interrelated and interdependent. As the temperature rises, more water enters the atmosphere, and dehydration increases the content of carbon dioxide which, in turn, should facilitate further increase in temperature due to the greenhouse effect. At high temperatures, there can be no biosphere in the familiar form, while the absence of a biosphere essentially eliminates the possibility of a high content of free oxygen in the atmosphere.

The comparative content of the commonest volatile components on Earth and Venus is presented in Table 4 [88]. The quantity of carbon dioxide on the Earth is approximately the same as on Venus. However, in the terrestrial atmosphere, its quantity is negligible ( $0.0003 \text{ kg/cm}^2$ ); the main mass is found in the upper envelope of the solid Earth. This relationship, in the contents of carbon dioxide between atmosphere and lithosphere, corresponds to the equilibrium state at the current temperature of the Earth, determined by reactions between carbonates and

silicates in the presence of liquid water. The carbon dioxide on the Earth is bonded into carbonates in sedimentary rock, primarily due to the activity of living organisms. On the hot planet Venus—with no water—carbon dioxide could not go over into the lithosphere and is retained in the atmosphere, creating the extremely high pressure of the planet's gas envelope. If the temperature on the Earth increased to the temperature of Venus, the pressure of the terrestrial atmosphere would become even higher than the current atmospheric pressure on Venus. This is because the pressure of some 100 atm resulting from liberation of carbon dioxide from carbonates would be supplemented by an additional 300 atm, corresponding to the mean depth of the world oceans, by evaporation of the water.

In the light of modern concepts about the nature of Venus it is natural to question if this planet is of exobiologic interest. This question has been discussed in a number of works (cf, e.g., [164, 204, 205, 206]). The authors mentioned possible existence of biologically active forms, both on the surface and in the clouds. Relative to the surface, it can be affirmed that the majority of organic molecules which compose biologic structures evaporate at temperatures which are essentially lower than  $500^\circ \text{ C}$ . The properties of proteins also change; and there is no liquid water on the surface. Therefore, it seems that Earth types of life can be excluded. Other possibilities, including so-called "biological refrigerators" or structures based on silicon-organic compounds, seem to be fairly artificial.

The conditions in the clouds at a level of about 50–55 km, which correspond more closely to Earth conditions, are far more favorable except for the prevailing content of  $\text{CO}_2$  and practical absence of  $\text{O}_2$  and  $\text{N}_2$ . Nonetheless, in the clouds, conditions exist for the formation of photoautotrophs. In the mixing atmosphere, the essential difficulty is retention of such organisms at a favorable altitude from which they cannot be displaced into the lower hot atmosphere. To resolve this difficulty, Morowitz and Sagan [156] hypothesized the presence of isopyknic cylinders filled with photosynthetic hydrogen. According to their assessments, the diameters of such cylinders, which would determine the size of orga-

TABLE 4.—*Volatile Compounds (Pressure as  $\text{kg/cm}^2$ ) on Earth, Venus, and Mars* [88, 135]

Volatile	Atmosphere of Earth	Total on Earth	Atmosphere of Venus	Atmosphere of Mars
$\text{CO}_2$	$3 \cdot 10^{-4}$	$70 \pm 30$	$90 \pm 15$	$(1.4 \pm 0.2) \cdot 10^{-2}$
$\text{H}_2\text{O}$	$10^{-2} \text{--} 10^{-3}$	$375 \pm 75$	$10^{-1} \text{--} 10^{-4}$	$(1.5 \text{--} 2.5) \cdot 10^{-6}$
$\text{O}_2$	0.23	$\approx 0.23$	$< 10^{-3}$	$< 2.5 \cdot 10^{-5}$
$\text{N}_2$	0.75	$\approx 0.75$	$< 2$	$< 0.8 \cdot 10^{-3}$
$\text{A}_g$	$10^{-2}$	$\approx 10^{-2}$	?	$< 0.3 \cdot 10^{-2}$
CO	$10^{-6} \text{--} 10^{-7}$	$\approx 10^{-6}$	$< 10^{-3}$	$0.7 \cdot 10^{-5}$
Cl	—	5.7	$2 \cdot 10^{-5}$	—
F	—	$3 \cdot 10^{-4}$	$10^{-7}$	—

nisms, would be several cm (assuming a shell thickness corresponding to the membrane thickness of Earth organisms). Such purely speculative ideas, although attractive, seem quite artificial. They can hardly be considered reasonable from the viewpoint of emerging life in clouds, or as certain kinds of "residues" of biologic forms which had existed on the planet. This does not, of course, exclude the possibility that at a certain period in its history, Venus possessed conditions favorable for manifestation of biologic activities.

The peculiarities of the evolution, heat exchange, and nature of the clouds and surface do not exhaust the problem of Venus, which continues quite justifiably to be called the mystery planet, in spite of tremendous successes achieved in the past few years of study.

Venus hides many secrets, the discovery of which will doubtless enrich planetology with new fundamental knowledge. The thickness of the gas envelope, its unique thermal regime, the unusual nature of its rotation—these and other peculiarities make Venus truly different among the family of planets in the solar system. What has caused these unusual conditions? Is the atmosphere of Venus a "primeval" atmosphere, characteristic of a young planet, or did these conditions arise later, as a result of irreversible geochemical processes caused by the proximity of Venus to the Sun? These questions merit close attention and require further comprehensive study.

## MARS

Mars is the fourth and last of the planets of the Earth group, in order of increasing distance from the Sun. It moves in an external orbit (contrasted to the "inner planets"—Mercury and Venus), therefore turns its day side toward the Earth as it approaches it, and is seen quite easily. Nevertheless, the possibility for producing new information by observation from the Earth's surface is limited. Knowledge of Mars in recent years has grown at unforeseen rates, primarily due to the use of space technology.

Only spacecraft can observe Mars closely. The obvious advantages are: a great increase in detailed images of Mars; elimination of interference of the Earth's atmosphere, since observa-

tions are performed from beyond the atmosphere; and use of simple apparatus instead of huge telescopes. All of this allows studies which are impossible from ground observatories.

The first attempts to utilize these advantages led to new discoveries. All automatic spacecraft sent to Mars were flyby vehicles until 1971; the great capabilities of their apparatus were strongly limited by the short time spent near the planet. The desire to use the advantages of spacecraft more fully led to more complex equipment in 1971, which was designed to place spacecraft in orbit around Mars. The US Mariner 9, on November 16, 1971, began to orbit Mars, followed by Soviet Mars 2 and Mars 3 on November 27 and December 2. The Mars 3 descent vehicle made the first soft landing on the surface of the planet on December 2. The Soviet automatic spacecraft landed in the martian desert, Phaethontis, at about 45° south latitude and 158° west longitude. Difficult landing conditions prevented performing the planned sequence of measurements.

A powerful dust storm of global scale took place on Mars at the time. The clouds of dust, rising in the martian atmosphere, made it almost opaque to rays in the visible portion of the spectrum. Therefore, in the first photographs transmitted by Mars 3 and Mariner 9, the Mars surface looks completely smooth, without noticeable contrast. The limb of the planet is seen clearly (indicating accuracy of the image transmitted), the terminator (boundary between day and night hemispheres) can be clearly seen, but no relief details are visible. On larger scale photographs, the wavy surface of the clouds can be distinguished and over the horizon, a thin layer of cloud as a narrow bright strip. Local clear spots began to appear in the second half of December, satisfactory atmospheric transparency was observed after about January 23, and the atmosphere became fully transparent in February. The dustiness of the martian atmosphere at first prevented photographing the planet's surface. However, a unique opportunity was provided to study a strong martian storm at close range.

Through the use of spacecraft and new methods of observation from the Earth's surface, the quantity of information on Mars has increased

tremendously in recent times. In particular, television images of the Mars surface and of its satellites, transmitted by Mariner 9, are of great interest. Combined analysis of mutually complementary experiments performed by the three artificial satellites of Mars has contributed greatly to understanding the physical, geological, and morphological peculiarities of this planet and the physics of its surrounding space.

### Global Characteristics of Mars

#### *Dimensions, Figure, and Gravitational Field*

Measurements of the Mars radius by different methods agree closely. A summary of the latest optical measurements and an extensive bibliography are available [48]. The results indicate an ellipsoid with equatorial radius,  $R_{eq} = 3398 \pm 3$  km, and polar,  $R_{pol} = 3371 \pm 4$  km. The combined results of terrestrial radar during the oppositions of 1967, 1969, and 1971 [181] indicated  $R_e = 3394 \pm 2$  km, which is the mean radius within limits of the planet's tropical belt.

Measurements of the planet's radius on the basis of blocking radio signals from spacecraft flying behind Mars apparently yielded the greatest accuracy (mean square error on the order of 1 km). Measurements from Mariner 9 showed that the physical surface of Mars can be approximated by: a triangular ellipsoid  $x^2/A^2 + y^2/B^2 + z^2/C^2 = 1$ , with a polar radius  $C = 3375.45$  km; and in the plane of the Equator: large half axis  $A = 3400.12$  km, small half axis  $B = 3394.19$  km, and longitude of large axis  $L_A = 99.7^\circ$  [19]. Significant asymmetry of Mars along the polar axis has been discovered: the level of the surface, almost throughout the southern hemisphere, is 3–4 km higher than in the northern hemisphere.

Precise analysis of the movements of Mariner 9 in its orbit around Mars has revealed heterogeneity of the planet's gravitation field [126]. These heterogeneities indicate local fluctuations in density beneath the surface. The results of measurement can be arbitrarily expressed as positive and negative mass concentrations or equivalent altitudes of the Mars physical surface over the surface of a spherical body of homogeneous density. Some mass concentrations are

easy to identify with local fluctuations in the radius of the planet.

The degree of Mars polar compression, determined by occultation of radio signals, does not agree with dynamic compression (i.e., compression of the ellipsoid of inertia of the planet)—determined from precession of the orbits of Mars satellites, and calculated on the basis of hydrostatic theory in the model of a homogeneous Mars. The disagreement can be explained by convection of solids within Mars [198].

The total mass of the planet, calculated from the motion of its satellites [248], is about  $6.423 \cdot 10^{23}$  kg. Analysis of motion of Mariner 6 and 7 flyby spacecraft allowed US specialists to refine the constant, consisting of the product of the constant of gravity times the mass of the planet [1]:  $GM_\sigma = 42\ 828.1 \pm 1.38$  km<sup>3</sup>/s<sup>2</sup>. The mass of the planet, unfortunately, can only be concluded from this expression with loss of accuracy, since the constant of gravity itself requires refinement. Not more than four significant digits can be given with confidence, and figures are usually limited to this accuracy.

The parameters derivative from the mass and radius are: mean density of the planet around 3.94 g/cm<sup>3</sup>; acceleration of the force of gravity on the surface of Mars 38% of its value on Earth—critical velocity 5.0 km/s.

### Magnetic Field

The magnetometer installed on the Mariner 4 flyby spacecraft (in 1965) to determine the dipole moment and properties of the martian magnetosphere reported a jump in intensity of 5 gamma near the planet. The experimenters assumed that this jump was related to passage through the leading edge of a shock wave in the solar wind, not to the field of the planet. Based on the results of this experiment, estimates of the upper limit of magnetic moment of Mars indicate that it is  $10^{-3}$  to  $2 \cdot 10^{-4}$  times the terrestrial field [226].

Ferroprobe magnetometers on Mars 2 and Mars 3 (1971–1972) recorded a three-component change in field intensity in the orbital sections closest to the planet, exceeding the natural background of the interplanetary field in this region at the maximum point on the magnetogram by 7 to

10 times [44]. The effect observed was possibly caused by reinforcement of the solar wind magnetic field due to two factors: (1) currents induced in the ionosphere of the planet, and (2) compression of the plasma between the shock wave and the planet. However, Dolginov et al [44] who performed the experiment consider that the data available on the topology and measured magnetic field can be best coordinated with the data of Gringauz on the intensity of the solar wind, and data on the shock wave position near the planet only if existence of a martian magnetic field is assumed with a dipole moment of  $2.4 \cdot 10^{22} \text{ G} \cdot \text{cm}^3$  with an intensity at the magnetic equator of about 60 gamma, i.e.,  $2 \cdot 10^{-3}$  times the terrestrial field.

#### *Parameters of Axial Rotation and the Martian Seasons*

The telescopic observations by several generations of astronomers provided the first source of information on the direction of the Mars axis and rate of diurnal rotation. Axial rotation is at a constant angular velocity relative to the fixed stars; the sidereal period is equal to 24 h 37 min 22.668 s. The length of a solar day varies slightly due to the unevenness of Mars movement in its orbit, averaging 24 h, 39 min, 35 s. The number of solar days in a martian year is  $668 \frac{2}{3}$ , one less than the number of stellar days.

The axis of Mars rotation is tilted from the perpendicular to the plane of the orbit by  $25^\circ$ , i.e., almost the same as for the Earth. However, similarity is limited to the tilt, and does not include the direction of the axis of diurnal rotation. The polar axis of Mars is tilted with its northern end in the constellation Cygnus, at the point with these coordinates: right ascension  $317.3^\circ \pm 0.3^\circ$ , declination  $+52.6^\circ \pm 0.2^\circ$  (epoch 1971.9, equinox 1950.0 [126]). There is no notable star near the pole which could act as a North Star.

The considerable inclination of the martian equator plane to the orbit plane means that the northern and southern hemispheres of the planet receive varying amounts of solar heat: in some parts of the orbit, the northern hemisphere is primarily illuminated and heated while in other parts it is the southern hemisphere. In other words, there is change of seasons on Mars.

The Sun passes approximately the same height in the martian sky as in the corresponding latitudes on Earth at each time of year. However, in contrast to our seasons, the martian northern seasons differ quite markedly from the southern seasons in length and temperature conditions. Spring and summer in the southern hemisphere of Mars are considerably shorter than those seasons in the northern latitudes (Table 5), due to considerable ellipticity of the martian orbit and resulting differences in the travel rate of the planet over different portions of its orbit.

The significant difference in duration of the warm time of year in the two hemispheres of Mars is explained by difference in solar illumination brightness, resulting from cyclical changes in the distance of the planet from the Sun. At perihelion, Mars is  $43.10^+ \text{ km}$  closer to the Sun, and the mean temperature at the subsolar point and over the entire day-hemisphere is  $25^\circ\text{--}30^\circ$  higher than at aphelion. This leads to differences in the climate in the northern and southern hemispheres.

The martian calendar (if it were constructed like the Julian and dates identified by the argument of declination of the Sun) would show the aphelion at the end of May, the perihelion in early December. Thus, autumn and winter in the northern latitudes on Mars are less severe than in the corresponding southern latitudes.

Precession of the axis of the planet's rotation in combination with the perihelion motion of the orbit causes a "drift" of the perihelion date along the entire Mars calendar with a period of 51 000 years, according to Murray et al [173]. During the same period, the difference in the insolation regime of the northern and southern hemispheres changes its polarity. Furthermore, the oscillation amplitude of insolation pulsates between an annual maximum (in the perihelion) and minimum

TABLE 5.—*Length of the Year on Mars between Moments of Equinoxes and Solstices in Our Epoch, in Mean Solar Days Universal Time*

Northern spring and southern fall	199
Northern summer and southern winter	182
Northern fall and southern spring	146
Northern winter and southern summer	160
Duration of 1 cycle	687

(in the aphelion). Such pulsation results from the variations of the Mars' orbit eccentricity with a period of about 2 million years [173].

The most essential age-old changes in the seasonal insolation of the polar regions of Mars must be caused, it seems, by variations of the inclination of the Mars axis toward the orbit plane. Ward [247] found that there are large-scale variations of inclination as a result of the combination of two known motions:

1. The precession of the polar Mars axis caused by the impact of solar gravitation on the equatorial swelling of the planet.
2. The motion of the orbital plane, caused by gravitational disturbances from planets.

Ward showed that the inclination oscillates, reaching a maximum every 120 000 years. Additionally, the amplitude of these oscillations changes with a period that is ten times larger; the average level also changes within small limits. The inclination amounted to  $33^\circ$  750 000 years ago; it decreased to  $16^\circ$  650 000 years ago. Now it is slowly increasing from a value of  $25^\circ$ . The extreme change limits are:  $14.9^\circ$  and  $35.5^\circ$ . Correspondingly, this is the angular height of the Sun in the sky above the Mars pole during the polar day.

### **Atmosphere of Mars**

#### *Optical Properties*

During telescopic visual observations, the atmosphere of Mars in the low and moderate latitudes appears transparent most frequently, with yellow turbidity and white clouds visible only occasionally. When observed through a blue filter, the atmosphere scatters sunlight quite strongly, and the surface details of the planet are poorly seen. The effect of reduced contrast with decreasing wavelength of reflected light is sometimes explained [185] by peculiarities of the surface color. However, during terrestrial telescopic photography on unsensitized photographic film, sensitive only to blue, violet, and ultraviolet light, all that can be seen most frequently is a cloudy fog of uneven density with extremely bright spots along the edges of the disk of the planet.

#### *Pressure at the Surface*

The martian atmosphere's ability to raise and hold dust in the suspended state for a long period creates an impression of significant gas density, which, however, is false, and one reason for long-standing confusion. Rough estimates of the atmospheric pressure at the surface of Mars, generally expressed in millibars (mbar) in planetary astronomy until 1963, averaged around 80 mbar (60 mm Hg according to an aneroid barometer). Recent improved methods of remote measurement by both terrestrial and spacecraft-borne apparatus have indicated that the true pressure is 10 to 20 times less than estimated earlier, some 200 times less than on Earth. Here the normal atmospheric pressure at sea level is 1013 mbar. On Mars, it varies from 3 mbar at high altitude (about 1 mbar on the highest peak) to 10 mbar in the lowlands [29, 102]. On Mars it amounts, on the average, to about 5.5 mbar. At each location on Mars, atmospheric pressure may also undergo temporary deviations which are listed in the section about barometric relief (under **The Relief of Mars**).

#### *Chemical Composition of the Lower Atmosphere*

The primary component of the lower atmosphere, carbon dioxide ( $\text{CO}_2$ ), can be identified easily by the characteristic lines in the sunlight spectrum scattered by Mars. The abundance of gases in planetary atmospheres is usually expressed in the form of the thickness of a layer, adjusted to a pressure of 1 atm. New estimates by various authors indicate that approximately  $75 \pm 15 \text{ m} \cdot \text{atm}$   $\text{CO}_2$  is present in the martian atmosphere. Estimates and bibliographies are available [160, 250]. Terrestrial high-resolution spectrographs have provided for using Doppler shift to separate some weak details belonging to martian water vapor from the background of great telluric bands [95], a result which has been confirmed and refined by new terrestrial observations [212]. Attempts were made to use the artificial satellites of Mars to study the moisture content of the lower atmosphere, not averaged over the entire visible portion of the day hemisphere, but rather for individual areas of the planet [29, 161].

The content of  $H_2O$  in the martian atmosphere undergoes seasonal variations in each hemisphere of the planet and changes from an undetectable quantity to some tens of microns of precipitated water. The wettest region in 1972 was the north polar area during the northern spring, where the atmosphere was found to be saturated with water vapor (i.e., 100% relative humidity) with some  $20\text{--}30 \mu\text{m}$  of precipitated  $H_2O$  [29]. The episodic appearance of clouds consisting of ice crystals also testifies to cases of saturation of the Mars atmosphere with water vapor over certain points.

Terrestrial Fourier spectroscopy using a Michelson interferometer has been used to detect carbon monoxide (CO) [94] in a quantity of  $5.6 \pm 1.0 \text{ cm} \cdot \text{atm}$ , i.e., less than 0.1% by volume. A new estimate [251] of the CO quantity disagrees with earlier estimates, showing  $42 \pm 0.6 \text{ cm} \cdot \text{atm}$  [13].

A report which appeared in 1968 on the discovery of molecular oxygen on Mars was later criticized [133]. Finally, in 1972 a more reliable estimate of  $O_2$  quantity showed  $9.5 \pm 0.6 \text{ cm} \cdot \text{atm}$  [13].

Observations by Mariner 7 and 9 in the polar areas of Mars indicated presence of ozone ( $O_3$ ) up to  $57 \mu\text{m} \cdot \text{atm}$ , appearing in late autumn, and disappearing in early summer [116]. It was assumed at first that it is absorbed on the solid surface of the winter polar cap. However, in 1971–1972, ozone absorption was observed in the Hartley continuum (between 2000 and 3000 Å) beginning at  $30^\circ$  north latitude, where there was no polar cap. The strong annual course of ozone is apparently related to changes in the content of water vapor [116]. Ozone is not observed in the equatorial regions.

No other components have been detected in the lower atmosphere of Mars in addition to those listed; only the upper limits of their possible content can be noted, below which they become undetectable [35, 82]. It is probable, theoretically, that Argon is present in relatively large quantities [158], although this question remains open, and current studies cannot answer it yet. If there is life on the planet, products of its metabolism may be present [57, 127]; however, attempts to find them on Mars have not yet been successful [75]. Further development of research methods is continuing [191].

### *Chemical-Dynamic Model of the Martian Atmosphere*

There have been indications in recent years [84, 152] of a difficult contradiction between the low content of CO and  $O_2$  in the martian atmosphere on the one hand, and contemporary theories on the other hand. Carbon monoxide is formed as a result of dissociation of  $CO_2$  under the influence of solar UV radiation at  $\lambda < 2270 \text{ \AA}$ , which penetrates to the lower atmosphere, and under the influence of electron shock with an energy  $E > 11.5 \text{ eV}$ . The reverse action does not occur. Nevertheless, the low observed content of CO indicates that there must be a rather effective recombination reaction. Such reaction cannot yet be named nor, consequently, can the conditions under which it might occur.

The recombination of carbon monoxide to carbon dioxide is believed to occur in the martian atmosphere under the catalytic influence of water vapor [151]; therefore, the content of CO and  $O_2$  in an atmosphere of  $CO_2$  should vary as a function of water content and mixing intensity. Rates of the 15 basic reactions have been outlined [151], and a model of the martian atmosphere constructed indicating the rates of recombination at various altitudes and calculated concentrations of various components following from the model.

### *Thermal Mode*

The surface of Mars, absorbing solar energy, reradiates it in the infrared range. The martian atmosphere, when no dust clouds are present, transmits all solar radiation with  $\lambda > 1900 \text{ \AA}$  freely, but absorbs the thermal radiation of the planet's surface in the band around  $15 \mu\text{m}$  and is thus heated. The diurnal temperature wave is propagated by radiant transfer from the base of the atmosphere to an altitude on the order of 1 km [70]. The time of thermal relaxation is significantly less than in the atmosphere of the Earth. Thus, the temperature of the lowest layer in the clear martian atmosphere is determined by surface temperature and may vary by more than  $100^\circ \text{ K}$  during a day. Theoretical studies of the thermal regime and dynamics of the lower Mars atmosphere include those of Gierasch

and Goody, which are important in using the original method of calculating radiation heat exchange of the Mars atmosphere with the planet's surface and into outer space.

The experimental x-ray data of the Mars atmosphere were used by Rasool and Stewart, who found that at the local midday, there is a  $20^{\circ}$ - $25^{\circ}$  temperature drop between the warm surface of the planet and the cooler adjacent layer of the atmosphere [193]. However, their result may have been influenced to some extent by averaging of the temperature over a comparatively thick lower layer of the atmosphere which had not been heated by noon.

The amplitude of diurnal fluctuations in observed temperature decreases with altitude; in the clear atmosphere of an altitude of 10 km, the amplitude of fluctuations is  $15^{\circ}$  K [75]; while in the dusty atmosphere, it is significantly greater. The absolute temperature decreases with height, but at night an inversion was found [193] which was probably caused by the extremely fast cooling of the surface. Furthermore, Mariner 9 registered inversions above, and at the border of, the winter polar cap.

An extremely cold area has been found in the middle atmosphere of Mars, where CO<sub>2</sub> is present in saturation quantities, and condensation might occur [193]. These results were produced by the radio refraction method in 1969. Measurements on Mariner 9 [101] also showed a temperature consistent with condensation of CO<sub>2</sub> near the morning terminator in the high latitudes of the winter hemisphere of Mars.

In the upper atmosphere, the mean temperature increases with increasing altitude, reaching  $325^{\circ}$ - $350^{\circ}$  K at about 230 km [40, 231]. The temperature in the exosphere fluctuates widely. Analysis of the fluctuations indicates the influence of processes not directly related to solar activity [231]; however, a direct dependence has been mentioned [90].

#### *Vertical Temperature Gradient and Dust in the Mars Lower Atmosphere*

With subadiabatic vertical temperature gradient, stratification in the atmosphere is stable, while with superadiabatic temperature gradient, convection arises, tending to reduce the gradient.

In the clear atmosphere of Mars in daytime, the observed rate of decrease of temperature with increasing altitude averages  $2.3^{\circ}$  K/km, i.e., is subadiabatic [75, 102]. However, good measurements are lacking of the afternoon lapse rates, which should be closer to adiabatic. Some local factors probably cause temporary disruptions in stable stratification. Otherwise, it would be difficult to explain the development mechanism of the currents which have carried dust to great altitudes.

During a great dust storm in 1971-1972, according to data of Mariner 9, dust clouds reached a height of 45 km [119]. During daytime in the equatorial region, the lower atmosphere with the greatest dust content (about 10 km thick) was practically isothermal and, consequently, still more stable than with the subadiabatic gradient. Near the lower boundary of the dust-carrying layer (on the surface of Mars), the temperature was somewhat lower than usual, while at the diffuse upper boundary, it was somewhat higher than usual for those altitudes, which is explained by absorption of the Sun's rays by dust. The heating effect resulting from presence of the dust was noted up to at least 20 to 30 km above the surface [101].

The vertical temperature gradient is a very sensitive criterion for clarity of the martian atmosphere; it shows that dust may be present in the martian atmosphere even when the television images indicate that the atmosphere is clear. According to Ryan's calculations [199], the wind-speed must be significantly higher than the observed speed of motion of martian clouds, in order to raise dust from the surface. The dust clouds probably rise during squall-like gusts of wind, the velocity of which is significantly greater than the mean velocity, while the weaker circulation is sufficient to maintain the dust in its suspended state.

#### *Winds and General Circulation*

The dynamic and thermal structure of the Mars lower atmosphere was studied theoretically by Gierasch and Goody [62] and Golitsyn [68], who observed a temperature jump in the lowest layer, about 10 m thick. In a layer about 1 km

thick, it was believed that a free convection mode may obtain. Gierasch and Goody found that the primary component in the system of martian winds is a seasonal zonal wind (i.e., directed practically along the parallels) with a mean velocity of about  $40 \text{ m} \cdot \text{s}^{-1}$ . Golitsyn produced estimates of mean windspeed for an atmospheric model with  $p_0 = 5 \text{ mbar}$ :  $v = 20 \text{ m} \cdot \text{s}^{-1}$  at a height on the order of 10 m and  $v = 40 \text{ m} \cdot \text{s}^{-1}$  at a height of about 200 m. With further increases in altitude, the windspeed changes more in direction than in modulus, and approaches geostrophic at an altitude of 2 to 4 km. The total angle of rotation in daytime falls within limits of a few degrees, while at night it may reach several tens of degrees. An estimate [69] of windspeed in the martian atmosphere (based on the theory developed by Golitsyn of similarity of large scale motions in the atmospheres of planets) yields  $50 \text{ m} \cdot \text{s}^{-1}$ , i.e., a value similar to those produced by other methods.

Thus, theoretical estimates of the windspeed in the lower atmosphere of Mars yield figures of about  $40 \text{ m} \cdot \text{s}^{-1}$ ; however, they depend strongly on local relief and do not exclude the possibility of speeds exceeding  $100 \text{ m} \cdot \text{s}^{-1}$  [63].

Calculations have been made of various versions of the general circulation model in the martian atmosphere; numerical modeling of the atmospheric circulation of Mars [120] is quite interesting. The atmosphere was assumed to consist of  $\text{CO}_2$ ; the transfer of solar and thermal radiation was considered. At the moment of the equinox, cyclones are active in the moderate and high latitudes of both hemispheres; in the middle latitudes, the winds are from the west, and in the region of the equator—from the east. During the solstice season, east winds remain in the tropics, weaker in the summer hemisphere. In the winter hemisphere, the motions result from condensation of  $\text{CO}_2$  in the polar cap: this causes meridional transfer of gas across the equator, while baroclinic wave motions and strong west winds predominate in the middle and higher latitudes. In all cases, a diurnal tidal component is noted in the atmospheric circulation.

The fields of winds (Fig. 15), calculated in 1972 on the basis of temperature measurements

in the Mars atmosphere by Mariner 9, has confirmed the presence of both seasonal and strong diurnal winds [75], as predicted earlier [70, 120].

Information on the dynamics of the martian atmosphere, obtained directly from observations [154] has been sought. Windspeeds in the lower atmosphere of Mars are usually estimated by terrestrial telescopic observation using visible displacements of cloud systems relative to the planet's physical surface. The observation of yellow (probably dust) clouds indicates speeds of about  $15 \text{ m} \cdot \text{s}^{-1}$ . In the case of white clouds, it is apparently not always possible to identify windspeeds and speeds of movement of bright spots on Mars. One of the authors of this chapter (Davydov) has repeatedly encountered records of white spots observed moving at almost the speed of sound for many hours (in memoirs of well-known observers of Mars). In some cases, it was apparently not the mechanical motion of an object which was observed, but rather optical displacement of condensation conditions, or visibility conditions [37] of a bright spot. However, this possibility forces a cautious approach to the more acceptable estimates of windspeeds on Mars made by the same method.

In late spring in the southern hemisphere, the direction of the seasonal wind changes from west to east [154]. This season is usually accompanied by appearance of a global haze and a halt in retreat of the polar cap boundaries. Examples of the influence of topography on atmospheric circulation have been noted.

The mode of the general circulation, according to Miyamoto, is near symmetrical, whereas Tang [235] concluded that such a mode would not be stable on Mars, and that rather a wave mode should predominate.

#### *Luminescence of the Upper Atmosphere and Parameters of the Ionosphere*

Hard solar radiation causes ultraviolet luminescence of the upper atmosphere of Mars, brightest in the Cameron bands of CO ( $\lambda$  1900–2700 Å, up to 300 kR) [231]. Other bright emissions have been observed by Mariner 6, 7, and 9 [15, 230] (Fig. 16) and Mars 2 and 3 [40].

The data of on-board and terrestrial spectrometry, in combination with radio occultation measurements, have served as a basis for constructing a model of the composition and structure of the ionosphere and upper atmosphere of Mars [16] in the altitude range from 100 to 230 km, i.e., practically up to the lower boundary of the exosphere. The most important component of the martian ionosphere, according to UV spectrometry performed by Mariner 9, is nothing other than  $O_2^+$ , while  $CO_2^+$  is a secondary component. OI and HI are also present, at relative concentrations at the 135-km level of  $10^{-2}$  and  $10^{-6}$  respectively [16].

The results of radio occultation experiments by Mars 2 and Mariner 9 [101, 103] confirm the existence and refine the parameters of the martian atmosphere, observed earlier by Mariner 4, 6, and 7 flyby spacecraft.

At 134–140 km from the surface of Mars with zenith scattering of the Sun at about  $50^\circ$ , the electron ( $e$ ) concentration is  $(1.5-1.7) \cdot 10^5 e \cdot cm^{-3}$ , which correlates with the flux of shortwave solar radiation measured on the Earth. Furthermore, it is reported by Kolosov et al. [103] that observations by Mars 2 determined a second maximum at an altitude of 110 km with a concentration of  $7 \cdot 10^4 e \cdot cm^{-3}$ .

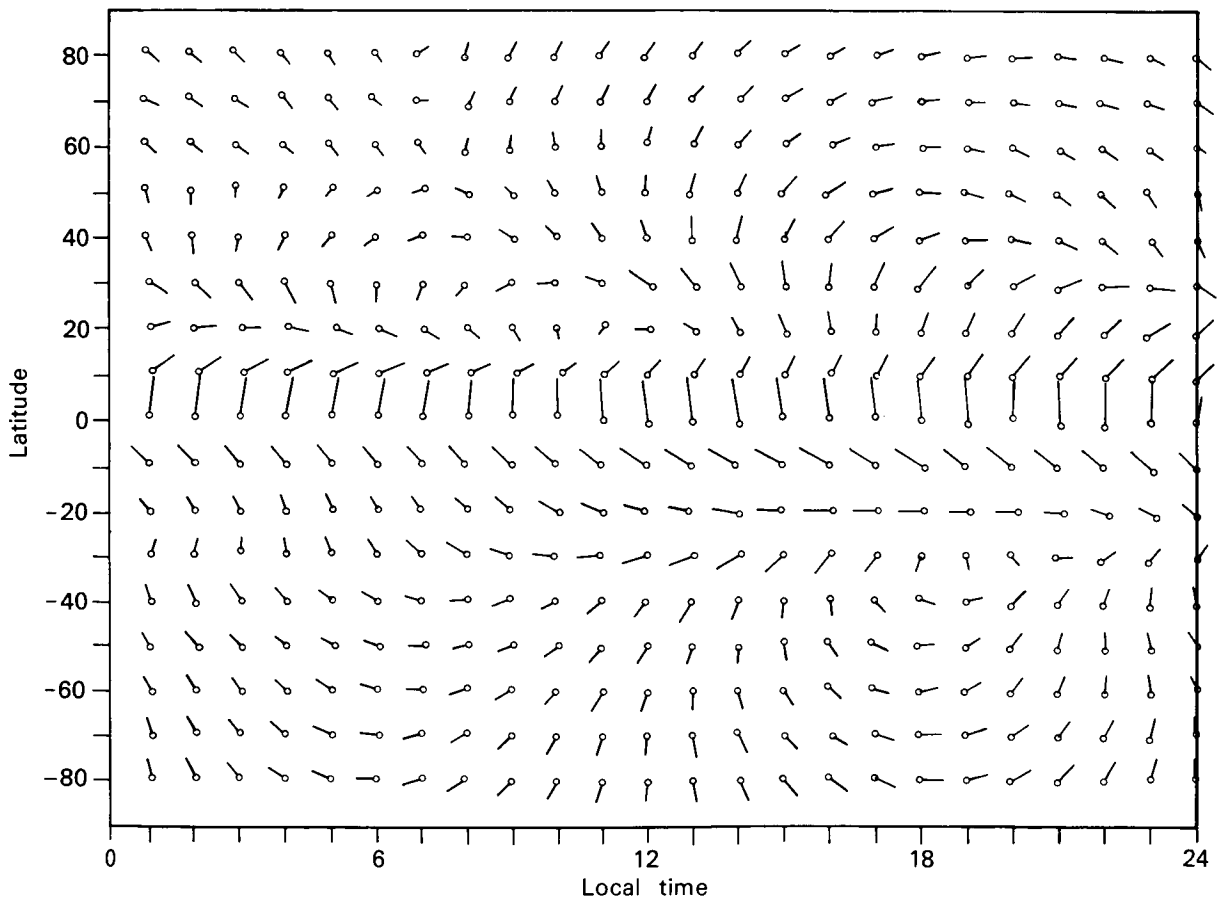


FIGURE 15.—Field of martian winds at 2.2 mbar atmospheric pressure level during global dust storm, calculated on the basis of temperature model of the atmosphere. Initial assumptions: hydrostatic equilibrium; smoothness of Mars; constant pressure at base of atmosphere. Direction and speed of wind shown by vectors departing from points. Length of vector equal to distance between two neighboring points corresponding to windspeed of 50 m/s.

*Concentration and Temperature  
of Neutral Hydrogen and Its  
Dissipation From the Exosphere*

The height distribution and atomic concentration of neutral hydrogen was determined by measurements of luminescence intensity of the higher layers of the Mars atmosphere in the spectral line  $L\alpha$  (121 Å). This was observed from Mariner 6 and 7 in 1969, and Mars 2 and 3, and Mariner 9 in 1971. If the concentration of atoms at the critical level (on Mars at a height of 230 km) and the average thermal speed  $\bar{v}$  of atoms in the exosphere (according to data of cosmic Mars probes) are known, it is possible to calculate the flow,  $F$ , of hydrogen atoms slipping away from Mars, according to Jean's equation:

$$F = n \cdot (\bar{v}/4) \cdot (Eg/Ek + 1) \exp(-Eg/Ek) \quad (3)$$

where  $Eg$  is the gravitation energy, equal to 0.123 eV for hydrogen atoms on Mars, and  $Ek = kT$  is the value which is proportional to the kinetic

energy of atoms. Using temperature  $T = 350^\circ$  K and density  $n = 3 \cdot 10^4 \cdot \text{cm}^{-3}$ , according to measurements of 1969, Barth and others [16] obtained a flow of dissipating hydrogen atoms  $F = 2 \cdot 10^8$  of atoms  $\cdot \text{cm}^{-2} \cdot \text{s}^{-1}$ . Observations of 1971 showed a lower temperature at the base of the exosphere than in 1969: according to data of Mariner 9 ( $325^\circ$  K) [16] and of Mars 2 and 3 ( $315^\circ$  K) [50].

Values used for calculating the flow of dissipating particles, obviously, may contain many errors. For example, Soviet specialists found the concentration of neutral hydrogen atoms in 1971 lower, but according to US calculations, it was greater than in 1969. Temperature, in turn, was measured along a vertical distribution scale of concentration. Izakov [90] showed that the temperature found by this method contained an error  $\pm 30^\circ$ - $50^\circ$  K, which, under certain conditions, reached  $100^\circ$  K. Contemporary assessments of dissipation speed based on such approx-

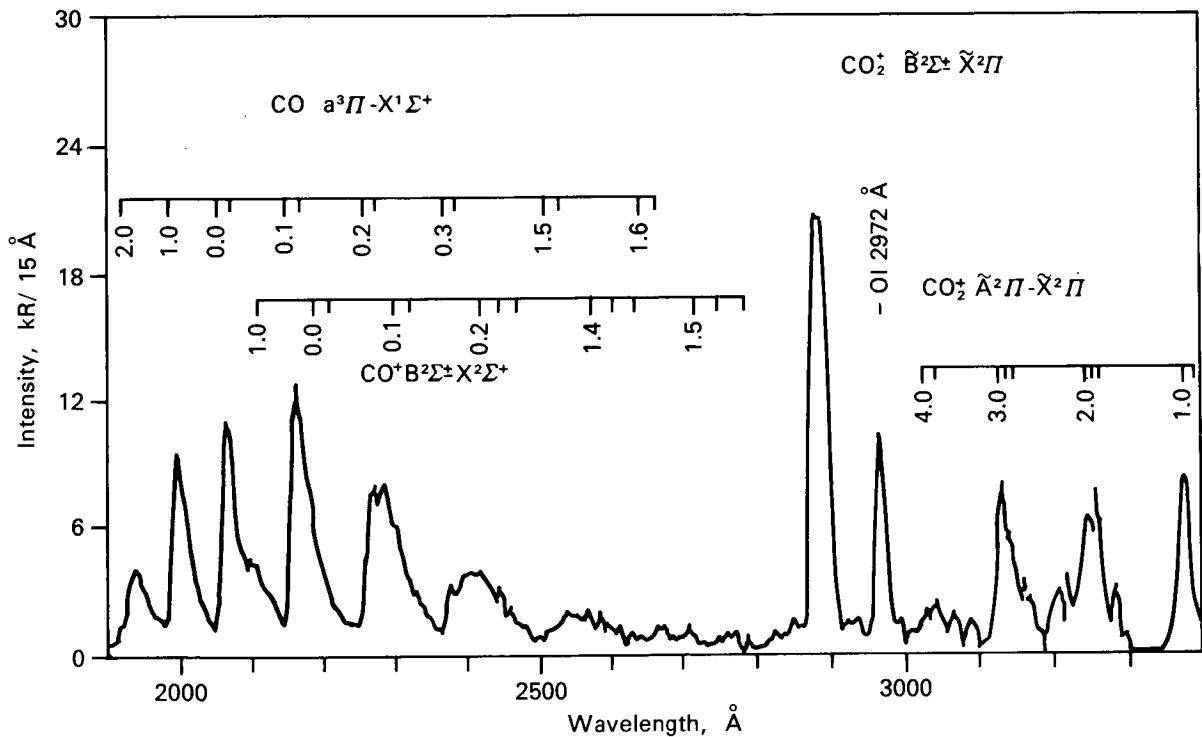


FIGURE 16.—Ultraviolet spectrum of atmosphere day glow of Mars, average of 120 recordings from Mariner 9 in November-December 1971. Cameron bands of CO, first negative system of bands of  $\text{CO}_2^+$ , intensive doublet and band of  $\text{C}_2^+$  and line of neutral atomic oxygen identified.

imate values probably cannot be used as a reliable basis for far reaching conclusions, e.g., determining how much water Mars could lose during its entire history.

### *The Surface of Mars*

*Surface temperature and thermophysical properties of the soil.* The temperature indicator is the natural thermal radiation intensity of the surface in areas of the spectrum where reflected solar radiation can be ignored. The results of ground measurements which agree satisfactorily with more detailed current data are graphically illustrated in Figure 17 (borrowed from [168]). Ground measurements of the martian temperature and of some parts of its surface can be carried out only with sufficiently large telescopes, and require the solution of considerable technological difficulties. Cosmic probes sent to Mars by the USSR and the US made it possible to come close to the planet by a factor of 50 000 which brought about a multiple enlargement of the quantity, and improvement of the quality, of data from initial observations. The advantage of the new data about the martian temperature is the low range amounting to several dozens of kilometers, and in some cases only 15 km—considerably different from  $10^3$  km for observations taken with the ground telescope. Temperature measurements, as well as studies of other martian features, indicate severe natural conditions.

It is very cold on Mars, from the point of view of inhabitants of moderate climatic belts of the Earth. Even in the tropics, there is a hard freeze each night, and the Sun's rays heat the surface above the freezing point only during the day. The maximum temperature is observed just after noon, reaching  $300^{\circ}$ – $305^{\circ}$  K in some areas; by evening (but still 2 hours before sundown), the surface cools to the point where frost is formed, and at night the temperature drops below  $200^{\circ}$  K. This is near the Equator. The sharp diurnal variations in surface temperature are attenuated beneath the outer layer of matter; at a depth of a few dozen centimeters, they are practically nil. The average day temperature is negative everywhere, with the exception, perhaps, of small geothermal segments (their possible existence on Mars will be discussed later). In the polar

zones, it is significantly colder than in the tropical belt, which would be expected; in winter, temperatures of around  $150^{\circ}$  K have been recorded here. This value is near the point of  $\text{CO}_2$  condensation under the conditions on Mars.

The thermophysical properties of the external martian cover (at least on a considerable part of the surface) are determined first by the fact that this cover consists of a finely ground substance. High dispersion of the substance is confirmed by the formation of dust clouds, by ground polarimetric observations, and by comparison of the surface temperature daily curve with the insolation regime. Temperature fluctuations in amplitude and stage correspond to the coefficient of thermal inertia which is characteristic for sand soil, and smaller, by far, than for rock. The conclusions of Soviet and US specialists about the thermophysical perimeters of martian soil, based on measurements from spacecraft, are in good agreement.

Radiometric observations from Mars 3 in a range of  $8$ – $40 \mu\text{m}$  can be interpreted within the framework of a homogeneous soil model which has these characteristics [162]: integral albedo is  $0.15 \leq A_i \leq 0.25$ ; heat inertia is  $0.004 \leq (\rho c)^{1/2} \leq 0.008 \text{ cal} \cdot \text{grad}^{-1} \cdot \text{cm}^{-2} \cdot \text{s}^{-1/2}$  (the last value is characteristic for crushed soil with average particle sizes from  $0.01$ – $0.05$  cm); and the depth of heat wave penetration amounts to  $4$ – $7$  cm. Dark fields are systematically warmer than light fields. No correlation between heat inertia and albedo was found, in opposition to the conclusions by Morrison and others [168]. Dots of increased heat inertia were found quite frequently which are probably connected with the fact that the route went through large craters. The limited accuracy of routing in this experiment lowers the reliability of comparing results with topography in relation to small details. More detailed data [99] resulted from infrared measurements from Mariner 9, carried out in two ranges;  $10$  and  $20 \mu\text{m}$ . The plotting of US results to topography was controlled by television. This essentially improved interpretation of radiometric data and made it possible, with analysis of soil thermophysical properties, to exclude “cold spots” from the study when correlation of such spots with local cloudiness was firmly established.

B  
C

For three large areas which differ greatly in visual albedo and are covered with craters, only small differences were found in the amplitude of daily temperature changes. In these cases, the absence of a connection between heat inertia and the reflective capacity in the visual part of the spectrum was established. On the contrary, the fields Syrtis Major and Masogaea showed a correlation between brightness and temperature. A 12-degree difference in midday temperature corresponds to a bolometric albedo difference of 0.1, whereas the difference of the visual reflective capacity in this case amounts to 0.15. In seeking limit values of the heat inertia of the soil in various martian regions, Kieffer and others [99] did not have an a priori method to select the corresponding regions for measurements. From all regions observed during the course of the experiment, Hellas is characterized by the smallest day variations of temperature. The heat inertia and the bolometric albedo for all observed fields do not go beyond the limits of these ranges:  $0.004 < I < 0.017$ ,  $0.2 \leq A_i \leq 0.4$ . Average particle sizes,

calculated according to the inertia value, are within limits from 0.006 to 0.5 cm [99].

One of the tasks of the infrared radiometer experiment on Mariner 9 was to look for volcanic activity. The temperature did not exceed 300° K in any part on Mars; it must be kept in mind that the registered temperature is lower than the real temperature if the "hot spot" occupies only part of the radiometer's field of vision. A lava lake with a temperature of 1500° K could be found from a height of about 2000 km only if the sizes were greater than 0.5 km; a 200-m lava lake will raise the radiometer indications only by 3° K. The probability of recognizing such details on Mars is very low; it depends considerably on both the size and temperature of "hot spots."

Local temperature deviations in some parts of the surrounding background temperature registered by Mariner 9 can be explained (according to conclusions of Kieffer and others [99]) as consequences of insignificant variations of heat inertia, of the bolometric albedo, or by topographical deviations of the surface from the local

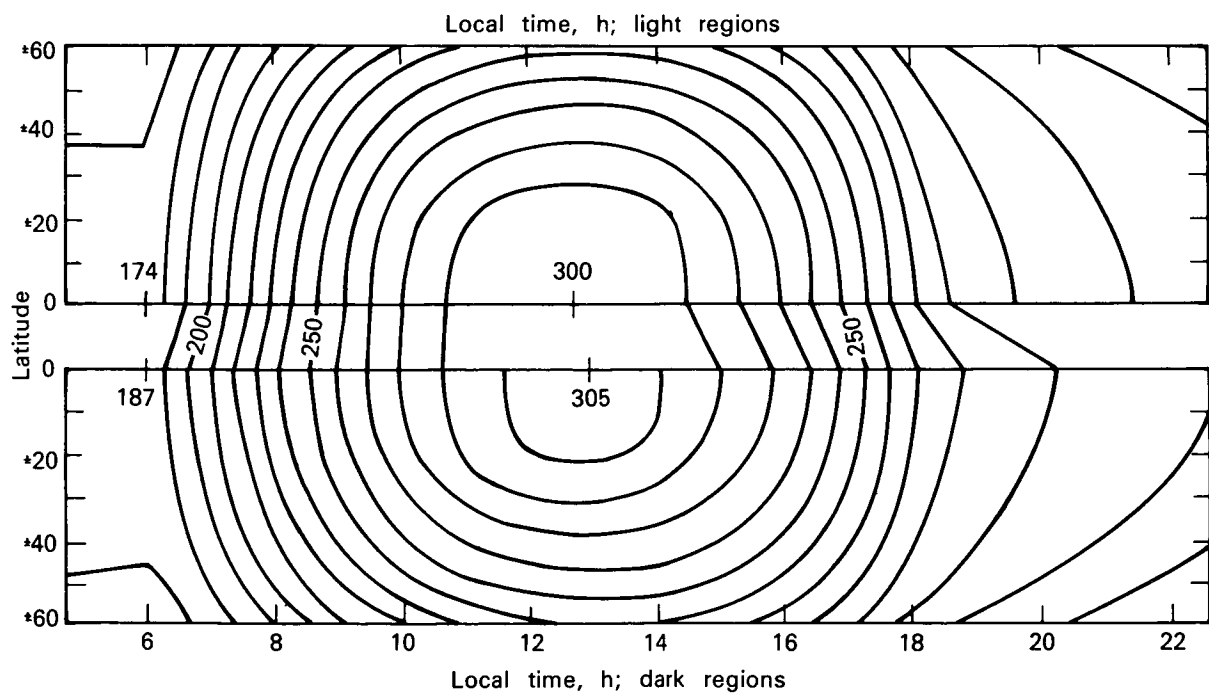


FIGURE 17.—Latitude distribution of temperature in light and dark areas of Mars surface as a function of local time (during season of Equinox, spring in southern hemisphere) determined by Morrison, Sagan, and Pollack [168] by processing of radiometric observations of Sinton and Strong [224].

horizontal, without attracting internal energy sources. However, if the same authors' ideas are taken into consideration about the difficulties in recognizing lava lakes of small area (particularly of simply warm parts), it would be incorrect to assume that the present data exclude the presence of such details on Mars. That they were not found does not negate their existence.

*Mineral composition of the Mars surface.* Meteorite material should have enriched the outer cover of Mars with iron. The reddish color of the surface of the planet is sometimes considered to result from at least an admixture of hydrated oxides of iron. Ocherous limonite was first named [54, 217]. Hematite or goethite, but not limonite, was shown to be formed under the conditions present [232]. Stinton's results contradict the "limonite" hypothesis; only a slight percentage content of iron oxide could be present [223]. Infrared spectroscopy data on-board Mariner 9 indicate that the dust raised by Mars surface wind contains silicon; its abundance corresponds to the content of  $60\% \pm 10\%$   $\text{SiO}_2$  [75], i.e., it is approximately equivalent to the abundance in the terrestrial desert sands [178].

*Surface albedo—light and dark areas relative to biological activity.* The monochromatic geometric albedo of the full disk of Mars in the visual area of the spectrum rises steeply from 0.05 in the violet to 0.25 in the red area, reaching its maximum of 0.30 around  $\lambda = 0.8 \mu\text{m}$ , then falling off slowly with further increases in wavelength of reflected radiation [158]. The reflective properties of various sectors on the Mars surface differ. The maximum geometric albedo for Arabia, one of the lightest areas, is 0.43—three times higher than for the dark area Syrtis Major [148]. The light areas, the so-called continents, occupy some two-thirds of the planet's surface on maps of Mars based on surface telescopic observations. Not more than one-third of the surface is covered with dark areas, earlier given the Latin names of seas, bays, lakes, and swamps, borrowed from geography and ancient Greek mythology. It is not necessary to explain that a classification consisting of bodies of water and continents is arbitrary, which is true for the lunar "seas" which contain no water.

The spectral reflective capacity of the light

areas and yellow clouds has been found similar, prompting the conclusion that the light areas are covered with a layer of fine powder, which is easily raised by the wind. However, the albedo of clouds of fine particles might be higher than the albedo of a surface made of the same material.

In regard to the nature of the dark areas, there is no single opinion. Since the publication by Lowell [128], containing the alluring but unconfirmed hypothesis of possible artificial origin of martian "canals," the probable relationship of the dark areas to biological activity on Mars has been discussed in various versions. Proponents of this idea base arguments on the obvious fact that a covering of plantlike organisms should be rather dark, since plants utilize the energy of solar rays and, furthermore, can make shade. The properties of the martian dark areas, which are difficult to explain, are frequently among the arguments set forth in favor of the hypothesis of a martian biosphere. For example, it has been reported that the dark areas which disappear in the yellow haze during dust storms reappear in the same locations when the atmosphere clears. The question is: Why are they not covered by a layer of the light material which falls to the surface as the dust storm dies? Furthermore, it has been established recently that outlines of the classical shaded areas, in many cases, have no relationship to the boundaries of different relief forms [34]. However, the most important argument is the long-discussed variability of the dark areas. Many works have been dedicated to rather fruitless discussion, as yet, of the causes of their curious behavior; significantly fewer works to careful and qualified observation of variability properties. Of what does it consist?

According to terrestrial telescopic observations [4],

The outlines of the dark areas are stable on the average, but in some places they change quite strongly in intensity and extent. The reality of these changes, doubted by Secci, was established by Flammarion; in some cases, the changes are secular in nature, but they may be seasonal as well.

Antoniadi [4] presents examples of various

types of changes, indicating that the broad, most clearly visible dark area, Syrtis Major, undergoes seasonal changes. However, this effect may be related to selectivity of the observations, since the expansion season of this detail correlates with increasing distance to Mars and increased minimum linear dimensions of parts studied near the threshold of angular resolution.

New facts concerning the secular and irregular changes were determined by de Mottoni on the basis of extensive observational material [169]. It should be noted here that in most cases it is possible to speak only of changes in the contrast of a given area with the surrounding background. Furthermore, Dollfus noted seasonal changes in polarization of both dark and light areas. In spring and early summer, an anomalous negative polarization is observed [46].

In considering the problem of Mars dark areas, it is, unfortunately, not always possible to separate solidly known facts from insufficiently confirmed opinions. Following the great opposition of 1909, a report on a seasonal darkening of the dark details on the Mars surface was widely published. Scientists, assuming the possibility of life on Mars, noted the external similarity of the martian "wave of darkening" to the annual development of vegetation oases. The martian "wave of darkening" became so popular, due to great repetition in the popular scientific literature over many years, that it began to be treated as a well-known fact. However, this is not quite correct. A recent attempt by Davydov to determine the seasonal course peculiarities of the "wave of darkening," on the basis of 200 of the best available terrestrial photographs from those published by various observers in the 1907–1971 interval, showed no such clear seasonal change. Apparently, the question not only of the causes, but also of the basic properties (including the regularity) of changes in the optical characteristics of the dark areas, must be considered insufficiently studied. Long series of spectrometric observations excluding optical illusions based on physiological properties of vision are required here. However, even by replacing the eye with the instrument, the influence of quality variability of the telescope image cannot be excluded; it depends greatly on

the turbulent motion of the air over the path of the beam through the Earth's atmosphere.

A terrestrial spectrometric comparison of dark and light areas of Mars in the spectral band from 0.3 to 2.5  $\mu\text{m}$  was made [148]. The light area became brighter and redder in 2 months, whereas the dark area remained the same. The changes determined differ from those which might be caused by the traditional "wave of darkening." However, even after determining falseness of the "wave of darkening" concept, the nature of the dark areas remains puzzling and requires careful study.

When attempts were made to compare the optical characteristics of the dark areas on Mars to the optical properties of terrestrial vegetation and organic substances [222, 237], and were discussed [194, 233], a parallel search was undertaken for an abiogenic mechanism for the changes in the dark areas. Many different explanations which were suggested are briefly reviewed [158]. For example, Cohen [25] relates the color of the dark areas and yellow clouds to coloration of chemical interaction products between Fe and CO:  $\text{Fe}(\text{CO})_5$  is yellow,  $\text{Fe}_2(\text{CO})_9$  is orange,  $\text{Fe}_3(\text{CO})_{12}$  is green.

The most acceptable criterion in recent years permits differentiating one group of similar hypotheses relating the variable surface properties of the dark areas to weathering and wind transfer processes of crushed material. The light products of weathering are periodically carried away by trade winds [216]. In summer, the dark surface is uncovered, which might serve as a reason for the anomalous polarization. A hypothesis was developed by Sagan and Pollack [208] on changes in dimensions of surface particles of certain Mars areas under the influence of seasonal variations in wind mode. Irregular changes in the dark spots are explained by the light dust blowing away from the dark surface (cf Sharonov hypothesis, using the same method to explain regular changes). These models are based on the conclusion that the dark areas are elevated and that the light areas are lower in elevation. However, radar does not confirm the existence of either this regularity or the reverse.

A new modification of an old idea developed in 1972. The visibility of the dark areas on Mars

probably changes only as a result of changes in dustiness or transparency of the martian atmosphere due to local seasonal variations in wind-speed. While this thought is interesting, it does not provide a final solution to the problem, since variations in transparency alone cannot explain the occasional appearance of new dark areas, not previously observed.

New information, bringing us closer to an understanding of the nature of the dark areas, resulted from the televised photograph of Mars by Mariner 9 (Fig. 18). The large dark area, Syrtis Major, on photographs taken from an altitude less than 2000 km, consisted of numerous dark "plumose" spots as well as light and dark bands which extend for tens, sometimes hundreds of kilometers with no topographic relief—even in photographs with the best angular resolution [146, 209]. The light bands are longer and narrower than the dark bands; both generally originate in craters or projecting relief details, indicating that the bands originate with winds

that blow in stable directions. One Mariner 9 photograph shows, with high resolution, a dark spot covering a portion of the crater floor. Figure 18 indicates the dark area covered with details of identical orientation, similar to dunes formed by winds of stable direction. The dark spots detected in other craters are possibly of the same nature. However, there is no reason to assume that all varieties of dark spots on Mars are, without exception, dune fields. Sagan and colleagues [210] assume that dark surface areas are often outcroppings of solid rock in areas covered with light powder ash. They also assume that both light and dark mobile material exist on Mars. A comparison of the same spots on photographs made at different times allowed US specialists to determine changes in the albedo of individual sectors, in comparison to the albedo of neighboring areas within the field of vision. The characteristic time of changes is not more than 2 weeks. The appearance of new bright bands or disappearance of old ones was not observed.

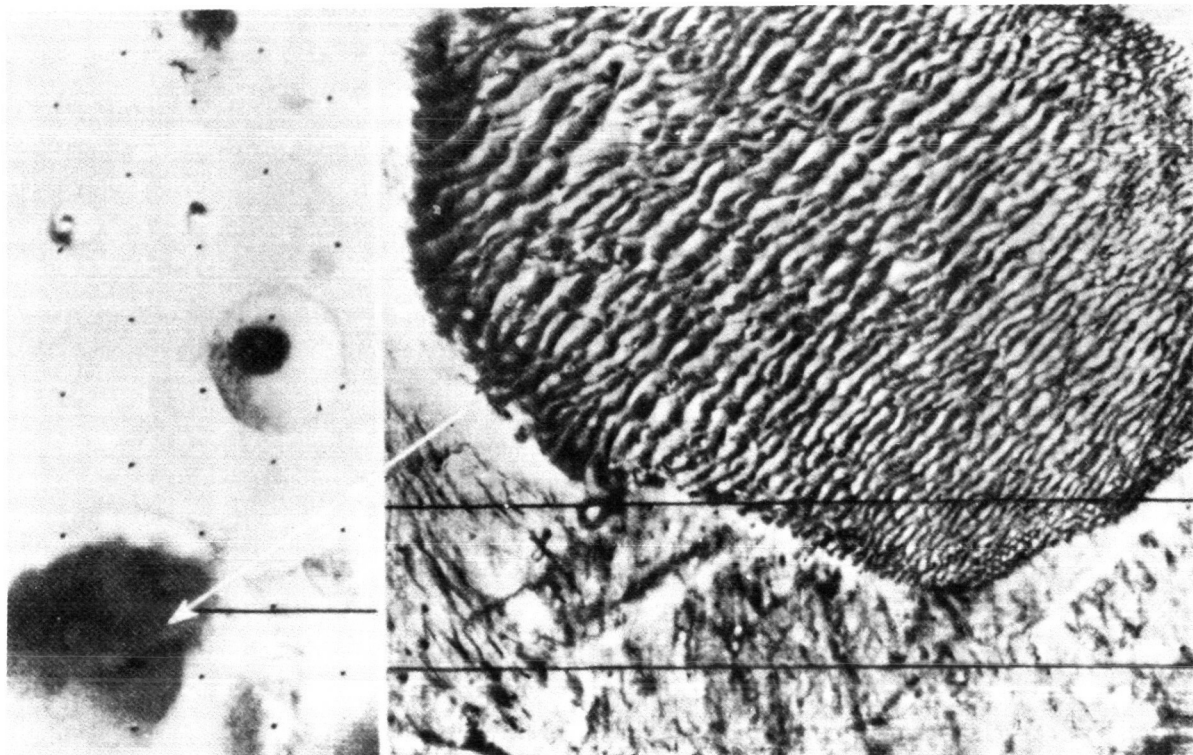


FIGURE 18.—Section of bottom of a 150-km crater in a region of hellespontus in zero-angle camera of Mariner 9. Photograph of a surface covered with dunes taken with wide-angle camera appears as very dark spot.

A review of the published photographs shows that the most noticeable changes are increases in area due to movement of dark spot boundaries, with conservation of all fine structure details unchanged within the limits of the previous boundaries. Sagan and colleagues defend the wind-dust genesis of the spots and bands and their changes with time [209]. They suggest that local changes in spots and bands cause the classical seasonal and secular changes in albedo of the Martian dark areas.

*Martian "canals."* The series of unusually straight, geometric lines observed on Mars are the result of a complex and insufficiently studied optical illusion, arising not only during visual observations, but also during photography of Mars through weak telescopes or with poor image quality. This can now be stated with assurance. The photographs from spacecraft show no network of "canals" on Mars. However, quasilinear natural formations are present, among which the large ones are not sufficiently regular and the small ones could not possibly be seen from Earth under any conditions.

*Polar caps.* A white spot around the pole can be clearly seen through a telescope in the winter hemisphere of the planet. Only a small part of the Mars polar cap is observable; its greater mass is located in the field of the polar night, in colder regions. In the spring and early summer, the white cap decreases rapidly in size, but another appears at the opposite pole, where winter is beginning. The process of fall and winter growth of the polar cap is usually obscured by a continuous layer of clouds, which arises at this time over the polar area.

The north polar cap is not as large as the south polar cap, which has a mean diameter by mid-winter of 3500 km, sometimes exceeding 5000 km. However, the huge south polar cap disappears almost completely during spring and summer, whereas the north polar cap shrinks more slowly and its remainder (varying from year to year) always exceeds 350 km diameter, according to ground observations. These differences are connected with insolation characteristics, discussed in a previous section, *Parameters of Axial Rotation and the Martian Seasons*.

In the late 19th century and the early 20th, it

was assumed that the polar caps of Mars consisted of ice and snow, and their spring thaw was the main source of moisture for the hypothetical martian biosphere. However, after spectroscopic observations showed the paucity of water vapor in the martian atmosphere, the opinion concerning the white polar cover changed: it was assumed to be a thin layer of water frost. The results of spectrophotometry indicated the presence of ice crystals. More recent data changed basically the classical concept of the nature of Mars polar caps. Mathematical modeling, followed by significant improvements in the spatial resolving capacity of instruments used for radiometric measurements of the Mars surface temperature, combined with results of spectrometry, showed that carbon dioxide is included in the composition of the white polar cover. Some specialists believe that the heart of the polar cap is made of ice, which may be covered by solid carbon dioxide during the winter. Carbon dioxide clathrates are probably present.

During the spring and summer reduction of the polar cap size, a dark border, several hundreds of kilometers wide, is observed around the polar cap; the reality of the dark border has been confirmed by Mariner 9 photographs. Certain specialists have thought that the dark border results from increased moisture in the soil due to thawing of glaciers. However, this connection could not be direct, only indirect, since the horizontal surface temperature at this point is below freezing, with only slopes that are turned toward the Sun rising above the freezing point. Sagan and colleagues suggested a hypothesis [210] for the development of the dark border: the possibility of light dust blowing away from the dark soil by the winds which are caused by temperature difference between the polar cap and its surroundings.

### The Relief of Mars

#### Methods of Altitude Measurement

The surface of Mars is mostly smooth and possibly quite free of slopes, according to recent assumption. No mountain shadows could be observed through telescopes; the lines of the twilight band between the day and night hemi-

spheres of the planet were smooth, without dark projections. Estimates of the upper limit of altitude of martian mountains with sharp shadows, which might remain unseen from the Earth, have been found to be too rough, which probably results from difficulties in accounting for atmospheric interference. New methods aid the astronomers. Radar observations of Mars from the Earth's surface permit measuring the distance to the subradar point (at the center of the planet's visible disk) with extremely high accuracy (down to  $\pm 75$  m) on the basis of delay time of the radio echo. The axial rotation of Mars causes the subradar point to shift along a single parallel. Continued operation of the radar set yields a profile of the planet's surface along the subradar parallel. As time passes, the aerographic latitude of the subradar point changes slowly; in this way, radar profiles of the martian relief have been made along several parallels [51, 181].

Radar, in principle, cannot compare the height of levels at points far apart on Mars, yielding only the altitude measured from the level of a sphere, the center of which corresponds to the center of the planet's mass. Also, any surface of equal altitudes (i.e., any gravitationally equipotential surface), from which the heights of mountains and depths of depressions on Mars could be measured, is definitely not precisely spherical, but rather will be quite complex in form, deviating up to 10 km from the approximation of a sphere. Comparisons of heights of radar profile details can be made only over a comparatively short sector without knowing the surface shape of equal altitudes.

Other methods, based on measurement of the gas content above the surface of Mars in a vertical column of unit cross section, can be used to relate all measured levels to a single common level for the entire planet. Obviously, there is more gas above a depression than above an elevated area. By comparing the atmospheric pressure over two different points, then using the known barometric formula, the difference can be found in levels (or difference in altitudes) of the planet's solid surface at the points observed. The surface heights produced by the barometric formula are barometric altitudes (or pressure altitudes); the method is barometric hypsometry.

The pressure at the surface (consequently, barometric altitude) can be found by at least three methods:

1. spectrometry based on peculiarities of the spectral lines;
2. scattering of light in the atmosphere;
3. the radio refraction method using spacecraft.

On-board hypsometry, using all these methods on Mariner 6, 7, and 9 as well as spectral hypsometry from terrestrial observatories and Mars 3, have yielded extensive material on which preliminary maps of Mars surface altitudes have been based [29, 80, 102].

What can be used as the zero altitude level on a planet which does not have such a convenient benchmark as "sea level"?

The origin of the reading has been taken as the 6.1 mbar barometric pressure level—the triple point of  $H_2O$ , corresponding to a reduction in boiling point of water to  $0^\circ C$ . Above this altitude level (i.e., at lower atmospheric pressures),  $H_2O$  can exist only as ice or vapor, whereas below this level it can exist as a liquid.

*Barometric altitude measurements.* There may be significant errors in measurements of barometric altitude resulting from variations in atmospheric pressure that are seasonal [30], diurnal [29], and meteorological [87], as well as a few unavoidable simplifications in the theory. The results produced at different moments in time do not belong to the same system of reference, since the zero level altitudes drift and the scale of altitude do not remain strictly constant. It is not possible at present to make corrections for many of these sources of error. Nevertheless, the method for measurement of barometric altitudes by measuring the atmospheric pressure both in the optical band (with preference to the long wave region of the spectrum, where aerosols have less influence) and in the radio-frequency band remains the only method for comparison of surface level altitudes at distant points on the planet, and production of such important relief characteristics as the full amplitude of altitudes.

*"Geological" forms on Mars.* Preliminary results of geological studies [146], based on television experiments by Mariner 9, 1971–1972, indicate that the surface of Mars is a result of a more

complex geological history than that of the Moon. Mars photographs show traces both of meteorite impacts and volcanic and tectonic activity, traces of many processes of surface erosion, movement, and sediment deposit.

#### *Main Types of Martian Relief [146]*

*Territories covered with craters.* Such territories are quite extensive on Mars, but are not the dominant type of surface, in contrast to the opinion formulated after the first Mars photographs by spacecraft. The morphology of craters and distribution by dimensions indicate that most are of meteorite origin. A few, possibly, are of volcanic origin, but such craters are difficult to distinguish from meteorite craters when both have been greatly altered.

*Mountainous territory.* One example of mountainous territory is the area from  $260^{\circ}$  to  $310^{\circ}$  west longitude along the 20th parallel in the southern hemisphere of Mars, which is multiple-peaked and has primarily smoothed mountains similar to the Apennine chain on the Moon. Volcanic mountains are also encountered on Mars, as well as high slopes of fault origin and waves of impact-explosive origin.

*Smooth planes.* Located around the higher relief forms, smooth planes occupy a significant portion of the northern hemisphere, as well as the surface of large basins in the central southern latitudes and floors of some very large craters. This relief form has several possible varieties, distinguished by one characteristic peculiarity: few or no traces of meteoritic bombardment.

*Volcanoes.* In the lower northern latitudes from  $90^{\circ}$  to  $140^{\circ}$  and around  $210^{\circ}$  west longitude (in the areas of Tharsis-Amazonis-Elysium), there are many volcanic domes. Four gigantic volcanic shields are among them, the largest (in volume) being in the area of Nix Olympica ( $18^{\circ}$ ,  $134^{\circ}$ ). A huge volcanic cone rises above it. At its peak, the caldera consists of several adjacent craters with floors at different levels (Fig. 19). The main crater, 65 km in diameter, is located at an altitude more than 25 km above the surrounding terrain or at an altitude of 29 km above the 6.1 mbar pressure level [81]. The foot of the mountain is of dark material, separated from the surrounding plain by steep cliffs, and the diameter

of its base is about 500 km. Nix Olympica is significantly larger than the world's largest volcanic formation, 225 km in diameter, in the Hawaiian Islands, with its main crater, Mauna Loa, being at an altitude of more than 4000 m above sea level and 9 km over the plane of the ocean floor.

Another of the highest Mars peaks, comparatively close to Nix Olympica, belongs to a volcano located at the center of a great dark spot, the middle spot ( $0^{\circ}$ ,  $112^{\circ}$ ). The caldera of the volcano rises 13.5 km above the level of the foot of the mountain, 19.2 km above the arbitrary zero level, and more than 23 km above the level of the lowest plains [75]. This caldera, 40 km in diameter, which has been photographed in large scale (Fig. 20), clearly shows vertical traces of slides and small meteorite craters on the inner slope of the circular rim. The bottom of the caldera is flat and smooth.

Around the volcanoes, many structures indicate an era of widespread volcanic activity following completion of the formation process of territory covered by the meteorite impact craters. A comparatively small volcanic complex was found beside the basic volcanic area, which, according to its type, shows special features. It is located in the Mare Tyrrhenum, approximately  $220^{\circ}$ ,  $253^{\circ}$ . A round depression in the center has a diameter of about 15 km, surrounded by a break crack, which outlines a territory of about



FIGURE 19.—Martian volcano Nix Olympica, 500 km in diameter at base. The edge of the volcanic shield is separated from adjacent plane by steep cliffs. Main crater, 65 km in diameter, is located at over 10 km altitude with several volcanic apertures. (Mariner 9 photograph)

45 km in diameter. Low mountain ridges and channels resembling the dandelion in design extend in radial directions for over 200 km. A broad channel, differing from other channels by its correct form, connects the central depression with the elliptic depression of similar size which is located 35 km to the southwest. Another volcanic formation with a broad channel, known on Mars, leaves the crater and becomes a sharply outlined depression. This complex is in the Ceraunius region next to  $24^{\circ}$ ,  $097^{\circ}$ —but in the latter case there is a typical volcanic dome.

The spectral search for volcanic gas, particularly water vapor, made by Mariner 9 in the calderas of martian volcanoes yielded no positive results. During the final stage of Mariner 9, infrared instruments indicated that the extensive white clouds near several of the volcanoes in the Tarsis area were composed of water ice.

*Grabens<sup>10</sup> and the Valley Marineris (Grand Canyon).* Some territories are cut by a network of wide, deep grabens—tracers of fractures and faults. The largest martian graben, the Grand (or Main) Canyon, extending for 2500 km in the region of Tithonius Lacus-Coprates-urorae Sinus-Eos, is 100–250 km wide. The canyon, in the area of Melas Lacus, is bordered by two trenches, the total width reaching 500 km. The slopes are cut by giant ravines (Fig. 21). Photographs along the Grand Canyon show chains of craters with no rims which appear to be strung along the great crack.

The depth of the Grand Canyon from the level of its edges is 6 km in some parts. The complex problem of removing rock from the canyon system has been noted [146]. Some of the material might have been carried along the canyon in the direction of the slope, from west to east; however, no details indicating such transfer have been discovered. Furthermore, on the north side of the canyon system a broad, deep, fully closed basin can be seen, which is, consequently, either a result of settling or removal of the material by the wind.

*Chaotic terrains* on Mars are in the form of large, isolated spots, containing blocks of rock intricately broken and split. The form is explained

by the outer layers settling after removal of material from beneath the surface. There are no known analogues on the Earth or Moon.

*Circular basins.* These have flat bottoms and are surrounded by mountain areas, reminiscent of giant craters. Formations of this type include, for example, Libya, Edom, Iapygia.

The greatest martian basin, Hellas, is some 1500 km in diameter, which is a depression, some 4 km below the 6.1 mbar barometric pressure level. Photographs made in 1969 and 1971 of the Hellas surface (or at least a significant part of it) indicate that it is unusually smooth, and different from neighboring regions. A few relief details can be distinguished only in the very border zone of the basin, close to mountainous areas. A drawing shows one crater close to the mountain and a small dome in the middle of a smooth plain [118]. At the same time, the cloud masses hiding the relief are clearly visible—not on this drawing, but on another of the same scale depicting a part 1000 km removed from here (Fig. 5). Leovy and

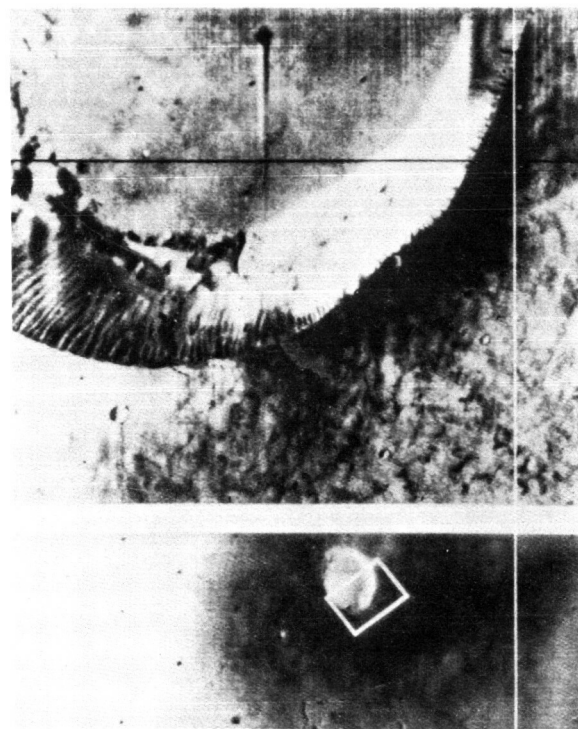


FIGURE 20.—Portion of rim and floor of a 40-km crater atop the highest martian peak in center of dark volcanic shield called middle spot. (Mariner 9 photograph)

<sup>10</sup>A graben is a trench limited by faults.

colleagues [118, 119] point out that the first of these areas looked completely smooth on all previous photographs. This is undoubtedly interesting but it is scarcely possible to generalize about the entire territory of the basin. It is not considered sufficient to propose a hypothesis that the absence of relief details in Hellas is an optical illusion; reasons for the absence of meteorite impact traces, which have severely bombarded neighboring areas, are not clear. Several different hypotheses have been set forth to explain the observed peculiarities of Hellas. Some specialists assume that clouds of dust exist here constantly [211], covering the true relief. Davydov's hypothesis [38] assumes that within Hellas there is a great water basin, covered with a solid layer of frost and wind sediment with a comparatively young outer surface. In this model, only small craters could be formed, the dimensions of which are small in comparison to the thickness of the

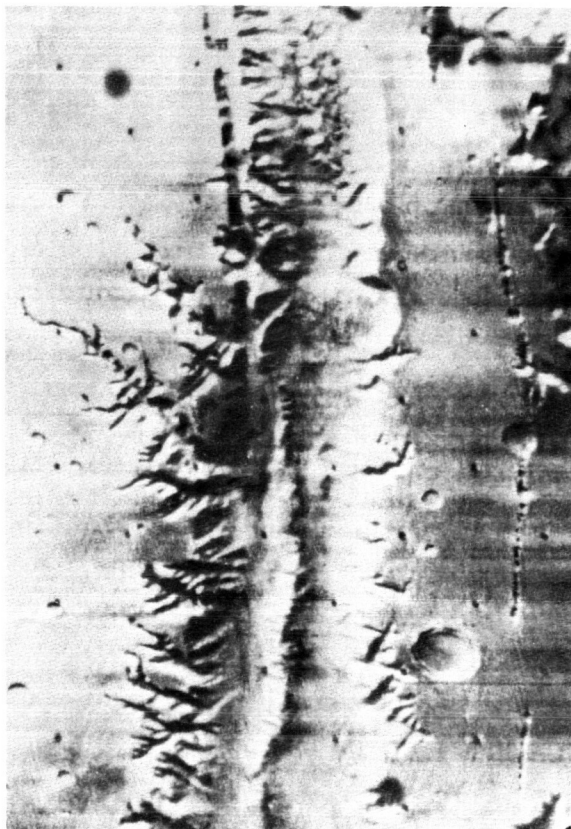


FIGURE 21.—Portion of the martian Grand Canyon. (Mariner 9 photograph)

solid crust on the surface of the water. A larger meteorite impact would cause a penetrating hole, which would be immediately filled with water to the Archimedes level, covered rapidly with ice, and in time "powdered" with dust.

*Streamlike formations.* According to current concepts, rivers could not flow on Mars at present—the mean daily surface temperature is below freezing in all climatic zones. Furthermore, due to the low atmospheric pressure, H<sub>2</sub>O can exist only as ice or vapor over the entire surface of Mars, except for depressions. Therefore, the discovery of channels, quite similar to riverbeds on the Earth, in photographs of Mariner 9, was quite surprising.

Figure 22 (a and b) shows three broad, winding valleys with "tributaries;" typical shoreline terraces, streambed sediments, and islands with their characteristic outlines are all visible on the photograph in Figure 22a. On the photograph in the valley (Fig. 22b), a dark "thread" several kilometers wide can be seen, i.e., hardly a Volga or Mississippi—probably traces of a streambed. Around all this, a typical martian scene: the ancient surface, broken over the centuries by young and old craters.

Several streamlike formations on Mars extend as much as 1500 km in length, and over 200 km in width. This is reality, and it requires an explanation which does not contradict other firmly established facts. To cut these streambeds would require a tremendous quantity of water or another liquid. It has been noted [146] that in addition to a stream of liquid, the possibility of erosion by a fluidized "solid-gas" system must be analyzed. The authors of this work assume that the source of the liquid more likely was the lithosphere rather than the atmosphere. This is indicated by some of the largest streambeds being found in the chaotic territory. In areas of elevated geothermal flow, the subsoil ice is probably thawed. The liquified material accumulates in a natural, impermeable reservoir until it bursts. Then, a brief but powerful flow develops. However, this idea requires further development [146].

Small streams are sometimes encountered in areas where the presence of ice beneath the surface is impossible, for example within me-

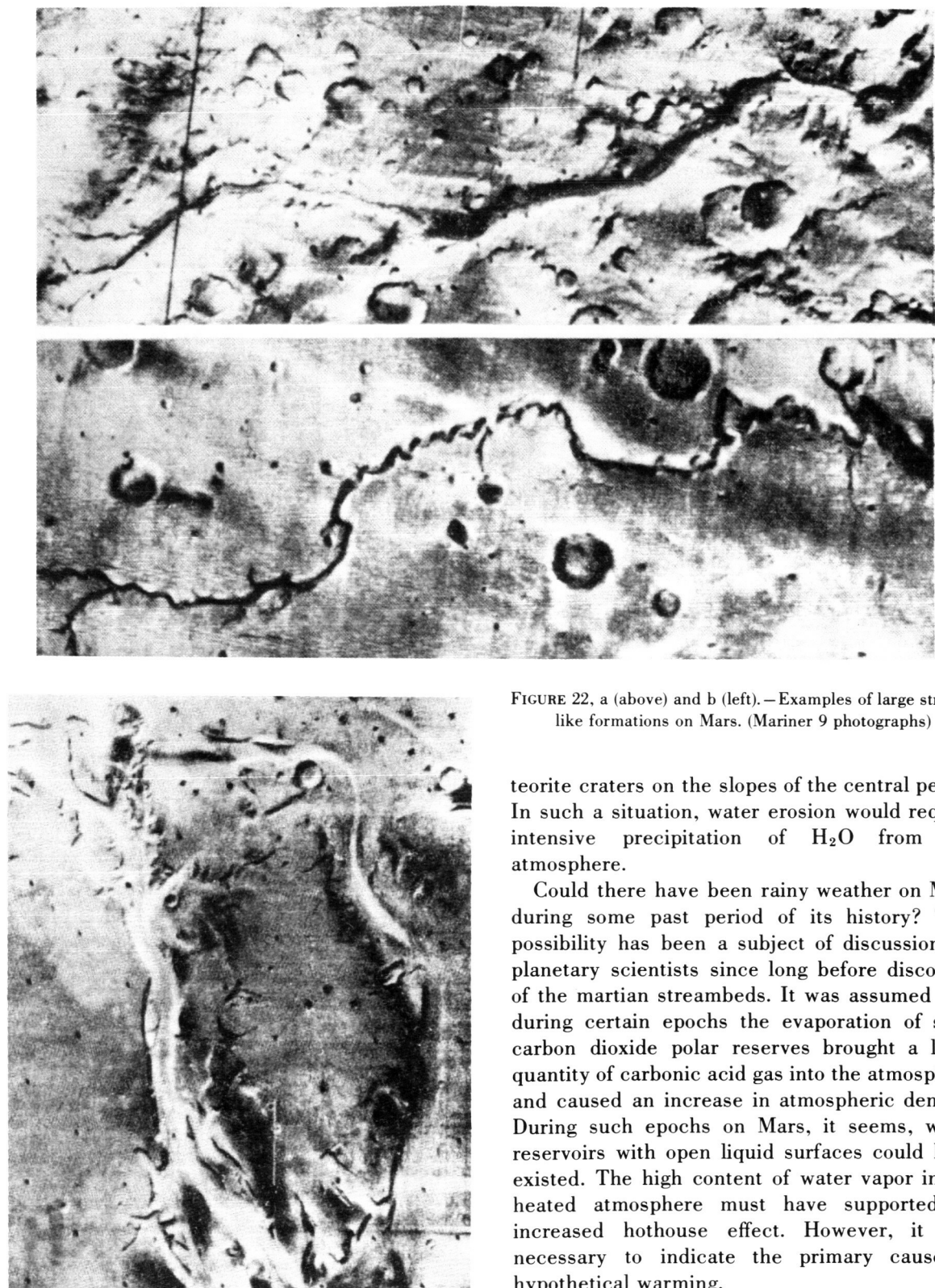


FIGURE 22, a (above) and b (left).—Examples of large stream-like formations on Mars. (Mariner 9 photographs)

teorite craters on the slopes of the central peaks. In such a situation, water erosion would require intensive precipitation of  $H_2O$  from the atmosphere.

Could there have been rainy weather on Mars during some past period of its history? This possibility has been a subject of discussion for planetary scientists since long before discovery of the martian streambeds. It was assumed that during certain epochs the evaporation of solid carbon dioxide polar reserves brought a large quantity of carbonic acid gas into the atmosphere and caused an increase in atmospheric density. During such epochs on Mars, it seems, water reservoirs with open liquid surfaces could have existed. The high content of water vapor in the heated atmosphere must have supported an increased hothouse effect. However, it was necessary to indicate the primary cause of hypothetical warming.

REPRODUCIBILITY OF THE  
ORIGINAL PAGE IS POOR

Studies were published in 1973 [173, 242] in which long, periodic changes of insolation on Mars were confirmed by sufficiently strict reasoning (cf. the section, *Parameters of Axial Rotation and the Martian Seasons*). Complicated changes of the insolation regime with the mutual imposition of several periods of cyclic recurrence permit the assumption that from time to time, there are epochs when the sums of the masses of the two martian polar caps become minimal. In this hypothesis, among other parameters, the possible amplitude of atmospheric pressure variations on Mars is not known, nor is the quantity of solid carbonic acid in the polar regions.

*Polar relief.* Original surface forms are encountered in the areas covered in winter by the polar caps. Even after the white cover retreats, the surface seems to be covered by multiple layers of sedimentation. These deposits give the impression of comparatively smooth polar relief, approximately the same in winter and summer, apparently replacing the depressions and covering the other varieties of geological structures observed in the lower latitudes.

### Water on the Planet

Spectral measurements indicate that the absolute content of water vapor in the martian atmosphere is very low (see section, *Chemical Composition of the Lower Atmosphere*). However, in some places during certain seasons, the relative humidity (RH) reaches 100%. From physics, it is known that the absolute quantity of water vapor in the atmosphere is limited by temperature, and at low temperatures, saturation occurs at extremely low absolute humidity. For this reason, the low content of moisture above the martian surface cannot be taken as a reliable indication of a shortage of water resources. It should be recalled that on Earth, water reserves are significantly greater than its content in the air.

The considerable quantity of H<sub>2</sub>O in the external layers of Mars can exist not only in the free state, but also in a chemically bonded and adsorbed state. Fanale and Cannon, basing their work on laboratory measurements of the adsorp-

tion of water vapors and other gases on ground basalt powders, concluded that the weathered products of geological rock on the martian surface may contain up to 15 g/cm<sup>2</sup> of adsorbed water. A decrease in atmospheric RH plus increased temperature during a day can bring about a partial desorption of H<sub>2</sub>O. From the point of view of contemporary geophysics, where the eruption of rock formed volcanic domes, a considerable quantity of water from martian depths must have been released. Most of the reserves of water on Mars at present may be concentrated in the layers of sediment in the form of permafrost [117] or, possibly, even in large bodies of water beneath a layer of permafrost [36], where the ordinary geothermal gradient would produce positive temperatures.

Certain peculiarities observed might indicate significant reserves of water in the outer layers of Mars:

- (a) streamlike formations;
- (b) indications of glaciers in the polar caps; and
- (c) large basins, at least in one of which is a completely smooth, sufficiently leveled low surface.

### Phobos and Deimos

The natural satellites of Mars were discovered visually by A. Hall through the US Naval Observatory telescope in 1877, and first photographed at the Pulkovo Observatory in 1896. They differ from the known satellites of all other planets in their extremely low altitude and small dimensions.

The information produced by terrestrial methods can be reduced primarily to determination and refinement of the parameters of orbital motion of Phobos and Deimos [221]. They revolve around Mars almost in the plane of the Equator. Phobos flies 70 times closer to the martian surface than the Moon to the Earth and makes a full orbital revolution each 7 h 39 min (sidereal period), i.e., more rapidly than the diurnal rotation of the planet. This is the only known case of this phenomenon in the solar system.

The unique photographs of the satellites of

Mars made by Mariner 9 [188] show that they are small, natural bodies; that they are not spherical; and in shape are more reminiscent of potatoes (Fig. 23). Phobos measures approximately  $21 \times 26$  km, Deimos— $12 \times 13\frac{1}{2}$  km. Both have the same albedo as basalts and carbonaceous chondrites. These two are the most abundant in the solar system in the relatively dark minerals. However, a selection cannot be made between them [188].

The surfaces of the Mars satellites show many craters, definitely of impact origin, since it is fundamentally impossible for centers of volcanism to exist within such tiny bodies. The largest crater on Phobos is 5.3 km in diameter. The power of an impact capable of forming such a crater is near the power necessary to destroy this satellite entirely.

The number of craters per unit surface area of Phobos and Deimos is approximately 100 times that of the surface of Mars. This indicates the effectiveness of the processes which smooth the relief on the surface of the planet, and the great age of its satellites.

Judging from the synchronism of the periods of axial rotation and of orbital rotation around the planet currently achieved, the last impact of a sizable meteorite on Phobos occurred more than  $10^6$  years ago, on Deimos— $10^8$  years ago.

### Again, the Problem of Life on Mars

Sufficient information has not been produced up to the present to prove the existence of biological activity on Mars. Whether the firmly established facts include any that could reliably

eliminate this possibility must be judged by biologists, not by astronomers. New information on Mars produced in 1971–1972 apparently has provided a foundation for further studies to solve this problem, which will be undertaken. There is hope that completion of this area of study will serve as a beginning for others to follow.

### Summary

Many problems related to the planets of the Earth group still await solution and are being solved at present by the combined efforts of astronomers and space scientists. Further growth of knowledge in this area will not only help to better understand the nature of our neighbors, but also will bring us closer to the solution of numerous geophysical problems, and thus broaden prospects to achieve results for the good of all mankind.

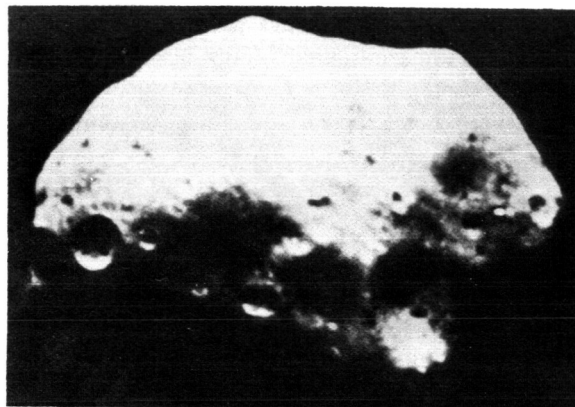


FIGURE 23.—The martian satellite Phobos.  
(Telephoto by Mariner 9)

### REFERENCES

1. ANDERSON, J. D., L. EFRON, and S. K. WONG. Martian mass and Earth-Moon mass ratio from coherent S-band tracking of Mariner 6 and 7. *Science* 167:277–279, 1970.
2. Anon. The velocity of light. *Sky Telesc.* 44(6):353, 365, 1972.
3. Anon. Venera 8, results of a space journey. *Pravda* No. 254(1972), 10 Sept., 1972.
4. ANTONIADI, E. M. *La Planète Mars*, Chap. 4–9. Paris, 1930. Transl. in, *Astronomy and Space*, Vol. 2, pp. 244–292. Newton Abbot, Engl., David & Charles;
5. ANTONIADI, E. M. *La Planète Mercure*. Paris, Gauthier-Villars, 1934. Transl. in, *Astronomy and Space*, Vol. 1, Pt. 1, pp. 43–64; Pt. 2, pp. 236–265; Pt. 3, pp. 348–374. Newton Abbot, Engl., David & Charles; New York, Neale Watson Academic Pubs., 1971/72.
6. ASH, M. E., D. B. CAMPBELL, R. B. DYCE, R. P. INGALLS, G. H. PETTENGILL, and I. I. SHAPIRO. Astronomical constants from analyses of inner-planet radar data. *Bull. Am. Astron. Soc.* 3(4, Pt. 1):474, 1971. (Abstr.)
7. ADVUYEVSKIY, V. S., M. Ya. MAROV, B. Ye. MOSHKIN,

New York, Neal Watson Academic Pubs., 1972.

- and A. P. EKONOMOV. Results of measurement of illumination in the atmosphere and on the surface of Venus by *Venera 8*. *Dokl. Akad Nauk SSSR* 210:799–802, 1973. Also in, *Astron. Astrophys. Abstr.* Pt. 1:230, 1973.
8. AVDUEVSKIY, V. S., M. Ya. MAROV, and M. K. ROZHDESTVENSKIY. Results of measurement of parameters of the atmosphere of Venus by the Soviet Probe *Venus 4*. *Kosm. Issled.* 7(3):233–246, 1969. (Transl: *Cosm. Res.*) 7(2):209–220, 1969.
  9. AVDUEVSKIY, V. S., M. Ya. MAROV, and M. K. ROZHDESTVENSKIY. Results of measurements of *Venera 5* and *Venera 6* and model of the atmosphere of Venus. *Kosm. Issled.* 8(6):871–881, 1970. A tentative model of the Venus atmosphere based on the measurements of *Veneras 5* and *6*. *J. Atmos. Sci.* (27):561–568, 1970.
  10. AVDUEVSKIY, V. S., F. S. ZAVELICH, M. Ya. MAROV, A. I. NOYKINA, and V. I. POLEZHAYEV. Numerical modeling of radiant-convective heat exchange in the atmosphere of Venus. *Kosm. Issled.* 9:280–291, 1971.
  11. BANKS, P. M., H. E. JOHNSON, and W. I. AXFORD. The atmosphere of Mercury. Comments. *Astrophys. Space Phys.* 2:214–220, 1970.
  12. BARABASHOV, N. P. *Priroda Nebesnykh tel i ikh Nablyudeniiye* (Transl: *The Nature of Heavenly Bodies and Their Observation*). Khar'kov, Khar'kov Univ. Press, 1969.
  13. BARKER, E. S. Detection of molecular oxygen in the Martian atmosphere. *Nature* 238(5365):447–448, 1972.
  14. BARTH, C. A. Interpretation of the Mariner 5 Lyman alpha measurements. *J. Atmos. Sci.* 25(1):564–567, 1968.
  15. BARTH, C. A., C. W. HORD, J. B. PEARCE, K. K. KELLY, G. P. ANDERSON, and A. I. STEWART. Mariner 6 and 7 ultraviolet spectrometer experiment: upper atmosphere data. *J. Geophys. Res.* 76:2213–2227, 1971.
  16. BARTH, C. A., A. I. STEWART, C. W. HORD, and A. L. LANE. Mariner 9 ultraviolet spectrometer experiment: Mars airglow spectroscopy and variations in Lyman alpha. *Icarus* 17:457–468, 1972.
  17. BROADFOOT, A. L., S. KUMAR, J. M. S. BELTON, and M. B. McELROY. Mercury's atmosphere from Mariner 10: preliminary results. *Science* 185:166–169, 1974.
  18. BULLEN, K. E. On internal structure of the planets. *Proc. Astron. Soc. Aust.* 1:2–3, 1967.
  19. CAIN, D. L., A. J. KLORE, B. L. SEIDEL, M. J. SYKES, and P. WOICESHYN. Approximations to the mean surface of Mars and Mars atmosphere using Mariner 9 occultations. *J. Geophys. Res.* 78:4352–4354, 1973.
  20. CAMICHEL, H., and A. DOLLFUS. La rotation et la cartographie de la planète Mercure (Transl: Rotation and cartography of the planet Mercury). *C. R. Acad. Sci. (B)* (Paris) 264:1765–1767, 1967.
  21. CAMICHEL, H., and A. DOLLFUS. La rotation et la cartographie de la planète Mercure (Transl: Rotation and cartography of the planet Mercury). *Icarus* 8:216–226, 1968.
  22. CAMPBELL, D. B., R. B. DYCE, R. P. INGALLS, G. H. PETTENGILL, and I. I. SHAPIRO. Venus: topography revealed by radar data. *Science* 175:514–515, 1972.
  23. CARPENTER, R. L. A radar determination of the rotation of Venus. *Astron. J.* 75(1):61–66, 1970.
  24. CHASE, S. C., E. D. MINER, D. MORRISON, G. MÜNCH, G. NEUGEBAUER, and M. SCHROEDER. Preliminary infrared radiometry of the night side of Mercury from Mariner 10. *Science* 185:142–145, 1974.
  25. COHEN, A. J. Seasonal color changes on Mars. *Astron. J.* 71:849–850, 1966. (Abstr.)
  26. COLOMBO, G. Rotational period of the planet Mercury. *Nature* 208:575, 1965.
  27. CONNES, P., J. CONNES, W. S. BENEDICT, and L. D. KAPLAN. Traces of HCl and HF in the atmosphere of Venus. *Astrophys. J.* 147(3):1230–1237, 1967.
  28. CONNES, P., J. CONNES, L. D. KAPLAN, and W. S. BENEDICT. Carbon monoxide in the Venus atmosphere. *Astrophys. J.* 152(3):731–743, 1968.
  29. CONRATH, B., R. CURRAN, R. HANEL, V. KUNDE, W. MAGUIRE, J. PEARL, J. PIRRAGLIA, J. WELKER, and T. BURKE. Atmospheric and surface properties of Mars obtained by infrared spectroscopy on Mariner 9. In, *Mariner Mars 1971 Project*, Vol. 4, pp. 299–213. Pasadena, Calif., Calif. Inst. Tech., Jet Propul. Lab., 1973. (NASA CR-135530; JPL-TR-32-1550-Vol. 4)
  30. CROSS, C. A. The heat balance of the Martian polar caps. *Icarus* 15:110–114, 1971.
  31. CRUIKSHANK, D. P. Sulphur compounds in the atmosphere of Venus. II: Upper limit for the abundance of COS and H<sub>2</sub>S. In, Kuiper, G. P., Ed. *Communications of the Lunar and Planetary Laboratory*, Vol. 6, Pt. 3, No. 97, pp. 199–200. Tucson, Ariz., Univ. Ariz., 1967. (NASA CR-97962)
  32. CRUIKSHANK, D. P., and C. R. CHAPMAN. Mercury's rotation and visual observations. *Sky Telesc.* 34:24–26, 1967.
  33. CRUIKSHANK, D. P., and G. P. KUIPER. Sulphur compounds in the atmosphere of Venus. I: An upper limit for the abundance of SO<sub>2</sub>. In, Kuiper, G. P., Ed. *Communications of the Lunar and Planetary Laboratory*, Vol. 6, Pt. 3, No. 97, pp. 195–197. Tucson, Ariz., Univ. Ariz., 1967. (NASA CR-97962)
  34. CUTTS, J. A., L. A. SODERBLOM, R. P. SHARP, B. A. SMITH, and B. C. MURRAY. The surface of Mars 3. Light and dark markings. *J. Geophys. Res.* 76:343–356, 1971.
  35. DALGARNO, A., and M. B. McELROY. Mars—is nitrogen present? *Science* 170:167–168, 1970.
  36. DAVYDOV, V. D. The behavior of the hydrosphere under the conditions of Mars and its observed manifestations. *Vopr. Kosmog.* (7):142–166, 1960.
  37. DAVYDOV, V. D. Halo-phenomena in the atmosphere of Mars in ice and unknown crystals. *Astron. Zh.* 47:172–178, 1970. (Transl: *Sov. Astron. AJ* 14:139–144, 1970.)
  38. DAVYDOV, V. D. The nature of the hellas area on Mars. *Astron. Vestn.* (5):232–239, 1971.
  39. DAVYDOV, V. D. Criteria of the presence of H<sub>2</sub>O crystals on Mars. *Fizika Luny i Planet* (Transl: *Physics of the*

- Moon and Planets*), pp. 423–424, Moscow, Nauka, 1972.
40. DEMENTYEVA, N. N., V. G. KURT, A. S. SMIRNOV, L. G. TITARCHUK, and S. D. CHUVAHIN. Preliminary results of measurements of UV emissions scattered in the Martian upper atmosphere. *Icarus* 17:475–483, 1972.
  41. DICKINSON, R. E. Infrared radiative heating and cooling in the Venusian mesosphere. I: Global mean radiative equilibrium. *J. Atmos. Sci.* 29:1531–1556, 1972.
  42. DICKINSON, R. E., and E. C. RIDLEY. Numerical solution for the composition of a thermosphere in the presence of a steady subsolar-to-antisolar circulation with application to Venus. *J. Atmos. Sci.* 29:1557–1570, 1972.
  43. DOLGINOV, Sh. Sh., Ye. G. YEROSHENKO, and L. N. ZHUGOV. Study of the magnetic field from the Venera 4 interplanetary spacecraft. *Kosm. Issled.* 6(4):561–575, 1968.
  44. DOLGINOV, Sh. Sh., Ye. G. YEROSHENKO, and L. N. ZHUGOV. The magnetic field in the immediate area of Mars based on data from the Mars 2 and Mars 3 satellites. *Dokl. Akad. Nauk SSSR* 207(6):1296–1299, 1972.
  45. DOLLFUS, A. Etude des planètes par la polarisation de leur lumière. *Ann. Astrophys. Suppl.*, No. 4, 1957. Washington, D.C., NASA, 1964. (NASA TT-F-188) (Thesis)
  46. DOLLFUS, A. Polarization studies of planets. In, Kuiper, G. P., and B. M. Middlehurst, Eds. *Planets and Satellites*, Chap. 9, pp. 343–399. Chicago, Univ. Chic. Press, 1961.
  47. DOLLFUS, A. Mesure du diamètre de Mercure lors de son passage devant le Soleil le 7 Novembre 1960. *Icarus* 3:219–225, 1963. (Fr.)
  48. DOLLFUS, A. New optical measurements of planetary diameters. IV. Planet Mars. *Icarus* 17:525–539, 1972.
  49. DONAHUE, T. M. Aeronomy of CO<sub>2</sub> atmospheres: a review. *J. Atmos. Sci.* 28(6):895–900, 1971.
  50. DOSTAVALOV, S. B., and S. D. CHUVAKHIN. About the distribution of neutral hydrogen in the upper Martian atmosphere. *Kosm. Issled.* 11(5):767–773, 1973.
  51. DOWNS, G. S., R. M. GOLDSTEIN, R. R. GREEN, G. A. MORRIS, and P. E. REICHLEY. Martian topography and surface properties as seen by radar: the 1971 opposition. *Icarus* 18:8–21, 1973.
  52. DRISCOLL, E. Our cratered sister planet. *Sci. News* 104 (Aug. 4):72–73, 1973.
  53. DYCE, R. B., G. H. PETTENGILL, and I. I. SHAPIRO. Radar determination of the rotation of Venus and Mercury. *Astron. J.* 72(3):351–359, 1967.
  54. EGAN, W. G., and K. M. FOREMAN. Evaluation of Mars surface simulation studies. *Astron. J.* 73(5, Pt. 2):S92, June 1968.
  55. EPSTEIN, E. E., J. W. MONTGOMERY, M. M. DWORETSKY, and W. G. FOGARTY. Mercury: epithil physical parameters and a hermocentric longitude dependence of its 3.3 mm radiation. *Radio Sci.* 5:401–409, 1970.
  56. FANALE, P. O., and W. A. CANNON. Adsorption on the Martian regolith. *Nature* 230:502–504, 1971.
  57. FANALE, F., C. STEMBRIDGE, and N. H. HOROWITZ. Biological studies of Mars: theoretical considerations and practical experiments. In, Tiffany, O. L., and E. Zaitzeff, Eds. *Advanced Space Experiments. Advances in the Astronautical Sciences*, Vol. 25, pp. 165–177. Washington, D.C., Tarzana, Calif., Am. Astronaut. Soc., 1969.
  58. FJELDBO, G., A. I. KLORE, and R. ESHLEMAN. The neutral atmosphere of Venus as studied with the Mariner V radio occultation experiments. *Astron. J.* 76:123–140, 1971.
  59. GALE, W. A., and A. C. E. SINCLAIR. Polar temperature of Venus. *Science* 165:1356–1357, 1969.
  60. GARY, B. Mercury's microwave phase effect. *Astrophys. J. Lett.* 149:L141–L145, 1967.
  61. GIERASCH, P. J. The 4-day rotation in the stratosphere of Venus: a study in radiative driving. *Icarus* 13(1):25–33, 1970.
  62. GIERASCH, P., and R. GOODY. A study of the thermal and dynamical structure of the Martian lower atmosphere. *Planet. Space Sci.* 16(5):615–646, 1968.
  63. GIERASCH, P., and C. SAGAN. A preliminary assessment of Martian wind regimes. *Icarus* 14:312–318, 1971.
  64. GOLDRICH, P., and S. PEALE. Spin-orbit coupling in the solar system. *Astron. J.* 71:425–438, 1966.
  65. GOLDSTEIN, R. M. Radio and radar studies of Venus and Mercury. *Radio Sci.* 5:391–395, 1970.
  66. GOLDSTEIN, R. M. Radar observations of Mercury. *Astron. J.* 76:1152–1154, 1971.
  67. GOLDSTEIN, R. M. Review of surface and atmosphere studies of Venus and Mercury. *Icarus* 17:571–575, 1972.
  68. GOLITSYN, G. S. Estimates of boundary layer parameters in the atmospheres of terrestrial planets. *Izv. Akad. Nauk SSSR, Fiz. Atmos. Okeana* 5(8):775–781, 1969.
  69. GOLITSYN, G. S. The similarity theory for large-scale movements of planetary atmospheres. *Dokl. Akad. Nauk SSSR* (190):323–326, 1970.
  70. GOODY, R., and M. J. S. BELTON. Radiative relaxation times for Mars. A discussion of Martian atmospheric dynamics. *Planet. Space Sci.* 15:247–256, 1967.
  71. GOODY, R. M., and A. R. ROBINSON. A discussion of the deep circulation of the atmosphere of Venus. *Astrophys. J.* 146:339–355, 1966.
  72. GRIFFITH, J. S. Constants of the solar system. *Spaceflight* 14:311–314, 1972.
  73. GRINGAUZ, K. I., V. V. BEZRUKIKH, G. I. VOLKOV, T. K. BREUS, I. S. MUSATOV, L. P. KHAVKIN, and G. P. SLOUTCHONOV. Preliminary results on plasma electrons from Mars 2 and Mars 3. *Icarus* 18:54–58, 1973.
  74. HÄMEEN-ANTTILA, K. A., T. PIKKARAINEN, and H. CAMICHEL. Photometric studies of the planet Mercury. *Moon* (1):440–448, 1970.
  75. HANEL, R., B. CONRATH, W. HOVIS, V. KUNDE, P. LOWMAN, W. MAGUIRE, J. PEARL, J. PIRRAGLIA, C. PRABHAKARA, B. SCHLACHMAN, G. LEVIN, P. STRAAT, and T. BURKE. Investigation of the Martian environment by infrared spectroscopy on Mariner 9. *Icarus* 17:423–442, 1972.

76. HANSEN, J. E. Information contained in the intensity and polarization of scattered sunlight. *Inst. Space Stud. Rep.*, Sept, 1972.
77. HANSEN, J. E., and A. ARKING. Clouds of Venus: evidence for their nature. *Science* 171:669–672, 1971.
78. HANSEN, J. E., and H. CHEYNEY. Comments on the paper by D. G. Rea and B. T. O'Leary, "On the composition of the Venus clouds." *J. Geophys. Res.* 73:6136–6137, 1968.
79. HARRIS, D. L. Photometry and colorimetry of planets and satellites. In, Kuiper, G. P., and B. M. Middlehurst, Eds. *Planets and Satellites*, Chap. 8, pp. 272–342. Chicago, Univ. Chicago Press, 1961.
80. HORD, C. W., C. A. BARTH, A. I. STEWART, and A. L. LANE. Mariner 9 ultraviolet spectrometer experiment: photometry and topography of Mars. *Icarus* 17:443–456, 1972.
81. HORD, C. W., K. E. SIMMONS, and L. K. McLAUGHLIN. Mariner 9 ultraviolet spectrometer experiment: pressure-altitude measurements on Mars. (Lab. Atmos. Space Phys., Univ. Colo.) *Icarus* 21(3):292–302, 1974.
82. HORN, D., J. M. McAFFEE, A. M. WINER, K. C. HERR, and G. C. PIMENTEL. The composition of the Martian atmosphere: minor constituents. *Icarus* 16:543–556, 1972.
83. HOWARD, H. T., G. L. TYLER, P. B. ESPOSITO, J. D. ANDERSON, R. D. REASENBERG, and I. I. SHAPIRO et al. Mercury: results on mass, radius, ionosphere, and atmosphere from Mariner 10 dual-frequency radio signals. *Science* 185:179–180, 1974.
84. HUNTER, D. M. Aeronomy of CO<sub>2</sub> atmospheres. *Comments Astrophys. Space Phys.* 4:1–5, 1972.
85. INGALLS, R. P., and J. V. EVANS. Scattering properties of Venus at 3.8 cm. *Astron. J.* 74:258–272, 1969.
86. INGALLS, R. P., and L. P. RAINVILLE. Radar measurements of Mercury: topography and scattering characteristics at 3.8 cm. *Astron. J.* 77:185–190, 1972.
87. INGERSOLL, A. P. Motions in planetary atmospheres and the interpretation of radio occultation data. *Icarus* 13:34–36, 1970.
88. INGERSOLL, A. P., and S. B. LEOVY. The atmospheres of Mars and Venus. In. Goldberg, L., Ed. *Annual Review of Astronomy and Astrophysics*, Vol. 9, pp. 147–182. Palo Alto, Calif., Annual Reviews, Inc., 1971.
89. IRVINE, W. M. Monochromatic phase curves and albedos for Venus. *J. Atmos. Sci.* 25(4):610–616, 1968.
90. IZAKOV, M. N. About the temperature of the Mars thermosphere. *Kosm. Issled.* 11(5):761–766, 1973.
91. JANSEN, M. A., R. E. HILLS, D. D. THORNTON, and W. J. WELCH. Venus: new microwave measurements show no atmosphere water vapor. *Science* 179:994–997, 1973.
92. JENKINS, E. B., D. C. MORTON, and A. V. SWEIGART. Rocket spectra of Venus and Jupiter from 2000 to 3000 Å. *Astrophys. J.* 157:913–924, 1969.
93. JURGENS, R. F. Some preliminary results of the 70 cm radar studies of Venus. *Radio Sci.* 5(2):435–442, 1970.
94. KAPLAN, L. D., J. CONNES, and P. CONNES. Carbon monoxide in the Martian atmosphere. *Astrophys. J.* 157(3):L187–L192, 1969.
95. KAPLAN, L. D., G. MÜNCH, and H. SPINRAD. An analysis of the spectrum of Mars. *Astrophys. J.* 139:1–15, 1964.
96. KERZHANOVICH, V. V. Wind velocity and turbulence in the Venusian atmosphere from Doppler measurements of the velocity of the Venera-4, Venera-5, and Venera-6, automatic interplanetary stations. *Kosm. Issled.* 10(2):261–273, 1971.
97. KERZHANOVICH, V. V., and M. Ya. MAROV. Circulation and dust content of the Venusian atmosphere according to wind velocity measurements from Venera 8. *Dokl. Akad. Nauk SSSR* 215(3):554–557, 1973.
98. KERZHANOVICH, V. V., M. Ya. MAROV, and M. K. ROZHDESTVENSKIY. Data on dynamics of the sub-cloud Venus atmosphere from Venera space probe measurements. *Icarus* 17:659–674, 1972.
99. KIEFFER, H. H., S. C. CHASE, Jr., E. MINER, G. MÜNCH, and G. NEUGEBAUER. Preliminary report of infrared radiometric measurements from the Mariner 9 spacecraft. *J. Geophys. Res.* 78(20):4291–4326, 1973.
100. KLEIN, M. J. Mercury: recent observations at 3.75 cm wavelength—summary. *Radio Sci.* 5:397–400, 1970.
101. KLIORÉ, A. J., D. L. CAIN, G. FJELDBØ, B. L. SEIDEL, M. J. SYKES, and S. I. RASOOL. The atmosphere of Mars from Mariner 9 radio occultation measurements. *Icarus* 17:484–516, 1972.
102. KLIORÉ, A. J., G. FJELDBØ, B. L. SEIDEL, M. J. SYKES, and P. M. WOICESHYN. S-band radio occultation measurements of the atmosphere and topography of Mars with Mariner 9—extended mission coverage of polar and intermediate latitudes. *J. Geophys. Res.* 78:4331–4351, 1973.
103. KOLOSOV, M. A., O. I. YAKOVLEV, Yu. M. KRUGLOV, B. P. TRUSOV, A. I. YEFIMOV, and V. V. KERZHANOVICH. Preliminary results of studies of the atmosphere of Mars by the Mars 2 satellite. *Dokl. Akad. Nauk SSSR* 206:1071–1073, 1972.
104. KOTEL'NIKOV, V. A., Yu. N. ALEKSANDROV, L. V. APRAKSIN, V. M. DUBROVIN, M. D. KISLIK, B. I. KUZNETSOV, G. M. PETROV, O. N. RZHIGA, A. V. FRANTSESSON, and A. M. SHAKHOVSKOY. Radiolocation observations of Venus in the Soviet Union in 1964. *Dokl. Akad. Nauk SSSR* 163:50–53, 1965.
105. KOTEL'NIKOV, V. A., V. M. DUBROVIN, B. A. DUBINSKIY, M. D. KISLIK, B. I. KUZNETSOV, I. V. LISHIN, V. A. MOROZOV, G. M. PETROV, O. M. RZHIGA, G. A. SYTSKO, and A. M. SHAKHOVSKOY. Radiolocation observations of Venus in the Soviet Union in 1962. *Dokl. Akad. Nauk SSSR* 151:532–535, 1963.
106. KOTEL'NIKOV, V. A., V. M. DUBROVIN, V. A. MOROZOV, G. M. PETROV, O. N. RZHIGA, Z. G. TRUNOVA, and A. M. SHAKHOVSKOY. Results of radiolocation of Venus in 1961. *Radiotekh. Elektron.* 7(11):1860–1872, 1962. (Transl: *Radio Eng. Electron.*) 7(11):1722–1733, 1962.

107. KOVALEVSKY, J. Détermination des masses des planètes et satellites. In, Dollfus, A., Ed. *Surfaces and Interiors of Planets and Satellites*, Chap. 1, pp. 1–44. London, New York, Academic, 1970.
108. KOZLOVSKAYA, S. V. The internal structure and chemical composition of Mercury. In, Martynov, D. Ya., and V. A. Bronshen, Eds. *Fizika Luny i Planet* (Transl: *Physics of the Moon and Planets*), pp. 228–231. Moscow, Nauka, 1972.
109. KROTIKOV, V. D., and V. S. TROITSKIY. Radio-frequency radiation and the nature of the Moon. *Usp. Fiz. Nauk* 81:589–639, 1963; Radio emission and nature of the Moon. *Sov. Phys. Usp.* (Transl.) 6(6):841–876, 1964.
110. KUIPER, G. P. The planet Mercury: summary of present knowledge. In, Kuiper, G. P., Ed. *Communications of the Lunar and Planetary Laboratory*, Vol. 8, Pt. 3, No. 142, pp. 165–174. Tucson, Ariz., Univ. Ariz., 1970.
111. KUIPER, G. P., D. P. CRUIKSHANK, G. T. SILL, and U. FINK. The infrared spectrum of carbon suboxide. II: Region 2–15 microns. In, Kuiper, G. P., Ed. *Communications of the Lunar and Planetary Laboratory*, Vol. 6, Pt. 3, No. 99, pp. 201–207. Tucson, Ariz., Univ. Ariz., 1967. (NASA CR-97962)
112. KUIPER, G. P., F. F. FORBES, D. L. STEINMETZ, and R. I. MITCHELL. High altitude spectra from NASA CV-990 jet. II. Water vapor on Venus. In, *Communications of the Lunar and Planetary Laboratory*, Vol. 6, Pt. 4, No. 100–104, pp. 209–228. Tucson, Ariz., Univ. Ariz., 1967. (NASA CR-97962)
113. KURT, V. G., S. B. DOSTOVALOV, and E. K. SHEFFER. The Venus far ultraviolet observations with Venera 4. *J. Atmos. Sci.* 25:668–671, 1968.
114. KUZ'MIN, A. D. *Radiofizicheskiye Issledovaniya Venery*. Moscow, VINITI, 1967. (Transl: *Radio Physical Studies of Venus*). Washington, D.C., NASA, 1969. (NASA TT-F-536)
115. KUZ'MIN, A. D., A. P. NAUMOV, and T. V. SMIRONVA. Estimates of the content of ammonia in the sub-cloud atmosphere of Saturn from radio astronomical measurements. *Astron. Vestn.* 6(1):13–18, 1972.
116. LANE, A. L., C. A. BARTH, C. W. HORD, and A. I. STEWART. Mariner 9 ultraviolet spectrometer experiment: observations of ozone on Mars. *Icarus* 18(1):102–108, 1973.
117. LEBEDINSKIY, A. I. Physical conditions on Mars. *Dokl. Akad. Nauk SSSR* 108:795–798, 1956.
118. LEOVY, C. B., G. A. BRIGGS, and B. A. SMITH. Mars atmosphere during the Mariner 9 extended mission: television results. *J. Geophys. Res.* 78(20):4252–4266, 1973.
119. LEOVY, C. B., G. A. BRIGGS, A. T. YOUNG, B. A. SMITH, J. B. POLLACK, E. N. SHIPLEY, and R. L. WILDEY. The Martian atmosphere: Mariner 9 television experiment progress report. *Icarus* 17(2):373–393, 1972.
120. LEOVY, C., and Y. MINTZ. Numerical simulation of the atmospheric circulation and climate of Mars. *J. Atmos. Sci.* 26:1167–1190, 1969.
121. LEVIN, B. J. Internal constitution of terrestrial planets. In, Dollfus, A., Ed. *Surfaces and Interiors of Planets and Satellites*. Chap. 8, pp. 462–510. London, New York, Academic, 1970.
122. LEWIS, J. S. Geochemistry of the volatile elements on Venus. *Icarus* 11:367–385, 1969.
123. LEWIS, J. S. Venus: atmospheric and lithospheric composition. *Earth Planet. Sci. Lett.* 10:73–80, 1970.
124. LEWIS, J. S. Refractive index of aqueous HCl solutions and the composition of the Venus clouds. *Nature* 230:295–296, 1971.
125. LOMONOSOV, M. V. The phenomenon of Venus on the Sun observed at the St. Petersburg Imperial Academy of Sciences, May 26, 1761. In *His, Polnoe Sobranie Sochinennii*, Vol. 4, pp. 361–376. (Trudy po fiziko, Astronomii), 1744–1765. Moscow, Akad. Nauk, SSSR, 1955.
126. LORELL, J., G. H. BORN, E. J. CHRISTENSEN, J. F. JORDAN, P. A. LAING, W. L. MARTIN, W. L. SJOGREN, I. I. SHAPIRO, R. D. REASENBERG, and G. L. SLATER. Mariner 9 celestial mechanics experiment: gravity field and pole direction of Mars. *Science* 175:317–320, 1972.
127. LOVELOCK, J. E., and C. E. GIFFRIN. Planetary atmospheres: compositional and other changes associated with the presence of life. In, Tiffany, O. L., and E. Zaitzeff, Eds. *Advanced Space Experiments. Advances in the Astronautical Sciences*, Vol. 25, pp. 179–193. Washington, D.C., Tarzana, Calif. Am. Astronaut. Soc., 1969.
128. LOWELL, P. *Mars and Its Canals*. New York, London, Macmillan, 1906.
129. LUKASHEVICH, N. L., M. Ya. MAROV, and Ye. M. FEYGELEN'SON. Interpretation of measurements of luminance in the atmosphere of Venus. *Kosm. Issled.* 12:272–278, 1974.
130. LUKIN, D. S., Yu. G. SPIRIDONOV, V. A. SHKOL'NIKOV, and S. I. FOMINYKH. Determination of the parameters of the atmosphere of Venus below the level of critical refraction from radio occultation measurements. *Kosm. Issled.* 10(2):274–278, 1972.
131. MALKUS, W. V. R. Hadley-Halley circulation on Venus. *J. Atmos. Sci.* 27:529–535, 1970.
132. MAMAKOV, A. S., and A. A. NEFED'YEV. Measurement of the diameter of Mercury. *Astron. Tsirk.* (Kazan AN SSSR) (669):3–4, 1972.
133. MARGOLIS, J. S., R. A. J. SCHORN, and L. D. G. YOUNG. High dispersion spectroscopic studies of Mars. V. A search for oxygen in the atmosphere of Mars. *Icarus* 15:197–203, 1971.
134. Mariner Stanford Group. Venus: ionosphere and atmosphere as measured by dual-frequency radio occultation of Mariner V. *Science* 158:1678–1683, 1967.
135. MARON, I., G. LUCHAK, and W. BLITZSTEIN. Radar observation of Venus. *Science* 134:1418–1421, 1961.
136. MAROV, M. Ya. A model of the atmosphere of Venus. *Dokl. Akad. Nauk SSSR* 196(1):67–70, 1971.
137. MAROV, M. Ya. Venus: a perspective at the beginning of planetary exploration. *Icarus* 16:415–461, 1972.
138. MAROV, M. Ya., V. S. AVDUYEVSKIY, N. F. BORODIN,

- A. P. EKONOMOV, V. V. KERZHANOVICH, V. P. LYSOV, B. Ye. MOSHKIN, M. K. ROZHDESTVENSKIY, and O. L. RYABOV. Preliminary results on the Venus atmosphere from the Venera 8 descent module. *Icarus* 20:407–421, 1973.
139. MAROV, M. Ya., V. S. AVDUYEVSKIY, V. V. KERZHANOVICH, M. K. ROZHDESTVENSKIY, N. F. BORODIN, and O. L. RYABOV. Measurement of temperature, pressure, and wind speed in the atmosphere of Venus by Venera 8. *Dokl. Akad. Nauk SSSR* 210(3):559–562, 1973.
140. MAROV, M. Ya., V. S. AVDUYEVSKIY, M. K. ROZHDESTVENSKIY, N. F. BORODIN, and V. V. KERZHANOVICH. Preliminary results of investigation of the atmosphere of Venus by Venera 7 automatic interplanetary station. *Kosm. Issled.* 9(4):570–579, 1971.
141. MAROV, M. Ya., and O. L. RYABOV. *A Model of the Atmosphere of Venus*. Moscow, Akad. Nauk SSSR, Inst. Prikl. Mat., 1972. (Preprint No. 39)
142. MAROV, M. Ya., and V. P. SHARI. *Transfer of Long Wave Radiation to the Lower Atmosphere of Venus*. Moscow, Akad. Nauk SSSR, Inst. Prikl. Mat., 1973. (Preprint No. 23) Washington, D.C., NASA, 1974. (NASA TT-F-15259)
143. MAYER, C. H., T. P. MCCULLOUGH, and R. M. SLOANAKER. Observations of Venus at 3.15 cm wavelength. *Astrophys. J.* 127(1):1–10, 1958.
144. MAYEVA, S. V. Some calculations of the thermal history of Mars and the Moon. *Dokl. Akad. Nauk SSSR* 159:294–297, 1964. (NASA TT-F-9624)
145. MAYEVA, S. V. Thermal history of the planets of the Earth group. In, Martynov, D. Ya., and V. A. Bronshtein, Eds. *Fizika Luny i Planet* (Transl: Physics of the Moon and Planets), pp. 223–228. Moscow, Nauka, 1972.
146. McCUALEY, J. F., M. H. CARR, J. A. CUTTS, W. K. HARTMANN, H. MASURSKY, D. J. MILTON, R. P. SHARP, and D. E. WILHELM. Preliminary Mariner 9 report on the geology of Mars. *Icarus* 17:289–327, 1972.
147. MCCORD, T. B., and J. B. ADAMS. Mercury: interpretation of optical observations. *Icarus* 17:585–588, 1972.
148. MCCORD, T. B., J. H. ELIAS, and J. A. WESTPHAL. Mars: the spectral albedo (0.3–2.5 $\mu$ ) of small bright and dark regions. *Icarus* 14:245–251, 1971.
149. McELROY, M. B. Structure of the Venus and Mars atmospheres. *J. Geophys. Res.* 74(1):29–41, 1969.
150. McELROY, M. B. Ionization processes in the atmospheres of Venus and Mars. *Ann. Geophys.* 26:643–652, 1970. Also, Tucson, Ariz., Kitt Peak Nat. Obs., 1970. (Preprint)
151. McELROY, M. B., and T. M. DONAHUE. Stability of the Martian atmosphere. *Science* 177:986–988, 1972.
152. McELROY, M. B., and J. C. McCONNELL. Dissociation of CO<sub>2</sub> in the Martian atmosphere. *J. Atmos. Sci.* 28:879–884, 1971.
153. McELROY, M. B., and D. F. STROBEL. Models for the nighttime Venus ionosphere. *J. Geophys. Res.* 74: 1118–1127, 1969.
154. MIYAMOTO, S. Martian atmosphere and crust. *Icarus* 5:360–374, 1966.
155. MOOS, H. W., W. G. FASTIE, and M. BOTTEMA. Rocket measurement of ultraviolet spectra of Venus and Jupiter between 1200 and 1800 Å. *Astrophys. J.* 155:887–897, 1969.
156. MOROWITZ, H., and C. SAGAN. Life in the clouds of Venus? *Nature* 215:1259–1260, 1967.
157. MOROZ, V. I. The infrared spectrum of Mercury ( $\lambda$ 1.0–319 $\mu$ ). *Astron. Zh.* 41:1108–1117, 1964. *Soviet Astron. J. (Transl.)* 8:882–889, 1965.
158. MOROZ, V. I. *Fizika Planet*. Moscow, Nauka, 1967. (Transl: *Physics of Planets*). Washington, NASA, 1968. (NASA TT-F-515)
159. MOROZ, V. I. The atmosphere of Venus. *Usp. Fiz. Nauk* 104(2):255–296, 1971.
160. MOROZ, V. I., and D. P. CRUIKSHANK. Spectroscopic determination of pressure in the atmosphere of Mars by the CO<sub>2</sub> bands. *Astron. Zh.* 48:1038–1045, 1971. (Transl: *Sov. Astron.*) 15:822–827, 1972.
161. MOROZ, V. I., and L. V. KSANFOMALITI. Preliminary results of astrophysical observations of Mars from Mars 3. *Icarus* 17:408–422, 1972.
162. MOROZ, V. I., L. V. KSANFOMALITI, A. M. KASATKIN, G. N. KRASOVSKIY, N. A. PARFENT'YEV, V. D. DAVYDOV, and G. N. FILIPPOV. Preliminary results of measurements of infrared temperature of the surface of Mars by Mars 3. *Dokl. Akad. Nauk SSSR* 208(2): 299–302, 1973.
163. MOROZ, V. I., L. V. KSANFOMALITI, G. N. KRASOVSKIY, V. D. DAVYDOV, N. A. PARFENT'YEV, V. S. ZHEGULEV, and G. F. FILIPPOV. *Mars III: Infrared Temperature and Thermal Properties of the Planet Surface*. Akad. Nauk SSSR, Inst. Space Stud., 1974. (Prepr.)
164. MOROZ, V. I., and O. G. TARANOVA. The height of dust clouds on Mars during the dust storm of 1971 from groundbased observations. *Astron. Tsir.* Kazan AN SSSR 697:1–3, 1972.
165. MORRISON, D. Martian surface temperature. *Astron. J.* 73(5, Pt. 2):S109, June 1968.
166. MORRISON, D. *Thermal Models and Microwave Temperatures of Planet Mercury*. Cambridge, Mass., Smithsonian Astrophys. Obs., 1969. (Spec. Rep. No. 292)
167. MORRISON, D. Thermophysics of the planet Mercury. *Space Sci. Revs.* 11:271–307, 1970.
168. MORRISON, D., C. SAGAN, and J. B. POLLACK. Martian temperatures and thermal properties. *Icarus* 11:36–45, 1969.
169. MOTTONI, G. DE. Prospettive di areografia basate sui documenti fotografici e sulle osservazioni visuali. In, *Atti 11 Conv. Soc. Astron. Ital.*, pp. 65–72. Padova, 1967.
170. MURDOCK, T. L., and E. P. NEY. Mercury: the dark side temperature. *Science* 170:535–537, 1970.
171. MURRAY, B. C., M. J. S. BELTON, G. E. DANIELSON, M. E. DAVIES, D. GAULT, B. HAPKE, B. O'LEARY,

- R. G. STROM, V. SUOMI, and N. TRASK. Venus: atmospheric motion and structure from Mariner 10 pictures. *Science* 183:1307-1315, 1974.
172. MURRAY, J. B., A. DOLLFUS, and B. SMITH. Cartography of the surface markings of Mercury. *Icarus* 17:576-584, 1972.
173. MURRAY, B. C., W. R. WARD, and S. C. YEUNG. Periodic insolation variations on Mars. *Science* 180:638-643, 1973.
174. MURRAY, B. C., R. L. WILDEY, and J. A. WESTPHAL. Infrared photometric mapping of Venus through the 8-14 micron atmospheric window. *J. Geophys. Res.* 68:4813-4818, 1963. (NASA CR-50149)
175. O'LEARY, B. T., and D. G. REA. On the polarimetric evidence for an atmosphere on Mercury. *Astrophys. J.* 148:249-253, 1967.
176. OWEN, T., and C. SAGAN. Minor constituents in planetary atmospheres: ultraviolet spectroscopy from the orbiting astronomical observatory. *Icarus* 16:557-568, 1972.
177. PARKINSON, T. D., and D. M. HUNTER. Martian dust storm: its depth on 25 November 1971. *Science* 175:323, 1972.
178. PETROV, M. P. *Pustyni Zemnogo Shara* (Transl: *Deserts of the Earth*). Leningrad, Nauka, 1973.
179. PETTENGILL, G. H., H. W. BRISCOE, J. V. EVANS, E. GEHRLETS, G. M. HYDE, L. G. KRAFT, R. PRICE, and W. B. SMITH. A radar investigation of Venus. *Astron. J.* 67(4):181-190, 1962.
180. PETTENGILL, G. H., and R. B. DYCE. A radar determination of the rotation of the planet Mercury. *Nature* 206:1240, 1965.
181. PETTENGILL, G. H., I. I. SHAPIRO, and A. E. E. ROGERS. Topography and radar scattering properties of Mars. *Icarus* 18:22-28, 1973.
182. PETTIT, E. Planetary temperature measurements. In, Kuiper, G. P., and B. M. Middlehurst, Eds. *Planets and Satellites*, Chap. 10, pp. 400-428. Chicago, Univ. Chic. Press, 1961.
183. POLLACK, J. B., E. E. ERICKSON, F. C. WITTEBORN, CH. CHACKERIAN, A. L. SUMMERS, W. VAN CAMP, B. J. BALDWIN, G. C. ANGASON, and L. J. CAROFF. *Aircraft Observations of Venus. Near Infrared Reflection Spectrum: Implications for Cloud Composition*. Moffett Field, Calif., NASA Ames Res. Cent., Space Sci. Div. (Prepr.)
184. POLLACK, J. B., and D. MORRISON. Venus: determination of atmospheric parameters from the microwave spectrum. *Icarus* 12:376-390, 1970.
185. POLLACK, J. B., and C. SAGAN. *An Analysis of Martian Photometry and Polarimetry*. Cambridge, Mass., Smithsonian Astrophys. Obs., 1967. (Spec. Rep. 258)
186. POLLACK, J. B., and C. SAGAN. The case for ice clouds on Venus. *J. Geophys. Res.* 73:5943-5949, 1968.
187. POLLACK, J. B., and C. SAGAN. Studies of the surface of Mars. *Radio Sci.* 5:443-464, 1970.
188. POLLACK, J. B., J. EVERETTA, M. NOLAND, C. SAGAN, W. K. HARTMANN, T. C. DUXBURY, G. H. BORN, D. J. MILTON, and B. A. SMITH. Mariner 9 television observations of Phobos and Deimos. *Icarus* 17:394-403, 1972.
189. PRICE, R., P. E. GREEN, Jr., T. J. GOBLICK, Jr., R. H. KINGSTON, L. G. KRAFT, Jr., G. H. PETTENGILL, R. SILVER, and W. B. SMITH. Radar echoes from Venus. *Science* 129:751-753, 1959.
190. RABE, E. Derivation of fundamental astronomical constants from the observations of Eros during 1926-1945. *Astron. J.* 55:112-126, 1940.
191. RADMER, R., and B. KOK. A unified procedure for the detection of life on Mars. *Science* 174:233-239, 1971.
192. RASOOL, S. I. The structure of Venus clouds—summary. *Radio Sci.* 5:367-368, 1970.
193. RASOOL, S. I., and R. W. STEWART. Results and interpretation of the S-band occultation experiments on Mars and Venus. *J. Atmos. Sci.* 28:869-878, 1971.
194. REA, D. G., B. T. O'LEARY, and W. M. SINTON. Mars: the origin of the 3.58- and 3.69-micron minima in the infrared spectra. *Science* 147:1286-1288, 1965.
195. REYNOLDS, R. T., and A. L. SUMMERS. Calculations on the composition of the terrestrial planets. *J. Geophys. Res.* 74:2494-2511, 1969.
196. RÖSCH, J. Un problème: la densité de Mercure. *Astronomie* 85:207-221, 1971.
197. RÖSCH, J., H. CAMICHEL, F. CHAUVEAU, M. HUGON, and G. RATIER. An attempt to measure the diameter of Mercury by Hertzsprung's method. *Icarus* 16:321-327, 1972.
198. RUNCORN, S. K. On the implications of the shape of Mars. *Icarus* 18:109-112, 1973.
199. RYAN, J. A. The Martian yellow clouds. In, *Geological Society of America Abstracts for 1965*, Spec. Paper No. 87, p. 316. New York, Geol. Soc. Am., 1966.
200. RZHIGA, O. N. Results of radar probing of planets. *Kosm. Issled.* 7(1):84-91, 1969.
201. SAGAN, C. *The Radiation Balance of Venus*. Presented at 105th Meet., Am. Astron. Soc., Univ. Pittsburgh, 1960. Pasadena, Calif., Calif. Inst. Technol., Jet Propul. Lab., 1960. (JPL Rep. 32-24). The surface temperature of Venus. *Astron. J.* 65:352-353, 1960. (Abstr.)
202. SAGAN, C. The photometric properties of Mercury. *Astrophys. J.* 144:1218-1221, 1966.
203. SAGAN, C. Atmospheres, origins of the Earth and planets. In, Runcorn, S. K., Ed. *International Dictionary of Geophysics*, Vol. 1, pp. 97-104. Oxford, Pergamon, 1967.
204. SAGAN, C. Life on the surface of Venus? *Nature* 216:1198-1199, 1967.
205. SAGAN, C. Life. *Encyclopedia Britannica*, Vol. 13, pp. 1083-1088. Chicago, 1970.
206. SAGAN, C. The trouble with Venus. In, Sagan, C., T. C. Owens, and H. J. Smith, Eds. *Planetary Atmospheres*, pp. 116-127. Proc., Int. Astron. Union Symp., No. 40. Dordrecht, Neth., Reidel, 1971.
207. SAGAN, C., and J. B. POLLACK. Anisotropic nonconservative scattering and the clouds of Venus. *J. Geophys. Res.* 72(2):469-477, 1967.
208. SAGAN, C., and J. B. POLLACK. A wind-blown dust model

- of Martian surface features and seasonal changes. Cambridge, Mass., *Smithsonian Astrophys. Obs.*, 1967. (Spec. Rep. 255)
209. SAGAN, C., J. VEVERKA, P. FOX, R. DUBISCH, J. LEDERBERG, E. LEVINTHAL, L. QUAM, R. TUCKER, J. B. POLLACK, and B. A. SMITH. Variable features on Mars: preliminary Mariner 9 television results. *Icarus* 17:346-372, 1972.
210. SAGAN, C., J. VEVERKA, P. FOX, R. DUBISCH, R. FRENCH, P. GIERASCH, L. QUAM, J. LEDERBERG, E. LEVINTHAL, R. TUCKER, B. EROSS, and J. B. POLLACK. Variable features on Mars. II: Mariner 9 global results. *J. Geophys. Res.* 78:4163-4196, 1973.
211. SAGAN, C., J. VEVERKA, and P. GIERASCH. Observational consequences of Martian wind regime. *Icarus* 15:253-278, 1971.
212. SCHORN, R. A., H. SPINRAD, L. P. GIVER, R. C. MOORE, and H. J. SMITH. High-dispersion spectroscopic observations of Mars. II. The water-vapor variations. *Astrophys. J.* 147:743-752, 1967.
213. SCHUBERT, G., and R. E. YOUNG. The 4-day Venus circulation driven by periodic thermal forcing. *J. Atmos. Sci.* 27:523-528, 1970.
214. SHARI, V. P. Fluxes of thermal radiation in the lower atmosphere of Venus. *Kosm. Issled.* (In print)
215. SHARONOV, V. V. *Priroda Planet* (Transl: *The Nature of the Planets*). Moscow, Fizmatgiz, 1958.
216. SHARONOV, V. V. La nature de la surface et de l'atmosphère de la planète Mars d'après les données photométriques et colorimétriques. *Mem. Soc. Roy. Sci. Liège* 7:386-392, 1963.
217. SHARONOV, V. V. Direct color comparison of the disc of Mars with terrestrial specimens. *Izv. Kom. Fiz. Planet.* (Moscow) (5):44-48, 1965.
218. SHIMIZU, M. *Exospheric Temperature of Venus*, Vol. 35, pp. 449-457. Tokyo, Inst. Space Aeronaut. Sci., Univ. Tokyo, 1970. (Rep. No. 455)
219. SILL, G. T. Sulfuric acid in the Venus clouds. In, *Communications of the Lunar and Planetary Laboratory*, Vol. 9, No. 171, pp. 191-198. Tucson, Ariz., Univ. Ariz., 1972.
220. SINCLAIR, A. C. E., J. P. BASART, D. BUHL, W. A. GALE, and M. LIWSCHITZ. Preliminary report on interferometer observations of Venus at 11.1 cm wavelength. *Radio Sci.* 5(2):347-354, 1970.
221. SINCLAIR, A. T. The motions of the satellites of Mars. *Mon. Not. Roy. Astron. Soc.* 155:249-274, 1972.
222. SINTON, W. M. Further evidence of vegetation on Mars. *Science* 130:1234-1237, 1959.
223. SINTON, W. M. On the composition of Martian surface materials. *Icarus* 6:222-228, 1967.
224. SINTON, W. M., and J. STRONG. Radiometric observations of Mars. *Astrophys. J.* 131:459-469, 1960.
225. SMITH, B. A. Fast movements of ultraviolet clouds on Venus. In, *Proceedings, International Symposium on Physics of the Moon and of Planets*, Oct. 1968, Kiev, pp. 324-325. Moscow, 1972.
226. SMITH, E. J., L. DAVIS, Jr., P. J. COLEMAN, Jr., and D. E. JONES. Magnetic field measurements near Mars. *Science* 149:1241-1242, 1965.
227. SMITH, W. B., R. P. INGALLS, I. I. SHAPIRO, and M. E. ASH. Surface-height variations on Venus and Mercury. *Radio Sci.* 5:411-423, 1970.
228. SMITH, B. A., and E. J. REESE. Mercury's rotation period: photographic confirmation. *Science* 162:1275-1277, 1968.
229. SPREITER, J. R., A. W. RIZZI, and A. L. SUMMERS. Solar wind flow past nonmagnetic planets—Venus and Mars. *Planet. Space Sci.* 18(9):1281-1299, 1970.
230. STEWART, A. I. Mariner 6 and 7 ultraviolet spectrometer experiment: implications of  $\text{CO}_2^+$ , CO and O airglow. *J. Geophys. Res.* 77:54-68, 1972.
231. STEWART, A. I., C. A. BARTH, C. W. HORD, and A. L. LANE. Mariner 9 ultraviolet spectrometer experiment: structure of Mars' upper atmosphere. *Icarus* 17:469-474, 1972.
232. STRAKHOV, N. M. The question of the possibility of formation of iron hydroxides on the surface of Mars. *Astron. Zh.* 43:1267-1272, 1966.
233. STRUGHOLD, H. The green and red planet. Albuquerque, Univ. New Mex. Press, 1953; London, Sidgwick & Jackson, 1954.
234. SURKOV, Yu. A., B. M. ANDREYCHIKOV, and O. M. KALINKINA. About the ammonia content in the Venus atmosphere according to data of the automatic station Venus 8. *Dok. Akad. Nauk SSSR* 213(2):296-298, 1973.
235. TANG, W. A study of the general circulation of the Martian atmosphere based upon the result of the occultation experiment from Mariner 4. Presented at 7th Int. Space Sci. Symp., Vienna, Austria, May, 1966. In, Dollfus, A., Ed. *Moon and Planets*, pp. 246-252. Amsterdam, North Holland, 1967.
236. THOMSON, J. H., J. E. B. PONSONBY, G. N. TAYLOR, and R. S. ROGER. A new determination of the solar parallax by means of radar echoes from Venus. *Nature* 190:519-520, 1961.
237. TIKHOV, G. A. *Astrobiologiya* (Transl: *Astrobiology*). Moscow, Molodaya Gardiya, 1953.
238. UREY, H. C. The origin and development of the Earth and other terrestrial planets. *Geochim. Cosmochim. Acta* (1):209-277, 1951.
239. UREY, H. C. The atmospheres of the planets. In, Flügge, S., Ed. *Handbuch der Physik*, Vol. 52, pp. 363-418. Berlin, Springer, 1959.
240. VAUCOULEURS, G. DE. Geometric and photometric parameters of the terrestrial planets. *Icarus* 3:187-235, 1964.
241. VAUCOULEURS, G. DE, and D. H. MENZEL. Results of the occultation of Regulus by Venus July 7, 1959. *Nature* 188:28-33, 1960.
242. VICTOR, W. K., and R. STEVENS. The 1961 JPL Venus radar experiment. *IRE Trans. Space Electron. Telem. SET-8(2):84-97*, 1962.
243. VINOGRADOV, A. P. *Vvedeniye v Geokhimiyu Okeana* (Transl: *Introduction to the Geochemistry of the Ocean*). Moscow, Nauka, 1967.

244. VINOGRADOV, A. P. The atmospheres of the planets of the solar system. *Vestn. Mosk. Univ. (Geol. Ser.)* 24(4):3–14, 1969.
245. VINOGRADOV, A. P., Yu. A. SURKOV, B. M. ANDREY-CHIKOV, O. M. KALINKINA, and I. M. GRECHISHCHEVA. The chemical composition of the atmosphere of Venus. *Kosm. Issled.* 8(4):578–587, 1970.
246. VINOGRADOV, A. P., Yu. A. SURKOV, F. F. KIRNOZOV, and V. N. GLAZOV. The content of natural radioactive elements in the Venusian rock; results of experiment with Venera 8 station. *Dokl. Akad. Nauk SSSR* 208:576–579, 1973. (Transl. in *Sov. Phys.*) 18:7–9, 1973.
247. WARD, W. R. Large-scale variations in the obliquity of Mars. *Science* 181:260–262, 1973.
248. WILKINS, G. A. The determination of the mass and oblateness of Mars from the orbits of its satellites. In, Runcorn, S. K., Ed. *Mantles of the Earth and Terrestrial Planets* (NATO Advanced Study Inst., Univ. Newcastle-upon-Tyne, 1966), pp. 77–84. New York, Interscience, 1967.
249. YOUNG, A. T. Are the clouds of Venus sulfuric acid? *Icarus* 18:564–582, 1973.
250. YOUNG, L. D. G. Interpretation of height resolution spectra of Mars. II. Calculations of CO<sub>2</sub> abundance, rotational temperature and surface pressure. *J. Quant. Spectrosc. Radiat. Transfer* 11:1075–1086, 1971.
251. YOUNG, L. D. G. Interpretation of high resolution spectra of Mars. III. Calculation of CO abundance and rotational temperature. *J. Quant. Spectrosc. Radiat. Transfer* 11:385–390, 1971.
252. ZILITINKEVICH, S. S., A. S. MONIN, V. G. TURIKOV, and D. V. CHALIKOV. Numerical modeling of the circulation of the Venusian atmosphere. *Dokl. Akad. Nauk. SSSR* 197(6):1291–1294, 1971.

## Chapter 5

# PLANETS AND SATELLITES OF THE OUTER SOLAR SYSTEM, ASTEROIDS, AND COMETS<sup>1</sup>

RAY L. NEWBURN, Jr. AND SAMUEL GULKIS

Jet Propulsion Laboratory, California Institute of Technology, Pasadena USA

### OUTER SOLAR SYSTEM

The outer solar system beyond Mars, which contains more than 99% of the nonsolar mass in the solar system, is of major cosmogonic significance. Here are most of the asteroids and comets—the giant planets: Jupiter, Saturn, Uranus, and Neptune, and their 29 satellites as well as the planet Pluto which is more like a satellite than a companion planet to the giants. The giant planets and probably their satellites differ markedly from the planets and satellites of the inner solar system. In contrast to mean

densities near 5 g/cm<sup>3</sup> for the terrestrial planets, mean densities of the major planets range from 0.7 g/cm<sup>3</sup> for Saturn to 1.6 g/cm<sup>3</sup> for Neptune. The giant planets are large with radii ranging 3.7–11.2 times that of the Earth; all rotate rapidly with periods from ca 10–ca 15 h. This rapid rotation produces a pronounced oblateness, particularly of Jupiter and Saturn. Rotational effects are also important in determining the distribution of plasma in the Jovian magnetosphere.

Earth-type planets and the giant planets differ, too, in the chemical nature of their atmospheres which are, respectively, oxidizing and reducing. The larger satellites of the giant planets also appear significantly different from the Moon, some of them, it is believed, being composed of large fractions of various ices or at least ice covered. Three satellites, Io, Ganymede, and Titan, are thought to have atmospheres, with that of Titan being quite substantial.

The major planets and their satellites are considered to be of considerable biologic interest, in addition to their importance toward understanding the formation of the solar system. Sagan [404] and other workers have shown that synthesis of complex organic compounds takes place most effectively in a reducing atmosphere. Major steps leading to the origin of life on Earth are believed to have occurred when the Earth's atmosphere was richer in hydrogen than at

<sup>1</sup> We wish to thank the many people who, either directly or indirectly, helped to compile quickly data used in this chapter, in particular, J. D. Anderson, T. D. Carr, O. V. Dobrovolskiy, F. P. Fanale, R. Goldstein, H. C. Grabske, A. S. Grossman, M. Janssen, T. V. Johnson, G. Null, R. J. Olness, E. Olsen, J. B. Pollack, R. Smoluchowski, V. G. Teifel, L. Trafton, D. L. Watson, and S. K. Wong for material for use prior to publication. B. Gary is thanked for assistance in compiling radio brightness temperature data used in the figures. We are especially grateful to F. Taylor who read the entire manuscript and commented critically on its contents. M. Owen and D. Mahoney are thanked for professional assistance in typing and editing the manuscript. We also thank the D. Reidel Publishing Company for permission to use historical and descriptive material from an earlier article we authored [343] which they published.

This paper presents results of one phase of research carried out at the Jet Propulsion Laboratory, California Institute of Technology, under NASA Contract No. NAS 7-100, sponsored by the National Aeronautics and Space Administration.

present. Large quantities of hydrogen would be lost from the Earth during geologic time due to the planet's inability to retain lighter gases. In contrast, major planets could retain any gas, including hydrogen. Their primitive reducing atmospheres may therefore be of major exobiologic significance [404]. The satellite Titan, for example, is a likely site of simple organic compounds, having both a reducing atmosphere and a solid surface on which complex molecules can form and accumulate.

Numerous environmental differences between inner and outer solar system objects are bases for anticipating that atmosphere and surface processes, totally different from those observable on the planets of the inner solar system, may be operative. In order to develop hypotheses about these processes, an adequate understanding of probable conditions on the planets and satellites is needed.

The purpose of this chapter is to present the best available knowledge of the outer solar system in mid-1974 to serve as a guide for studying the outer solar system. Only observational results and direct interpretation are discussed, with

results of a more speculative nature limited to literature references. Emphasis is placed upon planets and larger satellites of greatest biologic interest; comets, asteroids, and the smaller satellites are also discussed but in less detail.

The principal physical and rudimentary photometric data for the five outer planets are presented in Tables 1 and 2; when using these, it is useful to remember that some data are still uncertain, especially for the outer three planets. Such uncertainties are usually indicated in the tables and, where important, are generally discussed in some detail.

Important information on planetary motions is in Table 3; many of these quantities are known to higher accuracy than those given, and additional figures can be found in the original references. Sufficient information is included for most calculations in physical planetology, but not for studies in celestial mechanics.

## JUPITER

Jupiter, being the largest and nearest giant planet, is the most studied. With the flyby by

TABLE 1.—*Physical Data*

Parameter <sup>1</sup>	Jupiter	Saturn	Uranus	Neptune	Pluto
Reciprocal mass <sup>2</sup> [128]	1 047.357	3 498.1	22 759	19 332	3 000 000
Mean error in mass <sup>3</sup> [128]	±0.005	±0.4	±87	±27	±500 000
Mass (Earth)=1) <sup>2,4</sup>	317.89	95.18	14.63	17.22	0.11
Mass, kg <sup>2,5</sup>	$1.8989 \times 10^{27}$	$5.6854 \times 10^{26}$	$8.739 \times 10^{25}$	$1.029 \times 10^{26}$	$6.6 \times 10^{23}$
Equatorial radius (km)	71 600 [219]	60 000 [120]	25 900 [102]	24 750 [152] <sup>6</sup>	ca 3 200 <sup>7</sup>
Equatorial radius (Earth=1) <sup>8</sup>	11.23	9.41	4.06	3.88	ca 0.5 <sup>7</sup>
Oblateness <sup>9</sup>	1/16.7 [219]	1/9.3 [120]	1/100 [102]	1/38.6 [152]	Unknown
Mean density, g cm <sup>-3</sup> <sup>10</sup>	1.314	0.704	1.21	1.67	ca 4.9 <sup>7</sup>
Equatorial surface gravity, m s <sup>-2</sup> <sup>11</sup>	22.88	9.05	7.77	11.00	ca 4.3
Equatorial escape velocity, km s <sup>-1</sup> <sup>12</sup>	59.5	35.6	21.22	23.6	ca 5.3

<sup>1</sup> Where the same source was used for all five planets, the reference number is given in this (parameter) column. In all other cases, it follows the individual datum. Additional information is given in footnotes.

<sup>2</sup> Includes the mass of satellite systems and atmosphere.

<sup>3</sup> Mean error from residuals of group means, groups being formed from results having a common method of derivation. The error for Pluto is estimated only.

<sup>4</sup> Calculated using 328 900.12 for the reciprocal mass of the Earth-Moon system and 81.3025 for their mass ratio [128].

<sup>5</sup> Calculated using data above,  $G=6.673 \times 10^{-20} \text{ km}^3 \text{ s}^{-2} \text{ kg}^{-1}$ , and  $GM_{\odot}=1.327125 \times 10^{11} \text{ km}^3 \text{ s}^{-2}$  [320].

<sup>6</sup> Improved analysis by light curve inversion [491] requires a larger scale height for Neptune's atmosphere. This would decrease the radius to optical depth unity by about 200 km. No change was made because of comparable uncertainties in several quantities.

<sup>7</sup> See discussion in section on PLUTO.

<sup>8</sup> Calculated using  $R_{\oplus}=6378.160 \text{ km}$  [320].

<sup>9</sup> Oblateness or optical flattening is defined as  $(R_{\text{equatorial}} - R_{\text{polar}})/R_{\text{equatorial}}$ .

<sup>10</sup> Calculated assuming all are oblate spheroids.

<sup>11</sup> Including centrifugal term,  $g_{\oplus}=9.78 \text{ ms}^{-2}$  at the Equator.

<sup>12</sup> No rotational contribution included.

Pioneer 10 on December 4, 1973, Jupiter also became the first of the giants to be studied at close range by spacecraft. In spite of this attention, knowledge of Jupiter still lags behind that of Mars or Venus, and intensive study is scheduled during the coming decade. In the pages that follow, an effort will be made to present an overview of current knowledge of Jupiter and to point out gaps in fundamental data and understanding.

### Atmosphere

#### *Background Information*

The first report on dark absorption bands in the spectrum of Jupiter apparently was made by Secchi in 1863. Shortly after the turn of the century, Slipher photographed these bands in some detail. In the early 1930s, Wildt suggested, and the work of Dunham confirmed, that they were due to the presence of methane and ammonia. Pioneering measurements of temperatures of the planets were made using vacuum thermocouples, in the mid-1920s, by Menzel, Coblenz, and Lampland at Lowell Observatory

and by Pettit and Nicholsen at Mt. Wilson Observatory. These showed that Jupiter was definitely a cold body, as Jeffries had argued in 1923 on theoretical grounds. Model studies analogous to the modern paper of Zapsolsky and Salpeter [534] indicated that the bulk of Jupiter must be hydrogen and helium, since no other substances have sufficiently low density at low temperatures to explain the observed mean density. Baum and Code [32], in 1952, observed photoelectrically an occultation of the star  $\sigma$ -Arietis by Jupiter, deriving from these observations a mean molecular weight of 3.3 for the Jovian atmosphere. Although recent studies have shown that large errors are possible using Baum and Code's curve-fitting technique [504], their basic conclusion that Jupiter's atmosphere must consist mainly of hydrogen and helium remains valid. Actual spectroscopic detection of molecular hydrogen was made by Kiess et al [248] in 1960.

The classic assumption was that gases in a planetary atmosphere could be considered a uniform transparent layer, except for pure absorption at some discrete wavelengths, above a

TABLE 2.—*Photometric Data*

Parameter <sup>1</sup>	Jupiter	Saturn	Uranus	Neptune	Pluto
Mean opposition magnitude, $V_0$ [194]	−2.55	0.75	5.52	7.84	14.90 <sup>9</sup>
Mean surface brightness at zero phase <sup>2</sup> $V_{mag}/(\text{arc sec})^2$	5.6	6.9	8.2	9.6	ca 18.2
Mean surface brightness at zero phase ( $\text{Earth}=1$ )	$3.98 \times 10^{-2}$	$1.20 \times 10^{-2}$	$3.63 \times 10^{-3}$	$1.00 \times 10^{-3}$	ca $3.6 \times 10^{-7}$
Color index <sup>3</sup> B-V [194]	0.83	1.04	0.56	0.41	0.80
Bolometric bond albedo, Å	0.45 [454]	0.61 [495]	0.33 [532] <sup>5</sup>	0.33 <sup>6</sup>	0.14? <sup>7</sup>
Calculated effective temperature <sup>4</sup> °K	105	71	57	45	42 <sup>8</sup>

<sup>1</sup> Photometric data in this table are in the widely used UBV photometric system. The broad passbands of this system were designed for stellar work, but the V-band gives a fair approximation to naked eye response. Detailed photometric properties are given in the main body of the text from modern narrow-band photometry.

<sup>2</sup> Calculated from  $V_0$  and data in Tables 1 and 3.

<sup>3</sup> Color index of the Sun is 0.63 [194].

<sup>4</sup> Calculated from A, data in Tables 1 and 3, and a value for the solar constant of  $1353 \text{ W m}^{-2}$ . This is the effective temperature each planet would have, if solar insolation were the only energy source.

<sup>5</sup> Original value scaled to radius in Table 1.

<sup>6</sup> Estimated as discussed in the subsection, *Visible Surfaces*, under URANUS AND NEPTUNE.

<sup>7</sup> Harris' [194] value for the visual albedo. It assumes a phase integral equal to that of Mars and a radius of 0.45 times that of the Earth.

<sup>8</sup> Effective temperature of a rapidly rotating body with the (very uncertain) properties listed. Pluto rotates slowly enough so that a relatively large difference between dayside and nightside temperatures can be expected. The effective temperature of a nonrotating body would be  $50.5^\circ \text{ K}$ .

<sup>9</sup> Andersson and Fix [12] have shown strong evidence of long period change in this mean magnitude; they find 15.07 for 1972 at zero phase. See discussion in the section, PLUTO.

well-defined reflecting layer (clouds or solid surfaces). Abundances were determined from absorption line strengths, with allowance for mean path length through the atmosphere. The early Jovian models of Kuiper [261] were of this reflection-layer type, for indeed, with information available even 20 years ago, no other assumption was feasible. Many atmospheric abundances are still quoted as though this assumption were valid, even while recognizing that in most cases it is not.

In a dense atmosphere, especially such as that of Uranus, Rayleigh scattering begins to contribute significantly to atmospheric opacity in visible light. As long as scatterers and absorbers are homogeneously mixed, and the properties of the scatterers are constant with height, and known, the abundance and atmospheric albedo problems are still quite tractable, although in reality this is never the case. Whenever a condensable gas is a minor component in saturation equilibrium, scattering density changes independently of gas density as a function of altitude. Spectral line formation and continuum albedo values in the resulting inhomogeneous atmosphere require a major numerical effort in a large computer.

While theory is adequate for most parts of the direct problem of predicting the behavior of radiation interacting with a simple, static, one-dimensional (vertical) atmosphere of known properties, the inverse problem, requiring definition of an

atmosphere from observed radiation, is far more difficult. Solution of this "atmospheric sounding" problem for Jupiter definitely requires data over a wide range of wavelengths and from point to point on the disk, which can only be obtained with adequate spatial resolution by special spacecraft experiments [456]. Up to the present, most work has consisted of solving the direct problem for families of "reasonable" models and comparing these to observations.

Further complications are of two types. One, already implied, is that Jupiter does not have a uniform atmosphere (nor does Saturn). There are obvious belts, zones, and spots (to be discussed later), and even the limited quantitative information now available indicates definite variation in many physical parameters from point to point on the Jovian disk. Attempts at temperature sounding with Earth-based spatial resolution, such as the recent work of Ohring [346], at best can give only an average over large areas of a very nonuniform planet. The second complication is that Jupiter is a dynamic body with obvious changes from month to month visible on even the poorest photographs.

Improvements in knowledge of planetary atmospheres follow a sort of iterative process, hopefully one which ultimately converges to the correct answer. The general procedure is to calculate preliminary models based upon the best estimates of atmospheric composition and temperatures. Data are then interpreted in terms

TABLE 3.—*Mechanical Data*

Parameter	Jupiter	Saturn	Uranus	Neptune	Pluto
Mean heliocentric distance, AU [341] <sup>1</sup>	5.203	9.539	19.182	30.058	39.439
Orbital eccentricity [341] <sup>1</sup>	0.0484	0.0557	0.0472	0.0086	0.2502
Orbital inclination [341] <sup>1</sup>	1° 18'	2° 29'	0° 46'	1° 46'	17° 10'
Sidereal period [341] <sup>2</sup>	11.862	29.458	84.013	164.793	247.686
Mean orbital velocity, km s <sup>-1</sup> [400]	13.06	9.65	6.80	5.43	4.74
Orbital angular momentum, kg km <sup>2</sup> s <sup>-1</sup> , calculated	$1.929 \times 10^{37}$	$7.813 \times 10^{36}$	$1.700 \times 10^{36}$	$2.514 \times 10^{36}$	ca. $1.8 \times 10^{34}$
Inclination of Equator to orbit	3.07° [369]	26.74° [369]	97.93° [369]	28.80° [369]	>50° [12]
Period of rotation	(see <sup>4</sup> )	(see <sup>5</sup> )	10.8 h [328] <sup>3</sup>	15.8 h [327] <sup>3</sup>	6.3874 d [342]

<sup>1</sup> Mean elements for the epoch 1960 January 1.5 ET.

<sup>2</sup> Tropical years.

<sup>3</sup> These periods are not accurately known. See subsection,

*The Visible Surfaces*, under URANUS AND NEPTUNE.

<sup>4</sup> See subsection, *The Visible Surfaces*, under JUPITER.

<sup>5</sup> See subsection, *The Visible Surfaces*, under SATURN.

of such models. Specifically, visible and thermal (infrared) opacities, which control energy transfer, are calculated for the best available abundances, and an attempt is made to study the energy balance of the atmosphere and derive temperature and pressure profiles, perhaps for a uniform, one-dimensional atmosphere in radiative equilibrium. Trafton published details of this major step in 1967 [465] for the four giant planets. Analysis of spectroscopic data and limb-darkening curves, using improved models, confirmed the inadequacy of the reflecting-layer theory and that an inhomogeneous model was required, at least to explain the observed center to limb variations. With resulting improvements in one-dimensional models, progress is now being made toward understanding the real, three-dimensional, dynamic Jupiter and toward models of the Jovian ionosphere, but these areas constitute the research frontier and are discussed in following sections.

### *Composition*

Molecular hydrogen is the major constituent of the Jovian atmosphere, and theoretical understanding of its properties is the best of any neutral molecule. Since it is a homopolar molecule,  $H_2$  has no normal dipole spectrum. A dipole moment can be induced by sufficient pressure but the resulting lines are broad, with small central intensity, and their equivalent widths are difficult to determine. Only the fundamental induced band at  $2.4 \mu m$  has been seen on Jupiter by Stratoscope II [99]. Molecular hydrogen does have a small quadrupole moment, and hydrogen abundances on Jupiter result largely from studies of lines in the second and third overtone (3.0 and 4.0) quadrupole rotation-vibration bands. These lines are intrinsically very weak and appear only because the  $H_2$  abundance on Jupiter is very large. An additional observational problem is introduced because these lines undergo observable collisional narrowing before ordinary pressure broadening sets in, making it difficult to determine accurate shapes and therefore pressures. The correct shape of such a line, narrowed by weak collisions, is believed to be given by

the Galatry profile [221, 233]. Unfortunately, such lines saturate while still very weak, and the highest possible resolution is required to obtain reasonable precision in abundance. The best  $H_2$  abundance available presently is about 65 km-amagat above a pressure near 1.7 atm [301].

Methane has a rich dipole rotation-vibration spectrum extending from  $7.8 \mu m$  well into the visible. Unfortunately, easily observed high overtones in the visible and near infrared are so complex that they have yet to be theoretically analyzed. No rotational quantum number assignments exist for any overtones higher than the  $3\nu_3$  band at  $1.1 \mu m$ , and only the *R* branch of that band has been analyzed, by Margolis and Fox in 1968 [299]. Laboratory line strengths are available from Bergstrahl and Margolis [46]; the Lorentz half-width from Bergstrahl [45]. Abundance of methane appears to be about 45 m-amagat above a pressure level near 1.7 atm [220, 298, 301]. An independent result, using the technique of Fourier spectroscopy, which averaged over a large part of the visible disk, gave  $38 \pm 8$  m-amagat above a pressure of about 2 atm [295].

Ammonia also has a rich dipole spectrum. Vibrational quantum numbers have been assigned to 42 bands in a recent analysis by McBride and Nicholls [314], who also carried out a rotational analysis of the  $5\nu_1$  band of ammonia at  $6450 \text{ \AA}$  [315]. The  $5\nu_1$  band is quite complex, with many blended features, and it is not clear that accurate abundance and temperature results for Jupiter can be obtained from assignments at available laboratory and observatory resolution. An empirical curve-of-growth analysis by Mason [310] suggests an abundance of  $13 \pm 3$  m-amagat and appears to be the best published result. This abundance should refer to the level above about 1.7–2.0 atm pressure as in methane and hydrogen, since a dense cloud deck is believed to be at that level (see section, **Atmospheric Structure**). The recent much higher abundance of Ohring [346] seems incompatible with other observations and with models assuming a solar abundance of nitrogen [506]; (see section, **Atmospheric Structure**). This result may be due to neglecting the clouds in the analysis.

Measurements of Jovian thermal disk temperatures at radio wavelengths provide data on ammonia abundance below the ammonia clouds [115, 137, 184, 525] as well as above them [183, 525]. Ammonia manifests itself through inversion-splitting of the molecule's rotational energy states. These transitions are believed to provide the principal source of radio opacity in the Jovian atmosphere. Gulkis and Poynter [184] have derived an ammonia mixing ratio of ca  $1.5 \times 10^{-4}$  below the clouds, based on the observed temperature spectrum (see next section, *Temperature*). This value is close to that expected for an atmosphere which contains a solar cosmic abundance of elements [278], thereby supporting the view that Jupiter's atmosphere is composed of primitive solar nebula material.

Direct spectroscopic detection of helium on a cold body is not possible from Earth's surface and is very difficult even from an Earth-orbiting satellite. The traditional assumption has been that helium is present on Jupiter in near solar abundance, but the first direct observational evidence of its presence was detection, by Pioneer 10 [239], of the 584 Å helium resonance line with a strength of 10–20 Rayleighs. Unfortunately, this measurement cannot be converted easily to a deep atmospheric abundance. Two crude abundance values for the region below the turbopause became available recently, however. Light curve inversion of multi-wavelength observations of the occultation of the star  $\beta$ -Scorpii by Jupiter allowed Sagan et al [406] to derive a helium fraction of  $0.16^{+0.19}_{-0.16}$  by number. The solar fraction is  $\text{He}/(\text{H}_2 + \text{He}) \cong 0.12$  [73]. A helium fraction can also be determined from the pressure effects of helium on the  $\text{H}_2$  rotation and translation spectrum in the far infrared [223]. The Pioneer 10 infrared radiometer experiment thus definitely indicated the presence of helium, the preliminary ratios being given as  $\text{He}:\text{H}_2 = 0.6$  in the south equatorial belt and 0.8 in the south tropical zone [88]. Until more complete experimental results including an error analysis are available, continued use of the solar fraction, ca 9 km-amagat, seems reasonable.

Three new molecules have been identified recently on Jupiter by Ridgway, using a Fourier

spectrometer on the 150-cm McMath solar telescope [392]. He estimates 10 cm-amagat<sup>2</sup> ethane ( $\text{C}_2\text{H}_6$ ) and 0.2 cm-amagat acetylene ( $\text{C}_2\text{H}_2$ ) as preliminary values from available data [392]. Roughly 0.9 cm-amagat phosphine ( $\text{PH}_3$ ) was also detected [393]. Presence of nonequilibrium species such as  $\text{C}_2\text{H}_6$ ,  $\text{C}_2\text{H}_2$ , and  $\text{PH}_3$  in these abundances strengthens the possibility that more complex organic species are also present.

Two isotopes have been detected on Jupiter. Beer and Taylor [34] found  $1.3 \pm 0.3$  cm-amagat  $\text{CH}_3\text{D}$  in their Fourier spectra of the 4.65  $\mu\text{m}$  region. With allowance for deuterium fractionation, they derived the ratio  $\text{D:H} = 4.8 \times 10^{-5}$  with error bounds of roughly  $\pm 50\%$  [34]. Their results are somewhat model-dependent, that being the source of most of the probable error. Fox et al [148] reported the probable detection of  $^{13}\text{CH}_4$  in Jupiter with an isotopic abundance ratio  $^{12}\text{C} : ^{13}\text{C} = 110 \pm 35$ .

All the abundances quoted in the previous paragraphs are some form of mean in both time and space. An attempt is always made to reduce the data to a one atmosphere path. Average limb-darkening results are discussed in a section, *The Visible Surface*. However, an entire series of papers at the 1974 annual meeting of the Division of Planetary Sciences, American Astronomical Society, gave evidence of additional spatial and temporal variations in the strengths of various Jovian atmospheric components. For example, variation in the strength of the 3-0 S (1) line of  $\text{H}_2$  by 40% in a week was reported [479]. Until such changes are clearly understood and reported, all abundance data must be treated with caution.

A number of rocket and satellite studies have been made of Jupiter at ultraviolet wavelengths. Atomic hydrogen has been detected several times by means of its Lyman- $\alpha$  emission at 1216 Å. In a recent rocket study by Rottman et al [399], a disk brightness of 4.4 krayleighs in this line was found, while Pioneer 10 found 1 krayleigh [239]. The difference may be a real time fluctuation or could be due to interference in the rocket experiment from the bright hydrogen torus in Io's orbit (see section, *SATELLITES*

<sup>2</sup> Later corrected to 1 cm-amagat (*Astrophys. J.* 192:L51, 1974).

AND RINGS). Other features exist in these and other spectra (see Jenkins [235]), but resolution is still low and identification uncertain.

Spectroscopic searches have placed *upper limits* on other species in Jupiter's atmosphere. The limits depend upon the molecular band wavelength as well as its intrinsic strength, since the Jovian atmosphere is much more transparent in some regions (near 5  $\mu\text{m}$ , for example) than others. More than one upper limit is given in Table 4 to provide information corresponding to different spectral regions.

Large-scale computer calculations have been carried out on the probable molecular composition of the Jovian atmosphere, assuming it is in thermodynamic chemical equilibrium. The most extensive work has been undertaken by Lewis and coworkers. Beginning with cosmic abundances, Lewis [278] showed that at temperatures from the freezing point of water to above 1000° K, virtually all oxygen is contained in  $\text{H}_2\text{O}$  molecules, all carbon in  $\text{CH}_4$ , all nitrogen in  $\text{NH}_3$ , and all sulfur in  $\text{H}_2\text{S}$ . At lower temperatures,  $\text{H}_2\text{O}$  freezes out and  $\text{H}_2\text{S}$  is removed through the formation of  $\text{NH}_4\text{SH}$  clouds [506].

TABLE 4.—*Upper Limits on Undetected Gases in the Jovian Atmosphere*

Gas	Wavelength, $\mu\text{m}$	Upper abundance, limit cm atm	Reference
$\text{C}_2\text{H}_4$ (ethylene)	10.5	0.5	[163]
	5.3	5	[163]
	0.8715	200	[354]
$\text{CH}_3\text{NH}_2$ (methylamine)	12.8	0.05	[163]
	1.52	2	[98]
	1.0325	300	[354]
HCN (hydrogen cyanide)	14	1	[163]
	4.75	70	[163]
	1.53	5	[98]
	1.0385	200	[354]
$\text{C}_2\text{N}_2$ (cyanogen)	4.7	2	[163]
$\text{H}_2\text{S}$ (hydrogen sulfide)	8.0	300	[163]
	1.58	25	[98]
	0.22	0.08	[9]
SiH <sub>4</sub> (silane)	10.5	1	[163]
	0.9738	2000	[354]

Molecules such as  $\text{PH}_3$ ,  $\text{C}_2\text{H}_2$ , and  $\text{C}_2\text{H}_6$  are distinctly nonequilibrium species, however, and indicate the occurrence of dynamic processes to some extent.

#### Temperature

Fundamental improvements in detectors of middle- and far-infrared radiation became available in the early 1960s; during this same period, the sensitivity of radio telescopes to millimeter waves was also improved, making studies of Jupiter practical at these wavelengths. Temperatures at wavelengths shorter than 1 mm are given in Table 5 in two groups: disk brightness temperatures and subsolar-point blackbody temperatures from thermal maps.

Thermal radio radiation from Jupiter was first detected at 3.15 cm wavelength in 1956 and 1957 [313]. These early observations gave a temperature of  $145^\circ \pm 26^\circ \text{ K}$  which was reasonably consistent with the estimated equilibrium temperature of Jupiter and with infrared measurements. Subsequent observations of Jupiter at longer wavelengths revealed rapid increase in temperature with increasing wavelength. It was suggested by Drake [125] and later confirmed by observations that the longer wavelength radiation from Jupiter is generated by high energy electrons trapped in the magnetic field of Jupiter in regions similar to those of the Van Allen belt around Earth.

Thermal emission from Jupiter's atmosphere and radiation belt (synchrotron) emission are now known to contribute equally to Jupiter's total emission near 7-cm wavelength. Presence of the synchrotron emission component makes it difficult to measure accurately the planet's thermal disk spectrum. Attempts have been made to separate disk from nonthermal emissions by using radio interferometric techniques and by making certain assumptions about the polarization properties of synchrotron emission. The interferometric method of separation is the most reliable of the two methods although there are few measurements using this technique. Berge [39, 40], Branson [63], and Olsen have used the interferometric technique to derive atmospheric emission at wavelengths from 2–21 cm. Dickel [115] combined his polarimetric observations of

Jupiter with interferometric results and atmospheric modeling to derive the thermal spectrum from short millimeter wavelengths to 21 cm. The resultant disk spectrum of Jupiter is shown in Figure 1. (For data used in this figure see [179, 343, 483]). The observed spectrum (after removal of synchrotron emission) rises from a value near 140° K at 1.25 cm to over 350° K at 21 cm. The generally accepted interpretation of this spectrum is that it is due to a deep convective atmosphere, in which ammonia exists as a trace constituent and is the principal source of radio-opacity.

A large number of rotational temperatures have been derived for Jupiter. Since the atmosphere is not isothermal, temperatures so derived are obviously a form of weighted mean over the absorbing region. The Curtis-Godson approximation is frequently employed to determine the appropriate weighting factor in a vertically inhomogeneous model atmosphere, so that the model can be compared directly to observations. This is a valid procedure, even for the collision-narrowed lines in the quadrupole spectrum of

$H_2$  [301]. In applying it to Jupiter, however, proper allowance must be made for the effects of absorption and scattering in the cloud layers, which requires that these be modeled also.

Margolis [298] showed that a simple reflecting layer model could be used for temperature, pressure, and abundance determinations as long as observations were strictly limited to the center of the disk. Apparently, this is because the upper cloud deck is strongly forward scattering and of moderate optical depth in the infrared, while the second cloud layer is very dense and behaves like a reflecting layer [301]. Explanation of center-to-limb variations requires a full inhomogeneous atmosphere treatment, however. Therefore, most of the rotational temperatures reported are of little quantitative value, since they combine data taken all over the disk. It can be stated, however, that temperature at the second (main) cloud deck must be higher than any of the measured rotational temperatures, and several of these are  $\geq 180^\circ K$  [300, 358].

The width of the pressure-induced fundamental band of  $H_2$  required a temperature of  $200^\circ -$

TABLE 5.—*Jovian Brightness Temperatures to 1 mm*

Wavelength, $\mu m$	Disk brightness temperature, $^\circ K$	Reference	Remarks
7.5–8.2	140	[163]	In $\nu_4$ band of $CH_4$ ; covered 65% of disk
9.2–12.0	127	[163]	In $\nu_2$ band of $NH_3$ ; covered 65% of disk
30–45	$136 \pm 1$	[16]	Calibration assumes Mars is a $235^\circ K$ blackbody
45–80	$150 \pm 5$	[16]	Do.
65–110	$153 \pm 7$	[16]	Do.
30–300	$133 \pm 1$	[16]	Do.
1.5–350	$134 \pm 4$	[23]	Stellar calibration
Wavelength, $\mu m$	Subsolar point temp., $^\circ K$	Reference	Remarks
5	See remarks	[241, 357, 508]	Radiation primarily from discrete sources with temperature perhaps ca $300^\circ K$
7.9	See remarks	[165]	Limb-brightening curve only, normalized to disk center $\Delta\lambda/\lambda$ ca 0.015
8.4	See remarks	[165]	Limb-darkening curve only, normalized to disk center $\Delta\lambda/\lambda$ ca 0.015
8.2–9.2	130–135	[507]	Correlated with surface features; higher values in belts than in zones
8–14	129	[516]	Temperature shown is average of 5 nights; individual nights shown in reference
17.5–25	150?	[163, 285]	Low reports variation in time and over disk, but complete details unpublished
14–25	126	[88]	Pioneer 10 result for the South Equatorial Belt
28–40	123	[288]	Calibrated with $\alpha$ Boo and $\alpha$ Her but Jupiter observations made at large air mass
30–55	145	[88]	Pioneer 10 result for the South Tropical Zone

225° K, according to Danielson [99]. Since absorption in such bands varies as the square of the density, this temperature presumably would refer to a better defined level near the main cloud deck. The meaning of all temperature measurements is understood much more plainly in terms of the models discussed later in this section.

### The Visible Surface

**Clouds.** The surface of Jupiter is shown to consist of alternating bright "zones" and dark "belts," even through a small telescope, with the zones generally whitish or yellowish and the belts more often brownish or reddish. The better photographs taken from Earth and those of Pioneer 10 show an intricate structure of spots, festoons, plumes, and waves [146]. Grays, blues, and blacks show up locally. The overall impression is one of pastels, although local areas can have considerable saturation.

The clouds of Jupiter have been "known" for many years to be of ammonia cirrus, i.e., clouds of small frozen ammonia particles. It will be indicated in the discussion of atmospheric structure that indeed, there must be a layer of

ammonia cirrus clouds, but recent work indicates that this layer must be rather tenuous. At longer wavelengths, one apparently sees through these clouds, at least near the center of the planetary disk, and through a clear region below them to a second, more substantial cloud deck that is perhaps made up of ammonium hydrosulfide particles.

The source of colors and cause of the banded appearance of Jupiter are not known in detail, although there are a number of hypotheses about the former. For example, Owen and Mason [356] suggest that the dominant yellowish color might be caused by a dilute mixture of  $(\text{NH}_4)_2\text{S}$  in the  $\text{NH}_4\text{SH}$  cloud deck. Lewis and Prinn [282] added the suggestion of  $(\text{NH}_4)_2\text{S}_x$ , or elemental sulfur. A detailed study by Prinn of ultraviolet ( $\lambda \leq 2700 \text{ \AA}$ ) radiation transfer and photolysis in the Jovian atmosphere [374] indicates that some radiation of wavelength greater than 1600  $\text{\AA}$  should penetrate through the atmosphere to the clouds and may result in photolysis of  $\text{NH}_3$  and  $\text{H}_2\text{S}$ . He suggests that these begin chain reactions which may result in a freezing out of such colored material.

Sagan and Khare [246, 405] reported on laboratory experiments in which various mixtures of  $\text{CH}_4$ ,  $\text{C}_2\text{H}_6$ ,  $\text{NH}_3$ ,  $\text{H}_2\text{S}$ , and liquid  $\text{H}_2\text{O}$  were irradiated by mercury emission at 2537 or 2537 and 1849  $\text{\AA}$ . Reaction products included a high molecular weight reddish-brown polymer and various amino acids. Another nonequilibrium process, electrical discharge, may result in complex organic molecules. Ponnamperuma and coworkers [81, 325, 523] studied the products of electrical discharges in mixtures of  $\text{CH}_4$  and  $\text{NH}_3$ . Hydrogen and nitrogen were liberated, and  $\text{HCN}$  and various nitriles were found among the volatile products, which was of considerable biological interest because nitriles hydrolyze to amino acids. A reddish nonvolatile reactant was also formed which yielded, upon acid hydrolysis, a number of amino and imino acids.

If the Jovian atmosphere is convective to great depths, as suggested by radio data, then the high temperatures will tend to destroy any complex organic molecules. Whether a steady state is possible, with sufficiently rapid production by photolysis and/or discharge to maintain visible

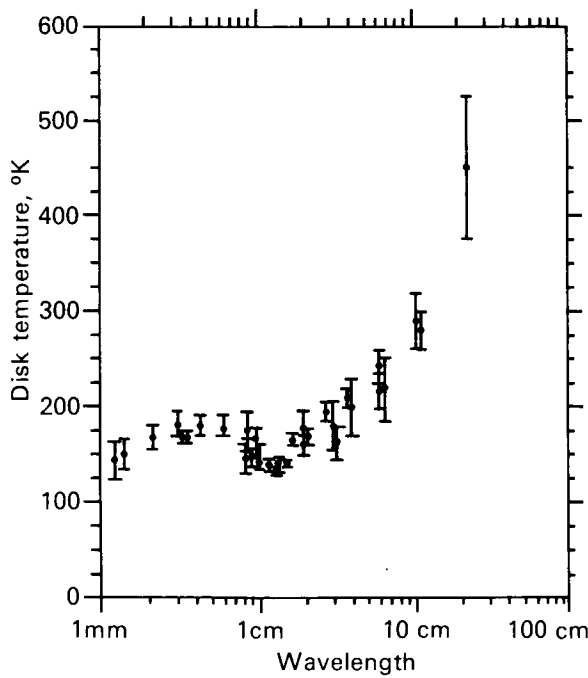


FIGURE 1.—Microwave spectrum of Jupiter's disk radiation.

amounts of them, depends on a number of completely unknown factors. The prominent ideas of a decade ago, that colors are caused by free radicals or solutions of sodium in ammonia, have fallen into disfavor as the atmospheric structure of Jupiter has become better known.

The detailed structure and motions of the Jovian clouds are direct evidence of extremely complex dynamic behavior. Although they remain in alternating dark belts and light zones parallel to the Equator of the planet, complex phenomena occur, particularly at the edges of the belts. A tremendous amount of data on the visible appearance of Jupiter over a long period has been collected and described by Peek [361]; his book should also be consulted for standard nomenclature for the visible surface.

Information on the rotation period within individual belts and zones has been gathered by Chapman [83], Reese [383], and Inge [224]. For example, these data show that since 1917, the north temperate current at the south edge of the north temperate belt has rotated even more rapidly than the equatorial belt. Over the years, there have been many attempts to correlate solar activity with activity in Jovian cloud belts or the Great Red Spot, as variously defined. A sampling of recent papers seems to say yes [25], no [144], and maybe [26, 376, 377].

It is not absolutely certain which phenomenon, if either, belts or zones, lies higher in the atmosphere. There is agreement that the upper cloud deck is nonuniform; but Teifel [460] finds more absorption in the  $\lambda$ -6190 methane band above dark belts, and Owen and Westphal [357] find less absorption in the even stronger  $\lambda$ -8940 methane band above the belts. The hottest spots on the planet are in belts, localized blue to black areas showing temperatures of 300° K or greater [508], although these may be holes where radiation from deeper regions easily penetrates. Temperature maps indicate that belts have higher temperatures than zones, however, even where there are no hot spots, which may indicate they are lower than the light-colored zones. The origin of belts is a complex hydrodynamic problem [for example, see 159, 207, 447, 477], and even an empirical description of them still lacks physical detail.

*Rotation.* One of the interesting problems of Jovian meteorology is that clouds making up the visible surface rotate as two rather distinct systems. Points within about 10° of the Equator constitute System I, whose standard meridian rotates with a period of 9 h 50 min 30.003 s. Points lying more than 10° from the Equator in either hemisphere constitute System II, whose standard meridian rotates with a period of 9 h 55 min 40.632 s [361]. Cloud motions relative to standard meridians make a choice of period completely arbitrary; however, some exact standard is needed for reference, and the numbers used have historical significance. The so-called equatorial jet which constitutes System I has been a particularly vexing meteorologic problem. It rotates more rapidly than any other visible surface part (except for the small north temperate current), and apparently more rapidly than the body of Jupiter (System III).

A true rotation period is difficult to define unless a body has a solid surface for reference, and Jupiter may not have such a surface (see section, **Body Structure**). The most likely true period seems to be that in which the magnetosphere rotates. This rate has been measured by radio astronomers at both decameter and decimeter wavelengths, and it is generally referred to as System III. A modern value of the System III period, based upon both decimeter and decameter studies, is 9 h 55 min 29.75 s  $\pm$  0.04 s [78]. If Jupiter should be fluid throughout, the concept of average or body rotational period will be difficult to define and of little use.

*Great Red Spot.* The most permanent feature of Jupiter's visible surface is the famous red spot. An elongated area of some 38 500 km in length by 13 800 km in width when at its largest in the 1880s [382], the Great Red Spot was probably seen 300 years ago and definitely noted in observations made more than 120 years ago [361]. The spot became most famous during the period 1879–1882, when its color was quite intense. Since that time, its visibility and color have waxed and waned, and even though the color has disappeared entirely at times, the location of the spot, the so-called red-spot hollow, has always been obvious. The red spot was very

prominent during 1962 and 1963, and remained quite "healthy" through 1965. It started to fade in 1966, and by February 1968 was extremely weak. Then, it suddenly began to strengthen and soon was back to its old prominence of 4 years earlier [382, 384, 388, 435, 436, 437]. This can be seen from the isodensitometry of Banos and Alissandrakis [27]. During 1969, its size averaged about 28 200 by 13 700 km [382].

The remarkable feature of the spot is that it does not seem to be solidly attached to any fixed surface but has wandered through  $1200^{\circ}$  of longitude during the past century (movement with respect to a mean motion of Jupiter which minimizes the red spot motion). There have been numerous short-period oscillations in regard to the steadier motion. Solberg [436] found a 3-month periodicity in these smaller excursions, and data for 7 consecutive years now give the oscillation a mean amplitude of  $0.8^{\circ}$  and a period of  $89.89 \pm 0.11$  d [382]. The circulating current has had a rotational period of 90 d with respect to System II during this time and may be driving the red spot in this oscillation. Meanwhile, the spot's center latitude remained nearly fixed, as always. During 1968–69, it had a mean value of  $-22.25^{\circ} \pm 0.03^{\circ}$  and always remained between  $-22.0^{\circ}$  and  $-22.5^{\circ}$  [382]. New data for 1969–71 have been given by Reese [384, 386].

It is interesting that at  $5 \mu\text{m}$  and at  $8-14 \mu\text{m}$ , the red spot is cooler than its surroundings [241, 515]. This is compatible with several observations showing less absorption above it [53, 329, 356] and suggests the feature penetrates to a high atmospheric level.

In January 1966, a small dark spot moving along the north edge of the south temperate belt approached the red spot, started around its south side, and circled it almost 1.5 turns before it disappeared [387]. Its period of circulation was 9 d. During the following year, four other dark spots, at least two from the south equatorial belt, showed similar behavior, though seen through only part of a turn around the red spot. These four spots had a circulation period of 12 d. Reese and Smith [387], reporting these fascinating observations, suggest that perhaps different atmospheric levels were involved.

Older hypotheses on the nature of the red

spot were variations of a solid island floating in dense atmosphere [361], but increased knowledge of physical conditions in the Jovian atmosphere has made such theories highly improbable [402]. No known substance can be both solid and have a lower density than the Jovian atmosphere at temperatures and pressures thought to exist there. If the floating object is supposed to have sufficient vertical extent to reach a depth where phase changes offer a level in which to float, then it would almost certainly be disrupted by the stresses at pressure levels of 0.1–10 Mbar [208]. Furthermore, an object floating in a density discontinuity would tend to be moved in latitude (toward the Equator) by the Eötvös force [402].

It was proposed by Hide in 1961 that the red spot might be the upper end of a Taylor column, a stagnant column of fluid caused by a two-dimensional atmospheric flow unable to surmount a topographic feature [202, 203]. The gross longitudinal motion is attributed to actual change in the rotation period of Jupiter's mantle caused by hydrodynamic motions in the core [202]. Of course, if Jupiter has no solid surface, then additional hypotheses must be invoked to save the Taylor column, such as the topographic feature being a magnetic loop or the upper end of an internal convection cell. Smoluchowski [431] has suggested that the topographic feature, causing the Taylor column, could be nearly pure solid hydrogen floating in helium-rich liquid hydrogen. However, there would still be the problem of explaining the latitude constraint. There have also been fluid-dynamic objections to the Taylor column hypothesis. The "original" Taylor column was considered as an application of the Taylor-Proudman theorem for a homogeneous fluid. Such columns, which have been produced in the laboratory [208], are completely stagnant with no vorticity or exchange with their surroundings. The question arises whether a similar structure can exist in a real baroclinic atmosphere and perhaps have some exchange with its surroundings. Hide [206] considers it likely, while Stone and Baker [448] consider it unlikely, as do Sagan [403] and Kuiper [265, 266]. In part, this becomes a question of semantics: Should the resulting structure be called a Taylor

column even if it exists? Hide [204, 206] continues to study the problem while viewing his hypothesis cautiously.

Colitsyn [170] suggests that the characteristic period for major changes in Jovian circulation may be  $3 \times 10^5$  yr or more, and, therefore, the red spot may simply be "a large long-lived eddy." Streett et al [450] have been studying the so-called Cartesian diver hypothesis in which a mass of hydrogen-rich solid floats in neutral buoyancy in a stratified fluid mixture of hydrogen and helium deep in the atmosphere and changes the surface appearance, perhaps through its effect on atmospheric convection or even creation of a Taylor column. Kuiper [266] studied a model of "organized cumulus convection" for the red spot and made persuasive arguments in its behalf, although Maxworthy [312] found considerable fault with the dynamics of his description.

The Great Red Spot of Jupiter is, at present, a fascinating, mysterious object, unique in its size and stability among atmospheric phenomena in the solar system. Until some hard, quantitative knowledge of Jovian atmospheric dynamics is obtained, it will remain one of the solar system's intriguing puzzles.

*Photometric properties.* Acquisition of photometric data on Jupiter is not an easy task. Complex atmospheric absorption and scattering cause rapid changes in photometric properties with wavelength. Rapid rotation limits the time available for detailed study and secular changes in the visible surface alter even disk-integrated properties as well as detailed properties. Finally, the phase angle of Jupiter, as observed from Earth, never exceeds 12°, so it is not possible to measure the phase function, phase integral, or complete photometric function. Jupiter's mean opposition magnitude has ranged over 0.45 magnitude at various oppositions since 1862 [194]. The value in Table 1 is the mean of these, although during 1963–65 [529] the actual value was  $V_0 = -2.70$ , 0.15 magnitude brighter. Harris [194] suggests that a phase coefficient of 0.005 magnitude/degree is appropriate at small phase angles for visual data. This implies that current observations will always be needed whenever the best possible photometric data are required.

A group associated with Harvard College Observatory carried out extensive photometry of Jupiter and Saturn from 1962 through 1965 in southern France and South Africa [230, 231], using 10 narrowband filters as well as UBV. Their detailed response curves are given by Young and Irvine [529]. The effective wavelengths and geometric albedos which resulted for the 10 narrow passbands are given in Table 6, having been corrected to agree with data in Table 1 and a visual solar magnitude of  $-26.8$ . The magnitudes given are an average of South African [231] and French [230] data. When tabulated chronologically, these data show a change in Jovian color from 1963 to 1965 [210].

TABLE 6.—*Jovian Geometric Albedos*

Passband	Effective wavelength, Å	Geometric albedo
v	3147	0.261
u	3590	0.305
s	3926	0.350
p	4155	0.404
m	4573	0.449
l	5012	0.483
k	6264	0.547
h	7297	0.415
g	8595	0.305
e	10635	0.295

Good reflected light, integrated photometry of Jupiter at wavelengths beyond  $1.1\text{ }\mu\text{m}$  does not exist, one reason being that the extensive absorptions by  $\text{CH}_4$  and  $\text{NH}_3$  beyond that wavelength leave only a few windows through to the continuum. Spectra at longer wavelengths have been taken [35, 98, 99, 163, 236], but none give absolute integrated results (although Danielson's [99] wide-slit measurements come close).

Satellite and sounding rocket studies of the Jovian ultraviolet spectrum have been made, in addition to the Pioneer 10 experiment, but calibration has been a difficult problem; many of the early results are not mutually compatible. Recent photometry, benefiting from improved measurements of the solar ultraviolet, has been obtained by Wallace et al [496]. Their Orbiting Astronomical Observatory (OAO-2) results covered the wavelength region from 2100 to

3600 Å at a resolution of 20 Å and showed a radiance factor of 0.25 at 3000 Å and 10° phase, rising to 0.31 at 2500 Å, and dropping back to 0.25 between 2000 and 2100 Å. True geometric albedos would perhaps be 5% larger, while corrections to the solar absolute magnitude and Jovian radius used in this document would decrease the final result by about 7%. Fluctuations in ultraviolet flux within about 0.05 magnitudes occur in one 10-h rotation of Jupiter, the planet being faintest when the red spot is on the central meridian [408]. There are no accurate albedos below about 2000 Å because the solar continuum is falling rapidly to nearly zero below 1800 Å. Rocket spectra show some faint emission, due possibly to H<sub>2</sub>, throughout the region from 1250 Å to about 1600 Å [399].

Since the phase angle of Jupiter never exceeds 12°, the phase integral  $q$  cannot be measured from Earth. Limb-darkening curves have been used to derive approximate values for  $q$ :  $q(U) = 1.55$ ,  $q(B) = 1.60$ , and  $q(V) = 1.65$ , but there is no unique relation between limb darkening and phase integral, and these values could be grossly in error [194]. Taylor assumed a phase integral of 1.6 at all wavelengths, to derive a bolometric Bond albedo of 0.45 [454]. The uncertainty in the latter was considered to be about  $\pm 0.07$ .

Limb-darkening curves have been derived by a number of observers both in and out of specific molecular bands [24, 201, 329, 337, 354, 459, 460]. Infrared equatorial and meridional limb-darkening curves have been taken from 0.6 to 2.0 μm [56]. Detailed photoelectric photometry has been carried out in 24 bands from 0.30 to 1.10 μm [364], in which the north and south tropical zones have been compared with the combined north equatorial belt and equatorial zone, with sizable differences found. Even more detailed work has been done [53], using 8 bands from 1.4 to 1.63 μm, taking data at 41 points on the Jovian disk and at three phase angles, from which an NH<sub>3</sub> absorption map of Jupiter, limb-darkening coefficients, and some CH<sub>4</sub> distributional data have been derived.

Polarimetry is a rather neglected technique for atmospheric study. Morozhenko and Yanovitskiy studied the entire disk of Jupiter as well

as the disk center in seven passbands [330, 331]. They derived a refractive index for atmospheric aerosols (1.36), which is that of ammonia, and particle diameters ca 0.4 μm. In detailed polarimetry, much stronger polarization was found at Jupiter's poles than near the equator, for example [187], and even considerable asymmetry is found between the two poles [154, 156]. At short wavelengths near the Equator, the polarization is typical of molecular scattering, while at longer wavelengths, there is evidence for aerosols. Much larger optical depths appear to be reached near the poles, perhaps indicating fewer ammonia particles there. With careful interpretation and improved models of the Jovian atmosphere, polarization measurements should offer fairly direct, local information on cloud heights and atmospheric aerosol content at the time of observation; this is information difficult to obtain in any other way.

The recent report of circularly polarized visible (6800 Å) light from Jupiter [243, 244, 245] was unexpected. At first, polarization was positive in the south polar region, and twice as large and negative in the north polar region, with fractional values a few times 10<sup>-5</sup>. Then, as Jupiter approached opposition, magnitude decreased to zero; after opposition, it increased but with opposite sign, indicating atmospheric multiple scattering to be responsible for the effect.

### *Energy Balance*

An apparent discrepancy between solar energy absorbed by Jupiter and energy emitted by the planet was emphasized by Opik [349]. A bolometric albedo for Jupiter of 0.45 implies that the effective temperature should be 105° K [454]. Brightness temperatures have been measured at virtually every wavelength in the infrared, and an effective temperature as low as 105° K seems impossible. The very broadband measurement covering 1.5–350 μm yielded a temperature of 134° K [23] which is revealing, since more than 99% of the energy of a 105° K blackbody is emitted in this wavelength range. It can be argued that the bolometric Bond albedo for Jupiter could be seriously in error (see subsection *Photometric properties*), but even if Jupiter were a blackbody

(with zero bolometric albedo), which it clearly is not, its effective temperature would only be 121° K. Only 15% (or  $0.45 \pm 0.07$ ) total uncertainty in the bolometric Bond albedo is estimated [454]. An albedo of 0.38 would raise the effective temperature to 109° K.

Jupiter rotates in less than 10 h. If the thermal relaxation time of the radiating "surface" of Jupiter is long compared with 5 h, it must radiate effectively from the total surface of the planet. If it relaxed to a very low temperature in much less than 5 h, then it would effectively radiate only from the lighted hemisphere, whose radiation balance temperature could be a factor of as much as 20<sup>25</sup> greater than 105° K (or 124° K). In fact Pioneer 10 showed that there is no difference between day and night side temperatures [88], as was expected from theoretical calculations and from thermal limb-darkening curves.

An effective temperature of even 125° K implies contribution from an internal energy source of  $7 \times 10^{-4}$  W cm<sup>-2</sup>, an amount of power equal to that absorbed from the Sun (assuming the Bond bolometric albedo of 0.45 is correct). An effective temperature of 134° K corresponds to an internal source of  $1.2 \times 10^{-3}$  W cm<sup>-2</sup>. This internal source has large effects upon both models of the Jovian interior and model atmospheres.

### Atmospheric Structure Models

Pressure-temperature-altitude profiles for the Jupiter atmosphere have been calculated by a number of authors. These models are based on many simplifying assumptions, meant to be representative of average conditions. Local variations of atmospheric parameters (weather) are ignored. Dynamics are included in calculations only insofar as they determine the average static structure.

Standard model atmospheres generally consist of a tropospheric region in which the deep atmosphere is in convective equilibrium with an upper troposphere in radiative equilibrium. An accurate model of the thermal opacity of the upper atmosphere is required to compute models

of the radiative region. The dominant source of thermal opacity in this region has been shown to be pressure-induced translational and rotational absorption by molecular hydrogen [465]. Ammonia furnishes some additional opacity, the greatest amount coming from the  $\nu_2$  rotation-vibration band at 10 μm [160, 467]. Other sources of atmospheric opacity are the  $\nu_4$  methane band at 7.5 μm, cloud layers, and any aerosols present in the atmosphere. The methane band provides complete absorption of more than 100 cm<sup>-1</sup> of spectrum even above the effective temperature level of 134° K in the Jovian atmosphere [455], but this is a very small fraction of total opacity. Polarization measurements of Morozhenko and Yanovitskiy [331] noted only small concentrations of aerosols but may have referred to strictly high atmospheric levels. Stratoscope II observations of the 3.0 μm bands of NH<sub>3</sub> require many larger solid particles for satisfactory explanation of the observed band strengths [409].

Almost two-thirds of the energy enters the Jupiter troposphere by convection, driven by the internal energy source. About 45% of incident solar energy is reflected, more than 10% is absorbed fairly high in the atmosphere in strong methane bands [476], a very small amount is absorbed in gaseous ammonia and molecular hydrogen, and the remainder—slightly more than 40%—must be absorbed by clouds at various levels.

A model atmosphere for Jupiter was published recently which includes thermal opacity of molecular hydrogen and ammonia and takes proper account of dynamic effects [477]. This model is reproduced as Table 7. It assumes an effective temperature of 135° K, He:H<sub>2</sub> = 0.1; CH<sub>4</sub>:H<sub>2</sub> =  $3 \times 10^{-3}$ ; maximum NH<sub>3</sub>:H<sub>2</sub> =  $1.7 \times 10^{-4}$ ; and surface gravity 2500 cm s<sup>-2</sup>. Omission of cloud layers is the model's most obvious deficiency. Methane was also not included; hence, there is no atmospheric heating or opacity and no modeling of the temperature inversion region of the atmosphere above the tropopause. Also, there is still some disagreement as to best values for the pressure-induced opacity of H<sub>2</sub> [426], and changes could result.

It is necessary to mention at this point that

REPRODUCIBILITY OF THE  
ORIGINAL PAGE IS POOR

temperature and pressure profiles were obtained from the S-band (2.3 GHz) occultation experiment [250] on Pioneer 10, which produced measurements deep into the neutral atmosphere, reaching a level of 2.8 atm for daytime entry and about 2.4 atm for nighttime exit. Assuming a composition of 85% H<sub>2</sub> and 15% He, atmospheric temperature at these pressures was found to exceed 700° K, considerably higher than convective equilibrium models and ground-based infrared and radio observations had predicted. This result now appears to be incorrect; the discrepancy is believed to be due to an incorrect inversion procedure which resulted from neglecting the oblateness of the planet. For example, the Trafton-Stone model has a temperature of 180° K near 1 atm whereas the occultation result gives a temperature near 500° K at this same pressure level. Most infrared

and radio measurements from Earth have indicated a temperature about 130°–150° K at pressure levels about 0.3–1 atm, whereas the Pioneer 10 occultation result yielded temperatures between 300°–450° K over this pressure range.

Another important difference between the models and occultation data is the temperature lapse rate. Pioneer 10 measured a temperature lapse rate of about 2.5° K/km which is substantially greater than adiabatic for the assumed composition. It is not currently understood how these discrepancies can be reconciled. Kliore et al [250] suggest that the presence of cloud or dust particles in the 1–30 mbar pressure altitude range could confuse interpretation of infrared data. However, they correctly point out, this would not explain observations at microwave frequencies.

TABLE 7.—*Radiative Dynamical Model Atmosphere for Jupiter*<sup>1</sup>

Depth, km	Temperature, °K	Pressure, log dynes cm <sup>-2</sup>	Density, g cm <sup>-3</sup>	H <sub>2</sub> abundance, km-amagat	Optical depth at 520 cm <sup>-1</sup>
0.0	105.6	3.843	1.694(−6)	0.26	0.000
14.4	105.6	4.231	4.263(−6)	0.63	0.003
22.3	106.1	4.444	6.927(−6)	1.03	0.008
29.7	106.8	4.643	1.088(−5)	1.63	0.020
34.2	107.5	4.764	1.430(−5)	2.16	0.035
41.0	109.4	4.945	2.129(−5)	3.27	0.080
46.3	111.8	5.083	2.862(−5)	4.49	0.15
53.1	115.7	5.270	4.215(−5)	6.91	0.30
57.0	119.9	5.349	4.933(−5)	8.30	0.50
60.2	123.3	5.425	5.707(−5)	9.87	0.70
63.7	127.6	5.505	6.636(−5)	11.9	1.00
67.2	132.4	5.582	7.624(−5)	14.2	1.40
69.9	136.9	5.639	8.422(−5)	16.2	1.80
71.1	139.0	5.664	8.768(−5)	17.1	2.00
73.8	144.8	5.717	9.521(−5)	19.3	2.61
76.7	150.9	5.773	1.039(−4)	22.0	3.37
79.2	156.2	5.819	1.116(−4)	24.5	4.16
81.5	160.9	5.859	1.188(−4)	26.8	4.95
85.7	169.7	5.930	1.362(−4)	31.6	6.88
89.0	176.5	5.984	1.444(−4)	35.8	8.65
95.2	189.1	6.079	1.677(−4)	44.5	13.3
100.4	199.5	6.153	1.885(−4)	52.8	18.2
109.1	216.6	6.269	2.268(−4)	69.0	30.1
116.1	230.3	6.356	2.606(−4)	84.3	42.6
122.1	241.9	6.427	2.922(−4)	99.2	55.8
127.3	252.1	6.486	3.212(−4)	113.7	69.7
131.9	261.1	6.537	3.487(−4)	127.8	84.3

<sup>1</sup> From Trafton and Stone [477].

A two-cloud layer model for that part of the Jovian atmosphere accessible to optical astronomy is now almost unanimously accepted. Although suggested at least as early as 1966 by Savage and Danielson [409], the theoretical studies of Lewis [277, 278] gave a firm physical basis for two distinct cloud layers. The Lewis models have strongly influenced interpretations. All current models show the upper cloud layer as ammonia cirrus in saturation equilibrium with its base near 150° K (the exact value a function of ammonia abundance) and extending upward with rapidly decreasing density to the tropopause (ca 106° K). In simple one-dimensional models, such as we are considering here, the optical depth of this upper cloud layer in visible light is 1.5–3.0 [220]. Therefore, much of Jupiter seen through a telescope is this upper layer, and the obvious two-dimensional structure of belts, zones, and so forth, implies the strong possibility of considerable variation in its thickness over the disk. The lower layer is usually assumed to be a classic reflecting layer of great density, probably NH<sub>4</sub>SH as suggested by Lewis with a base near 225° K [277]. The latest results of Weidenschilling and Lewis [506] for the Trafton and Stone model [477] suggest that the base may be near 200° K and the clouds no thicker than the upper deck of NH<sub>3</sub> clouds. Thus, it may be possible to see to even deeper levels in the Jovian atmosphere in areas where NH<sub>3</sub> clouds may be very thin, perhaps to water ice clouds with a base near 270° K. The 5 μm radiation in dark belts may, in large part, come from these lower levels. Abundances, base pressures, and even crude rotational temperatures given in the composition section are in general agreement with the Trafton-Stone model. The greatest uncertainties remain the lack of aerosol data and poor spatial resolution of most observations over an obviously inhomogeneous planet, although continued improvement in all optical parameters for atmospheric gases also can be expected.

Above the tropopause, there is a minimum of observational data at present. There is a temperature inversion caused by methane band absorption, especially at 3.3 μm, heating the upper atmosphere. Clearest observational evidence is in the 7.9 μm limb *brightening* observed by

Gillet and Westphal [165]. The light curve inversion of data from β-Scorpii occultation by Jupiter [406] indicates a temperature near 180° K at  $10^{15}$  molecules cm<sup>-3</sup> density and rising to 220° K near  $5 \times 10^{13}$  molecules cm<sup>-3</sup>. Theoretical models by Wallace et al [497] tie onto the Trafton-Stone model nicely at the 30 mbar level and show a rise to 140° K at  $3 \times 10^{-2}$  atm and 155° K above  $10^{-3}$  atm. There are a number of theoretical studies on the ionosphere above the  $10^{13}$  molecule cm<sup>-3</sup> level [76, 319, 420, 451].

The radio brightness temperature disk spectrum of Jupiter (Fig. 1) provides data on the thermal structure and composition of Jupiter's atmosphere beneath the clouds in the region inaccessible to optical and infrared observations. Although interpretation of radio data is model-dependent, these observations provide important constraints on possible models. For example, an atmosphere with a temperature profile which is isothermal immediately beneath the clouds is inconsistent with the observed spectrum. Gulkis and Poynter [184] have shown that the observed spectrum is consistent with a H<sub>2</sub>-He convective model atmosphere in which temperature rises to at least 400° K and in which ammonia is present in solar cosmic abundance. Gulkis et al [183] analyzed pressure-broadened ammonia absorption in the Jovian microwave spectrum and derived a pressure of 0.48 atm at 130° K.

### Dynamics

The banded structure of Jupiter is clear evidence that dynamic forces play an important role in its atmospheric structure. Evaluation of the problem by Stone [446] has shown that the mean temperature structure (previously indicated) is very near radiative-convective equilibrium. He finds static stability very low, advection a very weak, large-scale effect because of the internal heat source and size of the planet, and departures from equilibrium damping out with a time constant of decades [446]. The nature of the instability which causes Jupiter to take on its observed zonal flow pattern is still unknown. Trafton and Stone [477] have discussed various dynamic modes, suggesting three not ruled out by observation, which singly or in

combination may be responsible for Jupiter's behavior: "an inertial instability regime," considered by Stone [445]; a "radiation-condensation instability regime," discussed by Gierasch [159]; and "a forced convection regime" which appears not to have been studied. Thus, even the cause of the basic zonal structure of Jupiter remains unknown in detail, while the causes of such features as the equatorial jet and Great Red Spot are totally speculative. Dynamics is a frontier of Jovian research.

### Body Structure Interior Models

For two major reasons, in a few decades the interior of Jupiter may be better understood than any planet except, possibly, Earth. Jupiter must be composed almost entirely of hydrogen and helium, since only these gases can make up a structure of sufficiently low density at nonstellar temperatures. These are the simple species most likely soon to be described quantitatively in the difficult range of pressure and temperature immediately beyond easy laboratory attainment. Further, Jupiter has a large internal energy source. The explanation of this source and the means by which its energy is transported to mean optical depth unity in the atmosphere provide additional strong boundary conditions not present in most planets. As the equation of state and transport properties of hydrogen and helium mixtures improve and are coupled with accurate boundary conditions of energy flux, atmospheric composition and state, magnetic field, and gravitational potential obtained from future space missions, a unique structure is likely to result.

There are two basic types of Jupiter models, both linked closely with two basic ideas about the planet's origin. The gravitational instability hypothesis assumes fluctuations in the primordial nebula occurred which were of sufficient magnitude that self-gravitation became comparable to disruptive solar tidal forces in some areas and materials in the nebula began to collapse [75]. The process of collapse is essentially that of stellar formation, except that bodies with 0.07 solar masses or less never start nuclear fusion, and just continue to collapse and cool [175]. Initial

evolutionary studies of a homogeneous body of Jovian mass showed that, after reaching an early maximum temperature of  $40\,000^\circ\text{K}$ , the body would rapidly cool and collapse, reaching the present Jupiter's state of radius and luminosity (energy production) in just under  $2 \times 10^9$  years [172, 173]. A more realistic calculation, including Smoluchowski's [433], recommended changes to include stratification and heating effects caused by hydrogen and helium immiscibility, is expected to stretch this time out to ca  $4 \times 10^9$  years.<sup>3</sup>

Static models of Hubbard [215] which fit into this logical framework, are homogeneous, completely convective (adiabatic) models for current Jovian boundary conditions. Temperature, pressure, and hydrogen to helium ratio at any point completely specify the model [216]. The hydrogen to helium ratio required is about 2 (by mass), however, which is considerably smaller than solar abundance (of more than 3), though not obviously in conflict with present crude observations of atmospheric ratio.

The second origin hypothesis assumes gravitational capture of gas by a high-density core [75]. Such theories commonly assume a solar ratio of hydrogen to helium, since it is difficult to understand how these could have been fractionated in the outer planets [75]. Models, such as Hubbard's, can be applied equally here, simply by terminating the convective calculation at the core surface, which gives more freedom for change in the hydrogen-to-helium ratio by picking a proper core size.

All homogeneous models can be subject to the criticism that they ignore complex details of the phase diagram of the H<sub>2</sub>-He system which are now becoming available. Hydrogen and helium have very limited mutual solubility in the liquid and metallic states [432, 449]. Smoluchowski [432] expects stable boundaries to exist between phases, with heat flow across the boundaries by conduction and within each phase by convection. If the central temperature is a "cool"  $7500^\circ\text{K}$ , he then expects the sequence of phases shown in Figure 2 [432]. A "hot" model with a  $10\,000^\circ\text{K}$  central temperature would be fluid throughout but would consist of a helium rich core (containing

<sup>3</sup> H. C. Grabske, Jr., private communication.

dissolved hydrogen) topped by a metallic hydrogen mantle (containing dissolved helium), and finally a supercritical molecular hydrogen atmosphere (containing helium, perhaps with separation of hydrogen and helium phases) [432, 433]. To either of these, a heavy element core could also be added. Thus, the question remains open of Jupiter having a solid surface anywhere. The complex hydrogen-helium phase diagram, which remains quantitatively uncertain, is today's major source of uncertainty in Jovian models.

The ultimate source of the internal energy radiated from Jupiter may be largely gravitational. Several authors have pointed out that straight gravitational contraction of ca  $1 \text{ mm yr}^{-1}$  with a current central temperature ca  $10\,000^\circ\text{K}$  could supply the observed luminosity [143, 215, 430]. If gravitational unmixing occurs, perhaps resulting in formation of a core, then the present luminosity is possible with a lower central temperature, but the core must grow each year by about  $2 \times 10^{-11}$  of Jupiter's total mass [143]. Separation of the

hydrogen-rich and helium-rich layers is considered a likely contributor to luminosity [407, 432], although its importance relative to straight contraction cannot be assessed quantitatively. Any actual phase changes are also contributing to the overall energy balance in some manner. At present, simple cooling may well be the major contributor to the energy production [218]. Yet the high interior temperatures, which probably exist today to make this true, ultimately are themselves most likely gravitational in origin. The primordial nebula itself was probably very cool at Jupiter's distance from the Sun [280].

Detailed physics of model building is complex, largely because the equation-of-state and transport properties of the material involved are not well-understood and rely almost entirely on theoretical derivations. A comprehensive outline of most of the theoretical methods has been given by Hubbard and Smoluchowski [218], and details of the theory behind evolutionary calculations have been provided by Grabske et al [173]. A typical Jupiter model [218] is in Table 8; it fits no particular set of boundary conditions, and does not include the complex hydrogen-helium phase details. It does show the general trend of pressure and density in the interior of Jupiter.

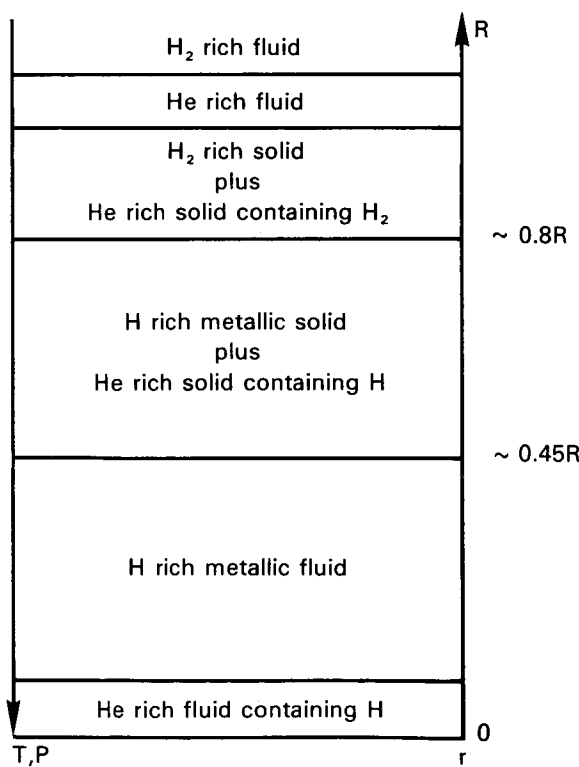


FIGURE 2.—Schematic ordering of H and He phases in the interior of a cool model of Jupiter. (After [432])

### Magnetosphere

The existence of a Jovian magnetosphere, first inferred from Earth-based radio observations [79], was confirmed by the first in situ measurements [186] of Pioneer 10. The Jovian magnetosphere, as inferred from Pioneer 10 magnetic field and particle measurements, is substantially different from the Earth's. In particular, the magnetic field exhibits a large outward extension, approaching a disk-shaped configuration, at distances greater than  $20 R_j$ . Figure 3 is a schematic diagram of the disk model of Jupiter's magnetosphere [486]. Highly energetic electrons and protons exist throughout the magnetosphere, concentrated in a thin disklike configuration at radial distances greater than  $20 R_j$ . Inside  $20 R_j$ , the magnetic field becomes more dipolar in form and energetic particle-trapping appears to be similar to Earth's Van Allen belt.

In the following sections, nonthermal radio

emissions from Jupiter are described, followed by discussions of magnetic field, energetic particles, and plasma contained within the magnetosphere.

### *Nonthermal Radio Emission*

Radio emission from Jupiter has been observed over the wavelength range from 1 mm to ca 650 m. A representative flux density spectrum of the observed emission is shown in Figure 4. The observed spectrum at wavelengths greater than 7 cm is dominated by nonthermal radiation; at shorter wavelengths the emission is dominated by atmospheric thermal radiation. Details of the thermal portion of the spectrum are shown in Figure 1 and discussed in the sections on Composition and Temperature. The nonthermal portion of the spectrum has at least two clearly distinguishable components, a centimeter and decimeter component, extending from ca 0.1 to ca 1 m, and a decametric and hectometric component, important at wavelengths longer than 7.5 m.

The centimetric/decimetric component is due to synchrotron emission from high-energy electrons trapped in Jupiter's magnetic field. The origin of the hectometric/decametric com-

ponent is not yet well-understood. Current knowledge of Jovian nonthermal radiation has been summarized [79, 444, 502, 503]. Dickel et al [115] summarized all available brightness temperature observations of Jupiter's microwave spectrum.

### *Decametric and Hectometric Radiation*

The behavior of decametric radiation has become quite clear in the 20 years since its discovery, although understanding of its mechanism generation is still vague. Decametric activity has been detected at ground-based observatories at frequencies between 3.5 [533] and 39.5 MHz [501], with possible detection at 43 MHz [255]. Recent observations of Jupiter with Earth-orbiting radio-telescopes tuned to frequencies well below the ionospheric critical frequency have extended the range of frequencies at which Jupiter has been detected from 3.5 MHz downward to 450 kHz [114]. Unlike synchrotron emission which is continuous, the decametric component is emitted sporadically, with intense bursts lasting short intervals. The flux density spectrum of the bursts shows rapid increase in flux density with decreasing frequency over the range from 40–10 MHz (7.5–60 m), peaks near 10 MHz, and then decreases at still lower frequencies.

On Earth reception, decametric radiation usually consists of noise which is intensity-modulated to form randomly occurring bursts characterized by a hierarchy of time structure. An entire activity period containing many bursts is known as a Jovian noise storm, which ordinarily lasts from several minutes to several hours. Quiescent periods between storms may last for hours, days, or weeks. Bursts generally have durations of 0.5 to 5 s, but occasionally bursts are much shorter or much longer. The bandwidths of individual bursts are usually between 0.05 and 2 MHz. Bursts with durations of 0.5 to 5 s are known as "L" bursts, while those of shorter duration are called "S" bursts. The L-burst waveform is believed to be due to diffraction effects in the interplanetary medium [124]. The S-burst waveform, on the other hand, is presumably of Jovian origin.

Measurements of all four polarization param-

TABLE 8.—“Typical” Model of Jupiter<sup>1</sup>

Radius, $10^4$ km	Fractional mass	Pressure, Mbars	Density, $\text{g cm}^{-3}$
6.9	0.99	0.004	0.03
6.5	0.97	0.24	0.4
6.0	0.90	1.1	0.7
5.5 <sup>2</sup>	0.80	2.5	1.1
5.0	0.70	4.5	1.6
4.5	0.60	7.6	1.9
4.0	0.40	11	2.3
3.5	0.30	15	2.6
3.0	0.20	20	3.0
2.5	0.10	24	3.4
2.0	0.06	28	3.7
1.5	0.03	32	3.9
1.0	0.01	35	4.1
0.5	0.001	36	4.2
0.0	0.0	37	4.2 <sup>3</sup>

<sup>1</sup> From [218].

<sup>2</sup> Approximate radius at which the molecular hydrogen-metallic hydrogen transition is assumed to occur in most models.

<sup>3</sup> Not including a possible dense core.

eters have been made by Sherrill [419], and Barrow and Morrow [29]. Sherrill concluded that the degree of polarization is usually at least 0.8 above 15 MHz and is practically 1.0 above 20 MHz. Polarization is always right-handed at 22.2 MHz and higher frequencies. The left-handed circular component becomes relatively more prominent as frequency is reduced, but the right-handed component is still predominant down to 10 MHz. The average axial ratio of individual bursts is approximately |0.5|, but occasionally bursts appear to be purely circular, with an axial ratio of unity. The true meaning of polarization data is not known at this time, although a likely interpretation is that radiation is being emitted into some characteristic mode of polarization at the point of origin and is modified substantially as it propagates out through the Jovian magnetosphere on its trip to Earth. Thus, polarization measured on Earth probably reflects both initial conditions of polarization at its point of origin and superposed propagation effects.

A characteristic feature of Jovian bursts is their tendency to recur at nearly the same central meridian longitude (CML), measured in System II. Characteristic histograms of occurrence probability as a function of CML are shown in Figure 5 for two different frequencies. In the vicinity of 18 MHz, emission appears to originate from at least three longitude zones,

generally referred to as sources A, B, and C (as indicated in Figure 5), or as the main source, the early source, and the late or third source. The characteristic structure of histograms allows definition of a rotation period for Jupiter. In 1962, the International Astronomical Union [225] adopted the rotational period of 9 h 55 min 29.37 s as the "best-fit" period to histogram data. This period has been named System III (1957.0). It has become clear more recently that this period is incorrect [78, 80, 180, 443]. The mean value of Jupiter's decametric rotation period is estimated [78] to be 9 h 55 min 29.75 s  $\pm 0.04$ . This period is

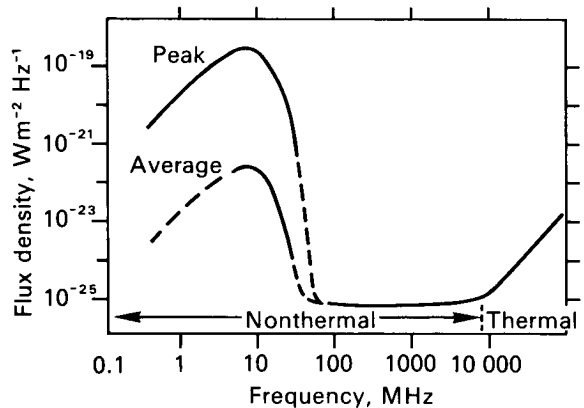


FIGURE 4.—Schematic appearance of Jupiter's observed radio spectrum.

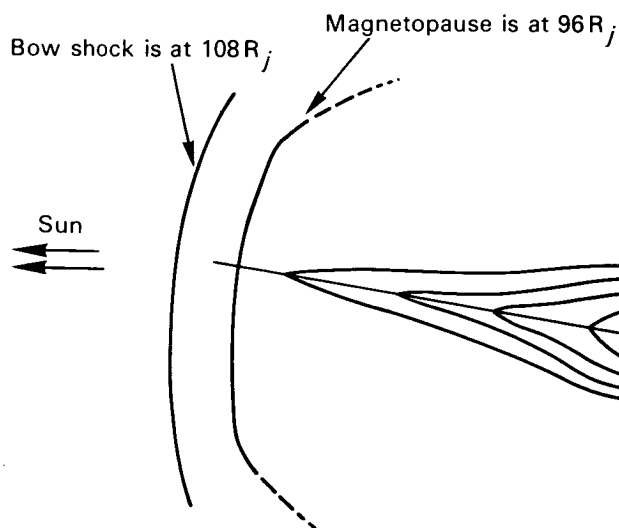
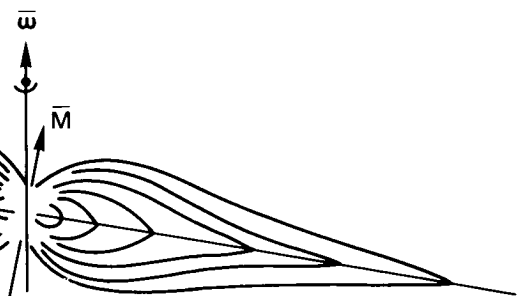


FIGURE 3.—Magnetodisk model of Jupiter's magnetosphere. (Adapted from [486])



0.4 s longer than System III (1957.0). Such correction implies that features on Jupiter in the System III (1957.0) longitude system will drift to higher longitudes at a rate of ca 3.6°/yr.

Upper limits on source sizes of individual Jovian emission events have been determined with long baseline interferometers. Dulk [126], using baselines up to 487 000  $\lambda$ , obtained an upper limit to the size of an incoherent source of 0.1'' (400 km at Jupiter) at 34 MHz. Carr et al [80] observed individual S-bursts at 18 MHz with interferometers having baselines up to 450 000  $\lambda$ .

Their preliminary results indicate that if S-burst sources are incoherent, at least some of them must be smaller than 0.1''. Despite the high angular resolution achieved, the positional uncertainties of the source of emission are still very great.

An unusual property of decametric emission discovered by Bigg [52] is the modulating effect of the satellite Io. Recently Desch and Carr [114] reported a similar modulating effect of the satellite Europa, which shows up at frequencies less than 1.3 MHz. Bigg found that the majority

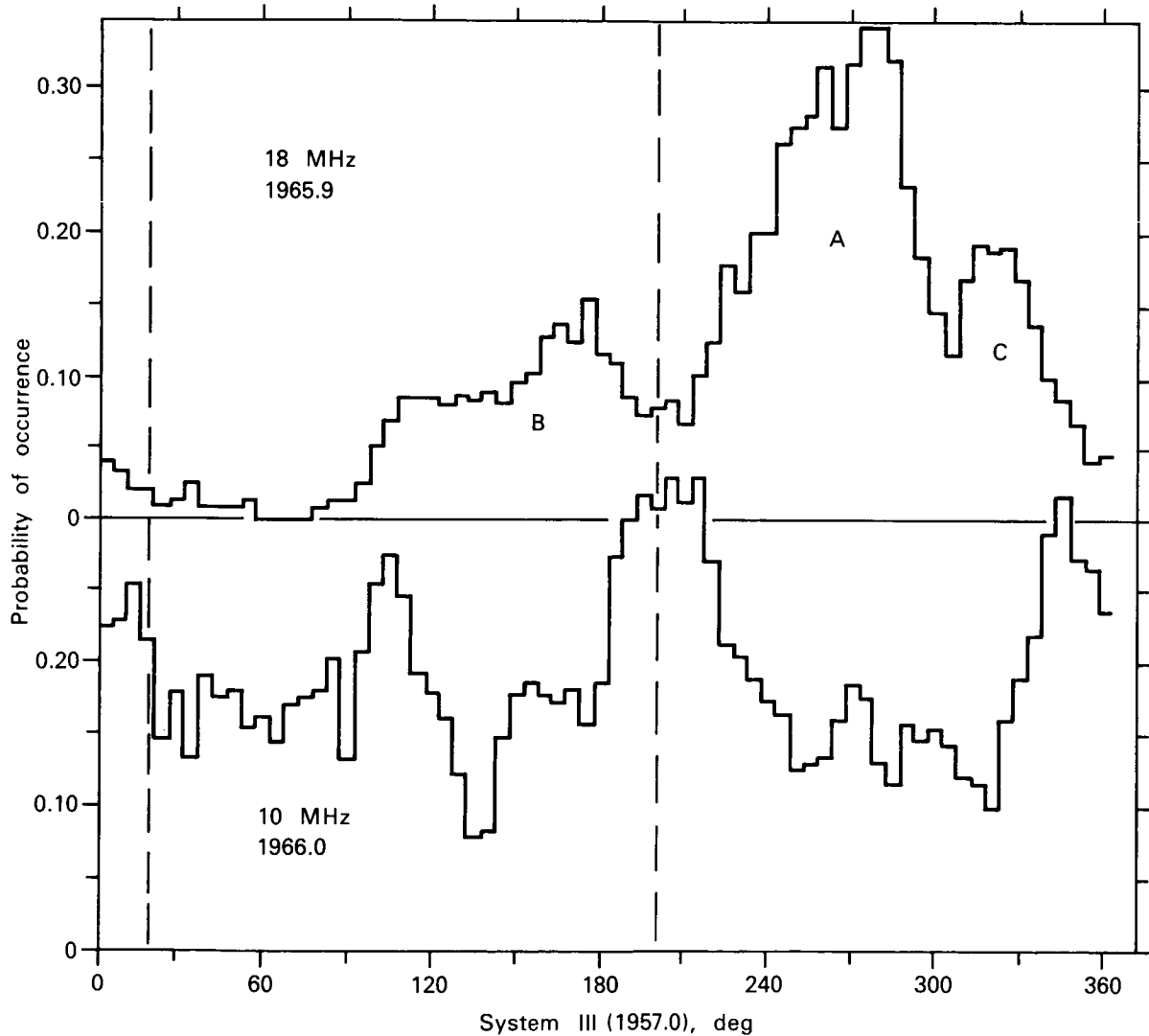


FIGURE 5.—Histograms of occurrence probability as a function of central meridian longitude (CML); CML values of magnetic poles are indicated by vertical dashed lines [79]. (See text)

of the stronger source B emission events occur when the orbital position of Io is within a few degrees of 93° from superior geocentric conjunction, and that most source A events occur when Io is near 246°. This effect has been well-verified [79, 502]; however, it is now apparent that while many source A events depend on Io's position, many do not.

Conseil et al [91] have recently shown a close relationship between solar wind velocity and the phase of Io during radio bursts from Jupiter. Most source B emission is Io-dependent. The Io effect is apparently much less pronounced at 10 MHz [127, 389] than at higher frequencies. There is no widely accepted theory which explains how Io modulates emission, although a number of ideas have been advanced [71, 132, 140, 167, 168, 308, 410, 502]. Gurnett [185] has recently suggested that photoelectrons are emitted from Io's surface and accelerated in a sheath surrounding Io. This suggestion is interesting in light of the Io ionosphere detected by Pioneer 10.

Understanding of the complete mechanism of creation of decametric radiation is still highly speculative. Two phenomena probably occur: (1) generation of an anisotropic distribution of particles or waves; and (2) generation of decametric radiation by them. Measurements of true source positions relative to Jupiter's disk would help to eliminate a number of the many conflicting theories.

#### *Centimetric and Decimetric Radiation*

Jupiter emits a nearly constant flux density of about  $6.0 \pm 1.0 \times 10^{-26} \text{ W m}^{-2} \text{ Hz}^{-2}$  (4.04 AU) at wavelengths from about 5 to 300 cm. Interferometric observations at wavelengths of 10 to 20 cm indicate that radiation is coming from an area much larger than that of the planetary disk.

Figure 6 shows Berge's [39] suggested brightness contours of the 10-cm radiation. An interesting result of this study is that the disk temperature for the thermal component at 2880 MHz appears to be ca 260°K, nearly twice the effective temperature of Jupiter. Branson [63] obtained brightness temperature maps of emitting regions at 1407 MHz at each of three values of CML

spaced 120° apart. They illustrate strikingly the large emitting region, and its rocking as the planet rotates. At wavelengths above 21 cm, the belt structure has not been measured accurately, and there is considerable disagreement in available experimental data as to whether or not the overall extent of emission increases with increasing wavelength [178].

Throughout most of the decimetric spectrum, radiation is linearly polarized, the degree of linear polarization reaching a maximum of ca 25% at 21 cm and decreasing toward longer and shorter wavelengths [115]. The direction of the electric vector rocks back and forth  $\pm 10^\circ$  relative to the rotational Equator as the planet rotates. Radiation also shows a small degree of circular polarization [38, 252, 413]. Observations of circular polarization provided information about polarity of the dipole and magnetic field strength within the Jovian magnetosphere. Circular polarization measurements of Komesaroff et al [252] have been used to derive a field strength in the radiation belts between 0.4 and 1.9 G. These measurements agree well with the magnetic field model based on Pioneer 10 measurements, predicting a field strength of 0.7 G at 1.8 R<sub>J</sub>. The results also confirm that Jupiter's magnetic dipole is antiparallel to that of the Earth, which was first pointed out by Warwick [500] and corroborated by Berge [38].

Accurate position measurements of decimetric centroid emission relative to the optical disk have been made [40, 317, 394, 443] which indicate that the Jovian magnetic field is well-centered

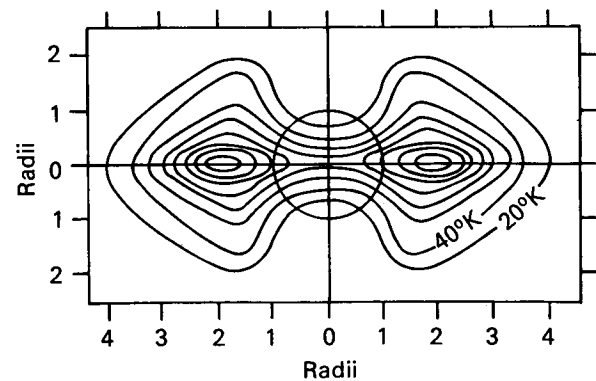


FIGURE 6.—Brightness temperature model of Berge [39]; contour interval is 20° K; CML (System III) is 20°.

and reasonably symmetric. Results rule out displacements greater than several tenths of a diameter.

The possible dependence of decimetric flux density on solar activity has been discussed by many authors (e.g., [79]). Investigation of the possible dependence of total flux density on solar activity was carried out by Gerard [158] from December 1967 to August 1968; he found evidence for positive correlation between the 11.13 cm Jovian total flux and solar activity as measured by the 10.7 cm solar flux. Measurements made in 1971 at 12.7 cm wavelength showed that Jupiter's flux density had varied by ca 20% over a period of 8 years [249], although this change could not be correlated with solar activity.

A mean rotation period of Jupiter can be determined at decimetric wavelengths by comparing longitudinal distribution, of either polarization angle or total intensity, with similar distribution obtained several years later. More precise decimetric results are given in Table 9. The weighted mean of decimetric measurements is estimated to be 9 h 55 min 29.71 s  $\pm$  0.07 s [78], which is not notably different from the period obtained at decametric wavelengths, but is a significant departure from System III (1957.0). There is no indication that the period has changed over the interval for which observations have been made. Decimetric determinations of the rotation period are as shown in Table 9.

TABLE 9.—*Decimetric Determinations of Jupiter's Rotation Period*

Reference	Rotation period
Bash, Drake, Gundermann, and Heiles [31]	09 h 55 min 29.70 s $\pm$ 0.04 s
Davies and Williams [105]	09 h 55 min 29.50 s $\pm$ 0.29 s
Komesaroff and McCulloch [251]	09 h 55 min 29.83 s $\pm$ 0.16 s
Whiteoak, Gardner, and Morris [514]	09 h 55 min 29.69 s $\pm$ 0.05 s
Gulkis, Gary, Klein, and Stelzried [181]	09 h 55 min 29.74 s $\pm$ 0.05 s
Stannard [443]	09 h 55 min 29.74 s $\pm$ 0.03 s

In summary, the distinguishing characteristics of this component are its flat nonthermal spec-

trum, the large, distinctive shape of the emitting region, relatively high degree of linear polarization, very small degree of circular polarization, and variations of all of these with rotation. Shortly after discovery of this component, it was suggested [125] that synchrotron radiation from relativistic electrons was the source of this radiation. A number of authors can be credited for having laid the groundwork which proved conclusively that the synchrotron mechanism was indeed responsible for this radiation [82, 137, 138, 139, 463]. In 1974, previous models were reviewed and a new model developed for electron and proton fluxes in radiation belts [444], based on knowledge of Jupiter prior to the Pioneer 10 encounter with Jupiter.

#### *Magnetic Field*

A single bow shock crossing was observed with the Pioneer 10 magnetometer [428] at 108 R<sub>J</sub> during the inward passage of the spacecraft. Magnetic field strength increased from 0.5 to 1.5  $\gamma$  ( $1 \gamma = 10^{-5}$  G) at the bow shock. The magnetopause was first observed at 96 R<sub>J</sub> as a well-defined boundary, with the magnetic field strength increasing to 5  $\gamma$ . Magnetic field strength remained near 5  $\gamma$  from 90 to 50 R<sub>J</sub> but was very irregular, frequently dipping to 1  $\gamma$ . As evidence for the large variability of the outer magnetosphere, the magnetopause boundary first encountered near 96 R<sub>J</sub> appeared to move in past the spacecraft as it neared 50 R<sub>J</sub>. Similar multiple encounters with the magnetopause boundary were seen on both the inbound and outbound spacecraft passage.

The field strength rises monotonically beginning at about 25 R<sub>J</sub> and going inward, and the direction becomes more dipolar. Data acquired between 2.84 and 6.0 R<sub>J</sub>, enabled Smith et al [429] to fit an eccentric dipole model to the data. The dipole has a moment of 4.0 G R<sub>J</sub><sup>3</sup> and a tilt angle with respect to Jupiter's rotation axis of 11°. The System III (1957.0) longitudes of the magnetic pole in the northern hemisphere are 222°. The field is directed in the opposite sense to that of Earth. The dipole is displaced from the center of Jupiter by 0.11 R<sub>J</sub> in the direction of latitude 16° North and System III (1957.0) longi-

tude  $176^\circ$ . The dipole tilt and longitude of the pole are in reasonable agreement with values inferred from radio astronomy measurements.

The large outward extension of the magnetic field is evident by comparing measured field strength between  $50$  and  $90 R_J$  with the  $4 G$  surface dipole field measured inside  $6 R_J$ . The latter would yield a field which varied as the inverse cube of the radial distance from the dipole with a strength of  $3.2 \gamma$  at  $50 R_J$ , whereas the measured field was ca  $5 \gamma$  throughout the region, which suggests that the magnetic field is inflated or being pulled out away from the planet. The inflation is probably due to stress produced by a corotating plasma in a magnetosphere dominated by centrifugal forces. The view that additional pressure must dominate magnetic pressure is supported by the observation that magnetic energy density just inside the magnetosphere ( $10^{-10} \text{ erg/cm}^3$ ) is less than the estimated solar wind energy density ( $5 \times 10^{-10} \text{ erg/cm}^3$ ).

### *Energetic Particles*

Prior to the first detection of the Jovian bow shock by Pioneer 10, energetic particles were detected by the spacecraft when it was about  $360 R_J$  from the planet [421]; the particles appeared in the form of sudden increases in electron fluxes, with energies ranging from about 1 to  $30 \text{ MeV}$ . Peak intensities were  $\geq 100$  times interplanetary quiet time levels and events lasted about 2 d. These particles, it is believed, escaped into the interplanetary medium from the bow shock or magnetosphere of Jupiter.

Within the magnetosphere at Jovicentric distances from ca  $20$  to  $100 R_J$ , high-energy electrons and protons, like the magnetic field, are concentrated in a disklike region near the magnetic equatorial plane. Stable trapping of particles in this region is doubtful, so that some authors refer to this region as the quasi-trapping region. Inside ca  $20 R_J$ , where the magnetic field becomes more dipolar, energetic electrons and protons appear to be stably trapped. Particles are not tightly confined near the magnetic Equator in this region. Detailed spectra of electrons and protons in the trapped particle region are not available at this time, although individual experi-

menters have given preliminary values. Simpson et al [422] find that the peak omnidirection electron flux greater than  $3 \text{ MeV}$  is ca  $2.5 \times 10^8 \text{ electrons cm}^{-2} \text{ sec}^{-1}$  (at  $L=3.1$ ). Peak omnidirection flux of protons greater than  $35 \text{ MeV}$  is  $6 \times 10^6 \text{ protons cm}^{-2} \text{ sec}^{-1}$  at  $L=3.4$ . Van Allen et al [485] give the following provisional expression for omnidirectional intensity  $J_0$  of electrons with energy  $\geq 21 \text{ MeV}$  within the region  $3.5 < L < 12 R_J$

$$J(E_c > 21 \text{ MeV}) = 3 \times 10^8 \exp \left[ -\frac{L}{1.45} \right] \left( \frac{\cos^6 \Lambda}{\sqrt{4 - 3 \cos^2 \Lambda}} \right)^{m/2} \quad (1)$$

In this expression,  $J$  is in electrons/cm<sup>2</sup> s,  $L$  is the magnetic shell parameter in units of  $R_J$ ,  $\Lambda$  is the magnetic latitude, and  $m=3.5 + \left( \frac{3.86}{L} \right)^8$  is the pitch angle parameter.

### *Plasma Density*

A "thermal plasma" must also exist in addition to energetic particles contained with the magnetosphere. Plasma density is an important parameter in theories of satellite-magnetosphere interactions, decametric and decimetric radiation, and configuration of the magnetosphere itself. The Pioneer 10 payload was not able to provide direct unambiguous data on this plasma distribution; hence it is necessary to rely almost solely on theoretical considerations to determine this quantity [64, 167, 226, 321, 322]. These theories have recently been reviewed by Mendis and Axford [322], who reached the general conclusions:

- the thermal plasma should corotate with the planet,
- thermal plasma should be concentrated toward the equatorial plane,
- centrifugal forces due to rotation of the planet are important in determining distribution of plasma,
- a nonthermal component of plasma in the ionosphere is responsible for populating the magnetosphere,
- recombination sets the limit of maximum plasma density.

Both Ioannidis and Brice [226], and Mendis and Axford [322] derived models in which maximum plasma density is ca  $30 \text{ cm}^{-3}$ . This occurs around  $L=10$  ( $10 R_j$  in the equatorial plane).

## SATURN

Saturn appears similar to Jupiter in many ways, with the obvious exception of its ring system. A magnetic field has not yet been detected on Saturn but this could have escaped detection thus far. With mean density of only  $0.70 \text{ g cm}^{-3}$ , the bulk of this planet once again must be dominated by hydrogen and helium as, presumably, is its atmosphere, although no measurement of its mean molecular weight exists. Theoretically, the problems of atmosphere and interior are essentially the same as those discussed for Jupiter, and will not be repeated.

Ground-based observation of Saturn is much more difficult; Saturn has only one-third the surface brightness of Jupiter, and all means of detection relying upon surface brightness require at least three times the exposure or integration time. The planet is nearly twice as far from the Sun as Jupiter and twice as far from Earth, so that the total flux received from Saturn on Earth is down by a factor of roughly 16 from that received from Jupiter. Also, geometric resolution of Saturn's surface seen from Earth is only half as great as that for Jupiter. It is not surprising that knowledge of Saturn is less extensive.

### Atmosphere

#### *Composition*

Molecular hydrogen was first positively identified in the Saturn atmosphere through detection of two lines of the 4-0 overtone in its quadrupole spectrum by Münch and Spinrad in 1962 [336]. Lines in both the 3-0 and 4-0 overtones have since been used to derive abundances, temperatures, and pressures in the usual way. The most recently published work suggests an abundance of  $76 \pm 20 \text{ km-amagat}$  of  $\text{H}_2$  at an effective pressure<sup>4</sup> of between 0.4 and 1.0 atm

[133]. A study of 14 plates [47], each containing the S(0) and S(1) lines of the 3-0 band, taken over a 3-month period suggests that the apparent abundance is variable between perhaps 75 and 140 km-amagat or more.

Detection of methane on Saturn followed the same historical sequence as on Jupiter. There have been three recent high-dispersion studies of the R branch of the  $3\nu_3$  methane band at  $1.1 \mu\text{m}$ : photographically recorded slit spectroscopy [44], photoelectrically scanned slit spectroscopy [471], and Fourier spectroscopy of most of the disk [106]. Each took reasonable care to exclude the ring. Trafton's result is larger by a factor of 3 than Bergstrahl's for the same half-width, while the result of de Bergh et al falls in between. There is some indication of temporal variation, as in the  $\text{H}_2$  lines. Part of the variation is probably due to differences in techniques used to locate the continuum. The best choice at present appears to be using the result of de Bergh et al [106],  $42 \pm 11 \text{ m-amagat}$  above a reflecting layer base pressure of  $2.8 \pm 0.6 \text{ atm}$ , recognizing that this is a planetwide average and that the reflecting layer model is very questionable for Saturn. All results are much smaller than the early estimate, 350 m-amagat (of Kuiper [261]) made empirically using shorter wavelength bands. The difference is certainly caused in part by comparison of Kuiper's spectra with laboratory results originating at far higher temperatures, but it may also be, in part, an indication of a complex inhomogeneous atmosphere.

The abundance of  $\text{NH}_3$ , on Saturn remains a matter of considerable debate. Dunbar reported its presence in an amount "probably not more than 2 m at atmospheric pressure" [130]. Later, when ammonia could not be detected [351, 440], it was suggested that there had been confusion with weak methane lines. Ammonia was again reported [166] in 1966, the lines being about  $0.15 \pm 0.06$  the strength of the corresponding band ( $6450 \text{ \AA}$ ) in Jupiter. Small temperature changes on Saturn would cause considerable change in the amount of gaseous ammonia in the atmosphere "above the clouds." There is "fairly impressive evidence for short-period changes (occurring in a few years) in the atmosphere of Saturn" [166]. Spectra at  $6450 \text{ \AA}$  taken in

<sup>4</sup>The effective pressure is half the base pressure in a reflecting layer model atmosphere.

December 1970 [97] showed no ammonia, and an upper limit of 7 m-atm was derived.

Cruikshank [97] also reported that observations of the strong 1.5  $\mu\text{m}$  ammonia band in 1969 by Kuiper, Cruikshank, and Fink failed to detect ammonia, and allowed an upper limit in abundance of only 20 cm-atm above optical depth unity to be set at that wavelength. An upper limit of about 2 cm-amagat was reported from studies [309] in the 4150-cm<sup>-1</sup> region during 1973–74, while in the  $\lambda$ 6450 band, an amount was detected “an order of magnitude less than on Jupiter”<sup>5</sup> (ca 1 m amagat?). These observations are not as different as they might seem, since apparent abundance on Jupiter in the former band is 50–100 times less than in the latter, and none of these measurements is precise.

There is a hint of the strong  $\nu_2$  band of ammonia at 10.5  $\mu\text{m}$  in the spectrum of Gillett and Forrest [161]. Measurements of the thermal disk temperature of Saturn at radio wavelengths provide strong support for the presence of ammonia in its atmosphere. Interpretation of radio data implies a relative concentration of ammonia beneath the clouds of  $3 \times 10^{-5}$  [269] to  $1.5 \times 10^{-4}$  [184].

There is no observational evidence for helium on Saturn, but with proof of its presence on Jupiter, confirming earlier theoretical expectations, there is little doubt that it will be found eventually on Saturn as well.

The medium resolution spectrum ( $\Delta\lambda/\lambda \approx 0.015$ ) of Saturn in the 7.5–13.5 region [161] gives a hint of two other species found on Jupiter, perhaps 2 cm-amagat of phosphine (PH<sub>3</sub>) and a small amount of ethane (C<sub>2</sub>H<sub>6</sub>). High-resolution spectra will be required for definite proof that these gases are present.

#### *Temperature*

Modern temperature measurements on Saturn, in the infrared and microwave regions of the spectrum, were first made at about the same time as those on Jupiter. A compilation of infrared results is given in Table 10. Radio emission

from Saturn has been observed over the wavelength range from ca 1 mm longward to ca 94 cm. Figure 7 shows disk brightness temperatures at radio wavelengths [343, 483, 528]. A distinct feature of Saturn’s spectrum is the wavelength dependence of the measured temperature. The temperature increases from near 130° K at millimeter wavelengths to close to 540° K at 94 cm; this behavior is qualitatively similar to the thermal radio spectrum of Jupiter.

Suggestions have been advanced to explain the marked increase in temperature with wavelength. Excess radiation may be due to (1) nonthermal emission from a trapped radiation belt, (2) thermal radiation from Saturn’s rings, (3) free-free emission from Saturn’s ionosphere, or (4) emission from Saturn’s atmosphere. There is little experimental evidence so far to support the first three mechanisms. Interferometric measurements have been made [41, 43, 66] over the wavelength range 3.7 to 21 cm which rule out strong emission from either a radiation belt or the rings. It is estimated [41] that at 21-cm wavelength no more than 6% of

TABLE 10.—*Saturn Brightness Temperatures to 1 mm*

Wave-length, $\mu\text{m}$	Brightness temperature, <sup>1</sup> °K	Refer- ence	Remarks
5	ca. 120	[286]	
7.7–7.9	129	[161]	15% of disk obscured by rings
8.5–11.5	ca. 103	[161]	Do.
10–14	$100 \pm 3$	[5]	
10–14	c $99 \pm 3$	[5]	Measures actually refer to + 17° latitude
17–25	c $97.3 \pm 2$	[338]	Limb was $95.5^\circ \pm 2^\circ$ K
30–45	$89 \pm 4$	[16]	All of rings as well as disk
45–80	$94 \pm 2$	[16]	Do.
65–110	$97 \pm 5$	[16]	Do.
125–300	$93 \pm 4$	[16]	Do.
30–300	$88 \pm 1$	[16]	Do.
45–300	$91 \pm 1$	[16]	Do.
1.5–350	$97 \pm 4$	[23]	Do.

<sup>1</sup> Values preceded by a “c” are center of disk temperatures. Others refer to averages over most or all of the disk. Possible ring contributions are noted in the remarks column.

<sup>5</sup> E. Barker, D.P.S. Meeting, Palo Alto, 1974.

the total radiation can come from visible rings, nor more than 5% from a radiation belt.

In order to explain the spectrum on the basis of free-free emission from Saturn's ionosphere, an emission measure many orders of magnitude larger than expected for Jupiter would be required [182]. Since solar ionizing flux is less at Saturn than at Jupiter, and their compositions are similar, it is expected that the emission measure of Saturn's ionosphere is less than Jupiter's. Therefore, it is unlikely that free-free emission from a hot ionosphere can explain the observed spectrum. A number of authors [182, 269, 524] have shown that the gross features of Saturn's centimeter wavelength spectrum can be explained in terms of thermal emission by an atmosphere whose opacity is wavelength-dependent and in which ammonia is assumed to be the principal source of opacity at radio wavelengths. A deep convective atmosphere is required to explain the observations. Saturn's spectrum was also measured [524] in the vicinity of the 1.25-cm inversion band of ammonia; evidence was found of ammonia as a constituent gas in the upper atmosphere.

Three studies of the  $3\nu_3$  methane band on Saturn [44, 106, 471] resulted in rotational temperatures between 130° and 140° K in spite of diverse abundances. A rotational temperature ca 80° K from hydrogen quadrupole lines was found [133], and departures from equilibrium

by hydrogen at these temperatures were noted. This problem is probably even more acute on Uranus. Any apparent hydrogen rotational temperature in a region where kinetic temperature is under 100° K likely cannot be given the usual interpretation as an equilibrium thermodynamic temperature.

### The Visible Surface

The clouds on Saturn appear to be in a state of differential rotation, the period increasing from 10 h 2 min ( $\pm 4$  min) at the Equator to 6% greater at 27° latitude, 8% greater at 42° latitude, and 11% greater at 57° latitude, as determined from Doppler spectroscopy [326]. Saturn has a so-called equatorial band, which is dark in blue light and bright in red light, six named cloud belts in each hemisphere, and light zones between these, for a total of at least 25 distinct degrees of shading under optimum observing conditions [385].

White spots appear on Saturn on rare occasions, persisting for a few days or weeks, never achieving the prominence or lifetime of the sporadic spots on Jupiter [1]. A recent spot at latitude  $-57.3^\circ$  set a record for both persistence and high south latitude. Its motion during a 490-d period from October 1969 to February 1971 appeared to be a damped 169-d sinusoid about a mean rotation period of 10 h 36 min  $27.9 \text{ s} \pm 0.2 \text{ s}$  [385]. The spot measured 8000 km north and south by 6000 km east and west.

Data were collected [117] on motions of eight earlier, well-observed spots which showed that three high-latitude objects ( $+57^\circ$ ,  $+36^\circ$ , and  $-36^\circ$ ) had rotation periods around 10 h 38 min, while four spots within  $8^\circ$  of the Equator had periods between 10 h 12 min and 10 h 15 min. A spot at  $-12.3^\circ$  had a period of 10 h 21 min. Thus, spot motions are not in good agreement with the spectroscopic rotation period. Moore recognized possible sizable errors in his work. Also, it is known that typically a spot may be driven at a distinctly atypical rotation rate (or at least such is true on Jupiter), so perhaps the results are not surprising. Nine spots and one spectroscopic study are not sufficient data to

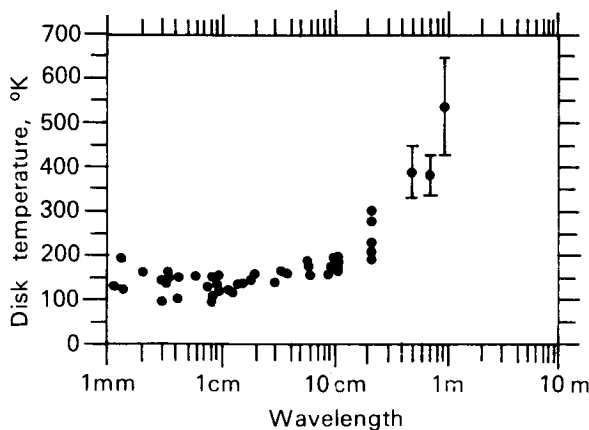


FIGURE 7.—Microwave spectrum of Saturn. Error bars are only shown for longest wavelengths where there are few measurements.

suggest a firm hypothesis. Hide [205] suggests that better observations will show a discrete equatorial jet similar to the one on Jupiter.

Shades of orange, blue, and so forth have been reported on Saturn by experienced observers, but all colors are extremely subtle, except for predominating variations from white to pale yellow to brownish yellow [1]. Their origin is unknown, but speculation is similar to that about Jupiter. Visible clouds are probably ammonia cirrus but somewhat more dense than on Jupiter (see section, **Atmospheric Structure**).

It is extremely difficult to obtain good integrated (full disk) photometry of Saturn because of the rings. Utilizing the 3 years of Harvard photometry [230, 231] obtained with the ring inclination varying relative to Earth, Irvine and Lane [228] reduced it to "no-ring" data. The resulting geometric albedos are in Table 11. These authors also derived approximate no-ring phase coefficients of  $0.013 \pm 0.007 \text{ mag deg}^{-1}$  for  $\lambda\lambda 3500 - 5000$  and  $0.035 \pm 0.010 \text{ mag deg}^{-1}$  for  $\lambda\lambda 6200 - 10600$ . In the infrared from 2–3.2  $\mu\text{m}$ , Saturn has a higher reflectivity than Jupiter, while from 3.2–4.2  $\mu\text{m}$  the reflectivity of both planets is very low [236]. The combined reflectivity of planet and ring is about 30% higher at 2500 than at 3500 Å and seems to decline at still shorter wavelengths [496].

Much of the detailed photometry for Saturn is in the form of polar or equatorial scans. Binder and McCarthy, [56] in particular, have furnished both equatorial and meridional limb-darkening curves in nine passbands from 0.6–1.55  $\mu\text{m}$ . Normal albedos (or close approximations) as a function of wavelength for the center of the

disk, at a resolution of about 500, were obtained by Teifel in 1968 [461]. Selected values from this work are in Table 12. In yellow and red light, the equatorial band is the brightest region on Saturn, and the north polar region, the darkest [461]. In blue to violet light, the polar region becomes quite bright and the equatorial band fades [461]. Both weak and strong methane bands show decreasing absorption from center to limb along the Equator and increasing absorption from center to pole along the central meridian [354, 461]. Methane absorption at  $-20^\circ$  latitude is 25–28% greater than at the Equator, much more than a straight air mass (secant) effect [461]. These effects can be interpreted in terms of varying density of ammonia aerosols with latitude.

#### *Energy Balance*

Photometry of Saturn is far more difficult than for Jupiter, because of the rings. No near-infrared, integrated photometry has been published beyond 1.06  $\mu\text{m}$ ; many energy balance studies have simply used the bolometric Bond albedo of Jupiter, although existing data tend to indicate a somewhat higher value for Saturn.

Calculations in this chapter are based upon Walker's [495] unpublished value of 0.61, resulting in a calculated effective temperature of  $71^\circ \text{ K}$ . A rapidly rotating body of zero albedo at Saturn's distance from the Sun would have an effective temperature of  $90^\circ \text{ K}$ . The broadband measurement of Aumann et al [23] is  $97^\circ \text{ K}$ . Thus, it appears that Saturn, like Jupiter, is radiating more energy than it receives from the Sun—three and a half times as much, accepting the 0.61 bolometric albedo and the  $97^\circ \text{ K}$  temperature. It

TABLE 11.—*Integrated Photometry of Saturn*<sup>1</sup>

Passband	Geometric albedo	Passband	Geometric albedo
U	0.169	4573 Å	0.318
B	0.302	5012 Å	0.377
V	0.436	6264 Å	0.498
3590 Å	0.184	7297 Å	0.376
3926 Å	0.199	8595 Å	0.297
4155 Å	0.240	10 635 Å	0.417

<sup>1</sup> Data from [228].

TABLE 12.—*Detailed Photometry of Saturn*<sup>1</sup>

Wavelength, Å	Normal albedo	Wavelength, Å	Normal albedo
4100	0.26	6050	0.67
4400	0.31	6200	0.50
4800	0.42	6400	0.72
5200	0.48	6600	0.71
5600	0.52	6800	0.67
5850	0.67		

<sup>1</sup> Center of disk data from [461].

has been pointed out that the rings are not as cold as was once thought, and that the measurement of Aumann et al undoubtedly includes a ring contribution. However, at the time of that measurement (Dec. 2, 1968) the rings were inclined only  $13.2^\circ$  to the Sun and not intercepting as much energy as in recent years.

Also, Murphy's recent work [338] indicates a temperature for the disk center at  $17\text{--}25\ \mu\text{m}$  of  $97.3^\circ\text{ K}$ , with little decrease toward the limb. Thermal opacity in this passband is less than immediately on either side of it, but it does not appear that the  $17\text{--}25\ \mu\text{m}$  brightness temperature could be sufficiently higher than the true effective temperature of Saturn to otherwise explain the apparent energy imbalance.

#### *Atmospheric Structure (Models)*

Thermal opacity in Saturn is dominated by pressure-induced  $\text{H}_2$  absorption, as for Jupiter [476]. Thermal structure is more uncertain because the magnitude of the internal energy source is less well-determined, the hydrogen to helium ratio is unknown, and the temperature lower (making the relative amounts of ortho- and parahydrogen a factor). The  $\text{NH}_3$  abundance is also uncertain and has not been included as an

opacity source in the existing radiative equilibrium calculations of Trafton and Münch [476]. There is evidence of methane absorption in the high atmosphere of Saturn as for Jupiter, the  $7.7\text{--}7.9\ \mu\text{m}$  temperature rising to  $129^\circ\text{ K}$  [161].

A nominal radiative-convective model constructed for Saturn [359] is given as Table 13. A major difference between the structure of Saturn's and Jupiter's atmospheres is caused by much smaller local gravity, which greatly increases scale height. Palluconi assumed a wet adiabatic gradient wherever it exceeded the radiative gradient, a good approximation to the effects of dynamics [359], especially when other uncertainties are so much greater. His assumed composition (footnote in Table 13) did not include  $\text{H}_2\text{S}$ , so no  $\text{NH}_4\text{SH}$  clouds are shown. Actually, such a layer might be expected at the very top of the solid  $\text{H}_2\text{O}$  cloud layer, which is shown. The effective pressure of  $\text{H}_2$  and  $\text{CH}_4$  line formation has been given as ca  $0.5\text{--}1.5$  atm. This is the region within the ammonia cloud layer and matches the  $130\text{--}140^\circ\text{ K}$  methane rotational temperature in Palluconi's model. A  $5\text{-}\mu\text{m}$  temperature of ca  $120^\circ\text{ K}$  [286] fits well enough as the temperature of the cloud tops. Microwave studies in the  $\text{NH}_3$  inversion line at  $1.25\text{ cm}$  indicate optical depth unity is reached at a temperature

TABLE 13.—*A Nominal Saturn Model Atmosphere*<sup>1</sup>

Pressure, atm	°K	Density, $\text{g cm}^{-3}$	Altitude, <sup>2</sup> km	$H_p$ , km	$H_{p^*}$ , km	w, $\text{mg l}^{-1}$	Comments
0.100	77.0	$3.59 \times 10^{-5}$	81.1	26.9	26.9		
0.168	77.0	$6.04 \times 10^{-5}$	67.1	26.9	26.9		Tropopause
0.300	95.0	$8.37 \times 10^{-5}$	49.8	33.1	51.7		
0.727	130.0	$1.55 \times 10^{-4}$	15.3	45.4	69.7	0.003377	
1.00	145.2	$1.91 \times 10^{-4}$	0.0	50.7	77.3	0.0762	Zero altitude <sup>2</sup>
1.12	151.0	$2.05 \times 10^{-4}$	-5.9	52.7	80.2	0.205	$\text{NH}_3$ cloud base
3.00	210.0	$3.95 \times 10^{-4}$	-67.5	73.4	109.5		
3.94	230.0	$4.74 \times 10^{-4}$	-88.4	80.3	119.1	0.0743	
5.10	250.0	$5.64 \times 10^{-4}$	-109.9	87.2	128.0	0.574	Solid $\text{H}_2\text{O}$
6.92	275.9	$6.94 \times 10^{-4}$	-138.1	96.3	141.3	4.82	Solution $\text{H}_2\text{O-NH}_3$ cloud base
10.0	309.9	$8.93 \times 10^{-4}$	-175.5	108.1	157.6		
30.0	434.1	$1.91 \times 10^{-3}$	-317.0	151.5	216.4		
100.0	617.8	$4.48 \times 10^{-3}$	-536.0	215.6	302.1		
300.0	841.3	$9.99 \times 10^{-3}$	-813.7	293.6	405.5		
1000.0	1166.2	$2.37 \times 10^{-2}$	-1232.1	406.9	554.9		

<sup>1</sup> From Palluconi [359]. The composition used is  $\text{H}_2$ , 88.572%, He, 11.213%,  $\text{H}_2\text{O}$ , 0.105%,  $\text{CH}_4$ , 0.063%, Ne, 0.013%,  $\text{NH}_3$ , 0.015%, and others, 0.019% by number;  $H_p$  is

the pressure scale height,  $H_{p^*}$  is the density scale height, and w is the mass of cloud per unit volume of gas.

<sup>2</sup> The zero altitude is arbitrarily selected at 1 atm pressure.

near 135° K and a pressure of about  $\frac{2}{3}$  atm [524]. All of this fits together as well as can be expected, given the present limited number of observations upon which to base model calculations.

No optical observations show any evidence of penetration of radiation from below the top cloud deck, such as was true for Jupiter. Nor is this any surprise, given the greater cloud density expected. The previously discussed limb-darkening curves for the equatorial belt would indicate that a simple reflecting layer model for spectral line formation is inappropriate, because they show decreasing rather than increasing absorption from center to limb. It may well be that a reflecting layer model can be used for relative abundances at the center of the disk, while scattering must be included to explain limb darkening, as for Jupiter. Finally, it must be remembered that there is considerable spatial variation over the disk of Saturn [56] and probably temporal variations as well. A single static atmospheric model can hardly be expected to explain such changes.

### Body Structure (Model Interiors)

The contemporary philosophy behind model interiors of Saturn is the same as for Jupiter. In practice, however, it is difficult to derive a com-

TABLE 14.—*A typical Saturn Model*<sup>1</sup>

Radius, $10^4$ km	Fractional mass	Pressure, Mbar	Density, $\text{g cm}^{-3}$
5.7	0.98	0.001	0.01
5.5	0.95	0.01	0.06
5.0	0.84	0.1	0.3
4.5	0.8	0.4	0.6
4.0	0.7	0.9	0.9
3.5	0.6	1.9	1.1
3.0 <sup>2</sup>	0.5	2.5	1.4
2.5	0.4	4	1.7
2.0	0.3	5	1.9
1.5	0.25	6	2.0
1.0	0.2	7	ca 3
0.5	0.05	ca 10	ca 3
0.0	0.0	ca 10	ca 3 <sup>3</sup>

<sup>1</sup>From Hubbard and Smoluchowski [218].

<sup>2</sup>Approximate radius at which the molecular hydrogen-metallic hydrogen transition is assumed to occur in most models.

<sup>3</sup>Not including a possible dense core.

pletely convective Saturn model. Even though its mean density is much lower than Jupiter's, Saturn's mass, and therefore its gravitational compression, are sufficiently smaller that models of Saturn have always required a much larger helium-to-hydrogen ratio than Jupiter and often a high molecular weight core as well [218]. Hubbard's completely convective models [214] required a mass fraction of only 27% hydrogen and a very high central temperature. If the internal energy source is somewhat smaller than previously thought, because of confusion with flux from the rings (see section, *Energy Balance*), and a core is included, then a perfectly satisfactory hydrogen-to-helium ratio can presumably be accommodated, whatever the ratio may be.

A typical Saturn model interior by Hubbard and Smoluchowski [218], in Table 14, is only meant to show the general trend of probable physical conditions inside Saturn. (Refer to the original literature for specific models.)

## URANUS AND NEPTUNE

Uranus and Neptune have proven rather intractable bodies, for obvious reasons. Uranus has a visual surface brightness less than  $\frac{1}{10}$  Jupiter's. Its total visual flux at opposition is less by a factor of more than 1000, while Neptune's visual flux is less by an even larger factor. Infrared and microwave flux densities are also less than for Jupiter. Nevertheless, steady improvement in optical and microwave instruments has made possible significant progress in understanding these unique bodies, especially during the past 5 years.

### Atmospheres

#### Composition

The existence of hydrogen on Uranus and Neptune was first inferred observationally by Herzberg [200] in 1952 by comparing a planetary feature seen by Kuiper [261] in Uranus and Neptune with laboratory spectra showing the  $\lambda 8270$  pressure-induced dipole  $S_3(0)$  line of  $H_2$ . In 1963, Spinrad [439] reported observation of the first  $H_2$  quadrupole line in Uranus,  $S(0)$  of the 4-0 band, and finally in 1973 the quadrupole lines in Neptune were detected by Trafton [473].

There are now several sets of observations at present of the Uranian quadrupole lines, and these do not agree particularly well. It is not now clear whether these differences could be caused by real variations, as for Jupiter and Saturn, or whether they reflect observational difficulty, since it is particularly hard even to locate the continuum accurately on Uranus and Neptune. Because attempts to derive actual abundances are strongly model-dependent, only equivalent widths are given in Table 15, and the abundance problem is considered in the section, *Atmospheric Structure (Models)*. The pressure-induced dipole lines of H<sub>2</sub> are all very broad, shallow features, and particularly difficult to measure accurately in a spectrum with strong CH<sub>4</sub> absorption everywhere. Approximate equivalent widths for three of these lines in each planet have been given by Belton and Spinrad [36].

The first to report absorption bands in the spectrum of Uranus was Secchi, in 1869. Wildt suggested in 1932 that these might be caused by CH<sub>4</sub>; in 1933, Dunham proved this for an infrared band on Jupiter; and by 1934, Adel and Slipher showed it to be true for Uranus. Slipher's work in the first decade of the 20th century confirmed earlier conjectures that Neptune's spectrum was very like that of Uranus, except that absorptions seemed even stronger. The work of Wildt, Dunham, Slipher, and Adel therefore confirmed the presence of methane on Neptune.

Each laboratory study of CH<sub>4</sub> at increased path-length and resolution seems to result in identifica-

tion of previously unexplained features in the spectra of Uranus and Neptune. Owen's 1967 study [353] of the  $\lambda 7500$  (Kuiper) CH<sub>4</sub> bands at path-lengths of 5.15 km-amagat suggested the presence of 3.5 km-amagat of methane on Uranus and 6 km-amagat on Neptune. These numbers were necessarily crude because of unknown effects, on the line equivalent widths, of temperature differences between laboratory and planet. Laboratory spectra of methane at 8.45 km-amagat and new spectra of Uranus in the  $\lambda 7500$  band by Lutz and Ramsay [290] gave line strengths and improved wavelengths, suggesting even greater methane abundance on Uranus.

It has been shown very recently [355] that the  $\lambda 6420$  feature usually attributed to an induced dipole transition in H<sub>2</sub> was at least largely caused by methane. Even a 10.1 km-amagat laboratory column of CH<sub>4</sub> was inadequate to match this and other Uranian features. Assuming spectra result from a mean atmospheric path in the Uranian atmosphere of three times a vertical column again suggests even more than 3.5 km-amagat of methane. The actual abundance is both temperature- and model-dependent but is certainly very large. Many very high overtone bands show considerable strength even below 5000 Å, which can be seen in the spectra of Galkin et al [153]. Photometry by Wamsteker [499] suggests that methane abundance on Neptune may be smaller than on Uranus, rather than larger as is usually assumed. Additional observations of both planets are acutely needed.

TABLE 15.—*Equivalent Widths (m Å) of H<sub>2</sub> Quadrupole Lines in Uranus and Neptune*

Planet	Uranus						Neptune
Observer and reference	Giver & Spinrad [166]		Lutz [289]	Price [373]	Trafton [472] <sup>1</sup>	Encrenaz & Owen [133]	Trafton [473]
Dateline	Dec. 1964	Mar. 1965	May-July 1971	May 1972	3-0 1972 4-0 1972-73	Feb. 1973	May-July 1973
S(0), 4-0 $\lambda 6435$	$26 \pm 10$	$37 \pm 12$		$62 \pm 19$	$30 \pm 3$	$30_{-3}^{+4}$	$28 \pm 4$
S(1), 4-0 $\lambda 6368$	$37_{-10}^{+25}$	$49 \pm 15$		$58 \pm 13$	$29 \pm 3$	$29_{-3}^{+6}$	$31 \pm 4$
S(0), 3-0 $\lambda 8273$			$95 \pm 25$		$170 \pm 18$		
S(1), 3-0 $\lambda 8151$			$114 \pm 15$		$167 \pm 20$		

<sup>1</sup>Also private communication.

Ammonia has not been identified in optical spectra of Uranus or Neptune. Its presence is expected theoretically, but only deep in their atmospheres [280]. There is some observational evidence of its presence in the rather uniform brightness temperatures of all the major planets near the ammonia inversion band at 1.25 cm [184].

There is no direct observational evidence of helium on Uranus and Neptune. The thermospheric temperature of Neptune (discussed in the next section) suggests that helium abundance can be *no higher than 50%* by number.

Trafton [475] has found a number of strong unidentified lines in the spectrum of Uranus between 1.04 and 1.07  $\mu\text{m}$ . It is suggested that these might be caused by a methane isotope or one of the simple hydrocarbons produced from methane, although they may equally be caused by some other new atmospheric gas.

### Temperatures

Low [284] made the first thermal infrared measurements of Uranus in 1966, reporting a temperature of  $55^{\circ}\pm 3^{\circ}$  K in the 17.5–25  $\mu\text{m}$  window. Harper et al [193] found a value of 45° K for the 350  $\mu\text{m}$  region and Low et al [288] measured  $49^{\circ}\pm 3^{\circ}$  K between 28 and 40  $\mu\text{m}$ . Recently working at the high altitude (4200 m) Mauna Kea Observatory, Morrison and Cruikshank were able to measure the flux from both Uranus and Neptune between 17 and 28  $\mu\text{m}$ . They report

$54.7^{\circ}\pm 1.8^{\circ}$  K for Uranus and  $57.2^{\circ}\pm 1.6^{\circ}$  K for Neptune [333]. These temperatures are all based upon slightly different planetary radii, but a one percent change in radius causes a temperature change of only about  $0.1^{\circ}\text{K}$  at these temperatures and wavelengths.

Radio emissions from Uranus and Neptune have been observed over the wavelength range 1.4 mm to 11 cm. The representative disk brightness temperature spectra for these planets are given in Figures 8 and 9. Most of the data used to compile these figures are in references [179, 343, 483]. Similar to Jupiter and Saturn, brightness temperatures of these planets are near 130° K near 1 cm wavelength, and increase at longer wavelengths. Based on solar heating alone, these planets would have a temperature near 50° K. A simple explanation for these planets being so warm at radio wavelengths is that radio emission originates deep in the atmosphere where it is warmer and denser than in the infrared radiation level. Trace amounts of ammonia are believed to provide atmospheric opacity [179]. While a great number of molecules absorb near 1-cm wavelength and become progressively more transparent at longer wavelengths, only two,  $\text{NH}_3$  and  $\text{H}_2\text{O}$ , have very strong absorption lines in this wavelength region and are likely constituents of the major planet atmospheres. Hydrogen ( $\text{H}_2$ ) and helium may also contribute to the opacity through their induced dipole moments.

The only spectral lines observed on Uranus

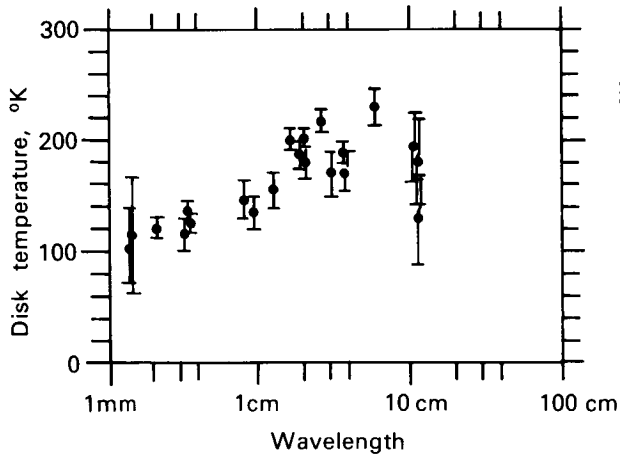
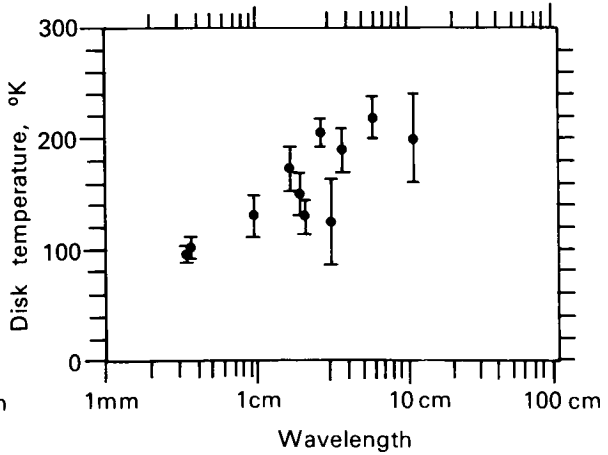


FIGURE 8.—Microwave spectrum of Uranus.



or Neptune with definitely known quantum numbers are the molecular hydrogen lines. Rotational temperature can be derived for each pair of lines in a given band (listed in Table 15) if H<sub>2</sub> is assumed to be equilibrium hydrogen rather than normal hydrogen. These temperatures generally fall in the 110–120° K range. Scatter in measurements and the peculiar behavior (already discussed) of the more extensive Saturn data suggest cautious interpretation.

Tentative quantum number assignments by Owen in the  $\lambda 6800$  band of methane suggest a rotational temperature of  $60^\circ \pm 15^\circ$  K [352]. Since this is some  $25^\circ$  K lower than the temperature to be expected for the observed amount of methane in saturation equilibrium, its meaning is quite uncertain.

The star BD-17° 4388 was occulted by Neptune in 1968, observations being made in Australia and Japan. The original results from Australia were reported by Freeman and Lynga [152], from Japan by Kovalevsky and Link [254]. A complete analysis of the Australian observations by means of light curve inversion, recently published [491], indicates an upper atmospheric scale height of 55–58 km. This implies a temperature of  $150^\circ$  K for a pure H<sub>2</sub> atmosphere and higher yet in direct proportion for larger values of molecular weight. Veverka et al [491] suggest that the large methane abundance on Neptune should assure effective radiative cooling of the thermosphere, implying that the H:He ratio can be no greater than 50% by number density.

Uranus is unique in the solar system in its axial inclination of 98°. The axis of Uranus was practically in the plane normal to the solar radius vector in 1966, all parts of the planet exposed to the Sun during one 10.8-h rotation. In 1985, the north pole of Uranus (assuming north is defined by the angular velocity vector) will face the Sun continuously, and temperatures in this visible hemisphere might rise as much as 20%, assuming no effective heat exchange between northern and southern hemispheres. Stone [447] suggests the radiative relaxation time for Uranus is so long that substantial seasonal effects are unlikely. He predicts that the polar regions, receiving more heat from the Sun per orbit, will be hotter than the Equator.

### *The Visible Surfaces*

Uranus normally appears as a small bluish-green disk, even through a large telescope, and is featureless except for a reasonable amount of limb-darkening. The Stratoscope II balloon telescope during its flight of March 26–27, 1970, found no surface features, i.e., an upper limit of 5% contrast on any beltlike feature at wavelengths  $\lambda\lambda 3800$ – $5800$  [102]. Yet the best of the classic visual observers, using large refracting telescopes (aperture > 50 cm) at times of superior “seeing” [2], usually reported two faint equatorial belts on either side of a bright equatorial zone and darker poles. Almost all observers found these belts inclined somewhat to the plane of the satellites [2]. Perhaps the belts vary in contrast.

Neptune is almost always described as a small, featureless bluish-green disk when seen through a moderate to large telescope. Dollfus described it as showing pronounced limb darkening and very weak spots of irregular shape, but no band structure [116].

In determining rotation periods, astronomers turned to spectroscopic and photometric techniques, since there were no obvious surface features to use. In spectroscopy, rotational velocity is measured from the Doppler shift of spectral lines. In 1930, Moore and Menzel [328] published a spectroscopic rotation period for Uranus of 10.8 h (the period generally quoted today). They noted it could be in error by as much as a half hour, although it was in substantial agreement with the 1912 spectroscopic result of Lowell and Slipher. Similarly, Moore and Menzel [327] published in 1928 the rotational period still quoted for Neptune,  $15.8 \pm 1.0$  h.

Campbell [2]<sup>6</sup> reported that in 1916 the light from Uranus fluctuated by 0.15 magnitudes in a period of 10 h 49 min 26.4 s, although the variation seemed to disappear later.

A long list [194] gives positive and negative reports on light fluctuations from Uranus since that time. Whether any of these variations were real, perhaps related to belt activity, or the product of inadequate early photometry is still not

<sup>6</sup>This is a secondary reference.

certain, but variations using a modern photoelectric photometer have not been reported. The situation for Neptune is similar.

The large amount of methane in the atmospheres of Uranus and Neptune causes tremendous absorption in the red and near-infrared and is at least partially responsible for the bluish-green colors of these planets. It appears that some hydrogen pressure-induced absorption is also required to match the geometric albedo of each [499]. Matching the geometric albedo data is the most important constraint available in constructing model atmospheres.

There are three important sets of albedo data: Wamsteker [499] covers completely  $0.3\text{--}1.1 \mu\text{m}$  at a resolving power  $\lambda/\Delta\lambda$  ca 30 on both planets; Appleby and Irvine [15] and Appleby [14] cover 10 wavelengths on Uranus and seven on Neptune at slightly higher resolution; and Younkin [530] covers completely  $0.33\text{--}1.11 \mu\text{m}$  at  $50 \text{ \AA}$  ( $\lambda < 0.7 \mu\text{m}$ ) and  $100 \text{ \AA}$  ( $\lambda > 0.7 \mu\text{m}$ ) resolution for Uranus only. Scaled to the same planetary radii, the three sets of results agree reasonably well.

Younkin's data have the highest peaks and troughs in the red and infrared, of course, since it has the highest resolution in this region of strong methane bands. His geometric albedo curve for Uranus scaled to the radius of Table 1 is shown in Figure 10. Neptune is shown to be nearly identical to Uranus at wavelengths shorter than  $0.54 \mu\text{m}$  but with lower peaks and shallower troughs in the region of methane absorption, perhaps indicating broader methane bands [499]. The albedo of Uranus was measured at wavelengths of  $1.26, 1.62, 1.74, 2.17$ , and  $2.27 \mu\text{m}$  with  $0.098$  to  $0.062 \mu\text{m}$  passbands, resulting in values of  $0.02$  or less at each wavelength [55]. Ultraviolet albedos have become available from the orbiting astronomical observatory. The albedos for Uranus and Neptune were found to be about the same at  $\lambda 2590$  as at  $\lambda 4000$ , while Uranus appears to have a still higher albedo (ca 0.7) at  $\lambda 2110$  [408].

The bolometric geometric albedo for Uranus has a value of  $0.32$  [530, 532]. When scaled to the radius of Table 1, this becomes  $0.27$ . Adopting Younkin's suggested value of  $1.25$  for the phase integral at all wavelengths, a bolometric Bond albedo for Uranus of  $0.33$  can be derived. The existing photometry of Neptune is sufficiently

similar to that of Uranus to adopt the same value. Since the maximum phase angle achieved by Uranus is only  $3.1^\circ$ , as viewed from Earth, and that of Neptune only  $1.9^\circ$ , it is obvious that accurate radiation balance studies can only be carried out from space probes.

The limb-darkening curve is one final important type of data which furnishes an important boundary condition on atmospheric models. Difficulties in obtaining meaningful results on bodies only  $4$  and  $2.5$  arc seconds in angular diameter are obvious, and, in fact, no data exist for Neptune. Danielson et al [102] obtained excellent curves for  $\lambda\lambda 3800\text{--}5800$  from their Stratoscope II photographs of Uranus. Sinton has shown there is some limb-brightening at  $8870 \text{ \AA}$  in the middle of a strong methane band where the albedo is only  $1\%\text{--}2\%$  [424].

#### *Atmospheric Structure (Models)*

The thermal atmospheric opacities of Uranus and Neptune are dominated by molecular hydrogen, as are Jupiter and Saturn [465, 468]. Additional opacity induced by methane, as suggested by Fox and Ozier [147], would become important only if either planet proved to have a large internal energy source. The measured infrared temperatures discussed above for Uranus all seem compatible with expected effective temperature calculated from purely solar heating except for the  $300\text{--}500 \mu\text{m}$  result, which is anomalously low. The  $17\text{--}28 \mu\text{m}$  value for Neptune seems high, however, and Trafton [474] suggests an internal heat source which may be tidal dissipation caused by Triton, Neptune's very large, close satellite.

Definite sources of visible opacity in the Uranus and Neptune atmospheres include Rayleigh and Raman scattering of  $\text{H}_2$ , very weak quadrupole and stronger induced dipole absorption of  $\text{H}_2$ , and very strong methane absorption. A pure molecular atmosphere containing only these opacities cannot match measured geometric albedos and  $\text{H}_2$  and  $\text{CH}_4$  line equivalent widths on either planet [36, 499]. A dense cloud layer of solid  $\text{NH}_3$  particles must form at about  $170^\circ \text{ K}$  and  $8$  bars on Uranus, if that gas is present, as expected [375], and if Trafton's temperature profile from his thermal opacity work is a rea-

sonable first approximation [465]. There should also be a thin CH<sub>4</sub> haze with a base at about 60° K and 0.4 bar. Such a model is consistent with the Stratoscope II limb-darkening curves [102], and the amount of H<sub>2</sub> above the NH<sub>3</sub> cloud tops ( $\gtrsim 370$  km-amagat) is reasonably consistent with measured equivalent widths of H<sub>2</sub> quadrupole lines [36] and with observed geometric albedos [499]. Recent work indicates the mixing ratio of CH<sub>4</sub> cannot be above about 10<sup>-2</sup>, or too thick a CH<sub>4</sub> cloud layer will result [100]. The case for Neptune is less clear because few observations are available. With higher surface gravity, pressure at the NH<sub>3</sub> cloud deck would be higher, the amount of H<sub>2</sub> above this deck larger, and any reflection from the deck less important than on Uranus. There may be thin argon clouds high in Neptune's atmosphere [475].

Detailed inversion of the light curve obtained when Neptune occulted the star BD-17° 4388 in 1968 furnishes the only quantitative observational data on the upper atmosphere of Neptune. Veverka et al [491] found the "quasi-linear" scale height to be 55–58 km, although there is localized structure showing swings between about 30 and 80 km. At a number density of 10<sup>15</sup> cm<sup>-3</sup>, the temperature would be about 130° K in a pure H<sub>2</sub> atmosphere, with a small positive temperature gradient reaching to higher elevations. Any mixture of heavier gases raises this temperature in direct proportion to the mean molecular weight. No analysis of the complex details of the refractivity profile has been made because too much data is missing. The ionosphere of Neptune is expected to be somewhat cooler than that of Jupiter [491] because of the greater amounts of methane and its photoproducts, which are efficient radiators, and the lower effective temperature of Neptune. No observational data exist for the upper atmosphere of Uranus.

### Body Structures

Real models, analogous to those for Jupiter and Saturn, do not exist for the interiors of Uranus and Neptune. Calculation of the unique mass-radius relationship for homogeneous, cold bodies [534] indicates that these planets probably contain large amounts of lighter elements but are

not so hydrogen-rich as Jupiter and Saturn [217]. A number of models containing large amounts of metallic ammonium (NH<sub>4</sub>) or a mixture of CH<sub>4</sub>, NH<sub>4</sub>, H<sub>2</sub>O, and Ne in solar abundances were constructed during the 1960s [370, 380, 390], but recent radical changes (ca 10%) in the best values for the radii of Uranus and Neptune have rendered them obsolete, even as crude models.

Makalkin [296] has reintegrated the cold (equation of state at 0° K) Neptune models of Reynolds and Summers [390] using the new radius. The resulting best fit occurs in a model with a larger fluid envelope and smaller solid core of higher central density, although it actually does not fit observed data well. Makalkin [296] suggests a hot model as the best possibility to improve the fit, although he notes that the composition could also be juggled. Zharkov and Trubitsyn [537] have run hot models for Uranus and Neptune with adiabatic temperature gradients. In such models, heavy element cores must be liquid, starting with atmospheric temperature even as low as 50° K at 1 bar pressure level.

It is not possible to state at present if Uranus and Neptune have solid surfaces, however, if they do, the surfaces are probably at depths of at least 5000 km. Improved values for radius, oblateness and higher order gravitational terms, rotation period, and atmospheric composition and structure are all needed as boundary conditions before interior model-building can produce convincing results.

## PLUTO

### General Background and Physical Data

Pluto was discovered by Tombaugh on February 18, 1930, after 25 years of deliberate, intense search [464]. Its orbit is the most eccentric and most highly inclined of any planet. Near perihelion, which it reaches next in 1989, it is nearer the Sun than Neptune can ever come, and midway between its nodes, it lies a billion and a quarter km above the ecliptic plane. Because of that inclination, there is no chance at present of a catastrophic encounter with Neptune.

A special perturbation study covering 120 000 years was presented in 1965 by Cohen and

Hubbard [90]; it uncovered an apparently stable libration in the Pluto-Neptune couple over 19 670 years. The study indicated that Neptune and Pluto never approach nearer than about 18 astronomical units (AU) to each other, and that the closest approach always occurs when Pluto is near aphelion. More recent studies have reinforced this conclusion. Williams and Benson [520] carried out a  $4.5 \times 10^6$  yr integration which confirms the 20 000-yr oscillation over the longer period, and which has uncovered other resonances, in particular, an important one with a period of 3 955 000 years. The total effect of these terms is to increase the minimum Pluto-Neptune distance and the apparent stability of the outer solar system. Wilkins and Sinclair [517] have noted the minimum distance (16.7 AU) between Pluto and Neptune is much greater than the minimum distance (10.6 AU) between the planets Pluto and Uranus.

The supposition that Pluto might be an escaped

satellite of Neptune was originated by Lyttleton [291]. The escape hypothesis was later championed by Kuiper [264] and Rabe [378, 379] as a likely outcome of Kuiper's protoplanet theory of the origin of the solar system. The two escape mechanisms proposed are completely different, however. Pluto seems physically more like a satellite of a giant planet than one of the planets themselves. On the other hand, resonance studies noted in the previous paragraph seem to indicate extreme stability of Pluto's orbit. It has been suggested as unlikely that the 20 000-yr libration began more recently than the time at which planetary masses stabilized at their present values [520]. The current stability and earlier escape from Neptune are not necessarily incompatible, but these studies inevitably make the escape hypothesis seem less attractive than previously. Only detailed study and comparison of Pluto and Triton seem likely to indicate if they might have had a common origin.

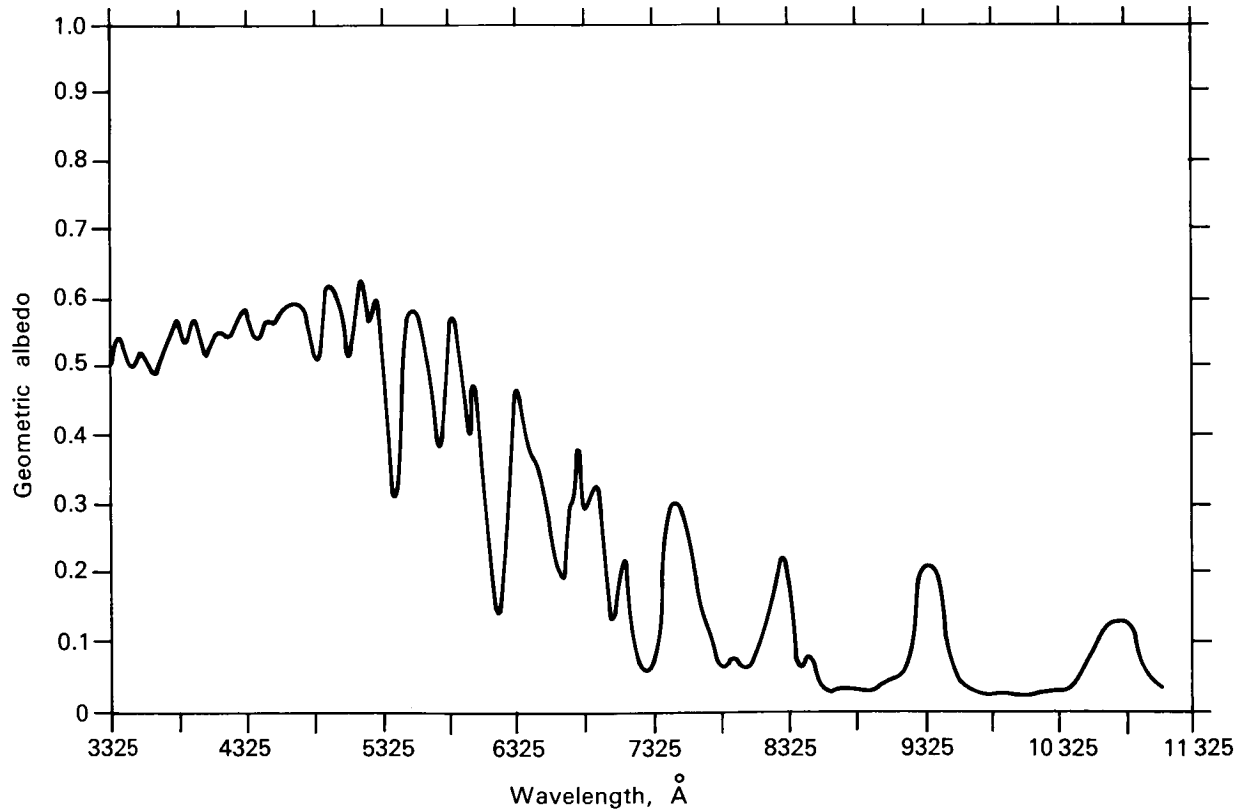


FIGURE 10.—Geometric albedo of Uranus,  $\lambda 3325-11\ 100$ . (Adapted from [530])

Pluto appears as a point source in all but the largest telescopes, and even in the largest telescopes it can be resolved only under the finest observational conditions. Kuiper made a direct measurement in 1950 of 0.23'' (about 5860 km) for Pluto's diameter [260], which may be subject to uncertainties approaching 50%. A far more accurate technique for measuring such small angles is photometric observation of a stellar occultation, but such occultations occur rarely. A "very near miss" recently fixed the extreme upper limit of Pluto's diameter at 6800 km [189].

The mass of Pluto has been difficult to determine, since it requires measuring perturbations on a large body, Neptune, by a smaller one, Pluto. Pluto has made only half a revolution including all known prediscovery observations back to 1846, further complicating determination of its mass. The best available mass figure for Pluto presently is 0.11 that of Earth [414], which, together with a 6400-km diameter, implies density of  $4.9 \text{ g cm}^{-3}$ . The history of attempts to determine the mass of Pluto has been one of continuous uncertainty, with the "best" value being 0.91 that of Earth until as recently as 1968. Halliday [188] suggested that a small change in the mass of either Saturn or Uranus could easily cause a large change in the mass determined for Pluto. The safest conclusion may be that of Ash et al [22], that "Pluto's mass cannot be determined reliably from existing data."

The rotation period of Pluto was first measured photometrically in 1955 by Walker and Hardie [494]. The latest period for Pluto obtained from phasing more than 20 years of data is  $6.38737 \pm 0.00018 \text{ d}$  [342]. Although the rotation period is quite constant, amplitude and mean opposition V magnitude of the light curves have not been. Andersson and Fix [12] find that the mean brightness of Pluto has decreased 0.20 magnitudes and amplitude of the light curves increased from 0.11 magnitudes 20 years ago to 0.22 magnitudes today. Attributing these changes to variation in the sub-Earth point on a Pluto with albedo features as the latter planet moves along its orbit, they solved for the obliquity of Pluto's axis and found it "probably greater than  $50^\circ$ ."

### Atmosphere

Pluto's low mass and temperature suggest that it may not have an atmosphere. Many potential atmospheric molecules, such as  $\text{CO}_2$ ,  $\text{H}_2\text{O}$ , and  $\text{NH}_3$ , would lie frozen on the surface, while others, such as  $\text{H}_2$  and  $\text{He}$ , would escape. The atmosphere might contain extremely small amounts of  $\text{CH}_4$  and/or  $\text{N}_2$ , but even at  $50^\circ \text{ K}$ , the vapor pressure of these species is extremely low. Heavier inert gases, such as neon and argon, could form a permanent atmosphere, but these are difficult to detect spectroscopically. Hart [196] finds that the spectrophotometry of Fix et al [142] would allow 1 atm of neon but this seems incompatible with 3 atm pressure because of increase in ultraviolet albedo that would result from Rayleigh scattering.

No evidence of an atmosphere could be detected on Pluto in a low-dispersion ( $720$  and  $340 \text{ \AA mm}^{-1}$ ) spectroscopic study of the visible red [258]. Much higher dispersion is certainly available today, but the best hope for detecting an atmosphere, which might be largely inert gases, would be by means of a spacecraft occultation experiment.

### Photometric Properties

As noted previously (in the discussion on rotation period and axial obliquity), the magnitude of Pluto reduced to mean opposition distance seems to be increasing, as is the amplitude of its diurnal variation. Pluto, because of its large orbital eccentricity, would be more than a magnitude brighter at perihelion than at its mean distance, were it not for this effect attributed to bright polar caps by its discoverers [12]. They [12] also suggested a phase coefficient of 0.05 magnitude/degree be applied to all Pluto photometry.

The relative brightness of Pluto has been measured between  $3400$  and  $5900 \text{ \AA}$  in 21 passbands having a full width of  $128 \text{ \AA}$  at half-maximum transmission [142]. This work showed a slowly increasing albedo toward the red from  $\lambda 3800$  as well as a steeper increase toward the blue from that point and some hint of structure at  $4800$  and  $5800 \text{ \AA}$ . Harris' photometry [194] shows a body considerably redder than the Sun at  $\lambda 6900$  and  $8200$ .

The radius of Pluto is so poorly known that attempts to quote a geometric albedo based on the radius are almost meaningless. Harris [194] picked a radius of 0.45 that of Earth, which gives  $p_v=0.13$ . He then chose a phase integral equal to that for Mars ( $q_v=1.04$ ), to derive a visual Bond albedo  $A_v=0.14$ . The albedo of Pluto seems to change only slowly with wavelength, so this value was inserted in Table 1 as a guess at the bolometric Bond albedo. It is obvious that an accurate radius and phase integral for at least 1 wavelength must be measured before such numbers can have real meaning. It seems likely that the bolometric Bond albedo for Pluto is sufficiently smaller than Neptune's to give Pluto the higher effective temperature. However, Pluto's slow rotation will assure considerable difference in actual dayside and nightside temperatures, the former reaching perhaps 50°K.

Polarimetry of Pluto by Kelsey and Fix [242] indicates that the planet probably has a microscopically rough surface, and their value of 0.27% polarization at a phase angle of only 0.8° is certainly compatible with a low albedo, since it hints at a deep negative branch for the polarization curve.

### Body Structure

Since even density of Pluto is grossly uncertain, meaningful work on the structure of the planet is unlikely until a spacecraft has accurately determined at least its basic physical measurements with some accuracy. A large magnetic field seems unlikely, since Pluto is small and rotates slowly, but after Mercury, who knows?

### SATELLITES AND RINGS

Less than a decade ago, satellites of the solar system (except the Moon) were in the backwater of astrophysical research. The extensive photoelectric photometry of Harris [194] and occasional studies by Kuiper and his students constituted the majority of modern knowledge, other than that of their masses and motions. During the past 5 years, satellite study has burgeoned into one of the most active fields of solar system physical research, one which required 100 pages to en-

compass in the recent review of Morrison and Cruikshank [335]. The emphasis here will be upon the Galilean satellites of Jupiter, and Titan, the bodies most likely to be of biological interest. The aforementioned review is recommended for additional physical information. Reviews of celestial mechanics are in papers by Wilkins and Sinclair [517] and Porter [369]. No review of satellites, however brief, would be complete without some description of the innumerable small satellites seen as the rings of Saturn, which will be discussed along with Saturn's satellites.

### Jupiter's Satellites

Jupiter has 12 known satellites, 5 near the planet in circular orbits in the equatorial plane and 7 in far out, highly eccentric, highly inclined orbits.<sup>7</sup> The basic orbital elements are given in Table 16, together with mean brightness and change of brightness caused by rotation. JV, sometimes called Amalthea, and the four large Galilean satellites (discovered by Galileo in 1610) appear to keep one face toward their primary [237, 335], rotating on their axes in the same period as they revolve about Jupiter. Almost nothing is known about the other seven bodies, or even Amalthea, which is so close to Jupiter (1.54 radii from the planetary surface) as to virtually prohibit accurate photometry.

The Galilean satellites are large, important bodies in their own right. Ganymede is larger than the planet Mercury, and all but Europa are larger than the Moon. In understanding these bodies, it is of great importance that accurate physical data are finally becoming available. In 1971, Io occulted  $\beta$ -Scorpii C [219, 347, 457], and in 1972, Ganymede occulted SAO 186800 [77], giving greatly improved radii for the two satellites. With these radii forming a base, it became possible to derive further data from mutual occultations occurring every 6 years when Earth is in the plane of the satellite orbits [67]. Finally, new masses have come from the flight of Pioneer 10 [8]. These data and quantities derived from them are in Table 17.

---

<sup>7</sup>A thirteenth satellite, lying just inside JVI, was discovered in Sept. 1974.

The occultation by Ganymede, besides an improved radius, apparently gave the first direct evidence of an atmosphere on a Galilean satellite, suggesting a surface pressure on Ganymede of at least  $10^{-6}$  bar but probably not as great as  $10^{-3}$  bar [77]. The star occulted was quite faint, how-

ever; and there are some questions on the reliability of the pressure data. The Pioneer 10 S-band radio occultation experiment [250] detected an electron density of  $6 \times 10^4 \text{ cm}^{-3}$  at  $100 \pm 40 \text{ km}$  above the surface of Io and a neutral atmosphere corresponding to surface pressure of  $10^{-8}$  to  $10^{-10}$

TABLE 16.—*Jupiter's Satellites*

Satellite	Semimajor axis, km	Eccentricity <sup>1</sup>	Inclination <sup>1,2</sup>	Sidereal period	V magnitude at mean opposition <sup>5</sup>	Rotational change in V <sup>6</sup>
JV <sup>3</sup>	181 500	0.0028	0°27.3'	11 h 57 min 22.70 s	ca 13.0	(?)
JI (Io) <sup>3</sup>	422 000	0.0000	0°1.6'	1 d 18 h 27 min 33.51 s	4.80	0.16
JII (Europa) <sup>3</sup>	671 400	0.0003	0°28.1'	3 d 13 h 13 min 42.05 s	5.17	0.31
JIII (Ganymede) <sup>3</sup>	1 071 000	0.0015	0°11.0'	7 d 3 h 42 min 33.35 s	4.54	0.15
JIV (Callisto) <sup>3</sup>	1 884 000	0.0075	0°15.2'	16 d 16 h 32 min 11.21 s	5.50	0.15
JVI <sup>4</sup>	11 487 000	0.158	27.6°	250.57 d	14.88	U
JVII <sup>4</sup>	11 747 000	0.207	24.8°	259.65 d	16.	N
JX <sup>4</sup>	11 861 000	0.130	29.0°	263.55 d	18.6	K
JXII <sup>4</sup>	21 250 000	0.169	147°	631 d	18.8	N
JXI <sup>4</sup>	22 540 000	0.207	164°	692 d	18.1	O
JVIII <sup>4</sup>	23 510 000	0.378	145°	739 d	18.8	W
JIX <sup>4</sup>	23 670 000	0.275	153°	758 d	18.3	N

<sup>1</sup> Eccentricities and inclinations for regular satellites are slightly variable. Those for irregular satellites are extremely variable.

<sup>2</sup> To the equatorial plane of Jupiter.

<sup>3</sup> From [400], except photometric data.

<sup>4</sup> From [369], except photometric data.

<sup>5</sup> From [194], except JVI which is from [10, 11].

<sup>6</sup> From [335].

<sup>7</sup> Possibly variable with leading edge brighter.

TABLE 17.—*Galilean Satellites: Physical Data*

Parameter <sup>1</sup>	Io (JI)	Europa (JII)	Ganymede (JIII)	Callisto (JIV)
Mass (Jupiter = 1) [8]	$4.696 \times 10^{-5}$ ± 0.06	$2.565 \times 10^{-5}$ ± 0.06	$7.845 \times 10^{-5}$ ± 0.08	$5.603 \times 10^{-5}$ ± 0.17
Mass (Moon = 1) <sup>2</sup>	1.213	0.663	2.027	1.448
Mean diameter, km	$3636 \pm 5$ [347]	$2980 \pm 100$ <sup>3</sup>	$5270 \pm 30_{-200}$ [77]	$5000 \pm 150$ [119]
Mean density, g cm <sup>-3</sup> <sup>4</sup>	3.54	3.51	1.94	1.63
Mean surface gravity, m s <sup>-2</sup> <sup>4</sup>	1.80	1.46	1.43	1.14
Escape velocity, km s <sup>-1</sup> <sup>4</sup>	2.56	2.09	2.75	2.38
Bolometric Bond albedo [335]	$0.62 \pm 0.13$	$0.74 \pm 0.14$ <sup>5</sup>	$0.35 \pm 0.08$	$0.11 \pm 0.03$
Effective temperature, K <sup>6</sup>	96	87	109	118
Maximum temperature, K <sup>7</sup>	135	123	155	167

<sup>1</sup> Where the same source was used for all four satellites, the reference number is given in the parameter column. In all other cases, it follows the individual datum.

<sup>2</sup> Calculated from value above, mass of Moon =  $7.347 \times 10^{22}$  kg [190], and mass of Jupiter =  $1.8985 \times 10^{27}$  kg [8]. Unlike the figure in Table 1, this does not include the satellites' mass.

<sup>3</sup> This figure is the average of three values from mutual occultation observations reported at the 1974 AAS Division of Planetary Sciences Meeting, Palo Alto, Calif.

<sup>4</sup> Calculated from mass and diameter given above. G =

$6.673 \times 10^{20} \text{ km}^3 \text{ s}^{-2} \text{ kg}^{-1}$ .

<sup>5</sup> Corrected from 0.68 for new value of radius given above.

<sup>6</sup> Calculated from  $F = 4(1-A)^{-1} \sigma T^4$ , assuming the flux  $F = 1353 \text{ W m}^{-2}$  at 1 AU and the Stefan-Boltzmann constant  $\sigma = 5.669 \times 10^{-8} \text{ W m}^{-2} \text{ deg}^{-4}$ . A is the bolometric Bond albedo.

<sup>7</sup> Calculated from  $F = (1-A)^{-1} \sigma T^4$ . This is the maximum equilibrium temperature that a body of the given albedo, normally illuminated, can have at 5.203 AU from the Sun without an internal heat source.

bar (depending upon composition) on that satellite. The Io optical occultation observations had only resulted in an atmospheric upper limit of about  $10^{-7}$  bar [30, 427].

In 1964, Binder and Cruikshank [54] reported an apparent excess brightness on Io of about 0.1 magnitude as it reappeared after solar eclipse by Jupiter, the excess disappearing in about 15 min. It was suggested that this might be evidence for an atmosphere condensing during eclipse and evaporating in sunlight. It was estimated that about  $2 \times 10^{-7}$  bar of evaporate would be required to satisfy the observations [279]. Since 1964, there have been many photometric studies of Io eclipses, some positive, some negative. If the phenomenon is real, it is certainly intermittent, and the Pioneer 10 results on atmospheric pressure would indicate it is not caused by atmospheric condensation. The results for 1973, using photometers specially designed to reject scattered light from Jupiter, were all negative (no brightening) [151, 324].

The discovery by Brown [69] of sodium D-line emission from the satellite was the most unexpected and spectacular result on the atmosphere of Io. Confirming observations were soon reported by Brown and Chaffee [70], and then Trafton et al [478] found that the sodium radiation came from a large area around Io (more than 10 arc seconds in radius). The amount often averaged ca  $10^{11}$  atoms  $\text{cm}^{-2}$ , assuming it to be uniform and optically thin over the field of view, although it apparently is variable in time. Meanwhile, Judge and Carlson [239] reported an apparent torus of hydrogen around Jupiter in the orbit of Io with a surface brightness of 10 kilo-Rayleighs (assuming it is all Lyman  $\alpha$ -radiation). Presumably, the torus of hydrogen around Io is similar to the torus which McDonough and Brice suggested would be found around Titan [318]. The most acceptable explanation so far suggested for the observations is sputtering of Io's surface by charged particles from the Jovian magnetosphere, followed by resonance fluorescence within the sodium and hydrogen clouds thus created [311].

Photometry of the Galilean satellites has indicated that their surface properties vary considerably from satellite to satellite. This is well illustrated by the broadband photometry of Lee

[274], shown in Figure 11 with Morrison and Cruikshank's normalization [335]. More detailed studies at higher spectral resolution have shown that Europa and Ganymede are coated largely with  $\text{H}_2\text{O}$  frost [141, 365] at a temperature near 150° K and of ca 0.1 mm grain size [247]. Kieffer and Smythe [247] estimate fractional abundance at 75% and 60% on JII and JIII, respectively, while  $\text{H}_2\text{O}$  frost is at most a minor constituent on JI and JIV. Io retains its very high and largely featureless albedo even at 5  $\mu\text{m}$  [164]. Kieffer and Smythe [247] suggest strongly hydrated minerals as candidates for the JI surface.

Polarization results also indicate differences among the Galilean satellites, with Callisto standing out with a strong negative branch more than twice as deep as any of its companions [122, 488].

A number of brightness temperature measures have been made through the 8–14  $\mu\text{m}$  and 17–28  $\mu\text{m}$  windows in Earth's atmosphere. Table 18 is taken from Morrison and Cruikshank, with Europa temperatures corrected for the new radius given in Table 17. The 10  $\mu\text{m}$  temperatures are consistently 10° K higher than those at 20  $\mu\text{m}$ , a surprising result. Hansen [192] has shown what appears to be a distinct emission feature at 12  $\mu\text{m}$  on the three Galilean satellites he observed (JI, JIII, and JIV), which may account for the difference but this also needs explanation. Flux curves during eclipse have been obtained by Hansen at 10  $\mu\text{m}$  [191], and Morrison and Cruikshank at 20  $\mu\text{m}$  [334]. In general, results can best be explained by a thin low-conductive layer over a thick layer of high conductivity for JI, JII, and JIII, with some additional complexity for JIV.

The brightness temperatures of Ganymede and Callisto at millimeter and centimeter short wavelengths are given in Table 19. Temperatures have been adjusted (where possible) to the satellite radii given in Table 17; temperatures in parentheses are those published. These measurements are quite difficult to make because of the usual problem of detecting a weak signal in the presence of a nearby strong signal. Of the four measurements shown for Callisto, it is expected that interferometric measurements at 3.71 cm and high signal/noise measurements at

2.82 cm using the 100-m Bonn radio telescope are the most reliable. These are also the most interesting because they indicate brightness temperatures significantly lower than infrared temperatures. Also, the difference in brightness temperatures of the two satellites is larger than would be expected from their albedos [360].

The low brightness temperatures can be explained [360] by radio emission originating below the surface, where the variation of temperature with phase is lower. This implies, if correct, that interior of the satellites is colder than the surface. Brightness temperature measurements at 3.55 mm and 8.2 mm (in contrast to centimeter wave measurements) are considerably higher than both infrared and centimeter radio measurements; their statistical uncertainties, however, are large. The idea has been advanced that high brightness temperatures are the result of a nearly transparent ice surface on these satellites

[271]. In the Lewis [279] models, the lapse rate in the ice crust is ca  $1^{\circ}$  K/km, and a crustal thickness of ca 100 km is required to explain the observations. This theory predicts that brightness temperature does not depend on wavelength, which is inconsistent with available data.

The formation, internal structure, and chemistry of the Galilean satellites have been considered by two groups [279, 280, 281, 368]. These studies indicate that all four bodies are likely to have a core of hydrated silicates, and Ganymede and Callisto may well have thick mantles of frozen or liquid water (liquid, if there is even a small amount of radioactive decay in their interiors). Each should have at least a thin solid crust, possibly ice on all but Io, although on Callisto, the low albedo obviously requires an additional dark material on the surface.

All the Galilean satellites are very interesting, apparently quite different from bodies nearer the

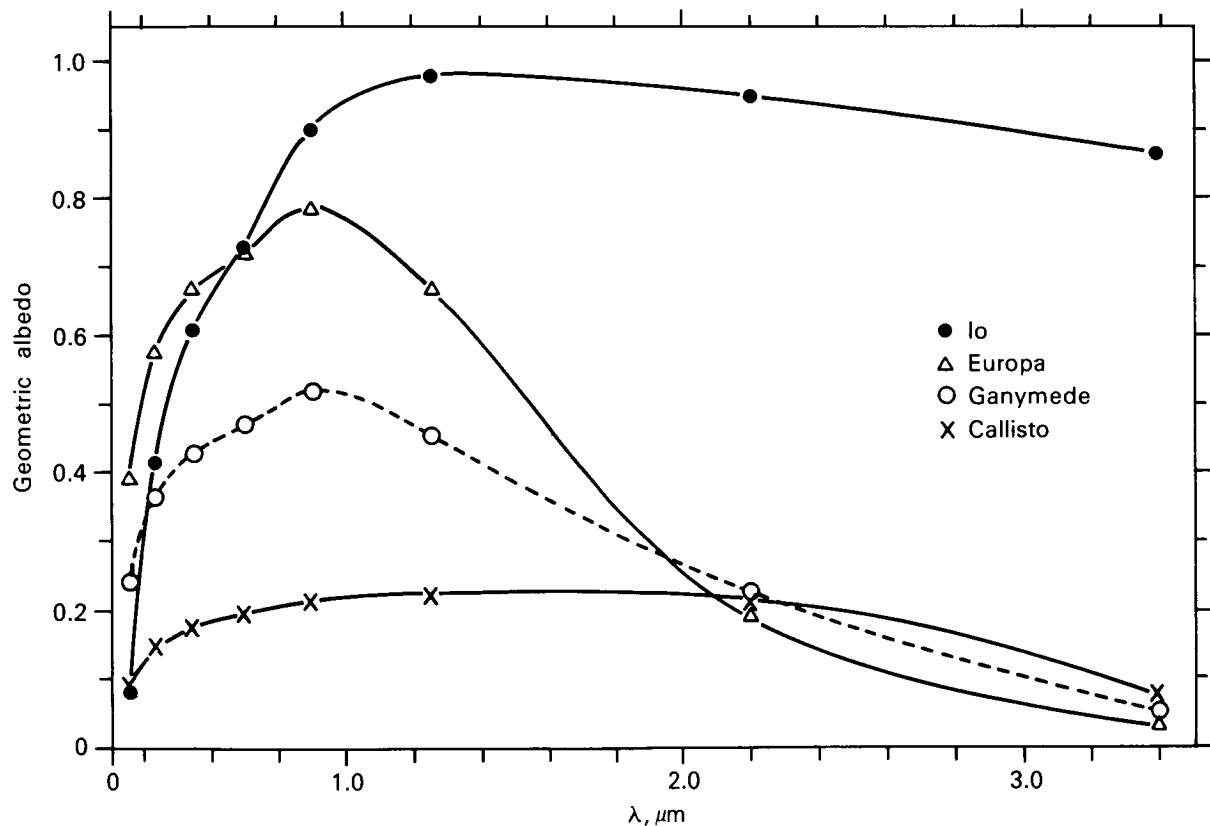


FIGURE 11.—Geometric albedo of the Galilean satellites, 0.4–3.4  $\mu\text{m}$ . (Adapted from [274] as normalized by [335])

Sun. Only Io and Europa have densities similar to the terrestrial planets (or perhaps the asteroids), and their albedos are many times higher than nearer, airless bodies. Io also exhibits a number of unique phenomena apparently associated with the Jovian magnetosphere. These satellites are sure to receive increased attention from space probes and ground-based observers during the next decade.

### Saturn's Rings and Satellites

#### *The Rings*

Saturn has 10 satellites, all but the outermost (Phoebe) in fairly regular orbits, and a glorious set of rings. The rings around Saturn, which appear to be unique in the solar system, were first seen by Galileo in 1610 as queer appendages on either side of the planet. The real nature of the appendages as part of a flat ring around the planet was discovered by Huygens in 1655. In the 1670s, Cassini found that the ring was double, a dark line separating it into two concentric rings. The dark line is now called Cassini's division, the outer ring A, and the inner ring B. In 1850, Bond at Harvard and Davies in England independently discovered a very tenuous third ring, a "crape ring" or Ring C, inside the first two. For many years, there has been considerable controversy about the existence of a fourth, extremely tenuous ring outside the A ring. Some positive evidence of this D ring's existence was obtained by Feibelman during the most recent [136] edge-on aspect, and was recently confirmed by Kuiper [267] who found evidence of material extending nearly to Dione.

Similarly, there have been reports of material

inside the crape ring [60, p 382]. Guerin has presented most convincing evidence of this [96, 176, 177] from photographs of Saturn which seem to confirm the presence of at least a small amount of ring material almost to the planet's atmosphere. He calls this material, which is separated from the C ring by a dark division, the D ring. To avoid confusion with material external to the A ring, it has been suggested that any material external to the A ring be called the D' ring [149]. Radial dimensions of the rings are given in Table 20.

The thickness of the rings is not easily determined, since they are very thin. The only times the rings have been observed when Earth was exactly in their plane occurred in October and December 1966 [60]. Then, through large telescopes, the rings did not completely disappear as it sometimes had been predicted they would. Photometry was undertaken at that time [61, 145] with somewhat discordant results. Both sets of data were analyzed and each found internally consistent. The thickness cannot be less than 500 m, nor is it likely to be greater than about 4 km. Systematic errors seem likely to cause the value to be underestimated [61], consequently a value of 2–3 km seems best until additional observations become available.

It is certain that the rings are not solid. Maxwell showed theoretically in 1857 that a solid ring rotating around a planet would not be stable, and Keeler showed spectroscopically in 1895 that the rings were in differential rotation. On at least six occasions, stars have been seen through the A ring, even though of magnitude 7.2 or fainter [59], giving rather direct proof of the rings' particulate nature. On at least two

TABLE 18.—*Galilean Satellite Temperatures*<sup>1</sup>

Authority	Wavelength, μm	Io (J1)	Europa (JII) <sup>2</sup>	Ganymede (JIII)	Callisto (JIV)
Gillett, Merrill, and Stein	11–12	139 ± 3	132 ± 3	142 ± 3	157 ± 3
Hansen	8–14	137 ± 3	131 ± 3	142 ± 3	152 ± 4
Morrison	8–14	138 ± 4	130 ± 4	145 ± 4	153 ± 5
Morrison, Cruikshank, and Murphy	17–28	128 ± 5	123 ± 5	138 ± 5	151 ± 7
Hansen	17–25	124 ± 4	122 ± 4	132 ± 5	142 ± 6
Morrison	17–28	130 ± 3	123 ± 3	143 ± 4	155 ± 5

<sup>1</sup>From Morrison and Cruikshank [335].

<sup>2</sup>Corrected for new radius of Europa, 1490 ± 50 km.

occasions, eighth magnitude stars were seen part of the time during passage behind the brighter, more dense B ring [59]. The troublesome problem of the mechanical stability of the ring will not be discussed here. (See references [60, 92, 93, 527] for further information.)

Additional information on the rings has come from four sources. Only photometry has been available for a considerable time; infrared radiometry, microwave radiometry, and radar information are very new. The large body of photometric work (reviewed by Morrison and Cruikshank [335]) will only be summarized here.

The visual surface brightness of the B ring and parts of the A ring are somewhat higher than the mean surface brightness of Saturn [95], indicating individual particles of very high albedo, since the rings are not optically thick. Several studies of ring optical depth converge on values of 0.7–1.0 for the B ring and 0.4–0.5 for the A

ring [335]. There is a very large opposition effect of 0.2 magnitude in the yellow up to 0.4 magnitude in the infrared and ultraviolet [229]. Since large opposition surges are usually identified with dark surfaces, the effect in Saturn's rings classically (since the 1880s) has been associated with mutual shadowing of the particles but such an effect should be independent of color, which is not what Irvine and Lane observed. The effect may be a combination of shadowing and backscattering.

Recent infrared spectrophotometry has shown that ring particles are largely ice or at least ice-covered [363], accounting for high yellow, red, and infrared albedo. However, a sharp drop in the ring albedo below 6000 Å, very much like the Io's behavior [28, 273], is not the behavior of ordinary pure ice.

Radiometry in the 8–14 μm windows is given in Table 21. It seems clear that ring temperature has increased with increasing Sun angle, implying shadowing was occurring at low angles. Most surprising is the high temperature for bodies of such high albedo. The effective temperature of a blackbody at Saturn's distance from the Sun is only 90° K. This would be raised to about 94° K for the B ring by including radiation from Saturn [338]. Estimates of the bolometric Bond albedo for ring particles generally lie between 0.5 and 0.8 or higher [335], implying fairly large, non-isothermal particles which are much warmer on the Sun-Earth side.

Recently, Goldstein and Morris demonstrated that the rings of Saturn are remarkably efficient radar reflectors by transmitting and receiving strong echoes from the rings at 12.6 cm [169]. The measured Doppler spread of echoes matches that expected from the particles in the bright

TABLE 19.—*Microwave Brightness Temperatures of Ganymede and Callisto*

Wavelength [reference]	Ganymede	Callisto
3.55 mm [171]		276 (255 ± 80)
8.2 mm [272]		233 (280 ± 120)
2.82 cm [360]	55 ± 14 (55 ± 14)	88 ± 18 (88 ± 18)
3.71 cm [42]		101 (101 ± 25)

TABLE 20.—*Saturn's Rings, Dimensions<sup>1</sup>*

Parameters	Radii, km	Saturn radii
Equatorial radius, Saturn	60 000 ± 240	1.00
Outer edge, ring D	72 600 ± 2000 <sup>2</sup>	1.21
Guerin division	Width ca 4200 km <sup>2</sup>	
Inner edge, ring C	76 800 ± 2000	1.28
Inner edge, ring B	92 000 ± 850	1.54
Outer edge, ring B	117 800 ± 350	1.97
Cassini division	Width ca 2600 km <sup>3</sup>	
Inner edge, ring A	120 400 ± 400	2.01
Outer edge, ring A	136 450 ± 350	2.28
Semimajor axis, orbit of Janus	168 700 <sup>2</sup>	2.81

<sup>1</sup> From [120], except where otherwise indicated.

<sup>2</sup> From [149].

<sup>3</sup> The edges of A and B rings are not sharp. Direct measurements of the width of the Cassini division often result in much larger values (i.e., ca 3500 km, Dollfus, [120]).

TABLE 21.—*Temperature of Saturn's Rings*

Wavelength, μm	Saturnicentric latitude of the Sun	Ring observed	Brightness temperature, °K	Reference
20	≤ 5°	A and B?	< 60	[23]
12.7	18°	A and B	82.7	[5]
20	26°	A	89	[338]
20	26°	B	94	[338]
11	26°	B	91	[335]
20	26°	B	96	[335]

inner ring, thereby strongly supporting the results. The received radar echo power was  $62 \pm 6\%$  of what would have been received from an isotropic reflector, without loss, in the same projected geometric cross section as the A and B rings and at the same distance—an entirely unexpected result. This reflectivity compares to 6% for Mercury, 12% for Venus, 8% for Mars, and 5 to 15% for the asteroids, Icarus and Toro. Interpretation is still very speculative, although it is generally agreed that radar observations require that reflecting objects be a centimeter-size or larger.

Goldstein and Morris [169] hypothesize that the scattering objects are likely to be rough with diameters on the order of a meter or larger. Pollack et al postulate that centimeter-sized particles of high albedo yield the observed high reflectivity through multiple scattering [367], and it is pointed out that radio brightness temperatures of the rings provide important constraints to the models. A third hypothesis proposed does not require a large single-scattering albedo. Pettengill and Hagfors [362] point out that backscattering from transparent spheres can show considerable gain over simple external reflection from the front surface of an equivalent sphere. Such gain results from internal scattering processes. For Saturn's rings, it is proposed, smooth ice fragments larger than 8 cm in radius will reproduce the radar result.

There are a number of single antenna and a few interferometer brightness temperature measurements of Saturn and its rings. Single antenna measurements yield the combined radiation from the Saturn-ring system, whereas interferometric measurements allow the ring brightness contribution to be separated and measured directly. One method of studying the ring influence is to observe dependence of the single disk antenna brightness temperatures on the planetocentric latitude of Earth (relative to the plane of the rings). A second method is to estimate the disk contribution from atmospheric models and attribute the residuals to the rings.

In a recent compilation of single antenna data [234] which relate to brightness temperature of the rings, it is shown that, with the exception of data at 1-mm wavelength, there are no statisti-

cally significant variations of brightness temperature with planetocentric angle. Measurements are consistent with absence of the rings, thereby showing that brightness temperatures of the rings must be low. Observing at a wavelength of 1 mm, Rather et al [381] measured a brightness temperature for Saturn that is  $45^\circ \pm 15^\circ$  K larger than that observed for Jupiter, inferring a brightness temperature of  $35^\circ \pm 15^\circ$  K for the rings. Because of the large size of the scatterers implied by radar observations, Pollack et al [367] infer that low brightness temperature must be due to emissivity effect. Janssen [234] combining the Rather et al data with earlier data, finds that the 1-mm data are consistent with an emissivity of 0.4. Briggs [66] estimates an upper limit of 80 cm to the particle size by assuming they are pure water ice.

High resolution interferometric observations of Saturn have been carried out at 3.7, 11, and 21 cm wavelengths [41, 43, 66] showing that nearly all of Saturn's emission originates from the planetary disk. Berge and coworkers estimate brightness temperature of the rings to be less than  $10^\circ$  and  $40^\circ$  K at 20 cm and 10 cm, respectively. Briggs, in agreement with Berge, found that average ring brightness temperature is less than  $20^\circ$  K at 3.7, 11, and 21 cm. Further, he found that when his interferometric fringes were perpendicular to Saturn's polar axis, the apparent size of the planet decreased. Such effect was not seen when the fringes were aligned with the polar axis. Briggs interpreted these data by a model in which the rings obscure part of Saturn's disk, thereby reducing the apparent size of the disk. Ring particles which are good scatterers and poor emitters can diffuse radiation from the disk while having a low brightness, which is consistent with both radio and radar data.

Several lines of evidence have converged to indicate that ring particles must be at least a few centimeters in diameter. Two not previously mentioned are the Poynting-Robertson effect which would sweep the ring free of all original particles smaller than about 3 cm in  $5 \times 10^9$  years [61, 505], and sputtering which would erode several centimeters of ice in a similar time [195]. Thus any small particles would have to be of more recent origin, nor can the rings be a monolayer, since shadowing and multiple scattering appear

to be required. Thus a number of "classical" models suggesting micron-sized particles or a monolayer of various thicknesses apparently have been ruled out by recent studies. No completely consistent ring models exist as yet, however, and there may still be surprises in physical study of one of the most beautiful objects of the solar system.

### The Satellites

The satellites of Saturn are laid out fairly regularly except for Phoebe, which is in an elongated retrograde orbit. The basic orbital elements are given in Table 22. Janus was discovered in 1966 when Saturn's rings were "edge-on." Even with the ring lights almost zero, Janus is difficult to see, with a magnitude of only 13.5 or 14, located next to a very bright planet [118, 425, 462]. Absolute confirmation that the object observed is indeed a satellite and not a ring condensation will probably have to wait until the rings are again edge-on, although the best of the photographs are very convincing.

The satellites of Saturn are rather substantial bodies, for the most part, all larger than the seven irregular satellites of Jupiter, and at least five (perhaps seven) of them of greater size than the largest asteroid. Titan (to be discussed in detail) is more massive and somewhat larger than the Moon. The basic physical data for all the satellites (except Janus) will be found in Table 23. Addi-

tional photometric and radiometric data for a number of Saturn's satellites are reviewed in Morrison and Cruikshank [335] and will not be repeated, except for mention of Iapetus and Titan.

### Iapetus

Iapetus was discovered by Cassini in 1671, who immediately reported a great brightness variation, suggesting . . . "but it seems, that one part of his surface is not so capable of reflecting to us the light of the Sun which maketh it visible, as the other part is" [1]. That, indeed, has proved to be the case. Murphy et al [339] found anticorrelation between visible brightness and infrared flux, with Iapetus having a temperature of  $117^\circ \pm 4^\circ \text{ K}$  and visual albedo of  $0.04 \pm 0.01$  near minimum light, and a temperature of  $110^\circ \pm 4^\circ \text{ K}$  and  $0.25 \pm 0.05$  visual albedo near maximum light. They suggest that the albedo at maximum is about 0.28. Zellner's [535] polarization studies are consistent with a bright trailing hemisphere and a dark leading hemisphere. Neither of the above studies is consistent with an elongated shape.

The most detailed photometry of Iapetus (that of Millis [323]) showed successive minima differing by 0.3 magnitude, which is attributed to change in solar phase angle, the resulting phase coefficient and opposition effect being comparable to that of the Moon, Callisto, and some asteroids—all having dark surfaces. A much smaller phase coefficient was found for the bright side, comparable to bright Io and Europa. The first good color curves obtained [323] showed 0.07 variation in B-V and 0.045 in U-B. Iapetus, then, is truly a remarkable object with one hemisphere six times as bright as the other. The best theory so far, proposed by Cook and Franklin [94], is that a thin ice crust was largely eroded from one side by meteoroidal bombardment of its leading hemisphere.

### Titan

Titan is certainly the most interesting of Saturn's satellites because of its extensive atmosphere. In 1944 Kuiper [258] first discovered methane on the satellite, empirically estimating its abundance in a presumed pure methane atmosphere at 200 m-amagat in 1952

TABLE 22.—*Saturn's Satellites*<sup>1</sup>

Satellite	Semimajor axis, km	Eccentricity	Inclination <sup>2</sup>	Period, d
Janus <sup>3</sup>	168 700	ca 0	ca 0	0.815
Mimas	185 800	0.0201	1°31.0'	0.942422
Enceladus	238 300	0.00444	0°01.4'	1.370218
Tethys	294 900	0	1°05.6'	1.887802
Dione	377 900	0.00221	0°01.4'	2.736916
Rhea	527 600	0.00098	0°21'	4.517503
Titan	1 222 600	0.029	0°20'	15.945452
Hyperion	1 484 100	0.104	(17°-56') <sup>4</sup>	21.276665
Iapetus	3 562 900	0.02828	14.72°	79.33082
Phoebe	12 960 000	0.16326	150.05°	550.45

<sup>1</sup> From [369], except data for Janus.

<sup>2</sup> To plane of ring.

<sup>3</sup> From [149].

<sup>4</sup> Varies from 17' to 56' [400].

[261]. There the matter stood for 20 years until Trafton's [469] surprising announcement of the possible presence of H<sub>2</sub> on Titan. He further suggested [470] that even the spectrophotometric observations of McCord et al [316] showed that either methane must be an order of magnitude more abundant than previously thought or a minor constituent. Hydrogen observations [469] suggested the presence of ca 5 km-amagat of H<sub>2</sub> (with a very large uncertainty).

Very recent radiometry by Low and Rieke [287], however, shows no evidence of the 17 μm pressure-induced H<sub>2</sub> feature, so the abundance is probably much lower than 5 km-amagat. Trafton also found [475] that there is at least one additional spectroscopically active gas on Titan absorbing in the 1.05–1.1 μm area. There is evidence of an additional absorber near 1.65 μm [297]. Further, there is a prominent emission feature near 12 μm [162], probably best explained as the 12.2 μm ethane (C<sub>2</sub>H<sub>6</sub>) band [101].

Both ethane (C<sub>2</sub>H<sub>6</sub>) and ethylene (C<sub>2</sub>H<sub>4</sub>) have bands in the 1.65 μm region, but Trafton [475] was unable to find evidence for absorptions of either in the 1.06 μm region. He suggests an isotope of CH<sub>4</sub> as one possible explanation of these lines [475].

Evidence of clouds on Titan further complicates spectroscopic interpretation. Polarization observations [489, 536] suggest the presence of an opaque cloud deck. Further, there is a rapid decrease in Titan's albedo through blue, violet, and near ultraviolet [25, 72], entirely opposite to the effect of molecular (Rayleigh) scattering. Albedo decrease virtually requires the presence of an aerosol, preferably a fine dust which absorbs ca λ<sup>-1</sup> [28].

A major boundary condition on models of Titan's atmosphere is furnished by photometric and thermal data. Younkin's [531] high resolution spectrophotometry from 0.50 to 1.08 μm permitted derivation of geometric albedos. With

TABLE 23.—*Saturn's Satellites, Physical Data*

Parameter <sup>1</sup>	Mimas	Enceladus	Tethys	Dione	Rhea
Mass (Saturn=1) <sup>2</sup>	6.59 ± 0.15 × 10 <sup>-8</sup>	1.48 ± 0.61 × 10 <sup>-7</sup>	10.95 ± 0.22 × 10 <sup>-7</sup>	20.39 ± 0.53 × 10 <sup>-7</sup>	3.2 ± 5.6 × 10 <sup>-6</sup>
Mass (Moon=1) <sup>3</sup>	0.00051	0.001	0.0085	0.0158	ca 0.025
Mean diameter, km <sup>16</sup>	ca 400 <sup>5</sup>	550 ± 300 <sup>4</sup>	1200 ± 200 <sup>4</sup>	1150 ± 231	1450 ± 200 <sup>4</sup>
Mean diameter (Moon=1) <sup>8</sup>	ca 0.1	0.16	0.35	0.33	0.42
Mean density, g cm <sup>-3</sup> <sup>9</sup>	ca 1.0	ca. 1.0	0.7	1.5	ca 1.1
V mag at mean opposition <sup>10</sup>	12.1	11.77	10.27	10.44	9.76
Rotational change in V	Unknown	ca 0.4 <sup>12</sup>	0.16 <sup>5</sup>	0.20 <sup>5</sup>	0.19 <sup>5</sup>
Parameter <sup>1</sup>	Titan		Hyperion	Iapetus	Phoebe
Mass (Saturn=1) <sup>2</sup>	2.4619 ± 0.0029 × 10 <sup>-4</sup>		ca 2.0 × 10 <sup>-7</sup>	3.94 ± 1.93 × 10 <sup>-6</sup>	Unknown
Mass (Moon=1) <sup>3</sup>	1.905		0.0015	0.02	
Mean diameter, km	4850 ± 300 <sup>4</sup>		160–920 <sup>5, 7</sup>	1800 ± 200 <sup>5</sup>	60–320 <sup>5, 7</sup>
Mean diameter (Moon=1) <sup>8</sup>	1.40			0.52	
Mean density, g cm <sup>-3</sup> <sup>9</sup>	2.34			ca 0.7	
V mag at mean opposition <sup>10</sup>	8.35 <sup>15</sup>		14.16	11.03	16.56 <sup>11</sup>
Rotational change in V	0.00 <sup>5</sup>		Unknown	1.92 <sup>13</sup>	0.25 <sup>11, 14</sup>

<sup>1</sup> All references are given in these footnotes.

<sup>2</sup> From Duncombe, Klepczynski, and Seidelmann [128].

<sup>3</sup> Calculated using mass of Moon = 7.347 × 10<sup>22</sup> kg [190].

<sup>4</sup> From Dollfus [119].

<sup>5</sup> From Morrison and Cruikshank [335].

<sup>6</sup> From Murphy, Cruikshank, and Morrison [339].

<sup>7</sup> Lower limit assumes a geometric albedo of 1.0; the upper limit, 0.03.

<sup>8</sup> Calculated using diameter of Moon = 3475 km [190].

<sup>9</sup> Calculated from data above.

<sup>10</sup> From Harris [194] except for Titan and Phoebe.

<sup>11</sup> From Andersson [10, 11].

<sup>12</sup> From Franz and Millis [150].

<sup>13</sup> From Millis [323]. (See discussion in text).

<sup>14</sup> Phoebe is apparently not "locked" to Saturn. Its period of rotation is apparently less than 1 d [10, 11].

<sup>15</sup> From Blanco and Catalano [58].

<sup>16</sup> Elliot, Veverka, and Goguen reported new radii for five satellites at IAU Colloquium No. 28, Planetary Satellites, Ithaca, N.Y., Aug. 1974. These will cause major changes in all physical data. For example, their values for Titan and Iapetus are 5832 ± 53 and 1595 ± 139 respectively.

existing measurements from 0.30 to 0.50  $\mu\text{m}$  and a synthetic spectrum based upon similar Jupiter and Saturn results from 1.08 to 4.0  $\mu\text{m}$ , Younkin [531] derives a bolometric geometric albedo of 0.21 and suggests using a bolometric Bond albedo of  $0.27 \pm 0.04$ . The effective temperature of Titan then is  $84^\circ \pm 2^\circ \text{ K}$ .

Detailed thermal measurements (from Low and Riecke [287]), given in Table 24, show a surprising picture. Even a nonrotating blackbody (zero albedos) normal to the Sun can reach only  $127^\circ \text{ K}$  at Titan's distance from the Sun. It would appear that there must be either a fairly effective atmospheric greenhouse mechanism or an atmospheric nonequilibrium radiator in operation. The peak at  $8\mu\text{m}$  is to be expected from methane inversion as on Jupiter and Saturn. The peak at  $12\mu\text{m}$  may be  $\text{C}_2\text{H}_6$  as noted above. The rest can potentially be modeled in at least two ways.

A series of greenhouse models for Titan was computed [366] in which the best fit to the data then available suggested roughly a 50–50 mix of  $\text{H}_2$  and  $\text{CH}_4$  with a surface temperature and pressure of at least  $150^\circ \text{ K}$  and 0.4 atm. The greenhouse was created by pressure-induced transitions in the gases, but there was visible opacity from methane clouds. The biggest problem is that the pressure-induced  $\text{H}_2$  feature that would then fill the region near  $17\mu\text{m}$  simply does not seem to be present [287].

Danielson, Caldwell, and Larach suggest that an aerosol layer of micron-sized particles would absorb a large part of incident thermal radiation [101], but could not reradiate it effectively at wavelengths several times their size, hence creating thermal inversion and explaining high  $5\mu\text{m}$  temperatures. The surface would be near  $80^\circ \text{ K}$ , heated by direct solar radiation and reemitted atmospheric radiation. The greatest problem is that the Bond albedo appears to be higher (0.27) than they assumed (0.20).

Low and Rieke suggest a slight modification: retaining the particle inversion layer but adding a bit of greenhouse would keep the surface temperature up to  $80^\circ\text{--}90^\circ \text{ K}$ , as required to keep too much  $\text{CH}_4$  from condensing out in spite of the higher albedo [287]. Detailed calculations have not yet been made for a combined green-

house-inversion model of Titan's atmosphere, but it seems plausible. Reliable quantitative models must await radio surface temperatures and positive identification of the unknown absorbers in Titan's atmosphere.<sup>8</sup>

The nature of Titan's crust is expected to be the factor which determines the presence and composition of the atmosphere. This problem and that of hydrogen escape have been considered by Hunten [222], who showed that a pure  $\text{H}_2$  atmosphere would escape extremely rapidly but that 10–25%  $\text{H}_2$  could probably be retained in a steady state, produced perhaps from photolysis of  $\text{NH}_3$ . Although an atmosphere on Titan may have a sufficient velocity to escape from Titan, it probably does not have a Saturn escape velocity [318]. Consequently, atoms and molecules lost by Titan are forced by the planet's gravitational field to orbit Saturn until ionized, or until recaptured by Titan.

There is no direct observational knowledge of the surface and interior of Titan. For example, in spite of very high precision photometry, no variation in Titan's brightness has been detected which could be attributed to rotation. Titan is usually assumed to keep one face toward Saturn, rotating and revolving synchronously, but this is no more than an educated guess. According to Lewis' models [279, 281], the surface may be largely methane hydrate ice, although obviously this is a function of what the surface temperature proves to be. The interior may contain a hydrous silicate mantle overlain with a hydrous ammonia solution immediately below the solid crust [279, 281], while there may be a troilite ( $\text{FeS}$ ) core. The uncomfortable fact remains that the only real observational datum on the interior of Titan is its density, and even that is uncertain by perhaps 20% because of the uncertainty in the satellite's radius.<sup>8</sup>

### Satellites of Uranus

Uranus has five satellites which form an extremely regular system, for which basic data is

<sup>8</sup> The new 5832 km radius for Titan (see Table 23) reduces the temperature discrepancy significantly and decreases the density by 60%.

given in Table 25. The satellites are too small for direct measurement of size at the distance of Uranus, and none has been detected in the middle infrared to allow a radiometric radius determination. If ice-covered, with a very high albedo, they could be as small as 200 km (Miranda) to 700 km (Titania) in diameter. Given extremely dark surfaces, diameters could be 1300 km (Miranda) to 4000 km (Titania). If Kuiper's uncertain masses (see Table 25) are taken literally, the true diameters must be near the lower limits to keep the densities above 1 g/cm<sup>3</sup>.

### Satellites of Neptune

Neptune has only two satellites. The apparently large and massive Triton is in retrograde motion in an orbit with no detected eccentricity, while tiny Nereid is in direct motion in a large, highly eccentric orbit. Basic data for the two satellites are given in Table 26. Very rough mass and diameter figures exist for Triton,  $1.3 \pm 0.3 \times 10^{-3}$  of Neptune [253] and  $3770 \pm 1300$  km [119], respectively.

Triton is apparently large enough to hold an atmosphere, although none has yet been de-

tected; an upper limit of 8 m-amagat of methane has been set [441].

The maximum surface temperature on Triton (assuming little atmospheric opacity) is noted at below the condensation temperature of methane hydrate [335], but above that of pure methane. Any atmosphere may have to consist largely of inert gases.

## ASTEROIDS

### Discovery and Logistics

A belief in basic order in the universe is inherent in science. Especially strong in the past was a corollary belief in simple mathematical symmetry in all things as well. This led in 1766 to Titius' discovery of a simple mathematical progression describing the distances of the then known planets from the Sun. The regularity (highly publicized later by Bode) is often known as Bode's law. Uranus, discovered in 1781, fit the law very well with one exception: the law predicted a planet at a heliocentric distance of 2.8 AU and none was known.

A cooperative search for the "missing planet" was then proposed. Even before the letter asking his cooperation reached him, Piazzi discovered a small planet while working on a star catalog [283]. This body was discovered January 1, 1801 and found to be at a mean distance of 2.77 AU. It was named Ceres. The next year, while making additional observations of Ceres, Olbers discovered a second small planet which was named Pallas [283]. He immediately suggested they might be parts of a larger planet which had exploded [283]. The same year, Huth suggested that between Mars and Jupiter the matter which formed the planets had simply collected into many smaller bodies rather than one large one [283]. In 1804, Harding found Juno; in 1807, Olbers added Vesta; and in 1845 and 1847, Hencke added Astraea and Hebe [283]. Two more small bodies were found in 1847, and no year since then has passed without at least one discovery [400].

Astronomers agreed in 1851 to officially designate the small planets, *minor planets* [283], but Herschel's term *asteroid* (starlike) has been more commonly used. When an asteroid is discovered and reported, it is given a provisional

TABLE 24.—*Infrared Photometry of Titan*<sup>1</sup>

$\lambda, \mu\text{m}$	$\Delta\lambda, \mu\text{m}$	$p^2$	$T_B^3, ^\circ\text{K}$
1.65	0.3	ca. 0.01	--
2.2	0.6	0.05	--
3.6	1.0	0.01	--
5.0	1.0	$\leq 0.10$	165
8.8	1.0	--	136
10.3	1.3	--	125
10.6	5.0	--	124
11.6	0.8	--	128
12.6	1.0	--	129
17	2	--	101
19	1	--	97
21	8	--	93
22.5	5	--	91
24.5	1	--	86
34	12	--	82

<sup>1</sup> From [287].

<sup>2</sup> Geometric albedo.

<sup>3</sup> Assumes a diameter of 5100 km rather than 4850 km as given in Table 23. The new value of 5832 km (see footnote 16, Table 23) will reduce all of these significantly.

designation [157]. If recovered at a second apparition, it is given a number in chronological order on the list of confirmed objects and named by its discoverer [157]. All names were feminized at one time, but this convention is no longer followed [157]. By early 1974, the list of numbered asteroids had reached 1846. An annual ephemeris of the numbered asteroids is published by the Institute for Theoretical Astronomy in Leningrad, while all minor planet observations, ephemerides of objects which have not yet received numbers, and lists of orbital elements and residuals of differential corrections are published by the Cincinnati Observatory in *Minor Planet Circulars* [198].

### Statistics and Groups

There have been two systematic searches for asteroids, from which statistical conclusions are relatively free from the selection effects resulting from using only the catalog of numbered objects. The first was the McDonald Survey, from 1950 through 1952, with a 25-cm f/7 four element photographic objective [268]. It reached to about the 16th apparent magnitude (in the blue). The second was the Palomar-Leiden Survey using

plates taken in 1960 with a 122-cm f/2.5 Schmidt camera [212]. It reached through the 20th apparent magnitude, but only in a small group of selected areas which biased against high eccentricity and high inclination objects [256]. The total number of asteroids brighter than photographic (B) magnitude 21.2 at mean opposition is  $4.8 \pm 0.3 \times 10^5$  [157]. Schubart [411] estimates the total mass of *all* asteroids to be only about  $2.4 \times 10^{21}$  kg, which is  $4 \times 10^{-4}$  of Earth's mass.

The great majority of asteroids have orbits with semimajor axes lying between 2.17 and 3.3 AU, the lower limit apparently the result of interactions with Mars. Williams [518] suggests that the asteroid belt once extended to much smaller heliocentric distances but was swept clean by collisions and close approaches to Mars, except for isolated groups. The upper limit of the main belt is the 2:1 resonance with Jupiter, the location where the mean daily motion of a body is exactly half that of Jupiter. The average inclination of asteroid orbits is about  $4^\circ$  near the inner edge of the main belt rising to  $11^\circ$  near the outer edge, with the larger asteroids less well-confined to the ecliptic than the smaller ones [157]. The mean orbital eccentricity of asteroids

TABLE 25.—*Satellites of Uranus*<sup>1</sup>

Satellite	Semimajor axis, km	Eccentricity	Inclination <sup>2</sup> , deg	Period, d	Mass <sup>3</sup> (Uranus = 1)	V magnitude at mean opposition <sup>4</sup>
Miranda <sup>5</sup>	129 800	0.017	3.4	1.41348	$1 \times 10^{-6}$	16.5
Ariel	190 900	0.0028	ca 0	2.52038	$15 \times 10^{-6}$	14.4
Umbriel	266 000	0.0035	ca 0	4.14418	$6 \times 10^{-6}$	15.3
Titania	436 000	0.0024	ca 0	8.70587	$50 \times 10^{-6}$	14.01
Oberon	583 400	0.0007	ca 0	13.46325	$29 \times 10^{-6}$	14.20

<sup>1</sup> Adapted from [263], except as otherwise noted.

<sup>2</sup> To what is thought the plane of Uranus' Equator. Dunham [129] reports that small mutual inclinations, in fact, exist for all the satellite orbits.

<sup>3</sup> Very uncertain values, derived with the assumption of equal densities and albedos for all five bodies.

<sup>4</sup> Taken from [194].

<sup>5</sup> Orbital elements from [513].

TABLE 26.—*Satellites of Neptune*<sup>1</sup>

Satellite	Semimajor axis, km	Eccentricity	Inclination, deg	Period, d	V magnitude at mean opposition <sup>2</sup>
Triton	355 550	0	159.945	5.876844	13.55
Nereid	5 567 000	0.74934	27.71	359.881	ca 18.7

<sup>1</sup> From [369], except as otherwise noted. <sup>2</sup> From [194].

in the Palomar-Leiden Survey is 0.147, the complete range being 0 to 0.385 [212, 256].

Numerous asteroid groups are of special interest both within and outside the main asteroid belt. The Trojan asteroids occupy the L<sub>4</sub> and L<sub>5</sub> Lagrangian solutions to the three-body problem in the Sun-Jupiter system, following and preceding Jupiter by roughly 60° in its orbit. A special search of the preceding (L<sub>5</sub>) point indicated it contained about 700 members brighter than mean opposition magnitude of 20.9 [213]. Preliminary results show only about 300 near the following point.<sup>9</sup> There is a stable resonance at the 3:2 commensurability with Jupiter (at 4.0 AU), which contains 23 numbered members and 10 discoveries of the Palomar-Leiden survey known as the Hilda group [211]. One asteroid called (279) Thule is in the 4:3 commensurability (at 4.3 AU) [211]; two asteroids (1362) Griqua, and (1101) Clematis are librating about the 2:1 resonance [302]; and 24 known members (15 numbered) in the Hungaria group are in the 9:2 resonance (at 1.9 AU) [302].

Asteroids crossing Earth's orbit are called Apollo asteroids after the first one discovered to do this. Seventeen are known, but several will be recovered only by chance [155, 305]. Apollo itself was recovered in a deliberate search by McCrosky in 1973, the first time it was seen since its discovery in 1932 [305]. Asteroids coming nearer than the perihelion distance of Mars (1.38 AU) but not crossing Earth's orbit, are called Amor asteroids [155]. Sixteen are known, but at least one, and perhaps two or more are lost [155]. One very special object is (944) Hidalgo; at the greatest mean distance of any known asteroid (5.8 AU) with an eccentricity of 0.66, it moves in to 2.0 and out to 9.7 AU [302], is the only minor planet known to come closer than 1 AU to Jupiter; it reached 0.38 AU in 1673 [302]. Hidalgo's orbit is also at high inclination, 42.5°, the largest known for many years. Hidalgo shares with Apollo and Amor asteroids the virtually ubiquitous property of high-eccentricity orbits. Only (433) Eros (eccentricity 0.22) of these groups has an eccentricity less than 0.36; (1566) Icarus holds the record at 0.83.

<sup>9</sup> T. Gehrels, private communication.

Most Apollo and Amor asteroids do not have particularly high inclination orbits, but this may have been a partially observational selection. Recent discoveries include Apollos 1973 EA at 40°, 1972 XA at 41°, and 1973 NA at 67° [305]. One Amor asteroid, (1580) Betulia, has an inclination of 52°. It was found that a number of the lower inclination Apollo and Amor asteroids are in resonance with, or librate about a resonance with Earth, although the "captures" may not be of very long duration [227].

In 1866, Kirkwood noted an apparent structure in the main asteroid belt, notably gaps at commensurabilities with Jupiter's period. The "Kirkwood gaps" at 2:1, 3:1, and 5:2 are particularly prominent [84], although (as previously noted) there are occasional asteroids exactly in, or librating about, a commensurability.

In a series of papers from 1918 through 1933, Hirayama recognized families of asteroids within the main belt with very similar "proper" orbital elements. "Proper" elements represent the motions of a body freed from most secular perturbations ([68], pp. 524–529). These Hirayama families are generally assumed to be collision fragments [211]. When clustering occurs in the angular variables as well, Alfvén has called the result a "jet stream." A complete listing of the Hirayama families and of many jet streams among the numbered asteroids has been given by Arnold [19]. Additional families were found in the Palomar-Leiden survey [211].

### Origin and Evolution

Classical theories of the origin of asteroids were those enunciated by Olbers and Huth within a year after the discovery of Ceres. Kuiper [262] consolidated these ideas, suggesting perhaps 100 (originally 5–10 [259]) bodies were formed by accretion while the rest resulted from collisions. In 1953, Kuiper [262] noted that some accretion must still be continuing while Alfvén, going much farther, describes gravitational focusing into "jet streams" as a major accretion mechanism still operating to the present [3]. A number of scientists have worked on the mechanics of the problem [33, 103, 480, 482]. A recent comprehensive study by Napier and Dodd

[340] indicates that collisions among some of the original asteroids are the most probable origin of the main belt.

The source of asteroids crossing into the inner solar system and of meteorites recovered on Earth is of great importance. There is evidence that some, but probably not all, of the Apollo asteroids may be nuclei of extinct comets [302, 303]. Evidence from spectrophotometry of asteroids (to be discussed) indicates that at least one Apollo, 1685 Toro, shares characteristics with main belt asteroids of the Flora group and with common chondritic meteorites [86, 238]. There has been a severe problem, however, that cosmic ray exposure ages of stone meteorites are very short compared to the time normally required to perturb them from the main belt into an Earth-crossing orbit without an extreme collision, which would create an obviously shocked body.

Two mechanisms have been suggested very recently which seem to supply sufficient stony meteorites from low velocity collisions with low exposure to cosmic rays [519, 538]. Both mechanisms furnish material only from the immediate vicinity of resonances, which would imply that all stony meteorites may originate from a limited number of asteroidal sources. Most iron meteorites are old enough to come from several places in the belt. Many meteors, entering Earth's atmosphere from well-known streams associated with comets, appear generally to be quite fragile and burn up long before reaching the ground. More substantial bodies could exist in cometary debris, however, and there is no problem dynamically in bringing them to Earth. There is quite general agreement, then, that meteorites originate in the asteroid belt and/or comets, but which types come from where is still a much debated and researched question. Standard references on the subject include [7, 17, 18, 197, 509, 510].

### Physical Data

The masses and diameters of the asteroids are of fundamental importance, but masses exist for only three asteroids, and one of those is very uncertain. In 1968, Hertz [199] published a mass of  $1.2 \pm 0.1 \times 10^{-10}$  solar masses for (4) Vesta determined from a series of close encounters

with (197) Arete. In 1974, Schubart [412] reported new masses for (1) Ceres and (2) Pallas derived from their mutual interaction, that for Ceres being  $5.9 \pm 0.3 \times 10^{-10}$  solar masses and for Pallas  $1.3 \pm 0.4 \times 10^{-10}$  solar masses. The mass of Ceres is roughly half the total mass of the asteroid belt [411].

Useful direct measurements of diameters have been made only for the first four asteroids. There are two other known methods to determine diameters: one using both infrared radiometry and visual photometry to determine albedo and diameter [332], the other, polarimetry to determine albedo, which, when coupled with visual photometry, gives a diameter [490]. Results from all three methods are compared in Table 27. Infrared and polarization results agree well but are obviously systematically larger than direct measures. Ceres has also been detected at 3.7 cm [65]. Use of the polarization diameter gives a disk brightness temperature of  $160^\circ \pm 53^\circ$  K, which is in good agreement with the expected temperature from solar insolation [65]. The larger diameters for Ceres and Vesta imply densities of  $2-2\frac{1}{2}$  g cm $^{-3}$ , but uncertainty in both masses and radii is sufficient to make this number of little value. Diameters have been measured for other asteroids and used to determine geometric albedos (to be discussed).

A great deal of information about asteroids has come from their light curves at one or more wavelengths. Since most asteroids have either an irregular shape or variation in reflectivity over their surfaces (or both), it usually requires careful photometry to find the period in which light fluctuations repeat (to phase the light curve), hence the rotation period. This has been accom-

TABLE 27.—Asteroid Diameters

Asteroid	Direct measurement <sup>1</sup> , km	Infrared measurement <sup>2</sup> , km	Polarization measurement <sup>3</sup> , km
(1) Ceres	770	1000	1050
(2) Pallas	490	530	560
(3) Juno	195	240	225
(4) Vesta	390	530	515

<sup>1</sup> Barnard's values as quoted by Dollfus [122].

<sup>2</sup> From Chapman and Morrison [84].

<sup>3</sup> Zellner's values as quoted by Chapman and Morrison [84].

plished to varying accuracy for some 50 asteroids; results through 1971 have been summarized by Taylor [458]. Well-determined rotation periods vary from 2.273 for (1566) Icarus to 18.813 for (532) Herculina [458], but a few objects appear to have much longer periods. Different aspects of the asteroid are seen by observing over a reasonable fraction of a revolution period—the amplitude of the light curve decreasing as one looks more at the pole.

Techniques have been developed for measuring the coordinates of the pole and the sense of rotation [458, 487] and results have been summarized by Vesely [487]. Some of the techniques used for small amounts of data unfortunately do not lead to unique answers when the shape is somewhat extreme, which is true for many asteroids. Determination of shape as well as rotation axis is considered by Dunlap [131]. In principle, albedo variations on the surface can also be modeled from light curves of sufficient detail and accuracy. Here, curves at more than 1 wavelength are useful, since albedo markings may vary with wavelength while shape will not.

Some description of the composition of asteroids has become possible for the first time, with the advent of precision spectrophotometry, placed on an absolute scale by means of polarization or infrared radius determinations. A summary of work through mid-1972 has been given by Chapman et al [87], while Chapman and Morrison provide a popular account of more recent work [84]. Two gross classes of asteroids are: red objects with moderate blue geometric albedo (0.1–0.2) and higher red geometric albedo (0.14–0.23); and dark, neutral objects with nearly flat spectral response, having geometric albedos from 0.09 down to 0.03. The latter sometimes show slight slope or structure and a decreasing albedo below 4000 Å. The former often show distinct spectral features. The first (red) class is of largely silicate-type material, and the second (dark, neutral) class is of carbonaceous chondritic-type material.

Chapman and Salisbury [85] have made detailed comparisons of laboratory spectral reflectivities between 41 meteorites and 36 asteroids. Only the Earth orbit crosser (1685) Toro [86] and (43) Ariadne [238] and (8) Flora [84] from the

inner edge of the main belt resemble ordinary chondritic meteorites. Matches to enstatite chondrites were found [85] for (16) Psyche and (29) Amphitrite, to a basaltic achondrite for (4) Vesta, to a carbonaceous chondrite for (2) Pallas, and to Chantonay (a shocked, brecciated L6 chondrite) for (192) Nausikaa. However, it is most striking that many asteroids resemble no known meteorite while many meteorites resemble no studied asteroid [85]. This is consistent with the idea that most common stony meteorites are derived from a very few atypical asteroids. Research on asteroids is only beginning to reach maturity. Detailed studies have been under way for only 5 years and many important new geochemical results can be expected in the near future.

## COMETS

### History and Nomenclature

Ancient Chinese records contain the earliest clear reference to a comet, one which appeared during a war about 1055 BC [209]. Records of Halley's Comet go back, possibly, to 240 BC or even to 467 BC [209, 304], and no apparition has gone unreported since it was seen in 86 BC [283, 304].

Two schools of thought existed among the ancient Chaldeans [283]: one group held that comets were like planets but moving far enough from Earth to be invisible most of the time; the other group believed comets were “fires produced by an eddy of violently rotating air.” Aristotle considered them atmospheric, the *product* of dry and windy weather [283]. In peoples’ minds they soon came to be the *cause* of winds, and then of things associated with winds, such as floods and severe fires. At first they were omens, later only bad omens, so that for 2 millennia people were frightened of comets. As late as 1910, during the appearance of P/Halley, confidence men did a large business in comet pills and gas masks to ward off “its noxious influence” [6].

Comets had been “respectable” among educated people for several hundred years before 1910. Tycho Brahe showed that the great comet of 1577 was more distant than the Moon because observations over all Europe clearly indicated the comet’s smaller parallax [283]. As early as

1665, Borelli observed that the comet of 1664 had apparently moved in an elliptical orbit "or another curved line" rather than a straight line [283]. However, using the new gravitational theory of his friend Newton, it was Edmond Halley, who showed that comets were relatively well-behaved members of the solar system. He demonstrated that the comet of 1682 had an orbit nearly identical to comets sighted in 1607 and 1531, and that four earlier comets had appeared at intervals of about 76 years [283]. He then predicted its reappearance in 1758, which, of course, occurred.

In current practice each comet, in order of discovery or recovery in a given calendar year, is provisionally designated by that year and successive letters of the alphabet, i.e., 1974a, 1974b. In about 2 years, after their orbits are well-determined, comets are redesignated with the year and a roman numeral in the order of their perihelion passages, i.e., 1971 I, 1971 II. Each comet is also designated by the name of its discoverer(s) but not by more than three names. If the comet's period is less than 200 years, the name is usually preceded by P (for periodic), and it may often be preceded or followed by its most recent observed perihelion passage designation, i.e., 1910 II P/Halley. If the discoverer has more than one periodic comet to his credit, the name is followed by a number, i.e. P/Temple 1 and P/Temple 2. In a few instances, where a comet has been lost for several returns, the name of its recoverer has been added, thus P/Swift 1, having been lost for eight successive apparitions and recovered by Gehrels on the ninth in 1973, is now designated P/Swift-Gehrels. At times a comet has been designated by the name of a scientist who has intensively investigated its orbit, the most prominent being P/Halley and P/Encke.

### Cometary Orbits

Edmond Halley proved that at least one or more comets moved in orbits that were highly eccentric ellipses. Other comets, apparently the great majority, seemed to move in parabolas or even hyperbolas. Comets were therefore designated periodic and nonperiodic, but as astrometry became more precise, this dichotomy

began to seem more and more artificial. Marsden's recent catalog [304] lists 503 comets with periods greater than 200 years. Of the 392 observed from 1800 through 1969, only 10 orbits were even formally hyperbolic when traced back beyond Neptune and referred to the solar system barycenter. Only 1899 I had a hyperbolic excess greater than three times the formal standard error, and Marsden feels this one would be removed from the hyperbolic list if allowance were made for nongravitational effects [304]. Marsden, along with the majority of orbit specialists (but by no means all) believes that all comets are initially bound to the solar system, although they may be lost (given a hyperbolic velocity) through planetary perturbations. Comets today are usually termed short period (periodic) or long period, the split being at a period of 200 years, although this is an arbitrary, nonphysical distinction. Five known comets have periods between 100 and 200 years and seven between 200 and 300 years; but this does mean the short period category includes all comets seen more than once.

A more physical distinction of comets could be based upon orbital characteristics. Table 28 groups the inclinations and periods of all comets seen at more than one return. Clearly, the vast majority of short period comets are very short period and show great preference for the plane of the ecliptic. No comet with a period of less than 13 years has an inclination greater than 32°. The long period comets, on the other hand, show absolutely no preference for the ecliptic orbit. Their lines of apsides are located almost randomly, though showing some clumpiness and a slight (many say significant) preference toward the galactic plane [292, 521] (see also, Volume I, Part 1, Chapter 1). Another significant difference is that the median perihelion distance of the 503

TABLE 28.—*Orbital Characteristics of 65 Comets Appearing More than Once*

Inclination	No.	Period	No.
i < 30°	55	P < 10 yr	46
i < 60°	60	P < 20 yr	55
i < 90°	62	P < 50 yr	58

long period comets is 0.84 AU, only about half that of the short period comets (1.5 AU) [304]. The meaning of these dynamical differences will be considered in the section, **Origin and Evolution.**

### Empirical Behavior of Comets

A comet, at very great distances from the Sun, is usually completely stellar in appearance, if it can be seen at all. As it reaches heliocentric distance of about 3 AU, it begins to develop a small nebulosity, called the coma. Spectroscopically, the initial nebulosity is largely emission from the (0–0) band of the violet system of CN near 3880 Å [453]. At about 2 AU, emission from the complex  $\lambda$ 4050 group of C<sub>3</sub> begins to develop, as does the  $\alpha$ -ammonia system of NH<sub>2</sub> (with weak bands scattered throughout the visible and near-infrared), but these bands are seen only in a much smaller area around the nucleus than CN [453]. At 1.8 AU, the Swan bands of C<sub>2</sub> begin to develop (primarily (1–0) at  $\lambda$ 4737, (0–0) at  $\lambda$ 5165, and (0–1) at  $\lambda$ 5636), having a greater spatial extent than C<sub>3</sub> but not so great as CN [21, 453]. By 1.5 AU, all radicals normally present can be seen (OH, CH, NH), as well as other overtones of C<sub>2</sub> and CN (0–1 of CN usually appears at about 2 AU) [453].

In 1970, Code et al [89] reported the presence of a large corona of H about Comet Tago-Sato-Kosaka, detected from its Lyman- $\alpha$  emission at 1216 Å by the Orbiting Astronomical Observatory. Since that time, hydrogen has been observed about comets Bennett, Encke, and Kohoutek, and it is obvious that atomic hydrogen is a major feature of all active comets, although its time of onset has not been reported observationally. Lines of metastable oxygen [OI] in the region  $\lambda$ 6300–6400 have been observed in comets since the available spectral dispersion became high enough to separate them from terrestrial airglow lines and other cometary emissions. These have now been observed at more than 1.5 AU [442]. At about 0.7 AU, the D-lines of Na usually appear in emission [453]. Comets approaching very close to the Sun, such as Ikeya-Seki 1965 VIII, also show emission lines of K, Cr, Mn, Fe, Ni, and Cu, plus ionized Ca [372].

The coma, although brightening as it approaches the Sun, generally shrinks in apparent size after reaching a maximum near 1.4 AU [453]. Meanwhile, the continuum of reflected sunlight, completely dominant beyond 3 AU and corresponding only to the stellarlike nucleus or occasionally a small area around it [123, 257], may grow in extent and dominate the entire central spectrum (as for comet Bennett), or, it may remain so weak as to be virtually undetectable (as for P/Encke), making the spectrum seem to be pure emission features.

The brighter comets nearer the Sun than 1.5 AU usually develop tails (type I) which seem to be composed largely, if not totally, of ions, emission features of CO<sup>+</sup> and N<sub>2</sub><sup>+</sup> being dominant [453]. CO<sub>2</sub><sup>+</sup>, CH<sup>+</sup>, NH<sup>+</sup>, and H<sub>2</sub>O<sup>+</sup> are also seen in ion tails. On rare occasion, an outstanding ion tail may develop even at a far greater distance. Comet Humason 1962 VIII showed great tail activity at more than 2.5 AU, with CO<sup>+</sup> and N<sub>2</sub><sup>+</sup> completely dominating the coma spectrum as well as that of the tail [174, 396]. Strong CO<sup>+</sup> emission was seen even at 5 AU [452]. Normally, beginning at about 1 AU, a comet may also develop a tail (type II) which shows only a continuum of reflected sunlight, apparently scattered from very small particles (ca 1  $\mu$ m). Apparent type II tails have occasionally also been observed at very great distances (3.95–5.0 AU) [350, 417]. The ion tails usually appear very straight, often with intricate filamentary structure and/or a turbulent appearance, while the “dust” tails are more featureless and often curved. Depending upon geometry, the two tails may appear separate or superimposed, in cases where a comet exhibits both types.

Any attempt to discuss an “average” comet or to predict its behavior is valid only in a statistical sense. Comets are individual entities. Their behavior is a complex function of dust-to-gas ratio, gas composition, and age (number of times they have come nearer than ca 4 AU to the Sun) at the very least; many additional variables can be hypothesized. The early attempts to forecast the brightness of comet Kohoutek (1973f) near perihelion are excellent examples. Long-period comets almost always brighten less rapidly with distance than short-period ones, and any hope

that Kohoutek would brighten as  $r^{-6}$ , or even  $r^{-4}$ , all the way from 5 AU was extremely optimistic. Long-period comets typically brighten at ca  $r^{-2.8}$  [123] to the extent that a simple power law can describe their behavior. The complexities of the situation have been well described by Sekanina [416] for one comet, P/Encke.

### Cometary Models

There is no universally accepted model of comets. The most widely accepted one by far is the icy conglomerate model of Whipple [511], which has been amplified considerably, especially by Delsemme and coworkers [108] and Sekanina [415]. It works well for the average comet, and cometary observations will be discussed here in terms of this model. Competing ideas about comets will be discussed briefly in the section, Origin and Evolution.

A comet has been pictured by Whipple [511] as a solid, low-density structure of frozen gases well-mixed with dust and larger debris. As it approaches the Sun, volatile substances begin to vaporize, forming a dust and gas atmosphere which is seen as the coma. Streaming back under the influences of radiation pressure and the solar wind, the dust and ionized gases form tails. The relatively sudden onset of activity at 3 AU has been explained by the discovery that water is the major component of comets, which controls the vaporization rate [108]. Whipple was led to the icy conglomerate model in order to explain the apparent secular acceleration of P/Encke. The nongravitational "jet propulsion" effect of gases vaporizing from part of the sunward hemisphere of a rotating nucleus seems quite an adequate explanation for Encke as well as other comets [307]. Sekanina has suggested that some or all comets may have a rocky core [415]. Thus, as comets grow older their activity would decline, being dependent toward the end upon the amount of gas which could diffuse to the surface. The end product then might be an Apollo-type asteroid, as discussed previously [303].

A major problem is the determination of the parent molecules of all radicals and ions actually observed in comets, that is, the composition of the

frozen gases in the nucleus. Observed abundances and extent of H and OH are compatible with photodissociation of an  $\text{H}_2\text{O}$  parent [48]. Water was finally detected, at 22.23 GHz, in 1974 [232]. Microwave studies also revealed the presence of two other stable, neutral species in comet Kohoutek: methyl cyanide ( $\text{CH}_3\text{CN}$ ) [484] and hydrogen cyanide (HCN) [434]. It is not clear whether either can be the parent of CN, since the photodissociation lifetime of  $\text{CH}_3\text{CN}$  seems too long [371] and that of HCN is unknown. The parent molecules could be much more volatile than water and still controlled by water vaporization if trapped as clathrates, as suggested by Delsemme and coworkers [110]. The interesting possibility of releasing a halo of icy grains from the nucleus, thereby increasing the effective area of release of material, is considered by Delsemme and Miller [110, 111, 112]. This has the added attraction of explaining the photometric nucleus, an optically thick region in the coma much larger than the "real" nucleus could possibly be.

As soon as the radical or ion is formed, its excitation is well-understood for most species. It is resonance fluorescence excitation of a collisionless gas [452], except possibly in the innermost region of the coma [297]. This has been shown quantitatively in CN, for example, where the strength of individual rotational lines in the comet is completely dependent upon the heliocentric velocity of the comet, as the Doppler effect shifts the wavelength and therefore the available intensity of exciting solar radiation, particularly when shifting through a Fraunhofer line [21, 104, 297, 452]. The intensity shift with changing velocity is known as the Swings effect. The Greenstein effect is similar but much smaller, resulting from the actual velocities (ca  $1 \text{ km s}^{-1}$ ) of the gases in the comet [21, 297, 452]. Rotational temperatures for  $\text{C}_2$  are always quite high ( $3000^\circ\text{--}5000^\circ \text{ K}$ ) as compared to heteronuclear molecules ( $200^\circ\text{--}500^\circ \text{ K}$ ) because a homopolar molecule cannot make pure rotational transitions, but there is no fundamental difference in excitation mechanism [452]. Resonance fluorescence works well for ions, too, as demonstrated by Arpigny for  $\text{CO}^+$  [20]. Only for metastable oxygen does resonance fluorescence seem completely inadequate [452]. It is generally believed that this

excitation results directly from the dissociation of the parent [51].

The flow of hydrogen from comet Bennett 1970 II was measured after perihelion from 0.6 to 1.04 AU [48]. The flow rate followed roughly an  $r^{-2}$  law ( $r$ =heliocentric distance), being  $0.7 \times 10^{29}$  H atoms  $s^{-1}$  sterad $^{-1}$  at 0.81 AU [48]. P/Encke produced ca  $5 \times 10^{26}$  H atoms  $s^{-1}$  sterad $^{-1}$  at 0.715 AU before perihelion in 1970 [48]. Assuming that all hydrogen comes from water and all water finally is completely broken down (OH also dissociates), the number of water molecules emitted by the nuclei was half these values. An old periodic comet, Encke, a bit closer to the Sun and before perihelion, was producing less than  $10^{-2}$  as much water as a "new" comet, Bennett, after perihelion. This clearly indicates that either Encke is much smaller than Bennett, or no longer "an infinite source" controlled only by solar insolation, or both.

Limits on cometary nuclei size can be set by measuring their apparent brightness at an inactive time (beyond 3 AU) and assuming various reflectivities. A compilation of such data by Roemer [397] suggests P/Encke is between 1.2 and 7.0 km in diameter, for example, while Humason is a giant between 19 and 110 km, and Tuttle-Giacobini-Kresák, a dwarf between 0.2 and 0.8 km. Studies by Delsemme and Rud [113] suggest Bennett has a diameter of about 7.5 km and a Bond albedo of 0.66, while the mean Bond albedo of Encke must be much smaller, with water-ice covering only a small fraction of the surface or no longer controlling H production. A nucleus of density  $1 \text{ g cm}^{-3}$  and 4 km in diameter would have a mass of  $3 \times 10^{13}$  kg, one 50 km in diameter, a mass of  $5 \times 10^{17}$  kg. The range  $10^{12}$ – $10^{18}$  kg is about that usually given for the smallest to largest possible comets.

Modeling of cometary tails has a long history. The mechanical theory of dust tails was well-developed by Soviets Bredikhin, Orlov, and others many years ago. The problem is essentially that of the motion of particles given various initial conditions moving under the dual forces of gravitation and solar radiation pressure [62], although details of dust emission mechanisms are still very much open to question [37, 526]. Apparent objections to the purely mechanical theory

stemming from observations [350] of nonradial tails at great distances can be explained by emission of icy grains at very large heliocentric distances [417].

Levin [275] has suggested that dust tails should remain divided into two categories, Bredikhin's type II and type III, and that one of these contains a large amount of neutral gas as well as dust, but this does not create a severe physical theory crisis. Type I tails are altogether different. Their structures appear to show accelerations far too large to have been induced by radiation; in fact, Biermann [49] was led to predict the solar wind, long before its actual detection, to explain these accelerations. A fairly detailed model of the interaction of a typical long-period comet with the solar wind has been presented by Biermann, Brosowski, and Schmidt [50]. It predicts the existence of a shock front about  $10^6$  km in front of the nucleus where the flow becomes subsonic and of a contact surface at about  $10^5$  km inside which the solar wind cannot penetrate. Wallis [498], on the other hand, suggests a collisionless charge exchange that slows the solar wind. Others have suggested that the contact surface may be unstable. Photoionization is insufficient to explain ion densities observed in a comet, and so apparently is charge exchange [107]. A critical velocity theory of ionization has been proposed (e.g., [418]). No real understanding exists of the mechanisms of interaction between a comet and the solar wind, hence there is no generally accepted mechanism for the formation and behavior of ion tails.

A discussion of comets within the framework of the icy conglomerate model should not neglect mention of a few of its problems. Some comets (previously noted) show activity at a heliocentric distance of 5 AU or more, much too distant to be caused by  $\text{H}_2\text{O}$  vaporization. If a comet has never before been near the Sun, then it could easily have a layer of more volatile species which would be activated at great distance. A comet with an excess ratio of volatile substances to water could not trap them all as clathrates, and would exhibit activity outside of control by water. These are the explanations usually offered for "new" comets. There are, however, "problem children," the best known being P/Schwassmann-Wachmann 1,

which is known to be in a nearly circular orbit (eccentricity 0.132) *beyond* Jupiter (perihelion 5.54 AU, aphelion 7.21 AU). This object, normally of magnitude ca 19, suddenly, in less than a day, brightens by as much as 7 magnitudes (a factor of more than 600) [391]. At least 20 outbursts were observed between 1939 and 1950, and these must be fairly common, since the comet is observed only rarely [391]. Crude spectra obtained on two occasions showed only a pure continuum of scattered sunlight; the cause of these outbursts is unknown.

The only other comet in nearly circular orbit at large distance, P/Oterma ( $e=0.144$ ,  $q=3.39$  until recent perturbations by Jupiter) has never shown such activity [391]. There have been rather extreme brightness fluctuations in a number of comets nearer the Sun. P/Tuttle-Giacobini-Kresák flared by 8–10 magnitudes in less than 5 days in May 1973 [398], just a day or two before its perihelion passage at 1.15 AU. It continued lesser outbursts for several weeks. “Pockets of gas,” or sometimes solar activity are occasionally used as explanations [13]. Even rather prosaic objects such as P/d’Arrest cause occasional problems. P/d’Arrest appears to have a well-condensed photometric nucleus after perihelion, but before perihelion, it is extremely difficult to locate and is invariably faint and diffuse [492]. This behavior has no reasonable explanation in terms of the icy conglomerate model. At least three diffuse comets (P/Westphal 1913 VI, Ensor 1926 III, and Pajdusakova 1954 II) have disappeared as they approached the Sun. Perhaps they simply “ran out of gas.” It will be most interesting to find if P/Westphal reappears on schedule in late 1975.

### Origin and Evolution

The nature and origin of comets has a long if not too satisfactory history. The idea that comets originate in interstellar space is often called the Laplace hypothesis, since Laplace made the first mathematical study of capture probabilities. However, the idea of interstellar formation goes at least back to Kepler [391]. The idea of formation within the solar system by ejection from the major planets is usually attributed to Lagrange [391]; at times all forms of origin within the solar system are

termed Lagrangian, although Vsekhsvyatskiy [493] is virtually alone in still championing the Lagrangian hypothesis in its original form. Until Whipple’s icy conglomerate model, it was generally agreed that comets were a loose swarm of separate particles with slight mutual gravitation [400]. At about the same time as Whipple’s theory appeared, Lyttleton [292] presented a study of origin by accretion from interstellar clouds. In the resulting comet, mutual gravitation is unimportant near the Sun, and each tiny particle pursues its own independent Keplerian orbit except for collisions.

Respected scientists, during the past 6 years, have advocated all four combinations of interstellar and solar system origin with “compact” and “loose-swarm” nucleus, plus various in-between theories. Witkowski supports a compact nucleus of interstellar origin [522]; Lyttleton, a very loose swarm of interstellar origin [292, 294]; Robey, a loose structure of plasma created from the Sun [395]; Alfvén, current creation of compact structures from loose ones by his jetstream mechanism [4, 481]. However, a large majority of comet specialists now favor compact structures created somewhere within the gravitational influence of the Sun, and further discussion is limited to such theories.

There are apparently two distinct dynamic families of comets (noted previously, under Cometary Orbits). Everhart [134, 135] has shown that there is no evolutionary path linking the two families, but suggests that both distributions (and a third group with very large perihelia, which we could never observe) could be derived from a source at near infinity (relative to solar binding energy) with all comets entering the system in near parabolic orbits [135]. Those with perihelia near Jupiter and Saturn could then be perturbed into short-period comets, while those with smaller perihelia would remain almost unperturbed and constitute the long-period family [135]. Between  $3 \times 10^4$  and  $10^5$  comets would be required, with perihelia near Jupiter at present, in order to keep the supply of short-period comets in steady state [109].

The question then arises: What is the origin and behavior of the possible source of comets “near infinity?” Oort [348] proposed that comets

originated at the same time and in the same general region as planets, and that perturbations threw them outward into a vast cloud between 30 000 and 100 000 AU. The orbits would there be randomized by stellar perturbations so that all sense of their origin in the ecliptic plane would be lost [348]. Whipple [512], Safronov [401], Nezhinskiy [344], and others have supported this idea. One big drawback is the inefficiency of the process. Another is that the resulting distribution of comets in heliocentric distance apparently would be completely unlike that observed today [135]. Cameron [74] suggests that comets originated in independent subdisks of the solar nebula already far beyond Pluto and reached even greater aphelion distances as a result of mass loss in the solar nebula and Sun during the Sun's T Tauri stage. O'Dell [345] has considered an interesting variation in which comets form as a vast cluster (ca  $10^{33}$ ) of small bodies (radius ca 70  $\mu\text{m}$ ) at great distance, accumulating interstellar volatile substances on their surfaces. Approaching the Sun, they collapse into a structure not readily distinguishable from Whipple's icy conglomerate comet.

Purported observational evidence for the existence of the "Oort Cloud" [348] has been strongly challenged by Lyttleton [293]. Improved evidence of its existence [306] is based upon improved orbital elements for comets of very long period and with relatively large perihelion distance (so nongravitational forces from escaping volatile substances are insignificant), but even the improved result isn't terribly convincing, being based upon too few data points. In part, the argument is semantic. Lyttleton has clearly

shown that there is no evidence for a "shell" in which the number of comets per unit volume is very high, but there does seem to be a grouping in "binding energy space" ( $E \propto 1/a$ , where  $a$  is the semimajor axis). Whether this is considered a mathematical artifact or physically significant depends upon the author.

The possibility of storing some comets nearer the Sun, perhaps among the giant planets, has been considered. The action on them by the giant planets is so strong that such orbits are soon transformed [135, 240]. Everhart [135] estimates that most orbits between Jupiter and Neptune would be emptied in about  $10^7$  years with no new supply available. The best theory at present, then, seems to be one in which the comets originated as a part of the primordial nebula, at least in the region beyond Saturn, and more probably beyond Pluto, and are kept in "cold storage" most of their lives. They are never seen at all unless their perihelion distance falls below about 6 AU, and they are seen regularly only if captured into short-period orbits by the action of the giant planets.

The average short-period comet, with a period of 10 years, may live  $10^4$  years or so before all its volatile substances are lost. What becomes of it then? It may totally dissipate, leaving nothing but a meteor stream. In Sekanina's [415] mantle-core model, there should be a rocky remnant, however, perhaps appearing as an Apollo asteroid [302, 303] (as discussed previously). Until there has been more study of both comets and asteroids, from the ground and from spacecraft, there can be no final answer to this question.

## REFERENCES

1. ALEXANDER, A. F. O'D. *The Planet Saturn*. London, Faber and Faber, 1962.
2. ALEXANDER, A. F. O'D. *The Planet Uranus*. New York, Am. Elsevier, 1965.
3. ALFVÉN, H., and G. ARRHENIUS. Structure and evolutionary history of the solar system. I. *Astrophys. Space Sci.* 8:338-421, 1970.
4. ALFVÉN, H., and A. MENDIS. Nature and origin of comets. *Nature* 246:410-411, 1973.
5. ALLEN, D. A., and T. L. MURDOCK. Infrared photometry of Saturn, Titan, and the rings. *Icarus* 14:1-2, 1971.
6. ALTER, D. Comets and people. *Griffith Obs.* XX:74-82, 1956.
7. ANDERS, E. Interrelations of meteorites, asteroids, and comets. In, Gehrels, T., Ed. *Physical Studies of Minor Planets*, pp. 429-446. Washington, NASA, 1971. (NASA SP-267)
8. ANDERSON, J. D., G. W. NULL, and S. K. WONG. Gravity results from Pioneer 10 Doppler data. *J. Geophys. Res.* 79:3661-3664, 1974.
9. ANDERSON, R. C., J. G. PIPES, A. L. BROADFOOT, and L. WALLACE. Spectra of Venus and Jupiter from 1800 to 3200 Å. *J. Atmos. Sci.* 26:874-888, 1969.
10. ANDERSSON, L. Photometry of Jupiter VI and Phoebe

- (Saturn IX). *Bull. Am. Astron. Soc.* 4:313, 1972.
11. ANDERSSON, L. New findings about Jupiter's and Saturn's satellites. *Sky Telesc.* 45:22-23, 1973.
  12. ANDERSSON, L. E., and J. D. FIX. Pluto: new photometry and a determination of the axis of rotation. *Icarus* 20:279-283, 1974.
  13. ANDRIENKO, D. A., A. A. DEMENKO, I. M. DEMENKO, and I. D. ZOSIMOVICH. Comet brightness variations and the conditions in interplanetary space. *Sov. Astron.-A. J.* 15:666-671, 1972.
  14. APPLEBY, J. F. Multicolor photoelectric photometry of Neptune. *Astron. J.* 78:110-112, 1973.
  15. APPLEBY, J. F., and W. M. IRVINE. Multicolor photoelectric photometry of Uranus. *Astron. J.* 76:617-619, 1971.
  16. ARMSTRONG, K. R., D. A. HARPER, Jr., and F. J. LOW. Far-infrared brightness temperatures of the planets. *Astrophys. J.* 178:L89-L92, 1973.
  17. ARNOLD, J. R. The origin of meteorites as small bodies. II. The model. *Astrophys. J.* 141:1536-1547, 1965.
  18. ARNOLD, J. R. The origin of meteorites as small bodies. III. General considerations. *Astrophys. J.* 141:1548-1556, 1965.
  19. ARNOLD, J. R. Asteroid families and "jet streams." *Astron. J.* 74:1235-1242, 1969.
  20. ARPIGNY, C. The resonance-fluorescence excitation of the CO<sup>+</sup> comet-tail bands in comet Humason (1961e). *Ann. Astrophys.* 27:406-416, 1964.
  21. ARPIGNY, C. Comet spectra. In, Kuiper, G. P., and E. Roemer, Eds. *Comets, Scientific Data and Missions, Proceedings of the Tucson Comet Conference*, Apr., 1970, pp. 84-111. Tucson, Univ. Ariz., 1972.
  22. ASH, M. E., I. I. SHAPIRO, and W. B. SMITH. The system of planetary masses. *Science* 174:551-556, 1971.
  23. AUMANN, H. H., C. M. GILLESPIE, Jr., and F. J. LOW. The internal powers and effective temperatures of Jupiter and Saturn. *Astrophys. J.* 157:L69-L72, 1969.
  24. AVRANCHUK, V. V. Spectrophotometry of the  $\lambda\lambda 6190$  methane and  $\lambda\lambda 6441$  and 6478 ammonia absorption bands on the disk of Jupiter. *Sov. Astron.-A. J.* 14:462-468, 1970.
  25. BALASUBRAHMANYAN, V. K., and D. VENKATESAN. Solar activity and the great red spot of Jupiter. *Astrophys. Lett.* 6:123-126, 1970.
  26. BANOS, C. J. Contribution to the study of Jupiter's atmosphere. *Icarus* 15:58-67, 1971.
  27. BANOS, C. J., and C. E. ALISSANDRAKIS. Isodensitometry of Jupiter's red spot and Jupiter. *Astron. Astrophys.* 15:424-432, 1971.
  28. BARKER, E. S., and L. M. TRAFTON. Ultraviolet reflectivity and geometrical albedo of Titan. *Icarus* 20:444-454, 1973.
  29. BARROW, C. H., and D. P. MORROW. The polarization of the Jupiter radiation at 18 Mc/S. *Astrophys. J.* 152:593-608, 1968.
  30. BARTHOLDI, P., and F. OWEN. The occultation of Beta Scorpii by Jupiter and Io. II. Io. *Astron. J.* 77:60-65, 1972.
  31. BASH, F. N., F. D. DRAKE, E. GUNDERMANN, and C. E. HEILES. 10-cm observations of Jupiter, 1961-1963. *Astrophys. J.* 139:975-985, 1964.
  32. BAUM, W. A., and A. D. CODE. A photometric observation of the occultation of  $\sigma$  Arietis by Jupiter. *Astron. J.* 58:108-112, 1953.
  33. BAXTER, D. C., and W. B. THOMPSON. Jetstream formation through inelastic collisions. In, Gehrels, T., Ed. *Physical Studies of Minor Planets*, pp. 319-326. Washington, D.C., NASA, 1971. (NASA SP-267)
  34. BEER, R., and F. W. TAYLOR. The abundance of CH<sub>3</sub>D and the D/H ratio in Jupiter. *Astrophys. J.* 179:309-327, 1973.
  35. BEER, R., C. B. FARMER, R. H. NORTON, J. V. MARTONCHIK, and T. G. BARNES. Jupiter: observation of deuterated methane in the atmosphere. *Science* 175:1360-1361, 1972.
  36. BELTON, M. J. S., and H. SPINRAD. H<sub>2</sub> pressure-induced lines in the spectra of the major planets. *Astrophys. J.* 185:363-372, 1973.
  37. BENVENUTI, P. Dust emission structure in comets with type II tails. *Astrophys. Space Sci.* 27:203-209, 1974.
  38. BERGE, G. L. Circular polarization of Jupiter's decimeter radiation. *Astrophys. J.* 142:1688-1693, 1965.
  39. BERGE, G. L. An interferometric study of Jupiter's decimeter radio emission. *Astrophys. J.* 146:767-798, 1966.
  40. BERGE, G. L. Some recent observations and interpretations of the Jupiter decimeter emission. In, *Proceedings of the Jupiter Radiation Belt Workshop*, pp. 223-242. Pasadena, Calif., Jet Propul. Lab., 1972.
  41. BERGE, G. L., and D. O. MUHLEMAN. High-angular-resolution observations of Saturn at 21.1 cm wavelength. *Astrophys. J.* 185:373-381, 1973.
  42. BERGE, G. L., and D. O. MUHLEMAN. The brightness temperature of Callisto at 3.71 cm wavelength. Presented at 5th Annu. Meet., Am. Astron. Soc., Planet. Sci. Div., Palo Alto, April 1974. *Am. Astron. Soc. Bull.* 6(3, pt. 2), 1974. (Abstr. No. 106)
  43. BERGE, G. L., and R. B. READ. The microwave emission of Saturn. *Astrophys. J.* 152:755-764, 1968.
  44. BERGSTRALH, J. T. Methane absorption in the atmosphere of Saturn: rotational temperature and abundance from the  $3\nu_3$  band. *Icarus* 18:605-611, 1973.
  45. BERGSTRALH, J. T. Methane absorption in the Jovian atmosphere. I. The Lorentz half-width in the  $3\nu_3$  band at 1.1  $\mu$ m. *Icarus* 19:499-506, 1973.
  46. BERGSTRALH, J. T., and J. S. MARGOLIS. Recomputation of the absorption strengths of the methane  $3\nu_3$  J-manifolds at 9050 cm<sup>-1</sup>. *J. Quant. Spectrosc. Radiat. Transfer* 11:1285-1287, 1971.
  47. BERGSTRALH, J. T., and J. W. YOUNG. Spectroscopic evidence of variability in Saturn's atmosphere. *Am. Astron. Soc. Bull.* 6(3, pt. 2), 1974. Abstr. No. 88
  48. BERTAUX, J. L., J. E. BLAMONT, and M. FESTOU. Interpretation of hydrogen Lyman-alpha observations of comets Bennett and Encke. *Astron. Astrophys.* 25:415-430, 1973.
  49. BIERMANN, L. Comet tails and solar corpuscular radiation. *Z. Astrophys.* 29:274-286, 1951. (Ger.)

50. BIERMANN, L., B. BROSOWSKI, and H. U. SCHMIDT. The interaction of the solar wind with a comet. *Solar Phys.* 1:254-284, 1967.
51. BIERMANN, L., and E. TREFFTZ. On the mechanisms of ionization and excitation in cometary atmospheres. *Z. Astrophys.* 59:1-28, 1964.
52. BIGG, E. K. Influence of the satellite Io on Jupiter's decametric emission. *Nature* 203:1008-1010, 1964.
53. BINDER, A. B. Spectrophotometry of the 1.5  $\mu\text{m}$  window of Jupiter. *Astron. J.* 77:93-99, 1972.
54. BINDER, A. B., and D. P. CRUIKSHANK. Evidence of an atmosphere on Io. *Icarus* 3:299-305, 1964.
55. BINDER, A. B., and D. W. McCARTHY, Jr. The infrared spectral albedo of Uranus. *Astrophys. J.* 171:L1-L3, 1972.
56. BINDER, A. B., and D. W. McCARTHY, Jr. IR spectrophotometry of Jupiter and Saturn. *Astron. J.* 78:939-950, 1973.
57. BISHOP, E. V., and W. C. DE MARCUS. Thermal histories of Jupiter models. *Icarus* 12:317-330, 1970.
58. BLANCO, C., and S. CATALANO. Photoelectric observations of Saturn satellites Rhea and Titan. *Astron. Astrophys.* 14:43-47, 1971.
59. BOBROV, M. S. On the observation of the occultation of stars by Saturn's rings. *Sov. Astron.-A.J.* 6:525-531, 1963.
60. BOBROV, M. S. Physical properties of Saturn's rings. In, Dollfus, A., Ed. *Surface and Interiors of Planets and Satellites*, pp. 377-461. New York, Academic, 1970.
61. BOBROV, M. S. Thickness of Saturn's rings from observations in 1966. *Sov. Astron.-A.J.* 16:348-354, 1972.
62. BOBROVNIKOFF, N. T. Comets. In, Hynek, J. A., Ed. *Astrophysics: A Topical Symposium*, pp. 302-356. New York, McGraw-Hill, 1951.
63. BRANSON, N. J. B. A. High resolution radio observations of the planet Jupiter. *Mon. Not. Roy. Astron. Soc.* 139(2):155-162, 1968.
64. BRICE, N. M., and G. A. IOANNIDIS. The magnetosphere of Jupiter and Earth. *Icarus* 13:173-183, 1970.
65. BRIGGS, F. H. Radio emission from Ceres. *Astrophys. J.* 184:637-639, 1973.
66. BRIGGS, F. H. The microwave properties of Saturn's rings. *Astrophys. J.* 189:367-377, 1974.
67. BRINKMANN, R. T. Jovian satellite-satellite eclipses and occultations. *Icarus* 19:15-29, 1973.
68. BROUWER, D., and G. M. CLEMENCE. *Methods of Celestial Mechanics*. New York, Academic, 1961.
69. BROWN, R. A. Optical line emission from Io. In, *Exploration of the Solar System, 65th Symposium, International Astronomical Union*, Torun, Pol., Sept. 1972.
70. BROWN, R. A., and F. H. CHAFFEE, Jr. High-resolution spectra of sodium emission from Io. *Astrophys. J.* 187:L125-L126, 1974.
71. BURNS, J. A. Jupiter's decametric radio emission and the radiation belts of its Galilean satellites. *Science* 159:971-972, 1967.
72. CALDWELL, J., D. R. LARACH, and R. E. DANIELSON. The continuum albedo of Titan. *Bull. Am. Astron. Soc.* 5:305, 1973.
73. CAMERON, A. G. W. Abundances of the elements in the solar system. *Space Sci. Rev.* 15:121-146, 1973.
74. CAMERON, A. G. W. Accumulation processes in the primitive solar nebula. *Icarus* 18:407-450, 1973.
75. CAMERON, A. G. W. Formation of the outer planets. *Space Sci. Rev.* 14:383-391, 1973.
76. CAPONE, L. A., and S. S. PRASAD. Jovian ionospheric models. *Icarus* 20:200-212, 1973.
77. CARLSON, R. W., J. C. BHATTACHARYYA, B. A. SMITH, T. V. JOHNSON, B. HIDAYAT, S. A. SMITH, G. E. TAYLOR, B. O'LEARY, and R. T. BRINKMANN. An atmosphere on Ganymede from its occultation of SAO 186800 on 7 June 1972. *Science* 182:53-55, 1973.
78. CARR, T. D. Jupiter's magnetospheric rotation period. *Astrophys. Lett.* 7:157-162, 1971.
79. CARR, T. D., and S. GULKIS. The magnetosphere of Jupiter. In, Goldberg, L., D. Layzer, and J. G. Phillips, Eds. *Annual Review of Astronomy and Astrophysics*, Vol. 7, pp. 577-618, 1969.
80. CARR, T. D., A. G. SMITH, F. F. DONIVAN, and H. I. REGISTER. The twelve-year periodicities of the decametric radiation of Jupiter. *Radio Sci.* 5(2): 495-503, 1970.
81. CHADHA, M. S., J. J. FLORES, J. G. LAWLESS, and C. PONNAMPERUMA. II. Organic synthesis in a simulated Jovian atmosphere. *Icarus* 15:39-44, 1971.
82. CHANG, D. B., and L. DAVIS, Jr. Synchrotron radiation as the source of Jupiter's polarized decimeter radiation. *Astrophys. J.* 136:567-581, 1962.
83. CHAPMAN, C. R. Jupiter's zonal winds—variation with latitude. *J. Atmos. Sci.* 26:986-990, 1969.
84. CHAPMAN, C. R., and D. MORRISON. The minor planets: sizes and mineralogy. *Sky Telesc.* 47:92-95, 1974.
85. CHAPMAN, C. R., and J. W. SALISBURY. Comparisons of meteorite and asteroid spectral reflectivities. *Icarus* 19:507-522, 1973.
86. CHAPMAN, C. R., T. B. MCCORD, and C. PIETERS. Minor planets and related objects. X. Spectrophotometric study of the composition of (1685) Toro. *Astron. J.* 78:502-505, 1973.
87. CHAPMAN, C. R., T. B. MCCORD, and T. V. JOHNSON. Asteroid spectral reflectivities. *Astron. J.* 78:126-140, 1973.
88. CHASE, S. C., R. D. RUIZ, G. MÜNCH, G. NEUGEBAUER, M. SCHROEDER, and L. M. TRAFTON. Pioneer 10 infrared radiometer experiment: preliminary results. *Science* 183:315-317, 1974.
89. CODE, A. D., T. E. HOUCK, and C. F. LILLIE. Comet Tago-Sato-Kosaka (1969g). *IAU Circ.* (Cambridge, Mass.), No. 2201, Jan. 21, 1970.
90. COHEN, C. J., and E. C. HUBBARD. Libration of the close approaches of Pluto to Neptune. *Astron. J.* 70:10-13, 1965.
91. CONSEIL, L., Y. LEBLANC, G. ANTONINI, and D.

- QUEMADA. The effect of the solar wind velocity on the Jovian decametric emission. *Astrophys. Lett.* 8:133-137, 1971.
92. COOK, A. F., and F. A. FRANKLIN. Rediscovery of Maxwell's Adams Prize Essay on the stability of Saturn's rings. *Astron. J.* 69:173-200, 1964.
93. COOK, A. F., and F. A. FRANKLIN. Rediscovery of Maxwell's Adams Prize Essay on the stability of Saturn's rings, II. *Astron. J.* 71:10-19, 1966.
94. COOK, A. F., and F. A. FRANKLIN. An explanation of the light curve of Iapetus. *Icarus* 13:282-291, 1970.
95. COOK, A. F., F. A. FRANKLIN, and F. D. PALLUCONI. Saturn's rings—a survey. *Icarus* 18:317-337, 1973.
96. COUPINOT, G. The rings of Saturn in 1969. Morphological and photometric studies. II. Deconvolution of the raw photometric curves. *Icarus* 19:212-223, 1973.
97. CRUIKSHANK, D. P. A search for ammonia in the atmosphere of Saturn. *Bull. Am. Astron. Soc.* 3:282, 1971.
98. CRUIKSHANK, D. P., and A. B. BINDER. Minor constituents in the atmosphere of Jupiter. *Astrophys. Space Sci.* 3:347-356, 1969.
99. DANIELSON, R. E. The infrared spectrum of Jupiter. *Astrophys. J.* 143:949-960, 1966.
100. DANIELSON, R. E. The structure of the Uranus atmosphere. Presented at 5th Annu. Meet., Planet. Sci. Div., Am. Astron. Soc., Palo Alto, Calif., Apr. 1974. *Am. Astron. Soc. Bull.* 6(3, Pt. 2):380, 1974. (Abstr. No. 076)
101. DANIELSON, R. E., J. J. CALDWELL, and D. R. LARACH. An inversion in the atmosphere of Titan. *Icarus* 20:437-443, 1973.
102. DANIELSON, R. E., M. G. TOMASKO, and B. D. SAVAGE. High-resolution imagery of Uranus obtained by stratoscope, II. *Astrophys. J.* 178:887-900, 1972.
103. DANIELSSON, L. The profile of a jetstream. In, Gehrels, T., Ed. *Physical Studies of Minor Planets*, pp. 353-362. Washington, D.C., NASA, 1971. (NASA SP-267)
104. DANKS, T., and C. ARPICNY. Relative band intensities in the red and violet systems of CN in comets. *Astron. Astrophys.* 29:347-356, 1973.
105. DAVIES, R. D., and D. WILLIAMS. Observations of the continuum emission from Venus, Mars, Jupiter, and Saturn at 21.2 cm wavelength. *Planet. Space Sci.* 14:15-32, 1966.
106. DEBERGH, C., M. VION, M. COMBES, J. LECACHEUX, and J. P. MAILLARD. New infrared spectra of the Jovian planets from 12 000 to 4000  $\text{cm}^{-1}$  by Fourier transform spectroscopy. II. Study of Saturn in the  $3 \nu_3 \text{CH}_4$  band. *Astron. Astrophys.* 28:457-466, 1973.
107. DELSEMME, A. H. Review of cometary science. In, Roberts, D. L., Ed. *The Proceedings of the Cometary Science Working Group*. Chicago, Ill. Inst. Tech. Res., 1971.
108. DELSEMME, A. H. Gas and dust in comets. *Space Sci. Rev.* 15:89-101, 1973.
109. DELSEMME, A. H. Origin of the short-period comets. *Astron. Astrophys.* 29:377-381, 1973.
110. DELSEMME, A. H., and D. C. MILLER. Physico-chemical phenomena in comets. II. Gas absorptions in the snows of the nucleus. *Planet. Space Sci.* 18:717-730, 1970.
111. DELSEMME, A. H., and D. C. MILLER. Physico-chemical phenomena in comets. III. The continuum of comet Burnham (1960 II). *Planet. Space Sci.* 19:1229-1257, 1971.
112. DELSEMME, A. H., and D. C. MILLER. Physico-chemical phenomena in comets. IV. The  $\text{C}_2$  emission of comet Burnham (1960 II). *Planet. Space Sci.* 19:1259-1274, 1971.
113. DELSEMME, A. H., and D. A. RUD. Albedos and cross-sections for the nuclei of comets 1969 IX, 1970 II and 1971 I. *Astron. Astrophys.* 28:1-6, 1973.
114. DESCH, M. D., and T. D. CARR. Decametric and hectometric observations of Jupiter from the RAE-1 satellite. Presented at 5th Annu. Meet., Am. Astron. Soc., Planet. Sci. Div., Palo Alto, Calif., April 1974. *Am. Astron. Soc. Bull.* 6(3, Pt. 2):378, 1974. (Abstr. No. 068)
115. DICKEL, J. R., J. J. DEGIOANNI, and G. C. GOODMAN. The microwave spectrum of Jupiter. *Radio Sci.* 5:517-527, 1970.
116. DOLLFUS, A. Visual and photographic studies of planets at the Pic du Midi. In, Kuiper, G. P., and B. M. Middlehurst, Eds. *Planets and Satellites, The Solar System*, Vol. 3, pp. 534-571. Chicago, Univ. Chicago Press, 1961.
117. DOLLFUS, A. Movements in the atmosphere of Saturn in 1960. Coordinated observations by the International Astronomical Union. *Icarus* 2:109-114, 1963. (Fr.)
118. DOLLFUS, A. Saturn X (Janus). *IAU Circ.* (Cambridge, Mass.), No. 1995, Feb. 1, 1967.
119. DOLLFUS, A. Diameters of the planets and satellites. In, Dollfus, A., Ed. *Surfaces and Interiors of Planets and Satellites*, pp. 45-139. New York, Academic, 1970. (Fr.)
120. DOLLFUS, A. New optical measurements of the diameters of Jupiter, Saturn, Uranus, and Neptune. *Icarus* 12:101-117, 1970.
121. DOLLFUS, A. Diameter measurements of asteroids. In, Gehrels, T., Ed. *Physical Studies of Minor Planets*, pp. 25-31. Washington, D.C., NASA, 1971. (NASA SP-267)
122. DOLLFUS, A. Physical studies of asteroids by polarization of the light. In, Gehrels, T., Ed. *Physical Studies of Minor Planets*, pp. 95-116. Washington, D.C., NASA, 1971. (NASA SP-267)
123. DONN, B. The characteristics of distant comets. *Ann. Astrophys.* 25:319-323, 1962.
124. DOUGLAS, J. N., and H. C. SMITH. Interplanetary scintillation in Jovian decametric radiation. *Astrophys. J.* 148:885-903, 1967.
125. DRAKE, F. D., and H. HVATUM. Nonthermal microwave radiation from Jupiter. *Astron. J.* 64:329-330, 1959.
126. DULK, G. A. Characteristics of Jupiter's decametric radio source measured with arc-second resolution. *Astrophys. J.* 159:671-684, 1970.

127. DULK, G. A., and T. A. CLARK. Almost-continuous radio emission from Jupiter at 8.9 and 10 MHz. *Astrophys. J.* 145:945-948, 1966.
128. DUNCOMBE, R. L., W. J. KLEPCZYNSKI, and P. K. SEIDELMANN. The masses of the planets, satellites, and asteroids. *Fundam. Cosm. Phys.* 1:119-165, 1974.
129. DUNHAM, D. Motions of the satellites of Uranus. *Bull. Am. Astron. Soc.* 3:415, 1971.
130. DUNHAM, T., Jr. Spectroscopic observations of the planets at Mount Wilson. In, Kuiper, G. P., Ed. *The Atmospheres of the Earth and Planets*, rev. ed., pp. 288-305. Chicago, Univ. Chicago Press, 1952.
131. DUNLAP, J. L. Laboratory work on the shapes of asteroids. In, Gehrels, T., Ed. *Physical Studies of Minor Planets*, pp. 147-154. Washington, D.C., NASA, 1971. (NASA SP-267).
132. ELLIS, G. R. A. The decametric radio emissions of Jupiter. *Radio Sci.* 69D:1513-1530, 1965.
133. ENCRENAZ, T., and T. OWEN. New observations of the hydrogen quadrupole lines on Saturn and Uranus. *Astron. Astrophys.* 28:119-124, 1973.
134. EVERHART, E. The origin of short-period comets. *Astrophys. Lett.* 10:131-135, 1972.
135. EVERHART, E. Examination of several ideas of comet origins. *Astron. J.* 78:329-337, 1973.
136. FEIBELMAN, W. A. Concerning the 'D' ring of Saturn. *Nature* 214:793-794, 1967.
137. FIELD, G. B. The source of radiation from Jupiter at decimeter wavelengths. *J. Geophys. Res.* 64:1169-1177, 1959.
138. FIELD, G. B. The source of radiation from Jupiter at decimeter wavelengths. 2. Cyclotron radiation by trapped electrons. *J. Geophys. Res.* 65:1661-1671, 1960.
139. FIELD, G. B. The source of radiation from Jupiter at decimeter wavelengths. 3. Time dependence of cyclotron radiation. *J. Geophys. Res.* 66:1395-1405, 1961.
140. FIELD, G. B. REMARKS ON JUPITER. In, Brown, H., G. J. Stanley, D. O. Muhleman, and G. Münch, Eds. *Proceedings, CalTech-JPL Lunar and Planetary Conference*, Sept. 1965, pp. 141-142. Pasadena, Calif. Inst. Tech., Jet Propul. Lab., 1966. (NASA CR-76142; JPL-TM-33-266)
141. FINK, U., H. P. LARSON, and N. H. DEKKERS. Infrared spectra of the Galilean satellites of Jupiter. *Astrophys. J.* 179:L155-L159, 1973.
142. FIX, J. D., J. S. NEFF, and L. A. KELSEY. Spectrophotometry of Pluto. *Astron. J.* 75:895-896, 1970.
143. FLASAR, F. M. Gravitational energy sources in Jupiter. *Astrophys. J.* 186:1097-1106, 1973.
144. FOCAS, J. H. Activity in Jupiter's atmospheric belts between 1904 and 1963. *Icarus* 15:56-57, 1971.
145. FOCAS, J. H., and A. DOLLFUS. Optical properties and thickness of the rings of Saturn observed on edge in 1966. *Astron. Astrophys.* 2:251-265, 1969. (Fr.)
146. FOUNTAIN, J. W., D. L. COFFEEN, L. R. DOOSE, T. GEHRELS, W. SWINDELL, and M. G. TOMASKO. Jupiter's clouds: equatorial plumes and other cloud forms in the Pioneer 10 images. *Science* 184:1279-1281, 1974.
147. FOX, K., and I. OZIER. The importance of methane to pressure-induced absorption in the atmospheres of the outer planets. *Astrophys. J.* 166:L95-L100, 1971.
148. FOX, K., T. OWEN, A. W. MANTZ, and K. N. RAO. A tentative identification of  $^{13}\text{CH}_4$  and an estimate of  $^{12}\text{C}/^{13}\text{C}$  in the atmosphere of Jupiter. *Astrophys. J.* 176:L81-L84, 1972.
149. FRANKLIN, F. A., G. COLOMBO, and A. F. COOK. A dynamical model for the radial structure of Saturn's rings, II. *Icarus* 15:80-92, 1971.
150. FRANZ, O. G., and R. L. MILLIS. UV photometry of Enceladus, Tethys, and Dione. *Bull. Am. Astron. Soc.* 5:304, 1973.
151. FRANZ, O. G., and R. L. MILLIS. A search for post-eclipse brightening of Io with an area-scanning photometer. Presented at 5th Annu. Meet., Am. Astron. Soc., Planet. Sci. Div., Palo Alto, Calif., April 1974. *Am. Astron. Bull.* 6(3, Pt. 2):383, 1974. (Abstr. No. 096)
152. FREEMAN, K. C., and G. LYNCA. Data for Neptune from occultation observations. *Astrophys. J.* 160:767-780, 1970.
153. GALKIN, L. S., L. A. BUGAENKO, O. I. BUGAENKO, and A. V. MOROZHENKO. The spectrum of Uranus in the region 4800-7500 Å. In, Sagan, C., T. C. Owen, and H. J. Smith, Eds. *Planetary Atmospheres*, pp. 392-393. Dordrecht, Holland, D. Reidel, 1971. (IAU Symp. No. 40)
154. GEHRELS, T. The transparency of the Jovian polar zones. *Icarus* 10:410-411, 1969.
155. GEHRELS, T. Physical parameters of asteroids and interrelations with comets. In, Elvius, A., Ed. *From Plasma to Planet*, pp. 169-178. Stockholm, Almqvist & Wiksell; New York, Wiley, 1972. (Nobel Symp. Ser. No. 21)
156. GEHRELS, T., B. M. HERMAN, and T. OWEN. Wavelength dependence of polarization. XIV. Atmosphere of Jupiter. *Astron. J.* 74:190-199, 1969.
157. GEHRELS, T., J. R. GILL, and J. W. HAUGHEY. Introduction. In, Gehrels, T., Ed. *Physical Studies of Minor Planets*, pp. xiii-xxvii. Washington, D.C., NASA, 1971. (NASA SP-267)
158. GERARD, E. Long-term variations of the decimeter radiation of Jupiter. *Radio Sci.* 5:513-516, 1970.
159. GIERASCH, P. J. Jupiter's cloud bands. *Icarus* 19:482-494, 1973.
160. GILLE, J. C., and T. LEE. The spectrum and transmission of ammonia under Jovian conditions. *J. Atmos. Sci.* 26:932-940, 1969.
161. GILLETT, F. C., and W. J. FORREST. The 7.5- to 13.5-micron spectrum of Saturn. *Astrophys. J.* 187:L37-L39, 1974.
162. GILLETT, F. C., W. J. FORREST, and K. M. MERRILL. 8-13 micron observations of Titan. *Astrophys. J.* 184:L93-L95, 1973.
163. GILLETT, F. C., F. J. LOW, and W. A. STEIN. The 2.8-

- 14-micron spectrum of Jupiter. *Astrophys. J.* 157:925-934, 1969.
164. GILLETT, F. C., K. M. MERRILL, and W. A. STEIN. Albedo and thermal emission of Jovian satellites I-IV. *Astrophys. Lett.* 6:247-249, 1970.
165. GILLETT, F. C., and J. A. WESTPHAL. Observations of 7.9 micron limb brightening on Jupiter. *Astrophys. J.* 179:L153-L154, 1973.
166. GIVER, L. P., and H. SPINRAD. Molecular hydrogen features in the spectra of Saturn and Uranus. *Icarus* 5:586-589, 1966.
167. GLEDHILL, J. A. Magnetosphere of Jupiter. *Nature* 214:155-156, 1967.
168. GOLDREICH, P. An explanation of the frequent occurrence of commensurable mean motions of the solar system. *Mon. Not. Roy. Astron. Soc.* 130:159-181, 1965.
169. GOLDSTEIN, R. M., and G. A. MORRIS. Radar observations of the rings of Saturn. *Icarus* 20:260-262, 1973.
170. GOLITSYN, G. S. A similarity approach to the general circulation of planetary atmospheres. *Icarus* 13:1-24, 1970.
171. GORGOLEWSKI, S. Possible detection of thermal radio emission at 3.5 mm from Callisto. *Astrophys. Lett.* 7:37, 1970.
172. GRABOSKE, H. C., Jr., J. B. POLLACK, A. S. GROSSMAN, and R. J. OLNESS. *The Structure and Evolution of Jupiter: The Fluid Contraction Stage*. Livermore, Calif., Lawrence Livermore Lab., 1973. (Prepr. UCRL-74860)
173. GRABOSKE, H. C., Jr., R. J. OLNESS, and A. S. GROSSMAN. *Thermodynamics of Dense Hydrogen-Helium Fluids*. Livermore, Calif., Lawrence Livermore Lab., 1973. (Prepr. UCRL-74859)
174. GREENSTEIN, J. The spectrum of comet Humason (1961e). *Astrophys. J.* 136:688-690, 1962.
175. GROSSMAN, A. S., and H. C. GRABOSKE, Jr. Evolution of low-mass stars. III. Effects of nonideal thermodynamic properties during the pre-main-sequence contraction. *Astrophys. J.* 164:475-490, 1971.
176. GUERIN, P. The new ring of Saturn. *Sky Telesc.* 40:88, 1970.
177. GUERIN, P. The rings of Saturn in 1969. Morphological and photometric study. I. Photograph acquisition and evaluation. *Icarus* 19:202-211, 1973.
178. GULKIS, S. Lunar occultation observations of Jupiter at 74 cm and 128 cm. *Radio Sci.* 5:505-511, 1970.
179. GULKIS, S. *Radio Emission from the Major Planets—The Thermal Component*. Presented at 17th Annu. Meet., Am. Astronaut. Soc., Seattle, Wash., June 1971. (AAS 71-109)
180. GULKIS, S., and T. D. CARR. Radio rotation period of Jupiter. *Science* 154:257-259, 1966.
181. GULKIS, S., B. GARY, M. KLEIN, and C. STELZRIED. Observations of Jupiter at 13-cm wavelength during 1969 and 1971. *Icarus* 18:181-191, 1973.
182. GULKIS, S., T. R. McDONOUGH, and H. CRAFT. The microwave spectrum of Saturn. *Icarus* 10:421-427, 1969.
183. GULKIS, S., M. J. KLEIN, and R. L. POYNTER. Jupiter's microwave spectrum—implications for the upper atmosphere. In, *Exploration of the Solar System*, Torun, Pol., 1973, pp. 273-280. (In press)
184. GULKIS, S., and R. POYNTER. Thermal radio emission from Jupiter and Saturn. *Phys. Earth Planet. Inter.* 6:36-43, 1972.
185. GURNETT, D. A. Sheath effects and related charged-particle acceleration by Jupiter's satellite Io. *Astrophys. J.* 175:525-533, 1972.
186. HALL, C. F. Pioneer 10. *Science* 183:301-302, 1974.
187. HALL, J. S., and L. A. RILEY. Polarization measurements of Jupiter and Saturn. *J. Atmos. Sci.* 26:920-923, 1969.
188. HALLIDAY, I. Comments on the mean density of Pluto. *Pub. Astron. Soc. Pac.* 81:285-287, 1969.
189. HALLIDAY, I., R. H. HARDIE, O. G. FRANZ, and J. B. PRISER. An upper limit for the diameter of Pluto. *Pub. Astron. Soc. Pac.* 78:113-124, 1966.
190. HAINES, E. L., Ed. Selenodesy and lunar dynamics. In, *Lunar Scientific Model*, Vol. 1. Pasadena, Calif., Jet Propul. Lab., 1971. (JPL Intern. Work. Doc. 900-278)
191. HANSEN, O. L. Ten micron observations of Io, Europa, and Ganymede. *Icarus* 18:237-246, 1973.
192. HANSEN, O. L. 12-micron emission features of the Galilean satellites and Ceres. *Astrophys. J.* 188:L31-L33, 1974.
193. HARPER, D. A., Jr., F. J. LOW, G. H. RIEKE, and K. R. ARMSTRONG. Observations of planets, nebulae, and galaxies at 350 microns. *Astrophys. J.* 177:L21-L25, 1972.
194. HARRIS, D. L. Photometry and colorimetry of planets and satellites. In, Kuiper, G. P., and B. M. Middlehurst, Eds. *Planets and Satellites, The Solar System*, Vol. III, pp. 272-342. Chicago, Univ. Chic., 1961.
195. HARRISON, H., and R. I. SCHOEN. Evaporation of ice in space: Saturn's rings. *Science* 157:1175-1176, 1967.
196. HART, M. H. A possible atmosphere for Pluto. *Icarus* 21:242-247, 1974.
197. HARTMANN, W. K., and A. C. HARTMANN. Asteroid collisions and evolution of asteroidal mass distribution and meteoritic flux. *Icarus* 8:361-381, 1968.
198. HERGET, P. The work at the minor planet center. In, Gehrels, T., Ed. *Physical Studies of Minor Planets*, pp. 9-12. Washington, D.C., NASA, 1971. (NASA SP-267)
199. HERTZ, H. G. The mass of Vesta. *Science* 160:299-300, 1968.
200. HERZBERG, G. Laboratory absorption spectra obtained with long paths. In, Kuiper, G. P., Ed. *The Atmospheres of the Earth and Planets*, rev. ed., pp. 406-416. Chicago, Univ. Chic., 1952.
201. HESS, S. L. Variations in atmospheric absorption over the disks of Jupiter and Saturn. *Astrophys. J.* 118:151-160, 1953.
202. HIDE, R. Origin of Jupiter's great red spot. *Nature* 190:895-896, 1961.
203. HIDE, R. On the hydrodynamics of Jupiter's atmosphere.

- Mem. Soc. Roy. Sci. Liège*, Ser. 5, 7:481–505, 1963.
204. HIDE, R. Dynamics of the atmospheres of the major planets with an appendix on the viscous boundary layer at the rigid bounding surface of an electrically-conducting rotating fluid in the presence of a magnetic field. *J. Atmos. Sci.* 26:841–853, 1969.
  205. HIDE, R. Motions in planetary atmospheres: a review. *Meteorol. Mag.* 100:268–276, 1971.
  206. HIDE, R. On geostrophic motion of a non-homogeneous fluid. *J. Fluid Mech.* 49:745–751, 1971.
  207. HIDE, R. Jupiter and Saturn. *Proc. Roy. Soc. London A* 336:63–84, 1974.
  208. HIDE, R., and A. IBBETSON. An experimental study of “Taylor columns.” *Icarus* 5:279–290, 1966.
  209. HO PENG YOKE. Ancient and mediaeval observations of comets and novae in Chinese sources. In, Beer, A., Ed. *Vistas in Astronomy*, Vol. 5, pp. 127–225. Oxford, Pergamon, 1962.
  210. HOPKINS, N. B., and W. M. IRVINE. Variations in the color of Jupiter. In, Sagan, C., T. C. Owen, and H. J. Smith, Eds. *Planetary Atmospheres, 40th Symposium, International Astronomical Union*, pp. 349–352. Dordrecht, Holland, D. Reidel, 1971.
  211. HOUTEN, C. J. VAN. Descriptive survey of families, Trojans, and jetstreams. In, Gehrels, T., Ed. *Physical Studies of Minor Planets*, pp. 173–175. Washington, D.C., NASA, 1971. (NASA SP-267)
  212. HOUTEN, C. J. VAN, I. VAN HOUTEN-GROENEVELD, P. HERGET, and T. GEHRELS. The Palomar-Leiden survey of faint minor planets. *Astron. Astrophys. Suppl.* 2:339–448, 1970.
  213. HOUTEN, C. J. VAN, I. VAN HOUTEN-GROENEVELD, and T. GEHRELS. Minor planets and related objects. V. The density of Trojans near the preceding Langrangian point. *Astron. J.* 75:659–662, 1970.
  214. HUBBARD, W. B. Thermal models of Jupiter and Saturn. *Astrophys. J.* 155:333–344, 1969.
  215. HUBBARD, W. B. Structure of Jupiter: chemical composition, contraction, and rotation. *Astrophys. J.* 162:687–697, 1970.
  216. HUBBARD, W. B. Observational constraint on the structure of hydrogen planets. *Astrophys. J.* 182:L35–L38, 1973.
  217. HUBBARD, W. B. The significance of atmospheric measurements for interior models of the major planets. *Space Sci. Rev.* 14:424–432, 1973.
  218. HUBBARD, W. B., and R. SMOLUCHOWSKI. Structure of Jupiter and Saturn. *Space Sci. Rev.* 14:599–662, 1973.
  219. HUBBARD, W. B., and T. C. VAN FLANDERN. The occultation of beta Scorpii by Jupiter and Io. III. Astrometry. *Astron. J.* 77:65–74, 1972.
  220. HUNT, G. E. Interpretation of hydrogen quadrupole and methane observations of Jupiter and the radiative properties of the visible clouds. *Mon. Not. Roy. Astron. Soc.* 161:347–363, 1973.
  221. HUNT, G. E., and J. S. MARCOLIS. Formation of spectral lines in planetary atmospheres. V. Collision narrowed profiles of quadrupole lines in hydrogen atmospheres. *J. Quant. Spectrosc. Radiat. Transfer* 13:417–426, 1973.
  222. HUNTER, D. M. The escape of H<sub>2</sub> from Titan. *J. Atmos. Sci.* 30:726–732, 1973.
  223. HUNTER, D. M., and G. MÜNCH. The helium abundance on Jupiter. *Space Sci. Rev.* 14:433–443, 1973.
  224. INGE, J. L. Short-term Jovian rotation profiles, 1970–1972. *Icarus* 20:1–6, 1973.
  225. [International Astronomical Union] *IAU Inf. Bull.* (Cambridge, Mass.), No. 8, Mar. 1962.
  226. IONNIDIS, G. A., and N. M. BRICE. Plasma densities in the Jovian magnetosphere: plasma slingshot or Maxwell demon? *Icarus* 14:360–373, 1971.
  227. IP, W.-H., and R. MEHRA. Resonances and librations of some Apollo and Amor asteroids with the Earth. *Astron. J.* 78:142–147, 1973.
  228. IRVINE, W. M., and A. P. LANE. Monochromatic albedos for the disk of Saturn. *Icarus* 15:18–26, 1971.
  229. IRVINE, W. M., and A. P. LANE. Photometric properties of Saturn's rings. *Icarus* 18:171–176, 1973.
  230. IRVINE, W. M., T. SIMON, D. H. MENZEL, J. CHARON, G. LECOMTE, P. GRIBOVAL, and A. T. YOUNG. Multicolor photometry of the brighter planets. II. Observations from Le Houga Observatory. *Astron. J.* 73:251–264, 1968.
  231. IRVINE, W. M., T. SIMON, D. H. MENZEL, C. PIKOOS, and A. T. YOUNG. Multicolor photoelectric photometry of the brighter planets. III. Observations from Boyden Observatory. *Astron. J.* 73:807–828, 1968.
  232. JACKSON, W. M., T. CLARK, and B. DONN. Comet Bradford (1974b). *IAU Circ.* (Cambridge, Mass.), No. 2674, May 24, 1974.
  233. JAMES T. C. Calculations of collision narrowing of the quadrupole lines in molecular hydrogen. *J. Opt. Soc. Am.* 59:1602–1606, 1969.
  234. JANSEN, M. A. Short wavelength radio observations of Saturn's rings, pp. 83–96. In, *The Rings of Saturn. Proceedings of the Saturn's Rings Workshop*, Pasadena, Calif., 1974. (NASA SP-343)
  235. JENKINS, E. B. Far-ultraviolet spectroscopy of Jupiter. *Icarus* 10:379–385, 1969.
  236. JOHNSON, H. L. The infrared spectra of Jupiter and Saturn at 1.2–4.2 microns. *Astrophys. J.* 159:L1–L5, 1970.
  237. JOHNSON, T. V. Galilean satellites: narrowband photometry 0.30–1.10 microns. *Icarus* 14:94–111, 1971.
  238. JOHNSON, T. V., and D. L. MATSON. Spectrophotometry of (43) Ariadne: a possible chondritic composition. *Bull. Am. Astron. Soc.* 5:308, 1973.
  239. JUDGE, D. L., and R. W. CARLSON. Pioneer 10 observations of the ultraviolet glow in the vicinity of Jupiter. *Science* 183:317–318, 1974.
  240. KAZIMIRCHAK-POLONSKAYA, E. I. The major planets as powerful transformers of cometary orbits. In, Chebotarev, G. A., E. I. Kazimirchak-Polonskaya, and B. G. Marsden, Eds. *The Motion, Evolution of Orbits, and Origin of Comets*, pp. 371–397. Dordrecht,

- Holland, D. Reidel, 1972.
241. KEAY, C. S. L., F. J. LOW, G. H. RIEKE, and R. B. MINTON. High-resolution maps of Jupiter at five microns. *Astrophys. J.* 183:1063–1073, 1973.
242. KELSEY, L. A., and J. D. FIX. Polarimetry of Pluto. *Astrophys. J.* 184:633–636, 1973.
243. KEMP, J. C., J. B. SWEDLUND, R. E. MURPHY, and R. D. WOLSTENCROFT. Circularly polarized visible light from Jupiter. *Nature* 231:169–170, 1971.
244. KEMP, J. C., and R. D. WOLSTENCROFT. Elliptical polarization by surface-layer scattering. *Nature* 231:170–171, 1971.
245. KEMP, J. C., R. D. WOLSTENCROFT, and J. B. SWEDLUND. Circular polarization—Jupiter and other planets. *Nature* 232:165–168, 1971.
246. KHARE, B. N., and C. SAGAN. Red clouds in reducing atmospheres. *Icarus* 20:311–321, 1973.
247. KIEFFER, H. H., and W. D. SMYTHE. Frost spectra: comparison with Jupiter's satellites. *Icarus* 21:506–512, 1974.
248. KIESS, C. C., C. H. CORLISS, and H. K. KIESS. High dispersion spectra of Jupiter. *Astrophys. J.* 132:221–231, 1960.
249. KLEIN, M. J., S. GULKIS, and C. T. STELZRIED. Jupiter: new evidence of long term variations of its decimeter flux density. *Astrophys. J.* 176:L85–L88, 1972.
250. KLORE, A., D. L. CAIN, G. FJELDBO, and B. L. SEIDEL. *The Atmospheres of Io and Jupiter Measured by the Pioneer 10 Radio Occultation Experiment*. Presented at 17th COSPAR meet., Sao Paulo, Brazil, June 1974.
251. KOMESAROFF, M. M., and P. M. MCCULLOCH. The radio rotation period of Jupiter. *Astrophys. Lett.* 1:39–41, 1967.
252. KOMESAROFF, M. M., D. MORRIS, and J. A. ROBERTS. Circular polarization of Jupiter's decimetric emission and the Jovian magnetic field strength. *Astrophys. Lett.* 7:31–36, 1970.
253. KOVALEVSKY, J. Determination of the masses of the planets and satellites. In, Dollfus, A., Ed. *Surfaces and Interiors of Planets and Satellites*, pp. 1–44. New York, Academic, 1970. (Fr.)
254. KOVALEVSKY, J., and F. LINK. Diameter, flattening and optical properties of the upper atmosphere of Neptune as derived from the occultation of the star BD-17° 4388. *Astron. Astrophys.* 2:398–412, 1969. (Fr.)
255. KRAUS, J. D. Planetary and solar radio emission at 11 meters wavelength. *Proc. IRE* 46:266–274, 1958.
256. KRESÁK, L. Orbital selection effects in the Palomar-Leiden asteroid survey. In, Gehrels, T., Ed. *Physical Studies of Minor Planets*, pp. 197–210. Washington, D.C., NASA, 1971. (NASA SP-267)
257. KRESÁK, L. Short-period comets at large heliocentric distances. *Bull. Astron. Inst. Czech.* 24:264–283, 1973.
258. KUIPER, G. P. Titan: a satellite with an atmosphere. *Astrophys. J.* 100:378–383, 1944.
259. KUIPER, G. P. On the origin of asteroids. *Astron. J.* 55:164, 1950.
260. KUIPER, G. P. The diameter of Pluto. *Pub. Astron. Soc. Pac.* 62:133–137, 1950.
261. KUIPER, G. P. Planetary atmospheres and their origins. In, Kuiper, G. P., Ed. *The Atmospheres of the Earth and Planets*, rev. ed., pp. 306–405. Chicago, Univ. Chic., 1952.
262. KUIPER, G. P. Note on the origin of the asteroids. *Proc. Natl. Acad. Sci.* 39:1159–1161, 1953.
263. KUIPER, G. P. On the origins of the satellites and the Trojans. In, Beer, A., Ed. *Vistas in Astronomy*, Vol. 2, pp. 1631–1666. New York, Pergamon, 1956.
264. KUIPER, G. P. Further studies on the origin of Pluto. *Astrophys. J.* 125:287–289, 1957.
265. KUIPER, G. P. Lunar and planetary laboratory studies of Jupiter, I. *Sky Telesc.* 43:4–8, 1972.
266. KUIPER, G. P. Lunar and planetary laboratory studies of Jupiter, II. *Sky Telesc.* 43:75–81, 1972.
267. KUIPER, G. P. On the origin of the solar system, I. *Celestial Mech.* 9:321–348, 1974.
268. KUIPER, G. P., Y. FUJITA, T. GEHRELS, I. GROENEVELD, J. KENT, G. VAN BIESBROECK, and C. J. VAN HOUTEN. Survey of asteroids. *Astrophys. J. Suppl.* 3:289–427, 1958.
269. KUZ'MIN, A. D., A. P. NAUMOV, and T. V. SMIROVA. Estimate of ammonia concentration in subcloud atmospheres of Saturn from radio-astronomy measurements. *Sol. Syst. Res.* 6:10–13, 1972.
270. KUZ'MIN, A. D., and B. Ya. LOSOVSKIY. Measurements of 8.2 mm radio emission from Saturn and estimates of the rings' optical thickness. *Sol. Syst. Res.* 5:62–65, 1971.
271. KUZ'MIN, A. D., and B. Ya. LOSOVSKIY. On the radio emission of Callisto. *Icarus* 18:222–223, 1973.
272. KUZ'MIN, A. D., and B. Ya. LOSOVSKIY. Measurements of the radio emission of Jupiter's satellite Callisto. *Sov. Phys. Dokl.* 18:511–512, 1974.
273. LEBOFSKY, L. A., T. V. JOHNSON, and T. B. MCCORD. Saturn's rings: spectral reflectivity and compositional implications. *Icarus* 13:226–230, 1970.
274. LEE, T. Spectral albedos of the Galilean satellites. *Commun. Lunar Planet. Lab.* (Univ. Ariz.) 9(3):179–180, 1972.
275. LEVIN, B. J. On the Bredikhin's classification of cometary tails and the nature of the type II tails. *Mem. Soc. Roy. Sci. Liège*, Ser. 5, XII:323–328, 1966.
276. LEVIN, B. Yu. Some remarks on the liberation of gases from cometary nuclei. In, Chebotarev, G. A., E. I. Kazimirchak-Polonskaya, and B. G. Marsden., Eds. *The Motion, Evolution of Orbits, and Origin of Comets*, pp. 260–270. Dordrecht; Holland, D. Reidel, 1972.
277. LEWIS, J. S. The clouds of Jupiter and the NH<sub>3</sub>-H<sub>2</sub>O and NH<sub>3</sub>-H<sub>2</sub>S systems. *Icarus* 10:365–378, 1969.
278. LEWIS, J. S. Observability of spectroscopically active compounds in the atmosphere of Jupiter. *Icarus* 10:393–409, 1969.
279. LEWIS, J. S. Satellites of the outer planets: their physical and chemical nature. *Icarus* 15:174–185, 1971.
280. LEWIS, J. S. Chemistry of the outer solar system. *Space*

- Sci. Rev.* 14:401-411, 1973.
281. LEWIS, J. S. The chemistry of the solar system. *Sci. Am.* 230(3):51-60, 65, 1974.
  282. LEWIS, J. S., and R. G. PRINN. Jupiter's clouds: structure and composition. *Science* 169:472-473, 1970.
  283. LEY, W. *Watchers of the Skies*. New York, Viking, 1963.
  284. LOW, F. J. The infrared brightness temperature of Uranus. *Astrophys. J.* 146:326-328, 1966.
  285. LOW, F. J. Observations of Venus, Jupiter, and Saturn at  $\lambda 20\mu$ . *Astron. J.* 71:391, 1966.
  286. LOW, F. J., and A. W. DAVIDSON. The thermal emission of Jupiter and Saturn. *Bull. Am. Astron. Soc.* 1:200, 1969.
  287. LOW, F. J., and G. H. RIEKE. Infrared photometry of Titan. *Astrophys. J.* 190:L143-L145, 1974.
  288. LOW, F. J., G. H. RIEKE, and K. R. ARMSTRONG. Ground-based observations at 34 microns. *Astrophys. J.* 183:L105-L109, 1973.
  289. LUTZ, B. L. Molecular hydrogen on Uranus. Observation of the 3-0 quadrupole band. *Astrophys. J.* 182:989-998, 1973.
  290. LUTZ, B. L., and D. A. RAMSAY. New observations on the Kuiper bands of Uranus. *Astrophys. J.* 176:521-524, 1972.
  291. LYTTLETON, R. A. On the possible results of an encounter of Pluto with the Neptunian system. *Mon. Not. Roy. Astron. Soc.* 97:108-115, 1936.
  292. LYTTLETON, R. A. *The Comets and Their Origin*. London, Cambridge Univ. Press, 1953.
  293. LYTTLETON, R. A. On the distribution of major-axes of long-period comets. *Mon. Not. Roy. Astron. Soc.* 139:225-230, 1968.
  294. LYTTLETON, R. A. Does a continuous solid nucleus exist in comets? *Astrophys. Space Sci.* 15:175-184, 1972.
  295. MAILLARD, J. P., M. COMBES, T. ENCRENAZ, and J. LECACHEUX. New infrared spectra of the Jovian planets from 12 000 to 4000 cm<sup>-1</sup>. I. Study of Jupiter in the  $3\nu_3$  CH<sub>4</sub> band. *Astron. Astrophys.* 25:219-232, 1973.
  296. MAKALKIN, A. B. The structure of models of Neptune. *Solar Syst. Res.* 6:153-157, 1973.
  297. MALAISE, D. J. Collisional effects in cometary atmospheres. I. Model atmospheres and synthetic spectra. *Astron. Astrophys.* 5:209-227, 1970.
  298. MARGOLIS, J. S. Studies of methane absorption in the Jovian atmosphere. III. The reflecting-layer model. *Astrophys. J.* 167:553-558, 1971.
  299. MARGOLIS, J. S., and K. FOX. Infrared absorption spectrum of CH<sub>4</sub> at 9050 cm<sup>-1</sup>. *J. Chem. Phys.* 49:2451-2452, 1968.
  300. MARGOLIS, J. S., and K. FOX. Studies of methane absorption in the Jovian atmosphere. I. Rotational temperature from the  $3\nu_3$  band. *Astrophys. J.* 157:935-943, 1969.
  301. MARGOLIS, J. S., and G. E. HUNT. On the level of H<sub>2</sub> quadrupole absorption in the Jovian atmosphere. *Icarus* 18:593-598, 1973.
  302. MARSDEN, B. G. On the relationship between comets and minor planets. *Astron. J.* 75:206-217, 1970.
  303. MARSDEN, B. G. Evolution of comets into asteroids? In, Gehrels, T., Ed. *Physical Studies of Minor Planets*, pp. 413-421. Washington, D.C., NASA, 1971. (NASA SP-267)
  304. MARSDEN, B. G. *Catalogue of Cometary Orbits*. Cambridge, Mass., Smithsonian Astrophys. Obs., 1972.
  305. MARSDEN, B. G. The recovery of Apollo. *Sky Telesc.* 46:155-158, 1973.
  306. MARSDEN, B. G., and Z. SEKANINA. On the distribution of "original" orbits of comets of large perihelion distance. *Astron. J.* 78:1118-1124, 1973.
  307. MARSDEN, B. G., Z. SEKANINA, and D. K. YEOMANS. Comets and nongravitational forces, V. *Astron. J.* 78:211-225, 1973.
  308. MARSHALL, L., and W. F. LIBBY. Stimulation of Jupiter's radio emission by Io. *Nature* 214:126-128, 1967.
  309. MARTIN, T. Z., D. P. CRUIKSHANK, and C. B. PILCHER. Ammonia in the atmosphere of Saturn. Presented at 5th Annu. Meet., Am. Astron. Soc., Planet Sci. Div., Palo Alto, April 1974. *Am. Astron. Bull.* 6(3, Pt.2):380, 1974. (Abstr. No. 074)
  310. MASON, H. P. The abundance of ammonia in the atmosphere of Jupiter. *Astrophys. Space Sci.* 7:424-436, 1970.
  311. MATSON, D. L., T. V. JOHNSON, and F. P. FANALE. Sodium D-line emission from Io: sputtering and resonant scattering hypothesis. *Astrophys. J.* 192:L43-L46, 1974.
  312. MAXWORTHY, T. A review of Jovian atmospheric dynamics. *Planet. Space Sci.* 21:623-641, 1973.
  313. MAYER, C. H., T. P. MCCULLOUGH, and R. M. SLOANAKER. Observations of Mars and Jupiter at a wavelength of 3.5 cm. *Astrophys. J.* 127:11-16, 1958.
  314. McBRIDE, J. O. P., and R. W. NICHOLLS. The vibrational-rotational spectrum of ammonia gas, I. *J. Phys. B* 5:408-417, 1972.
  315. McBRIDE, J. O. P., and R. W. NICHOLLS. The vibrational-rotational spectrum of ammonia gas. II. A rotational analysis of the 6450 Å band. *Can. J. Phys.* 50:93-102, 1972.
  316. MCCORD, T. B., T. V. JOHNSON, and J. H. ELIAS. Saturn and its satellites: narrow-band spectrophotometry (0.3-1.1  $\mu$ ). *Astrophys. J.* 165:413-424, 1971.
  317. MCCULLOCH, P. M., and M. M. KOMESAROFF. Location of the Jovian magnetic dipole. *Icarus* 19:83-86, 1973.
  318. McDONOUGH, T. R., and N. M. BRICE. A new kind of ring around Saturn? *Nature* 243:513, 1973.
  319. McGOVERN, W. E., and S. D. BURK. Upper atmospheric thermal structure of Jupiter with convective heat transfer. *J. Atmos. Sci.* 29:179-189, 1972.
  320. MELBOURNE, W. G., J. D. MULHOLLAND, W. L. SJOGREN, and F. M. STURMS, Jr. *Constants and Related Information for Astrodynamical Calculations*. Pasadena, Calif., Jet Propul. Lab., 1968. (NASA CR-9766; JPL TR-32-1306)
  321. MELROSE, D. B. Rotational effects on the distribution

- of thermal plasma in the magnetosphere of Jupiter. *Planet. Space Sci.* 15:381-393, 1967.
322. MENDIS, D. A., and W. I. ALEXANDER. Satellites and magnetospheres of the outer planets. In, Donath, F. A., F. G. Stehli, and G. W. Wetherill, Eds. *Annual Review of Earth and Planetary Sciences*, Vol. 2, pp. 419-474. Palo Alto, Calif., Univ. Calif., 1974.
323. MILLIS, R. L. UBV photometry of Iapetus. *Icarus* 18:247-252, 1973.
324. MILLIS, R. L., D. T. THOMPSON, B. J. HARRIS, P. BIRCH, and R. SEFTON. A search for post-eclipse brightening of Io with multiple-aperture photometers. Presented at 5th Annu. Meet., Am. Astron. Soc., Planet. Sci. Div., Palo Alto, Apr. 1974. *Am. Astron. Soc. Bull.* 6(3, pt. 2):383, 1974. (Abstr. No. 095)
325. MOLTON, P. M., and C. PONNAMPERUMA. Organic synthesis in a simulated Jovian atmosphere. III. Synthesis of aminonitriles. *Icarus* 21:166-174, 1974.
326. MOORE, J. H. Spectroscopic observations of the rotation of Saturn. *Pub. Astron. Soc. Pac.* 51:274-281, 1939.
327. MOORE, J. H., and D. H. MENZEL. Preliminary results of spectrographic observations for rotation of Neptune. *Pub. Astron. Soc. Pac.* 40:234-238, 1928.
328. MOORE, J. H., and D. H. MENZEL. The rotation of Uranus. *Pub. Astron. Soc. Pac.* 42:330-335, 1930.
329. MOROZ, V. I., and D. P. CRUIKSHANK. Distribution of ammonia on Jupiter. *J. Atmos. Sci.* 26:865-869, 1969.
330. MOROZHENKO, A. V. Polarimetric observations of the giant planets. III. Jupiter. *Sov. Astron.-A.J.* 17:105-107, 1973.
331. MOROZHENKO, A. V., and E. G. YANOVITSKIY. The optical properties of Venus and the Jovian planets. I. The atmosphere of Jupiter according to polarimetric observations. *Icarus* 18:583-592, 1973.
332. MORRISON, D. Determination of radii of satellites and asteroids from radiometry and photometry. *Icarus* 19:1-14, 1973.
333. MORRISON, D., and D. P. CRUIKSHANK. Temperatures of Uranus and Neptune at 24 microns. *Astrophys. J.* 179:329-331, 1973.
334. MORRISON, D., and D. P. CRUIKSHANK. Thermal properties of the Galilean satellites. *Icarus* 18:224-236, 1973.
335. MORRISON, D., and D. P. CRUIKSHANK. Physical properties of the natural satellites. *Space Sci. Rev.* 15:641-739, 1974.
336. MÜNCH, G., and H. SPINRAD. On the spectrum of Saturn. *Mem. Soc. Roy. Sci. Liège, Ser. 5*, 7:541-542, 1963.
337. MÜNCH, G., and R. L. YOUNKIN. Molecular absorptions and color distributions over Jupiter's disk. *Astron. J.* 69:553, 1964.
338. MURPHY, R. E. Temperatures of Saturn's rings. *Astrophys. J.* 181:L87-L90, 1973.
339. MURPHY, R. E., D. P. CRUIKSHANK, and D. MORRISON. Radii, albedos, and 20-micron brightness temperatures of Iapetus and Rhea. *Astrophys. J.* 177:L93-L95, 1972.
340. NAPIER, W. McD., and R. J. DODD. On the origin of the asteroids. *Mon. Not. Roy. Astron. Soc.* 166:469-489, 1974.
341. [Nautical Almanac Office]. *Explanatory Supplement to the Astronomical Ephemeris*. London, HMSO, 1961.
342. NEFF, J. S., W. A. LANE, and J. D. FIX. An investigation of the rotational period of the planet Pluto. *Pub. Astron. Soc. Pac.* 86:225-230, 1974.
343. NEWBURN, R. L., Jr., and S. GULKIS. A survey of the outer planets Jupiter, Saturn, Uranus, Neptune, Pluto and their satellites. *Space Sci. Rev.* 14:179-271, 1973.
344. NEZHINSKIY, E. M. On the stability of the Oort cloud. In, Chebotarev, G. A., E. I. Kazimirchak-Polonskaya, and B. G. Marsden, Eds. *The Motion, Evolution of Orbits, and Origin of Comets*, pp. 335-340. Dordrecht, Holland, D. Reidel, 1972.
345. O'DELL, C. R. A new model for cometary nuclei. *Icarus* 19:137-146, 1973.
346. OHRING, G. The temperature and ammonia profiles in the Jovian atmosphere from inversion of the Jovian emission spectrum. *Astrophys. J.* 184:1027-1040, 1973.
347. O'LEARY, B., and T. C. VAN FLANDERN. Io's triaxial figure. *Icarus* 17:209-215, 1972.
348. OORT, J. H. Empirical data on the origin of comets. In, Middlehurst, B. M., and G. P. Kuiper, Eds. *The Moon, Meteorites, and Comets, The Solar System*, Vol. IV, pp. 665-673. Chicago, Univ. Chic., 1963.
349. ÖPIK, E. J. Jupiter: chemical composition, structure, and origin of a giant planet. *Icarus* 1:200-257, 1962.
350. OSTERBROCK, D. E. A study of two comet tails. *Astrophys. J.* 128:95-105, 1958.
351. OWEN, T. Comparisons of laboratory and planetary spectra. III. The spectrum of Jupiter from 7750 to 8800 Å. *Astrophys. J.* 142:782-786, 1965.
352. OWEN, T. An identification of the 6800 Å methane band in the spectrum of Uranus and a determination of atmospheric temperature. *Astrophys. J.* 146:611-613, 1966.
353. OWEN, T. Comparisons of laboratory and planetary spectra. IV. The identification of the 7500 Å bands in the spectra of Uranus and Neptune. *Icarus* 6:108-113, 1967.
354. OWEN, T. The spectra of Jupiter and Saturn in the photographic infrared. *Icarus* 10:355-364, 1969.
355. OWEN, T., B. L. LUTZ, C. C. PORCO, and J. H. WOODMAN. On the identification of the 6420 Å absorption feature in the spectra of Uranus and Neptune. *Astrophys. J.* 189:379-381, 1974.
356. OWEN, T., and H. P. MASON. New studies of Jupiter's atmosphere. *J. Atmos. Sci.* 26:870-873, 1969.
357. OWEN, T., and J. A. WESTPHAL. The clouds of Jupiter: observational characteristics. *Icarus* 16:392-396, 1972.
358. OWEN, T., and J. H. WOODMAN. On the atmospheric temperature of Jupiter derived from the  $3\nu_3$  methane band. *Astrophys. J.* 154:L21-L23, 1968.
359. PALLUCONI, F. D. The planet Saturn (1970). In, NASA

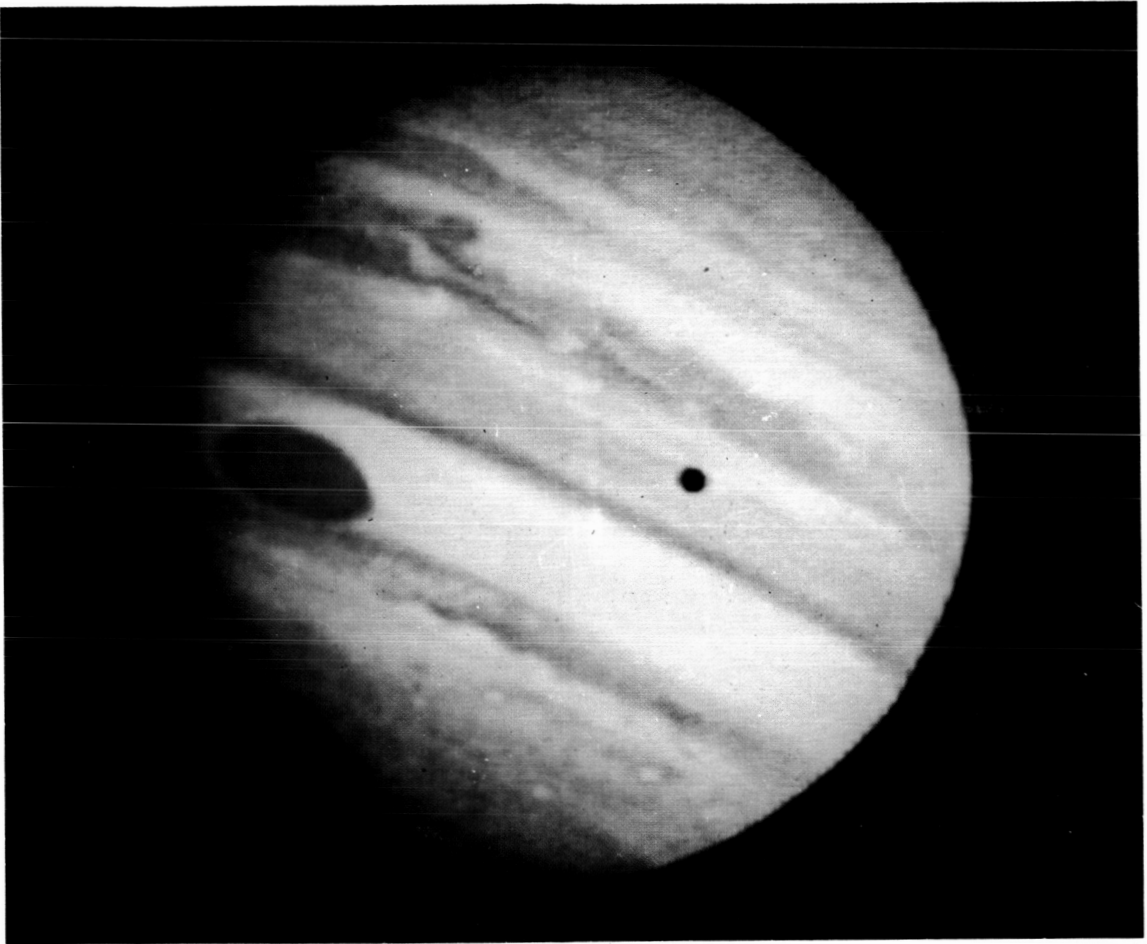
- Space Vehicle Design Criteria (Environment).* Washington, D.C., NASA, 1972. (NASA SP-8091)
360. PAULINY-TOTH, I. I. K., A. WITZEL, and S. GORGOLIEWSKI. The brightness temperatures of Ganymede and Callisto at 2.8 cm wavelength. *Astron. Astrophys.* 34:129-132, 1974.
361. PEAK, B. M. *The Planet Jupiter.* London, Faber and Faber, 1958.
362. PETTENGILL, G. H., and T. HAGFORS. Comments on radar scattering from Saturn's rings. *Icarus* 21:188-190, 1974.
363. PILCHER, C. B., C. R. CHAPMAN, L. A. LEBOFSKY, and H.H. KIEFFER. Saturn rings: identification of water frost. *Science* 167:1372-1373, 1970.
364. PILCHER, C. B., and T. B. MCCORD. Narrow-band photometry of the bands of Jupiter. *Astrophys. J.* 165:195-201, 1971.
365. PILCHER, C. B., S. T. RIDGWAY, and T. B. MCCORD. Galilean satellites; identification of water frost. *Science* 178:1087-1089, 1972.
366. POLLACK, J. B. Greenhouse models of the atmosphere of Titan. *Icarus* 19:43-58, 1973.
367. POLLACK, J. B., A. SUMMERS, and B. BALDWIN. Estimates of the size of the particles in the rings of Saturn. *Icarus* 20:263-278, 1973.
368. POLLACK, J. B., and R. T. REYNOLDS. Implications of Jupiter's early contraction history for the composition of the Galilean satellites. *Icarus* 21:248-253, 1974.
369. PORTER, J. G. The satellites of the planets. *Br. Astron. Assoc. J.* 70:33-59, 1960.
370. PORTER, W. S. The constitutions of Uranus and Neptune. *Astron. J.* 66:243-245, 1961.
371. POTTER, A. E., and B. DEL DUCA. Lifetime in space of possible parent molecules of cometary radicals. *Icarus* 3:103-108, 1964.
372. PRESTON, G. W. The spectrum of comet Ikeya-Seki (1965f). *Astrophys. J.* 147:718-742, 1967.
373. PRICE, M. J. The scattering mean free path in the Uranian atmosphere. *Icarus* 20:455-464, 1973.
374. PRINN, R. G. UV radiative transfer and photolysis in Jupiter's atmosphere. *Icarus* 13:424-436, 1970.
375. PRINN, R. G., and J. S. LEWIS. Uranus atmosphere: structure and composition. *Astrophys. J.* 179:333-342, 1973.
376. PRINZ, R. The atmospheric activity of the planet Jupiter. I. From 1964 to 1968 in yellow light. *Icarus* 15:68-73, 1971.
377. PRINZ, R. The atmospheric activity of the planet Jupiter. II. Short-term variations in five spectral ranges. *Icarus* 15:74-79, 1971.
378. RABE, E. On the origin of Pluto and the masses of the protoplanets. *Astrophys. J.* 125:290-295, 1957.
379. RABE, E. Further studies on the orbital development of Pluto. *Astrophys. J.* 126:240-244, 1957.
380. RAMSEY, W. H. On the constitutions of Uranus and Neptune. *Planet. Space Sci.* 15:1609-1623, 1967.
381. RATHER, I., P. ADE, and P. CLEGG. *Brightness Temperature Measurements of Saturn, Jupiter, Mars, and Venus at 1 mm Wavelength.* (To be published)
382. REESE, E. J. Jupiter's red spot in 1968-1969. *Icarus* 12:249-257, 1970.
383. REESE, E. J. *Summary of Jovian Latitude and Rotation-Period Observations from 1898 to 1970.* Las Cruces, N. Mex. State Univ., Dep. Astron., 1971. (TN-71-36)
384. REESE, E. J. Jupiter: its red spot and other features in 1969-1970. *Icarus* 14:343-354, 1971.
385. REESE, E. J. Recent photographic measurements of Saturn. *Icarus* 15:466-479, 1971.
386. REESE, E. J. Jupiter: its red spot and disturbances in 1970-1971. *Icarus* 17:57-72, 1972.
387. REESE, E. J., and B. A. SMITH. Evidence of vorticity in the great red spot of Jupiter. *Icarus* 9:474-486, 1968.
388. REESE, E. J., and H. G. SOLBERG, Jr. *Recent Measures of the Latitude and Longitude of Jupiter's Red Spot.* Las Cruces, N. Mex. State Univ., 1965. (TN-557-65-7)
389. REGISTER, H. I. *Decameter-Wavelength Radio Observations of the Planet Jupiter, 1957-1968.* Gainesville, Fla., Univ. Fla., 1968. (Doct. diss.)
390. REYNOLDS, R. T., and A. L. SUMMERS. Models of Uranus and Neptune. *J. Geophys. Res.* 70:199-208, 1965.
391. RICHTER, N. B. *The Nature of Comets.* London, Methuen, 1963.
392. RIDGWAY, S. T. Jupiter: identification of ethane and acetylene. *Astrophys. J.* 187:L41-L43, 1974.
393. RIDGWAY, S. T. The infrared spectrum of Jupiter, 750-1200  $\text{cm}^{-1}$ . Presented at 5th Annu. Meet., Am. Astron. Sci., Planet. Sci. Div., Palo Alto, Apr. 1974. *Am. Astron. Soc. Bull.* 6(3, pt.2):376, 1974. (Abstr. No. 056)
394. ROBERTS, J. A., and R. D. EKERS. The position of Jupiter's Van Allen belt. *Icarus* 5:149-153, 1966.
395. ROBEY, D. H. *A Theory on the Nature and Origin of Comets with Implications for Space Mission Planning.* Presented at Annu. Meet., Am. Astronaut. Soc., Anaheim, Calif., June 1970. New York, AAS, 1970. (AAS-70-029)
396. ROEMER, E. Comet notes. *Pub. Astron. Soc. Pac.* 74:537-539, 1962.
397. ROEMER, E. The dimensions of cometary nuclei. *Mem. Soc. Roy. Sci. Liège*, Ser. 5, XII:23-28, 1966.
398. ROEMER, E. Comet notes. *Mercury* 2(4):19-21, 1973.
399. ROTTMAN, G. J., H. W. MOOS, and C. S. FREER. The far-ultraviolet spectrum of Jupiter. *Astrophys. J.* 184:L89-L92, 1973.
400. RUSSELL, H. M., R. S. DUGAN, and J. Q. STEWART. *Astronomy,* Vol. 1, rev. ed. Boston, Mass., Ginn, 1945.
401. SAFRONOV, V. S. Ejection of bodies from the solar system in the course of the accumulation of the giant planets and the formation of the cometary cloud. In, Chebotarev, G. A., E. I. Kazimirchak-Polonskaya, and B. G. Marsden, Eds. *The Motion, Evolution of Orbits, and Origin of Comets,* pp. 329-334. Dordrecht, Holland, D. Reidel, 1972.
402. SAGAN, C. On the nature of the Jovian red spot. *Mem. Soc. Roy. Sci. Liège*, Ser. 5, 7:506-515, 1963.

403. SAGAN, C. A truth table analysis of models of Jupiter's great red spot. *Comments Astrophys. Space Phys.* 3:65-72, 1971.
404. SAGAN, C. The solar system beyond Mars: an exobiological survey. *Space Sci. Rev.* 11:827-866, 1971.
405. SAGAN, C., and B. N. KHARE. Experimental Jovian photochemistry: initial results. *Astrophys. J.* 168:563-569, 1971.
406. SAGAN, C., J. VEVERKA, L. WASSERMAN, J. ELLIOT, and W. LILLER. Jovian atmosphere: structure and composition between the turbopause and the mesopause. *Science* 184:901-903, 1974.
407. SALPETER, E. E. On convection and gravitational layering in Jupiter and in stars of low mass. *Astrophys. J.* 181:L83-L86, 1973.
408. SAVAGE, B. D., and J. J. CALDWELL. Ultraviolet photometry from the orbiting astronomical observatory. XIII. The albedos of Jupiter, Uranus, and Neptune. *Astrophys. J.* 187:197-208, 1974.
409. SAVAGE, B. D., and R. E. DANIELSON. Models of the atmosphere of Jupiter. In, Brancazio, P. J., and A. G. W. Cameron, Eds. *Infrared Astronomy*, pp. 211-244. New York, Gordon and Breach, 1968.
410. SCHATTEN, K. H., and N. F. NESS. The magnetic-field geometry of Jupiter and its relation to Io-modulated Jovian decametric radio emission. *Astrophys. J.* 165:621-632, 1971.
411. SCHUBART, J. Asteroid masses and densities. In, Gehrels, T., Ed. *Physical Studies of Minor Planets*, pp. 33-39. Washington, D.C., NASA, 1971. (NASA SP-267)
412. SCHUBART, J. The masses of the first two asteroids. *Astron. Astrophys.* 30:289-292, 1974.
413. SEAQUIST, E. R. Circular polarization of Jupiter at 9.26 cm. *Nature* 224:1011-1012, 1969.
414. SEIDELMANN, P. K., W. J. KLEPCZYNSKI, R. L. DUNCOMBE, and E. S. JACKSON. Determination of the mass of Pluto. *Astron. J.* 76:488-492, 1971.
415. SEKANINA, Z. Dynamical and evolutionary aspects of gradual deactivation and disintegration of short-period comets. *Astron. J.* 74:1223-1234, 1969.
416. SEKANINA, Z. Secular decrease in the absolute brightness of the comet Encke. In, Konoplyeva, V. P., Ed. *Astrometry and Astrophysics, No. 4, Physics of Comets*, pp. 43-62. Washington, D.C., NASA, 1970. (NASA TT-F-599)
417. SEKANINA, Z. Existence of icy comet tails at large distances from the Sun. *Astrophys. Lett.* 14:175-180, 1973.
418. SHERMAN, J. C. The critical velocity of gas-plasma interaction and its possible heterogenic relevance. In, Elvius, A., Ed. *From Plasma to Planet*, pp. 315-341. Stockholm, Almqvist & Wiksell (New York, Wiley), 1972. (Nobel Symp. Ser. No. 21)
419. SHERRILL, W. M. Polarization measurements of the decameter emission from Jupiter. *Astrophys. J.* 142:1171-1185, 1965.
420. SHIMIZU, M. The upper atmosphere of Jupiter. *Icarus* 14:273-281, 1971.
421. SIMPSON, J. A., D. HAMILTON, G. LENTZ, R. B. MCKIBBEN, A. MOGRO-CAMPERO, M. PERKINS, K. R. PYLE, A. J. TUZZOLINO, and J. J. O'GALLAGHER. Protons and electrons in Jupiter's magnetic field: results from the University of Chicago experiment on Pioneer 10. *Science* 183:306-309, 1974.
422. SIMPSON, J. A., D. C. HAMILTON, R. B. MCKIBBEN, A. MOGRO-CAMPERO, K. R. PYLE, and A. J. TUZZOLINO. The protons and electrons trapped in the Jovian dipole magnetic field region and their interaction with Io. *J. Geophys. Res.* 79:3522-3544, 1974.
423. SINTON, W. M. *Physical Researches on the Brighter Planets*. Bedford, Mass., AF Cambridge Res. Lab., 1964. (AFCRL-64-926) (Final rep.)
424. SINTON, W. M. Limb and polar brightening of Uranus at 8870 Å. *Astrophys. J.* 176:L131-L133, 1972.
425. Sky and Telescope. A tenth satellite of Saturn? *Sky Telesc.* 33(2):71, 93, 1967.
426. SLATTERY, W. L., and W. B. HUBBARD. Statistical mechanics of light elements at high pressure. III. Molecular hydrogen. *Astrophys. J.* 181:1031-1038, 1973.
427. SMITH, B. A., and S. A. SMITH. Upper limits for an atmosphere on Io. *Icarus* 17:218-222, 1972.
428. SMITH, E. J., L. DAVIS, JR., D. E. JONES, D. S. COLBURN, P. J. COLEMAN, JR., P. DYAL, and C. P. SONETT. Magnetic field of Jupiter and its interaction with the solar wind. *Science* 183:305-306, 1974.
429. SMITH, E. J., A. M. A. FRANDSEN, L. DAVIS, JR., D. E. JONES, P. J. COLEMAN, JR., D. S. COLBURN, P. DYAL, and C. P. SONETT. The planetary magnetic field and magnetosphere of Jupiter: Pioneer 10. *J. Geophys. Res.* 79:3501-3513, 1974.
430. SMOLUCHOWSKI, R. Internal structure and energy emission of Jupiter. *Nature* 215:691-695, 1967.
431. SMOLUCHOWSKI, R. Jupiter's convection and its red spot. *Science* 168:1340-1342, 1970.
432. SMOLUCHOWSKI, R. Dynamics of the Jovian interior. *Astrophys. J.* 185:L95-L99, 1973.
433. SMOLUCHOWSKI, R. *The Interior Structure of Jupiter (Consequences of Pioneer 10 Data)*. Presented at USA-USSR Conf. on Cosmochem. of the Moon and Planets, Moscow, June 1974.
434. SNYDER, L. E., D. BUHL, and W. F. HUEBNER. Detection of HCN in Comet Kohoutek (1973f). Presented at 5th Annu. Meet., Am. Astron. Soc., Planet. Sci. Div., Palo Alto, Apr. 1974. *Am. Astron. Soc. Bull.* 6(3, pt.2):389, 1974. (Abstr. No. 152)
435. SOLBERG, H. G., JR. Jupiter's red spot in 1965-1966. *Icarus* 8:82-89, 1968.
436. SOLBERG, H. G., JR. Jupiter's red spot in 1965-1966. *Icarus* 9:212-216, 1968.
437. SOLBERG, H. G., JR. Jupiter's red spot in 1967-1968. *Icarus* 10:412-416, 1969.
438. SOLBERG, H. G., JR. A three-month oscillation in the longitude of Jupiter's red spot. *Planet. Space Sci.* 17:1573-1580, 1969.

439. SPINRAD, H. Pressure-induced dipole lines of molecular hydrogen in the spectra of Uranus and Neptune. *Astrophys. J.* 138:1242-1245, 1963.
440. SPINRAD, H. Spectroscopic research on the major planets. *Appl. Opt.* 3:181-186, 1964.
441. SPINRAD, H. Lack of a noticeable methane atmosphere on Triton. *Pub. Astron. Soc. Pac.* 81:895-896, 1969.
442. SPINRAD, H., H. E. SMITH, and J. LEIBERT. Comet Kohoutek (1973f). *IAU Circ.* (Cambridge, Mass.), No. 2591, Nov. 7, 1973.
443. STANNARD, D. *The Radio Astronomy of Jupiter*. Presented at Neil Brice Mem. Symp., Frascati, Italy, May 1974.
444. STANSBERRY, K. G., and R. S. WHITE. Jupiter's radiation belt. *J. Geophys. Res.* 79:2331-2342, 1974.
445. STONE, P. H. The symmetric baroclinic instability of an equatorial current. *Geophys. Fluid Dyn.* 2:147-164, 1971.
446. STONE, P. H. A simplified radiative-dynamical model for the static stability of rotating atmospheres. *J. Atmos. Sci.* 29:405-418, 1972.
447. STONE, P. H. The dynamics of the atmospheres of the major planets. *Space Sci. Rev.* 14:444-459, 1973.
448. STONE, P. H., and D. H. BAKER, Jr. Concerning the existence of Taylor-columns in atmospheres. *Q. J. Roy. Meteorol. Soc.* 94:576-580, 1968.
449. STREETT, W. B. Phase equilibria in molecular hydrogen-helium mixtures at high pressures. *Astrophys. J.* 186:1107-1125, 1973.
450. STREETT, W. B., H. I. RINGERMACHER, and G. VERONIS. On the structure and motions of Jupiter's red spot. *Icarus* 14:319-342, 1971.
451. STROBEL, D. F., and G. R. SMITH. On the temperature of the Jovian thermosphere. *J. Atmos. Sci.* 30:718-725, 1973.
452. SWINGS, P. Cometary spectra. *Q. J. Roy. Astron. Soc.* 6:28-69, 1965.
453. SWINGS, P., and L. HASER. *Atlas of Representative Cometary Spectra*. Louvain, Belg., Univ. Liège, 1956.
454. TAYLOR, D. J. Spectrophotometry of Jupiter's 3400-10 000 Å spectrum and a bolometric albedo for Jupiter. *Icarus* 4:362-373, 1965.
455. TAYLOR, F. W. Methods and approximations for the computation of transmission profiles in the  $\nu_4$  band of methane in the atmosphere of Jupiter. *J. Quant. Spectrosc. Radiat. Transfer* 12:1151-1156, 1972.
456. TAYLOR, F. W. Temperature sounding experiments for the Jovian planets. *J. Atmos. Sci.* 29:950-958, 1972.
457. TAYLOR, G. E. The determination of the diameter of Io from its occultation of  $\beta$  Scorpii C on May 14, 1971. *Icarus* 17:202-208, 1972.
458. TAYLOR, R. C. Photometric observations and reduction of lightcurves of asteroids. In, Gehrels, T., Ed. *Physical Studies of Minor Planets*, pp. 117-131. Washington, D.C., NASA, 1971. (NASA SP-267)
459. TEIFEL, V. G. Spectrophotometry of the methane absorption bands at 0.7-1.0  $\mu$  on the disk of Jupiter. *Sov. Astron.-A. J.* 10:121-123, 1966.
460. TEIFEL, V. G. Molecular absorption and the possible structure of the cloud layers of Jupiter and Saturn. *J. Atmos. Sci.* 26:854-859, 1969.
461. TEIFEL, V. G., L. A. USOLTZEEVA, and G. A. KHARITONOVA. The spectral characteristics and probable structure of the cloud layer of Saturn. In, Sagan, C., T. C. Owen, and H. J. Smith, Eds. *Planetary Atmospheres*, pp. 375-383. Dordrecht, Holland, D. Reidel, 1971. (IAU Symp. No. 40)
462. TEXEREAU, J. Observing Saturn's edgewise rings, October 1966. *Sky Telesc.* 33:226-227, 1967.
463. THORNE, K. S. Dependence of Jupiter's decimeter radiation on the electron distribution in its Van Allen belts. *Radio Sci.* 69D:1557-1560, 1965.
464. THOMBAUGH, C. W. The trans-Neptunian planet search. In, Kuiper, G. P. and B. M. Middlehurst, Eds. *Planets and Satellites, The Solar System*, Vol. III, pp. 12-30. Chicago, Univ. Chic., 1961.
465. TRAFTON, L. Model atmospheres of the major planets. *Astrophys. J.* 147:765-781, 1967.
466. TRAFTON, L. M. Photometric observations of Saturn's 1.1  $\mu$  CH<sub>4</sub> band. *Bull. Am. Astron. Soc.* 3:282, 1971.
467. TRAFTON, L. A semiempirical model for the mean transmission of a molecular band and application to the 10  $\mu$  and 16  $\mu$  bands of NH<sub>3</sub>. *Icarus* 15:27-38, 1971.
468. TRAFTON, L. On the methane opacity for Uranus and Neptune. *Astrophys. J.* 172:L117-L120, 1972.
469. TRAFTON, L. On the possible detection of H<sub>2</sub> in Titan's atmosphere. *Astrophys. J.* 175:285-293, 1972.
470. TRAFTON, L. The bulk composition of Titan's atmosphere. *Astrophys. J.* 175:295-306, 1972.
471. TRAFTON, L. Saturn: a study of the 3  $\nu_3$  methane band. *Astrophys. J.* 182:615-636, 1973.
472. TRAFTON, L. Scanner observations of the quadrupole H<sub>2</sub> lines in the spectrum of Uranus. *Bull. Am. Astron. Soc.* 5:290-291, 1973.
473. TRAFTON, L. Neptune: observations of the H<sub>2</sub> quadrupole lines in the (4-0) band. In, *Exploration of the Solar System, 65th Symposium, International Astronomical Union*, Torun, Pol., Sept. 1973.
474. TRAFTON, L. Neptune's internal heat source: an explanation in terms of the dissipation of Triton's orbit. Presented at 5th Annu. Meet., Am. Astron. Soc., Planet. Sci. Div., Palo Alto, Calif., Apr. 1974. *Am. Astron. Soc. Bull.* 6(3, pt. 2):380, 1974. (Abstr. No. 078)
475. TRAFTON, L. Titan: unidentified strong absorptions in the photometric infrared. *Icarus* 21:175-187, 1974.
476. TRAFTON, L., and G. MÜNCH. The structure of the atmospheres of the major planets. *J. Atmos. Sci.* 26:813-825, 1969.
477. TRAFTON, L., and P. H. STONE. Radiative-dynamical equilibrium states for Jupiter. *Astrophys. J.* 188:649-655, 1974.
478. TRAFTON, L., T. PARKINSON, and W. MACY, Jr. The spatial extent of sodium emission around Io. *Astrophys. J.* 190:L85-L89, 1974.
479. TRAUB, W. A., and N. P. CARLETON. Observations of spatial and temporal variations of the Jovian H<sub>2</sub>

- quadrupole lines. Presented at 5th Annu. Meet., Am. Astron. Soc., Planet. Sci. Div., Palo Alto, Apr. 1974. *Am. Astron. Soc. Bull.* 6(3, pt. 2):376, 1974. (Abstr. No. 054)
480. TRULSEN, J. Collisional focusing of particles in space causing jetstreams. In, Gehrels, T., Ed. *Physical Studies of Minor Planets*, pp. 327-335. Washington, D.C., NASA, 1971. (NASA SP-267)
481. TRULSEN, J. Formation of comets in meteor streams. In, Chebotarev, G. A., E. I. Kazimirchak-Polonskaya, and B. G. Marsden, Eds. *The Motion, Evolution of Orbits, and Origin of Comets*, pp. 487-490. Dordrecht, Holland, D. Reidel, 1972.
482. TRULSEN, J. Numerical simulation of jetstreams. II. The two-dimensional case. *Astrophys. Space Sci.* 18:3-20, 1972.
483. Ulich, B. L. Absolute brightness temperature measurements at 2.1 mm wavelength. *Icarus* 21:254-261, 1974.
484. Ulich, B. L., and E. K. CONKLIN. Detection of methyl cyanide in comet Kohoutek. *Nature* 248:121-122, 1974.
485. VAN ALLEN, J. A., D. N. BAKER, B. A. RANDALL, and D. D. SENTMAN. The magnetosphere of Jupiter as observed with Pioneer 10. I. Instrument and principal findings. *J. Geophys. Res.* 79:3559-3577, 1974.
486. VAN ALLEN, J. A., D. N. BAKER, B. A. RANDALL, M. F. THOMSEN, D. D. SENTMAN, and H. R. FLINDT. Energetic electrons in the magnetosphere of Jupiter. *Science* 183:309-311, 1974.
487. VESELY, C. D. Summary on orientations of rotation axes. In, Gehrels, T., Ed. *Physical Studies of Minor Planets*, pp. 133-140. Washington, D.C., NASA, 1971. (NASA SP-267)
488. EVERKA, J. Polarization measurements of the Galilean satellites of Jupiter. *Icarus* 14:355-359, 1971.
489. EVERKA, J. Titan: polarimetric evidence for an optically thick atmosphere. *Icarus* 18:657-660, 1973.
490. EVERKA, J., and M. NOLAND. Asteroid reflectivities from polarization curves: calibration of the "slope-albedo" relationship. *Icarus* 19:230-239, 1973.
491. EVERKA, J., L. WASSERMAN, and C. SAGAN. On the upper atmosphere of Neptune. *Astrophys. J.* 189:569-575, 1974.
492. VSEKHSVYATSKIY, S. K. *Physical Characteristics of Comets*. Jerusalem, Isr. Prog. Sci. Transl., 1964. (NASA T-80; OTS 62-11031)
493. VSEKHSVYATSKIY, S. K. The origin and evolution of the comets and other small bodies in the solar system. In, Chebotarev, G. A., E. I. Kazimirchak-Polonskaya, and B. G. Marsden, Eds. *The Motion, Evolution of Orbits, and Origin of Comets*, pp. 413-425. Dordrecht, Holland, D. Reidel, 1972.
494. WALKER, M. F., and R. HARDIE. A photometric determination of the rotational period of Pluto. *Pub. Astron. Soc. Pac.* 67:224-231, 1955.
495. WALKER, R. G. *Infrared Photometry of Stars and Planets*. Cambridge, Mass., Harvard Univ., 1967. (Doct. diss.)
496. WALLACE, L., J. J. CALDWELL, and B. D. SAVAGE. Ultraviolet photometry from the orbiting astronomical observatory. III. Observations of Venus, Mars, Jupiter, and Saturn longward of 2000 Å. *Astrophys. J.* 172:755-769, 1972.
497. WALLACE, L., M. PRATHER, and M. J. S. BELTON. The thermal structure of the atmosphere of Jupiter. Presented at 5th Annu. Meet., Am. Astron. Soc., Planet. Sci. Div., Palo Alto, Apr. 1974. *Am. Astron. Soc. Bull.* 6(3 pt.2):377, 1974. (Abstr. No. 060)
498. WALLIS, M. K. The physics of cometary plasma. *Planet. Space Sci.* 15:1407-1418, 1967.
499. WAMSTEKER, W. The wavelength dependence of the albedos of Uranus and Neptune from 0.3 to 1.1 micron. *Astrophys. J.* 184:1007-1016, 1973.
500. WARWICK, J. W. The position and sign of Jupiter's magnetic moment. *Astrophys. J.* 137:1317-1318, 1963.
501. WARWICK, J. W. Radio emission from Jupiter. *Ann. Rev. Astron. Astrophys.* 2:1-22, 1964.
502. WARWICK, J. W. Radiophysics of Jupiter. *Space Sci. Rev.* 6:841-891, 1967.
503. WARWICK, J. W. *Particles and Fields Near Jupiter*. Washington, D.C., NASA, 1970. (NASA CR-1685)
504. WASSERMAN, L., and J. EVERKA. On the reduction of occultation light curves. *Icarus* 20:322-345, 1973.
505. WATSON, K., B. C. MURRAY, and H. BROWN. The stability of volatiles in the solar system. *Icarus* 1:317-327, 1963.
506. WEIDENSCHILLING, S. J., and J. S. LEWIS. Atmospheric and cloud structures of the Jovian planets. *Icarus* 20:465-476, 1973.
507. WESTPHAL, J. A. Observations of Jupiter's cloud structure near 8.5 μ. In, Sagan, C., T. C. Owen, and H. J. Smith, Eds. *Planetary Atmospheres*, pp. 359-362. Dordrecht, Holland, D. Reidel, 1971. (IAU Symp. 40)
508. WESTPHAL, J. A., K. MATTHEWS, and R. J. TERRILE. Five micron pictures of Jupiter. *Astrophys. J.* 188: L111-L112, 1974.
509. WETHERILL, G. W. Collisions in the asteroid belt. *J. Geophys. Res.* 72:2429-2444, 1967.
510. WETHERILL, G. W. Cometary versus asteroidal origin of chondritic meteorites. In, Gehrels, T., Ed. *Physical Studies of Minor Planets*, pp. 447-460. Washington, D.C., NASA, 1971. (NASA SP-267)
511. WHIPPLE, F. L. On the structure of the cometary nucleus. In, Middlehurst, B. M., and G. P. Kuiper, Eds. *The Moon, Meteorites, and Comets, The Solar System*, Vol. IV, pp. 639-664. Chicago, Univ. Chic., 1963.
512. WHIPPLE, F. L. The origin of comets. In, Chebotarev, G. A., E. I. Kazimirchak-Polonskaya, and B. G. Marsden, Eds. *The Motion, Evolution of Orbits, and Origin of Comets*, pp. 401-408. Dordrecht, Holland, D. Reidel, 1972.
513. WHITAKER, E., and R. GREENBERG. Eccentricity and inclination of Miranda's orbit. *Comm. Lunar Planet. Lab.* 10:70-80, 1973.
514. WHITEOAK, J. B., F. F. GARDNER, and D. MORRIS. Jovian linear polarization at 6 cm wavelength. *Astrophys. Lett.* 3:81-84, 1969.

515. WILDEY, R. L. Hot shadows of Jupiter. *Science* 147:1035-1036, 1935.
516. WILDEY, R. L., B. C. MURRAY, and J. A. WESTPHAL. Thermal infrared emission of the Jovian disk. *J. Geophys. Res.* 70:3711-3719, 1965.
517. WILKINS, G. A., and A. T. SINCLAIR. The dynamics of the planets and their satellites. *Proc. Roy. Soc. London A* 336:85-104, 1974.
518. WILLIAMS, J. G. Proper elements, families, and belt boundaries, In, Gehrels, T., Ed. *Physical Studies of Minor Planets*, pp. 177-181. Washington, D.C., NASA, 1971. (NASA SP-267)
519. WILLIAMS, J. G. Meteorites from the asteroid belt? EθS (*Trans. Am. Geophys. Union*) 54:233, 1973.
520. WILLIAMS, J. G., and G. S. BENSON. Resonances in the Neptune-Pluto system. *Astron. J.* 76:167-177, 1971.
521. WITKOWSKI, J. M. On the origin of comets. *Solar Syst. Res.* 5:66-71, 1971.
522. WITKOWSKI, J. M. On the problem of the origin of comets. In, Chebotarev, G. A., E. I. Kazimirchak-Polonskaya, and B. G. Marsden, Eds., *The Motion, Evolution of Orbits, and Origin of Comets*, pp. 419-425. Dordrecht, Holland, D. Reidel, 1972.
523. WOELLER, F., and C. PONNAMPERUMA. Organic synthesis in a simulated Jovian atmosphere. *Icarus* 10:386-392, 1969.
524. WRIXON, G. T., and W. J. WELCH. The millimeter wave spectrum of Saturn. *Icarus* 13:163-172, 1970.
525. WRIXON, G. T., W. J. WELCH, and D. D. THORNTON. The spectrum of Jupiter at millimeter wavelengths. *Astrophys. J.* 169:171-183, 1971.
526. WURM, K. The substructure in the heads of comets with type I and type II tails. *Astrophys. Space Sci.* 27:211-216, 1974.
527. YABUSHITA, S. Stability analysis of Saturn's rings with differential rotation. *Mon. Not. Roy. Astron. Soc.* 133: 247-263, 1966.
528. YERBURY, M. J., J. J. CONDON, and D. L. JAUNCEY. Observations of Saturn at a wavelength of 49.5 cm. *Icarus* 15:459-465, 1971.
529. YOUNG, A. T., and W. M. IRVINE. Multicolor photoelectric photometry of the brighter planets. I. Program and procedure. *Astron. J.* 72:945-950, 1967.
530. YOUNKIN, R. L. *Spectrophotometry of the Moon, Mars, and Uranus*. Los Angeles, Calif., Univ. Calif., 1970. (Doct. diss.)
531. YOUNKIN, R. L. The albedo of Titan. *Icarus* 21:219-229, 1974.
532. YOUNKIN, R. L., and G. MÜNCH. Spectrophotometry of Uranus from 3300 to 11 000 Å. *Astron. J.* 72:328-329, 1967.
533. ZABRISKIE, F. R., W. A. SOLOMON, and J. P. HAGAN, Jr. Low-frequency observations of Jupiter. *Astron. J.* 70:151, 1965.
534. ZAPOLSKY, H. S., and E. E. SALPETER. The mass-radius relation for cold spheres of low mass. *Astrophys. J.* 158:809-813, 1969.
535. ZELLNER, B. On the nature of Iapetus. *Astrophys. J.* 174:L107-L109, 1972.
536. ZELLNER, B. The polarization of Titan. *Icarus* 18:661-664, 1973.
537. ZHARKOV, V. N., and V. P. TRUBITSYN. Adiabatic temperatures in Uranus and Neptune. *Phys. Solid Earth* (Izv.) (7):496-500, 1972.
538. ZIMMERMAN, P. D., and G. W. WETHERILL. Asteroidal source of meteorites. *Science* 182:51-53, 1973.



Jupiter. The Great Red Spot, a shadow of the moon, Io, and Jupiter's cloud structure are shown in this photograph taken at 0702 GMT on December 2, 1973, as NASA's Pioneer 10 spacecraft was 2 500 000 kilometers from the giant planet. (NASA 73-H-1164)

REPRODUCIBILITY OF THE  
ORIGINAL PAGE IS POOR

## Part 3

# PROBLEMS OF EXOBIOLOGY

## Chapter 6

# BIOLOGICAL EFFECTS OF EXTREME ENVIRONMENTAL CONDITIONS<sup>1</sup>

A. A. IMSHENETSKIY

Institute of Microbiology, Academy of Sciences USSR, Moscow

The development of new scientific disciplines begins with setting new trends in experimental research. This applies to space biology, which involves study of the effect of extreme factors on living matter, evaluation of various methods of detection of extraterrestrial life, and development of the most promising methods of sterilizing devices to be sent into space. The development of a new scientific discipline is impossible without preliminary generalization of all data obtained previously which are directly related. In regard to the effects of the majority of extreme factors found in free space and on the planets, researchers have a great scientific inheritance at their disposal, handed down by ecology, biophysics, biochemistry, and microbiology.

Systematization of these data made it evident that an extensive body of literature deals with a number of physical factors found in space: the effects of low and high temperatures, ionizing and UV radiation, the effects of various gases, vibration, desiccation, and acceleration. At the same

time, space biology is obliged to begin study of the physical factors in space which have not been studied previously.

This situation is complicated by some of these factors not being completely reproducible under laboratory conditions. This is particularly true of weightlessness, and of vacuum which may reach  $10^{-16}$  mm Hg in space. However, this has not prevented the obtaining of interesting results in the study of these extreme factors. A number of physical and chemical factors are of no special interest in space biology such as ultrasound, effects of various chemicals (including surfactant substances), and concentrations of hydrogen ions. Investigation has centered principally on microorganisms for many reasons. The universal distribution of microorganisms indicates their exclusive ability to accommodate to the most diverse ecological niches. Another reason is the unusually high resistance of microorganisms to the action of extreme factors. Finally, the majority of methods for detecting extraterrestrial life are based on seeking microorganisms that inhabit the soil of planets and multiply on a nutrient medium that is brought to the planet along with the biological station. Thus, microorganisms have become the favored subject in studying the action of extreme factors, although other studies have been performed that include higher plants and lower animals.

There are several ways of studying the action

<sup>1</sup> Translation of, *Biologicheskiye effekty ekstremal'nykh usloviy okrukhayushchey sredy*, Volume I, Part 3, Chapter 1, *Osnovy Kosmicheskoy Biologii i Meditsiny* (*Foundations of Space Biology and Medicine*), Moscow, Academy of Sciences USSR, 1973, 81 pages.

The author expresses sincere gratitude for the valuable contributions of L. K. Lozino-Lozinskii and E. I. Zaar (USSR), and D. W. Jenkins, S. M. Siegel, and C. E. Zobell (USA), who prepared surveys on national materials, and to all colleagues who collaborated in preparing this chapter.

of extreme factors: tests in the laboratory, in deep space, on the surfaces of planets or their satellites, and finally inside a flying spacecraft. The walls of a spacecraft in flight shield the living materials under study considerably against action of some extreme factors; however, under these conditions it is quite possible to study the influence of weightlessness and vibration.

Generalization of data in the extensive literature on the action of extreme factors on living matter involves considerable difficulties. There is considerable lack of agreement between the results obtained in describing the resistance of living objects to a given external factor. Only those results can be used which have been established repeatedly by several investigators; data which differ markedly may be mentioned as available in the literature but as yet unconfirmed.

In this chapter, limits of the biosphere and characteristics of extreme factors will be discussed, then the effect of individual physical and chemical factors on living organisms.

### LIMITS OF THE BIOSPHERE

The concept of the biosphere would be incomplete without a definition of its limits, which are also a function of living matter being able to withstand the powerful action of various physical and chemical factors. Several limits are of no interest in space biology, while others are of direct significance.

Many extreme factors affect various types of living matter on Earth. Therefore, the ecology of microorganisms, plants, and animals provides valuable data for space biology. The theory of the biosphere developed by Vernadskiy includes in the Earth's biosphere all organisms plus the abiotic medium in which they exist [159]. This is a complete unit but it is full of contradictions; both organisms and the inorganic conditions under which they exist undergo changes. A conclusion in ecology reached long ago is that the lowest life forms are those most resistant to extreme effects: bacteria, actinomycetes, microscopic fungi, certain algae, and protozoa.

In discussing the limits of the biosphere, the distribution of life vertically has been studied only slightly. The upper limit of the biosphere

has not been established; in collecting samples in the stratosphere by means of stratospheric balloons, the necessary technical requirements were not observed, and the collection of samples at high altitudes has been complicated by the admixture of soil microorganisms from the surface of the balloon, the envelope of which lay on the ground while being filled with gas. The only exception is the studies carried out some time ago using the Explorer II stratospheric balloon, where samples were collected under sterile conditions. At an altitude of 20 km, spore-forming bacteria and microscopic fungi were found, but only in small amounts. Hence, microorganisms can retain viability under stratospheric conditions despite low temperature, UV and ionizing radiation. Consequently, air currents may lift microorganisms to heights of 20 km. No data are available yet on the ability of microorganisms to be elevated to great heights.

For the detection of microorganisms at high altitudes, certain changes are necessary in our views regarding the possibility of transporting microorganisms in space [9]. The well-known forms of microorganisms weigh too much to move around under stratospheric conditions or in deep space under the influence of light pressure. In this connection, the attention of biologists has been attracted to the discovery of microorganisms with life cycle forms invisible under the light microscope. This is particularly true of mycoplasms and viruses. The possibility of transport in space of such light particles cannot be ruled out. However, the very long action of extreme factors in space makes such transport of small microorganisms highly unlikely. During this new stage of scientific development, the theory of panspermia has been revived. The possibility of transport of very small embryos in nonscientific space is not antiscientific in itself. However, the theory of panspermia does not solve the basic problem of the origin of life, which has ceased to be simply a philosophical problem and has become an orderly theory in conjunction with the establishment of chemical evolution in space and successes in chemical synthesis.

The lower limit of the biosphere, too, has been inadequately defined. Living microorganisms are frequently found on the ocean floor; samples

have been collected at depths of 11 km. At such great depths, microorganisms are subjected to a pressure equal to 1100 kg/cm<sup>2</sup>. Purple sulfur bacteria have also been found in oil reservoir water flowing from great depths [31, 82, 106]. Microorganisms have been found in cores from depths of 4 km. Living microorganisms in permafrost zones or in rock salt have not been confirmed so far.

Life which exists at high and low temperatures has been studied with extraordinary thoroughness. It may be considered firmly established that living microorganisms that multiply at 75°–90° C live in geysers and hot springs. The influence of low and high temperatures on living matter is discussed in greater detail in a subsequent section in this chapter, under TEMPERATURE.

Marine biology was the first area in science to establish that certain bacteria in the seas can reproduce very well at pressure of 400 atm. Such barotolerant microorganisms have been subjected to special study; barotolerant bacteria have also been found in soil in flower pots and greenhouses, which must be considered slightly paradoxical.

In modern ecology of microorganisms, a great deal of information is available on the life of microbes at very low and very high pH values. Bacteria and fungi which form various organic acids are naturally quite resistant, presenting a simultaneous resistance to both the specific action of acids and to low pH. However, the low pH values formed by readily dissociating mineral acids are withstood much better by the microorganisms. Thus, *Thiobacillus thioparus* and other species of *Thiobacillus*, which oxidize various reduced compounds of sulfur to form sulfuric acid, multiply at pH 1.0, and some at pH 0.5. These microorganisms are found in ore refuse which contains sulfides and in heaps of extracted sulfur. On the other hand, there are soda lakes inhabited by various prokaryotes and eukaryotes. In such lakes, found in Asia and Africa, the water reaction reaches a pH of 8.0–9.0. Still more alkaline reactions are produced under industrial conditions, in particular, in the leather industry in the fluids of lime pits which have a pH of 11.0 where *Bacillus mesentericus*, which is resistant to this reaction, can multiply.

The gas composition on Earth can vary within wide limits. At the bottom of the seas and oceans there is little free oxygen, but active life can be observed. On the ocean ground at a depth of 10 000 m, Polychaeta, Isopoda, Bivalvia, Holo-thorioidea, and others were found in addition to microorganisms, which must be remembered when discussing life on planets which contain almost no oxygen. Anaerobic bacteria occurring in various layers of soil is less certain; aerobic soil microorganisms can utilize oxygen to create anaerobic conditions.

The content of various gases in the atmosphere or in bodies of water is accompanied by multiplication of special physiologic groups of microorganisms that utilize these gases. This applies to the bacteria which oxidize hydrogen, methane, hydrogen sulfide, carbon monoxide, those which use carbon dioxide, nitrogen, and so forth. Hence, composition of the atmosphere or nature of gases dissolved in water can lead to complete lack of life only in unusual cases, which is true of the dead hydrogen sulfide zone in the Black Sea.

Ionizing radiation under natural conditions does not exert any pernicious influence on microorganisms, inasmuch as the available doses are insufficiently high. On the other hand, the sterilizing effect of UV radiation is quite evident. The effects of various types of radiation on living organisms are described in subsequent sections of this chapter, ULTRAVIOLET RAYS, and IONIZING RADIATION.

Highly diverse biological niches are populated by microorganisms, and they occupy the extreme limits of the biosphere (indicated in data already presented). However, an understanding of the biosphere requires involvement of active interaction between organisms and the conditions of their existence. Lower and higher plants are very important in the circulation of chemical elements on Earth; participation of plant organisms in breaking up rocks, and in pedogenic processes has long attracted naturalists' attention. There has been less interest in ecological changes which result from the vital activity of living matter, in particular of microorganisms. The hydrogen sulfide zones in the oceans, formed from the reduction of sulfates,

are completely empty of life; the considerable liberation of hydrogen and methane from the mud of fresh water reservoirs governs the nature of the microbiocenosis in these areas. Certain products of vital activity act as "means of protection," which applies particularly to lactic acid, certain pigments released into the surrounding medium, antibiotics, and toxins. These substances, which inhibit other species, enable the species which form them to compete better in the battle for survival.

Hence, the basic development of the biosphere is the adaptation of living matter to various living conditions and the active change in these conditions.

### NATURE OF EXTREME FACTORS

The task of space biology involves the study of extreme factors which act on the planets, in deep space and on objects in space; some of these factors have been long studied in biophysics and ecology. This applies to the action of high and low temperatures, ionizing and UV radiation, magnetic field, pressure, environmental reactions, and various chemical substances. The study of certain factors which includes weightlessness and others was begun recently, only after space biology acquired the rank of a science.

The great majority of extreme factors may be created under laboratory conditions with appropriate devices. Such devices are so powerful that the researcher is able to subject the test objects to the effect of UV radiation in doses which cells receive in deep space. The same is true of many other extreme factors; however, certain factors cannot be reproduced under laboratory conditions.

Any physical or chemical factor may be extreme and everything depends on its energy, dose, duration of action, and means of application. Suffice it to say that high pressure produced by such inert gases as argon or nitrogen can cause the death of bacteria in a fluid. The experimenter can study the influence of each factor individually as well as in combination, which is highly important since one factor may influence the sensitivity to another factor. Thus, increasing the pressure reduces the sensitivity to high temperature. Preliminary loss of moisture makes the cell resistant to a number of external influences.

In studying the interaction of various factors it becomes clear that some lead to synergism while others have an antagonistic or protective effect, and finally, it is possible that a certain factor has no influence on the activity of another.

The complex action of several factors can be reproduced in special climatologic stations where the conditions on a given planet or in deep space can be simulated. Living objects have been studied most frequently by means of the "Artificial Mars" station, in which the living conditions correspond to those on the planet Mars. There are also devices which simulate the conditions in deep space or on the Moon.

The number of extreme factors of interest to space biology is far less than the number investigated in ecology and biophysics. Thus, the interests of space biology are in the effects of vacuum, low temperature, temperature variation, weightlessness, vibration, and acceleration, the action of high doses of ionizing and UV radiation, low moisture content in the substrate, and gases. At the same time, the action of toxic substances, the influence of various salts, high osmotic pressure, and other factors are generally of little interest to space biology, but the possibility must be included that this depends on the limited information on the soil and atmosphere of the planets.

The first detailed chemical analyses of the soil and atmosphere of the planets will probably require study of the physiologic effect of various chemical compounds and new factors. During spacecraft flight, biological objects are subjected to the action of numerous flight factors including weightlessness, acceleration, vibration and ionizing radiation. The researcher must deal with the combined action of many factors; all efforts to analyze this complex into its individual elements have failed thus far. A principal reason is that under experimental conditions on Earth, it is not possible to reproduce weightlessness and study its interaction with other flight factors. Interesting studies are conducted along this line to explain the physiologic effects of vibration, influence of weightlessness, resulting action of ionizing radiation, and so forth. However, none of these will permit the necessary classical

analysis of each of the factors acting during flight, and recreate the necessary synthesis of a combination of all existing flight factors acting on the biological objects.

In determining the effect of a factor, three physiologic points are established: minimum, optimum, and maximum. Insufficient attention is usually given to the fact that during the action of a factor of a given intensity, the object in question is able to multiply but the biologic object gradually dies under repeated exposure to the same factor at the same dose. An example is the relationship of a culture of microorganisms to high temperature; they can grow once at a relatively high temperature, but the culture dies following repeated passages at the same temperature. Thus, in determining maximum and minimum physiologic points, the objects must be exposed to them several times in order to determine if the organism really can exist under these conditions. In studying the extreme factors, their effects on viability (ability to survive), growth and multiplication, and variation (frequency of development of mutations) are determined.

In ascertaining the influence of any extreme factor on growth, development, multiplication, and so forth, there is no difficulty involved. It is more complex to determine the dose of a factor which leads to the death of the cell. The cell may be inactivated and not grow under the conditions usually employed, but if the factors are changed, it may undergo reactivation and the cell will reproduce. Spores subjected to the action of high temperature will not grow on some nutrient media, while some spores will grow on other nutrient media with other compositions. This is fully applicable to photoreactivation which is possible following the action of UV radiation and in other cases.

Considerable experimental data have been accumulated which indicate that various extreme factors can act in different ways on functions of the living organism described. Thus, very low temperatures prevent reproduction of microorganisms, but in conjunction with additional dehydration of the cells, their existence can be prolonged. The effect of any factor depends on its specificity, dose (amount of energy), and dura-

tion of action. Rapid changes in conditions of existence usually have a profound effect on living organisms. With a slow drop in temperature, certain species of bacteria will grow at  $-5^{\circ}\text{C}$ , while a rapid drop of temperature from  $+30^{\circ}$  to  $0^{\circ}\text{C}$  may be lethal for some bacteria. To a certain extent, this is true of rapid increases in pressure alternating with conditions corresponding to atmospheric pressure. However, for most microorganisms, desiccation of cells at low temperature does not cause the death of the entire population. This is the basis for lyophilization of cultures used for their preservation.

The number of cells dying during lyophilization varies greatly with species of microorganisms: for *Staphylococcus aureus* 11.9%, for *Pseudomonas fluorescens* 41.0%, and for *Saccharomyces carlsbergensis* 92.0%. For the most part, biological objects studied have been subjected to the action of a complex of factors, which is true of all experiments aboard spacecraft or satellites. It is also the reason that in laboratory studies, it is necessary to study the effect of each factor separately. However, these studies are not always capable of determining the interaction of various factors which act simultaneously upon the living object; there may be a neutralization of one factor by another, intensification of action, change in mechanism of action, and so forth.

Problems in space biology include a comparative study of the effect of a given factor on both more complex and less complex organized life forms. Such an evolutionary approach makes it possible not only to confirm different degrees of sensitivity in various objects, but also to start a means for comparative study of the mechanism of action of extreme factors. Thus, anaerobic organisms do not react to the action of oxidative phosphorylation inhibitors. Poisons which act on the nervous system or the hemopoietic organs of animals often fail to exert any kind of inhibiting effect on microorganisms. The study of the action of extreme factors yields results that are valuable in many respects.

First, these data are valuable for space medicine with the principal task of creating conditions to insure safety of both the flight and the cosmonauts on planets and satellites.

Second, these studies will make it possible to investigate the action of these extreme factors and their combinations which may exist on other planets on terrestrial materials, thus facilitating the search for extraterrestrial life.

Third, the intensity of the action of extreme factors observed in space and on the planets governs their ability to sterilize objects in space and determines whether or not the terrestrial organisms which are conveyed to a planet will be able to reproduce.

Fourth, research in this direction will provide new scientific data on the action of factors which have not been studied previously. This relates to a high vacuum, weightlessness, superhigh doses of UV radiation, and the like.

Study of the action of extreme factors is directly related to the general biological problem of living matter adapting to various living conditions. In most cases development of different biological races differs in some particular feature. For example, marine and fresh-water forms of sulfate-reducing bacteria can be used which belong to the same species, or mesophilic and thermophilic variants of *Bacillus mycoides*. It is certain, however, that an ecotype can be a newly created species, since in the future, it will become markedly different from the original form in many other ways. In regard to the mechanism of adaptation, there is still no basis for assuming that there will be such accommodation on other planets in ways different from those on Earth.

Another problem of similar importance biologically concerns the temporary complete or nearly complete cessation of metabolism in living matter which leads to anabiosis (with which many studies have dealt). The periodically developing state of anabiosis which has no effect on subsequent transition to active life is extremely important in space biology. Thus, variations from +20° to -90° C during the martian day produces a brief anabiotic state which develops at low temperature. However, according to experiments with terrestrial organisms, this has no effect on living organisms' ability to metabolize, to grow and multiply when the

temperature rises again. Short-term cessation of life may be a widespread phenomenon. The seeds of certain plants with a dense, hermetically sealed exocarp are thought to retain their viability for a long time. However, all attempts to detect vital activity in the cells of algae which have been preserved in rock salt for 250 million years have been unsuccessful. Searches for living matter in meteorites have been equally fruitless. Apparently, retention of the normal structure of protein for millions of years is impossible, which explains the lack of data on very long anabiosis.

## TEMPERATURE

### Effects of Low Temperatures

Of great interest to space biology is the effect of low temperatures which may be very low in deep space and on the planets. (See Part 2, Chapters 4 and 5 of this volume.) Microorganisms and the seeds of higher plants remain viable at very low temperatures. This was demonstrated experimentally long ago. Later, a special science, cryobiology, dealt with the relationship of various living substances to low temperatures, the mechanism of their action, and the influence on growth and reproduction [10, 11, 102]. Many higher plants and animals on Earth live at temperatures from -10° to -20° C and some species retain viability at still lower temperatures (-20° to -50° C); comparatively few living substances can survive at temperatures below -50°. Liquefied gases are usually employed in testing the resistance of various organisms; thus, the temperature of liquid air is -195° C, liquid hydrogen is -250° C, and liquid helium is between -269° and -271° C. Test results of the resistance of various living substances are shown in Table 1 [31, 33, 35, 46, 47, 159, 162, 166, 167, 168, 170, 172], which indicate these conclusions.

1. Temperatures below -190° C are withstood by many bacteria, yeasts, microscopic fungi, algae, protozoa, worms, insects, human spermatozoa, and higher plants.
2. Various species of bacteria are particularly resistant, retaining viability at absolute zero (-273° C).

3. Terrestrial microorganisms in space or on planets that have very low temperatures have not died. Consequently, low temperature in space does not have a bactericidal effect and the microflora which are on the surfaces of satellites and spacecraft remain viable.

Study of the Moon has confirmed the latter view, inasmuch as living terrestrial bacteria were found on the Moon which had been transported there earlier aboard spacecraft. The extreme resistance of microorganisms to superlow temperatures is generally recognized. Considerable interest attaches to the ability of higher plants to withstand such conditions [92]. Figure 1 shows European black currant bushes, grown from grafts, which were hardened at  $-253^{\circ}$  or  $-195^{\circ}$  C [155, 156]. Cell cultures from malignant tumors have also been found to be extremely resistant. The preservative capacity of low temperatures has been reflected in the widespread storage of collection cultures in liquid nitrogen, in hermetically sealed refrigerators. The combination of very low temperature (liquid helium) with evacuation of the test tube containing the microorganisms to  $10^{-7}$  mm Hg has a particularly favorable effect.

The ability to withstand a temperature of absolute zero ( $-273^{\circ}$  C) may be considered proved. However, there are no data to indicate how long such a temperature can be withheld

by living objects; extrapolation could be made on the basis of these observations: in rapid freezing of bacteria in collected milk and subsequent dehydration at 77–100 mm Hg, bacteria retained their viability after 10 years.

Freezing influences retention of viability considerably, but in this regard, there are no characteristics common to all biological objects. With very rapid freezing to very low temperatures, a number of the viable cells are preserved in individual cases, while others require initially



FIGURE 1.—Black currant bushes (*Ribes nigrum* L.) grown from grafts cooled to  $-195^{\circ}$  C (center) or  $-253^{\circ}$  C (left) with control (right) [48].

TABLE 1.—*Superlow Temperatures Withstood by Various Organisms*

Temperature, °C	Objects	Reference
$-252^{\circ}$	Microscopic fungi, yeasts, bacteria	[105]
$-273^{\circ}$	Species of bacteria	[13]
$-269^{\circ}$ to $-271^{\circ}$	Spores of bacteria and fungi, seeds of higher plants	[10, 11]
$-190^{\circ}$	<i>Staphylococcus aureus</i> , <i>Salmonella typhi</i> , <i>Bacillus subtilis</i>	[161]
$-269^{\circ}$	Human spermatozoa	[83]
$-269.5^{\circ}$	Spirochetes and trypanosomes	[83]
$-197^{\circ}$	<i>Treboxia erici</i> (from lichen)	[110]
$-197^{\circ}$	Protozoa, <i>Anguillula aceti</i> (vinegar eel)	[59]
$-253^{\circ}$	European black currant, birch	[155, 156]
$-75^{\circ}$	<i>Aerobacter aerogenes</i>	[163]
$-272^{\circ}$	Dried rotifers	[84]
$-195^{\circ}$ to $-209^{\circ}$	<i>Morus lombrycis</i> (mulberry)	[132]
$-195^{\circ}$	<i>Porphyra yezensis</i>	[152]
$-195^{\circ}$	<i>Trichinocamus populi</i>	[151]
$-150^{\circ}$	<i>Escherichia coli</i>	[115]

gradual cooling to not very low temperatures and then rapid cooling to ultralow temperatures. As for thawing, rapid thawing insures preservation of more living cells than does slow thawing. Depending on the means of freezing and the nature of the biological object, from 10%–70% of the cells remain alive following exposure to ultralow temperatures. In contrast to single freezing at ultralow temperatures, alternate multiple freezing and thawing leads to the death of a great many of the objects under study. In this connection, a method of sterilizing soil has been proposed which has the advantage of physical and chemical properties of the soil changing less than when sterilization is done by means of an autoclave.

There is dehydration of the cells under ultralow temperatures [102]. If the water freezes, forming crystals outside the cell, this creates favorable conditions for living organisms, but when biological objects freeze, crystals may develop inside the cells causing their death. At the beginning of thawing or the end of cooling a

living organism, recrystallization may be observed during which many large crystals of water appear inside the cell (Fig. 2). Electron-microscopic study of objects has revealed cavities or spaces containing ice crystals.

The least damage is observed in vitrification, where individual ice crystals are not found, but all of the water congeals, retaining its amorphous state. If the cells have a small relative surface, for example in bacteria, vitrification is usually observed and no crystals develop inside the cells. The finer mechanism of the effect of freezing is interesting. Denaturing the protoplasm leads to a higher content of salts in the cell, has an effect on the spatial position of the molecules, and affects separation of hydrogen bonds and formation of SH or SS bonds. In the final analysis, denaturing and conformational changes may occur in protein complexes.

The instantaneous action of low temperatures may cause mutational variability. Such temperature shocks produce, in particular, the well-known mutations in *drosophila* and microorganisms.

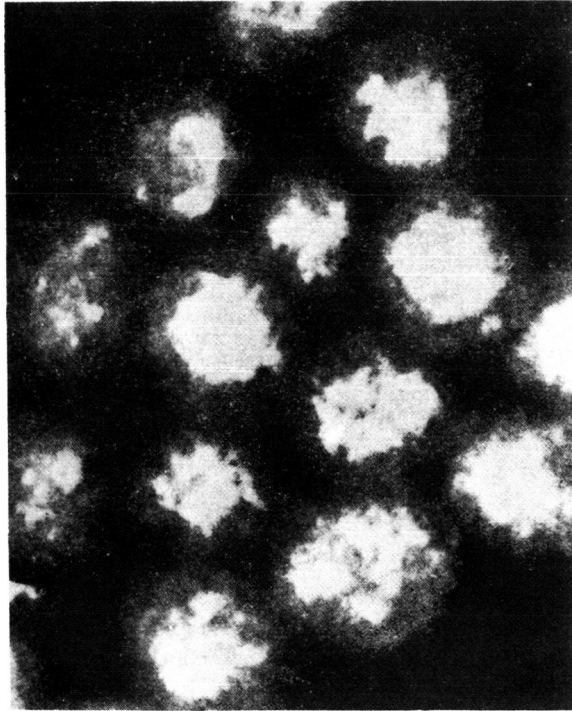


FIGURE 2.—Recrystallization of water in dormant spores during rapid cooling [35].

### Life at Low Temperatures

The ability to produce a great deal of heat explains why certain homiothermic animals can obtain food and reproduce at low temperatures from  $-20^{\circ}$  to  $-50^{\circ}$  C. This is true of penguins, polar bears, and others. In contrast, the higher plants and poikilothermal animals usually cannot survive at very low temperatures. However, the ability to live and multiply at temperatures from  $+5^{\circ}$  to  $-2^{\circ}$  C is characteristic of many marine plant and animal organisms. Their number is enormous if it is taken into account that 90% of the water in the World ocean is at this temperature. Psychrophilic microorganisms growing at temperatures from  $-6^{\circ}$  to  $-9^{\circ}$  C have been found in the waters of the North and South Arctic Ocean.

Nival (snow) flora and fauna which live in the Himalayas at altitudes of 6000 meters are also capable of existing at  $-5^{\circ}$  C, even at  $-17^{\circ}$  C, without becoming anabiotic. This is true of the beetle *Astagobius angustatus*, the snowfly (*Chiona*), several species of needletails and spiders

(*Hypogastra*, *Poistoma*). The red or orange coatings which cover snow or glaciers are formed by accumulations of algae (*Chlamydomonas nivalis*), red yeasts (*Rhodotorula*) and microscopic fungi [6, 47]. These microorganisms can also multiply at temperatures below  $-5^{\circ}\text{ C}$ . It is much more difficult to determine the ability to live and grow at low temperatures than to establish the resistance of an organism to a single exposure at very low temperatures.

In studying the growth of microorganisms, any liquid or solid nutrient medium will freeze when the temperature drops. The freezing point of the nutrient medium may be lowered by sharply increasing the content of salts or sugars in the medium, which may be favorable for studying the growth of halophilic or osmophilic microorganisms. It must be added that as the temperature decreases, there is a significant drop in the rate of cell reproduction. Physiological activity can also be evaluated on the basis of ability of the cells to move about in the liquid medium. A reliable indicator also is the study of photosynthesis at low temperatures.

Data on physiological processes at low temperatures are in Table 2, which permit these conclusions:

1. In both conifers and lichens, photosynthesis is definitely possible at  $-20^{\circ}\text{ C}$ , and perhaps at still lower temperatures.
2. From discussion in the scientific literature, it can be concluded that the minimum temperature at which growth of microorganisms is possible is  $-12^{\circ}\text{ C}$ . Reports of growth at lower temperatures would best be considered unproven, although an exception is *Dunaliella salina* which, as a halophilic form, may be found in solutions of sodium chloride cooled to  $-15^{\circ}\text{ C}$ .

Reports in the literature also state that red yeasts and microscopic fungi have grown, and the latter have formed spores, at temperatures from  $-34^{\circ}$  to  $-44^{\circ}\text{ C}$ . (These data have not been included in the table.)

The ability of high-mountain fauna and flora to remain viable at minus temperatures has already been described. Natural adaptation to other

ecological conditions has taken place simultaneously. These organisms are more resistant to the action of UV radiation, low atmospheric pressure, and periodic temperature changes that occur in night and day, as well as low atmospheric humidity. The soil of Antarctica also contains low moisture which sometimes does not exceed 10%. All of these conditions bear a certain degree of similarity to those on Mars. However, any part of the Earth is not as harsh as the living conditions on Mars.

### High Temperature

There is no ecological factor to which living organisms have adapted as exclusively as to low and high temperatures. It must apparently be considered proven that life is possible within limits from  $-12^{\circ}$  to  $+80^{\circ}\text{ C}$ . Accordingly, lethal high temperatures can vary markedly. Fish that live in Antarctic waters of a temperature of  $+2^{\circ}\text{ C}$ , will die in water at  $+6^{\circ}\text{ C}$ . The majority of nonsporeforming bacteria lose their vital capacity at  $60^{\circ}\text{ C}$  in the course of 10 min. Sporeforming bacteria, which are very resistant to desiccation and moist sterilization, usually can withstand  $150^{\circ}$ – $160^{\circ}\text{ C}$  for 30 min during dry sterilization and will die at  $120^{\circ}\text{ C}$  after being autoclaved for 1 h. However, dry heat at  $180^{\circ}\text{ C}$  will kill all sporeforming bacteria.

The higher the temperature, the sooner all the cells will die. Thus, spores of thermophilic *Bacillus stearothermophilus* die at  $120^{\circ}\text{ C}$  in 100 min, and in 1 min at  $188^{\circ}\text{ C}$ . The more resistant the cells are to drying, or the less water they contain, the more resistant they are to heat. This may explain precisely why dried rotifers die only at  $170^{\circ}$ – $200^{\circ}\text{ C}$  after being exposed for 5 min.

It is not simple to show that all bacterial spores died during sterilization. First, spores grew 10–15 d after seeding following heat treatment. Second, the chemical composition of the nutrient media influences the number of germinating spores, especially certain amino acids. Hence, it is not possible to demonstrate the sterility of a sample under examination by using only standard nutrients for the cultures, if these media are of incomplete composition.

The resistance of microorganisms to high tem-

peratures is influenced by many factors: total numbers of cells in the sterilized material; age of the cells and stage of their development; composition of the nutrient medium on which the microorganisms are grown; amount of water in the cells; hydrostatic pressure, and others. The sterilizing effect of high temperatures is discussed in greater detail in Chapter 9 of this volume, "Planetary Quarantine, Principles, Methods, and Problems," which discusses the sterilization of spacecraft.

Thermophilic microorganisms, which are widely distributed in nature, are found in hot springs with various water composition, and in piles of organic matter (peat, hay, manure), where the temperature rises sharply from their vital activity. Thermophiles were formerly believed to be primarily sporeforming bacteria and actinomycetes, but it was shown later that there are also thermophilic blue-green algae and non-sporeforming bacteria. Geysers are usually inhabited by microorganisms which, after a pure culture has been isolated, will grow on nutrient media at temperatures from 60° to 75° C depending on the species.

Slides submerged in water of hot springs show growth of flexibacteria cells after 10 d at 93.5°–95.5° C. Foulings formed by the cells of the true bacteria have been found in water at 85°–88° C. Pure cultures of thermophiles will not grow in nutrient media at such high temperatures. Assimilation of carbon dioxide by hydrogen

bacteria has been confirmed by means of carbon dioxide labeled at the carbon; these bacteria live in geyser water at 73° C. Thermophilic sulfate-reducing bacteria have been isolated from cores taken from depths of 4000 m, where the temperature reached 105° C; these cultures grew at 65° C.

Thermophiles can multiply at high temperatures, which is associated with adaptation to altered life conditions created by high temperature. There is considerably less oxygen in the water of hot springs, greater solubility of various substances, a more pronounced unfavorable effect of harmful chemical compounds, and all biochemical processes involved in vital activity are sharply accelerated. Generation time in thermophiles at 70° C is 13–14 min, while for *Bacillus stearothermophilus* it is 10–11 min. Correspondingly, the lifetime is shortened and autolysis of cells begins earlier. Observations indicate that when water salinity is increased or osmotic pressure rises, bacteria can grow at higher temperatures. At pressures of 1000 atm, sulfate-reducing bacteria can grow at 104° C.

Reports on the action of high temperatures on living organisms indicate that at the temperature on Venus (400° C), life is completely impossible. It is sometimes assumed that the great amount of clouds on Venus consist of water, have considerably lower temperatures, and may contain unicellular microorganisms capable of reproducing under these conditions. This assumption is less than likely, but it cannot be completely

TABLE 2.—Physiologic Processes in Different Organisms at Low Temperatures

Temperature, °C	Organism	Vital activity, indication	Reference
–20° to –40°	Lichens, conifers	Photosynthesis	[88]
–24°	<i>Geotrichum candidum</i>	Growth	[14]
–7.5°	Bacteria on the surface of fish	Growth	[12]
–12.2°	Microscopic fungi on frozen raspberry	Growth	[8]
–12°	Bacteria and microscopic fungi	Growth	[87]
–17.8°	Microscopic fungi, yeasts	Growth	[87]
–15°	<i>Pyramimonas</i> , <i>Dunaliella salina</i>	Movement in liquid	[165]
–20°	Bacteria	Growth and luminescence	[129]
–30°	Algae	Photosynthesis	[85]
–20° to –24°	Insect eggs	Development	[160]
–18° to –20°	Microscopic fungi, <i>Pseudomonas</i> (in fruit juice)	Growth	[16]
–18°	<i>Aspergillus glaucus</i> "red yeasts"	Growth in glycerine	[16]
–30°	Lichens	Photosynthesis	[140]

rejected, since reproduction of microorganisms in a fog of very fine nutrient medium droplets has been demonstrated.

### VACUUM

Very low pressure is a typical extreme factor in space; its influence on biological objects was not studied before the development of space biology. However, the best instruments still cannot produce the vacuum in space which is about  $10^{-16}$  mm Hg. The vacuums that are created usually do not rise above  $10^{-9}$  or  $10^{-10}$  mm Hg. Experiments with greater vacuums might provide new results, but the vacuum that can be created with existing apparatus suffices to provide some idea of the effect.

In ordinary devices, the influence of the vacuum (for technical reasons) usually is combined with simultaneous exposure to low temperatures,  $-23^{\circ}$  to  $-35^{\circ}$  C. In other devices [28] with different designs, temperature can be established between  $-190^{\circ}$  and  $+120^{\circ}$  C. The experiments may vary from several days to several years.

The retention of viability is usually studied in highly diverse microorganisms and some protozoa and viruses following exposure to a vacuum. The influence of the vacuum on certain physiological processes in microorganisms and certain enzymes has also been studied. Most of

the high-vacuum studies are shown in Table 3, the data of which are reviewed here.

1. All sporeforming bacteria retained viability at high vacuum and low temperature not only for days but for 5 years. These results were obtained in the majority of the studies and only two reported the death of spores. Spores of *B. subtilis* are 10 times more resistant than vegetative cells.
2. Nonsporeforming bacteria are less resistant, their deaths varying within wide limits of 4.7%–95%, and in 4 species of yeasts from 0.64% to 33.9%. Under high-vacuum conditions and low temperature, cells are better able to retain their viability than in laboratory desiccators, therefore the viability of experimental microorganisms in comparison with controls may reach 147%.
3. The high resistance to vacuum by various algae, conidia of *Aspergillus*, and mycelia of fungi (lacking spores or conidia) was quite unexpected. There is only one report of death of the conidia of *Penicillium*. Under the influence of vacuum, the titer of various bacteriophages decreased from  $3 \cdot 10^{-7}$ – $1 \cdot 10^{-9}$  to  $1 \cdot 10^{-7}$ – $5 \cdot 10^{-7}$ , i.e., by 2–4 orders. Protozoa retained viability for a long period.

TABLE 3.—Effect of a Vacuum on Microorganisms

Organism	Vacuum	Temperature, °C	Duration, d	Results	Reference
<i>B. subtilis</i> , <i>Bacillus cereus</i> , <i>B. mycoides</i> , <i>A. niger</i> , <i>Aspergillus flavus</i> (Lyophilized spores of bacteria and conidia of <i>Aspergillus</i> )	$1 \times 10^{-5}$ – $5 \times 10^{-7}$ mm Hg	—	2, 4, 7, 16, 32	All microorganisms re-tained viability except <i>B. cereus</i> , which died after 32 d in a vacuum	[128]
<i>B. subtilis</i> , <i>Myco-bacterium smegmatis</i> , <i>Aspergillus fumigatus</i>	$5.0 \times 10^{-9}$ – $3.6 \times 10^{-10}$ mm Hg	$+23^{\circ}$ to $+24^{\circ}$	5	Did not die	[127]
<i>B. subtilis</i> , <i>A. niger</i> , <i>Aspergillus terreus</i> , <i>Penicillium citrinum</i>	$1 \times 10^{-6}$ – $6 \times 10^{-9}$ mm Hg	—	10, 30 40 45	Only conidia <i>P. citrinum</i> died after 10 d, all microorganisms died after 30 d	[19]

TABLE 3.—Effect of a Vacuum on Microorganisms—Continued

Organism	Vacuum	Temperature, °C	Duration, d	Results	Reference
<i>B. subtilis</i> var. <i>niger</i>	$1 \times 10^{-8}$ – $6 \times 10^{-9}$ mm Hg	—	35	Spores remained viable	[112]
<i>Bacillus megaterium</i> , <i>B. subtilis</i> var. <i>niger</i> , <i>B. stearothermophilus</i> , <i>Clostridium sporogenes</i> , <i>A. niger</i>	$1 \times 10^{-8}$ – $1 \times 10^{-10}$ mm Hg	–190° to +120°	4 & 5	At –190° and –110°C and in a vacuum they survive; at +60° death sharply increases; 40% of <i>B. subtilis</i> var. <i>niger</i> , and 25% of <i>A. niger</i> survive	[28, 29]
<i>B. subtilis</i> var. <i>niger</i> , <i>Mycobacterium phlei</i> , <i>A. niger</i>	$1 \times 10^{-7}$ – $1 \times 10^{-10}$ mm Hg	+25°	140	Significant number of microorganisms survived	[44, 45]
<i>Sarcina flava</i> , <i>Brevibacterium linens</i> , <i>B. subtilis</i> , <i>B. mesentericus</i> var. <i>niger</i> , <i>B. mycoides</i> , <i>B. megaterium</i> , <i>Arthrobacter simplex</i> , <i>Aspergillus oryzae</i>	$1 \times 10^{-9}$ mm	–23° to –35°	3	Viability depends on the species and varied from 57.5% to 147% <sup>1</sup>	[67]
<i>S. flava</i> , <i>Pseudomonas pyocyannea</i> , <i>P. fluorescens</i> , <i>E. coli</i> , <i>Serratia marcescens</i> , <i>B. linens</i> , <i>B. subtilis</i> , <i>B. mesentericus</i> , <i>B. mesentericus</i> var. <i>niger</i> , <i>B. mycoides</i> , <i>B. megaterium</i> , <i>A. simplex</i> , <i>Vibrio metchnikovii</i> , <i>A. oryzae</i> , <i>Chaetomium globosum</i> , <i>Fomes fomentarius</i> , <i>Coriolus pubescens</i>	$1 \times 10^{-8}$ – $1 \times 10^{-9}$	–23° to –35°	3	13 of 17 species did not die; their viability varied 0.34%–147% <sup>1</sup> vegetative mycelia of the fungi showed growth; these died: <i>V. metchnikovii</i> , <i>S. marcescens</i> , <i>P. fluorescens</i>	[68]
<i>Saccharomyces vini</i> , <i>Saccharomyces rouxii</i> , <i>Torulopsis aeria</i> , <i>Candida tropicalis</i> , <i>Rhodotorula rubra</i>	$1 \times 10^{-9}$ mm Hg	–23° to –35°	3	Viability depends on species and varied 0.64%–33.9%	[63, 69, 96]
<i>Streptococcus faecalis</i> , <i>S. aureus</i>	$1 \times 10^{-9}$ – $1 \times 10^{-10}$ mm Hg	+4° to +80°	5	Number of living cells decreases as a function of temperature increase; 4%–10% present at 40°	[142]
<i>E. coli</i>	$1 \times 10^{-1}$ – $1 \times 10^{-6}$ mm Hg	—	—	1% cells survived; inactivation of cells by UV and x-rays in vacuum increased	[22]

See footnote at end of table.

TABLE 3.—Effect of a Vacuum on Microorganisms—Continued

Organism	Vacuum	Temperature, °C	Duration, d	Results	Reference
<i>E. coli</i>	$2 \times 10^{-6}$	—	—	At 1 mm Hg pressure or less, cellular division was inhibited and radiosensitivity of the cells increased	[61]
<i>Chlorella vulgaris</i> , <i>Zyngbia aestuarii</i> , <i>Scenedesmus acuminatus</i> , <i>Mastigocladus laminosus</i> , <i>Amorphonostoc punctiforme</i>	$1 \times 10^{-8}-1 \times 10^{-9}$ mm Hg	-23° to -35°	3	All the algae retained viability	[72, 73]
Phages of <i>E. coli</i> , T2, CgF 74, f-2	$1 \times 10^{-8}-1 \times 10^{-9}$ mm Hg	-23° to -35°	3	Inactivation of phages in vacuum varied $3 \times 10^7-1 \times 10^9$ to $1 \times 10^5-5 \times 10^7$	[75]
Desert soil containing aerobic, anaerobic, microaerophilic bacteria, fungi, algae, and protozoa were subjected to the action of a vacuum	$1 \times 10^{-6}-1 \times 10^{-8}$ mm Hg	4° 20° 55°	4 years 5 years	After 4–5 years the number of viable aerobes and micro-aerophilic bacteria decreased; number of algae decreased from $10^6$ to $10^2$ /g soil; after 4 years, protozoa retained viability but died after 5 years	[24]
<i>E. coli</i> , <i>B. subtilis</i>	$2 \times 10^{-7}-5 \times 10^{-9}$	80°	From 1 to 7 d, from 1 to 3 h	Vegetative cells of <i>B. subtilis</i> were 10 times less resistant than spores, whose viability was 23%–56%	[62]
<i>E. coli</i>	$1 \times 10^{-1}-1 \times 10^{-10}$ mm Hg	—	—	About 95% of the cells died	[23]
<i>S. flava</i> , <i>B. megaterium</i> , <i>A. terreus</i>	$1 \times 10^{-9}$ mm Hg	+20° to -190°	21	Viability retained	[81]
<i>B. megaterium</i> , <i>B. subtilis</i> , <i>B. stearothermophilus</i> , <i>C. sporogenes</i> , <i>A. niger</i> , Soil actinomycetes	$1 \times 10^{-8}-1 \times 10^{-10}$ mm Hg	+25° to -190°	2–5	All sporeforming bacteria survived; temperature had no effect on viability; only actinomycetes survived heating to 120° C under vacuum conditions	[29, 111]

<sup>1</sup> In the vacuum and low temperature, cells retain viability better in a test than in the control, i.e., in a desiccator with usual pressure and room temperature.

4. When temperature is increased to plus values, the number of surviving microorganisms in the vacuum drops sharply, but even at 60° C, spores of *B. subtilis* and conidia of *Aspergillus niger* retain viability.
5. Microorganisms in desert soil are protected considerably against the effects of a vacuum, since various bacteria, fungi, algae, and protozoa remained alive in the soil for 4–5 years [24]. In this connection, the cells in a vacuum became more radiosensitive. Thus, at an x-ray dose of 145 kV, 1 krad/min in a single-cell layer of cells of *E. coli* at 10<sup>-5</sup> mm Hg kills more bacteria than at 760 mm Hg

[139, 140]. (See Figure 13 in a subsequent section, under IONIZING RADIATION.)

In a vacuum, the effect of UV-rays (245 nm) on bacteria is more pronounced than at normal pressure, and photoreactivation of the cells becomes impossible following vacuum exposure. If pressure is increased, cell division is inhibited. In short, these are the actual data on the effect of a high vacuum (Table 4). Yet very little is known about the mechanism of its action, and it is not possible to assume complete dehydration of the cells under these conditions. This would require determination of the bound water with the aid of nuclear magnetic resonance. A description of the cytological changes would be simplified

TABLE 4.—Effect of High Vacuum on the Oxidation Capacity, Resistance of Iron Porphyrin Enzyme and ATP of Microorganisms<sup>1</sup>

No. of experiment	Organism	Vacuum	Temperature, °C	Oxidation of glucose and alcohol	Iron porphyrin enzymes		Activity of ATP on subcellular level	Reference
					On cellular level, %	On subcellular level, %		
1.	<i>S. flava, A. simplex</i>	1 × 10 <sup>-3</sup> –1 × 10 <sup>-10</sup> mm Hg	–23° to –35°	Oxidation capacity retained; <i>A. simplex</i> oxidizes glucose and ethyl alcohol more intensively than <i>S. flava</i>	—	—	—	[74]
2.	<i>S. flava, S. marescens, A. simplex, S. rouxii</i>	1 × 10 <sup>-8</sup> –1 × 10 <sup>-9</sup> mm Hg	–23° to –35°	—	93 78 93 87	78 70 68 68	—	[79]
3.	<i>S. flava, S. marescens, A. simplex, S. rouxii, C. tropicallis</i>	1 × 10 <sup>-8</sup> –1 × 10 <sup>-9</sup> mm Hg	–23° to –35°	—	—	—	95 101 100 92 89	[77]

<sup>1</sup> Duration of experiment: 3 d; activity in the control assumed to be 100%.

by experimenting with a well-studied cytological model such as the yeast cell.

Some data indicate that bacteria retain the ability to oxidize glucose and ethyl alcohol following a stay in a vacuum. ATP in three species of bacteria and one species of yeast is not inactivated by a high vacuum. Cells may lose ATP from boiling or disintegration; in either instance, following a stay in a vacuum, this may be detected by luminescence. In these species, activity of the iron porphyrin protein following exposure to the vacuum is decreased 14%–32% (the control is assumed to be 100%). The resistance of cells to high vacuum is in complete agreement with the fact that the vacuum has almost no inactivating effect on trypsin, peroxidase, cytochrome C, or ATP, and reduces activity of catalase, ribonuclease,  $\alpha$ -amylase, and urease to a comparatively insignificant degree (Table 5).

Although unicellular organisms are relatively resistant to high vacuum, there are no data on the possibility of growth under these conditions. Theoretically, such a possibility would clearly be excluded. It can be assumed that bacteria spores in a micrometeorite, which protects them against solar radiation, could retain their viability in space.

The effect of a high vacuum is of great interest to space biology. Various living organisms in the soil have survived under high vacuum conditions for 4–5 years, which indicates that the vacuum does not have a sterilizing effect. This cannot be the cause of rapid death of microorganisms on the surface of Mars or the Moon, which is confirmed

by detection of microorganisms on the Moon brought there previously by spacecraft. It is also obvious that microorganisms on the surface of spacecraft in flight through space will be kept viable under vacuum conditions. Resistance to high vacuum makes it understandable that, with comparatively slight decrease in pressure (4.5–7.6 mbar), many microorganisms can reproduce very well.

## PRESSURE

Mud of the Pacific Ocean is inhabited by various microorganisms subjected to 1000 atm pressure. The area of the globe occupied by oceans and their depths makes it necessary to conclude that high pressure is unquestionably one of the most widespread ecological factors acting on various animals and plants. Studies have been pursued for 100 years on the resistance of cells to single exposure to high pressure, and the influence of the high pressure on growth and physiology of various species of microorganisms. These studies have progressed in two directions. First, the influence of high hydrostatic pressure has been investigated under laboratory conditions as it applies to various microorganisms. Modern presses make it possible to study pressures of 50 000 atm or more. The second direction involves raising samples of mud from the deep ocean bottom and determining the physiological features of the microorganisms living in the mud. All other living creatures inhabiting dry land, except bacteria, microscopic fungi, actinomycetes, and algae, perish rapidly at high pressure.

TABLE 5.—*Effect of High Vacuum on Crystalline Enzymes, Cytochrome C and ATP<sup>1</sup>*

Vacuum	Results of Activity, %								Reference
	$\alpha$ -amylase	Trypsin	Urease	Ribo-nuclease	Catalase	Peroxidase	Cytochrome C	ATP	
$1 \times 10^{-8}$ – $1 \times 10^{-10}$ mm Hg	51	103	65	79					[71]
$1 \times 10^{-8}$ – $1 \times 10^{-9}$ mm Hg					88 69 82	86 79 —	98 69 63	97 97 99	[76]

<sup>1</sup> Duration of experiment 3 d at  $-25^{\circ}$  to  $-35^{\circ}$  C; activity in the control assumed to be 100%.

The resistance of microorganisms to a single exposure of high hydrostatic pressure has been shown repeatedly [95, 161, 177, 178, 179]. The results of these experiments in Table 6 permit these conclusions:

1. Various species of microorganisms possess different degrees of sensitivity to high pressure. Thus, yeast (*Saccharomyces cerevisiae*) at a pressure of 7000 atm dies in several seconds, while not all spores of *B. subtilis* die at a pressure of 17 600 atm for 75 h.
2. The higher the pressure and the longer the exposure, the more pronounced the

effect of high hydrostatic pressure. Thus, in a single exposure to 3750–7500 atm pressure, nonsporeforming bacteria retained their viability. When the exposure was lengthened to 1.5–3 h, pressures above 3000 atm were sufficient to kill these species.

3. In the majority of cases, Table 6 shows only the maximum pressure used which led to the death of cells; at lower pressures (200–400 atm), microorganisms showed only inhibition of growth.

Under high pressure, cultures of various bacteria (*E. coli*, *Pseudomonas*, *S. marcescens*)

TABLE 6.—Resistance of Microorganisms to High Pressure

Organisms	Pressure, atm	Duration of exposure	Results	Reference
<i>Micrococcus agilis</i> , <i>S. aureus</i> , <i>Thiosarcina rosea</i> , <i>Bacterium pyocyanum</i> , <i>Bacterium prodigiosum</i> , <i>S. typhi abdominalis</i> , <i>Corynebacterium pseudodiphtheriae</i> , <i>Mycobacterium tuberculosis hominis</i> , <i>Bacillus anthracis</i> , <i>Vibrio comma</i> , <i>Oidium lactis</i>	3000	4 h to 4 d	Did not die	[25]
<i>S. marcescens</i> , <i>Streptococcus lactis</i> , <i>Aerobacter aerogenes</i> , <i>P. fluorescens</i>	2040–3060 3400–4220 5780–6800	60 min 40 min 4 min	All died	[60]
<i>Saccharomyces cerevisiae</i> , <i>Saccharomyces albicans</i>	2040–2380 3674–4080 5780	60 min 10 min 5 min		
<i>B. subtilis</i>	3000–12 000	14 h	Did not die	[99]
<i>B. subtilis</i>	17 600	75 h	Some died	[7]
<i>S. cerevisiae</i>	7000	Several s	All died	[104]
30 sp bacteria	600	2 d	Many survived	[173]
56 sp bacteria	1000–2000	Min to several years	33 cultures died	[173, 174]
63 sp bacteria	600	4 d	23 cultures died	[119]
Deep-water mud, containing microorganisms	800		Reproduction inhibited	[93]
Sporeforming bacteria in milk	1000	9 min	Viability retained	[154]
Mixed microflora from deep water mud	400	18 mo; reinoculated after 1–2 mo	Normal growth	[26]

formed long threads reaching 200  $\mu\text{m}$  which may be considered the result of inhibited cell division. The transition to normal pressure led to breakdown of the threads into fragments. DNA was found only at the ends of the threads, but its content in the cell at atmospheric pressure remained normal.

There is not uniform opinion concerning the dimensions of the cells. The size of the cell decreases, according to some data, while other data indicate that it increases. As the hydrostatic pressure rises, various physiological characteristics of the microorganisms change. Initially, reproduction is suspended, while mobile forms, for example *Pseudomonas aeruginosa*, retain active mobility even after exposure to pressure of 12 000 atm. Those cells with suspended reproduction do not lose respiratory ability while glucose, mannose, fructose, malate, lactate, succinate, or other substances are present. Respiration was lost in *P. aeruginosa* after pressure of 800 atm for 30 min [68].

The establishment of maximum tolerable pressure is quite complex. Evidently nonsporeforming bacteria which retain viability after exposure to 600–1000 atm for 3–4 d may be included among the barotolerant forms. In comparison with bacteria, algae are somewhat more resistant; *Chlorella pyrenoidosa* began a slower rate of reproduction only at 500 atm; *Hydrodictyon reticulatum* proved somewhat less resistant. After 26 hours' exposure to 400 atm, the yield decreased 50%. At prolonged pressures of 100–200 atm, the multiplication rate of *Chlorella* increases [149]. In the study of temperature influence on bacteria resistance to high pressure there is no clear picture. In isolated experiments involving temperature increases to 40° C, the number of species that grew under a pressure of 400 atm decreased markedly, while in others, as the temperature rose, the unfavorable influence of high pressure on growth decreased.

The properties of certain food products change during sterilization and heating. A number of patents have been granted which are applicable to the sterilization of such products by means of multiple exposure to high pressure. However, these sterilization methods do not apply to spore resistance and barotolerant forms.

Increased pressure may play a role as a mutagenic factor, inasmuch as mutations formed following its action on the fungus *Neurospora crassa*, which is well-known genetically [107]. After tadpoles of *Rana temporaria* have been exposed to high pressure once, they become more resistant to subsequent high pressure, it has been reported.

Under terrestrial conditions, microorganisms that grow and multiply at atmospheric or slightly reduced pressure are predominantly species that inhabit mountains at high altitudes.

A mud sample taken from the Philippine deep in 1952 at a depth of 10 000 meters was cultured, and results obtained differed as a function of the pressure employed. In cultures kept under a pressure of 1000 atm, from 16 to 100 times more bacteria grew than in the same medium at normal atmospheric pressure [176]. This was the first demonstration of barophilic bacteria growing better under high pressure. Barophilic bacteria were found in the intestines of deep-water animals, and in mud collected at a depth of 7400 m. It was also shown that deep-water denitrifying bacteria reduced nitrates at high pressure, while denitrifiers isolated from shallow water ceased to reduce nitrates at 400–600 atm pressure. A similar pattern was observed with sulfate-reducing bacteria—they failed to grow at atmospheric pressure and reduced sulfates at 1000 atm. An observation on barophilic bacteria is that culture of *Pseudomonas* sp., isolated from marine water, at 28° C and a 300–350 atm pressure, accumulated 30% more biomass than at normal atmospheric pressure [94].

However, a number of studies have yielded negative results. In similar experiments with mud collected from deep waters in another deep (the Kermadec-Tonga), no barophilic bacteria could be found; nor were there any in cultures of mud taken from the Kurile-Kashgat deep. It would not be correct, however, to doubt that there are barophilic forms in deep-lime mud.

In studying the physiology of barotolerant bacteria, it was found that some formed more organic acids by fermenting hydrocarbons at high pressure, and at the same time secreted less carbonic acid. At high pressure, the process

of decarboxylation is probably inhibited, which is concerned with formation of a great deal of acid. The influence of one physical factor generally may influence the results of action of another factor. Thus, all spores of *B. subtilis* die within 90 min at 93.6° C and 1 atm pressure, while at the same temperature but at 600 atm, 20% of the spores will survive.

### WEIGHTLESSNESS

The development of life on Earth probably took place in a primal ocean, the water containing organic substances that resulted from chemical evolution. Living matter that inhabited the water during the transition to the terrestrial form of life had to adapt to a biologically more powerful gravitation than there had been in the water. This left its impression on the entire evolution of living matter on Earth. There was a relative increase in the weight of the skeleton and marrow, as well as an increase in the amount of blood. This is confirmed by comparing these parameters in fish, amphibians, reptiles, birds, and mammals [91]. It would be erroneous, however, to state that this is the only change in animals and plants which have abandoned the ocean and taken up life on Earth. Various functions changed and gravitation became one of the conditions necessary for the normal existence of terrestrial organisms. This is confirmed by space medicine data; changes produced by weightless-

ness were observed during the flights of cosmonauts and included hypokinesia and excessive excretion of calcium related to decalcification of bone tissue. Exposure to weightlessness seems to change the physiology of the organism, requiring gradual readaptation to normal conditions of weight.

Complete weightlessness cannot be simulated experimentally on Earth. However, its action aboard spacecraft and satellites is never isolated. The clinostat made a significant contribution to the problem of weightlessness (Fig. 3). It is possible to simulate weightlessness in the horizontal clinostat [30, 48, 49]. The growth of young monocotyledonous and dicotyledonous plants has been best studied. Rotation in the clinostat combined with weightlessness cause the root of the growing plant to change its orientation, which is shown in Figure 4. Normal growth direction is deflected up to 5 h after the test.

Moistened oat seeds were placed in cylindrical blocks of agar, and the agar blocks were fastened to a clinostat combined with a centrifuge; it was shown that the threshold force of gravity equaled  $10^{-3}$  G. A plant growing on such a clinostat is shown in Figure 5. Effects are different, de-

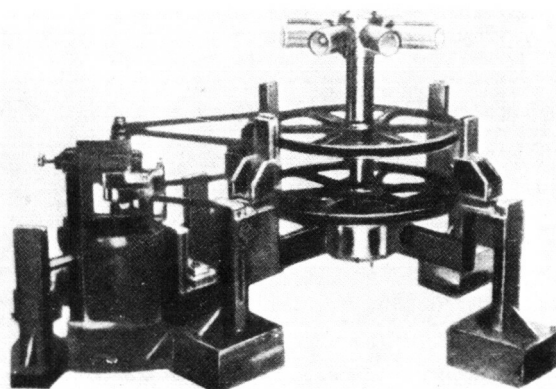


FIGURE 3.—Clinostat with reduced vibration combined with centrifuge [163].

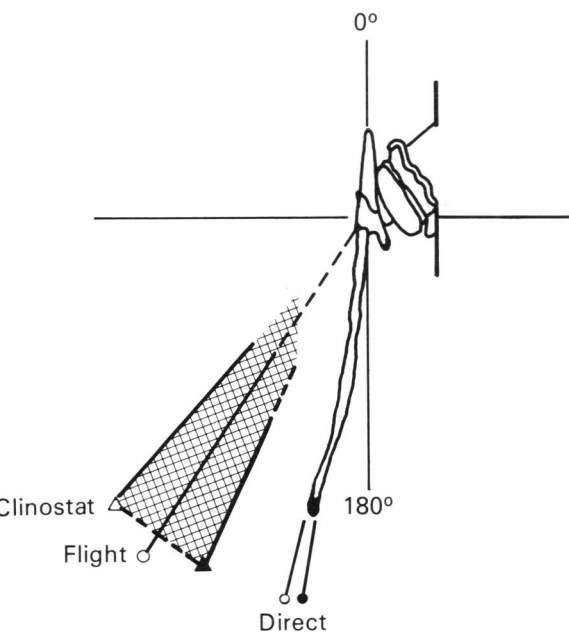


FIGURE 4.—Flight effect of Biosatellite II on orientation of primary roots [78].

pending on the size of the centrifugal force. The size of the gravitropic reaction, determined by the under- and above-Earth parts of the plants, is shown in Figure 6. Thus, some effects in plants caused by Earth gravitation can be reduced to zero with the aid of a clinostat. In particular, the usual geotropism of roots is not observed in the plants.

A comparative study of the growth of dicotyledonous plants, such as *Capsicum annuum* (pepper), aboard Biosatellite II or in a clinostat on Earth [37], indicated that in both cases all the leaves had epinasty, with the interaxial angle of a plant on a satellite reduced by 20°–60°. In wheat sprouts, orientation of the coleoptile and of the primary and secondary roots as well as cytological changes were similar, but not the same, aboard a satellite and in the clinostat [38].

A theory previously held then forgotten, that intracellular grains may play the role of statoliths which insure normal reaction to gravitation, has again acquired validity. In control plants, starch grains were found in the lower parts of cells of the coleoptile and roots, while in experimental plants (in-flight or in the clinostat), these grains were located in no particular order. In contrast to the plants, giant amoebas (*Pelomyxa cardiensis*) and fertilized eggs of the frog (*Rana pipiens*), aboard Biosatellite II, changed very little.

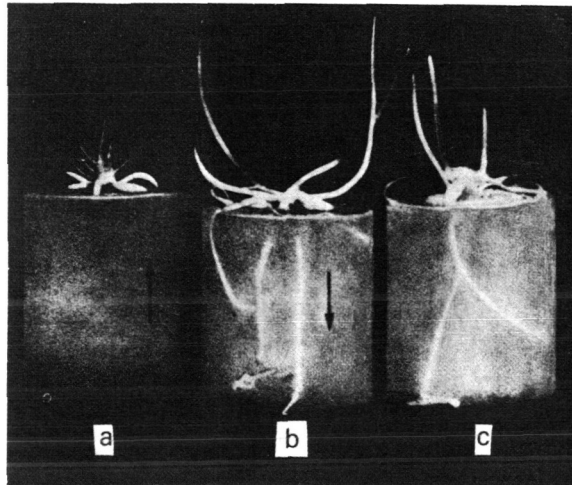


FIGURE 5.—Oat sprouts and roots grown on the centrifugal clinostat [163]. Arrows indicate direction of acceleration—0.1 G on seeds; a and b, rotation of the clinostat at 2 rpm; c, control.

The division of fertilized frog eggs that had been under conditions of weightlessness aboard the Gemini 8 and 12 spacecraft also took place normally [78, 164].

Animals that live in water are perhaps less sensitive to weightlessness than those that live on land; by living in water they become accustomed to gravitation in liquid, a characteristic which has been reinforced by evolution. Changed gravitation may also influence the results of ionizing radiation action. Thus, the secondary roots of bean sprouts (*Vicia faba*), grown in a clinostat, were subjected to x-irradiation. This led to a shift of phases in the cell cycle of the roots, increase in the number of micronuclei, change in the mitotic index, and other abnormalities [49].

Lower organisms can withstand considerable increases in gravitation quite well; the bacteria *E. coli* grow when exposed to 100 000 G for 40 d. The effect of 400 000 G on ascarid eggs for 1 h has no influence on emergence of larvae from the eggs. In more complexly organized living matter (birds, rodents), body size decreases and growth lags in comparison with controls. Rats accelerated for 4–6 hours at the 2-G level for 2–3 months showed a decrease in weight of the experimental animals, shown in Figure 7. At the same time,

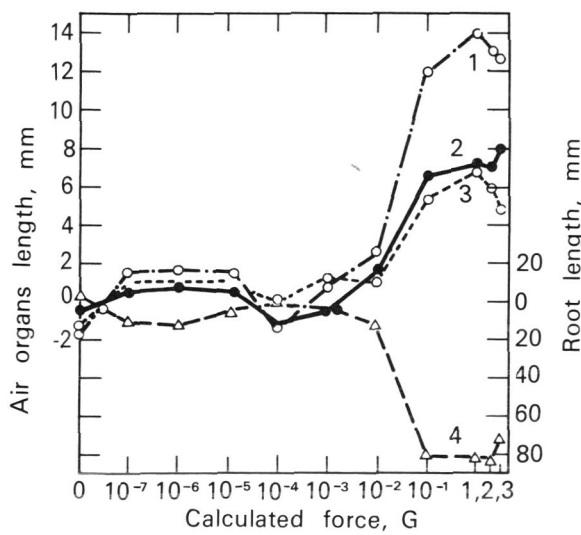


FIGURE 6.—Orientation of plants grown in a clinostat with simultaneous rotation on a centrifuge [163]. 1, sprouts; 2, coleoptile; 3, mesocotyls; 4, roots.

creatinine and total nitrogen excreted in the urine increased (Fig. 8).

### VIBRATION

Vibration is a spaceflight factor that can affect biological objects aboard a satellite or spacecraft. The intensity of the vibration varies within wide limits. The purpose of laboratory experiments on vibration is to clarify its influence on the object under study and thereby come close to interpreting the total effect produced by spaceflight factors. Studies conducted on a vibrating stand permit variation in the intensity of the vibration; an effort is usually made to simulate vibration during flight.

Experiments were carried out with a Goodman motor 8/600, frequency 5–500, maximum amplitude 12.5 mm, and maximum load 20 kg. Acceleration and amplitude were constant and the vibration was sinusoidal. Vibrations were imposed on mice examined cytologically to determine changes in marrow after 24 h. Among the experimental animals, 9.79% showed pathologic mitosis, while the controls showed only 2.61% [101]. Similar experiments with mice were under less rigorous conditions (frequency 70 Hz, amplitude  $\pm 0.4$  mm). The mice were infected with cells of Erlich's carcinoma and subjected to vibration for 7–30 min after 6 d. After the vibration was terminated, 24 h later, the ascitic fluid was fixed and the total number of anaphases and pathologic anaphases was counted by fluorescence microscopy [101]. After 15 min of vibration, pathologic anaphases were 42.3%, while the controls showed only 13.6%.

There is a basis for concluding that vibration causes restructuring of the chromosomes in mouse cells, which may have to do with agglutination of chromosomes and ultimately with incor-

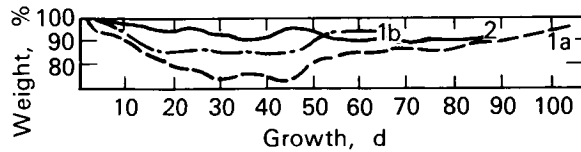


FIGURE 7.—Effect of acceleration on the weight of rats (in % of weight of control animals) [84]. 1a, 2 G; 1b, 0.8 G; (animals fed during rotation); 2, 2 G (animals not fed during rotation).

rect chromosome division. Vibration may have a favorable influence on the development and metabolism of mice. Thus, at a frequency of 70 and 1500 Hz and exposure for 1 h, there is a considerable increase in body growth of mice (Fig. 9). Vibration at 35–700 Hz with 0.4–0.05 mm amplitude increases the effect of irradiation, which is observed in lysogenic bacteria. In laboratory experiments, low-frequency vibration induces crossing over in cells of male *Drosophila*. Following exposure to vibration there is increased activity of the antigen-antibody reaction; this

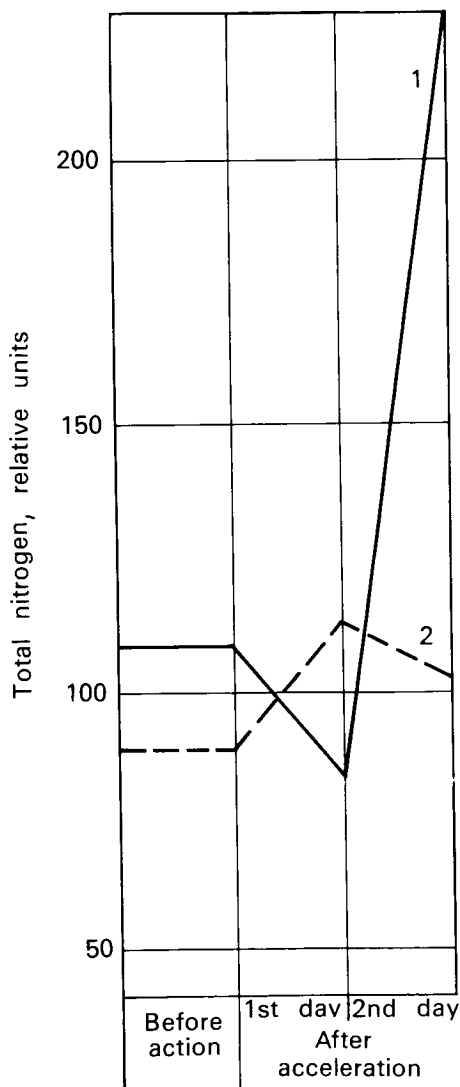


FIGURE 8.—Increase of amount of nitrogen excreted with urine by rats during acceleration [84]. Acceleration 10 G, 50 min. 1, control; 2, experimental.

effect is similar to the action of chemical mutagens or ionizing radiation. Vibration may have a definite and significant stimulating effect which leads, in particular, to sharp acceleration of the growth of onions ([31] Fig. 10).

In summary, certain conclusions can be drawn. First, vibration is one of the dynamic factors which act independently on biological objects. Second, vibration is one of the flight factors that change the effect of radiation or other influences. Thus, an increase in weightlessness removes the unfavorable effect of vibration [51]. Third, the nature of changes produced by vibration have been only slightly studied scientifically, which refers to data of cytology, physiology, biophysics, and biochemistry. The fine details of the mechanism of the action of vibration have not yet been ascertained.

### ULTRAVIOLET RAYS

Only a portion of ultraviolet radiation reaches the surface of the Earth which is shielded by water vapor, dust, and ozone in the atmosphere [133]. Microorganisms enter the air from the Earth's surface, but microflora that live in the air are constantly subjected to selection under the influence of UV-rays. The most resistant microorganisms are those whose cells contain pigments; analysis of microflora that inhabit the air reveals a considerable majority of colonies of bacteria and fungi that are colored yellow, orange, red, green, brown, purple, or black. Most of these pigments are carotenoids, while some are melanins which can protect the cell against the lethal effects of UV-radiation. Colorless (apigmented) mutants obtained in these

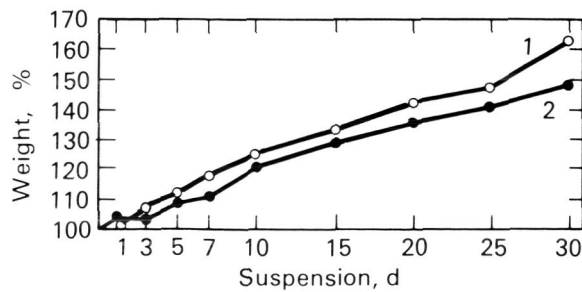


FIGURE 9.—Change of body weight in mice after vibration (170 Hz, 60 min, 10 units [7]). 1, experimental; 2, control.

cultures are far less resistant to UV-radiation than are the original form. The pigments are not secreted from the cell into its surrounding medium.

The pigmented bacteria that form pigments (primarily phenazinic) liberated by the cell into the liquid nutrient medium are not resistant to UV-radiation. The screening protection of pigments is supported by the fact that high mountain and desert soils show a wide distribution of fungi that form dark pigments, and at an altitude of 4000–5000 m they are the only inhabitants of the soil. The pigment protects the cells against increased radiation levels by absorbing the light quanta. In addition to the pigments, the protoplasts of cells of microorganisms and their cell walls contain substances which are also protective. Thus, a 2% aqueous solution of polysaccharide synthesized by *Bacillus mucilaginosum* completely protects the cells against the lethal action of radiation.



FIGURE 10.—Effect of vibration on growth of onion bulbs in a clinostat [7]. 1, experimental; 2, control.

The effect of UV-rays is better withstood by microorganisms at rest, multiplying slowly, acid-resistant, forming spores or conidia, containing ribonucleate of magnesium, wax, or lipids, and also those in a dehydrated state [40]. Sensitivity to UV-radiation varies in different but similar species. Thus, *Paramecium bursaria* is twice as resistant as *P. caudatum*. Within the limits of a single genus of yeast, *Rhodotorula*, the most resistant and most sensitive species differ from one another by a factor of 300. Resistance may be an ecological factor, inasmuch as the mountain strains of red yeasts are more resistant than forms in the valley [147]. Resistance to UV-radiation may be increased by numerous, repeated exposures to radiation, so that in this way in 2 years, *Rhodotorula* was used to produce a much more resistant form than the original [146]. During a number of years, *Bodo marina* was subjected to radiation action at a wavelength of 253.4 nm; the adapted form was able to withstand  $38.5 \times 10^3$  ergs/mm<sup>2</sup>, while the control could withstand only  $2.75 \times 10^3$  ergs/mm<sup>2</sup>.

Photoreactivation means that objects exposed to daylight following UV-radiation recover viability to varying degrees. The enzyme systems that participate in photoreactivation can carry out their function even after living objects have been irradiated with rays that do not reach the Earth's surface. The preliminary effect of cosmic radiation on higher plants does not destroy their capacity for photoreactivation after being exposed to UV-radiation [137].

Photoreactivation is accomplished with visible light (4200–5400 Å), but external conditions affect the degree of photoreactivation; thus, for example, at temperatures below the optimum for a given object, it proceeds more satisfactorily. Observations that photoreactivation can take place directly under simultaneous exposure to UV-radiation and daylight are of great interest. Thus, *P. caudatum*, irradiated for 16–18 h with doses of 1.5–40 and 120 μW (2537 Å), shows retarded division and dies after 25 d. At the same radiation level, but simultaneous irradiation with visible light (2.8–15 thousand lx), division proceeds normally for 42 d. The ability of various microorganisms to achieve photoreactivation varies markedly, but in the case of *Streptomyces*

*griseus*, photoreactivation increases viability by a factor of 300 [133].

UV-radiation with a wavelength of 2537 Å is generally recognized to have the greatest bactericidal effect. Under deep space conditions or on surfaces of celestial bodies which lack atmospheres, living cells would die rapidly from the effects of ultraviolet-radiation. However, UV-radiation can easily be cut off by very thin shields. Thus, the stony meteorite known as the Kunashak was broken up and very small cones with bases of 36 μm, 145 μm high were made from the resulting sand by adding a very small amount of clay. Spores of *B. megaterium* were added to the central portions of these cones while they were being manufactured. These cones were then subjected to UV-radiation in doses equal to that received had they been in space for a year:  $2.6 \times 10^7$  ergs/cm<sup>2</sup> to  $7.8 \times 10^8$  ergs/cm<sup>2</sup> [69].

Subsequent inoculation of the broken-up cones showed that all spores retained viability. Since it was necessary to define the possible minimum thickness of the shield, spores of *Bacillus cereus* were covered with a film of chrome, the thickness of which gradually increased [70]. If the film reached a thickness of 800 Å, the spores would not die from a dose corresponding to  $7.8 \times 10^7$  ergs/cm<sup>2</sup>. Consequently, a relatively thin layer of Martian dust would completely protect living cells from the effects of UV-radiation.

This conclusion is supported by various biological objects that have been raised to high altitudes by rockets, spacecraft, and stratospheric balloons and which died rapidly from the effect of the solar radiation. However, it was sufficient to cover them by a thin protein film to protect their viability; all of the studies that were conducted with the "Artificial Mars" confirm that microorganisms exist in the outermost layers of the soil, or, the crushed mineral limonite completely protects them against death. Several doses of UV-radiation used in these experiments were  $33.6 \times 10^8$  ergs/cm<sup>2</sup> for 3 weeks, a total dose of  $10^9$  ergs/cm<sup>2</sup> in the other experiments. With 10 xenon arc lamps it was possible to deliver a dose of 7000 ergs/cm<sup>2</sup> s<sup>-1</sup> at wavelengths from 2000–3000 Å. All of this indicates that if there are living organisms in the soil of Mars, they are

QUALITY OF THIS  
PAGE IS POOR

well-protected against the lethal effect of UV-radiation.

The luminance on Mars is 0.44 of the terrestrial solar constant. However, there is a shift on this planet in the quantum maximum of solar radiation to the shortwave region: on the Earth it is 680 m $\mu$ m and on Mars 550–565 m $\mu$ m. Wavelengths of this order on Earth are absorbed considerably by anthocyanins [148], which is precisely the way high-altitude vegetation shows an intensified absorption of radiant energy in the green and infrared regions of the spectrum. This is related, in turn, to intensification of the synthesis of anthocyanins.

### IONIZING RADIATION

Resistance to ionizing radiation and the mechanism of its action on warm-blooded animals have been discussed in Volume II, Part 3, Chapter 12, "Ionizing Radiation," of this publication. Space biology has considerable interest in lower organisms that are resistant to ionizing radiation. With an increased level in natural radiation, as the result of adaptation, resistant forms will develop [50]. Thus, microorganisms isolated from water in radioactive springs are 3–10 times more resistant to radiation than cultures extracted from water of nonradioactive springs [90]. These are inherited changes and their development is only possible at a sufficiently high, natural radioactivity level (for example, 194–362 mrad/h).

Forms that are resistant to ionizing radiation are also found in mines, where minerals contain radioactive elements. The practical activity of man is accompanied by the development of conditions under which high doses of ionizing radiation are received. Thus, the water of nuclear reactors contains forms that developed at doses of millions of rad. The development of such resistant forms is reflected in the names of such species, e.g., *Micrococcus radiodurans*.

Ionizing radiation usually cannot be listed among the factors which are dangerous to biological objects inside satellites and spacecraft [134]. Ionizing radiation inside spacecraft does not exceed 30–40 rad, even when passing through the Earth's internal radiation belt and during solar flares. There are two points of view concerning the influence of different forms of

ionizing radiation. According to one, in case of action of protons with a broad activity spectrum (50–630 MeV or  $^{60}\text{Co}$  rays), the death of yeasts will be the same (Figs. 11 and 12). Similar results were obtained with the phage *E. coli*, and cultures of animal and human tissues [123].

Supporters of the second theory feel that  $\beta$ -particles have less effect on *B. mesentericus* than  $\gamma$ -rays, while other data indicate that neutrons are less fatal to *E. coli* than x-rays. This is also supported by the fact that, to obtain mutations in *Drosophila*, the dose of neutrons must be 1.5 times greater than the dose of hard x-rays. It is important, however, that the bactericidal effect is not directly proportional to radiation intensity, but is a function of the dose expressed in roentgens per minute. This may be illustrated by the data in Table 7 [98].

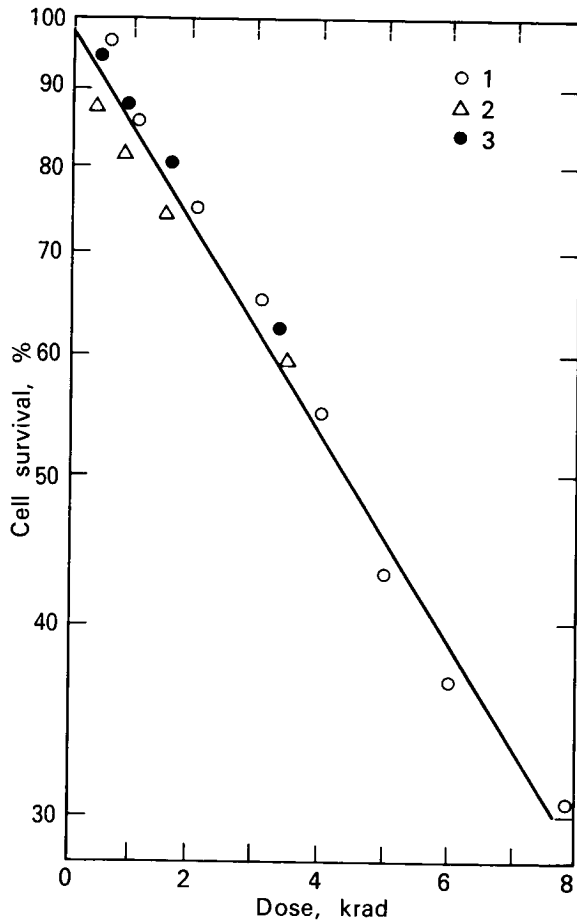


FIGURE 11.—Effect of protons on haploid yeasts (*Saccharomyces*). 1, 24 MeV; 2, 510 MeV; 3,  $\gamma$ -rays from  $^{60}\text{Co}$ .

The bactericidal effect has nothing to do with the intensity of the radiation but only with its dose. Consequently, the dose absorbed by the organism is of critical significance [98]. In studying radiation effects, the term Relative Biological Effectiveness (RBE) is frequently employed, i.e., the effectiveness of one kind of radiation in regard to another.

Unicellular organisms exposed to ionizing radiation for a long period can be subjected to the influence of a very high total dose. Thus, a culture of *P. caudatum*, when exposed to a single dose of 10 krad for 5 months, received 7000 krad, and the inhibition of division by *Paramecium* was independent of the total dose; rather, it was a reaction to the direct dose received.

The easily reproduced action of  $\alpha$ -,  $\beta$ -,  $\gamma$ -rays and neutrons does not provide the answer to the effect of the spectrum of protons with the 15–200 MeV range which are captured by the geomagnetic field [153]. Unprotected biological objects have not been directly elevated to the necessary altitude. However, it is completely feasible to study the effect of components that consist of heavy ions [109]. At an altitude of 30 km, black mice and rabbits developed areas of white fur corresponding to the track which was left after exposure to heavy ions. Histological examination of the white areas did not reveal any melanin or melanocysts, and the deep-lying hair follicles had vanished.

The resistance to ionizing radiation is in-

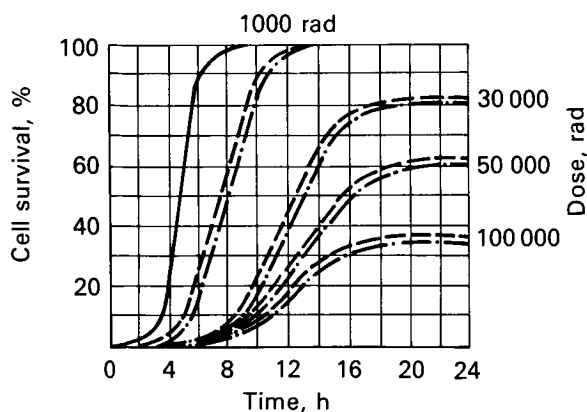


FIGURE 12.—Inhibiting action of 630 MeV protons and  $\gamma$ -rays on mitosis in yeasts [130].

fluenced by a great number of factors. The resting stages, particularly spores of bacteria, are much more resistant than vegetative cells, which is precisely one of the factors preventing the use of ionizing radiation for spacecraft sterilization. Algae cells are quite resistant; thus,  $\gamma$ -rays in doses of  $2.45 \times 10^6$  rad have a lethal effect on *Microcoleus*, *Phormidium*, and *Synechococcus*. The nonpigmented forms of *Gliocladium fimbriatum* are more sensitive to  $\gamma$ -rays than all the pigmented, darkly colored strings of the fungus, which is difficult to explain when discussing ionizing radiation [108]. Cultures of microorganisms in the exponential phase of growth are more sensitive to radiation than when in the lag phase, stationary phase, or slowing-of-growth phase. Conditions under which the organisms existed before, during, or after irradiation have considerable influence on the results. Thus, under conditions which lead to decrease in molecular oxygen during x-irradiation, the resistance of organisms rises.

Irradiation at low temperatures decreases the lethal action of ionizing radiation. This has been proven by many observations. Yeasts are more resistant at  $-33^\circ\text{C}$ , the action of  $\gamma$ -rays on spores of *Phycomyces nitens* and cells of *Salmonella schottmuelleri* is weaker at  $-192^\circ\text{C}$ . Sensitivity of *B. megaterium* spores decreases as a function of temperature decrease from  $+37^\circ$  to  $-195^\circ\text{C}$ . Other studies established the protective action of deep cooling on radioreistance of seeds of various plants, spores of lower fungi, yeast, bacteria, and certain tissue cultures.

The movements of ions and radicals are decreased in the frozen state, so that radiation

TABLE 7.—Effect of X-Rays on *B. mesentericus* Spores [98]

Rays	Intensity, R/min	MLD,R (37% of living cells remain)
X-rays, 8 Å	$6.24 \times 10^3$	$1.5 \times 10^5$
	$6.02 \times 10^4$	$1.2 \times 10^5$
	$7.70 \times 10^5$	$1.7 \times 10^5$
X-rays, 0.15 Å	65	$5.6 \times 10^3$
	209	$5.7 \times 10^3$

resistance of bacteria increases by a factor of 9, in comparison with resistance of bacteria at the same temperature but in a liquid medium. This involves the temperature at which water changes to ice. The influence of external conditions on radiation resistance may be illustrated by *E. coli* being more resistant to ionizing radiation under anaerobic conditions by a factor of 3 (Fig. 13), by 2.5 times in the presence of cysteine, by 3–6 times when cells are frozen in air, and by 10–12 times during freezing in the absence of oxygen. Dried cells of organisms are less sensitive to radiation than those which contain the normal amount of water. Increasing the sensitivity under aerobic conditions is related to the radicals which develop:  $H \cdot + O_2 \rightarrow H_2O$ . Water, however, is the principal source of harmful radicals and oxidative compounds:  $H_2O \rightarrow H \cdot + HO^-$ ,  $2H_2O \rightarrow H_2O_2 + H_2$ .

A number of substances are protective against radiation on all lower organisms, if used before or during irradiation. These include thiols, alcohols, glycols, and other organic compounds which are radioprotective. The latter are sometimes used to demonstrate that the decrease in mutations aboard a spacecraft is a function of radiation. Use of these substances reduces the effect. Any physical factor which acts on living matter living on the Earth can be included among those factors to which organisms adapt in the course of evolution. In this connection, *P. caudatum* and *P. aurelia*, which are completely

protected against radiation, begin to multiply more slowly and normal growth is observed only at a dose of 700 mrad/yr. Ionizing radiation has a stimulating effect on these objects; with a dose of  $^{60}Co$  of 600–39 000 mrad/yr there is an increase in the growth of the culture.

With x-rays, the rate of ionizing is 10 000–150 000 eV, i.e., at much higher values than ionization under the influence of UV-radiation. Higher doses of UV cause various, numerous changes: oxidation of unsaturated bonds, breakup of hydrogen bonds, and polymerization. All of this leads to disrupting the synthesis of nucleic acids, inactivation of enzymes, formation of toxic substances, and lethal mutations.

The "life" duration of forming radicals is short, but they may move out of the zone of irradiation and react with nucleic acids or proteins. Bactericidal action of radiation, it should be noted again, is not caused by the intensity of radiation but only by the number of rads absorbed by the organism. A single irradiation may damage a vitally important molecule and once damaged, in an organism which already has irreparable injuries, all subsequent radiation will not have a biological effect. Some time is required for the death of a bacterial cell following the beginning of its radiation; during this time, the harmful action of ionizing radiation is realized.

The target theory has aroused lively discussion in radiobiology—there are arguments pro and con. In examining this theory in conjunction with the action of ionizing radiation on lower organisms, it is natural that the sizes of micro-organisms make it possible for the rays to penetrate any part of the cell. The chances of a lethal dose of radiation from random incidence are the same for all parts of the cell. Consequently, the number of cells which die must be directly proportional to the number of cells which have absorbed quanta of energy. However, the number of cells which actually die is always less than the radiation absorbed by the micro-organisms, which has led to the concept of the sensitive zone of bacteria. This zone, in that part of the cell where the absorbed quanta lead to death, is equal to 5% of the total volume of the microorganism.

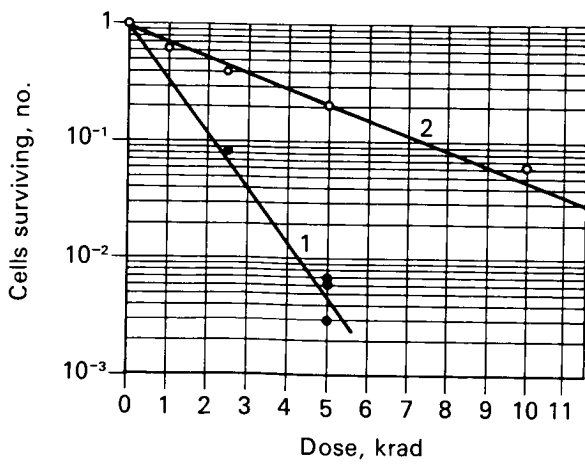


FIGURE 13.—Increase in number of cells killed by x-rays [67].  
1, experimental— $10^{-5}$  mm Hg; 2, control—760 mm Hg.

If the dimensions of the target for each type of radiation and the volume of the sensitive zone are known, by dividing the latter by the former, the total number of sensitive targets in the bacteria is obtained. Death of bacteria from ionizing radiation is reminiscent of first-order reactions. However, there are five arguments against the theory of targets.

1. The curve of mortality is not exponential and the nature of the curve changes easily.
2. There is no direct relationship between the mortality curve and the received dose (mentioned above).
3. The contents of the cell are inhomogeneous and penetration of the ray into vitally important molecules of the latter will result in death of the cell. For example, 250 genes are found in the cell of *E. coli*. It is also possible for radiation to damage the supply of lipids which does not lead to death of the microorganism.
4. When irradiating diploids and polyploids, all the alleles of the gene must be inactivated in order for death to occur; this is impossible, however, since according to target theory the changes are in a single molecule.
5. The target theory requires a relationship between the curve of formation of mutations and the curve of death of cells. Indeed, the curve of mutation development may not increase after reaching a certain level, but the death of the cells can always increase.

The target theory has been a strong stimulus to research in experimental radiobiology, and has yielded many valuable results for science.

### MAGNETIC FIELD

In a study of the physiologic effect of the magnetic field, the results were contradictory. The magnetic field on Earth is equal to 0.5 oersted; artificially generated magnetic fields may be equal to 167 000 oersteds or more. In studying the action of a magnetic field corresponding to 140 000 oersteds for 2 hours on the

fruit fly, *Drosophila melanogaster*, and the fungus, *N. crassa*, no mutants developed. The fluorescent bacteria, *Photobacterium fischeri*, showed no change in the intensity of its luminescence. However, eggs of the sea urchin developed more slowly after being subjected to this influence than those of the control. The effect of the magnetic field of 100 000 Oe failed to produce any pathologic reactions in white rats, and in *C. pyrenoidosa*, neither photosynthesis nor respiration changed. However, the physiology of higher plants was affected by a weak magnetic field [116]. Low-frequency magnetic fields (3–5 Hz, 500–2000 Oe) produced pathologic changes in rats [35].

The duration of exposure is extremely important. When bacteria are exposed to 14 000 Oe for 24 h, growth is suppressed. Following exposure for 28 d at 5900 Oe, young mice lost weight and some of the males died. The higher the organization of the object under study, the more easily the changes develop. Thus, in man, 35 Oe is sufficient to produce a mild toothache and an unpleasant taste in the mouth. The magnetic field on Earth, weak as it may be, must be included among the normal factors constantly acting on all life. In this regard, the development of conditions under which the effects of the magnetic field are absent can lead to disruption of normal physiologic conditions in experimental animals. This problem requires further study.

### DESICCATION OF CELLS AND THE BIOLOGY OF XEROPHYTES

Cells may lose water for different reasons. Thus, dehydration is observed at high vacuum, very low temperatures, or during ordinary drying, which takes place at normal pressure and low temperature, but in a dry atmosphere. Only the latter possibility will be discussed.

Prolonged viability with considerable loss of moisture is not known in animals. Higher plants, e.g., *Myrothamnus flabellifolia*, can be desiccated to an air-dry state and retain growth capacity for a long time [46]. Dried blue-green algae have remained viable for 7 years. Seeds of plants may remain alive for a long time under

these conditions. The fertility of wheat seeds after storage for 2–3 thousand years in Egyptian tombs has not been confirmed. However, seeds of *Nelumbo nucifera*, which have a very dense and hermetically sealed exocarp, grew after being in Asian tombs for 1000 years [89].

The viability of microorganisms that have been isolated from soil particles adhering to the roots of plants, kept for 200–300 years in herbaria, is completely reliable information. These typical soil microorganisms have been able to withstand prolonged desiccation. Still more convincing are cultures prepared from spore-forming bacteria cultures, stored for 100–110 years in collections of cultures of microorganisms, which grew. The most resistant are spores of bacteria, and those species of nonsporeforming bacteria which contain wax and lipids (microbacteria, actinomycetes), or which have a mucous capsule, e.g., *Azotobacter*.

Whether desiccated cells contain some bound water remains an open question; only recently the use of nuclear magnetic resonance for detecting residual water was begun. Microbiology, a comparatively young science, does not have at its disposal the results of special studies devoted to preservation of viability of cells that have been stored in the dried state for a long time. The biochemistry of proteins and nucleic acids still cannot provide an answer to how long they can continue to possess properties necessary for retaining cell viability when the cell remains anabiotic for a long time. In this regard, all attempts have been unsuccessful to discover living microorganisms in rock salt 250 million years old, or in meteorites [1, 15, 73]. On the other hand, extensive experience has been gained on preserving viability in cells of various microorganisms that have been desiccated in a vacuum at low temperature (lyophilization). This, of course, does not prove that when lyophilized cells are stored for a very long time, the denaturing or breakdown of the protein structure does not occur.

No living substance can survive, grow, and reproduce without water. Because of the magnitude of the area the oceans and seas occupy on the globe, a shortage of water cannot arise for many plants and animals. The situation is

completely different on land, where there are deserts. Water in the soil may be physically bound, i.e., held by particles of soil. This kind of water surrounds the particles with a film of several layers of water molecules so firmly bound that the water takes on new properties: it will not conduct electrical current and it will not freeze at  $-78^{\circ}\text{C}$ .

The maximum amount of water in the physically bound state is the maximum hygroscopicity. Water which is less firmly bound to soil particles will enter the free state. Thermodynamically active water in a solution ( $A_w$ ) can be expressed as the ratio of the pressure of the solution ( $P_s$ ) and the vapor pressure of pure water

$$\left( P_w : A_w = \frac{P_s}{P_w} \right).$$

Determination of  $A_w$  makes it possible to establish the accessibility of a given substrate for various microorganisms. In the majority of known bacteria,  $A_w$  is between 0.90–0.99; in halophilic bacteria,  $A_w$  is 0.75. All living substances that are capable of reproduction at values of  $A_w$  lower than 0.75 are xerophytes [98]. The values of  $A_w$  at which the following will grow are *Aspergillus glaucus*, 0.70; *Saccharomyces rouxii*, 0.62; fungi isolated from the surface of plums, 0.60; *Xenopsylla cheopis*, 0.5; *Pleurococcus vulgaris*, 0.48; *Lepisma domestica*, 0.45.

The term *xerophile* which is sometimes used has no basis in fact; both higher and lower plants grow better when the moisture in the substrate is significant. *Xerophiles* were formerly designated plants which grow in soil with a relative moisture content of 85%–90%. The  $A_w$  value is more accurate than soil relative moisture. In determining the reaction of organisms to humidity, the concept of maximum hygroscopicity is used widely, but in this connection it must be kept in mind that it changes as a function of soil composition, therefore it is preferable to express water content in weight percent. Thus, the maximum hygroscopicity of sandy soil is 1%, that of loam is 3%–5%, and chernozems that are rich in humus have a value of 10% [75].

Some samples of sandy soil from the Sahara

Desert are totally lacking in water, while in others its content varies from 0.8%–1.8%. In the In-Salakha region, 1 mm of precipitation fell in 4 years. Throughout the central Sahara, total annual precipitation is 16 mm. Nevertheless, the sands of the Sahara contain highly diverse micro-organisms (to be pointed out later), which relates to daily changes in temperature of 36° C in the shade and 50° C in the Sun. When the temperature falls, vaporlike water in the air condenses and precipitates in the form of liquid droplets. In this way, the Sahara soil can receive an additional 60–100 mm precipitation per year.

The still greater daily temperature variations on Mars, which reach 120° C, could possibly lead to similar results. Soils with moisture content close to maximum hygroscopicity yield fungi and actinomycetes [117]. Xerophytes usually are found more rarely among bacteria. In the Turkmen Desert sand, the moisture content of which is 0.1%–2.7%, viable microflora have been found [172]. When slides are buried in the soil using the Kholodny-Rossi method, and the moisture of the soil is 2.11%, the mycelia of fungi are visible on the slides after 7 days [162]. If slides containing small soil particles are placed in a desiccator to which 10% H<sub>2</sub>SO<sub>4</sub> has been added, after 10–60 days at 18°–20° C, hyphae of fungi and mycelia of actinomycetes will be found growing on the slides. These conditions are shown in Table 8.

TABLE 8.—Soil Conditions and Moisture Content

Soil	Maximum hygroscopic moisture (weight, %)	Experimental moisture (weight, %)
Light chestnut loam	4.29	2.6; 3.6; 4.9
Solonchak solonets	10.2	5.7; 3.1; 8.5
Dark garden	9.1	5.1; 6.9; 8.0

Under the microscope, the slides show the fine hyphae of the fungi; *Penicillium* and *Fusarium* are particularly numerous. Less water is required for hyphae growth than for formation

of conidia or sporangia. While the xerophytic fungi grow well at 80%–85% maximum hygroscopicity, the growth of actinomycetes requires more moist conditions. Formation of slight accumulations of bacteria occurs at 4.43%–6.20%, while in solonchak solonets it takes place at 10.51%–11.20% moisture. At low values of A<sub>w</sub>, the growth rate decreases and development of the organism is retarded.

Data indicating that bacteria are not as xerophytic as fungi and actinomycetes have stimulated systematic searches for bacteria in the sandy soils of Kara-Kum and Nubian Deserts, to find the forms which would grow at the very lowest moisture content of the substrate. Many strains were isolated, some were found to be xerophytic [78, 97], among which were *Mycococcus oligonitrophilus*, *Mycobacterium rubrum*, and *M. smegmatis*. Small test tubes containing a mixture of crushed limonite to which 2% garden soil had been added were placed on the bottom of a large test tube to which a saturated solution of K<sub>2</sub>SO<sub>4</sub> had been added. One of the above-mentioned bacteria was added to the crushed limonite, then the large test tubes were evacuated and sealed. The moisture in the crushed limonite in the presence of the K<sub>2</sub>SO<sub>4</sub> solution was equal to the maximum hygroscopicity, corresponding to 3.8% moisture. At the beginning and end of the experiments, inoculations showed that desert soils contain xerophytic bacteria which grow at such low levels of moisture [80]. Bacteria were formerly considered to develop only at higher levels of moisture. The methodology in these experiments has been discussed in greater detail in the description of the studies conducted with the "Artificial Mars."

Xerophytic microorganisms clearly must possess two physiological characteristics. First, an intracellular osmotic pressure must develop so that they will be able to overcome the forces that retain water on the surface of the soil particles. An ecological niche determines the osmotic pressure of the cell. In bacteria that live in the north in podzol soil, osmotic pressure does not exceed 4 atm, while in the southern areas it is equal to several tenths atm. Among the halophilic microorganisms which have increased osmotic pressure, the halophilic form of *B.*

*megaterium* can be included. Strains of this species in the soil do not grow on media containing salt. In an experiment, the halophilic form of *B. megaterium* was xerophytic at the same time. The osmotic pressure in osmophilic yeasts that grow in honey and jam have been studied in considerable detail. The xerophyticity of halophilic and osmophilic microorganisms has not yet been studied. It must not be forgotten that in the halophilic state, microorganisms adapt not only to a high salt concentration, but also to the specific effect of salt. The majority of halophiles develop (Table 9) on a 50% glucose medium; their osmophilic nature has confirmed this. However, several species did not grow.

The second physiological characteristic of

xerophytic microorganisms is that they have developed an accommodative mechanism which keeps water in the cell. Thus, in the yeast *Cryptococcus albidus*, isolated from dry desert soil, considerable water is retained when the cells are dried; the presence of this water was confirmed by nuclear-magnetic resonance. When the cells were dried, they became impermeable to the water "held" in them. Various chemical methods of processing the cells failed to extract it. This impermeability of the cell wall or cell contents has to do with compaction of the protein structures and changes in their conformation which arise during desiccation [2].

Microbiocenoses can form in sandy desert soils only through microorganisms which synthesize

TABLE 9.—*Growth of Halophilic and Halotolerant Bacteria on a Nutrient Medium with Maximum Concentration of NaCl and on a Medium with Glucose<sup>1</sup> [80]*

No. of culture	Culture	Growth on a NaCl nutrient medium, %	Growth on a nutrient medium, 50% glucose
1	<i>Micrococcus aurantiacus</i>	30	+
2	<i>M. aurantiacus</i>	25	+
3	<i>Micrococcus tetragenes</i>	20	+
4	<i>M. tetragenes</i>	25	+
5	<i>Micrococcus corallinus</i>	20	+
6	<i>Mycococcus rubens</i>	20	+
7	<i>M. smegmatis</i>	20	-
8	<i>Pseudomonas sinuosa</i>	15	+
9	<i>Bacterium album</i>	15	+
10	<i>Pseudobacterium maris</i>	20	-
11	<i>Haemophilus aegyptius</i>	20	+
12	<i>Bacillus amaricans</i>	20	+
13	<i>Flavobacterium breve</i>	25	+
14	<i>B. megaterium</i> —halotolerant variety	20–25	+
15	<i>Bacillus pseudococcus</i>	20–25	-

<sup>1</sup> Cultures were collected from Kara-Bogaz-Gol by O. Ye. Timuk.

organic material by photosynthesis. The sands of the Sahara contain large amounts of microscopic algae capable of multiplying during a comparatively short period, and are able to remain anabiotic for a long period. Algae usually grow in the surface layers of soil, among which are various species of *Chlorella* and *Dictyococcus cocomyxa*, as well as *Phormidium*, *Microcystis*, and other blue-green algae. To a lesser degree, chemoautotrophic bacteria participate in the primary synthesis of organic substances in the desert. The heterotrophic microflora are extremely diverse, and 38 species of fungi have been found in the sands of the Sahara, primarily *Aspergillus* and *Penicillium* as well as a number of actinomycetes species.

In less dry soils, highly diverse bacteria include those that are nitrifying, nitrogen-fixing, urea-decomposing, denitrifying, and cellulose-decomposing. The majority are aerobes; only a few are anaerobes [41, 113, 118, 162]. Hence, the expression "lifeless Sahara" has no meaning. All deserts on the Earth have soil in which numerous diverse and active microflora flourish. In areas of the desert where plants are found, there are symbiotic relationships between the microorganisms and the plants. Thus, in the soil of Saudi Arabia, taken from the rhizosphere of *Artemisia*, there are several million microorganism cells per gram of soil, while outside the rhizosphere, there are only several thousand cells. Living conditions in the deserts have a direct relationship to space biology, since the small amount of water is the principal factor which limits life of terrestrial microorganisms under conditions simulating those on Mars.

### EFFECT OF GASES

The action of various gases on biologic objects is of interest for a number of reasons.<sup>2</sup> The gas composition of the atmosphere of various planets differs and this has a direct relationship to space biology, since the atmosphere participates in the energetic and structural exchange of living organisms thereby playing a considerable role

<sup>2</sup>On Earth there are a number of gases including oxygen, nitrogen, ammonia, methane, hydrogen, hydrogen sulfide, carbonic acid, carbon oxide, and sulfur gases.

in circulating certain elements in nature. Some of the general viewpoints will be discussed.

The poisonous effect of some gases is so strong that all living organisms are killed. Such gases include hydrogen cyanide, sulfur dioxide, chlorine, ethylene oxide, and methyl bromide. Gas sterilization has come into wide use in recent years, particularly for sterilization of spacecraft. Related problems are treated in some detailed modern handbooks [66]. Inert gases which do not have an unfavorable effect on biological substances at ordinary pressures include argon, neon, krypton, helium, and nitrogen.

Louis Pasteur was the first to refute the firm conviction of his time that life was impossible without air. He not only discovered anaerobic butyrate bacteria, but also proved experimentally that the oxygen in the atmosphere affects them like a poison. Later, other strictly anaerobic bacteria were discovered that were incapable of living in the presence of oxygen, which is harmful to many living substances when its partial pressure increases. Thus, an oxygen pressure of 15–44 atm suppresses growth of microorganisms in meat. The maximum resistance of microbes and higher organisms is 2–10 atm oxygen pressure or 10–50 atm air containing 21% oxygen. The sensitivity of microaerophilic forms of microorganisms is less.

The resistance of bacteria to oxygen in nutrient media in a quantity up to 35 g/ml decreases sharply when hydrostatic pressure rises [160]. Thus, microorganisms grow well in nutrient media subjected to oxygen at 3 atm pressure or 45 atm air pressure. However, if the nutrient medium contains 105 mg/l of oxygen dissolved in it, bacteria will not grow in this medium at 25 atm hydrostatic pressure. Some cultures, after exposure to these conditions for 4 d at 25°C, die completely. In other forms of microorganisms, increased oxygen content has an inhibiting effect even at lower hydrostatic pressures, 5–10 atm.

Certain aerobic life forms can utilize oxygen traces in the atmosphere. Thus, protozoan flagellata multiply in nitrogen containing only 0.0005% oxygen [103]. Aerobic microorganisms are capable of using low oxygen concentrations for breathing before its content in the medium

is reduced by diffusion. In particular, *Micrococcus candidans* can reproduce with 0.001% oxygen content in the medium. If the oxygen content of the medium is replaced as it is used up, aerobic bacteria can reproduce in liquid media that contain 0.02 mg/l oxygen; this is the smallest amount which can be determined by the well-known Winkler method.

These data indicate that a very low oxygen content in the martian atmosphere would not be a reason for excluding the possibility of life on this planet. The influence of each of the physical factors on Mars must be studied in conjunction with the other factors. Thus, ecologists usually consider that anaerobiosis or micro-aerophilia in organisms correlates to a higher degree of resistance to low temperature. Obligate aerobic forms are less resistant to cold. The biologic effect of atomic and molecular oxygen, as well as ozone in concentrations detected on Mars, remains an open question.

Carbon dioxide action on biological objects is extremely important. The CO<sub>2</sub> in the Earth's atmosphere is assimilated by photosynthesizing higher and lower plants as well as by chemo-autotrophs. However, CO<sub>2</sub> concentration in the atmosphere increased to a certain limit will increase photoassimilation, on which the feeding of higher plants on carbon dioxide is based. Microorganisms which form CO<sub>2</sub> when they ferment, e.g., yeasts, reproduce very well in liquid media saturated with carbon dioxide. On the other hand, aerobic microscopic fungi are markedly inhibited by carbon dioxide. Special hermetically sealed containers have been suggested in which berries or fruits could be stored in a CO<sub>2</sub> atmosphere. The bactericidal effect of CO<sub>2</sub> is clearly evident if this gas is used at 50 atm pressure. In this case, *E. coli*, *Pseudomonas aeruginosa*, *Salmonella typhi*, *Staphylococcus*, *Streptococcus*, *Diplococcus pneumoniae*, *Mycobacterium tuberculosis* and other species of yeasts will be completely killed in several hours. The nature of the gas is very significant; thus, cells of *E. coli* completely retain viability when in nitrogen at 120 atm pressure, while at the same hydrogen pressure, 10%–40% of the cells die.

A rapid rise in pressure has a particularly unfavorable effect. Thus, pressure rising rapidly

to 160 atm caused the death of up to 90% of the bacteria cells suspended in water [42]. Nitrogen and carbon dioxide had less significant effects, while nitrous oxide and argon had more pronounced effects. It is natural that carbon dioxide may have an inhibiting effect only when it is used at a certain partial pressure. Although the martian atmosphere contains a great deal of CO<sub>2</sub>, the pressure is only 4.5–7.5 mbar, which permits two conclusions. First, regardless of the high content of CO<sub>2</sub>, it cannot have an unfavorable effect on living objects. Second, if living organisms exist on Mars, capable of photo- or chemosynthesis, both will differ from similar processes on Earth with regard to physical chemistry, energetics, and biochemistry.

From the standpoint of evolution, the observations of ecologists are interesting: if certain microorganisms form gases as the result of their vital activity, and the gases are more or less poisonous, these species will have much higher resistance to these gases and to the changes in the medium under their influence. The concentrations of ammonia which can be withstood by bacteria that decompose urea and the associated high pH value of the medium will only be mentioned, as well as the considerable quantities of poisonous hydrogen sulfide formed by sulfate-reducing bacteria. On the other hand, bacteria which oxidize methane, hydrogen, hydrogen sulfide, carbon monoxide, and other gases are much more resistant to these gases than are the other microorganisms. Such an increase in resistance is naturally accommodative and creates an ecological niche which is inaccessible to other microorganisms.

## STUDIES CONDUCTED ABOARD SPACECRAFT AND SATELLITES

A great number of biologic studies have been conducted aboard satellites and spacecraft, about which there are survey articles [34, 39, 43, 44, 122, 125, 138, 141, 144, 166, 167, 169]. These data form the basis of studies in space medicine which have ensured cosmonauts' safety in flight. Besides the construction of the spacecraft or satellite, the conditions within them are markedly different from those in space. Vacuum, low

temperature, ultraviolet radiation, and similar conditions do not influence the interiors of satellites. The biologic objects inside the satellites are subjected to weightlessness, vibration, acceleration, and comparatively low doses of cosmic radiation. The total effect of spaceflight factors must be mentioned since they exert pronounced influences on one another. In order to define these factors, Earth experiments have been performed to study separately the influence of acceleration, vibration, and other factors.

Some factors complicate acquiring unconditionally precise and unambiguous data in these experiments. During flight, radiation is very low, usually several tenth parts of rad [52], and in experiments, radiobiologists use much higher doses and work with objects lacking the necessary increased radiosensitivity. It is difficult to establish "classical" controls on Earth, and random temperature changes may complicate comparison of experiments with the controls. The sensitivity of biological objects to various classical factors is a function of the inhomogeneity of the material used in the various experiments. Much depends upon the type of seeds, kind of insects, and similar factors. All this explains the lack of reproducibility of results involving repeated tests, and the considerable diversity in findings of various authors.

All biological studies which deal with the effect of spaceflight factors may be conditionally divided into two groups. The first, the results of experiments that have been repeated more than once, may be classified as generally recognized. The second, the data of experiments which are of considerable interest and must be reproduced by other researchers.

The first group includes studies with *Chlorella* whose viability of cells in flight is 75.0%, and 94.6% in the controls [157, 158]. Statistically reliable induction of the bacteriophage *E. coli* K-12 has been observed repeatedly, but there is not always a direct relationship between the satellite flight duration and induction of the phage [5, 34, 167, 168, 169, 170].

The well-known antiradiation substances,  $\beta$ -mercaptopropylamine and 5-methoxytryptamine, reduce the level of phage production activity of lysogenic bacteria [4]. Stimulation of growth in

*Allium cepa* has been observed during flight [5], which is interesting because a similar effect was obtained from vibration under laboratory conditions. Interesting results were obtained with dry seeds of *Crepis*: flight conditions had nothing to do with the fertility and growth of the seeds, but a statistically reliable increase in the number of chromosomal changes was noted [36]. A stay in space increased mutagenic sensitivity and seeds which had been in flight and subsequently processed with ethyleneimine yielded 15.4% chromosomal aberrations, while the effect of ethyleneimine alone was 6.5%. In experiments with barley seeds, the combined effect of flight factors and ethyleneimine yielded a greater mutagenic effect than each of the factors separately.

Formation of mutations in the corn plant [122] was established by using precise methods of recording. When microspores of *Tradescantia paludosa* were flown in satellites, mitosis was disrupted (Fig. 14), along with changes in chromosomes and disruption of growth processes [3, 5, 122, 135]. The sprouts of wheat, carrots, tomatoes, peas, and others showed chromosomal changes in cells of the primary roots [32], which was also

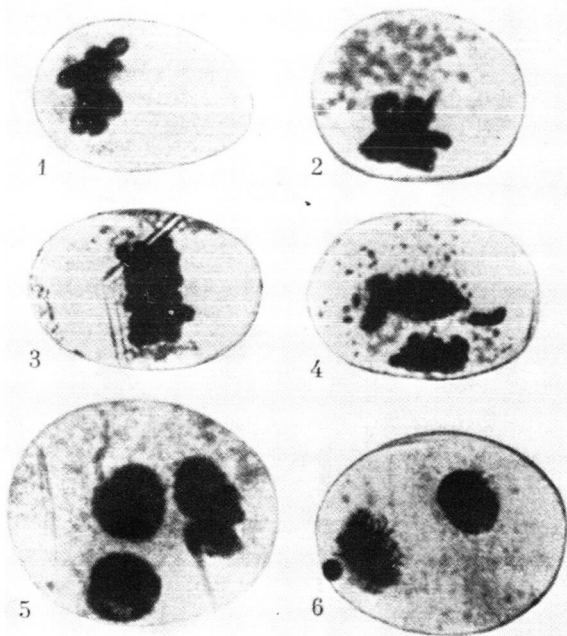


FIGURE 14.—Disruption of mitosis in microspores of *Tradescantia paludosa* postflight [52].

observed in barley and pine seeds following flight [4, 32]. Spaceflight factors increased the frequency of dominant lethals and failure of chromosomes to divide in *Drosophila* [4, 17, 120, 122].

The second group includes experiments, the results of which have not been confirmed on each flight. Thus, chromosomal aberrations in peas were observed in 4 of 14 cases, and in wheat in three of nine cases [122]. An increase in the frequency of chromosomal changes in sprouts of pine, bean, lettuce, cucumber, wheat, and mustard were not always statistically reliable [143]. During the flight of the Discoverer-17 satellite, only 30% of *Clostridium sporogenes* spores survived [122]. Even if it is taken into account that there was a flare during the flight and cosmic radiation increased to 33 rad, mainly due to neutrons, it is difficult to explain such a high percentage of mortality of the resistant spores.

In studies involving *Drosophila*, three experiments showed reliable increases in frequency of recessive lethals, but this was not observed in four other experiments [122]. The number of such examples could be increased considerably. For the experimenter, any failure to repeat previously obtained data requires indicating the reasons for such diverse results. At present, no such explanation is possible. Increasing mutability of *E. coli* does not correlate with lack of the same effect in other bacterial species on the flight [122].

Spaceflight factors cannot be considered highly influential, which is supported by failure to produce any significant disruptions in the vital activity of biological objects in many space flights. Neither a decrease in viability nor a change in metabolism was found in *E. coli*, *S. aureus*, or *Clostridium butyricum* during flight. Likewise, there was no change in viability of influenza or tobacco mosaic viruses, nor in particles of T-2 and 1321 phages. There were no mutations in the haploid or diploid yeasts and *F. breve*; the number of auxotrophic mutations in bacteria did not change [122]. The number of pigment spots or morphologic mutations in *Drosophila* were the same in experiments and controls. There were no genetic effects noted in wet, radiosensitive onion seeds, diploid and tetra-

ploid buckwheat; the frequency of chromosomal aberrations in violet stock did not increase. *Tradescantia* showed coloration after flight (Fig. 15).

Flight conditions did not have a significant influence on chromosomes of sprouts from dry seeds of pine, carrot, spring and winter wheat, lettuce, and mustard [122]. The sprouting and growth of seeds of a number of plants proceeded normally and there were no changes in contents of protein, lipids, starch, and amino acids. After flight, the frequency of regressive lethals was determined in chromosomes of male and female *Drosophila*; frequency of mutations in experimentals and controls was the same. *Drosophila* eggs did not die during flight, and embryonal development of the eggs of horse ascarid, *Parascaris equorum*, was normal after flight. Usually there are no dominant lethal mutations for *Habrobracon*. After flight, cells in culture of HeLa, fibroblasts, and cells of the human amnion were found capable of growth and reproduction.



FIGURE 15.—*Tradescantia* with flowers blooming during flight [7].

Pieces of rabbit and human skin demonstrated enormous resistance, inasmuch as they retained viability following a stay in space (autotransplantation). No obvious pathologic changes were observed in steppe tortoises which were flown [150].

Spaceflight factors had a definite stimulating effect in some experiments. Dry seeds of wheat, lettuce, mustard, barley, beans, peas, carrots, cucumbers, and tomatoes grew better postflight than the controls. Growth of onion bulbs definitely increased [31]. Stimulation of spore growth and mycelia development in actinomycetes were also observed [122]. The influence of a number of flight factors made itself felt at a later stage, whereas radiation damage is directly linked to the physiologic processes in cells. In this connection, certain objects under investigation were irradiated repeatedly before, during, or after flight, which made it possible (but only partially) to explain the relationship between the flight factors. The eggs or larvae of insects were convenient objects for this study. Pupae of the flour beetle, *Tribolium confusum*, were irradiated with  $\gamma$ -rays during a satellite flight. In comparison with a control (irradiation on Earth), the number of insects with wing anomalies increased from 29.9% to 44.8% [20, 145]. Hence, flight factors increased variability.

In similar experiments with larvae of *Drosophila melanogaster*, those which had been irradiated and were aboard the satellite had chromosome breaks, frequently accompanied by loss of part of the chromosome, recessive lethal mutations, and earlier development, all of which were found more frequently than in irradiated larvae left on Earth. Weightlessness aboard the satellite evidently causes failure of chromosomes to divide and formation of chromosomal translocations [17].

The eggs of *Habrobracon* were subjected to  $\gamma$ -radiation during the flight of the satellite, which led to failure of the chromosomes to divide and consequently to a decrease in larvae hatching in comparison with controls. In the nonirradiated sperm of this insect aboard the flight, there was a threefold increase in the number of recessive lethal mutations. In irradiated insects aboard the flight, there was a sharp drop in activity of the

enzyme xanthidehydrogenase. Because of the vibration that accompanied launching and landing, the frequency of sperm mutations increased by a factor of 3 in comparison with controls [18].  $\beta$ -Irradiation (180 rad) of a culture of leukocytes led to increased frequency of one-hit aberrations, including chromosomal deletions postflight.

Irradiation during flight had a definite effect. However, in experiments with diploid yeasts *Saccharomyces ellipsoideus*, haploid *Saccharomyces bailii*, hydrogen bacteria, seeds of lettuce and peas, it was shown that flight factors have no influence on the result of subsequent irradiation at a dose up to 160 krad [52]. This result contradicts the observations in which irradiation postflight also had a genetic effect. Irradiation of dry lettuce seeds (*Lactuca sativa*) preflight (1–10 krad) leads to an increased number of cells with chromosomal aberrations and development of other radiobiological effects.

The cells of haploid and diploid yeast *S. cerevisiae*, and dry seeds of *Crepis capillaris*, *Arabidopsis thaliana*, and *Chlorella vulgaris* were subjected to  $\gamma$ -rays preflight ( $^{137}\text{Cs}$ ), with the dose varying 3.0–30 krad. Compared to the controls, spaceflight factors reduced viability of *Arabidopsis* sprouts and *Chlorella* fertility; increased mutability of *Chlorella* and yeasts and frequency of chromosomal aberrations in meristem cells of *Crepis* root. The flight increased the negative effect of irradiation in these objects according to all indicators. At the same time, spaceflight factors did not affect the radiosensitivity of the investigated objects genetically [36]. Aluminum or copper shields used in satellites protect objects from ionizing radiation [153].

Similar studies were performed with *Tradescantia*, irradiated with  $^{85}\text{Sr}$ , aboard the satellite. A few control plants aboard the satellite were protected by a tungsten shield; other control plants were on Earth. The sizes of cells, numbers of somatic mutations, and chromosomal aberrations turned out to be the same in the experimental and control plants. However, there was disruption of pollen formation, and the cells of the root tip and microspora showed disruption of mitosis, which evidently had to do with the influence of weightlessness on the irradiated object [34].

There are few definite data on the interaction of spaceflight factors, despite the large number of studies performed. Evidently the principal reason is that it is impossible to reproduce weightlessness on Earth. It is interesting to compare parallel data obtained on a clinostat. Under true weightlessness, the length of wheat sprouts increased 14%–17%, the number of dividing cells dropped 20%–43%, and the nucleus volume increased by 13%–26%. This is not observed on a clinostat [30, 32].

This effect is due to considering only weightlessness without the complex of factors in operation under satellite flight conditions. Weightlessness aboard a spacecraft does not disturb *Drosophila* growth and laying eggs, but larvae developed far more poorly in the male than in the female [3]. *Tradescantia* cells showed far more frequent mitotic disturbance than the controls, which is also related to weightlessness [3]. Experiments with oat seeds on a biaxial clinostat showed that in a 3-d exposure, the threshold acceleration for stems was  $10^{-3}/g$ , and for the root,  $10^{-4}/g$ . Biologic objects subjected to extreme factors in deep space has been researched a great deal less. Rockets were used for research purposes in addition to stratospheric balloons and satellites, which incorporated the capacity for exposing the objects in space. After the rockets were launched, and at an altitude of 150 km for 3 min, viability was partially retained in spores of *B. subtilis*, conidia of *Pencillium roqueforti*, coliphage T<sub>1</sub>, and the poliomyelitis virus.

Solar radiation was the principal reason for death and fine screens of metal (880 Å Au and 1400 Å Al) completely protected the objects under investigation against death [63, 65]. In a similar experiment with the T<sub>1</sub> coliphage (Fig. 16), rapid death occurred; if the control is taken as unity, 0.00002 phage particles remained following brief exposure [64]. Experiments on Earth established that at 1633 Å, the T<sub>1</sub> coliphage dies earlier than at 2537 Å, i.e., the wavelength considered most bactericidal [100].

The most significant influence on *E. coli* and *B. subtilis* is in the ionosphere and stratosphere by UV-radiation (200–300 nm), while the vacuum and low temperature do not produce this effect, according to experiments with rockets and

stratospheric balloons. Penetrating radiation has a comparatively low level of importance in this regard. Following irradiation in the stratosphere, *E. coli* is capable of photoreactivation [124].

The insignificant effect observed in the experiments (described above) is evidently due to brevity of the experiment. Studies aboard a spacecraft showed much lower resistance of various biologic objects. Thus, 6-h exposure of bacterial spores, conidia of fungi and phages to factors in deep space indicated that only  $10^{-4}$  remained viable. Various viruses were quite resistant. If viability in the controls is used as unity, viability of smallpox virus is 0.2, that of PR 8 influenza is 1.0, tobacco mosaic virus is 1.0, canine hepatitis is 1.0, and infectious bovine rhinotracheitis has only a trace value. The activity of the enzyme lactic dehydrogenase is 0.2 [58]. However, in another series of experiments at an altitude of 300 km, lasting 16 h 47 min, viability of *P. roqueforti* conidia was 0.00003 and that of the coliphage T<sub>1</sub> was 0.000002 [59]. The natural conclusion is that prolonged exposure in space is lethal to living organisms not protected against the Sun's rays.

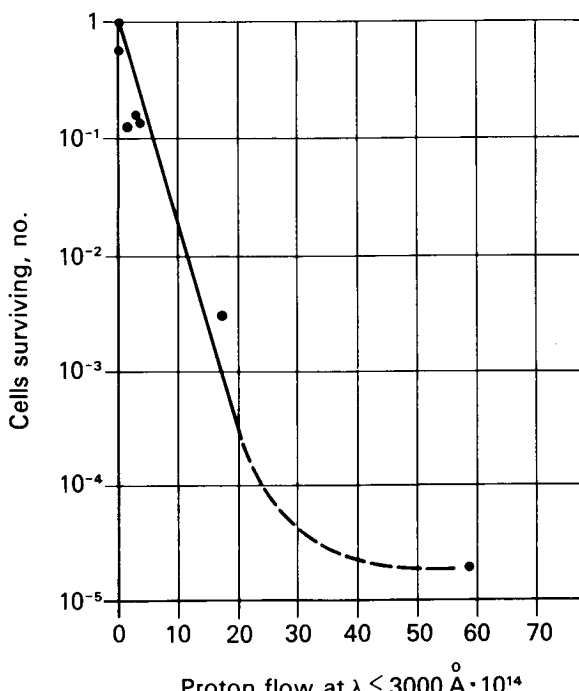


FIGURE 16.—Effect of solar radiation on coliphage T<sub>1</sub> [116].

## SIMULATION OF CONDITIONS ON PLANETS

Creating the conditions that exist on other planets and investigating the viability of terrestrial beings under these conditions was a problem which was solved only after space biology developed as an independent science. These studies were conducted primarily using apparatus which simulates conditions on Mars, and should provide answers to four questions.

1. Can terrestrial organisms retain viability under these conditions?
2. Does the complex organization of living matter have any effect on its resistance?
3. Are there organisms which not only will live but also will reproduce under these conditions?
4. How do individual factors influence terrestrial matter, and which have the most unfavorable effects?

Studies in this direction must deal in particular with the possibility of microorganisms reproducing under martian conditions, which, to a certain extent, would give an idea of possible existence of life on Mars. At the same time, the possibility of reproduction of terrestrial microorganisms reaching the surface of Mars aboard spacecraft would be solved, which is directly related to the sterilization of spacecraft.

The principal characteristics of devices aboard the "Artificial Mars" station, described in the literature, are in agreement, which is easily explained by the necessity of creating identical physical and physicochemical conditions in the apparatus [53, 55, 70, 97]. It should be made clear that as more and more new information is gained about Mars by means of spacecraft flying past Mars or landing on its surface, conditions in the apparatus will have to be changed.

The "Artificial Mars" is usually a device with a glass chamber in which martian conditions are created. A programing mechanism in the device changes the parameters of conditions within the chamber.

First, there are temperature variations from +30° C to -60° C every 12 h, corresponding to the martian day. These changes must not

be abrupt; they take place gradually. For technical reasons, it is very convenient to place the material to be studied on the end of a copper rod, in the glass chamber, characterized by a high degree of thermal conductivity.

Second, a vacuum pump creates reduced atmospheric pressure in the glass chamber corresponding to martian levels.

Third, the chamber is filled with a gas mixture. In the initial experiments, this mixture was composed of carbon dioxide, nitrogen, and argon. On the basis of new data concerning the martian atmosphere, a mixture composed mainly of carbon dioxide is now used.

Fourth, terrestrial organisms subjected to martian conditions are UV-irradiated. To irradiate the material under study, it is most convenient to have a small quartz window in the glass chamber wall, which transmits UV-radiation. The total UV-radiation dose received by the objects under study sometimes reached  $33.6 \times 10^8$  ergs/cm<sup>2</sup> in 3 weeks, corresponding to the "martian dose." A general idea of the structure of the entire apparatus is shown in Figure 17 and its external appearance is in Figure 18. UV-irradiation was not carried out in research by a number of authors.

In research with the Artificial Mars, particular emphasis is placed on the humidity of the atmosphere and the substrate on which the objects to be studied are located. A wide variety of microorganisms have usually been studied, located in different substrates: solid or liquid nutrient medium; on the surface of membrane filters; in soil or crushed limonite.

Creating the four conditions (described above) posed no difficulties, but maintaining a constant low level of moisture in the substrate was extremely difficult. This problem will be discussed subsequently with the results of experimental research. Brief reports on the conditions and results of the experiments (described in the literature) are in Table 10.

These data indicate that many microorganisms,

including various bacteria and fungi, retain viability after being kept in the Artificial Mars. In some experiments, viability was maintained for 6–10 months. The majority of the experiments were performed at pressures much greater than those on Mars. In the earliest experiments, nitrogen was predominant in the atmosphere, while in reality there should have been a large amount of carbon dioxide. Higher plants withstand the influence of martian conditions only when the experiment is performed at plus or not very low temperatures. Simulated martian conditions are not suitable for reproduction of protozoa.

The study of each of these physical factors separately or in combination indicated that UV-radiation in doses found on the surface of Mars is absolutely lethal for all microorganisms studied. However, cells of microorganisms covered with a very thin layer of crushed soil are completely protected from UV-radiation. In experiments, microorganisms were mixed with soil, which is precisely the reason that in the majority of experiments, UV-irradiated objects were not studied. Variations in temperature, composition of the atmosphere, and reduced pressures in the Artificial Mars did not have a lethal effect on the organisms under study.

Data on the reproduction of various terrestrial microorganisms under martian conditions are limited [163]. The low level of moisture of the atmosphere and substrate is always the factor which limits bacteria growth. Thus, experiments

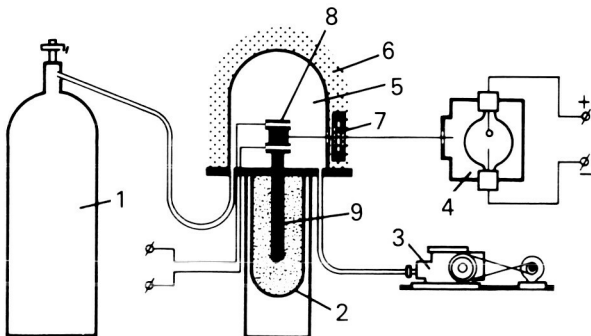


FIGURE 17.—“Artificial Mars” device [165]. 1, gas mixture cylinder; 2, vessel containing cooling mixture; 3, pump; 4, lamp producing UV-rays; 5, chamber for test objects; 6, thermally insulated chamber; 7, quartz glass “window”; 8, heating element; 9, copper rod.

where the object under study was in a liquid or very moist medium are of less interest, since such conditions are very unlikely on Mars.

Studies in this direction encountered methodological difficulties. The crushed limonite contained 2% garden soil and bacterial cells had 3.0%–3.8% moisture; when it was exposed to a moistened atmosphere of Mars, i.e., mixtures of carbon dioxide and nitrogen or argon, the limonite was desiccated. It was decided to place a bottle of water and another bottle containing a solution of potassium chloride in the Artificial Mars chamber, which made it possible to maintain a constant moisture level in the limonite equal to maximum hygroscopic moisture, i.e., 3.8%. The cells of nonsporeforming or sporeforming bacteria in the limonite, isolated from desert soil, reproduced at this low level of substrate moisture (3.0%–3.8%). The organisms were *Streptomyces*

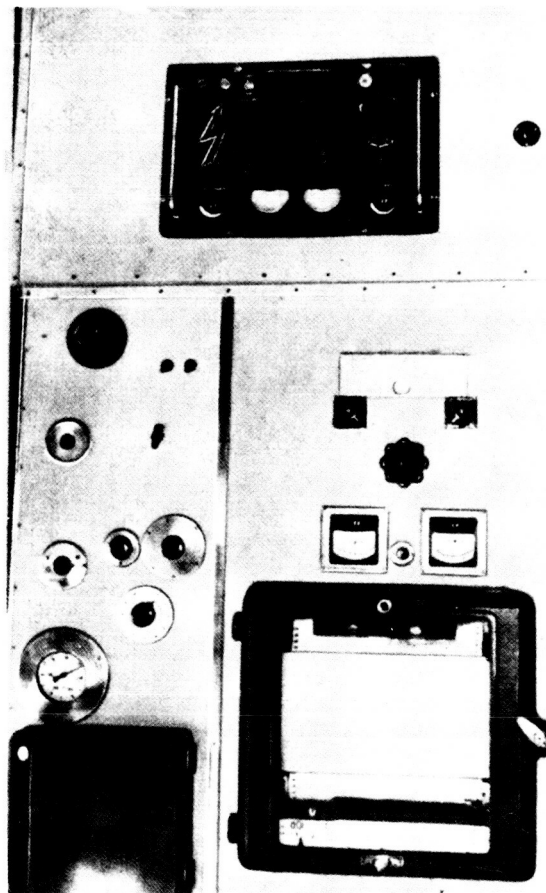


FIGURE 18.—External view of “Artificial Mars” device [165].

TABLE 10.—*Viability and Growth of Organisms under Simulated Martian Conditions*

Organism	Viability, months	Moisture, %	Temperature, °C	P, mm Hg	N <sub>2</sub> , %	CO <sub>2</sub> , %	Substrate	Reference
<i>Clostridium, Corynebacterium</i> , thin short rods	10	1.0 or less	-25 to +25	65	100		Soil	[27]
<i>Clostridium tetani</i>	2	1.0	-60 to +25	85	95	0.3	Soil	[55]
<i>B. cereus</i>	2	0.5% of soil weight	-20 to +25	65	94	2.2	Soil	[130]
<i>Clostridium botulinum, Klebsiella pneumoniae</i>	10	Lyophilization	-25 to +25	65	95	0.5	Lava with soil	[56]
Anaerobic spore-forming organisms	6	Low	-60 to +20	76	95	5	Soil	[121]
<i>Clostridium</i>								
Anaerobic nonspore-forming bacteria:								
<i>Pseudomonas, Rhodopseudomonas</i>								
<i>C. sporogenes</i>	Growth	8.4	-25 to +23	65	94	2.0	Soil	[131]
Winter wheat	0.6	Moist	-10 to +23	76	98	0.24	Soil	[139]
Peas, beans, onions, wheat sorghum, rice	0.3	Moist	+25	75	100	0	Paper	[141]
<i>B. subtilis</i> var. <i>globigii</i>	3	< 0.5 of substrate weight	-60 to +25	85	93.8	2.2	Felsite + limonite (1:1)	[53]
<i>A. niger, A. oryzae, Mucor plumbeus, R. rubra</i>	6h	Very dry	-60 to +25	76	95.5	0.25	—	[171]
Vegetative bacteria cells	Die	—	—	—	—	—	—	
Spores of <i>B. subtilis, B. cereus</i>	Growth	7.0	—	8.5	93.8	2.2	—	[57]
<i>B. subtilis</i>	Growth	More than 8.0	-65 to +25	Po <sub>2</sub> no less than 15 mm	—	—	—	[58]
Nonsporeforming bacteria	Growth	In presence of water	-70 to +25	Simulated martian conditions	—	—	—	
Sporeforming bacteria	Die	Absence of moisture	—	—	—	—	—	[163]
Sporeforming bacilli	0.5	3.0	-60 to +28	7	40	50	Limonite with soil	[70]
<i>Micrococcus</i> sp., <i>Haemophilus aegyptius, B. zooglieicus, Mycococcus oligonitrophilus</i>	0.5	3.8	-60 to +28	7	10	—	Limonite with soil	[34]
Nonsporeforming bacteria and <i>M. oligonitrophilus</i>	0.5	3.0	-60 to +28	7	20	80	Limonite with soil	[78]
<i>M. ruber, B. megaterium</i>	3 Growth	3.8	-60 to +28	5.3	20	80	Thin dry films of agar	[80]

*cylindrosporus*, *M. ruber*, *Mycococcus oligonitrophilus*, *M. smegmatis*, and the halophilic strain of *B. megaterium* (Figs. 19, 20, 21, 22).

The ability to reproduce at very low moisture levels in the substrate is apparently the most prominent characteristic of martian organisms, if they actually exist on Mars. For this reason, particular emphasis was placed on xerophytic

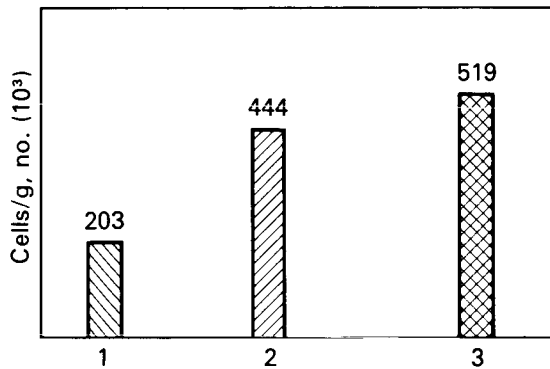


FIGURE 19.—Reproduction of *Streptomyces cylindrosporus* under simulated martian conditions; substrate moisture content, 3.8% [101]. 1, initial amount; 2, control; 3, in the "Mars" device.

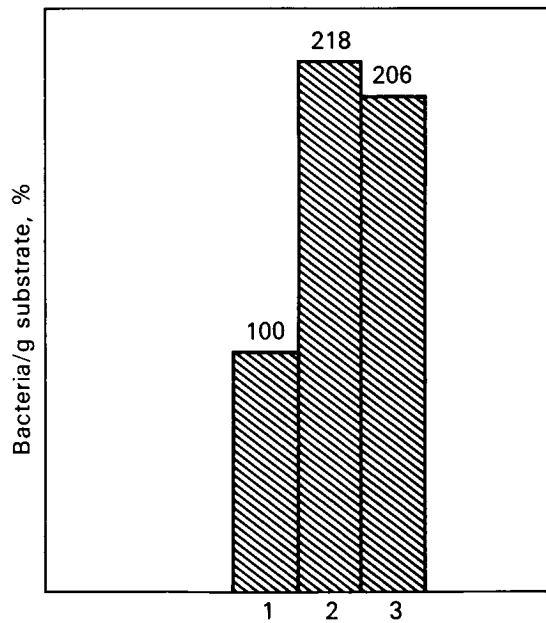


FIGURE 20.—Reproduction of pigmented microorganisms isolated from Antarctic soil; substrate moisture content, 4%. 1, control (initial number of cells introduced into substrate); 2, *Mycococcus ruber*; 3, *M. smegmatis*.

soil bacteria which multiply at very low substrate moisture levels. Microorganisms collected from desert soil and the Arctic were studied. The best method proved to be:

A saturated solution of potassium sulfate was placed on the bottom of a test tube. A small test tube containing a long slide was placed in the large test tube. This slide carried a dried film of agar containing a suspension of microorganism cells. Later, the air in the test tube was replaced by martian atmosphere, then the pressure in the test tube was reduced to 7 mm Hg by evacuation. The test tubes were sealed and placed in a thermostat at 30° C (Fig. 23).

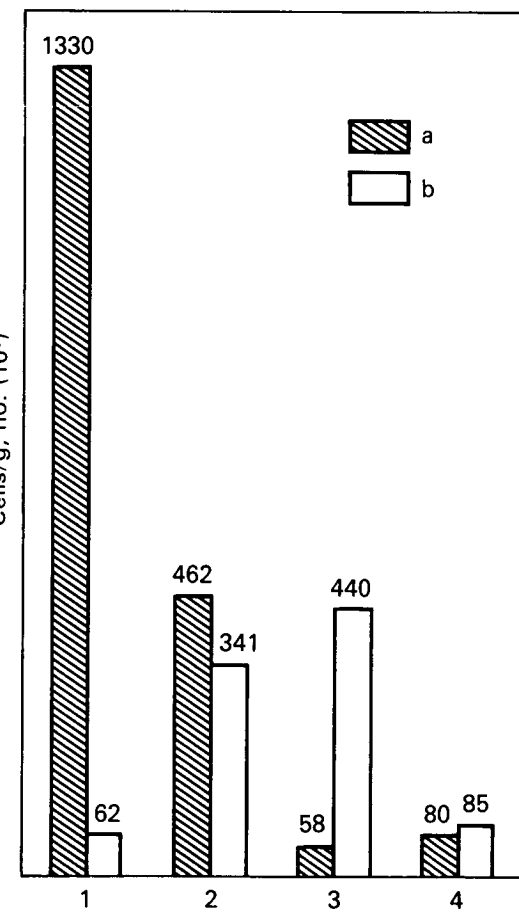


FIGURE 21.—Bacteria reproduction in "Artificial Mars" device; moisture content of ground limonite, 3.8% [103]. a, initial number of cells; b, number of cells after 14 d; 1, *B. zooglieicus*; 2, *Micrococcus* sp.; 3, *Mycococcus oligonitrophilus*; 4, *Haemophilus aegyptius*.

After several days, microscopy and photomicrography of the cell cultures and similar operations revealed that under these conditions, bacteria were capable of reproducing (Figs. 24, 25). The moisture level of the agar film did not exceed 3.8%, since such moisture level is established above a saturated solution of potassium sulfate. With the same method, but instead of the glass slide, crushed limonite and bacteria can be put in the small tube which is then placed in a large test tube with a saturated solution of potassium sulfate. After lowering the

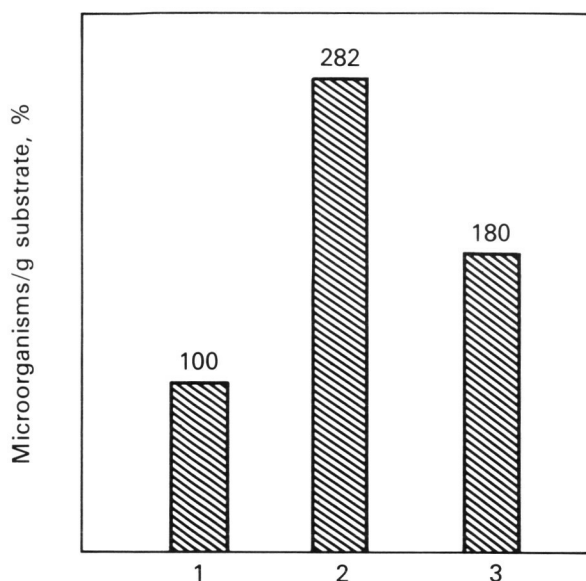


FIGURE 22.—Reproduction of halotolerant strain of *Bacillus megaterium* in the "Artificial Mars" device. 1, control (initial number of cells/g of substrate, 100%); 2, seeding in the mixture: limonite + felsite (1:1) + garden soil (2%); 3, seeding in the mixture: limonite + felsite (1:1) + peat (2%).

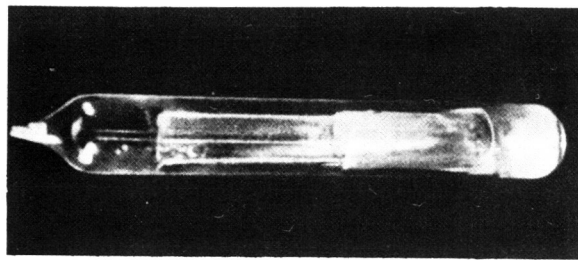


FIGURE 23.—Growth of *Mycococcus ruber* on agar film in a sealed test tube containing 10% K<sub>2</sub>SO<sub>4</sub> solution [104]; film moisture content, 3.8%.

pressure and admitting the gas mixture, the test tube is sealed.

These studies in space biology have established new facts for soil microbiology. Xerophytic bacteria were previously thought to be capable of reproducing only in soil which has a higher moisture content.

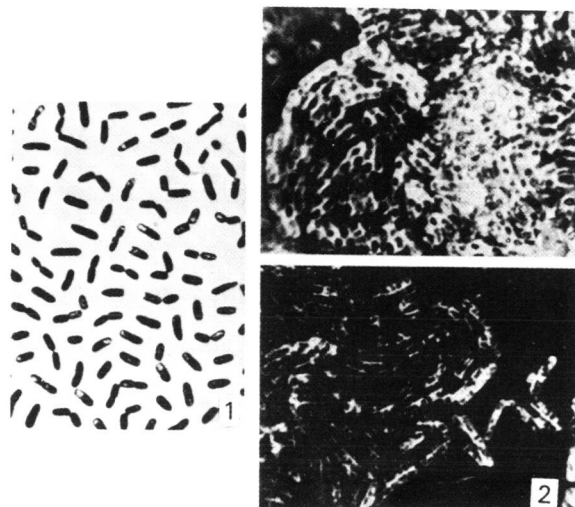


FIGURE 24.—Reproduction of *B. megaterium* on substrate containing 3.8% water [104]. 1, initial number of cells; 2, reproducing cells.



FIGURE 25.—Reproduction of *Mycococcus ruber* cells on substrate containing 3.8% water. 1, initial number of cells; 2, reproducing cells.

A special chamber was constructed to simulate the frequent dust storms on Mars. The barometric pressure, temperature, and gas composition of the atmosphere could be varied. As the result of the artificial storm, cells of *B. cereus*, *B. subtilis*, *E. coli*, *S. marcescens* and *S. aureus*, in suspension with soil particles, were subjected to UV-radiation (2400–2800 Å). In order to obtain the martian dose, it was sufficient to expose the organisms for 55 min at a dose level of  $2.6 \times 10^4$  ergs/s. The bacteria died rapidly at higher doses ( $10^5$ – $10^6$  ergs/cm<sup>2</sup>) (Fig. 26).

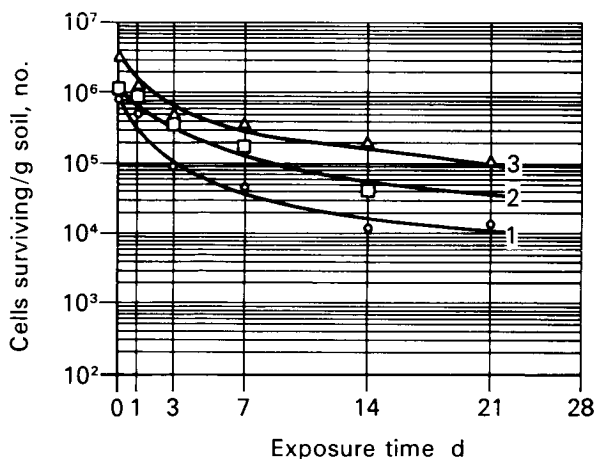


FIGURE 26.—Survival rate of *B. subtilis* cells under different conditions when dust clouds were formed [89]. 1, 25%, terrestrial atmosphere, 760 mm Hg; 2, freezing and thawing, terrestrial atmosphere 760 mm Hg (action of UV-rays); 3, freezing and thawing, artificial martian atmosphere, pressure of 15 mm Hg (action of UV-rays).

### EFFECT OF EXTREME FACTORS AND THE SEARCH FOR EXTRATERRESTRIAL LIFE

Data on the relationship of terrestrial organisms to extreme conditions are very valuable for the study of life on other planets. Extreme conditions vary on different planets, but the interaction of these conditions and organisms must be very similar to that on Earth. This relates to the general assumption that the search for life beyond Earth must proceed on the basis of terrestrial concepts regarding life. Xerophytic terrestrial microorganisms will reproduce under the Artificial Mars conditions (already stated);

thus, the extreme factors on Mars will not inhibit reproduction of certain terrestrial microorganisms. Two conclusions are possible.

First, conditions on Mars are not unfavorable enough to completely exclude, categorically, the existence of life. Second, the possibility cannot be excluded of reproduction of terrestrial microorganisms that reach Mars aboard spacecraft. The nature of the extreme factors on Mars permits several assumptions to be made regarding the possibility of life. Layers of soil closest to the surface can scarcely contain living cells because of the very high doses of UV-radiation that reach Mars. New mechanisms of resistance may have arisen in addition to those which are familiar (pigments and the like), or, all life is beneath a thin layer of soil [54]. This cannot disturb photosynthesis, since terrestrial algae photosynthesize in soil whose surface layers absorb UV-radiation completely. If photosynthetic organisms exist on Mars, apparently they photosynthesize without giving off oxygen, similar to photoautotrophic bacteria.

Traces of oxygen in the atmosphere may be sufficient to support protozoa life; it is also possible that there are organisms capable of anaerobic respiration due to compounds containing oxygen, and possibly there are anaerobes. Further, on the basis of terrestrial microorganisms' resistance to ionizing radiation, this cannot be the reason for lack of life on Mars, which is equally true of the reduced pressure and temperature variations that are readily withstood by many plant and lower animal organisms.

The most unfavorable extreme conditions on Mars must definitely include the nearly complete absence of water, both in the atmosphere and in the soil. For this reason, a profound study has started, dealing with the propagation, physiology, and biochemistry of xerophytic organisms. There is still no basis for concluding that the moisture level of the martian soil is 3.8%, i.e., the moisture level for the growth of terrestrial xerophytes. The possibility cannot be excluded that soil is moistened periodically by water contained in the atmosphere when the temperature falls; the basis for this assumption is that the polar caps on Mars are evidently composed of water and carbon dioxide.

Most of the methods suggested for observing extraterrestrial life, particularly on Mars, are based on culturing soil in nutrient media and recording subsequent reproduction of microorganisms. To create conditions for growing martian microflora, if such exist, two means are possible. First, conditions similar to those on Mars can be simulated. Soil cultures must be grown in very poor nutrient media, and the temperature must be low (+10° C). The atmosphere above the soil particles must consist of nitrogen and carbon dioxide. The experiment must be of considerable duration and may reach 90 days.

Theoretically, creating ecological conditions simulating those on Mars must be considered completely justified. Another possible approach is based on data from terrestrial ecology. Microorganisms can multiply under conditions that are close to extreme, but this does not mean that they cannot grow under more favorable conditions. A narrow, very strict ability to adapt to certain conditions of life is generally not true of microorganisms. Thus, all xerophytes grow on liquid nutrient media. Stenothermic thermophiles grow at 75° C, but can also grow at 35° C, as can

osmophiles, psychrophiles, and other microorganisms capable of adapting to certain life conditions [114].

The relationship of microorganisms to extreme conditions makes the use of nutrient media valuable for observing extraterrestrial life, and for culturing the media at 20°–30° C in the absence of a martian atmosphere [96]. Support for this method is that microorganisms inhabit the soil of deserts, the Antarctic, and the Arctic and multiply well under these conditions. The necessity of using more favorable conditions for growth is also governed by the brief duration of the functioning of the automatic biological station, 72 hours for example. Under strictly martian conditions, the reproduction of microorganisms will be quite negligible within this time frame. At the same time, media with both rich composition and higher temperatures will create conditions for more rapid reproduction of microorganisms, if they do exist on Mars. The search for extraterrestrial life is discussed in greater detail in Volume I, Part 3, Chapter 8 of this work, "Search for and Investigation of Extraterrestrial Forms of Life."

## REFERENCES

1. ABYSOV, S. S., C. A. ZAVARZIN, M. V. IVANOV, V. I. SERECIN, and O. G. SHIROKOV. Survival of microorganisms in potassium salt deposits. *Mikrobiologiya* 35(5):885–889, 1966.
2. AKSENOV, S. I. The limits of the adaptation of life to extreme conditions in connection with problems of exobiology. In, Tarusov, V. B., Ed. *Problemy Kosmicheskoy Biologii*, Vol. 19, pp. 7–89. Moscow, Nauka, 1971. (Transl: *Problems of Space Biology*). Vol. 19, pp. 1–76. Washington, D.C., NASA, 1973. (NASA TT-F-761)
3. ANTIPOV, V. V., N. L. DELONE, G. P. PARFENOV, and V. G. VYSOTSKIY. Results of biological experiments carried out under conditions of "Vostok" flights with the participation of cosmonauts A. G. Nikolayev, P. R. Popovich, and V. F. Byovskiy. In, Florkin, M., Ed. *Life Sciences and Space Research*, Vol. 3, pp. 215–229. Presented at 5th COSPAR Int. Space Sci. Symp., Florence, Italy, May 1964. Amsterdam, North-Holland; New York, Wiley, 1965.
4. ANTIPOV, V. V., V. A. KOZLOV, G. P. PARFENOV, and P. P. SAKSONOV. The results of biological studies made on board the *Voskhod* and *Voskhod-2* space-ships. In, Brown, A. H., and F. G. Favorite, Eds. *Life Sciences and Space Research*, Vol. 5, pp. 119–121. Presented at 7th COSPAR Int. Space Sci. Symp., Vienna, Austria, May 1966. Amsterdam, North-Holland, 1967.
5. ANTIPOV, V. V., N. L. DELONE, M. D. NIKITIN, G. P. PARFENOV, and P. P. SAKSONOV. Some results of radiobiological studies performed on *Cosmos-110* biosatellite. In, Vishniac, W., and F. G. Favorite, Eds. *Life Sciences and Space Research*, Vol. 7, pp. 207–209. Proc., Open Meet. Working Group 5, 11th COSPAR Plenary Meet., Tokyo, May 1968; Symp. Biological Effects of Radiation in Space, Tokyo, May 1968. Amsterdam, North-Holland, 1969.
6. BAB'YEVA, I. P., and V. I. GOLUBEV. Psychrophilic yeasts in the oases of Antarctica. *Mikrobiologiya* 38(3):518–524, 1969.
7. BASSET, J., and M. A. MACHEBOEUF. Études sur les effets biologiques des ultra-pressions. Études sur l'immunité: influence des pressions très élevées sur certains antigènes et anticorps (Transl: Studies on biological effects of high pressures. Studies on immunity: influence of very high pressures on some antigens and antibodies). *C. R. Acad. Sci. (Paris)* 196:67–69, 1933. (Fr.)
8. BECKWITH, T. D. Molds in cold storage. *Ice Refrig.* 90:159–160, 1936.

9. BECQUEREL, P. La vie terrestre provient-elle d'un autre monde? (Transl: Does terrestrial life come from another world?) *Bull. Soc. Astron. Fr.* 38:393-417, 1924. (Fr.)
10. BECQUEREL, P. La suspension de la vie au-dessous de 1/20° K absolu par démagnetisation adiabatique de l'alun de fer dans le vide le plus élevé. *C. R. Acad. Sci. (Paris)* 231:261, 1950. (Fr.)
11. BECQUEREL, P. La suspension de la vie des spores de bactéries et des moisissures desséchées dans la vide le zero absolu. Ses conséquences pour la dissemination et la conservation de la vie dans l'Univers. *C. R. Acad. Sci. (Paris)* 231:392, 1950. (Fr.)
12. BEDFORD, R. H. Salt as a control of bacterial decomposition of halibut. *Bull. Biol. Board Can.* (29):1-16, 1932.
13. BELEHRADEK, J. *Temperature and Living Matter.* (Portoplasma monographs), Vol. 8. Berlin, Gebrüder Borntraeger, 1935.
14. BERRY, J. A. Growth of yeast below zero. *Science* 80:341, 1934.
15. BIEN, E., and W. SCHWARTZ. Geomikrobiologische untersuchungen. VI. Über das vorkommen konservierter, toter und lebender bakterien-zellen in Salzgesteinen. *Z. Allg. Mikrobiol.* 5:185, 1965.
16. BORGSTROM, G. Unsolved problems in frozen food microbiology. In, *Proceedings, Low Temperature Microbiology Symposium*, pp. 197-257. Camden, N.J., Campbell Soup Co., 1962.
17. BORSTEL, VON R. C., R. H. SMITH, A. R. WHITING, D. S. GROSCH, L. S. BROWNING, I. LOSTER, J. V. SLATER, and B. BUCKHOLD. Mutational aspects of insects in the Biosatellite II experiment. In, Vishniac, W., and F. G. Favorite, Eds. *Life Sciences and Space Research*, Vol. 7, pp. 70-76. Proc., Open Meet. Working Group 5, 11th COSPAR Plenary Meet., Tokyo, May 1968. Amsterdam, North-Holland, 1969.
18. BORSTEL, VON R. C., R. H. SMITH, A. R. WHITING, and D. S. GROSCH. Biological responses to habrobracon to spaceflight. In, Vishniac, W., and F. G. Favorite, Eds. *Life Sciences and Space Research*, Vol. 8, pp. 6-11. Proc., Open Meet. Working Group 5, 12th COSPAR Plenary Meet., Prague, May 1969. Amsterdam, North-Holland, 1970.
19. BRUESCHKE, E. E., R. H. SUESS, and M. WILLARD. The viability of microorganisms in ultra-high vacuum. *Planet. Space Sci.* 8(1):30-34, 1961.
20. BUCKHOLD, B. Biosatellite II - physiological and somatic effects on insects. In, Vishniac, W., and F. G. Favorite, Eds. *Life Sciences and Space Research*, Vol. 7, pp. 77-83. Proc., Open Meet. Working Group 5, 11th COSPAR Plenary Meet., Tokyo, May 1968; Symp. Biological Effects of Radiation in Space, Tokyo, May 1968. Amsterdam, North-Holland, 1969.
21. BUECKER, H., and G. HORNECK. Survival of microorganisms under simulated space conditions. In, Vishniac, W., and F. G. Favorite, Eds. *Life Sciences and Space Research*, Vol. 8, p. 33. Presented at 12th COSPAR Plenary Meet., Prague, May 1969. Amster-
- dam, North-Holland, 1970.
22. BUECKER, H., G. HORNECK, and H. WOLLENHAUPT. Radiation sensitivity of *Escherichia coli* in vacuum. Presented at 3rd Int. Biophys. Congr., Cambridge, Mass., 1969.
23. BUECKER, H., G. HORNECK, R. FACIUS, M. SCHWAGER, C. THOMAS, G. TURCU, and H. W. WOLLENHAUPT. Effects of simulated space vacuum on bacterial cells. In, Vishniac, W., Ed. *Life Sciences and Space Research*, Vol. 10, pp. 191-195. Proc., Open Meet.. Working Group 5, 14th COSPAR Plenary Meet., Seattle, Wash., June 1971. Berlin, East Ger., Akademie, 1972.
24. CAMERON, R. E., F. A. MORELLI, and H. P. CONROW. *Survival of Microorganisms in Desert Soil Exposed to Five Years of Continuous Very High Vacuum.* Pasadena, Calif., Jet Propul. Lab., 1970. (JPL Rep. 32-1454) (NASA CR-109763)
25. CHLOPIN, G. W., and G. TAMMANN. Influence of high pressure on microorganisms. *Z. Hyg. Infekts.* (Leipzig) 45:171-204, 1903. (Ger.)
26. CHUMAK, M. D., T. P. BLOKHINA, and A. E. KRISS. The effect of prolonged cultivation of barotolerant bacteria under pressure on their propagation rate under these conditions. *Dokl. Akad. Nauk SSSR* 181(1):727-729, 1968.
27. DAVIS I., and J. D. FULTON. The reactions of terrestrial microorganisms to simulated martian conditions. In, *Proceedings, 10th International Astronautical Congress*, London, 1959, Vol. 2, pp. 778-785. Vienna, Springer, 1960.
28. DAVIS, N. S., G. J. SILVERMAN, S. A. GOLDBLITH, and W. H. KELLER. Survival of spores at several temperatures in ultrahigh vacuum. In, *Bacteriological Proceedings*, p. 31. Presented at 62d Annual Meet., Am. Soc. Microbiol., May 1962. (Abstr.)
29. DAVIS, N. S., G. J. SILVERMAN, and W. H. KELLER. Combined effects of ultrahigh vacuum and temperature on the viability of some spores and soil organisms. *Appl. Microbiol.* 11:202-210, 1963.
30. DEDOLPH, R. R. The influence of simulated low-gravity environments on growth, development and metabolism of plants. In, Brown, A. H., and F. G. Favorite, Eds. *Life Sciences and Space Research*, Vol. 5, pp. 217-228. Presented at 7th COSPAR Int. Space Sci. Symp., Vienna, Austria, May 1966. Amsterdam, North-Holland, 1967.
31. DELONE, N. L., V. V. ANTIPOV, E. N. MOROZOVA, P. P. SAKSONOV, and A. S. TRUSOVA. Growth stimulation of certain biological specimens subjected to vertical vibrations. *Kosm. Issled.* 6:788-792, 1968. (Transl: *Cosmic Res.*) 6:663-666, 1968.
32. DELONE, N. L., E. M. MOROZOVA, and V. V. ANTIPOV. A cytological study of some higher plants whose seeds and bulbs were on board 5, 6, and 7 probes. In, Vishniac, W. *Life Sciences and Space Research*, Vol. 9, p. 111. Proc., Open Meet., Working Group 5, 13th COSPAR Plenary Meet., Leningrad, May 1970. Berlin, East Ger., Akademie, 1971.

33. DELONE, N. L., A. S. TRUSOVA, E. M. MOROZOVA, V. V. ANTIPOV, and G. P. PARFENOV. The influence of space flights on board the spacecraft Kosmos-110 on microspores *Tradescantia paludosa*. *Kosm. Issled.* 6(2):299-303, 1968.
34. DE SERRES, F. J. Effects of radiation during space flight on microorganisms and plants on the Biosatellite II and Gemini XI missions. In, Vishniac, W., and F. G. Favorite, Eds. *Life Sciences and Space Research*, Vol. 7, pp. 62-66. Proc., Open Meet., Working Group 5, 11th COSPAR Plenary Meet., Tokyo, May 1968; Symp. Biological Effects of Radiation in Space, Tokyo, May 1968. Amsterdam, North-Holland, 1969.
35. DRUZ', V. A., and Yu. M. MADIYEVSKIY. Effect of constant magnetic and low-frequency electromagnetic fields on the hydration capacity of living tissues. *Biofizika* 11:631-637, 1966.
36. DUBININ, M. P., E. N. VAULINA, K. V. KOSIKOV, and I. D. ANIKEEVA, et al. Space flight effects on the heredity of higher plants and lower plants. In, *Life Sciences and Space Research*, Vol. 11, pp. 105-110. Presented at 15th COSPAR Plenary Meet., Madrid, May 1972. Berlin, E. Ger., Akademie, 1973.
37. EDWARDS, B. F. Weightlessness experiments on Biosatellite II. In, Vishniac, W., and F. G. Favorite, Eds. *Life Sciences and Space Research*, Vol. 7, pp. 84-92. Proc., Open Meet., Working Group 5, 11th COSPAR Plenary Meet., Tokyo, May 1968; Symp. Biological Effects of Radiation in Space, Tokyo, May 1968. Amsterdam, North-Holland, 1969.
38. EDWARDS, B. F., and S. W. GRAY. Cellular changes in wheat seedlings during orbital flight. In, Vishniac, W., Ed. *Life Sciences and Space Research*, Vol. 9, pp. 113-118. Proc., Open Meet., Working Group 5, 13th COSPAR Plenary Meet., Leningrad, May 1970. Berlin, East Ger., Akademie, 1971.
39. EDWARDS, B. F. Effects of weightlessness on cells and tissues. In, Vishniac, W., Ed. *Life Sciences and Space Research*, Vol. 10, p. 119. Proc., Open Meet., Working Group 5, 14th COSPAR Plenary Meet., Seattle, Wash., June 1971. Berlin, East Ger., Akademie, 1972.
40. FEDOROVA, R. I. Effect of ultraviolet radiation on microorganisms as a principal external factor of space environment. In, Florkin, M., and A. Dollfus, Eds. *Life Sciences and Space Research*, Vol. 2, pp. 305-310. Presented at 4th COSPAR Int. Space Sci. Symp., Warsaw, Pol., June 1963. Amsterdam, North-Holland; New York, Interscience, 1964.
41. FEHER, D. *Der Wuestenboden als Lebensraum* (Transl: *The Desert Floor as an Environment*). Sopron, Hung., 1939.
42. FRASER, D. Bursting bacteria by release of gas pressure. *Nature* 167:33-34, 1951.
43. GAZENKO, O. G., and A. A. GYURDZHIAN. On the biological role of gravity; some results and prospects of space research on satellites and spaceships. In, Florkin, M., Ed. *Life Sciences and Space Research*, Vol. 3, pp. 241-257. Presented at 5th COSPAR Int. Space Sci. Symp., Florence, Ital., May 1964. Amster-
- dam, North-Holland; New York, Wiley, 1965.
44. GAZENKO, O. G., and A. A. GYURDZHIAN. Physiological effects of gravitation. In, Brown, A. H., and M. Florkin, Eds. *Life Sciences and Space Research*, Vol. 4, pp. 1-21. Presented at 6th COSPAR Int. Space Sci. Symp., Mar del Plata, Argent., May 1965. Washington, D.C., Spartan, 1966.
45. GEIGER, P. J., F. A. MORELLI, and H. P. CONROW. Effects of ultrahigh vacuum on three types of microorganisms. In, *Supporting Research and Advanced Development Space Programs Summary*, Vol. 4, p. 109, Pasadena, Calif., Jet Propul. Lab., 1963.
46. GENKEL', P. A., and N. D. PRONINA. Anabiosis with desiccation of the floral poikiloxerophytic plant *Myrothamnus flabellifolia*. *Fiziol. Rast.* 16:896-901, 1969.
47. GOLLERBAKH, M. M., and V. B. SOCHAVA. Glaciers and snowflakes. In, Lavrenko, E. M., and V. B. Sochava, Eds. *Rastitel'nyi Pokrov SSSR* (Transl: *The Plant Cover of the USSR*), Vol. 2, pp. 835-839. Moscow, Editio Academiae Scientiarum, 1956.
48. GORDON, S. A., and J. SHEN-MILLER. On the thresholds of gravitational force perception by plants. In, Brown, A. H., and M. Florkin, Eds. *Life Sciences and Space Research*, Vol. 4, pp. 22-34. Presented at 6th COSPAR Int. Space Sci. Symp., Mar del Plata, Argent., May 1965. Washington, D.C., Spartan, 1966.
49. GORDON, S. A., and E. M. BUESS. Radiation-induced chromosome aberrations and rhythms in roots of gravity-compensated vicia. In, Vishniac, W., and F. G. Favorite, Eds. *Life Sciences and Space Research*, Vol. 7, p. 69. Proc., Open Meet., Working Group 5, 11th COSPAR Plenary Meet., Tokyo, May 1968; Symp. Biological Effects of Radiation in Space, Tokyo, May 1968. Amsterdam, North-Holland, 1969.
50. GRAVSKIY, E. A., and Ye. G. ZINOVIEVA. An investigation of the radiosensitivity in the cells repeatedly exposed to ionizing radiation. *Dokl. Akad. Nauk SSSR* 121:837-840, 1958.
51. GRAY, S. W., and B. F. EDWARDS. An effect of weightlessness following exposure to vibration. In, Vishniac, W., and F. G. Favorite, Eds. *Life Sciences and Space Research*, Vol. 8, pp. 25-32. Proc., Open Meet., Working Group 5, 12th COSPAR Plenary Meet., Prague, May 1969. Amsterdam, North-Holland, 1970.
52. GRIGORYEV, Yu. G., V. P. BENEVOLENSKY, Yu. P. DRUZHININ, Yu. I. SHIDAROV, V. I. KOROGODIN, L. V. NEVZGODINA, A. T. MILLER, and L. S. TSARAPKIN. Influence of Cosmos 368 spaceflight conditions on radiation effects in yeasts, hydrogen bacteria and seeds of lettuce and pea. In, Vishniac, W., Ed. *Life Sciences and Space Research*, Vol. 10, pp. 113-118. Proc., Open Meet., Working Group 5, 14th COSPAR Plenary Meet., Seattle, Wash., June 1971. Berlin, East Ger., Akademie, 1972.
53. HAGEN, C. A., E. J. HAWRYLEWICZ, and R. EHRLICH. Survival of microorganisms in a simulated Martian environment. *Appl. Microbiol.* 12:215-218, 1964.

54. HAGEN, C. A., E. J. HAWRYLEWICZ, B. T. ANDERSON, and M. L. CEPHUS. Effect of ultraviolet on the survival of bacteria airborne in simulated martian dust clouds. In, Vishniac, W., and F. G. Favorite, Eds. *Life Sciences and Space Research*, Vol. 8, pp. 53–58. Presented at 12th COSPAR Plenary Meet., Open Meet., Working Group 5, Prague, May 1969. Amsterdam, North-Holland, 1970.
55. HAWRYLEWICZ, E. J., and R. EHRLICH. *Studies with Microorganisms under a simulated Martian environment and Space Research*, Vol. 6, pp. 108–114. Proc., Open Biochemistry and Biology, 128th Meet., Am. Assoc. Adv. Sci., Denver, Dec. 1961.
56. HAWRYLEWICZ, E. J., B. B. GOWDY, and R. EHRLICH. Microorganisms under a simulated Martian environment. *Nature* 193:497, 1962.
57. HAWRYLEWICZ, E. J., C. A. HAGEN, and R. EHRLICH. Response of microorganisms to a simulated Martian environment. In, Florkin, M., Ed. *Life Sciences and Space Research*, Vol. 3, pp. 64–73. Presented at 5th COSPAR Int. Space Sci. Symp., Florence, Ital., May 1964. Amsterdam, North-Holland; New York, Wiley, 1965.
58. HAWRYLEWICZ, E. J., C. A. HAGEN, and R. EHRLICH. Survival and growth of potential microbial contaminants in severe environments. In, Brown, A. H., and M. Florkin, Eds. *Life Sciences and Space Research*, Vol. 4, pp. 166–175. Presented at 6th COSPAR Int. Space Sci. Symp., Mar del Plata, Argent., May 1965. Washington, D.C., Spartan, 1966.
59. HESS, E. In, Jenkins, D. W., S. M. Siegel, and C. E. ZoBell, *Compendium*. 1956.
60. HITE, B. H., N. J. GIDDINGS, and C. E. WEAKLEY, Jr. The effect of pressure on certain microorganisms encountered in the preservation of fruits and vegetables. *W. Va. Univ. Agric. Exp. Stn. Bull.* 146:1–67, 1914.
61. HORNECK, G., H. BUECKER, and H. WOLLENHAUPT. Survival of bacterial spores under some simulated lunar surface conditions. In, Vishniac, W., Ed. *Life Sciences and Space Research*, Vol. 9, pp. 119–124. Presented at 13th COSPAR Plenary Meet., Open Meet., Working Group 5, Leningrad, May 1970. Berlin, E. Ger., Akademie, 1971.
62. HORNECK, G., H. BUECKER, and H. W. WOLLENHAUPT. Survival of bacterial spores under some simulated lunar space conditions. In, Vishniac, W., Ed. *Life Sciences and Space Research*, Vol. 9, pp. 119–124. Proc., Open Meet., Working Group 5, 13th COSPAR Plenary Meet., Leningrad, May 1970. Berlin, East Ger., Akademie, 1971.
63. HOTCHIN, J., P. LORENZ, A. MARKUSEN, and C. HEMENWAY. The survival of microorganisms in space. Further rocket and balloon-borne exposure experiments. In, Brown, A. H., and F. G. Favorite, Eds. *Life Sciences and Space Research*, Vol. 5, pp. 1–6. Presented at 7th COSPAR Int. Space Sci. Symp., Vienna, Austria, May 1966. Amsterdam, North-Holland, 1967.
64. HOTCHIN, J., P. LORENZ, and C. L. HEMENWAY. The survival of terrestrial microorganisms in space at orbital altitudes during Gemini satellite experiments. In, Brown, A. H., and F. G. Favorite, Eds. *Life Sciences and Space Research*, Vol. 6, pp. 108–114. Proc., Open Meet., Working Group 5, 10th COSPAR Plenary Meet., London, Eng., July 1967. Amsterdam, North-Holland, 1968.
65. HOTCHIN, J., F. D. BAKER, and L. BENSON. Survival of RNA and DNA viruses in space on the Gemini XII satellite. In, Vishniac, W., and F. G. Favorite, Eds. *Life Sciences and Space Research*, Vol. 7, pp. 67–68. Proc., Open Meet., Working Group 5, 11th COSPAR Plenary Meet., Tokyo, May 1968; Symp. Biological Effects of Radiation in Space, Tokyo, May 1968. Amsterdam, North-Holland, 1969.
66. HUGO, W. B., Ed. *Inhibition and Destruction of the Microbial Cell*. London, New York, Academic, 1971.
67. IMSHENETSKIY, A. A., N. I. BOGROV, and S. V. LYSENKO. Resistance of microorganisms to a high vacuum. *Dokl. Akad. Nauk SSSR* 154(5):1188–1190, 1964.
68. IMSHENETSKIY, A. A., and S. V. LYSENKO. Ultra-high vacuum and microorganisms. In, Florkin, M., Ed. *Life Sciences and Space Research*, Vol. 3, pp. 142–148. Presented at 5th COSPAR Int. Space Sci. Symp., Florence, Ital., May 1964. Amsterdam, North-Holland; New York, Wiley, 1965.
69. IMSHENETSKIY, A. A., S. S. ABYZOV, G. T. VORONOV, A. I. ZHUKOVA, and S. V. LYSENKO. The possibility of life in outer space. In, Brown, A. H., and M. Florkin, Eds., *Life Sciences and Space Research*, Vol. 4, pp. 121–130. Presented at 6th COSPAR Int. Space Sci. Symp., Mar del Plata, Argent., May 1965. Washington, D.C., Spartan, 1966.
70. IMSHENETSKIY, A. A., S. S. ABYZOV, G. T. VORONOV, L. A. KUZHURINA, S. V. LYSENKO, G. G. SOTNIKOV, and R. I. FEDOROVA. Exobiology and the effect of physical factors on microorganisms. In, Brown, A. H., and F. G. Favorite, Eds. *Life Sciences and Space Research*, Vol. 5, pp. 250–260. Presented at 7th COSPAR Int. Space Sci. Symp., Vienna, Austria, May 1966. Amsterdam, North-Holland, 1967.
71. IMSHENETSKIY, A. A., G. S. KOMOLOVA, S. V. LYSENKO, and G. D. GAMULYA. Influence of a high vacuum on the activity of certain enzymes. *Dokl. Akad. Nauk SSSR* 182:971–972, 1968.
72. IMSHENETSKIY, A. A., and S. S. ABYZOV. Microbiological investigations of meteorites. In, Imshenetskiy, A. A., Ed. *Zhizn' Vne Zemli i Metody Yeye Obnaruzheniya* (Transl: *Extraterrestrial Life and Methods of Detecting It*), pp. 157–166. Moscow, Nauka, 1970.
73. IMSHENETSKIY, A. A., and S. V. LYSENKO. Effect of deep vacuum on microorganisms. In, Imshenetskiy, A. A., Ed. *Zhizn' Vne Zemli i Metody Yeye Obnaruzheniya* (Transl: *Extraterrestrial Life and Methods of Detecting It*), pp. 106–118. Moscow, Nauka, 1970.
74. IMSHENETSKIY, A. A., and S. V. LYSENKO. The effect of high vacuum on the oxidative processes in *Sarcina flava* and *Bacillus simplex*. *Mikrobiologiya* 39:480–483, 1970.

75. IMSHENETSKIY, A. A., A. M. LYSENKO, and S. V. LYSENKO. The effect of lyophilizing and high vacuum on bacteriophages of *E. coli*. *Mikrobiologija* 39:694–696, 1970.
76. IMSHENETSKIY, A. A., S. V. LYSENKO, G. G. SOTNIKOV, and G. D. GAMULYA. The effect of high vacuum on crystalline preparations of catalase, peroxidase, cytochrome c and ATP. *Mikrobiologija* 39:788–791, 1970.
77. IMSHENETSKIY, A. A., S. V. LYSENKO, and G. G. SOTNIKOV. The effect of high vacuum on ATP stability in microorganisms. *Mikrobiologija* 39:986–989, 1970.
78. IMSHENETSKIY, A. A., L. A. KUZHURINA, and V. M. YAKSHINA. Multiplication of certain soil microorganisms under simulated martian conditions. In, Vishniac, W., and F. G. Favorite, Eds. *Life Sciences and Space Research*, Vol. 8, pp. 59–61. Proc., Open Meet., Working Group 5. 12th COSPAR Plenary Meet., Prague, May 1969. Amsterdam, North-Holland, 1970.
79. IMSHENETSKIY, A. A., S. V. LYSENKO, and G. G. SOTNIKOV. The effect of high vacuum on the activity of iron-porphyrin enzymes in microorganisms. *Mikrobiologija*, 40:289–292, 1971.
80. IMSHENETSKIY, A. A., L. A. KUZHURINA, and V. M. YAKSHINA. On the multiplication of xerophilic microorganisms under simulated martian conditions. In, Sneath, P. H. A., Ed. *Life Sciences and Space Research*, Vol. 11, pp. 63–66. Proc., 15th COSPAR Plenary Meet., Madrid, May 1972. Berlin, East Ger., Akademie, 1973.
81. IMSHENETSKIY, A. A., S. V. LYSENKO, V. F. UDOVENKO, and A. M. BUTENKO. Long-term effect of high vacuum on microorganisms. *Mikrobiologija* 42:836–838, 1973.
82. ISACHENKO, B. L. Microorganisms from the lower layers of the biosphere in connection with the genesis of petroleum. In, his *Selected Works*, Vol. 2, pp. 218–225. Moscow, Akad. Nauk. SSSR, 1951.
83. JAHNEL, F. The survival of trypanosomes and spirochetes of recurrent fever after freezing in liquid helium at  $-269.5^{\circ}\text{C}$ . *Z. Immunitaetsforsch.* 94:328–341, 1938. (Ger.)
84. JAMES, P. E. The limits of life. *J. Br. Interplanet. Soc.* 14:265–266, 1955.
85. JAMES, P. E. In, Jenkins, D. W., S. M. Siegel, and C. E. ZoBell, *Compendium*. 1965.
86. JAZUDA and HIROSHI. *Okayama-Gakkai-Zasshi* 71:6761, 1959.
87. JENSEN, L. B. Bacteriology of ice. *Food Res.* 8:265–272, 1943.
88. JUMELL, H. Sur la dégagement d'oxygène par les plantes, aux basses températures. *C. R. Acad. Sci.* 112:1462, 1891.
89. KEILEN, D. The problem of anabiosis or latent life: history and current. *Concept. Proc. Roy. Soc. (B)* 150:149, 1959.
90. KISELEY, P. N., K. P. KASHKIN, J. B. BOLTAKS, and G. A. VITOVSAYA. The acquisition of radiore sistivity by a microbe cell inhabiting media with an increased level of natural radiation. *Mikrobiologija* 30:206–213, 1961.
91. KORZHUYEV, P. A. Life, gravitation, weightlessness. In, Pekelis, V. D., Ed. *Naselennyi Kosmos* (Transl: *Inhabited Space*), pp. 133–141. Moscow, Nauka, 1972.
92. KRASAVTSEV, O. A. Resistance of hardened woody plants to dehydration at low temperatures. *Fiziol. Rast.* 14:512–519, 1967.
93. KRISS, A. E., V. I. BIRYUZOVA, and S. S. ABYSOV. Microorganisms propagating under high pressure. *Izv. Akad. Nauk SSSR, Ser. Biol.* (6):677–689, 1958.
94. KRISS, A. E., and N. D. KOSHTOYANTS. Glucose metabolism in the pressure-tolerant bacterium *Pseudomonas* under conditions of high pressure and non-optimal temperatures. *Mikrobiologija* 38:945–951, 1969.
95. KRISS, A. E. Biological action of high pressure. *Usp. Mikrobiol.* 6:128–152, 1970.
96. KUZHURINA, L. A. Nutrient media which can be used to detect microorganisms on Mars. In, Imshenetskiy, A. A., Ed. *Zhizn' Vne Zemli i Metody Yeye Obnaruzheniya* (Transl: *Extraterrestrial Life and Methods of Detecting It*), pp. 41–47. Moscow, Nauka, 1970.
97. KUZHURINA, L. A., and V. M. YAKSHINA. Behavior of various soil microorganisms in the "Artificial Mars" chamber. In, Imshenetskiy, A. A., Ed. *Zhizn' Vne Zemli i Metody Yeye Obnaruzheniya* (Transl: *Extraterrestrial Life and Methods of Detecting It*), pp. 118–125. Moscow, Nauka, 1970.
98. LAMANNA, C., and M. F. MALLETT. *Basic Bacteriology*. Baltimore, Williams & Wilkins, 1965.
99. LARSON, W. P., T. B. HARTZELL, and H. S. DIEHL. The effect of high pressures on bacteria. *J. Infect. Dis.* 22:271–279, 1918.
100. LORENZ, P. R., C. L. HEMENWAY, and J. HOTCHIN. The biological effectiveness of solar electromagnetic radiation in space. In, Brown, A. H., and F. G. Favorite, Eds. *Life Sciences and Space Research*, Vol. 6, pp. 100–107. Proc., Open Meet., Working Group 5, 10th COSPAR Plenary Meet., London, Eng., July 1967. Amsterdam, North-Holland, 1968.
101. LOUBIERE, R., P. GROGNOT, and F. VIOLETTE. A note on changes in anaphase induced by mechanical vibration. In, Brown, A. H., and M. Florkin, Eds. *Life Sciences and Space Research*, Vol. 4, pp. 221–224. Presented at 6th COSPAR Int. Space Sci. Symp., Mar del Plata, Argent., May 1965. Washington, D.C., Spartan, 1966. (Abstr.)
102. LOZINA-LOZINSKIY, L. K. *Ocherki po Kriobiologii* (Transl: *Fundamentals of Cryobiology*). Leningrad, Nauka, 1972.
103. LOZINA-LOZINSKIY, L. K., V. N. BYCHENKOVA, E. I. ZAAR, V. L. LEVIN, and V. M. RUMYANTSEVA. Some potentialities of living organisms under simulated martian conditions. In, Vishniac, W., Ed. *Life Sciences and Space Research*, Vol. 9, pp. 159–165. Proc., Open Meet., Working Group 5, 13th COSPAR Plenary Meet., Leningrad, May 1970. Berlin, East Ger., Akademie, 1971.
104. LUYET, B. Sur le mécanisme de la mort cellulaire par

- les hautes pressions: l'intensité et la durée des pressions léthales pour la levure. *C. R. Acad. Sci. (Paris)* 204:1214-1215, 1937. (Fr.)
105. MACFAYDEN, A., and S. ROWLAND. Influence of temperature of liquid hydrogen on bacteria. *Proc. Roy. Soc. (London)* 66:488-489, 1900.
106. MALYSHEK, V. T., and A. A. MALIYANTZ. Sulphur bacteria in the "pink" waters of the Surukhani oil fields and their significance in the geochemistry of water. *Dokl. Akad. Nauk SSSR N.S.3:221-224*, 1935.
107. MCELROY, W. D., and G. DE LA HABA. Effect of pressure on induction of mutations by nitrogen mustard. *Science* 110:640-642, 1949.
108. MIRCHINK, T. G., G. B. KASHKINA, and Yu. D. ABATUROV. Stability of pigmented fungi *Stemphylium botyosum Wallr.* and *Cladosporium cladosporioides* (Fries) de Vries towards gamma-irradiation. *Mikrobiologiya* 37(5):865-869, 1968.
109. MIRO, L., G. DELTOUR, A. PFISTER, R. KAISER, and R. GRANDPIERRE. Current status of French research of the biological effects of heavy ions in cosmic radiation as observed in high altitude balloons. In, Vishniac, W., and F. G. Favorite, Eds. *Life Sciences and Space Research*, Vol. 8, pp. 39-44. Proc., Open Meet., Working Group 5, 12th COSPAR Plenary Meet., Prague, May 1969. Amsterdam, North-Holland, 1970.
110. MISH, L. B. *Biological Studies of Symbiosis Between the Algae and Fungus in the Rock Lichen Umbilicaria papillosa*. Cambridge, Mass. Harvard Univ. Press, 1953.
111. MORELLI, F. A., F. P. FEHLNER, and C. H. STEMBRIDGE. Effect of ultra-high vacuum on *Bacillus subtilis* var. *Niger*. In, *JPL Research Summary*, No. 36-14, pp. 1-4. Pasadena, Calif., Calif. Inst. Technol., Jet Propul. Lab., May 1962.
112. MORELLI, F. A., F. P. FEHLNER, and C. H. STEMBRIDGE. Effect of ultra-high vacuum on *Bacillus subtilis* var. *Niger*. *Nature* 196:106-107, 1962.
113. MURZAKOV, B. G. Problems of microflora ecology of desert soils in connection with problems of space microbiology. *Usp. Mikrobiol.* 9:96, 1974.
114. MURZAKOV, B. G. Methods for detecting extraterrestrial life. *Usp. Mikrobiol.* 11, 1975.
115. NEI, T., T. ARAKI, and T. MATSUSAKA. The mechanism of cellular injury by freezing microorganisms. In, Asahina, E., Ed. *Proceedings, International Conference on Low Temperature Science*, Vol. 2, pp. 157-169. Presented at Conf. on Cryobiology-Cellular Injury and Resistance in Freezing Organisms, Sapporo, Jap., Aug. 1966. Sapporo, Hokkaido Univ., 1966.
116. NOVITSKIY, Yu. I. Biomagnetism and plant life. *Izv. Akad. Nauk SSSR, Ser. Biol.* (2):257-261, 1967.
117. NOVOGRUDSKIY, D. M. *Pochvennaya Mikrobiologia* (Transl: *Soil Microbiology*). Alma-Ata, Akad. Nauk Kazakh SSR, 1956.
118. OPFELL, J. B., and G. P. ZEBAL. Ecological patterns of microorganisms in desert soils. In, Brown, A. H., and F. G. Favorite, Eds. *Life Sciences and Space Research*, Vol. 5, pp. 187-203. Presented at 7th COSPAR Int. Space Sci. Symp., Vienna, Austria, May 1966. Amsterdam, North-Holland, 1967.
119. OPPENHEIMER, C. H., and C. E. ZOBELL. The growth and viability of sixty-three species of marine bacteria as influenced by hydrostatic pressure. *J. Mar. Res.* 11:10-18, 1952.
120. OSTER, I. I. Genetic effects produced by the space environment. In, Vishniac, W., and F. G. Favorite, Eds. *Life Sciences and Space Research*, Vol. 7, pp. 95-96. Proc., Open Meet., Working Group 5, 11th COSPAR Plenary Meet., Tokyo, May 1968; Symp. Biological Effects of Radiation in Space, Tokyo, May 1968. Amsterdam, North-Holland, 1969.
121. PACKER, E., S. SCHER, and C. SAGAN. Biological contamination of Mars II. Cold and aridity as constraints on the survival of terrestrial microorganisms, in simulated martian environments. *Icarus* 2:293-316, 1963.
122. PARFENOV, G. P. Genetic studies in space. *Kosm. Issled.* 5(1):140-155. 1967. (NASA TT-F-11251)
123. PARIN, V. V., Yu. G. GRIGORYEV, E. E. KOVALEV, N. I. RYZHOV, N. N. DERBENEVA, V. I. POPOV, and M. G. PETROVNIN. Characteristics of biological effects of cosmic radiation, model investigations. In, Vishniac, W., and F. G. Favorite, Eds. *Life Sciences and Space Research*, Vol. 7, pp. 160-170. Proc., Open Meet., Working Group 5, 11th COSPAR Plenary Meet., Tokyo, May 1968; Symp. Biological Effects of Radiation in Space, Tokyo, May 1968. Amsterdam, North-Holland, 1969.
124. PETRAS, E., and K. BISA. Microbiological studies on the radiation environment of the ionosphere and stratosphere. In, Brown, A. H., and F. G. Favorite, Eds. *Life Sciences and Space Research*, Vol. 6, pp. 115-122. Proc., Open Meet., Working Group 5, 10th COSPAR Plenary Meet., London, Eng., July 1967. Amsterdam, North-Holland, 1968.
125. PITTEDRIGH, C. S. On the biological problems to be attacked with a series of U.S. satellites in 1966. In, Florkin, M., Ed. *Life Sciences and Space Research*, Vol. 3, pp. 206-214. Presented at 5th COSPAR Int. Space Sci. Symp., Florence, Italy, May 1964. Amsterdam, North-Holland; New York, Wiley, 1965.
126. PLANEL, H., I. P. SOLEILHAVOUP, and R. TIXADOR. Biological effect of cosmic and Telluric radiations. In, Vishniac, W., Ed. *Life Sciences and Space Research*, Vol. 10, p. 187. Proc., Open Meet., Working Group 5, 14th COSPAR Plenary Meet., Seattle, Wash., June 1971. Berlin, East Ger., Akademie, 1972.
127. PORTNER, D. M., D. R. SPINER, R. K. HOFFMAN, and C. R. PHILLIPS. Effect of ultrahigh vacuum on viability of microorganisms. *Science* 134(2):2047, 1961.
128. PRINCE, A. E., and S. BAKANAUSKAS. In, *Survival of Microorganism Spores Exposed to High Vacuum*, Append. I. Dayton, Ohio, USAF Wright Air Dev. Cent., Air Res. Dev. Command, 1958.
129. RECORD, B. R., and R. TAYLOR. Some factors influencing the survival of *Bacterium coli* on freeze-drying. *J. Gen. Microbiol.* 9:475, 1953.

130. ROBERTS, T., and E. S. WYNNE. *Studies with a Simulated Martian Environment: Bacterial Survival and Soil Moisture Content*. Brooks AFB, Tex., Sch. Aerosp. Med., 1962. (SAM-TDR-62-121.)
131. ROBERTS, T. L., and L. A. IRVINE. *Studies with a Simulated Martian Environment. Germination and Growth of Bacterial Spores*. Brooks AFB, Tex., Sch. Aerosp. Med., 1963. (SAM-TDR-63-75.)
132. SAKAI, A. Survival of plant tissue at super-low temperatures by rapid cooling and rewarming. In, Asahina, E., Ed. *Proceedings, International Conference on Low Temperature Science*, Vol. 2, pp. 119-130. Presented at Conf. on Cryobiology-Cellular Injury and Resistance in Freezing Organisms, Sapporo, Jap., Aug. 1966. Sapporo, Hokkaido Univ., 1966.
133. SAMOYLOVA, K. A. *Deystviye Ul'trafioletovoy Radiatsii na Kletku* (Transl: *Effect of Ultraviolet Radiation on the Cell*). Leningrad, Nauka, 1967.
134. SAVENKO, I. A., N. F. PISARENKO, P. I. SHAVRIN, and V. E. NESTEROV. Control over cosmic radiation level during flight of space vehicles Vostok 3, Vostok 4, Vostok 5, and Vostok 6. In, Florkin, M., Ed. *Life Sciences and Space Research*, Vol. 3, pp. 23-28. Presented at 5th COSPAR Int. Space Sci. Symp., Florence, Ital., May 1964. Amsterdam, North-Holland; New York, Wiley, 1965.
135. SCHAIRER, L. A., A. H. SPARROW, and K. M. MARI-MUTHU. Radiobiological studies of plants orbited in Biosatellite II. In, Vishniac, W., and F. G. Favorite, Eds. *Life Sciences and Space Research*, Vol. 8, pp. 19-24. Proc., Open Meet., Working Group 5, 12th COSPAR Plenary Meet., Prague, May 1969. Amsterdam, North-Holland, 1970.
136. SCHWARTZ, W., and F. ZEITSCHR. *Fiftür Allgemeine Mikrobiologie*.
137. SHAKHOV, A. A. Influence of cosmic radiation on vital activity of plants. *Zh. Obshch. Biol.* 23(2):81-89, 1962.
138. SHEN-MILLER, J. Reciprocity in geotropic response and acceleration constraints of the biosatellites. In, Vishniac, W., and F. G. Favorite, Eds. *Life Sciences and Space Research*, Vol. 7, pp. 93-94. Proc., Open Meet., Working Group 5, 11th COSPAR Plenary Meet., Tokyo, May 1968; Symp. Biological Effects of Radiation in Space, Tokyo, May 1968. Amsterdam, North-Holland, 1969.
139. SIEGEL, S. M., L. A. HALPERN, C. GIUMARRO, G. RENWICK, and G. DAVIS. Martian biology: the experimentalists approach. *Nature* 197:329-331, 1963.
140. SIEGEL, S. M. *The General and Comparative Biology of Terrestrial Organism Under Experimental Stress Conditions*. Tarrytown, N.Y., Union Carbide Res. Inst., 1964. (Q. Rep. 3) (NASA CR-56272)
141. SIEGEL, S. M., C. GIUMARRO, and R. LATTERELL. Behavior of plants under extraterrestrial conditions: seed germination in atmosphere containing nitrogen oxides. *Proc. Nat. Acad. Sci. USA* 52:11-13, 1964.
142. SILVERMAN, G. J., and N. BEECHER. Survival of cocci after exposure to ultrahigh vacuum at different temperatures. *Appl. Microbiol.* 15(1):665-667, 1967.
143. SISAKYAN, N. M., O. G. GAZENKO, and V. V. ANTIPOV. Satellite biological experiments. Major results and problems. In, Florkin, M., Ed. *Life Sciences and Space Research*, Vol. 3, pp. 185-205. Presented at 5th COSPAR Int. Space Sci. Symp., Florence, Ital., May 1964. Amsterdam, North-Holland; New York, Wiley, 1965.
144. SISAKYAN, N. M. Several problems of exophysiology. In, Sisakyan, N. M., Ed. *Problemy Kosmicheskoy Biologii*, Vol. 6, pp. 5-21. Moscow, Nauka, 1967. (Transl: *Problems of Space Biology*), Vol. 6, pp. 1-18. Washington, D.C., NASA, 1968. (NASA TT-F-528.)
145. SLATER, J., B. BUCKHOLD, I. SILVER, and C. TOBIAS. Environmental studies with the beetle, *Tribolium confusum*. In, Vishniac, W., and F. G. Favorite, Eds. *Life Sciences and Space Research*, Vol. 8, p. 5. Proc., Open Meet., Working Group 5, 12th COSPAR Plenary Meet., Prague, May 1969. Amsterdam, North-Holland, 1970.
146. SOLNTSEVA, I. O. Results of the prolonged exposure of *Rhodotorula glutinis* to weak doses of UV-light. *Tr. Inst. Biol. Vnutr. Vod. Akad. Nauk SSSR* 14(17):84-86, 1967.
147. SOLNTSEVA, I. O. Resistance of mountain strains of yeast-like organisms to UV-irradiation. *Tr. Inst. Biol. Vnutr. Vod. Akad. Nauk SSSR* 14(17):91-93, 1967.
148. STANKO, S. A. Problems of the habitability of Mars and the photoenergetics of plants. In, *Tezisy Dokladov VI Sovesh. po Probleman Planetol.* (Transl: *Sixth Congress on Problems of Planetology*), Vol. 2, pp. 96-98. Leningrad, 1968.
149. STURM, G. Effect of hydrostatic pressure on algae. *Arch. Mikrobiol.* 28:109-125, 1957.
150. SUTULOV, L. S., S. G. KULKIN, P. P. SAKSONOV, J. L. SUTULOV, N. I. KONNOVA, L. V. TRUCHINA, E. S. SEVERGINA, L. L. SAMSONOVA, S. N. SONINA, T. V. SELIVANOVA, and V. I. SOLOV'YEV. Post-flight histological analysis of turtles aboard Zond 7. In, Vishniac, W., Ed. *Life Sciences and Space Research*, Vol. 9, pp. 125-128. Proc., Open Meet., Working Group 5, 13th COSPAR Plenary Meet., Leningrad, May 1970. Berlin, East Ger., Akademie, 1971.
151. TANNO, K. Freezing injury in fat-body cells of the poplar sawfly. In, Asahina, E., Ed. *Proceedings, International Conference on Low Temperature Science*, Vol. 2, pp. 245-257. Presented at Conf. on Cryobiology-Cellular Injury and Resistance in Freezing Organisms, Sapporo, Jap., Aug. 1966. Sapporo, Hokkaido Univ., 1966.
152. TERUMOTO, I. Frost resistance in algae cells. In, Asahina, E., Ed. *Proceedings, International Conference on Low Temperature Science*, Vol. 2, pp. 191-209. Presented at Conf. on Cryobiology-Cellular Injury and Resistance in Freezing Organisms, Sapporo, Jap., Aug. 1966. Sapporo, Hokkaido Univ., 1966.
153. THEDE, A. L., and G. S. RADKE. Correlation of dose, rate and spectral measurements in the inner Van Allen belt. In, Brown, A. H., and F. G. Favorite, Eds. *Life Sciences and Space Research*, Vol. 6, pp. 59-68. Proc., Open Meet., Working Group 5, 10th COSPAR

- Plenary Meet., London, Eng., July 1967. Amsterdam, North-Holland, 1968.
154. TIMSON, W. J., and A. J. SHORT. Resistance of microorganisms to hydrostatic pressure. *Biotechnol. Bioeng.* 7:139-159, 1965.
155. TUMANOV, I. I. Frost resistance of fruit trees. *News of the USSR Academy of Sciences, Biology*, No. 3:459, 1963.
156. TUMANOV, I. I., O. A. KRASAVTSEV, and N. N. KHVALIN. An increase in frost resistance to -235°C attained in the birch and black currant by the hardening method. *Dokl. Akad. Nauk SSSR* 127(2):1301-1303, 1959.
157. VAULINA, E. N., and I. D. ANIKEEVA. The influence of space flight on *Chlorella*. In, Vishniac, W., and F. G. Favorite, Eds. *Life Sciences and Space Research*, Vol. 8, pp. 12-18. Proc., Open Meet., Working Group 5, 12th COSPAR Plenary Meet., Prague, May 1969. Amsterdam, North-Holland, 1970.
158. VAULINA, E. N., I. D. ANIKEEVA, I. G. GUBAREVA, and G. A. STRAUCH. Survival and mutability of *Chlorella* aboard the Zond vehicles. In, Vishniac, W., Ed. *Life Sciences and Space Research*, Vol. 9, pp. 105-110. Proc., Open Meet., Working Group 5, 13th COSPAR Plenary Meet., Leningrad, May 1970. Berlin, East Ger., Akademie, 1971.
159. VERNADSKIY, V. I. *Biosfera* (Transl: *The Biosphere*). Leningrad, 1926.
160. WAY, M. I. The effects of freezing temperatures on the developing egg of *Leptohylemyia coarctata Fall.* (Diptera, Muscidae) with special reference to diapause development. *J. Inst. Physiol.* 4:92, 1960.
161. WINCHESTER, G., and T. J. MURRAY. Effect of liquid air temperature on bacteria. *Proc. Soc. Exp. Biol. Med.* 35:165-166, 1936.
162. YENIKEYEVA, M. G. Moisture of the soil and activity of microorganisms: experiments with pure cultures of microorganisms. *Tr. Inst. Mikrobiol. Akad. Nauk SSSR* 2:130-138, 1952.
163. YOUNG, R. S. Differential survival of bacteria under Martian conditions. In, Brown, A. H., and M. Florkin, Eds. *Life Sciences and Space Research*, Vol. 4, pp. 131-132. Presented at 6th COSPAR Int. Space Sci. Symp., Mar del Plata, Argent., May 1965. Washington, D.C., Spartan, 1966.
164. YOUNG, R. S., and J. W. TREMOR. Weightlessness and the developing frog egg. In, Brown, A. H., and F. G. Favorite, Eds. *Life Sciences and Space Research*, Vol. 6, pp. 87-93. Proc., Open Meet., Working Group 5, 10th COSPAR Plenary Meet., London, Eng., July 1967. Amsterdam, North-Holland, 1968.
165. ZERNOV, S. A., and O. I. SHMAL'GAUZEN. Life limits at negative temperatures. *Reports of the USSR Academy of Sciences, Biology* 44:84, 1944.
166. ZHUKOV-VEREZHNICKOV, N. N., A. A. ANTIPOV, R. I. BAYEVSKIY, O. G. GAZENKO, A. M. GENIN, A. A. GYURDZHIAN, B. A. ZHURALEV, A. Sh. KARPOV, G. P. PARFENOV, A. D. SERYAPIN, Ye. Ya. SHEPELEV, and V. I. YAZDOVSKIY. Some results of biomedical investigations on the second and third Sputnik spacecraft. In, Sisakyan, N. M., Ed. *Problemy Kosmicheskoy Biologii*, Vol. 1, pp. 267-284. Moscow, Akad. Nauk SSSR, 1962. (Transl: *Problems of Space Biology*), Vol. 1, pp. 295-313. Washington, D.C., NASA, 1963. (NASA TT-F-174)
167. ZHUKOV-VEREZHNICKOV, N. N., I. N. MAYSKIY, V. I. YAZDOVSKIY, A. P. PEKKOV, N. I. RYBAKOV, N. N. KLEMPARSKAYA, A. A. GYURDZHIAN, G. P. TRIBULEV, N. P. NEVED'YEVA, M. M. KAPICHNIKOV, I. I. PODOPLELOV, V. V. ANTIPOV, I. S. NOVIKOVA, and V. Ya. KOP'YEV. Problems of space microbiology and cytology. In, Sisakyan, N. M., Ed. *Problemy Kosmicheskoy Biologii*, Vol. 1, pp. 118-136, 1962. Moscow, Akad Nauk SSSR, 1962. (Transl: *Problems of Space Biology*), Vol. 1, pp. 133-151. Washington, D.C., NASA, 1963. (NASA TT-F-174)
168. ZHUKOV-VEREZHNICKOV, N. N., M. N. VOLKOV, I. N. MAYSKIY, M. A. GUBERNIEV, N. I. RYBAKOV, V. V. ANTIPOV, V. A. KOZLOV, P. P. SAKSONOV, G. P. PARFENOV, A. V. KOLOBOV, K. D. RYBAKOVA, and E. D. ANISKIN. Genetic experimental studies of lysogenic bacteria during the Cosmos 110 flight. *Kosm. Issled.* 6:144-149, 1968.
169. ZHUKOV-VEREZHNICKOV, N. N., M. N. VOLKOV, I. N. MAYSKIY, N. I. RYBAKOV, M. A. GUBERNIEV, I. I. PODOPLELOV, A. N. KULAGIN, E. D. ANISKIN, K. D. RYBAKOVA, N. I. SHARYI, I. P. VORONKOVA, P. P. SAKSONOV, V. Ya. KOP'YEV, V. V. ANTIPOV, V. A. KOZLOV, G. P. PARFENOV, and V. I. ORLOVSKIY. Experiments with microorganisms and human cell cultures in the Zond 5 and Zond 7 flights. In, Vishniac, W., Ed. *Life Sciences and Space Research*, Vol. 9, pp. 99-103. Proc., Open Meet., Working Group 5, 13th COSPAR Plenary Meet., Leningrad, May 1970. Berlin, East Ger., Akademie, 1971.
170. ZHUKOV-VEREZHNICKOV, N. N., M. N. VOLKOV, N. I. RYBAKOV, I. N. MAYSKIY, P. P. SAKSONOV, M. A. GUBERNIEV, I. I. PODOPLELOV, V. V. ANTIPOV, V. A. KOZLOV, A. N. KULAGIN, E. D. ANISKIN, K. D. RYBAKOVA, N. I. SHARYI, Z. P. VORONKOVA, G. P. PARFENOV, V. I. ORLOVSKIY, and V. A. GUMENIUK. Biological action of space flight factors on lysogenic bacteria *E. Coli* K-12 (lambda) and human cells in a culture. *Kosm. Issled.* 9:292-299, 1971. (Transl: *Cosmic Res.*) 9:267-273, 1971.
171. ZHUKOVA, A. I., and I. I. KONDRA'T'YEV. On artificial martian conditions reproduced for microbiological space research. In, Florkin, M., Ed. *Life Sciences and Space Research*, Vol. 3, pp. 120-126. Presented at 5th COSPAR Int. Space Sci. Symp., Florence, Ital., May 1964. Amsterdam, North-Holland; New York, Wiley, 1965.
172. ZHUKOVA, A. I., and V. Kh. KOZLOVA. Viability of microorganisms in the desert soils of Turkmeniya. *Mikrobiologiya* 35:503-508, 1966.
173. ZOBELL, C. E., and F. H. JOHNSON. The influence of hydrostatic pressure on the growth and viability of terrestrial and marine bacteria. *J. Bacteriol.* 57:179-

- 189, 1949.
174. ZOBELL, C. E., and C. H. OPPENHEIMER. Some effects of hydrostatic pressure on the multiplication and morphology of marine bacteria. *J. Bacteriol.* 60:771-781, 1950.
175. ZOBELL, C. E. Occurrence and importance of bacteria in Indonesian waters. *J. Sci. Res. (Indones.)* 1:2-6, 1952.
176. ZOBELL, C. E. Bacterial life at the bottom of the Philippine trench. *Science* 115:507-508, 1952.
177. ZOBELL, C. E., and A. B. COBET. Growth, reproduction and death rates of *Escherichia coli* at increased hydrostatic pressures. *J. Bacteriol.* 84:1228-1236, 1962.
178. ZOBELL, C. E. Hydrostatic pressure as a factor affecting the activities of marine microbes. In, Miyake, Y., and T. Koyama, Eds. *Recent Researches in the Fields of Hydrosphere, Atmosphere and Nuclear Geochemistry* (Ken Sugawara Festival Volume), Water Res. Lab., Nagoya Univ., pp. 83-116. Tokyo, Maruzen, 1964.
179. ZOBELL, C. E., and A. B. COBET. Filament formation by *Escherichia coli* at increased hydrostatic pressures. *J. Bacteriol.* 87:710-719, 1964.
180. ZOBELL, C. E., and L. L. HITTLE. Some effects of hyperbaric oxygenation on bacteria at increased hydrostatic pressures. *Can. J. Microbiol.* 13:1311-1319, 1967.

## Chapter 7

# THEORETICAL AND EXPERIMENTAL PREREQUISITES OF EXOBIOLOGY<sup>1</sup>

A. I. OPARIN

Institute of Biochemistry imeni A. N. Bakh, Academy of Sciences USSR, Moscow

### EXOBIOLOGY AND THE ORIGIN OF LIFE: THE INSEPARABLE CONNECTION

The world we live in is constantly changing through a process of evolutionary development that is gradual, and which leads to emergence of ever newer, more complex, more diverse, and richly differentiated forms of reality. This process may not occur simultaneously and identically everywhere, but in different ways at different rates in various places in the universe and on various objects in the celestial world. Thus, evolution must not be diagramed as a single direct line, but rather as a cluster of various paths, whose separate branches may lead to very complex and complete forms of organization and movement of matter. Nothing is known about many of these forms, and in numerous instances, their existence is not even suspected. Any one form should not be considered prematurely as a special category of life, only because of its complexity or perfection. Life is far from a result

of all the numerous branches in the development of matter; its specific qualities and ways of emerging and improving are inherent. Only a single example of life, terrestrial life, is known at present, from which judgments must proceed of other possible forms of biological organization. The Earth and the events which originated on it must, to a great extent, serve as a model for broader judgments of life in the universe.

As long as the origin of life on Earth was considered a kind of rare "happy accident," there was little stimulus to discuss life beyond our planet, apart from calculations of the degree of probability of such an "improbable" event, which was scarcely intellectually satisfying. However, there is every reason now to see in the origin of life not a "happy accident" but a completely regular phenomenon, an inherent component of the total evolutionary development of our planet. The search for life beyond Earth is thus only a part of the more general question, which confronts science, of the origin of life in the universe. Study of the conception of life on Earth amounts to an investigation of only one example of an event which must have occurred countless times in the world. Therefore, an explanation of how life appeared on Earth should strongly support the theory of existence of life on other bodies in the universe.

The problem of the origin of life, almost completely ignored by the scientific world at the

<sup>1</sup> Translation of, *Teoreticheskiye i eksperimental'nyye predposyolki ekzobiologii*, Volume I, Part 3, Chapter 2 of *Osnovy Kosmicheskoy Biologii i Meditsiny (Foundations of Space Biology and Medicine)*, Moscow, Academy of Sciences USSR, 1972, 154 pages.

The valuable compilations for this chapter made by R. M. Lemmon and G. C. Pimental of the USA are gratefully acknowledged, as well as the contributions by I. A. Egorov, V. N. Florovskov, T. E. Pavlovskov, K. B. Serebrovskov, and V. P. Vdovskin of the USSR.

beginning of this century, now attracts many investigators with different specialities and from various countries. The related scientific literature has thus increased greatly. It is expedient to cite from the literature those monographs [40, 41, 75, 76, 261, 305, 368, 369, 371, 374, 375, 376, 440, 486, 487] and thematic collections [71, 120, 148, 246, 263, 320, 373, 381, 438, 502, 511] published in recent years which contain generalized data and broad summaries.

Terrestrial life originated specifically through the evolutionary development of hydrocarbons (organic compounds). The proposal is often made in scientific, and particularly in popular literature, that life could have emerged on other bodies of our celestial world based on compounds of other elements (silicon, germanium, and so forth). Since signs of the existence of such forms of life have in fact not been observed, this proposition is general and purely theoretical, but even in such form it meets very solid theoretical objections. Quantum chemistry, which provides an understanding of the specific electron structure of molecules [459, 463, 464, 625], nowhere favors the possibility of a noncarbon form of life. The most important vital functions are impossible without conjugate or resonant molecular systems, which are rich in electrons and highly delocalized [460, 461]. No other element may replace carbon in this respect. In particular, silicon—close to carbon in Mendeleev's table—could not serve as the basis for the structural components of life despite its abundance on the surface of the Earth [115; 232, 624]. This prediction, according to modern quantum chemistry, is based on electronic delocalization, which is inherent in carbon compounds but lacking in silicon compounds [282, 462]. Thus, in the summary works cited and in this review, attention is concentrated on the evolutionary development of carbon compounds, which led to the origin of life on Earth.

### **EMERGENCE AND EVOLUTION OF CARBON COMPOUNDS IN THE UNIVERSE**

Modern astronomical data reveal surprising interconnections within the galactic system as

a whole. The evolution of the universe appears at present as a single development, where each subsequent stage is inseparably bound to the preceding one and understood only in that light. An arbitrarily selected starting point of evolution, which has lasted many billions of years, is the process of nucleosynthesis, i.e., formation of the atomic nuclei of all the known elements. The evolution of nucleosynthesis is normally set in parallel with the evolutionary development of the stars [64, 144, 145, 162, 208, 555], since it has become clear that the process of star formation has occurred and continues without interruption in the universe [17, 131, 184, 514].

That our galaxy consists of five different types of star population [329] is conditionally accepted. Stars of an age close to that of the galaxy [146, 236, 240] belong to the first and most ancient type—from 12 to 20 billion years old. The Sun, a younger star of the third generation, is calculated to be about 5 billion years old, i.e., it originated after our galaxy had existed for a long time [58]. Even younger star populations are in our galaxy, among which, in particular, are stars located directly in the vicinity of the spiral branches of the galaxy [11, 65]. The elemental composition of stars of the first generation differs from that of younger stars in having a much higher ratio of hydrogen over metals. This graphically indicates that the initial medium from which stars of the first generation were formed consisted almost exclusively of hydrogen, which even now is the most prevalent element in space (98% of all atoms in the universe are hydrogen atoms) [144, 566]. The stars of later generations (in particular the Sun), however, were formed from a mixture of light and heavy elements, which must have originated long after the galaxy began to form [239, 248].

### **Nucleosynthesis**

Modern data show that two paths of nucleosynthesis are possible: one, stable, is related to the mechanism of stellar radiation in stable stars; and the other, unstable, is related to supernova bursts [77, 79, 558, 559]. The nucleosynthesis of light elements is exoergic; the energy liberated supports the stellar radiation. Be-

cause electrostatic repulsion during the joining of hydrogen nuclei is relatively small, a conversion of hydrogen into helium may occur at temperatures of a million degrees. Nucleosynthesis of light elements is even possible in a contracting gas sphere which consists of only hydrogen, and it may begin immediately after this sphere reaches the indicated temperature due to its compression and the liberation of gravitational energy. For the origin of heavier elements, however, a temperature of several billion degrees is necessary, which is lacking in the interiors of stable stars and arises only during supernova bursts.

Carbon did not require supernova bursts for its nucleosynthesis, but originated long before the formation of the heavy elements in the stable process of stellar radiation. The carbon-nitrogen reaction, along with proton-proton transformation, is the basic thermonuclear source of the stars' energy. Hydrogen, helium, carbon, nitrogen, and oxygen comprise the group of nucleogenetically related elements. Hydrogen is the most primordial chemical element in the universe, and all other elements are formed from it. The nuclear fusion of hydrogen, as a result of the action of the proton-proton cycle, led to the formation of helium at the beginning of stellar evolution.

The carbon-nitrogen cycle, during the process of "combustion" of helium and the capture of  $\alpha$ -particles, leads to the formation of carbon, nitrogen, and oxygen in correspondingly more developed celestial bodies, particularly in the so-called carbon stars [64, 65]. Therefore, carbon, like other light elements (H, He, N, O), is extensively distributed in the universe. It could have been detected comparatively long ago in studying the spectra of all classes of stars, including the most ancient generations [272]. In stellar atmospheres which have the highest surface temperatures, carbon is present in the ionized or neutral atomic state [210, 433], but even beginning with type-A stars, g-bands appear in their spectra, which indicate the origin of primary carbon compounds—hydrocarbons (methane, CH, [627]). In the spectra of subsequent types of stars, the hydrocarbon bands appear with increasingly greater clarity as the surface temperature

of the stars decreases, and reaches maximal clarity in the M, N, and R spectra. The spectra mentioned also show, in the atmosphere of the stars, the presence of compounds of carbon with nitrogen (CN<sub>1</sub>) and the so-called Swan bands, which are determined by molecules consisting of two connected atoms of carbon (C<sub>2</sub>) [497, 526], and the presence of (C<sub>3</sub>) and (CH<sub>2</sub>) [217].

The formation of water, molecular hydrogen, nitrogen, and oxygen, and of these six diatomic compounds—C<sub>2</sub>, CN, CO, CH, NH, OH [11]—is an unavoidable consequence of the interaction of carbon with nitrogen and oxygen which are produced by it in stellar atmospheres which are exceptionally rich in hydrogen. Thus, in the atmospheres of relatively cold stars [11, 217], including the Sun [4], hydrogen, carbon, nitrogen, and oxygen exist mainly as atoms and as homo- and heteronuclear diatomic combinations. The triatomic molecules H<sub>2</sub>O, C<sub>3</sub>, and C<sub>2</sub>H are found in relatively large quantities in the atmospheres of carbon stars, which, it has been proposed, were the sources of interstellar carbon kernels or graphite particles [241]. The presence of HCN, HCO, CH<sub>4</sub>, and NH<sub>3</sub> in dwarf stars was proposed by Vardya [596] on the basis of his calculations and a number of theoretical concepts. However, not one of these compounds has actually been detected so far. The stars of various generations must be viewed, therefore, as the starting place for the synthesis of original carbon compounds which are predecessors of organic substances.

### Star Formation

Stars are in constant interaction with their surrounding interstellar space. This interstellar medium is far from uniform. Turbulent processes are observed in it, including local warmings due to the effect of gas ionization. The bursts of supernova stars create shock waves, at which time the gas density in such a wave increases by several orders, and this may be highly significant for the formation of gravitationally related condensations and subsequent formation of stars [134]. If a high-density gas-dust cloud appears on the path of the shock wave which characterizes the propagation of an ionization front, it is com-

pressed due to the pressure of hot gas and converted into a dense dark formation—a globule. This is the embryo of a star, which then, in a quite short time, may be compressed even more as a result of gravitational collapse and be converted into a self-luminous body. A large number of such globules, normally connected to nebulae, are known at present [132]. A graphic example of such a process is represented by filaments in the constellation Cygnus. Studies of various photographs of this region, taken during half a century, show that these filaments, which include a certain amount of stellar chains, are fleeing at great speed from some general center, shown to be the source of radio emissions. A phenomenon of such a type is interpreted by Fesenkov as proof of a supernova star burst in the past at a given point of the galaxy [132]. Many similar filaments have been photographed by Shayn [527] in various regions of the sky.

Quickly developing condensations, in which noticeable changes have appeared for several years, are also encountered in the region of the Orion nebula, where even now an intensive star formation is occurring [32, 212]. In the spectrum of this nebula, narrow interstellar absorption bands of CH, CH<sup>+</sup>, CN, and a number of other molecular bands have been detected. Solid particles with dimensions in fractions of microns are also scattered in these condensations. The composition of these particles is unknown, but in their spectral characteristics they identify with graphite and, as recently suggested, even with diamonds [498, 605].

Star formation from interstellar matter occurs constantly in our galaxy [17, 131, 184, 514]; but in line with this, the stars are constantly giving off part of their substance into the surrounding medium, enriching it particularly with carbon compounds. They create favorable conditions in space for the synthesis of various organic compounds, radiating cosmic rays and plasma clouds which contain ionized atoms of different elements. For example, the Sun creates the so-called solar wind, which washes the upper layers of its atmosphere with intense radiation at great velocity. They comprise a gaseous component of the solar corona which, however, contains solid particles of varying origin [135].

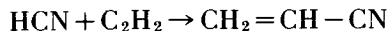
N-type red giants, on an enormous scale, generate a very fine carbon dust which is constantly expelled into space by radiation pressure and forms the chief component in space clouds [109]. The total mass of these particles does not exceed 1% of the gas composition of the interstellar environment. However, these particulates are responsible for the very high light absorption which determines the overall appearance of the Milky Way. These particulates may also give rise to molecular systems, because they are highly irradiated by cosmic rays and stellar emanations [238, 241, 247]. Therefore, it is not surprising that radiometric determinations give evidence of the presence, here, of different organic compounds in various regions of interstellar space [29, 49, 107, 114, 217, 465, 529].

### Interstellar Space

Thermodynamic data show that in the presence of hydrogen, carbon is reduced to methane, nitrogen to ammonia, and oxygen to water [345]. Actually, recent radioastronomic observations have shown ammonia [82] and water vapors [83, 540] to be in interstellar space. Carbon monoxide (CO) has been detected in various regions of the Milky Way [249, 636]. Molecular hydrogen in interstellar space was predicted by Knaap et al before its actual detection [273]. HCN was also observed in Milky Way emissions [59, 541], and formaldehyde was the first organic molecule detected in space [411, 542, 654]. The region where it was found is considered dusty, and it has been suggested that this organic substance is a consequence of the particulate protection of molecules from ultraviolet light; but it is more probable that this is related to an increased rate of formation of formaldehyde.

Complex chemical processes must undoubtedly occur in interstellar dust clouds, which prompted the suggestion that large particles of carbon capture other atoms (H, N, and O) in interstellar dust and form more complex organic molecules [58]. One of such molecules detected in interstellar space is the molecule of cyanoacetylene [584, 585]. Its formation consists of 5 atoms of 3 different elements, which cannot be explained by simple gas-phase reactions capable of syn-

thesizing diatomic molecules; however, cyanoacetylene could be formed in the reaction between HCN and acetylene:



Hodgson [222] suggests a possible reaction for the formation of pyrrole from an unsaturated four carbon chain and ammonia. The interaction of pyrrole with formaldehyde could be the mechanism for formation of porphyrins in plasma reactions [226]. There are also indications here of the presence in interstellar space of other polymer organic substances, interpreted by some authors [251, 252, 253] as porphyrins, and by others as polyaromatic hydrocarbons [106, 107, 211, 626].

### Comets

Studies of comets provide a great deal of information on carbon compounds in interstellar matter. There is not yet a completely clear concept of the mechanism of origin of comets; however, there is no doubt that such unstable small bodies could not be generated within the solar system. Condensations of similar composition, obviously, arise universally in space from typical interstellar material. Comets, in their chemical composition, reflect principally the composition of primordial solar nebulae [291], containing large amounts of carbon compounds, and thus may be considered space models for the abiotic synthesis of biochemically important compounds [393, 395]. The nucleus of comets is seen as a discrete mass of solid particles which could be formed from typical interstellar material at a temperature on the order of 10°–100° K [631, 632]. When comets approach the Sun at a distance less than 3 astronomical units (AU), it is possible to observe their spectrum, which reveals fluorescent emission bands corresponding to molecules of CN, CH, CH<sub>2</sub>, C<sub>2</sub>, C<sub>3</sub>, NH, NH<sub>2</sub> and OH, and also to radicals CH<sup>+</sup>, OH<sup>+</sup>, CO<sup>+</sup>, N<sub>2</sub> and CO<sub>2</sub><sup>+</sup> [32, 313, 475, 573, 574, 641]. These compounds supposedly exist in the comet nuclei in one of these forms:

1. As frozen free radicals [108, 174].
2. As “ice”—water, ammonia, and methane [631, 632].
3. As clathrate-type hydrates [342].

A fourth probable form consists of the so-called parent compounds, which comprise the internal parts of the comets and must be complex organic compounds such as HCN, NH<sub>2</sub>, H<sub>2</sub>O, CO, C<sub>2</sub>N<sub>2</sub>, CH<sub>4</sub>, C<sub>2</sub>H<sub>2</sub> and other hydrocarbons [200, 217, 234, 574].

The importance of these comet substances for formation of biochemical compounds at the preplanetary and planetary stages of the Earth has been particularly emphasized by Oró [393, 395, 397]. Comets can, even at present, “fatten” the Earth with organic substances to some degree. Of course, their role in this connection was more significant in the past when the population density of a near-solar comet cloud was much greater. Even with the present abundance of comets, it could be expected that the Earth, in the course of its history, collided with comets no less than a hundred times, thereby receiving various organic compounds from them [394].

Thus, the atmospheres of stars, the accumulations of gas-dust matter, the comet clusters and interstellar space contain an abundant amount of carbon and its compounds—organic substances which alone are completely capable of supporting all chemical evolution toward living substances similar to those on Earth [303]. These organic substances may originate, exist, and evolve in a wide range of temperatures from 3000° K and greater which are prevalent in the atmosphere of carbon stars [11, 434, 573] down to 1.8° K in dust clouds [58]. However, this evolution could scarcely lead to the emergence of life here, for which the necessary condition is the formation of planetary systems. Heavenly bodies with a sufficiently large mass, such as stars, may be formed almost entirely from pure hydrogen. However, the existence of bodies the size of Earth with only this element is inconceivable because the mass of these bodies would not be sufficient to prevent its dissemination in space. Accordingly, it is possible to conclude that during the first billions of years of the existence of our galaxy, when heavy elements had not yet been formed in a sufficient quantity, planetary systems similar to ours could not exist. Therefore, life could not exist during the evolutionary process of these planets, which makes it possible to conclude that propagation

of life in the universe is limited to stellar populations of sufficiently late types. However, it cannot be assumed that our solar system is extraordinary in any way. A great multitude of similar systems must exist in our galaxy. Of course, not all planets of this or any system may be abodes of life, for which they must meet a number of conditions in terms of dimensions, chemical composition, distance from a central light source, temperature, illumination, and so forth. These conditions can evidently be fulfilled by only one or two planets in a given system. After considering all these conditions, Shapley [524] calculated that there are  $10^8$  places in the universe suitable for the emergence and existence of life. However, Huang increases this figure to  $10^{18}$  [242]. Brown's calculations show that a great number of the visible stars may have planetary systems with one or two planets with necessary parameters for the existence of life. Even if stricter limitations are applied to the conditions for spontaneous emergence of life than have been considered normal until the present, life could have evolved at least 10 billion times in our galaxy, according to Brown's calculations [55].

### **EVOLUTION OF CARBON COMPOUNDS IN THE SOLAR SYSTEM**

The formation of the solar system and the mechanism of this process cannot, at present, be regarded as completely explained. However, starting with Russell [485], it has been accepted that the basis for the formation of the Sun and its surrounding planets is the process of fusion of diffuse space matter particles [94, 163, 237, 289, 557, 564, 580, 587, 588, 630, 640]. According to these concepts, the starting point for formation of the solar system was the formation of a cloud of gas-dust matter with a size commensurate with the scale of a modern planetary system, a temperature on the order of 50° K, and a weak magnetic field. It contained approximately 1000 hydrogen atoms per 1 cm<sup>3</sup>, a significantly smaller amount of helium, and other inert elements, which together with hydrogen formed the gas component of the cloud. Methane, which is preserved in a gaslike state even at comparatively low temperatures, may also have been

present [29]. The remaining elements of the Mendeleev table were present mainly as components of the dust, comprising only thousandths or even smaller fractions of a percent of the total mass of the accumulation.

The gas-dust cloud was gravitationally unstable; it had a known turbulence and certain central condensation which finally led to its general disintegration. When the mass of the central body precipitously increased, it quickly became very dense and hot due to gravitational energy. The hydrogen-helium reaction then caused it to be transformed into our Sun. The rest of the matter which did not become part of the Sun formed into a discoidal cloud which gave rise to formation of the "protoplanets" [9, 78, 290, 307, 525, 592, 594, 633]. Because of this method of formation, the atomic composition of the Sun is in direct proportion to the composition of the gas-dust nebula which gave birth to it. Hydrogen comprises the main mass, followed by helium, oxygen, nitrogen, and carbon. Subsequent heavier elements are represented in thousandths, tens of thousandths, and smaller fractions of a percent [177, 330, 524].

All substances which were part of the original gas-dust solar nebula can be divided into three groups [53]. In the so-called *gas group* belong hydrogen, helium, and inert gases which preserve their gaslike state at temperatures close to absolute zero. Next comes the *ice group*, which includes compounds formed from carbon, nitrogen, oxygen, and hydrogen, such as water, ammonia, and methane (the latter might also be partially assigned to the first group). Finally, a group arbitrarily called the *earth group* composed of compounds of silicon, magnesium, iron, and other heavier elements. The ratio of the relative mass of these groups in the Sun may be approximated as:

If the *earth group* is taken as unity, then the substances in the *ice group* will contain 4–7 times more and those in the *gas group* 300–600 times more mass [53, 56, 565].

Different ratios were created in the protoplanetary discoidal cloud [590, 591, 633]. Its temperature depended strongly, first, on the ever-increasing solar radiation, and second, on

the loss of heat from the cloud by radiation into interstellar space. Its temperature at the periphery thus differed strongly from the central regions of the gas-dust disk. This gradient must have determined the nature of distribution of protoplanetary material in the disk [54]. Nearer the periphery, where intensive cooling occurred, substances of the ice group condensed at a great rate and froze to the earth group particles, forming the so-called *comet clusters*. In the region of Jupiter's orbit and farther towards the periphery, gas, dust, and the comet clusters quickly fused into large planets, thus determining their chemical composition [633].

### Formation of Planets

The planetary building processes must have developed differently in those regions of the discoidal cloud closer to the Sun and in the region of the Earth-type planets. Here the gas component of the cloud was almost entirely lost. The ice group was preserved only partially, and the principal material was the earth group. The accumulation of live dust particles consisting of this material led to formation of planet clusters—small bodies whose composition included all the nonvolatile substances of a primary dust cloud—silicates and their hydrates, metals (in particular iron), their oxides, sulfides, carbides, and live particles of natural carbon, plus components from the ice group—water in the form of hydrates of ammonia salts and organic substances (hydrocarbons). The later fusion of planet clusters led to formation of Earth-type planets and asteroids [230, 328, 536, 565, 593].

Planets which emerged in this way already differed from one another in the initial material of which they were formed. This difference was magnified later by each one having had its own subsequent complex history before becoming what it is now observed to be [469, 489]. This also influenced decisively the evolution of carbon compounds belonging to the planets. Jupiter in its very deep and turbulent atmosphere contains large quantities of ammonia, methane, hydrogen, and possibly also water vapor [6, 389, 556, 634, 635]. Based on the presence of these substances, Jupiter might serve as a natural model for study

of the evolution of organic substances [488], especially because within its enormous cloud layer there must be a zone where relatively mild temperatures prevail [338].

Recent laboratory tests simulating conditions possible for Jupiter have shown that under these conditions, coupled with electrical charges and ultraviolet light, complex and polymerized organic substances are formed within corresponding gas mixtures [437, 451, 499, 637]. However, Lewis and Prinn [310] conclude that the results of these laboratory tests cannot be directly applied to the modern atmosphere of Jupiter. Conditions actually existing there contradict possibilities of the preservation of organic substances and, even more so, preclude the emergence of life. Conditions similar to those on Jupiter evidently exist on Saturn and on other large planets, but for them, it should be taken into account that as the distance from the Sun increases, their illumination by solar radiation decreases [207, 288, 349, 481, 489].

Different composition and different evolutionary paths for the carbon compounds are inherent on the Earth-type planets. Mercury is the least studied planet. It is bare rock, devoid of atmosphere, and thus is open to the entire spectrum of solar radiation. Its surface facing the Sun is heated to 350° C, while the opposite side is cooled to -170° C, which not only prevents the emergence of life, but also makes doubtful any further evolution of carbon compounds which would be blown away by the solar wind [5, 36, 105, 235].

*Venus.* In contrast to Mercury, Venus has a very extensive atmosphere, closed at the top by a dense cloud layer which has prevented direct telescopic study of its surface. Only radioastronomical investigations have permitted some degree of knowledge on composition of the atmosphere and temperature which prevail [50, 254, 276, 327, 388, 431, 535]. Such data show that although Venus was formed from the same planet cluster material as the Earth, is approximately the same size, and is in an orbit located next to the Earth's, it cannot serve as a natural model for the study of evolutionary paths of Earth (see, however, [354]). Venus, initially a cold body, did not undergo internal stratification, according

to Fesenkov. Therefore, in contrast to what took place on Earth, the long-lived radioactive elements on Venus remained distributed more or less uniformly throughout the entire mass, which caused a gradual heating which has continued to this day [133].

*Mars.* This planet has greater promise, with more similarities to Earth [442, 652]. It has long attracted attention because of possible emergence and existence of life; consequently, the scientific literature on Mars is exceptionally large [175]. However, numerous early suggestions had to be rejected, for example, the proposed biologic indications of seasonal changes resulting from intense summer development of vegetation on the surface of Mars. A summary of the pertinent data [28, 35, 81, 175, 214, 268, 304, 337, 361, 430, 491, 539, 571] permits characterization of the planet Mars:

The principal component of the martian atmosphere is carbon dioxide ( $\text{CO}_2$ ), which is judged to comprise 50–100% of the atmosphere [35, 270, 355]. Nitrogen does not exceed 5% [92], and very small amounts of water [409, 583] and CO [255] have been observed. The presence of argon in amounts comparable to  $\text{CO}_2$  is theoretically probable; however, there are no observational data.

The martian atmosphere is rarefied, approximately 100 times less dense than the Earth's atmosphere at its surface [213, 267, 269, 470]. The mean temperature over the planet at the bottom of the atmosphere is approximately equal to 200°–210° K. In the summer at the Equator, the temperature may reach +30° C in the daytime, but may fall the same night to –70° or –80° C. Ultraviolet radiation from the Sun with a wavelength of 1900 Å reaches the surface of Mars if its atmosphere is not obscured by sandstorms. The surface layer of Mars is formed of a sand-dust cover, which contains a significant amount of limonite. The external appearance of Mars greatly resembles the Moon. Basically, it is a desert devoid of water with significant elevations and depressions, entirely covered by craters of various sizes, ages, and origins, which in many cases have more gentle slopes than those

on the Moon, indicating their active disintegration by winds and great thermal extremes.

The poles of Mars are covered with white caps which consist of solid  $\text{CO}_2$  with a water-ice underlayer [214, 361]. The white caps thaw in summer, which is related to the darkening of so-called seas which extends to the Equator. The small amount of water, complete permeability of the atmosphere for shortwave ultraviolet light, and the low temperatures with their great even drops would create very severe conditions for life of terrestrial organisms. But these conditions do not exclude completely the possibility of the existence of life on Mars. Some authors have suggested that Mars has undergone substantial changes in the course of its planetary history. In the initial periods, it may have been more like Earth, and the emergence of life occurred there the same as on our planet. Once emerged, the organisms may have gradually adapted to the increasingly bleak conditions of the martian surface [528, 590].

### Meteorites

Recent extensive studies of meteorites have provided the most significant information on the material from which the Earth was formed and, in particular, on those initial carbon compounds whose evolution in our planet led to the emergence of life. This is true since until recently, meteorites were the only extraterrestrial objects which could be subjected to direct chemical and mineralogical analysis. Their composition must be very similar to that of the planet clusters which serve as initial material for formation of Earth-type planets. Extensive reviews of modern works on meteorites comprise hundreds of articles and books [12, 13, 263, 356, 603].

The origin of meteorites is a problem that cannot be considered completely solved. But it is accepted as highly probable that they were formed in our solar system in the zone of the asteroids which apparently are the "parent bodies" for them. The time of their formation is near that of the solar system. All meteorites can be divided basically into two groups—iron and stone. The first ones supposedly originated from the central part of the "parent bodies" and the

second ones from the peripheral part. All contain some amount of carbon and its compounds [293, 331]. Iron meteorites contain carbon in its natural form or in a compound with metal (cohenite—FeNi,  $\text{CO}_3\text{C}$ ). Stony meteorites contain an average of about 1% carbon. Carbonaceous chondrites, in which the content of carbon may reach almost 5%, are even richer; a significant part of chondrite carbon is in the form of organic substances [206, 601, 612] which may amount to 7% of the carbon; approximately 10% are soluble in organic solvents. These are called bitumenlike substances—basically a complex mixture of hydrocarbons [600].

The hydrocarbons of carbonaceous chondrites were studied by Studier [562] and Oró [293, 366, 407] with the aid of a combination gas chromatograph and mass spectrometer. They showed that the distribution of hydrocarbons in carbonaceous chondrites is somewhat similar to their distribution in ancient sedimentary rocks, also to products of abiogenic synthesis according to Fischer-Tropsch. In all the carbonaceous chondrites which Oró studied, isoprenoid hydrocarbons were detected in a small amount, in particular pristap, thytat, and norpristap, which at one time were considered indicators of the biogenic origin of given mixtures of organic substances [75]. However, using the meteorite Groznaya, Vdovykin [603] and Oró [400] showed that these substances have an abiogenic nature and are not the result of contamination under terrestrial conditions. In a model experiment, these substances may even be formed by means of inorganic synthesis [357]. Other organic substances have been detected along with hydrocarbons in the carbonaceous chondrites [202, 203, 206, 224, 299, 308, 365, 366, 398, 560, 561, 600, 606, 617, 650], in particular aromatic and fatty acids, sulfur- and chlorine-containing organic substances (phiophenes and alkylchlorides), cyclic nitrogen compounds, purines and triazines, prophyrrins [223] and amino acids [256]. Detection of the latter substances evoked especially heated discussions in the literature, because they could easily have been terrestrial contaminants—in particular as traces from the fingers of the experimenters. In numerous instances the amino acid composition of meteoritic

samples corresponded to that of such contamination [188, 540].

The extraterrestrial origin of amino acids has been proved often. Particularly persuasive are studies of the Murchison meteorite which fell in Australia and was immediately subjected to analysis. Along with the predominant amino acids normally encountered in chondrites—glycine, alanine, glutamic acid, and proline—small amounts were found of 2-methylalanine and sarcosine, which are not component parts of Earth proteins, but arise during abiogenic syntheses. Twelve nonprotein amino acids were later found which could have originated only in the meteorite itself or, more accurately, even before its formation during the action of solar radiation on primordial dust [296, 297]. All the amino acids found in meteorites are optically inactive, with the exception of those that were injected with terrestrial contaminants. A number of other signs distinguish meteoritic organics from substances of the most ancient deposits on the Earth. The age of meteoritic substances is calculated at approximately 4.5 billion years [332]; consequently, they are 1 billion years older than the carbon compounds found on Earth.

On the basis of morphologic similarity in carbon chondrites, Claus and Nagy [85, 359], in the early 1960s, described microinclusions which luminesce in ultraviolet rays, which might be expected of residues from space microorganisms which could have been generators of organic substances in meteorites. However, now it can be considered sufficiently well-established [137, 602] that the so-called organized elements of carbonaceous chondrites are sometimes morphologically very similar to the residues of microbes, or in some cases, are particles of mineral origin or small clumps or carbonaceous matter, or in other cases, the results of terrestrial contamination.

Almost all carbonaceous compounds which have been identified in carbonaceous chondrites may be produced in the Fischer-Tropsch reaction from a mixture of  $\text{CO}$ ,  $\text{H}_2$  and  $\text{H}_3$  in the presence of nickel, iron, or a magnetite catalyst [562]. A number of organic compounds of great biological interest, detected in meteorites, were also synthesized by Hayatsu, Studier, and Anders

from CO, D<sub>2</sub> and ND<sub>3</sub> in the presence of nickel-iron and aluminum catalysts. They were able to identify p-alkanes, iso-, anti-iso, and dimethyl-alkanes, adenine, guanidine, xanthine, glycine, alanine, asparagine acid, glutamic acid, tyrosine, histidine, pyrrolic polymers, and other organic compounds [202]. It is very important that the substances obtained in this manner show carbon-isotope fractionation of the same sign and of the same amounts as observed in carbonaceous compounds of meteorites. These studies show that the organic substances in meteorites could have been produced in a catalytic reaction between CO, hydrogen, and ammonia in the solar nebula [299]. Thus, the organic substances of carbonaceous chondrites differ from biogenic organic substances of rocks by their carbon-isotope composition, absence of optic activity, different ratios of separate components of their compounds, presence of chlorine, and by a number of other peculiarities [604]. All characteristics point to their abiogenic nature and that they were formed during agglomeration of the initial material for meteorites.

### Lunar Samples

The second nonterrestrial objects, after meteorites, subjected to direct chemical and mineralogical study were lunar soil samples supplied by US astronauts and the Soviet automatic stations Luna 16 and 20 [80, 118, 294, 308, 554, 570, 616, 639]. The age of the lunar dust samples from the Sea of Tranquillity lies within 3.7 to 4.6 billion years. In this respect, they occupy a place between the oldest samples of rocks on the Earth and meteoritic material. Thus, lunar organic substances, if they were found, would be of special interest, because they would belong to the period which has not been studied so far. They could have either an abiotic character [653] (abiogenetically formed on the Moon itself) or have accumulated with meteorites which have fallen on the lunar surface, or, they might have originated as a result of the vital activity of organisms which exist or did exist on the Moon [170]. Unfortunately, analyses of the lunar material yielded disappointing results in this regard.

The total carbon content in lunar dust is not slight; on the average, it is expressed as 150 ppm [127, 257, 350]. For comparison with terrestrial rocks, this amount is approximately equal to 200 ppm on Earth [333]. However, per portion of organic substances in lunar dust, it is less than 2 ppm. No sugars, nucleic acids, fatty acids, or amino acids could be detected [167, 295, 408]. However, with the aid of a very sensitive amino acid analyzer, Fox et al determined the presence of a minimal amount of amino acids (20–70 parts per billion of lunar soil) in samples taken by Apollo 11 and Apollo 12 from trenches, among which the presence of glycine, alanine, and so forth can be presumed [157, 195, 358]. Traces of porphyrins were also detected in lunar dust (Apollo 11), but it turned out that these did not belong to the Moon but were synthesized in the rocket gases [225, 226]. The hydrocarbons detected in lunar dust during acid hydrolysis could have been generated from carbides, which are important components of the carbonaceous complex of the lunar surface [15].

No microstructures were detected on the Moon which would confirm the presence of organisms living at present or in the past [24, 504]. The isotopic composition of the lunar carbon is very unusual; evidently lunar carbon is a mixture of carbon of local origin, meteorites, and solar wind [299, 323]. The abnormally high content of <sup>13</sup>C in lunar dust cannot be assigned to a carbonate phase because the amount of carbonates, if present at all, is exceptionally small. Present-day carbon on the Moon, on the basis of the chemical and isotopic composition, evidently did not originate from carbonaceous chondrites, which have continuously fallen onto the lunar surface for billions of years. Possibly lunar carbon compounds came from iron meteorites which contained these substances. However, mineralogical studies show only very small inclusions of nickel-iron meteoritic material [258]. Since carbon on the Moon is represented not by carbon-hydrogen heteroatomic compounds, but principally by carbides, oxides, elementary carbon, and a high enrichment of <sup>13</sup>C, there are grounds to propose that it had a unique history on the surface of the Moon. In this connection, the organic substances of the original matter and of

the carbonaceous chondrites were strewn on the completely unprotected lunar surface by solar wind and were not retained. Only the more stable and heavy compounds of carbon were preserved.

Thus, both interstellar space and clouds of gas-dust matter are quite rich in carbon and organic substances, which were also present in the protoplanetary discoidal solar nebula. But in those regions where prevailing higher temperature formed, the gaseous components—hydrogen, helium, and other inert elements—must have escaped to the peripheral regions of the nebula in significant amounts. Methane also must have met such a fate.

The content of inert gases on the Earth is very small in comparison with their content in space [52, 563]; their abundance was highly depleted as a result of volatilization from that part of the protoplanetary cloud in which the Earth was formed. This volatilization occurred even before the Earth was formed as a planet, under a very low gravitational field. According to Urey [589], this explains depletion of the neon content on our planet to a significantly greater degree than the heavier xenon. But if the depletion proceeded entirely by means of fractionation by mass, i.e., if volatilization from a gravitational field took place according to molecular weight, then CH<sub>4</sub> would be expected to be as depleted as neon, but in fact carbon is preserved on the Earth to a much greater degree. This indicates that it was retained during the formation of our planet not as methane, but in the form of heavier chemical compounds—in particular as organic substances which had been synthesized under conditions of the interstellar medium in the protoplanetary nebula. These cosmic organic substances, according to their origin, entered the composition of the planet clusters which served as material for the formation of Earth-type planets and asteroids. Each of the planets which arose in such a manner from a similar material later had its individual, long, and complex thermal history, during the course of which the initial organic substances evolved in a specific manner for each planet. This history determined the composition of its modern carbonaceous compounds. The thermal history

of the asteroids, because of their small weight, was less significant and therefore the meteorites which arose during their crushing evidently retained their original composition and structure to a great degree.

Space research provides information, to a great degree, on those abiogenic carbon compounds which were starting compounds for the further evolution of Earth organics on the path to the emergence of life. However, research is still insufficient to understand these paths well. In order to understand them, the modern geochemistry of carbon compounds may be studied and the behavior of organic substances modified under conditions which might have taken place on the Earth at the beginning of its existence.

## **EVOLUTION OF ORGANIC SUBSTANCES ON THE EARTH**

The formation and initial stages in the evolution of the Earth as a planet are being extensively studied at present, from both the geological and geochemical points of view [22, 29, 49, 117, 130, 309, 487, 587, 588, 593, 594, 607, 608, 614, 615]. Nevertheless, this stage of evolution is still far from adequately understood and evokes strong differences of opinion. According to current widely held concepts, our planet was formed by accumulation of cold solid bodies with varying contents of iron and silicates, but basically lacking such free gases and volatile compounds as molecular hydrogen, light inert elements, and methane. They were lost previously in that region of the gas-dust nebula in which the Earth was formed. Only a small number of these gases could be preserved in the Earth's composition to the degree that they were adsorbed by solid components of the nebula. They could have formed the primary atmosphere of the Earth. However, this atmosphere could not have been long-lasting because its component gases could not be retained by the Earth's gravitation. Because of such loss, the Earth developed its modern mass and the composition which is now characteristic of it—one which is close to the average composition of meteorites.

The remaining compact mass of the Earth continued to evolve through its internal energy,

at which time the mass divided into the core, mantle, and crust. The mechanism for such differentiation is quite characteristic of our planet, but remains far from clear. A hypothetical secondary melting due to the initial gravitational heat and radiogenic warming is advanced most frequently as an explanation. However, complete melting of the Earth by such means would require several billion years. Actually, the differentiation occurred within an incomparably shorter time. It has been proposed that "short-lived" and presently "frozen" isotopes, such as  $^{10}\text{Be}$ ,  $^{26}\text{Al}$ ,  $^{129}\text{U}$ ,  $^{244}\text{Ri}$ , and so forth, played an important part in the complete or partial melting of the Earth. In any case, the entire subsequent course of the evolution of the planet was determined by its thermal history. During its formation, the principal sources of internal heat were gravitational energy given off during agglomeration and compression of the Earth's matter, and energy formed during the decay of radioactive elements which were not distributed throughout the entire mass, but basically displaced toward the Earth's periphery.

The most important boundary in the Earth's development was the surface formation of a crust, atmosphere, and hydrosphere. The modern Earth crust consists of a granite and basalt shell. The so-called mantle, of low-grade silicon and ultrabasic rocks (dunites), underlies the crust. On the basis of tests on the zonal fusion of the substance of stony meteorites, Vinogradov [609] became convinced that the dunites of the mantle are residues from melting of the original substance of the Earth, which is similar to the composition of chondrites. Light basalt rocks melting from a mantle stratum due to the effect of radiogenic heat should have been accompanied by a discharge of various vapors and gases due to their evaporation as the temperature increased, or due to their formation in solid ground shells during radioactive, radiochemical, and chemical processes. Therefore, the formation of aqueous and gaseous shells of the Earth (its hydrosphere and atmosphere) was closely connected to processes in the lithosphere from the very beginning.

The amount of water on the surface of the Earth

during its early existence was not great [483, 588]. The basic mass of water which formed the world oceans appeared only at the very beginning of the Archean era, immediately after formation of the Earth's crust. It developed gradually during formation of the lithosphere from silicate hydrates or generally from bound constitutional water of the Earth's interior [482, 613]. Archean waters differed substantially in chemical composition from modern waters. Acid gaslike products—HCl, HF, boric acid,  $\text{H}_2\text{S}$ ,  $\text{CO}_2$ ,  $\text{CH}_4$ , and other hydrocarbons which had been discharged by volcanoes were dissolved in them, thus they had an acid reaction. The composition of the water of the ancient oceans began to approximate modern composition only toward the middle of the Archean age. The acids became neutralized after being subjected to the action of silicates of sedimentary deposits and carbonates of K, Na, Ca, Mg [553] (see, however, [484, 534]). In spite of the Earth not having free, molecular hydrogen during its formation, it retained this element in the form of diverse compounds which imparted a regenerative character to both the lithosphere and to the secondary atmosphere which had arisen.

Molecular oxygen, characteristic of the modern atmosphere, was practically lacking [87, 230]. Only a very small amount of it could appear during photolysis of water vapors by short-wave ultraviolet rays [199]. However, even in this case, oxygen could not accumulate in the atmosphere to any significant amount, because it was absorbed very quickly and completely by rocks which were unsaturated with respect to it [302]. Such a process of  $\text{O}_2$  absorption can be observed even now. For example, lava masses ejected onto the Earth's surface during modern volcanic eruptions are normally very rich in metal oxides, so that lava and basalts are of black and green color. The sedimentary formations from them (red or yellow sands or clays) are rich in the higher oxide form of iron. Thus, when free oxygen is abundant in the modern atmosphere, it oxidizes only the very surface film of the Earth's crust; if it were not for the constant biogenic formation of this gas, it would have disappeared from our atmosphere in a very short time, since it is absorbed by rocks [179].

Thus, before the formation of biogenic oxygen [47, 610], the secondary atmosphere had no free oxygen and was reducing in nature. This may be ascertained from direct geologic data obtained by studying ancient Precambrian deposits. Rutten [486] divides the history of our planet into two basic periods: actualistic, similar to the modern, and preactualistic, the period preceding it. During these periods, geologic processes which occurred on the Earth's surface differed a great deal. For example, during the modern actualistic era, in an atmosphere rich in free oxygen, chemical processes play the chief role in weathering basic rocks. Minerals already oxidized were transported and deposited elsewhere. On the contrary, if the atmosphere had a reducing nature (proposed for the preactualistic era), minerals of the basic rocks were only worked over physically and deposited in a chemically unchanged form. Studies from this point of view of a number of deposits more than 2 billion years old show convincingly that they formed under conditions which lacked free oxygen [230, 260, 306, 467, 468].

Studies of gases discharged by modern volcanoes and fumaroles provide some concept of the possible enrichment of the ancient atmosphere of the Earth by  $\text{CO}_2$  and CO. In these discharges, carbon is represented principally in its oxidized form, and methane comprises only a small admixture [324, 543, 544]. Their source could have been graphite scattered in basalts, also organic substances of cosmic origin. Carbon could oxidize due to  $\text{H}_2\text{O}$ . The gases  $\text{CO}_2$ , CO,  $\text{CH}_4$  and  $\text{H}_2$  which are frequently detected in cavities of ejected rocks also originated in this way. At high temperatures, the equilibrium shifted in favor of  $\text{CH}_4$ , and at lower temperatures, in favor of  $\text{CO}_2$ . Therefore, ancient volcanoes ejected  $\text{CH}_4$  as well as  $\text{CO}_2$  and CO. Methane and carbon monoxide shifted principally to the atmosphere, and  $\text{CO}_2$  was distributed between the atmosphere and water [611, 613]. However, a significant part of the carbon monoxide dissolved in ocean water interacted with silicates and then shifted to residues in the form of carbonates. This was in contrast to what might have happened in the atmosphere of Mars, which lacked open water.

In summary, it is possible to conclude that the Earth, from the very beginning of its formation, was enriched by both natural and carbide carbon as well as by cosmogenic organic substances—frequently by quite complex, heavy molecules. Miller and Urey [346] noted that these organic substances, during gravitational and radiogenic warming of the Earth, had to be subjected to pyrolysis to some degree. The equilibrium mixture which originated on this occasion ( $\text{CH}_4$ ,  $\text{CO}_2$ , CO,  $\text{NH}_3$ ,  $\text{N}_2$ ,  $\text{H}_2\text{O}$ ,  $\text{H}_2$ ) was sublimated onto the Earth's surface and served as material for secondary synthesis of organic compounds under the action of radiant energy and other energetic factors. However, it has become obvious that even in the very depths of the Earth there was not only decay (which evidently continues), but also synthesis of organic substances as a result of the Fischer-Tropsch reaction [202, 299] and similar abiotic processes [110].

### Abiogenic Synthesis

To understand the totality of these complex, abiogenic, organochemical transformations which occurred at some time on the Earth has been rendered extremely difficult. Life originated and developed luxuriantly on the surface of our planet, where it forms a zone of life—the biosphere. Within the limits of this zone, the prebiochemical evolution of organic substances under natural conditions cannot be directly observed.

After emergence and further development of life, an abrupt change of conditions on the Earth's surface excluded any possibility of prolonged evolution of organic substances in the same ways that this evolution had occurred during the abiotic epoch. If abiotic organic substances could somehow now emerge, they would quickly be destroyed, eaten by microorganisms which populate the soil, water, and air everywhere. Charles Darwin pointed this out in one of his letters [93]. No matter how paradoxical it may sound, the main reason that life originates on Earth is the fact that it has already done so [367] (see, however, [262]). Since life developed hundreds of millions of years ago, the possibility is eliminated of studying abiogenic

syntheses in a pure form under natural conditions not only within limits of the biosphere, but also in the most ancient deposits of the Earth's crust. Organic substances of biogenic origin accumulate here, resulting from the vital activity of organisms—a process which is exceptionally vigorous and completed at much faster rates than abiogenic synthesis.

The basic difficulty is that there are no available chemical methods to distinguish reliably between biogenic and abiogenic organics. Only a few years ago, the detection of porphyrins or other complex organic compounds, not only on the Earth but on any space object, was considered convincing proof of the presence of life. For example, in 1966 Urey wrote concerning organic substances found in carbonaceous meteorites: "evidently, it is safe to say that if such material would have been found on the Earth, nobody would have raised the question of biological origin" [595].

This position has changed radically. At present, not one organic compound discovered in ancient terrestrial deposits could, by itself, serve as a reliable indicator of its biotic or abiotic origin. This concerns the isoprenoids in particular, e.g., pristane or phytane, which at one time Calvin [73] considered indicators of biologic origin. These substances may be synthesized in an abiogenic way [33]. The more ancient the rocks which are studied, the clearer the indication of abiotic processes should be. In a study of petroleum samples from different deposits, Robinson noted that crude petroleum of more ancient origin contains substances which lag far behind biochemical compounds, but arise easily by abiogenic means [477, 478, 479].

However, this position is now far from being universally convincing. The lack of reliable chemical criteria for the biogenic or abiogenic origin of natural organic substances has caused serious arguments between proponents of the mineral and biologic origin of petroleum [119, 209, 285, 286, 453, 454, 575, 598, 599]; both viewpoints are extreme and cannot be considered acceptable. It is understood that organic substances which are synthesized by organisms and entered the composition of sedimentary rocks, after having undergone a number of changes in

the process of geochemical decay and secondary synthesis, provide a beginning for the formation of petroleum sources. It cannot be denied that under the complex conditions of the Earth's crust, numerous abiogenic syntheses occurred (and continue), which are based on mineral, catalytic processes for which both inorganic forms of carbon as well as products of the decay of modern and ancient organics have been, and are, the initial raw material.

As life developed, biogenic processes acquired increasingly greater importance during the synthesis of organic substances; but in the ancient periods of the Earth's existence, in particular before the emergence of life, abiogenic processes had an exclusive importance and only later were obscured by biosynthesis. From the viewpoint of the origin of life, organic substances which formed in basic rocks could be considered examples of inorganic synthesis that are particularly interesting. Works on the geochemistry of organic substances are reviewed extensively in *Organic Geochemistry* [120], so that only supplementation is needed with references to the proposed inorganic syntheses. Specific finds in this area are fully described in the scientific literature; only summary mention of them will be made here.

Kropotkin and Shakhvarstova [283] describe petroleum occurrence in basic rocks of various countries and regions—Cuba, Mexico, California, South America, Turkey, New Caledonia, France, Brazil, Australia, South America, and the Soviet Union. Florovskaya et al [140, 143], give data on the distribution of carbon substances in different formations of the Earth's crust, including magmatic rocks, pegmatites, and hydrothermal veins. There are important monographs on hydrocarbon gases and bitumens in rocks of the khibinite alkaline massif, on the inclusion of organic substances in minerals, of carbonaceous compounds in rocks or crystalline shields and of the crystalline foundation of plates [141, 142, 245, 284, 428, 429]. Hydrocarbons from Lake Trinidad asphalt and formations of Mount Sorrel, which evidently do not have a biological origin, are of great interest [446, 447]. Most of these authors consider such finds proof of the abiogenic origin of the organic compounds

detected; but since there are no reliable chemical features in the substances found, these conclusions are made only on the basis of geological concepts and in certain instances can be interpreted otherwise.

### Biogenic Synthesis

Solving the problem of emergence of life on Earth involving attempts to trace the consecutive stages of chemical evolution and its transformation into a biological form of organization appears to be a good approach, and is on the same basis as that which paleontologists follow to study the Darwinian evolution of life. Such investigations seek simpler forms of organic materials which have been preserved in the more ancient zones of the Earth's crust. The basic purpose of all related work is to link the increasingly complex chemical formation with the most primitive forms of life. Serious difficulties are encountered in this method. On the one hand, the assumption is that the further back in paleontological time, the more primitive will be the morphological structure of the formations discovered. In addition, many colloid substances which have no relationship to life might, under artificial and natural conditions, easily form structures which externally are very similar to microorganisms. The "artificial cells" of Herrera [215, 216] are examples. This author mixed solutions of sulfocyanates and formaldehyde, then fixed the colloids obtained with alcohol. Residues were formed which even expert cytologists recognized as fixed microorganisms belonging to various classes of living substances. Therefore, in examining the most ancient structural formations, great care must be exercised to determine whether they are residues of primitive organisms or artifacts which originated from organic or inorganic colloidal mixtures. On the other hand, when any organic substances in the most ancient deposits of the Earth's crust are discovered, it can never be said with complete certainty whether they originated abiogenically or are products of the vital functioning of organisms which might have lived at one time. Extensive reviews are devoted to the most ancient fossils [25, 75, 88, 261, 487, 505, 619, 620].

Petrified remains of animals and plants preserved from the beginning of the Cambrian period clearly picture the irreversible process in development of the organic world, ongoing continuously over 550 million years. Not long ago, it was still thought that the paleontological chronicle had been broken off during the Cambrian age, and that the remains of organisms which had populated the Earth more than a half billion years ago had not been preserved to the present because the rocks which contained them had been subjected to profound alterations and metamorphosis which completely destroyed all biological structures. However, it has been possible recently to establish that in many places on the Earth, for example in Southern Australia and Africa, on such platforms as the Russian, Siberian, and Chinese, and beneath layers with the most ancient Cambrian complexes, there are strata closely related to them which contain more ancient fossil remains.

Investigation indicated that late Precambrian life was a direct predecessor of the Cambrian. The fossils discovered here point to the existence, at that time, of not only a rich flora, but also fauna, represented by comparatively highly developed unicellular as well as multicellular organisms. In particular, in deposits 650 million years old, in the region of Ediacara Hills (South Australia), impressions and petrified fossils were discovered of frozen embryonic jellyfish, soft corals, platyhelminthes and other extinct forms of animals [171, 173, 178]. In the Precambrian deposits of the USSR and China, Vologdin found the most primitive needles of silicon sponges, impressions of worms, and so forth [619]. However, in deeper layers with an age of 800–1000 million years, animal remains are not present, but, in contrast, the vegetative world is represented by numerous fragments and accumulations of varied algae and spores of primitive plants [23, 171].

### *Stromatolitic Periods*

All periods preceding the Proterozoic were evidently an era of bacteria and algae, the most important of which were the so-called stromatolitic formative periods. Stromatolites are unique

limestone formations in the form of relatively rectilinear cupolas consisting of a number of cones built on top of one another. They are products of the vital activity of ancient photosynthesizing organisms, principally blue-green algae [172, 198, 259, 492, 618]. Early stromatolite-formers played an essential role in the gradual enrichment of the Earth's atmosphere with oxygen. However, in their initial existence, the oxygen they formed did not necessarily go into the atmosphere but could have been entirely absorbed by chemosynthetic iron bacteria also present in the stromatolite, which were in symbiosis with the blue-green algae. As a result of seasonal fluctuation, a laminated structure of stromatolites formed in which limestone alternates with iron hydroxide [621].

Deposits of limestone secreted by organisms which have been found in the Sahara are classified as the beginning of stromatolites, which are about 1.5 billion years old [42, 181]. Formations similar to the stromatolites were found by MacGregor in dolomite series of Southern Rhodesia [317], with age determined at 2.7 billion years [363]. Actual remains of organisms were not present. The conclusion that these formations developed from algae is based only on external similarity to stromatolites. However, it is completely possible that the producers of limestone secretion in Rhodesia had no definite morphological structure but were only masses of abiogenic colloidal material or probionts which preceded life.

The most representative accumulation of fossil remains of authentic organisms of the Precambrian period were discovered in layers of black shale near the foundation of Gunflint iron ore deposits around Lake Ontario [23, 27, 86, 90, 586], whose age has been estimated at 1.9 billion years [243]. Numerous unicellular and colonial forms were detected (both branched and unbranched), which closely resemble modern blue-green algae. Numerous spherical formations resembling spores, as well as the remains of organisms are found which have no similarity to modern living creatures. Bacterialike formations, in particular, similar to modern iron bacteria, were also discovered electron-microscopically with the aid of the replica method [506].

The Sudan formation (Minnesota, USA)

belongs to carbon-rich ancient sedimentary formations, with an age of about 2.7 billion years [16]. Structures which might be taken for the remains of algae or bacteria were found here in gray pyrite globules, but these could be simply structures of abiogenic colloidal material [89]. Even more ancient finds (3.1 billion years old) were found in Fig Tree deposits (Eastern Transvaal). Although the fossil forms found here are very sparse, nevertheless some of them recall modern small bacteria when shown singly on replicas [26]. Barghorn called them *Eubacterium isolatum*. However, there is no certainty that these formations are true fossils and not artifacts. Thus, Rutten [487] cautiously suggested calling them "organized elements." There is even more doubt about the carbon structures found in the Onverwacht deposits (approximate age—3.7 billion years) [126, 360].

All the material presented on the development of life before the Cambrian age shows that it took place according to the same principle (from simple to complex) as during the later epochs which have been well studied by paleontologists. The forms of life discovered are simpler and more uniform the further back in time one goes. During the late Precambrian age, life was represented by various multicellular creatures, by both plants and animals (Ediacara Hills). A flourishing development of stromatolite producers—blue-green algae and bacteria—was found in the earlier epoch of the Proterozoic (1–1.5 billion years ago). During the Gunflint epoch, various representatives of these organisms were both unicellular and confervoid in shape. However, at the beginning of the Archean era, there were evidently only unicellular forms. Much earlier finds—"organized elements"—may have represented probionts or even accumulations of abiogenic colloidal material. Thus, the beginning of life is considered a transition from the preceding chemical evolution to a biological one.

#### *Molecular Paleontology*

It is tempting to link those investigations based only on morphological data with a chemical study—the so-called "molecular paleontology." Such investigation in the area of molecular

paleontology has begun comparatively recently, but numerous works already exist in the scientific literature in which both the oldest deposits mentioned above, as well as the many other formations of later origin, have been subjected to detailed chemical analysis for the purpose of establishing the intramolecular structure of the organic substances contained within them [3, 23, 34, 37, 48, 66, 67, 68, 74, 116, 119, 160, 187, 197, 227, 228, 250, 336, 406, 432, 455, 500, 519, 520, 521, 522]. In this way, many classes of organic compounds have been subjected to analysis: carbons, fats, amino acids, with special attention paid to hydrocarbons as the substances which have been preserved for the longest time.

In *Chemical Evolution* [75, 76], Calvin summarizes extensively works on the molecular paleontology of hydrocarbons, giving the results of analyses with gas chromatography and mass spectroscopy of many hydrocarbons extracted from comparatively ancient objects:

Site	Age, years
San Joaquin petroleum	30 million
Green River shale	60 million
Nonesuch ancient rocks	1 billion
Gunflint	1.9 billion
Sudan	2.7 billion
Fig Tree	3.1 billion
Onverwacht deposits	3.7 billion

Various compounds related to normal hydrocarbons, isoalkanes, anti-isoalkanes, cyclohexylalkanes, isoprenoids, and polycyclic isoprenoids were found in these deposits.

Isoprenoid phytane ( $C_{19}$ ) and pristane ( $C_{20}$ ) were given particular attention since they were once considered substances of exclusively biological origin similar to the so-called biological markers. However, it has since become known that these isoprenoids may also originate in abiogenic reactions and even in space objects. In general, it is not known at present if the molecular structure alone of such hydrocarbon compounds may be reliable proof of their biogenic origin. In order to discover the biogenic or abiogenic nature of hydrocarbon mixtures which have been isolated from objects of various geological age, Calvin uses the following approach.

For modern living creatures, it is characteristic that they synthesize organic sub-

stances selectively. Of a large number of thermodynamically possible isomers in the process of biological metabolism, only very few are synthesized, and that is determined by the specificity of the action of enzymes. In analyzing hydrocarbon mixtures which have been obtained from known biological objects, gas chromatograms are produced with clearly pronounced sharp peaks, each of which corresponds to a specific compound. In contrast, a nonspecific formation of all possible isomers might be expected during inorganic syntheses. Thus, the gas chromatogram of such a complex mixture would be expected to have the appearance of a continuous curve characteristic of the statistical distribution of hydrocarbons.

Such a chromatogram is actually produced from a mixture of hydrocarbons generated in carbide solution in hydrochloric acid [229] or during a spark discharge in methane. A similar continuous chromatogram is also characteristic of the natural abiogenic hydrocarbons of Lake Trinidad and the formation of Montsorrel [447].

The specificity of hydrocarbons found in ancient rocks could, conceivably, confirm convincingly their biological origin [336]; however, the total fraction of alkanes obtained in a Fischer-Tropsch reaction, i.e., by abiogenic means, also gives a gas chromatogram with clearly pronounced discrete peaks for hydrocarbons, which might be judged as biogenic. Calvin obtained data on the composition and properties of hydrocarbon mixtures isolated from comparatively young deposits (San Joaquin and the Green River) of clearly biogenic origin, and uses these data as the standard of biological formation for more ancient formations as well. In particular, he believes indicators of biogenic nature are: the discrete character of the chromatogram; prevalence of  $\alpha$ -alkanes with an odd number of hydrocarbon atoms; interrelationship of cyclic and open isoprenoid chains; presence of pristane and phytane; and others.

This similarity with the younger rocks is obvious for the shales of Nonesuch and Gunflint, but the matter is slightly more complex because the Sudan and the Fig Tree shales did not reveal any predominance of "odd" over "even" hydro-

carbons. In addition, Oró and Nooner discovered here the presence of the isoprenoid C<sub>17</sub>, which is lacking in the younger deposits of biological origin (for which there are biochemical reasons); but this hydrocarbon is formed in the Fischer-Tropsch reaction [405]. This raises doubt about the biological origin of the Fig Tree hydrocarbons, although the discovery there of optically active amino acids favors their biogenic origin [298]. Finally, there is a comparatively continuous chromatogram for the extracts from the Onverwacht deposits, saturated with hydrocarbons, which is characteristic of abiogenically synthesized substances [318].

These studies in molecular paleontology, despite their significance, unfortunately cannot provide a clear picture of molecular evolution or the process of making organic substances more complex. This was accomplished in the earliest periods of the Earth's existence which led to the emergence of those ancient organisms whose residues we now discover in deep deposits of the Earth's crust. Model experiments, however, which reveal the chemical potential of organic substances in various degrees of complexity, and the possible realization of these potentials under conditions near those which existed on the primitive Earth, will help in solving this problem.

### MODEL TESTS FOR REPRODUCING ABIOPHIC SYNTHESIS

Many works at present on laboratory abiogenic syntheses of organic substances lead to the subsequent complication of these substances and, thus, to modeling of those processes which might lie at the basis of chemical evolution, which preceded life on Earth. Summaries of these articles are in recent monographs, collections, and review articles [71, 75, 122, 148, 261, 263, 305, 320, 381, 421, 438, 450, 511], and characterize chemical and thermodynamic potentials in carbonaceous compounds from the most primitive representatives to the most complex polymers. These potentials have remained unchanged both in the past and present, but developed differently under varied conditions. Therefore, in the model tests, there is normally considerable effort to reproduce conditions which supposedly existed

on the primitive Earth. However, abiogenic syntheses of biologically important substances could take place within very wide limits of these conditions, in particular at the first stages of chemical evolution. For example,  $\alpha$ -amino acids are formed in different gaseous mixtures, with varied energy sources on various space objects. As further evolution moved toward complication of organic compounds, the effect of the external conditions was evermore significant; and in different local areas of the Earth's surface, this evolution proceeded differently. It is generally possible now to enumerate those general conditions which must always be taken into consideration in attempts to reproduce, in model tests, abiogenic syntheses of primary organic substances on the surface of the still lifeless Earth.

*Initial carbonaceous compounds.* The Earth, during its formation, obtained a significant reserve of abiogenic organic substances of varying degrees of complexity which originated in space. Some, of course, were subjected to pyrolysis during the process of warming of the Earth's interior, and the gaslike products of this pyrolysis were sublimated onto the Earth's surface and entered the composition of the secondary (preactualistic) atmosphere, and partially the hydrosphere of our planet [346]. These gaslike products were CH<sub>4</sub>, CO<sub>2</sub>, CO, N<sub>2</sub>, NH<sub>3</sub>, H<sub>2</sub>O, and H<sub>2</sub>, which in one combination or another, serve principally as the starting material for model abiogenic syntheses. Processes which occur in an aqueous medium are studied in smaller dimensions. These investigations are frequently connected to more complex organic compounds which originated on the basis of the primary abiogenic syntheses. The possible abiogenic syntheses which could have taken place in the Earth's crust as a result of catalytic reactions, for example the Fischer-Tropsch reaction, have been even more poorly reproduced [204, 642].

*Reductive conditions on the surface of the pre-actualistic Earth.* The Earth's atmosphere was devoid of free oxygen for a long time, which is shown by the geologic data presented [486]. This is confirmed by anaerobic processes being the basis for the energetic metabolism of all modern living creatures. Oxygen-respiration units in aerobes were added on to these processes later

[51, 321, 368], "Among all natural systems," correctly wrote Tsukerkendl and Poling, "only living matter differs by the fact that, in spite of the very essential transformations which it has undergone, it preserves by means of recording within its own organization, a large quantity of information which reflects its history" [581]. Analysis of the modern organization of life shows convincingly that its beginnings were under anaerobic conditions.

*Source of energy needed for syntheses.* Interaction of organic substances could occur under the preactualistic conditions of the Earth spontaneously, due to fundamental potential energy or in conjugate reactions. In particular, this is probable under conditions of the Earth's crust at increased temperature and in the presence of corresponding catalysts [43, 110]. However, external sources of energy must have played an important role in the organochemical syntheses of that time. Shortwave ultraviolet rays, which reach the Earth's surface due to the absence of an ozone screen in the atmosphere of that time, are predominant [103, 186, 345, 425, 445, 577]. Later, according to Calvin, radioactive emissions of a number of elements and in particular of  $^{40}\text{K}$  (in which the primitive Earth crust was very rich [572]) must have been an important source of energy for the abiogenic syntheses. A number of authors have achieved the synthesis of many biologically important substances by bombarding a mixture of primitive gases with very high-energy electrons and, in this manner, simulating radiation by  $^{40}\text{K}$  [73, 164, 410, 443]. In this connection, radiation of uranium and thorium might also have played an important role both in syntheses in the Earth's crust and in the hydrosphere [357, 450].

The energy of electrical discharges in the Earth's atmosphere, although relatively small, has been most widely used to this day for abiogenic syntheses. This form of energy was first used in Miller's basic tests [339], then in different variations by others [1, 185, 219, 396, 425]. Biologically important compounds also form during simple heating of exhaust gases and solutions [190, 192, 193, 316, 392, 402, 404]. Undoubtedly, such local heating took place in the primitive Earth on a wide scale, and to a great degree, continues in volcanic activity and hydrothermal

phenomena. To these basic sources of energy, it is possible to add the shock wave in gas during the fall of meteorites [182, 221] and ultrasonic waves which can be an aqueous medium [123, 124, 125, 545].

*Decomposition of organic substances.* The decomposition of organic substances as well as the synthesis must have been caused by such energy. Thermodynamic equilibrium is eventually established but does not work to the advantage of synthesis. For example, calculations for the surface layer of ocean waters subject to prolonged action of shortwave ultraviolet light would indicate that during onset of thermodynamic equilibrium only negligible amounts of organic substances could be preserved [533]. However, under natural conditions, thermodynamic equilibrium could not become established on the Earth's surface because of a continuous displacement of substances synthesized in one place to another. For example, under hydrospheric conditions, these substances easily pass from the decomposing action of shortwave rays to deeper layers of the water and become absorbed in ground particles, and so forth [379]. Therefore, an indispensable condition for model tests is displacement of substances which are synthesized in one place and accumulate in another. This condition was met in Miller's device [339], in the synthesis of proteinoids by Fox [149], and in Young and Ponnamperuma's model tests [652].

### Abiogenic Synthesis of Biomonomers

Various organic substances have been synthesized in laboratory tests—sugars, fats, organic alcohols, aldehydes, acids, and a number of heterocyclic compounds. Particular attention was paid to the formation of biomonomers, i.e., those molecules which are component parts of biologically important polymers—proteins and nucleic acids. Some are amino acids, purine and pyrimidine bases, nucleosides and nucleotides.

*Amino acids.* Amino acids are formed from primitive gases more easily than any other biomonomers. In particular, this means that  $\alpha$ -amino acids are synthesized in significantly larger quantities than  $\beta$ -compounds (for example,  $\beta$ -alanine) [192, 316, 339, 340, 341]. Amino

acids, which are not incorporated in proteins (and mentioned in connection with the Australian meteorite [296, 297]) are synthesized in even smaller quantities. Several chemical means for their abiogenic formation have been proposed in the literature. Miller proposed a cyanohydrin mechanism, which is confirmed by the presence of aldehydes and HCN in its reaction products. Ponnamperuma and Weller [452] show  $\alpha$ -aminonitrile as an intermediate reaction product. Sanchez et al [494] grant that cyanoacetylene plays an important role; they emphasize the leading role of oligomers of HCN, like other authors [2, 190, 334, 335].

Experiments were carried out in modeling abiogenic synthesis in a mixture of gases of CH<sub>4</sub>, NH<sub>3</sub>, H<sub>2</sub>O and H<sub>2</sub>, in certain cases with the exclusion of H<sub>2</sub> or with the addition of CO, CO<sub>2</sub>, N<sub>2</sub>, ethane (in place of CH<sub>4</sub>) or H<sub>2</sub>S. With this method, the following amino acids were synthesized: cysteine, serine, threonine,  $\alpha$ -amino-butyric acid, N-methylglycine (sarcosine), asparagine, asparaginic acid, glycine, alanine,  $\beta$ -alanine, glutamic acid, valine, leucine, isoleucine, alloisoleucine, lysine, phenylalanine, and tyrosine [84, 104, 397, 424, 427, 580]. There are other works in the literature where the synthesis of amino acids was carried out in an aqueous medium with the use of other types of compounds (for example, HCHO, HCN, NH<sub>4</sub>CL, NH<sub>4</sub><sup>+</sup>, NO<sub>3</sub><sup>-</sup>, formamide, paraformaldehyde, malonic acid and urea, N-acetylglycine, and so forth [19, 112, 147, 201, 218, 274, 364, 415, 426, 472, 530, 531]).

*Components of nucleic acids.* In the synthesis of purines and pyrimidines, achievements are less significant than successes with the synthesis of amino acids. In an experiment simulating the primitive Earth atmosphere, Ponnamperuma et al discovered adenine after irradiating a mixture of CH<sub>4</sub>, NH<sub>3</sub>, H<sub>2</sub>O and H<sub>2</sub> by an electron beam [443]. No other purine or pyrimidine bases have been synthesized under these conditions, which is interesting to compare with the preeminent position of adenine in all biological systems. Molecular orbital calculations indicate that adenine, of all nucleic bases, has the most resonance energy [459], which, of course, makes its abiogenic synthesis highly probable.

Oró was the first to report on adenine synthesis in 1960 [392]; this work was illustrated in more detail in subsequent publications [402, 403] and confirmed by Lowe et al [316]. The synthesis was carried out under moderate heating (from 30° to 100° C) of a mixture of hydrogen cyanide, ammonia, and water. Oró and others studied the mechanism of this reaction and showed that this condensation occurs through aminomalonitrile (a trimer of HCN) and diaminomalonitrile, or 4-amino-4-cyanoimidazole, (a tetramer of HCN) [129, 402, 495, 496]. Adenine, like another nucleic purine, guanine, was synthesized during irradiation of a weak solution of HCN by UV light [436]. Both these purines are reaction products of 4-amino-4-cyanoimidazole with HCN or cyanogen in an aqueous solution [493, 495], which emphasizes the great importance of HCN in primary abiogenic syntheses. Of the three pyrimidines—cytosine, uracil, and thymine—the first two were obtained in model tests, which simulated primitive Earth conditions to some degree.

Uracil was synthesized during heating of malic acid, urea, and polyphosphoric acid up to 130° C [156]. Oró shows the formation of uracil during heating of urea with acrylonitrile [397]. Sanchez et al discovered the formation of cytosine during the heating of ethylenedinitrile in an aqueous solution of KCN [494]. In a number of these syntheses, other bases were also detected which normally do not enter the compositions of nucleic acids—hypoxanthine, diaminopurine, and xanthine [493].

The carbon components of nucleotides—ribose and 2-deoxyribose—have been synthesized under conditions similar to primitive [159, 323, 399]. Ponnamperuma et al were able to carry out fusion of nucleotide components in an aqueous medium by using ethyl metaphosphate. The syntheses were made in aqueous solutions of adenine, adenosine, and adenylic acid of ribose and ethyl metaphosphate; mixtures were illuminated by ultraviolet light with a wavelength of 2537 Å at 40° C. In this way, conversion of adenine into adenosine, adenosine into AMP, AMP into ADP, and finally ADP into ATP was established [441, 444, 449]. Even more promising results were obtained by the use of ionizing radiation [436]. There are also other indications

of model tests on the synthesis of varied nucleosides and nucleotides [31, 244, 622] and because of the important role of polyphosphates in model tests, other works should be mentioned [20, 292, 343, 344, 439, 466, 507, 508, 510, 512].

*Other monomer substances.* The possibility of abiogenic synthesis of other biologically significant compounds has been demonstrated in model tests on a much smaller scale than for amino acids and nucleic components. The syntheses of fatty acids [10, 164, 552] might be indicated here—imidazole heterocyclics [532], isoprenoids [357], and porphyrin [128, 226, 279, 280, 576]. The latter are of great interest to researchers because of their importance in the syntheses of chlorophyll and cytochromes. Optically inactive (racemic) mixtures of organic substances are formed in all abiogenic syntheses in model tests. In contrast, the biogenically formed compounds are always optically active [166], which has attracted attention since the time of Pasteur. At present, asymmetrical syntheses are carried out in the laboratory under the action of circularly polarized ultraviolet light [287] and on the surface of nonsymmetrical quartz crystals [39, 578, 579]. However, Wald doubts that any of the indicated abiogenic factors may create conditions for the emergence of stable asymmetry. In his opinion, this could occur not during the synthesis of monomers, but particularly during the process of higher order structures forming; for example, during selection of proteins and polypeptides which form spirals. The problem of asymmetry has been extensively studied [8, 191, 264, 265, 266, 476].

### Abiogenic Synthesis of Biopolymers

The evolutionary step toward the emergence of life following the formation of polymers was their uniting into biopolymers, in particular, into compounds similar to proteins and nucleic acids, which are exceptionally important in organization of living substances [30, 121]. In a number of modern model tests, this association has been carried out by means of dehydration condensation, in which two methods are used to verify the possibility of such condensation under primitive Earth conditions.

The first method uses high temperatures in corresponding nonaqueous solutions; and the second, in searching for compounds whose free energy (also whose affinity for water) might enable them to carry out dehydration condensation of amino acids or mononucleotides even in diluted aqueous solutions. Basically, attention will be concentrated here on model abiogenic syntheses of polypeptides and polynucleotides, although there are similar experiments in the syntheses of polyglycosides, melanine, and so forth [44]. There are extensive summaries of the abiogenic synthesis of biopolymers [75, 261].

### Polypeptides and Proteinlike Substances

Fox et al, simulating volcanic conditions, heated a mixture of 18 amino acids to 170° C on a piece of lava for 6 h. An excess amount of dicarboxylic amino acids melted the mixture until it was carbonized. Heating, also in the presence of polyphosphates, permitted reducing the heating temperature to 100° C [155, 158, 194]. Under this temperature, an amber-colored polymer formed with molecular weight of several thousands (from 5000 to 10 000) which contains all amino acids used in the test typical of protein (it lost its optical activity, however). Fox called this polymer proteinoid because a number of features were similar to proteins.

Two very interesting properties of proteinoids were revealed in later studies: first, a high internal molecular uniformity which is repeated by the coherence of amino acid residues (which will be treated in more detail later); and second, a completely, although weakly, detectable experimentally enzymatic activity (catalysis of hydrolysis, decarboxylation, amination, and deamination) [150, 151, 152]. Among numerous works on the synthesis of polypeptides in an aqueous medium, these should be noted: polycondensation of glycine during its heating in an aqueous solution of ammonia [541], during  $\gamma$ -irradiation of N-acetyl-glycine [112], during thermal treatment of solutions of ammonia cyanide [316], during heating of the mixture of HCN, NH<sub>3</sub> [271, 335], during polymerization of aminoacetonitrile [7, 8, 189, 473], cyanamide [448, 501, 550] and dicyanamide [183, 548, 549, 551].

The sequence in which amino acid residues are bound in a polypeptide chain is a very important problem in the synthesis of polypeptides and proteinlike compounds. In modern biological synthesis of proteins, this sequence, which is characteristic of each individual protein (primary structure), is determined by the nucleic code, but, as shown, even during Fox's thermal synthesis, a certain constant order of proximity of amino acids was created in the absence of nucleic acids [153, 194]. Steinman [547] attached the first amino acid in the row to granules of a high-molecular polymer (chlormethylated polystyrol) and, in that way, obtained a resin to which one amino acid was attached. He then studied the relative effectiveness of attaching to it a number of other amino acids, with a protected amino group. After determining experimentally the yields of different dipeptides, Steinman compared these results to the rate of amino acid pairs as defined in the "atlas of protein structures" [95, 96, 523] in modern proteins, and found a significant conformity.

In *Chemical Evolution* ([76], p. 175), Calvin comments on this subject: "There are reasons to suppose that the mechanism which determines the sequence of amino acids in polypeptides includes some component for which the presence of a code system was at first not necessary." He then gives a model for a reproduction system of a polypeptide without a matrix based on control from the growing end [582]. It is interesting to compare these views with the remarkable synthesis of cyclopeptide (gramicidin S) carried out by Lipmann in the absence of a nucleic code [314, 315].

#### Nucleic Acids

The possibility of synthesizing nucleic acids *in vitro* has been shown [180, 275]. However, these syntheses may take place only in the presence of a corresponding specific enzyme, therefore cannot serve as a model for abiogenic processes on the primitive Earth. The probability of such a synthesis was first mentioned by Schramm [508] in his works with polyphosphorus ether. It was later shown that cytidine-phosphate may condense into oligonucleotides with the aid of polyphosphoric acid [513]. The capacity of carbo-

diimide to induce the formation of di- and tri-nucleotides from a mixture of nucleosides and nucleotides in dilute aqueous solution was shown in model tests, which more closely approximated conditions of the primary Earth [352, 567, 568, 569]. Thus, current model tests on abiogenic synthesis of organic substances under conditions which simulate primordial Earth permit (with great probability) imagining the sequential course of chemical evolution from the simplest carbon compounds to high-polymer substances from which were formed those "organized elements" or primitive organisms whose residues are discovered in deposits of the Earth's crust. At this stage of the development of matter, the transition from chemical evolution to biological evolution occurred on our planet when individual whole systems—living organisms—separated from the homogeneous solution of organic substances. A concept of this transition can be formed by comparing modern data of comparative biochemistry [138] to laboratory models.

#### MODEL TESTS WITH INDIVIDUAL OPEN SYSTEMS

Life on Earth is now represented by various organisms—individual complete systems with a specific complex structure and metabolism, and a definite order for mutually compatible biochemical reactions. Naturally, such complex systems could not arise suddenly in the simple, more or less homogeneous, aqueous solution of the hydrosphere, in the so-called "primordial soup." The systems must have been preceded by much simpler formations which, in the evolutionary process, gradually acquired newer and newer features of organization specific only to the living world [380]. First and foremost, they must have acquired the capacity to counteract the growth of entropy—a characteristic of all living creatures. Second, there must be a mechanism for adaptation to existence under given conditions of an external environment. In fact, all parts of the organism (its molecules, cellular organoids, and organs) must adapt to the functions they carry out in the process of living. Third and finally, there must be a special, perfected form of preserving transmission of information

based on the intramolecular organization of high-polymer compounds.

At first glance, it seems that the capacity of living organisms to counteract the growth of entropy contradicts the second law of thermodynamics [38], although this apparent contradiction is known. This was solved by Schroedinger (descriptively, although not completely accurately), who showed that the living organism "attempts" in a way "negative entropy" due to the external environment. In this way, the local reduction of entropy in any individually viewed living object is compensated for by increased entropy in the surrounding environment. Actually, this matter is much more complex within organisms. But in order to carry out even such a simplified arrangement, an organism-and-environment complex is necessary, that is the most primitive formation of phase relationships in a homogeneous solution [325, 418, 419, 471]. The emergence of multiple phases, separation from the starting uniform solution by individual systems which have separated from the surrounding medium by definite interfaces, is extremely widespread in nature and constantly encountered during laboratory studies. Without doubt, such separation on a vast scale also occurred repeatedly on the surface of a lifeless Earth.

In different sections of the hydrosphere with varied chemical composition and natural conditions, countless variegated individual systems could form, which would differ greatly from modern living creatures [72]. Numerous models of such phase-separated systems cannot only be imagined, but also reproduced in laboratory tests. For example, Goldacre [176] described the formational process for small closed vesicles which are contained in a protein-lipoid membrane on the surface of modern bodies of water. They emerged simply because of the effect of wind on protein-lipid film which had formed from products of decomposed bodies of modern organisms which had collected on the surface of the water [98]. In essence, these are simply sections of water removed from the surrounding environment by a definite interface. Even in such simple systems, conditions are created for potential independent interaction with the external environment [21, 97, 99, 413, 414].

In another example, Fox dissolved proteinoids produced by heating a mixture of amino acids in hot water. After cooling this solution, there was a formation of numerous microscopic spherules 2–7  $\mu\text{m}$  in diameter, which he called microspheres. These proteinoid microspheres have an electron-microscopic structure, particularly a double membrane, with a number of biologically interesting properties [149, 153, 651]. Bahadur, the Indian scientist, observed the synthesis of polymers in sunlight. In his tests under sterile conditions, small spherical bodies which had separated from the surrounding solution were formed with an external shape, internal structure, and a number of other properties which, in his opinion, make them like living organisms. Thus, he called them "jeewanu," which translated from Sanskrit means "particles of life" [18, 19].

In working with such artificial systems which automatically separate from solution, particular attention is often paid to their external morphologic similarity to living objects. The problem of counteracting the growth of entropy in phase-separated systems is not to be solved by this, but by interaction with the surrounding medium—as open systems do, whose thermodynamics differ principally from classical thermodynamics. The thermodynamics and kinetics of open systems have been well-developed [70, 353, 416, 417, 456, 457, 458].

In closed systems (on which classical thermodynamics was principally developed), only substances included in the system are capable of chemical reaction. The constancy of the system's properties is characterized by a state of equilibrium in which the reaction rate goes in one direction equal to the rate of the reverse reaction. A thermodynamic criterion of this equilibrium is the minimum role of free energy and the maximum importance of entropy (in other words, its transition to the most probable of all possible states). Spontaneous processes in a closed system are not capable of transferring to a less probable state; that is, they can only keep the entropy of the system constant or increase it, depending on whether reversible or irreversible processes are being dealt with. When the entropy in the system increases, equilibrium is absent. On the contrary, during the onset of equilibrium, the rate

of increase of entropy is equal to zero. Conversely, in an open system, substances entering from the external medium are balanced somehow by chemical compounds returning to the external medium. Therefore, the constancy of such an open system is not characterized by thermodynamic equilibrium (as observed in closed systems), but by the onset of a steady state in which rate is achieved unilaterally by the chemical changes going on and the diffusion of substances into and out of the system.

Thermodynamic equilibrium and the steady state are similar in that in both, the system preserves its properties constant in time. A radical difference is that generally there are not changes of the free energy during equilibrium ( $\alpha F = 0$ ); but during the steady state, this happens continuously, at a constant rate ( $\alpha F = \text{const}$ ). Thus, the steady state is not constant because the free energy is at a minimum (as during the formation of a crystal), but because the system constantly receives free energy from the external medium in an amount which compensates for its decrease internally. The kinetics of the processes in open systems are also complex and unique. This is particularly important in the study of living objects, inasmuch as they are chemical open systems in which, for example, the introduction of a catalyst changes not only the reaction rate, but also the steady-state concentrations of components (hydrodynamic model [69], chemical models [101, 220, 417, 420]).

To solve the problem of reproducing systems which have the capacity to counteract the growth of entropy, it is important that models for this purpose pass easily from the static to a steady, continuous state characteristic of open systems [377]. The most promising (but not the only possible) models in this regard may be coacervate droplets produced at the beginning of the 1930s by Bungenberg-de-Jong which were studied later in detail [45, 46, 60, 61, 62, 63]. In initial tests, dilute aqueous solutions of gelatin were mixed with gum arabic, and observed under normal temperature and acidity. Droplets visible under an optical microscope, in which the molecules of both polymers had concentrated, separated by phase from this solution, while they were lacking entirely in the surrounding solution.

A number of subsequent investigations showed that the coacervate droplets might be formed from various substances, especially from organic polymers and lipoids.

### Coacervate Systems

About 200 examples of coacervate systems formed from varied proteins, nucleic acids, polyglycosides, phosphatides, chlorophyll, and so forth, are given by Yevreinova in *Concentration of Substances and the Action of Enzymes in Coacervates* [646]. In the formation of coacervates, the degree of polymerization of the substances chosen is of great importance. They can be obtained not only from natural biochemical compounds, but also from artificial polymers, for example, polyadenine and polylysine [370, 385]. The volume of droplets (from 5 to several thousand  $10^{-12} \text{ cm}^3$ ) fluctuates greatly as a function of the components and coacervation conditions selected. The concentration of polymers in the droplets exceeds their concentration in the starting solutions by many tens and hundreds of times. The study of droplets in interference, ultraviolet, or electron microscopes, reveals a certain structure and a clearly pronounced external interface (surface film) [386, 643, 644, 645, 647, 648].

Coacervate droplets can selectively adsorb and concentrate interiorly different substances from the surrounding solution (dyes, amino acids, mononucleotides, and so forth [649]). A colloidal-chemical study of cellular protoplasm shows that it and a number of its structures are found in the coacervate state lying between salts and gels [311, 312, 319, 515]. By including different catalysts (particularly enzymes) in the coacervate droplets, a number of varied reactions can be obtained (oxide reduction, polymerization, photochemical transformation, and so forth) because of substances entering from the external medium. Thus, substances of the external medium, undergoing chemical changes, either accumulate in the drops as polymers or are destroyed (freeing the energy enclosed in them), while products of their decomposition are liberated to the external medium. A continuous stream of substances is thus created through the droplets which simulate

biological metabolism in an elementary form. The droplets, interacting with the external medium according to type of open systems, take on a dynamic stability or a capacity for prolonged existence. Under certain conditions, they even increase in volume and weight, which can be directly observed under a microscope and established by chemical analysis (specifically, this was observed in the synthesis of amylose in protein-glycosylic coacervates or of polyadenine in protein-nucleic droplets) [370, 377, 382, 383, 387, 420, 422, 516, 518].

In coacervate droplets in which several intercombined reactions take place, the more complete the union of the catalysts included in the droplets, the faster the droplets will grow. In comparing the growth curves of two differently organized kinds of drops in the same medium, the more perfect drops grow according to a rapidly rising curve, while the less perfect ones are suppressed then halted in growth [384, 597]. These tests made it possible to demonstrate the rudiments of a new law—prebiological natural selection of the predecessors of life probionts—which originated at some time on the surface of the Earth. The second of characteristic properties of life could have arisen only on the basis of this law—the “expediency” adaptability of a living system to conditions of its existence and adaptability of its parts (molecules, organoids, and organs) to the functions carried out by them in the life process.

In the scientific literature, the widespread concept of the initial formation of living systems is still encountered. There must be organized and functional nucleic acids and proteins within the aqueous solution of the Earth's hydrosphere. An automatic collection of their molecules would then have led to the formation of primary organisms similar to the assembling of a machine from previously manufactured parts [347, 348]. Such a concept echoes former mechanistic views which liken the organism to a machine. The adaptability of a machine part to the work it carries out is apt, because the part was manufactured according to a previously thought-out plan or drawing. It is in no way possible to imagine how, in the absence of such a plan, polymers could have been formed with a molecular structure

geared to carrying out specific functions in the complete living systems formed from them.

This adaptability could originate only as a result of natural selection which only complete, phase-separated, open systems could have undergone. These systems had to be capable of overcoming the increase of entropy on the basis of their interaction with the external medium. Individual molecules of the primordial soup could not have done so [351]. Model tests with coacervate droplets have shown that such individual systems may also arise from chaotically or uniformly constructed polymers [385]; these polymers may sometimes have different catalytic functions [151] or the capacity for replication. Efficient functions could be formed only in complete systems which have been subjected to selection. It is precisely from these systems (and not simply in the primordial soup), from the multiplicity of possible variants of polymer structures, that those chosen were best adapted to carrying out functions important to the preservation and more rapid growth of a system (under given conditions of the external medium). Later, they were able to reinforce the properties of these systems during the process of their proliferation and simulation [378].

### Probionts

The evolutionary development of probionts is based mainly on data of comparative biochemistry. It is predominantly concerned with their catalytic apparatus as the most important factor in the organization of metabolism and is based on the relationships of the rates of its constituent reactions. At the stage of evolution under discussion, the only available catalysts for the probionts were inorganic salts and organic substances in the primordial soup and whose catalytic activity is very small. However, in mutual combination, this activity may be increased by many hundreds and thousands of times [300, 301].

A colossal number of different atomic groupings and their combinations can be supposed which, to one degree or another, were able to catalyze the reactions necessary for the existence of probionts. As a result of natural selection always

having eliminated the less perfect complexes, only very few, the most perfect—the coenzymes widely known to biochemistry—have survived. While their number is comparatively small, they are universal catalysts for all living beings, which indicates very early formation during emergence and evolution of life.

The essential constancy of concentration of coenzymes in the proliferating probiots could easily be supported by means of the simple entrance of these compounds (or the components which form them) from the external medium (such as modern vitamins, which also act as coenzymes). However, the capacity of the probiots to form these catalysts through their metabolism had to be developed later [231, 233]. Proteins—enzymes whose catalytic activity is closely related to their intramolecular organization, and above all to their primary structure, with regular location of amino acid residues in their polymer chain—only began a decisive role substantially later [102, 111, 372, 423, 538]. Even during simple thermal production of proteinlike polymers (proteinoids), their primary structure may have a specific order in the arrangement of the component amino acids. Moreover, they manifest a specific catalytic activity [113, 154, 196, 277, 290].

The possibility of such abiogenic synthesis of polypeptides with an ordered chain of amino acid fragments in the absence of a nucleic code is confirmed by Lipmann's work [315] on non-ribosomal synthesis of gramicidin and tyrocidine. Steinman [322] also found in the synthesis of peptides that specific amino acid fragments adjoin one another with the same degree of frequency as in modern proteins [96]. The possibility of fixed repetition in syntheses by replication based on control from the growing end was shown by Calvin [75], who advanced the proposition that the modern system of coding amino acids has its beginning, to some extent, in an ancient synthesis system of polypeptides in which the growing amino acid sequence determined itself. The existence of purely protein evolving systems can, then, be theorized.

The characteristic correspondence of the intramolecular structure of modern enzymes to the catalytic functions which they carry out arose

because of prebiological selection of complete systems, not of individual protein molecules. In systems of this type, numerous and varied combinations of amino acid fragments could be generated which would determine their various functions. The system gained an advantage, under conditions of the external medium, only when the internal protein structures which arose accelerated those reactions, which, in harmonic combination with other processes occurring in the system, were beneficial for the whole and promoted survival and continued proliferation of the entire system. If such were not the case, the system was destroyed by natural selection. Thus, it is understandable how at a given stage of evolution, that efficiency of organization of living systems arose which has been designated the second characteristic property of life.

The third peculiarity of life, the capacity for transmission of hereditary information, was only rudimentary because the direct replication of proteins was still very imperfect and easily disturbed. In modern organisms, enzymatic proteins synthesize by an extremely complex and perfect mechanism through which amino acids are sequentially linked to the polypeptide chain, in precisely that order. This is required for a specific, rigorously regular combination of mononucleotide fragments in DNA and RNA molecules. Such a mechanism could arise only during the process of prolonged evolution of probiots and the living systems which were then formed [474]. The first link in this evolution was the abiogenic formation of polynucleotides, a capability which was shown in a number of model syntheses [508, 568]. Of course, polymers arose in these which were much more primitive in intramolecular structure than those which now exist. They had to evolve, the same as the polypeptides. In examining this evolution, facts must be taken into consideration:

Polynucleotides have a clearly pronounced capacity for direct or complementary replication, and consequently for comparatively accurate self-reproduction of a specific intramolecular organization [628].

Polynucleotides, in contrast to polypeptides, do not have catalytic activity which would

permit them to participate directly in the organization of metabolism of probionts or of any other initial systems. They mediate this only by means of proteins.

The evolution of nucleic acids discussed by Orgel [390], deals with two problems:

The possibility of replication of polynucleotides without enzymes, and the evolution of polynucleotides without proteins.

While current model tests give a positive answer to the first question [391], the second is much more complex, which concerns the possibility of an evolution of polynucleotides oriented to the emergence of life in the absence of proteins. The "natural selection without function" proclaimed by Orgel is internally contradictory, because natural selection may only be compared to definite functions. With the capacity for quite perfect replication (although only in the presence of proteins and enzymes), nucleic acids which are found simply in aqueous solution might accumulate only in definite local places on the Earth's surface in the form of evolutionarily immobile organic deposits. In addition, the combination of proteins with catalytic functions and nucleic acids with perfect capacity for replications is extremely favorable for evolution. Union of these substances into phase-separated formations occurs (in model tests) even during simple mixing of intramolecularly poorly organized polypeptides and polynucleotides (which still do not carry genetic information). Under primitive Earth conditions, interaction of originally independent protein and nucleic systems and the subsequent evolution of the "genetic code," which later determined the preservation and ideal transmission of hereditary information, must have occurred also in such formations.

In generalizing much material in the literature,

Crick [91] proposes two possible pathways for the origin of modern nucleic code:

1. This code was derived simply on the basis of purely stereochemical relationships between triplets of bases (by codes) and amino acids. (In this case, its current universality has been determined by purely chemical structure and in principle it cannot be otherwise.)
2. Originally, the code was more primitive and became perfected during the process of its evolution on the basis of natural selection, i.e., by the attraction of biological regularity. It is now universal not because no other code could exist for purely chemical reasons, but "because at the present time *any change in it would be fatal* or strongly counterselective."

A number of factors and concepts favor the second solution of the problem, and Crick provides a possible picture for subsequent evolution of the code which could have taken place only in complete systems formed from primitive polypeptides and polynucleotides subjected to natural selection, but which were capable of perfecting their organization on the basis of prebiological selection of the systems, not of the individual molecules. Thus, at a comparatively late stage in the evolution of the probionts, these systems reached a new, previously unachieved height of precise self-reproduction which is characteristic of all modern living beings [165, 638]. Further improvement was on this basis, with regard to both metabolic organization, and intracellular structure. This matter has been discussed on the basis of comparative biochemical and cytological data [75, 96, 100, 139, 161, 168, 169, 261, 278, 279, 281, 321, 322, 368, 371, 412, 435, 502, 523, 546, 629].

## REFERENCES

1. ABELSON, P. H. Paleobiochemistry: inorganic synthesis of amino acids. *Carnegie Inst. Wash. Yearb.* 55:171-174, 1956.
2. ABELSON, P. H. Chemical events on the primitive Earth. *Proc. Nat. Acad. Sci.* 55:1365-1372, 1966.
3. ABELSON, P. H., and P. L. PARKER. Fatty acids in sedimentary rocks. *Carnegie Inst. Wash. Yearb.* 61:181-184, 1962.
4. ABETTI, G. *The Sun.* New York, Macmillan, 1957.
5. ADAMS, W. S., and T. DUNHAM. Note on the spectrum of Mercury. *Publ. Astron. Soc. Pac.* 44:380, 1932.
6. ADEL, A., and V. M. SLIPHER. Constitution of the

- atmospheres of the giant planets. *Phys. Rev.* 46:902–906, 1934.
7. AKABORI, Sh. On the origin of the fore-protein. In, Oparin, A. I., et al, Eds. *Proceedings, First International Symposium on the Origin of Life on Earth*. Moscow, 1957. Clark, F., and R. L. M. Syng, Eds., pp. 189–196. New York, Pergamon, 1959.
  8. AKABORI, Sh. Asymmetrical hydration of carbonyl compounds. In, Oparin, A. I., Ed. *Proiskhozhdeniye Prebiologicheskikh Sistem* (Transl: *Origin of Prebiological Systems*), pp. 135–143. Moscow, Mir, 1966. Also in, Fox, S. W., Ed. *The Origins of Prebiological Systems and of Their Molecular Matrices*, pp. 127–135. New York, Academic, 1965.
  9. ALFVEN, H. On the early history of the Sun and formation of the solar system. *Astrophys. J.* 137: 981–990, 1963.
  10. ALLEN, W. V., and C. PONNAMPERUMA. A possible prebiotic synthesis of monocarboxylic acids. *Curr. Mod. Biol.* 1:24–28, 1967.
  11. ALLER, L. H. *The Abundance of the Elements*. New York, Interscience, 1961.
  12. ANDERS, E. Meteorites and the early history of the solar system. In, Jastrow, R., and A. G. W. Cameron, Eds. *On the Origin of the Solar System*, pp. 95–142. New York, Academic, 1963.
  13. ANDERS, E. Meteorites and the early solar system. *Ann. Rev. Astron. Astrophys.* 9:1–34, 1971.
  14. ANDERS, E. Interstellar molecules: formation in solar nebulae. In, Gordon, M. A., and L. E. Snyder, Eds. *Molecules in the Galactic Environment*. Proc., symp. sponsored by Nat. Radio Astron. Obs. and Univ. Va., Charlottesville, Nov. 1971, pp. 429–442. New York, Wiley, 1973.
  15. ANDERSON, A. T., Jr., A. V. CREWE, J. R. GOLDSMITH, P. B. MOORE, J. C. NEWTON, E. J. OLSEN, J. V. SMITH, and P. J. WYLIE. Petrologic history of Moon suggested by petrography, mineralogy and crystallography. *Science* 167:587–589, 1970.
  16. ANDERSON, D. H. *Uranium-Thorium-Lead Ages of Zircons and Model Lead Ages of Feldspars from the Saganaga Snowbank and Giants Range Granites of Northeastern Minnesota*. Minneapolis, Univ. Minn., 1965. (PhD thesis) (Diss. Abstr. 26:308, 1965–1966)
  17. ARP, H. C. The evolution of galaxies. *Sci. Am.* 208(1):71–84, 1963.
  18. BAHADUR, K. Photosynthesis of amino acids from paraformaldehyde and potassium nitrate. *Nature* 173:1141, 1954.
  19. BAHADUR, K. *Synthesis of Jeewanu, the Protocell*. Allahabad, Ram Narain Lal Beni Prasad, 1966.
  20. BALTSCHEFFSKY, H. Inorganic pyrophosphate and the origin and evolution of biological energy transformation. In, Buvet, R., and C. Ponnamperuma, Eds. *Chemical Evolution and the Origin of Life*, Vol. 1, pp. 466–474. New York, Am. Elsevier, 1971.
  21. BANGHAM, A. D., J. DEGIER, and G. D. GREVILLE. Osmotic properties and water permeability of phospholipid liquid crystals. *Chem. Phys. Lipids* 1:225–246, 1967.
  22. BARANOV, V. I. Thermal history of the Earth. In, Maevich, A. G., Ed. *Voznikoveniye Zhizni vo Vselennoy* (Transl: *Origin of Life in the Universe*), pp. 39–44. Moscow, Akad. Nauk SSSR, 1963.
  23. BARGHOORN, E. S., W. MEINSCHEIN, and J. SCHOPF. Paleobiology of Precambrian shale. *Science* 148:461–472, 1965.
  24. BARGHOORN, E. S., D. PHILLPOTT, and C. TURNBILL. Micropaleontological study of lunar material. *Science* 167:775, 1970.
  25. BARGHOORN, E. S., and J. W. SCHOPF. Microorganisms from the late Precambrian of central Australia. *Science* 150:337–339, 1965.
  26. BARGHOORN, E. S., and J. W. SCHOPF. Microorganisms three billion years old from the Precambrian of South Africa. *Science* 152:758–763, 1966.
  27. BARGHOORN, E. S., and S. A. TYLER. Microorganisms from the Gunflint chert. *Science* 147:563–577, 1965.
  28. BARTH, C. A., W. G. FASTIE, C. W. HORD, J. B. PEARCE, K. K. KELLEY, A. I. STEWART, G. E. THOMAS, G. P. ANDERSON, and O. W. F. RAPER. Ultraviolet spectroscopy. In, *Mariner-Mars 1969. A Preliminary Report*, pp. 97–104. Washington, D.C., NASA, 1969. (NASA SP-225)
  29. BATES, D. R., and L. SPITZER, Jr. The density of molecules in interstellar space. *Astrophys. J.* 113:441–463, 1951.
  30. BAYER, E., G. JUNG, and H. HAGENMAIER. Investigation of a total synthesis of ferredoxin. In, Kimball, A. P., and J. Oró, Eds. *Prebiotic and Biochemical Evolution*, pp. 223–232. Amsterdam, North-Holland, 1971.
  31. BECK, A., R. LOHRMANN, and L. E. ORGEL. Phosphorylation with inorganic phosphates at moderate temperatures. *Science* 157:952, 1967.
  32. BECKLIN, E., and G. NEUGEBAUER. Infrared observations of the galactic center at 5 and 10  $\mu$ . In, *Abstracts of Papers*, 128th meet., Am. Astron. Soc., Univ. Tex., Dec. 1968, p. 14. New York, AAS, 1968. (Abstr. 3.03)
  33. BELSKY, T. *Chemical Evolution and Organic Geochemistry*. Berkeley, Univ. Calif., Lawrence Radiat. Lab., 1966. (UCRL-16605) (PhD thesis)
  34. BELSKY, T., R. JOHNS, A. McCARTHY, A. L. BURLINGAME, W. RICHTER, and M. CALVIN. Evidence of life processes in a sediment two and a half billion years old. *Nature* 206(5):446–447, 1965.
  35. BELTON, M. J. S., A. L. BROADFOOT, and D. M. HUNTER. Abundance and temperature of CO<sub>2</sub> on Mars during the 1967 opposition. *J. Geophys. Res.* 73:4795–4806, 1968.
  36. BELTON, M. J. S., D. M. HUNTER, and M. B. McELROY. A search for an atmosphere on Mercury. *Astrophys. J.* 150:1111–1124, 1967.
  37. BENDORAITIS, J. G., B. L. BROWN, and L. S. HEPNER. Isolation and identification of isoprenoids in petroleum. In, *Proceedings*, 6th World Petrol. Congr.,

- Sect. 5, Paper 15. Frankfurt/Main, 1963. *Also in, Abstracts of Technical Papers*, p. 158, 1963.
38. BERGSON, H. L. *L'Evolution Créatrice* (Transl: *Creative Evolution*). Paris, Alcan, 1907.
  39. BERNAL, J. D. *The Physical Basis of Life*. London, Routledge, 1951.
  40. BERNAL, J. D. *The Origin of Life*. London, Weidenfeld and Nicolson, 1967.
  41. BERNAL, J. D. *Vozniknoveniye Zhizni* (Transl: *The Origin of Life*). Moscow, Mir, 1969. (Russ.)
  42. BERTRAND, J. Precambrian stromatolithic artifacts of the stromatolith series of the northwest of the Ahaggar (Sahara). *Bull. Soc. Geol. (France)* 7(10): 168-178, 1968.
  43. BIRD, C. W. Synthesis of organic compounds by direct carbonylation reactions using metal carbonyls. *Chem. Rev.* 62:283-302, 1962.
  44. BLOIS, M. S., and S. RAMDORN. Random polymers as a matrix for chemical evolution. In, Fox, S., Ed. *The Origin of Prebiological Systems*, pp. 19-39. New York, Academic, 1965.
  45. BOOIJ, H. L. Colloid chemistry of living membranes. In, *Conference on Permeability*, Wageningen, Neth., 1962, pp. 5-35. Wageningen, Agric. Univ., 1963.
  46. BOOIJ, H. L., and H. G. BUNGENBERG-DE-JONG. Biocolloids and their interactions. In, *Protoplasmatologia; Handbuch der Protoplasmaforschung*, Bd. 1, Grundlagen 2. Vienna, Springer, 1956.
  47. BOYCHENKO, Ye. A., T. M. UDEL'NOVA, and S. G. YUFEROVA. Evolution of reduction functions of the biosphere. *Geokimya* (11):1392-1396, 1969.
  48. BRADLEY, P. The geology of juvenile carbon. In, Ponnamperuma, C., Ed. *Exobiology, Frontiers of Biology*, Vol. 23, pp. 62-94. New York, Am. Elsevier, 1972.
  49. BRIGGS, M. H. Origin of the solar system. *Nature* 187:1102-1103, 1960.
  50. BRIGGS, M. H., and G. MAMIKUNIAN. Venus—a summary of present knowledge. *J. Br. Interplanet. Soc.* 19:45-52, 1963.
  51. BRODA, E. The origins of bacterial respiration. In, Buvet, R., and C. Ponnamperuma, Eds. *Chemical Evolution and the Origin of Life*, Vol. 1, pp. 447-452. New York, Am. Elsevier, 1971.
  52. BROWN, H. Rare gases and the formation of the Earth's atmosphere. In, Kuiper, G. P., Ed. *The Atmospheres of the Earth and Planets*, pp. 260-268. Chicago, Univ. Chicago Press, 1949.
  53. BROWN, H. The composition and structure of the planets. *Astrophys. J.* 111:641-653, 1950.
  54. BROWN, H. Rare gases and the formation of the Earth's atmosphere. In, Kuiper, G. P., Ed. *The Atmospheres of the Earth and Planets*, 2nd ed., pp. 258-266. Chicago, Univ. Chicago Press, 1952.
  55. BROWN, H. Planetary systems associated with main-sequence stars. *Science* 145:1177-1181, 1964.
  56. BROWN, H., and M. G. INGRAHAM. The isotopic composition of meteoritic copper. *Phys. Rev.* 72:347, 1947.
  57. BROWNLEE, R. R., and A. N. COX. Early solar evolution. *Sky Telesc.* 21:252-256, 1961.
  58. BUHL, D. News notes. *Res. Dev.* 21(10):6, 1970.
  59. BUHL, D., and L. E. SNYDER. Hydrogen cyanide can be added to the list of molecules discovered in interstellar space. *Chem. Eng. News* 28(26):57, 1970.
  60. BUNGENBERG-DE-JONG, H. G. Coacervation and its meaning for biology. *Protoplasma* 15:110-173, 1932.
  61. BUNGENBERG-DE-JONG, H. G. *La Coacervation, les Coacervates et Leur Importance en Biologie*. I. Généralités et Coacervates Complex. II. Coacervates Autocomplex (Transl: *Coacervation of Coacervates and Their Importance in Biology*. I. Regularities and Complex Coacervates. II. Autocomplex coacervates). Paris, Hermann, 1936.
  62. BUNGENBERG-DE-JONG, H. G. Coacervation, I., II. *Kolloid-Z.* 79:223-232, 334-344, 1937; 80:221-231, 350-360, 1937.
  63. BUNGENBERG-DE-JONG, H. G., and C. MALEE. V. Contributions to the problem of the association between proteins and lipids. *Proc. K. Ned. Akad. B* 56:203-217, 1953.
  64. BURBIDGE, E. M., and G. R. BURBIDGE. Formation of elements in stars. *Science* 128:387-399, 1958.
  65. BURBIDGE, E. M., G. R. BURBIDGE, W. A. FOWLER, and F. HOYLE. Synthesis of the elements in stars. *Revs. Mod. Phys.* 39:547-650, 1957.
  66. BURLINGAME, A. L., P. HAUG, T. BELSKY, and M. CALVIN. Occurrence of biogenic steranes and pentacyclic triterpanes in an Eocene shale (52 million years) and in an early Precambrian shale (2.7 billion years). A preliminary report. *Proc. Nat. Acad. Sci.* 54:1406-1412, 1965.
  67. BURLINGAME, A. L., P. A. HAUG, H. K. SCHNOES, and B. R. SIMONEIT. Fatty acids derived from the Green River formation oil shale by extractions and oxidations. In, Schenk, P. A., and I. Havenaar, Eds. *Advances in Organic Geochemistry 1968*, pp. 85-129. New York, Pergamon, 1969.
  68. BURLINGAME, A. L., and B. R. SIMONEIT. High resolution mass spectrometry of Green River kerogen oxidations. *Nature* 222:741-747, 1969.
  69. BURTON, A. C. The properties of the steady state compared to those of equilibrium as shown in characteristic biological behavior. *J. Cell. Physiol.* 14:327-349, 1939.
  70. BUVET, R., E. ETAIX, F. GODIN, P. LEDUC, and L. LE PORT. Energetic continuity between present-day and primeval syntheses of biological compounds. In, Buvet, R., and C. Ponnamperuma, Eds. *Chemical Evolution and the Origin of Life*, Vol. 1, pp. 51-62. New York, Am. Elsevier, 1971.
  71. BUVET, R., and C. PONNAMPERUMA. Eds. *Chemical Evolution and the Origin of Life*, Vol. 1. New York, Am. Elsevier, 1971.
  72. CAIRNS-SMITH, A. G. The origin of life and the nature of the primitive gene. *J. Theor. Biol.* 10:53-88, 1966.
  73. CALVIN, M. Chemical evolution. *Proc. Roy. Soc. (London)*, Ser. A. 288:441-466, 1965.

74. CALVIN, M. Molecular paleontology. *Bennet Lect. Trans. Leicester Lit. Phil. Soc.* 42:45–69, 1968.
75. CALVIN, M. *Chemical Evolution: Molecular Evolution Towards the Origin of Living Systems on the Earth and Elsewhere*. New York, Oxford Univ. Press, 1969.
76. CALVIN, M. *Khimicheskaya Evolyutsiya* (Transl: *Chemical Evolution*), Oparin, A. I., Ed. Moscow, Mir, 1971. (Russ.)
77. CAMERON, A. G. W. Chemical evolution of the stars: introductory report; neutron star models. Presented at 9th Colloq. Int. Astrophys., Univ. Liège, July, 1959. In, *Mem. Soc. Roy. Sci. Liège*, 5th Ser., Vol. 3, pp. 163–206; 461–465. Liège, Univ. Liège, 1960.
78. CAMERON, A. G. W. The formation of the Sun and planets. *Icarus* 1:13–69, 1962.
79. CAMERON, A. G. W., Ed. *Interstellar Communication*. New York, W. A. Benjamin, 1963.
80. CHANG, S., and K. KVENVOLDEN. Distribution and significance of carbon compounds on the Moon. In, Ponnampерума, C., Ed. *Exobiology, Frontiers of Biology*, Vol. 23, pp. 400–430. New York, Am. Elsevier, 1972.
81. CHAPMAN, C. R., J. B. POLLACK, and C. SAGAN. An analysis of the Mariner-4 cratering statistics. *Astron. J.* 74:1039–1051, 1969.
82. CHEUNG, A. C., D. M. RANK, C. H. TOWNES, D. D. THORNTON, and W. J. WELCH. Detection of NH<sub>3</sub> molecules in the interstellar medium by their microwave emission. *Phys. Rev. Lett.* 21:1701–1705, 1968.
83. CHEUNG, A. C., D. M. RANK, C. H. TOWNES, D. D. THORNTON, and W. J. WELCH. Detection of water in interstellar regions by its microwave detection. *Nature* 221:626–628, 1969.
84. CHOUGHLEY, A. S., and R. M. LEMMON. Production of cysteic acid, taurine, and cystamine under primitive Earth conditions. *Nature* 210:628–629, 1966.
85. CLAUS, G., and B. NAGY. A microbiological examination of some carbonaceous chondrites. *Nature* 192:594–596, 1961.
86. CLOUD, P. E., Jr. Significance of the Gunflint (Precambrian) microflora. *Science* 148:27–35, 1965.
87. CLOUD, P. E., Jr. Atmospheric and hydrospheric evolution on the primitive Earth. *Science* 160(5):729–736, 1968.
88. CLOUD, P. E., Jr. Pre-Paleozoic sediments and their significance for organic geochemistry. In, Eglington, G., and M. T. J. Murphy, Eds. *Organic Geochemistry: Methods and Results*, pp. 727–736. Berlin, Springer, 1969.
89. CLOUD, P. E., Jr., J. W. GRUNER, and H. HAGEN. Carbonaceous rock of the Soudan iron formation (early Precambrian). *Science* 148:1713–1716, 1965.
90. CLOUD, P. E., Jr., and H. HAGEN. Electron microscopy of the Gunflint microflora: preliminary results. *Proc. Nat. Acad. Sci.* 54:1–8, 1965.
91. CRICK, F. H. C. The origin of the genetic code. *J. Mol. Biol.* 38:367–379, 1968.
92. DALGARNO, A., and M. B. MC ELROY. Mars: Is nitrogen present? *Science* 170:167–168, 1970.
93. DARWIN, F., Ed. *The Life and Letters of Charles Darwin*, Vol. 3, p. 18. London, Murray, 1887.
94. DAUVILLIER, A. *Cosmologie et Chimie*. Paris, Presses Univ. de France, 1956.
95. DAYHOFF, M. O. *Atlas of Protein Sequence and Structure*, 2nd ed. Washington, D.C., Georgetown Univ. Med. Cent., Nat. Biomed. Res. Found., 1969.
96. DAYHOFF, M. O. Evolution of proteins. In, Ponnampерума, C., Ed. *Exobiology, Frontiers of Biology*, Vol. 23, pp. 266–300. New York, Am. Elsevier, 1972.
97. DEBORIN, G. A. *Balkovo-Lipidnyye Plenki kak Prototip Biologicheskikh Membran* (Transl: *Protein-Lipid Films as a Prototype of Biological Membranes*). Moscow, 1967. (Abstr. Doct. diss).
98. DEBORIN, G. A. and V. Z. BARANOVA. Study of artificial lipovitellin films. In, Kretovich, V. L., Ed. *Problemy Evolyutsionnoy i Tekhnicheskoi Biokhimii* (Transl: *Problems of Evolutionary and Technical Biochemistry*), pp. 147–153. Moscow, Nauka, 1964.
99. DEBORIN, G. A., V. Z. BARANOVA, and I. G. ZHUKOVA. Study of surface films of a lipoprotein complex from membranes of *Micrococcus lysodeicticus*. *Dokl. Akad. Nauk SSSR* (Moscow) 166:231–234, 1966.
100. DEBORIN, G. A., I. P. TYURINA, T. I. TORKHOVSKAYA, and A. I. OPARIN. Fermentative cleavage of ribonucleic acid isolated from ribonuclease of a lipid membrane. *Zh. Evol. Biokhim. Fiziol.* (Leningrad) 1(6): 550–556, 1965.
101. DENBIGH, K. G., M. HICKS, and F. M. PAGE. Kinetics of open reaction systems. *Trans. Faraday Soc.* 44:479–494, 1948.
102. DIXON, M., and E. C. WEBB. *Enzymes*, 2nd ed. New York, Academic, 1964.
103. DODONOVA, N. Ya., and A. I. SIDOROVA. Photosynthesis of amino acids from a mixture of gases under the action of vacuum ultraviolet radiation. *Biofizika* 6:149–158, 1961.
104. DODONOVA, N. Ya., and A. I. SIDOROVA. On the role of ethyl radicals in the synthesis of amino acids under the action of vacuum ultraviolet radiation. *Biofizika* 7:31–33, 1962.
105. DOLLFUS, A. Observation of an atmosphere around the planet Mercury. *C. R. Acad. Sci. (Paris)* 231: 1430–1432, 1950.
106. DONN, B. Polycyclic hydrocarbons, Platt particles and interstellar extinction. *Astrophys. J.* 152:L129–L133, 1968.
107. DONN, B. Organic molecules in space. In, Ponnampерума, C., Ed. *Exobiology, Frontiers of Biology*, Vol. 23, pp. 431–448. New York, Am. Elsevier, 1972.
108. DONN, B., and H. C. UREY. On the mechanism of comet outbursts and the chemical composition of comets. *Astrophys. J.* 123:339–342, 1956.
109. DONN, B., N. C. WICKRAMASINGHE, J. P. HUDSON, and T. P. STECHER. On the formation of graphite grains in cool stars. *Astrophys. J.* 153:451–464, 1968.
110. DOSE, K. Catalysis. In, Schwartz, A. W., Ed. *Theory and Experiment in Exobiology*, Vol. 1, pp. 41–71.

- Groningen, Neth., Wolters-Noordhoff, 1971.
111. DOSE, K. Evolution of prebiotic catalytic functions. In, *Origin of Life and Evolutionary Biochemistry*, pp. 31–36. Presented at Int. Symp. Yarna, Bulg., 1971. (Abstr.)
112. DOSE, K., and C. PONNAMPERUMA. The effect of ionizing radiation on N-acetyl-glycine in the presence of ammonia. *Radiat. Res.* 31:650, 1967.
113. DOSE, K., and L. ZAKI. The peroxidatic and catalatic activity of hemoproteinoids. *Z. Naturforsch.* 26B:144–148, 1971.
114. DUFAY, J. *Galactic Nebulae and Interstellar Matter*. (Pomerans, A. J., transl.) New York, Philosophical Libr., 1957.
115. EDSELL, J. T., and J. WYMAN. *Biophysical Chemistry: I. Thermodynamics, Electrostatics and the Biological Significance of the Properties of Matter*. New York, Academic, 1958.
116. EGLINTON, G. Hydrocarbons and fatty acids in living organisms and recent and ancient sediments. In, Schenk, P., and I. Havenaar, Eds. *Advances in Organic Geochemistry for 1968*, pp. 1–24. London, Pergamon, 1969.
117. EGLINTON, G. Organic geochemistry; the organic chemist's approach. In, Eglinton, G., and M. T. J. Murphy, Eds. *Methods and Results*, pp. 20–73. Berlin, Springer, 1969.
118. EGLINTON, G. Carbon chemistry of the Moon. In, Buvet, R., and C. Ponnampерума, Eds. *Chemical Evolution and the Origin of Life*, Vol. 1, pp. 523–540. New York, Am. Elsevier, 1971.
119. EGLINTON, G., and M. CALVIN. Chemical fossils. *Sci. Am.* 216(1):32–43, 1967.
120. EGLINTON, G., and M. T. J. MURPHY, Eds. *Organic Geochemistry: Methods and Results*. Berlin, Springer, 1969.
121. EIGEN, M. The evolution of biological micromolecules. *Naturwiss. Rundsch.* 24(1):22–23, 1971.
122. EL'PINER, I. Ye. Ultrasonics and synthesis of organic substances. *Priroda* (Moscow) (11):64–70, 1968.
123. EL'PINER, I. Ye., and A. V. SOKOL'SKAYA. Synthesis by ultrasonic waves in water saturated with reducing gases. *Dokl. Akad. Nauk SSSR* 119:1180–1182, 1958.
124. EL'PINER, I. Ye., A. V. SOKOL'SKAYA, and F. I. BRAGINSKAYA. Abiogenic synthesis of biologically active substances in a field of ultrasonic waves. *Zh. Evol. Biokhim. Fiziol.* (Moscow) 4:307–322, 1968.
125. EL'PINER, I. Ye., A. V. SOKOL'SKAYA, and A. V. KOLOCHEVA. On the synthesis of peptides, heterocyclic compounds and amino acids in a field of ultrasonic waves. *Dokl. Akad. Nauk SSSR* (Moscow) 181:737–740, 1968.
126. ENCEL, A. E., B. NAGY, L. NAGY, C. ENGEL, G. KREMP, and C. DREW. Alga-like forms in Onverwacht series, South Africa: oldest recognized lifelike forms on Earth. *Science* 161:1006–1008, 1968.
127. EPSTEIN, S., and H. P. TAYLOR.  $^{18}\text{O}/^{16}\text{O}$ ,  $^{30}\text{Si}/^{28}\text{Si}$ , D/H, and  $^{13}\text{C}/^{12}\text{C}$  studies of lunar rocks and minerals. *Science* 167:533–535, 1970.
128. FALK, J. E. *Porphyrins and Metalloporphyrins*, Chap. 10, pp. 154–161. Amsterdam, North-Holland, 1964.
129. FERRIS, J. P., and L. E. ORGEL. Studies in prebiotic synthesis I. Amino-malononitrile and 4-amino-5-cyanoimidazole. *J. Am. Chem. Soc.* 88:3829–3831, 1966.
130. FESENKOВ, V. G. Some considerations about the primeval state of the Earth. In, Oparin, A. I., et al., Eds. *Proceedings, First International Symposium on the Origin of Life on Earth*, Moscow, 1957, Clark, F., and R. L. M. Syngе, Eds. pp. 9–15. New York, Pergamon, 1959.
131. FESENKOВ, V. G. Unity and interconnection of a galactic system as a condition for the origin of life on planets. In, Masevich, A. G., Ed. *Vozniknoveniye Zhizni vo Vselennoy* (Transl: *Origin of Life in the Universe*), pp. 77–93. Moscow, Akad. Nauk SSSR, 1963.
132. FESENKOВ, V. G. Meteorites and the origin of the solar system. *Priroda* (Moscow) (10):2–7, 1964.
133. FESENKOВ, V. G. Space conditions of the possibility of life in the universe. In, Kretovich, V. L., Ed. *Problemy Evolyutsionnoy i Tekhnicheskoy Biokhimii* (Transl: *Problems of Evolutionary and Technical Biochemistry*), pp. 5–11. Moscow, Nauka, 1964.
134. FESENKOВ, V. G. Conditions for life in the universe. In, Imshenetskiy, A. A., Ed. *Zhizn' vne Zemli i Metody yeye Obnaruzheaniya* (Transl: *Life Beyond the Earth and Methods of Detecting It*), pp. 7–16. Moscow, Nauka, 1970.
135. FESENKOВ, V. G. Organic substances in the universe. In, Buvet, P., and C. Ponnampерума, Eds. *Chemical Evolution and the Origin of Life*, pp. 495–498. New York, Am. Elsevier, 1971.
136. FESENKOВ, V. G., and D. ROZHKOВSKIY. *Atlas Gazovo-Pylevykh Tumannostey* (Transl: *Atlas of Gas-Dust Nebulae*). Moscow, Nauka, 1953.
137. FITCH, F. W., and E. ANDERS. Current status of the analysis of organized elements in carbonaceous chondrites. In, Florkin, M., Ed. *Life Sciences and Space Research*, Vol. 3, p. 154. New York, Wiley, 1965.
138. FLORKIN, M. *Biochemical Evolution*. New York, Academic, 1949.
139. FLORKIN, M., and H. S. MASON. An introduction to comparative biochemistry. In, Florkin, M., and H. S. Mason, Eds. *Comparative Biochemistry: A Comprehensive Treatise*, Vol. 1, pp. 1–14. New York, Academic, 1960.
140. FLOROVSKAYA, V. N. Abiogenic carbon substances of the Earth's crust. Presented at Second All-Union Biochem. Congr., Tashkent, Oct., 1969, pp. 5–7. Akad. Nauk Uzb. SSR, 1969.
141. FLOROVSKAYA, V. N., T. A. TEPLITSKAYA, R. ZEZIN, and L. OVCHINNIKOVA. Coloring and luminescence of hackmanite. *Dokl. Akad. Nauk SSSR* 163:450–453, 1965.
142. FLOROVSKAYA, V. N., R. B. ZEZIN, L. I. OVCHINNIKOVA, Yu. I. PIKOVSKIY, and T. A. TEPLITSKAYA. *Diagnostika Organicheskikh Veshchestv v Gornykh Porodakh i Mineralakh Magmaticheskogo i Gidrotermicheskogo*

- Proiskhozhdeniya* (Transl: *Diagnosis of Organic Substances in Rocks and Minerals of Magnetic and Hydrothermal Origin*. Moscow, Nauka, 1968.
143. FLOROVSKAYA, V. N., R. ZEZIN, L. OVCHEINNIKOVA, Yu. PIKOVSKIY, and T. TEPLITSKAYA. Carbon substances in different genetic types of rocks and valuable minerals. *Byull. Mosk. Ova Ispyt. Prir. Otd. Geol.* 10:110–120, 1969.
  144. FOWLER, W. A. The origin of the elements. *Proc. Nat. Acad. Sci.* 52: 524–548, 1964.
  145. FOWLER, W. A., J. L. GREENSTEIN, and F. HOYLE. Nucleosynthesis during the early history of the solar system. *Geophys. J.* 6:148–220, 1962.
  146. FOWLER, W. A., and F. HOYLE. Nuclear cosmochronology. *Ann. Phys.* 10:280–302, 1960.
  147. FOX, S. W. How did life begin? *Science* 132(3421):200–208, 1960.
  148. FOX, S. W., Ed. *The Origins of Prebiological Systems and of Their Molecular Matrices*. Conference proceedings, Wakulla Springs, Fla., Oct. 1963. New York, Academic, 1965.
  149. FOX, S. W. Simulated natural experiments in spontaneous organization of morphological units from proteinoid. In, Fox, S., Ed. *The Origins of Prebiological Systems and of Their Molecular Matrices*, pp. 361–382. New York, Academic, 1965.
  150. FOX, S. W. Self-assembly of the protocell from a self-ordered polymer. *J. Sci. Ind. Res.* 27(7):267–274, 1968.
  151. FOX, S. W. Self-ordered polymers and propagative cell-like systems. *Naturwissenschaften* 56:1–9, 1969.
  152. FOX, S. W. Explanation of some aspects of the origin of life based on experimental data. *Zh. Evol. Biokhim. Fiziol.* 6(2):131–147, 1970.
  153. FOX, S. W. Self-assembly of the protocell from a self-ordered polymer. In, Kimball, A. P., and J. Oró, Eds. *Prebiotic and Biochemical Evolution*, pp. 8–30. Amsterdam, North-Holland, 1971.
  154. FOX, S. W. Self-ordering in and self-assembly of thermal polymers of amino acids. In, *Origin of Life and Evolutionary Biochemistry*, pp. 37–43. Presented at Int. Symp., Varna, Bulg., 1971. (Abstr.)
  155. FOX, S. W., and K. HARADA. The thermal copolymerization of amino acids common to protein. *J. Am. Chem. Soc.* 82:3745–3751, 1960.
  156. FOX, S. W., and K. HARADA. Synthesis of uracil under conditions of a thermal model of prebiological chemistry. *Science* 133:1923–1924, 1961.
  157. FOX, S. W., K. HARADA, P. E. HARE, G. HINSCH, and G. MUELLER. Bio-organic compounds and glassy microparticles in lunar fines and other materials. *Science* 167:767–770, 1970.
  158. FOX, S. W., and S. YUYAMA. Abiotic production of primitive protein and formed microparticles. *Ann. N.Y. Acad. Sci.* 8:487, 1963.
  159. GABEL, N. W., and C. PONNAMPERUMA. A model for the primordial origin of monosaccharides. *Nature* 216:453–455, 1967.
  160. GABEL, N. W., and C. PONNAMPERUMA. Primordial organic chemistry. In, Ponnampерума, C., Ed. *Exobiology, Frontiers of Biology*, Vol. 23, pp. 95–135. New York, Am. Elsevier, 1972.
  161. GAFFRON, H. On dating stages in photochemical evolution. In, Kasha, M., and B. Pullman, Eds. *Horizons in Biochemistry*, pp. 59–89. New York, Academic, 1962.
  162. GAMOW, G. *The Creation of the Universe*. New York, Viking, 1952.
  163. GAMOW, G., and J. HYNEK. A new theory by C. F. Von Weizsäcker of the origin of the planetary system. *Astrophys. J.* 101:249–254, 1945.
  164. GARRISON, W. M., D. C. MORRISON, J. G. HAMILTON, A. A. BENSON, and M. CALVIN. Reduction of carbon dioxide in aqueous solutions by ionizing radiation. *Science* 114:416–418, 1951.
  165. GAVAUDAN, P. The genetic code and the origin of life. In, Buvet, R., and C. Ponnampерума, Eds. *Chemical Evolution and the Origin of Life*, Vol. 1, pp. 432–435. New York, Am. Elsevier, 1971.
  166. GAZE, V. F. *Asimmetriya Protoplazmy* (Transl: *Asymmetry of Protoplasm*). Moscow, Akad. Nauk SSSR, 1940.
  167. GEHRKE, C. W., R. W. ZUMWALT, W. A. AUE, D. L. STALLING, A. DUFFIELD, K. A. KVENVOLDEN, and C. PONNAMPERUMA. Carbon compounds in lunar fines from Mare Tranquillitatis. III. Organo siloxanes in hydrochloric acid hydrolysates. In, Levinson, A. A., Ed. *Proceedings, Apollo 11 Lunar Science Conference*, Houston, Tex., Jan. 1970, Vol. 2, pp. 1845–1846. New York, Pergamon, 1970. Also in, *Geochim. Cosmochim. Acta*, Suppl. 1.
  168. GEL'MAN, N. S. Molecular organization of biological membranes. *Usp. Sovrem. Biol.* (Moscow) 64:379–398, 1967.
  169. GEL'MAN, N. S., M. A. LUKYANOVA, and D. N. OSTROVSKIY. *Membrany Bakteriy i Dykhatel'naya tsep'* (Transl: *Membranes of Bacteria and the Respiratory Chain*). Moscow, Nauka, 1972.
  170. GILVARRY, J. J. Observability of indigenous organic matter on the Moon. *Icarus* 5:228–236, 1966.
  171. GLAESNER, M. F. Precambrian animals. *Sci. Am.* 204(3):72–78, 1961.
  172. GLAESNER, M. F., W. V. PREISS, and M. R. WALTER. Precambrian columnar stromatolites in Australia. Morphological and stratigraphical analysis. *Science* 164:1056–1058, 1969.
  173. GLAESNER, M. F., and M. WADE. The late Precambrian fossils from Ediacara, South Australia. *Palaeontology* 9:599–628, 1966.
  174. GLASEL, J. A. Stabilization of NH in hydrocarbon matrices and its relation to cometary phenomena. *Proc. Nat. Acad. Sci.* 47:174–180, 1961.
  175. GLASTONE, S. *The Book of Mars*. Washington, D.C., NASA, 1968. (NASA SP-179)
  176. GOLDACRE, R. J. Surface film, their collapse on compression, the shapes and sizes of cells and the origin of life. In, Danielli, J. F., K. G. A. Pankhurst, and

- A. C. Riddiford, Eds. *Surface Phenomena in Chemistry and Biology*, pp. 278-298. London, Pergamon, 1958.
177. GOLDBERG, L., E. A. MUELLER, and L. H. ALLER. The abundance of the elements in the solar system. *Astrophys. J. Suppl. Ser.* 5:1-138, 1960.
178. GOLDRING, R., and C. N. CURNOW. The stratigraphy and facies of the late Precambrian at Ediacora, South Australia. *J. Geol. Soc. Aust.* 14:195-214, 1967.
179. GOLDSCHMIDT, V. M. Geochemical distribution of the elements. IX. The relative abundances of the elements and of the atomic species. *Skr. Nor. Vidensk. Akad. Oslo* 4:1938. (Monogr.)
180. GOULIAN, M., A. KORNBERG, and R. L. SINSHEIMER. Enzymatic synthesis of DNA. XXIV. Synthesis of infectious phage DNA  $\phi \times 174$  #DNA. *Proc. Nat. Acad. Sci.* 58:2321-2328, 1967.
181. GRAVELLE, M., and M. LELUBRE. Discovery of stromatoliths of the conophyton group in the Pharusian of Western Ahaggar (Central Sahara). *Bull. Soc. Geol. (France)*, 6(7):435-442, 1957.
182. GREENE, E. F., and J. P. TOENNIES. *Chemical Reactions in Shock Waves*. New York, Academic, 1964.
183. GREENLAND, D. J., R. H. LABY, and J. P. QUIRK. Adsorption of glycine and its di-, tri- and tetra-peptides by montmorillonite. *Trans. Faraday Soc.* 58:829-841, 1962.
184. GREENSTEIN, J. L. Stellar evolution and the origin of chemical elements. *Am. Scientist* 49:449-473, 1961; The history of stars and galaxies. *Proc. Nat. Acad. Sci.* 52:549-565, 1964.
185. GROSSENBACHER, K. A., and C. A. KNIGHT. Amino acids, peptides and spherules obtained from "primitive Earth" gases in a sparking system. In, Fox, S. W., Ed. *The Origins of Prebiological Systems and of Their Molecular Matrices*, pp. 173-186. New York, Academic, 1965.
186. GROTH, W. E., and H. V. WEYSENHOFF. Photochemical formation of organic compounds from mixtures of simple gases. *Planet. Space Sci.* 2:79-85, 1960.
187. HAN, J., and M. CALVIN. Occurrence of fatty acids and aliphatic hydrocarbons in 3-4 billion-year-old sediment. *Nature* 224:576-577, 1969.
188. HAN, J., B. R. SIMONEIT, A. L. BURLINGAME, and M. CALVIN. Organic analysis on the Pueblito Allende meteorite. *Nature* 222:364-365, 1969.
189. HANABUSA, H., and S. AKABORI. Polymerization of aminoacetonitrile. *Bull. Chem. Soc. Jap.* 32:626-630, 1959.
190. HARADA, K. Formation of amino-acids by thermal decomposition of formamide-oligomerization of cyanide. *Nature* 214(5087):479-480, 1967.
191. HARADA, K. Origin and development of optical activity of bio-organic compounds on the primordial Earth. In, Buvet, R., and C. Ponnamperuma, Eds. *Chemical Evolution and the Origin of Life*, Vol. 1, pp. 71-79. New York, Am. Elsevier, 1971.
192. HARADA, K., and S. W. FOX. Thermal synthesis of natural amino acids from a postulated primitive terrestrial atmosphere. *Nature* 201(4917):335-336, 1964.
193. HARADA, K., and S. W. FOX. The thermal synthesis of amino acids from a hypothetically primitive terrestrial atmosphere. In, Fox, S., Ed. *The Origins of Prebiological Systems and of Their Molecular Matrices*. Conference proceedings, Wakulla Springs, Fla., Oct. 1963, pp. 187-194. New York Academic, 1965.
194. HARADA, K., and S. W. FOX. Thermal polycondensation of free amino acids with polyphosphoric acid. In, Fox, S. W., Ed. *The Origins of Prebiological Systems and of Their Molecular Matrices*, pp. 289-298. New York, Academic, 1965.
195. HARADA, K., P. E. HARE, C. R. WINDSOR, and S. W. FOX. Evidence for compounds hydrolyzable to amino acids in aqueous extracts of Apollo 11 and Apollo 12 lunar fines. *Science* 173:433-435, 1971.
196. HARDEBECK, H. G., G. KRAMPITZ, and L. WULF. Decarboxylation of pyruvic acid in aqueous solution by thermal proteinoids. *Arch. Biochem. Biophys.* 123:72-81, 1968.
197. HARE, P. E. Amino acid artifacts in organic geochemistry. *Carnegie Inst. Wash. Yearb.* 64:232-235, 1965.
198. HÄRME, M., and V. PERTTUNEN. Stromatolite structures in Precambrian dolomite in Tervola, North Finland. *C. R. Soc. Geol. Finl.* 35:79-81. *Bull. Comm. Geol. Finl.*, No. 212, 1963.
199. HARTECK, P., and J. H. D. JENSEN. The oxygen content of the atmosphere. *Z. Naturforsch.* 3A:591-595, 1948.
200. HASER, L. The conservation of free radicals at low temperature and the structure of comet nuclei. *C. R. Acad. Sci. (Paris)* 241:742-743, 1955.
201. HASSELSTROM, T., M. HENRY, and B. MURR. Synthesis of amino acids by beta radiation. *Science* 125(3243):350-351, 1957.
202. HAYATSU, R., M. H. STUDIER, and E. ANDERS. Possible origin of organic matter in meteorites and the Earth. In, *Abstracts of Papers (EF 1-70-48)*, 1970 International Symposium on Hydrogeochemistry and Biogeochemistry, Sept. 1970, Tokyo, Jap., p. 73.
203. HAYATSU, R., M. H. STUDIER, and E. ANDERS. Origin of organic matter in the early solar system. IV. Amino acids: confirmation of catalytic synthesis by mass spectrometry. *Geochim. Cosmochim. Acta* 35:939-951, 1971.
204. HAYATSU, R., M. H. STUDIER, S. MATSUOKA, and E. ANDERS. Origin of organic matter in early solar system. VI. Catalytic synthesis of nitriles, nitrogen bases and porphyrin-like pigments. *Geochim. Cosmochim. Acta* 36:555-571, 1972.
205. HAYATSU, R., M. H. STUDIER, A. ODA, K. FUSE, and E. ANDERS. Origin of organic matter in early solar system. II. Nitrogen compounds. *Geochim. Cosmochim. Acta* 32:175-190, 1968.
206. HAYES, J. M. Organic constituents of meteorites—a review. *Geochim. Cosmochim. Acta* 31:1395-1440, 1967.

207. HEATH, M. B. B. Saturn in 1958. *J. Br. Astron. Assoc.* 70:29–32, 1960.
208. HEISENBERG, W. The development of the uniform field theory of elementary particles. *Naturwissenschaften* 50:3–7, 1963.
209. HENDERSON, W., G. EGLINTON, P. SIMMONDS, and J. E. LOVELOCK. Thermal alteration as a contributory process to the genesis of petroleum. *Nature* 219:1012–1016, 1968.
210. HENROTEAU, F., and J. HENDERSON. A spectrographic study of early class B stars. *Pub. Dom. Astron. Obs. Ottawa* 5:1–23, 1920; HENROTEAU, F. A spectrographic study of early class B stars. *Pub. Dom. Astron. Obs. Ottawa* 5(8):331–364, 1922. (Third paper)
211. HERBIG, G. H. The diffuse interstellar bands. III. The situation in 1966. In, van Woerden, H., Ed. *Radio Astronomy and the Galactic System*, pp. 85–89. New York, Academic, 1967. (IAU Symp. No. 31)
212. HERBIG, G. H. The youngest stars. *Sci. Am.* 217(2):30–36, 1967.
213. HERR, K. C., D. HORN, J. M. McAFFEE, and G. C. PIMENTEL. Martian topography from the Mariner 6 and 7 infrared spectra. *Astron. J.* 75:883–894, 1970.
214. HERR, K., and G. PIMENTEL. Infrared spectroscopy. In, *Mariner-Mars 1969—A Preliminary Report*, pp. 83–96. Washington, D.C., NASA, 1969. (NASA SP-225)
215. HERRERA, A. L. Cellules artificielles, figures mitosiques et chromosomes. *Bull. Lab. Plasmogen. Mex.* 1(49):97–98, 1936; Importance plasmogénique des savons. *Bull. Lab. Plasmogen. Mex.* 1(32):63–64, 1934; Formes organiques produites par le formol, le phénol, et sulfo-cyanate d'ammonium. *Bull. Lab. Plasmogen. Mex.* 1(36):71–72, 1934.
216. HERRERA, A. L. A new theory of the origin and nature of life. *Science* 96:14, 1942.
217. HERZBERG, G. *Molecular Spectra and Molecular Structure*, 2nd ed. I. *Spectra of Diatomic Molecules*. Princeton, Van Nostrand, 1951.
218. HEYNS, K., and K. PAVEL. I. Thermal conversion products of amino acids. *Z. Naturforsch.* 12b:97–109, 1957.
219. HEYNS, K., W. WALTER, and E. MEYER. Model tests for construction of an organic compound in the atmosphere by means of electric charge. *Naturwissenschaften* 44:385–389, 1957.
220. HINSHELWOOD, C. N. *The Chemical Kinetic of the Bacterial Cell*. Oxford, Clarendon, 1946.
221. HOCHSTIM, A. R. Hypersonic chemosynthesis and possible formation of organic compounds from impact of meteorites on water. *Proc. Nat. Acad. Sci.* 50(2):200–208, 1963.
222. HODGSON, G. W. Exobiology of porphyrins. In, Schwartz, A. W., Ed. *Theory and Experiment In Exobiology*, Vol. 1, pp. 83–103. Groningen, Neth., Wolters-Noordhoff, 1971.
223. HODGSON, G. W., and B. BAKER. Evidence for porphyrins in the Orgueil meteorite. *Nature* 202:125–131, 1964.
224. HODGSON, G. W., and B. L. BAKER. Porphyrins in meteorites: metal complexes in Orgueil, Murray, cold Bokkeveld and Mokoia carbonaceous chondrites. *Geochim. Cosmochim. Acta* 33:943–958, 1969.
225. HODGSON, G. W., E. PETERSON, K. A. KVENVOLDEN, E. BUNNENBERG, B. HALPERN, and C. PONNAMPERUMA. Search for porphyrins in lunar dust. *Science* 167:763–765, 1970.
226. HODGSON, G. W., and C. PONNAMPERUMA. Prebiotic porphyrin genesis: porphyrins from electric discharge in methane, ammonia, and water vapor. *Proc. Nat. Acad. Sci.* 59:22–28, 1968.
227. HOERING, T. C. The isolation of organic compounds from Precambrian rocks. *Carnegie Inst. Wash. Yearb.* 61:184–187, 1962.
228. HOERING, T. C. The extractable organic matter in Precambrian rocks and the problem of contamination. *Carnegie Inst. Wash. Yearb.* 64:215–218, 1965.
229. HOERING, T. C. Criteria for suitable rocks in Precambrian organic geochemistry. *Carnegie Inst. Wash. Yearb.* 65:365–372, 1966.
230. HOLLAND, H. D. Model for the evolution of the Earth's atmosphere. In, Engel, A. E. J., H. L. James, and B. F. Leonard, Eds. *Petrologic Studies: A Volume in Honor of A. F. Buddington*, pp. 447–477. New York, Geol. Soc. Am., 1962.
231. HOROWITZ, N. H. On the evolution of biochemical syntheses. *Proc. Nat. Acad. Sci.* 31:153–157, 1945.
232. HOROWITZ, N. H. Study of the cosmos and the origin of life. In, Kretovich, V. L., Ed. *Problemy Evolyutsionnoy i Tekhnicheskoy Biokhimii* (Transl: *Problems of Evolutionary and Technical Biochemistry*), pp. 12–16. Moscow, Nauka, 1964.
233. HOROWITZ, N. H., and S. L. MILLER. Current theories on the origin of life. In, Zechmeister, L., Ed. *Fortschr. Chem. Org. Naturstoffe*, pp. 423–459. Vienna, Springer, 1962.
234. HOUCK, T. E., and C. F. LILLIE. Ultraviolet “pictures” of comets taken from space. *Chem. Eng. News* 48(14):33, 1970.
235. HOWARD, W. E., III, A. H. BARRETT, and F. T. HADDOCK. The measurement of microwave radiation from the planet Mercury. *Astron. J.* 66:287, 1961.
236. HOYLE, F. *The Nature of the Universe*. Oxford, B. Blackwell, 1950; rev. ed., New York, Harper-Row, 1960.
237. HOYLE, F. On the origin of the solar nebula. *Quart. J. Roy. Astron. Soc.* 1:28–55, 1960.
238. HOYLE, F. *Galaktika, Yadra i Kvazary* (Transl: *Galaxies, Nuclei and Quasars*). Moscow, Mir., 1968.
239. HOYLE, F., W. A. FOWLER, G. R. BURBIDGE, and E. M. BURBIDGE. On relativistic astrophysics. *Astrophys. J.* 139:909–928, 1964.
240. HOYLE, F., and J. V. NARLIKAR. Steady state model and the ages of galaxies. *Observatory (London)* 82:13–14, Feb. 1962.
241. HOYLE, F., and N. C. WICKRAMASINGHE. Graphite particles as interstellar grains. *Mon. Not. Roy. Astron. Soc.* 124:417–433, 1962.

242. HUANG, S. S. Occurrence of life in the universe. *Am. Scientist* 47:397-402, 1959.
243. HURLEY, P. M., H. W. FAIRBAIRN, W. H. PINSON, Jr., and J. HOWER. Unmetamorphosed minerals in the Gunflint formation used to test the age of the animikie. *J. Geol.* 70:489-492, 1962.
244. IBANEZ, J., A. P. KIMBALL, and J. ORO. The effect of imidazole, cyanamide and polyornithine on the condensation of nucleotides in aqueous systems. In, Buvet, R., and C. Ponnampерuma, Eds. *Chemical Evolution and the Origin of Life*, Vol. 1, pp. 171-179. New York, Am. Elsevier, 1971.
245. IKORSKIY, S. V. *Organicheskoye Veshchestvo v Mineralakh Izyerzhennykh Gornykh Porod na Primere Khibinskogo Shchelochnogo Massiva* (Transl: *Organic Matter in Minerals of Ejected Rocks Exemplified by the Khibina Alkaline Massif*). Leningrad, Nauka, 1967.
246. IMSHENETSKIY, A. A., Ed. *Zhizn'vne Zemli i Metody yeye Obnaruzheniya*. (Transl: *Life Beyond the Earth and Methods of Detecting It*). Moscow, Nauka, 1970.
247. IRELAND, J. G., K. NANDY, H. SEDDON, and R. D. WOLSTENCROFT. Role of impurities in interstellar graphite grains. *Nature* 215:377-378, 1967.
248. JASTROW, R., and A. G. W. CAMERON, Eds. *Origin of the Solar System*. New York, Academic, 1963.
249. JEFFERTS, K. B., A. A. PENZIAS, and R. W. WILSON. Carbon monoxide found. *Chem. Eng. News* 48(17):14-15, 1970.
250. JOHNS, R. B., T. BELSKY, E. D. McCARTHY, A. L. BURLINGAME, P. HAUG, H. K. SCHNOES, W. RICHTER, and M. CALVIN, II. The organic geochemistry of ancient sediments. *Geochim. Cosmochim. Acta* 30:1191-1222, 1966.
251. JOHNSON, F. M. Diffuse interstellar lines and the chemical characterization of interstellar dust. In, Greenberg, J. M., and T. P. Roark, Eds. *Interstellar Grains*, pp. 229-240. Washington, NASA, 1967. (NASA SP-140)
252. JOHNSON, F. M. Interstellar matter. In, Enzmann, R. D., Ed. *Use of Space Systems for Planetary Geology and Geophysics*, pp. 51-66. Tarzana, Calif., Am. Astron. Soc., 1968.
253. JOHNSON, F. M., and G. W. HODGSON. Preliminary low temperature absorption and scattering data of organic powders simulating interstellar dust. In, *Abstracts of Papers*, 129th Meet. Am. Astron. Soc., Honolulu, Mar. 1969, p. 8. New York, AAS, 1969. (Abstr. 2.01)
254. KAPLAN, L. D. A new interpretation of the structure and CO<sub>2</sub> content of the Venus atmosphere. In, *Planetary and Space Science*, Vol. 8, pp. 23-29. New York, Pergamon, 1961.
255. KAPLAN, L. D., J. CONNES, and P. CONNES. Carbon monoxide in the Martian atmosphere. *Astrophys. J.* 157:1187-1192, 1969.
256. KAPLAN, I. R., E. DEGENS, and J. REUTER. Organic compounds in stony meteorites. *Geochim. Cosmochim. Acta* 27:805-834, 1963.
257. KAPLAN, I. R., and J. W. SMITH. Concentration and isotopic composition of carbon and sulfur in Apollo 11 lunar samples. *Science* 167:541-543, 1970.
258. KEIL, K., M. PRINZ, and T. E. BUNCH. Mineral chemistry of lunar samples. *Science* 167:597-599, 1970.
259. KELLER, B. Problems of the late Precambrian. *Priroda* (Moscow) (9):30-38, 1959.
260. KELLOGG, H. H., and S. K. BASU. Thermodynamic properties of the system lead-sulfur-oxygen to 1100°K. *Am. Inst. Min. Met. Eng. Trans.* 218:70-81, 1960.
261. KENYON, D., and G. D. STEINMAN. *Biochemical Predestination*. New York, McGraw-Hill, 1969.
262. KEOSIAN, J. *The Origin of Life*. New York, Reinhold, 1964.
263. KIMBALL, A. P., and J. ORO, Eds. *Prebiotic and Biochemical Evolution*. Amsterdam, North-Holland, 1971.
264. KLABUNOVSKIY, Ye. I. *Asimmetricheskiy Sintez* (Transl: *Asymmetrical Synthesis*). Moscow, Goskhimizdat, 1960.
265. KLABUNOVSKIY, Ye. I. The origin of optically active compounds in nature. *Usp. Sovrem. Biol.* (Moscow) 55:378-390, 1963.
266. KLABUNOVSKIY, Ye. I. *Stereospetsklicheskiy Kataliz* (Transl: *Stereospecific Catalysis*). Moscow, Nauka, 1968.
267. KLORE, A., D. L. CAIN, and G. S. LEVY. Radio occultation measurement of the Martian atmosphere over two regions by the Mariner IV space probe. In, Dollfus, A. Ed. *Moon and Planets; A Session of the Seventh International Space Science Symposium*, Vienna, May 1966, pp. 226-239. Amsterdam, North-Holland, 1967.
268. KLORE, A., D. L. CAIN, G. S. LEVY, V. R. ESHLEMAN, G. FJELDBO, and F. D. DRAKE. Occultation experiment: results of first direct measurement of man's atmosphere and ionosphere. *Science* 149:1243-1248, 1965.
269. KLORE, A. J., G. FJELDBO, and B. L. SEIDEL. Summary of Mariner 6 and 7 radio occultation results on the atmosphere of Mars. In, Kondratyev, K. Ya., M. J. Rycroft, and C. Sagan, Eds. *Space Research XI* (COSPAR), Leningrad, May 1970, pp. 165-175. Berlin, Akademie, 1971.
270. KLORE, A., G. FJELDBO, B. SEIDEL, and S. I. RASOOL. S-band occultation. In, *Mariner-Mars 1969, A Preliminary Report*, pp. 111-126. Washington, NASA, 1969. (NASA SP-225)
271. KLASS, R., and C. N. MATTHEWS. Hydrogen cyanide dimer and chemical evolution. *Proc. Nat. Acad. Sci.* 48:1300-1306, 1962.
272. KLÜBER, H. von. *Das Vorkommen der chemischen Elemente im Kosmos* (Transl: *The Predecessor of Chemical Elements in the Cosmos*). Leipzig, Barth, 1931.
273. KNAAP, H. F., C. J. N. VAN DEN MEIJKENBERG, J. J. M. BEENAKKER, and H. C. VAN DE HULST. Formation of

- molecular hydrogen in interstellar space. *Bull. Astron. Inst. Neth.* 18:256–258, 1966. See also: Molecular H found using camera developed by Dr. George K. Carruthers, NRL physicist, and Harry Merchant. *Chem. Eng. News* 48(25):12, 1970.
274. KOLOMIYCHENKO, M. A. The photochemical synthesis of amino acids. *Ukr. Biokhim. Zh.* 36:216–225, 1964.
275. KORNBERG, A. *Enzymatic Synthesis of DNA*, pp. 69–103. New York, Wiley, 1962.
276. KOTEL'NIKOV, V. A., V. M. DUBROVEIN, M. D. KISLIK, E. B. KORENBERG, V. P. MINASHIN, V. A. MOROZOV, N. J. NIKITOKII, G. M. PETROV, O. N. RZHIGA, and A. M. SHAKHOVSKOI. *Radio Location of the Planet Venus in April 1961 in the Soviet Union*. Moscow, Akad. Nauk SSSR, 1961. (Rep.)
277. KRAMPITZ, G., S. DIEHL, and T. NAKASHIMA. Amino-transferase activity of polyanhydro- $\alpha$ -amino acids (proteinoids). *Chem. Abstr.* Dec. 1967; *Naturwissenschaften* 54:516–517, 1967.
278. KRASNOVSKIY, A. A. Development of a method in the action of a photocatalytic system of organisms. In, Oparin, A. I., Ed. *Vozniknoveniye Zhizni na Zemle* (Transl: *Origin of Life on Earth*), pp. 351–362. Moscow, Akad. Nauk SSSR, 1957.
279. KRASNOVSKIY, A. A. The evolution of photochemical electron transfer systems. In, Kimball, A. P., and J. Oró, Eds. *Prebiotic and Biochemical Evolution*, pp. 209–216. Amsterdam, North-Holland, 1971.
280. KRASNOVSKIY, A. A., and A. V. UMRIKHINA. Abiogenic formation of porphin and its participation in processes of photochemical electron transfer. *Dokl. Akad. Nauk SSSR* (Moscow) 155:691–693, 1964.
281. KREBS, H. A., and H. KORNBERG. *Energy Transformations in Living Matter*. Berlin, Springer, 1957.
282. KREPS, Ye. M. Conference on evolutionary biochemistry in Liège; report of Prof. B. Pullman (Paris), "Electron factors and biochemical evolution." *Zh. Evol. Biokhim. Fiziol.* (Leningrad) 7(1):110–117, 1971.
283. KROPOTKIN, P. N., and K. SHAKHVARSTOVA. Solid bitumens, petroleum and hot gases in intrusions of hyperbasites in traps and volcanic cores. In, *Problemy Migratsii Nefti i Formirovaniye Neftyanykh i Gazovykh Skopleniy* (Transl: *Problems of the Migration of Petroleum and Formation of Petroleum and Gas Accumulation*), pp. 151–164. Moscow, Gostoptekhizdat, 1959.
284. KUDRYAVTSEV, N. A. Petroleum, gas and some bitumens injected in metamorphic rock. In, *Trudy Vsesoyuznogo Neftyanogo Geologo-Razvedyvatel'nogo Instituta (VNUGRI)*, No. 142. Leningrad, Nedra, 1959.
285. KUDRYAVTSEV, N. A. Present state of the problem of the genesis of petroleum in 1966. In, *Genezis Nefti i Gaza* (Transl: *Genesis of Petroleum and Gas*), pp. 262–291. Moscow, Nedra, 1967.
286. KUDRYAVTSEV, N. A. Petroleum as an abiogenic substance. *Priroda* (Moscow) (3):70–72, 1971.
287. KUHN, W., and E. BRAUN. Photochemical preparation of optically active substances. *Naturwissenschaften* 17:227–228, 1929.
288. KUIPER, G. P. New absorptions in the Uranus atmosphere. *Astrophys. J.* 109:540–541, 1949.
289. KUIPER, G. P. On the origin of the solar system. In, Hynek, J. A., Ed. *Astrophysics, A Topical Symposium*, pp. 357–424. New York, McGraw-Hill, 1951.
290. KUIPER, G. P. Planetary atmospheres and their origin. In, Kuiper, G. P., Ed. *The Atmospheres of the Earth and Planets*, 2nd ed., pp. 306–405. Chicago, Univ. Chic. Press, 1952.
291. KUIPER, G. P. Comets and the dissipation of the solar nebula. 4th Int. Colloq. Astrophys., Sept. 1952, Liège. *Mem. Soc. Roy. Sci. (Liège)*, Ser. 4 (*Physics of Comets*) 13(1–2):401–425, 1953.
292. KULAEV, I. S. Inorganic polyphosphates in evolution of phosphorus metabolism. In, Buvet, R., and C. Ponnamperuma, Eds. *Chemical Evolution and the Origin of Life*, Vol. 1, pp. 458–465. New York, Am. Elsevier, 1971.
293. KVASHA, L. G. Carbonaceous chondrites. In, Masevich, A. G., Ed. *Vozniknoveniye Zhizni vo Vselennoy* (Transl: *Origin of Life in the Universe*), pp. 44–55. Moscow, Akad. Nauk SSSR, 1963.
294. KVENVOLDEN, K. A. Analyses of lunar samples for carbon compounds. In, Schwartz, A. W., Ed. *Theory and Experiment In Exobiology*, Vol. 1, pp. 105–121. Groningen, Neth., Wolters-Noordhoff, 1971.
295. KVENVOLDEN, K. A., S. CHANG, J. W. SMITH, J. FLORES, K. PERING, C. SAXINGER, F. WOELLER, K. KEIL, I. BREGER, and C. PONNAMPERUMA. Carbon compounds in lunar fines from Mare Tranquillitatis. I. Search for molecules of biological significance. In, Levinson, A. A., Ed. *Proceedings, Apollo 11 Lunar Science Conference*, Houston, Tex., Jan. 1970, Vol. 2, pp. 1813–1828. New York, Pergamon, 1970. Also in, *Geochim. Cosmochim. Acta*, Suppl. 1.
296. KVENVOLDEN, K., J. LAWLESS, K. PERING, E. PETERSON, J. FLORES, C. PONNAMPERUMA, I. R. KAPLAN, and C. MOORE. Evidence for extraterrestrial amino acids and hydrocarbons in the Murchison meteorite. *Nature* 228:923–926, 1970.
297. KVENVOLDEN, K. A., J. G. LAWLESS, and C. PONNAMPERUMA. Nonprotein amino acids in the Murchison meteorite. *Proc. Nat. Acad. Sci.* 68:486–490, 1971.
298. KVENVOLDEN, K. A., E. PETERSON, and G. E. POLLOCK. Optical configuration of amino acids in Precambrian Fig Tree chert. *Nature* 221:141–143, 1969.
299. LANCET, M. S., and E. ANDERS. Carbon isotope fractionation in the Fischer-Tropsch synthesis and in meteorites. *Science* 170:980–982, 1970.
300. LANGENBECK, W. *Die Organischen Katalysatoren und ihre Beziehungen zu den Fermenten* (Transl: *The Organic Catalysts and Their Relationships to Enzymes*), 2nd ed. Berlin, Springer, 1949.
301. LANGENBECK, W. Chemistry of organic catalysis. In, Nord, F. F., Ed. *Advances in Enzymology*, Vol. 14, pp. 163–192. New York, Interscience, 1953. (Ger.)

302. LATIMER, W. M. Astrochemical problems in the formation of the Earth. *Science* 112:101–104, 1950.
303. LAWDEN, D. F. Chemical evolution and the origin of life. *Nature* 202:412, 1964.
304. LEIGHTON, R. B., N. H. HOROWITZ, B. C. MURRAY, R. P. SHARP, A. H. HERRIMAN, A. T. YOUNG, B. A. SMITH, M. E. DAVIES, and C. B. LEOVY. Mariner 6 and 7 television pictures: preliminary analysis. *Science* 166:49–67, 1969.
305. LEMMON, R. M. Abiogenic synthesis of biologically-relevant organic compounds. In, Calvin, M., Ed. *Chemical Evolution; Molecular Evolution Towards the Origin of Living Systems on the Earth and Elsewhere*, p. 8. New York, Oxford Univ. Pr., 1969.
306. LEPP, H., and S. S. GOLDICH. Chemistry and origin of iron formations. *Geol. Soc. Am. Bull.* 70:1637, 1959.
307. LEVIN, B. J. Origin of the solar system. *New Sci.* 13 (Feb. 8):323–325, 1962.
308. LEVIN, B. Yu. Development of the Moon in the light of current data. *Priroda* (Moscow) (12):2–9, 1971.
309. LEVIN, B. Yu. and S. V. MAYEVA. On the thermal history of the Earth. *Izv. Akad. Nauk SSSR, Ser. Geofiz.* (Moscow) (2):243–252, 1960.
310. LEWIS, J. S., and R. G. PRINN. Chemistry and photochemistry of the atmosphere of Jupiter. In, Schwartz, A. W., Ed. *Theory and Experiment in Exobiology*, Vol. I, pp. 123–142. Groningen, Neth., Wolters-Noordhoff, 1971.
311. LIEBL, V., I. CHALOUPKA, and I. MALEK. Study of proteolysis of complex coacervates and flocculates. In, Kretovich, V. L., Ed. *Problemy Evolyutsionnoy i Tekhnicheskoy Biokhimii* (Transl: *Problems of Evolutionary and Technical Biochemistry*), pp. 131–146. Moscow, Nauka, 1964.
312. LIEBL, V., and J. SIEBLOVA. Coacervate systems and life. *J. Br. Interplanet. Soc.* 21:295–312, 1968.
313. LILLER, W. The nature of the grains in the tails of comets 1956 h and 1957 d. *Astrophys. J.* 132:867–882, 1960.
314. LIPMANN, F. Gramicidin S and tyrocidine biosynthesis: a primitive process of sequential addition of amino acids on polyenzymes. In, Buvet, R., and C. Ponnamperuma, Eds. *Chemical Evolution and the Origin of Life*, Vol. 1, pp. 381–383. New York, Am. Elsevier, 1971.
315. LIPMANN, F. Aspects of the evolution of polypeptide synthesis. In, *Origin of Life and Evolutionary Biochemistry*, pp. 27–30. Presented at Int. Symp., Varna, Bulg., 1971. (Abstr.)
316. LOWE, C. U., M. REES, and R. MARKHAM. Synthesis of complex organic compounds from simple precursors: formation of amino acids, amino acid polymers, fatty acids and purines from ammonium cyanide. *Nature* 199(4890):219–222, 1963.
317. MACGREGOR, A. M. A Precambrian algal limestone in Southern Rhodesia. *Trans. Geol. Soc. S. Afr.* 43:9–15, 1940.
318. MACLEOD, W. D., Jr. Combined gas chromatography–mass spectrometry of complex hydrocarbon trace residues in sediments. *J. Gas Chromatogr.* 6:591–594, 1968.
319. MACOVSKI, E. Living matter and its origin. *Rev. Chim. (Roumania)* 4:11–20, 1959.
320. MAMIKUNIAN, G., and M. BRIGGS, Eds. *Current Aspects of Exobiology*. New York, Pergamon, 1965.
321. MARGULIS, L. Microbial evolution on the early Earth. In, Buvet, R., and C. Ponnamperuma, Eds. *Chemical Evolution and the Origin of Life*, Vol. 1, pp. 480–484. New York, Am. Elsevier, 1971.
322. MARGULIS, L. Early cellular evolution. In, Ponnamperuma, C., Ed. *Exobiology, Frontiers of Biology*, Vol. 23, pp. 342–368. New York, Am. Elsevier, 1972.
323. MARIANI, E., and G. TORRACA. The composition of formose. A chromatographic study. *Int. Sugar J.* 55:309–311, 1953.
324. MARKHININ, Ye. K. *Rol'vulkanizma v Formirovani Zemonoy Kory* (Transl: *The Role of Vulcanism in the Formation of the Earth's Crust*). Moscow, Nauka, 1967.
325. MARKINA, Z. N., A. V. CHINNIKOVA, and P. A. REBINDER. *Fiziko-Khimicheskaya Mekhanika Dispersnykh Struktur* (Transl: *Physical-Chemical Mechanics of Dispersed Structures*). Moscow, Nauka, 1966.
326. MAROV, M. Ya. Some results of and prospects for physics studies of space. *Priroda* (Moscow) (4):18–34, 1971.
327. MARTYNOV, D. Ya. Venus—the physical nature of the planet. *Vestn.-Mosk. Univ., Ser. 3 (Fiz. Astron.)* (5):23–38, 1961.
328. MARTYNOV, D. Ya. Recent data on the physical conditions on Earth-type planets. In, Masevich, A. G., Ed. *Voznikoveniye Zhizni vo Vselennoy* (Transl: *The Origin of Life in the Universe*), pp. 56–76. Moscow, Akad. Nauk SSSR, 1963.
329. MARTYNOV, D. Ya. *Kurs Obshchey Astrofiziki* (Transl: *A Course in General Astrophysics*). Moscow, Fizmatgiz, 1965.
330. MASON, B. H. *Principles of Geochemistry*, 2nd ed. New York, Wiley, 1958.
331. MASON, B. H. The origin of meteorites. *J. Geophys. Res.* 65:2965–2970, 1960.
332. MASON, B. H. Carbonaceous chondrites. *Space Sci. Rev.* 1:621–646, 1963.
333. MASON, B. H. *Principles of Geochemistry*, 3rd ed. New York, Wiley, 1966.
334. MATTHEWS, C. N., and R. MOSER. Prebiological protein synthesis. *Proc. Nat. Acad. Sci.* 56(4):1087–1094, 1966.
335. MATTHEWS, C. N., and R. MOSER. Peptide synthesis from hydrogen cyanide and water. *Nature* 215(5107): 1230–1234, 1967.
336. McCARTHY, E., and M. CALVIN. Organic geochemical studies. I. The molecular criteria for hydrocarbon genesis. *Nature* 216:642–647, 1967.
337. MCCORD, T. B., and J. ADAMS. Spectral reflectivity of

- Mars. *Science* 163:1058–1060, 1969.
338. MICHaux, C. M. *Handbook of the Physical Properties of the Planet Jupiter*. Washington, NASA, 1967. (NASA SP-3031)
339. MILLER, S. L. A production of amino acids under possible primitive Earth conditions. *Science* 117:528–529, 1953.
340. MILLER, S. L. Production of some organic compounds under possible primitive Earth conditions. *J. Am. Chem. Soc.* 77:2351–2361, 1955.
341. MILLER, S. L. The formation of organic compounds on the primitive Earth. *Ann. NY Acad. Sci.* 69:260–275, 1957.
342. MILLER, S. L. Occurrence of gas hydrates in the solar system. *Proc. Nat. Acad. Sci.* 47:1798–1808, 1961.
343. MILLER, S. L., and M. PARRIS. Synthesis of pyrophosphate under primitive Earth conditions. *Nature* 204:1248–1250, 1969.
344. MILLER, S. L., and M. PARRIS. Synthesis of pyrophosphate under primitive Earth conditions. In, Kimball, A. P., and J. Oró, Eds. *Prebiotic and Biochemical Evolution*, pp. 83–88. Amsterdam, North-Holland, 1971.
345. MILLER, S. L., and H. C. UREY. Organic compound synthesis on the primitive Earth. *Science* 130:245–251, 1959.
346. MILLER, S., and H. C. UREY. Extraterrestrial sources of organic compounds in the origin of life. In, Kretovich, V. L. Ed. *Problemy Evolyutsionnoy i Tekhnika Biokhimii* (Transl: *Problems of Evolutionary and Engineering Biochemistry*), p. 357. Moscow, Nauka, 1964.
347. MONOD, J. Les frontières de la biologie. *Recherche* (Paris) (5):415–422, 1970.
348. MONOD, J. *Chance and Necessity*. Paris, Seuil, 1970. New York, Knopf, 1971.
349. MOORE, J. H. Spectroscopic observations of the rotation of Saturn. *Publ. Astron. Soc. Pac.* 51:274–281, 1939.
350. MOORE, C. B., C. F. LEWIS, E. K. GIBSON, and W. NICHIPORUK. Total carbon and nitrogen abundances in lunar samples. *Science* 167:495–497, 1970.
351. MORA, P. T. The folly of probability. In, Fox, S. W., Ed. *The Origins of Prebiological Systems and of Their Molecular Matrices*, pp. 39–64. New York, Academic, 1965.
352. MORAVEK, J. Formation of oligonucleotides during heating of a mixture of uridine-2'-(3') phosphate and uridine. *Tetrahedron Lett.* (18):1707–1710, 1967.
353. MOROWITZ, H. J. An energetic approach to pre-biological chemistry. In, Buvet, R., and C. Ponnamperuma, Eds. *Chemical Evolution and the Origin of Life*, Vol. 1, pp. 37–41. New York, Am. Elsevier, 1971.
354. MOROWITZ, H., and C. SAGAN. Life in the clouds of Venus? *Nature* 215:1259–1260, 1967.
355. MOROZ, V., and D. KRYUYKSHEK. *Astron. Zh.* (In press)
356. MUELLER, G. Carbonaceous meteorites and the origin of life. In, Bernal, J. D. *The Origin of Life*, pp. 255–279. London, Weidenfeld and Nicolson, 1967.
357. MUNDAY, C., K. PERING, and C. PONNAMPERUMA. Synthesis of acyclic isoprenoids by the  $\gamma$ -irradiation of isoprene. *Nature* 223:867–868, 1969.
358. NAGY, B., C. M. DREW, P. B. HAMILTON, V. E. MODZELESKI, M. E. MURPHY, W. M. SCOTT, H. C. UREY, and M. YOUNG. Organic compounds in lunar samples: pyrolysis products, hydrocarbons, amino acids. *Science* 167:770–772, 1970.
359. NAGY, B., W. G. MEINSCHEIN, and D. J. HENNESSY. Review of earlier work on carbonaceous material and organized elements in meteorites. *Science* 150:380, 1965.
360. NAGY, B., and H. C. UREY. Organic geochemical investigations in relation to the analysis of returned lunar rock samples. In, Vishniac, W., and F. G. Favorite, Eds. *Life Sciences and Space Research*, Vol. 7, pp. 31–46. New York, Wiley, 1969.
361. NEUGEBAUER, G., G. MUENCH, S. CHASE, Jr., H. HATZENBEKER, E. MINER, and D. SCHOFIELD. Infrared radiometry. In, *Mariner-Mars, 1969: A Preliminary Report*, pp. 105–109. Washington, NASA, 1969. (NASA SP-225)
362. NICHOLSON, I. Chemical evolution of protein sequence. *J. Macromol. Sci. Chem.* 4(7):1619–1625, 1970.
363. NICOLAYSEN, L. O. Stratigraphic interpretation of age measurements in southern Africa. In, Engel, A. E. J., H. L. James, and B. F. Leonard, Eds. *Petrologic Studies: A Volume in Honor of A. F. Buddington*, pp. 569–598. New York, Geol. Soc. Am., 1962.
364. NISKANEN, R. A., T. Ye. PAVLOVSKAYA, T. A. TELEGINA, V. S. SIDOROV, and V. A. SHARPATY. The mechanisms of photochemical synthesis of amino acids under ultraviolet irradiation on formaldehyde and ammonia salt solutions. *Izv. Akad. Nauk SSSR, Ser. Biol.* 2:238–245, 1971.
365. NOONER, D. W., and J. ORÓ. Organic compounds in meteorites. I. Aliphatic hydrocarbons. *Geochim. Cosmochim. Acta* 31(9):1359–1394, 1967.
366. OLSON, R. J., J. ORÓ, and A. ZLATKIS. Organic compounds in meteorites. II. Aromatic hydrocarbons. *Geochim. Cosmochim. Acta* 31(10):1935–1948, 1967.
367. OPARIN, A. I. *The Origin of Life*. New York, Macmillan, 1938.
368. OPARIN, A. I. *Vozniknoveniye Zhizni na Zemle*, 3rd ed. Moscow, Akad. Nauk SSSR, 1957. (Transl: *The Origin of Life on the Earth*). New York, Academic, 1957.
369. OPARIN, A. I. *Life: Its Nature, Origin and Development*. New York, Academic, 1961.
370. OPARIN, A. I., and K. B. SEREBROVSKAYA. The formation of coacervate droplets in the synthesis of polyadenylic acid by polynucleotide phosphorylase. *Dokl. Akad. Nauk. SSSR* (Moscow) 148:943–944, 1963.
371. OPARIN, A. I. *The Chemical Origin of Life*. Springfield, Ill., C. C. Thomas, 1964.
372. OPARIN, A. I. The origin of life and the origin of enzymes. In, Nord, F. F., Ed. *Advances in Enzymology*, Vol. 27, pp. 347–380. New York, Interscience, 1965.
373. OPARIN, A. I., Ed. *Proiskhozhdeniye Predbiologicheskikh*

- Sistem* (Transl: *The Origin of Prebiological Systems*). Moscow, Mir, 1966.
374. OPARIN, A. I. *Vosniknoveniye i Nachal'noye Razvitiye Zhizni* (Transl: *The Origin and Beginning Development of Life*). Moscow, Meditsina, 1966.
375. OPARIN, A. I. *Genesis and Evolutionary Development of Life*. New York, Academic, 1968.
376. OPARIN, A. I. *Zhizn', yeye Priroda, Proiskhozhdeniye i Razvitiye* (Transl: *Life, Its Nature, Origin and Development*), 2nd ed. Moscow, Nauka, 1968.
377. OPARIN, A. I. Coacervate drops as models of prebiological systems. In, Kimball, A. P., and J. ORÓ, Eds. *Prebiotic and Biochemical Evolution*, pp. 1-7. Amsterdam, North-Holland, 1971.
378. OPARIN, A. I. Modern aspects of the problem of the origin of life. *Scientia* (Milan), Ser. 7. 65(3-4):195-206, 1971.
379. OPARIN, A. I. Problem of the origin of life: present state and prospects. In, Buvet, R., and C. Ponnamperuma, Eds. *Chemical Evolution and the Origin of Life*, Vol. I, pp. 3-9. New York, Am. Elsevier, 1971.
380. OPARIN, A. I. Routes for the origin of the first forms of life. *Subcell. Biochem.* 1:75-81, 1971.
381. OPARIN, A. I., et al. *Vozniknoveniye Zhizni na Zemle, Trudy Mezhdunarodnogo Simpoziuma*, Moscow, 1957 (Transl: *The Origin of Life on Earth, Proceedings, First International Symposium*). New York, Pergamon, 1959.
382. OPARIN, A. I., K. B. SEREBROVSKAYA, and T. L. AUERMAN. The synthesis of polyadenylic acid in a coacervate. In, *Abstracts, 5th International Biochemical Congress*, Moscow, 1961, p. 78. Oxford, Pergamon, 1961. (Abstr. 3.77.459)
383. OPARIN, A. I., K. B. SEREBROVSKAYA, and S. A. PANTSCHAVA. Oxidation-reduction processes in coacervate drops: dehydrogenation of reduced diphenylphosphopyridine nucleotide (DPNH). *Dokl. Akad. Nauk SSSR* (Moscow) 151:234-236, 1963.
384. OPARIN, A. I., K. V. SEREBROVSKAYA, and N. V. VASIL'YEVA. Modelling of prebiological selection of supermolecular systems (coacervate drops). *Dokl. Akad. Nauk SSSR* (Moscow) 181:744-746, 1968.
385. OPARIN, A. I., K. B. SEREBROVSKAYA, N. V. VASIL'YEVA, and T. O. BALAYEVSKAYA. Formation of coacervates from polypeptides and polynucleotides. *Dokl. Akad. Nauk SSSR* (Moscow) 154(2):471-472, 1964.
386. OPARIN, A. I., I. G. STOYANOVA, K. B. SEREBROVSKAYA, and T. A. NEKRASOVA. Electronmicroscopic study of coacervates. *Dokl. Akad. Nauk SSSR* (Moscow) 150:684-685, 1963.
387. OPARIN, A. I., T. N. YEVREINOVA, T. I. LARIONOVA, and I. M. DAVYDOVA. Synthesis and decomposition of starch in coacervate drops. *Dokl. Akad. Nauk SSSR* (Moscow) 143:980-983, 1962.
388. ÖPIK, E. J. The aeosphere and atmosphere of Venus. *J. Geophys. Res.* 66:2807-2819, 1961.
389. ÖPIK, E. J. Jupiter: chemical composition, structure and origin of a giant planet. *Icarus* 1:200-257, 1962.
390. ORGEL, L. E. Evolution of the genetic apparatus. *J. Mol. Biol.* 38:381-393, 1968.
391. ORGEL, L. E., and J. E. SULSTON. Polynucleotide replication and the origin of life. In, Kimball, A. P., and J. ORÓ, Eds. *Prebiotic and Biochemical Evolution*, pp. 89-94. Amsterdam, North-Holland, 1971.
392. ORÓ, J. Synthesis of adenine from ammonium cyanide. *Biochem. Biophys. Res. Comm.* 2:407-412, 1960.
393. ORÓ, J. Comets and formation of biochemical compounds on the primitive Earth. *Nature* 190(4774):389-390, 1961.
394. ORÓ, J. Experimental organic cosmochemistry: the formation of biochemical compounds. In, Fallone, E. M., Ed. *Proceedings, Lunar and Planetary Exploration Colloquium*, Santa Monica, Calif., May 1962, Vol. 3, No. 2, pp. 9-28. Downey, Calif., North Am. Aviat., 1963. (Pub. 513-W-12)
395. ORÓ, J. Studies in experimental organic cosmochemistry. *Ann. NY Acad. Sci.* 109:464-481, 1963.
396. ORÓ, J. Synthesis of organic compounds by electric discharges. *Nature* 197(4870):862-867, 1963.
397. ORÓ, J. Stages and mechanisms of prebiological organic synthesis. In, Fox, S. W., Ed. *The Origins of Prebiological Systems and of Their Molecular Matrices*, pp. 137-171. New York, Academic, 1965.
398. ORÓ, J. Organic matter in meteorites. In, Ponnamperuma, C., Ed. *Exobiology, Frontiers of Biology*, Vol. 23, p. 446. New York, Am. Elsevier, 1972.
399. ORÓ, J., and A. C. COX. Non-enzymatic synthesis of 2-deoxyribose. *Proc. Fed. Am. Soc. Exp. Biol.* 21:80, 1962.
400. ORÓ, J., and E. GELPI. Gas-chromatographic mass-spectrometric studies on the isoprenoids and other isomeric alkanes in meteorites. In, Millmann, P. M., Ed. *Meteorite Research: Symposium on Meteorite Research*, Vienna, 1968, pp. 518-523. Dordrecht, Reidel, 1969.
401. ORÓ, J., and C. L. GUIDRY. Direct synthesis of polypeptides. I. Polycondensation of glycine in aqueous ammonia. *Arch. Biochem. Biophys.* 93:166-171, 1961.
402. ORÓ, J., and A. P. KIMBALL. Synthesis of purines under possible primitive Earth conditions. I: Adenine from hydrogen cyanide. *Arch. Biochem. Biophys.* 94:217-227, 1961.
403. ORÓ, J., and A. P. KIMBALL. Synthesis of purines under possible primitive Earth conditions. II: Purine intermediates from hydrogen cyanide. *Arch. Biochem. Biophys.* 96:293-313, 1962.
404. ORÓ, J., A. P. KIMBALL, R. FRITZ, and F. MASTER. Amino acid synthesis from formaldehyde and hydroxylamine. *Arch. Biochem. Biophys.* 85(1):115-130, 1959.
405. ORÓ, J., and D. W. NOONER. Aliphatic hydrocarbons in Precambrian rocks. *Nature* 213:1082-1085, 1967.
406. ORÓ, J., D. W. NOONER, and A. ZLATKIS. Hydrocarbons of biological origin in sediments about two billion years old. *Science* 148:77-79, 1965.
407. ORÓ, J., D. W. NOONER, A. ZLATKIS, and S. A. WIK-

- STRÖM. Paraffinic hydrocarbons in the Orgueil, Murray, Mokoia and other meteorites. In, Brown, A. H., and M. Florkin, Eds. *Life Sciences and Space Research*, Vol. 4, pp. 63–100. Washington, D.C., Spartan; London, Macmillan, 1966.
408. ORO, J., W. S. UPDEGROVE, J. GILBERT, J. McREYNOLDS, E. GIL-AV, J. IBANEZ, A. ZLATKIS, D. A. FLORY, R. L. LEVY, and C. WOLF. Organogenic elements and compounds in surface samples from the Sea of Tranquility. *Science* 167:765–767, 1970.
409. OWEN, T., and H. MASON. Mars: water vapor in its atmosphere. *Science* 165:893–895, 1969.
410. PALM, C., and M. CALVIN. Primordial organic chemistry. I. Compounds resulting from electron irradiation of  $C^{14}H_4$ . *J. Am. Chem. Soc.* 84(11):2115–2121, 1962.
411. PALMER, P., B. ZUCKERMAN, D. BUHL, and L. E. SNYDER. Formaldehyde absorption in dark nebulae. *Astrophys. J.* 156:L147–L150, 1969.
412. PANTSCHAVA, E. Some information on the possibility of preglycolytic ways in evolution. In, Buvet, R., and C. Ponnamperuma, Eds. *Chemical Evolution and the Origin of Life*, Vol. 1, pp. 475–479. New York, Am. Elsevier, 1971.
413. PAPAHADJOPoulos, D., and N. MILLER. Phospholipid model membranes. I. Structure characteristics of hydrated liquid crystals. *Biochim. Biophys. Acta* 135:624–638, 1967.
414. PAPAHADJOPoulos, D., and J. C. ATKINS. Phospholipid model membranes. II. Permeability properties of hydrated liquid crystals. *Biochim. Biophys. Acta* 135:639–652, 1967.
415. PASCHKE, R., R. W. H. CHANG, and D. YOUNG. Probable role of gamma irradiation in origin of life. *Science* 125:881, 1957.
416. PASYNSKIY, A. G. The theory of open systems and its importance for biology. *Usp. Sovrem. Biol.* 43:263–279, 1957.
417. PASYNSKIY, A. G. Enzymatic reaction in steady open systems. In, *Proceedings, Symposium on Enzyme Chemistry*, pp. 350–355. Tokyo, Maruzen, 1958. (I.U.B. Symp. Ser. V.2)
418. PASYNSKIY, A. G. *Kolloidnaya Khimiya* (Transl: *Colloidal Chemistry*). Moscow, Vysshaya Shkola, 1959.
419. PASYNSKIY, A. G. *Biofizicheskaya Khimiya* (Transl: *Biophysical Chemistry*), 2nd ed. Moscow, Vysshaya Shkola, 1968.
420. PASYNSKIY, A. G., and V. P. BLOKHINA. Fermentative oxidation of ascorbic acid under conditions of open systems. *Biokhimiya* 21:826–833, 1956.
421. PASYNSKIY, A. G., and T. Ye. PAVLOVSKAYA. Formation of the biologically important compounds in the prebiological stage of Earth formation. *Usp. Khim.* 33: 1198–1215, 1964.
422. PASYNSKIY, A. G., and V. P. SLOBODSKAYA. Dynamic stability of enzymic coacervates in substrate solutions. *Dokl. Akad. Nauk SSSR* 153:473–476, 1963.
423. PATTEE, H. Experimental approaches to the origin of life problem. In, Nord, F., Ed. *Advances in Enzymology*, Vol. 27, pp. 381–415. New York, Interscience, 1965.
424. PAVLOVSKAYA, T. E., and A. G. PASYNSKIY. The original formation of amino acids under the action of ultraviolet rays and electric discharges. In, Oparin, A. I., et al, Eds. *Vosnikoveniye Zhizni na Zemle, Trudy Mezhdunarodnogo Simpoziuma*, Moscow, 1957 (Transl: *The Origin of Life on Earth, Proceedings, First International Symposium*), pp. 151–157. New York, Pergamon, 1959.
425. PAVLOVSKAYA, T. E., and A. G. PASYNSKIY. The primary formation of amino acids in ultraviolet rays and electrical discharge. In, Oparin, A. I., et al, Eds. *Vosnikoveniye Zhizni na Zemle, Trudy Mezhdunarodnogo Simpoziuma*, Moscow, 1957 (Transl: *The Origin of Life on Earth, Proceedings, First International Symposium*), pp. 161–167. New York, Pergamon, 1959.
426. PAVLOVSKAYA, T. E., A. G. PASYNSKIY, and A. GRABENNIKOVA. Formation of amino acids by the action of ultraviolet light on solutions of formaldehyde and ammonium salts in the presence of adsorbants. *Dokl. Akad. Nauk SSSR* (Moscow) 135:743–746, 1960.
427. PAVLOVSKAYA, T. E., A. G. PASYNSKIY, V. SIDOROV, and A. LADYZHENSKAYA. Prebiological synthesis of biochemically important compounds. In, Oparin, A. I., Ed. *Abiogenez i Nachal'nye Stadii Evolyutsii Zhizni* (Transl: *Abiogenesis and the Initial Stages of the Evolution of Life*), pp. 41–48. Moscow, Nauka, 1968.
428. PETERSIL'YE, I. A. *Geologiya i Geokhmiya Prirodnnykh Gazov i Dispersnykh Bitumov Nekotorykh Geologicheskikh Formatsiy Kol'skogo Poluoastrova* (Transl: *Geology and Geochemistry of Natural Gases and Dispersed Bitumens of Certain Geological Formations of Kola Peninsula*). Leningrad, Nauka, 1964.
429. PETERSIL'YE, I. A., M. A. PAVLOVA, V. T. MALASHKINA, and M. D. PETERSIL'YE. Organic matter in ejected and metamorphic rocks. In, *Genezis Nefti i Gaza* (Transl: *Genesis of Petroleum and Gas*), pp. 342–350. Moscow, Nedra, 1967.
430. PETROV, G., and V. MOROZ. Observatory study of the "red" planet. *Pravda*, Dec. 26, 1971.
431. PETTENGILL, G. H. Radar measurements of Venus. In, Priester, W., Ed. *Space Research III; Proceedings, 3d International Space Science Symposium*, Washington, D.C., 1962, pp. 872–885. New York, Wiley, 1963.
432. PFLUG, H. D., W. MEINEL, K. NEUMANN, and M. MEINEL. Entwicklungstendenz des Frühen Lebens auf der Erde (Transl: Development of early life on the Earth). *Naturwissenschaften* 56:10–14, 1969.
433. PLASKETT, J. S. The spectroscopic binary  $\theta^2$  Tauri. *Pub. Dom. Astron. Obs. Ottawa* 2(2):63–85, 1915.
434. PLOOSTER, M. N., and T. B. REED. Carbon-hydrogen-acetylene equilibrium at high temperatures. *J. Chem. Phys.* 31:66–72, 1950.
435. POGLAZOV, B. F. *Sborka Biologicheskikh Struktur* (Transl: *Assembly of Biological Structures*). Moscow, Nauka, 1970.

436. PONNAMPERUMA, C. Abiological synthesis of some nucleic acid constituents. In, Fox, S. W., Ed. *The Origins of Prebiological Systems and of Their Molecular Matrices*, pp. 221-242. New York, Academic, 1965.
437. PONNAMPERUMA, C. Some recent work on prebiological synthesis of organic compounds. *Icarus* 5:450-454, 1966.
438. PONNAMPERUMA, C., Ed. *Exobiology, Frontiers of Biology*, Vol. 23. New York, Am. Elsevier, 1972.
439. PONNAMPERUMA, C., and S. CHANG. The role of phosphates in chemical evolution. In, Buvet, R., and C. Ponnamperuma, Eds. *Chemical Evolution and the Origin of Life*, Vol. 1, pp. 216-223. New York, Am. Elsevier, 1971.
440. PONNAMPERUMA, C., and N. GABEL. Current status of chemical studies on the origin of life. In, *Space Life Sciences*, Vol. 1, pp. 64-96. Dordrecht, Holl., Reidel, 1968.
441. PONNAMPERUMA, C., and P. KIRK. Synthesis of deoxyadenosine under simulated primitive Earth conditions. *Nature* 203:400-401, 1964.
442. PONNAMPERUMA, C., and H. P. KLEIN. The coming search for life on Mars. *Q. Rev. Biol.* 45(3):235-258, 1970.
443. PONNAMPERUMA, C., R. LEMMON, R. MARINER, and M. CALVIN. Formation of adenine by electron irradiation of methane, ammonia and water. *Proc. Nat. Acad. Sci.* 49(5):737-740, 1963.
444. PONNAMPERUMA, C., and R. MACK. Nucleotide synthesis under possible primitive Earth conditions. *Science* 148:1221-1223, 1965.
445. PONNAMPERUMA, C., R. MARINER, and C. SAGAN. Formation of adenosine by ultraviolet irradiation of a solution of adenine and ribose. *Nature* 198:1199-1200, 1963.
446. PONNAMPERUMA, C., and K. L. PERING. Possible abiogenic origin of some naturally occurring hydrocarbons. *Nature* 209:979-982, 1966.
447. PONNAMPERUMA, C., and K. L. PERING. Aliphatic and alicyclic hydrocarbons isolated from Trinidad Lake Asphalt. *Geochim. Cosmochim. Acta* 31:1350-1354, 1967.
448. PONNAMPERUMA, C., and E. PETERSON. Peptide synthesis from amino acids in aqueous solution. *Science* 147:1572-1574, 1965.
449. PONNAMPERUMA, C., C. SAGAN, and R. MARINER. Synthesis of adenosine triphosphate under possible primitive Earth conditions. *Nature* 199(4890):222-226, 1963.
450. PONNAMPERUMA, C., and M. SWEENEY. The role of ionizing radiation in primordial organic synthesis. In, Schwartz, A. W., Ed. *Theory and Experiment In Exobiology*, Vol. I, pp. 1-40. Groningen, Neth., Wolters-Noordhoff, 1971.
451. PONNAMPERUMA, C., and F. WOELLER. Differences in the character of C<sub>6</sub> to C<sub>9</sub> hydrocarbons from gaseous methane in low-frequency electric discharges. *Nature* 203:272-274, 1964.
452. PONNAMPERUMA, C., and F. WOELLER.  $\alpha$ -aminonitriles formed by an electric discharge through a mixture of anhydrous methane and ammonia. *Curr. Mod. Biol.* 1:156-158, 1967.
453. PORFIR'YEV, V. B. On the nature of petroleum. In, *Problema Proiskhozhdeniya Nefti i Gaza v Usloviyakh Formirovaniya ikh Zalezhey* (Transl: *Problem of the Origin of Petroleum and Gas Under Conditions of the Formation of Their Beds*), p. 26. Moscow, Gostoptekhizdat, 1960.
454. PORFIR'YEV, V. B. Present state of the problem of petroleum formation. In, *Genesis Nefti i Gaza* (Transl: *Genesis of Petroleum and Gas*), pp. 292-314. Moscow, Nedra, 1967.
455. PRASHNOWSKY, A. A., and M. SCHIDLOWSKI. Investigations of Precambrian thucholite. *Nature* 216:560-563, 1967.
456. PRIGOGINE, I. *Introduction to Thermodynamics of Irreversible processes*. Springfield, Ill., C. C. Thomas, 1955.
457. PRIGOGINE, I. Problems of evolution in the thermodynamics of irreversible phenomena. In, Clark, F., and R. L. M. Syng, Eds. *The Origin of Life on the Earth*, pp. 418-427. New York, Pergamon, 1959.
458. PRIGOCINE, I., and A. BABLOYANZ. Coherent structures and thermodynamic stability. In, Buvet, R., and C. Ponnamperuma, Eds. *Chemical Evolution and the Origin of Life*, Vol. 1, pp. 29-36. New York, Am. Elsevier, 1971.
459. PULLMAN, A., and B. PULLMAN. Molecular orbitals and the processes of life. In, Löwdin, P. O., and B. Pullman, Eds. *Molecular Orbitals in Chemistry, Physics and Biology*, pp. 547-571. New York, Academic, 1964.
460. PULLMAN, B. Electronic factors in biochemical evolution. In, Schoffeniels, E. Ed. *Biochemical Evolution and the Origin of Life* (Proc. Int. Conf. Biochem. Evol., Liège, 1970), Vol. 2, pp. 1-2. Amsterdam, North-Holland, 1971. Also in, *Exobiology, Frontiers of Biology*, Vol. 23, pp. 136-139. New York, Am. Elsevier, 1972.
461. PULLMAN, B. Electronic factors in biochemical evolution. In, Ponnamperuma, C., Ed. *Exobiology, Frontiers of Biology*, Vol. 23, pp. 136-169. New York, Am. Elsevier, 1972.
462. PULLMAN, B., and A. PULLMAN. Electronic delocalization and biochemical evolution. *Nature* 196:1137-1142, 1962.
463. PULLMAN, B., and A. PULLMAN. *Quantum Biochemistry*. New York, Interscience, 1963.
464. PULLMAN, B., and A. PULLMAN. *Kvantovaya Biokhimiya* (Transl: *Quantum Biochemistry*). Moscow, Mir, 1965.
465. PURCELL, E. M. *Radioastronomy and Communication Through Space*. Long Island, N.Y., US Brookhaven Nat. Lab. Lect. No. 1, 1960. (BNL 658). Also in, *Lectures in Science. Vistas in Research*, Vol. 1,

- pp. 1-13. Long Island, N.Y., Brookhaven Nat. Lab., 1967.
466. RABINOWITZ, J., S. CHANG, and C. PONNAMPERUMA. Possible mechanisms for prebiotic phosphorylation. In, Kimball, A. P., and J. Oró, Eds. *Prebiotic and Biochemical Evolution*, pp. 70-77. Amsterdam, North-Holland, 1971.
467. RAMDOHR, P. The uranium-gold deposits of Witwatersrand, Blind River District, Dominion Reef, and Serra de Jacobina: ore microscopic investigation and geological comparison. *Abh. Deut. Wiss. Berl. Kl. Chem. Geol. Biol.* 3:1958. (Monogr.)
468. RANKAMA, K. Geologic evidence of chemical composition of the Precambrian atmosphere. *Geol. Soc. Am.* 62:651-664, 1955. (Spec. paper)
469. RASOOL, S. I. Planetary atmosphere. In, Ponnamperuma, C., Ed. *Exobiology, Frontiers of Biology*, Vol. 23, pp. 369-399. New York, Am. Elsevier, 1972.
470. RASOOL, S. I., J. S. HOGAN, R. W. STEWART, and L. H. RUSSEL. Temperature distribution in the lower atmosphere of Mars from Mariner 6 and 7 radio occultation data. *J. Atmos. Sci.* 27:841-843, 1970.
471. REBINDER, P. A. *Fiziko-Khimicheskaya Mekhanika* (Transl: *Physico-Chemical Mechanics*). Moscow, Znanii, 1958.
472. REID, C. The relation between primitive and present-day photobiological processes. In, Oparin, A. I., et al, Eds. *Vosnikoveniye Zhizni na Zemle, Trudy Mezhdunarodnogo Simpoziuma*, Moscow, 1957 (Transl: *The Origin of Life on Earth, Proceedings, First International Symposium*), pp. 619-625. New York, Pergamon, 1959.
473. REUTER, J. H. On the synthesis of peptides under primitive Earth conditions. In, Hobson, G. D., and G. C. Speers, Eds. *Advances in Organic Geochemistry; Proceedings, 3d International Congress on Organic Geochemistry*, London, 1966, pp. 539-545. New York, Pergamon, 1969. (Earth Sci. Ser., Monogr. 32)
474. RICH, A. On the problems of evolution and biochemical information transfer. In, Kasha, M., and B. Pullman, Eds. *Horizons in Biochemistry*, pp. 103-126. New York, Academic, 1962.
475. RICHTER, N. B. *Statistik und Physik der Kometen*. Leipzig, J. A. Barth, 1954. (Ger.)
476. RITCHIE, P. D. *Asymmetric Synthesis and Asymmetric Induction*. New York, Oxford Univ. Pr., 1933. (St. Andrews Univ. Pub. No. 36)
477. ROBINSON, R. The duplex origins of petroleum. In, Colombo, U., and G. D. Hobson, Eds. *Advances in Organic Geochemistry; Proceedings, International Meeting*, Milan, 1962, pp. 7-10. New York, Macmillan; Oxford, Eng., Pergamon, 1964. (Earth Sci. Ser., Monogr. 15)
478. ROBINSON, R. The origins of petroleum. *Nature* 212: 1291-1295, 1966.
479. ROBINSON, R. Origins of oil. A correction and further comment on the Brunnock even C-number pre-
- dominance in certain higher alkanes of African crudes and on the biogenesis of nonacosane. *Nature* 214:263, 1967.
480. ROHLFING, D. L., and S. W. FOX. Catalytic activities of thermal polyanhydro-d-amino acids. In, *Advances in Catalysis and Related Subjects*, Vol. 20, pp. 373-418. New York, Academic, 1969.
481. ROSE, W. K., J. M. BOLOGNA, and R. M. SLOANAKER. Linear polarization of the 3200 Mc/sec radiation from Saturn. *Phys. Rev. Lett.* 10:123-125, 1963.
482. RUBEY, W. W. Geological history of sea water. *Bull. Geol. Soc. Am.* 62:1111-1148, 1951.
483. RUBEY, W. W. Development of the hydrosphere and atmosphere, with special reference to the probable composition of the early atmosphere. *Geol. Soc. Am.* 62:631-650, 1955. (Spec. paper)
484. RUBEY, W. W. Geologic history of sea water. In, Brancazio, P. J., and A. G. W. Cameron, Eds. *The Origin and Evolution of Atmospheres and Oceans*, pp. 1-63. New York, Wiley, 1964.
485. RUSSELL, H. N. *The Solar System and Its Origin*. New York, Macmillan, 1935.
486. RUTTEN, M. G. *The Geological Aspects of the Origin of Life on Earth*. Amsterdam, Neth., Am. Elsevier, 1962.
487. RUTTEN, M. G. *The Origin of Life by Natural Causes*. Amsterdam, Neth., Am. Elsevier, 1971.
488. SAGAN, C. Exobiology—a critical review. In, Florkin, M., and A. Dollfus, Eds. *Life Sciences and Space Research*, Vol. 2, pp. 35-53. New York, Interscience, 1964.
489. SAGAN, C. The solar system as an abode of life. In, Pittendrigh, C. S., W. Vishniac, and J. P. T. Pearman, Eds. *Biology and the Exploration of Mars*, pp. 73-113. Washington, D.C., Nat. Acad. Sci., 1966. (Publ. 1296)
490. SAGAN, C. Life on the surface of Venus? *Nature* 216 (5121):1198-1199, 1967.
491. SAGAN, C., and J. B. POLLOCK. Windblown dust on Mars. *Nature* 223:791-794, 1969.
492. SALOP, L. I. *Pre-cambrian of USSR*. In, Hejtman, B., Ed. *Proceedings, 23d International Geological Congress*, Prague, 1968, Sect. 4, pp. 61-73. Prague, Academia, 1968.
493. SANCHEZ, R. A., J. P. FERRIS, and L. E. ORGEL. Conditions for purine synthesis: did prebiotic synthesis occur at low temperatures? *Science* 153:72-73, 1966.
494. SANCHEZ, R. A., J. P. FERRIS, and L. E. ORGEL. Cyanooctyne in prebiotic synthesis. *Science* 154(3750): 784-785, 1966.
495. SANCHEZ, R. A., J. P. FERRIS, and L. E. ORGEL. Studies in prebiotic synthesis. II. Synthesis of purine precursors and amino acids from aqueous hydrogen cyanide. *J. Mol. Biol.* 30(2):223-253, 1967.
496. SANCHEZ, R. A., J. P. FERRIS, and L. E. ORGEL. Studies in prebiotic synthesis. IV. Conversion of 4-amino-imidazole-5-carbonitrile-derivatives to purines. *J. Mol. Biol.* 38:121-128, 1968.
497. SANFORD, R. F. Carbon isotopes in class N stars. *Publ.*

- Astron. Soc. Pac.* 41:271–272, 1929.
498. SASLAW, W. C., and J. E. GAUSTAD. Interstellar dust and diamonds. *Nature* 221:160–162, 1969.
499. SASLAW, W. C., and R. L. WILDEY. On the chemistry of Jupiter's upper atmosphere. *Icarus* 7:85–93, 1967.
500. SCHIDLOWSKI, M. Metallogenesis in the southwestern Witwatersrand Basin, Oranje Freistgoldfeld Sudfrrika (Free State Goldfield, South Africa). *Geol. Jahrb. Beih.* 85:1–80, 1970.
501. SCHIMPL, A., R. M. LEMMON, and M. CALVIN. Cyanamide formation under primitive Earth conditions. *Science* 147:149–150, 1965.
502. SCHOFFENIELS, E., Ed. *Biochemical Evolution and the Origin of Life* (Proc. Int. Conf. Biochem. Evol., Liège, 1970). Amsterdam, North-Holland, 1971. Also in, *Exobiology, Frontiers of Biology*, Vol. 23. New York, Am. Elsevier, 1972.
503. SCHOPF, J. W. Antiquity and evolution of Precambrian life. In, *McGraw-Hill Yearbook of Science and Technology*, pp. 47–55, 1967. New York, McGraw-Hill, 1967.
504. SCHOPF, J. W. Micropaleontological studies of lunar samples. *Science* 167:779–780, 1970.
505. SCHOPF, J. W. Precambrian paleobiology. In, Ponnamperuma, C., Ed. *Exobiology, Frontiers of Biology*, Vol. 23, pp. 16–61. New York, Am. Elsevier, 1972.
506. SCHOPF, J. W., E. S. BARGHOORN, M. D. MASER, and R. O. GORDON. Electron microscopy of fossil bacteria two billion years old. *Science* 149(3690):1365–1367, 1965.
507. SCHRAMM, G. Synthesis of nucleosides and polynucleotides with metaphosphate esters. In, Fox, S. W., Ed. *The Origin of Prebiological System and of Their Molecular Matrices*, pp. 299–315. New York, Academic, 1965.
508. SCHRAMM, G., H. GRÖTSCH, and W. POLLMAND. Non-enzymatic synthesis of polysaccharides, nucleosides and nucleic acid and the origin of self-reproducing systems. *Agnew. Chem.* 74:53–59, 1962.
509. SCHROEDINGER, E. *What Is Life? The Physical Aspect of the Living Cell*. Cambridge, Eng., Univ. Press, 1945.
510. SCHWARTZ, A. W. Phosphate: solubilization and activation on the primitive Earth. In, Buvet, R., and C. Ponnamperuma, Eds. *Chemical Evolution and the Origin of Life*, Vol. 1, pp. 207–215. New York, Am. Elsevier, 1971.
511. SCHWARTZ, A. W., Ed. *Theory and Experiment in Exobiology*, Vol. 1. Groningen, Neth., Wolters-Noordhoff, 1971.
512. SCHWARTZ, A. W., and H. DEUSS. Concentrative processes and origin of biological phosphates. In, Schwartz, A. W., Ed. *Theory and Experiment in Exobiology*, Vol. 1, pp. 73–81. Groningen, Neth., Wolters-Noordhoff, 1971.
513. SCHWARTZ, A. W., and S. W. FOX. Condensation of cytidylic acid in the presence of polyphosphoric acid. *Biochim. Biophys. Acta* 134:9–16, 1967.
514. SCHWARZSCHILD, M. *Structure and Evolution of the Stars*. Princeton, Princeton Univ. Press, 1958.
515. SEREBROVSKAYA, K. B. *Koatservativ i Protoplazma* (Transl: *Coacervates and Protoplasma*). Moscow, Nauka, 1971.
516. SEREBROVSKAYA, K. B., G. I. LOZOVARA, and T. O. BALAYEVSKAYA. The study of reactions of photo-sensitization in phosphatide-protein coacervates. *Zh. Evol. Biokhim. Fiziol.* 2:302–307, 1966.
517. SEREBROVSKAYA, K. B., and N. VASIL'YEVA Conversion of coacervate drops into dynamically stable systems. *Dokl. Akad. Nauk SSSR* 155:212–215, 1964.
518. SEREBROVSKAYA, K. B., V. B. YEVSTIGNEYEV, V. A. GAVRILOVA, and A. I. OPARIN. Photosensitizing activity of chlorophyll in coacervates. *Biofizika* 7(1): 34–41, 1962. Washington, D.C., NASA, 1967. (NASA TT-F-10711)
519. SERGIYENKO, I. Z., and M. I. BOBYLEVA. Amino acids and carbohydrates in Precambrian rocks. In, *Abstracts, Int. Geochim. Congr.*, July 1971, Vol. 2, p. 922. Moscow, 1971.
520. SERGIYENKO, I. Z., M. I. BOBYLEVA, I. A. YEGOROV, and V. D. FONIN. Amino acid and carbohydrate composition of organic matter in a tenial archeocyathes skeleton. *Dokl. Akad. Nauk SSSR* 190(3):725–728, 1970.
521. SERGIYENKO, I. Z., S. A. SIDORENKO, and M. I. BOBYLEVA. Amino acids and carbohydrates in the oldest deposits (such as kyanite shists of the Kola Peninsula). *Dokl. Akad. Nauk SSSR* 215(2):474–477, 1974.
522. SERGIYENKO, I. Z., A. G. VOLOGDIN, I. A. YEGOROV, and M. I. BOBYLEVA. Discovery of amino acids and carbons in Precambrian rocks. In, *Tezisy Doklada Vtorogo Vsesoyuznogo Seminara "Organicheskiye Veshchestva Sovremennykh i Isokopayemykh Osadkov"* (Transl: *Reports, 2nd All-Union Seminar on Organic Substances of Modern and Fossil Residues*), pp. 70–71. Moscow, Mosc. State Univ. Press, 1970.
523. SHAN, D. O. Origin of membranes and related surface phenomena. In, Ponnamperuma, C., Ed. *Exobiology, Frontiers of Biology*, Vol. 23, pp. 235–265. New York, Am. Elsevier, 1972.
524. SHAPLEY, H. *Of Stars and Men, the Human Response to an Expanding Universe*. Boston, Beacon, 1958.
525. SHAUMAN, E. Critical review of cosmogonic theories propagated in Western Europe and America. In, *Voprosy Kosmogonii* (Transl: *Problems of Cosmogony*), Vol. 3, pp. 227–308. Moscow, Akad. Nauk SSSR, 1954.
526. SHAYN, G. A., and V. F. GAZE. *Dokl. Akad. Nauk SSSR* 68:661, 1949.
527. SHAYN, G. A., and V. F. GAZE. *Atlas Diffuznykh Gazouykh Tumannostey* (Transl: *Atlas of Diffuse Gas Nebulae*). Moscow, 1952.
528. SHKLOVSKIY, I. S., and C. SAGAN. *Intelligent Life in the Universe*. San Francisco, Holden-Day, 1966.
529. SIDGWICK, N. V. *The Chemical Elements and Their Compounds*, Vol. 1, p. 490. Oxford, Eng., Univ.

- Press, 1950.
530. SIDOROV, V. S. Change in the composition of amino acids during their abiogenic synthesis depending on the length of action of ultraviolet rays on solutions of formaldehyde and ammonium salts. *Dokl. Akad. Nauk SSSR* 164(3):692–696, 1965.
531. SIDOROV, V. S. Pathways of abiogenic formation of certain amino acids and heterocyclic compounds. In, *Petrozavodsk*, 1965. (Abstr. Diss.)
532. SIDOROV, V. S., T. Ye. PAVLOVSKAYA, and A. G. PASYNSKIY. Formation of imidazole and its derivatives during the action of ultraviolet rays on solutions of formaldehyde and ammonia salts. *Zh. Evol. Biokhim. Fiziol.* 2:293–301, 1966.
533. SILLEN, L. G. How has sea water got its present composition? *Sven. Kem. Tidskr.* 75:161–167, 1963.
534. SILLEN, L. G. The ocean as a chemical system. *Science* 156:1189–1197, 1967.
535. SINTON, W., and J. STRONG. Radiometric observations of Venus. *Astrophys. J.* 131:470–490, 1960.
536. SMART, W. M. *Origin of the Earth*. Baltimore, Penguin, 1959.
537. SMITH, J. W., and I. R. KAPLAN. Endogenous carbon in carbonaceous meteorites. *Science* 167:1367–1370, 1970.
538. SMITH, A. E., K. RAAB, and J. A. EKPAHA-MENSAH. Origin of enzymic and photosynthetic activity in a prebiotic system. *Experientia* 27:648–650, 1971.
539. SMOLUCHOWSKI, R. Mars: retention of ice. *Science* 159:1348–1350, 1968.
540. SNYDER, L. E., and D. BUHL. Water-vapor clouds in the interstellar medium. *Astrophys. J.* 155:L65–L70, 1969.
541. SNYDER, L. E., and D. BUHL. Radio emission from hydrogen cyanide. *IAU Circ.* 2251, June 10, 1970.
542. SNYDER, L. E., D. BUHL, B. ZUCKERMAN, and P. PALMER. Microwave detection of interstellar formaldehyde. *Phys. Rev. Lett.* 22:679–681, 1969.
543. SOKOLOV, V. A. Evolution of the atmosphere of the Earth. In, Oparin, A. I., et al, Eds. *Vozniknoveniye Zhizni na Zemle, Trudy Mezhdunarodnogo Simpoziuma*, Moscow, 1957 (Transl: *The Origin of Life on Earth, Proceedings, First International Symposium*), pp. 59–69. New York, Pergamon, 1959.
544. SOKOLOV, V. A. *Geokhimiya Gazov Zemnoy Kory i Atmosfery* (Transl: *Geochemistry of Gases of the Earth's Crust and Atmosphere*). Moscow, Nedra, 1966.
545. SOKOL'SKAYA, A. V., and I. Ye. EL'PINER. Synthesis of amino acids during the action of ultraviolet waves. In, *Abstracts, 5th International Biochemical Congress*, Moscow, 1961, p. 51. Oxford, Pergamon, 1961. (Abstr. 2.150.547)
546. SPIRIN, A. S., and L. P. GAVRILOVA. *Ribosoma* (Transl: *Ribosome*). Moscow, Nauka, 1971.
547. STEINMAN, G., and M. COLE. Synthesis of biologically pertinent peptides under possible primordial conditions. *Proc. Nat. Acad. Sci.* 58:735–742, 1967.
548. STEINMAN, G., D. H. KENYON, and M. CALVIN. Dehydration condensation in aqueous solution. *Nature* 206:707–708, 1965.
549. STEINMAN, G., D. H. KENYON, and M. CALVIN. The mechanism and protobiochemical relevance of dicyanamide-mediated peptide synthesis. *Biochim. Biophys. Acta* 124:339–350, 1966.
550. STEINMAN, G., R. M. LEMMON, and M. CALVIN. Cyanamide: a possible key compound in chemical evolution. *Proc. Nat. Acad. Sci.* 52:27–30, 1964.
551. STEINMAN, G., R. M. LEMMON, and M. CALVIN. Dicyanamide: possible role in peptide synthesis during chemical evolution. *Science* 147:1574–1575, 1965.
552. STOOPS, C. E., and C. L. FURROW. Radiation-induced reaction of carbon dioxide with ethylene. *Science* 134:839–840, 1961.
553. STRAKHOV, N. M. *Tipy Litogeneza i Ikh Evolyutsiya v Istorii Zemli* (Transl: *Types of Lithogenesis and Their Evolution in the History of the Earth*). Moscow, Gosgeoltekhizdat, 1969.
554. STROM, R. G., and G. FIELDER. Multiphase eruptions associated with the lunar craters Tycho and Aristarchus. *Comm. Lunar Planet. Lab.* 8(149–152):235–288, 1970.
555. STRUVE, O. *Stellar Evolution, An Exploration from the Observatory*. Princeton, Princeton Univ. Press, 1950.
556. STRUVE, O. The atmospheres of Jupiter and Saturn. *Sky Telesc.* 13:336–368, 1954.
557. STRUVE, O. McCrea's theory of the solar system's origin. *Sky Telesc.* 19:154–156, 1960.
558. STRUVE, O. Observational data of interest in the study of stellar evolution; introductory report. Presented at 9th Int. Astrophys. Colloq., Liège, July 1959. *Mem. Roy. Soc. Sci. (Liège)*, 5th Ser. 3:17–40, 1960.
559. STRUVE, O., and V. ZEBERGS. *Astronomy of the 20th Century*. New York, Macmillan, 1962.
560. STUDIER, M. H., R. HAYATSU, and E. ANDERS. *Origin of Organic Matter in Early Solar System. I. Hydrocarbons*. Washington, D.C., NASA, 1965. (NASA CR-69930)
561. STUDIER, M. H., R. HAYATSU, and E. ANDERS. Origin of organic matter in early solar system. V. Further studies of meteoritic hydrocarbons and a discussion of their origin. *Geochim. Cosmochim. Acta* 36:189–215, 1972.
562. STUDIER, M. H., R. HAYATSU, and K. FUSE. Analyses of pyrimidine and purine bases by a combination of paper chromatography and time-of-flight mass spectrometry. *Anal. Biochem.* 26:320–324, 1968.
563. SUÈSS, H. E. Die Häufigkeit der Edelgase auf der Erde und im Kosmos (Transl: Abundance of rare gases on the Earth and in the cosmos). *J. Geol.* 57:600–607, 1949. (Ger.)
564. SUÈSS, H. E. *Nuclear Geology*, p. 28. Varenna, Ital., Sc. Int. Fis., 1960. (Summer course)
565. SUÈSS, H. E. Thermodynamic data on the formation of solid carbon and organic compounds in primitive planetary atmospheres. *J. Geophys. Res.* 67:2029–2034, 1962.
566. SUÈSS, H. E., and H. C. UREY. Abundances of the elements. *Rev. Mod. Phys.* 28:53–74, 1956.
567. SULSTON, J., R. LOHRMANN, L. E. ORGEL, and H. T.

- MILES. Specificity of oligonucleotide synthesis directed by polyuridylic acid. *Proc. Nat. Acad. Sci.* 60:409-415, 1968.
568. SULSTON, J., R. LOHRMANN, L. E. ORGEL, and H. T. MILES. Nonenzymatic synthesis of oligoadenylates on a polyuridylic acid template. *Proc. Nat. Acad. Sci.* 59:726-733, 1968.
569. SULSTON, J., R. LOHRMANN, L. E. ORGEL, H. SCHNEIDER-BERNLOEHR, and B. J. WEIMANN. Nonenzymic oligonucleotide synthesis on the polycytidylate template. *J. Mol. Biol.* 40:227-237, 1969.
570. Summary of Apollo 11 Lunar Science Conference, Houston, Tex., Jan. 1970. *Science* 167(3918):449-455, 1970. (Reports, pp. 456-784)
571. SURKOV, Yu. Revealing the secrets of the universe. *Pravda* Dec. 18, 1971.
572. SWALLOW, A. J. *Radiation Chemistry of Organic Compounds*, p. 244, New York, Pergamon, 1960.
573. SWINGS, P. Introduction. 4th Int. Colloq. Astrophys., Sept., 1952, Liège. *Mem. Soc. Roy. Sci. (Liège)*, Ser. 4 (*Physics of Comets*) 13(1-2), 1953.
574. SWINGS, P., and L. HASER. *Atlas of Representative Cometary Spectra*. Louvain, Univ. Liège, Astrophys. Inst., 1956.
575. SYLVESTER-BRADLEY, P. C., and R. J. KING. Evidence for abiogenic hydrocarbons. *Nature* 198:728-731, 1963.
576. SZUTKA, A. Formation of pyrrolic compounds by ultraviolet irradiation of  $\delta$ -aminolevulinic acid. *Nature* 212:401-402, 1966.
577. TERENIN, A. N. Photosynthesis in the shortest ultraviolet. In, Oparin, A. I., et al, Eds. *Vosniknoveniye Zhizni na Zemle, Trudy Mezhdunarodnogo Simpoziuma*, Moscow, 1957 (Transl: *The Origin of Life on Earth, First International Symposium*), pp. 136-139. New York, Pergamon, 1959.
578. TERENT'YEV, A. P., and Ye. I. KLABUNOVSKIY. Problem of absolute asymmetrical synthesis. *Uch. Zap.* (Moscow Gos. Univ.) 151:145, 1951.
579. TERENT'YEV, A. P., and Ye. I. KLABUNOVSKIY. The role of dysymmetry in the origin of living matter. In, Oparin, A. I., et al, Eds. *Vosniknoveniye Zhizni na Zemle, Trudy Mezhdunarodnogo Simpoziuma*, Moscow, 1957 (Transl: *The Origin of Life on Earth, Proceedings, First International Symposium*), pp. 99-108. New York, Pergamon, 1959.
580. TER HAAR, D., and A. G. W. CAMERON. Historical review of theories of the origin of the solar system. In, Jastrow, R., and A. G. W. Cameron, Eds. *On the Origin of the Solar System*, pp. 4-37. New York, Academic, 1963.
581. TSUKERKENDL, E., and L. POLING. Molecules as documents of the evolutionary process. In, Kretovich, V. L., Ed. *Problemy Evolyutsionnoy i Tekhnicheskoy Biokhimii* (Transl: *Problems of Evolutionary and Technical Biochemistry*), pp. 54-62. Moscow, Nauka, 1964.
582. TSURUTA, T., S. INOUE, and K. MATSURA. Asymmetric selection in the copolymerization of N-carboxyl-L- and D-alanine anhydride. *Biopolymers* 5:313-319, 1967.
583. TULL, R. G. High-dispersion spectroscopic observations of Mars. IV. Latitude distribution of atmospheric water vapor. *Icarus* 13:43-57, 1970.
584. TURNER, B. E. Cyanoacetylene is the largest molecule yet to be discovered in interstellar space. *Chem. Eng. News* 48(34):31, 1970.
585. TURNER, B. E. Radio emission from interstellar cyanoacetylene. *IAU Circ.* 2268, July 27, 1970.
586. TYLER, S. A., and E. S. BARGHOORN. Occurrence of structurally preserved plants in the Precambrian rocks of the Canadian Shield. *Science* 119:606-608, 1954.
587. UREY, H. C. On the early chemical history of the Earth and the origin of life. *Proc. Nat. Acad. Sci.* 38:351-363, 1952.
588. UREY, H. C. *The Planets, Their Origin and Development*. Silliman Mem. Lect., 1951. New Haven, Yale Univ. Press, 1952.
589. UREY, H. C. The dissipation of gas and volatilized elements from protoplanets. *Astrophys. J. Suppl.* Ser. 1:147-174, 1954.
590. UREY, H. C. The atmosphere of the planets. In, Flügge, S., Ed. *Handbuch der Physik*, Vol. 52, pp. 363-418. Berlin, Springer, 1959.
591. UREY, H. C. Primitive planetary atmospheres and the origin of life. In, Oparin, A. I., et al, Eds. *Vosniknoveniye Zhizni na Zemle, Trudy Mezhdunarodnogo Simpoziuma*, Moscow, 1957 (Transl: *The Origins of Life on Earth, Proceedings, First International Symposium*), pp. 16-22. New York, Pergamon, 1959.
592. UREY, H. C. The planets. In, Berkner, L. V., and H. Odishaw, Eds. *Science in Space*, pp. 199-217. New York, McGraw-Hill, 1961.
593. UREY, H. C. Evidence regarding the origin of the Earth. *Geochim. Cosmochim. Acta* 26:1-13, 1962.
594. UREY, H. C. The origin and evolution of the solar system. In, LeGally, D. P., Ed. *Space Science*, pp. 123-168. New York, Wiley, 1963.
595. UREY, H. C. Biological material in meteorites. *Science* 151:157-166, 1966. Also in, Rutten, M. G. *The Origin of Life by Causes*, p. 188. Amsterdam, Neth., Am. Elsevier, 1971.
596. VARDYA, M. S. March with depth of molecular abundances in the outer layers of K and M stars. *Mon. Not. Roy. Astron. Soc.* 134:347-370, 1966.
597. VASIL'YEVA, N. V., T. O. BALAYEVSKAYA, L. Z. GOGI-LASHVILI, and K. B. SEREBROVSKAYA. Comparative study of the kinetics of a joined reaction on colloidal models (coacervates). *Biokhimiya* 34:795-799, 1969.
598. VASSOYEVICH, N. B. The genetic nature of petroleum in the light of data from organic geochemistry. In, Sokolov, V. A., Ed. *Genezis Nefti i Gaza* (Transl: *Genesis of Petroleum and Gas*), pp. 25-53. Moscow, Nauka, 1968.
599. VASSOYEVICH, N. B. Biogenic carbonaceous substance

- as a source of petroleum. *Priroda* (Moscow) (3):58–69, 1971.
600. VDOVYKIN, G. P. Bitumens of carbonaceous chondrites Groznaya and Migei. *Geokhimiya* 2:134–138, 1962.
601. VDOVYKIN, G. P. Carbonaceous substances of meteorites and their origin. *Geokhimiya* (4):299–307, 1964.
602. VDOVYKIN, G. P. Organized elements in carbonaceous chondrites. *Geokhimiya* (7):678–682, 1964.
603. VDOVYKIN, G. P. *Uglerodistoe Veshchestvo Meteoritov* (Transl: *Carbonaceous Matter of Meteorites*). Moscow, Nauka, 1967.
604. VODOVYKIN, G. P. Carbon polytypism in meteorites. In, Schenck, P. A., and I. Havenaar, Eds. *Advances in Organic Geochemistry*, pp. 593–604. New York, Pergamon, 1969.
605. VDOVYKIN, G. P. Interstellar dust and aromatic carbon. *Nature* 225:254, 1970.
606. VDOVYKIN, G. P. Meteorites and life. In, Imshenetskiy, A. A., Ed. *Zhizn' vne Zemli i Metody yeye Obnaruzheniya* (Transl: *Life Beyond the Earth and Methods of Detecting It*), pp. 135–157. Moscow, Nauka, 1970.
607. VERNADSKIY, V. I. *Ocherki Geokhimii* (Transl: *Outlines of Geochemistry*). Moscow, Gorgeonefte, 1934.
608. VINOGRADOV, A. P. *Khimicheskaya Evolyutsiya Zemli* (Transl: *Chemical Evolution of the Earth*). Moscow, Izd. Akad. Nauk SSSR, 1959.
609. VINOGRADOV, A. P. On the origin of the Earth's crust matter. *Geokhimiya* (1):3–29, 1961. Zone melting as a method of studying some radial processes in the Earth. *Geokhimiya* (3):269–270, 1962.
610. VINOGRADOV, A. P. *Izotopy Kisloroda i Fotosintez* (Transl: *Isotopes of Oxygen and Photosynthesis*). Moscow, Izd. Akad. Nauk SSSR, 1962.
611. VINOGRADOV, A. P. Gas conditions of the Earth. In, *Khimiya Zemnoy Kory* (Transl: *Chemistry of the Earth's Crust*), Vol. 2, pp. 5–21. Moscow, Nauka, 1964.
612. VINOGRADOV, A. P. The matter of meteorites. *Geokhimiya* (11):1275–1312, 1965.
613. VINOGRADOV, A. P. *Vvedeniye v Geokhimiya Okeana* (Transl: *Introduction to Geochemistry of the Ocean*). Moscow, Nauka, 1967.
614. VINOGRADOV, A. P. The chemistry of planets. In, *Nauka i Chelovechestvo* (Transl: *Science and Humanity*), pp. 214–237. Moscow, Nauka, 1968.
615. VINOGRADOV, A. P. The atmosphere of planets of the solar system. *Vestn. Mosk. Univ., Geol.* 24(4):3–14, 1969.
616. VINOGRADOV, A. P. Preliminary data of lunar rock provided by the automatic station Luna-16. *Priroda* (3):8–15, 1971.
617. VINOGRADOV, A. P., and G. P. VDOVYKIN. Multi-molecular organic matter of carbonaceous chondrites. *Geokhimiya* (9):843–848, 1964.
618. VOLOGDIN, A. G. Discovery of the origin of stromatolites. *Priroda* (Moscow) (9):39–46, 1955.
619. VOLOGDIN, A. G. *Paleontologiya i Poiski Poleznykh Iskopayemykh* (Transl: *Paleontology and Searches for Mineral Resources*). Moscow, Znaniye, 1960.
620. VOLOGDIN, A. G. *Drevneyshiye Vodorosli SSSR* (Transl: *Ancient Algae of the USSR*). Moscow, Akad. Nauk SSSR, 1962.
621. VOLOGDIN, A. G. *Zemlya i Zhizn'* (Transl: *The Earth and Life*). Moscow, Akad. Nauk SSSR, 1963.
622. WACHNELDT, T. V., and S. W. FOX. Phosphorylation of nucleosides with polyphosphoric acid. *Biochim. Biophys. Acta* 134:1–8, 1967.
623. WALD, G. The origin of optical activity. *Ann. NY Acad. Sci.* 69:352–368, 1957.
624. WALD, G. Life in the second and third periods; or why phosphorus and sulfur for high-energy bonds? In, Kasha, M., and B. Pullman, Eds. *Horizons in Biochemistry*, pp. 127–142. New York, Academic, 1962.
625. WALD, G. The origins of life. *Proc. Nat. Acad. Sci.* 52:595–611, 1964.
626. WALKER, G. A. H., J. B. HUTCHINGS, and P. F. YOUNGER. Interstellar extinction anomalies and the diffuse interstellar bands. *Astron. J.* 74:1061–1066, 1969.
627. WATERMAN, E. P. The visual region of the spectrum of brighter Class A stars. *Lick Obs. Bull.* 8(243):1–17, 1913.
628. WATSON, J. D., and F. H. C. CRICK. Genetical implications of the structure of DNA. *Nature* (London) 171:964–967, 1953.
629. WATTS, D. C. Functional organization and molecular evolution. In, Kimball, A. P., and J. Oró, Eds. *Precambrian and Biochemical Evolution*, pp. 189–199. Amsterdam, North-Holland, 1971.
630. WEIZSACKER, C. F. von. *The History of Nature*. Chicago, Univ. Chicago Press, 1949.
631. WHIPPLE, F. L. A comet model. I. The acceleration of Comet Enke. *Astrophys. J.* 111:375–394, 1950.
632. WHIPPLE, F. L. On the structure of the cometary nucleus. In, Middlehurst, B. M., and G. P. Kuiper, Eds. *The Moon, Meteorites, and Comets. IV. The Solar System*, pp. 639–664. Chicago, Univ. Chicago Press, 1963.
633. WHIPPLE, F. L. The history of the solar system. *Proc. Nat. Acad. Sci.* 52:565–594, 1964.
634. WILDT, R. *Absorptionsspektren und Atmosphären der grossen Planeten* (Transl: *Absorption Spectra and Atmospheres of the Giant Planets*), No. 22. Goettingen, Univ. Sternwarte Veröff., 1932.
635. WILDT, R. Methane in the atmospheres of the giant planet. *Naturwissenschaften* 20:851, 1932.
636. WILSON, R. W., K. B. JEFFERTS, and A. A. PENZIAS. Carbon monoxide in the Orion nebula. *Astrophys. J.* 161:L43–L44, 1970.
637. WOELLER, F., and C. PONNAMPERUMA. Organic synthesis in a simulated Jovian atmosphere. *Icarus* 10:386–392, 1969.
638. WOESE, C. R. The emergence of genetic organization. In, Ponnamperuma, C., Ed. *Exobiology, Frontiers of Biology*, Vol. 23, pp. 301–341. New York, Am. Elsevier, 1972.
639. WOOD, J. A., J. S. DICKEY, Jr., U. B. MARVIN, and B. N. POWELL. Lunar anorthosite sites. *Science* 167:602–604, 1970.

640. WOOLFSON, M. M. Origin of the solar system. *Nature* 187:47-48, 1960.
641. WURM, K. The physics of comets. In, Middlehurst, B. M., and G. P. Kuiper, Eds. *The Moon, Meteorites and Comets, IV. The Solar System*, pp. 573-617. Chicago, Univ. Chicago Press, 1963.
642. YANG, C. C., and J. ORÓ. Synthesis of adenine, guanine, cytosine and other nitrogen organic compounds by a Fischer-Tropsch-like process. In, Buvet, R., and C. Ponnamperuma, Eds. *Chemical Evolution and the Origin of Life*. Vol. 1, pp. 152-167. New York, Am. Elsevier, 1971.
643. YEVREINOVA, T. N. Coacervates. In, Oparin, A. I., et al, Eds. *Proceedings, First International Symposium on the Origin of Life on Earth*, Moscow, 1957. Clark, F., and R. L. M. Synge, Eds., pp. 493-494. London, Pergamon, 1959.
644. YEVREINOVA, T. N. Distribution of nucleic acids in coacervate droplets. *Dokl. Akad. Nauk SSSR* 141:1224-1227, 1961.
645. YEVREINOVA, T. N. Distribution of nucleic acids on coacervate drops. In, Oparin, A. I., Ed. *Evolutionary Biochemistry*, Vol. 3, Proc. 5th Int. Congr. Biochem., Moscow, 1961, pp. 110-113. New York, Macmillan, 1963.
646. YEVREINOVA, T. N. *Kontsentrirovaniye Veshchestv i Deystviye Fermentov v Koatsetvatakh*. (Transl: Concentration of Substances and the Action of Enzymes in Coacervates. Moscow, Nauka, 1966.
647. YEVREINOVA, T. N., H. N. KARNAUKHOV, T. W. MAMONTOVA, and G. R. IVANITSKIY. The interaction of biological macromolecules in coacervate systems. *J. Colloid Interface Sci.* 36(1):18-23, 1971.
648. YEVREINOVA, T. N., and A. F. KUZNETSOVA. Use of interferential microscopy for coacervates. *Biofizika* 6:288-293, 1961.
649. YEVREINOVA, T. N., A. V. POGOSTOVA, T. I. CHUKANOVA, and T. I. LARIONOVA. Injection of amino acids into coacervates. *Nauchn. Dokl. Vyssh. Shk. Biol. Nauk* 1:159-164, 1962.
650. YOSHINO, D., R. HAYATSU, and E. ANDERS. Origin of organic matter in early solar system. 'III. Amino acids: catalytic synthesis. *Geochim. Cosmochim. Acta* 35:927-938, 1971.
651. YOUNG, R. S. Morphology and chemistry of microspheres from proteinoid. In, Fox, S. W., Ed. *The Origins of Prebiological Systems and of Their Molecular Matrices*, pp. 347-357. New York, Academic, 1965.
652. YOUNG, R. S., C. PONNAMPERUMA, and B. McCAW. Abiogenic synthesis on Mars. In, Florkin, M., Ed. *Life Sciences and Space Research*, Vol. 3, pp. 127-138. New York, Wiley, 1965.
653. ZELLER, E. J., and G. DRESCHHOFF. Formation of organic compounds in solid bodies by solar and cosmic proton bombardment. In, Millmann, P. M., Ed. *Meteorite Research: Symposium on Meteorite Research*, Vienna, 1968, pp. 524-533. Dordrecht, Holl., Reidel, 1969.
654. ZUCKERMAN, B., D. BUHL, P. PALMER, and L. E. SNYDER. Observation of interstellar formaldehyde. *Astrophys. J.* 160:485-506, 1970.

## Chapter 8

# SEARCH FOR AND INVESTIGATION OF EXTRATERRESTRIAL FORMS OF LIFE<sup>1</sup>

A. B. RUBIN

Biology Faculty, Problem Laboratory of Space Biology, Moscow State University USSR

### PROBLEMS OF EXOBIOLOGY

The detection of life on planets other than the Earth is a continuing challenge to those concerned with the larger problem of the origin of life. The presence or absence of life may have significant influence on the composition of planetary atmospheres and other physical conditions. Study of the surface layers of other planets makes it possible to refine concepts regarding the role of biological processes on Earth, which may even lead to consideration of the consequences of human activity. Therefore, exobiological research may prove valuable in solving contemporary human problems. The transport of foreign life forms could also lead to highly unexpected consequences on Earth, which would be difficult to anticipate.

The existence of life outside Earth is also important for the handling of fundamental problems concerning the origin and essence of life. The immediate goal of exobiological experiments

conducted in automatic biologic laboratories (ABL) is to answer the question of the presence or absence of life on a planet. The investigation of extraterrestrial life forms should contribute to understanding of the vital processes and phenomena of life as a whole. The absence of life on other planets would also be of scientific significance, demonstrating the specific role of terrestrial conditions in the origin and evolution of living forms. It is not clear to what extent extraterrestrial forms could resemble Earth organisms in their main biochemical properties.

In detecting extraterrestrial life, various evolutionary stages of organic matter which could theoretically be encountered on other planets must be taken into account. For example, on Mars there are a number of possibilities from the existence of complex, abiogenic organic compounds to the presence of developed life forms [96]:

1. Chemical evolution terminated on Mars with abiogenic formation of amino acids, sugars, fatty acids, carbohydrates, and possibly proteins, but life is not present on the planet.
2. These substances differ from similar compounds found on Earth.
3. Primary probiologic open systems are

<sup>1</sup> Translation of, Poisk i Issledovaniye Vnezemnykh Form Zhizni, Volume 1, Part 3, Chapter 8 of *Osnovy Kosmicheskoy Biologii i Meditsiny* (*Foundations of Space Biology and Medicine*), Moscow, Academy of Sciences USSR, 1973. 122 pages.

Data presented in this chapter are based on material prepared by N. Horowitz (USA) and S. I. Aksenov (USSR). The author expresses profound gratitude to them.

- separated from the environment by membranes.
4. Simple primitive life forms resemble Earth microorganisms.
  5. More complex forms are analogous to simple plants and insects on Earth.
  6. Life existed and died out on Mars much earlier, reaching one of these stages and leaving only insignificant traces.
  7. There are signs of highly developed life (civilization).
  8. There is, and always has been, complete absence of life on Mars.

The experimental investigation of these possibilities constitutes the basic problem in the biological study of Mars. Theoretical prerequisites, criteria for the existence of life, and proposed methods of detecting living systems on other planets are discussed in this chapter.

### **CRITERIA FOR EXISTENCE AND SEARCH FOR LIVING SYSTEMS**

Concepts of the essence of life are based on studies of vital processes on Earth. However, the search for life on other planets requires identification of vital phenomena under conditions markedly different from those on Earth. Consequently, theoretical methods and appropriate devices for detecting life must be based upon scientific criteria pertinent to the phenomenon of life as a whole.

Fundamental properties peculiar to living systems of terrestrial origin which can be used to characterize extraterrestrial organisms include [19]: response of organisms to changes in external conditions, metabolism, growth, development, reproduction, properties of inheritance and variation, and finally, the process of evolution. There would be no doubt about an unknown object being a living system if these properties were found to apply.

The principal difficulty is that many characteristics of life can be simulated *in vitro*. For example, reactions to external stimulation are also possessed by nonliving systems, which change their physical and chemical states under the influence of external factors. The ability to grow is also a characteristic of crystals, while

exchanging energy and matter with the external environment is characteristic of open chemical systems.

Searches for extraterrestrial life must be based upon a combination of different criteria of existence and methods of detecting living forms. This approach should lead to an increase in the reliability of detecting life on other planets. The question arises: which of those important general criteria would reflect characteristic properties of life? From this standpoint the principal properties of living systems will be examined.

### **Chemical Basis of Life**

Recent studies have shown a possibility for synthesizing biologically important substances from simple compounds, such as ammonia, methane, water vapor, and so forth, which are included in the composition of the primary atmosphere of Earth. Under laboratory conditions, the energy required for carrying out such syntheses comes from ionizing radiation, electrical discharges, and ultraviolet light, from which amino acids, organic acids, sugar nucleotides, nucleoside phosphates, lipids, materials of a porphyritic nature, and others have been obtained. The majority of molecules characteristic of life originated on Earth by abiogenic means, and, more important, their synthesis can occur on other planets without participation of living systems. Consequently, the mere detection of organic substances on other planets cannot serve as a reliable index of the existence of life, inasmuch as these substances may be products of abiogenic synthesis.

An example of abiogenic synthesis is provided by carbonaceous chondrites of meteoritic origin, containing 5%–7% organic matter [88], which include diverse compounds occurring under terrestrial conditions, such as polynuclear hydrocarbons, aromatic and fatty acids, derivatives of purine such as adenine and guanine, amino acids, and others. Under conditions different from those on Earth, the chemical evolution of compounds may also form complex organic substances which constitute the chemical basis of living systems on Earth.

The most characteristic feature of the chemical

composition of living systems of terrestrial origin is that they all incorporate carbon. This element forms molecular chains as the basis for all important bioorganic compounds—proteins and nucleic acids in particular—with water the biologic solvent. Hence, the only known basis for life is carbon-organic and includes protein, nucleic acids, and water. The theoretical possibility of constructing living systems on another basis, however, is discussed in the literature. For example, the skeleton of molecules might incorporate silicon instead of carbon, and the role of water as the biologic solvent may be played by ammonia [17]. However, this possibility would be very difficult to take into account in selecting detection methods and designing appropriate apparatus, since our scientific concepts are based on the study of terrestrial organisms only. On the other hand, a careful analysis of complex biopolymers containing carbon indicates the unique properties of carbon as the basic element for living systems.

Conditions for synthesis of carbon-organic compounds already existed at the protoplanetary cloud stage, which explains the extensive distribution of organic carbon compounds throughout the universe [15, 55]. In organic compounds, carbon atoms form much stronger chemical bonds with each other and with adjacent atoms than silicon, which cannot form strong double bonds, so that giant inert polymers with single bonds develop ( $\text{SiO}_2$ ). Finally, the instability of silicon chains and its compounds in the presence of water or oxygen also limits its role as the basis for vital processes [93]. Carbon-based macromolecules obviously have greater thermal stability with respect to maintaining their spatial structure (secondary, tertiary) in comparison with silicon-based analogs [1].

The role of water can be discussed in regard to its possible replacement by ammonia or other fluids that boil at low temperatures (hydrogen sulfide, hydrogen fluoride). In fact, water has a number of properties that provide for its role as a biologic solvent. Such properties are: its amphoteric nature, ability to perform autodissociation into the cation ( $\text{H}^+$ ) and anion ( $\text{OH}^-$ ), a higher dipolar moment and dielectric constant, low viscosity, and finally high specific thermal

capacity and latent conversion heat which protect organisms against rapid temperature changes. Many of these properties may be provided by ammonia or hydrogen sulfide, especially at limit temperatures where water would either evaporate or freeze, while other substances retain properties as liquid solvents [17]. However, respiration efficiency based upon ammonia would only be about 10% in comparison with respiration on Earth since the free energy of water formation is approximately 10 times greater than the same value for ammonia. The advantages of using liquid ammonia at temperatures of  $-40^\circ$  to  $-50^\circ$  C lose much of their value since there are no known catalysts capable of carrying out effective synthesis of ammonia from nitrogen and hydrogen in this temperature range [58]. The role of water in biologic systems also includes macromolecule stabilization factors provided by the general structural characteristics of water [1]. On the whole, carbon and water as the basis for life can be considered a general characteristic of living systems on other planets as well.

The striking biochemical uniqueness of terrestrial organisms is due to a limited number of complex compounds which have been synthesized in an abiogenic fashion under conditions of a primary reducing atmosphere on Earth. The further interaction of these compounds has led to the formation of biologic polymers (macromolecules) at the expense of the same forms of energy as in primary reactions of abiogenic synthesis [60]. A characteristic physical feature of biologic macromolecules is a system of conjugated double bonds formed by  $\pi$ -electrons. Delocalization of  $\pi$ -electrons determines the functional characteristics and stabilization of biopolymer structure and may be one of the most important physical factors influencing the molecular processes of metabolism. Macromolecules of terrestrial type may be considered then as the basis of the structural organization of living matter and consequently necessary for life under extraterrestrial conditions. A characteristic feature of living systems is inclusion in their composition, not only of basic chemical elements (C, H, O, N), but a number of others, especially sulfur and phosphorus. This property may also be viewed as necessary for living matter.

The chemical specificity of terrestrial life is a unique phenomenon of life as a whole and includes carbon-based organic compounds. However, physical and chemical characteristics of its basic constituents, the building blocks of life, are of abiogenic origin.

### Dynamic Properties of Living Systems

The dynamic properties of living systems should be considered as the starting point in interpretation of exobiologic experimental data. The evolution of biologic systems has been connected with development of types of interaction between its elements and regulation of the system.

Life is inseparably connected with the existence of open systems in which the exchange of substances and energy governs the properties of the system [57]. Mathematical modeling of the dynamic properties of open systems has made it possible to explain a number of characteristic features, in particular, the establishment of a stationary oscillating state under constant external conditions, observed at various levels of biologic organization. This property is an important feature of the high degree of organization which, in turn, may be viewed as the necessary condition for life. In an open system, entropy change can be split into two parts: one due to interactions with the environment, and the other to changes inside the system [61]. If a system is far from equilibrium, special space dissipative structures can be formed which are highly important in developing biologic systems [62].

Biologic systems possess special internal control processes. The transfer of small amounts of substance or quantities of energy in the control process itself leads to response reactions during which much larger amounts of energy and mass are handled [46]. This also forms the energy basis for the regulation of living systems according to the "feedback" principle. It is clear that a process of "active regulation" is only possible when there are certain reserves of available free energy which can be readily mobilized [11, 71]. In this respect, the unique genetic property of living systems for self-replication resulted from evolution of open systems in which all processes are eventually directed toward reproduction.

Another important dynamic property of living systems is that several groups of processes differ in their rates. In fact, there are three basic types of processes in cells: enzyme reactions with characteristic times of  $10^{-3}$ – $10^{-1}$ , of  $10^{-2}$  s– $10^2$  s, and processes of reproduction where characteristic times may reach several hours. Stability of a living system is achieved by dynamic balancing of these processes.

These characteristics of dynamic organization of life (outlined briefly) are the result of relatively simple open systems evolving into self-reproducing open living systems. The internal tendency toward organization can be found on many levels of biologic organization [5]. This has definitely played the critical role in evolution of primary protobiologic systems capable of combining individual reactions into a self-regulating system of cellular metabolism.

### Role of Light

An important aspect of extraterrestrial life is the requirement for external influx of energy to maintain development. Some of the properties of photobiologic processes, in particular photosynthesis, and their significance in the development of methods and criteria for life detection will be discussed.

Sunlight, primarily in the ultraviolet region of the spectrum, has already been significant in abiogenic formation of the most important organic compounds. However, the role of light is not limited merely to the flow of free energy necessary for abiogenic synthesis, but also contributes to photochemical acceleration of further conversions of complex organic compounds.

The activity of the primary living system can also be largely determined by photochemical reactions between constituent compounds. Many modern organisms with no direct relationship to photosynthesis nevertheless change their activity when illuminated. Thus, photoreactivation of cells by visible light after the damaging influence of ultraviolet radiation is clearly an ancient process having taken place when the first living systems developed protective mechanisms against the destructive effects of ultraviolet radiation reaching Earth. Blue light also has an activating

effect on flavin and cytochrome enzymes, leading to an increase in respiratory processes in plants [92].

New data have appeared recently on the influence of visible light on growth, development, and morphogenesis of heterotrophic organisms [73]. The effect of light on nonphotosynthesizing organisms definitely indicates a broad spectrum of photoregulatory reactions in which (in contrast to photosynthesis) there is no important storage of light energy. The primary pigmented photosynthesizing organisms, such as modern photosynthesizing purple bacteria, may possibly use photochemical reactions of porphyrins to speed up certain metabolic processes, rather than for direct photosynthesis of organic matter [38]. Later, these photochemical properties of porphyrins formed the basis of bacterial type photosynthesis and then photosynthesis of higher green plants, involving photolysis of water and evolution of free molecular oxygen. The appearance of free molecular oxygen in the Earth's atmosphere marked a new era of aerobic respiration in the development of life. It should be pointed out that light may not be the only source of energy at early evolutionary stages of organic compounds. This role could be played as well by chemical energy released, for example, in condensation reactions in inorganic polyphosphate [45].

Life requires for its origin and development, on the whole, a constant external influx of free energy which is supplied on Earth by sunlight. That is the reason why light is so important at all stages in the evolution of life, beginning with abiogenic synthesis of primary compounds, their further conversions, vital activity of primary living systems, and finally in modern photosynthesis which provides organic substances on Earth. Evidently photosynthesis in some form, as a process for the utilization of light energy in biologic systems, is an important criterion for the existence of developed life. Primary processes of photosynthesis include an open system of electron flow from external sources of electrons (water or hydrogen donor), along a chain of intermediate compounds; the driving force for their transfer provided by light energy. Circulation of the electron flow is coupled with formation of adenosine triphosphate (ATP) [12].

Among some peculiar features of photosynthetic mechanisms is the oxidation of cytochrome by bacteriochlorophyll in photosynthetic purple bacteria proceeding at the temperature of liquid nitrogen [10, 21]. It can be concluded that regardless of the concrete chemical structure of the photosynthetic apparatus, a common feature of photobiologic processes for the utilization of light energy is this sequence of reactions: absorption of light and excitation of pigment molecules, delocalization of the electron, transfer of the electron along the open chain of oxidation-reduction compounds, and formation of the final products where light energy is accumulated. This photosynthetic chain may be considered a necessary condition for the existence of life; this is completely valid with respect to developed life forms in which there is a complex chain for transferring electrons from the substrate to the final acceptor. In heterotrophic anaerobes, which predominated at various stages of evolution on Earth, a simple system exists for the transfer of the electron, synthesizing macroergs in the reactions involving substrate phosphorylation of the donor-carrier-acceptor type.

On the basis of the data presented, general principles can be developed for guidelines in determining criteria for the existence and search for extraterrestrial life [24, 25, 30, 54, 70, 76, 78].

1. The principal property of living matter is its ability to exist in the form of open self-reproducing systems, which possess structures for the collection, storage, transmission, and utilization of information.
2. Organic compounds containing carbon and water as a solvent form the chemical basis of life.
3. A necessary condition of life is utilization of light energy, since other sources of energy provide several orders less power.
4. Conjugate chemical processes occur in living systems involving transmission of energy.
5. Asymmetrical molecules which perform optical rotation may predominate in biologic systems.
6. The various organisms on a planet must

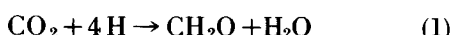
of necessity possess a number of similar basic features.

### Biologic Problems on Mars

The limits of adaptation of living systems to external influences and physical conditions on other planets, especially Mars, under which life could exist, have been discussed in detail in previous chapters. There is considerable material in the literature on theoretical analysis of possible types of metabolism of hypothetical organisms on Mars.

For the existence of active life on the planet, a necessary condition is the presence of an external nutrient medium, in which exchange of substances must take place, making accessible to the organism a rather broad variety of compounds required for its function [1]. This is also valid with regard to life forms which move about in search of materials necessary for their activity. The general energy requirements of communities of organisms must be satisfied by external sources, especially light.

The utilization of light on Mars for maintaining intensive abiogenic synthesis of organic compounds was considered difficult, since the atmosphere on the planet is in a primarily oxidized state. However, photocatalytic production on surfaces of organic compounds from CO and H<sub>2</sub>O was recently shown in simulated martian atmosphere [28]. There is another possibility of abiogenic synthesis of organic compounds as the result of capture of protons contained in solar radiation by CO<sub>2</sub> molecules:



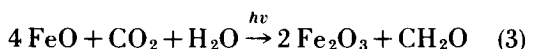
However, calculations indicate that with this source of organic compounds, with a proton flux intensity of  $3 \times 10^{19}$  particles/m<sup>2</sup> yr<sup>-1</sup>, it would be possible to have no more than a few thousand bacterial cells appear per cm<sup>2</sup>/yr, which is insufficient for the maintenance of active life [33]. Evidently on Mars the utilization of light energy by organisms, if such exist, can proceed intensively in the course of the biologic process of photosynthesis. As far as biochemical conversions of photosynthetic products are concerned, their nature may be highly diverse as a function of external conditions.

The low amount of free oxygen (0.1% of CO<sub>2</sub>) [9] in the atmosphere of Mars indicates at first glance that martian organisms could have only the anaerobic type of metabolism. However, in the absence of free oxygen in the atmosphere, other compounds containing oxygen, and even oxygen itself, may be stored inside organisms in the same way as some Earth plants with special organs for storing gaseous oxygen [1]. Utilization of compounds with high oxygen content in oxidation processes may also be possible. On Earth, the involvement of nitrates of oxygen and their reduction to nitrites in the respiration of roots of higher plants serves as an example [1]. Instead of free oxygen, therefore, it may be possible on Mars to use such compounds as sulfates, nitrates, or carbonates [90].

Hence, the low content of free oxygen does not exclude oxidation and liberation of energy by organic compounds formed in photosynthesis under martian conditions. According to another hypothesis [90], the role of oxygen in aerobic respiration for martian microorganisms may be served by iron: this element in the oxidized state is contained in limonite (Fe<sub>2</sub>O<sub>3</sub> × nH<sub>2</sub>O). The entire process may be represented as:



where the direct acceptor of the electron is Fe<sup>+3</sup>. This hypothesis has been tested experimentally with bacteria from bottom mud cultured in an oxygen-free nutrient medium, to which iron oxide (limonite) has been added. A similar process could maintain vital activity of microorganisms on Mars with simultaneous utilization of FeO as an electron donor in photosynthetic reactions. Hence, the reverse reaction occurs under the influence of light:



Under conditions of low moisture limonite may theoretically serve as a source of water for martian organisms; water is contained in this crystalline hydrate.

The martian atmosphere, containing significant amounts of CO<sub>2</sub> and CO, may be the basis for relatively simple biologic cycles occurring, in addition to photosynthesis, in which there is also utilization of carbon; the carbon is contained in

these compounds and the formation of organic substances could take place [96]. Microorganisms on Earth are known to grow in media containing CO as the sole source of carbon [84]. It is assumed that in the martian atmosphere, under the influence of sunlight, the CO<sub>2</sub> molecule dissociates as



The exothermal reaction of oxidation of CO to form CO<sub>2</sub>, taking place within the organism is:



This in turn provides energy for metabolic processes in which fixation of carbon leads to the formation of organic substances:



It is possible to combine this cycle with photosynthesis, in which water molecules splitting under the influence of light leads to production of oxygen, which oxidizes CO to form CO<sub>2</sub> and hydrogen, and reduces CO to CH<sub>2</sub>O. The theory of utilization of both CO and CO<sub>2</sub> in metabolic reactions is supported by this hypothesis.

However, there are obvious difficulties in the need for a close relationship between the photochemical reaction for dissociation of CO<sub>2</sub> in the martian atmosphere and the process of reverse oxidation of CO to CO<sub>2</sub> within the organisms. It must also be assumed that martian organisms have the ability to bind CO and O<sub>2</sub> in special complexes that interact to transform oxidized CO into CO<sub>2</sub>. The possibility of operating a carbon cycle of this type does not exclude the need for photosynthesis in maintaining vital activity of martian organisms. On the basis of modern physical and chemical conditions on Mars—low temperature, low pressure, low concentration of free oxygen, and low moisture and water vapor content—it can be assumed that the most probable forms of microorganisms are anaerobic, xerophytic, and psychrophilic [30]. Life may be concentrated in areas most suitable for its existence and not distributed uniformly over the planet's surface.

Distinctive and harsh conditions on Mars have not necessarily led to fundamental changes in the nature of biologic processes from those existing on Earth. It is entirely possible that

evolution may have followed exactly the same path in developing specialized accommodative organs and reactions which allow special metabolic processes to go on under harsh conditions, resembling those on Earth. The theory has been mentioned that special organs can retain gaseous oxygen in the organisms of martian plants, from which can be derived their hypothetical ability to utilize various aqueous mixtures at low temperatures as biologic solvents. On the other hand, the suggested ability of microbial organisms to develop special mechanisms for obtaining water under severe conditions seems somewhat exaggerated, since no such phenomena were found in microorganisms of Antarctic deserts [26]. These hypotheses show, in any case, that it is very difficult to predict in an unambiguous, theoretical fashion the existence of certain characteristics of organisms on the basis of modern conditions on a certain planet.

The final answer may only be found by taking into account the influence of external conditions under which living systems developed at all previous evolutionary stages of life forms [55]. Otherwise, it will be necessary to remain within the framework of hypothetical models of types of metabolism of extraterrestrial organisms, including those on Mars. These models can be interesting in a scientific sense, but their proximity to actual systems, and consequently the degree of reliability, must remain far from clear.

## METHODS OF DETECTING EXTRATERRESTRIAL LIFE

The practical solution of the problem, the existence and detection of extraterrestrial life forms, can only be found by direct space experiments on Mars, planned for the 1970s and 1980s. An intensive program is underway to develop life-detection methods, strategies, and tactics for use beyond the Earth. The principal goal is to obtain information on the existence of one or more characteristic properties of life. Since there is no necessary, adequate index of life, this problem can only be solved by complex utilization of a number of methods.

Although different detection methods may be used to study various aspects of vital activity of

hypothetical martian microorganisms, these methods must possess certain general features. Under conditions of space experiment, automatic functioning of each apparatus without direct human intervention must be ensured. Collected data must be encoded in a certain fashion and transformed into radio signals to be transmitted to Earth. Finally, the process of obtaining the information must not change the original condition of the sample, or, in any case, only those interventions will be allowed where influence on the sample can be predicted in advance. Clearly, not every method of laboratory investigation in biology satisfies these requirements. For example, excluded are the very fine but tedious methods of biochemical analysis suitable for specially equipped laboratories, but not suitable under conditions of experiment in space. No doubt, when it becomes possible to send sterile samples of martian soil to Earth, which was done with lunar material, these objects will be carefully studied by modern biologic methods. However, researchers must now be limited only to those methods of detecting life which lend themselves to the automatic mode and, if possible, yield unambiguous results.

The suggested methods may be divided conditionally into three major groups:

1. Remote methods of observation of planets to determine the general situation on the planet from the standpoint of signs of life.
2. Analytic methods to perform direct physical-chemical analyses of soil and atmosphere on the planet, when an automatic station lands, will ascertain the theoretical possibility of the existence of life, at least in the area where the automatic station lands.
3. Functional methods are intended for direct detection and study of samples containing basic features of living matter. By these means, questions can be answered on growth and multiplication, metabolism, ability to capture nutrient substances, and other features of life.

It is clear that optimum strategy will require correct combinations of remote, analytic, and functional detection methods at different stages in the study of the planet.

A discussion follows on individual methods, their reliability, scientific value, and the strategy and tactics of their use in exobiologic studies.

### Remote Methods

Remote methods of detecting life include techniques and instruments available both on Earth and aboard spacecraft and artificial planetary satellites. Direct detection of life by remote methods is possible only if properties of living systems cause noticeable changes in the atmosphere or on the surface of the planet.

On the surface of a planet, individual details smaller than 100 km cannot be resolved by optical methods at interplanetary distances, therefore individual organisms generally cannot be directly observed. However, as the result of vital activity of organisms, deviations from stationary conditions may be detected in the atmosphere of a planet or on its surface. A reliable sign of life could be detection on the surface of ordered structures which are difficult to explain within the framework of inorganic stationary processes [76]. Similar information on the structure of the "continents" and "seas" of Mars, the seasonal color changes on the planet's surface at various times of year, and so forth, are of considerable interest for the biologic study of Mars. Such studies, in addition to purely scientific interest, could determine the most convenient landing site for an automatic station to be used for detecting life on the surface of the planet.

The direct source of information in remote methods consists of data from passive observation of luminescence and the reflection of planets in various portions of the electromagnetic spectrum while flying around the planet. For example, it is possible to utilize infrared spectroscopy to determine the presence in the planet's atmosphere (and therefore estimate the content on the surface) of CO<sub>2</sub>, CO, O<sub>2</sub>, O, H, O<sub>3</sub>, and H<sub>2</sub>O. One of the devices is a scanning infrared sensor meant to determine concentrations of water vapor and above average temperatures. The three-channel scanning photometer is intended for studying thermal radiation of the planet's surface in the 8–12 μm range, for evidence of water vapor in the 2, 7 μm region, and for recording light

intensity in the visible region of the spectrum from 0.55 to 1.1  $\mu\text{m}$ .

An important source of information is the emission spectrum of the light from planets in the ultraviolet (UV) range due to resonance or fluorescence scattering of light by atoms in the atmosphere. The absorption spectra in the UV region are the combined result of reflection of light from the surface and scattering in the atmosphere. The emission and absorption spectra are recorded by observing the brightly illuminated or dark limb or illuminated disk of the planet by means of a telescope and a scanning UV spectrometer mounted aboard a spacecraft.

Detection of oxygen in the atmosphere on the basis of UV absorption by ozone in the 2000–3000 Å region is important. By this means, detection of molecular oxygen amounts which are excessive in comparison with photochemical equilibrium may indicate a process of photosynthesis as the source of this oxygen on Mars [2]. It is also recommended that active radar measurements be made of the planet's surface or the passage of radiation from the spacecraft located near the planet through the atmosphere to Earth. In this connection, it will be promising to employ complex utilization of an orbiting space station with an optical telescope [64]. Another powerful instrument in the study of the surface is photography of separate areas of the surface with high resolution and optimum contrast. The scientific value of the photographic method is governed primarily by correct interpretation of the pictures obtained. This is possible if a specialist expresses in advance certain information or reliable hypotheses concerning the nature of the planetary surface, thus making it possible to determine new structural characteristics on the photograph [53] for scientific evaluation.

### Analytic Methods

Analytic methods are intended for detailed investigation of the properties of a planet's soil and detection of signs of living matter in the samples. External morphologic signs of life can be studied, and the presence of complex organic substances in these samples, which are essential signs of life, can be established.

The results of analytic studies of soil samples form a necessary basis for planning subsequent biologic experiments involving the study of functional properties of hypothetical organisms. A number of diverse instruments and methodological approaches for investigating the planet have been proposed.

### *Transmission of Panoramas*

The transmission of panoramas will be conducted for a given period to determine basic topographic characteristics of the planet's surface. It will be particularly valuable to obtain and transmit stereoscopic images to serve as the basis for charts and three-dimensional topographic models of large surface areas [3].

At least two kinds of devices for obtaining and transmitting images of the martian surface are: a flow-scan television camera and an optical-mechanical scanning device. The latter, which is reliable, is based on the principle of direct conversion of a light into an electrical signal with subsequent scanning of the planetary surface by means of the optical system. The photogrammetric measurements of the size of objects, distances, and elevations on the surface obviously are necessary for a general description of the planet, not to mention the advantages from preliminary selection of the future investigation site by a mobile automatic station.

Transmitting pictures from a camera located on the surface of the planet is particularly important. A special vidicon stereoscopic camera has been developed with interchangeable objectives, capable of moving over the surface [16]. These devices have a particularly important feature: the ability to study the surrounding area in various surface regions, searching for moving objects and thereby obtaining information about possible large forms of life. Transmission of pictures for a long time, showing areas of the soil surface (even at comparatively low magnifications), could, theoretically, provide information about organisms such as insects, mollusks, and worms. Inasmuch as existence of large life forms on Mars is controversial at present, methods of obtaining pictures cannot be considered the source of direct information

on the existence of organisms, but are merely auxiliary.

#### *Sample Collection Methods*

Collection of samples is undertaken for direct study of soil from the surface or subsurface layers of the planet by special devices connected to analytic devices, which must not change sample characteristics. Obtaining the required amount of soil, and its preliminary processing prior to measurement, are necessary steps in investigating properties of the sample by analytical and functional methods usually performed on Earth under laboratory conditions. On another planet, these comparatively simple operations, that must be carried out automatically with high reliability, present tremendous difficulties.

The total weighed amount of collected soil required for analysis is governed by the sensitivity of analytic devices and the concentration of organic compounds or microbial cells in the soil to be studied.

These factors obviously influence the answer to the question of to what depth (beginning with the external surface layer), and in what mechanical condition the soil samples must be obtained. For example, in soil microbiology the technique of collecting samples determines their consistency and the type of microorganisms associated with soil particles.

Under martian conditions it will be necessary to collect not only finely dispersed "dust" samples from the surface, but also to examine subsurface layers to depths of 10 cm. From experience in terrestrial studies, subsurface layers contain not only large numbers of microorganisms, but more important, may be protected against lethal effects of UV radiation.

Biologic studies, in contrast to geologic, give preference to samples containing relatively small particles of low density. The collection of samples for biologic purposes may be divided into two categories [27]:

1. Samplers of a total mass to collect samples with particles of different linear dimensions not exceeding some upper limit ( $< 300 \mu\text{m}$ ). An example is the miniature soil drill which is driven in

and withdrawn, without rotating, bringing with it a soil sample.

2. Selective samplers to insure collection of samples with particles of certain sizes appropriate for direct analytic examination. The sampling operation is carried out by pneumatic suction and mechanical drilling with subsequent retrieval. Selection of particles is achieved by means of small openings of a certain size at the sampler output and creation of aerodynamic suction forces which will allow sampling of particles of specific sizes and densities. Selective samplers are mechanically rather simple and more suitable for collecting material for biologic and analytic studies than total mass samplers. Transmission of the sample from the sampling device to the analytic unit can be accomplished in different ways: pneumatic transport, through the influence of pressure differential, mechanical screw transmission, and mechanical lifting devices.

Prior to direct examination, samples may require additional crushing, homogenization, and sorting of particles. In studies using x-ray structural analysis, as well as gas chromatography, the sample material must be converted into a specific form to insure transportation into chambers of appropriate size and shape.

Samples must be collected at some distance from the landing site of the automatic station; this is particularly important in soft landings by braking engines, which cause undesirable increase in surface temperature and creation of chemical compounds resulting from rocket fuel combustion. Apparatus used in a hard landing also produces local damage to the surface. These facts are useful in determining the advantages of mobile samplers which are capable of moving about under control or at will over the surface, covering a large area and providing statistical reliability of sample collection from the chosen area.

Various types of sampling devices have been developed [27, 47]:

"Sticky strip" sampler (adhesion); fan collector (suction fan); aerosol collector

(suction fan); surface sample collector (backhoe); soil drill (hollow drill); rubbing conical screen (drill); rotating metallic brush on a telescoping arm (street sweeper); screw-type transport collector (drill with screw transporter); scraper-chain conveyor (grab bucket).

The most preferred methods of mechanical sampling are [61]:

The "sticky strip" method, in which long strips covered with a special substance to which dust particles will adhere, are thrown to significant distances from the landing site of the station. The samples are studied directly on the surface of the sticky strip after it is returned to the station.

Boring in the soil layer, very similar to regular methods of sampling under terrestrial conditions, enabling the largest amount of soil to be obtained.

Pneumatic aerosol collection, essentially a modification of the vacuum cleaner, which uses suction to obtain soil samples.

There is not, at present, a universal sampler suitable for all types of exobiologic studies. Therefore, the optimum method of collecting samples and the type of sampler will be determined as a function of the purpose and tasks of the specific exobiologic experiment, conditions existing on the planet, construction of the landing station, and means by which landing is made on the planet, as well as the landing site itself.

#### *Microscopy*

The microscopic method is one of the most universal and widely used in biologic studies. In exobiologic experiments, it is used to examine special preparations for external morphologic features characteristic of living forms and cells of microscopic organisms.

The possibility of detecting living forms from external morphologic features is based on fundamental concepts of the firm relationship of function and form in biologic systems at all levels of organization. In this context, for example, are special structures for providing the flow of substances through cell membranes, or clear

architectonics in the cell arrangement in organs and tissues, or a specialized plan for geometric structure of the multicellular organism as a whole. Regardless of the absence of terrestrial forms, it is believed that the existence of extraterrestrial organisms will be necessarily linked to certain geometric structures which would ensure their vital activity at all levels of organization. From this standpoint, the detection of formations with specific form, shape, color, and appearance of branched, symmetrical, regular, or aggregate structures may indicate the presence of living organisms.

A more reliable indication would be detection of internal structures in individual microscopic formations. This is a necessary feature of hypothetical martian organisms for which physiological functions, under complex conditions existing on the planet, would be necessarily linked to special morphologic structures. Discovery of mobile forms under the microscope and cessation of their movements under the influence of poison would be a definite basis for concluding that there were living forms in the sample.

The difficulty in interpreting photomicrographs should not be underestimated; even under terrestrial conditions the correct and unambiguous determination of the nature of the pictures is highly problematical.

Other arguments involve the nature of regular structures and microorganisms found in meteorites (carbonaceous chondrites) [81]. There is no doubt that these microorganisms are actually of terrestrial origin and the consequence of contamination of the meteorite substance on Earth. Thus, it is important to emphasize space-craft sterilization in seeking extraterrestrial life.

The scientific significance in exobiology which might be gained by using the microscope with other analytic and functional methods of detecting life need not be demonstrated. The microscope may be used to obtain answers to some of the fundamental questions concerning cellular forms of life, the structure of cell membranes and organelles, and reduplication processes of special morphologic structures associated with physiologic functions of the organism. Microscopy used in exobiologic studies is characterized

by a number of specific features connected with the automatic mode of operation of the station on the planet's surface.

The transmission of pictures to Earth is limited by the scope of information which can be handled by the communication channel between the automatic station and Earth. Simple calculations will show that at the usual image-scanning rate on a microscope equipped with a television attachment, a flow of information of about  $10^7$  bits/s is generated, i.e., approximately the same amount that could be transmitted through space in an entire day using radio communications between a station on Mars and a receiver on Earth [81]. This illustrates the importance of automatic methods of preliminary selection for transmitting to Earth only those pictures which may be of specific interest to the biologist.

Preliminary enrichment of the sample by mechanical selection of the most volatile particles, primarily those associated with biologic functions, may, under certain circumstances, increase the population of microorganisms and consequently the probability of finding them in the sample under the microscope. As an example, the simplified microscope can be used which weighs 0.295 kg, for biologic studies of aerosol samples of the martian atmosphere (Fig. 1). Another method is to stain the sample material with biologic fluorescent dyes (fluorogens), look at all the images under the microscope and transmit to Earth only those which show fluorescent particles.

Under the cytochemical microscope (Fig. 2), it is possible to scan strips, excited by a beam of light, containing material which has been stained with acridine orange dye. The stained area, which is the structure to be transmitted to Earth, is determined by recording through the differential method the difference in currents from two

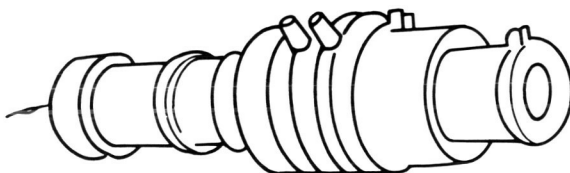


FIGURE 1.—Biological microscope for studies on Mars [81].

photomultipliers receiving the light passing through the stained and unstained parts of the sample. In this way, it is also possible to determine small concentrations of proteins and nucleic acids [59]. The method of staining biological preparations is discussed in greater detail in the section, *Optical Detection Methods*.

The use of an electron microscope has been evaluated for the study of structural elements of the microbial cell which are not visible under a light microscope [14]. Its use, in conjunction with the miniature microscope, may expand morphologic studies considerably, which are particularly important for investigating the internal molecular structure of the component elements of a living being. Use of the electron microscope combined with television technology is an important possibility, since both of these have elements in common—source of electrons, electromagnetic focusing lenses, and vidicons.

The electron image can be converted directly into electrical signals, transmitted to Earth in this form, or captured in films of ultrafine photographic emulsion, which are then transmitted to Earth by means of television technol-

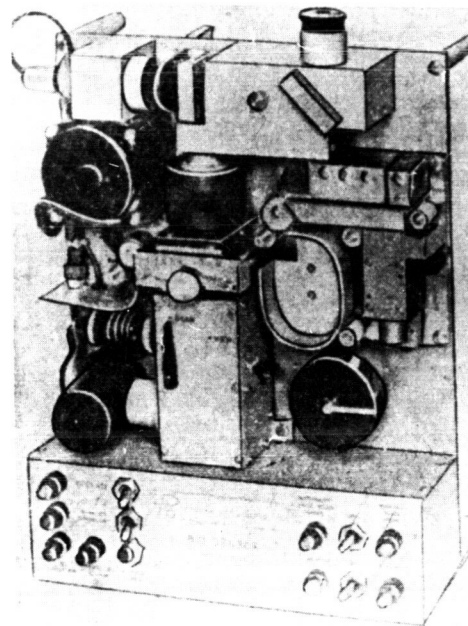


FIGURE 2.—Cytochemical microscope for exobiological research [81].

ogy. The principal technical condition for successful use of this method in exobiology is to develop types of miniature electron microscopes that can be operated under superlow temperature in liquid helium ( $1^{\circ}$ – $4^{\circ}$  K) in which the phenomenon of superconductivity can be employed. Diamond drills to obtain superthin sections can be used to collect material rapidly and directly for studies under the electron microscope. In conjunction with other methods and especially with the light microscope, the electron microscope can be a special device in exobiologic research.

#### *Gas Chromatography–Mass Spectroscopy*

Complex organic substances present in a soil sample is a necessary but not sufficient condition for the existence of life. A number of methods to determine bioorganic compounds in solutions are based on interaction of these solutions with chemical reagents (ninhydrin). Some of these methods, such as amino acid analyzers, have been automated for mass laboratory analysis.

Devices based on ion-exchange chromatography, still in the developmental stage, will be able to analyze the content, in eluents, of amino acids, purines, pyrimidines, nucleosides, nucleotides, and other compounds which absorb light in the UV region of the spectrum. Preliminary acid hydrolysis of soil samples to separate amino acids may expand considerably the possibilities of this method [4].

However, the difficulties of analyzing the absorption spectrum of a mixture of substances in the UV region, as well as the need for chemical reagents whose strict specificity for extraterrestrial organic compounds is highly problematical (they may be analogs of terrestrial amino acids, proteins, bases of nucleic acids), make such methods less suitable, at least in the first stages of investigation when acquisition of data from a broad spectrum of organic compounds is required simultaneously. The use of liquid solutions also involves considerable technical difficulties, especially under the low atmospheric pressure on Mars and therefore, is justifiable when the task is to find specific bioorganic compounds.

These considerations triggered a search for other approaches to organic analysis in extra-planetary exobiologic experiments and resulted in final development of miniature instruments using a combination of gas chromatography and mass spectrometry.

In the gas chromatography method, material in the sample is converted to a gaseous state, and its components, then carried in a stream of carrier gas, are adsorbed on chromatographic columns. Each compound in the original gas mixture is determined by comparing its relative delay time in the column with corresponding data for previously known compounds.

Hence, by using various columns, it is possible to determine the components of a gas mixture such as  $\text{CO}_2$ ,  $\text{N}_2$ ,  $\text{O}_2$ ,  $\text{H}_2$ ,  $\text{CO}$ ,  $\text{CH}_3$ ,  $\text{NH}_3$ ,  $\text{H}_2\text{O}$ , and  $\text{C}_2\text{H}_4$ . The simplest and most reliable method for primary analysis of sample material is to heat it to several hundred degrees (pyrolysis), although this procedure causes difficulties in determining the original biologic compounds on the basis of the nature of the pyrolysates which are found. Advantages of the gas chromatographic method are its simplicity, nonspecificity with respect to chemical structure of the original compounds, and comparatively small weight and size of the apparatus. The combined effect on the sample material of various solvents and extraction with subsequent thermal heating is intended to determine not only simple original compounds, but also classes of organic substances in the material under study.

Successive extractions of soil samples by hot aqueous solutions of ethanol [20] are employed to determine amino acids and carbohydrates. After triple rinsing of the extracted amino acids and carbohydrates, volatile extracts are added to them by siliconizing, and the extracts are then set into the gas chromatograph column. Another physical method of detecting organic compounds is to determine their mass spectra directly by mass spectroscopy. Mass spectroscopic study also requires evaporation of the original substance of the sample and its preliminary division into separate component parts. Both methods are highly sensitive and enable information to be obtained with  $10^{-6}$ – $10^{-9}$  g raw material. Because of these features, the mass spectrometer

and gas chromatograph may be combined in a single instrument. The essence of this combined method is that after passing through the gas chromatograph and before the sample is fed into the ion source of the mass spectrometer, most of the carrier gas is removed in a special enriching device, which simultaneously increases concentration of the substance under study. A block diagram of the device is shown in Figure 3[4].

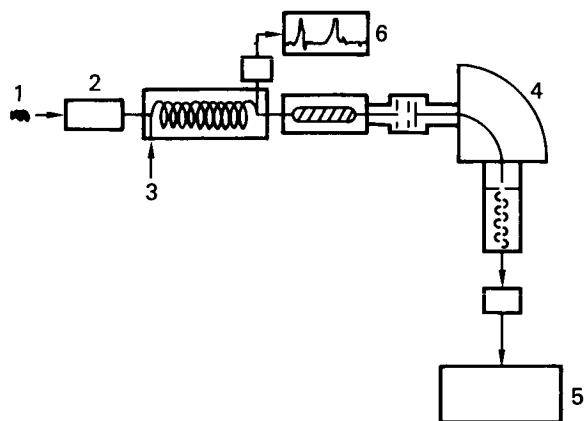


FIGURE 3.—Gas chromatograph-mass spectrometer [4]. 1, sample; 2, soil; 3, gas inlet; 4, mass spectrometer; 5, mass-spectrum recording unit; 6, chromatograph recorder.

Approximately 15 mg soil are sufficient in this kind of apparatus to determine some 70 different organic compounds. Figure 4 shows the result of a study using gas chromatography on desert soil samples. As each peak appears in turn on the chromatogram, mass spectrometric analysis is performed to determine organic substances [80].

The combined method has considerable advantages for the rapid separation of components in a complex mixture; continuous mass spectrometric analysis having high resolution— $\Delta m = 1$  with molecular weight  $M \sim 500$ —permits definition of a broad class of organic compounds in a solid, liquid, or gaseous sample. Determination of such biologically important compounds as amino acids, derivatives of sugar (hexose, pentose), fatty acids, and porphyrins makes this a very promising method in exobiology. Tests of desert soil under terrestrial conditions have shown the presence of proteins, fats, carbohydrates, and practically no hydrocarbons, and material in shale and certain meteorites is a mixture of aliphatic and aromatic hydrocarbons but no heterocyclic compounds [80].

The further development of this method for exobiologic research involves overcoming mechanical difficulties, such as a limited amount of carrier gas needed for mass analysis of the

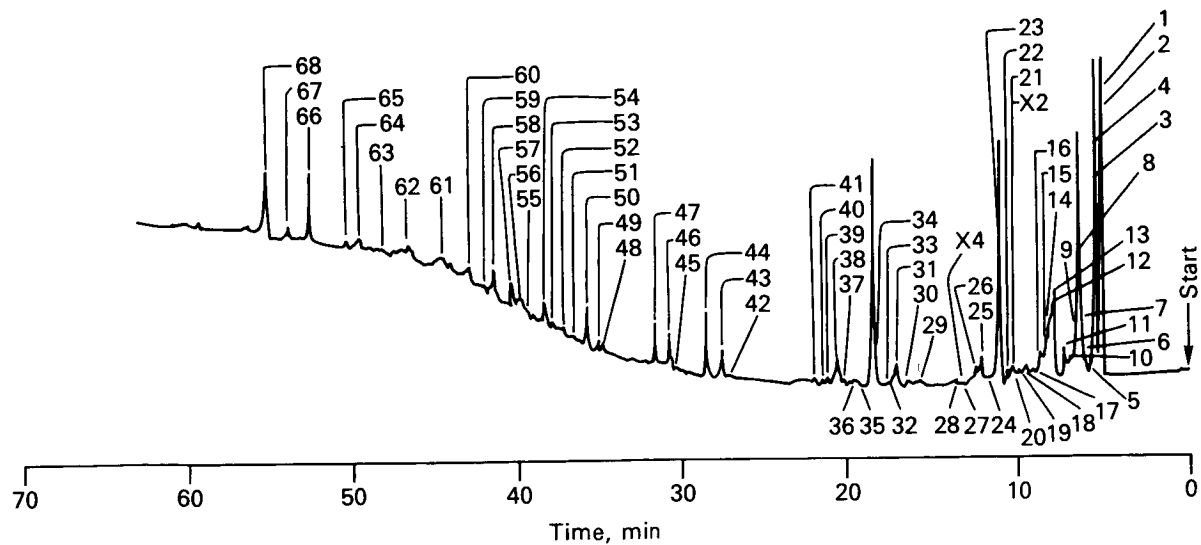


FIGURE 4.—Gas chromatogram of pyrolysis products at 500° C for a sample of desert soil. Numbers correspond to units determined on the mass spectrometer [80]: 7, acrolein; 13, propionitrile; 23, benzene; 46, furfural; 60, phenylacetonitrile; 68, indole.

substances aboard spacecraft, providing low pressure in the mass spectrometer chamber connected to the gas chromatograph, and many others. On the whole, this is unquestionably the most promising method in exobiologic research for determining, with a high degree of sensitivity, the presence of a great many diverse organic compounds on the surface of Mars.

#### *Optical Detection Methods*

Optical methods are powerful tools in modern biology for obtaining information about the state of living systems; they do not disrupt the integrity of the biologic object. Optical methods are based on the ability of molecules of bio-organic compounds to absorb or emit light with a certain spectral composition under various conditions. Depending on the purposes and conditions of the exobiologic investigation and the methods of analyzing the sample, analytic optical methods can provide information on the presence of complex organic compounds or can serve as a source of data on specific biologic processes in the study of functional properties of microorganisms. The principal optical methods proposed in exobiology and their place in the overall system of exobiologic experiments will be discussed.

A common feature of optical methods is a system for recording light fluxes, with the principal contributor a photosensitive device (photomultiplier). The types of small-scale vibration-resistant photomultipliers developed in recent years ensure high integral sensitivity with a wide spectral range and low dark current, and make it possible to record small light fluxes up to several hundred quanta/s which strike the surface of the photocathode. The same is true of modern radio electronic circuits which have been designed using the principle of differential amplifiers or memories combined with computers.

#### **Functional Methods**

It has already been mentioned that the detection of certain substances in a mixture of complex organic molecules directly on the basis of their absorption spectra in the UV region is complicated by the overlap of absorption bands. The

recording of spectra of intensities of luminescence of the molecules of organic compounds is considerably more promising.

#### *Fluorescence Methods*

*Natural fluorescence.* Absorption of a quantum of light by a system of optical electrons changes the molecule into a singlet-electron excited state, which returns to the original state in approximately  $10^{-8}$  s, accompanied by emission of quanta of fluorescence. If intramolecular conversion to the triplet state occurs during  $10^{-8}$  s, return of the molecule from the triplet level may lead to fluorescence lasting from about  $10^{-4}$  to several seconds.

The presence of characteristic peaks in luminescence spectra facilitates detection of fluorescent molecules in complex mixtures of organic compounds. This applies in particular to such molecules as chlorophyll and its derivatives, flavine enzymes, and a number of other fluorescent compounds that are important in biologic processes.

In mixtures of organic compounds, especially in biopolymer proteins and nucleic acids, the absorption of light quanta leads to migration of energy, electron excitation between adjacent molecules, so that molecules that have absorbed light and chromophoric groups that are responsible for luminescence differ from each other. In this way, bioorganic complexes can be detected by characteristic fluorescence bands under conditions where the absorption spectra cannot be resolved due to the powerful screening background of the medium and other impurities.

In biopolymers, the principal chromophores, in the case of nucleic acids, are nitrous bases of nucleotides (purines; adenine, and guanine; and pyrimidines; cytosine and thymine in DNA, cytosine and uracil in RNA). The chromophores of proteins are the aromatic amino acids: tryptophan and, to a lesser degree, tyrosine and phenylalanine [39, 91]. Excitation of proteins and nucleic acids in the near UV region of the spectrum ( $\lambda \sim 280$  nm) causes them to fluoresce in the 300–400 nm region, the nature of which is highly dependent upon the pH of the medium.

Derivatives of nucleic acids, nucleic acid bases,

or products of their interaction with other substances may also possess characteristic fluorescence patterns which make possible their detection.

On the basis of these considerations, methods have been devised for determining ribonucleotides in the alkaline hydrolysates of RNA, which contains adenosine and guanosine mononucleotides. The intensity of fluorescence of guanine and adenine in an acid medium (pH 2), and guanine in an alkaline medium (pH 10.5) makes it possible to estimate RNA content in the cells of microorganisms in soil samples. By this method, RNA can be detected in amounts as small as 10 ng, or approximately  $1-3 \times 10^5$  cells of microorganisms [65]. The fluorescence of tryptophan-containing proteins indicates their presence in a sample. It has been shown that intensity of protein fluorescence in a cell culture of *E. coli* is proportional to the concentration in the range from  $2 \times 10^7$  to  $5 \times 10^8$  cells/ml. Similar experiments with soil samples have yielded like results after preliminary centrifuging of the soil suspension to precipitate heavy colloid particles interfering with recording of protein fluorescence in the cells of the soil microflora [63, 64]. Similar measurements of fluorescence intensity of chlorophyll make it possible to determine the number of cells containing this pigment [66].

If the fluorescence intensities are measured as a function of development of a cell culture, the increase in fluorescence will be an index of cell growth in the sample. In this way, the recording of fluorescence may not only insure detection of certain bioorganic compounds, but can also act as a functional method for the study of parameters accompanying processes of vital activity (growth of cells). A great deal must still be done to increase the sensitivity of fluorescence methods under conditions intended to detect individual cells in the sample.

**Fluorescence stains.** Detection of biologic macromolecules, especially nucleic acids, by optical methods is also possible by fluorochrome, acridine orange dye, the molecules of which form bonds with nucleic acid molecules. As a result, the complex of DNA with the dye fluoresces under photoexcitation in the green area of the spectrum and RNA in the red.

The method of staining with fluorochrome detects differences in optical properties of complexes of bioorganic and inorganic compounds formed with this substance, and thereby permits use of such detection methods as fluorescence, microscopy, and others. These properties are also manifested when living cells are stained, and in light of the method's high sensitivity, opens up possibilities of detecting individual microorganisms weighing up to  $10^{-12}$  g [6, 52]. This method, used in tests to ascertain the content of nucleic acids, have given positive results on the spores of various microorganisms (*Bacillus cereus*) and vegetative cells of *Bacterionema matruchotii*, *E. coli*, *Sarcina lutea*, *Proteus OX-19*, and *Shaschaos* [6].

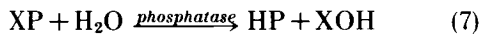
Other dyes can be used in addition to acridine orange, for example, 4,5,4,5-dibenzo-3,3'-diethyl-9-methylthiacarbocyanine bromide, which when correctly processed, reacts only with organic matter in a soil extract, producing shifts in the absorption spectrum of the dye [34]. The sensitivity of this method in detecting polypeptides, nucleotides, and so forth, is much less than with proteins, nucleic acids, and polysaccharides (< 0.002%), while purine and pyrimidine bases, amino acids, and nucleosides cannot be detected by this means. Samples must be processed in advance to remove inorganic matter, which can also cause changes in the spectrum of the dye.

The most convenient method of detecting microbial cells stained by fluorochrome is luminescence microscopy, which is used to detect, quantitatively estimate, and investigate cenoses of microorganisms. When examining a soil suspension stained with acridine orange under the microscope, after the suspension has been exposed to an exciting blue light, a color image is obtained: soil particles shine with a red color, and microorganisms are green [98, 99]. The results and pictures are usually on color or black and white film, the brightness and clarity of the images depend on the concentration of dye which must be prepared specially or combined with quenchers to suppress the luminescence of the substrate, and thereby reveal the glow of the cells of microorganisms. In many instances, living and dead cells can be differentiated by

this method. Living and surviving cells glow with a green color while dead cells are red. Under terrestrial conditions, the luminescence method reveals all groups of soil microorganisms: bacteria, actinomycetes, fungi, yeasts, algae, protozoa, and so forth.

Another optical method of determining DNA is based on reactions with desoxyribose separated from the DNA molecule with 3,5-diaminobenzoic acid in an acid medium (4N HCl). This reaction results in products which fluoresce with a maximum in the 510 nm region when excited by light with a wavelength of 410 nm. The sensitivity of this method makes possible the detection of as little as 3–4 ng DNA by fluorescence, i.e.,  $10^5$  cells of *E. coli*. One advantage of this method is that soil samples can be tested without preliminary extraction of DNA and RNA [67].

*Enzyme-phosphatases* are widely distributed among terrestrial microorganisms because of their participation in phosphate metabolism and energy transfer in cell metabolism. Determination of phosphatase activity in soil extracts may provide information concerning the existence of living systems especially since, when phosphatase is extracted in a soil medium by cells of microorganisms, their fermentative activity is retained. A general principle for determining phosphatase activity is that phosphatases in the sample catalyze the hydrolysis of the dye substrate, which is bound to the remainder of phosphoric acid in a single complex. During the reaction, free dye is liberated; unlike its phosphate derivative, it possesses the ability to fluoresce under an exciting light. Schematically, this process may be represented as:



where P is the remainder of phosphoric acid, X is the dye substrate, XP is the fluorescent complex, and XOH is the fluorescent form of the dye-fluorogen. As fluorogen (X), fluorescein dyes can be used; their derivatives (3-methoxydihydrofluoran), and  $\alpha$ -naphthol ( $C_{10}H_7OH$ ) [79, 95], possess high quantum yields of fluorescence up to 0.90–0.95 in solution of 0.1 M  $NaHCO_3$ . This explains the general high sensitivity of the method.

Figure 5 shows the curves representing the relationship between the intensity of fluorescence in the presence of the fluorescein derivative, 3-methoxydihydrofluoran-6-O, 1,6 phosphate, and the concentration of phosphatase in the medium with different periods of incubation [79]. The minimum amount of enzyme found in this experiment was  $10^{-3}$  mg/ml, which corresponds to the total activity of  $10^4$  cells of *B. subtilis*/ml in 100 min of incubation [79]. The hydrolysis rate of phosphate derivatives of this substance under the influence of phosphatase, and the fluorescence yield of free fluorogens may be markedly dependent upon reaction conditions, the pH of the medium, and other factors in this method of exobiologic research.

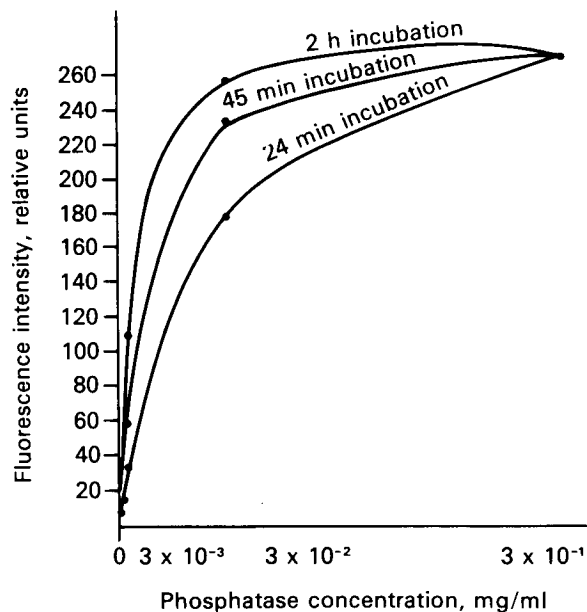


FIGURE 5.—Intensity of fluorescein dyes fluorescence vs phosphatase concentration.

The method of fluorogen staining of biochemical compounds—substrates of specific enzymes to detect enzyme activity—may be used when determining desoxyribonuclease (DNAase). The heterocyclic part of the DNA-substrate molecule for DNAase is labeled with fluorogen. Under the influence of the enzyme, low molecular products which have strong fluorescence are stripped away [85]. Derivatives of fluorescein

dye can also be used as the fluorogens, particularly sulfon of fluorescein ( $C_{19}H_{12}O_6S$ ).

Similar methods suggested for use in special devices for exobiologic experiments are called "multivators," which are intended primarily to detect phosphate activity and aminopeptidase using  $\beta$ -naphthylamides of amino acids [44]. In addition to fluorometric measurements, the multivator may also be used for colorimetric, and nephelometric analyses of reactions occurring in the 300–600 nm wavelength range, also for potentiometric measurements of the oxidation-reduction potential (see below).

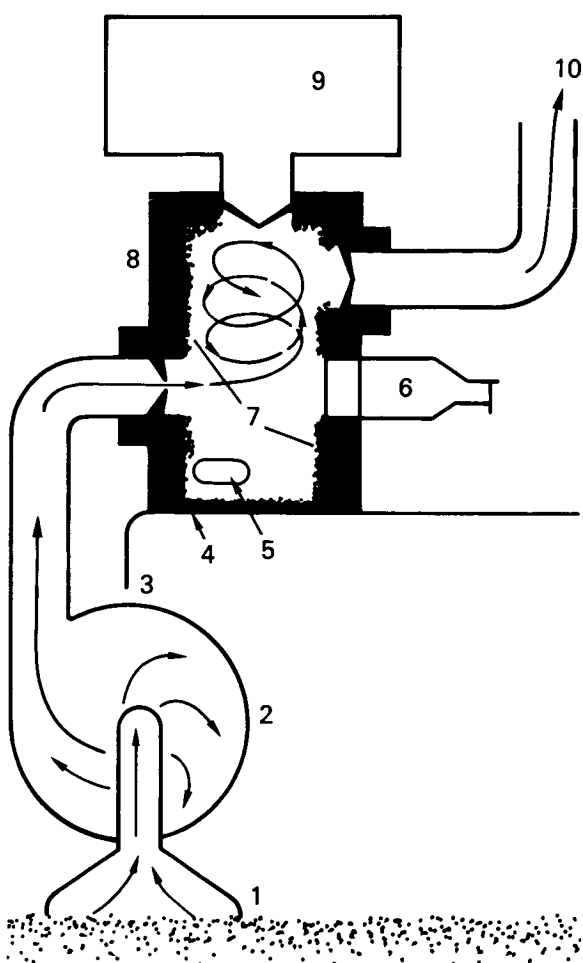


FIGURE 6.—"Multivator" chamber for determining phosphatase. 1, device for dust capture; 2, sand (air pump); 3, photomultiplier; 4, fluorescence detector; 5, substrate; 6, pilot light; 7, dust; 8, reaction chamber; 9, working fluorescein solution; 10, gas outlet.

Figure 6 shows a diagram of the multivator chamber into which dust will be drawn from the surface of Mars to determine phosphatase activity by an interaction with the phosphate derivative of fluorescein. The multivator can detect up to  $10^3$  cells in 1–10 mg of soil in 5–15 min. The device weighs 380 g, is 25 cm long, and 7 cm in diameter.

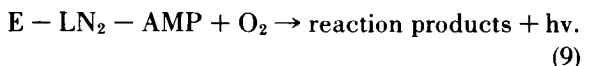
*Adenosine triphosphoric acid* (ATP) is a universal substance for storing and transferring energy in metabolic processes. ATP detected in exobiologic experiments on Mars may be due to either abiogenic origin or the presence of living forms. If the latter, as in detection of phosphatase activity, considerable similarity between biochemical systems of terrestrial and martian organisms would be indicated.

A biochemiluminescence method, based on the luciferin-luciferase reaction responsible for the chemiluminescent glow of fireflies, may be employed to detect ATP [48, 68]. The specific reducing substrate luciferin (L) is oxidized by oxygen in the atmosphere, liberating energy in the form of light under the influence of the enzyme luciferase (E). This reaction takes place in the presence of ATP, and its intensity (and consequently the number of quanta of light) is proportional to the ATP concentration.

Although details of the glow reaction have not yet been completely explained, there may be activation of the reductive luciferin ( $LN_2$ ) in the first stage and formation of an active complex of luciferyladenylate with luciferase (E) and liberation of pyrophosphate.



Further oxidation of this complex by oxygen in the air is accompanied by luminescence which can be recorded by a photomultiplier:



This method for determining ATP is convenient, precise, and widely used in biochemical investigations. Its sensitivity is a function of the possibility of detecting low light fluxes. Under laboratory conditions, the bioluminescent method may be used to determine concentrations of ATP from  $10^{-12}$  to  $10^{-17}$  g/ml; but in the  $10^{-17}$ –

$10^{-18}$  g/ml range there is a disturbance of the direct proportional relationship between intensity of light and amount of ATP in the sample valid for higher concentrations of this substance [82].

Modern technology makes it possible to record up to 100–200 photons striking the cathode of the photomultiplier. Inasmuch as one bacterial cell contains an average of  $10^3$  molecules of ATP, it is possible to detect one living cell.

To increase the glow, it is necessary to break the cell wall and release ATP into the luciferin and luciferase solution. In laboratory tests, various methods have been used, such as chemical processing of the material with perchloric acid, lysozyme, boiling, and the action of ultrasound [31]. Figure 7 shows a typical curve corresponding to the increase in the brightness of ATP extracted by boiling from the cells of soil microflora. The "diogenes" device has a mechanism

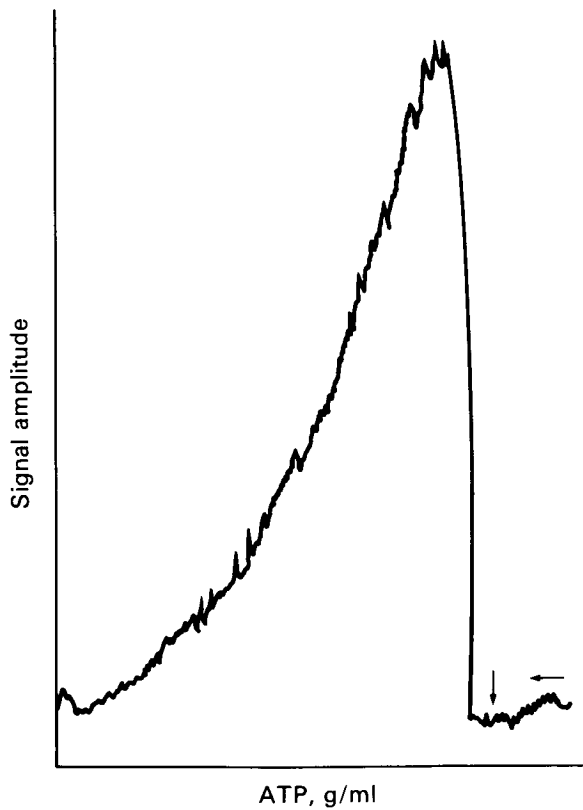


FIGURE 7.—Kinetics of luciferin-luciferase reaction (recording) with ATP in microflora from a soil sample. Value of the signal amplitude is  $10^{-11}$  g/ml ATP or  $10^6$  cells/g soil [82].

for extracting ATP from the collected sample, ampoules containing luciferin-luciferase and a standard solution of ATP, a measuring cuvette with a volume of 0.1 ml, a photomultiplier, and radio device.

#### *Incubation of Soil Samples*

To avoid indeterminacy in the composition of the nutrient medium, soil extracts can be used since the soil contains all necessary substances for the growth of natural microorganisms. This kind of natural nutrient medium may be prepared by dissolving a small amount of material from the planet surface in a small volume of fluid. Technically, this collection can be accomplished by means of a special two-layered cuvette, with the upper section containing the soil sample and the lower one, connected with it by capillaries, containing the aqueous solution [50]. By this system favorable conditions can be produced for the growth of microorganisms in the upper level and their transition into the lower level. In addition, according to data from soil microbiology, preliminary solution or mixing of the soil sample will significantly increase the number of microorganisms after sowing.

Such preliminary preparation prior to incubation of an alkaline extract from desert soil samples increases manyfold ( $2 \times 10^5$ ) the number of microorganisms in comparison with a soil sample in distilled water. The method of soil enrichment by external nutrient substances can also be used to aid natural microorganisms to adapt more easily to artificially introduced nutrients and to speed their development. In addition, the thickness of the film of soil surrounding the particles is small compared to the expected size of microorganisms ( $0.5\text{--}2 \mu\text{m}$ ), and under these conditions, cells are capable of creating favorable conditions in the microenvironment and accommodating to them [56].

Finally, exobiologic experiments are also planned without use of artificial nutrient substances or the addition of solvents (water) which, of course, may have a harmful effect on martian organisms accustomed to a small amount of moisture in their environment. These experi-

ments are intended mainly to study gas exchange between a sample of soil and the external environment and to detect changes in the composition of the surrounding atmosphere. (This will be discussed in greater detail.)

Modern exobiology assumes the use of nutrient media rich in simple organic and mineral substances in a water base. Regardless of harsh conditions existing on Mars (lack of moisture, low temperatures) to which microorganisms have become adjusted, they must obviously develop intensively when encountering rich nutrient media.

On Earth, situations have been encountered where laboratory conditions that insure optimum growth of microorganisms differ markedly from their natural medium, especially with forms that have adapted to harsh conditions. However, increased moisture content may be more harmful for martian microorganisms than an excess of nutrient media, and exobiologic experiments must take this into account.

### *Thermogenesis*

Biochemical changes that form the basis of vital activity of living systems are accompanied by irreversible dissipation of chemical energy and production of heat. From the standpoint of thermodynamics of irreversible processes, heat production may be viewed as a general functional criterion for the existence of living systems regardless of their concrete structural and chemical base.

The microcalorimetry method has long been important in studying the growth of microorganisms and seeds, and the vital activity of certain invertebrates and small vertebrates [8]. The sensitivity of modern microcalorimetry allows determination of heat production in the growth of  $10^4$  cells of bacteria in 1 ml medium. Similar measurements, carried out with soil samples, have shown that heat production curves correspond to growth curves of microflora cells [49].

A device to determine growth of soil microorganisms, presently being designed, will allow use of a sample containing  $10^6$  cells/g. Heat production can be measured during metabolism, and thermogenesis levels can be compared be-

tween living cells and the control sample of cells killed by  $HgCl_2$ . On an ordinary nutrient medium (trypsin, proteins from soybeans, glucose), up to  $10^3$  soil microorganisms have been determined. Total heat production was 47.6 cal/d which means that the rate of heat production reached 1200 mcal/s. Moisture added to dry soil samples also increased intensity of metabolism with a consequent increase in the thermogenesis rate to 10–40 mcal/s. In such water-moistened soil samples it was possible to determine up to  $10^5$ – $10^6$  cells without addition of nutrient medium.

The most sensitive method of determining thermogenesis is differential microcalorimetry, where thermocouples connected opposite one another record thermoelectric current differentials arising between two chambers containing control and experimental samples. This method has obvious advantages, the most important of which are that it is not limited with respect to the chemical nature of the processes being recorded and high sensitivity; however, microcalorimetry in exobiology still has a number of technical difficulties. These are the need for ensuring steady temperature conditions and uniform distribution of temperature between two chambers located in a cylindrical metallic tank of comparatively large size. Requirements concerning economy of weight of the apparatus, which are unavoidable in the initial stages of exobiologic experiments on Mars, clearly limit the use of this method at the start.

### *Studies of Microorganism Growth*

The simplest way to determine growth of microorganisms in liquid media is to measure the turbidity of the nutrient solution. The growth of microorganisms is accompanied by changes in absorption and scattering of light at various wavelengths, a phenomenon which has long been exploited in microbiologic research. In the near UV region of the spectrum, absorption is due mainly to proteins (280 nm) and nucleic acids (260–265 nm). In the visible region of the spectrum, light is absorbed by molecules of pigments and cytochromes; but in particular, there is a scattering of light, which is a function of the size,

concentration, refractive indices, and so forth of microorganism cells.

Changes in the scattering of light accompanying growth of microorganisms are not related to the chemical nature of the processes, which is an advantage of this method. Its use for exobiologic research is based on the assumption that martian microorganisms can live and multiply in aqueous nutrient media. The apparatus for studying the scattering of light is shown in Figure 8.

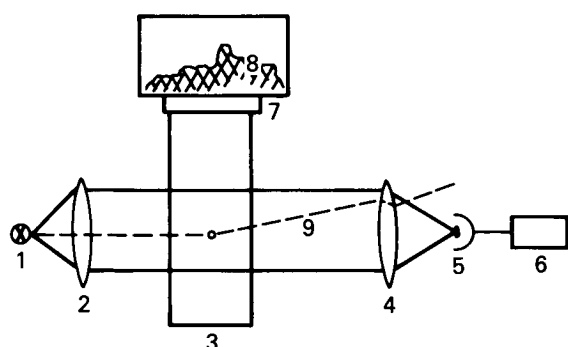


FIGURE 8.—Apparatus for measuring light scattering by cells of microorganisms. 1, measuring light source; 2, 4, fixed lenses; 3, optical cuvette with aqueous solution (lower compartment); 5, photomultiplier; 6, radiation measuring device; 7, porous filter; 8, cuvette with soil sample (upper compartment); 9, scattered beam.

A control sample consists of a suspension of cells that have been killed by poison so that their optical properties will not change with time. Comparison of optical characteristics of a sample containing living cells with a dead cell control at given intervals makes it possible to follow the dynamics of soil microflora development and to detect the minimum number of cells in the nutrient solution. The study of the time characteristics of the light scattering curves requires correct interpretation of experimental results in which the scattering of light as a function of cell growth has been determined.

One disadvantage of this and of other single-beam methods of recording optical effects in biologic objects is the strong influence exerted on instrument readings by side effects. For example, the precipitation or clumping of particles, which is not related to growth of cells in the sample, would also cause a change in their

light scattering properties. The effect of these factors can be taken into account if the control and experimental suspensions are compared periodically, at short intervals. In theory, this can be done in more complicated differential two-beam devices where a measuring beam, modulated at a frequency of several tenths of a Hz, passes alternately through both cuvettes. However, in spite of lower accuracy, single-beam measuring methods are simpler, reliable, and therefore still preferred in exobiologic research. The absolute sensitivity of proposed single-beam methods of determining light scattering properties is  $10^3$ – $10^4$  cells in 1 ml suspension,  $10^{-8}$  g/ml of protein with absorption of 280 nm [7, 82].

An important technical improvement is utilization of the above-mentioned two-section cuvettes. Microorganisms growing in the upper section in a soil sample will pass through a porous steel filter, which will prevent colloidal soil particles from reaching the measuring optical cuvette; thus, they will not disturb periodic determination of light scattering by bacterial cells. As cells grow in the soil sample, their number will increase and consequently the concentration and scattering of light in the optical cell will increase and be recorded by a spectrophotometer. The basis for this type of design is the multi-channel laboratory nephelometer (Fig. 9), which permits simultaneous measurement of light scattering in several different soil samples.

Figures 10 and 11 show curves representing the changes in the scattering and absorption of light with time at  $\lambda = 280$  nm that accompany the growth of microflora in soil samples. The nature of the dynamics of this index is the principal source of information regarding the progress of microorganism growth.

Another method of determining the growth of microorganisms is the recording of pH changes during the growth of microflora. In addition to moisture content, the pH level of soil solutions is important for development and population distribution of various groups of microorganisms. The majority of microorganisms are capable of reproducing in a neutral or nearly neutral pH, but some groups can grow at pH values between 0.6 and 11. The reproduction of microorganisms,

in turn, causes changes in pH of the medium in which they are living because of the utilization of substances and excretion into the medium of certain metabolic products. Thus, in media containing carbohydrates, the fermentation process involves the formation of acid and neutral products, while growth on protein media generally leads to alkalinization due to excretion of ammonia.

Studies [82] have shown that reproduction of microflora of different soil types in media containing glucose always led to acidification of the medium and displacement of pH toward the acid side, while in protein media there was alkalinization of the culture fluid. Thus, the growth of desert microflora from  $2 \times 10^3$  to  $3.9 \times 10^8$  cells/ml over 28 h caused a shift in pH from 6.95 to 5.4.

Similar changes depend primarily on the composition of the nutrient medium, inasmuch as this is the major factor that determines which groups of organisms can grow under

certain conditions and thus undergo changes in pH as a function of the nature of their metabolism.

The method of measuring changes in pH during growth of microorganisms requires no less than  $10^6$  cells/ml and is slightly less sensitive than the photometric method described. However, this method does have the advantage of not requiring an optically transparent medium. Determination of the growth of microorganisms is also possible by using various optical methods, which is discussed in greater detail in the section, **Analytic Methods**.

The dynamics of changes in the content of biologically important compounds during incubation of a soil sample may be an important indicator of microflora development. An increase in optical activity of the medium upon consumption of one of the optical antipodes of developing microflora can also be very indicative. This is true of sensitive methods of recording fluorescence of pigments (chlorophyll) in cells of

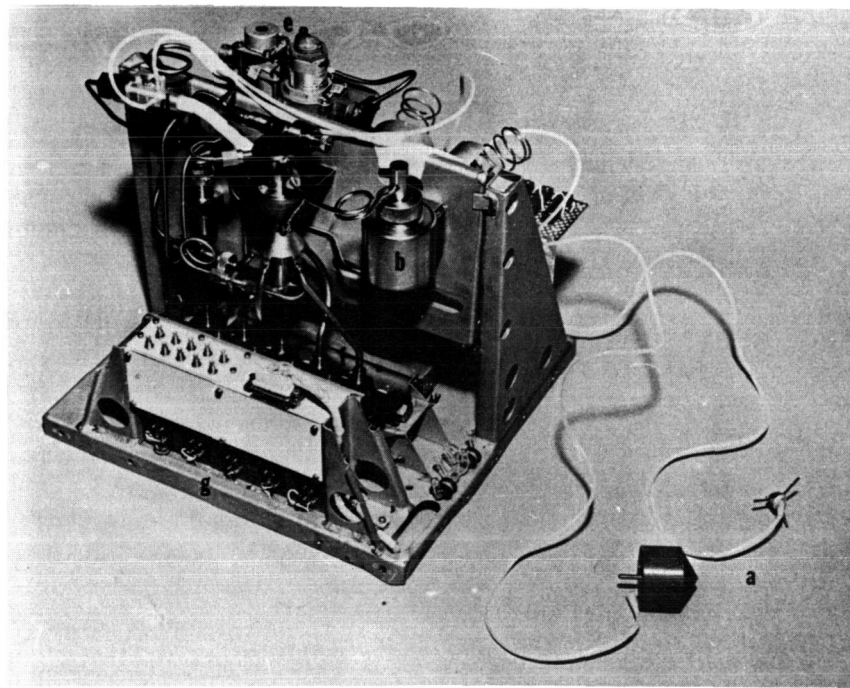


FIGURE 9.—External view of 12-channel laboratory nephelometer (Wolf Trap). a, two types of soil collector; b, reservoir containing water; c, bunker with soil distributor; d, system using a Venturi to insert soil sample (up to 25 mV); e, reduction valve for compressed nitrogen tank; f, container with five cells and tubes through which soil passes; g, container with five light sources with adjustment of intensity on feedback principle.

photosynthesizing algae (*Chlorella*), making it possible to detect an increase in the number of cells by 100–200 cells/ml during the initial few hours of growth of the culture [66].

Without exception, in all experiments involving determination of the growth of microorga-

nisms, the control must be a sample containing microflora that have been killed in one way or another, the basic indicator being the dynamics of the change in the recorded parameter during the entire growth period of the microorganisms under study.

#### Metabolism

The general biologic activity in a soil sample can be conveniently detected by measuring changes in the gaseous composition of the surrounding atmosphere resulting from the vital activity of soil microflora. On Earth, the current composition of the atmosphere is due primarily to vital activity of living systems, especially green plants. On the other hand, although the lowly microflora cannot significantly influence the general composition of the atmosphere, gaseous products of their metabolic processes may be detected in experiments with soil samples in small closed volumes. In these experiments, using gas chromatography and mass spectroscopy, there will be periodic measurement of the content of  $H_2$ ,  $CH_4$ ,  $CO_2$ ,  $Kr$  ( $He$ ) in the atmosphere surrounding the soil sample in a small closed volume [51]. These experiments are therefore intended for recording changes in composition of the martian atmosphere during a long period in a closed system, in which a sample of martian soil with nutrient medium is enclosed.

At the end of this period, and after recording any changes, the remaining gas mixture is replaced above the sample by a new portion of martian atmosphere, and the entire cycle is repeated. If the changes observed in the gaseous composition during the first incubation period are the consequence of purely physical and chemical processes involving interaction of soil components, or the nutrient medium with gaseous elements of the martian atmosphere, the corresponding reactions will be reduced as a measure of the consumption of these components and addition of new amounts of fresh martian atmosphere to the closed chamber.

On the other hand, changes in the atmosphere due to growth and vital activity of soil microorganisms will be repeated in each cycle and will increase as microflora grow. As the control, samples used have been heated to high temperatures to inactivate living systems.

FIGURE 10.—Recording of change in light scattering in microflora growth in garden soil. 1, growth curve; 2, curve corresponding to sterilized soil sample.

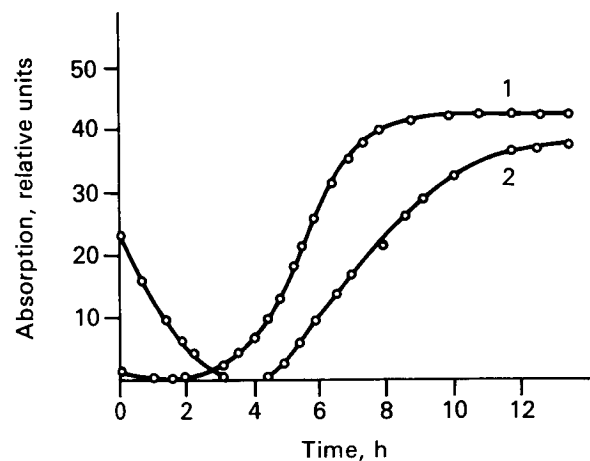


FIGURE 11.—Change in absorption of monochromatic light with  $\lambda = 280$  nm in reproduction of microflora in desert soil (+ 37° C) [83]. 1, 2.5 mg soil + 2.5 mg limonite/10 ml medium; 2, 25 mg soil + 25 mg of limonite/10 ml medium.

Similar experiments under terrestrial conditions have shown that samples contain organisms producing  $H_2$ ,  $N_2$ ,  $CH_4$  under anaerobic conditions. Other important metabolic gaseous products ( $NH_3$ ,  $H_2S$ ,  $CO_2$ ) are excreted by organisms, but they are readily soluble in an aqueous nutrient medium, so that their determination in the gaseous phase may be slightly complicated.

On the basis of the composition of the gaseous products, especially in simple nutrient media, it is possible to identify individual physiologic groups of microorganisms responsible for a specific type of metabolism, such as ammonifiers, sulfate-reducing and methane-forming bacteria, denitrifiers, and so forth. Under anaerobic conditions, denitrifying bacteria are able to use nitrates as electron acceptors in the oxidation of various respiratory substrates. This type of metabolism may be important on Mars, under conditions of a severe oxygen shortage in the atmosphere.

In order to detect denitrifiers on Mars, use of an appropriate medium with nitrate is proposed, and to detect organisms by means of the appearance of nitric oxide ( $NO$ ), nitrous oxide ( $N_2O$ ) and molecular nitrogen ( $N_2$ ) in the gaseous phase [13]. If instead of the nitrate, the intermediate product of denitrification  $N_2O$  is used, then the two gaseous components,  $N_2O$  and  $N_2$ , can be used to estimate intensity of their reduction process of  $N_2O$  by denitrifying microorganisms.

An important part in the nitrogen cycle on Earth is nitrogen fixation, which is carried out by various groups of microorganisms capable of reducing substances with a triple bond ( $N_2$ ,  $N_2O$ ,  $HCN$ ,  $C_2H_2$ ). In the reduction of these compounds, a role is probably facilitated by the same enzyme systems that participate in the reduction of molecular nitrogen. Obviously, these metabolic reactions can also be carried out by martian organisms in the course of their vital activity. Introduction of acetylene  $C_2H_2$  as an electron donor stimulates the process of nitrate ( $NO_2$ ) reduction, leading to simultaneous liberation of  $CO_2$  and nitrous oxide ( $N_2O$ ). Addition of glucose also speeds up the denitrification processes but causes development of new gas

components ( $H_2$ ,  $C_2H_4$ ). Thus, as a function of the nitrogen fixing activity and denitrifying forms of microorganisms, the content and composition of the organic substrates, and the initial concentrations of products  $NO_2$ ,  $NO$ ,  $N_2O$ ,  $N_2$ , the dynamics of the changes in the gaseous components over the soil sample will have a different nature as a consequence of these factors.

*Dynamics of gas exchange experiment.* In an experiment involving a soil sample from a greenhouse [13], the dynamics of gas exchange are shown in Figure 12 (a and b).

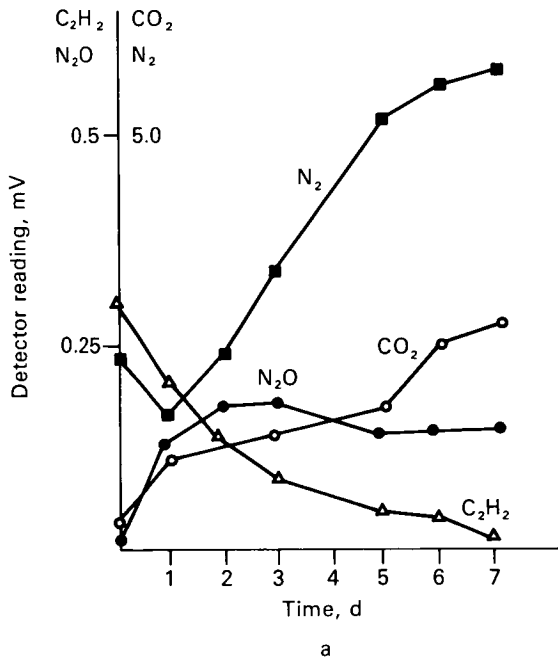
During the first few days, there is intensive release of  $N_2O$  and  $CO_2$ . Beginning with the 2nd day (in the version with glucose), the  $N_2O$  level drops off steeply until it disappears completely on the 6th day. This indicates a high degree of activity of the denitrifiers. As the result of the reduction of  $N_2O$  (2nd and 3rd days) there is an increase in  $N_2$  content in both varieties. The decrease observed in the amount of  $N_2$  during the first 24 hours—regardless of the experimental conditions—is obviously the consequence of its absorption by soil particles. However, in the course of 3 days, the nature of the dynamics of nitrogen in different versions of the experiment differed. Thus, in the absence of glucose, during the entire experiment (7 days) consumption of  $N_2$  was not observed. Introduction of glucose, however, led to its decrease during this period (3rd to 7th day).

The use of molecular nitrogen coincided with the appearance of new components in the gaseous phase— $H_2$  and ethylene ( $C_2H_4$ ). Decrease in  $N_2$  and increase in  $C_2H_4$  content indicate the nitrogen-fixing activity of soil microorganisms. Hence, the method of gas exchange in a closed system composed of soil and atmosphere makes it possible not only to determine the presence of active microorganisms, but also in many cases, to identify the important biologic processes of denitrification and nitrification in the sample under study.

*Gulliver experiment.* There is considerable use of labeled atoms in modern biology to learn the details of processes and to identify intermediate and final products. This principle, used as the basis for the method of detecting metabolism of microorganisms, has been given the

conditional name of "Gulliver" [42, 43]. In the experiment, to a nutrient medium, intended for growing martian soil microflora, organic compounds are added which have been labeled with  $^{14}\text{CO}_2$  and  $^{35}\text{S}$ . In the course of their metabolism, organisms will use the labeled substrate and excrete the gases  $^{14}\text{CO}_2$  and  $\text{H}_2^{35}\text{S}$  into the culture medium, which will be recorded by means of a soft  $\beta$ -radiation counter. This method has the advantage of a high degree of sensitivity, making it possible to observe several hundred cells/mg soil, which is very important if the possible low level of metabolism of martian organisms is taken into account. Tests on Earth have shown that even during the first 1–2 h of incubation, it is possible to detect excretion of  $^{14}\text{CO}_2$  by growing microorganisms. As the nutrient medium, labeled with  $^{14}\text{C}$  (in addition to glucose), the sodium salt of formic acid can be used as well as amino acids, proteins, and other components.

The "Gulliver" device for studying Mars consists of a sample collector, a vessel containing a nutrient medium, an incubation chamber, and a  $\beta$ -radiation counter. The sample

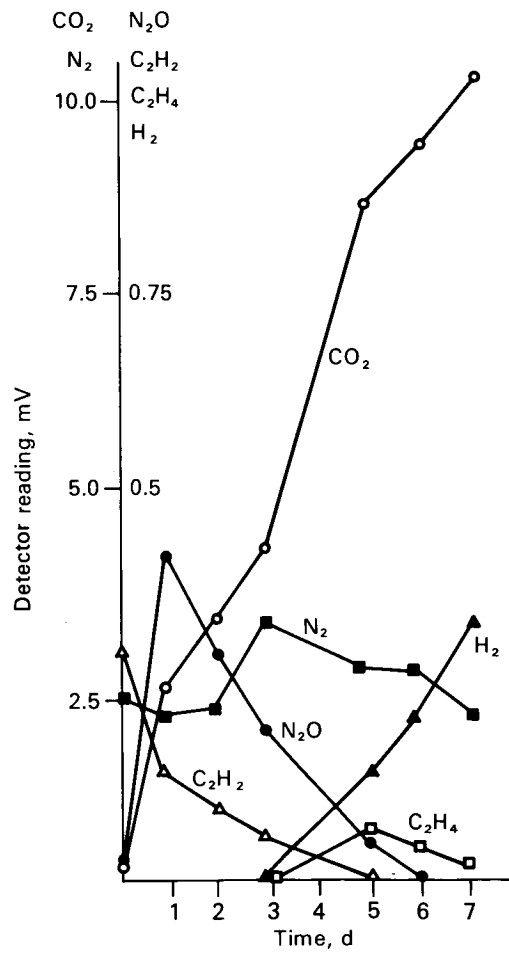


a

is collected from the soil surface by sticky strips, 6–8 m long, covered with silicon lubricant; the strips are ejected onto the surface and then drawn back into the incubation chamber, where they are submerged in the radioactive nutrient medium.

In other "Gulliver" models, experiments will be conducted directly on the planet's surface. In both cases, radioactive gas emitted  $^{14}\text{CO}_2$ , to be fixed by barium hydroxide, will be located on the surface of the counter.

The virtual absence of water on the martian surface will necessitate certain changes in preparing for future experiments on Mars. In this connection, preliminary tests of soil samples



b

FIGURE 12.—Dynamics of content change of components of a gaseous mixture above a greenhouse soil sample [13]. a, without glucose; b, with glucose.

weighing several g, which have been mixed with only 1 ml of an aqueous solution, have also shown vital activity of microorganisms. Additional studies will be necessary to determine the possibility of spontaneous decay of labeled compounds and the excretion of radioactive gas during the flight to Mars.

*Labeled nutrient media experiment.* The development and use of the method of labeled nutrient media have shown that it is possible to determine various soil microorganisms living under certain conditions (deserts, tundra, Krasnozem<sup>2</sup> [32]). The curves for the increase in  $^{14}\text{CO}_2$  may differ in shape; in all cases, they indicate vital activity in the soil in comparison with controlled inactivated samples.

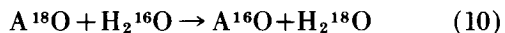
To develop methods of recording  $^{14}\text{CO}_2$  by radioactive counters, which should be highly sensitive, is another important problem. These should have a low intrinsic background and be able to function over wide temperature ranges, under mechanical stress. The use of diamond detectors is promising [40].

Determination of metabolism and particularly carbon metabolism by means of labeled atoms may be made by inclusion of radioactive  $^{14}\text{CO}_2$  or  $^{14}\text{CO}$  in organic compounds as the result of vital activity of microorganisms [29]. This approach is based on the assumption that martian organisms are capable of assimilating CO and  $\text{CO}_2$  which is contained in the atmosphere. Under CRITERIA FOR EXISTENCE AND SEARCH FOR LIVING SYSTEMS, possible types of metabolic reactions responsible for these processes were discussed, the most important of which is photosynthesis. The suggested experiment consists of a soil sample incubated in an atmosphere which contains small amounts of  $^{14}\text{CO}_2$  and  $^{14}\text{CO}$ . After several hours of incubation, the initial atmosphere is replaced by an inert gas, and the soil subjected to pyrolysis at 600° C. The gas which is then formed contains products of pyrolysis of the bioorganic compounds containing labeled  $^{14}\text{C}$ , and to some extent, remains of the original gases  $^{14}\text{CO}_2$  and  $^{14}\text{CO}$ . These are captured in a special trap and recorded

separately, while the organic products of pyrolysis are collected in a column of refractory material and heated to 700° C.

The radioactivity of their oxidation products is measured, the amount indicating the biologic activity of the assimilation processes of soil microorganisms. Under terrestrial conditions, this method can detect the fixation of  $^{14}\text{CO}_2$  in light by photosynthetic organisms in the amount of  $10^2\text{--}10^3$  cells, and in darkness by nonphotosynthetic bacteria up to  $10^5\text{--}10^6$  cells. The same method can be used to detect assimilation of  $^{14}\text{CO}$  from the atmosphere. Experiments have not given positive results if the sample was previously dried, but addition of water vapor to the chamber reactivated the microorganisms. Hence, the method suggested is capable of detecting xerophytic forms of martian organisms.

*Oxygen exchange.* Another well-known property of organisms, the ability to catalyze the exchange of oxygen between phosphate, nitrate, and sulfate anions and water, forms the foundation of a method for determining metabolism based on the stable oxygen isotope  $^{18}\text{O}$  [37]. The reaction takes place between anions labeled with  $^{18}\text{O}$  and water which contains  $^{16}\text{O}$ :



Isotope  $^{18}\text{O}$  appearing in water indicates biologic activity of the preparation. The determination is made with the aid of a mass spectrometer, into the receiving vacuum chamber of which water and dissolved gases are diffused from the sample through a teflon membrane. Experiments have yielded positive results and have shown that the most diverse cultures of cells as well as soil samples contain microflora ( $10^5\text{--}10^7$  cells/g) capable of performing catalysis of oxygen metabolism. Inactivated samples of soil and bioorganic compounds were used as controls (amino acids, purines, acetates, glycine) which did not catalyze metabolism of  $^{18}\text{O}$ .

### Photosynthesis

In exobiologic research, one of the approaches to detect photosynthesis is to study metabolism by isotopic methods (already described) applied to soil samples subjected to the action of light.

<sup>2</sup> Krasnozem—a Russian term for a zonal red soil developed in a Mediterranean climate [18a].

In this case, the controls are completely inactivated samples (by heating to 160° C), or the experiments are performed in darkness. Another possible approach is to identify the processes of light energy utilization in which the photosynthetic chain is viewed as an open system for electron transport by means of intermediate carriers (see the section, CRITERIA FOR EXISTENCE AND SEARCH FOR LIVING SYSTEMS). In this approach, an important possibility is not taking into account the concrete physicochemical nature of the products, the substrate of photosynthesis, and components of the photosynthetic apparatus, and to pose the problem of determining the functional activity of the photosynthetic chain. Most of the data on the complexity of electron transport processes in photosynthesis have been obtained by differential and pulse spectroscopy, the use of which is based on changes in the coefficient of absorption of certain wavelengths of light by carriers in oxidation-reduction processes.

Illumination of a suspension of photosynthetic organisms by exciting light or a change in its intensity causes, in turn, a change in the stationary concentration of electrons in the intermediate chain of photosynthetic carriers. In Figure 13, a recording, as a function of time, of several curves represents the transition between "dark" and "light" steady states of the photosynthetic chain during illumination by various wavelengths of exciting light. It should be noted, without going into detailed analysis of the mechanism of oxidation-reduction conversions, that the form of the transitional curves indicates the successive nature of reactions in a complex system of carriers which are responsible for these conversions.

The nature of these curves as well as the properties of the steady state which is established in the cell is a function of the physiologic state of the organism, the influence on the cell of various metabolic poisons, the gaseous composition of the surrounding atmosphere (Fig. 14), and temperature. These peculiarities make it possible to differentiate between open living systems and other complicated systems which are of nonbiologic origin.

An important parameter in evaluating the

complex nature of photo-induced pigments of the reaction is made up of induction curves, i.e., time curves showing change in intensity and average duration of fluorescence of pigments during transition of cells from the dark state to stationary light mode. In the case of ordinary dye solutions, including chlorophyll, and bacterial chlorophyll, the transitional curves have a smooth monotonic nature, and the time of the transient period is approximately  $5 \times 10^{-8}$  s. In intact living cells, the transient process time is on the order of several seconds, while the curves themselves have a complex nature [69]. It is obvious that in living systems the shape of transient curves is determined not so much by purely physical processes of deactivation of exciting molecules of pigments, as with solutions, but rather by electron transfer reactions induced by pigment. The presence of such induction curves is an indication that the molecules of pigments are included in the complex system of reactions where utilization of energy in their excited state is involved.

Chemiluminescence is another important

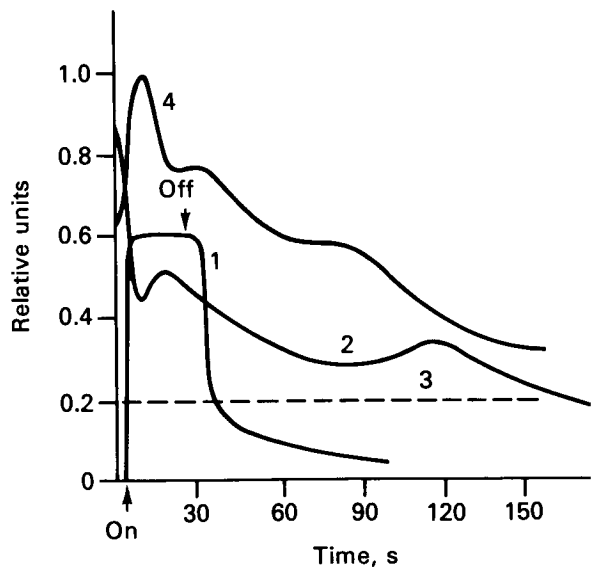


FIGURE 13.—Kinetics of transitional processes in photosynthesis chain between light and dark steady states [70]. 1, transitional curve in photosynthesis of higher plants (cytochrome absorption); 2, the same, for afterglow intensity; 3, curves 1, 2 following inactivation of sample; 4, induction curve of fluorescence with light on.

feature of living systems, in particular, photosynthetic systems, in which numerous chemical reactions are accompanied by the emission of light.

In living biologic systems, chemiluminescence has been observed in cells of photosynthetic organisms [86] and in cells of animal tissues [87]; the nature of luminance is dependent upon the state of the organism. Thus, inhibitors of metabolism change chemiluminescence intensity. In photosynthetic organisms, saturation of luminescence occurs at the same intensities of exciting light as does the saturation of photosynthesis by light. Temperature dependence of the afterglow is similar to temperature dependence of the fermentative processes, while the temperature optimum is close to the optimum for photosynthesis. When heated to temperatures above optimum, but less than + 45° C, the afterglow is reversibly suppressed; at temperatures above 45° C, there is an irreversible suppression of afterglow. Clearly, the autoemission of light quanta takes place during reversible recombination of certain intermediate products in the photosynthetic chain

with molecules of pigments. The kinetics of change in intensity of chemiluminescence in the intermediate period following extinguishing of the light (transition from light to darkness), or following exciting light turning on (transition from darkness to light), reflects the nature of the time sequence of the reactions involved in electron transfer leading to emission of a light quantum (Fig. 14).

The afterglow decay curve may be rather complex, which is the consequence of interaction of primary electron transfer reactions in photosynthesis [72].

The complicated transient curves, shown in Figure 14, indicate that the processes responsible for the appearance of chemiluminescence and fluorescence occur in an organized open system and are linked not only to the final physical act of emission of a light quantum, but also are determined by the time and spatial sequence of reactions involved in electron transport in a heterogeneous living system.

A number of parameters (chemiluminescence, fluorescence) studied under certain conditions will make it possible to confirm the presence

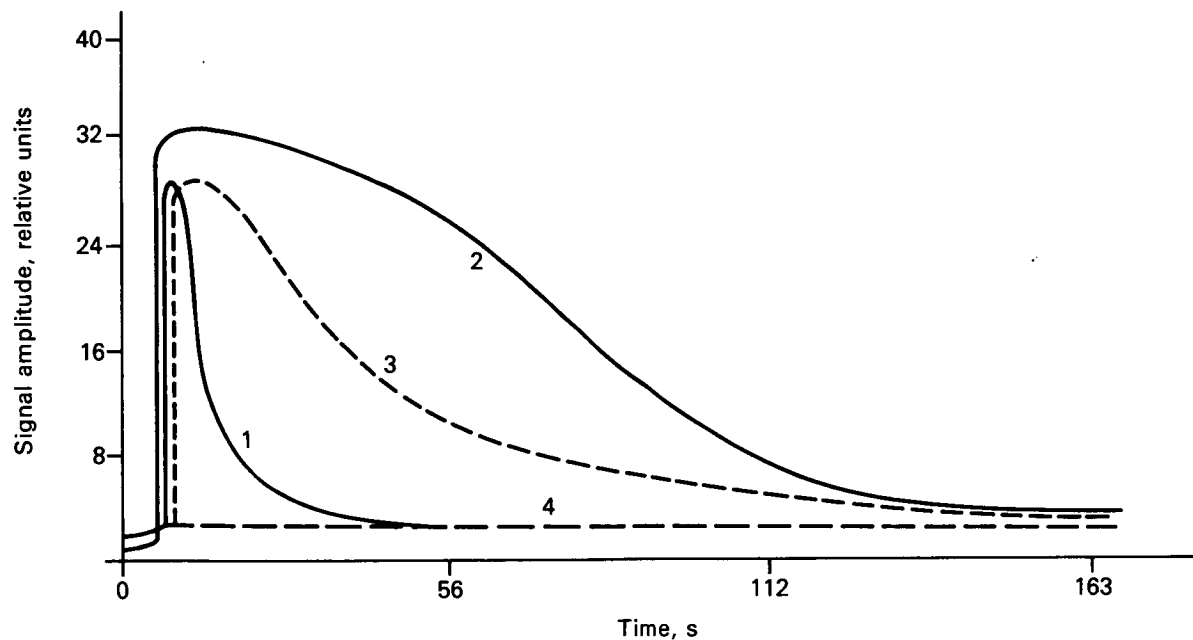


FIGURE 14.—Kinetics of chemiluminescence in reaction of luminol+H<sub>2</sub>O<sub>2</sub> [83]. 1, FeSO<sub>4</sub>, 10<sup>-4</sup> M; 2, catalase 10<sup>-6</sup> M; 3, cells of *E. coli*, 1.5×10<sup>8</sup> cells/ml; 4, limonite, sterile soil.

of certain kinds of complexly organized photobiological systems. An important requirement in such study is to have only a change in the conditions of light excitation (intensity and spectral region) in regard to the pigments contained in living systems. The range of light excitation changes is of the same order as the range of natural changes in illumination of corresponding organisms. In conjunction with the use of various reagents, inhibitors, and temperature effects, these methods may detect photosynthetic organisms and thus yield very important information about the presence of life on the planet.

### EXOBIOLOGIC STUDIES—AUTOMATIC BIOLOGIC LABORATORIES (ABL)

The exobiologic methods of detecting life (discussed in the previous section) are completely feasible from the present technologic point of view. Use of these methods will make it theoretically possible not only to detect extraterrestrial life forms, but also to learn about some of their specific characteristics. However, it has been noted that none of these detection methods, when used individually, will provide data that allow unambiguous interpretation of the presence of life.

This viewpoint differs significantly from what is encountered in experiments in space to measure physical parameters of other celestial bodies or interplanetary space. For example, the questions of the existence of a magnetic field, radiation belt in the atmosphere of a planet, and so forth, are solved by measuring the appropriate parameters, and the reliability of the data is totally a function of the accuracy and statistical reliability of the quantitative results obtained. Thus, it is sufficient to measure mass, velocity, and other physical parameters in order to have an idea of the characteristics of micrometeorites.

If reasons for a physical phenomenon and its parameters are not clear, they can be ascertained by new measurements, but the actual existence of a phenomenon is determined by the accuracy of the initial experiment. On the other hand, in exobiologic studies, separate experiments such as the increase in accuracy

of measurements, do not help to answer the basic question of the existence of life in the sample under study. The best approach (previously stated) is to combine individual methods to study the dynamics of microflora metabolism with time.

The close interrelationship of exobiologic experiments creates another difference from physical experiments. For example, experiments in growing martian microflora on artificial media must follow those involving detection of organic substances and must precede metabolic studies. On the other hand, a negative result from growing martian organisms on liquid nutrient media means that a considerable change must be made in further studies; this possibility must be allowed for on Earth.

These facts indicate that the only correct approach to exobiologic studies is to construct an automatic biologic laboratory (ABL) in which individual methods aimed at detection of life can be structurally combined, and their use controlled by a single program in the functioning of the ABL.

At present, ABLs which would include all known methods of detection are not easy to build. Therefore, depending on concrete goals, periods of launching, and lifetimes of space stations on the planet's surface, ABL designs must incorporate different kinds of instruments to reflect their usage for actual projects.

So far, these biologic laboratories have been used to answer the basic question of the existence of life, so that all appropriate projects for the ABL have many features in common. The ABL must have a collecting device or be able to provide samples by means of a collecting device which will be useful for the entire space station. After the sample is collected it will be placed in a doser-distributor, then into an incubation section where microflora will be grown at certain temperatures and light levels, enriching the sample material.

These processes can be carried out in different modes, beginning with total preservation of the initial martian conditions and terminating with the creation of temperature, pressure, and moisture similar to those on Earth. Provision must be made in the ABL system design for adding

gases at a certain pressure, and a system of vacuum valves for emptying the ABL of external atmosphere after the sample has been collected. A device for maintaining a certain temperature is also necessary both in the area where micro-organisms are grown and directly in the measuring cell where the optical parameters of the sample are determined. After specified time intervals, as microflora grow, the sample material in both solid and dissolved form will be analyzed by functional as well as analytical methods. Information on the prerequisites for the existence of life being on the planet will be obtained, presumably, by remote and analytical methods (temperature, atmospheric composition, presence of organic matter). A brief discussion will follow on some of the most highly developed ABL projects or their individual functional components.

### Viking Project

The Viking project for 1975 [36] has a plan to land a heavy station on the surface of Mars, which will carry out such exobiologic experiments as: determination of metabolism (see the section, METHODS OF DETECTING EXTRATERRESTRIAL LIFE), assimilation of CO and CO<sub>2</sub>, decomposition of the substrate labeled with <sup>14</sup>C, experiments involving gas exchange, and measurement of light scattering.<sup>3</sup> All four experiments are being conducted in parallel using data from the same sample (Fig. 15). This is very important because changes in each characteristic may reflect purely physical and chemical processes that are not related to biologic activity. A change in gas composition may be the result of chemical processes, sorption and desorption, and changes in the solubility of gases; scattering of light may vary as a function of formation of crystals and decomposition of precipitates; finally, a change in the accumulation of <sup>14</sup>C in organic products may be due to photochemical reactions. However, the probability of a synchronous change in these three parameters is practically equal to zero if active organisms are missing from the sample [56].

Nine measurement chambers are planned,

three for the experiment involving gas exchange, and two chambers each for the remaining three experiments [36]. The total weight of the ABL is to be 8.5 kg. The station will function for 90 days on the surface of the planet and will include at least three 15-day measurement cycles and one control test for each of the four experiments.

As a control, it is proposed to use samples that have been inactivated by heating to 160° C for 3 hours. The station will have injectors for pulling in the martian atmosphere, water vapor, gases with radioactive labels, and  $\beta$ -radiation counters to measure <sup>14</sup>C. A special device will monitor the sequence of experiments and change it on command from Earth. Information will be transmitted to Earth or stored first in a memory unit for the entire spacecraft.

### *Life Detection Devices*

Three characteristic methods will form the basis of another project<sup>4</sup>: photometry of the culture medium while microorganisms are developing in it, the bioluminescent method of determining iron porphyrin compounds, and the radiometric method of determining decomposition of glucose labeled with <sup>14</sup>C in the course of vital activity of microorganisms [35]. The latter method is readily modified for simultaneous determination of photosynthesis on the basis of decay of <sup>14</sup>CO<sub>2</sub> in the gaseous phase during illumination of the sample. The device has two locks for collecting soil from the planet, and the actual sample collecting will be with a sticky strip. The soil sample, weighing 1 g, will enter a dosing device which will distribute it through the operating cuvettes—25 mg to the photometric channel, 500 mg to the bioluminescent channel, and 100 mg to the radiometric channel.

After the soil has been distributed, the lock opening will be hermetically sealed and pressure in the device raised to a set value. On command from the program device, ampoules with nutrient medium and the inhibitors will enter the working and control cuvettes, and cultivation of micro-organisms will begin. The measurements will be

<sup>3</sup> According to the latest data, the method of the scattering of light has been dropped from the Viking project.

<sup>4</sup> The latest ABL project involves five methods of detecting life and makes extensive use of optical measuring devices.

carried out in six reaction cuvettes, where the light will be recorded by vibration-resistant photomultipliers and the radiometric channel will use radiation counters. The instrument will provide three measurement cycles with two repetitions each; the program device will set the time between cycles.

### *Optical Measuring Unit*

The measuring cuvette for determining optical characteristics of the material under study is one of the most important functional units in the ABL. This is apparent when analytic methods of determining complex organic compounds based on their optical characteristics are used in studying microorganism properties and individual metabolic processes by functional methods. In all these very different cases, regardless of preliminary processing of samples, whether living cells or organic compounds, investigation by optical methods in the measuring cuvette will generally be the same. Consequently, a measuring optical unit is suggested for the ABL to determine life by photobiological methods and complex

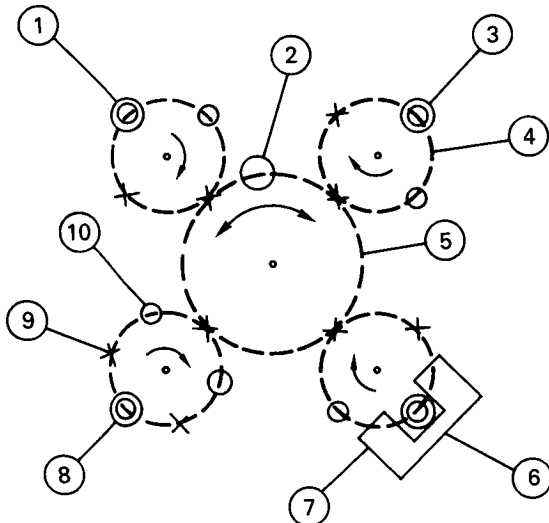


FIGURE 15.—Experiments aboard the ABL for Viking project in 1975 [36]. 1, unit for gas exchange experiments; 2, bunker for soil; 3, experiment for decomposition of  $^{14}\text{C}$  substrate; 4, measuring chamber; 5, pathway for distribution of sample material; 6, unit for experiment on light scattering; 7, optical system; 8, experimental block for  $\text{CO}_2$  and CO assimilation; 9, cell for dumping; 10, measuring chamber.

utilization of optical characteristics of the sample under study [70].

Figure 16 shows a schematic of an apparatus to obtain simultaneously several parameters of a sample from the surface of the soil. The system for exciting the object with monochromatic light and simultaneous recording by photoelectronic multipliers will allow recording in the measuring cell after automatic collection and preparation of samples of these parameters:

1. spectrum and intensity of light absorption in the 250–1000 nm range;
2. spectrum and intensity of light reflection in the 250–1000 nm range;
3. spectrum and intensity of fluorescence;
4. spectrum, intensity, and kinetics of spontaneous and photo-induced chemiluminescence;
5. bioluminescence in the presence of ATP;
6. dynamics of change in optical density in the presence of reproduction of microorganisms;
7. dynamics of change in the contents of  $\text{O}_2$ ,  $\text{CO}_2$ , and pH by means of electrodes inserted into the medium;
8. content of reduced nicotinamide-adenine dinucleotide.

Introducing various substances to the measuring cell may allow recording of practically any reaction aimed at detecting certain biologically

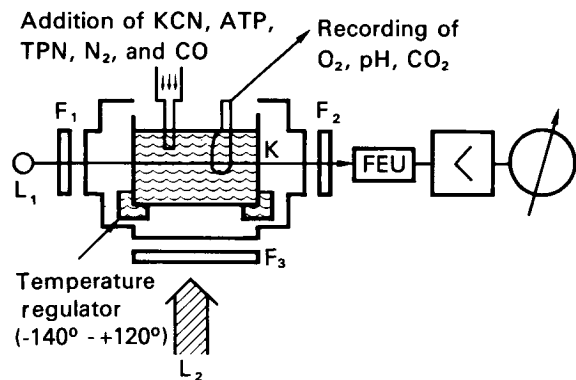


FIGURE 16.—Optical measuring unit of ABL for detecting life by photobiological methods [70].  $L_1$ , source of measuring light;  $L_2$  source of exciting light;  $F_1$ ,  $F_2$ ,  $F_3$ , light filters;  $K$ , cuvette with sample; FEU, photoelectric multiplier in circuit with amplifier and recorder.

important compounds, including complex organic molecules accompanied by a change in absorption or emission of light by the reaction medium.

It is also easy to change illumination conditions of the object in order to detect reactions of photosynthesis and other organisms whose vital activity is a function of light action. It is important to change the temperature of the sample within wide limits (+120° to -140° C), because the distinguishing feature of living systems is temperature dependence of a number of parameters.

Recording the optical characteristics not only of the solutions, but also of soil samples is an important feature. Although the sensitivity of such a device is limited by boundaries characteristic of ordinary single-beam systems ( $10^2$ - $10^3$  cells of photosynthetic organisms,  $10^{-14}$  g/ml ATP), it can be increased by modern radio-electronic means. This device has the advantage of simultaneous recording in time of a number of parameters for the same sample, which will considerably increase reliability of scientific information, lead to economy of weight, and quantity of individual instrument packages.

The current development of exobiology is very closely linked to the development of fundamental problems of biology which are of primary

importance for understanding the essence of vital processes and principles of organization of living systems.

The designs described in this chapter of the ABL and individual devices for extraterrestrial biologic research reflect the current level of knowledge in this area of natural science. This contribution can scarcely be overestimated in the detection of extraterrestrial life forms. However, the lack of life on Mars and other planets in the solar system does not exclude development of exobiology as a science, nor is it an obstacle to further improvement of automatic detection methods and collection of characteristics of living systems. The results in this area, constituting part of biologic instrument construction, will apply to modern biologic science and other branches of human activity, as well as to problems on the conquest of space, and the need for automatic monitoring of living systems under such conditions. Exobiologic experiments on Mars must take into account the possibility of detecting various precellular forms reflecting evolutionary stages of prebiologic systems, which irreversibly disappeared on Earth long ago. There is no doubt that the study of this kind of object might make invaluable contributions to the development of biologic science.

## REFERENCES

- AKSENOV, S. I. The limits of adaptation of life to extreme conditions (in connection with problems of exobiology). In, Tarusov, B. N., Ed. *Problemy Kosmicheskoy Biologii*, Vol. 19, pp. 7-89. Moscow, Nauka, 1971. (Transl: *Problems of Space Biology*), Vol. 19, pp. 1-76. Washington, D.C., NASA, 1973. (NASA TT-F-761)
- BARTH, C. A. Planetary ultraviolet spectroscopy. *Appl. Opt.* 8(7):1295-1304, 1969.
- BATSON, R. M. Photogrammetry with surface-based images. *Appl. Opt.* 8(7):1315-1322, 1969.
- BEIMANN, K. Organic analysis. *Appl. Opt.* 9(6):1282-1288, 1970.
- BERNAL, J. D. *The Origin of Life*. London, Weidenfeld and Nicolson, 1967.
- BOTAN, E. A., and H. P. HOVNANIAN. The detection of extraterrestrial life by means of a quantitative fluorescent nucleic acid acridine orange reaction. Presented at 5th Int. Space Sci. Symp., Florence, Italy, May 1964. In, Florkin, M., Ed. *Life Sciences and Space Research*, Vol. 3, pp. 95-99. New York, Wiley, 1965.
- BUCKENDAHL, D. E., L. REID, Jr., and E. LEMBERG. *Engineering Breadboard Model, Wolf Trap Microbe Detection Device*. Boulder, Colo., Ball Bros. Res. Corp., 1965. (Final rep. BBRC F65-6) (NASA CR-74214)
- CALVET, E., and H. PRAT. *Macrocalorimetrie; Applications Physicochimiques et Biologiques*. Paris, Masson, 1956.
- CARLETON, N. P., and W. A. TRAUB. Detection of molecular oxygen on Mars. *Science* 177:988-991, 1972.
- CHANCE, B., and M. NISHIMURA. On the mechanism of chlorophyll-cytochrome interaction: the temperature insensitivity of light-induced cytochrome oxidation in chromotomium. *Proc. Nat. Acad. Sci.* 46: 19-24, 1960.
- DECHEV, G., and A. MASKONA. Optimum self-adjustment of metabolic processes in the cell. *Dokl. Akad. Nauk SSSR* 162:201-204, 1965.
- DUYSENS, L. N. M. Photosynthesis. In, Butler, J. A. V., and H. E. Huxley, Eds. *Progress in Biophysics*, Vol. 14. New York, Macmillan, 1964.
- FEDOROVA, R. I. The possibility of the method of gas exchange for detecting extraterrestrial life—identifica-

- tion of denitrifying microorganisms. *Izv. Akad. Nauk SSSR, Ser. Biol.* (5):717–722, 1972.
14. FERNANDEZ-MORAN, H. *Exobiological Study: Analytical Systems for Biological Study of Mars. The Role of Electron Microscopy and Electron Optical Techniques in Exobiology*. Washington, D.C., NASA, 1965. (NASA CR-75702)
  15. FESENKOV, V. G. Conditions of life in the universe. In, Imshenetskiy, A. A., Ed. *Zhizn' Vne Zemli i Metody Yeye Obnaruzheniya*, pp. 7–16. Moscow, Nauka, 1970. (Transl: *Extraterrestrial Life and Its Detection Methods*), pp. 1–12. Washington, D.C., NASA, 1972. (NASA TT-F-710)
  16. FIELD, R. K. Electronic frog eyes may search for life on Mars. *Electron. Design* 14(Oct. 25):17, 1966.
  17. FIRSOFF, V. A. *Life Beyond the Earth; A Study in Exobiology*. London, Hutchinson, 1963.
  18. FRANK, G. M., Ed. *Kolebatel'nyye Protessy v Biologicheskikh i Khimicheskikh Sistemakh* (Transl: *Oscillatory Processes in Biological and Chemical Systems*). Symposium, Pushchino, 1966. Moscow, Nauka, 1967.
  - 18a. GARY, M., R. McAFFEE, Jr., and C. L. WOLF, Eds. *Glossary of Geology*, p. 389. Washington, D.C., Am. Geol. Inst., 1972.
  19. GIESE, A. C. *Cell Physiology*. Philadelphia, Saunders, 1962.
  20. GORYAYEV, P. P. Extraction of organic matter from soil for purposes of exobiology. *Izv. Akad. Nauk SSSR, Ser. Biol.* (5):672, 1972.
  21. GRIGOROV, L. N., A. A. KONONENKO, and A. B. RUBIN. Study of low-temperature photo-induced reactions of cytochromes and cellular sulfobacteria. *Mol. Biol.* 4:483–490, 1970.
  22. HALPERN, B. Optical activity for exobiology and the exploration of Mars. *Appl. Opt.* 8(7):1349–1353, 1969.
  23. HALPERN, B., J. W. WESTLEY, E. C. LEVINTHAL, and J. LEDERBERG. The Pasteur probe: an assay for molecular asymmetry. In, *Life Sciences and Space Research*, Vol. 5, pp. 239–249. Amsterdam, North-Holland, 1967.
  24. HOROWITZ, N. H. Study of space and the origin of life. In, Kretovich, V. L., Ed. *Problemy Evolyutsionnoy i Tekhnicheskoy Biokhimii* (Transl: *Problems of Evolutionary and Technical Biochemistry*), pp. 12–16. Moscow, Nauka, 1964.
  25. HOROWITZ, N. H. The search for extraterrestrial life. *Science* 151:789–792, 1966.
  26. HOROWITZ, N. H., R. E. CAMERON, and J. S. HUBBARD. Microbiology of the dry valleys of Antarctica. *Science* 176:242–245, 1972.
  27. HOTZ, G. M. Sampling. *Appl. Opt.* 8(7):1329–1339, 1969.
  28. HUBBARD, J. S., J. P. HARDY, and N. H. HOROWITZ. Photocatalytic production of organic compounds from CO and H<sub>2</sub>O in simulated Martian atmosphere. *Proc. Nat. Acad. Sci.* 68:574–578, 1971.
  29. HUBBARD, J. S., G. L. HOBBY, N. H. HOROWITZ, P. J. GEIGER, and F. A. MORELLI. Measurement of C<sup>14</sup> assimilation in soils: an experiment for the biological exploration of Mars. *Appl. Microbiol.* 19:32–38, 1970.
  30. IMSHENETSKIY, A. A. Detection of extraterrestrial life. In, Imshenetskiy, A. A., Ed. *Zhizn' Vne Zemli i Metody Yeye Obnaruzheniya*, pp. 27–41. Moscow, Nauka, 1970. (Transl: *Extraterrestrial Life and Its Detection Methods*), pp. 27–44. Washington, D.C., NASA, 1972. (NASA TT-F-710)
  31. IMSHENETSKIY, A. A., S. A. BUTENKO, L. A. KUZYURINA, L. M. MAKHIN, G. G. SOTNIKOV, and R. I. FEDOROVA. A comparative evaluation of different methods for detection of extraterrestrial life. Presented at 10th COSPAR Plenary Meet., London, July 1967. In, Brown, A. H., and F. G. Favorite, Eds. *Life Sciences and Space Research*, Vol. 6, pp. 170–182. Amsterdam, Holl., North-Holland, 1968.
  32. IMSHENETSKIY, A. A., B. G. MURZAKOV, A. G. VOSKANYAN, and V. K. SUROVOV. Dynamics of the decomposition of 1,6-C<sup>14</sup>-glucose by microflora from desert soil. *Mikrobiologiya* 41:727–732, 1972.
  33. Jet Propulsion Laboratory. *The Biological Exploration of Mars*. Pasadena, Calif., Calif. Inst. Technol., Jet Propul. Lab., 1967. (JPL Intern. Rep. 900–44)
  34. KAY, R. E., and E. R. WALWICK. Philco Labs developing protein detector to probe for life on Mars. *Missiles Rockets* 14(9):26, 1962.
  35. KAZAKOV, G. A. Device for detecting extraterrestrial life. In, Imshenetskiy, A. A., Ed. *Zhizn' Vne Zemli i Metody Yeye Obnaruzheniya*, pp. 76–80. Moscow, Nauka, 1970. (Transl: *Extraterrestrial Life and Its Detection Methods*), pp. 90–96. Washington, D.C., NASA, 1972. (NASA TT-F-710)
  36. KLEIN, H. P., J. LEDERBERG, and A. RICH. Biological experiments: the Viking Mars lander. *Icarus* 16:139–146, 1972.
  37. KOK, B., and J. E. VARNER. Extraterrestrial life detection based on oxygen isotope exchange reactions. *Science* 155:1110–1112, 1967.
  38. KONDRA'T'YEVA, Ye. N. *Fotosinteziryushchiye Bakterii* (Transl: *Photosynthetic Bacteria*). Moscow, Akad. Nauk SSSR, 1963.
  39. KONEV, S. V., and I. D. VOLOTOVSKIY. *Vvedeniye v Molekulyarnuyu Fotobiologiyu* (Transl: *Introduction to Molecular Photobiology*). Minsk, Nauka i Tekhnika, 1971.
  40. KOZLOV, S. F., R. I. FEDOROVA, E. A. KONOROVA, and L. M. MAKHIN. The use of diamond radiation counters in the detection of extraterrestrial life. In, *Life Sciences and Space Research*, Vol. 9, pp. 153–158. Berlin, Akad. Verlag, 1971.
  41. KUZYURINA, L. A., and V. M. YAKSHINA. Nutrient media applicable to microorganism detection on Mars. In, Imshenetskiy, A. A., Ed. *Zhizn' Vne Zemli i Metody Yeye Obnaruzheniya*, pp. 41–47. Moscow, Nauka, 1970. (Transl: *Extraterrestrial Life and Its Detection Methods*), pp. 45–52. Washington, D.C., NASA, 1972. (NASA TT-F-710)
  42. LEVIN, G. V., A. H. HEIM, J. R. CLENDENNING, and M. F. THOMPSON. "Gulliver" a quest for life on Mars. *Science* 138:114, 1962.
  43. LEVIN, G. V., and G. R. PEREZ. *Life Detection by Means*

- of Metabolic Experiments.* Presented at 12th Annu. Meet., Am. Astron. Soc., Anaheim, Calif., May 1966. New York, AAS, 1966.
44. LEVINTHAL, E., J. LEDERBERG, and L. HUNDLEY. Multivator—a biochemical laboratory for Martian experiments. Presented at 4th Int. Space Sci. Symp., Warsaw, June 1963. In, Florkin, M., and A. Dollfus, Eds. *Life Sciences and Space Research*, Vol. 2, pp. 112–123. New York, Wiley (Interscience), 1964.
45. LIPMANN, F. The current stage of evolution of biosynthesis and the development preceding it. In, Oparin, A. I., Ed. *Proiskhozhdeniye Prebiologicheskikh Sistem* (Transl: *Origin of Prebiological Systems*). Moscow, Mir, 1966. Also, Projecting backward from the present stage of evolution of biosynthesis. In, Fox, S. W., Ed. *The Origins of Prebiological Systems and Their Molecular Matrices*, pp. 259–273. New York, Academic, 1965.
46. LYAPUNOV, A. A. Control systems in organic nature. In, Lyapunov, A. A., Ed. *Problemy Kibernetiki*, Vol. 10, p. 179. Moscow, State Pub. House Phys. Math. Lit., 1963. (Transl: *Problems of Cybernetics*), Vol. 10, pp. 282–302. Washington, D. C., US Dept. Comm., 1964. (JPRS-26341)
47. *Mars Biological Sample Collection and Processing Study Program.* Final rep. St. Paul, Minn., Litton Syst. Appl. Sci. Div., 1965. (JPL-2703) (NASA CR-57724)
48. McELROY, W. D., and B. L. STREHLER. Factors influencing the response of bioluminescent reaction to adenosine triphosphate. *Arch. Biochem.* 22:420–433, 1949.
49. McLaren, A. D., and A. NOVICK. Calorimetry. In, Pittendrigh, C. S., W. Vishniac, and J. P. T. Pearman, Eds. *Biology and the Exploration of Mars*, Chap. 20, pp. 349, 406–409 (Rea, D. G., Ed. Analytical methods for landers). Washington, D. C., Nat. Acad. Sci., 1966. (NAS Publ. No. 1296; NASA CR-77938)
50. MEREK, E. L., and V. I. OYAMA. Analysis of methods for growth detection in the search for extraterrestrial life. *Appl. Microbial.* 16:724–731, 1968.
51. MEREK, E. L., and V. I. OYAMA. Integration of experiments for the detection of biological activity in extraterrestrial exploration. In, *Life Sciences and Space Research*, Vol. 8, pp. 108–115. Amsterdam, North-Holland, 1970.
52. MEYSEL', M. N. Fluorescent microscopy and cytochemistry in general microbiology. *Usp. Mikrobiol.* (7):3–32, 1971.
53. MURRAY, B. C., and M. E. DAVIES. Space photography and the exploration of Mars. *Appl. Opt.* 9(6):1270–1281, 1970.
54. OPARIN, A. I. *Zhizn', Yeye Priroda, Proiskhozhdeniye i Razvitiye* (Transl: *Life: Its Nature, Origin and Development*). Moscow, Akad. Nauk SSSR, 1960.
55. OPARIN, A. I. The development of life on Earth and beyond. In, Imshenetskiy, A. A., Ed. *Zhizn' Vne Zemli i Metody Yeye Obnaruzheniya*, pp. 16–27. Moscow, Nauka, 1970. (Transl: *Extraterrestrial Life and Its Detection Methods*), pp. 13–26. Washington, D.C., NASA, 1972. (NASA TT-F-710)
56. OYAMA, V. I., B. J. BERDAHL, G. C. CARLE, and E. L. MEREK. Experimental concepts of life detection for planetary exploration. Presented at Space Technol. and Heat Transfer Conf., Los Angeles, Calif., June 1970. In, *Space Systems and Thermal Technology for the 70's*, Pt. 1. New York, ASME, 1970. (70-AV/SPT-3)
57. PASYNISKIY, A. G. *Biofizicheskaya Khimiya* (Transl: *Biochemical Chemistry*). Moscow, Vysshaya Shkola, 1963.
58. PASYNISKIY, A. G. Some problems of the theory of the origin of life on Earth. In, Kretovich, V. L., Ed. *Problemy Evolyutsionnoy i Tekhnicheskoy Biologii* (Transl: *Problems of Evolutionary and Technical Biology*), pp. 26–30. Moscow, Nauka, 1964.
59. PETERSON, R. E., R. GINSBERG, V. W. GREENE, D. LUNDGREN, and D. ROTENBERG, et al. *Microscopic System for Mars Study Program (Feasibility Study)*. Washington, D.C., NASA, 1962. (NASA CR-50429) (JPL-2274)
60. PONNAMPERUMA, C. Life in the universe—intimations and implications for space science. *Astron. Astronaut.* 3(10):66–69, 1965.
61. PRIGOGINE, I. *Introduction to Thermodynamics of Irreversible Processes*. New York, Wiley (Interscience), 1967.
62. PRIGOGINE, I., and G. NICOLIS. Biological order, structure and instabilities. *Q. Rev. Biophys.* 4:107–148, 1971.
63. RHO, J. H. Fluorometric measurement of growth: II. Fluorescence of soil as a measure of bacterial growth. In, *Space Programs Summary 37–25*, Vol. 4, pp. 243–248. Pasadena, Calif., Jet Propul. Lab., 1964.
64. RHO, J. H. Fluorometric measurement of growth: III. The interference of soil with the fluorescence of proteins in a neutral aqueous solution. In, *Space Programs Summary 37–27*, Vol. 4, pp. 116–126. Pasadena, Calif., Jet Propul. Lab., 1964.
65. RHO, J. H. Fluorometric determination of nucleic acids. II. Assay of purines and purine nucleotides of biological samples of chemical hydrolysis. In, *Space Programs Summary 37–42*, Vol. 4, pp. 153–157. Pasadena, Calif., Jet Propul. Lab., 1966. (NASA CR-81966) (JPL-SPS-37-42)
66. RHO, J. H., and J. V. BEHAR. Fluorometric measurement of growth: I. fluorescence of chlorophyll  $\alpha$  measure of algae growth. In, *Space Programs Summary 37–24*, Vol. 4, p. 262. Pasadena, Calif., Jet Propul. Lab., 1966.
67. RHO, J. H., and J. R. THOMPSON. Fluorometric determination of nucleic acids. I. Deoxyribose assay of biological material. In, *Space Programs Summary 37–41*, Vol. 4, pp. 170–173. Pasadena, Calif., Jet Propul. Lab., 1966. (NASA CR-81201) (JPL-SPS-37-41)
68. RICH, E., and C. J. PLAKAS. Flight instrumentation for extraterrestrial detection of adenosine triphosphate. *Aerospace Med.* 39:879, 1968.
69. RUBIN, A. B. *Processes of Deactivation of Excited Molecules of Pigments in Photosynthetic Organisms*. Moscow, 1962. (Diss.)

70. RUBIN, A. B. Photobiological processes and criteria for the existence of extraterrestrial life. In, *Life Sciences and Space Research*, Vol. 9, p. 12. Berlin, Akad. Verlag, 1971.
71. RUBIN, A. B., and A. S. FOKHT. Determining the rate of growth of entropy for systems far from thermodynamic equilibrium. *Biofizika* 17:96–102, 1972.
72. RUBIN, A. B., and P. S. VENEDIKTOV. The relationship between chemiluminescence of photosynthetic organisms with light reactions of photosynthesis. *Fiziol. Rast. (Moscow)* 15(1):34–40, 1968.
73. RUBIN, L. B., O. V. YEREMEYeva, and V. V. AKHOBADZE. The influence of light on the metabolism of non-photosynthetic microorganisms. *Usp. Sovrem. Biol.* 71:220–234, 1971.
74. RUDENKO, A. P. *Teoriya Samorazvitiya Otkrytykh Kataliticheskikh Sistem* (Transl: *The Theory of the Spontaneous Development of Open Catalytic Systems*). Moscow, Mosc. State Univ. Press, 1969.
75. SAGAN, C. Biological exploration of Mars. Presented at Am. Astron. Soc. Symp. on the Exploration of Mars, Denver, June 1963. In, Morgenthaler, G. W., Ed. *Exploration of Mars*, pp. 571–581. North Hollywood, Western Period., 1963.
76. SAGAN, C. Exobiology: a critical review. Presented at 4th Int. Space Sci. Symp. (COSPAR), Warsaw, June 1963. In, Florkin, M., and A. Dollfus, Eds. *Life Sciences and Space Research*, Vol. 2, pp. 35–53. New York, Wiley (Interscience), 1964.
77. SELIGER, H. H., and W. D. McELROY. Spectral emission and quantum yield of firefly bioluminescence. *Arch. Biochem. Biophys.* 88:136–141, 1960.
78. SHNEOUR, E. A. Criteria for the detection of biological systems. Presented at Am. Astronaut. Soc. Symp., Denver, Feb. 1965. In, Morgenthaler, G. W., and R. G. Morra, Eds. *Unmanned Exploration of the Solar System*, pp. 215–223. North Hollywood, Calif., Western Period., 1965. Also in, *Advances in the Astronautical Sciences*, Vol. 19. Baltimore, Am. Astronaut. Soc., 1965.
79. SHNEOUR, E. A. *3-Methoxy-Dihydrofluoran-6-ol-6-Phosphate: A Fluorogenic Substrate for the Detection of Enzymatic Activities*. Palo Alto, Calif., Stanford Univ., Sch. Med., 1965. (IRL-1015)
80. SIMMONDS, P. G., G. P. SHULMAN, and C. H. STEM-BRIDGE. Organic analysis by pyrolysis—gas chromatography—mass spectrometry: a candidate experiment for the biological exploration of Mars. *J. Chromatogr. Sci.* 7(1):36–41, 1969.
81. SOFFEN, G. A. Extraterrestrial optical microscopy. *Appl. Opt.* 8(7):1341–1347, 1969.
82. SOTNIKOV, G. G. *The Possibility of Detecting Extraterrestrial Life by Several Physical-Chemical Methods*. Moscow, 1971. (Diss.)
83. SOTNIKOV, G. G., and S. A. BUTENKO. Detection of iron porphyrin proteins in a search for extraterrestrial life. In, Imshenetskiy, A. A., Ed. *Zhizn' Vne Zemi i Metody Yeye Obnaruzheniya*, pp. 61–71. Moscow, Nauka, 1970. (Transl: *Extraterrestrial Life and Its Detection Methods*), pp. 70–82. Washington, D.C., NASA, 1972. (NASA TT-F-710)
84. STEPHENSON, M. *Bacterial Metabolism*, 3d ed. London, Longmans, Green, 1949.
85. STEVENS, V. L. *Fluorometric Assay for Nuclease Activity*. Palo Alto, Calif., Stanford Univ., Sch. Med., 1965. (IRL-1029)
86. STREHLER, B. L., and W. ARNOLD. Light production by green plants. *J. Gen. Physiol.* 34:809–820, 1951.
87. TARUSOV, B. N., A. I. POLIVODA, and A. I. ZHURAVLEV. Detection of chemiluminescence in the liver of irradiated mice. *Radiobiologiya* 1:150–151, 1961.
88. VDOVYKIN, G. P. *Uglerodistoye Veshchestvo Meteoritov* (Transl: *The Carbonaceous Substance of Meteorites*). Moscow, Nauka, 1967.
89. VISHNIAC, W. Bacterial ecologies in limonite. Presented at 5th Int. Space Sci. Symp. (COSPAR), Florence, Italy, May 1964. In, Florkin, M., Ed. *Life Sciences and Space Research*, Vol. 3, pp. 139–141. New York, Wiley, 1965.
90. VISHNIAC, W., and D. E. BUCKENDAHL. Detection of microorganisms on the planet Mars. Presented at Am. Astronaut. Soc. Symp., Denver, Feb. 1965. In, Morgenthaler, G. W., and R. G. Morra, Eds. *Unmanned Exploration of the Solar System*, Vol. 19, pp. 325–336. North Hollywood, Calif., Western Period., 1965.
91. VLADIMIROV, Yu. A. *Fotokhimiya i Lyuminestsentsiya Belkov* (Transl: *Photochemistry and Luminescence of Proteins*). Moscow, Nauka, 1965. Jerusalem, Isr., Program Sci. Transl., 1969. (AEC-TR-6717) (TT-69-55013)
92. VOSKRESENSKAYA, N. P. *Fotosintez i Spektral'nyy Sostav Sveta* (Transl: *Photosynthesis and the Spectral Composition of Light*). Moscow, Nauka, 1965.
93. WALD, G. The origins of life. *Proc. Nat. Acad. Sci.* 52:595–611, 1964.
94. WEST, S. S., J. LISKOWITZ, V. R. USDIN, and E. A. WELCH. A polarimeter for detection of extraterrestrial life. *Proc. 18th Annu. Conf. Eng. Med. Biol.* 7:176, 1965. (NASA Contract NASw-842)
95. WESTLEY, J. *Fluorescein and Naphthol Substrates for Phosphatase Assays*. Palo Alto, Calif., Stanford Univ., Sch. Med., 1964. (IRL-1010)
96. WOLFGANG, R. Carbon monoxide as a basis for primitive life on the other planets. *Nature* 225:876, 1970.
97. YOUNG, R. S. *Extraterrestrial Biology*, p. 60. New York, Holt, Rinehart and Winston, 1966.
98. ZVYAGINTSEV, D. G. Study of adhesive microorganisms by means of fluorescence microscopy. *Biol. Nauk.* 3:11, 1965.
99. ZVYAGINTSEV, D. G. *Adsorption of Microorganisms by Soil and Its Influence on Their Vital Activity*. Moscow, 1970. (Doct. diss.)

## Chapter 9

# PLANETARY QUARANTINE: PRINCIPLES, METHODS, AND PROBLEMS<sup>1</sup>

LAWRENCE B. HALL

National Aeronautics and Space Administration, Washington, D.C. USA

### FOUNDATIONS OF PLANETARY QUARANTINE

#### The Contamination Problem

Mankind has been fascinated since ancient times by the prospect of discovering and studying extraterrestrial life forms. Now that space exploration has become a reality, the detection of planetary life or its precursors has been established as a major objective of the planetary programs of both the United States of America and the Union of Soviet Socialist Republics.

The success of these space explorations, however, is threatened by the possibility that undesired life forms might accompany man and his vehicles from one planet to another and establish themselves with unforeseeable consequences. The introduction and proliferation of terrestrial life forms could destroy the once-in-forever opportunity to examine the planets in their pristine condition. Planetary quarantine is intended to safeguard this opportunity.

Perhaps Earth is the only planet in the solar system where life can exist. Should this prove to be so, some of our efforts will have been wasted. For the present, however, planetary quarantine appears to be the proper course of action for three reasons:

(1) Terrestrial microbial life carried to a

planet by an automated or manned spacecraft may reproduce and spread on that body, confuse follow-on studies forever, and possibly mask or destroy life indigenous to that planet. The environment of the planet may be so changed that the planet's usefulness to mankind in future centuries will be seriously reduced.

- (2) An automated spacecraft intended to detect biological life on a planet must not carry terrestrial microbial life, or the instruments may detect it rather than extraterrestrial life.
- (3) The Earth may be adversely affected by organisms or materials brought back from another planet or from outer space.

Although these reasons for quarantine focus on microbial life forms as the primary contamination threat, because of their recognized ability to withstand environmental extremes and to reproduce singly, the interests of science in extraterrestrial life are not entirely confined to these forms. For example, the discovery of organic molecules that were the precursors or remnants of viable life would be of tremendous scientific significance. Accidental introduction of organic molecules or terrestrial life forms other than viable microorganisms could cause erroneous conclusions about life in the solar system. The quarantine program must address these possibilities.

The possibility of back-contamination of the

<sup>1</sup> The author expresses gratitude to V. I. Vashkov, N. V. Ramkova, T. V. Shcheglova, and B. B. Polyakov—Soviet authors of the review used in writing this chapter.

Earth by extraterrestrial life has applied so far only to manned flights to the Moon. The Lunar Receiving Laboratory (LRL), provided isolation for the returning Apollo astronauts and lunar samples. As information on martian environmental conditions accumulates, the importance of isolating and decontaminating returning Mars missions will become more evident. Meanwhile, plans must proceed on the assumption that quarantine against back-contamination will be necessary. The techniques required differ considerably from those necessary for prevention of outbound contamination by terrestrial organisms. One potential technique for unmanned missions involves remote inspection of returned samples while in Earth orbit—quarantine to be lifted and the samples brought to Earth only if tests for biological activity are negative. Another candidate technique involves encapsulation of the returned samples prior to Earth entry; a biologic barrier would then maintain quarantine during investigation of the samples on Earth.

The first significant discussions on planetary back-contamination were in Washington, D.C., in 1964, when the US National Academy of Sciences (NAS) held a conference on the potential hazards of back-contamination from the planets [17]. The recommendations of this conference, although weighted toward manned exploration of the Moon, have served as the basic guide in developing the philosophy and broad policies for the US program for control of back-contamination.

### **Development of International Planetary Quarantine Programs**

Concern over planetary contamination led to international cooperation in a program of Planetary Quarantine (PQ). In 1957 the NAS in the US expressed deep concern that contamination by early space exploration could endanger scientific investigation of the planets. The International Council of Scientific Unions (ICSU) was urged to assist in evaluating contamination hazards and to encourage development of preventive measures. Subsequently, the ICSU formed an ad hoc committee, Contamination by Extraterrestrial Exploration (CETEX) [24], to review

this issue. The committee recommended, in 1958, adoption of a code of conduct aimed at achieving a compromise between all-out lunar and planetary exploration on the one hand, and, on the other, providing maximum protection against terrestrial contamination of the Moon and planets.

At its meeting in 1959 [25], CETEX took the position that the contamination problem was an integral part of the duties of the ICSU Committee on Space Research (COSPAR), established the preceding October. As a result, COSPAR assumed responsibility for consideration of the contamination problem and has since issued a series of resolutions defining planetary quarantine objectives for launching nations.

### **Development of National Planetary Quarantine Programs**

In response to these actions developing and clarifying the meaning of planetary quarantine, the USSR and US have undertaken planetary quarantine programs. This program is administered in the US by the National Aeronautics and Space Administration (NASA).

Those directing PQ operations in both nations strive to meet the objectives set by COSPAR by first establishing realistic PQ requirements and then monitoring spaceflight projects to verify that the requirements are satisfied. A primary quarantine objective was adopted by COSPAR in 1964 in a resolution recommending an upper bound of  $1 \times 10^{-3}$ —one chance in a thousand—for the probability that a given planet will be contaminated by a program of terrestrial space exploration consisting of a number of missions over a stated time period.

Acceptance of this definitive objective opened the way for development of quantitative PQ requirements for each spaceflight mission. In the procedure developed in the US, the PQ authority subdivides the upper bound of  $1 \times 10^{-3}$  on the basis of COSPAR's estimate of the number of flights capable of causing contamination and issues to each flight project an allocation limiting the probability that that mission will result in planetary contamination. The computation of these allocations recognizes the differing con-

tamination risks of the various types of missions such as landers, orbiters, and flybys. The allotment method employed generally favors orbiter and flyby missions at the expense of landers, since the former can frequently satisfy allocations through the use of highly reliable guidance components without resort to the expensive, though effective, decontamination procedures needed by landers. The allocations assigned to several US missions are in Table 1.

### PLANETARY QUARANTINE METHODOLOGY

Planetary quarantine places constraints on planetary flight missions to minimize the probability of contamination of the planet and of the scientific experiments carried aboard the spacecraft. These constraints may affect the preparation of spacecraft and equipment for flight and the spacecraft trajectory. Since the spacecraft and equipment must be as reliable as possible to maximize the probability of mission success, care must be exercised in the selection of PQ techniques to assure that their application does not detract from the mission success.

This potential conflict of goals must be recognized both by those who establish PQ requirements and by those who select and implement contamination control measures. Effective administration and management of the PQ program must also include reasonable sensitivity to the technologic and budgetary constraints on flight projects. For these reasons, analytical and experimental studies are carried out to develop PQ techniques that have minimum impact on mission effectiveness and maximum cost effectiveness.

A major achievement of the United States PQ program has been the development of an analytical structure interrelating the various factors involved in the contamination estimation. Expanding upon a mathematical formulation of contamination probabilities first suggested by Sagan and Coleman [107], analytical models [53, 111, 119] now exist to facilitate the establishment of PQ requirements, measure their impact upon mission objectives, estimate potential contamination, determine decontamination needs, and select contamination control measures.

### Models for Probability of Contamination

The manner in which the various factors interact, in determining the extent of contamination control needed, can be illustrated with the aid of a risk allocation model. Risk is defined in terms of the probability of occurrence of the various events that can lead to planetary contamination by each of the many distinct, potentially contaminating sources.

One such model, useful in determining the extent of decontamination needed during the assembly and test of a planetary lander, is based upon an analytical formulation by a working committee of COSPAR undertaken during its 1967 meeting in London [22]. It expresses the probability that at least one of the  $N_i(o)$ <sup>2</sup> organisms present on a spacecraft at launch contaminates the planet. It is a simplification of a more rigorous formulation and assumes that the product of the probability terms on the right side of the equation is much smaller than unity.

$$P(c) = \sum_i N_i(o) \cdot P(st) \cdot P(uv) \cdot P(sa) \cdot P(r) \cdot P(g) \quad (1)$$

The value of  $P(c)$  is equal to the summation, over  $i$  distinct sources of microbial contamination, of the product of the number of microorganisms in each source and the probabilities of events occurring that effect contamination. In this equation [46]:  $N_i(o)$  is the number of viable terrestrial organisms at launch. The events of concern in this example are:

<sup>2</sup> The microbial contamination in spacecraft, before terminal sterilization procedures are applied, is determined through assay and estimation procedures, which are described in the next section of this chapter under **Estimation of Microbial Contamination Levels**. In practice, the surface contamination is determined by assaying a large number of random surface samples and statistically treating the results to obtain a conservative value of the average number of microorganisms per unit surface area. This value is then applied to the total spacecraft surface area. Applying the same assay results to the portions of spacecraft surface areas which will be joined together determines the mated microbial burden. Buried contamination is generally determined by applying the value for the mean density of organisms—similarly developed as explained in the section, **Estimation of Microbial Contamination Levels**—to the total volume of nonmetallic spacecraft materials. Reference [31] provides examples of spacecraft surface assays and resulting total surface bio-burdens for past US flight missions.

- $P(st)$ —probability that a microorganism on the spacecraft survives the stresses of interplanetary space travel
- $P(uv)$ —probability that a microorganism on the spacecraft survives the stresses of ultraviolet radiation in space
- $P(sa)$ —probability that a microorganism that has survived the stresses of space travel will survive entry into the atmosphere of the target planet
- $P(r)$ —probability that an organism on the spacecraft will be released in a viable state onto the planet's surface or into its atmosphere, given that it has survived space travel and atmospheric entry
- $P(g)$ —probability that a viable organism, deposited at random on the planet's surface or in its atmosphere, will grow and proliferate

Each of the parameters on the right side of Equation (1) can be broken down into many subparameters. For example, the probability of growth,  $P(g)$ , can include the probabilities that the species of organism can grow on the planet, that a suitable growth environment exists on the planet, and that the organism will survive transfer from the spacecraft to a favorable environ-

TABLE 1.—*Probability of Contamination Allocations for US Missions*<sup>1</sup>

Mission	Probability of contamination
Mariner Venus 1	$1 \times 10^{-4}$
Mariner Venus 2	$1 \times 10^{-4}$
Mariner Mars 3	$4.5 \times 10^{-5}$
Mariner Mars 4	$4.5 \times 10^{-5}$
Mariner Venus 5	$3 \times 10^{-5}$
Mariner Mars 6	$3 \times 10^{-5}$
Mariner Mars 7	$3 \times 10^{-5}$
Mariner Mars 8	$7.1 \times 10^{-5}$
Mariner Mars 9	$7.1 \times 10^{-5}$
Pioneer 10	$6.4 \times 10^{-5}$
Mariner Venus Mercury for Venus	$7 \times 10^{-5}$
Viking '75 (each launch)	$1 \times 10^{-4}$

<sup>1</sup> Planetary Quarantine Status Board, NASA Headquarters, Planetary Quarantine Office of Space Science, Washington, D.C.

ment. The final summation is a probability that can be compared directly with the probability-of-contamination allocation issued to that mission. This approach defines the limits of the probability of occurrence of undesirable events. A knowledge of this value and of expected fallout and indigenous levels then establishes the need for contamination control during spacecraft manufacture and preparation for launch.

In this evaluation process, space survival terms must be determined, which is accomplished by the PQ authority with the aid of scientists and researchers in space microbiology and environment studies. Many special studies are initiated under the auspices of the PQ authority to gain insight into the pertinent phenomena and reduce the uncertainty in quantitative evaluations.

### Studies of Space Survival Parameters

Studies have been conducted for the evaluation of space survival parameters by both the US and USSR. Experiments simulating deep space have proved that interplanetary environments are far less lethal to microorganisms than to other, more complex forms of life. However, some inactivation can be expected due to radiation, and to some extent from the stresses of temperature and vacuum.

The Jet Propulsion Laboratory (JPL) of the California Institute of Technology is investigating microbial survival in long-duration exposure (up to 180 days) to simulated spaceflight temperature and vacuum conditions. It appears [45] that the lethality attributable to these conditions is neither dramatic nor consistent, suggesting that reliance upon the combined effects of vacuum and temperature for significant microbial kill in deep space is not realistic. A slight initial reduction of the vegetative microbiologic population on the spacecraft can be expected, but vacuum and temperature stresses of deep space cannot be categorically regarded as sterilizing or decontaminating agents, particularly for spores.

Experimenters in the USSR as well as in the US have incubated various organisms under conditions simulating the environments of Mars, Venus, and the Moon. Under martian conditions of daily temperature alternation between  $-60^{\circ}\text{C}$

and +26° C, atmospheric pressure of 7 mm Hg, and gas composition of 80% carbon dioxide and 20% nitrogen, several desert organisms [60] were able to grow at a relative humidity as low as 3.8%. The ability of such terrestrial life forms to exist on Mars probably depends on whether this minimal amount of moisture is available.

Outer space simulation tests in the USSR [59] showed that some microorganisms and enzymes are very resistant to vacuum pressures as low as  $10^{-10}$  mm Hg. Furthermore, certain US tests [36, 95] indicate that vacuum may stabilize microorganisms. In interpreting the results of simulation experiments with vacuum, two factors must be considered. The first is that a relatively long time is involved in reaching a vacuum equivalent to space, especially if elevated temperatures are also required. The test organisms are therefore desiccated at a much slower rate than those located on the surface of a space probe during exit from the Earth's atmosphere. The second consideration, which is difficult to resolve satisfactorily, is the question of adequate controls. Even when moderate vacuums ( $10^{-3}$  mm Hg) are employed as controls, it is often difficult to establish the exact stage (application of the vacuum, extent of drying, or rehydration process) at which a cell either loses viability or is stabilized.

Ionizing space radiation other than that from solar flares and in trapped belts is not considered a significant inactivation stress; it is doubtful whether such radiation can be depended upon to destroy surface contaminants on space probes. For example, microorganisms inhabiting the water of nuclear reactors have adapted to millions of roentgens of radiation.

Ultraviolet light is a highly lethal agent in outer space. Table 2 lists the dosages necessary for 80 to 100% inactivation of unprotected microorganisms. These data are based upon US and USSR experimentation [21, 78, 109]. Despite a high degree of reflection, ultraviolet radiation is easily blocked by dust or other opaque material, such as an outer layer of microorganisms shielding underlying cells.

Experience in thermal effects of Earth reentry has been combined with postulated models of planetary atmospheres in estimating the probability that microbial contamination on landing

vehicles will survive entry into the atmosphere. These analyses are generally performed by planetary spaceflight projects since many of the trajectory and engineering parameters involved are unique to a particular mission. The results, therefore, have limited applicability to other missions.

An analysis of survivability during entry into the atmosphere of Jupiter has recently been completed [116]. Extensive surface heating and ablation is predicted, based upon the high atmospheric density and vehicle trajectories that give high entry velocities.

TABLE 2.—*Resistance of Various Microorganisms to Ultraviolet Radiation* [34]

Microorganism	UV Dosage required for 80–100% inactivation in ergs/cm <sup>2</sup> × 10 <sup>4</sup>		
	Ref [21]	Ref [78]	Ref [109]
<i>Actinomyces</i> sp	—	—	4.0–8.0
<i>Aspergillus nidulans</i>	—	—	54
<i>Aspergillus niger</i>	—	—	90–160
<i>Bacillus megaterium</i>	—	2.9	1.13
<i>Bacillus megaterium</i>	—	6.0	2.73
<i>Bacillus pyocyanum</i>	—	4.4	—
<i>Bacillus subtilis</i>	7	—	6–7
<i>Bacillus subtilis</i>	12	—	12
<i>Bacterium aertrycke</i>	—	0.048	—
<i>Escherichia coli</i>	3	1.55	1–2.5
<i>Micrococcus candidans</i>	—	3.67	—
<i>Micrococcus lysodeikticus</i>	—	—	27–50
<i>Micrococcus pyogenes aureus</i>	—	—	6.0
<i>Micrococcus radiodurans</i>	—	—	80–160
<i>Micrococcus sphaeroides</i>	—	—	10
<i>Oospora lactis</i>	5	—	—
<i>Penicillium digitatum</i>	44	—	—
<i>Pseudomonas aeruginosa</i>	—	—	1.8–3.6
<i>Pseudomonas fluorescens</i>	—	—	3.0–3.5
<i>Saccharomyces</i> sp	—	14.7	—
<i>Saccharomyces cerevisiae</i>	6	6.5	—
<i>Saccharomyces</i> (diploids)	—	—	30
<i>Saccharomyces</i> (haploids)	—	—	8.4
<i>Saccharomyces turbidans</i>	—	9.0	—
<i>Saccharomyces vini</i> (diploids)	—	—	30
<i>Salmonella typhimurium</i>	—	—	1.9
<i>Sarcina lutea</i>	—	—	19.7
<i>Serratia marcescens</i>	—	0.7	1.8–4.0
<i>Staphylococcus albus</i>	—	—	1.84–3
<i>Staphylococcus aureus</i>	—	1.54	2.18–4.95
<i>Streptococcus hemolyticus</i>	—	—	2.16
<i>Streptococcus lactis</i>	—	—	6.15
<i>Streptococcus ridans</i>	—	—	2.0

Research has recently been completed on improved estimation of the probability that organisms buried in, or on, an arriving spacecraft will be released on a planet surface in a viable state. Of the several potential release mechanisms pertinent to landings on Mars, release resulting from material fracturing on impact and from aeolian erosion were assessed in a test program conducted by the Boeing Co. [82]. Inoculated pellets of spacecraft material were fractured in high-velocity impact tests and eroded by sand blasting. The tests have supported the specification of these parameters issued for use by US flight projects<sup>3</sup> (see Table 3).

TABLE 3.—*Values Specified for Probability of Microbial Release Parameters for Martian Missions under Conditions of Fracturing Impact and Aeolian Erosion* [30, 105]

Probability of release	Landing	Value
Surface contamination	Nominal	1 to $1 \times 10^{-2}$
Surface contamination	Non-nominal	0.5
Mated surface contamination	Nominal	$10^{-3}$
Mated surface contamination	Nominal	$10^{-1}$
Buried contamination	Nominal	$10^{-4}$
Buried contamination	Non-nominal	$10^{-4}$

The estimation of  $P(g)$ , the probability that a terrestrial microorganism reaching a given planet will grow and proliferate, has received considerable attention. Laboratory tests of the ability of terrestrial organisms to grow in simulated martian environment were carried out with inconclusive results due to lack of knowledge of the availability of water in the microenvironments of the atmosphere. The Space Science Board of the NAS reviewed the evaluation of  $P(g)$  for Mars in July 1970 and recommended using a value of  $1 \times 10^{-4}$ , admitting, however, that this estimate reflected incomplete knowledge of the martian environment, and would be subject to reevaluation when further data became available. Data from US and USSR missions to Mars may support such a reevaluation.

<sup>3</sup> *Planetary Quarantine Specification Sheets*. Sept. 28, 1972, Revision 1, Nov. 1972. Issued by NASA Headquarters, Planetary Quarantine Officer.

These few examples illustrate how a laboratory-based research program has eliminated information gaps and helped develop quantitative space survival probabilities that can be technically substantiated and effectively utilized in establishing valid contamination control procedures.

## STANDARDS AND GUIDELINES

In determining the need for contamination reduction and control procedures, microbial contamination levels must be anticipated. The effect of spacecraft assembly and test operations upon these levels must also be estimated.

The PQ authority assists, on the basis of laboratory research, in the estimation of these parameters and guides flight project groups by issuing contamination control technology information with guidelines for its application.

### Estimation of Microbial Contamination Levels

Microorganisms can be enumerated through assay, in the case of accessible surface contamination, or by estimation, for those levels which cannot be directly sampled without damaging the spacecraft.

*Accessible contamination.* The accurate enumeration of microorganisms on surfaces requires recognition and consideration of a number of factors. Surfaces associated with spacecraft are composed of a wide variety of materials with many surface finishes. In addition, some of the materials contain substances that inhibit the growth of microorganisms. Consequently, assay procedures for space hardware have been designed to separate microbial contamination from surfaces for subsequent culturing.

Microorganisms that have been present on surfaces for long periods, or that have survived decontamination treatments, tend to adhere quite tenaciously. The consequent difficulty of removal can markedly affect the accuracy of the assay. In addition, microorganisms in nature usually do not occur as single cells but rather in clumps and aggregates made up of many cells. Standard techniques for the microbiologic sampling of surfaces [32, 100] such as the rinse, swab-rinse, and direct contact plate [48], do not dis-

tinguish between individual cells and aggregates of cells and hence can lead to enumeration inaccuracies. Although the rinse and swab-rinse tests do allow for some breaking up of clumps by manual or mechanical shaking, there is variation in detection counts. Recovery efficiencies vary not only according to size, composition, and finish of the surfaces, but also among personnel performing the assays.

New techniques have been developed not only to reduce this variability, but also to increase recovery of microorganisms from space hardware. One technique, the vacuum probe, resulted from a study initiated to develop a surface sampler that could be used on large surface areas [76, 103].

Puleo et al [100] used an ultrasonic vacuum probe to effectively recover microorganisms from a variety of surfaces, even when bacterial spores were "heat fixed" to the test surfaces. Ultrasonic energy broke up clumps of microbial cells into smaller aggregates and single cells. Both factors, removal and declumping, markedly improved the accuracy of the assay. Subsequent studies [99] showed that ultrasonic baths produced the same recovery efficiencies as the ultrasonic probe. Also, the ultrasonic baths were easy to use and permitted processing more samples in a given period. This procedure works equally well for spores and vegetative microorganisms and does not produce any detectable lethal effects on microorganisms. Consequently, ultrasonic energy is employed in assaying microbial surface contamination, whether on stainless steel fallout strips, piece parts, swabs from the surfaces of space hardware or filters, or probe tips of vacuum probes. Vacuum probes and ultrasonic collectors cannot be used on spacecraft, however, since the ultrasonic energy can damage sensitive parts. As a result, there is almost complete reliance on the swab-rinse technique in detecting surface contamination levels. Ultrasonic energy can be applied as soon as the sample has been recovered from the spacecraft material surface. A second innovative collection technique, capable of removing a large sample of surface contamination, has been developed by the Phoenix Laboratories of the US Public Health Service, Center for Disease Control. The sample is collected by wiping

the entire surface of interest with a sterile, rayon cloth (commercially available in the US). Micro-organisms collected by the cloth are recovered by sonication in a rinse solution which is then assayed. This wipe-rinse technique exhibits a sampling efficiency comparable to that of other techniques but has the marked advantage of recovery from larger surfaces and consequently produces more valid results [33].

*Inaccessible contamination.* Contamination located between joints (mated contamination) or encapsulated within material is generally inaccessible for direct assay; its levels are estimated by methods and guidelines established through experimentation and experience. Mated contamination is accessible on the surfaces of the parts prior to hardware assembly, and can be assayed at that time. The usual approach to its enumeration is to establish, by assay, the surface contamination density existing at the time of assembly, and to use this value in conjunction with the extent of mated surface areas to develop a conservative estimate for the total mated surface contamination level. In this approach the assumption is made that there is no growth or die-off once the parts have been permanently mated.

Viable organisms encapsulated within solid materials can be released to a planet surface if the solid should be fractured, eroded, or deteriorate. In an effort to provide a basis for estimation of microorganisms contained within space-craft materials, several research groups have attempted quantitative recovery of viable microorganisms from solid materials. US investigators showed in 1960 [87] that certain types of electronic piece parts contained viable microorganisms internally. As a result of this work, JPL investigators and their subcontractors in the Dynamic Science Corp. initiated studies to define both microbiologic and engineering problems of interior contamination assay [76, 103]. Subsequently, similar studies were initiated by workers in the Phoenix Laboratories, US Public Health Service (USPHS), Center for Disease Control [101], the USPHS in Cincinnati [4, 5, 6], and at the University of Minnesota [43]. The pertinent results of these studies can be summarized in the following paragraphs.

In conducting assays of encapsulated microorganisms, the objective is to reduce solid material to a size small enough to ensure release of embedded microorganisms without harming them. If microorganisms are killed, the extent of kill should be consistent from test to test.

No single assay system is suitable for measuring the internal contamination of all potentially contaminated materials. Hard materials can usually be ground or pulverized, but the rate of kill for embedded microorganisms may be high.

Some polymers can be dissolved by nontoxic solvents to free embedded microorganisms which can then be plated out and counted [49]. Relatively soft materials which do not lend themselves easily to pulverization at ambient temperatures can be treated with liquid nitrogen, which makes them brittle enough for pulverization. However, this problem is far from solved.

Some materials contain toxic substances which must be chemically neutralized or physically removed from the microenvironment prior to culturing.

Solidification, polymerization, and storage of solids can contribute to a significant die-off of embedded test microorganisms when model systems are used to evaluate various recovery techniques.

Recent work in the US conducted jointly by the USPHS and Exotech Systems, Inc., resulted in an estimation technique for buried bioburden based upon an analytical model that accounts for the uncertainties of assay techniques [73]. The model was exercised using all known data obtained by laboratory fracturing, grinding, dissolving, and disassembling, as appropriate, various samples of solid materials and spacecraft piece parts. The results led to a specification conservatively stated as 130 spores/cc as a mean density of organisms in nonmetallic spacecraft materials.

This conservative specification can be used in estimating the contamination encapsulated in materials produced in the US as they are received for fabrication and assembly. Such information can eliminate the need for extensive bioassay by flight projects. As further aids to flight projects,

standards and advisory procedures have been issued by the PQ authority which include selection of a standard test microorganism, decontamination and sterilization methods, standards for microbiologic assay, and values for microbial death rates. These standards are based upon experimental investigations sponsored, in the main, by the PQ authorities of the USSR and the US.

The *Bacillus subtilis* var. *niger* spore has been selected in the US as a representative organism for testing the effectiveness of decontamination or sterilization procedures used in a planetary flight program [80]. Extensive knowledge exists about this microorganism and standardized cultures are readily available from the Phoenix Laboratories, Center for Disease Control. Its dry-heat inactivation characteristics are well-known from extensive studies and are being compared with those of naturally occurring contamination experienced in spacecraft fabrication and testing in substantiating sterilization processes [120].

Spore inactivation in dry-heat sterilization is specified in terms of a *D*-value, the time required to reduce the mean viable microbial population by a factor of 10. An important question in using a *D*-value to describe the die-off behavior of microorganisms is whether or not inactivation kinetics are exponential, i.e., linear on a semilogarithmic plot, or instead possess either a shoulder or a tailing effect. The presence of a shoulder suggests the need for additional time to reach a specified level of decontamination and a tailing effect indicates that a portion of the population will survive a given treatment, independent of the duration of exposure. Either effect may negate much of the usefulness of the *D*-value concept in establishing sterility requirements. Despite the current uncertainty of the validity of the exponential approximation, the *D*-value concept has been found operationally useful in the design, implementation, and verification of heat sterilization measures. Further research to detect any tailing effect in naturally occurring populations is underway in the US.

The *D*-value is a function of the accessibility of the microbial population and the temperature and moisture content of the surroundings. In

practice,  $D$ -values are specified at 125°C with a maximum allowable moisture content. A scaling factor, defined as a  $Z$ -value, permits extrapolation of  $D$ -values to other sterilizing temperatures. Table 4 presents dry-heat sterilization specifications currently in use in the US.

TABLE 4.—Dry Heat Specifications

Temperature	100°C min.
Max. RH	25% at 0°C and 76 mm Hg
$D$ -Values	
Buried burden	5 h
Mated surface burden	1 h
Exposed surface burden	1/2 h
$Z$ -Value	21°C
Temperature scaling function	$D_T = D_{125} \cdot 10^{\frac{125-T}{Z}}$ where $D_T$ is $D$ -value at temperature $T$ in °C

Other standards have been issued to cover contamination control methods. Both heat and ethylene oxide are acceptable decontamination techniques for US spaceflight programs. The USSR employs these and other techniques (described in a later section). Guidelines resulting from experimentation describe the use of barriers to limit microbial accumulation in and on spacecraft. A description of the methods for reducing the number of microbes in spacecraft assembly areas is given in the next section, CONTAMINATION CONTROL TECHNIQUES.

### Contamination Source Analysis

A probability-of-contamination analysis is performed by flight projects to determine the need for contamination control and to assist in selection of proper control measures. Determining the probability of contaminating a planet requires: (1) identifying all possible contamination sources associated with a mission; (2) determining the initial contamination levels associated with each source; (3) determining the contamination level at time of launch; (4) determining whether this level—or some fraction of it—can physically reach the planet; and, (5) determining what fraction of the contamination level which does

reach the planet will survive the environmental stresses encountered prior to reaching the planet.

An illustration of contamination source identification [26, 80] for a planetary lander project is in Figure 1. The key points of this contamination analysis by the JPL are:

- (1) All aspects of the flight program, including the interactions of flight hardware with the interplanetary environment, are examined to identify possible sources of contamination.
- (2) Sources of contamination are examined individually to yield an adequate understanding of the processes through which they occur.
- (3) Where possible, mathematical models are formulated which characterize the probability of contamination. The models are based on standard probabilistic techniques, and the limitations inherent in their formulation are described.

The major possible sources of contamination [52] for an orbiting mission are shown in Figure 2. Hall [47] pointed out that the quarantine constraints for accidental impact of the nonsterilized spacecraft can have a dominant effect on the trajectory biasing requirements and the orbit altitudes; consequently, close scrutiny of acceptable risks for flyby and orbiter missions is warranted.

The initial burden of viable organisms on the vehicle is determined by extrapolation from microbial assay and can be expressed in any of several ways. It can be stated as an average of the several measurements of the bioburden. A more conservative approach is to state it as an upper or maximum value of several measurements of the microbial contamination level. A system model, used by Ingram [61], treats this number as several ranges of values, each with an associated probability—i.e., a histogram. Implementation of Ingram's model, however, is complex, requiring a knowledge of every contaminating event during assembly and of the associated environments. A stochastic model has been developed which avoids these difficulties [106]; this approach is being considered for use

by the US Viking 1975 project. Methods have been developed for systematically dealing with histogram data in probabilistic computations with parameters of variable uncertainty [51, 110].

### Documentation

Flight project groups are required to document the results of their analyses and the measures used for contamination control. US projects prepare planning documents (including a PQ plan, microbiologic assay and monitoring plan, and sterilization plan) and analysis reports. Planning documents are submitted to the PQ authority for

review to ensure adequate attention to decontamination needs and measures. Analysis reports document the analytical development of decontamination requirements and quantify the constraints, if any, to be applied during spacecraft fabrication.

Prior to approval for launch, a report is submitted to the PQ authority describing both the compliance measures undertaken by the flight project, and their effectiveness in limiting the microbial burden during manufacture. Based upon the acceptability of these data as well as an independent verification conducted by the PQ authority, an approval for launch is granted.

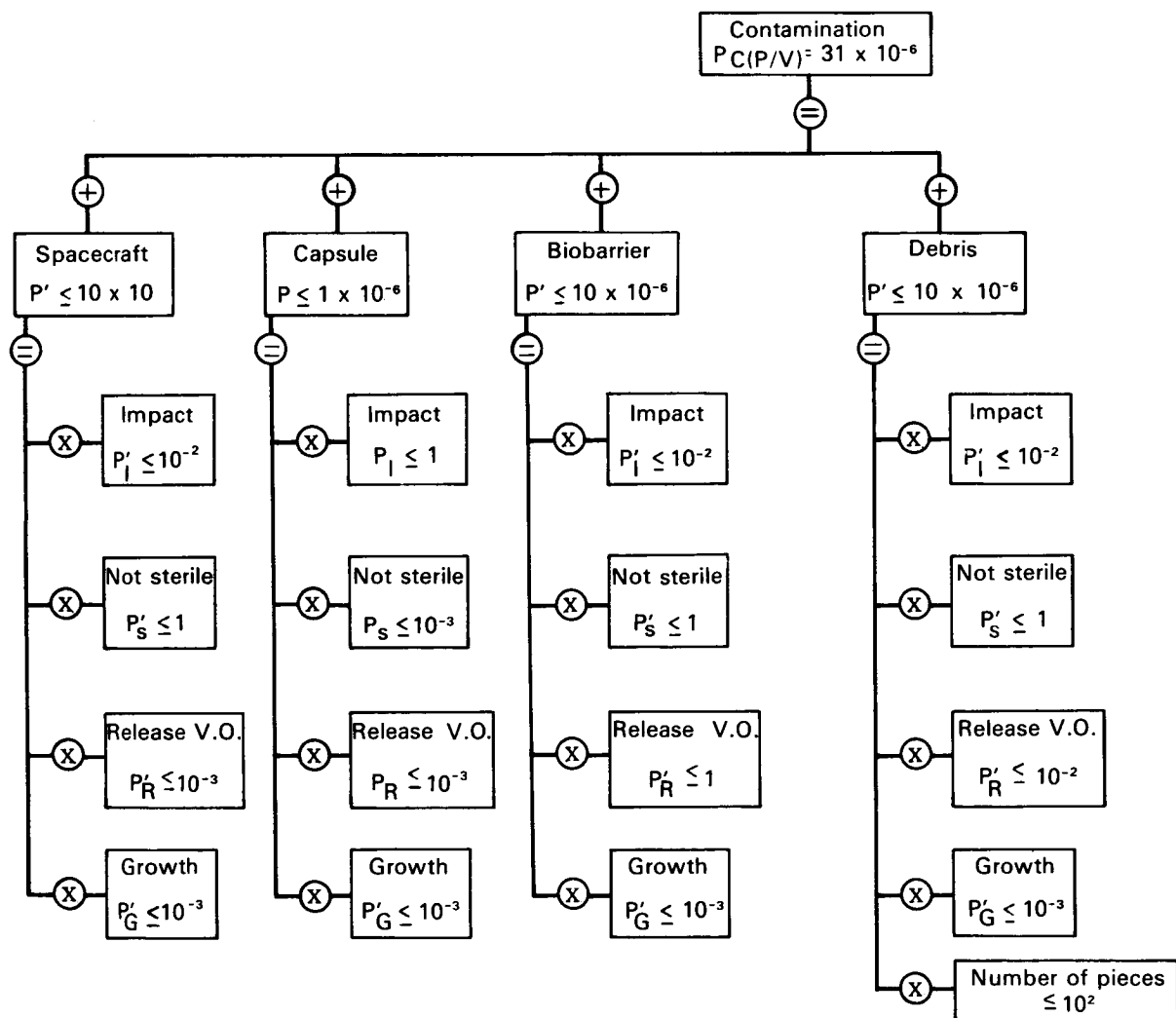


FIGURE 1.—Contamination source identification for planetary lander mission.

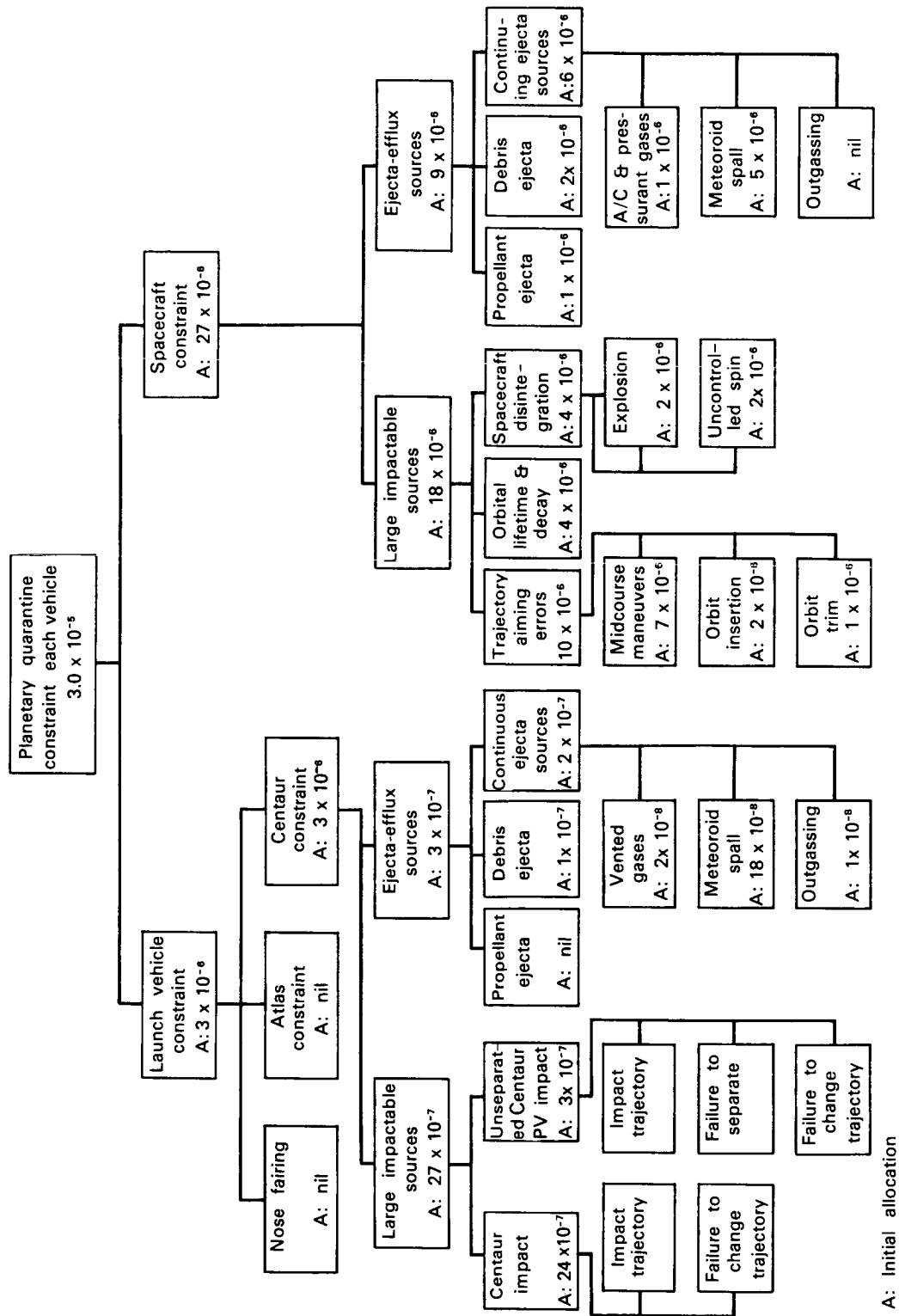


FIGURE 2.—Mariner Mars 1971 planetary quarantine model.

Launching nations are urged to submit to COSPAR a report stating the degree to which spaceflight missions have satisfied quarantine requirements. The data are summarized to aggregate the estimated probability that the total space exploration programs of all nations have contaminated each planet. Current results are examined by the COSPAR Panel on Planetary Quarantine at each annual meeting to assess the progress of the total Planetary Quarantine program and to determine the need for policy revisions. Complete international cooperation in this matter has not yet been attained by COSPAR, but full participation should result when all launching nations accept the importance of adequate PQ measures.

### CONTAMINATION CONTROL TECHNIQUES

The value to successful quarantine of measures such as a constituted PQ authority, an awareness of the problem to be solved, and development of the quantitative requirements and implementation guidelines have been illustrated in preceding sections. However, it is the adequacy of the measures taken by the spaceflight group to control the level of contamination of space vehicles and to produce the operational reliability needed to minimize the chances of a contaminating accident that assures that the quarantine goals are met. On the basis of a contamination analysis, contamination control needs can be determined and related to measured bioburdens at key times during the assembly process. To meet these needs, control measures can be selected to be applied during assembly stages. In similar fashion, operational reliability goals can be quantified and used to specify design quality, workmanship standards, and reliability assurance levels to be achieved when the number of microorganisms does not exceed the level established as the highest acceptable limit. Obviously, the most stable and desirable level of control from a microbiologic viewpoint would be sterility—the absence of viable microorganisms. Although sterility is the objective of spacecraft decontamination measures, it is always a matter of probability whether this absolute level is achieved.

Because of the possible adverse effects of stringent sterilization techniques on system performance it is undesirable to apply treatments to realize extreme probability of sterility. The probability of contamination achieved in recent US missions is illustrated in Table 5, which summarizes the estimated surface bioburden at the time of launch. Comparison with the surface contamination levels of products manufactured without biologic control indicates that a very low level of contamination has been achieved.

Preventive and corrective tactics are used in combination for contamination control: techniques for limiting the introduction of contamination and for reducing extant contamination levels of facilities, personnel, and hardware. Techniques have been adapted from medicine, food processing, environmental control, and other areas. Many have been further developed, and some new techniques have been devised. Undoubtedly, the advances in contamination control made for Planetary Quarantine will be used in turn by those areas from which the technology was adapted.

#### Contamination Prevention

Contamination prevention involves consideration of potential sources of contamination and the use of barriers to shield the spacecraft from these sources [74].

*Biologic barriers.* The objective of a biologic barrier is to keep the number of microorganisms within an enclosure at an acceptably low level. This can be accomplished by using an air shield as in a clean room or a solid microbial barrier.

Clean rooms reduce or eliminate microbiologic contaminants, at a site or on equipment, thus increasing the probability that subsequent decontamination will be successful. Functional reliability is also improved because of increased chemical and particulate cleanliness [79]. The effectiveness of a clean room in limiting the microbial level accumulated on the surfaces of spacecraft material depends upon the air-handling system employed and upon operational procedures. The control of airborne contamination is specified in terms of the maximum number of particles permitted in the air stream;

e.g., a Class 100 clean room has less than  $3.5 \times 10^3$  particles/m<sup>3</sup> (100 particles/cu ft). This low level is usually achieved by a vertical laminar flow, as opposed to turbulent flow air systems. Laminar-flow clean rooms and work areas successfully hold intramural microbial contamination to a very low level and drastically reduce soil-type microorganisms, such as bacterial and mold spores, from the extant microorganism population.

A vertical laminar-flow clean room usually has a full ceiling filter bank of high efficiency particulate air (HEPA) filters. The retention efficiency for typical HEPA filters often exceeds 99.6% for particles of 0.3  $\mu\text{m}$  and larger. Exhaust air exits through a grated floor. The airflow is high volume and downward throughout the entire cross section of the room. A laminar horizontal, or crossflow clean room is somewhat less effective downstream from any source of contamination,

TABLE 5.—*Status of Probability of Planetary Contamination*<sup>1</sup>

Mars missions	Launch date	Type mission	Weight kgm	Probability of planetary contamination			Sterilized	Surface microbial spore load	Mission results
				Prelaunch allocation	Postflight estimate	Cumulative probability			
Mariner 3	11/5/64	Flyby	261	$4.5 \times 10^{-5}$	NIL	NIL	No	$2 \times 10^5$	Unsuccessful-failed to jettison
Mariner 4	11/28/64	Flyby	261	$4.5 \times 10^{-5}$	NIL	NIL	No	$2 \times 10^5$	Passed Mars at 9850 km 7/14/65
Mariner 6	2/24/69	Flyby	380	$3 \times 10^{-5}$	approx. $3.2 \times 10^{-8}$	approx. $3.2 \times 10^{-8}$	No	$2 \times 10^4$	Passed Mars at 3400 km 7/31/69
Mariner 7	3/27/69	Flyby	380	$3 \times 10^{-5}$	approx. $3.2 \times 10^{-8}$	approx. $6.4 \times 10^{-8}$	No	$3 \times 10^5$	Passed Mars at 3540 km 8/5/69
Mariner 8	5/8/71	Orbiter	990	$7.1 \times 10^{-5}$	NIL	approx. $6.4 \times 10^{-8}$	No	$1 \times 10^4$	Failed to achieve Earth orbit
Mariner 9	5/30/71	Orbiter	990	$7.1 \times 10^{-5}$	$3.9 \times 10^{-5}$	approx. $3.9 \times 10^{-5}$	No	$1 \times 10^3$	Achieved Mars orbit 10/14/71
Venus missions									
Mariner 1	7/22/62	Flyby	202	$1 \times 10^{-4}$	NIL	NIL	No	$2 \times 10^5$	Unsuccessful—mission abort at launch by safety officer
Mariner 2	8/27/62	Flyby	203	$1 \times 10^{-4}$	$3 \times 10^{-17}$		No	$5 \times 10^5$	Flyby passed Venus at 34826 km 12/14/62
Mariner 5	6/14/67	Flyby	245	$3 \times 10^{-5}$	$3 \times 10^{-17}$	NIL	No	assayed $1 \times 10^5$	Flyby at 3200 km 10/19/67

<sup>1</sup> Exotech Systems, Inc. *Contamination Logs for Mars and Venus*. Washington, D.C., Exotech Systems, 1971. (Rep. Contr. NASw-2062)

such as workers. There are also portable clean rooms—vertical laminar airflow units with plastic curtains for side walls, blowers, a ceiling HEPA filter bank, and support legs on casters to facilitate movement.

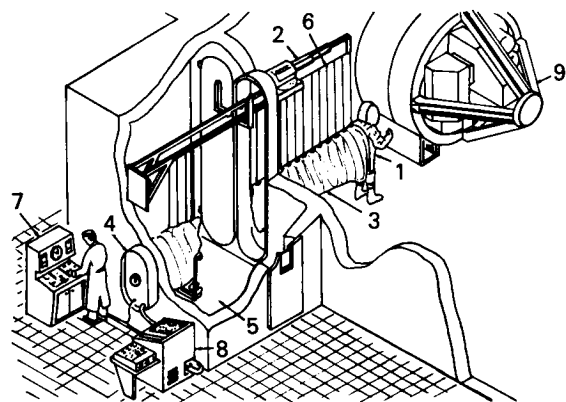
The JPL developed an Experimental Assembly and Sterilization Laboratory (EASL) [65, 75, 84] having an extremely low level of airborne microbial contamination in the bioassay room and laminar downflow work areas [74]. JPL later enlarged and improved the EASL and constructed a Sterilization Assembly and Development Laboratory (SADL) [102], a complete spacecraft assembly facility incorporating (1) a 130-m<sup>2</sup> laminar downflow room with a 10-m high bay; (2) an operational support equipment area; (3) a 75-cm ethylene oxide decontamination chamber; (4) a 75-cm dry-heat sterilization chamber, and (5) all equipment needed to conduct microbiologic assays.

Microbiologic barriers, from cabinet size to very large installations, prevent passage of microorganisms into or out of the barrier [88, 89]. In planetary quarantine, protection of the equipment or material inside the barrier is usually of primary interest, but occasionally a barrier that works in both directions is needed. The absolute barrier cabinets used in the US Lunar Receiving Laboratory prevented escape of potentially harmful lunar material during quarantine, and also prevented contamination of lunar samples by terrestrial microorganisms. Absolute barriers permit no interchange of protected and unprotected environments. Isolation is accomplished by placing material or work within a gas-tight enclosure, through the walls of which operations are conducted by means of flexible gloves or remotely operated instruments. In fact, such enclosures can be evaluated for microbiologic integrity with a gas leak detector.

The partial barrier principle uses enclosures, rooms, or cabinets that are not gastight and depend on air pressure differentials through working openings. Inlet or outlet air (or both) may be filtered. Pressurization of such barrier systems depends on whether work or personnel is to be protected. When work within the barrier is to be protected from outside contamination, the enclosure is maintained at positive pressure.

Negative pressure is used in the enclosure to inhibit escape of microorganisms.

A Bio-Isolator Suit System (BISS), part of the assembly sterilizer facility designed in the US for the isolation of sterile spacecraft, has an outer suit, and an inner suit which is sealed to a flexible pleated tunnel large enough to permit operator access and egress (see Fig. 3) [38, 136]. The BISS is complete with life-support and monitoring subsystems. All human operations are topologically and biologically isolated by the suit and tunnel from the spacecraft after the beginning of the sterilization operations.



1. BISS outer suit	6. Stringers
2. Boom	7. Director's console
3. Tunnel	8. Life-support console
4. Hatch	9. Spacecraft
5. Antechamber	

FIGURE 3.—Bioisolator suit system and assembly/sterilizer interface concept [74].

A comprehensive review of absolute barrier devices for personnel protection has been made by Gremillion [44], whose description of barriers includes incubators, refrigerators, centrifuges and balances, and covers disinfectant dunk baths and autoclaves for the entrance and exit of materials. Similar cabinets have been described by Blickman and Lanahan [13], and McDade [74] discussed barriers for aerospace application.

Flexible plastic barriers for the absolute containment of germ-free animals are largely the result of development work by Trexler [121]. A negative-pressure safety hood made of flexible

plastic film was developed by Phillips et al [91]. Subsequently, rigid plastic absolute barriers were also developed [90]. The types of barriers or isolators for germ-free animal experimentation have been summarized by Trexler [122, 123].

*Preventing contamination by personnel.* The primary source of microorganisms in spacecraft assembly is the personnel associated with the fabrication processes. Human skin surfaces provide a fertile site for the survival and growth of microorganisms [29, 72]. Bacterial studies have shown that microorganisms may be found on the skin surface, throughout the stratum corneum, and in the ducts of most excretory glands.

The removal of microorganisms from skin surfaces, or their sterilization, has been attempted many times by a variety of techniques. Surgeons rely upon the scrub-rinse technique generally employing hexachlorophene to reduce the number of organisms on the skin. Fingertips, of special interest, are the body surfaces most frequently in contact with spaceflight hardware. While the scrub-rinse technique tends to remove considerable numbers of skin microorganisms, sterility cannot be obtained [132].

Germicidal soaps help to suppress the bacterial skin flora for a time (as shown by Ulrich [125]) although the bacterial skin numbers eventually return to the level that is normal for the specific individual. It is quite probable that bacterial populations lying deep in the skin are well protected from biocidal concentrations of germicide, as well as against mechanical removal. Most probably, too, these organisms constitute the source of the eventual return to the normal bacterial skin level for that individual. Fortunately for the purposes of planetary quarantine, few, if any, spores or sporeforming bacteria are disseminated by the human body, although a few survive passage through the digestive tract and can be released to the occupied environment.

A noninjurious method of sterilizing skin is not known at present. Since bacteria are constantly shed or removed from the skin, a mechanical barrier such as surgical gloves, combined with the use of germicidal soaps, appears to be the best method of reducing or preventing microbial transfer from skin surfaces to spaceflight hardware.

### Decontamination Techniques

Many techniques for reducing microbial levels on spacecraft and their components have been investigated. None is ideal, but several are presently in use and others show promise. Tests show that a higher degree of sterilization can be achieved when these techniques are used on a smooth surface. Contaminant survival becomes significant as surface roughness increases. The techniques described in this section include: direct contact disinfectant cleaning using solvents and decontaminants, remote surface decontamination with chemicals or radiation, and heat sterilization with and without radiation.

*Disinfectant cleaning.* Direct contact disinfectant cleaning involves washing the exposed surfaces of spacecraft materials with disinfectants such as ethyl alcohol, isopropyl alcohol, formaldehyde in methanol, paracetic acid, and hydrogen peroxide. NASA's AIMP Project [70] employed a disinfectant cleaning program including brush-washing electronic modules with ethyl alcohol, rinsing electronic components in 85–95% isopropyl alcohol baths, sponging surfaces with cotton swabs and wipers saturated with isopropyl alcohol. It was estimated that at launch a microbial surface level of  $1.5 \times 10^4$  organisms was achieved.

Similar techniques have been used to limit the microbial surface contamination levels on the US Mariner program. Polypropylene pads saturated with a solvent selected for compatibility with the material being cleaned were employed in the Mariner Mars '71 program. Residues were removed by rubbing the surfaces with sterile flannel. On delicate parts, such as the solar panels, cotton-tipped toothpicks were used to minimize damage to the delicate electrical connection network.

Hydrogen peroxide, used in industrial applications for its biocidal properties, is suitable for use on some spacecraft materials. A concentration of 3 to 5% is effective for microorganisms in the vegetative state, 3 to 10% for spores (depending upon type), and a concentration of 1 to 5% will kill viruses [129]. A disadvantage of hydrogen peroxide is a high surface tension, 73 dyn/cm. This can be reduced by adding surfactants, such as 0.5% sulfanol, and achieve

cleaning through more complete coating on the surfaces. The addition of anionic detergents can reduce the surface tension of the solution to as low as 28.8 dyn/cm. Treatment of surfaces with such a mixture will have a lethal effect on vegetative and sporogenous forms of microorganisms, according to Shumayeva [113]. Immersion in a 6% solution can decontaminate surfaces infected with spores of malignant anthrax; and by increasing the temperature of the solution to 50° C, the concentration of the hydrogen peroxide can be reduced by a factor of two without decreasing the effectiveness.

*Surface sterilization.* The techniques refer to the use of chemicals or radiation without direct contact with the surface. Decontaminants used include gases (ethylene oxide, methyl bromide and formaldehyde) and radiation (laser beams, gaseous plasma, ultraviolet and ionizing radiation).

Ethylene oxide (ETO) has been used for many years in the pharmaceutical and food processing industries as a microbial decontaminant. Its effectiveness is a function of time, temperature, concentration, and relative humidity [115]. As a surface decontaminant for reducing microbial populations on spacecraft [66, 85], several factors must be considered. ETO is both toxic and hazardous. A small percentage (3%) in air will support combustion, and if ignited in a closed space will explode. However, a noncombustible mixture can be made by adding an inert substance. ETO mixed with carbon dioxide or various fluorinated hydrocarbons is available in the US. These mixtures do not support combustion with air in any proportion. Adverse effects of ETO include proneness to corrosion of materials; polymerization caused by catalytic properties of some materials; chemical reaction with some materials [37, 64, 67]; and parameter drift of some electronic devices [11, 14]. Such effects are overcome by proper handling and precautions.

Space scientists in the USSR currently consider a mixture of 40% ETO and 60% methyl bromide (referred to as OB mixture) the most suitable means of surface decontamination of space hardware. It is reported to be five times more effective against *Staphylococcus aureus* and two-and-a-half times more effective against spores of *B. mesentericus* than a mixture of 12%

ETO and 88% Freon (referred to as cryoxide). The combination of ETO and methyl bromide exceeds cryoxide in bactericidal properties because of the bactericidal capacity of both components. USSR research indicates that the OB mixture does not harm materials being sterilized [83], but this remains an open question in the US.

Methyl bromide by itself has several valuable attributes. It is widely used as a refrigerant and in fire extinguishers, and is an excellent fumigant for stored grain, seeds, and nursery stocks. It is not as effective a sterilant as ETO, but adds a penetrating effect so that the combination of ETO and methyl bromide kills microorganisms more rapidly than either constituent alone, according to Soviet reports [127].

Recent research using formaldehyde gas generated from paraformaldehyde [86] suggests that it may have some use in the sterilization of spacecraft components. Formaldehyde as a gaseous sterilizing agent is advantageous in that the space to be sterilized need not be tightly enclosed nor hermetically sealed, a condition often impossible to achieve when large volumes are to be treated. Formaldehyde gas has a slow rate of penetration, a significant feature when residual action is required. The absorbed surface film of the polymer will continue to release formaldehyde gas slowly, often for several days after the sterilization cycle has been completed. If sterilization is carried out in a vacuum chamber, penetration can be accelerated. The principal disadvantages using formaldehyde as a surface sterilant for spacecraft are its interaction with some commonly used materials and its potential as an organic contaminant of life-detection experiments.

There has been renewed interest in formaldehyde sterilization recently because of the availability of a highly purified form of paraformaldehyde which apparently increases ease of production of the gas and reduces problems of residuals. Heating of this polymer results in the release of pure formaldehyde gas with little or no waste. An odorless formaldehyde-based sporicide is under development by Sandia Laboratories.<sup>4</sup>

<sup>4</sup> Presentation by R. E. Trujillo at the Spacecraft Sterilization Technology Seminar, San Francisco, July 1972. (NASA contract W-12-853)

Both gel and liquid forms have been produced which have bactericidal effects similar to simple formaldehyde and accelerated effects with modest heating.

Researchers at MIT [97] have found that bacteria can be destroyed by irradiation with laser light. Heat-resistant spores (*Bacillus subtilis*) became entirely inactive within a hundredth of a second in a 50-W, unfocused CO<sub>2</sub> laser beam. The laser beam method does not disturb the substrate materials used (copper, aluminum, glass, and paper). This quality would make it possible to sterilize the surfaces of materials that are quite sensitive to heat—materials, in addition to those of spacecraft, include medical and surgical materials, foods, metals, paper, and probably even the surfaces of wounds during operations, as well as the air in the operating room. A wide range of wavelengths (from 2 to 10.6 μm) has been found effective in sterilizing spores. The high reflective energy produces extensive kill, mitigating possible structural shielding effects.

Gaseous discharge or plasma sterilization has been investigated as a means for complete elimination of contamination from medical products and foods [56]. The Boeing Co.<sup>5</sup> has tested the effectiveness of radio-frequency-generated oxygen plasmas on inoculated strips. A surface cleaning effect has been observed with plasma temperatures of 50° C. Sterilization appears to be complete without material degradation. The plasma is an extremely rich source of ultraviolet light, which may be the actual sterilizing agent.

Both plasma and laser beam sterilization are surface treatments with limited penetration ability. The applicability of these techniques is questionable to sterilization of surface films of thickness greater than 1 μm and of contamination resident in deep pores or sharp recesses.

Ionizing radiation [58] in the form of gamma rays, high-energy electrons and protons, is a decontaminant. Imshenetskiy and Abyzov reported in 1972 that in many cases where heating could damage electrical apparatus, the use of gamma rays is becoming increasingly popular in the USSR [56]. According to the data of Jaffe [62, 63] the γ-radiation dose required for sterilization

of materials and apparatus on a spacecraft is 10 million rads. However, Astafayeva et al [8] feel that these doses are much too high. Their data indicate that sterilization of radio parts, even those containing spores of *B. mesentericus*, which are relatively resistant to the action of gamma rays, can be accomplished with a dose of 2.5 million rads. The same dose proved effective for sterilization of porous rubber and certain liquids that were considerably contaminated by a test culture.

Tests conducted in the USSR [126] of radiation-sterilized materials and radio parts after storage for various durations (from 1 day to 3 months) showed that physical and chemical properties of the materials and the electrical parameters of the devices tested remained unchanged. These studies indicated that the use of radiation sterilization is suitable in many cases for sterilizing spacecraft but would necessitate special attention to parts selection and design for radiation resistance.

High-energy electrons and protons, while not possessing the penetrating power of γ-rays, can sterilize surface contamination. Through reflection and scattering, they can also be effective on hidden surfaces. Both electron and proton beams can be focused in concentrated patterns, thereby speeding the decontamination process. Tests [3] underway at the JPL to investigate the lethal properties of the trapped radiation belts of Jupiter, should provide further data on the effectiveness of electron and proton beam sterilization.

Considerable information exists on radiation damage to materials similar to those used on spacecraft. A large segment of this information concerns nuclear reactor radiations (mixed neutron-gamma fields) which are believed unsuitable for spacecraft sterilization application since they can produce radioactivity in the irradiated material [12, 35, 71, 81].

Materials most susceptible to damage from x-ray, γ-ray, and electron beam radiation include electronic semiconductors and organic polymers. Semiconductors are subject to interface surface deterioration which can affect electrical properties [18, 19, 77, 114, 117]. Damage requires that a radiation energy threshold be exceeded. Radiation damage to organic polymers is principally

<sup>5</sup> Informal communication with Dr. Richard Olson, The Boeing Co., Seattle, Wash.

due to ionization [15]. Covalent bonds are broken and subsequent recombination of the free radicals is random and can lead to scission and cross-linking. Damage is generally directly proportional to dose.

The technical feasibility of spacecraft radiation sterilization in a program which includes careful selection of electronic parts, organic materials, manufacturing processes, and screening tests has been investigated in detail [10]. Further study is necessary to evaluate the economics of spacecraft radiation sterilization and to compare its effectiveness and applicability to currently used techniques.

**Thermal sterilization.** Terrestrial microorganisms are susceptible to high temperatures. Autoclaving, a standard sterilizing process in industry and food preparation, utilizes high temperature steam (dry heat) as the active ingredient.

Space scientists in the US currently consider dry-heat sterilization the most suitable means of decontaminating space hardware. Dry heat effectiveness depends upon:

- temperature
- time
- water activity
- open or closed system
- physical and chemical properties of the microorganism
- adjacent support material
- surrounding atmosphere

A simple logarithmic model [85], useful in defining conservative operational characteristics, expresses microbial destruction as a function of time and temperature:

$$\log N_U = \frac{-U}{D_T^z} + \log N_o \quad (2)$$

where  $N_o$  is the initial microbial population,  $D_T^z$  is the time in units of time required to reduce the population by 90% at temperature  $T$  and for a temperature coefficient  $z$ , and  $N_U$  is the expected mean population after  $U$  units of time of heating.

Microbial heat inactivation, however, is more complex than this simplified model suggests and a rigorous treatment must consider water activity, population mix, and equilibration characteristics. The effect of a mixed population of

several microbial groups, each with different initial population levels and  $D$ -values, is to produce a composite inactivation characteristic which tails out as destruction progresses. This increasing resistance to destruction necessitates close examination of the composite inactivation characteristic when high levels of decontamination are to be achieved.

Open and closed systems represent the two extremes in water movement to or from the microorganisms during heating. In closed systems, characterizing encapsulated and, in some cases, mated surface contamination, the microorganisms are located so that they are completely surrounded by a solid material impervious to water vapor transmission. In open systems, characterizing surface contamination, the microbes are in intimate and continuous contact with the surrounding atmosphere while they undergo dry-heat sterilization. Mated surface organisms, depending upon their physical situation and the degree of water transmission, are in either open or closed systems. The water vapor content immediately surrounding the organisms is all-important in this biocidal process, and the nature of the remainder of the surrounding gas atmosphere has little effect on the rate of dry-heat sterilization.

In the temperature range of 100°–125° C, inactivation is strongly dependent upon the relative humidity (RH), with lethality above 50% RH and below 0.2% RH much greater than the kill rates in the intermediate range [16]. This dramatic effect [7] of water activity upon inactivation of *Bacillus subtilis* at 125° C is shown in Figure 4.

For efficient sterilization, either the wet or dry extremes should be chosen. From a reliability standpoint, wet sterilization, although used earlier in the USSR [126], is felt unsuitable for delicate components; hence, the dry end of this spectrum has been selected for use by US flight projects. Studies are currently underway to determine a realistic minimum RH achievable during sterilization of typical spacecraft to take maximum advantage of this effect. Because of the heat sensitivity of much spacecraft material, the dry thermal sterilization temperature must be carefully selected. Recent

research [126] indicates that temperatures of 110–140° C are best suited for spacecraft sterilization. The US space program approves temperatures of 100° C and above and provides the set of specifications given in Table 4 for dry heat use [80].

Other factors involved in the design of a dry-heat sterilization process are the thermodynamic characteristics of the space vehicle and the heating environment, the numbers of organisms to be killed, and the distribution of the microbial burden on the spacecraft. Many factors in the design and configuration of the space vehicle strongly influence the temperature profile of the vehicle. Three of these factors are: location of the thermal control paths, placement of thermal insulation, and the physical properties of constituent materials.

In one of several alternative methods for applying heat to the vehicle, a canister containing the lander is sealed and the unit placed in an

oven and heated. Heat flows from the atmosphere in the oven through the canister to the lander. In another more favored system, sterile gas is heated in a heat exchanger and recirculated through the canister. To optimize the thermal process, the heat lethality above the US specified minimum limit of 100° C should be integrated over the sterilization cycle—heat-up, temperature maintenance, and cool-down. In order to satisfy a wide range of designs, it is necessary to establish a range of processing conditions, all of which will produce the desired decontamination of a space lander. Clearly, the final selection of the sterilization process must be the result of a trade-off study between spacecraft design factors and process parameters.

Nonsterile vehicles and components that have served their useful life, such as flyby or orbiting buses, can, theoretically, be sterilized by the activation of on-board exothermic heating agents such as Thermit, a mixture of aluminum powder and iron oxide. When ignited, it generates high sterilizing temperatures. However, using this technique forces basic spacecraft design constraints to ensure transfer of sufficient heat to all parts of the vehicle before the heat paths are destroyed, and imposes a weight penalty.

Sterilization at the end of a lander capsule's useful life would be too late to protect life-detection experiments or to prevent release of terrestrial life on a planet, eliminating the method from serious consideration.

*Thermoradiation.* Thermoradiation is attractive for contamination control [96] in spacecraft assembly because it exposes components to less heat than dry heat sterilization and less radiation than radiation alone.

The lethal effects of biologic systems of combined heat and ionizing radiation have been observed by many experimenters. Radiation sensitivity increases with a rise in temperature in such varied biologic systems as proteins [9, 20, 93, 94], viruses [1, 27, 55, 92, 124], spores [56, 57, 97, 113, 126], bacteria [62, 63], yeast [8], paramecia [94], insects [39], vertebrate cells [69, 118], and human tumors [2, 23, 27, 40, 50, 54, 55, 68, 98, 133, 134]. Sterilization in a composite heat and radiation environment can be ascribed to in-

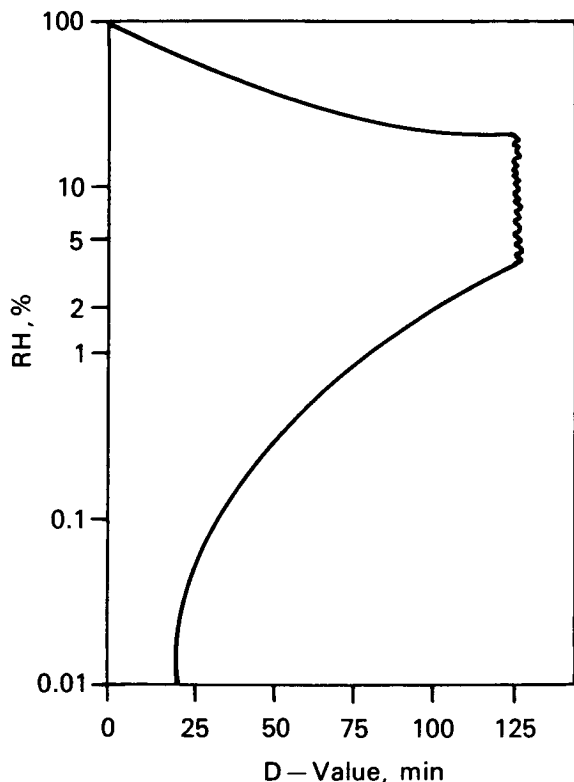


FIGURE 4.—Heat inactivation at 125° C as a function of R.H.

creased radiation sensitivity. Temperatures at which the increased rates of inactivation occur are below those temperatures at which thermal inactivation becomes effective.

To evaluate the lethal synergism of heat and radiation, Sandia Laboratories<sup>6</sup> conducted experiments in the temperature range of 60°–125° C with radiation doses believed acceptable for typical spacecraft materials and components.

The sterilization effectiveness of ionizing radiation, dry heat, and then the simultaneous application of ionizing radiation and dry heat at various temperatures were compared. Figure 5, typical of these experiments, compares the inactivation of these sterilization agents singly, and in combination [104]. Additional experiments have revealed that this synergistic relationship of heat and radiation exists at temperatures as low as 60° C. Thermoradiation *D*-values at a dose rate of 8 krad/h varied from 1.5 h at 105° C to 3 h at 90° C and 6 h at 69° C [104]. These *D*-values represent a rather significant reduction in time required for sterilization. For example, the dry-heat *D*-values for *B. subtilis* var. *niger* at 60° C range from 53 to 274 h [130], depending on the moisture condition of the spores.

Graikoski [42], working with gamma radiation from Cobalt-60 and with several sporeforming species, concluded that a common mechanism is probably responsible for spore survival and radiosensitization. He postulated that the nucleoprotein deoxyribonucleic acid (DNA) component is important in this regard.

Samoylenko and Ivanov [108], comparing the sensitivity of bacteria to  $\gamma$ -irradiation and heat (50° C), showed that the radioresistant cultures tested were also more thermal-resistant. The DNA composition of the resistant strains had greater mole percent fractions of adenine and thymine than nonresistant strains.

The correlation of radiosensitivity with nucleic acid content has been verified by Sandia [28]; this correlation provides further evidence that the nucleic acid component of biosystems is responsible for the intrinsic radiosensitivity of a given biosystem.

<sup>6</sup>Thermoradiation—Experimentation Task in Contract W-12, 853. Technical Assistance (Systems Analysis and Clean Room Monitoring) for Planetary Quarantine Program.

**Autosterilization.** An autosterilizing material is one which contains an ingredient toxic to microorganisms. Studies by Astafyeva et al [8] have shown that various materials used in spacecraft, as well as oxide films produced under industrial conditions, possess autosterilizing properties. Such materials include alloys of magnesium, aluminum, copper, silver, surfaces covered with silver or copper, and certain types of rubber. There are also enamels which can cause reductions in microbial infection tens of thousands of times; however, test cultures remain viable beneath the coatings.

According to the data of Shank et al (1962) [112], Zsolnai (1962) [135], Godding and Lynch (1965) [41], the liquid fuels used in spacecraft

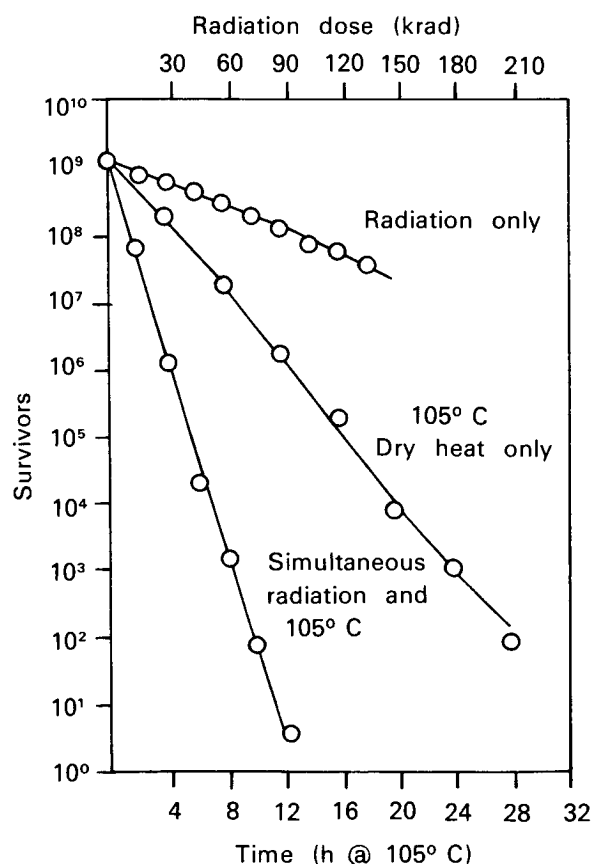


FIGURE 5.—Comparison of inactivation of *Bacillus subtilis* var. *niger* using  $\gamma$ -radiation at room temperature, dry heat alone at 105° C, then simultaneous dry heat and  $\gamma$ -radiation [104].

have autosterilizing properties on bacteria to varying degrees, while the solid fuel components do not.

The data of Opfell [83] indicate that when small amounts of paraformaldehyde are added to dyes, plastics, greases, and other compounds, they acquire bactericidal and autosterilizing properties. Willard and Alexander [131] showed that the addition of 3-7% formaldehyde to various dyes and coatings confers bactericidal properties on these materials. In order to obtain bactericidal cellulose cloth for a spacecraft, Vashkov and Sheglova [128] chemically combined the macromolecule of cellulose with various bactericidal metals, quaternary-ammonium bases, and phenol preparations. These materials produced death in 70-100% of the gram-positive and gram-negative microorganisms placed on their surfaces.

Heat generated in manufacturing or testing parts can also produce internal sterility of parts. An example is the heat generated by exothermic reactions in polymerization.

In decontaminating spacecraft, difficulties have been encountered frequently because certain materials cannot tolerate the doses of radiation or temperatures that would ensure the necessary degree of sterility. Therefore, autosterilizing materials are of considerable interest in planetary quarantine and this characteristic can be evaluated during materials selection accompanying spacecraft design.

## VERIFICATION PROCEDURES

The success of a spacecraft contamination control program is measured by enumeration of the microbial levels, especially bacterial spores, in and on space hardware. Although this general approach is practiced in other fields, spacecraft sterilization presents unique problems. In the food and pharmaceutical industries, for example, sterility tests can be performed on statistically significant samples of the final product. On spacecraft, where large numbers of items do not exist, a postcycle sterility test would be inconclusive, could produce recontamination, and might degrade flight hardware. Consequently, presterilization assays are used in combination with laboratory-verified inactivation character-

istics in estimating the limit of post-sterilization contamination levels. This process requires knowledge of the microbial population mix on the spacecraft to assure that the inactivation characteristics for the sterilization technique selected do not radically differ from the laboratory values. Microbial samples, collected by flight project personnel, are cultured and counted by an assay laboratory certified for this purpose.

A manual describing assay procedures, published by NASA in 1967, revised 1968, specifies techniques for assay of space hardware and intramural environments used for assembly and testing. The general procedure for enumerating aerobic and anaerobic microorganisms and spores is illustrated in Figure 6.

Most assay systems for spore enumeration involve heating the microbial suspension prior to plating, which is referred to as heat shock or heat activation. It has been shown repeatedly that many spores require such treatment for maximal germination. Counts of one variety of *Bacillus subtilis* have shown two- to threefold increases with heat shock [31]. However, certain spores germinate without heat shock and some can be adversely affected by heat shock. For example, viable counts of *Bacillus subtilis* var. *niger* spores are consistently reduced two to three times after heat shocking. In a mixed, naturally occurring spore population (the type of contamination with which spacecraft assays are concerned), some spores may not survive heat shock, others would survive, and still others would be stimulated.

Research in this area is in two main directions. The Center for Disease Control Laboratory in Phoenix has suggested that an ideal system for assaying spores in a mixed microbial population would be a technique that utilizes a nonthermal treatment for killing vegetative cells without harming spores, and a nontoxic chemical stimulus to induce maximal spore germination. The procedure for enumerating anaerobic microorganisms is essentially the same as that for aerobic microorganisms, with the exception that the culture plates are incubated under strict anaerobic conditions. Experience has shown that there are very few strictly anaerobic bacteria on spacecraft. Hence, this procedure is seldom used.

Organism enumeration, knowledge of the effects of sterilants used, and physical measurement of the parameters affecting the sterilants applied to the spacecraft are the bases on which the PQ authority can confidently certify that the mission, when launched, will comply with COSPAR requirements. Verification of flight project compliance with the PQ requirements enables each launching nation to assure concerned organizations that biologic safeguards have been established, and that a course is being followed which will result in the planets being maintained as biologic preserves for scientific investigations.

## OUTLOOK FOR THE FUTURE

Throughout the recorded history of planet Earth, invasions of a species of plant or animal often resulted in regional changes of catastrophic proportions. Early man often interposed crude barriers, frequently only distance, between the invader and himself when he was the susceptible host. Developing trade and commerce in the world bridged natural barriers to life forms. The time has come to consider insuring the maintenance of interplanetary barriers.

The huge and presumably hostile space between the planets has served as a natural

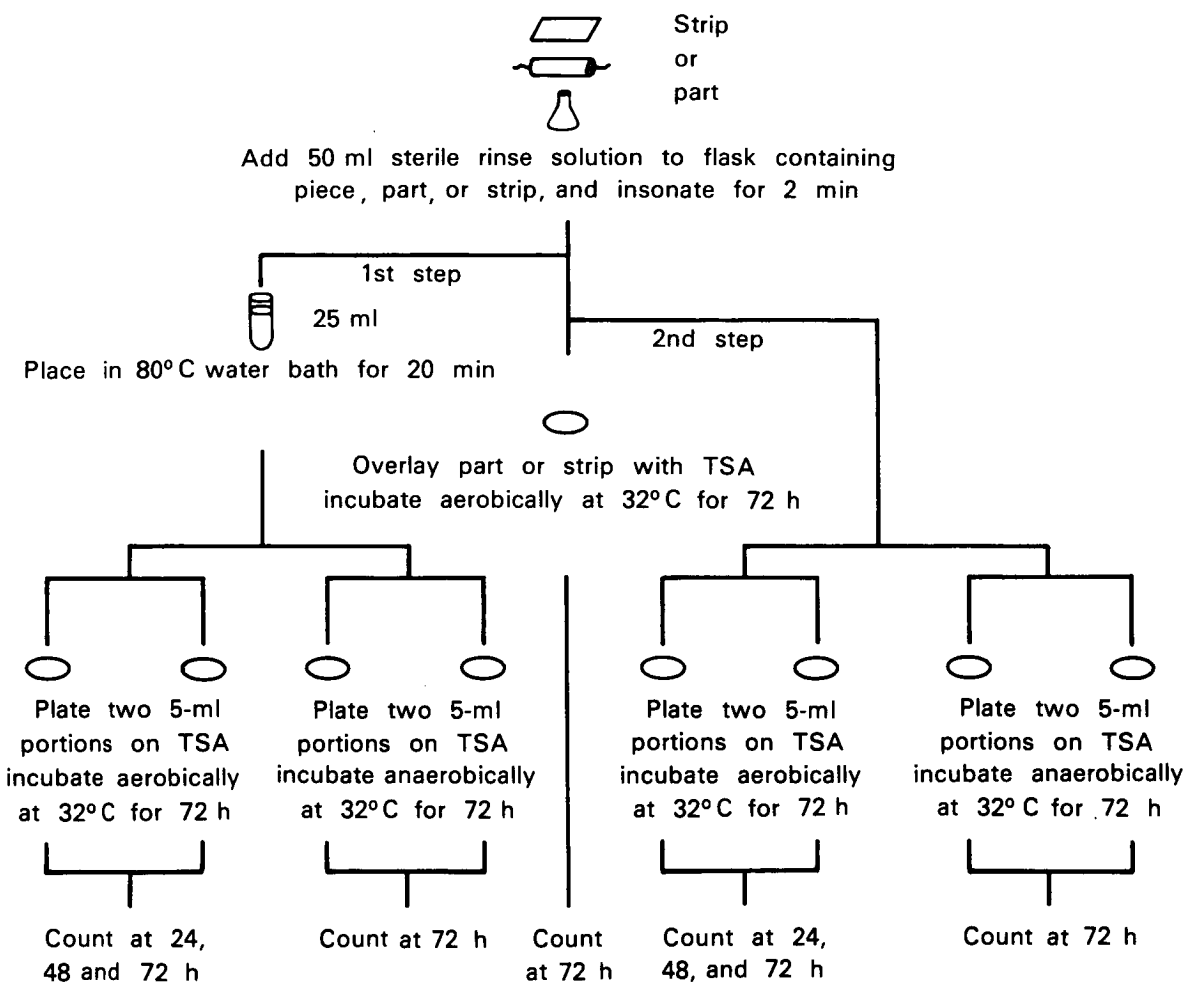


FIGURE 6.—Schematic of piece, part, and fallout strip analysis.

barrier throughout the ages to prevent the transfer of pathogenic agents, if they exist, between the celestial bodies. With the advent of space travel this natural barrier has been transcended. An artificial barrier, planetary quarantine, has now been instituted to effect the required degree of protection.

The US planetary exploration program has been guided by NASA's Planetary Quarantine Program. In accordance with international agreements, the COSPAR has been kept informed of the measures employed to control contamination within the specified limits for each spacecraft launch.

As space exploration programs have advanced, knowledge has been accumulated regarding the biological and physical characteristics of the planets. We are now quite confident of the estimates of the environmental characteristics of Venus, and similar data concerning Mars are being assimilated from flights of Mars 1, Mars 2, and Mariner 9.

Such knowledge has resulted in reducing the uncertainty in the estimation of key PQ parameters and in supporting the relaxation of PQ constraints. For example, following the flight of Venera 7, a 5-decade reduction in the value of the probability of growth on the surface of the planet was effected in the light of the very high temperatures found to exist on the surface. Quarantine has now been lifted in the US program from Mercury and from Venus, with the exception of possible microenvironments in the atmosphere of the latter.

It is expected that similar modifications will follow as space exploration proceeds. The forthcoming martian landings by the space

launching nations should provide insight into the important question of the availability of water in the microenvironments on the martian surface. With these data, the requirement for quarantine of Mars can be realistically reviewed. The Pioneer missions to Jupiter may provide insight into the existence and abundance of similar life-supporting factors for the Jovian planets and their satellites, hence bear upon the issue of quarantine for these bodies.

The success of planetary quarantine can be assured only by rigorous measures, to make sure that no errors have been made and that no factor has been overlooked. Only by the use of such rigid measures, burdensome as they may be, can the planets be undisturbed awaiting future scientific investigations.

The program of planetary quarantine conceived by the ICSU, and administered by proper authorities within the launching nations, includes rigorous measures and combines the scientific and technical knowledge necessary to formulate requirements with the authority needed to ensure compliance. Thus, PQ is safeguarding the planets of our solar system from possible irreversible loss associated with our newly developed exploration ability. Until such time as space exploration can show that quarantine is no longer necessary, planetary spacecraft must continue to be governed by quarantine requirements. In this way, mankind can continue the exploration of space, confident that the threat of irreversible contamination of the planets has been contained and that their environments will remain pristine awaiting the coming of mankind and the uses, in the dim future, that man may design for these planets.

## REFERENCES

1. ADAMS, W. R., and E. C. POLLARD. Combined thermal and primary ionization effects on a bacterial virus. *Arch. Biochem. Biophys.* 36:311-322, 1952.
2. ALTMAN, K. I., G. B. GERBER, and S. OKADA. Radiation effects on molecules. In, Okada, S. *Radiation Biochemistry*, Vol. 1, pp. 1-76. New York, Academic, 1970.
3. American Institute of Biological Sciences (AIBS). *Minutes, Semi-Annual NASA Spacecraft Sterilization Technology Seminar*. Washington, D.C., AIBS, 1972.
4. ANGELOTTI, R., K. H. LEWIS, et al. *Ecology and Thermal Inactivation of Microbes in and on Interplanetary Space Vehicle Components*. Cincinnati, USPHS, Robt. A. Taft Sanit. Eng. Cent., 1965. (First quart. rep.)
5. ANGELOTTI, R., K. H. LEWIS, et al. *Ecology and Thermal Inactivation of Microbes in and on Interplanetary Space Vehicle Components*. Cincinnati, USPHS, Robt. A. Taft Sanit. Eng. Cent., 1965. (Second quart. rep.)
6. ANGELOTTI, R., K. H. LEWIS, et al. *Ecology and Thermal Inactivation of Microbes in and on Interplanetary Space Vehicle Components*. Cincinnati, USPHS, Robt. A. Taft Sanit. Eng. Cent., 1966. (Fifth quart. rep.)
7. ANGELOTTI, R., J. H. MARYANSKI, T. F. BUTLER, J. T. PEELER, and J. E. CAMPBELL. Influence of spore

- moisture content on the dry heat resistance of *Bacillus subtilis* var. *niger*. *Appl. Microbiol.* 16(5): 735-745, 1968.
8. ASTAFYeva, A. K., V. I. VASHKOV, E. N. NIKIFOROVA, and N. V. RAMKOVA. Methods for a spacecraft sterilization. In, Brown, A. H., and F. G. Favorite, Eds. *Life Sciences and Space Research*, Vol. 5, pp. 38-43. Amsterdam, North-Holland, 1967.
  9. AUGENSTEIN, L. G., T. BRUSTAD, and R. MASON. The relative roles of ionization and excitation processes in the radiation inactivation of enzymes. In, Augenstein, L. G., R. Mason, and H. Quastler, Eds. *Advances in Radiation Biology*, Vol. 1, pp. 227-266. New York, Academic, 1964.
  10. BARRETT, M. J., and W. C. COOLEY. *On the Feasibility of Radiation Sterilization of Planetary Spacecraft*. Washington, D.C., Exotech Inc., 1966. (TR-012)
  11. BARTHOLOMEW, C. S., and D. C. PORTER. Reliability and sterilization. *J. Spacecr. Rockets*. 3(12):1762-1766, 1966.
  12. Battelle Memorial Institute. *Radiation Effects State-of-the-Art*, 1964-1965 (Hamman, D. J., E. N. Wyler, R. K. Thatcher, W. H. Veagie, Jr., F. R. Shober, et al.). Columbus, Ohio, Battelle Mem. Inst., 1965. (REIC-38)
  13. BLICKMAN, B. I., and T. B. LANAHAN. Ventilated work cabinets reduce lab risks. *Saf. Maint.* 120:34-36, 44-45, 1960.
  14. BOEING CO. *The Effects of Ethylene Oxide upon Operating Electronic Devices with Breached Hermetic Seals*. Seattle, Boeing Co., 1967. (Rep. D2-36527-1)
  15. BOLT, R. O., and J. G. CARROLL, Eds. *Radiation Effects on Organic Materials*. New York, Academic, 1963.
  16. BRANNEN, J. P., and D. M. GARST. Dry heat inactivation of *Bacillus subtilis* var. *niger* spores as a function of relative humidity. *Appl. Microbiol.* 23(6):1125-1130, 1972.
  17. BROWN, A. H. *Conference on Potential Hazards of Back Contamination from the Planets*. Washington, D.C., Nat. Acad. Sci. USA, Space Sci. Board, 1965.
  18. BROWN, R. R. Proton and electron permanent damage in silicon semi-conductor devices. In, *Radiation Effects in Electronics*. Philadelphia, Am. Soc. Test. Mat., 1964. (Spec. Tech. Publ. No. 384)
  19. BRUCKER, G., W. DENNEHY, and A. HOLMES-SIEDLE. High energy radiation damage in silicon transistors. *IEEE Trans. Nucl. Sci.* NS-12(5):69-71, 1965.
  20. BRUSTAD, T. Heat as a modifying factor in enzyme inactivation by ionizing radiations. In, *Biological Effects of Neutron and Proton Irradiations*, Vol. 2, pp. 404-410. Vienna, Int. At. Energy Agency, 1964.
  21. CLEMEDSON, C.-J. Sterilization of lunar and planetary space vehicles. *XIII Int. Astronaut. Congr.* (Varna, 1962), Vol. 1, pp. 292-313. Vienna-New York, Springer, 1964.
  22. COSPAR Study Group on Standards for Space Probe Sterilization. The value of agreed standards of sterility (Heden, C. G.). Appendix B. Tentative nomenclature and analytical basis for use in planetary quarantine. *COSPAR Tech. Man. Ser.*, No. 4, pp. 29-34. Paris, Muray Print, 1968.
  23. CONCAR, A. D., and M. L. RANDOLPH. Magnetic centers (free radicals) produced in cereal embryos by ionizing radiation. *Radiat. Res.* 11:54-66, 1959.
  24. CETEX. Contamination by extraterrestrial exploration. *Nature* 183:925-928, 1959.
  25. CETEX. Development of international efforts to avoid contamination of extraterrestrial bodies. *Science* 128:887-889, 1958.
  26. CRAVEN, C. W. Planetary quarantine analysis, Part 1. *Astronaut. Aeronaut.* 6(8):20-24, 1968.
  27. DIGIOIA, G. A., J. J. LICCIARDELLO, J. T. R. NICKERSON, and S. A. GOLDBLITH. Effect of temperature on radio-sensitivity of Newcastle disease virus. *Appl. Microbiol.* 19:455-457, 1970.
  28. DUCAN, V. L., and R. TRUJILLO. Synergistic inactivation of viruses by heat and ionizing radiation. *Biophys. J.* 12:92-113, 1972.
  29. EVANS, C. W., W. M. SMITH, E. A. JOHNSON, and E. R. GIBLETT. Bacterial flora of the normal human skin. *J. Invest. Dermatol.* 15:305-324, 1950.
  30. Exotech Systems, Inc. *Planetary Quarantine Specification Sheets*. Issued by direction of NASA Planet. Quar. Off. Washington, D.C., Exotech Syst., 1972.
  31. FAVERO, M. S. In, Hall, L. B., Ed. *Planetary Quarantine: Principles, Methods, and Problems*, pp. 27-36. New York, Gordon and Breach, 1971.
  32. FAVERO, M. S., J. J. McDADE, J. A. ROBERTSEN, R. K. HOFFMAN, and R. W. EDWARDS. Microbiological sampling of surfaces. *J. Appl. Bacteriol.* 31:336-343, 1968.
  33. FAVERO, M. S., and N. J. PETERSON. *Recovery of Surface and Buried Contamination*. Presented at AIBS/NASA Semi-Ann. NASA Spacecr. Steriliz. Technol. Semin., San Francisco, July 1972.
  34. FEDEROVA, R. I. Possibility of the spreading of viable germs in outer space. In, Imshenetskiy, A. A., Ed. *Extraterrestrial Life and Its Detection Methods*, pp. 154-167, Washington, D.C., NASA, 1971. (NASA TT-F-710)
  35. FRANK, M., C. D. TAULBEE, and H. L. CHAMBERS. Influence of operating conditions on radiation damage to transistor gain. In, *Radiation Effects in Electronics*. Philadelphia, Am. Soc. Test. Mat., 1964. (Spec. Tech. Publ. No. 384)
  36. GEIGER, P. J., F. A. MORELLI, and H. P. CONROW. Effects of ultrahigh vacuum on three types of micro-organisms. In, *Space Programs Summary*, Vol. IV, pp. 109-115. Pasadena, Calif., Jet Propul. Lab., 1964. (JPL 37-27)
  37. General Electric Company. *The Effects of Ethylene Oxide Sterilization in Typical Spacecraft Materials*. Program Information Request Release. N.D.
  38. General Electric Co. *A Research Study To Definitize a Bio-Isolator Suit System (BISS)*. Philadelphia, General Electric Co., 1967. (Final Rep. 67SD888)
  39. GINOZA, W. The effect of ionizing radiation on nucleic acids of bacteriophages and bacterial cells. *Ann. Rev. Microbiol.* 21:325-368, 1967.

40. GINOZA, W. Inactivation of viruses by ionizing radiation and by heat. In, Maramorosch, K., and H. Koprowski, Eds. *Methods in Virology*, Vol. IV, pp. 139-209. New York, Academic, 1968.
41. CODDING, R. M., and V. H. LYNCH. Viability of *Bacillus subtilis* spores in rocket propellants. *Appl. Microbiol.* 13(1):10-14, 1965.
42. GRAIKOSKI, J. T. The simultaneous lethal effect of temperature and gamma radiation on bacterial spores. *Diss. Abstr.* 22(2):394, 1961.
43. GREENE, V. W., B. WALKER, Jr., and O. A. ANDERSON. *Methodology of Measuring Internal Contamination in Spacecraft Hardware*. Minneapolis, Univ. Minn., Sch. Public Health, 1967. (Final Rep.)
44. GREMILLION, G. G. The use of bacteria-tight cabinets in the infectious disease laboratory. In, *Proceedings, Second Symposium Gnotobiotic Technology*, pp. 171-182. Terre Haute, Ind., Notre Dame Univ. Press, 1960.
45. HAGAN, C. A., J. F. GODFREY, and R. H. GREEN. The effect of temperature on the survival of microorganisms in deep space vacuum. *Space Life Sci.* 3(2): 108-117, 1971.
46. HALL, L. B. *A Decade of Development in Sterilization Technology by the United States Space Program*. Presented at Int. Steriliz. Conf., Amsterdam, Sept. 1972.
47. HALL, L. B. The importance of sterilization techniques in space exploration. *COSPAR Tech. Man.*, No. 4, pp. 3-18. Paris, Muray Print, 1968.
48. HALL, L. B., and M. J. HARTNETT. Measurement of the bacterial contamination on surfaces in hospitals. *Public Health Rep.* 79(11):1021-1024, 1964.
49. HILL, L. W. *Quantitation of Buried Contamination by Use of Solvents*. Fargo, N.D., Univ. N. Dak., 1972.
50. HOFF, A. J., and D. C. KONINGSBERGER. Production of free radicals in DNA and inactivation of its biological activity by gamma-rays. *Int. J. Radiat. Biol.* 17(5): 459-465, 1970.
51. HOFFMAN, A. R. Microbial burden prediction model. In, *Planetary Quarantine* (Semi-ann. rev., space res. and technol., July-Dec., 1970). Pasadena, Calif., Jet Propul. Lab., 1971. (Doc. 900-484)
52. HOFFMAN, A. R., and R. J. REICHERT, *Mariner Mars 1971 Planetary Quarantine Plan*, Part 1. Pasadena, Calif., Jet Propul. Lab., 1970. (JPL Rep. PD 610-18)
53. HOFFMAN, A. R., and D. A. WINTERBURN. *Microbial Burden Prediction Model for Unmanned Planetary Spacecraft*. Pasadena, Calif., Jet Propul. Lab., 1972. (JPL Rep. 900-566)
54. HORAN, P. K., and W. SNIPES. The temperature dependence of radiation-induced free-radical destruction. *Int. J. Radiat. Biol.* 19(1):37-43, 1971.
55. HOTZ, G., and A. MÜLLER. The action of heat and ionizing radiation on the infectivity of isolated  $\phi\lambda$ -174 DNA. *Proc. Natl. Acad. Sci. USA* 60:251-257, 1968.
56. HUNT, R. E., and R. R. ERNST. *A Study of the Requirements, Preliminary Concepts and Feasibility of a New System to Process Medical/Surgical Supplies in the Field*, Vol. 1 (Technical Summary), Part 1 (Technical Investigation). Cambridge, Mass., Arthur D. Little, 1971. (Final rep., Phase 1 No. 72688; Contr. DADA-17-70-C-0072)
57. HUNT, R. E., and R. R. ERNST. Analysis of candidate sterilizers and sterilization processes. In, *A Study of the Requirements, Preliminary Concepts, and Feasibility of a New System to Process Medical/Surgical Supplies in the Field*, Vol. 1 (Technical Summary). Appendix 6.2. Cambridge, Mass., Arthur D. Little, 1971. (Final rep. 72688, Phase 1; Contr. DADA 17-70-C-0072)
58. IMSHENETSKIY, A. A., and S. ABYZOV. Sterilization of spacecraft. In, Imshenetskiy, A. A., Ed. *Extraterrestrial Life and Its Detection Methods*, pp. 230-252. Moscow, Nauka, 1970. (NASA TT-F-710)
59. IMSHENETSKIY, A. A., and S. V. LYSENKO. Effect of a high vacuum on microorganisms. In, Imshenetskiy, A. A., Ed. *Extraterrestrial Life and Its Detection Methods*, pp. 129-143. Washington, D.C., NASA, 1972. (NASA TT-F-710)
60. IMSHENETSKIY, A. A., S. S. ABYZOV, G. T. VORONOV, L. A. KUZJURINA, and S. V. LYSENKO. In, Brown, A. H., and F. G. Favorite, Eds. *Life Sciences and Space Research*, Vol. 5, pp. 250-260. Amsterdam, North-Holland, 1967.
61. INGRAM, G. E., M. A. MARTIN, E. BERGER, and T. F. GREEN, *Voyager Mars Planetary Quarantine-Basic Math Model Report*. Philadelphia, General Electric Co., 1967. (Rep. VOY-C2-TR8)
62. JAFFE, L. D. Sterilizing unmanned spacecraft. *Aeronaut. Aerosp. Eng.* 1:22-29, 1963.
63. JAFFE, L. D. Problems in sterilization of unmanned space vehicles. In, Florkin, M., and A. Dollfus, Eds. *Life Sciences and Space Research II*, pp. 406-432. Amsterdam, North-Holland, 1964.
64. Jet Propulsion Laboratory. *Effects of Decontamination and Sterilization on Spacecraft Polymeric Materials* (Lee, S. M., and J. J. Licari), Pasadena, Calif., Jet Propul. Lab., 1968. (NASA CR-94312)
65. KAPELL, G. F., J. J. McDADE, and T. R. GAVIN. *Experimental Assembly and Sterilization Laboratory (EASL) Operations: Phase I*. Pasadena, Calif., Jet Propul. Lab., 1966. (Tech. Rep. TR32-941)
66. KAUTZ, G. P., and P. TARVER. Plan for sterilization of Voyager capsule. In, *Spacecraft Sterilization Technology*, pp. 559-567. Washington, D.C., NASA, 1966. (NASA SP-108)
67. KOHORST, D. P., and H. HARVEY. Polymers for use in sterilized spacecraft. In, *Spacecraft Sterilization Technology*, pp. 327-342. Washington, D.C., NASA, 1966. (NASA SP-108)
68. KÜRZINGER, K. Temperature-dependence of radiation sensitivity in the dry state: a model derived from experiments using atomic hydrogen II. *Int. J. Radiat. Biol.* 19(1):45-50, 1971.
69. LEA, D. E. *Actions of Radiations on Living Cells*, 416 pp. London, Cambridge Univ. Pr., 1955.
70. LEDOUX, F. N. *Decontamination of the AIMP-D Space-*

- craft.* Greenbelt, Md., NASA/Goddard Space Flight Cent., 1967. (Doc. X-723-67-171)
71. LEVY, P. W. Radiation effects in glass and other materials. *Phys. Today* 15(9):19-23, 1962.
  72. LOVELL, D. L. Skin bacteria; their location with reference to skin sterilization. *Surg. Gynecol. Obstet.* 80(2):170-174, 195, 1945.
  73. LYLE, R. G., and I. JACOBY. *Estimation of Encapsulated Microbial Burden.* Washington, D.C., Exotech Syst., 1972. (TR 72-13)
  74. McDADE, J. J. Control of microbial contamination. In, Hall, L. B., Ed. *Planetary Quarantine: Principles, Methods, and Problems*, pp. 37-62. New York, Gordon and Breach, 1971.
  75. McDADE, J. J., M. S. FAVERO, G. S. MICHAELSEN, and D. VESLEY. Environmental microbiology and the control of microbial contamination. In, *Spacecraft Sterilization Technology*, pp. 51-86. Washington, D.C., NASA, 1966. (NASA SP-108)
  76. McNALL, E. G., W. T. DUFFY, and J. J. IANDOLO. Microbiological techniques for recovery from interiors of solids. In, *Spacecraft Sterilization Technology*, pp. 155-176. Washington, D.C., NASA, 1966. (NASA SP-108)
  77. MESSENGER, G. C. Displacement damage in silicon and germanium transistors. *IEEE Trans. Nucl. Sci.* NS-12(2):53-65, 1965.
  78. MEYER, A., and E. SEITZ. *Ultraviolet Radiation. Production, Measurement and Use in Medicine, Biology and Technology.* Moscow, Inostrannay Lit., 1952.
  79. NASA. *NASA Standards for Clean Rooms and Work Stations for the Microbiologically Controlled Environment.* Washington, D.C., NASA, 1967. (NHB 5340.2)
  80. NASA. *Planetary Quarantine Provisions for Unmanned Planetary Missions.* Washington, D.C., NASA, 1969. (NHB 8020.12)
  81. National Bureau of Standards. *Shielding for High-Energy Electron Accelerator Installations.* Washington, D.C., Natl. Bur. Stand., 1964. (NBS Handb. 97) (Presently available from Natl. Counc. Rad. Prot. & Meas., Bethesda, Md., No. 31)
  82. OLSON, R. L., and S. J. FRASER. *Release of Micro-organisms from Solids after Simulated Hard Landings.* Seattle, Boeing Co., 1970. (Final rep.)
  83. OPFELL, J. B. A general review of chemical sterilization in space research. In, Florkin, M., and A. Dollfus, Eds. *Life Sciences and Space Research II*, pp. 385-405. Amsterdam, North-Holland, 1964.
  84. PAIK, W. W., and J. A. STERN. *The Microbiological Aspects of Sterilization Assembly Development Laboratories EASL and SADL.* Pasadena, Calif., Jet Propul. Lab., 1968. (Tech. Rep. TR 32-1207)
  85. PFLUG, I. J. Sterilization of space hardware. *Environ. Biol. Med.* 1:63-81, 1971.
  86. PHILLIPS, C. R. Gaseous sterilization. In, Lawrence, C. A., and S. S. Block, Eds. *Disinfection, Sterilization and Preservation.* Philadelphia, Lea & Febiger, 1968.
  87. PHILLIPS, C. R., and R. K. HOFFMAN. Sterilization of interplanetary vehicles. *Science* 132:991-995, 1960.
  88. PHILLIPS, G. B. Microbiological barrier techniques. Ft. Detrick, Md., US Army Biol. Labs., 1965. (Tech. Manuser. 260)
  89. PHILLIPS, G. B. Microbiological barrier techniques. In, *Spacecraft Sterilization Technology*, pp. 105-135. Washington, D.C., NASA, 1966. (NASA SP-108)
  90. PHILLIPS, G. B., and E. HANEL, Jr. Use of ultraviolet radiation in microbiological laboratories. *US Gov't. Res. Rep.* 34:122, 1960.
  91. PHILLIPS, G. B., F. E. NOVAK, and R. L. ALG. Portable inexpensive plastic safety hood for bacteriologists. *Appl. Microbiol.* 3:216-217, 1955.
  92. POLLARD, E. C. The action of ionizing radiation on viruses. In, Smith, K. M., and M. A. Lauffet, Eds. *Advances in Virus Research*, Vol. 2, pp. 109-151. New York, Academic, 1954.
  93. POLLARD, E. C. Thermal effects on protein, nucleic acid and viruses. In, Duchesne, J., Ed. *Advances in Chemical Physics. Vol. 7: The Structure and Properties of Biomolecules and Biological Systems*, pp. 201-237, New York, Interscience, 1964.
  94. POLLARD, E. C., and W. SOLOSKO. The thermal inactivation of  $T_4$  and  $\lambda$  bacteriophage. *Biophys. J.* 11(1): 66-74, 1971.
  95. PORTNER, D. M., D. R. SPINER, R. K. HOFFMAN, and C. R. PHILLIPS. Effect of ultrahigh vacuum on viability of microorganisms. *Science* 134:2047, 1961.
  96. POTTER, R. C., C. SCHNEIDER, M. RYSKA, and D. O. HUMMEL. Trends in radiation polymerization. *Angew. Chem. Engl.* 7:845-856, 1968.
  97. [PRATT]. The cleansing light (by "M.S."). In, *MIT Reports on Research*, pp. 3-4. Cambridge, Mass., MIT, 1972.
  98. PRYOR, W. A. Free radicals in biological systems. *Sci. Am.* 223(2):70-83, 1970.
  99. PULEO, J. R., M. S. FAVERO, and N. J. PETERSON. Use of ultrasonic energy in assessing microbial contamination of surfaces. *Appl. Microbiol.* 15(11):1345-1351, 1967.
  100. PULEO, J. R., M. S. FAVERO, and G. J. TRITZ. Feasibility of using ultrasonics for removing viable microorganisms from surfaces. *Contam. Control* 6(4):58-67, 1967.
  101. PULEO, J. R., and G. S. OXBORROW. *Recovery of Viable Microorganisms from Solids: I. Model Systems.* Phoenix, Ariz., USPHS, 1966. (Natl. Commun. Dis. Cent. Rep. 13)
  102. REDMANN, G. H. *Experimental Assembly and Sterilization/Sterile Assembly and Development Laboratory Test and Operation.* Pasadena, Calif., Jet Propul. Lab., 1967. (TM-33-322)
  103. REED, L. I. Microbiological analysis techniques for spacecraft sterilization. In, *Space Programs Summary 37-32*, Vol. IV, pp. 35-42. Pasadena, Calif., Jet Propul. Lab., 1965.
  104. REYNOLDS, M. C., and D. M. GARST. Optimizing thermal

- and radiation effects for bacterial inactivation. *Space Life Sci.* 2:394-399, 1970.
105. REYNOLDS, O. E. Developments in the analysis of planetary quarantine requirements. In, Sneath, P. H. A., Ed. *Life Sciences and Space Research XI*, pp. 3-7. Berlin, Akademie, 1973.
  106. ROARK, A. L. *A Stochastic Approach to Bioburden Estimation and Prediction-A Preliminary Report*. Albuquerque, N. Mex., Sandia Labs., 1970. (SC-RR-70-561)
  107. SAGAN, C., and S. COLEMAN. Spacecraft sterilization standards and contamination of Mars. *J. Astronaut. Aeronaut.* 3(5):22-27, 1965.
  108. SAMOYLENKO, I. I., and K. K. IVANOV. Bacterial resistance to radiation and heat effects. *Zh. Mikrobiol. Epidemiol. Immunobiol.* (2):113-115, 1972.
  109. SAMOYLOVA, K. A. *Deystviye Ul'trafioletovoy Radiatsii na Kletku* (Transl: *Effect of Ultraviolet Radiation on the Cell*). Leningrad, Nauka, 1967.
  110. SCHALKOWSKY, S., and I. JACOBY. *Safety Margins in the Implementation of Planetary Quarantine Requirements*. Washington, D.C. Exotech Syst., 1972. (Interim Rep. TR72-14)
  111. SCHALKOWSKY, S., and R. C. KLINE, Jr. Analytical basis for planetary quarantine. In, Hall, L. B., Ed. *Planetary Quarantine: Principles, Methods and Problems*, pp. 9-26. New York, Gordon and Breach, 1971.
  112. SHANK, J. L., J. H. SILLIKER, and R. H. HARPER. The effect of nitric oxide on bacteria. *Appl. Microbiol.* 10:185-189, 1962.
  113. SHUMAEVA, Yu. F. *Use of Certain Surfactants for Purposes of Disinfection*. Moscow, 1966. (Candidate diss.)
  114. SONDER, E., and L. C. TEMPLETON. Gamma irradiation of silicon. *J. Appl. Phys.* 31(7):1279-1286, 1960; 36(6):1811-1815, 1965.
  115. STROUD, R. H., and R. G. LYLE. *Contamination Control by Use of Ethylene Oxide*. Washington, D.C., Exotech Syst. (Tech. Summ. TR72-11)
  116. SWENSON, B. L. *Spacecraft Component Survivability during Entry into the Jovian Atmosphere*. Washington, D.C., NASA, 1971. (NASA TM-X-2276)
  117. TRW Space Technology Laboratory. *The Energy Dependence of Electron Damage in Silicon*. Redondo Beach, Calif., TRW Space Technol. Lab., 1964.
  118. TIMOFEEV-RISOVSKIY, N. W., and K. G. ZIMMER. *Das Trefferprinzip in der Biologie* (Transl: *The Thrust Principle in Biology*), Bd. 1, Leipzig, Hirzel, 1947.
  119. TRAUTH, C. A., Jr. A multistage decision model for mission non-contamination requirements. *Space Life Sci.* 1:135-149, 1968.
  120. TRAUTH, C. A., Jr., and A. L. ROARK. *Dry Heat Sterilization of Heterogeneous Bacterial Populations*. Presented to PQAP, March 1972.
  121. TREXLER, P. C. Flexible-wall plastic film isolators. In, *Proceedings, Second Symposium Gnotobiotic Technology*, pp. 55-60. Terre Haute, Ind., Notre Dame Univ. Pr., 1960.
  122. TREXLER, P. C. Germ-free isolators. *Sci. Am.* 211(1):78-84, 86, 88, 1964.
  123. TREXLER, P. C. The gnotobiote-review and future. *Bio-Med. Purv.* 1:47-58, 1961.
  124. TRUJILLO, R. E. *Preparation and Assay of T4 Bacteriophage*. Albuquerque, N. Mex., Sandia Labs., 1971. (Tech. Rep. SC-RR-710107)
  125. ULRICH, J. A. Skin carriage of bacteria in the human. In, *Spacecraft Sterilization Technology*, pp. 87-95. Washington, D.C., NASA, 1966. (NASA SP-108)
  126. VASHKOV, V. I. Modern methods and means of sterilization of spacecraft. In, Imshenetskiy, A. A., Ed. *Extraterrestrial Life and Its Detection Methods*, pp. 207-219. Moscow, Nauka, 1970. (NASA TT-F-710)
  127. VASHKOV, V. I., and A. G. PRISHCHEP. Efficiency of sterilization by making use of ethylene oxide and methyl bromide mixture. In, Brown, A. H., and F. G. Favorite, Eds. *Life Sciences and Space Research*, Vol. V, pp. 44-50. Amsterdam, North-Holland, 1967.
  128. VASHKOV, V. I., and G. SHCHEGOLOVA. Imparting antimicrobial properties to various materials. In, *COSPAR Tech. Manual*, No. 4, pp. 127-131. Paris, Muray Print, 1968.
  129. VASHKOV, V. I., N. V. RASHKOVA, and G. V. SHCHEGOLOVA. Planetary quarantine. In, *Karantin Planet: Printsipy, Metody i Problemy, Osnovy Kosmicheskoy Biologii i Meditsiny* (Transl: *Principles, Methods, Problems, and Means of Sterilization of Spacecraft*), Vol. 1, Part 3, Chap. 4, pp. 3-156. Washington, D.C., NASA, 1970. (NASA TT-F-13769)
  130. VESLEY, D., G. SMITH, J. HAUGEN, and Y. THUN. Survival of microbial spores under several temperature and humidity conditions. In, Pfleg, I. J., Ed. *Environmental Microbiology as Related to Planetary Quarantine*. Minneapolis, Univ. Minn., Sch. Public Health, 1969. (Semi-Ann. Rep. 3)
  131. WILLARD, M., and A. ALEXANDER. A self-sterilizing coating for spacecraft surfaces. *Nature* 202:658-659, 1964.
  132. WILLIAMS, R. E. O. Healthy carriage of *Staphylococcus aureus*: its prevalence and importance. *Bacteriol. Rev.* 27:56-71, 1963.
  133. ZIMMER, K. G. From target theory to molecular radiobiology. *Phys. Med. Biol.* 14(4):545-553, 1969.
  134. ZIMMER, K. G., L. EHRENBERG, and A. EHRENBERG. Nachweis langlebiger maanetischer zentren in bestrahlten biologischen medien und oaren bedeutung fur die strahlenbiologie. (Transl: Determination of long-lived magnetic centers in irradiated biological media and their significance for radiation biology.) *Strahlentherapie* 103:3-15, 1951.
  135. ZSOLNAI, T. Versuche zur entdeckung neuer fungistatika-VI (Transl: Experiments for the development of new fungistatics). *Biochem. Pharmacol.* 11:995-1016, 1962.
  136. ZWERLING, S. *A research Study to Definitize a Bio-Isolator Suit System (BISS)*. Philadelphia, General Electric Co., 1967. (Final Rep. 67SD660)

## BIBLIOGRAPHY

- ADAMS, M. H. *Bacteriophages*, 592 pp. New York, Interscience, 1959.
- BRANNEN, J. P. A rational model for thermal sterilization of microorganisms. In, *Mathematical Biosciences*, Vol. 2 (1/2), pp. 165-179. New York, Elsevier, 1968.
- DAVIS, N. S., G. J. SILVERMAN, and W. H. KELLER. Combined effects of ultra-high vacuum and temperature on the viability of some spores and soil organisms. *Appl. Microbiol.* 11(3):202-209, 1963.
- DECKER, H. M., and L. M. BUCHANAN. Filter applications for spacecraft sterilization program. In, *Spacecraft Sterilization Technology*, pp. 259-268. Washington, D.C., NASA, 1966. (NASA SP-108)
- DUGAN, V. L. A kinetic analysis of spore inactivation in a composite heat and gamma radiation environment. *Space Life Sci.* 2:498-505, 1971.
- DUGAN, V. L. *Principles of Operation of the Vacuum Probe Microbiological Sampler*. Albuquerque, Sandia Labs., 1967. (SC-RR-67-688)
- DUGAN, V. L., W. J. WHITFIELD, J. J. McDADE, J. W. BEAKLEY, and F. W. OSWALT. *A New Approach to the Microbiological Sampling of Surfaces: The Vacuum Probe Sampler*. Albuquerque, Sandia Labs., 1967. (SC-RR-67-114)
- FAVERO, M. S. Dual meanings of activation. *Space Newsletter* (Ryde, Aust.) 2(12):163-164, 1967.
- FREIFELDER, D., and B. TRUMBO. Matching of single-strand breaks to form double-strand breaks in DNA. *Biopolymers* 7:681-693, 1969.
- General Services Admin. *Clean Room and Work Station Requirements, Controlled Environments*. Washington, D.C., GSA, 1966. (Fed. Stand. No. 209a)
- GINOZA, W. Radiosensitive molecular weight of single-stranded virus nucleic acids. *Nature* (London) 199:453-456, 1963.
- GREEN, R. H. *Environmental Simulation Studies/Molsini* JPL Planetary Quarantine Program Status Review, June 1968.
- HUTCHINSON, F., and E. POLLARD. In, Errera M., and A. Forsberg, Eds. *Mechanisms in Radiobiology*, Vol. 1, pp. 71-92. New York, Academic, 1961.
- IMSHENETSKIY, A. A., and S. V. LYSENKO. Ultra-high vacuum and microorganisms. In, *Life Science and Space Research*, Vol. 3, pp. 142-148. Amsterdam, North-Holland, 1965.
- KAPLAN, H. S., and L. E. MOSES. Biological complexity and radio-sensitivity. *Science* 145:21-25, 1964.
- LEA, D. E., and K. M. SMITH. The inactivation of plant viruses by radiation. II. The relation between inactivation dose and size of virus. *Parasitology* (London) 34(2):227-237, 1942.
- MAHLER, H. R., and E. H. CORDES. *Biological Chemistry*, 2nd ed., pp. 177-183. New York, Harper & Row, 1966.
- MITRA, S., M. D. ENGER, and P. KAESBERG. Physical and chemical properties of RNA from the bacterial virus R 17. *Proc. Natl. Acad. Sci. USA* 50:68-75, 1963.
- MORELLI, F. A., F. P. FEHLNER, and C. H. STEMBRIDGE. Effect of ultrahigh vacuum on *Bacillus subtilis* var. *niger*. *Nature* (London) 196:106-107, 1962.
- PHILLIPS, G. B. Back contamination. *Environ. Biol. Med.* 1(2):121-160, 1971.
- REYNOLDS, M. C., K. F. LINDELL, and N. LAIBLE. *A Study of the Effectiveness of Thermoradiation Sterilization*. Albuquerque, Sandia Labs., 1970. (SC-RR-70-423)
- RUBBO, S. D., and J. F. GARDNER. Efficiency of sterilants in terrestrial and extraterrestrial environments. In, Sneath, P. H. A., Ed. *COSPAR Tech. Man. No. 4*, pp. 37-50. Paris, Muray Print, 1968.
- SCHACHMAN, H. K., and R. C. WILLIAMS. The physical properties of infective particles. In, Burnet, F. M., and W. M. Stanley, Eds. *The Viruses*, Vol. 1, pp. 223-327. New York, Academic, 1959.
- SCHUSTER, H. The ribonucleic acids of viruses. In, Chargaff, E., and J. N. Davidson, Eds. *The Nucleic Acids: Chemistry and Biology*, Vol. 3, pp. 245-301. New York, Academic, 1960.
- SILVERMAN, G. J. Microbial survival in deep space environment. *Environ. Biol. Med.* 1(1):83-97, 1971.
- SINSHEIMER, R. L. a single-stranded deoxyribonucleic acid from bacteriophage  $\phi$ X 174. *J. Mol. Biol.* 1:43-53, 1959.
- STENT, G. S. Mating in the reproduction of bacterial viruses. In, Smith, K. M., and M. A. Lauffer, Eds. *Advances in Virus Research*, Vol. 5, pp. 95-149. New York, Academic, 1958.
- TAYLOR, D. Effect of planetary trapped radiation belt on microorganisms. Presented at AIBS/NASA semi-annual Spacecraft Sterilization Technology Seminar, San Francisco, Calif., July 1972.
- TERZI, M. Comparative analysis of inactivating efficiency of radiation of different organisms. *Nature* (London) 191:461-463, 1961.

## AUTHORS' ADDRESSES

### VOLUME EDITORS

Robert W. Krauss, Dean, College of Science, Oregon State University, Corvallis, Oregon 97331

A. A. Imshenetskiy, Institute of Microbiology, Academy of Sciences USSR, Profsoyuznaya ul. 7, korpus 2, Moscow V-312, USSR 117312

G. I. Petrov, Institute of Space Research, Academy of Sciences USSR, Profsoyuznaya ul. 88, Moscow V-485, USSR 117901

### AUTHORS

#### US

Cameron, A. G. W. Harvard College Observatory, Cambridge, Massachusetts 02138

Gulkis, Samuel. Jet Propulsion Laboratory, California Institute of Technology, Pasadena, California 91103

Hall, Lawrence B. Planetary Programs, Office of Space Sci-

ences, National Aeronautics and Space Administration, Washington, D.C. 20546

Newburn, Ray L., Jr. Jet Propulsion Laboratory, California Institute of Technology, Pasadena, California 91103

Urey, Harold C. Department of Chemistry, University of California, San Diego, La Jolla, California 92307

#### USSR

Davydov, V. D. Institute of Space Research, Academy of Sciences USSR, Profsoyuznaya ul. 88, Moscow GSP-I, USSR 117810

Imshenetskiy, A. A. Institute of Microbiology, Academy of Sciences USSR, Profsoyuznaya ul. 7, korpus 2, Moscow V-312, USSR 117312

Logachev, Yu. I. Scientific Research Institute of Nuclear Physics, Moscow State University, Leninskiye gory, Moscow V-234, USSR 117234

Marov, M. Ya. Institute of Applied Mathematics, Academy of Sciences USSR, Miusskaya ploshchad' 4, Moscow A-47, USSR 125047

Oparin, A. I. Institute of Biochemistry imeni A. N. Bakh, Academy of Sciences USSR, Leninskiy pr-t 33, Moscow V-71, USSR 117071

Pisarenko, N. F. Institute of Space Research, Academy of Sciences USSR, Profsoyuznaya ul. 88, Moscow, GSP-I, USSR 117810

Rubin, A. B. Biology Faculty, Problem Laboratory of Space Biology, Moscow State University, Leninskiye gory, Moscow V-234, USSR 117234

Vernov, S. N. Scientific Research Institute of Nuclear Physics, Moscow State University, Leninskiye gory, Moscow V-234, USSR 117234

## INDEX

- Abiogenic compounds**, 368

**Abiogenic synthesis**, 325, 329–331, 333–335, 337, 346, 369, 371, 373

of biomonomers, 339–341

of biopolymers, 341–342, 370

energy sources needed, 339

model tests, 338–342

**Acceleration**, physiological effects of, 271, 290, 291

**Actinomycetes**, 272, 285, 298, 304

**Adenine**, 330, 340, 382

**Adenosine triphosphate (ATP)**, 284, 285, 340, 372, 385, 386, 398

**Albategnius** (lunar crater), 117, 118, 124, 125

**Algae**, 272, 276, 300, 302, 304

detection of, 384, 389

low-temperature effects, 279

pressure effects, 285, 287

Stromatolytic period, 335, 336

$\alpha$ -amylase, 285

$\alpha$ -particles, 84–88

**Aluminum (Al)**, 21, 28, 121, 133

**Amalthea** (Jupiter satellite), 234

**Amino acids**, 338–342, 346, 368, 369, 380, 381, 382

on Mars, 368

in meteorites, 329

on Moon, 330

**Ammonia**, 369, 370

in interstellar space, 324, 325

on Jupiter, 199, 201

on Saturn, 221, 222

**Amor** (asteroid group), 246

**Amphitrite** (asteroid), 248

**Anabiosis**, 276

**Anaerobic processes**, 338

**Animals**, 272

ionizing radiation, effects on, 293

**Anisotropic diffusion**, 70–71

**Anisotropy**, 61, 62, 63–64, 65, 67

**Anorthosite**, 121, 124, 125

**Antibaryons**, 6, 8

**Antimatter**, 5, 6, 8, 9

**Antineutrinos**, 6, 7

**Apollo** (asteroid group), 246, 247, 251

**Apollo 11 mission**, 119, 330

**Apollo 12 mission**, 119, 330

**Apollo 13 mission**, 119

**Apollo 14 mission**, 121

**Apollo 15 mission**, 122

**Apollo 16 mission**, 122, 124

**Apollo 17 mission**, 122

**Apollo program**, 119, 404

**Arabia** (Mars), 178

*Arabidopsis thaliana*, 304

**Argon (Ar)**, 26, 139, 140, 328

**Ariadne** (asteroid group), 248

**Ariel** (Uranus satellite), 245

*Artemisia*, 300

**Artificial Mars device**, 306–312

*Aspergillus*, 281, 300

*Aspergillus glaucus*, 297

**Assay**, microbiologic, 409, 411

poststerilization, 405

procedures manual, 423

standards, 410

**Asteroids**, 72, 124, 125, 129, 197, 244–248, 327, 328

belt, 124, 125, 245

classes, 246

collisions, 246

diameters, 247

discovery, 244–245

families, 246

groups, 245–246

Kirkwood gaps, 246

logistics, 244–245

mass, 247

orbits, 245, 246

origin and evolution, 246–247

physical data, 247–248

statistics, 245–246

*Astagobius angustatus*, 278

**Astraea** (asteroid), 244

**Auroras**, 99–104

disturbances, 97, 98, 99

electron, 100

homogenous, 99

physical properties, 99

polar, 99, 100

polar cap glow, 100, 101

proton, 100

ray type, 99

subauroral red arcs, 101

substorms, 100, 101

**Autoclaving**, 420

**Automatic biologic laboratories (ABL)**, 368, 375, 396–399

life-detection devices in, 297–398

**Automatic biologic laboratories—Continued**

optical measuring unit, 398–399

**Autosterilization**, 422–423

**Azotobacter**, 297

**Bacillus cereus**, 311, 383

**Bacillus mesentericus**, 273, 294, 418, 419

**Bacillus mycoides**, 276

**Bacillus stearothermophilus**, 279, 280

**Bacillus subtilis**, 311

decontamination of, 419, 420, 423

high-temperature effects on, 281, 282

pressure effects on, 286, 288

spacecraft studies, 305

**Bacillus subtilis** var. *niger*, 422, 423

*B. megaterium*, 283, 309

*B. zooglieicus*, 309

**Back-contamination**, 403–404

**Background radiation**, 4–5

**Bacteria**, 272, 276, 285, 289, 298, 335, 336, 372, 384, 391, 417, 421, 423

anaerobic, 300

barotolerant, 273

growth, 307

halophilic, 299

halotolerant, 299, 310

high-temperature effects, 279

low-temperature effects, 279

reproduction of, 306–311

spacecraft experiments, 305

**Bacterionema matruhotii**, 383

**Balloon high-altitude experiments**, 55, 272, 305

**Barometric hypsometry**, 182

**Barriers**, microbiologic, 411, 414

**Baryons**, 6, 8

**Basalt**, lunar, 117, 120, 123–125, 127–128

**Bennett** (comet), 250, 252

**Beryllium**, 21

**Betulia** (asteroid), 246

“Big Bang” theory of universe, 3–4

**Bioassay room**, 414

**Bioburdens**, 414

**Biochemiluminescence sampling method**, 385

**Biogenic synthesis**, 335–338

**Biosolator suit system (BISS)**, 416

- Biomonomers, 339–340  
 Biopolymers, 341, 382  
 Biosatellite II experiment, 288  
 Biosphere, 164, 272–274, 334, 345  
 Bismuth, 21  
 Black holes, 11  
 Bode's law, 244  
*Bodo marina*, 292  
 Bond albedo, 136, 252  
 Boron, 21  
 Bremsstrahlung, 42, 45
- Calcium (Ca), 21, 28, 121, 133  
 Callisto (Jupiter satellite), 235, 236, 237  
   microwave brightness temperature, 239  
*Capsicum annum*, 289  
 Carbohydrates, 368, 380, 389  
 Carbon (C), 19, 57, 133, 331, 333, 370,  
   372  
   in interstellar space, 324–325  
   in solar system, 326–331  
 Carbon compounds, 121, 322–338, 370,  
   372  
   evolution of  
     in solar system, 326–331  
     in the universe, 322–326  
   initial, 338  
 Carbon dioxide ( $\text{CO}_2$ ), 139, 328, 333,  
   393, 407  
   on Mars, 170, 171  
   on Venus, 148, 150  
 Carbon monoxide (CO), 148, 171, 324,  
   328, 329, 333  
 Carbon-nitrogen cycle, 323  
 Catalase, 285  
 Centrimetric radiation, 215, 218  
 Ceraunius region (Mars), 184  
 Ceres (asteroid), 244, 247  
*Chaoschaos*, 383  
 Chemiluminescence, 394–395  
 Cherenkov radiation, 42  
*Chlorella*, 302, 304  
*Chlorella pyrenoidosa*, 287, 296  
*Chlorella vulgaris*, 283, 304  
 Chlorophyll, 341, 344, 382  
 Chondrites, carbonaceous, 21, 129,  
   329–331, 369  
 Chromospheric flare, 51, 53  
 Clean rooms, 414–415  
   laminar-flow, 415  
 Clematis (asteroid), 246  
 Clinostat, 288, 289  
 Closed systems, 343, 420  
*Clostridium butyricum*, 303  
*Clostridium sporogenes*, 303  
 Coacervate systems, 344–345  
 Coenzymes, 346  
 Comet clusters, 327
- Comets, 47, 72, 248–254, 325–326  
   chemical composition of, 325  
   core of, 251  
   empirical behavior of, 250–251  
   history, 248–249  
   long-period, 249–252  
   model of, 251, 253  
   new, 252  
   nomenclature, 248–249  
   nucleus, 251, 325  
   orbits, 249, 253, 254  
   origin and evolution of, 253–254, 325  
   periodic, 249  
   short-period, 249, 250, 253  
   and solar wind, 252  
   tails, 250, 252
- Compton radius, 6  
 Compton scattering, 7  
 Contamination, 403–404  
   accessible, 408–409  
   accident, 403, 414  
   back, 403–404  
   buried, 409, 410  
   control techniques, 405, 407, 408,  
    414–423  
   effectiveness of, 410  
   estimation of, 405  
   inaccessible, 409–411  
   levels of, 411, 414  
   of materials, 409–410  
   microbial, 405, 408–411  
   of personnel, 417  
   planetary, probability of, 415  
   prevention, 414–417  
   probability of, 411–412  
   models for, 405–406  
   sources of, 411–413  
   space survival study, 406–408  
   surface, 405, 407–409
- Coprates (Mars), 184  
 Cosmic rays, 15, 62, 324  
   galactic, 54–55, 66  
     chemical composition, 54  
   solar, 51, 55–60, 70, 71  
     flares, 67–68, 72  
     quiet periods, 67  
     shock waves, 66–67  
     spectrum, 57, 60
- Cosmobarometers, 25  
 Cosmologic constant, 4  
 Cosmology, 3–5  
   “Big Bang” theory of, 3–4  
   principles of, 3–4  
   steady state, 4  
   symmetric, 9  
   unsymmetric, 9
- Cosmos 470 experiment, 74  
 Cosmos 502 experiment, 74  
 Cosmothermometers, 25
- Crepis capillaris*, 304  
 Cryobiology, 276  
 Cuvette soil sampling device, 386, 388  
 Cyanoacetylene, 324–325  
 Cyclopeptide, 342  
 Cygnus (constellation), 169, 324  
 Cytochrome, 289, 372  
 Cytosine, 340
- d'Arrest (comet), 253  
 Davy (lunar rill), 118  
 Dawes (lunar crater), 119  
 Decametric radiation, 215–218  
 Decimetric radiation, 46, 215, 218–219  
 Decontamination techniques, 417–423  
   autosterilization, 422–423  
   disinfectant cleaning, 417  
   effectiveness of, 410  
   surface sterilization, 418–420  
   thermal sterilization, 420–421
- Deimos (martian satellite), 135, 187–188
- Density wave theory, 13
- Deoxyribonucleic acid (DNA), 382, 384,  
   422
- Descartes (lunar crater), 122  
 Desiccation of cells, 271, 296–300  
 Deuterium, 7, 9, 17, 23, 164  
 Dione (Saturn satellite), 241  
   physical data, 242
- Diplococcus pneumoniae*, 301  
 Discoverer-17 experiment, 303  
 Doppler shift, 4, 251  
*Drosophila*, 293, 303, 305  
*Drosophila melanogaster*, 296, 304  
 Dry-heat sterilization, 410, 411, 420–422  
*Dunaliella salina*, 279  
 Dunite, 120, 125, 332
- Earth (see also Sun-Earth connection),  
   21, 115, 116, 126, 133, 135, 139, 142  
   age of, 127, 129  
   Archean era, 332  
   atmosphere, 29, 38–40, 164, 331–  
    333, 336, 338, 339, 369, 372, 390  
   biosphere, 164, 272–274, 334, 345  
   Cambrian period, 335, 336  
   characteristics of, 105  
   comets and, 325–326  
   contamination of, 403–404  
   crust, 331, 334, 335, 338  
   density of, 121, 134, 136  
   diameter, 134  
   distance from Sun, 145  
   evolution of, 164, 335  
   formation, theories of, 28–29  
   geometric characteristics, 134  
   gravitational field, 135  
   Gunflint epoch, 336  
   history, 333

- Earth—Continued**
- hydrosphere, 331, 338, 342, 343
  - inert gases on, 331
  - interior, 28, 29
  - ionosphere, 95–98
    - disturbances, 98–99
  - life on, theories of, 29, 321–333, 335, 369–370
  - magnetic field, 79–83, 94, 135
  - magnetosphere, 51, 76–83, 90
    - disturbances, 104
    - electron distribution, 89
    - energy in, 104
  - mass, 127, 134, 331
  - melting of, 332
    - models, 80, 81
    - solar wind effect, 81
    - structure of, 83
  - oceans of, 29
  - organic substances, evolution of, 331–338
  - planets, 133, 135
  - plasmosphere, 82
  - Precambrian period, 335, 336
  - Protozoic period, 335, 336
  - radiation, 135
  - radiation belts, 83–88
    - $\alpha$ -particles in, 84–87
    - death of particles in, 88
    - protons of, 83–84
    - sources of particles in, 87–88
    - structure of, 83
  - rotation, 26, 145
  - sedimentary rocks, 115
  - spin characteristics, 134
  - Stromatolytic period, 335–336
  - temperature, 28
  - thermal history, 29
  - volatile components, 166
  - volcanoes, 333
    - water on, 332
- Earth-Moon system, 26–29, 128, 133**
- Earth sciences, 135**
- Edom (martian basin), 184**
- Electron beam radiation, 419**
- Electron detectors, 55**
- Electron microscope, 379–380**
- Electron-positron pairs, 6–7, 20, 21**
- Electrons, 16, 54–56, 59, 60, 64, 163, 214**
- cone of propagation, 64
  - distribution of, 89
  - high-energy, 58, 419
  - lifetime of, 90
  - low-energy, 58, 60, 61
  - precipitation of, 91
  - satellite, 85
  - spectra, 65
  - streams, 56, 62, 63, 65–67
- Electrostatic analysis, 47**
- Enceladus (Saturn satellite), 241**
- physical data, 242
- Encke (comet), 250**
- Ensor (comet), 253**
- Entropy, 342–344, 345, 371**
- Enzyme-phosphatases, 384**
- Enzymes, 284, 285, 346, 347, 407**
- reactions, 371
- Eos (Mars), 184**
- Eros (asteroid), 246**
- Escherichia coli*, 283, 286, 289, 295, 301, 303, 311, 383, 395**
- Ethyl alcohol, 417**
- Ethylene oxide (ETO), 418**
- Eubacterium isolatum*, 336**
- Europa (Jupiter satellite), 106, 234–236, 237**
- Europium, 121**
- Exobiology, 29, 142, 166, 188, 271, 301, 311–312, 321–347, 368–399, 403**
- investigation and search for extra-terrestrial forms of life, 368–399
  - prerequisites of, 321–347
- Explorer 10 (interplanetary probe), 92**
- Explorer 12 (interplanetary probe), 92, 104**
- Explorer 16 (interplanetary probe), 73, 74**
- Explorer 23 (interplanetary probe), 73, 74**
- Explorer 26 (interplanetary probe), 90**
- Explorer 33 (interplanetary probe), 53**
- Explorer 34 (interplanetary probe), 63, 66**
- Extraterrestrial life. *See* Exobiology**
- Extreme environmental conditions, biological effects of, 271–312**
- desiccation of cells, 296–300
  - gases, effects of, 300–301
  - ionizing radiation, 293–296
  - magnetic field, 296
  - pressure, 285–288
  - temperature, 281
  - ultraviolet rays, 293–296
  - vacuum, 281–285
  - vibration, 290–291
  - weightlessness, 288–290
- F. breve*, 303**
- Faculae, 34**
- Fats, 339**
- Fatty acids, 368, 369**
- Fischer-Tropsch reaction, 329, 333, 337, 338**
- Flocculi, 34, 36**
- calcium, 34
  - hydrogen, 34
- Flora (asteroid group), 248**
- Flow-scan television camera, 376**
- Fluorescein dyes, 384**
- Fluorescence, 382, 384**
- Fluorescence sampling methods, 382–386**
- Fluorochrome, 383**
- Flyby missions, 198–199, 405, 415, 421**
- Formaldehyde, 324, 325, 418, 423**
- Fossils, 335–336**
- Fra Mauro (lunar crater), 121**
- Fraunhofer absorption lines, 38–39**
- Friedmann expansion law, 3–5, 8**
- Fungi, 276, 285, 298, 306**
- Fusarium*, 298**
- Galaxies, 324, 325**
- angular momentum of, 12
  - clusters, 9, 10, 11
  - elliptical, 12, 16
  - evolution of, 12–13
  - formation of, 10, 11
  - irregular, 12
  - new systems, 12
  - nuclei formation of, 11
  - red shifts of, 4
  - spectra of, 4
  - spiral, 12–13
- Galilean satellites (Jupiter), 234–237**
- temperature of, 235, 238
- Gamma radiation, 54, 294, 419, 422**
- Ganymede (Jupiter satellite), 106, 197, 234–237**
- microwave brightness temperature, 239
- Gas chromatography, 329, 337, 380, 381**
- Gaseous plasma sterilization, 418**
- Gases, biologic effects of, 300–301**
- Gas exchange experiment, 391, 398**
- Geomagnetic disturbances, 89, 94–98, 103**
- Geostrophic wind, 159**
- Germicidal soaps, 417**
- Gliocladium fimbriatum*, 294**
- Globular clusters, 10**
- Glycine, 122**
- Grand Canyon (Valley Marineris) (Mars), 184, 185**
- Greenstein effect, 251**
- Griqua (asteroid), 246**
- Groznaya (meteorite), 329**
- Gulliver experiment, 391–393**
- Habrobracon*, 303, 304**
- Haemophilus aegyptius*, 309**
- Halley's Comet, 248**
- Heat inactivation, 420, 421**
- Hebe (asteroid), 244**
- Hectometric radiation, 215**
- Heisenberg uncertainty principle, 6**

- Helium (He), 331  
   in atmosphere of Mercury, 140  
   in interplanetary space, 53, 54, 56, 57  
   on Jupiter, 199, 202, 213, 222  
   on Saturn, 222  
   in solar system, 57, 323, 326, 331  
   in universe, 7, 9, 11, 14, 17–19, 21–22
- Hellas (martian basin), 185
- Hexachlorophene, 417
- Hidalgo (asteroid), 246
- High-efficiency particulate air (HEPA) filters, 415–416
- High-energy particles, 55, 59, 66, 67, 87, 419
- High temperature, effects of, 279–281
- Hilda (asteroid group), 246
- Histogram, 217, 411
- Hubble law, 4, 5
- Hubble radius, 5–6, 7
- Humason (comet), 250
- Hungaria (asteroid group), 246
- Hydrocarbons, 322, 329, 334, 337, 369
- Hydrodiction reticulatum*, 287
- Hydrogen, 5, 7, 9–11, 17, 53, 54, 133, 331, 333, 370  
   atoms, 7, 10  
   in comets, 250, 252  
   ionized, 14, 15  
   on Jupiter, 199, 201, 213, 236  
   on Moon, 122  
   negative ions, 10  
   neutral regions, 7, 14, 15  
   nuclei, 17  
   on Saturn, 221, 226  
   in solar system, 21, 326  
   in stars, 18, 19, 21, 325  
   in universe, 323–326
- Hydrogen ionization, 13–15
- Hydrogen peroxide, 417–418
- Hydrogen sulfide, 370
- Hyperion (Saturn satellite), 241  
   physical data, 242
- Iapetus (Saturn satellite), 241  
   physical data, 242
- Iapygia (martian basin), 184
- Icarus (asteroid), 246
- Ikeya-Seki (comet), 250
- IMP-1 (interplanetary probe), 49, 104
- Inert gases, 326, 331
- Infrared radiometry, 202, 247
- Infrared (IR) spectrophotometry, 148
- Infrared spectroscopy, 375
- Infrared thermometry, 140
- Insects, low-temperature effects on, 276
- Intercosmos 6 data, 74
- Interplanetary magnetic fields, 32, 48–50, 62, 68  
   sectorial structure of, 49–51
- Interplanetary medium, 34, 47–76  
   shock waves in, 51–54, 71, 77, 93, 323
- Interplanetary plasma, 47
- Interplanetary space, 32–111, 324–325
- Io (Jupiter satellite), 106, 197, 218, 234–238
- Ionizing radiation, 271, 273, 274, 293–296, 369  
   dose, 294  
   flux of, 96  
   low temperature and, 294  
   protection against, 295  
   resistance to, 294  
   solar flares, 39  
   spacecraft, factor in, 293  
   target theory, 295–296
- Ionizing radiation sterilization, 419, 420, 421, 422
- Ionospheric disturbances, 45, 98–99
- Iron (Fe), 21, 27, 133, 331  
   on Mercury, 136, 137  
   in meteorites, 329  
   on Moon, 121, 128
- Isoprenoid phytane ( $C_{19}$ ), 337
- Isoprenoids, 337, 338
- Isopropyl alcohol, 417
- Isotropic diffusion, 69–70
- Janus (Saturn satellite), 241
- Jeans length, 9, 10
- Jet streams, 23
- Juno (asteroid), 244, 247
- Jupiter (planet), 24, 126, 127, 129, 197–221, 245, 327, 407  
   albedo, 208, 209  
   atmosphere, 199–213  
   composition, 201–203  
   computer calculation, 203  
   dynamics, 212–213  
   energy balance, 209–210  
   structure models, 210–212  
   temperature, 203–205, 218  
   visible surface, 205–209
- body structure, 213–214
- characteristics, 105
- clouds on, 205–206
- density, 198
- energetic particles on, 220
- escape velocity, 198
- magnetic field, 214, 219–220
- magnetopause, 219
- magnetosphere, 106, 214–221, 236
- mass, 198, 235
- model of, 214, 215
- orbit, 200
- photometric data, 198–199, 208–209
- physical data, 198
- plasma density, 220–221
- radiation conditions near, 106, 205
- Jupiter (planet)—Continued  
   radio emission from, 203, 215  
   radius, 198  
   red spot 206–208  
   rocket and satellite studies, 199, 202, 204, 208–209  
   rotation, 200, 206, 219  
   satellites, 129, 234–238  
   spectrum, 205, 216, 223  
   troposphere, 210
- JV (Jupiter satellite), 234
- Kohoutek (comet), 250, 251
- Labeled nutrient media experiment, 393
- Lander spacecraft, 405, 412, 421
- Larmor rotation, 78
- Laser beam sterilization, 419
- Lead, 21, 123
- Lepisma domestica*, 297
- Libya (martian basin), 184
- Life  
   chemical basis, 369–371  
   dynamic properties of, 372  
   evolution of, 368  
   light, role of, 371–373  
   origin of, 29, 341–347, 368  
   search for, 369
- Life-detection methods, 374–396  
   analytic, 376–382  
   fluorescence, 382–386  
   functional, 382–386  
   gas chromatography, 380–382  
   mass spectroscopy, 380–382  
   metabolism studies, 390–393  
   microorganism growth studies, 387–390  
   microscopy, 378–380  
   optical, 382  
   panoramas, transmission of, 376–377  
   photosynthesis, 393–396  
   remote, 375–376  
   sample collection, 377–378  
   samples, incubation of, 386–387  
   thermogenesis, 387
- Light, role of, 371–373
- Light scattering, 376, 387, 388, 397
- Limestone, 336
- Limonite, 307, 390, 395
- Lipids, 369
- Lithium, 21
- Littrow (lunar crater), 122
- Low temperature, effects of, 276–279  
   life at, 278–279  
   physiologic processes in different organisms, 280
- Luciferin-luciferase reaction, 385, 386
- Luminescence, 382

- Luna 1 (lunar probe), 104  
 Luna 2 (lunar probe), 47, 104  
 Luna 3 (lunar probe), 47  
 Luna 16 (lunar probe), 330  
 Luna 19 (lunar probe), 74  
 Luna 20 (lunar probe), 330  
 Lunar Explorer, 74  
 Lunar module, 119  
 Lunar Orbiter, 74  
 Lunar Receiving Laboratory (LRL), 404, 416  
 Lunar samples, 28, 121, 122, 330–331, 404  
 Lyophilization, 275
- Macromolecules, 370, 383  
 Magnesium (Mg), 21, 133  
 Magnetic disturbances, 101  
 Magnetic field, 326, 396  
     physiologic effect of, 296  
 Magnetometer experiment, 168, 219  
 Magnetopause, 77, 92, 164  
 Mare Crisium (Moon), 115, 117  
 Mare Fecunditatis (Moon), 119  
 Mare Humorum (Moon), 115, 117  
 Mare Imbrium (Moon), 115, 117, 118  
 Mare Nectaris (Moon), 115, 117  
 Mare Nubium (Moon), 119  
 Mare Oceanus Procellarum (Moon), 119  
 Mare Orientale (Moon), 115, 117, 119  
 Mare Serenitatis (Moon), 115, 117, 118  
 Mare Tranquillitatis (Moon), 119, 330  
 Mare Tyrrhenum (Mars), 183  
 Marine biology, 273  
 Mariner 1 (Venus probe), 406, 415  
 Mariner 2 (Venus probe), 406, 415  
 Mariner 3 (Mars probe), 406, 415  
 Mariner 4 (Mars probe), 168, 406, 415  
 Mariner 5 (Venus probe), 142, 144, 149–152, 161–163, 406, 415  
 Mariner 6 (Mars probe), 168, 175, 182, 406, 415  
 Mariner 7 (Mars probe), 168, 171, 175, 182, 406, 415  
 Mariner 8 (Mars probe), 406, 415  
 Mariner 9 (Mars probe), 167, 168, 171, 175, 177, 178, 180, 181, 182, 183, 184, 185, 186, 406, 415  
 Mariner 10 (Mars probe), 136, 140, 141, 142, 149, 161  
 Mariner Mars '71 program, 417  
     quarantine model, 413  
 Mariner Venus Mercury for Venus mission, contamination, probability of, 406  
 Marius Hills (Moon), 118  
 Mars (planet), 126, 133, 167–188, 245  
     albedo, 176–181  
 Mars (planet)—Continued  
     atmosphere of, 162, 170–176, 328, 333, 373, 374, 380  
     chemical-dynamic model, 171  
     dayglow, 175  
     dynamics, 173  
     lower, 170–171, 172  
     middle, 172  
     model, 174  
     pressure, 170  
     upper, 172–174  
     biologic problems, 373–374  
     canals, 181  
     chaotic terrain, 184  
     characteristics of, 105  
     circular basins, 184–185  
     clouds, 171  
     contamination, probability of, 406  
     craters, 177, 180, 183, 184  
     density, 134, 168  
     desert, 167  
     diameter, 134  
     distance from Sun, 145, 167  
     dust storm, 167, 174  
     evolution of, 164, 374  
     exosphere, 175–176  
     geological studies, 182–183  
     geometric characteristics, 134  
     global characteristics, 168  
     grabens, 184  
     Grand Canyon, 184, 185  
     gravitational field, 168  
     hemispheres, 169  
     ionosphere, 174  
     life on, 188, 301, 311, 328, 368, 369, 397, 407  
     magnetic field, 168–170  
     magnetopause, 106  
     mass, 134, 168  
     models, 174  
     mountains, 183–184  
     observations of, terrestrial, 167  
     orbit, 145, 167  
     photographs of, 167, 170, 180, 181, 183  
     planes, 183  
     poles, 170–173, 181, 187, 328  
     probes, 397, 406, 415  
     quarantine program, 425  
     radar observations, 182  
     radiation conditions near, 106  
     radius, 168  
     rotation of, 145, 169–170  
     satellites, 133, 170, 187–188  
     seasons, 169–170, 173, 179, 328  
     simulation of conditions on, 306–311  
     soft landing on, 167  
     soil, 176–178  
 Mars (planet)—Continued  
     spacecraft data, 167–176, 182, 374–380, 397  
     spectrometer studies, 174  
     spin characteristics, 134  
     streamlike formations, 185–187  
     surface, 176–181, 328  
     mineral composition of, 178  
     temperature, 171, 172, 174, 175, 176, 177, 328  
     thermal mode, 171–172  
     volatile compounds, 166  
     volcanoes, 183  
     water on, 170, 176, 187, 328, 333  
     wave of darkening, 179  
     winds, 173–174  
 Mars 2 (Mars probe), 167, 168  
 Mars 3 (Mars probe), 167, 168, 176, 182  
 Masogaea (Mars), 177  
 Mass spectrometer, 329, 380–381, 393  
 Mass spectroscopy, 337–380  
 Mated microbial burden, 405  
 Mathematical models, 371, 411  
 Matter, 3–10, 21, 23  
     solar, 24  
 Melas Lacus (Mars), 184  
 Mercury (planet), 28, 129, 133, 135–142  
     atmosphere of, 139–140, 327  
     Bond albedo, 136  
     characteristics of, 105  
     chemical composition, 136  
     density, 134, 136, 142  
     diameter, 134–136  
     distance from Sun, 135, 145  
     escape velocity, 136  
     evolution of, 164  
     geometric characteristics, 134  
     infrared thermometry experiment, 140–141  
     interior, 136  
     life on, 327  
     maps of, 137, 138  
     mass, 134, 136  
     models, 136  
     nucleus, 136  
     observations of, terrestrial, 135  
     orbit, 145, 167  
     photographs of, 136, 139  
     poles, 140  
     radar studies, 138, 139  
     radioactivity, 136  
     radioastronomy experiments, 141  
     radius, 136  
     rotation, 138–139, 145  
     shape, 135  
     spacecraft data, 136  
     spectral reflectivity of, 137  
     spin characteristics, 134  
     Sun and, 138–140

- Mercury (planet)—Continued**
- surface, 136–138, 140, 142, 327
  - temperature, 136, 140, 141
  - thermal history, 136
  - thermal radiation, 140, 141
  - UV experiment, 140
- Mesons**, 6
- Metabolism**, 342, 369, 387, 390–393, 397
- Meteorites**, 22, 73, 122, 129, 185, 248, 328–330, 369
- composition, 21, 29, 74, 75, 129, 328, 331
  - density of, 121
  - iron, 328, 329
  - origin of, 24–26, 328
  - sporadic, 74
  - stone, 328, 329
- Methane**, 227, 333, 369
- in interstellar space, 324–326
  - on Jupiter, 199, 201, 221
  - on Saturn, 221, 223
- Methyl bromide**, 418
- Mice**
- acceleration effects on, 290, 291
  - vibration effects on, 291
- Microbiocenoses**, 274, 299
- Microbiology**, 297
- Microcalorimetry**, 387
- Micrococcus candidans*, 301
- Micrococcus radiodurans*, 293
- Microcoleus*, 294
- Microcystis*, 300
- Microflora**, 387–390, 396
- Micrometeorites**, 74–76, 396
- Micrometeoroids**, 119
- Microorganisms**, 271–273, 335, 369, 374, 377–379
- accessibility of, 410
  - aerobic, 423, 424
  - anaerobic, 423, 424
  - assay of, 409–410, 423
  - barotolerant, 273
  - barriers for, use of, 411, 414–417
  - contamination levels, 408–411
  - contamination models, 405–407
  - destruction of, 410, 420
  - detection of, 383
  - embedded, 409, 410
  - enumeration of, 424
  - growth studies, 386–390, 406, 408
  - on Mars, 373
  - metabolism of, 390–393
  - radiation effects on
    - ionizing, 273
    - ultraviolet, 305–307
  - reentry heating effect on, 407
  - removal of, 417–423
  - sampling, 408
  - sources, 411–413
- Microorganisms—Continued**
- space travel effects, 406
  - survival of, 406
  - temperature effects on
    - high, 275, 279–280, low, 276–279, 280
  - terrestrial, 403
  - thermophilic, 280
  - UV radiation effects on, 406, 407
  - vacuum effect on, 281–285
  - vacuum pressure experiments, 407
  - water factor in, 297–298
- Microscope sampling method**, 378–380
- biological, 379
  - cytochemical, 379
  - electron, 379–380
- Microspheres**, 343
- Microwave radiation**, 4, 5, 45
- Milky Way (galaxy)**, 324
- Mimas (Saturn satellite)**, 241
- physical data, 242
- Miranda (Uranus satellite)**, 244, 245
- Molecular paleontology**, 335–338
- Molnya (satellite) data**, 66
- Monomer substances**, 341
- Mononucleotides**, 344
- Moon**, 115–129, 140, 146, 277
- age of, 123–124
    - isochron, 123
  - atmosphere, 74, 122
  - caldera, 115
  - characteristics of, 105
  - chemical composition, 121–122, 124
  - core, 120
  - craters, 115, 118, 125, 137
    - collisional, 118
    - explosive, 115
    - halo, 118
    - ray, 115
    - volcanic, 118
  - density of, 26, 27, 116, 121, 129
  - dipole field, 126
  - far side, 119
  - genesis rock, 122, 124
  - gravitational field, 115–116, 123
    - anomalies, 116–118, 125
  - interior, 117–119, 120, 122, 124, 129
  - laser altimeter experiment, 118
  - lava flows, 115, 118–121, 124, 127
  - life on, 122, 330
  - magnetic field, 126
  - manned flights to, 404
  - maria, 116–118, 120, 121, 122, 124, 125
  - mascons, 116–118, 120, 124, 125
  - mass, 116, 117, 235
  - and Mercury, 142
  - micrometeorite impacts on, 74
  - moments of inertia, 116, 124
- Moon—Continued**
- moonquakes, 120, 121
  - mountains, 115, 116, 119, 120, 137
  - near side, 119
  - orbit, 26, 120, 127
  - origin of, 26–28
    - atmospheric condensation theory, 26–27
    - capture theory, 27, 128–129
    - fission theory, 26
    - model for, 128–129
    - twin planet theory, 27
  - physical constants, 115, 116
  - poles, 116
  - probe, 47, 73, 104, 121, 330
  - radiation conditions near, 105–106
  - radioactivity, 120, 125
  - radius, 116, 121
  - rills, 117, 118, 119
  - rotation, 120
  - seismic observations, 119–121
  - shape, 116, 120
  - spacecraft experiments, 115, 117, 119, 121, 122, 124
    - spectral reflectivity of, 137
  - surface, 115, 118–121, 127
    - samples, 28, 121, 330–331, 404
  - temperature, 116, 120
  - volcanoes, 121
    - water on, 115, 121, 123
- Multivator chamber**, 385
- Murchison (meteorite)**, 329
- Mycobacterium rubrum*, 298
- Mycobacterium smegmatis*, 298, 309
- Mycobacterium tuberculosis*, 301
- Mycococcus oligonitrophilus*, 298, 309
- Mycococcus ruber*, 308, 309, 310
- Mycoplasms**, 272
- Myrothamnus flabellifolia*, 296
- Nelumbo nucifera*, 297
- Neon (Ne)**, 14, 140, 331
- Nephelometer**, 385, 388, 389
- Neptune (planet)**, 24, 226–232
- atmosphere, 226–231
    - composition, 230–231
    - structure (models), 230–231
    - temperature, 228–230
  - body structure, 231
  - characteristics, 105
  - density, 198
  - hydrogen quadruple lines, 226–227
  - mass, 198
  - mechanical data, 200
  - photometric data, 199, 227
  - physical data, 198
  - rotation, 229
  - satellites, 244
  - spectrum, 227, 228

- Nereid (Neptune satellite), 244, 245  
*Neurospora crassa*, 287, 296  
 Neutrinos, 6, 7, 20  
 Neutron capture process, 21–22  
 Neutrons, 6, 7, 11  
     spallation-produced, 24  
 Nickel (Ni), 21, 329  
 Nitrogen (N), 133, 370, 391, 407, 410  
     in interstellar space, 323, 324  
     on Mars, 328  
     on Moon, 122  
     in solar system, 326  
 Nitrogen fixation, 391  
 Nix Olympica (martian volcano), 183  
 Nucleic acids, 340–341, 342, 344, 345,  
     370, 422  
     detection of, 380, 382  
     evolution of, 347  
     on Moon, 330  
 Nucleosynthesis, 7, 11, 12, 16–22, 322–  
     323  
     related elements, 323  
     stable, 322  
     stellar evolution and, 16–22  
     unstable, 322  
 Nucleotides, 340, 341, 369, 382, 383  
  
 Oberon (Uranus satellite), 245  
 OGO (Orbiting Geophysical Observatory), 74  
 Oort cloud, 254  
 Open systems, 342–347, 372, 420  
 Optical measuring unit, 398–399  
 Optical-mechanical scanning device, 376  
 Orbiter missions, 376, 405  
 Orbiting Astronomical Observatory (OAO), 150, 208–209, 250  
 Organic compounds, 370, 372, 377, 380  
 Orion (nebula), 324  
 Oterma (comet), 253  
 Oxygen (O), 14, 57, 133, 333, 338, 373  
     detection of, 376  
     in interstellar space, 323, 324  
     on Mars, 171, 373  
     molecular, 332, 372  
     on Moon, 122  
     in Sun, 326  
 Oxygen exchange experiment, 393  
 Ozone, 171  
  
 Pajdusakova (comet), 253  
 Paleontology, molecular, 335, 336–338  
 Pallas (asteroid), 244, 247, 248  
 Panspermia, 272  
 Paracetic acid, 417  
 Paraformaldehyde, 418, 423  
*Paramecium aurelia*, 295  
*Paramecium bursaria*, 292  
  
*Paramecium caudatum*, 292, 295  
*Parascaris equorum*, 303  
 Pegasus (satellite) data, 74, 75  
*Pelomyxa cardiensis*, 289  
*Penicillium*, 281, 298, 300  
*Penicillium roqueforti*, 305  
 Peroxidase, 285  
 Perturbation, 9, 12, 28  
 Petroleum, origin of, 334  
 Phaethontis (martian desert), 167  
 Phobos (martian satellite), 133, 187–188  
 Phoebe (Saturn satellite), 241  
     physical data, 242  
*Phormidium*, 294, 300  
 Phosphatase concentration, 384  
 Phosphates, 369  
 Phosphatides, 344  
 Phosphorus, 121, 370  
 Photometric studies, 227, 236, 247, 397  
 Photomicrographs, 378  
 Photomultiplier, 382, 386, 388  
 Photons, 5, 7, 9, 14, 386  
 Photoreactivation, 275, 292  
 Photosynthesis, 279, 371–374, 376,  
     393–396  
*Phycomyces nitens*, 294  
 Pioneer 1 (interplanetary probe), 74  
 Pioneer 8 (interplanetary probe), 66, 74  
 Pioneer 9 (interplanetary probe), 74  
 Pioneer 10 (interplanetary probe), 75,  
     106, 406  
     planet Jupiter data, 199, 202, 203,  
     204, 209, 214, 219, 220, 234–235  
 Planetary physics, 135  
 Planetary quarantine (PQ), 403–425  
     cost effectiveness, 405  
     documentation, 412–414  
     international programs, 404, 424, 425  
     management, 405  
     methodology, 405–408  
     model, 413  
     national programs, 404–405, 425  
     need for, 405  
     requirements, 404, 405  
     standards and guidelines, 408–414  
 Planets (*see also* individual planets,  
     such as Mars, Mercury, Venus,  
     etc.) 133–188, 197–234  
     atmosphere, 368  
     clusters, 327  
     Earth-type, 327  
     formation of, 327–328  
     soil samples, 376  
 Plants, 272, 273, 276, 291, 296, 302  
     acceleration effects on, 289, 305  
     low-temperature effects on, 276, 279  
     spacecraft studies, 302–303  
     vibration effects, 291  
     weightlessness effects on, 288–289  
  
 Plasma sterilization, 419  
*Pleurococcus vulgaris*, 297  
 Pluto (planet), 197, 231–234  
     albedo, 233, 234  
     atmosphere, 233  
     body structure, 234  
     characteristics, 105  
     diameter, 233  
     mass, 233  
     mechanical data, 200  
     and Neptune, 231–232  
     orbit, 232  
     photometric properties, 199, 233–234  
     physical data, 231–233  
     radius, 234  
     rotation, 233  
     temperature, 234  
 Pneumatic suction sampling techniques, 377  
 Polar caps (PCA), 101–102  
 Polarimetry, 209, 234, 247  
 Polyadenine, 344  
 Polyglycosides, 344  
 Polylysine, 344  
 Polymers, 343, 344, 345, 410, 418  
 Polynucleotides, 346–347  
 Polypeptides, 341–342, 346, 347  
 Polyphosphates, 341  
 Polypropylene, 417  
 Porphyrins, 325, 372  
 Potassium, 121  
 Pressure, effects of, 285–288  
     high, 286–287  
     hydrostatic, 285  
     microorganisms, effects on, 286–288  
     tolerable, 287  
 Primordial soup, 342  
 Pristane (C<sub>20</sub>), 337  
 Probiotics, 345–347  
 Prospero (satellite) data, 74  
 Proteinoids, 339, 341, 343  
 Proteins  
     detection of, 380, 382, 383  
     in exobiology, 342, 344–346, 368  
*Proteus OX-19*, 383  
 Proton-proton cycle, 323  
 Protons, 6, 7, 17, 52, 54–59, 66, 68, 214,  
     293, 294, 419  
     death of, 84, 88  
     distribution of, 85  
     flux of, 55, 66, 72, 106  
     high-energy, 56, 71–72, 84  
     long-lived, 64  
     low-energy, 51, 61–64, 84, 86  
     origin of, 84  
     solar, 53, 57, 71, 72  
     spectra, 61, 65  
     streams, 56, 60, 62, 64, 65, 67, 71–72  
 Protoplanets, 326, 370

- Protozoa, 272, 276, 305  
*Pseudomonas*, 286  
*Pseudomonas aeruginosa*, 287, 301  
 Psyche (asteroid), 248  
 Ptolemaeus (lunar crater), 117, 118, 124  
 Pyrolysis, 338  
 Pyroxene, 137  
 Pyrrole, 325
- Quantum chemistry, 322
- Radar planetary studies, 74, 138, 139, 182, 376  
 Radiation belts, 77, 83–88, 203, 396, 419  
      $\alpha$ -particles in, 84–88  
     death of particles in, 88  
 Radio radiation, 34, 35, 52, 55  
 Radioastronomy measurements, 141, 148, 149, 150  
 Radiolocation experiment, 144, 146  
 Radiometer, 141, 177  
 Radio waves, 41  
*Rana pipiens*, 289  
*Rana temporaria*, 287  
 Rare earths, 121  
 Rats  
     acceleration effects on, 290  
     magnetic field effects, 296  
 Rayleigh scattering, 7, 200, 233  
 Reentry survivability, 407  
 Relativity, general theory of, 3–5  
 Relic radiation, 5  
 Remote life-detection methods, 375–376  
 Rhea (Saturn satellite), 241  
     physical data, 242  
 Rheometers, 55  
*Rhodotorula*, 292  
 Ribonuclease, 285  
 Ribonucleic acid (RNA), 382, 383, 384  
 Rocket high altitude experiments, 41, 55, 56, 101, 305  
 Rubidium, 123
- Saccharomyces*, 293  
*Saccharomyces bailii*, 304  
*Saccharomyces cerevisiae*, 286, 304  
*Saccharomyces ellipoideus*, 304  
*Saccharomyces rouxii*, 297  
*Salmonella schottmuelleri*, 294  
*Salmonella typhi*, 301  
 Salyut (spacecraft) data, 74  
 Sample collection methods, 377–378  
     devices, 377–378  
*Sarcina flava*, 282, 284  
*Sarcina lutea*, 383  
 Saturn (planet), 24, 197, 221–226, 327  
     atmosphere, 221–226  
     composition, 221–222
- Saturn (planet)—Continued  
     energy balance, 224–225  
     structure models, 225, 226  
     temperature, 222–223  
     visible surface, 223–224  
 body structure, 226  
 characteristics, 105  
 clouds on, 223  
 density, 197, 198, 226  
 ionosphere, 223  
 mass, 198, 226  
 mechanical data, 200  
 photometry of, 199, 224  
     detailed, 224  
     integrated, 224  
 physical data, 198  
 radio emission from, 222  
 rings, 224, 238–241  
     dimensions, 239  
     temperature, 239  
 rotation, 200  
 satellites, 241–243  
 spectrum, microwave, 223  
 white spots, 223
- Scalar-tensor theory of general relativity, 5  
 Scanning photometer, 375  
 Schwassmann-Wachmann (comet), 252–253  
 Semiconductors, 419  
*Serratia marcescens*, 286, 311  
 Shock waves, interplanetary space, 51–54, 66–67, 71, 77, 93, 323  
 Silicates, 126, 331  
 Silicon (Si), 20, 21, 27, 133, 322  
 Sinus Iridum (Moon), 117  
 Skin, sterilization of, 417  
 Sodium, 21  
 Soil drill, 377  
 Soil samples, 376–378  
     collection methods, 377  
     incubation of, 386–387  
     metabolism in, 390–393  
 Solar constant, 38, 140  
 Solar flares, 34–35, 47, 52, 53, 55–72, 407  
     chromospheric, 51, 53  
     classification of, 34, 35  
     large, 34, 45, 56–58  
     levels of activity, 58  
     and solar cosmic rays, 67–69, 72  
     weak, 34  
 Solar nebulae, 23–26, 126, 129, 325, 326, 331  
     Earth group substances, 326, 327  
     gas group substances, 326, 327  
     ice group substances, 326, 327  
     massive, 23–25  
     minimum, 23–24, 26
- Solar nebulae—Continued  
     models of, 25, 26  
     primitive, 25, 26, 28  
     theories of, 23–26  
     turbulence factor, 23  
 Solar particles, 64–66  
 Solar plasma, 47–50  
 Solar protuberances, 35  
 Solar system, 126, 129, 133, 197–254  
     age of, 28  
     carbon compounds in, 326–331  
     constituent materials, 21–22  
     formation of, 22–26, 27, 326  
         current theories, 23  
         dualistic theory, 22  
         monistic theory, 22  
     life in, 403  
     nebula theories, 23–26  
     origin of, 22–26, 126–127  
     turbulence factor, 24  
 Solar wind, 22, 23, 47–48, 50–53, 55, 70, 71, 77, 123, 140, 164, 252, 324, 327  
     chemical composition of, 47  
     density, 50  
     Moon and, 105  
     perturbations in, 48, 50–51  
     quiet, 47–48  
     velocity, 50–53, 218  
 Space hardware, 420, 423  
 Space station, 375, 376, 396  
 Space survival studies, 406–408  
 Spacecraft  
     contamination of, 403, 408–411, 414, 423  
     decontamination of, 418, 420, 423  
     sterilization of, 378, 420  
 Spacecraft biological experiments and studies, 133, 135, 142, 167–171, 180, 182, 301–305, 406, 415  
 Spectrometer studies, 148, 154, 162, 174, 182, 202  
 Spectrophotometry, 162, 248, 388  
 Spectroscopy, 150, 171, 178, 221  
 Spermatozoa, 276  
 Spiral arm shock, 15  
 Spores, 294, 410, 421, 422, 423  
 Sporicide, 418  
*Staphylococcus*, 301  
*Staphylococcus aureus*, 303, 311, 418  
 Starfish explosion, 85  
 Stars, 49, 54, 199  
     atmosphere, 323, 325  
     carbon, 323  
     core, 18–21  
     density wave theory of, 13  
     dwarf, 323  
     energy of, 17–18  
     evolution of, 18–20

- Stars—Continued**
- formation of, 13, 16, 22, 323–324
  - horizontal branch, 18–19
  - hydrogen, 10, 11, 18, 21
  - hydrogen-helium, 17
  - hydrostatic equilibrium, 17
  - interior of, 17, 18
  - main sequence, 17–19
  - mass, 20
  - massive, 11, 21
  - neutron, 11, 20, 21
  - nuclear reaction, 17–20, 23
  - nucleosynthesis, 11, 21, 22
  - orbits, 12, 13, 20
  - pregalactic, 10–12
  - primitive globular clusters, 10
  - red giant, 18, 324
  - rotation of, 13
  - spectra, 323
  - spiral arm, 12, 13
  - structure of, 16, 17, 18
  - temperature, 17, 18
  - white dwarf, 19
- Steady state, 344, 394
- Sterilization Assembly and Development Laboratory (SADL), 416
- Sterilization methods, 414, 421, 422
- autosterilization, 422–423
  - dry, 420, 422
  - ionizing radiation, 419, 422
  - procedures, 410
  - skin, 417
  - spacecraft, 423
  - surface, 418–420
  - thermal, 420
- Stochastic model, 411
- Stratomesosphere, 152
- Stratoscope II balloon telescope, 229
- Streptococcus*, 301
- Streptomyces cylindrosporus*, 309
- Streptomyces griseus*, 292
- Stromatolites, 336
- Strontrium (Sr), 121, 123, 124
- Sugars, 368
- Sulphur, 21, 370
- Sun, 13, 15–17, 23–25, 32–47, 115, 116, 124, 126, 127, 133, 138–141, 142–145, 323, 325–328
- activity of, 32–37
    - centers of, 35–37
    - cycles, 37
    - indices, 37
  - atmosphere, 32, 33, 35, 37, 54
  - bursts, 43–46, 67
  - chromosphere, 35, 36, 39, 42
  - corona, 34, 36, 42, 47, 51, 67, 324
  - diagram, 36
  - energy distribution, 40, 41
  - faculae, 34
- Sun—Continued
- flares, 34–36, 56–68
  - flocculi, 34, 36
  - formation of, 326
  - magnetic field, 32–34, 49
    - bipolar (BM), 33
    - cycle, 33
    - unipolar (UM), 33
  - mass, 19, 25
  - noise storms, 43
  - photosphere, 34, 37, 38–39
  - proto, 24
  - protuberances, 35–36
  - radiation of, 38, 39
    - corpuscular, 46–47, 55
    - electromagnetic, 32, 37
    - flux, 39, 40
    - microwave, 45
    - radio, 41–45
      - bremsstrahlung, 34, 42, 45
      - Cherenkov radiation, 42
      - magnetic bremsstrahlung, 42
      - shortwave, 39–41
      - sporadic, 45, 46
    - rotation of, 22
    - spectrum, 38
    - spots, 33–34, 36, 37, 58, 72
  - Sun-Earth connections, 32, 76, 89–105
    - geomagnetic activity, 89–95
    - geomagnetic disturbances, 89, 94–99, 100–103
      - morphology of, 95
    - ionospheric disturbances, 89, 98–99
    - solar wind and Earth's magnetic field, 92–94
  - Sunlight, 371, 372
  - Sunspots, 33–34, 58, 72
    - bipolar, 33
    - penumbra of, 33, 34
    - umbra of, 33, 34
    - unipolar, 33, 34
  - Supernova explosions, 11, 19–20, 21, 324
  - Surveyor 3 (lunar probe), 74
  - Surveyor 5 (lunar probe), 121
  - Surveyor 6 (lunar probe), 121
  - Surveyor 7 (lunar probe), 121
  - Swings effect, 251
  - Synechococcus*, 294
  - Syrtis Major (Mars), 177, 178, 179, 180
  - Tago-Sato-Kosaka (comet), 250
  - Telescope, 376
    - balloon, 229
  - Temperature, effects of, 276–281
    - high, 279–281
    - low, 276–279
    - superlow, 277
  - Temple (comet), 249
  - Tethys (Saturn satellite), 241
    - physical data, 242
  - Thermal sterilization, 420–421
  - Thermit, 421
  - Thermodynamic equilibrium, 339, 343, 344
  - Thermogenesis, 387
  - Thermonuclear reactions, 7, 19, 20
  - Thermoradiation, 421, 422
  - Thorium (Th), 121, 123
  - Thule (asteroid), 246
  - Titan (Saturn satellite), 197, 198, 236, 241–244
    - greenhouse model, 243
    - infrared photometry of, 244
    - physical data, 242
  - Titania (Uranus satellite), 244, 245
  - Titanium (Ti), 28, 121, 128, 137
  - Tithonius Lacus (Mars), 184
  - Toro (asteroid), 248
  - Tradescantia*, 303–305
  - Tradescantia paludosa*, 302
  - Tribolium confusum*, 304
  - Tritium, 7
  - Triton (Neptune satellite), 232, 245
  - Trojan (asteroid group), 246
  - Trypsin, 285
  - Trypticase soy agar (TSA), 424
  - Turbulence, 23, 24
  - Tuttle-Giacobini-Kresák (comet), 253
  - Ultraviolet(UV)radiation, 11, 34, 97, 162, 329, 339
    - effects of, 271, 273–276, 284, 291–293, 306, 307, 371
  - Mariner 10 experiment, 140
  - microorganisms, resistance to, 406, 407
  - Ultraviolet(UV)region, 371, 380, 382
  - Umbriel (Uranus satellite), 245
  - Universe (*see also* Cosmology, Earth-Moon system, Solar system, and Stars), 3–31
    - age of, 6
    - chaotic state of, 6, 8
    - closed, 7
    - coalescence stage, 8, 9
    - contraction, 3, 5, 10
    - evolution of, 322–326
    - expansion of, 3, 4, 5, 6, 8–10
    - Hubble radius, 5–8
    - length of, 5–7
    - matter and, 3–4, 6, 9
    - model of, 3, 5
    - open, 5–9
    - origin of, 5
    - physics of, 5–9
    - pregalactic era, 9–12
    - symmetric, 5, 8–9, 11

- Universe—Continued  
 temperature, 6, 9, 11  
 unsymmetric, 5–8
- Uracil, 340
- Uranium, 121, 122, 123
- Uranus (planet), 24, 197, 226–231  
 albedo, 232  
 atmosphere, 200, 226–231  
 composition, 226–228  
 structure, 230–231  
 temperature, 228–229  
 visible surface, 226, 229–230
- body structure, 231
- characteristics, 105
- density, 198
- hydrogen quadruple lines, 226–227
- mass, 198
- photometric data, 199
- physical data, 198
- rotation, 229
- satellites, 243–244
- spectrum, 227, 228
- Urease, 285
- Vacuum, 271, 281–285  
 enzymes, effects on, 285  
 microorganisms, effects on, 281–283,  
 407  
 high-vacuum effects, 284
- Vacuum probe, 409
- Valley Marineris (Mars), 184
- Van de Graff (lunar crater), 118
- Vela-2A (satellite) experiment, 48
- Vela-3A (satellite) experiment, 52, 53
- Vela-3B (satellite) experiment, 52
- Venera 1 (Venus probe), 47
- Venera 2 (Venus probe), 65, 94
- Venera 4 (Venus probe), 94, 142, 149,  
 150, 151, 152, 160, 161
- Venera 5 (Venus probe), 142, 149, 150,  
 151, 152
- Venera 6 (Venus probe), 66, 94, 142,  
 149, 150, 151
- Venera 7 (Venus probe), 142, 146–147,  
 149, 151, 160, 425
- Venera 8 (Venus probe), 142, 147–151,  
 155, 156, 158, 160
- Venus (planet), 126–128, 133, 135,  
 142–167, 280  
 albedo, 153
- Venus (planet)—Continued  
 astronomical characteristics, 142–146  
 atmosphere of, 142, 148–164, 327  
 chemical composition of, 150  
 dynamics, 158–161  
 models of, 151, 155, 161, 165  
 upper, 161–164  
 characteristics of, 105  
 clouds, 142, 144, 153, 154, 155, 156,  
 158, 160  
 conjunction, 143, 144  
 contamination, probability of, 406  
 density, 134, 144, 145  
 diameter, 134  
 distance from Sun, 142, 143, 145, 165  
 emission characteristics, 153  
 evolution of, 164–167  
 formation of, 327  
 geometric characteristics, 134  
 hydrogen corona, 164  
 illumination, 156–157  
 induced ionopause, 164  
 ionosphere, 148  
 life on, 142, 166  
 magnetopause, 105  
 map, 146, 147  
 mass, 134, 144  
 models, 151, 155, 158, 161, 165  
 optical measurements, 157  
 orbit, 142, 145  
 origin of, 164–165  
 phases, 143  
 photographs, 144, 161  
 physical properties, 146  
 probes, 406, 415, 425  
 quarantine program, 425  
 radar studies, 144, 146  
 radiation, 159  
 radiation conditions near, 105  
 radioastronomy measurements, 148,  
 149, 327  
 radiolocation experiment, 144, 146  
 radius, 144  
 reflective characteristics, 147, 153  
 rotation, 127, 142–145  
 seasons, 143, 144  
 solar wind and, 105  
 spacecraft data, 142, 144, 146–152,  
 156, 158–163  
 spectrometer studies, 148
- Venus (planet)—Continued  
 spectrum, 148, 154, 160  
 spin characteristics, 134  
 surface, 146–148, 167  
 temperature, 148, 149, 150, 152, 157,  
 158, 165, 166, 327  
 thermal mode, 157–158  
 volatile compounds, 166  
 water on, 153, 155, 165, 166  
 wind on, 160
- Vesta (asteroid), 244, 247, 248
- Vibration, effects of, 271, 290–291  
 mice, effects on, 291  
 spacecraft factor, 290–291
- Vidicon stereoscopic camera, 376
- Viking project, 397–398, 406  
 life-detection devices, 397–398  
 optical measuring unit, 398
- Viruses, 272
- Visible light, 38–39, 372
- Vitrification, 278
- Water, 323–325, 327, 328, 339, 343, 369,  
 370, 372, 386, 397  
 on Mars, 170, 176, 328, 329, 333  
 on Moon, 115, 121, 123  
 properties of, 370  
 in soil, 297–298
- Weightlessness, effects of, 271, 288–290  
 physiological effect, 289  
 plants, effect on, 288–289  
 simulation of, 288
- Westphal (comet), 253
- Wolf number, 37
- Worms, 276
- X-ray radiation, 34, 52
- X-ray structural analysis, 377
- X-rays, 15, 34, 40, 63, 67, 68, 294, 295,  
 419
- Xenon (Xe), 331
- Xenopsylla cheopis*, 297
- Xerophiles*, 297
- Xerophytes*, 296–300, 311, 312
- Yeasts, 279, 285, 293, 294, 299, 384
- Zond 3 (space probe), 65